Mathematical Problems in Engineering

Mathematical Control of Complex Systems 2013

Guest Editors: Zidong Wang, Hamid Reza Karimi, Bo Shen, Jun Hu, Hongli Dong, and Xiao He

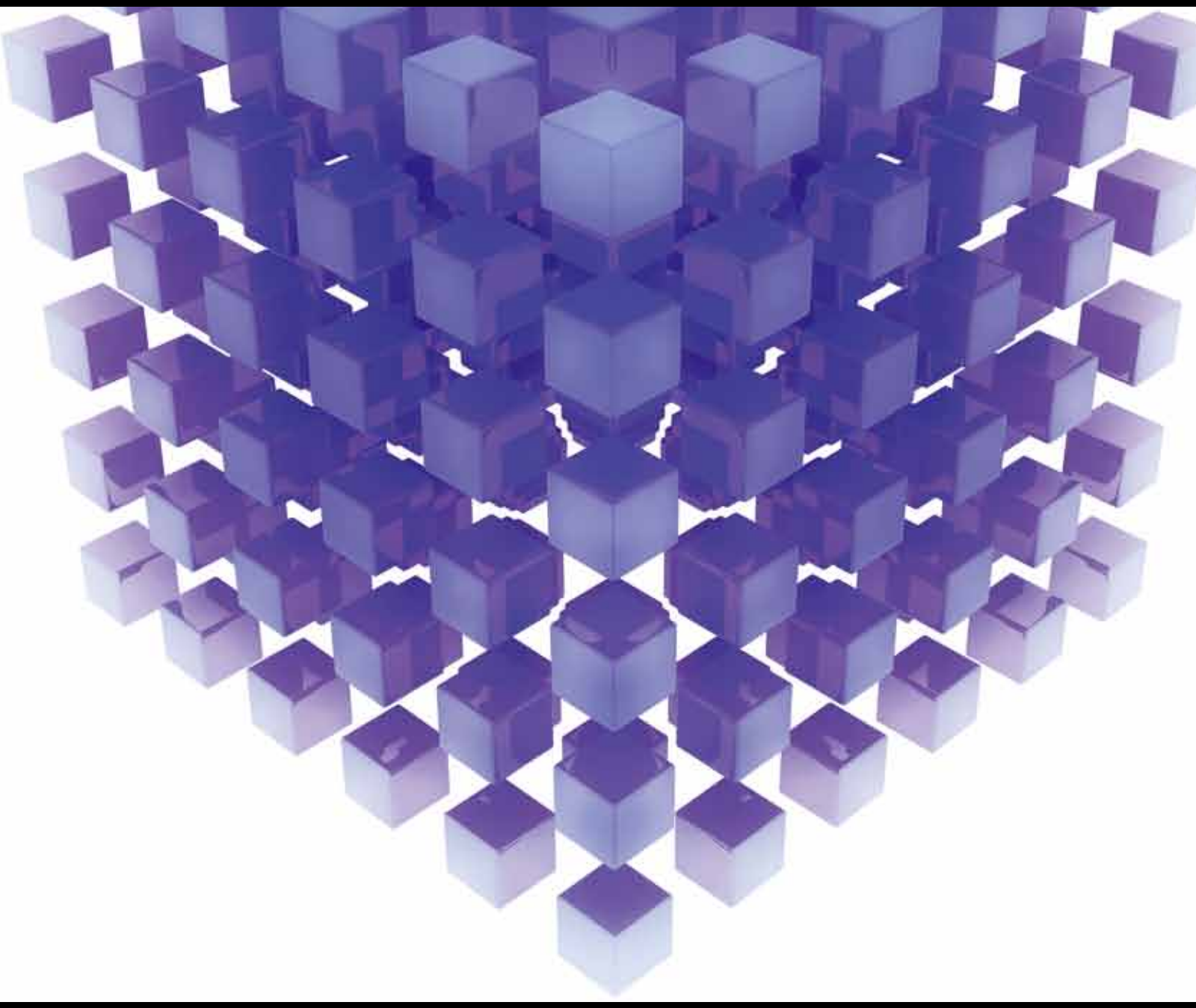

Mathematical Control of Complex Systems 2013

Mathematical Problems in Engineering

Mathematical Control of Complex Systems 2013

Guest Editors: Zidong Wang, Hamid Reza Karimi, Bo Shen, Jun Hu, Hongli Dong, and Xiao He

Editorial Board

Contents

Hindawi Publishing Corporation
Mathematical Problems in Engineering
Volume 2014, Article ID 825210, 4 pages
http://dx.doi.org/10.1155/2014/825210

Editorial
Mathematical Control of Complex Systems 2013

Zidong Wang,[1,2] Hamid Reza Karimi,[3] Bo Shen,[1] Jun Hu,[4,5] Hongli Dong,[5,6] and Xiao He[7]

[1] *School of Information Science and Technology, Donghua University, Shanghai 200051, China*
[2] *Department of Information Systems and Computing, Brunel University, Uxbridge, Middlesex UB8 3PH, UK*
[3] *Department of Engineering, Faculty of Engineering and Science, University of Agder, 4898 Grimstad, Norway*
[4] *Department of Applied Mathematics, Harbin University of Science and Technology, Harbin 150080, China*
[5] *Research Institute of Intelligent Control and Systems, Harbin Institute of Technology, Harbin 150001, China*
[6] *College of Electrical and Information Engineering, Northeast Petroleum University, Daqing 163318, China*
[7] *Department of Automation, Tsinghua University, Beijing 100084, China*

Correspondence should be addressed to Zidong Wang; zidong.wang@brunel.ac.uk

Received 1 December 2013; Accepted 1 December 2013; Published 23 January 2014

Mathematical control of complex systems have already become an ideal research area for control engineers, mathematicians, computer scientists, and biologists to understand, manage, analyze, and interpret functional information/dynamical behaviours from real-world complex dynamical systems, such as communication systems, process control, environmental systems, intelligent manufacturing systems, transportation systems, and structural systems. This special issue aims to bring together the latest/innovative knowledge and advances in mathematics for handling complex systems. Topics include, but are not limited to the following: control systems theory (behavioural systems, networked control systems, delay systems, distributed systems, infinite-dimensional systems, and positive systems); networked control (channel capacity constraints, control over communication networks, distributed filtering and control, information theory and control, and sensor networks); and stochastic systems (nonlinear filtering, nonparametric methods, particle filtering, partial identification, stochastic control, stochastic realization, system identification).

We have solicited submissions to this special issue from control engineers, electrical engineers, computer scientists, and mathematicians. After a rigorous peer review process, 31 papers have been selected that provide overviews, solutions, or early promises, to manage, analyze, and interpret dynamical behaviours of complex systems. These papers have covered both the theoretical and practical aspects of complex systems in the broad areas of dynamical systems, mathematics, statistics, operational research, and practical engineering.

This special issue starts with two survey papers on the recent advances of recursive filtering (sliding mode design) for networked nonlinear stochastic systems and distributed filtering (fault detection) for sensor networks. Specifically, in the paper entitled "*Recent advances on recursive filtering and sliding mode design for networked nonlinear stochastic systems: a survey*" by J. Hu et al., the focus is to provide a timely review on the recent advances of the recursive filtering and sliding mode design for nonlinear stochastic systems with network-induced phenomena. The network-induced phenomena under consideration include missing measurements, fading measurements, signal quantization, probabilistic sensor delays, sensor saturations, and randomly occurring nonlinearities. The recent developments of the network-induced phenomena are first summarized. Various filtering and sliding mode design for nonlinear stochastic systems are reviewed in great detail and some interesting yet challenging issues are raised. Latest results on recursive filtering and sliding mode designs for discrete-time nonlinear stochastic systems with network-induced phenomena are reviewed. Subsequently, a bibliographical review is provided in "*A survey on distributed filtering and fault detection for sensor networks*" by H. Dong et al. on distributed filtering and fault detection problems over sensor networks. The algorithms employed to study the distributed filtering and detection

problems are categorized and then discussed. In addition, some recent advances in distributed detection problems for faulty sensors and fault-events are also summarized in great detail. Finally, some concluding remarks are drawn and the future research challenges for distributed filtering and fault detection for sensor networks are pointed out.

During the past decades, the problems of performance analysis of complex systems have received significant research attention. In the paper entitled "*Numerical optimization design of dynamic quantizer via matrix uncertainty approach*" by K. Sawada and S. Shin, a numerical optimization method is proposed for the continuous-time dynamic quantizer under switching speed and quantized accuracy constraints. The design problem is discussed via sampled-data control framework and the case of temporal and spatial resolution constraints can be addressed in analysis and synthesis, simultaneously. Also, a new insight is presented for the two-step design of the existing continuous-time optimal quantizer. The performance monitoring and reliability analysis is discussed in "*Performance reliability prediction of complex system based on the condition monitoring information*" by H. Wang and Y. Jiang. Aircraft engine performance degradation process is described by using the Wiener process to forecast aeroengine performance reliability taking the condition monitoring information into account. The proposed method integrates the performance monitoring and reliability analysis into one framework by making full use of a variety of condition monitoring information. In the work entitled "*The method of Lyapunov function and exponential stability of impulsive delay systems with delayed impulses*" by P. Cheng et al., the problem of exponential stability is studied for a class of general impulsive delay systems with delayed impulses. By using the Lyapunov function method, some Lyapunov-based sufficient conditions are derived to ensure the exponential stability. Their applications to linear impulsive systems with time-varying delays are also proposed, and a set of sufficient conditions for exponential stability is provided in terms of matrix inequalities. The problem of global asymptotic stability is investigated for 2D discrete F-M systems with state saturation and time-varying delays in "*Stability analysis of state saturation 2D discrete time-delay systems based on F-M model*" by D. Chen and H. Yu. By constructing a delay-dependent 2D discrete Lyapunov functional and introducing a nonnegative scalar based on a row diagonally dominant matrix, a sufficient condition is proposed to guarantee the global asymptotic stability of the addressed systems by solving the linear matrix inequalities (LMIs). In the work entitled "*Impulsive vaccination SEIR model with nonlinear incidence rate and time delay*" by D. Li et al., a new impulsive vaccination SEIR epidemic model with time delay and nonlinear incidence rate is established. A sufficient condition is given to guarantee the stability of the disease-free periodic solution and the persistence of the model. Subsequently, in the paper entitled "*Synchronization of complex dynamical networks with nonidentical nodes and derivative coupling via distributed adaptive control*" by M. Shi et al., the distributed adaptive learning laws of periodically time-varying and constant parameters are designed and the distributed adaptive control is constructed.

The design of various controllers has long been the main stream of research topics and much effort has been made for complex systems. In the paper entitled "H_∞ *control of pairwise distributable large-scale TS fuzzy systems*" by A. Filasová and D. Krokavec, the partially decentralized control problems are studied for pairwise distributable large-scale TS fuzzy systems. Sufficient conditions are presented to ensure the stability and H_∞ performance. Subsequently, in the work entitled "*Stabilization of a class of stochastic nonlinear systems*" by N. Noroozi et al., two nonlinear controllers are given and applied to a guidance system in stochastic setting. Firstly, an adaptive control law for the guidance system is presented. Secondly, a robust finite-time control scheme is proposed to stabilize a class of nonlinear stochastic systems such that the closed loop system is stable. A new approach for self-triggered control is proposed in "*Self-triggered model predictive control using optimization with prediction horizon one*" by K. Kobayashi and K. Hiraishi from the viewpoint of model predictive control (MPC). The difficulty of self-triggered MPC is explained. Accordingly, the one-step input-constrained problem and the N-step input-constrained problem are formulated and solved. In the paper entitled "*Robust* H_∞ *control for discrete-time stochastic interval system with time delay*" by S. Yu et al., the robust H_∞ control problem is investigated for discrete-time stochastic interval system with time delay. By constructing appropriate Lyapunov-Krasovskii functional, sufficient conditions are given to ensure the existence of the robust H_∞ controller for addressed systems. By employing the Takagi-Sugeno (T-S) fuzzy linearization approach, the linear parameter varying (LPV) gain scheduling control problem is studied in "*State-feedback* H_∞ *control for LPV system using T-S fuzzy linearization approach*" by Y. Hu et al. By constructing the piecewise parameter-dependent Lyapunov function, the LPV T-S fuzzy gain scheduling control law is designed. In the paper entitled "H_∞ *control for two-dimensional Markovian jump systems with state-delays and defective mode information*" by Y. Wei et al., the problem of H_∞ control is discussed for a class of two-dimensional (2-D) Markovian jump linear systems (MJLSs) with state-delays and defective mode information. An extended model predictive control algorithm is given in "*LMI-based model predictive control for a class of constrained uncertain fuzzy Markov jump system*" by T. Yang and H. R. Karimi to address the problem of constrained robust model predictive control. By introducing two external parameters, new upper bounds on arbitrarily long time intervals are derived and less conservative results are given. In the work entitled "*Active control of oscillation patterns in the presence of multiarmed pitchfork structure of the critical manifold of singularly perturbed system*" by R. Vrabel et al., the possibility of control of oscillation patterns is analyzed for nonlinear dynamical systems without the excitation of oscillatory inputs. A general method is developed for the partition of the space of initial states to the areas allowing active control of the stable steady-state oscillations. The implementation of pair-wise decomposition is discussed in "*Coordinated control for a group of interconnected pairwise subsystems*" by C. Ma and X.-B. Chen for an interconnected system with uncertainties. The proposed controller scheme is applied on

a four-area power system to illustrate the effectiveness of the main results.

In the past decades, the issues of filter design and fault detection have received considerable research interests and have found successful applications in a wide range of practical engineering domains. In the paper entitled "*Robust H_∞ filtering for a class of uncertain Markovian jump systems with time delays*" by Y. Yang and J. Lu, the problem of robust H_∞ filtering is studied for a class of uncertain time-delay systems with Markovian jumping parameters and norm-bounded time-varying parameter uncertainties. The robust filter is designed in "*Finite-frequency filter design for networked control systems with missing measurement*" by D. Ye et al. for networked control systems (NCSs) with random missing measurements. A finite-frequency stochastic H_∞ performance is given and a sufficient condition is derived to guarantee desired performance. In the work entitled "*Intermittent fault detection for uncertain networked systems*" by X. He et al., the robust fault detection problem is studied for a class of discrete-time networked systems with multiple state delays and unknown input. Polytopic-type parameter uncertainty in the state-space model matrices is considered. A novel measurement model is employed to account for both the random measurement delays and the stochastic data missing (package dropout) phenomenon. By converting the addressed robust fault detection problem into an alternative robust H_∞ filtering problem of a certain Markovian jumping system, a sufficient condition for the existence of the desired robust fault detection filter is presented. The work entitled "*Adaptive fault detection with two time-varying control limits for nonlinear and multimodal processes*" by J. Li et al. is concerned with the two time-varying control limits design used for on-line fault detection for the multimode and nonlinear process. Mahalanobis distances among samples and super ball domains of mean and variance of samples are computed by a just-in-time (JIT) approach to reduce and update the training data set as queries being detected. In the paper entitled "*Fault diagnosis for linear discrete systems based on an adaptive observer*" by J. Liu et al., a fault diagnosis algorithm is developed to estimate the fault for a class of linear discrete systems based on an adaptive fault estimation observer. An observer gain matrix and adaptive adjusting rule of the fault estimator are designed. The proposed adaptive regulating algorithm can guarantee the negativity of the first order difference of a Lyapunov discrete function so that the observer is ensured to be stable and fault estimation errors are convergent. The problem of robust fault-tolerant tracking control is studied in "*Adaptive finite-time control for a flexible hypersonic vehicle with actuator fault*" by J. Wang et al. Simulation on the longitudinal model of a flexible air-breathing hypersonic vehicle (FAHV) with actuator faults and uncertainties is conducted. An adaptive fault-tolerant control strategy is presented based on practical finite-time sliding mode method such that the velocity and altitude track their desired commands in finite time with the partial loss of actuator effectiveness. The adaptive update laws are used to estimate the upper bound of uncertainties and the minimum value of actuator efficiency factor.

Over the past decades, the applications of various control schemes have received considerable research interests. In the work entitled "*An overview of distributed energy-efficient topology control for wireless adhoc networks*" by M. J. Abbasi et al., most recent energy efficient topology control algorithms in WSNs and adhoc network are classified and studied. The topology control aims of the existing algorithms are characterized into three main types: energy efficiency, network capacity, and energy balancing. The most famous and recent topology control algorithms based on their features are reviewed and compared in each goals category. In the paper entitled "*Proportional derivative control with inverse dead-zone for pendulum systems*" by J. Rubio et al., a proportional derivative controller with inverse dead-zone is proposed for the control of pendulum systems with dead-zone inputs. By using the Lyapunov analysis, the asymptotic stability of the proposed technique is guaranteed. Based on the hot rolling process, a load distribution optimization model is established in "*Load distribution of evolutionary algorithm for complex-process optimization based on differential evolutionary strategy in Hot Rolling Process*" by X. Yang et al. The rolling force ratio distribution and good strip shape are integrated as two indicators of objective function in the optimization model. The evolutionary algorithm for complex-process optimization (EACOP) is introduced. The paper entitled "*Nonlinear robust control of a hypersonic flight vehicle using fuzzy disturbance observer*" by L. Zehngdong et al. is concerned with a novel tracking controller design for a hypersonic flight vehicle in complex and volatile environment. The attitude control model is constructed with multivariate uncertainties and external disturbances. The nonlinear disturbance observer is introduced to estimate the influence of uncertainties and disturbances on the flight control system. Also, fuzzy theory is adopted to improve the performance of the nonlinear disturbance observer. By analyzing the topology of China Education and Research Network, it can be concluded that it is different from the common Internet in several aspects as in "*Study of evolution model of China education and research network*" by G. Mao and N. Zhang. The evolution model of the complex directed network is established which reflects some main characteristics of China Education and Research Network. In the work entitled "*On the multipeakon dissipative behavior of the modified coupled Camassa-Holm model for shallow water system*" by Z. Shen et al., the dissipative property is taken into account for the modified coupled two-component Camassa-Holm system after wave breaking. Based on the obtained global dissipative solutions to the modified coupled two-component Camassa-Holm system, the dissipative multipeakon solutions are constructed. In the paper entitled "*Analysis of the degradation of MOSFETs in switching mode power supply by characterizing source oscillator signals*" by X. Zheng et al., the focus is on the detection of incipient faults and on analyzing aging. The wiretap channel with action-dependent states and rate-limited feedback is established in "*Wiretap channel with action-dependent states and rate-limited feedback*" by X. Yin et al. The capacity-equivocation region and secrecy capacity of such a channel are obtained.

Acknowledgments

This special issue is a timely reflection of the recent research progress in the area of mathematical control of complex systems. We would like to acknowledge all authors for their efforts in submitting high-quality papers. We are also very grateful to the reviewers for their thorough and on time reviews of the papers.

Zidong Wang
Hamid Reza Karimi
Bo Shen
Jun Hu
Hongli Dong
Xiao He

Hindawi Publishing Corporation
Mathematical Problems in Engineering
Volume 2014, Article ID 427209, 10 pages
http://dx.doi.org/10.1155/2014/427209

Research Article

Adaptive Fault Detection with Two Time-Varying Control Limits for Nonlinear and Multimodal Processes

Jinna Li,[1,2] Yuan Li,[3] Yanhong Xie,[1] and Xuejun Zong[3]

[1] *The Lab of Operation and Control, Shenyang University of Chemical Technology, Liaoning 110142, China*
[2] *The Key Laboratory of Networked Control Systems, Shenyang Institute of Automation, Chinese Academy of Sciences, Liaoning 110016, China*
[3] *The College of Information Engineering, Shenyang University of Chemical Technology, Liaoning 110142, China*

Correspondence should be addressed to Jinna Li; lijinna_721@126.com

Received 11 September 2013; Accepted 17 November 2013; Published 20 January 2014

Academic Editor: Jun Hu

A novel fault detection method is proposed for detection process with nonlinearity and multimodal batches. Calculating the Mahalanobis distance of samples, the data with the similar characteristics are replaced by the mean of them; thus, the number of training data is reduced easily. Moreover, the super ball regions of mean and variance of training data are presented, which not only retains the statistical properties of original training data but also avoids the reduction of data unlimitedly. To accurately identify faults, two control limits are determined during investigating the distributions of distances and angles between training samples to their nearest neighboring samples in the reduced database; thus, the traditional k-nearest neighbors (only considering distances) fault detection (FD-kNN) method is developed. Another feature of the proposed detection method is that the control limits vary with updating database such that an adaptive fault detection technique is obtained. Finally, numerical examples and case study are given to illustrate the effectiveness and advantages of the proposed method.

1. Introduction

Fault detection has been one focus of recent efforts since there existed a growing need for the quality monitoring and safe operation in the practical process engineering [1–4]. The objective existences of dynamic change, multiple modes, and nonlinearity pose serious challenges for fault detection proceeding in most of the process engineering, such as semiconduction process [5–8]. Hence, an effective and adaptive fault detection technology is worth investigating in order to deal with these obstacles.

Note that nonlinear PCA method [9] dynamic PCA [10] have been reported to be used for tackling dynamic and nonlinear process. Following them, [11] investigated the fault detection for nonlinear systems based on T-S fuzzy-modeling theory. Reference [12] investigated the nonlinear systems modeling and fault detection for electric power systems. However, the aforementioned methods fail to work well for the dynamic systems with nonlinearity together with multiple modes. Recently, [5, 6, 13–15] proposed some detection techniques to jointly address the nonlinear, multimodal, and dynamic behaviors of systems. References [5, 6] applied kNN rule and improved PCA-kNN to fault detection for semiconductor manufactory process with nonlinear and multimode behaviors. Reference [14] proposed an adaptive local model based on the monitoring approach for online monitoring of nonlinear and multiple mode processes with non-Gaussian information. Reference [15] proposed a data-based just-in-time (JIT) SPC detection and identification technique, where the distance was calculated and checked every time when fault detection was conducted. Reference [13] reduced and updated training database, and it presented JIT fault detection method.

Note that it is the key how to determine the scale of reduced database for precise fault detection. However, to the best of the authors' knowledge, how to reduce and update the training samples set to lighten the computation load and realize high detection performance has not been investigated fully to date. Moreover, there are data drift and shift as well as circumstance disturbance involved in the practical

engineering application such that originally normal data may be mistaken for fault, or vice versa. Time-varying control limits design is a potential approach used to overcome the above-mentioned negative factors, while few results have been available in the literature so far, which motivates the present study.

This paper is concerned with the two time-varying control limits design used for online fault detection for the multi-mode and nonlinear processes. The key idea is that Mahalanobis distances among samples and super ball domains of mean and variance of samples are first computed by a JIT approach to reduce and update the training data set as queries being detected. Then, two control limits are computed in terms of both kNN distance and kNN angle rules such that we can accurately identify whether the current data is normal or not by on-line approach. It is worth pointing out that two control limits vary according to the updating database such that an adaptive fault detection technique that can effectively eliminate the impact of data drift and shift on the performance of detection process is obtained. Several distinguished differences from the existing solutions to deal with fault detection for industrial processes with nonlinear and multi-mode behaviors are given below.

(1) Compared with [5, 6], FD-kNN method is improved in the sense of the stochastic characteristic (mean) of training samples' angles to their k-nearest neighboring training samples being investigated to calculate control limit. Thus, two control limits are derived, which is the significant contribution in this paper.

(2) Different from [15], we propose a new fault detection framework used to reduce and update database, as well as vary control limits. Note that [5, 6] are not also focused on this framework.

(3) There exist two significant differences from [13]. The first one is that the method of reducing training database. Here, two thresholds are proposed to control the reduction of data. The second one is that two time-varying control limits used for detecting fault are presented, while only one time-varying control limit is derived in [13].

This paper is organized as follows. An algorithm of reducing training database is presented in Section 2. Section 3 is dedicated to describe the on-line fault detection method. Section 4 presents the results of experimental simulation. Conclusions are stated in Section 5.

2. Reducing the Training Data Set

In this section, we will describe a technique of reducing the training data set.

The need for reducing training samples in database originates from the need to reduce calculation load and cost expenditure for fault detection. However, the key is how to control the reduction degree, while guaranteeing high detection quality. Here, we try to utilize the property that the closer the Mahalanobis distance between two samples is, the more similar their basic features are. The basic idea is that the two data with the closest Mahalanobis in database are searched and substituted for the mean of them [16], and this process is repeated until both mean of samples and variance of samples exceed a specific threshold. Let $\mathbf{X}$ denote the training data matrix with n samples (rows) and m variables (columns), meanwhile, $\mathbf{X}$ also represents the raw data set that consists of n samples. The detailed algorithm is given as follows.

Algorithm 1. One has the following.

Step 1. Let $\mathbf{Z}(n\times m) = \mathbf{X}(n\times m)$ and $\mathbf{V} = (v_{ij}) = ((x_i - \overline{x}_i)'(x_j - \overline{x}_j)/(n-1))$ denote the covariance matrix of $\mathbf{X}$, where x_i and x_j $(i, j = 1, 2, \ldots, m)$ are the stochastic variables, and those means are denoted by $\overline{x}_i$ and $\overline{x}_j$, respectively.

Step 2. Calculate the variance and mean of samples as $\mathbf{V}_X = [v_{11} \quad v_{22} \cdots v_{mm}]^{\mathrm{T}}$ and $\mathbf{M}_X = [\overline{x}_1 \quad \overline{x}_2 \cdots \overline{x}_m]^{\mathrm{T}}$, where v_{ii} denotes the sample variance corresponded to stochastic variable x_i $(i = 1, 2, \ldots, m)$.

Step 3. For each sample, we calculate the Mahalanobis distances between it and all of the other samples stored in data set $\mathbf{Z}$, and we define a Mahalanobis distance matrix $\mathbf{MD}(n \times n) = (md_{ij})$, where md_{ij} $(i, j = 1, 2, \ldots, n)$ represents the Mahalanobis distance between sample i and sample j.

Step 4. The minimum and nonzero element in each raw in the matrix $\mathbf{MD}$ is searched and all of them construct a row vector $\mathbf{v}$ $(1 \times n)$. Moreover, we record the place (column number) of each minimum element in each row, and they are placed in a row vector $p(1 \times n)$. Based on it, finding out the minimum value in $\mathbf{v}(1 \times n)$, and if its place in $\mathbf{v}(1 \times n)$ is i and No. i element is j in vector $p(1 \times n)$, then md_{ij} is the minimum value in the matrix $\mathbf{MD}(n\times n)$, which means the Mahalanobis distance between the sample i and the sample j is the closest in training data set.

Step 5. Leting $\mathbf{M} = \mathbf{Z}$, the sample i is replaced by the mean of the sample i and the sample j, and the sample j is deleted; thus, the matrix $\mathbf{Z}$ is reduced a row. Similar to Step 2, the variance $\mathbf{V}_Z$ and mean $\mathbf{M}_Z$ of samples $\mathbf{Z}$ are calculated, respectively. Set a threshold ϵ, if the variance and mean of samples $\mathbf{Z}$ belong to the ε super ball domain of the variance and mean of samples $\mathbf{X}$; that is, $\|\mathbf{M}_Z - \mathbf{M}_X\| \le \varepsilon$ and $\|\mathbf{V}_Z - \mathbf{V}_X\| \le \varepsilon$, return to Step 3, where $0 \le \varepsilon < 1$; otherwise, $\mathbf{M}$ is the simplified data SET. Exit.

Remark 2. Note that the two similar samples are replaced by the mean of them based on Mahalanobis distance; however, the statistical characteristics of samples will remain essentially unchanged since the threshold ε that bounds the ranges of mean and variance-centered super ball domains limits the reduction degree of training data. Obviously, the smaller the threshold ε, the fewer the samples deleted, and then good detection results may be obtained since mean and variance of raw data change less. However, too much data will have heavy load on both storage cost and computation. Therefore, we advise that a proper small threshold should be determined

based on the compromise of lower cost and higher detection performance. Obviously, Algorithm 1 is a kind of logical and promising way of reducing training data.

Remark 3. As a matter of fact, our approach has obviously extended the methods used to reduce database in [13, 16] in the sense that the changes of mean and variance of raw data set are limited inside two specific super ball domains. Few changes in mean and variance of raw data set guarantee that the statistical characteristics of raw data are unchanged to some level.

3. Detection Method

The basic principle of the proposed fault detection method in this paper is that the trajectory of an incoming normal sample is similar to the trajectories of training samples that consist of normal data, which means that the trajectory of an incoming fault sample must exhibit some deviations from the trajectories of normal training samples [5, 6]. In other words, the distance between a fault sample and the nearest neighboring training samples must be greater than a normal sample's distance to the nearest neighboring training samples, and a fault sample's angle with the nearest neighboring training samples must also be greater than a normal sample's angle with the nearest neighboring training samples. Therefore, if we can determine the distribution of training samples' distances to their nearest neighboring training samples and the distribution of training samples' angles with their nearest neighboring training samples, we can define two control limits for given confidence levels. A query is considered abnormal if its distance to its nearest neighboring training samples is beyond the control limit CL_d or the control limit CL_θ. Otherwise, the query is normal.

In this section, we will give two fault detection methods. One is that queries are identified with fixed control limits as shown in Figure 1. In Figure 2, the other scheme in which control limits are updated along with normal query updating database also can be seen.

3.1. Fault Detection with Fixed Control Limits

(A) Offline Model Building

Algorithm 4. One has the following.

Step 1. Set $i = 1$ choose positive integers k_1, k_2, and s denotes the number of data in the reduced database Ω.

Step 2. Find k_1 neighbors with the nearest distance and k_2 neighbors with minimum angle for sample i in the database Ω, respectively.

Step 3. Calculate the squared distances between sample i and its k_1 nearest neighbors and the angles between sample i and its k_2 neighbors.

Step 4. Calculate the mean $\overline{X}_i$ of these squared distances and the mean θ_i of these angles.

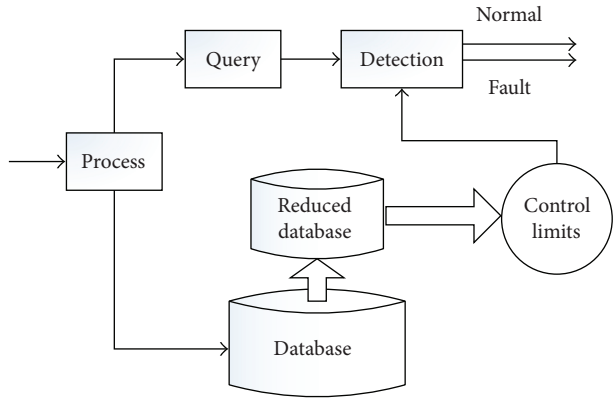

Figure 1: Fault detection with fixed control limits.

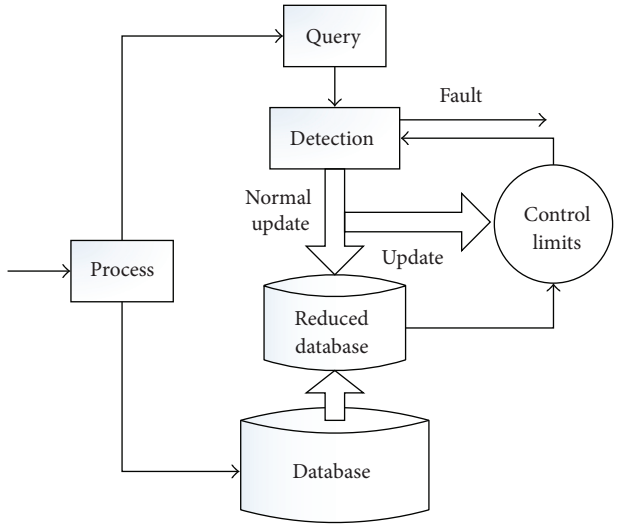

Figure 2: Fault detection with varying control limits.

Step 5. Set $i = i + 1$. If $i \leq s$, go to Step 2; otherwise, go to Step 6.

Step 6. Estimate the cumulative distribution functions of $\overline{X}_i$ and θ_i to obtain CL_d and CL_θ.

Remark 5. At Step 2, Euclidean distance is used since it is simple and easy, but any other distance is also suitable for the method proposed. For the choice of k_1 and k_2, an alternative approach is to try several different values of k_1 and k_2 on historical data and choose the values that give the best cross-validation [5, 6].

Remark 6. Two control limits CL_d and CL_θ proposed in this paper are determined in terms of cumulative distribution functions for given confidence levels, which means that the mean values of vast majority squared distance and angles based on kNN rule for the normal samples do not exceed it. For example, 95% control limit means a value within which 95% of population of normal operation data (calculated mean values) are included. Here, 95% is called confidence level based on probability and statistical theory.

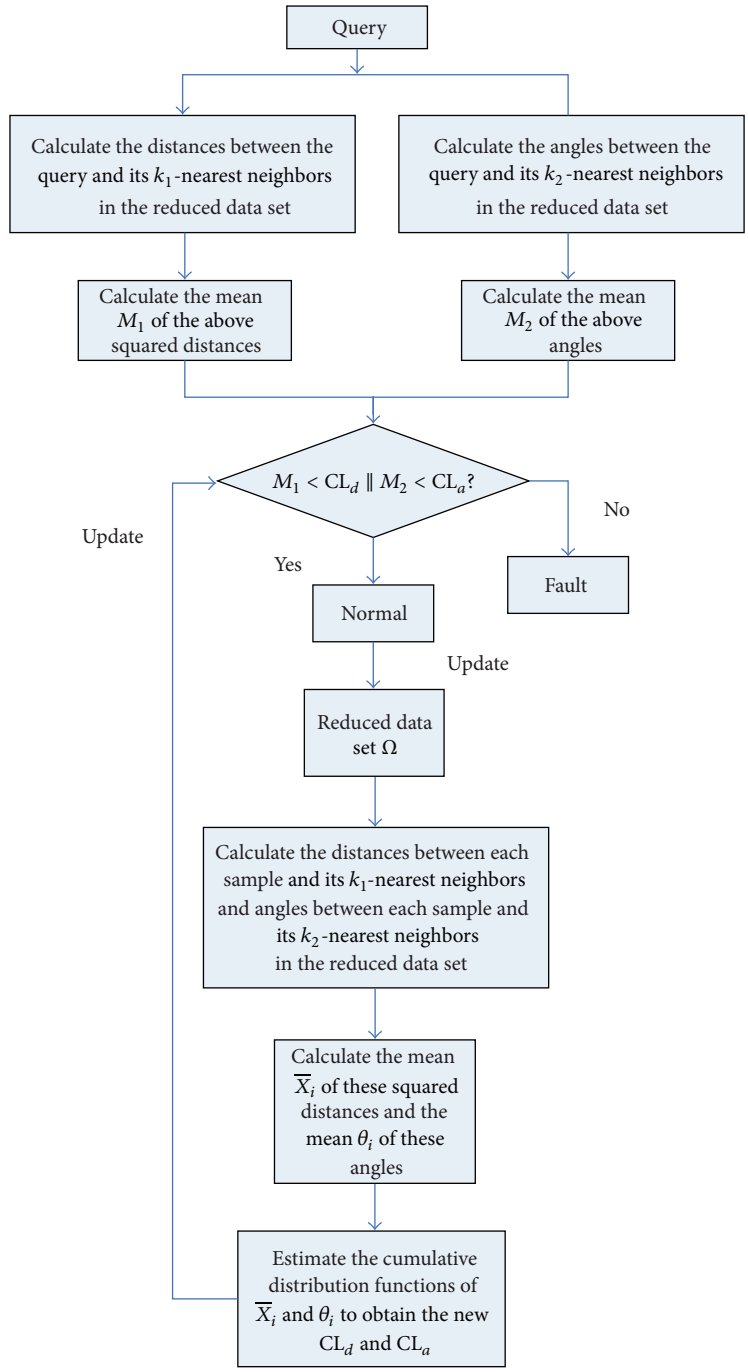

Figure 3: Flow chart of proposed method with varying.

(B) Online Detection

Algorithm 7. One has the following.

Step 1. Calculate the squared distances between the query i ($i = 1, 2, \ldots$) and its k_1-nearest neighbors and the angles between it and its k_2 neighbors in the reduced data set Ω.

Step 2. Calculate the means of the above squared distances and angles.

Step 3. The query is abnormal if the means are beyond either CL_d or CL_a; otherwise, this query is normal. $i = i + 1$, return to Step 1.

3.2. Fault Detection with Varying Control Limits. Firstly, we perform Algorithm 4 to obtain two control limits CL_d or CL_a based on the reduced training data. Next, we continue to carry out Algorithm 8 that is obtained by rewriting Algorithm 7.

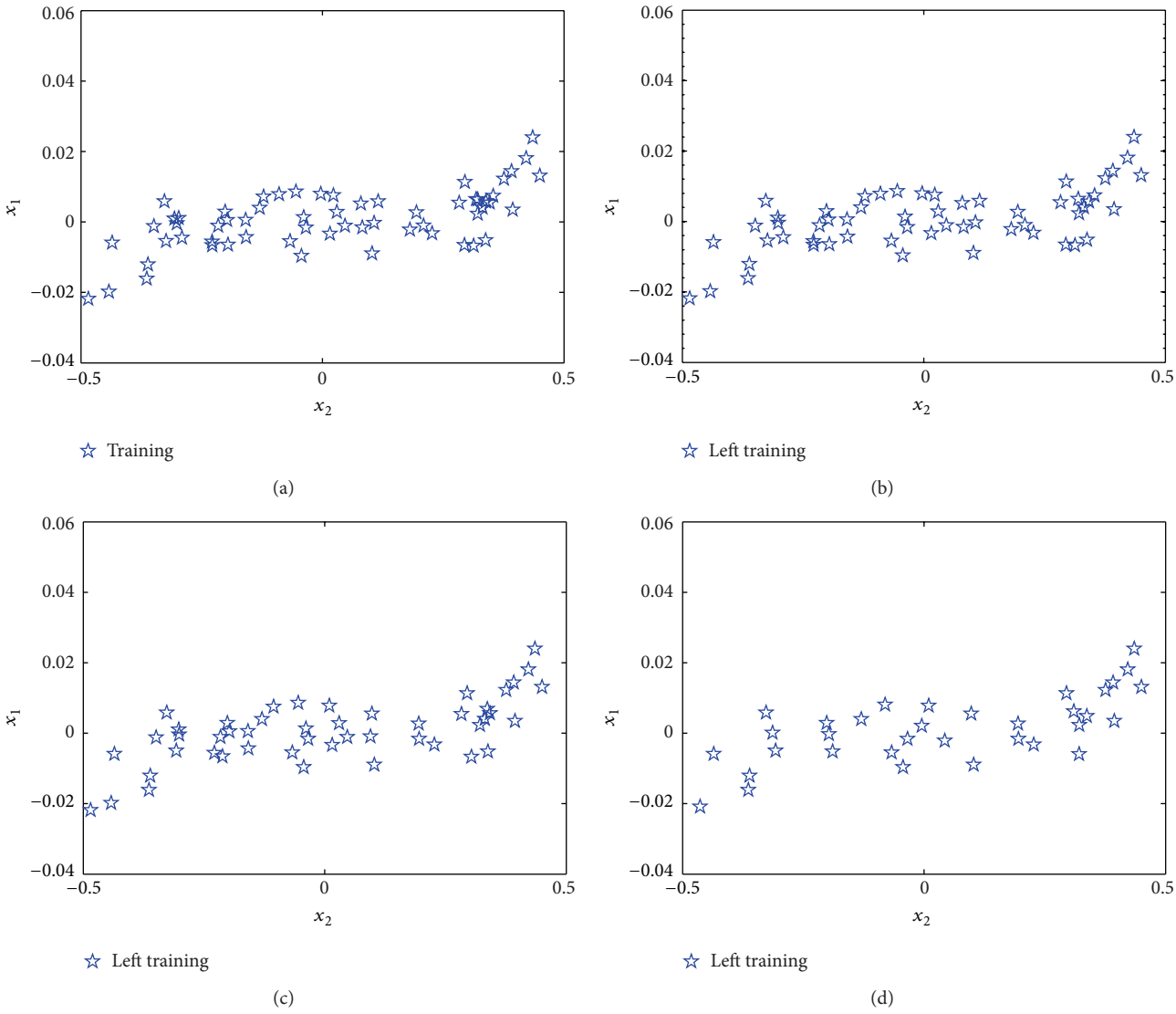

Figure 4: Training dataset (a) and left data under thresholds $\epsilon = 0.01$ (b), $\epsilon = 0.015$ (c), and $\epsilon = 0.02$ (d).

Algorithm 8. One has the following.

Step 1. Calculate the distances between the query i ($i = 1, 2, \ldots$) and its k_1-nearest neighbors and the angles between it and its k_2 neighbors in the reduced data set Ω.

Step 2. Calculate the means of the above squared distances and angles.

Step 3. The query is abnormal if the means are beyond either CL_d or CL_a; then, $i = i + 1$, return to Step 1. Otherwise, this query is normal and it can be put into the reduced database to updated database Ω.

Step 4. Continuing to perform Algorithm 1 and Algorithm 4, the new CL_d or CL_a are calculated. $i = i + 1$, return to Step 1.

More detailed implementation of Algorithm 8 is shown in Figure 3.

Remark 9. Obviously, time-varying control limits obtained by recalculating control limits when the new detected normal data are added into database can reduce the effect of drift and shift or circumstance disturbance on fault detection, compared with the fix control limit [5, 6, 15]. However, it may also increase computation complexity and cost expenditure. It should be pointed out that Algorithm 1 is implemented once the on-line detection process is completed as shown in Algorithm 8. Thus the updated database can be reduced, such that the low cost of storage and high fault detection quality can be guaranteed simultaneously.

Remark 10. Compared with [5, 6, 9–13, 15], the technique that reduces and updates training data set is a main contribution in this paper. More importantly, as shown in Figure 3, the varying control limits can be derived such that the adaptive fault detection can eliminate the impact of data drift and shift on the quality of fault detection to some extent. Moreover, we

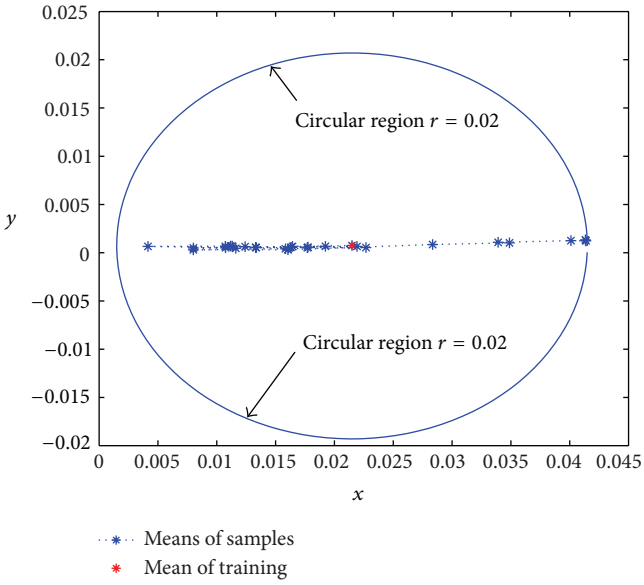

FIGURE 5: Means of samples with circular region.

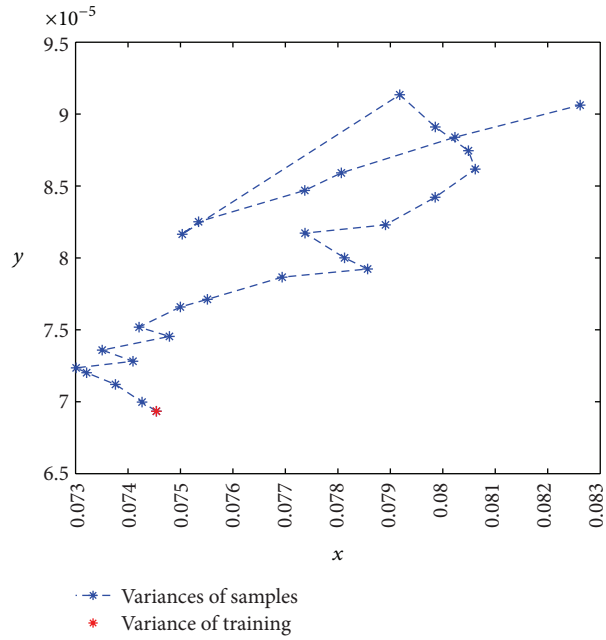

FIGURE 6: Variances of samples.

make use of two control limits to identify faults; it is natural that detection performance is better by the method proposed in this paper than that obtained in [5, 6].

Remark 11. Note that the database is updated by on-line approach and confidence limits of statistics used for detecting faults are also time-varying in [14]. For the sake of comparison, we give two differences. One is that the database is not only updated but also reduced during detection process. The other is that models of systems are not constructed, and two controls limits are presented by investigating the statistical characteristics.

Remark 12. In fact, the difficulties posed by nonlinearity, dynamic changes, and multiple modes of control process on fault detection have been addressed explicitly by the detection method proposed, which comes as no great surprise, since the kNN technique (handling nonlinearity and multiple modes), the on-line detection, and update scheme (adapting to dynamic changes) are integrated.

4. Numerical Examples

In this section, two examples are given to show the effectiveness of the proposed fault detection technique. In Example 1, firstly, we give the results of reducing training data set under different thresholds and the main aim is to show the effect of thresholds on the number of reducing training data; secondly, we not only verify the effectiveness of the detection method proposed in this paper for nonlinear process but also illustrate that faults can be identified better under two control limits than one control limit; in addition, comparative results are given to show the advantages of this paper. In Example 2, we verify the effectiveness of proposed detective technique under multiple modes. More importantly, the advantage of dynamic and varying control limit can be shown.

Example 1. Consider the following dominant nonlinear and single process mode:

$$x_1 = x_2^3 + \text{noise}. \tag{1}$$

(*A*) *Reduction of Training Data under Different Thresholds.* 60 normal runs are operated for verifying the method of reducing training data set. Here, three thresholds $\epsilon = 0.01$, $\epsilon = 0.015$, and $\epsilon = 0.02$ are set, corresponding to which Table 1 gives the number of left samples in the reduced data set, and the upper bounds of distance deviations between mean and variance of left data and those of the training data can also be seen in Table 1. Figure 4 shows the training data set and the reduced data set under different thresholds.

As shown in Table 1 and Figure 4, the left data become less and less and distance deviations of mean and variance increase with the threshold increasing. Then, a small threshold is favorable in order that the characteristics of training data is retained leading to better detection results. To clearly describe the reducing data process, we give Figures 5–7. In Figure 5, the red star denotes the mean of training data, and blue stars with dashed line describe the changes of means of training sample during reducing process under threshold $\epsilon = 0.02$. Similarly, Figures 6 and 7 show the changes of variance of sample under the aforementioned threshold. Moreover, the circular regions (when the dimension of sample exceeds 3, we use the supper ball regions) with radius of 0.02 are shown in Figures 5 and 7, respectively.

(*B*) *Verification of the Detection Method Proposed and Comparison with Relevant Results.* Continuing to operate

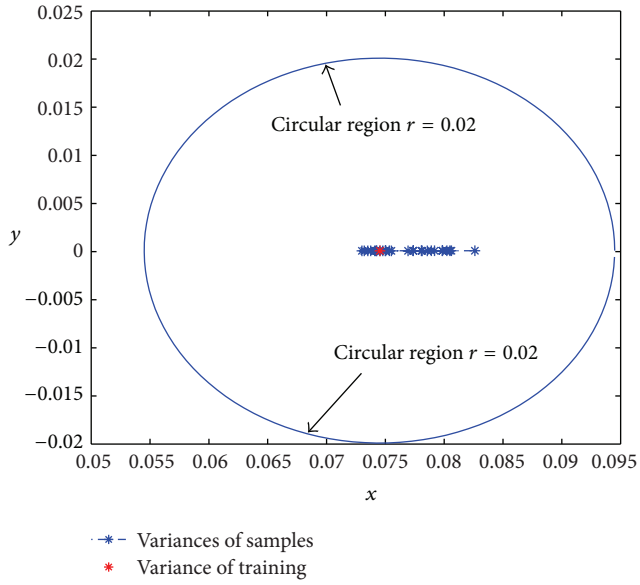

Figure 7: Variances of samples with circular region.

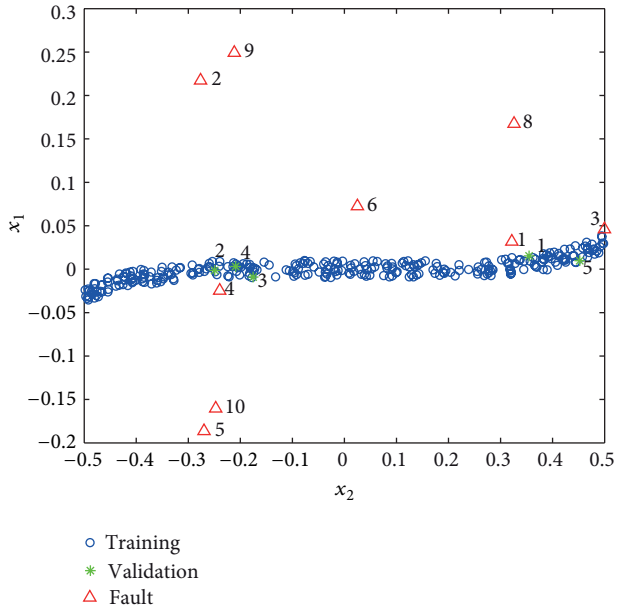

Figure 8: Training data set, validations, and faults.

Table 1: Reduction of Database.

Thresholds	Left data	$\|\mathbf{M}_Z - \mathbf{M}_X\|$	$\|\mathbf{V}_Z - \mathbf{V}_X\|$
0.01	57	0.0103	0.0015
0.015	48	0.0173	0.0036
0.02	34	0.0261	0.0092

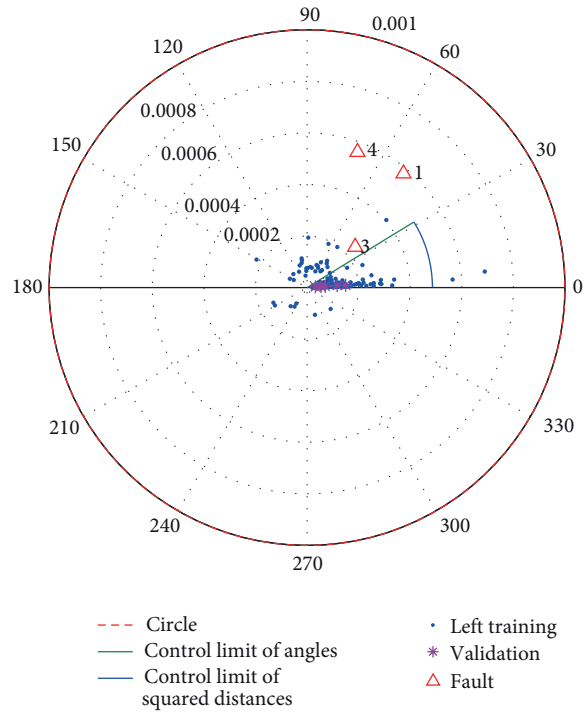

Figure 9: Fault detection by the method in this paper.

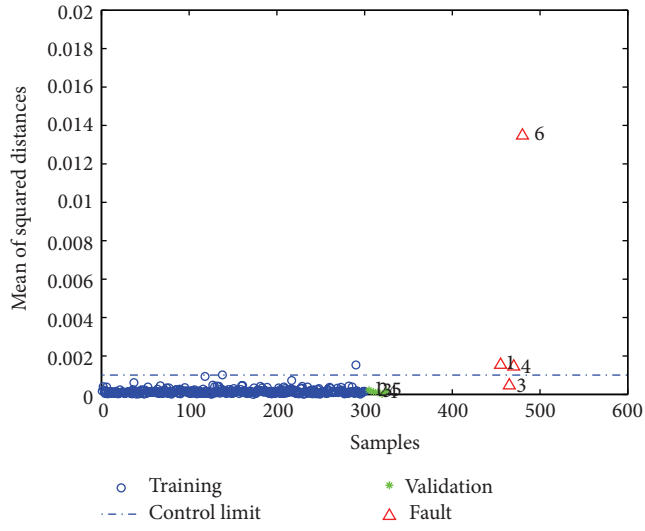

Figure 10: Fault detection by kNN method [5].

Table 2: Summary of parameters in Example 1.

ε	k_1	k_2	CL_d	CL_θ	Left data
0.01	5	5	$4.8628e-004$	0.5510	268

the system (1), we obtain 300 normal data used for training data, 5 normal runs used for validation, and 10 faults introduced and all of these data are shown in Figure 8. Some necessary parameters used in Algorithms 1 and 4 and obtained results are given in Table 2. Here, two confidence levels 99% and 85% are chosen to obtain the CL_d and CL_θ. The detection result by the method in this paper is presented in polar coordinates shown in Figure 9. Clearly, the normal data should belong to the area enclosed by the polar axis, a ray with polar angle CL_θ and polar radius CL_d based on

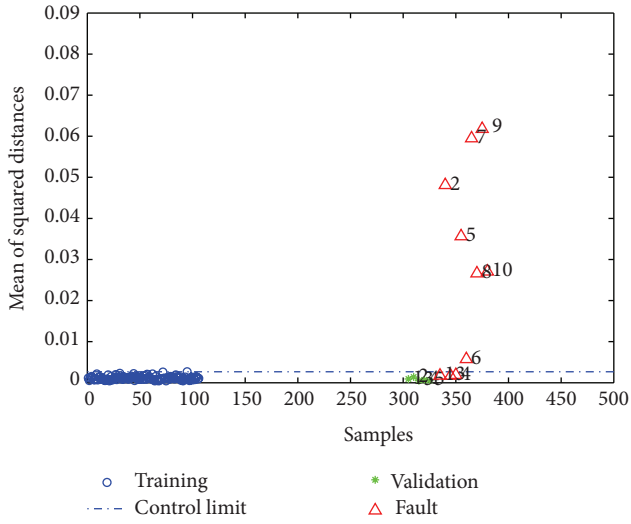

Figure 11: Fault detection by the method [13].

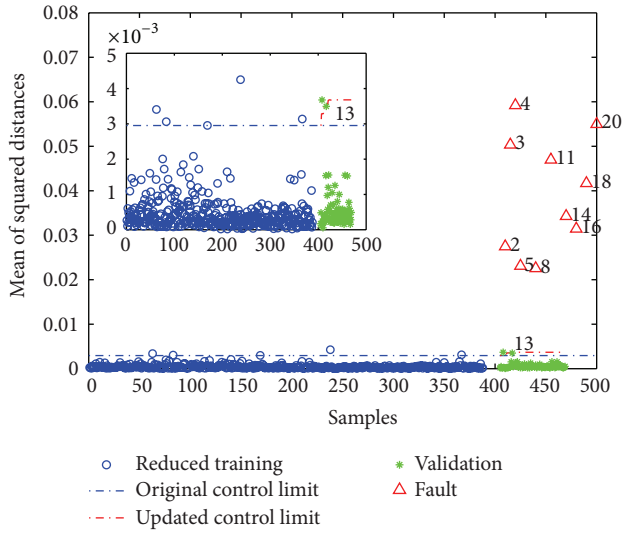

Figure 13: Fault detection by the proposed method.

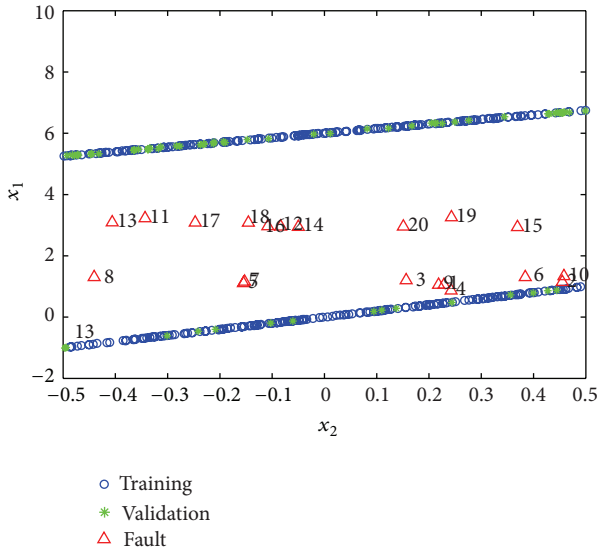

Figure 12: Training data set, validations, and faults.

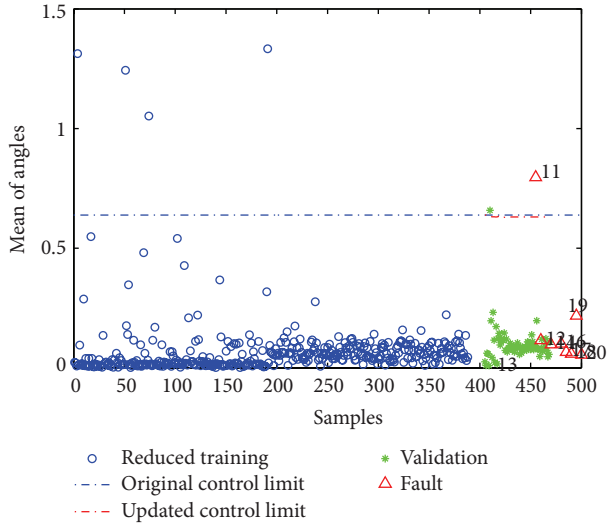

Figure 14: Fault detection by the proposed method.

Algorithm 7, and the data outside the area are faults. It should be pointed out that faults that do not appear in Figure 9 have exceeded the display extent. From Figure 9, all of faults are accurately identified. Simulation results presented illustrate that defection performance does not suffer degradation by virtue of the reduced data set, which will contribute to saving storage space and reducing the computational complexity. Figures 10 and 11 show the detection results by the method proposed in [5, 13], respectively. In Figure 10, fault 3 is identified as normal and faults 1, 3, and 4 are mistaken for normal data in Figure 11. The single control limit based on the nearest distances is used in [5, 13] to detect data, while two control limits obtained by utilizing the distributions of k-nearest distances and smallest angles are used in detective process in this paper. By comparison with the methods in [5, 13], the advantage of the detective technique with two control limits over one control limit is obvious.

Example 2. Considers the following bimodal cases [5, 6]:

$$\begin{aligned} &\text{(A)}\ x_1 = 2x_2 + \text{noise}, \\ &\text{(B)}\ x_1 = 1.5x_2 + 6 + \text{noise}. \end{aligned} \tag{2}$$

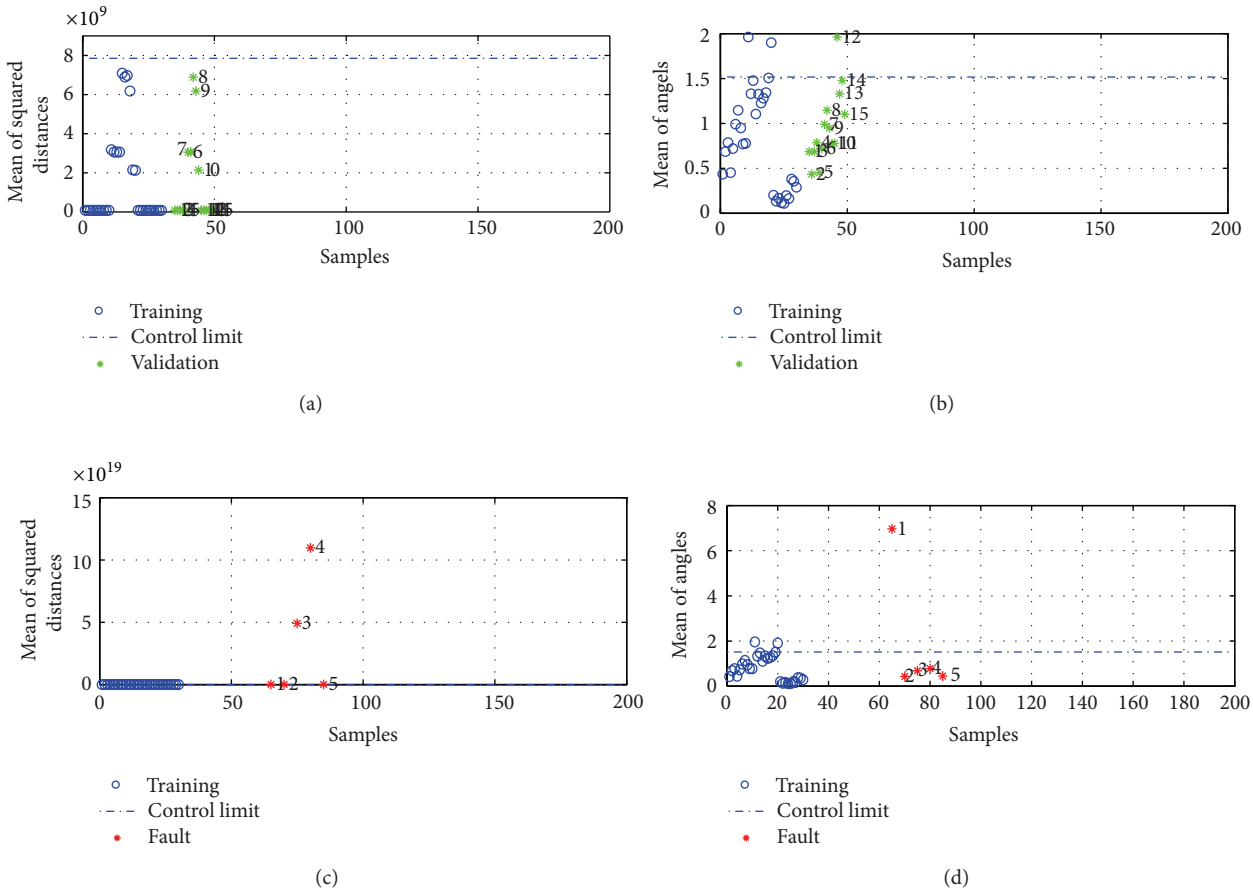

Figure 15: Fault detection by the proposed method.

The above two cases are operated to produce 200 normal data, respectively, and continue to be operated to produce 10 faults that are used for the defection, respectively. Moreover, the first case is operated to produce 10 normal data and 50 normal data are produced in operating the second case, then the total 60 normal data are used for validation. All data are given in Figure 12. Similar to Example 1, both k_1 and k_2 are set to be 10, and the confidence level is chosen as 99% and 90% to calculate the CL_d and CL_θ, respectively. Threshold $\epsilon = 0.03$ is set. When validations are detected, data set is updated and reduced, and control limits are also updated. At last, 299 normal samples are left to use for fault detection. The detection results by the proposed method in this paper is presented in Figures 13 and 14. As shown in Figures 13 and 14, control limits CL_d and CL_θ are updated as the validations are identified and all of faults are identified correctly. Note that the normal sample 13 used for validation is correctly identified, while it is mistaken for fault under the fix control limit (similar to [15]), which illustrates the advantage of the varying control limits.

5. Case Study

In this section, all of data used for training and validation are produced from an AL stack etch process that was performed on a commercial scale Lam 9600 plasma etch tool at Texas Instrument, Inc. [17]. It is well known that AL stack etch process is characterized by the multiple modes and nonlinearity, and it is usually accompanied by data drift and shift. By Algorithm 8, the control limits $\mathrm{CL}_d = 7.8537e+09$ and $\mathrm{CL}_\theta = 1.5165$ are calculated, respectively. Changing training data, 5 faults are obtained. Figure 15 shows the detection results by the proposed method in this paper. One can clearly see that almost all of validations are identified as normal data and all of faults exceed the control limit CL_d. This case illustrates the effectiveness of the proposed method.

6. Conclusions

This paper studies an adaptive fault detection method faced to process engineering with nonlinear and multimodal behaviors. The main idea is as follows: firstly, the training database is reduced and updated by on-line approach to lighten storage load and obtain varying control limits; next, two control limits are determined by investigating the distributions of the kNN squared distances and kNN angles of normal samples to guarantee high quality of detection. The developed FD-kNN method based on local neighborhoods naturally handles process nonlinearity and multimodal environment.

We highlight that two control limits are actively adjusted by on-line approach to overcome effect of drift and shift on the quality of detection. Thus, queries can be identify as correctly as possible. Finally, numerical examples and case study are given to illustrate the effectiveness and advantages of the proposed method. With the development of signal estimation technology of networked nonlinear stochastic systems [18–20], on-line and adaptive fault detection methods for these systems based on updated database will be discussed in the future.

Conflict of Interests

The authors do not have any conflict of interests regarding the content of the paper.

Acknowledgments

The authors would like to acknowledge the National Natural Science Foundation of China under Grants 61104093, 61174119, 61174026, 61104003, 60774070, and 61074029, the Special Program for Key Basic Research Founded by MOST under Grant 2010CB334705, the National High Technology Research and Development Program of China (863 Program) under Grant 2011AA040101, and the Scientific Research Project of Liaoning Province of China under Grants L2012141, L2011064. The authors also would like to acknowledge the Opening Project of Key Laboratory of Networked Control Systems, Chinese Academy of Sciences.

References

[1] C. Cheng and M. S. Chiu, "Nonlinear process monitoring using JITL-PCA," *Chemometrics and Intelligent Laboratory Systems*, vol. 76, no. 1, pp. 1–13, 2005.

[2] X. Wang, U. Kruger, and B. Lennox, "Recursive partial least squares algorithms for monitoring complex industrial processes," *Control Engineering Practice*, vol. 11, no. 6, pp. 613–632, 2003.

[3] Y. W. Zhang, L. J. Zhang, and H. L. Zhang, "Fault detection for industrial processes," *Mathematical Problems in Engineering*, vol. 2012, Article ID 757828, 18 pages, 2012.

[4] H. Li, H. Q. Zheng, and L. W. Tang, "Gear fault detection based on teager-huang transform," *International Journal of Rotating Machinery*, vol. 2010, Article ID 502064, 9 pages, 2010.

[5] Q. P. He and J. Wang, "Fault detection using the k-nearest neighbor rule for semiconductor manufacturing processes," *IEEE Transactions on Semiconductor Manufacturing*, vol. 20, no. 4, pp. 345–354, 2007.

[6] Q. P. He and J. Wang, "Principal component based k-nearest-neighbor rule for semiconductor process fault detection," in *Proceedings of the American Control Conference (ACC '08)*, pp. 1606–1611, Seattle, Wash, USA, June 2008.

[7] H. J. Gong and Z. Y. Zhen, "A neuro-augmented observer for robust fault detection in nonlinear systems," *Mathematical Problems in Engineering*, vol. 2012, Article ID 789230, 8 pages, 2012.

[8] J. Li, Q. Y. Su, L. F. Sun, and B. Li, "Fault detection for nonlinear impulsive switched systems," *Mathematical Problems in Engineering*, vol. 2013, Article ID 815329, 12 pages, 2013.

[9] D. Dong and T. J. Mcavoy, "Nonlinear principal component analysis—based on principal curves and neural networks," *Computers and Chemical Engineering*, vol. 20, no. 1, pp. 65–78, 1996.

[10] W. F. Ku, R. H. Storer, and C. Georgakis, "Disturbance detection and isolation by dynamic principal component analysis," *Chemometrics and Intelligent Laboratory Systems*, vol. 30, no. 1, pp. 179–196, 1995.

[11] Z. Q. Zhu and X. C. Jiao, "Fault detection for nonlinear networked control systems based on fuzzy observer," *Journal of Systems Engineering and Electronics*, vol. 23, no. 1, pp. 129–136, 2012.

[12] V. Torresa, S. Maximova, H. F. Ruiza, and J. L. Guardadoa, "Distributed parameters model for high-impedance fault detection and localization in transmission lines," *Electric Power Components and Systems*, vol. 41, no. 14, pp. 1311–1333, 2013.

[13] J. N. Li, Y. Li, H. B. Yu, and C. Zhang, "Adaptive fault detection for complex dynamic processes based on JIT updated data set," *Journal of Applied Mathematics*, vol. 2012, Article ID 809243, 17 pages, 2012.

[14] Z. Q. Ge and Z. H. Song, "Online monitoring of nonlinear multiple mode processes based on adaptive local model approach," *Control Engineering Practice*, vol. 16, no. 12, pp. 1427–1437, 2008.

[15] M. Kano, T. Sakata, and S. Hasebe, "Just-in-time statistical process control for flexible fault management," in *Proceedings of the SICE Annual Conference (SICE '10)*, pp. 1482–1485, Taipei, Taiwan, August 2010.

[16] X. Gao, G. Wang, and J. H. Ma, "An approach of building simplified multivariate statistical model based on mahalanobis distance," *Information and Control*, vol. 30, no. 7, pp. 676–680, 2001.

[17] E. R. Inc, "Metal Etch data for fault detection evaluation," 1999, http://software.eigenvector.com/Data/Etch/in-dex.html.

[18] J. Hu, Z. D. Wang, B. Shen, and H. J. Gao, "Quantised recursive filtering for a class of nonlinear systems with multiplicative noises and missing measurements," *International Journal of Control*, vol. 86, no. 4, pp. 650–663, 2013.

[19] J. Hu, Z. D. Wang, H. J. Gao, and L. K. Stergioulas, "Extended kalman filtering with stochastic nonlinearities and multiple missing measurements," *Automatica*, vol. 48, no. 9, pp. 2007–2015, 2012.

[20] J. Hu, Z. D. Wang, B. Shen, and H. J. Gao, "Gain-constrained recursive filtering with stochastic nonlinearities and probabilistic sensor delays," *IEEE Transactions on Signal Processing*, vol. 61, no. 5, pp. 1230–1238, 2013.

Hindawi Publishing Corporation
Mathematical Problems in Engineering
Volume 2014, Article ID 858624, 7 pages
http://dx.doi.org/10.1155/2014/858624

Review Article

A Survey on Distributed Filtering and Fault Detection for Sensor Networks

Hongli Dong,[1,2] Zidong Wang,[3,4] Steven X. Ding,[2] and Huijun Gao[5]

[1] *College of Electrical and Information Engineering, Northeast Petroleum University, Daqing 163318, China*
[2] *Institute for Automatic Control and Complex Systems, University of Duisburg-Essen, 47057 Duisburg, Germany*
[3] *School of Information Science and Technology, Donghua University, Shanghai 200051, China*
[4] *Department of Information Systems and Computing, Brunel University, Uxbridge, Middlesex UB8 3PH, UK*
[5] *Research Institute of Intelligent Control and Systems, Harbin Institute of Technology, Harbin 150001, China*

Correspondence should be addressed to Zidong Wang; zidong.wang@brunel.ac.uk

Received 22 September 2013; Accepted 19 October 2013; Published 2 January 2014

Academic Editor: Xiao He

In recent years, theoretical and practical research on large-scale networked systems has gained an increasing attention from multiple disciplines including engineering, computer science, and mathematics. Lying in the core part of the area are the distributed estimation and fault detection problems that have recently been attracting growing research interests. In particular, an urgent need has arisen to understand the effects of distributed information structures on filtering and fault detection in sensor networks. In this paper, a bibliographical review is provided on distributed filtering and fault detection problems over sensor networks. The algorithms employed to study the distributed filtering and detection problems are categorised and then discussed. In addition, some recent advances on distributed detection problems for faulty sensors and fault events are also summarized in great detail. Finally, we conclude the paper by outlining future research challenges for distributed filtering and fault detection for sensor networks.

1. Introduction

1.1. Sensor Networks. Sensor networks have recently been undergoing a quiet revolution in all aspects of the hardware implementation, software development, and theoretical research. In addition to the universal attributes of complex networks, sensor networks do possess their own characteristics due mainly to the large number of inexpensive wireless devices (nodes) densely distributed and loosely coupled over the region of interest. The past decade has seen successful applications of sensor networks in many practical areas ranging from military sensing, physical security, and air traffic control to distributed robotics and industrial and manufacturing automation. Accordingly, theoretical research on sensor networks has gained an increasing attention from multiple disciplines including engineering, computer science, and mathematics. Lying in the core part of the area are the distributed estimation and filtering problems that have recently been attracting growing research interests.

For distributed estimation/filtering problems, the inherently asynchronous sensor network is comprised of a large number of sensor nodes with computing and wireless communication capabilities, where the nodes are spatially distributed to form a wireless ad hoc network and every node has its own notion of time. Each individual sensor in a sensor network locally estimates/filters the system state from not only its own measurement but also its neighbouring sensors' measurements according to the given topology. The possible complexity of such a topology poses many challenges for scientists and engineers, and it is difficult to analyse these networks thoroughly with currently available estimation/filtering algorithms. Therefore, there is an urgent need to research on modelling, analysis of behaviours, systems theory, estimation, and filtering in sensor networks. Numerous fundamental questions have been addressed about the connections between sensor network topology and dynamic properties including stability, controllability, robustness, and other observable aspects. However, some major problems have not been fully investigated, such as the behaviour of stability, estimation, and filtering for sensor networks with incomplete/imperfect/stochastic topology, as well as their applications in, for example, distributed signal processing.

Sensor networks have already become an ideal research area for control engineers, mathematicians, and computer scientists to manage, analyze, interpret, and synthesize functional information from real-world sensor networks. Sophisticated system theories and computing algorithms have been exploited or emerged in the general area of distributed sensor networks, such as analysis of algorithms, artificial intelligence, automata, computational complexity, computer security, concurrency and parallelism, data structures, knowledge discovery, DNA and quantum computing, randomisation, semantics, symbol manipulation, numerical analysis, and mathematical software. This survey aims to bring together the latest approaches to understanding, estimating, and filtering complex sensor networks in a distributed way. The references discussed in this paper include, but are not limited to the following aspects of sensor networks: (1) systems analysis of distributed sensor networks; (2) distributed parameter identification of sensor networks; (3) robustness and fragility analysis of distributed sensor networks; (4) methods and algorithms for sensor network dynamics; and (5) distributed estimation and filtering with limited communication constraints.

1.2. Distributed Filtering. Over the past ten years or so, the sensor networks (SNs) have proven to be a persistent focus of research attracting an ever-increasing attention in the areas of systems and communication. A typical sensor network is composed of a large number of spatially distributed autonomous sensor nodes and also a few control nodes, where each sensor has wireless communication capability as well as some level of intelligence for signal processing and for disseminating data [1–7]. The development of sensor networks was originally motivated by military applications such as distributed localization, power spectrum estimation, and target tracking problems. With recent intensive research in this area, sensor networks have a wide-scope domain of applications in areas such as environment and habitat monitoring, health care applications, traffic control, distributed robotics, and industrial and manufacturing automation [1–3, 8, 9].

As one of the most fundamental collaborative information processing problems, the distributed filtering or estimation problem for sensor networks has gained particular concerns from many researchers and a wealth of the literature has appeared on this topic; see, for example, [10–19] and the references therein. For distributed filtering problems, the information available on an individual node of the sensor network is not only from its own measurement but also from its neighboring sensors' measurements according to the given topology. As such, the main difficulty in designing distributed filters lies in how to cope with the complicated coupling issues between one sensor and its neighboring sensors and how to reflect such couplings in the filter structure specification.

1.3. Distributed Fault Detection. On another research front, the fault detection problem has been an active field of research for the past decades because of the ever increasing demand for higher performance, higher safety, and reliability standards [20–33]. In sensor networks, sensor nodes have strong hardware and software restrictions in the light of processing power, memory capability, battery supply, and communication throughput, and faults are likely to occur frequently due to the low cost and the uncontrolled or even harsh environment where the sensor nodes are deployed. It is thus indispensable for the sensor networks to be able to detect, locate the faulty sensor nodes, and take actions to exclude them from the network during normal operation in order to ensure the network quality of service. Recently, some localized and distributed generic algorithms have been addressed in wireless sensor networks and a number of results about the distributed fault detection and fault tolerance have been published in the literature.

1.4. Structure of the Survey. The focus of this paper is to provide a timely review on the recent advances of the distributed filtering and fault detection issues for sensor networks. The rest of this paper is outlined as follows. In Section 2, the related results in the area of distributed filtering for wireless sensor networks are reviewed. The study contains a classification of different methods concerning distributed filtering. A comparison of different approaches is briefly summarized. Section 3 discusses the distributed fault detection problems over sensor networks. Both the distributed faulty sensors detection and distributed fault-event detection are carried out and explained separately. In Section 4, we give some concluding remarks and also point out some future directions.

2. Distributed Filtering for Sensor Networks

2.1. Traditional Kalman Filtering Approach. In recent years, the distributed filtering problem for sensor networks has received a fast growing research interest and some efficient distributed filtering/state estimation algorithms have been available in the literature; see, for example, [10, 11, 34–39] and the references therein.

The available algorithms, which can estimate stationary signals with low-cost and track nonstationary processes with reduced complexity, have a variety of engineering applications such as battlefield surveillance and target tracking. For example, a distributed Kalman filtering (DKF) algorithm has been introduced in [38] through which a crucial part of the solution is utilized to estimate the average of n signals in a distributed way. Accordingly, this elegant algorithm has been developed in [34–36, 40, 41] with different sensing models and dynamic consensus protocols. The notion of distributed bounded consensus filters has been introduced in [19] and the convergence analysis has been conducted for the corresponding distributed filters. In [14, 17, 42], the optimal distributed estimation algorithm has been proposed to adaptively update the weights for minimizing the estimated mean-square error. The diffusion-based Kalman filtering and smoothing algorithm has been established in [10, 11], where the information is diffused across the network through a sequence of Kalman iterations and data aggregation. In multisensor linear systems, several efficient algorithms including the centralised sensor fusion, distributed sensor fusion, and multialgorithm fusion to minimize the Euclidean estimation

error of the state vector have been presented in [43, 44]. In [45–47], the distributed particle filtering algorithm has been investigated as a response to offload the computation from the central unit as well as to reduce converge cast communication. References [48, 49] have introduced the maximum-likelihood approach in order to achieve the best possible variance for a given bandwidth constraint.

Looking into the issues discussed above, it can be observed that most available literature concerning the distributed filtering problems have been mainly limited to the traditional Kalman filtering theory that requires exact information about the plant model.

2.2. Robust and/or H_∞ Filtering Approach. In the presence of modeling errors, parameter uncertainties, and external disturbance, it is difficult to ensure the robustness of the traditional Kalman filters especially when the unavoidable parameter drifts or external disturbances occur. Note that the robust performance of the available distributed filters has not been paid adequate research attention despite its clear engineering significance. In this sense, it is of great significance to include the robust and/or H_∞ performance requirements for the distributed filtering problems.

Very recently, a new distributed H_∞-consensus performance has been defined in [50] to quantify bounded consensus regarding the filtering errors over a finite horizon, the distributed filtering problem has been addressed for a class of linear time-varying systems in the sensor network, and the filter parameters have been designed recursively by resorting to the different linear matrix inequalities. The H_∞-consensus performance presented in [50] has been utilized in [39] to deal with the distributed H_∞ filtering problem for a class of polynomial nonlinear stochastic systems in sensor networks. Subsequently, the desired distributed H_∞ filters have been designed in terms of the solution to certain parameter-dependent linear matrix inequalities. A stochastic sampled-data approach has been addressed in [16] to investigate the distributed H_∞ filtering in sensor networks. In [51], an H_∞-type performance measure of disagreement between adjacent nodes of the network has been included and a robust filtering approach has been proposed to design the distributed filters for uncertain plants.

2.3. Filtering with Incomplete Information. It is worth noting that most reported results concerning the distributed filtering/estimation algorithms are for linear and/or deterministic systems. Since nonlinearities are ubiquitous in practice, it is necessary to consider the distributed filtering problem for target plants described by nonlinear systems. On the other hand, distributed filtering in a sensor network inevitably suffers from the constrained communication and computation capabilities that would degrade the network performances.

It is well known that, accompanied by the rapid development of network technologies, the network-induced phenomena have been thoroughly investigated for filtering and control problems of networked systems [13, 21, 52–73]. Considering the case that the occurrence of incomplete information in sensor networks is more complex and severer due primarily to the network size, communication constraints, limited battery storage, strong coupling, and spatial deployment, the distributed filtering problem has been investigated in [74–76] for several classes of nonlinear stochastic systems over lossy sensor networks. The issue of average H_∞ performance constraints has been brought up in [74], and then the distributed H_∞ filtering problem has been investigated for system with repeated scalar nonlinearities and multiple probabilistic packet losses. Moreover, in [75], the distributed filtering problem has been further extended to the nonlinear time-varying systems with limited communication. The lossy sensor network suffers from quantization errors and successive packet dropouts that are described in a unified framework. A new distributed finite-horizon filtering technique by means of a set of recursive linear matrix inequalities has been proposed to satisfy the prescribed average filtering performance constraint.

In addition, the distributed H_∞ filtering problem has been investigated in [76] for a class of discrete-time Markovian jump nonlinear time-delay systems with deficient statistics of modes transitions. In [77], a new approach has been proposed in virtue of the solvability of certain coupled recursive Riccati difference equations (RDEs) to deal with the distributed H_∞ state estimation problem for a class of discrete time varying nonlinear systems with both stochastic parameters and stochastic nonlinearities.

3. Distributed Fault Detection for Sensor Networks

Wireless sensor networks (WSNs) are a multihop self-organized network system through wireless communication in which the failed nodes may decrease the service quality of the entire WSNs and create huge burden to the limited energy. In recent years, a growing number of efforts have been focused on the development of the fault detection methods for sensor nodes.

In [78], the online model-based detection of sensor faults has been first investigated by the cross-validation-based technique in which statistical methods are utilized to identify the sensors that are most likely to be faulty. This technique is centralized and can be applied to a broad set of fault models. A distributed fault detection scheme for sensor networks has been proposed in [79] to identify the faulty sensors, where each sensor node makes a decision based on the comparisons between its own sensing data and neighbors' data. The scheme, however, has the shortcoming of reducing the fault detection accuracy in the case that the number of neighbor's nodes to be diagnosed is small. In [80], an improved distributed fault detection algorithm based on weighted average value has been addressed by defining a new detection criterion to remedy the shortcoming that mentioned above. The scheme detects the sensor fault using spatial and time information simultaneously, where each sensor node identifies its own status based on local neighbor's average sensed data with some thresholds, hence maintaining low false alarm rate.

By using the spatial correlation of sensor measurements, a weighted median fault detection scheme has been introduced in [81] to detect the faults in WSNs. Reference [82]

has studied the problem of designing a distributed fault-tolerant decision fusion in the presence of sensor faults, where sensor fault detection scheme has been put forward to eliminate unreliable local decisions when performing distributed decision fusion. In [83], an agreement-based fault detection mechanism has been presented to detect cluster-head failures in clustered underwater sensor networks. Furthermore, a schedule generation scheme for a cluster head has been introduced to generate the transmission schedule of the forward and backward frames. The distributed fault detection problem has been investigated in [84] for WSNs, where each sensor node discerns its own status in view of local comparisons of sensed data with some thresholds and transfers the test results. It is well known that the basic idea of the distributed fault detection methods for sensor nodes is to check out the failed nodes by exchanging data and mutually testing among neighbor's nodes in this sensor networks.

It is worth pointing out that, apart from the development of distributed fault detection methods for sensor nodes, the distributed fault-event detection, which serves as a much more useful application in a sensor network, has also received much research attention. In [85], a distributed Bayesian fault recognition algorithm has been presented to solve the fault-event detection problem in sensor networks, where the randomized decision scheme and the threshold decision scheme have been used to derive analytical expressions for their detected performance. The proposed algorithm has the superiority of being completely distributed and localized each node by obtaining the information from neighboring sensors in order to make its decisions. A localized fault identification algorithm has been proposed in [86] to identify the faulty sensors and detect the reach of events in sensor networks, where each sensor node compares its own sensed data with the median of neighbors' data in order to determine its own status. In [87], a fault detection scheme for an event-driven wireless sensor network has been addressed by using an external manager, which can perform more complex functions compared to the sensor nodes. In [88], a fault-tolerant energy-efficient detection scheme has been presented to introduce the sensor fault probability into the optimal event detection process. For a given detection error bound, the minimum neighbors are selected to minimize the communication volume during the fault correction. It is also noted that the proposed distributed fault detection methods for sensor networks have a widely application fields such as the management of a reservoir [89] and integration of supply networks [90].

4. Conclusions and Future Work

In this paper, we have discussed and reviewed results, mostly from relatively recent work, on the problems of distributed filtering and fault detection for sensor networks. The various distributed filtering and fault detection technologies over sensor networks have been surveyed in great detail. Based on the literature review, some related topics for the future research work are listed as follows.

(i) A trend for future research is to generalize the methods obtained in the existing results to the distributed filtering and fault detection problems for nonlinear stochastic complex networks systems with randomly occurring incomplete information.

(ii) The nonlinearities considered in the existing results have some constraints that may bring somewhat conservative results. An additional trend for future research is to investigate the distributed filtering and fault detection problems for the general nonlinear systems for sensor networks.

(iii) Another future research direction is to further investigate the problems of nonparametric and robust sequential distributed detection for sensor networks.

(iv) The techniques such as conditional statistical tests and multivariate procedures in the presence of nonparametric hypotheses can be applied fruitfully in distributed fault detection applications.

Conflict of Interests

The authors declare that they have no conflict of interests related to this study.

Acknowledgments

This work was supported in part by the National Natural Science Foundation of China under Grants 61134009, 61329301, 61333012, 61374127 and 61004067, the Engineering and Physical Sciences Research Council (EPSRC) of the UK, the Royal Society of the UK, and the Alexander von Humboldt Foundation of Germany.

References

[1] A. Bertrand and M. Moonen, "Distributed adaptive node-specific signal estimation in fully connected sensor networks—part I: sequential node updating," *IEEE Transactions on Signal Processing*, vol. 58, no. 10, pp. 5277–5291, 2010.

[2] A. Bertrand and M. Moonen, "Distributed adaptive node-specific signal estimation in fully connected sensor networks—part II: simultaneous and asynchronous node updating," *IEEE Transactions on Signal Processing*, vol. 58, no. 10, pp. 5292–5306, 2010.

[3] P. Bianchi, J. Jakubowicz, and F. Roueff, "Linear precoders for the detection of a Gaussian process in wireless sensors networks," *IEEE Transactions on Signal Processing*, vol. 59, no. 3, pp. 882–894, 2011.

[4] E. Kokiopoulou and P. Frossard, "Distributed classification of multiple observation sets by consensus," *IEEE Transactions on Signal Processing*, vol. 59, no. 1, pp. 104–114, 2011.

[5] E. Kokiopoulou and P. Frossard, "Polynomial filtering for fast convergence in distributed consensus," *IEEE Transactions on Signal Processing*, vol. 57, no. 1, pp. 342–354, 2009.

[6] Y. Mostofi and M. Malmirchegini, "Binary consensus over fading channels," *IEEE Transactions on Signal Processing*, vol. 58, no. 12, pp. 6340–6354, 2010.

[7] A. Sundaresan and P. K. Varshney, "Location estimation of a random signal source based on correlated sensor observations," *IEEE Transactions on Signal Processing*, vol. 59, no. 2, pp. 787–799, 2011.

[8] B. Chen, K. Jamieson, H. Balakrishnan, and R. Morris, "Span: an energy-efficient coordination algorithm for topology maintenance in ad hoc wireless networks," in *Proceedings of the 7th Annual International Conference on Mobile Computing and Networking*, pp. 85–96, Rome, Italy, July 2001.

[9] R. Szewczyk, E. Osterweil, J. Polastre, M. Hamilton, A. Mainwaring, and D. Estrin, "Habitat monitoring with sensor networks," *Communications of the ACM*, vol. 47, no. 6, pp. 34–40, 2004.

[10] F. S. Cattivelli and A. H. Sayed, "Diffusion strategies for distributed Kalman filtering and smoothing," *IEEE Transactions on Automatic Control*, vol. 55, no. 9, pp. 2069–2084, 2010.

[11] F. S. Cattivelli and A. H. Sayed, "Diffusion strategies for distributed Kalman filtering: formulation and performance analysis," in *Proceedings of the Cognitive Information Processing*, pp. 36–41, Santorini, Greece, 2008.

[12] L. Chai, B. Hu, and P. Jiang, "Distributed state estimation based on quantized observations in a bandwidth constrained sensor network," in *Proceedings of the 7th World Congress on Intelligent Control and Automation (WCICA '08)*, pp. 2411–2415, Chongqing, China, June 2008.

[13] H. Dong, Z. Wang, D. W. C. Ho, and H. Gao, "Variance-constrained H_∞ filtering for a class of nonlinear time-varying systems with multiple missing measurements: the finite-horizon case," *IEEE Transactions on Signal Processing*, vol. 58, no. 5, pp. 2534–2543, 2010.

[14] M. Farina, G. Ferrari-Trecate, and R. Scattolini, "Distributed moving horizon estimation for sensor networks," in *Proceedings of the 1st IFAC Workshop on Estimation and Control of Networked Systems (NecSys '09)*, pp. 126–131, Venice, Italy, September 2009.

[15] J. Liang, Z. Wang, and X. Liu, "Distributed state estimation for discrete-time sensor networks with randomly varying nonlinearities and missing measurements," *IEEE Transactions on Neural Networks*, vol. 22, no. 3, pp. 486–496, 2011.

[16] B. Shen, Z. Wang, and X. Liu, "A stochastic sampled-data approach to distributed H_∞ filtering in sensor networks," *IEEE Transactions on Circuits and Systems I*, vol. 58, no. 9, pp. 2237–2246, 2011.

[17] A. Speranzon, C. Fischione, K. Johansson, and A. Sangiovanni-Vincentelli, "A distributed minimum variance estimator for sensor networks," *IEEE Journal on Selected Areas in Communications*, vol. 26, no. 4, pp. 609–621, 2008.

[18] J. Teng, H. Snoussi, and C. Richard, "Decentralized variational filtering for target tracking in binary sensor networks," *IEEE Transactions on Mobile Computing*, vol. 9, no. 10, pp. 1465–1477, 2010.

[19] W. Yu, G. Chen, Z. Wang, and W. Yang, "Distributed consensus filtering in sensor networks," *IEEE Transactions on Systems, Man, and Cybernetics B*, vol. 39, no. 6, pp. 1568–1577, 2009.

[20] S. X. Ding, T. Jeinsch, P. M. Frank, and E. L. Ding, "A unified approach to the optimization of fault detection systems," *International Journal of Adaptive Control and Signal Processing*, vol. 14, no. 7, pp. 725–745, 2000.

[21] H. Dong, Z. Wang, D. W. C. Ho, and H. Gao, "Robust H_∞ filtering for Markovian jump systems with randomly occurring nonlinearities and sensor saturation: the finite-horizon case," *IEEE Transactions on Signal Processing*, vol. 59, no. 7, pp. 3048–3057, 2011.

[22] Z. Gao and S. X. Ding, "Actuator fault robust estimation and fault-tolerant control for a class of nonlinear descriptor systems," *Automatica*, vol. 43, no. 5, pp. 912–920, 2007.

[23] F. Gökas, *Distributed control of systems over communication networks [Ph.D. dissertation]*, University of Pennsylvania, Philadelphia, Pa, USA, 2000.

[24] X. He, Z. Wang, and D. H. Zhou, "Robust fault detection for networked systems with communication delay and data missing," *Automatica*, vol. 45, no. 11, pp. 2634–2639, 2009.

[25] H. Dong, Z. Wang, and H. Gao, "Fault detection for Markovian jump systems with sensor saturations and randomly varying nonlinearities," *IEEE Transactions on Circuits and Systems I*, vol. 59, no. 10, pp. 2354–2362, 2012.

[26] H. Dong, Z. Wang, and H. Gao, "On design of quantized fault detection filters with randomly occurring nonlinearities and mixed time-delays," *Signal Processing*, vol. 92, no. 4, pp. 1117–1125, 2012.

[27] S. Yin, S. Ding, A. Haghani, H. Hao, and P. Zhang, "A comparison study of basic data-driven fault diagnosis and process monitoring methods on the benchmark Tennessee Eastman process," *Journal of Process Control*, vol. 22, no. 9, pp. 1567–1581, 2012.

[28] S. Yin, S. Ding, and H. Luo, "Real-time implementation of fault tolerant control system with performance optimization," *IEEE Transactions on Industrial Electronics*, vol. 61, no. 5, pp. 2402–2411, 2013.

[29] S. Yin, S. X. Ding, A. H. A. Sari, and H. Hao, "Data-driven monitoring for stochastic systems and its application on batch process," *International Journal of Systems Science*, vol. 44, no. 7, pp. 1366–1376, 2013.

[30] S. Ding, S. Yin, K. Peng, H. Hao, and B. Shen, "A novel scheme for key performance indicator prediction and diagnosis with application to an industrial hot strip mill," *IEEE Transactions on Industrial Informatics*, vol. 9, no. 4, pp. 2239–2247, 2012.

[31] S. Ding, P. Zhang, S. Yin, and E. Ding, "An integrated design framework of fault tolerant wireless networked control systems for industrial automatic control applications," *IEEE Transactions on Industrial Informatics*, vol. 9, no. 1, pp. 462–471, 2013.

[32] Y. Zheng, H. Fang, and H. O. Wang, "Takagi-Sugeno fuzzy-model-based fault detection for networked control systems with Markov delays," *IEEE Transactions on Systems, Man, and Cybernetics B*, vol. 36, no. 4, pp. 924–929, 2006.

[33] M. Zhong, S. X. Ding, and E. L. Ding, "Optimal fault detection for linear discrete time-varying systems," *Automatica*, vol. 46, no. 8, pp. 1395–1400, 2010.

[34] R. Carli, A. Chiuso, L. Schenato, and S. Zampieri, "Distributed Kalman filtering based on consensus strategies," *IEEE Journal on Selected Areas in Communications*, vol. 26, no. 4, pp. 622–633, 2008.

[35] M. Kamgarpour and C. Tomlin, "Convergence properties of a decentralized Kalman filter," in *Proceedings of the 47th IEEE Conference on Decision and Control (CDC '08)*, pp. 3205–3210, Cancun, Mexico, December 2008.

[36] R. Olfati-Saber, "Distributed Kalman filtering for sensor networks," in *Proceedings of the 46th IEEE Conference on Decision and Control (CDC '07)*, pp. 5492–5498, New Orleans, La, USA, December 2007.

[37] R. Olfati-Saber, "Kalman-Consensus filter: optimality, stability, and performance," in *Proceedings of the 48th IEEE Conference on Decision and Control held jointly with 28th Chinese Control Conference (CDC/CCC '09)*, pp. 7036–7042, Shanghai, China, December 2009.

[38] R. Olfati-Saber and J. S. Shamma, "Consensus filters for sensor networks and distributed sensor fusion," in *Proceedings of*

the 44th IEEE Conference on Decision and Control, and the European Control Conference (CDC-ECC '05), pp. 6698–6703, Seville, Spain, December 2005.

[39] B. Shen, Z. Wang, Y. S. Hung, and G. Chesi, "Distributed H_∞ filtering for polynomial nonlinear stochastic systems in sensor networks," *IEEE Transactions on Industrial Electronics*, vol. 58, no. 5, pp. 1971–1979, 2011.

[40] P. Alriksson and A. Rantzer, "Distributed Kalman filtering using weighted averaging," in *Proceedings of the 17th International Symposium on Mathematical Theory of Networks and Systems*, Kyoto, Japan, 2006.

[41] D. P. Spanos, R. Olfati-Saber, and R. M. Murray, "Approximate distributed kalman filtering in sensor networks with quantifiable performance," in *Proceedings of the 4th International Symposium on Information Processing in Sensor Networks (IPSN '05)*, pp. 133–139, Piscataway, NJ, USA, April 2005.

[42] T.-Y. Wang, L.-Y. Chang, and P.-Y. Chen, "A Collaborative sensor-fault detection scheme for robust distributed estimation in sensor networks," *IEEE Transactions on Communications*, vol. 57, no. 10, pp. 3045–3058, 2009.

[43] T. M. Berg and H. F. Durrant-Whyte, "Model distribution in decentralized multi-sensor data fusion," in *Proceedings of the American Control Conference*, pp. 2292–2293, Boston, Mass, USA, June 1991.

[44] X. Shen, Y. Zhu, E. Song, and Y. Luo, "Minimizing Euclidian state estimation error for linear uncertain dynamic systems based on multisensor and multi-algorithm fusion," *IEEE Transactions on Information Theory*, vol. 57, no. 10, pp. 7131–7146, 2011.

[45] M. Coates, "Distributed particle filters for sensor networks," in *Proceedings of the 3rd International Symposium on Information Processing in Sensor Networks (IPSN '04)*, pp. 99–107, New York, NY, USA, April 2004.

[46] M. Coates and G. Ing, "Sensor network particle filters: motes as particles," in *Proceedings of the IEEE/SP 13th Workshop on Statistical Signal Processing*, pp. 1152–1157, Novosibirsk, Russia, July 2005.

[47] H. Q. Liu, H. C. So, W. Chan, and K. W. K. Lui, "Distributed particle filter for target tracking in sensor networks," *Progress in Electromagnetics Research*, vol. 11, pp. 171–182, 2009.

[48] A. Ribeiro and G. B. Giannakis, "Bandwidth-constrained distributed estimation for wireless sensor networks—part I: gaussian case," *IEEE Transactions on Signal Processing*, vol. 54, no. 3, pp. 1131–1143, 2006.

[49] A. Ribeiro and G. B. Giannakis, "Bandwidth-constrained distributed estimation for wireless sensor networks—part II: unknown probability density function," *IEEE Transactions on Signal Processing*, vol. 54, no. 7, pp. 2784–2796, 2006.

[50] B. Shen, Z. Wang, and Y. S. Hung, "Distributed H_∞-consensus filtering in sensor networks with multiple missing measurements: the finite-horizon case," *Automatica*, vol. 46, no. 10, pp. 1682–1688, 2010.

[51] V. Ugrinovskii, "Distributed robust filtering with H_∞ consensus of estimates," *Automatica*, vol. 47, no. 1, pp. 1–13, 2011.

[52] H. Dong, Z. Wang, and H. Gao, "Robust H_∞ filtering for a class of nonlinear networked systems with multiple stochastic communication delays and packet dropouts," *IEEE Transactions on Signal Processing*, vol. 58, no. 4, pp. 1957–1966, 2010.

[53] H. Gao, Z. Fei, J. Lam, and B. Du, "Further results on exponential estimates of Markovian jump systems with mode-dependent time-varying delays," *IEEE Transactions on Automatic Control*, vol. 56, no. 1, pp. 223–229, 2011.

[54] H. Gao and X. Li, "H_∞ filtering for discrete-time state-delayed systems with finite frequency specifications," *IEEE Transactions on Automatic Control*, vol. 56, no. 12, pp. 2935–2941, 2011.

[55] H. Gao, T. Chen, and J. Lam, "A new delay system approach to network-based control," *Automatica*, vol. 44, no. 1, pp. 39–52, 2008.

[56] H. Gao and T. Chen, "A new approach to quantized feedback control systems," *Automatica*, vol. 44, no. 2, pp. 534–542, 2008.

[57] J. Hu, Z. Wang, H. Gao, and L. K. Stergioulas, "Extended Kalman filtering with stochastic nonlinearities and multiple missing measurements," *Automatica*, vol. 48, no. 9, pp. 2007–2015, 2012.

[58] J. Hu, Z. Wang, B. Shen, and H. Gao, "Quantised recursive filtering for a class of nonlinear systems with multiplicative noises and missing measurements," *International Journal of Control*, vol. 86, no. 4, pp. 650–663, 2013.

[59] J. Hu, Z. Wang, H. Gao, and L. K. Stergioulas, "Robust sliding mode control for discrete stochastic systems with mixed time delays, randomly occurring uncertainties, and randomly occurring nonlinearities," *IEEE Transactions on Industrial Electronics*, vol. 59, no. 7, pp. 3008–3015, 2012.

[60] X. Li and H. Gao, "Robust finite frequency H_∞ filtering for uncertain 2-D Roesser systems," *Automatica*, vol. 48, no. 6, pp. 1163–1170, 2012.

[61] X. Li and H. Gao, "Robust finite frequency H_∞ filtering for uncertain 2-D systems: the FM model case," *Automatica*, vol. 49, no. 8, pp. 2446–2452, 2013.

[62] B. Shen, Z. Wang, H. Shu, and G. Wei, "On nonlinear H_∞ filtering for discrete-time stochastic systems with missing measurements," *IEEE Transactions on Automatic Control*, vol. 53, no. 9, pp. 2170–2180, 2008.

[63] B. Shen, Z. Wang, J. Liang, and Y. Liu, "Recent advances on filtering and control for nonlinear stochastic complex systems with incomplete information: a survey," *Mathematical Problems in Engineering*, vol. 2012, Article ID 530759, 16 pages, 2012.

[64] H. Dong, Z. Wang, X. Chen, and H. Gao, "A review on analysis and synthesis of nonlinear stochastic systems with randomly occurring incomplete information," *Mathematical Problems in Engineering*, vol. 2012, Article ID 416358, 15 pages, 2012.

[65] Z. Wang, D. W. C. Ho, H. Dong, and H. Gao, "Robust H_∞ finite-horizon control for a class of stochastic nonlinear time-varying systems subject to sensor and actuator saturations," *IEEE Transactions on Automatic Control*, vol. 55, no. 7, pp. 1716–1722, 2010.

[66] Z. Wang, B. Shen, H. Shu, and G. Wei, "Quantized H_∞ control for nonlinear stochastic time-delay systems with missing measurements," *IEEE Transactions on Automatic Control*, vol. 57, no. 6, pp. 1431–1444, 2012.

[67] Z. Wang, B. Shen, and X. Liu, "H_∞ filtering with randomly occurring sensor saturations and missing measurements," *Automatica*, vol. 48, no. 3, pp. 556–562, 2012.

[68] Z. Wang, D. W. C. Ho, Y. Liu, and X. Liu, "Robust H_∞ control for a class of nonlinear discrete time-delay stochastic systems with missing measurements," *Automatica*, vol. 45, no. 3, pp. 684–691, 2009.

[69] Z. Wang, Y. Liu, and X. Liu, "H_∞ filtering for uncertain stochastic time-delay systems with sector-bounded nonlinearities," *Automatica*, vol. 44, no. 5, pp. 1268–1277, 2008.

[70] Z. Wang, Y. Wang, and Y. Liu, "Global synchronization for discrete-time stochastic complex networks with randomly occurred nonlinearities and mixed time delays," *IEEE Transactions on Neural Networks*, vol. 21, no. 1, pp. 11–25, 2010.

[71] G. Wei, Z. Wang, and H. Shu, "Robust filtering with stochastic nonlinearities and multiple missing measurements," *Automatica*, vol. 45, no. 3, pp. 836–841, 2009.

[72] D. Yue, E. Tian, Y. Zhang, and C. Peng, "Delay-distribution-dependent stability and stabilization of T-S fuzzy systems with probabilistic interval delay," *IEEE Transactions on Systems, Man, and Cybernetics B*, vol. 39, no. 2, pp. 503–516, 2009.

[73] H. Zhang, M. Li, J. Yang, and D. Yang, "Fuzzy model-based robust networked control for a class of nonlinear systems," *IEEE Transactions on Systems, Man, and Cybernetics A*, vol. 39, no. 2, pp. 437–447, 2009.

[74] H. Dong, J. Lam, and H. Gao, "Distributed H_∞ filtering for repeated scalar nonlinear systems with random packet losses in sensor networks," *International Journal of Systems Science*, vol. 42, no. 9, pp. 1507–1519, 2011.

[75] H. Dong, Z. Wang, and H. Gao, "Distributed filtering for a class of time-varying systems over sensor networks with quantization errors and successive packet dropouts," *IEEE Transactions on Signal Processing*, vol. 60, no. 6, pp. 3164–3173, 2012.

[76] H. Dong, Z. Wang, and H. Gao, "Distributed H_∞ filtering for a class of Markovian jump nonlinear time-delay systems over lossy sensor networks," *IEEE Transactions on Industrial Electronics*, vol. 60, no. 10, pp. 4665–4672, 2013.

[77] D. Ding, Z. Wang, H. Dong, and H. Shu, "Distributed H_∞ state estimation with stochastic parameters and nonlinearities through sensor networks: the finite-horizon case," *Automatica*, vol. 48, no. 8, pp. 1575–1585, 2012.

[78] F. Koushanfar, M. Potkonjak, and A. Sangiovanni-Vincentelli, "On-line fault detection of sensor measurements," in *Proceedings of the 2nd IEEE International Conference on Sensors*, vol. 2, pp. 974–979, October 2003.

[79] J. Chen, S. Kher, and A. Somani, "Distributed fault detection of wireless sensor networks," in *Proceedings of the Workshop on Dependability Issues in Wireless Ad Hoc Networks and Sensor Networks (DIWANS '06)*, pp. 65–71, New York, NY, USA, September 2006.

[80] S. Ji, S.-F. Yuan, T.-H. Ma, and C. Tan, "Distributed fault detection for wireless sensor based on weighted average," in *Proceedings of the 2nd International Conference on Networks Security, Wireless Communications and Trusted Computing (NSWCTC '10)*, vol. 1, pp. 57–60, Wuhan, China, April 2010.

[81] J.-L. Gao, Y.-J. Xu, and X.-W. Li, "Weighted-median based distributed fault detection for wireless sensor networks," *Journal of Software*, vol. 18, no. 5, pp. 1208–1217, 2007.

[82] T.-Y. Wang, L.-Y. Chang, D.-R. Duh, and J.-Y. Wu, "Distributed fault-tolerant detection via sensor fault detection in sensor networks," in *Proceedings of the 10th International Conference on Information Fusion*, pp. 1–6, Quebec, Canada, July 2007.

[83] P. Wang, J. Zheng, and C. Li, "An agreement-based fault detection mechanism for underWater sensor networks," in *Proceedings of the 50th Annual IEEE Global Telecommunications Conference (GLOBECOM '07)*, pp. 1195–1200, Washington, DC, USA, November 2007.

[84] M.-H. Lee and Y.-H. Choi, "Fault detection of wireless sensor networks," *Computer Communications*, vol. 31, no. 14, pp. 3469–3475, 2008.

[85] B. Krishnamachari and S. Iyengar, "Distributed Bayesian algorithms for fault-tolerant event region detection in wireless sensor networks," *IEEE Transactions on Computers*, vol. 53, no. 3, pp. 241–250, 2004.

[86] M. Ding, D. Chen, K. Xing, and X. Cheng, "Localized fault-tolerant event boundary detection in sensor networks," in *Proceedings of the 24th Annual Joint Conference of the IEEE Computer and Communications Societies*, vol. 2, pp. 902–913, March 2005.

[87] L. B. Ruiz, I. G. Siqueira, L. B. Oliveira, H. C. Wong, J. M. S. Nogueira, and A. A. F. Loureiro, "Fault management in event-driven wireless sensor networks," in *Proceedings of the 7th ACM Symposium on Modeling, Analysis and Simulation of Wireless and Mobile Systems*, pp. 149–156, New York, NY, USA, October 2004.

[88] X. Luo, M. Dong, and Y. Huang, "On distributed fault-tolerant detection in wireless sensor networks," *IEEE Transactions on Computers*, vol. 55, no. 1, pp. 58–70, 2006.

[89] Y. Chen and K. A. Hoo, "Stability analysis for closed-loop management of a reservoir based on identification of reduced-order nonlinear model," *Systems Science and Control Engineering*, vol. 1, no. 1, pp. 12–19, 2013.

[90] S. R. Desai and R. Prasad, "A new approach to order reduction using stability equation and big bang big crunch optimization," *Systems Science and Control Engineering*, vol. 1, no. 1, pp. 20–27, 2013.

Hindawi Publishing Corporation
Mathematical Problems in Engineering
Volume 2013, Article ID 126269, 16 pages
http://dx.doi.org/10.1155/2013/126269

Review Article

An Overview of Distributed Energy-Efficient Topology Control for Wireless Ad Hoc Networks

Mohammadjavad Abbasi, Muhammad Shafie Bin Abd Latiff, and Hassan Chizari

Department of Computer Science, Faculty of Computing, Universiti Teknologi Malaysia (UTM), 81310 Skudai, Johor, Malaysia

Correspondence should be addressed to Mohammadjavad Abbasi; mj_abbasi55@yahoo.com

Received 29 July 2013; Accepted 20 October 2013

Academic Editor: Hongli Dong

A wireless ad hoc network is composed of several tiny and inexpensive device such as wireless sensor networks (WSNs) which have limited energy. In this network energy, efficiency is one of the most crucial requirements. Data transmitting in minimum power level is one way of maximizing energy efficiency. Thus, transmission power level of nodes should be managed in a smart way to improve energy efficiency. Topology control is one of the main algorithms used in a wireless network to decrease transmission power level while preserving network connectivity. Topology control could improve energy efficiency by reasonably tuning the transmission power level while preserving network connectivity in order to increase network capacity and lifetime. In pursuit of energy efficiency and connectivity, nodes can be selfish and are conflicting with each other. Therefore to overcome the conflict, game theory is used to construct energy efficient topology, as well as minimizing energy consumption. In this paper, the main goal and most recent energy efficient topology control algorithms in WSNs and ad hoc network are classified and studied according to their specific goals.

1. Introduction

Wireless sensor networks (WSNs) are a particular type of ad hoc network, in which the nodes are autonomous. These nodes are tiny devices equipped with communication component, data computation, and sensing capability [1–3]. In this type of network, each node collects information from the target area and sends this information to a sink, through a multihop communication network. A wireless network consists of hundreds to thousands nodes, which are deployed either inside the target area or very close to the target area. Upon an event happening or during monitoring sessions, the wireless nodes will collect and report this information to the sink node for further analysis.

These wireless networks can be used for many important applications such as health care, intrusion detection and plants control, weather monitoring, security and tactical surveillance, disaster monitoring, and ambient conditions detection [1, 4]. As an example, in forest fire early detection system [5], wireless temperature and smoke wireless nodes are installed in the forest to detect fire or smoke in its early stage, without deploying complicated wired structures. Another application is in a battlefield, a soldier can be aware of the status of friendly troops or the availability of equipment by their information collected from wireless networks [6].

Energy efficiency is one of the main requirements in sensor networks [7]. Nodes in wireless sensor network are powered with limited energy resource for variety of applications and thus have limited lifetime. Therefore, the energy resource of sensor nodes must be managed efficiently to improve the network lifetime. Moreover, sensor nodes are equipped with storage device, communication radio, and computation device, all of which are powered with limited battery provision. Thus, it is mandatory that every node be energy efficient; this not only maximizes the node's lifetime but also maximizes the network performance. Designing an energy efficient algorithm for the desirable network performance is necessary.

Wireless networks performance can be enhanced by designing energy efficient algorithm. One way for maximizing energy efficiency is transmitting data with minimum power level. Topology control (TC), that is, the study of how

to adjust each node power level so as to increase network goals, is an algorithm used to improve network performance. In topology control, sensor network is abstracted as graph consisting of sets of wireless nodes and communication links between these nodes. The role of a topology control algorithm is to dynamically adjust transmission power level of defined set of neighbor nodes for each node. The aim is to construct efficient networks and satisfy energy efficiency, energy balancing, and network connectivity. By minimizing transmission power level, nodes collaboratively set their optimal transmission range instead of maximum transmission level and TC helps constructing energy efficient topology, thereby improving network lifetime. The most important challenges in topology control are briefly summarized below.

(1) Fully Distributed Control. In many scenarios, nodes, which execute a task selfishly to save energy, are expected to work unattended in remote geographic areas under critical environmental conditions. Therefore, topology control method should adopt a fully distributed control structure [8, 9].

(2) Transmission Power Selection. Deploying several hundreds to thousands of inaccessible and unattended wireless nodes, which are prone to failures, makes topology control as an ambitious task. Each node selects its own power range while preserving network connectivity by topology control [10–12]. This act must not intervene the formal service in the wireless networks and the system must be enough node degree to increase the network real-time packet delivery and adaptive to select transmission power range.

(3) Energy Balance Topology Control. In wireless network, each node chooses nodes with higher residual energy to minimize the energy consumption of nodes with low residual energy, even though more power is needed [13–15]. Hence, the constructed topology must have the properties such as balanced energy consumption.

(4) Energy Efficient Topology Control. Despite the capacity of battery, wireless networks should operate for a relatively long period of time, since it might be impossible to recharge or replace node batteries. The lifetime can be improved by utilizing the energy-efficient topology control algorithms [16–18].

From the above discussion, clearly good research is necessary to address topology control problem. Hence, during topology control, it is desired to obtain the minimum transmission power levels of the nodes while preserving the network connectivity capability. Although, the minimum transmission power levels of network is important during topology process, the energy efficiency and energy balance across the topology control should be maintained during the operation.

In wireless network, nodes act selfishly and conflict with each other in pursuit for energy efficiency and connectivity [19–21]. If the nodes select lower transmission range, the constructed topology will be disconnected. In reverse, if nodes select high transmission power level, the interference among nodes will raise, leading to high energy consumption. The main problem is how to establish a tradeoff between connectivity and energy efficiency for each node. Game theory is used to solve the conflicting objectives of nodes seeking to achieve connectivity and energy efficiency.

The rest of this paper discusses energy efficiency topology control issues in WSN and highlights the limitations of existing topology control algorithms. After describing the basics of ad hoc and wireless sensor networks in the following section with some examples for each category of the detailed topology control taxonomy presented in Figure 1, game theory is briefly elaborated in Section 2. Section 3 discusses heterogeneous transmission power. The homogeneous transmission power control is discussed in Section 4, which consists of centralized and distributed energy efficient topology control algorithms. Topology control algorithms are discussed in Section 5. Finally, Section 6 discussed conclusions.

2. Game Theoretic Definition and Preliminaries

Game theory is one of the fundamental mathematical tools that has been used for analyzing between rational and intelligent players. Game theory has been used in a system, with regard to action and pay-off. A review of some fundamental definitions and concepts in game theory that will be used and applied throughout this research are stated in the literature [22, 23].

2.1. Game, Strategy, and Equilibrium. A game consisted of players, the possible strategy of the players, and consequences of the strategy. The definition of the game is given in Definition 1.

Definition 1. A game Γ has three elements $\langle I, A, u\rangle$, where

(i) *player set* $I = 1, \ldots, n$, where n is number of players in game,

(ii) *action set* $A = \times_{i\in I} A_i$ is the space of all action vector, in which each a_i of the vector $a \in A$ belongs to the set A_i, the set of actions of player. It is the Cartesian product of an action for each player i,

(iii) u is a utility of player i over outcomes defined by strategy profile. For a particular action a, $u(a) = (u_i(a), u_2(a), \ldots, u_i(a))$ is called a individual utility function $u_i(a)$.

In wireless network infrastructure, the nodes are often the players during a game, in which the nodes are constructing a connected topology. Recall that some of the features under its control are classified by transmission power (action list) p. Thus, the best action might be chosen from the transmission power list p. In essence, the collection of the best actions determines the outcome of the game. Transmission power level considers the outcome with network connectivity by minimum energy consumption. However, some players are conflicting with each other by this outcome. Game theory

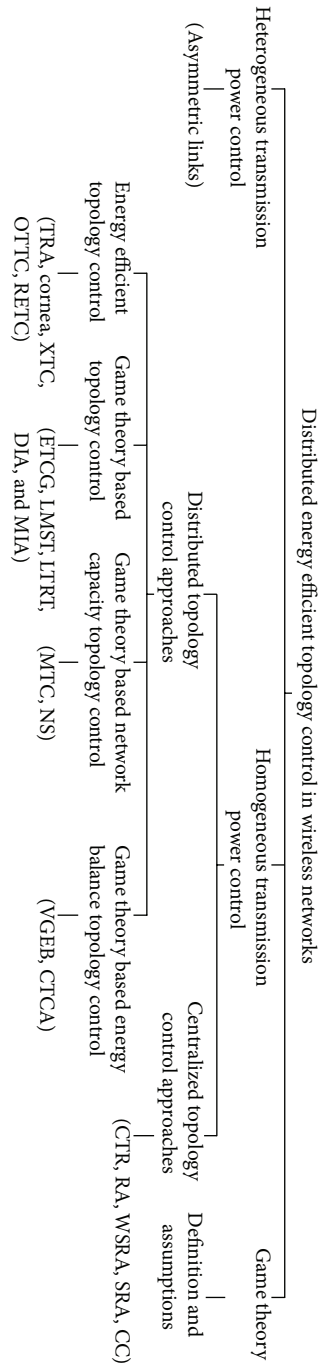

Figure 1: Taxonomy of energy-efficient topology construction protocols.

can predict this outcome among the game. Nash equilibrium (NE) is one of the best solutions for outcome problem in game theory [24, 25]. An NE has mean features and is a fixed point. From this fixed point, no player has any incentive to deviate from its action. Therefore, an NE can predict the outcome of a game.

Definition 2. The action profile a^* is an NE, if $u_i(a^*) \geq u_i(a_i, a^*_{-i})$ for every action a_i of a player i.

Based on Definition 2, the most action of a player is to avoid unstable strategy and play in the best strategy. When many strategies exist, it denotes a best response for each player, given the strategies of the other players. So that player can pick its best response accordingly.

Definition 3. An action $a' \in A_i$ is the best response of strategy for a player i if and only if $u_i(a'_i, a_{-i}) \geq u_i(a_i, a_{-i})$, for all $a_i \in A_i \setminus a'_i$.

Definition 3 elaborates why NE is the stable point of the best response. Based on existence of pure strategy of NE, stable point of NE can be found. Sometimes game has multiple equilibria. The task of getting rid of the undesirable ones is another issue which needs more attention. Furthermore, one player wants the convergence of the game properties and the problem is further compounded when some NE exists.

There is a special class of game theory for existence of the best strategy and convergence to the properties. Denote how Definition 3 can help for best strategy-based algorithm to come up with some NE of the game.

2.2. Potential Games. In a potential game, the consequences of any individual player's change in strategy are implied by the potential function. General games do not need to possess pure Nash equilibrium, while this is not the case for potential games [26]. Beyond merely possessing pure Nash equilibrium, potential games also provide a straightforward algorithm for agents to learn to play a pure Nash equilibrium and the best response dynamics. Moreover, the best response dynamic is the simplest of the learning dynamics.

Definition 4. Ordinal potential function (OPF): a game is an ordinal potential function $\Phi : A \rightarrow R$ such that for any player i, any joint action $a \in A$ and any action $a \in A_a$:

$$\begin{aligned} &u_i(a) - u_i(a_i, a_{-i}) \\ &\quad = \phi_i(a) - \phi_i(a_i, a_{-i}). \end{aligned} \tag{1}$$

ϕ is Exact Potential Function (EPF).

Definition 5. A game Γ is an ordinal potential game (OPG) $a \in A$ and any action $a \in A_i$:

$$\begin{aligned} &u_i(a) - u_i(a_i, a_{-i}) > 0 \\ &\quad \Longleftrightarrow \phi_i(a) - \phi_i(a_i, a_{-i}) > 0. \end{aligned} \tag{2}$$

According to Definitions 4 and 5, an EPG is an OPG with the similar potential function. Potential games with action vector are known to be fixed at least on one NE as the best strategies [26]. The following lemma shows how NE of the game can be classified.

Lemma 6. *Let Γ be an OPG and let ϕ be its corresponding OPF. If $a \in A$ maximizes ϕ, then it is a Nash equilibrium.*

Proof. From Definition 5 we have that Γ is an OPG. Γ is better response dynamic and has defined an improvement path, a sequential of improving action, which is finite. The equilibrium set of $\Gamma(u)$ coincides with equilibrium set of $\Gamma(\phi)$. Then, $a \in A$ is an equilibrium for Γ if and only if for every $i \in I$, $\phi(a) \geq \phi(a_i, a_{-i})$ for all $a_{-i} \in A_i$. Consequently, if ϕ used a maximal point in A, based on the finite improvement path (FIP) property of potential game [26], Γ can be converge to equilibrium. And each player can maximize its utility, as far as possible to maximize potential function. Based on Nash equilibrium, no node can maximize its utility by changing its action. Γ can converge to the Nash equilibrium. □

Based on Lemma 6, potential function is a subset of the NE of a potential game. For identification of NE in game, it is required to identify the potential functions. In addition to its NE, potential games have convergence properties, yet, selfish adaptations. The balance between efficiency and stability is fundamental for any dynamic system, specifically in a mutual system of independent selfish players. Moreover, in NE, sense stability is based on self-interest whereas system efficiency is based on general interest. Prisoners' Dilemma in [27] is a classical sample that demonstrates the inefficiency of the stable outcomes. The efficiency concept is called Pareto optimality in game theory.

Definition 7. An action set a' is Pareto optimality (OP) $a \notin A$ such that $u_i(a) > u_i(a')$ and $u_j(a) < u_j(a')$ for $j \in A$.

Definition 7 elaborates how, from a Pareto Optimal (PO) state, it is inconceivable to change into another state and increase the pay-off of agents without minimizing the pay-off of some other agents. The terminologies and definitions illustrated in this subsection are used as the preliminaries of review algorithms art of the misbehavior mitigation system. In the rest of the paper, the above terminologies and definitions will be used frequently.

3. Heterogeneous Transmission Power Control

In heterogeneous networks, nodes have different transmission power levels. The assumption of heterogeneous nodes does not hold the same type; therefore, they may have slightly different maximal transmission power. There also exist heterogeneous wireless networks in which devices have dramatically same capabilities. TC using per node transmission power method has been proven to be more efficient in improving the network lifetime. Asymmetric link algorithm which is used in heterogeneous nodes to efficiently adjust a power level had been proposed in [28]. Moreover, each node has different maximum transmission levels since they are heterogeneous. Furthermore, for node i, the current transmission power is p_i, P_{ij} as the transmission power required for node i to connect a node j, and $P_i(\max)$ as its maximum transmission power level. Since $P_i(\max) \neg P_j(\max)$ for $i \neg j$. In such a situation where $P_i(\max) \geq P_{ij} > P_j(\max)$, there exists a reverse link in the connected topology since $P_{ji} > P_j(\max)$. Consequently, the introduced algorithm seems to be stable. Each node based on its information adjusts the transmission powers. Thus, the topology converges to the final topology with minimum transmission power. However, the notion of the most existing topology control algorithms cannot be directly extended to heterogeneous networks where different nodes may have various transmission power level.

4. Homogeneous Transmission Power Control

In homogeneous topology control algorithms, the connected topology is constructed by adjusting the transmission power level of the nodes. In the first case considered in this section, all the nodes are homogeneous infrastructure in a network.

For this case, coverage, connectivity, and energy efficiency algorithms are presented.

The algorithm in the branch of transmission power control are more coverage oriented [29, 30]. However, in such cases, connectivity is not preserved. Moreover, the coverage oriented protocols used the different techniques for construction of topology control. Some algorithms are introduced to provide coverage of a set of predefined target areas. Furthermore, the algorithms in the branch transmission power control are focused only on construction of a connected network. The main aim of these algorithms is to decrease transmission power of the topology, while preserving connectivity.

The proposed algorithm in [31] used disk model algorithm and studied link connectivity. In summary, the disk model is Boolean: an edge (i, j) $\exists$ for all i & j only if power level $p_i > w(i, j)$, otherwise not. Energy efficiency is a key requirement in the design of wireless networks, since nodes have limited operational life. Hence, energy-efficient algorithms are required to adjust communication links between nodes. On the other hand, it has been shown that the topology of a sensor network greatly affects the nodes operational life [32].

Topology of each network depends on controlled and uncontrolled factors. Controlled factors are transmission power level and use of directional antennas. Uncontrolled factors are classified as node failure, node mobility, noise, and interference [46]. This section discusses controlled factors in wireless networks with focus on transmission power selection algorithms. The efficient topology control has significant effect on network capacity and network operation lifetime. Many TC algorithms have been introduced for homogeneous networks. Such algorithms deal with limitations of wireless networks, such as energy consumption and network capacity. Such proposed algorithms are analyzed critically. Comparisons of the energy efficient topology control algorithms are also given in Table 1. In the following subsection, centralized and distributed topology control algorithms are discussed.

4.1. Centralized Topology Control Algorithms. Centralized transmission power control method is stable topology construction algorithm. There are many algorithms from the topology control that can be applied as centralized transmission power control method. However, in centralize topology control, node needs the authority to control its power levels.

Authors in [47] applied minimum spanning tree (MST) on a graph that preserves connectivity. Furthermore, the transmission power level of each node is guaranteed as long as the greatest link of the MST is established and this is referred to as connected topology. In [47], authors investigated that for connected networks, the weight of the greatest link, from which the level of the critical transmission range (CTR) can be computed, is represented as being *with high probability* $(w : h : p)$ by

$$\mathrm{CTR}_{\mathrm{dense}} = \sqrt{\frac{\log n + f(n)}{n\pi}}, \tag{3}$$

where $f(n)$ is a nondecreasing function of n, such that $\lim_{n\to\infty} f(n) = +\infty$, and $\log n$ is the logarithm of $n(\log n)$.

However, $(w : h : p)$ of (3) works only for 2-D deployments. Authors in [3], used similar equation which works for 1-D and 3-D deployments. Moreover, $(w : h : p)$ has several limitations. It just can be used for connected networks and it is not precise.

Authors in [38] reformulated the CTR methods, which can preserve network connectivity in both sparse and dense graph. Moreover, it uses the size of the deployment area and computes the optimum radio range and number of nodes to establish a connectivity. For the one-dimensional case, the CTR is given by

$$\mathrm{CTR} = k\frac{l \log l}{n}, \tag{4}$$

where the value of k is a constant with $1 \geq k \geq 2$, and l is the size of the area. Moreover, the researchers also provided a partially proven objective for d-dimensional deployments.

For d-dimensional deployments, with $d = 2; 3; \ldots$, the authors in [3] introduced a partially demonstrated result to find the CTR for preserve connectivity as

$$\mathrm{CTR} = k\frac{l^d \log l}{n}, \tag{5}$$

where k is a constant with $0 \leq k \leq 2^d d^{d/(2+1)}$.

The CTR is generally a hard and costly operation, particularly when a full connection is required. Moreover, the CTR may be near to the maximum transmission power level and therefore there will be neither differences in the topology nor energy efficiency.

Authors in [48] proposed algorithms to find a solution for range assignment (RA) problem. The algorithms find a strongly connected graph and minimize the total energy usage of the network. An approach is proposed in [48, 49] for solving the RA problem in 2-D and 3-D. Furthermore, symmetry constraints have been added to the RA problem. Moreover, adding symmetry constraints has resulted in two new issues: first, weakly symmetric range assignment (WSRA) and second the symmetric range assignment (SRA). The solution to the SRA problem is required as all edges in the construction topology should be a reverse link. It has been assumed that some nodes have to maximize their power level to build the symmetric tree. On the other hand, the WSRA removes directed links and adjusts the RA for each node such that the comprised topology is connected and symmetric. The total energy usage of all the assignments is minimized. The WSRA method is more flexible to solve transmission range assignment because it constructs a connected backbone of reverse links. Furthermore, WSRA had been proposed in [3] which has a great gain compared to the SRA in terms of energy consumption.

The aim of TC algorithm is to specify the level of transmission power in order to ensure connectivity and minimize energy usage for each node. The researchers [32, 36, 41] proposed some TC algorithms to reduce power level and ensure network connectivity. In [39], authors studied cooperative communication (CC) algorithm which allow multiple nodes

Table 1: A comparative feature of topology control algorithms.

Author	Proposed algorithm	Topology construction	Topology maintenance	Control scheme	Reliable energy efficient	Energy efficiency	Energy balance	Information exchange
Eidenbenz et al. [19]	ETCG	Connectivity	None	Distributed	None	None	None	One-hop info
Kadivar et al. [33]	OTTC	Energy efficient	None	Distributed	None	Energy efficiency	None	Two-hop info
Sethu and Gerety [34]	STC	Energy efficient	None	Distributed	None	Energy efficiency	None	One-hop info
Komali et al. [7]	MIA and DIA	Energy efficient	None	Distributed	None	Energy efficiency	None	One-hop info
Zarifzadeh and Yazdani [21]	NS	Network capacity	None	Distributed/centralized	None	Energy efficiency	None	One-hop info
Zarifzadeh et al. [35]	MTC	Network capacity	None	Distributed/centralized	None	Energy efficiency	None	One-hop info
Li et al. [36]	LMST	Energy efficient	None	Distributed	None	Energy efficiency	None	One-hop info
Hao et al. [15]	VGEB	Energy balance	Energy balance	Distributed	None	Energy efficiency	Energy balance	Two-hop info
Wattenhofer and Zollinger [37]	XTC	Energy efficient	None	Distributed	None	Energy efficiency	None	One-hop info
Song et al. [13]	TRA	Energy balance	None	Distributed/centralized	None	Energy efficiency	None	One-hop info/global
Santi and Blough [38]	CTR	Connectivity	None	Centralized	None	None	None	Global
Yu et al. [39]	CC	Energy efficiency	None	Centralized	None	Energy efficiency	None	Global
Li and Mohapatra [40]	Unbalance energy	Energy efficiency	None	Distributed	None	Energy efficiency	Energy balance	One-hop info
Cardei et al. [41]	TCC	Connectivity	None	Distributed	None	Energy efficiency	None	One-hop info
Chu and Sethu [42]	CTCA	Energy efficiency	Energy efficiency	Distributed	None	Energy efficiency	None	One-hop info
Olariu and Stojmenović [43]	Corona	Energy efficiency	None	Distributed	None	Energy efficiency	None	One-hop info
Wu et al. [14]	N-Uniform	Energy efficiency	None	Distributed	None	Energy efficiency	Energy balance	One-hop info
Sun et al. [44]	WDTC	Energy efficiency	None	Distributed	None	Energy efficiency	Energy efficiency	One-hop info
Lee et al. [45]	RETC	Network capacity	Energy balance	Distributed	Minimum packet lost	Energy efficiency	Energy balance	One-hop info

to simultaneously forward the same packet. CC algorithm considers disconnected topology and the improvement of a centralized TC scheme, named Cooperative Bridges. CC minimizes the power levels as well as preserve network connectivity. The CC algorithm defines such a problem as follows. First, TC is considered as extended links caused by cooperative communication. Second, the energy efficiency link is extended with cooperative communication. The main aims of proposed centralized topology control technique in [39] are reducing the transmission power level of nodes and increasing connectivity for bipartite networks. Accordingly, simulation results show that CC technique has better performance than other techniques in terms of the connectivity to the energy consumption ratio. However, in CC algorithm, each node is responsible for constructing efficient topology based on global information.

4.2. Distributed Topology Control Algorithms. The main concern of the distributed topology construction algorithm is building a "quality" and efficient topology. In such topology, efficiency refers to minimal energy usage, minimum computational and information exchange complexity, and so on. The rest of this section discusses the energy-efficient topology control in wireless networks and highlights the limitations of existing topology control designed to handle energy efficiency in homogeneous networks.

4.2.1. Energy Efficient Topology Control Algorithms. In [50], the authors argue that, for large size of network, there is still amount of battery left unused after the operational life of the sensor network is over. This unused battery can be up to 90% of total initial energy. To balance the uneven energy consumption among the nodes in wireless networks, mixed routing algorithm (MRA) is proposed by authors in [51]. In MRA algorithm, each node is allowed to either forward a packet to one of its neighbors or to forward it directly to the destination. Furthermore, the decision is depending on its residual energy. The drawback of this algorithm is that it cannot be applied in networks when the node's maximal transmission level is smaller than the network area radius.

Authors in [43] discussed the relationship between the network operational life and the width of each corona C in concentric corona model. The researchers proposed algorithm that minimized the amount of energy usage on forwarding along some intermediate nodes, from a node in a corona and ending at the destination. Moreover, all the Cs in such algorithms must have the same width. However, authors in [43] assumed that all nodes in corona C_i should route along a path in C_{i-1}, and the power level in C_i is $(r_i - r_{i-1})$ and r_{i-1}. Furthermore, if each corona has similar width and similar power level, this assumption may result into the use of less energy for routing. Additionally, divide the corona C_i into two subcoronas; namely, s_1 and s_2 may lead to consume more energy for packet forwarding. The width of subcorona s_1 is equivalent to that of corona C_{i-1}, so nodes in s_1 will forward packets to C_{i-1}. Furthermore, the nodes in subcorona s_2 which are near to corona C_{i-1} with power level greater than the width of corona may result in routing across corona C_{i-1} to corona C_{i-2}, that is, more near to the destination. Moreover, as illustrated in [43], the packet forwarded from all nodes in corona C_i should be routed for the next intermediate in corona C_{i-1} rather than corona C_{i-1}. However, these nodes in s_2 with power level $(r_i - r_{i-1})$, which can forward packets to C_{i-2} but should send to C_{i-1}, will consume more energy for routing.

In [40], authors studied the problem of unbalance energy consumption in large-scale wireless networks. In such investigation the authors described the energy hole in a ring model. Ring model considers the per node energy consuming rate (ECR) and the per node traffic load. Based on ECR algorithm each node around destination needs to forward more packet as compared to the other nodes which are far away from destination. However, in such algorithm, energy consumption rate is higher in inner rings than outer rings and thus has much shorter operation life.

Authors in [14] proposed a nonuniform node distribution strategy to achieve subbalanced energy consumption based on Corona C models. The research studies show that if the total numbers of nodes in corona grow from C_{R-1} to C_1 with a common ratio $q > 1$ and there are $N_{R-1}/(q-1)$ nodes in C_R, then the network can improve sub-balanced uneven energy usage. Here, N_i represents the entire number of nodes in corona C_i. However, distribution strategy of nodes cannot work easily, because in most situations, the nodes are distributed randomly.

Corona (C) model with adjustable transmission power with circular multihop deployment is proposed by authors in [13]. The proposed model assumed that the decision factor for optimizing the network operational life minimizes the transmission power of nodes in each C. Based on this factor, it divides the maximal transmission level of nodes into several levels. Nodes in the similar Cs have the related transmission level, and different C has various transmission levels, which construct an order list in term of the transmission level order. They used multiobjective optimization problem (MOP) for searching of transmission power level between all Cs. Each node can adjust its transmission power for saving energy. The model divided t_{xZ} into k spaces, and sensors have k space transmission power level to choose. The unit length of transmission power range is represented by d. Furthermore, the model divides the whole network area with radius range R into m adjacent concentric parts termed C as shown in Figure 2. Authors in [13] also proposed distributed and centralized algorithm for adjusting transmission power of each node in each corona to extend the network lifetime as shown in Figure 3. However, searching the optimal transmission levels of nodes between all the coronas is an NP-complete problem.

The approach in [37] proposed eXtreme topology control (XTC) algorithm for topology control which operates with the neighbors' link qualities. The main features of XTC algorithms are relevant properties (symmetry, connectivity, sparseness, and planarity) of TC while being faster than any previous algorithms. The XTC algorithm does not require the node coordinate information.

The following explanation shows how nodes order list can be established in XTC algorithm. Based on maximum

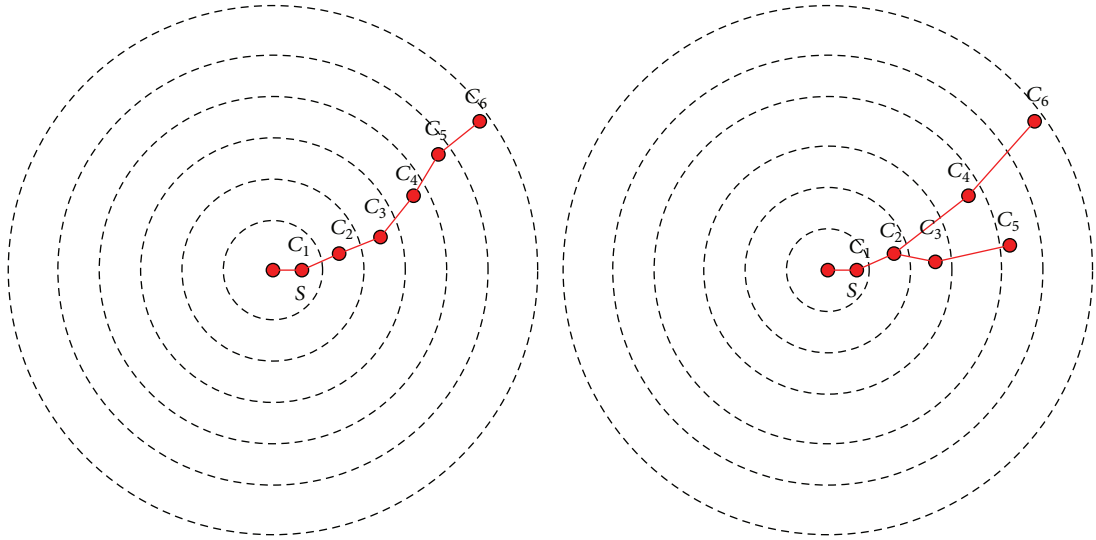

Figure 2: Two branches of transmission powers between all coronas: (a) $k = 1$. (b) $k > 1$.

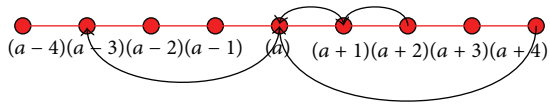

Figure 3: Adjacent coronas $k > 4$.

transmission power, information of each node can be realized by the weight of the links. With additional assumption, link between nodes is bidirectional. Moreover, the signal threshold can be calculated based on the Euclidean distance to the senders. If all nodes send a message with same transmission power range, the neighbor list of node u is also equivalent to the order list. The link qualities w_{uv}, w_{uw}, and w_{vw} reflect that the signal threshold between node u and node w is spoiled by a obstacle, where $w_{uv} < w_{uw}$ and $w_{vw} < w_{uw}$. In contrast, XTC algorithm does not include the link (u, w) in its result topology but applies connection that establishes order list via node v. However, the XTC algorithm does not consider the "power stretch mean" and "stretch factors."

One-hop two-hop topology control (OTTC) [33] is an improved algorithm of XTC which operates with weight of the links. Each node collects its one-hop neighborhoods in a neighbor list and exchanges the list between its neighbors. OTTC algorithm supplies connected subgraph with all properties of topology control (i.e., "connectivity," "symmetry," "spanner," and "low degree"). The OTTC works in fully distributed and low quality information. The main issue considered by OTTC algorithm is the "node degree," "stretch factor," and "power stretch mean" factors.

The following description shows how a node's neighbor list can be obtained in the OTTC as shown in Figure 4. Link quality of the node can be realized by having each initial transmission power of each node via hello message. With the additional assumptions, node u can establish its order list by calculating Euclidean distance and signal thresholds. After receiving the order list by each node, nodes u and v exchange their order list. Therefore, after exchanging the neighbor list, node u finds its two-hop neighbor nodes. Node u and node v are connected in the graph, so there exists a path $P : u = u_0 - u_1 - u_2 - \cdot u_k = v$ on graph G. Edge $u_j, u_{j+1} \in P$ with minimum weight $\|u_j, u_{j+1}\|$ between connected link in G which are not connected in the graph G_{OTTC}. Since u_j and u_{j+1} are not in topology $(u_j, u_{j+1} \notin G_{\mathrm{OTTC}})$, there are two case: First, there exists node $w \in (N(u_j)) \cup (\widetilde{N(u_j)}) \cap (N(u_{j+1})) \cup (\widetilde{N(u_{j+1})})$ such that $w \prec_{u_{j+1}} u_j$ and $w \prec_{u_j} u_{j+1}$. Since $u_j u_{j+1}$ is lower weight, it includes $w \in (N(u_j)) \cup (N(u_{j+1}))$. Moreover, path u_j, w, u_{j+1} is connected to u_j and u_{j+1}. Second, there exists $w \in (N(u_j)) \cup (\widetilde{N(u_{j+1})})$ such as $u_j u_{j+1} > \max\{u_j w, u_{j+1} z, wz\}$ for some z in second hop $(u_j, u_{j+1}) \cap (u_{j,w})$. Furthermore, nodes u_j and u_{j+1} are connected with path u_j, w, z, u_{j+1}.

The proposed OTTC algorithm is fully distributed and work based on low quality information. The main feature of OTTC compared to other algorithms is the use of two-hop information exchange between neighbors, which helps to minimize the power level and degree of the nodes. However, OTTC algorithm considers the low degree which reduces the robustness of topology in real-time application. Moreover, OTTC algorithm does not consider the remaining energy and it may result in consuming more energy.

The paper in [44] presents WDTC algorithm which considers residual energy information to the construction of connected topology. WDTC works based on link weight function. Then each node induces minimum spanning tree (MST) in the new weighted graph. At each iteration of T, the link weight is different, so that the induced MST is different as well as initial topology. WDTC algorithm can effectively improve the network operational lifetime and balance the nodes' energy usage.

Distributed and reliable energy-efficient topology control (RETC) algorithm is proposed by authors in [45].

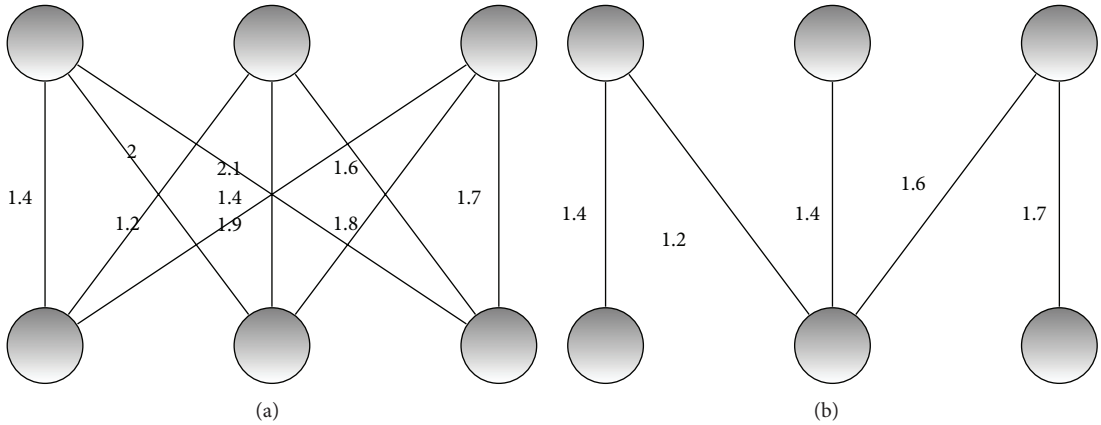

Figure 4: (a) The original graph $(k_3; k_3)$. (b) OTTC topology control.

The RETC algorithm assumed that nodes are connected to their neighbors with a certain packet loss probability. However, many intermediate nodes and congestion may result in packet loss. Thus, reliability must be achieved while designing topology control. Reliable topology can achieve energy balancing and connectivity. The authors argued that considering only topology control is not sufficient to improve an energy-efficient topology construction algorithm. They used maintenance phase that can balance the energy consumption in order to improve network lifetime. In maintenance phase, topology status and trigger topology construction are monitored by nodes when necessary to maximize network lifetime. Additionally, in RETC algorithm, nodes enable us to autonomously select reliable link which has high probability of packet forwarding. Therefore, in the new proposed topology control, a reliable topology is generated to maximize network reachable probability. However, RETC algorithm only considers the nodes residual energy and does not consider average energy of nodes, which may result in consuming more energy.

4.2.2. Game Theory Based Topology Control Algorithms. In [19], authors were the foremost to propose the equilibrium in topology control Game (ETCG) and studied strong connectivity properties. However, in the proposed algorithm, the stable point of NE is not guaranteed and also does not consider the energy efficiency. However, the work was assigned to the analysis of complexity in finding an NE.

The approach in [52, 53] used the game-theoretic concepts which is "mechanism design" to solve TC problem. Those algorithms are considered to develop globally energy efficient algorithms. Moreover, proposed algorithms are used for designing incentive compatible objective. The aims of those algorithms are global energy efficiency by cooperating the selfish user with the social outputs. "Mechanism design" is applied to provide the appropriate incentives to the individual player. "Mechanism design" can increase their objective function when the topology uses minimum energy consuming, subject to preserving network connectivity. Both authors adopted "mechanism design" algorithm by engineering a payment that leads selfish nodes to forward packets to other nodes. The utility function proposed by author in [53] eliminates that each player realized the per link price that it proposed to pay for forwarding packet. However, the algorithm of assigning price on per edge does not account for the wireless advantage. In addition, the communication cost is increased by a node when transmitting data via an edge as a function of transmission power that is required to obtain the edge. Furthermore, nodes increase uniform energy usage in constructing the edge to each of its accessible neighbor at the same transmission level.

The authors in [9] reformulated the ETCG algorithm as exact potential games (EPG). EPG responded to the existence of at least one NE. EPG responds to the existence of at least one NE. Authors in [7] investigated TC to adjust the per node power level such that the resulting topology was energy efficient and satisfies current global properties such as strong connectivity. The algorithm assumes that nodes are responsible to construct topology. The authors studied Nash equilibrium for constructing efficient topology, when nodes employ the greedy best response algorithm. Based on NE in such methods, a modified algorithm based on a better response dynamic is introduced.

The max-improvement algorithm (MIA) and δ-improvement algorithm (DIA) are proposed by authors in [7]. Both algorithms consist of three main phases: "initialization phase", "adaptation phase," and "update phase." However, such algorithms differ in adaptation phase. In MIA, nodes adjust their transmission power level abased on a "greedy" better response process. On the other hand, in the DIA algorithm, nodes adapt their transmission power range based on "restrained" best response process.

The three phases are discussed as follows.

(i) Initial Phase. Each node i adapts its transmission power to $p_i^{\max}$ and discovers its neighbor by sending "hello messages" and then receives the ACKs from each node in the $p_i^{\max}$ neighbor. Furthermore, when a node i receives a response ACKs from each transmission power of neighborhood nodes j, node i adapts its edge state quality between node i and

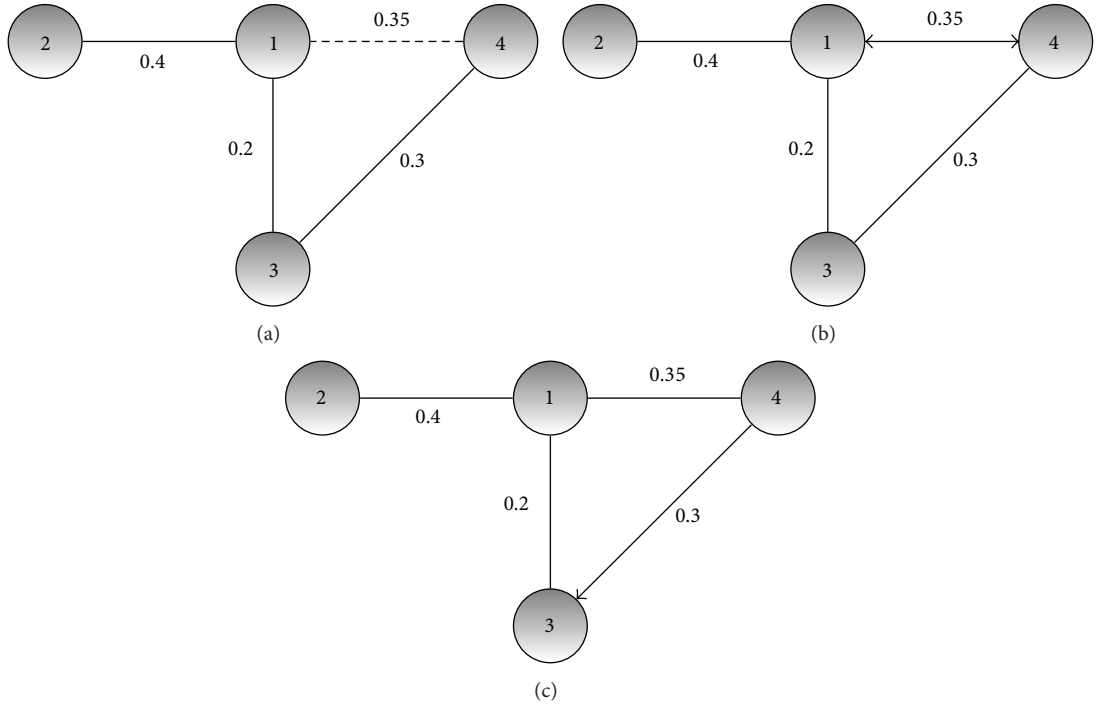

Figure 5: (a) The MST algorithm. (b) The PMST. (c) The G_{DIA} constructed by DIA.

node j, (m_{ij}) to 1. Intuitively, for each node i, determine a link quality e_{ij} as

$$e_{ij} = \begin{cases} 1, & \text{if } p_i \geq w(i,j) \\ 0 & \text{otherwise.} \end{cases} \tag{6}$$

Here, $w(i, j)$ is the power level required to reach an edge $ij = (i, j) \in E$. For each node $i \in N$, defines action set as

$$A = \left\{ p_{\max} = p^0, p^1, \ldots, p^k = p_{\min} \right\}, \tag{7}$$

where A is an ordered set (finite number of power levels); that is, $p^k < p^{k-1}$. One way to construct A is to let the transmission power level of all nodes be initialized maximum power level and minimize the power level in a step of predefined step size δ.

(ii) Adaption Phase. In adaption phase, each node is selected from permutation round robin to assign its transmit level. All those nodes produce either MIA or DIA during the game and only one node sets its transmission range. Node i, selected via some sequential orders, improves its pay-off as shown in (8), by adapting its transmission power from $p_i^{\max}$ based on $p_i < p_{\max}$:

$$u_i(p) = \varphi_i(g(p)) - \chi_i(p_i), \tag{8}$$

where $\varphi_i : G \rightarrow IR$ represents the pay-off node i proceed from graph g, and χ_i is the cost increased. Both algorithms determine the adaption phase in two categories. In the MIA adaptation phases, the game can be played as a normal game, where every node is chosen to increase its individually utility in that iteration. In the best response based algorithm, whenever a node has a chance to change its action, it chooses an action that increases its individual utility shown in (8), given the transmission power range as shown in Figure 5 of all other nodes based on the following

$$\begin{aligned} p_i &= \arg\operatorname*{Max}_{q_i \in A} u_i(q_i, p_{-i}), \\ &\min_{\widetilde{c}_i(a_{-i}) \in \Re(\Gamma_i^{c_i})} u_i(\widetilde{a}_i^*, \widetilde{c}_i(a_{-i}^*)) \\ &\geq \min_{\widetilde{c}_i(a_{-i}) \in \Re(\Gamma_i^{c_i})} u_i(\widetilde{a}_i, \widetilde{c}_i(a_{-i}^*)). \end{aligned} \tag{9}$$

On the other hand, in the DIA adaptation phases, power is in the discrete action list. More precisely, it is sufficient to search for the best transmission power over that action list which corresponds to the signal's threshold entries of Ω. In DIA algorithm, each node i selects a power level one less than its current power level if the selected transmission power results in a higher utility than its current power level. Otherwise, the node changes transmission power to the power level, that is, currently transmit at. Additionally, given the action of all other nodes, each node chooses to forward a packet to the next node, at power level given

$$\widetilde{p}_i = \arg\operatorname*{Max}_{q_i \in \{p_i^{k+1}, p_i^k\}} u_i(q_i, p_{-i}). \tag{10}$$

(iii) Update Phase. As illustrated from the MIA and DIA algorithms, nodes selected their power range in each iteration

and determined their neighborhoods. Based on the detection of its neighbors, the node updates the overall topology. Each node changes its transmission range to a certain connected topology state. Additionally, other nodes are informed of this change by some optimized broadcast algorithm.

In DIA algorithm, each node minimizes its transmission power level since this change results in maximizing its utility; otherwise, the player changes transmission power to its previous power level. Additionally, the researcher used potential game in TC game for globally energy efficient. The MIA converges to topologies that ensure the connectivity establishment. However, the MIA is not energy efficient. On the other hand, the DIA algorithm guarantees convergence to min-max energy efficiency and preserves the network connectivity. Additionally, to guarantee the convergence to NE, the nodes employ the best response algorithm to choose an adequate transmission power level. However, in DIA and MIA, nodes do not consider the residual energy and it may result in draining more energy.

Authors in [36] introduced a local minimum spanning tree (LMST) based algorithm for topology control. LMST is a localized algorithm to build minimum spanning tree based connected topology. Moreover, the LMST uses one-hop neighbor's information of nodes. Each node has an identification ID. In the LMST algorithm, each node from the information of one-hop calculates MST individually. The researcher constructed LMST with the following two phases.

(i) Initially, each node sends a "hello message" using the maximal power level $d_{\max}$ as the undirected graph $G = (V, E)$, where V is set of nodes and E is set of link, $E = \{(u, v), d_{(u,v)} < d_{\max}, u, v \in V\}$. Hello message as visible neighborhood contains its ID that helps node to construct its local graph.

(ii) In second phases, after obtaining visible neighborhood, each node u builds its local MST $T_u = (V(T_u), E(T_u))$ of G_u from its local graph. Each node uses "Bellman-Ford shortest" algorithm individually to obtain its local MST. Each link has a different weight; for example, edges (u_1, v_1) and (u_2, v_2) are different. The locally computed MST can preserve the network connectivity. To simply connectivity, authors in [36] defined neighborhood relation and neighborhood set. Node v is a neighborhood of node u's, denoted by $u \rightarrow v$, if and only if $(u, v) \in E(T_u)$. Moreover, $u \leftrightarrow v$, if and only if $u \rightarrow v$ and $v \rightarrow u$. In addition, that is, node v is a neighborhood of node u's if and only if the node v is on the node u's LMST, $T(u)$ and is one-hop away from node u as shown in Figure 6.

In addition, the proposed algorithm in [36] considered the pay-off of a node for adding a tree as a function of its transmission power. More accurately, every node is only concerned in minimizing its transmission level while being connected to the network. The one-hop neighborhood of each node is determined trivially based on its transmission power level. However, it is not an energy efficient solution for the large-scale network. Moreover, the node energy usage distribution in LMST is unbalance. Consequently, those nodes with high consumption rates may leading to the network operational lifetime fault prematurely. Therefore, the battery usage of each node should be balanced.

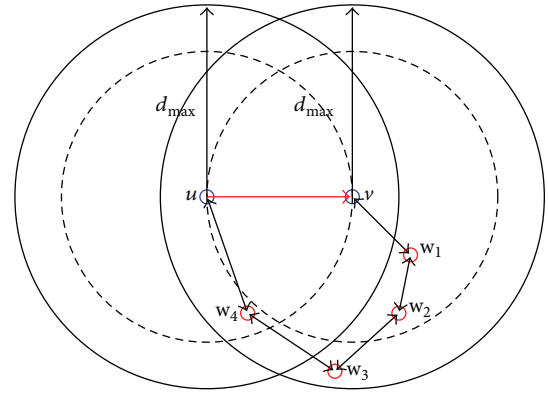

Figure 6: The LMST.

In [41], authors introduced an algorithm to optimize the traditional TC scheme. In such algorithm, each node repetitively maximizes its power level. This algorithm starts from a symmetric, connected network, assumed to be the output of conventional of TC algorithms. Accordingly, more reliable TC algorithms were investigated in [54], such as fault-tolerant local and local tree based reliable topology (LTRT). Such algorithms can preserve k-link connectivity; that is, topology cannot be disconnected if the numbers of disconnected edges are less than k and are referred to as k-link connected algorithm.

4.2.3. Game Theory Based Network Capacity Topology Control Algorithms. In [35], authors proposed multi-power topology control (MTC) game, where each node is capable to employ multichannel communications to minimize their energy consumption. Indeed, nodes do not adjust their transmission range for themselves, since it is assumed to have the capability of sending data at multiple power ranges simultaneously. However, the MTC algorithms are equipped with multiradio.

Authors in [21] proposed neighbor selection game (NS) with complete information of network. In NS algorithm, each node is interested to selfishly choose its neighbors such that their energy usage is reduced and the network capacity is improved. The NS algorithm considers the benefit of connectivity and energy cost of a node for connecting to a network. Each node is only trying to minimize its transmission range while being joined to other nodes as shown in Figure 7. The authors believed that the rate of energy consumed in a wireless network depends not only on transmission power but also on the amount of packets it forwards. Finally, in [21], authors introduced two distributed algorithms (global versus local) for obtaining a TC in a network in the presence of selfish nodes. In the global algorithm, each player knows the complete information about the network connectivity. While in the local model, each node gathers neighbor information within a limited hop. Then generalize the problem to the case where the transmission powers are the unknown variables and should be determined jointly with the neighbor sets. In addition, the authors consider the topology control and

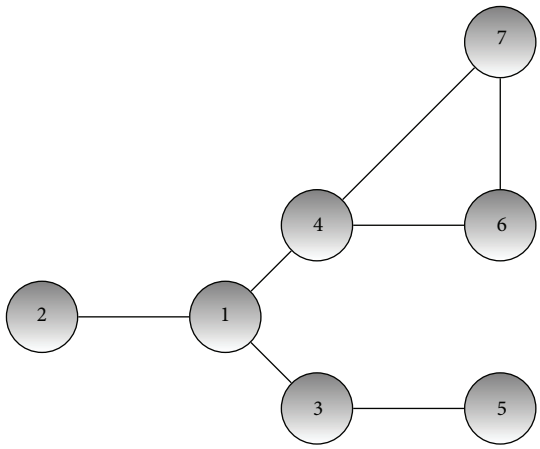

Figure 7: A sample NE topology in which no node benefits from removing any of the links.

neighbor selection as a joint process of joint neighbor Selection (JNS) algorithm in which both the transmission power and the neighbor set of nodes are unknown. The power list is not given as input to the problem; instead, nodes work on an initial topology to determine their transmission power and neighbor list together. In the JNS algorithms, players start with the max graph and in each repetition, one node takes turn and plays its best response and assumes that nodes have global knowledge about the connectivity of the whole network. Furthermore, the joint best response algorithm works similarly to the local method except that each node chooses the lightest link between itself and every k-hop strong component. The results of their simulations show that the global method yields about 20% higher total energy consumption than the approximated (stable) solution. However, refer to simulation results and the JNS algorithm needs fully global information to work properly. Based on the result, the local method can reduce this problem by more than 10%.

4.2.4. Game Theory Based Energy Balance Topology Control Algorithms. Authors in [15] introduced virtual game-based energy balanced topology control algorithm (VGEB) with incomplete information. VGEB algorithm considers balancing energy consumption which can drain nodes energy. In the virtual game (VG), each node exchanges its complete information only once within neighbor nodes. Furthermore, in VGEB algorithm, first, each node will select some neighbor nodes with more remaining energy as their other neighbors to mitigate the energy usage of nodes with less remaining energy as shown in Figure 8. Additionally, in VGEB algorithm, each node i constructs the VGEB $\Gamma^i = \langle N^{(i)}, P^{(i)}, u^{(i)} \rangle$ in which each node only makes a decision based on its power level. Following three phases describe the VGEB algorithm.

(i) Information Collection Phases. Each node i sets its transmission power $p^{\max}$ and propagates request message for its neighborhood in $p^{\max}$. Since the node i receives ACK from each responding neighborhood j, node i contains neighborhood j's ID, transmission power level to node js, p_{ij}, and residual energy into the order list. Based on the collected neighbor lists, each node i has each node k's ($k \in N(i)$) power action set $P_k^{(i)} = \{p_{k1}^{(i)}, p_{k2}^{(i)}, \ldots, p_{km_k}^{(i)}\}$, where k is a symbol in $N(i)$.

(ii) Virtual Game Phases. In this phase, each node has discretized the action vector. The action set of node $k \in N(i)$ is defined as

$$P_k^{(i)} = \left\{p_k^{\max} = p_{k1}^{(i)}, p_{k2}^{(i)}, \ldots, p_{km_k}^{(i)} = p_k^{\max}\right\}, \tag{11}$$

where k selects transmission level, one power levels less than the current level if the selected level gives higher utility than its certain power level. Otherwise, the node revers to the power range it is currently used. Given the transmission power level of all other nodes in N^i,

$$p_k^i = \arg \max_{q_k^i \in p_{kh}^i, p_{km}^i} u_k^i \left(q_{-k}^i, q_k^i\right), \tag{12}$$

where $u_k^i(q_{-k}^i, q_k^i)$ is utility function which is outcome of each transmission power level. Additionally, a utility function obtains the trade-off and sets the power level action to a benefit for each node, based on the following equation (13):

$$u_k^i \left(q_{-k}^i, q_k^i\right) = f_k^i \left(q_{-k}^i, q_k^i\right) \left(\frac{\alpha p_k^{\max}}{E_{rk}} + \beta \overline{E}_k \left(p_k^i\right)\right) - \left(\frac{\alpha p_k^i}{E_{rk}}\right), \tag{13}$$

where α and β are nondecreasing value. $f_k^i(q_{-k}^i, q_k^i) = 1$ if sensor node k is able to connect to its neighbors, else $f_k^i(q_{-k}^i, q_k^i) = 0$. Additionally, $E_k(p_k^i)$ is the average residual energy of a node j's, j is the node in which node k is able to be connected by one-hop distance with p_k^i, $E_0(j)$ and $E_r(j)$ are the initial energy allocated and the residual energy, respectively.

(iii) Maintenance Phase. As the operational time of the network goes by, energy usage of the nodes becomes unbalanced. It is possible for each node i to figure out its own residual energy. Furthermore, if its residual energy is less than a specified level (e.g., a level is 1/5 of its allocated battery), then node i executes the VG algorithm $\Gamma^{(i)}(p^{\max} \rightarrow p^{(i)})$ to readjust its transmission power level.

VGEB greatly minimizes the energy exhausting in the information exchange and considers the energy balance. However, if a topology only considers energy balancing without considering pursuing energy efficiency, node's lifetime may fail prematurely.

Traditional TC algorithms such as DRNG, DLSS [55], and STC [34] start the TC execution with each node's maximal transmission level to detect all of its neighbors. Local neighbor and transmission power range information is exchanged between nodes and their neighbors. Without further communication between nodes, the minimum power level of each node is calculated at each node. However, based on DRNG, DLSS and STC algorithms nodes do not have

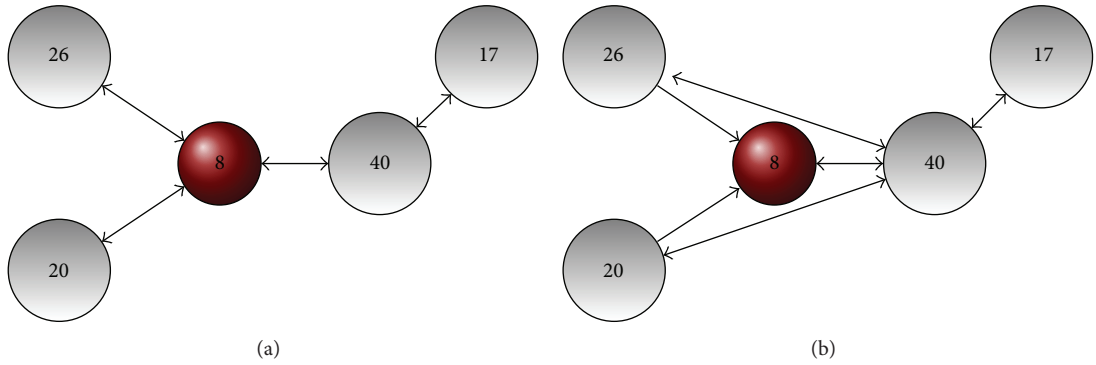

FIGURE 8: (a) The topology without considering remain energy (b) and the topology considering remaining energy.

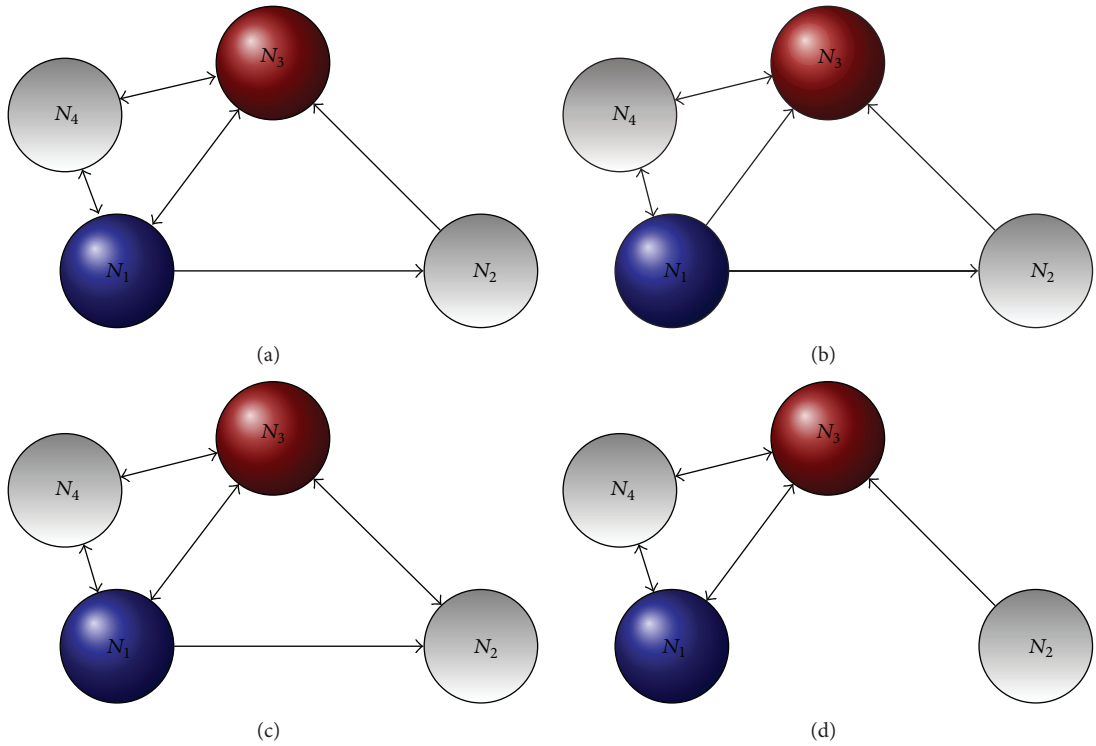

FIGURE 9: Transmission power selection in the CTCA algorithm. (a) Case 1: Node N_3's, where node N_1 is not able of minimizing its power level without being unconnected. (b) Case 2: Node N_3 minimizes its power level to its optimal power, but N_1's lifetime cannot be increased. (c) Case 3: Node N_3 maximizes its power level to $p(N_3; N_2)$. Now, node N_1 is capable to minimize its power without being unconnected. (d) Case 4: Node N_1 modifies its certain power level to its potential power and improves lifetime of the network.

permission to cooperate with neighbor nodes to improve the network functional lifetime.

The approach in [42] proposed cooperative topology control with Adaptation (CTCA) algorithm. CTCA algorithm is adaptive and allows cooperation among nodes to increase the network operational lifetime. The CTCA consists of two main phases.

(i) Neighbor List Phases. Each node sets its power at the maximum transmission level $p_{\max}$ and makes neighbor list of a node N_i, that is, equal to $R_i(0) = \{N_j p(N_i, N_j \leq p_{\max})\}$. Determine the action set for node N_i as $A_i = \{p_i^1, p_i^2, \ldots, p_i^n\}$, where, for node $N_j \in R_i(0)$, there exists a power range $p_k^i \in A_i$. Moreover, p_k is the lower power level required for N_i to connect N_j. The proposed CTCA algorithm assumed that $p_i^1 \leq p_i^2 \leq p_i^n \leq p_{\max}$. The CTCA algorithm uses DLSS algorithm [55] for determining p_i for transmission power level adjustment. Moreover, each node propagates message to its neighbor for current residual energy by mark "energy info shared" $W_i(t)$ and modifies W_j for $N_j \in I_i$.

(ii) Neighbor Assisted Power Adjusts Phases (NAPA). Each node tries to improve its neighbor's operational life, refereed by $N_{m_{(i)}}(t)$ the node in $O_i(t) = I_i(t) \cup N_i$ with the lower

functional life as shown in Figure 9. Moreover, its optimal transmission level at interval t is set as $Y_{m_{(i)}}(P_m(t))$, and its functional life at t is set as $Z_{m_{(i)}}(P_m(t))$. In addition, assumption $a_i \in A_i$ refers to the current transmission power for node N_i in time t. CTCA algorithm determines the utility u_i for node N_i with power level a_i as

$$u_i(a_i,t) = c_i(a_i,t)\,V_i(a_i,t)\,l_i(a_i,t) + c_i(a_i,t)\min\left(\min_{N_j\in I_i(t)} V_i(a_i,t), Z_j\left(P_j(t),t\right)\right), \tag{14}$$

where $c_i(a_i,t)$ denotes 0,1. If $c_i(a_i,t) = 1$ node, N_i can connect to a node N_j with power range a_i; otherwise, $c_i(a_i,t) = 0$. $c_i(a_i,t)$ is used to show the node N_i operational lifetime by transmission power a_i. If $N_{m_{(i)(t)}}$'s current power level can be minimized by N_i transmitting at power range a_i and $N_m(i)$ functional life in this case is greater than the neighbor's lifetime. Additionally, $N_m(i)$'s operational life is not considered, and therefore $l_i(a_i,t) = 0$. However, if transmitting at the transmission level a_i may not help increasing $N_{m_{(i)(t)}}$'s operational life, its operational life results in lower than the neighbor's operational lifetime in the connected network. In addition, node N_i should increase its operational life; that is, $l_i(a_i,t) = 1$.

If the CTCA algorithm meets all of the conditions illustrated above, then node N_i will be selected to maximize its transmission level in order to help increasing its neighbor's functional life. Furthermore, the author had proven the existence of a NE for the game theory and provided a algorithm which gains a NE. The simulation results of the CTCA algorithm show that the algorithm is able to increase the functional life and balance energy consumption. However, the proposed algorithm is not an energy efficient solution, which consume more energy with using high power level. Consequently, those nodes with high consumption rates are leading to the network operational lifetime over prematurely. Therefore, topology control should consider energy efficiency and energy balancing together.

5. Discussion

Topology control of wireless networks is unstructured to fluctuations. To tackle such unstable characteristics, a TC mechanism must overcome the variability in typologies. The fundamental aim of TC is that, instead of using the maximum transmission level, each node collaboratively adjusted its power level and constructed efficient topology, with the objective of improving the network functional lifetime. Table 1 shows the main characteristics of the existing TC algorithms. It identifies the algorithm of each algorithm and clarifies the class of these algorithms. The objectives of each algorithm are also included. Most current TC algorithms for energy conservation have inconsecutive assumptions.

Obviously, it is the connectivity at the edge that qualifies end-to-end connectivity. The well-known link connectivity is the protocol model or disk model. Connectivity problem is considered to minimize one of the power adjustments. The comprehensive feature of deterministic TC algorithms can be stated as an optimization problem. Additionally, the objective, mainly, is to specify a power adjustment, such that $p_i^{\max}$ to $p(i)$ is decreased, while preserving connectivity. Moreover, the objective could be desirable with following properties: k-connectivity, node degree, and spanner.

There are numerous topology control designed for WSNs and ad hoc networks such as homogeneous transmission power control and heterogeneous transmission power control. The homogeneous transmission power control can be characterized in two schemes, centralized and distributed topology control scheme. In centralized topology control, nodes need authority to control. In distributed topology control, each node act selfishly to save its limited energy in critical environment by using its neighbor information. Such information can be achieved by exchanging information between the nodes. On the other hand, there are several challenges for topology control in wireless networks such as node deployment, network capacity, and energy consumption. However, energy consumption can be considered as the main important technical challenge for topology control in wireless networks. Obviously, energy efficiency topology control can be improved in two ways: minimizing the energy consumption by selecting optimum transmission power level or balancing energy consumption among the nodes. In all TC algorithm as mentioned in the literature, the only consideration for each node is to reduce its power level while preserving network connectivity. However, existing algorithms do not consider the fact that various nodes are in various positions in the topology, and some may end up with a high transmission power level. Therefore, this high power level will consume more energy and disrupt network. Also, many algorithms have been investigated to construct an efficient topology such that balanced energy consumption, for example, by considering residual energy of the node during transmission power selection.

Most algorithms assumed that nodes are cooperative to each other, since, in wireless networks, there is no method to qualify nodes. However, this assumption may not always hold. Each node may compete with its neighbor to conserve its own limited energy and consequently degrade the whole network efficiency. If the nodes select too low transmission power level, the constructed topology will be disconnected. It is more reasonable to assume that nodes act selfishly and this selfish behavior can be modeled as noncooperative games. Game theory is a fundamental tool to achieve an energy balance and energy efficient while preserving network connectivity in the present of selfish nodes. Moreover, in such models, nodes interact with other nodes to maximize their individual utility. Currently, the fundamental algorithm for noncooperative TC is based on adapting the power level of nodes, while the topology remains connected. However, some algorithms consider only energy balance and do not consider energy efficiency and reliable neighbor selection.

Though, there is a significant improvement in the theoretical study of energy efficiency topology control in wireless networks. There is some evidence to confirm benefits of TC on improving network lifetime. In fact, distinguishing

optimal power selection and reliable neighbor selection that can forward packets through the network at rates close to capacity with minimum energy consumption is still an open issue.

6. Conclusions

In this paper, topology control aims of the existing algorithms are characterized into three main types: energy efficiency, network capacity, and energy balancing. The most famous and recent topology control algorithms based on their features are reviewed and compared in each goals category. According to this overview, most of the proposed algorithms consider minimizing the transmission power levels while preserving network connectivity in wireless network (DIA, MIA, and OTTC). Furthermore, some of them consider balanced energy consumption of nodes (VGEB, CTCA, and ECR) and a number of them aim to improve network capacity (NS, RETC). However, by increasing the application of wireless networks, the functions of wireless nodes will be so highlighted and they always seek to achieve conflicting objectives such as in the pursuit of energy efficiency and network connectivity. Therefore, scalable solutions which can perform topology control by considering multiobjective QoS requirements and high spatial reuse are greatly required for wireless networks.

References

[1] I. F. Akyildiz, W. Su, Y. Sankarasubramaniam, and E. Cayirci, "A survey on sensor networks," *IEEE Communications Magazine*, vol. 40, no. 8, pp. 102–105, 2002.

[2] P. Santi and J. Simon, "Silence is golden with high probability: maintaining a connected backbone in wireless sensor networks," in *Wireless Sensor Networks*, pp. 106–121, 2004.

[3] P. Santi, "Topology control in wireless ad hoc and sensor networks," *ACM Computing Surveys*, vol. 37, no. 2, pp. 164–194, 2005.

[4] S. E. Calvano, W. Xiao, D. R. Richards et al., "A network-based analysis of systemic inflammation in humans," *Nature*, vol. 437, no. 7061, pp. 1032–1037, 2005.

[5] N. Mladineo and S. Knezic, "Optimisation of forest fire sensor network using gis technology," in *Proceedings of the 22nd International Conference on Information Technology Interfaces (ITI '02)*, pp. 391–396, 2000.

[6] L. Ritchie, S. Deval, M. Reisslein, and A. W. Richa, "Evaluation of physical carrier sense based spanner construction and maintenance as well as broadcast and convergecast in ad hoc networks," *Ad Hoc Networks*, vol. 7, no. 7, pp. 1347–1369, 2009.

[7] R. S. Komali, A. B. MacKenzie, and R. P. Gilles, "Effect of selfish node behavior on efficient topology design," *IEEE Transactions on Mobile Computing*, vol. 7, no. 9, pp. 1057–1070, 2008.

[8] T. M. Chiwewe and G. P. Hancke, "A distributed topology control technique for low interference and energy efficiency in wireless sensor networks," *IEEE Transactions on Industrial Informatics*, vol. 8, no. 1, pp. 11–19, 2012.

[9] R. S. Komali and A. B. MacKenzie, "Distributed topology control in ad-hoc networks: a game theoretic perspective," in *Proceedings of the 3rd IEEE Consumer Communications and Networking Conference (CCNC '06)*, pp. 563–568, January 2006.

[10] Z. Mi and Y. Yang, "Topology control and coverage enhancement of dynamic networks based on the controllable movement of mobile agents," in *Proceedings of the IEEE International Conference on Communications (ICC '11)*, pp. 1–5, June 2011.

[11] S.-C. Wang, D. S. L. Wei, and S.-Y. Kuo, "An SPT-based topology control algorithm for wireless ad hoc networks," *Computer Communications*, vol. 29, no. 16, pp. 3092–3103, 2006.

[12] Y. Wang, "Topology control for wireless sensor networks," in *Wireless Sensor Networks and Applications*, pp. 113–147, 2008.

[13] C. Song, M. Liu, J. Cao, Y. Zheng, H. Gong, and G. Chen, "Maximizing network lifetime based on transmission range adjustment in wireless sensor networks," *Computer Communications*, vol. 32, no. 11, pp. 1316–1325, 2009.

[14] X. Wu, G. Chen, and S. K. Das, "Avoiding energy holes in wireless sensor networks with nonuniform node distribution," *IEEE Transactions on Parallel and Distributed Systems*, vol. 19, no. 5, pp. 710–720, 2008.

[15] X.-C. Hao, Y.-X. Zhang, N. Jia, and B. Liu, "Virtual game-based energy balanced topology control algorithm for wireless sensor networks," *Wireless Personal Communications*, pp. 1–20, 2012.

[16] C. Schurgers, V. Tsiatsis, and M. B. Srivastava, "Stem: topology management for energy efficient sensor networks," in *IEEE Aerospace Conference Proceedings*, vol. 3, pp. 1099–1108, 2002.

[17] S. Zarifzadeh, A. Nayyeri, and N. Yazdani, "Efficient construction of network topology to conserve energy in wireless ad hoc networks," *Computer Communications*, vol. 31, no. 1, pp. 160–173, 2008.

[18] S. Rizvi, H. K. Qureshi, S. Ali Khayam, V. Rakocevic, and M. Rajarajan, "A1: an energy efficient topology control algorithm for connected area coverage in wireless sensor networks," *Journal of Network and Computer Applications*, vol. 35, no. 2, pp. 597–605, 2012.

[19] S. Eidenbenz, V. S. A. Kumar, and S. Zust, "Equilibria in topology control games for ad hoc networks," *Mobile Networks and Applications*, vol. 11, no. 2, pp. 143–159, 2006.

[20] R. S. Komali, R. W. Thomas, L. A. Dasilva, and A. B. MacKenzie, "The price of ignorance: distributed topology control in cognitive networks," *IEEE Transactions on Wireless Communications*, vol. 9, no. 4, pp. 1434–1445, 2010.

[21] S. Zarifzadeh and N. Yazdani, "Neighbor selection game in wireless ad hoc networks," *Wireless Personal Communications-*, vol. 70, no. 2, pp. 617–640, 2013.

[22] M. J. Osborne, *An Introduction to Game Theory*, vol. 3, Oxford University Press, New York, NY, USA, 2004.

[23] J. Ratliff, "A folk theorem sampler. Lecture notes," 2010, http://www.virtualperfection.com/gametheory/5.3.FolkTheoremsampler.1.0.pdf.

[24] G. Arslan and J. S. Shamma, "Distributed convergence to nash equilibria with local utility measurements," in *Proceedings of the 43rd IEEE Conference on Decision and Control (CDC '04)*, pp. 1538–1543, December 2004.

[25] J. R. Marden, G. Arslan, and J. S. Shamma, "Joint strategy fictitious play with inertia for potential games," *IEEE Transactions on Automatic Control*, vol. 54, no. 2, pp. 208–220, 2009.

[26] D. Monderer and L. S. Shapley, "Potential games," *Games and Economic Behavior*, vol. 14, no. 1, pp. 124–143, 1996.

[27] W. Poundstone and N. Metropolis, "Prisoner's dilemma: John von neumann, game theory, and the puzzle of the bomb," *Physics Today*, vol. 45, article 73, 1992.

[28] J. Liu and B. Li, "Distributed topology control in wireless sensor networks with asymmetric links," in *IEEE Global Telecommunications Conference (GLOBECOM '03)*, pp. 1257–1262, December 2003.

[29] H. Zhang and J. C. Hou, "Maintaining sensing coverage and connectivity in large sensor networks," *Ad Hoc & Sensor Wireless Networks*, vol. 1, no. 1-2, pp. 89–124, 2005.

[30] X. Wang, G. Xing, Y. Zhang, C. Lu, R. Pless, and C. Gill, "Integrated coverage and connectivity configuration in wireless sensor networks," in *Proceedings of the 1st International Conference on Embedded Networked Sensor Systems (SenSys '03)*, pp. 28–39, November 2003.

[31] P. Gupta and P. R. Kumar, "The capacity of wireless networks," *IEEE Transactions on Information Theory*, vol. 46, no. 2, pp. 388–404, 2000.

[32] R. Ramanathan and R. Rosales-Hain, "Topology control of multihop wireless networks using transmit power adjustment," in *Proceedings of a IEEE 19th Annual Joint Conference of the Computer and Communications Societies (INFOCOM '00)*, vol. 2, pp. 404–413, March 2000.

[33] M. Kadivar, M. E. Shiri, and M. Dehghan, "Distributed topology control algorithm based on one- and two-hop neighbors' information for ad hoc networks," *Computer Communications*, vol. 32, no. 2, pp. 368–375, 2009.

[34] H. Sethu and T. Gerety, "A new distributed topology control algorithm for wireless environments with non-uniform path loss and multipath propagation," *Ad Hoc Networks*, vol. 8, no. 3, pp. 280–294, 2010.

[35] S. Zarifzadeh, N. Yazdani, and A. Nayyeri, "Energy-efficient topology control in wireless ad hoc networks with selfish nodes," *Computer Networks*, vol. 56, no. 2, pp. 902–914, 2012.

[36] N. Li, J. C. Hou, and L. Sha, "Design and analysis of an MST-based topology control algorithm," *IEEE Transactions on Wireless Communications*, vol. 4, no. 3, pp. 1195–1206, 2005.

[37] R. Wattenhofer and A. Zollinger, "XTC: a practical topology control algorithm for ad-hoc networks," in *Proceedings of the 18th International Parallel and Distributed Processing Symposium (IPDPS '04)*, pp. 2969–2976, April 2004.

[38] P. Santi and D. M. Blough, "The critical transmitting range for connectivity in sparse wireless ad hoc networks," *IEEE Transactions on Mobile Computing*, vol. 2, no. 1, pp. 25–39, 2003.

[39] J. Yu, H. Roh, W. Lee, S. Pack, and D. -Z. Du, "Topology control in cooperative wireless ad-hoc networks," *IEEE Journal on Selected Areas in Communications*, vol. 30, no. 9, pp. 1771–1779, 2012.

[40] J. Li and P. Mohapatra, "Analytical modeling and mitigation techniques for the energy hole problem in sensor networks," *Pervasive and Mobile Computing*, vol. 3, no. 3, pp. 233–254, 2007.

[41] M. Cardei, J. Wu, and S. Yang, "Topology control in ad hoc wireless networks using cooperative communication," *IEEE Transactions on Mobile Computing*, vol. 5, no. 6, pp. 711–724, 2006.

[42] X. Chu and H. Sethu, "Cooperative topology control with adaptation for improved lifetime in wireless ad hoc networks," in *Proceedings of the 28th IEEE International Conference on Computer Communications (INFOCOM '12)*, pp. 262–270, 2012.

[43] S. Olariu and I. Stojmenović, "Design guidelines for maximizing lifetime and avoiding energy holes in sensor networks with uniform distribution and uniform reporting," in *Proceedings of the 25th IEEE International Conference on Computer Communications (INFOCOM '06)*, vol. 6, pp. 1–12, April 2006.

[44] R. Sun, J. Yuan, I. You, X. Shan, and Y. Ren, "Energy-aware weighted graph based dynamic topology control algorithm," *Simulation Modelling Practice and Theory*, vol. 19, no. 8, pp. 1773–1781, 2011.

[45] C.-Y. Lee, L.-C. Shiu, F.-T. Lin, and C.-S. Yang, "Distributed topology control algorithm on broadcasting in wireless sensor network," *Journal of Network and Computer Applications*, vol. 36, pp. 1186–1195, 2013.

[46] V. Srivastava, J. Neel, A. B. MacKenzie et al., "Using game theory to analyze wireless ad hoc networks," *IEEE Communications Surveys and Tutorials*, vol. 7, no. 4, pp. 46–56, 2005.

[47] M. D. Penrose, "The longest edge of the random minimal spanning tree," *The Annals of Applied Probability*, vol. 7, no. 2, pp. 340–361, 1997.

[48] L. M. Kirousis, E. Kranakis, D. Krizanc, and A. Pelc, "Power consumption in packet radio networks," *Theoretical Computer Science*, vol. 243, no. 1-2, pp. 289–305, 2000.

[49] A. E. F. Clementi, P. Penna, and R. Silvestri, "Hardness results for the power range assignment problem in packet radio networks," in *Algorithms and Techniques of Randomization, Approximation, and Combinatorial Optimization*, pp. 197–208, 1999.

[50] J. Lian, K. Naik, and G. B. Agnew, "Data capacity improvement of wireless sensor networks using non-uniform sensor distribution," *International Journal of Distributed Sensor Networks*, vol. 2, no. 2, pp. 121–145, 2006.

[51] A. Jarry, P. Leone, O. Powell, and J. Rolim, "An optimal data propagation algorithm for maximizing the lifespan of sensor networks," in *Distributed Computing in Sensor Systems*, pp. 405–421, 2006.

[52] S. Yuen and B. Li, "Strategyproof mechanisms towards dynamic topology formation in autonomous networks," *Mobile Networks and Applications*, vol. 10, no. 6, pp. 961–970, 2005.

[53] P. Santi, S. Eidenbenz, and G. Resta, "A framework for incentive compatible topology control in non-cooperative wireless multihop networks," in *Proceedings of the Workshop on Dependability Issues in Wireless Ad Hoc Networks and Sensor Networks (DIWANS '06)*, pp. 9–18, September 2006.

[54] K. Miyao, H. Nakayama, N. Ansari, and N. Kato, "LTRT: an efficient and reliable topology control algorithm for ad-hoc networks," *IEEE Transactions on Wireless Communications*, vol. 8, no. 12, pp. 6050–6058, 2009.

[55] N. Li and J. C. Hou, "Localized topology control algorithms for heterogeneous wireless networks," *IEEE/ACM Transactions on Networking*, vol. 13, no. 6, pp. 1313–1324, 2005.

Hindawi Publishing Corporation
Mathematical Problems in Engineering
Volume 2013, Article ID 646059, 12 pages
http://dx.doi.org/10.1155/2013/646059

Review Article

Recent Advances on Recursive Filtering and Sliding Mode Design for Networked Nonlinear Stochastic Systems: A Survey

Jun Hu,[1] Zidong Wang,[2,3] Hongli Dong,[4,5] and Huijun Gao[6]

[1] *Department of Applied Mathematics, Harbin University of Science and Technology, Harbin 150080, China*
[2] *School of Information Science and Technology, Donghua University, Shanghai 200051, China*
[3] *Department of Information Systems and Computing, Brunel University, Uxbridge, Middlesex UB8 3PH, UK*
[4] *College of Electrical and Information Engineering, Northeast Petroleum University, Daqing 163318, China*
[5] *Institute for Automatic Control and Complex Systems, University of Duisburg-Essen, Duisburg 47057, Germany*
[6] *Research Institute of Intelligent Control and Systems, Harbin Institute of Technology, Harbin 150001, China*

Correspondence should be addressed to Zidong Wang; zidong.wang@brunel.ac.uk

Received 22 September 2013; Accepted 18 October 2013

Academic Editor: Xiao He

Some recent advances on the recursive filtering and sliding mode design problems for nonlinear stochastic systems with network-induced phenomena are surveyed. The network-induced phenomena under consideration mainly include missing measurements, fading measurements, signal quantization, probabilistic sensor delays, sensor saturations, randomly occurring nonlinearities, and randomly occurring uncertainties. With respect to these network-induced phenomena, the developments on filtering and sliding mode design problems are systematically reviewed. In particular, concerning the network-induced phenomena, some recent results on the recursive filtering for time-varying nonlinear stochastic systems and sliding mode design for time-invariant nonlinear stochastic systems are given, respectively. Finally, conclusions are proposed and some potential future research works are pointed out.

1. Introduction

In recent years, the networked control systems (NCSs) have become very prevalent owing to the advantage of decreasing the hard-wiring, the installation cost, and the implementation difficulties. Their applications could cover a wide range of industries such as space and terrestrial exploration, access in hazardous environments, factory automation, remote diagnostics and troubleshooting, experimental facilities, domestic robots, aircraft, automobiles and manufacturing plant monitoring [1, 2]. In the networked world nowadays, signals are typically transmitted through networks (e.g., Internet) which may undergo unavoidable communication delays, packet dropouts and disorder, quantization, saturations, and so on. These network-induced phenomena include, but are not limited to, missing measurements, fading measurements, signal quantization, time-delays, randomly occurring nonlinearities, probabilistic sensor delays, and sensor saturations. It is well known that these network-induced phenomena would lead to abrupt structural and parametric changes in practical engineering applications. Consequently, it is of important significance to tackle the filtering and sliding mode design problems for systems with network-induced phenomena.

The nonlinearity and stochasticity are ubiquitous features existing in almost all practical systems that contribute significantly to the complexity of system modeling. Since the occurrence of the nonlinearities and stochasticity which inevitably degrades the system performance and even leads to instability, the analysis and synthesis problems for nonlinear stochastic systems have long been the main stream of research topics and much efforts have been made to deal with the nonlinear stochastic systems. Accordingly, many control and filtering approaches have been successfully applied in many branches of practical domains such as computer vision, communications, navigation and tracking systems, and econometrics and finance. Over the past decade, with the rapid developments of the NCSs, the design of controller and filter for nonlinear stochastic systems with network-induced

phenomena has recently become a hot research focus that has attracted an increasing interest.

In this paper, we aim to provide a timely review on the recent advances of the recursive filtering and sliding mode design for nonlinear stochastic systems with network-induced phenomena. The network-induced phenomena under consideration include missing measurements, fading measurements, signal quantization, probabilistic sensor delays, sensor saturations, randomly occurring nonlinearities, and randomly occurring uncertainties. The recent developments of the network-induced phenomena are first summarized. Secondly, various filtering and sliding mode designs for nonlinear stochastic systems are reviewed in great detail and some interesting yet challenging issues are raised. Subsequently, latest results on recursive filtering and sliding mode design for discrete-time nonlinear stochastic systems with network-induced phenomena are reviewed. Finally, conclusions are drawn and some possible related research directions are pointed out.

The remainder of this paper is arranged as follows. In Section 2, the network-induced phenomena are discussed. In Section 3, the developments of filtering and sliding mode design problems for nonlinear stochastic systems are summarized. Some latest results on the recursive filtering and sliding mode design problems for nonlinear stochastic systems with network-induced phenomena are reviewed in Section 4. In Section 5, both the conclusions and some future research works are given.

2. Network-Induced Phenomena

Recently, much work has been done on the network-induced problems focusing on the missing measurements, fading measurements, signal quantization, sensor saturations, probabilistic sensor delays, randomly occurring nonlinearities, time delays, and so forth.

2.1. Missing Measurements. Most traditional controller/filter design approaches rely on the assumption that the measurement signals are perfectly transmitted. Such an assumption, however, is conservative in many engineering practices presented with unreliable communication channels. For example, due to temporal sensor failures or network congestions, the system measurements may contain noise only at certain time points and the true signals are simply missing. As such, the control and filtering problems with missing measurements have received considerable research attention and many important results have been reported in recent years; see, for example, [3–13]. To be more specific, the optimal estimation problems have been investigated in [5, 8] for linear systems with multiple packet dropouts. In [12], the stochastic stability has been analyzed for extended Kalman filtering (EKF) with intermittent observations. A common way for modeling the data missing is to introduce a random variable satisfying the Bernoulli binary distribution taking values on either 1 or 0, where 1 is for the perfect signal delivery and 0 represents the measurement missing. Most of the aforementioned results have been based on the hypothesis that all sensors have identical failure characteristics [5]. However, in practical applications, owing to the sensors aging, sensor temporal failure, or some of the data coming from a highly noisy environment, the measurement missing might be partial and individual sensor could have different missing probability in the data transmission process [11].

2.2. Fading Measurements. Fading measurements are now well known to be one of the most frequently occurring phenomena in networked systems [14, 15]. They refer to the cases when the perfect communication is not always available and the system measurement fades/degrades in a probabilistic way. To be specific, the linear state estimation problem has been investigated in [14], where single or multiple sensors amplify and forward their measurements of a common linear dynamical system to a remote fusion center via noisy fading wireless channels. It has been shown that the expected estimation error covariance (with respect to the fading process) at the fusion center remains bounded and converges to a steady state value. The estimation outage minimization problem has been studied in [15] for state estimation of linear systems over wireless fading channels. Obviously, the missing measurements mentioned above are extreme cases of the fading ones. Accordingly, the filtering problems with missing measurements have drawn considerable research interest [5, 12, 16–18]. Very recently, a more general description of the multiple missing measurements has been put forward in [11] and has already stirred some research interests where each sensor is allowed to have individual missing probability in data transmission. As mentioned above, a usual way for handling the missing measurements is to introduce the Bernoulli distributed white sequence specified by a conditional probability distribution, where the measurement signal is assumed to be either completely missing or completely available. However, such an assumption is quite restrictive in practice in case of fading measurements for an array of sensors.

2.3. Signal Quantization. At the forefront of networked system, the quantization issue has recently become a research focus that has attracted an increasing interest because, in a networked environment, signals are often quantized before being transmitted to other nodes due to the finite word length of the packets. Up to now, a series of results have been available in the literature on the quantization effects; see, for example, [19–25] and the references therein. In [21], the problem of quadratic stabilization has been studied for single-input-single-output linear time-invariant systems with logarithmic quantizers. Subsequently, by using the sector-bound approach, the quantized feedback control problems have been tackled in [23, 26] for linear discrete-time systems. Parallel to the quantized feedback control issue, the quantized estimation problem also has a wide range of applications, see for example, [27, 28] for more detailed discussions. Specifically, in the case when the measured signals are transmitted over a digital communication channel, the state estimator has been designed in [28] for linear system with quantized measurements. It is worth noticing that most published results

on the quantization effects have been dealt with for time-invariant systems over an infinite horizon. However, in reality, the majority of practical systems exhibiting the time-varying nature and the system dynamics are better quantified over a finite horizon, and this is particularly true for systems undergoing digital discretization. So far, the finite-horizon recursive filtering problem has not been properly investigated for nonlinear time-varying systems subject to quantization effects.

2.4. Randomly Occurring Nonlinearities and Randomly Occurring Uncertainties. Nonlinearities and uncertainties serve as two important kinds of complexities for system modeling. As is well known, many engineering systems in practice are influenced by additive nonlinear disturbances and/or uncertainties that are caused by environmental circumstances. Such unpredictable disturbances may be subject to random abrupt variations, for instance, random failures and repairs of components, changing subsystem interconnections, sudden environmental disturbances, and modification of the operating point of a linearized model of a nonlinear system. In other words, the nonlinear disturbances and the parameter uncertainties may occur in a probabilistic way with certain types and intensity. A typical example is the networked control systems where signals are transmitted through networks and the nonlinear disturbances and the uncertainties may occur according to the network conditions that are randomly changeable. In this case, both the randomly occurring nonlinearities (RONs) and the randomly occurring uncertainties (ROUs) should be taken into account when designing the practical control systems. Recently, in [29, 30], the concept of RONs has been introduced to model the randomly occurring nonlinear functions for complex networks, but ROUs has not yet received adequate research attention.

2.5. Probabilistic Sensor Delays. Most traditional filtering algorithms have been based on the measurement outputs that are supposed to contain information about the current state of the system. However, in engineering practice, the system measurements may be subject to unavoidable sensor delays, which is particularly true in a networked environment. In the past decade, a great number of results have been reported for filtering problems with deterministic/fixed sensor delays; see for example, [31–33]. On the other hand, because of limited bandwidth of the communication channel, it is often the case that the sensor delay occurs in a random way when, for example, the information is transmitted through networks in real-time distributed decision-making and multiplexed data communication environment [34]. Accordingly, the filtering problems with *random* sensor delays have recently received much research attention (see, e.g., [35–39]), where all sensors share the same type of delay characteristics [40, 41]. Nevertheless, in reality, the system measurements are usually collected through multiple sensors with different physical constraints. In this case, it is fairly conservative to assume that all sensors undergo random delays of the same probability distribution law. Rather, it would make more practical sense to consider individual features for randomly occurring sensor delays.

2.6. Sensor Saturations. It is well known that sensors may not always produce signals of unlimited amplitude mainly due to the physical constraints or technological restrictions. The sensor saturation, if not properly handled, will inevitably affect the implementation precision of the designed filtering/control algorithms and may even cause undesirable degradation of the filter/controller performance. Consequently, the actuator/sensor saturation problem has been gaining an increasing research interest that has led to many important results reported in the recent literature; see, for example, [42–48]. To be more specific, the output feedback H_∞ controllers have been synthesized in [43, 47, 48] and the robust H_∞ filters have been designed in [44, 45] for systems with sensor saturations. It is worth mentioning that most existing results concerning the sensor saturations have been concerned with time-invariant systems over the infinite-horizon. Unfortunately, in reality, almost all real-time systems should be time-varying especially those after digital discretization. Recently, motivated by the practical importance of the sensor saturation issues, the H_∞ control problem has been addressed in [48] and the set-membership filtering problem has been investigated in [46] for a class of time-varying systems with saturated sensors.

2.7. Random Parameter Matrices. Discrete-time systems with random parameter matrices arise in many application domains such as digital control of chemical processes, mobile robot localization, radar control, missile track estimation, navigation systems, and economic systems [49–51]. For this case, some system parameters might be randomly perturbed within certain intervals probably due to the abrupt phenomena such as random failures and repairs of the components, changes in the interconnections of subsystems, sudden environment changes, and modification of the operating point of a linearized model of nonlinear systems. Accordingly, some research efforts have been made on the filter design with random parameter matrices. For example, the recursive optimal estimation problem has been dealt with in [49] for linear discrete-time systems with random parameter matrices in the minimum variance sense. The distributed Kalman filtering fusion problem has been tackled in [50] for systems with random parameter matrices and the potential application has also been discussed. Nevertheless, probably due to its mathematical complexity, the recursive filtering problem for discrete time-varying nonlinear stochastic systems with random parameter matrices has not received adequate research attention yet.

2.8. Time Delays. It is well known that time-delays are frequently encountered in many industrial and engineering systems (e.g., chemical process, long transmission lines in pneumatic, and communication networks) due to the finite switching speed of amplifiers or finite speed of information processing [52, 53]. The existence of time delays may cause undesirable dynamic behaviors such as oscillation and instability [54, 55]. Over the past decades, much effort has been made to address the time-delay systems; see, for example, [56–64] and references cited therein. To mention a few, a sliding surface

has been constructed in [57] for the uncertain system with single/multiple state-delays and additive perturbations. In [58], by means of linear matrix inequality (LMI) technique, an integral sliding mode surface has been designed to address the sliding mode control (SMC) problem for the uncertain stochastic system with time-varying delays. In the case when the system states are not easily measured, the SMC problem has been investigated in [59] for systems with mismatched uncertainties via the output feedback approach. In [65], the SMC problem has been investigated for a class of nonlinear singular stochastic systems with Markovian switching. Actually, according to the occurrence way of time-delays, the time-delays can be generally classified into two types: discrete delays and distributed delays. Most of results mentioned above are applicable to continuous-time systems only, and the relevant results for discrete-time systems with mixed (i.e., both discrete and distributed) delays have been very few. The distributed time-delay in the discrete-time setting is an emerging concept that has been proposed in [30, 66] for complex networks.

3. Recursive Filtering and Sliding Mode Design for Nonlinear Stochastic Systems

In this section, we are in a position to review the approaches for handling the recursive filtering and sliding mode design problems for nonlinear stochastic systems.

3.1. Recursive Filter Design. The analysis and synthesis problems for nonlinear systems have been the mainstream of research topics and much effort has been made to deal with the nonlinear stochastic systems; see, for example, [11, 67–81]. It is worth pointing out that, in most literature, the nonlinearities are assumed to occur in a deterministic way. While this assumption is generally true especially for systems modeled according to physical laws, other kinds of nonlinearities, namely, stochastic nonlinearities, deserve particular research attention since they occur randomly probably due to intermittent network congestion, random failures and repairs of the components, changes in the interconnections of subsystems, sudden environment changes, and modification of the operating point of a linearized model of nonlinear systems. In fact, such stochastic nonlinearities include the state-multiplicative noises and random sequences as special cases. Recently, the filtering problem with stochastic nonlinearities described by statistical means has already stirred some research interests, and some latest results can be found in [11, 73, 82] and the references therein.

In the past few decades, the filtering or state estimation problems for stochastic systems have been extensively investigated and successfully applied in many branches of practical domains [83–86]. It is well known that the traditional Kalman filter (KF) serves as an optimal filter in the least mean square sense for *linear* systems with the assumption that the system model is exactly known. In the case when the system model is nonlinear and/or uncertain, there has been an increasing research effort to improve Kalman filters with hope to enhance their capabilities of handling nonlinearities and uncertainties. Along this direction, many alternative filtering schemes have been reported in the literature including the H_∞ filtering [87–89], mixed H_2/H_∞ filtering [90–92], and robust EKF design [93–97]. To mention a few, the optimal linear estimation problems have been intensively studied in [9] with multiple packet dropouts and in [40] for multiple sensors with different delay rates, the robust recursive KF algorithm has been developed in [98] for linear time-varying systems with stochastic parametric uncertainties, and the EKF problem has been dealt with in [94] for a class of uncertain systems with sum quadratic constraints. Note that almost all real-time systems are time-varying and therefore finite-horizon filtering problem is of practical significance [99]. However, there have been very few results in the literature regarding filtering problems over a finite horizon for time-varying nonlinear stochastic systems with network-induced phenomena.

In most of the available filtering algorithms, a conservative assumption is that the process and measurement noises are uncorrelated. In practical engineering, these two kinds of noises are often correlated. For example, for the target tracking problem, there may exists the cross correlation between the process noise and the measurement noise if both of them are dependent on the system state. Also, the process noise sequences of a discrete-time system sampled from a continuous-time system are inherently correlated across time, and there may be cross correlation between different sensor noises if the various sensors work in a common noisy environment. A typical example is the radar systems whose sampling frequency is high enough compared with the error bandwidth [100]. Recently, the filter design problems have been widely studied in [101–106] with autocorrelated noises and/or cross correlated noises. It should be mentioned that very little research effort has been made on the recursive filtering problem for time-varying nonlinear stochastic systems with correlated noises and network-induced phenomena.

For practical purposes, the filter design is inevitably subject to certain physical constraints. For example, in many applications, the system states should preserve the positivity, the system outputs experience saturations, and the filter gains may need to be of a specific structure for easy implementation. It should be pointed out that the filtering problems with constraints have been gaining a recurring research interest in the past decade; see, for example, [103, 107–111]. Very recently, in [110], a KF algorithm has been developed to cope with the constraints on the data injection gain. The gain-constrained filtering problem has been investigated for a broad class of real-time dynamical systems; see, for example, the tracking problem of a land based vehicle [103], the estimation problem of two state continuous stirred tank reactor [112], and the tracking problem of a vehicle along circular roads [113].

3.2. Probability Guaranteed H_∞ Filter Design. In traditional control theory, the performance objectives of a controlled system are usually required to be met accurately [114]. However, for many stochastic control problems, due to a variety of unpredictable disturbances, it is neither possible nor necessary to enforce the system performance with probability 1. Instead, it is quite common for practical control systems to

attain their individual performance objective with certain satisfactory probability. These kinds of engineering problems have given rise to great challenges for the realization of multiple control objectives with respect to individual probability constraints. In particular, as a newly emerged research topic, the probability-guaranteed H_∞ controller design problem has been raised in [115] and then thoroughly investigated in [116–119] in an elegant way. Specifically, the probability-guaranteed H_∞ analysis problem has been studied in [115, 119] for a class of linear continuous-time systems and in [116] for a class of linear discrete-time systems with structured disturbances. Recently, a new probability-guaranteed robust H_∞ filtering problem has been put forward in [118] for a class of linear continuous time-invariant systems. Despite the advances made on the research topic of probability-guaranteed design, there is still much room for further investigation on more comprehensive systems in order to cover more engineering practice. For example, in reality, most engineering systems are nonlinear and time-varying with saturated sensors, where the performances are usually evaluated over a finite-horizon for time-varying systems.

3.3. Sliding Mode Controller/Observer Design. Among various design methods for robust control, the sliding mode control (SMC) scheme appears to be a rather popular one that has been extensively studied and widely applied. This is because SMC possesses remarkable strong robustness against model uncertainties, parameter variations, and external disturbances [65, 120–122]. In the past two decades, SMC has become one of the most active branches of control theory that has found successful applications in a variety of practical engineering systems such as robot manipulators, aircrafts, underwater vehicles, spacecrafts, electrical motors, positioning systems, and automotive engines. For example, the adaptive sliding mode has been studied in [123, 124] for sensorless motor drives. The effective SMC schemes have been designed in [125] for high-speed positioning systems and in [126] for spacecraft-attitude-tracking maneuvers. Also, considerable research attention has been devoted to the theoretical research on SMC problems for different systems. For example, the concept of SMC has been widely employed in controller design problems for uncertain systems [61, 127, 128], stochastic systems [58, 59, 65, 129], and Markovian jump systems [65, 130].

Recently, many important results have been reported on the SMC problem for *discrete-time* systems; see [60, 61, 131–135]. In [136, 137], the SMC problems for a class of uncertain systems with mismatched uncertainty have been investigated. In the context of SMC for discrete-time systems, the quasisliding mode concept has been proposed in [133] and the discrete-time sliding mode reaching condition has been thoroughly studied based on a reaching law approach. Such a reaching condition has recently been shown in [60, 61, 138–140] to be a popular and convenient way of addressing the SMC problems for a class of discrete-time systems. Noting the advantages of the NCSs, it seems significantly important to investigate the SMC problem for discrete-time system with various network-induced phenomena.

On the other hand, it is well known that system states are not always available mainly due to the limit of physical conditions or expense for measuring in reality. Therefore, the state estimation problem has received a great deal of research attention. In recent years, the sliding mode observer (SMO) theory has been successfully applied to a wide range of areas such as induction motor drives, n-degree-of-freedom mechanical systems, and single-link flexible joint robot systems [141–143]. When designing the sliding mode observers (SMOs), a suitable nonlinear output injection is usually introduced to guarantee finite time convergence and induce a sliding motion. Most research on SMO design has been carried out along this line; see, for example, [141, 142, 144–149]. To be specific, by constructing an appropriate SMO, the fault reconstruction and estimation problems have been extensively studied in [143, 146–148, 150] for uncertain systems. It should be pointed out that almost all results mentioned above have been concerned with continuous-time systems, and the relevant results for *discrete-time* systems have been very few despite the fact that nowadays digitalized control systems are inherently discrete-time ones.

As mentioned above, the time-delays and nonlinearities are inevitably encountered in various industrial systems. The occurrence of time-delays and nonlinearities would cause great degradation of the system performance. Accordingly, the SMO problem for nonlinear and/or time-delay systems has gained considerable research interest and a variety of important results have been published in the literature; see [143, 148, 150–152]. To mention a few, in [151], an H_∞ SMO problem has been investigated for uncertain nonlinear Lipschitz-type systems with fault and disturbances and a sufficient condition has been given such that the H_∞ performance requirement is satisfied. By using Taylor series expansion and employing a nonlinear transformation, the discrete-time model has been derived in [150, 152] from its continuous-time counterpart and then the discrete-time sliding mode state estimation problems have been addressed for uncertain nonlinear systems. So far, very few results have been available for the SMO problem of discrete-time systems with time-delays.

4. Latest Progress

Very recently, the recursive filtering and sliding mode design problems have been widely investigated for nonlinear stochastic systems with network-induced phenomena and some interesting results have been reported. In this section, some of the newest works with respect to this topic are summarized.

(i) In [153, 154], the recursive filtering problems have been investigated for two classes of time-varying nonlinear stochastic systems. Firstly, the phenomenon of measurement missing occurs in a random way and the missing probability for each sensor is governed by an individual random variable satisfying a certain probability distribution over the interval $[0, 1]$. Such a probability distribution is allowed to be any commonly used distribution over the interval $[0, 1]$ with known conditional probability. Both deterministic and stochastic nonlinearities have been included in the system model, where the stochastic nonlinearities have been

described by statistical means that could reflect the multiplicative stochastic disturbances. A new filter has been first designed in [153] such that, in the presence of both the stochastic nonlinearities and multiple missing measurements, there exists an upper bound for the filtering error covariance which is minimized by properly designing the filter gain. Secondly, the recursive finite-horizon filtering problem has been investigated in [154] for a class of time-varying nonlinear systems subject to multiplicative noises, missing measurements, and quantization effects. The missing measurements have been modeled by a series of mutually independent random variables obeying Bernoulli distributions with possibly different occurrence probabilities. The quantization phenomenon has been described by using the logarithmic function and the multiplicative noises have been considered to account for the stochastic disturbances on the system states. By using similar techniques, the desired filter parameters have been obtained by solving two Riccati-like difference equations that are of a recursive form suitable for online applications.

(ii) In [155, 156], the recursive filtering problems have been studied for two classes of time-varying stochastic systems with stochastic nonlinearities. Firstly, the phenomenon of measurement fading occurs in a random way and the fading probability for each sensor is governed by an individual random variable obeying a certain probability distribution over the known interval $[\beta_k, \gamma_k]$. Such a probability distribution could be any commonly used discrete distribution over the interval $[\beta_k, \gamma_k]$ that covers the Bernoulli distribution as a special case. The process noise and the measurement noise are one-step autocorrelated, respectively. The process noise and the measurement noise are two-step cross correlated. An unbiased, recursive and locally optimal filter has been designed in [155] for a class of time-varying nonlinear stochastic systems with random parameter matrices, stochastic nonlinearity, and multiple fading measurements as well as correlated noises. Secondly, the proposed filtering method has been extended to deal with the gain-constrained recursive filter design problem in [156] for the systems subject to probabilistic sensor delays, stochastic nonlinearities, and finite-step correlated noises. Intensive stochastic analysis has been carried out to obtain the filter gain characterized by the solution to recursive matrix equations. It has been shown that the proposed scheme is of a form suitable for recursive computation in online applications.

(iii) The probability-guaranteed H_∞ finite-horizon filtering problem has been discussed in [157] for a class of time-varying nonlinear systems with uncertain parameters and sensor saturations. The system matrices are functions of mutually independent stochastic variables that obey uniform distributions over known finite ranges. By using the sector-bounded approach, a decomposition technique has been employed to facilitate the filter design in terms of difference linear matrix inequalities (DLMIs). Attention has been focused on the construction of a time-varying filter such that the prescribed H_∞ performance requirement can be guaranteed with prespecified probability constraint. By employing the DLMIs approach, sufficient conditions have been established to guarantee the desired performance of the designed finite-horizon filter. The time-varying filter gains have been obtained in terms of the feasible solutions to a set of DLMIs that can be recursively solved by using the semidefinite programming method. A computational algorithm has been specifically developed for the addressed probability-guaranteed H_∞ finite-horizon filtering problem.

(iv) The H_∞ SMO design problem has been studied in [158] for a class of nonlinear discrete time-delay systems. The nonlinear descriptions quantify the maximum possible derivations from a linear model and the system states are allowed to be immeasurable. Attention has been focused on the design of a discrete-time SMO such that the asymptotic stability as well as the H_∞ performance requirement of the error dynamics can be guaranteed in the presence of nonlinearities, time-delay, and external disturbances. Firstly, a discrete-time discontinuous switched term has been constructed to make sure that the reaching condition holds. Then, by constructing a new Lyapunov-Krasovskii functional based on the idea of "delay-fractioning" and introducing some appropriate free-weighting matrices, a sufficient condition has been established to guarantee the desired performance of the error dynamics in the specified sliding surface by solving a minimization problem. In particular, the so-called "weighting" scalar parameters have been constructively introduced to fit both the delay-fractioning idea and the sliding mode approach. It has been shown that the desired observer gains can be obtained in terms of the feasible solutions to a set of matrix inequalities that can be solved easily by using the semidefinite programming method.

(v) In [159, 160], the robust SMC problems have been investigated for discrete-time uncertain nonlinear stochastic systems with time-varying delays. Firstly, the randomly occurring nonlinearity (RON), which describes the phenomenon of a class of nonlinear disturbances occurring in a random way, has been modeled according to a Bernoulli distributed white sequence with a known conditional probability. By constructing a novel Lyapunov-Krasovskii functional, the idea of delay-fractioning has been applied to cope with the robust SMC problem with time-delays. Sufficient conditions have been derived in [159] to ensure the stability of the systems dynamics in the specified sliding surface. Such conditions have been characterized in terms of a set of LMIs with an equality constraint. A new discrete-time SMC law has been synthesized to guarantee the reaching condition of the discrete-time sliding surface. Moreover, the robust H_∞ SMC problem has been investigated in [160] for a general class of discrete-time uncertain systems with stochastic nonlinearities and time-varying delays. By constructing a similar sliding surface and designing the SMC law, sufficient conditions have been given to ensure that, for all parameter uncertainties, unmatched stochastic nonlinearities, time-varying delays, and unmatched external disturbance, the sliding mode dyna mics is asymptotically mean-square stable while achieving a prescribed disturbance attenuation level.

(vi) In [161, 162], the robust SMC problems have been studied for discrete-time uncertain nonlinear stochastic systems with mixed time-delays. Firstly, both the sector-like nonlinearities and the norm-bounded uncertainties enter into the system in random ways, and such ROUs and RONs

obey certain mutually uncorrelated Bernoulli distributed white noise sequences with known conditional probabilities. This description can reflect the fact that the ROUs and RONs can appear or disappear in a probabilistic way due to unpredictable changes of the environmental circumstances. The mixed time-delays consist of both the discrete and the distributed delays, and the stochastic disturbance is of the general Itô-type. An SMC law has been designed in [161] such that the mean-square asymptotic stability of the sliding mode dynamics can be guaranteed in the presence of ROUs and RONs as well as mixed time-delays. By employing the idea of delay-fractioning and constructing a new Lyapunov-Krasovskii functional, sufficient conditions have been established to achieve the desired performance in the specified sliding surface by solving certain semidefinite programming problem. Secondly, the robust SMC design problem has been investigated in [162] for a class of uncertain nonlinear systems with Markovian jumping parameters and mixed time-delays, and a set of parallel results has been derived.

5. Conclusions and Future Works

In this paper, we have summarized some recent advances on the recursive filtering and sliding mode design for nonlinear stochastic systems with network-induced phenomena. The developments of the network-induced phenomena have been surveyed. Subsequently, various recursive filtering and sliding mode design problems have been discussed for nonlinear stochastic systems. Furthermore, the recursive filtering and sliding mode design approaches of the nonlinear stochastic systems with network-induced phenomena have been given and the latest results have been reviewed. To conclude this survey paper, we highlight some related topics for the further research works as follows.

(i) The nonlinearities addressed have some constraints that may bring somewhat conservative results. The analysis and synthesis of more general nonlinear systems with network-induced phenomena would be one of the future research topics.

(ii) Another future research direction is to investigate the guaranteed-cost control problem for nonlinear time-varying systems with randomly occurring actuator failures over a finite time-horizon.

(iii) In case that the convergence analysis of the recursive filter approach becomes a concern, some additional assumptions can be made on the system parameters in order to ensure the global boundedness of the estimation errors, which constitutes one of the future research topics.

(iv) When the system states are immeasurable, the dynamic output feedback sliding mode design is desired for time-delay nonlinear stochastic systems with network-induced phenomena.

(v) An additional trend for future research is to generalize the current methods to the synchronization, control, and filtering problems for nonlinear stochastic complex networks with network-induced phenomena.

Acknowledgments

This work was supported in part by the National Natural Science Foundation of China under Grant nos. 61134009, 61329301, 61333012, 61374127 and 11301118, the Engineering and Physical Sciences Research Council (EPSRC) of the UK under Grant no. GR/S27658/01, the Royal Society of the UK, and the Alexander von Humboldt Foundation of Germany.

References

[1] H. Dong, Z. Wang, X. Chen, and H. Gao, "A review on analysis and synthesis of nonlinear stochastic systems with randomly occurring incomplete information," *Mathematical Problems in Engineering*, vol. 2012, Article ID 416358, 15 pages, 2012.

[2] B. Shen, Z. Wang, J. Liang, and Y. Liu, "Recent advances on filtering and control for nonlinear stochastic complex systems with incomplete information: a survey," *Mathematical Problems in Engineering*, vol. 2012, Article ID 530759, 16 pages, 2012.

[3] H. Dong, Z. Wang, and H. Gao, "Observer-based H_∞ control for systems with repeated scalar nonlinearities and multiple packet losses," *International Journal of Robust and Nonlinear Control*, vol. 20, no. 12, pp. 1363–1378, 2010.

[4] H. Dong, Z. Wang, D. W. C. Ho, and H. Gao, "Variance-constrained H_∞ filtering for a class of nonlinear time-varying systems with multiple missing measurements: the finite-horizon case," *IEEE Transactions on Signal Processing*, vol. 58, no. 5, pp. 2534–2543, 2010.

[5] F. O. Hounkpevi and E. E. Yaz, "Robust minimum variance linear state estimators for multiple sensors with different failure rates," *Automatica*, vol. 43, no. 7, pp. 1274–1280, 2007.

[6] M. Sahebsara, T. Chen, and S. L. Shah, "Optimal H_∞ filtering in networked control systems with multiple packet dropouts," *Systems & Control Letters*, vol. 57, no. 9, pp. 696–702, 2008.

[7] M. Moayedi, Y. K. Foo, and Y. C. Soh, "Adaptive Kalman filtering in networked systems with random sensor delays, multiple packet dropouts and missing measurements," *IEEE Transactions on Signal Processing*, vol. 58, no. 3, pp. 1577–1588, 2010.

[8] S. Sun, L. Xie, W. Xiao, and Y. C. Soh, "Optimal linear estimation for systems with multiple packet dropouts," *Automatica*, vol. 44, no. 5, pp. 1333–1342, 2008.

[9] S. Sun, L. Xie, W. Xiao, and N. Xiao, "Optimal filtering for systems with multiple packet dropouts," *IEEE Transactions on Circuits and Systems II*, vol. 55, no. 7, pp. 695–699, 2008.

[10] Z. Wang, D. W. C. Ho, and X. Liu, "Variance-constrained filtering for uncertain stochastic systems with missing measurements," *Institute of Electrical and Electronics Engineers*, vol. 48, no. 7, pp. 1254–1258, 2003.

[11] G. Wei, Z. Wang, and H. Shu, "Robust filtering with stochastic nonlinearities and multiple missing measurements," *Automatica*, vol. 45, no. 3, pp. 836–841, 2009.

[12] S. Kluge, K. Reif, and M. Brokate, "Stochastic stability of the extended Kalman filter with intermittent observations," *IEEE Transactions on Automatic Control*, vol. 55, no. 2, pp. 514–518, 2010.

[13] X. He, Z. Wang, X. Wang, and D. Zhou, "Networked strong tracking filtering with multiple packet dropouts: algorithms and applications," *IEEE Transactions on Industrial Electronics*, vol. 61, no. 3, pp. 1454–1463, 2014.

[14] S. Dey, A. S. Leong, and J. S. Evans, "Kalman filtering with faded measurements," *Automatica*, vol. 45, no. 10, pp. 2223–2233, 2009.

[15] A. S. Leong, S. Dey, G. N. Nair, and P. Sharma, "Power allocation for outage minimization in state estimation over fading channels," *IEEE Transactions on Signal Processing*, vol. 59, no. 7, pp. 3382–3397, 2011.

[16] B. Sinopoli, L. Schenato, M. Franceschetti, K. Poolla, M. I. Jordan, and S. S. Sastry, "Kalman filtering with intermittent observations," *IEEE Transactions on Automatic Control*, vol. 49, no. 9, pp. 1453–1464, 2004.

[17] Z. Wang, F. Yang, D. W. C. Ho, and X. Liu, "Robust H_∞ filtering for stochastic time-delay systems with missing measurements," *IEEE Transactions on Signal Processing*, vol. 54, no. 7, pp. 2579–2587, 2006.

[18] M. Sahebsara, T. Chen, and S. L. Shah, "Optimal H_2 filtering in networked control systems with multiple packet dropout," *IEEE Transactions on Automatic Control*, vol. 52, no. 8, pp. 1508–1513, 2007.

[19] Z. Wang, H. Dong, B. Shen, and H. Gao, "Finite-horizon H_∞ filtering with missing measurements and quantization effects," *IEEE Transactions on Automatic Control*, vol. 58, no. 7, pp. 1707–1718, 2013.

[20] R. W. Brockett and D. Liberzon, "Quantized feedback stabilization of linear systems," *IEEE Transactions on Automatic Control*, vol. 45, no. 7, pp. 1279–1289, 2000.

[21] N. Elia and S. K. Mitter, "Stabilization of linear systems with limited information," *IEEE Transactions on Automatic Control*, vol. 46, no. 9, pp. 1384–1400, 2001.

[22] M. L. Corradini and G. Orlando, "Robust quantized feedback stabilization of linear systems," *Automatica*, vol. 44, no. 9, pp. 2458–2462, 2008.

[23] M. Fu and L. Xie, "The sector bound approach to quantized feedback control," *IEEE Transactions on Automatic Control*, vol. 50, no. 11, pp. 1698–1711, 2005.

[24] W. P. M. H. Heemels, A. R. Teel, N. van de Wouw, and D. Nešić, "Networked control systems with communication constraints: tradeoffs between transmission intervals, delays and performance," *IEEE Transactions on Automatic Control*, vol. 55, no. 8, pp. 1781–1796, 2010.

[25] Z. Wang, B. Shen, H. Shu, and G. Wei, "Quantized H_∞ control for nonlinear stochastic time-delay systems with missing measurements," *IEEE Transactions on Automatic Control*, vol. 57, no. 6, pp. 1431–1444, 2012.

[26] D. F. Coutinho, M. Fu, and C. E. de Souza, "Input and output quantized feedback linear systems," *IEEE Transactions on Automatic Control*, vol. 55, no. 3, pp. 761–766, 2010.

[27] R. Carli, F. Fagnani, P. Frasca, and S. Zampieri, "A probabilistic analysis of the average consensus algorithm with quantized communication," in *Proceedings of the 17th World Congress, International Federation of Automatic Control (IFAC'08)*, Seoul, Korea, July 2008.

[28] M. Fu and C. E. de Souza, "State estimation for linear discrete-time systems using quantized measurements," *Automatica*, vol. 45, no. 12, pp. 2937–2945, 2009.

[29] Y. Wang, Z. Wang, and J. Liang, "Global synchronization for delayed complex networks with randomly occurring nonlinearities and multiple stochastic disturbances," *Journal of Physics A*, vol. 42, no. 13, article 135101, 2009.

[30] Z. Wang, Y. Wang, and Y. Liu, "Global synchronization for discrete-time stochastic complex networks with randomly occurred nonlinearities and mixed time delays," *IEEE Transactions on Neural Networks*, vol. 21, no. 1, pp. 11–25, 2010.

[31] H. Zhang, G. Feng, G. Duan, and X. Lu, "H_∞ filtering for multiple-time-delay measurements," *IEEE Transactions on Signal Processing*, vol. 54, no. 5, pp. 1681–1688, 2006.

[32] M. Basin, M. A. Alcorta-Garcia, and A. Alanis-Duran, "Optimal filtering for linear systems with state and multiple observation delays," *International Journal of Systems Science*, vol. 39, no. 5, pp. 547–555, 2008.

[33] M. Basin, P. Shi, and D. Calderon-Alvarez, "Joint state filtering and parameter estimation for linear stochastic time-delay systems," *Signal Processing*, vol. 91, no. 4, pp. 782–792, 2011.

[34] F. Yang, Z. Wang, G. Feng, and X. Liu, "Robust filtering with randomly varying sensor delay: the finite-horizon case," *IEEE Transactions on Circuits and Systems I*, vol. 56, no. 3, pp. 664–672, 2009.

[35] Y. I. Yaz and E. E. Yaz, "A new formulation of some discrete-time stochastic-parameter state estimation problems," *Applied Mathematics Letters*, vol. 10, no. 6, pp. 13–19, 1997.

[36] R. Caballero-Águila, A. Hermoso-Carazo, J. D. Jiménez-López, J. Linares-Pérez, and S. Nakamori, "Recursive estimation of discrete-time signals from nonlinear randomly delayed observations," *Computers & Mathematics with Applications*, vol. 58, no. 6, pp. 1160–1168, 2009.

[37] J. Linares-Pérez, A. Hermoso-Carazo, R. Caballero-Águila, and J. D. Jiménez-López, "Least-squares linear filtering using observations coming from multiple sensors with one- or two-step random delay," *Signal Processing*, vol. 89, no. 10, pp. 2045–2052, 2009.

[38] M. Chen, "Synchronization in complex dynamical networks with random sensor delay," *IEEE Transactions on Circuits and Systems II*, vol. 57, no. 1, pp. 46–50, 2010.

[39] J. Ma and S. Sun, "Optimal linear estimators for systems with random sensor delays, multiple packet dropouts and uncertain observations," *IEEE Transactions on Signal Processing*, vol. 59, no. 11, pp. 5181–5192, 2011.

[40] F. O. Hounkpevi and E. E. Yaz, "Minimum variance generalized state estimators for multiple sensors with different delay rates," *Signal Processing*, vol. 87, no. 4, pp. 602–613, 2007.

[41] R. Caballero-Águila, A. Hermoso-Carazo, J. D. Jiménez-López, J. Linares-Pérez, and S. Nakamori, "Signal estimation with multiple delayed sensors using covariance information," *Digital Signal Processing*, vol. 20, no. 2, pp. 528–540, 2010.

[42] D. Chen, S. Li, and Y. Shi, "The practical stabilization for a class of networked systems with actuator saturation and input additive disturbances," *Mathematical Problems in Engineering*, vol. 2012, Article ID 326876, 19 pages, 2012.

[43] Y.-Y. Cao, Z. Lin, and B. M. Chen, "An output feedback H_∞ controller design for linear systems subject to sensor nonlinearities," *IEEE Transactions on Circuits and Systems I*, vol. 50, no. 7, pp. 914–921, 2003.

[44] Y. Niu, D. W. C. Ho, and C. W. Li, "Filtering for discrete fuzzy stochastic systems with sensor nonlinearities," *IEEE Transactions on Fuzzy Systems*, vol. 18, no. 5, pp. 971–978, 2010.

[45] Y. Niu, D. W. C. Ho, and C. W. Li, "H_∞ filtering for uncertain stochastic systems subject to sensor nonlinearities," *International Journal of Systems Science*, vol. 42, no. 5, pp. 737–749, 2011.

[46] F. Yang and Y. Li, "Set-membership filtering for systems with sensor saturation," *Automatica*, vol. 45, no. 8, pp. 1896–1902, 2009.

[47] Z. Zuo, J. Wang, and L. Huang, "Output feedback H_∞ controller design for linear discrete-time systems with sensor nonlinearities," *IEE Proceedings on Control Theory & Applications*, vol. 152, no. 1, pp. 19–26, 2005.

[48] Z. Wang, D. W. C. Ho, H. Dong, and H. Gao, "Robust H_∞ finite-horizon control for a class of stochastic nonlinear time-varying systems subject to sensor and actuator saturations," *IEEE Transactions on Automatic Control*, vol. 55, no. 7, pp. 1716–1722, 2010.

[49] W. L. De Koning, "Optimal estimation of linear discrete-time systems with stochastic parameters," *Automatica*, vol. 20, no. 1, pp. 113–115, 1984.

[50] Y. Luo, Y. Zhu, D. Luo, J. Zhou, E. Song, and D. Wang, "Globally optimal multisensor distributed random parameter matrices Kalman filtering fusion with applications," *Sensors*, vol. 8, no. 12, pp. 8086–8103, 2008.

[51] E. Yaz and R. E. Skelton, "Parametrization of all linear compensators for discrete-time stochastic parameter systems," *Automatica*, vol. 30, no. 6, pp. 945–955, 1994.

[52] S. Elmadssia, K. Saadaoui, and M. Benrejeb, "New delay-dependent stability conditions for linear systems with delay," *Systems Science and Control Engineering*, vol. 1, no. 1, pp. 2–11, 2013.

[53] Y. Chen and K. A. Hoo, "Stability analysis for closed-loop management of a reservoir based on identification of reduced-order-nonlinear model," *Systems Science and Control Engineering*, vol. 1, no. 1, pp. 12–19, 2013.

[54] H. Gao, Z. Fei, J. Lam, and B. Du, "Further results on exponential estimates of Markovian jump systems with mode-dependent time-varying delays," *IEEE Transactions on Automatic Control*, vol. 56, no. 1, pp. 223–229, 2011.

[55] H. Gao, Y. Zhao, and W. Sun, "Input-delayed control of uncertain seat suspension systems with human-body model," *IEEE Transactions on Control Systems Technology*, vol. 18, no. 3, pp. 591–601, 2010.

[56] E. Fridman, U. Shaked, and L. Xie, "Robust H_∞ filtering of linear systems with time delays," *International Journal of Robust and Nonlinear Control*, vol. 13, no. 10, pp. 983–1010, 2003.

[57] F. Gouaisbaut, M. Dambrine, and J. P. Richard, "Robust control of delay systems: a sliding mode control design via LMI," *Systems & Control Letters*, vol. 46, no. 4, pp. 219–230, 2002.

[58] Y. Niu, D. W. C. Ho, and J. Lam, "Robust integral sliding mode control for uncertain stochastic systems with time-varying delay," *Automatica*, vol. 41, no. 5, pp. 873–880, 2005.

[59] Y. Niu and D. W. C. Ho, "Robust observer design for Itô stochastic time-delay systems via sliding mode control," *Systems & Control Letters*, vol. 55, no. 10, pp. 781–793, 2006.

[60] Y. Xia, G. P. Liu, P. Shi, J. Chen, D. Rees, and J. Liang, "Sliding mode control of uncertain linear discrete time systems with input delay," *IET Control Theory & Applications*, vol. 1, no. 4, pp. 1169–1175, 2007.

[61] M. Yan and Y. Shi, "Robust discrete-time sliding mode control for uncertain systems with time-varying state delay," *IET Control Theory & Applications*, vol. 2, no. 8, pp. 662–674, 2008.

[62] Z. Wang and D. W. C. Ho, "Filtering on nonlinear time-delay stochastic systems," *Automatica*, vol. 39, no. 1, pp. 101–109, 2003.

[63] Z. Wang, D. W. C. Ho, Y. Liu, and X. Liu, "Robust H_∞ control for a class of nonlinear discrete time-delay stochastic systems with missing measurements," *Automatica*, vol. 45, no. 3, pp. 684–691, 2009.

[64] Z. Wang, J. Lam, and X. Liu, "Filtering for a class of nonlinear discrete-time stochastic systems with state delays," *Journal of Computational and Applied Mathematics*, vol. 201, no. 1, pp. 153–163, 2007.

[65] L. Wu and D. W. C. Ho, "Sliding mode control of singular stochastic hybrid systems," *Automatica*, vol. 46, no. 4, pp. 779–783, 2010.

[66] Y. Liu, Z. Wang, J. Liang, and X. Liu, "Synchronization and state estimation for discrete-time complex networks with distributed delays," *IEEE Transactions on Systems, Man, and Cybernetics B*, vol. 38, no. 5, pp. 1314–1325, 2008.

[67] A. Mehrsai, H. R. Karimi, and K. D. Thoben, "Integration of supply networks for customization with modularity in cloudand make-to-upgrade strategy," *Systems Science and Control Engineering*, vol. 1, no. 1, pp. 28–42, 2013.

[68] M. Darouach and M. Chadli, "Admissibility and control of switched discrete-time singular systems," *Systems Science and Control Engineering*, vol. 1, no. 1, pp. 43–51, 2013.

[69] M. Basin, P. Shi, and D. Calderon-Alvarez, "Central suboptimal H_∞ filter design for nonlinear polynomial systems," *International Journal of Adaptive Control and Signal Processing*, vol. 23, no. 10, pp. 926–939, 2009.

[70] B. Shen, Z. Wang, H. Shu, and G. Wei, "On nonlinear H_∞ filtering for discrete-time stochastic systems with missing measurements," *IEEE Transactions on Automatic Control*, vol. 53, no. 9, pp. 2170–2180, 2008.

[71] B. Shen, Z. Wang, H. Shu, and G. Wei, "Robust H_∞ finite-horizon filtering with randomly occurred nonlinearities and quantization effects," *Automatica*, vol. 46, no. 11, pp. 1743–1751, 2010.

[72] K. Reif, S. Günther, E. Yaz, and R. Unbehauen, "Stochastic stability of the discrete-time extended Kalman filter," *IEEE Transactions on Automatic Control*, vol. 44, no. 4, pp. 714–728, 1999.

[73] E. E. Yaz and Y. I. Yaz, "State estimation of uncertain nonlinear stochastic systems with general criteria," *Applied Mathematics Letters*, vol. 14, no. 5, pp. 605–610, 2001.

[74] X. He, Z. Wang, Y. Liu, and D. Zhou, "Least-squares fault detection and diagnosis for networked sensing systems using adirect state estimation approach," *IEEE Transactions on Industrial Informatics*, vol. 9, no. 3, pp. 1670–1679, 2013.

[75] X. Li and H. Gao, "Robust finite frequency H_∞ filtering for uncertain 2-D systems: the FM model case," *Automatica*, vol. 49, no. 8, pp. 2446–2452, 2013.

[76] X. Li, H. Gao, and C. Wang, "Generalized Kalman-yakubovich-popov lemma for 2-D FM LSS model," *IEEE Transactions on Automatic Control*, vol. 57, no. 12, pp. 3090–3103, 2012.

[77] H. Gao and X. Li, "H_∞ filtering for discrete-time state-delayed systems with finite frequency specifications," *IEEE Transactions on Automatic Control*, vol. 56, no. 12, pp. 2935–2941, 2011.

[78] X. Li and H. Gao, "Robust finite frequency H_∞ filtering for uncertain 2-D roesser systems," *Automatica*, vol. 48, no. 6, pp. 1163–1170, 2012.

[79] S. Ding, S. Yin, P. Zhang, and B. Shen, "An integrated design framework of fault-tolerant wireless networked control systems for industrial automatic control applications," *IEEE Transactions on Industrial Informatics*, vol. 9, no. 1, pp. 462–471, 2013.

[80] S. Yin, S. Ding, A. Haghani, H. Hao, and P. Zhang, "A comparison study of basic data-driven fault diagnosis and process-monitoring methods on the benchmark Tennessee eastman process," *Journal of Process Control*, vol. 22, no. 9, pp. 1567–1581, 2012.

[81] S. Yin, X. Yang, and H. R. Karimi, "Data-driven adaptive observer for fault diagnosis," *Mathematical Problems in Engineering*, vol. 2012, Article ID 832836, 21 pages, 2012.

[82] E. Yaz, "On the optimal state estimation of a class of discrete-time nonlinear systems," *IEEE Transactions on Circuits and Systems*, vol. 34, no. 9, pp. 1127–1129, 1987.

[83] H. Gao, W. Zhan, H. R. Karimi, X. Yang, and S. Yin, "Allocation of actuators and sensors for coupled-adjacent-buildingvibration attenuation," *IEEE Transactions on Industrial Electronics*, vol. 60, no. 12, pp. 5792–5801, 2013.

[84] H. Gao, W. Sun, and P. Shi, "Robust sampled-data H_∞ control for vehicle active suspension systems," *IEEE Transactions on Control Systems Technology*, vol. 18, no. 1, pp. 238–245, 2010.

[85] H. Gao, X. Meng, T. Chen, and J. Lam, "Stabilization of networked control systems via dynamic output-feedback controllers," *SIAM Journal on Control and Optimization*, vol. 48, no. 5, pp. 3643–3658, 2009/10.

[86] S. R. Desai and R. Prasad, "A new approach to order reduction using stability equation and big bang big crunch optimization," *Systems Science and Control Engineering*, vol. 1, no. 1, pp. 20–27, 2013.

[87] H. Dong, Z. Wang, and H. Gao, "Robust H_∞ filtering for a class of nonlinear networked systems with multiple stochastic communication delays and packet dropouts," *IEEE Transactions on Signal Processing*, vol. 58, no. 4, pp. 1957–1966, 2010.

[88] H. Gao and C. Wang, "A delay-dependent approach to robust H_∞ filtering for uncertain discrete-time state-delayed systems," *IEEE Transactions on Signal Processing*, vol. 52, no. 6, pp. 1631–1640, 2004.

[89] B. Shen, Z. Wang, Y. S. Hung, and G. Chesi, "Distributed H_∞ filtering for polynomial nonlinear stochastic systems in sensor networks," *IEEE Transactions on Industrial Electronics*, vol. 58, no. 5, pp. 1971–1979, 2011.

[90] H. Gao, J. Lam, L. Xie, and C. Wang, "New approach to mixed H_2/H_∞ filtering for polytopic discrete-time systems," *IEEE Transactions on Signal Processing*, vol. 53, no. 8, pp. 3183–3192, 2005.

[91] H. Rotstein, M. Sznaier, and M. Idan, "H_2/H_∞ filtering: theory and an aerospace application," in *Proceedings of the 1994 American Control Conference*, pp. 1791–1795, July 1994.

[92] L. Xie, L. Lu, D. Zhang, and H. Zhang, "Improved robust H_2 and H_∞ filtering for uncertain discrete-time systems," *Automatica*, vol. 40, no. 5, pp. 873–880, 2004.

[93] M. R. James and I. R. Petersen, "Nonlinear state estimation for uncertain systems with an integral constraint," *IEEE Transactions on Signal Processing*, vol. 46, no. 11, pp. 2926–2937, 1998.

[94] A. G. Kallapur, I. R. Petersen, and S. G. Anavatti, "A discrete-time robust extended Kalman filter for uncertain systems with sum quadratic constraints," *IEEE Transactions on Automatic Control*, vol. 54, no. 4, pp. 850–854, 2009.

[95] X. Kai, C. Wei, and L. Liu, "Robust extended Kalman filtering for nonlinear systems with stochastic uncertainties," *IEEE Transactions on Systems, Man, and Cybernetics A*, vol. 40, no. 2, pp. 399–405, 2010.

[96] X. Kai, L. Liangdong, and L. Yiwu, "Robust extended Kalman filtering for nonlinear systems with multiplicative noises," *Optimal Control Applications & Methods*, vol. 32, no. 1, pp. 47–63, 2011.

[97] Z. Wang, X. Liu, Y. Liu, J. Liang, and V. Vinciotti, "An extended Kalman filtering approach to modelling nonlinear dynamic gene regulatory networks via short gene expression time series," *IEEE/ACM Transactions on Computational Biology and Bioinformatics*, vol. 6, no. 3, pp. 410–419, 2009.

[98] F. Wang and V. Balakrishnan, "Robust Kalman filters for linear time-varying systems with stochastic parametric uncertainties," *IEEE Transactions on Signal Processing*, vol. 50, no. 4, pp. 803–813, 2002.

[99] B. Shen, Z. Wang, and X. Liu, "Bounded H_∞ synchronization and state estimation for discrete time-varying stochastic complex networks over a finite horizon," *IEEE Transactions on Neural Networks*, vol. 22, no. 1, pp. 145–157, 2011.

[100] A. Ray, "Performance evaluation of medium access control protocols for distributed digital avionics," *ASME Journal of Dynamic Systems, Measurement and Control*, vol. 109, no. 4, pp. 370–377, 1987.

[101] J.-A. Guu and C.-H. Wei, "Tracking technique for manoeuvring target with correlated measurement noises and unknown parameters," *IEE Proceedings F-Radar and Signal Processing*, vol. 138, no. 3, pp. 278–288, 1991.

[102] E. Song, Y. Zhu, and Z. You, "The Kalman type recursive state estimator with a finite-step correlated process noises," in *Proceedings of the IEEE International Conference on Automation and Logistics (ICAL '08)*, pp. 196–200, Qingdao, China, September 2008.

[103] D. Simon, *Optimal State Estimation: Kalman, H_∞, and Nonlinear Approaches*, John Wiley & Sons, New York, NY, USA, 2006.

[104] A. Fu, Y. Zhu, and E. Song, "The optimal Kalman type state estimator with multi-step correlated process and measurement noises," in *Proceedings of the International Conference on Embedded Software and Systems (ICESS '08)*, pp. 215–220, Sichuan, China, July 2008.

[105] E. Song, Y. Zhu, J. Zhou, and Z. You, "Optimal Kalman filtering fusion with cross-correlated sensor noises," *Automatica*, vol. 43, no. 8, pp. 1450–1456, 2007.

[106] J. Feng, Z. Wang, and M. Zeng, "Optimal robust non-fragile Kalman-type recursive filtering with finite-step autocorrelated noises and multiple packet dropouts," *Aerospace Science and Technology*, vol. 15, no. 6, pp. 486–494, 2011.

[107] M. Darouach, M. Zasadzinski, and M. Boutayeb, "Extension of minimum variance estimation for systems with unknown inputs," *Automatica*, vol. 39, no. 5, pp. 867–876, 2003.

[108] J. Chandrasekar, D. S. Bernstein, O. Barrero, and B. L. R. De Moor, "Kalman filtering with constrained output injection," *International Journal of Control*, vol. 80, no. 12, pp. 1863–1879, 2007.

[109] S. J. Julier and J. J. LaViola, Jr., "On Kalman filtering with nonlinear equality constraints," *IEEE Transactions on Signal Processing*, vol. 55, no. 6, pp. 2774–2784, 2007.

[110] B. O. S. Teixeira, J. Chandrasekar, H. J. Palanthandalam-Madapusi, L. A. B. Tôrres, L. A. Aguirre, and D. S. Bernstein, "Gain-constrained Kalman filtering for linear and nonlinear systems," *IEEE Transactions on Signal Processing*, vol. 56, no. 9, pp. 4113–4123, 2008.

[111] J. M. Del Rincón, D. Makris, C. O. Uruñuela, and J.-C. Nebel, "Tracking human position and lower body parts using Kalman and particle filters constrained by human biomechanics," *IEEE Transactions on Systems, Man, and Cybernetics B*, vol. 41, no. 1, pp. 26–37, 2011.

[112] S. Kolås, B. A. Foss, and T. S. Schei, "Constrained nonlinear state estimation based on the UKF approach," *Computers and Chemical Engineering*, vol. 33, no. 8, pp. 1386–1401, 2009.

[113] C. Yang and E. Blasch, "Kalman filtering with nonlinear state constraints," in *Proceedings of the 9th International Conference on Information Fusion*, Seattle, Wash, USA, July 2006.

[114] S. Yin, H. Luo, and S. Ding, "Real-time implementation of fault-tolerant control systems with performance optimization," *IEEE Transactions on Industrial Electronics*, vol. 61, no. 5, pp. 2402–2411, 2014.

[115] I. Yaesh, S. Boyarski, and U. Shaked, "Probability-guaranteed robust H_∞ performance analysis," in *Proceedings of the 15th IFAC Congress*, Barcelona, Spain, 2002.

[116] S. Boyarski and U. Shaked, "Discrete-time H_∞ and H_2 control with structured disturbances and probability-relaxed requirements," *International Journal of Control*, vol. 77, no. 14, pp. 1243–1259, 2004.

[117] S. Boyarski and U. Shaked, "Robust H_∞ control design for best mean performance over an uncertain-parameters box," *System & Control Letters*, vol. 54, no. 6, pp. 585–595, 2005.

[118] S. Boyarski and U. Shaked, "Probability-guaranteed robust full-order and reduced-order H_∞-filtering," in *Proceedings of the IFAC SSSC*, Foz do Iguassu, Brazil, 2007.

[119] I. Yaesh, S. Boyarski, and U. Shaked, "Probability-guaranteed robust H_∞ performance analysis and state-feedback design," *Systems & Control Letters*, vol. 48, no. 5, pp. 351–364, 2003.

[120] L. Wu, P. Shi, and H. Gao, "State estimation and sliding-mode control of Markovian jump singular systems," *Institute of Electrical and Electronics Engineers*, vol. 55, no. 5, pp. 1213–1219, 2010.

[121] Y. Xia, G.-P. Liu, P. Shi, J. Chen, and D. Rees, "Robust delay-dependent sliding mode control for uncertain time-delay systems," *International Journal of Robust and Nonlinear Control*, vol. 18, no. 11, pp. 1142–1161, 2008.

[122] X. Yu and M. Zhihong, "Fast terminal sliding-mode control design for nonlinear dynamical systems," *IEEE Transactions on Circuits and Systems I*, vol. 49, no. 2, pp. 261–264, 2002.

[123] G. Foo and M. F. Rahman, "Sensorless sliding-mode MTPA control of an IPM synchronous motor drive using a sliding-mode observer and HF signal injection," *IEEE Transactions on Industrial Electronics*, vol. 57, no. 4, pp. 1270–1278, 2010.

[124] T. Orlowska-Kowalska, M. Dybkowski, and K. Szabat, "Adaptive sliding-mode neuro-fuzzy control of the two-mass induction motor drive without mechanical sensors," *IEEE Transactions on Industrial Electronics*, vol. 57, no. 2, pp. 553–564, 2010.

[125] B. K. Kim, W. K. Chung, and K. Ohba, "Design and performance tuning of sliding-mode controller for high-speed and high-accuracy positioning systems in disturbance observer framework," *IEEE Transactions on Industrial Electronics*, vol. 56, no. 10, pp. 3798–3809, 2009.

[126] C. Pukdeboon, A. S. I. Zinober, and M.-W. L. Thein, "Quasi-continuous higher order sliding-mode controllers for spacecraft-attitude-tracking maneuvers," *IEEE Transactions on Industrial Electronics*, vol. 57, no. 4, pp. 1436–1444, 2010.

[127] H. H. Choi, "LMI-based sliding surface design for integral sliding mode control of mismatched uncertain systems," *IEEE Transactions on Automatic Control*, vol. 52, no. 4, pp. 736–742, 2007.

[128] L. Wu and W. X. Zheng, "Passivity-based sliding mode control of uncertain singular time-delay systems," *Automatica*, vol. 45, no. 9, pp. 2120–2127, 2009.

[129] Y. Niu, D. W. C. Ho, and X. Wang, "Sliding mode control for Itô stochastic systems with Markovian switching," *Automatica*, vol. 43, no. 10, pp. 1784–1790, 2007.

[130] P. Shi, Y. Xia, G. P. Liu, and D. Rees, "On designing of sliding-mode control for stochastic jump systems," *IEEE Transactions on Automatic Control*, vol. 51, no. 1, pp. 97–103, 2006.

[131] K. Abidi, J.-X. Xu, and Y. Xinghuo, "On the discrete-time integral sliding-mode control," *IEEE Transactions on Automatic Control*, vol. 52, no. 4, pp. 709–715, 2007.

[132] A. Bartoszewicz, "Discrete-time quasi-sliding-mode control strategies," *IEEE Transactions on Industrial Electronics*, vol. 45, no. 4, pp. 633–637, 1998.

[133] W. Gao, Y. Wang, and A. Homaifa, "Discrete-time variable structure control systems," *IEEE Transactions on Industrial Electronics*, vol. 42, no. 2, pp. 117–122, 1995.

[134] N. O. Lai, C. Edwards, and S. K. Spurgeon, "Discrete output feedback sliding-mode control with integral action," *International Journal of Robust and Nonlinear Control*, vol. 16, no. 1, pp. 21–43, 2006.

[135] N. O. Lai, C. Edwards, and S. K. Spurgeon, "On output tracking using dynamic output feedback discrete-time sliding-mode controllers," *IEEE Transactions on Automatic Controll*, vol. 52, no. 10, pp. 1975–1981, 2007.

[136] X. G. Yan, S. K. Spurgeon, and C. Edwards, "Static output feedback sliding mode control for time-varying delay systems with time-delayed nonlinear disturbances," *International Journal of Robust and Nonlinear Control*, vol. 20, no. 7, pp. 777–788, 2010.

[137] X.-G. Yan, S. K. Spurgeon, and C. Edwards, "Decentralised sliding mode control for nonminimum phase interconnected systems based on a reduced-order compensator," *Automatica*, vol. 42, no. 10, pp. 1821–1828, 2006.

[138] Y. Xia, M. Fu, P. Shi, and M. Wang, "Robust sliding mode control for uncertain discrete-time systems with time delay," *IET Control Theory & Applications*, vol. 4, no. 4, pp. 613–624, 2010.

[139] L. F. Ma, Z. D. Wang, and Z. Guo, "Robust H_2 sliding mode control for non-linear discrete-time stochastic systems," *IET Control Theory & Applications*, vol. 3, no. 11, pp. 1537–1546, 2009.

[140] L. Ma, Z. Wang, Y. Niu, Y. Bo, and Z. Guo, "Sliding mode control for a class of nonlinear discrete-time networked systems with multiple stochastic communication delays," *International Journal of Systems Science*, vol. 42, no. 4, pp. 661–672, 2011.

[141] C. Lascu, I. Boldea, and F. Blaabjerg, "A class of speed-sensorless sliding-mode observers for high-performance induction motor drives," *IEEE Transactions on Industrial Electronics*, vol. 56, no. 9, pp. 3394–3403, 2009.

[142] C. P. Tan, X. Yu, and Z. Man, "Terminal sliding mode observers for a class of nonlinear systems," *Automatica*, vol. 46, no. 8, pp. 1401–1404, 2010.

[143] X.-G. Yan and C. Edwards, "Nonlinear robust fault reconstruction and estimation using a sliding mode observer," *Automatica*, vol. 43, no. 9, pp. 1605–1614, 2007.

[144] F. J. Bejarano and L. Fridman, "High order sliding mode observer for linear systems with unbounded unknown inputs," *International Journal of Control*, vol. 83, no. 9, pp. 1920–1929, 2010.

[145] C. Edwards and S. K. Spurgeon, "Sliding mode stabilization of uncertain systems using only output information," *International Journal of Control*, vol. 62, no. 5, pp. 1129–1144, 1995.

[146] C. Edwards, S. K. Spurgeon, and R. J. Patton, "Sliding mode observers for fault detection and isolation," *Automatica*, vol. 36, no. 4, pp. 541–553, 2000.

[147] B. Jiang, M. Staroswiecki, and V. Cocquempot, "Fault estimation in nonlinear uncertain systems using robust sliding-mode observers," *IEE Proceedings on Control Theory and Applications*, vol. 151, no. 1, pp. 29–37, 2004.

[148] C. P. Tan and C. Edwards, "Robust fault reconstruction in uncertain linear systems using multiple sliding mode observers in cascade," *IEEE Transactions on Automatic Control*, vol. 55, no. 4, pp. 855–867, 2010.

[149] S. K. Spurgeon, "Sliding mode observers: a survey," *International Journal of Systems Science*, vol. 39, no. 8, pp. 751–764, 2008.

[150] K. C. Veluvolu and Y. C. Soh, "Discrete-time sliding-mode state and unknown input estimations for nonlinear systems," *IEEE Transactions on Industrial Electronics*, vol. 56, no. 9, pp. 3443–3452, 2009.

[151] R. Raoufi, H. J. Marquez, and A. S. I. Zinober, "H_∞ sliding mode observers for uncertain nonlinear Lipschitz systems with fault estimation synthesis," *International Journal of Robust and Nonlinear Control*, vol. 20, no. 16, pp. 1785–1801, 2010.

[152] K. C. Veluvolu, Y. C. Soh, and W. Cao, "Robust discrete-time nonlinear sliding mode state estimation of uncertain nonlinear systems," *International Journal of Robust and Nonlinear Control*, vol. 17, no. 9, pp. 803–828, 2007.

[153] J. Hu, Z. Wang, H. Gao, and L. K. Stergioulas, "Extended Kalman filtering with stochastic nonlinearities and multiple missing measurements," *Automatica*, vol. 48, no. 9, pp. 2007–2015, 2012.

[154] J. Hu, Z. Wang, B. Shen, and H. Gao, "Quantised recursive filtering for a class of nonlinear systems with multiplicative noises and missing measurements," *International Journal of Control*, vol. 86, no. 4, pp. 650–663, 2013.

[155] J. Hu, Z. Wang, and H. Gao, "Recursive filtering with random parameter matrices, multiple fading measurements and correlated noises," *Automatica*, vol. 49, no. 11, pp. 3440–3448, 2013.

[156] J. Hu, Z. Wang, B. Shen, and H. Gao, "Gain-constrained recursive filtering with stochastic nonlinearities and probabilistic sensor delays," *IEEE Transactions on Signal Processing*, vol. 61, no. 5, pp. 1230–1238, 2013.

[157] J. Hu, Z. Wang, H. Gao, and L. K. Stergioulas, "Probability-guaranteed H_∞ finite-horizon filtering for a class of nonlinear time-varying systems with sensor saturations," *Systems & Control Letters*, vol. 61, no. 4, pp. 477–484, 2012.

[158] J. Hu, Z. Wang, Y. Niu, and L. K. Stergioulas, "H_∞ sliding mode observer design for a class of nonlinear discrete time-delay systems: a delay-fractioning approach," *International Journal of Robust and Nonlinear Control*, vol. 22, no. 16, pp. 1806–1826, 2012.

[159] J. Hu, Z. Wang, and H. Gao, "A delay fractioning approach to robust sliding mode control for discrete-time stochastic systems with randomly occurring non-linearities," *IMA Journal of Mathematical Control and Information*, vol. 28, no. 3, pp. 345–363, 2011.

[160] J. Hu, Z. Wang, H. Gao, and L. K. Stergioulas, "Robust H_∞ sliding mode control for discrete time-delay systems with stochastic nonlinearities," *Journal of the Franklin Institute*, vol. 349, no. 4, pp. 1459–1479, 2012.

[161] J. Hu, Z. Wang, H. Gao, and L. K. Stergioulas, "Robust sliding mode control for discrete stochastic systems with mixed time delays, randomly occurring uncertainties, and randomly occurring nonlinearities," *IEEE Transactions on Industrial Electronics*, vol. 59, no. 7, pp. 3008–3015, 2012.

[162] J. Hu, Z. Wang, Y. Niu, and H. Gao, "Sliding mode control for uncertain discrete-time systems withparameters and mixed delays," *Journal of the Franklin Institute*.

Hindawi Publishing Corporation
Mathematical Problems in Engineering
Volume 2013, Article ID 895895, 8 pages
http://dx.doi.org/10.1155/2013/895895

Research Article

Stabilization of a Class of Stochastic Nonlinear Systems

Valiollah Ghaffari,[1] Hamid Reza Karimi,[2] Navid Noroozi,[3] and S. Vahid Naghavi[4]

[1] *School of Electrical and Computer Engineering, Shiraz University, 7134851151 Shiraz, Iran*
[2] *Department of Engineering, Faculty of Engineering and Science, University of Agder, 4898 Grimstad, Norway*
[3] *Young Researchers and Elites Club, Najaf Abad Branch, Islamic Azad University, Najaf Abad, Isfahan, Iran*
[4] *Young Researchers and Elites Club, Zarghan Branch, Islamic Azad University, Zarghan, Iran*

Correspondence should be addressed to Navid Noroozi; navid.noroozi@ymail.com

Received 8 August 2013; Accepted 20 October 2013

Academic Editor: Xiao He

This paper addresses two control schemes for stochastic nonlinear systems. Firstly, an adaptive controller is designed for a class of motion equations. Then, a robust finite-time control scheme is proposed to stabilize a class of nonlinear stochastic systems. The stability of the closed-loop systems is established based on stochastic Lyapunov stability theorems. Links between these two methods are given. The efficiency of the control schemes is evaluated using numerical simulations.

1. Introduction

There has been conspicuous attention toward extending popular nonlinear control design in deterministic setting to stochastic framework. In particular, the integrator backstepping was generalized for stochastic nonlinear system in [1]. The author in [2] gave an extension of output feedback backstepping design for stochastic systems. Battiloti [3] investigated stabilization for a class of stochastic nonlinear systems in upper triangular. A stochastic version of nonlinear small gain was given in [4]. Using the small gain condition, the authors provided an adaptive backstepping controller. Other attempts toward this end have been reported in [5–10] and references therein.

Asymptotic stabilization is an important issue in many engineering applications. But for very demanding applications, finite-time stabilization offers an effective alternative, which yields, in some sense, fast response, high tracking precision, and disturbance-rejection properties [11]. Finite-time stability [12, 13] allows solving the finite-time stabilization problem. Finite-time stabilization method was introduced by Bhat and Bernstein [12] and then it has been developed by many other researchers (see, e.g., [13, 14]). As mentioned above, over the last few decades, considerable research works have been devoted to analysis and design of nonlinear stochastic systems. Recently, Chen and Jiao [15] have extended finite-time stability of deterministic systems to stochastic framework using the Itô differential equation.

In this paper, we provide two nonlinear control designs with applications to a guidance system in stochastic setting. The former gives an adaptive control law for the guidance system. The latter stabilizes a class of stochastic system in finite-time; as a special case, it is applied to the guidance system. Two numerical simulations illustrate the effectiveness of the proposed control schemes. Moreover, links between these two methods are given in Section 4.

The rest of this paper is organized as follows. In Section 2, notions for stochastic nonlinear systems are reviewed. In Section 3, a Lyapunov-based adaptive stochastic control is presented for the guidance system; then the result is verified with numerical simulations. In Section 4, a finite-time stochastic control is investigated. Using this control method, a robust finite-time guidance law is derived. In Section 5, concluding remarks are placed.

2. Preliminaries

List of Properties

(i) R_+ is the nonnegative real numbers.

(ii) C^n denotes the set of n-times differentiable functions R^n to R_+.

(iii) $|\mathbf{x}|$ stands for Euclidean norm.

(iv) A function $\alpha : R_+ \to R_+$ is of class-$\mathcal{K}$ ($\alpha \in \mathcal{K}$) if it is continuous, zero at zero and strictly increasing. Furthermore, it is of class-$\mathcal{K}_\infty$ ($\alpha \in \mathcal{K}_\infty$) if $|s| \to \infty$ as $s \to \infty$.

(v) A function $\beta : R_+ \times R_+ \to R_+$ is of class-$\mathcal{KL}$ if for each fixed $t \geq 0$, $\beta(\cdot, t) \in \mathcal{K}$ and for each fixed $s \geq 0$, $\beta(s, \cdot)$ is strictly decreasing and $\beta(s, t) \to 0$ as $t \to \infty$.

(vi) $E[\cdot]$ denotes the expectation of stochastic variable x.

Consider the following stochastic nonlinear system:

$$d\mathbf{x} = \left(\mathbf{f}(\mathbf{x}) + \mathbf{g}(\mathbf{x})\, u\right) dt + \mathbf{h}(\mathbf{x})\, d\mathbf{w}, \tag{1}$$

where $\mathbf{x} = [x_1, \ldots, x_n]^T \in R^n$ is the state of the system which is assumed to be available for measurement, $u \in R$ is the control input, $t \in R_+$ is time, $\mathbf{f} \in R^n, \mathbf{g} \in R^n$, and $\mathbf{h} \in R^{n \times r}$ are continuous functions, and $\mathbf{w}$ is an r-dimensional standard Brownian motion. Let $x(t, x_0)$ denote the solution to the system (1) starting from the initial value x_0. The system (1) can be thought of as a perturbation from the deterministic system $\dot{\mathbf{x}} = \mathbf{f}(\mathbf{x}) + \mathbf{g}(\mathbf{x})u$ by an additive white noise.

Let $V : R^n \to R^+$ with the property that $V \in C^2$. The differential operator L is defined by

$$LV := \frac{\partial V}{\partial \mathbf{x}} \left(\mathbf{f}(\mathbf{x}) + \mathbf{g}(\mathbf{x})\, u\right) + \frac{1}{2} \operatorname{Tr}\left\{\mathbf{h}^T \frac{\partial^2 V}{\partial \mathbf{x}^2} \mathbf{h}\right\}, \tag{2}$$

where $\operatorname{Tr}\{\cdot\}$ denotes the matrix trace. We borrow some notions on stability of stochastic system from [4, 15].

Definition 1 (see [4]). The system (1) is said to be input-to-state practically stable (ISpS) in probability if for any $\varepsilon > 0$, there exist some $\beta \in \mathcal{KL}$, $\gamma \in \mathcal{K}$, and $\delta > 0$ such that the following hold:

$$P\left\{|x| \leq \beta\left(\left|x_0\right|, t\right) + \gamma(|u|) + \delta\right\} \geq 1 - \varepsilon, \quad \forall t \geq 0, \quad x_0 \in R^n \setminus \{0\}. \tag{3}$$

Definition 2 (see [15]). For system (1), define $T(x_0, w) = \{T \geq 0 : x(t, x_0) \equiv 0\, \forall t > T\}$, which is called the stochastic settling time function.

Definition 3 (see [15]). For stochastic system (1), the origin $\mathbf{x} = 0$ is said to be globally stochastically finite-time stable, if for each $x_0 \in R^n$, the following conditions hold:

(i) stochastic settling time function $T(x_0, w)$ exists with probability one;

(ii) if $T(x_0, w)$ exists, then $E[T(x_0, w)] < +\infty$;

(iii) the origin is stable.

Theorem 4 (see [4]). *For system* (1)*, there exist* $V : R^n \to R_+$ *function with the property that* $V \in C^2$*, functions* $\alpha, \underline{\alpha}, \overline{\alpha} \in \mathcal{K}_\infty$ *and* $\gamma \in \mathcal{K}$*, and* $\delta > 0$ *such that the following hold:*

$$\underline{\alpha}(\mathbf{x}) \leq V(\mathbf{x}) \leq \overline{\alpha}(\mathbf{x}), \quad LV \leq -\alpha(|\mathbf{x}|) + \gamma(|\mathbf{x}|) + \delta; \tag{4}$$

then system (1) *is ISpS in probability sense. Such a function* V *is called an ISpS Lyapunov function for* (1).

Theorem 5 (see [15]). *Consider system* (1) *with* $u = 0$*. If there exist a positive definite, twice continuously differentiable, and radially unbounded Lyapunov function* $V : R^n \to R_+$ *and real numbers* $\beta > 0$ *and* $0 < \alpha < 1$*, such that*

$$LV(\mathbf{x}) \leq -\beta[V(\mathbf{x})]^\alpha, \tag{5}$$

then the origin of system (1) *is globally stochastically finite-time stable.*

Lemma 6 (Young's inequality). *For any* $(a, b) \in R \times R$*, for all* $(p, q) \in R_+ \times R_+$ *with* $(1/p) + (1/q) = 1$*, and for each* $\varepsilon > 0$*, the following holds:*

$$ab \leq \frac{\varepsilon^p}{p}|a|^p + \frac{1}{\varepsilon^q q}|b|^q. \tag{6}$$

3. Adaptive Control Design for a Guidance System

In this section, we design an adaptive control law for the guidance system below under the presence of noise. The geometry of planar interception is shown in Figure 1. The two-dimensional motion equation of the planar interception is [16]

$$\dot{r} = V_T \cos(q - \varphi_T) - V_M \cos(q - \varphi_M), \quad r\dot{q} = -V_T \sin(q - \varphi_T) + V_M \sin(q - \varphi_M), \tag{7}$$

where r is the relative range, q is LOS angle, φ_M and φ_T are flight-path angle for missile and target, and V_M and V_T are missile velocity and target velocity, respectively. Differentiating (7) with respect to time yields [16]:

$$\ddot{r} = r\dot{q}^2 + w - u, \quad \ddot{q} = -\frac{2\dot{r}}{r}\dot{q} + \frac{1}{r}w - \frac{1}{r}u, \tag{8}$$

where u and w are missile acceleration normal to line of sight and target acceleration normal to line of sight, respectively. Let u be the control input. Also, define $x(t) := \dot{q}(t)$ for all $t \geq 0$. So we get

$$\dot{x} = -\frac{2\dot{r}}{r}x + \frac{1}{r}w - \frac{1}{r}u. \tag{9}$$

Assumption 7. Suppose that $\dot{r}(t)$ and $w(t)$ are stochastic processes defined by

$$\dot{r}(t) = \dot{\overline{r}}(t) + \zeta(t), \quad w(t) = \overline{w}(t) + \zeta(t), \tag{10}$$

where $\dot{\overline{r}}(t)$ and $\overline{w}(t)$ are deterministic and $\zeta(t)$ is white noise degrading measurements. Using Assumption 7, the system (9) can be represented as

$$dx = \left(-\frac{2\dot{\overline{r}}}{r}x + \frac{1}{r}\overline{w} - \frac{1}{r}u\right) dt - \frac{1}{r}(2x - 1)\, dw. \tag{11}$$

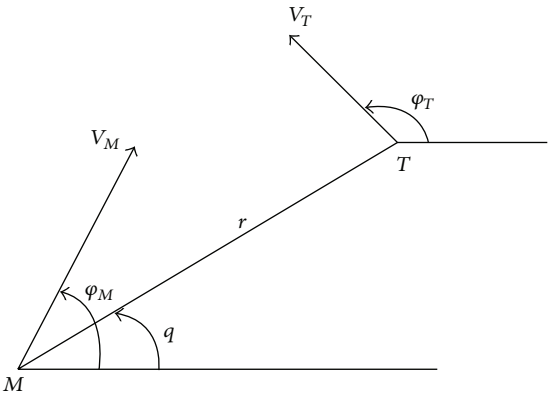

Figure 1: Planar interception geometry. M and T denote the missile and the target, respectively.

Theorem 8. *Consider the stochastic system* (11). *The following guidance law*

$$u = cx + \overline{w} - N\dot{\overline{r}}x + \widehat{\theta}\frac{x}{r} + 6\frac{x}{r} - \frac{6}{r}, \quad N > 2 \tag{12}$$

with the update law

$$\dot{\widehat{\theta}} = k\left[\sigma\left(\theta^{\circ} - \widehat{\theta}\right) + \frac{x^4}{r^2}\right] \quad c, \sigma, k > 0,\ \theta^{\circ} \in R \tag{13}$$

guarantees the boundedness of $\mathbf{x}(t)$ *and* $\widehat{\theta}(t)$ *and the convergence of* $\mathbf{x}(t)$ *to an arbitrary small neighborhood of the origin.*

Proof. Define the following Lyapunov function:

$$V\left(x, \widehat{\theta}\right) = \frac{1}{4}x^4 + \frac{1}{2k}\widetilde{\theta}^2, \tag{14}$$

where $\widetilde{\theta} = \theta - \widehat{\theta}$. According to the Itô differential rule [17], we have

$$\begin{aligned} LV = {} & \frac{\partial V}{\partial x}\left(-\frac{2\dot{\overline{r}}}{r}x + \frac{1}{r}\overline{w} - \frac{1}{r}u\right) \\ & + \frac{1}{2}\frac{\partial^2 V}{\partial x^2}\left(\frac{2x-1}{r}\right)^2 + \frac{\partial V}{\partial \widehat{\theta}}\dot{\widehat{\theta}}. \end{aligned} \tag{15}$$

Adding and subtracting $\sigma\widetilde{\theta}(\theta^{\circ} - \widehat{\theta})$ to the right-hand sight of (15) give

$$\begin{aligned} LV = {} & x^3\left(-\frac{2\dot{\overline{r}}}{r}x + \frac{1}{r}\overline{w} - \frac{1}{r}u\right) \\ & + \frac{3}{2}\left(\frac{x}{r}\right)^2\left(4x^2 - 4x + 1\right) \\ & - \frac{1}{k}\widetilde{\theta}\dot{\widetilde{\theta}} \pm \sigma\widetilde{\theta}\left(\theta^{\circ} - \widehat{\theta}\right). \end{aligned} \tag{16}$$

This can be simplified as

$$\begin{aligned} LV = {} & \frac{x^3}{r}\left(-2\dot{\overline{r}}x + \overline{w} - u + \frac{6x}{r} - \frac{6}{r}\right) \\ & + \frac{3}{2}\frac{x^2}{r^2} - \frac{1}{k}\widetilde{\theta}\dot{\widetilde{\theta}} \pm \sigma\widetilde{\theta}\left(\theta^{\circ} - \widehat{\theta}\right). \end{aligned} \tag{17}$$

Rewrite (17) as

$$\begin{aligned} LV = {} & \frac{x^3}{r}\left(-2\dot{\overline{r}}x + \overline{w} - u + \frac{6x}{r} - \frac{6}{r}\right) \\ & + \frac{3}{2}\frac{x^2}{r^2} - \frac{\widetilde{\theta}}{k}\left(\dot{\widehat{\theta}} - \sigma k\left(\theta^{\circ} - \widehat{\theta}\right)\right) - \sigma\widetilde{\theta}\left(\theta^{\circ} - \widehat{\theta}\right), \end{aligned} \tag{18}$$

so we get

$$\begin{aligned} LV = {} & \frac{x^3}{r}\left(-2\dot{\overline{r}}x + \overline{w} - u + \frac{6x}{r} - \frac{6}{r} + \widehat{\theta}\frac{x}{r}\right) \\ & - \widehat{\theta}\frac{x^4}{r^2} + \frac{3}{2}\frac{x^2}{r^2} - \frac{\widetilde{\theta}}{k}\left(\dot{\widehat{\theta}} - \sigma k\left(\theta^{\circ} - \widehat{\theta}\right)\right) - \sigma\widetilde{\theta}\left(\theta^{\circ} - \widehat{\theta}\right). \end{aligned} \tag{19}$$

Recalling the fact that $\widetilde{\theta} = \theta - \widehat{\theta}$, (19) can be written as

$$\begin{aligned} LV = {} & \frac{x^3}{r}\left(-2\dot{\overline{r}}x + \overline{w} - u + \frac{6x}{r} - \frac{6}{r} + \widehat{\theta}\frac{x}{r}\right) \\ & + \left(\widetilde{\theta} - \theta\right)\frac{x^4}{r^2} + \frac{3}{2}\frac{x^2}{r^2} - \frac{\widetilde{\theta}}{k}\left(\dot{\widehat{\theta}} - \sigma k\left(\theta^{\circ} - \widehat{\theta}\right)\right) \\ & - \sigma\widetilde{\theta}\left(\theta^{\circ} - \widehat{\theta}\right). \end{aligned} \tag{20}$$

Therefore, we have

$$\begin{aligned} LV = {} & \frac{x^3}{r}\left(-2\dot{\overline{r}}x + \overline{w} - u + \frac{6x}{r} - \frac{6}{r} + \widehat{\theta}\frac{x}{r}\right) \\ & - \theta\frac{x^4}{r^2} + \frac{3}{2}\frac{x^2}{r^2} - \frac{\widetilde{\theta}}{k}\left(\dot{\widehat{\theta}} - \sigma k\left(\theta^{\circ} - \widehat{\theta}\right) - k\frac{x^4}{r^2}\right) \\ & - \sigma\widetilde{\theta}\left(\theta^{\circ} - \widehat{\theta}\right). \end{aligned} \tag{21}$$

It follows with the following update law

$$\dot{\widehat{\theta}} = k\left[\sigma\left(\theta^{\circ} - \widehat{\theta}\right) + \frac{x^4}{r^2}\right] \tag{22}$$

that

$$\begin{aligned} LV = {} & \frac{x^3}{r}\left(-2\dot{\overline{r}}x + \overline{w} - u + \frac{6x}{r} - \frac{6}{r} + \widehat{\theta}\frac{x}{r}\right) \\ & - \theta\frac{x^4}{r^2} + \frac{3}{2}\frac{x^2}{r^2} - \sigma\widetilde{\theta}\left(\theta^{\circ} - \widehat{\theta}\right). \end{aligned} \tag{23}$$

The last term in (23) can be written as

$$2\widetilde{\theta}\left(\theta^{\circ} - \widehat{\theta}\right) = \widetilde{\theta}^2 + \left(\theta^{\circ} - \widehat{\theta}\right)^2 - \left(\theta^{\circ} - \theta\right)^2. \tag{24}$$

Substituting (24) into (21) gives

$$\begin{aligned} LV = {} & \frac{x^3}{r}\left(-2\dot{\overline{r}}x + \overline{w} - u + \frac{6x}{r} - \frac{6}{r} + \widehat{\theta}\frac{x}{r}\right) \\ & - \frac{\sigma}{2}\left(\widetilde{\theta}^2 + \left(\theta^{\circ} - \widehat{\theta}\right)^2 - \left(\theta^{\circ} - \theta\right)^2\right) - \theta\frac{x^4}{r^2} + \frac{3}{2}\frac{x^2}{r^2}. \end{aligned} \tag{25}$$

Pick the following control law:

$$u = cx + \overline{w} - N\dot{\overline{r}}x + \widehat{\theta}\frac{x}{r} + 6\frac{x}{r} - \frac{6}{r} \quad N > 2. \tag{26}$$

So we obtain

$$\begin{aligned} LV = & -c\frac{x^4}{r} + \frac{\dot{\overline{r}}x^4}{r}(N-2) - \theta\frac{x^4}{r^2} + \frac{3}{2}\frac{x^2}{r^2} \\ & - \frac{\sigma}{2}\left(\widetilde{\theta}^2 + \left(\theta^\circ - \widehat{\theta}\right)^2 - \left(\theta^\circ - \theta\right)^2\right). \end{aligned} \tag{27}$$

For $N > 2$, the second term on the right-hand side of (27) is negative (i.e., $(\dot{\overline{r}}x^4/r)(N-2) < 0$), thus

$$\begin{aligned} LV \le & -c\frac{x^4}{r} - \theta\frac{x^4}{r^2} + \frac{3}{2}\frac{x^2}{r^2} \\ & - \frac{\sigma}{2}\left(\widetilde{\theta}^2 + \left(\theta^\circ - \widehat{\theta}\right)^2 - \left(\theta^\circ - \theta\right)^2\right). \end{aligned} \tag{28}$$

A simplified but conservative version of (28) is

$$LV \le -c\frac{x^4}{r} - \theta\frac{x^4}{r^2} + \frac{3}{2}\frac{x^2}{r^2} - \frac{\sigma}{2}\left(\widetilde{\theta}^2 - \left(\theta^\circ - \theta\right)^2\right). \tag{29}$$

The last term in (29) on the right-hand side of (29) is negative (i.e., $-\sigma/2(\theta^\circ - \widehat{\theta})^2 < 0$), so

$$LV \le -c\frac{x^4}{r} - \theta\frac{x^4}{r^2} + \frac{3}{2}\frac{x^2}{r^2} - \frac{\sigma}{2}\widetilde{\theta}^2 + \frac{\sigma}{2}\left(\theta^\circ - \theta\right)^2. \tag{30}$$

The second and third terms on the right-hand side of (30) can be written as

$$\begin{aligned} -\theta\frac{x^4}{r^2} + \frac{3}{2}\frac{x^2}{r^2} &= -\frac{\theta}{r^2}\left(x^4 - \frac{3}{2\theta}x^2\right) \\ &= -\frac{\theta}{r^2}\left(x^4 - \frac{3}{2\theta}x^2 + \left(\frac{3}{4\theta}\right)^2 - \left(\frac{3}{4\theta}\right)^2\right) \\ &= -\frac{\theta}{r^2}\left(x^2 - \frac{3}{4\theta}\right)^2 + \frac{9}{16\theta r^2}. \end{aligned} \tag{31}$$

By substituting (31) into (30), we get

$$LV \le -c\frac{x^4}{r} - \frac{\theta}{r^2}\left(x^2 - \frac{3}{4\theta}\right)^2 + \frac{9}{16\theta r^2} - \frac{\sigma}{2}\widetilde{\theta}^2 + \frac{\sigma}{2}\left(\theta^\circ - \theta\right)^2. \tag{32}$$

So

$$LV \le -c\frac{x^4}{r} - \frac{\sigma}{2}\widetilde{\theta}^2 + \frac{9}{16\theta r^2} + \frac{\sigma}{2}\left(\theta^\circ - \theta\right)^2 \quad \theta > 0. \tag{33}$$

Let $\varepsilon = (9/16\theta r^2) + (\sigma/2)(\theta^\circ - \theta)^2$. Substituting (14) into the right-hand side of above inequality gives

$$LV \le -c_0 V + \varepsilon, \tag{34}$$

where $c_0 = \min\{k\sigma, 4c/r\}$. Inequality (34) implies that V is an ISpS Lyapunov function. Therefore, it ensures the boundedness of $\mathbf{x}(t)$ and $\widetilde{\theta}(t)$ and convergence of $\mathbf{x}(t)$ to an arbitrary small neighborhood of the origin. □

Corollary 9. *Under the assumption that $w(t)$ is a pure deterministic variable. The following guidance law*

$$u = cx + w - N\,\dot{\overline{r}}x + \widehat{\theta}\frac{x}{r}, \quad N > 2 \tag{35}$$

with an update law

$$\dot{\theta} = k\frac{x^4}{r^2} \quad k > 0 \tag{36}$$

guarantees the boundedness of $\mathbf{x}(t)$ and $\widehat{\theta}(t)$ and the convergence of $\mathbf{x}(t)$ to the origin.

Proof. The proof is a simple conclusion of Theorem 8. □

Three-Dimensional Case. With the same arguments, the result can be extended to the three-dimensional case. Consider the following stochastic system:

$$\begin{aligned} dx_1 &= \left(-\frac{2\dot{\overline{r}}}{r}x_1 + \frac{1}{r}\overline{w}_1 - \frac{1}{r}u_1\right)dt - \frac{1}{r}\left(2x_1 - 1\right)dw_1, \\ dx_2 &= \left(-\frac{2\dot{\overline{r}}}{r}x_2 + \frac{1}{r}\overline{w}_2 - \frac{1}{r}u_2\right)dt - \frac{1}{r}\left(2x_2 - 1\right)dw_2, \end{aligned} \tag{37}$$

where $w_1 = a_{T\theta}$ and $w_2 = a_{T\phi}$. The following guidance laws

$$\begin{aligned} u_1 &= c_1 x + \overline{w}_1 - N\dot{\overline{r}}x_1 + \widehat{\theta}_1\frac{x_1}{r} + 6\frac{x_1}{r} - \frac{6}{r}, \quad N > 2, \\ u_2 &= c_2 x + \overline{w}_2 - N\dot{\overline{r}}x_2 + \widehat{\theta}_2\frac{x_2}{r} + 6\frac{x_2}{r} - \frac{6}{r}, \quad N > 2 \end{aligned} \tag{38}$$

with the update laws

$$\begin{aligned} \dot{\widehat{\theta}}_1 &= k_1\left[\sigma_1\left(\theta_1^\circ - \widehat{\theta}_1\right) + \frac{x_1^4}{r^2}\right], \quad c_1, \sigma_1, k_1 > 0,\ \theta_1^\circ \in R, \\ \dot{\widehat{\theta}}_2 &= k_2\left[\sigma_2\left(\theta_2^\circ - \widehat{\theta}_2\right) + \frac{x_2^4}{r^2}\right], \quad c_2, \sigma_2, k_2 > 0,\ \theta_2^\circ \in R \end{aligned} \tag{39}$$

guarantee the boundedness of $\mathbf{x}(t)$ and the convergence of $\mathbf{x}(t)$ to an arbitrary small neighborhood of the origin.

3.1. Numerical Simulation. For the closed loop system, the mentioned stochastic differential equations governed by this guidance system can be simplified as

$$\begin{aligned} dx(t) = & \left(-(N+2)\frac{\dot{\overline{r}}(t)}{r(t)}x(t) - \frac{c + \widehat{\theta}(t)}{r(t)}x(t)\right. \\ & \left. + \frac{6}{r^2(t)}x(t) - \frac{6}{r^2(t)}\right)dt \\ & + \left(\frac{-2}{r(t)}x(t) + \frac{1}{r(t)}\right)dw(t), \end{aligned} \tag{40}$$

where $\dot{\widehat{\theta}}(t)$ and $r(t)$ are simultaneously solved by the following:

$$\dot{\widehat{\theta}}(t) = k\left[\sigma\left(\theta^{\circ} - \widehat{\theta}(t)\right) + \frac{x^4(t)}{r(t)}\right] \quad c, \sigma, k > 0 \quad \theta^{\circ} \in R,$$
$$\ddot{r}(t) = \left(r(t)\,x(t) - c - N\dot{r}(t) - \widehat{\theta}(t) + \frac{6}{r(t)}\right) \times x(t) + \zeta(t) - \frac{6}{r(t)}. \tag{41}$$

To solve these equations numerically, we follow the methods in [18, 19]. The guidance law and update law parameters are chosen as $N = 2$, $c = 500$, $\sigma = 2$, $K = 5$, and $\theta^0 = 0.2$. Initial conditions of system (11) and adaptive guidance law (13) are selected as $\dot{r}(0) = 200$, $r(0) = 1$, $\widehat{\theta}(0) = 0$, and $x(0) = 0.1$. Sampling time is set to the value $h = 0.005$. Applying our proposed method, the line of sight rate $x(t)$ is depicted in Figure 2.

The update parameter $\widehat{\theta}(t)$ is shown in Figure 3. As we expect, after some transient time (0.4 second), the update parameter stays close to the value of 0.2.

The control input $u(t)$ is shown in Figure 4.

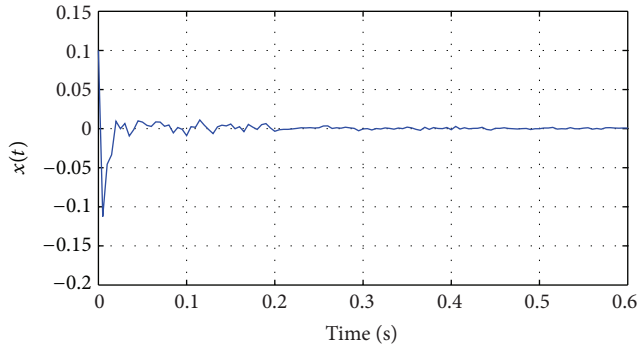

Figure 2: The line of sight rate $x(t)$.

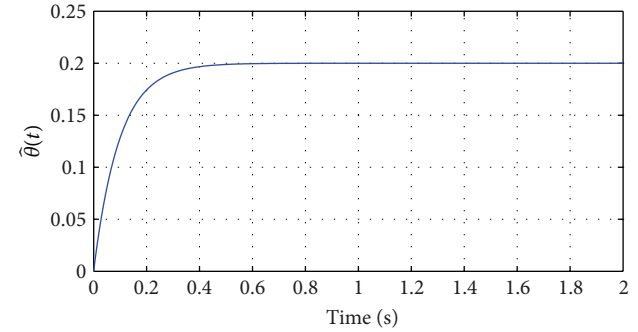

Figure 3: The adaptation parameter $\widehat{\theta}(t)$.

4. Finite-Time Control Law for Stochastic systems

In the previous section, the variable $\dot{q}$ is only controlled (see (9)). One expects to get better performance of the guidance system if both the LOS angle q and the angular velocity $\dot{q}$ are controlled. In this case, we get the following state-space equations:

$$\dot{x}_1 = x_2,$$
$$\dot{x}_2 = -\frac{2\dot{r}}{r}x_2 + \frac{1}{r}w - \frac{1}{r}u. \tag{42}$$

Using Assumption 7, the system (42) can be represented as

$$dx_1 = x_2 dt,$$
$$dx_2 = \left(-\frac{2\dot{\overline{r}}}{r}x_2 + \frac{1}{r}\overline{w} - \frac{1}{r}u\right)dt - \frac{1}{r}(2x_2 - 1)\,dw. \tag{43}$$

So we aim to develop a guidance law to stabilize the origin of the system (43). On the other hand, the notion of finite-time stability is very important in guidance problems since the guidance equations are valid as long as the intercept point is met in finite-time [16, 20, 21]. The adaptive guidance law proposed in the previous section does not provide the finite-time convergence of the guidance system although it gives the effective robustness. These motivate us to give a robust finite-time guidance law in stochastic setting.

Consider the following stochastic nonlinear system:

$$dx_1 = x_2 dt,$$
$$dx_2 = \left(f(\mathbf{x}, t) + u\right)dt + g(\mathbf{x}, t)\,dw, \tag{44}$$

where $w \in R$ and $\mathbf{x} = [x_1, x_2]^T \in R^2$ is assumed to be available for measurement. A guidance system can be modeled in this form. We emphasize that the guidance system (43) is a special case of the system (44).

Assumption 10. For any $\mathbf{x} \in R^2$, the nonlinear part of (42) can be bounded by

$$\left|f(\mathbf{x}, t)\right| \le \gamma(x_1, x_2)\left(|x_1| + |x_2|\right), \tag{45}$$

where $\gamma(x_1, x_2) \ge 0$ is a known C^1 function.

It should be noted that the function $f(\cdot, \cdot)$ is unknown, in general. We only need that the upper bound (45) is given.

Theorem 11. *Consider the stochastic system* (42) *with Assumption 10. The following control law*

$$u = -\beta(x_1, x_2)\left(x_2^{5/3} + 0.15x_1\right)^{1/5} - \left[\frac{7}{3}\varpi(x_1, x_2) + \frac{\delta^4}{4}x_2^{8/3}\right]\xi_2^{1/5} \tag{46}$$

guarantees the boundedness of $\mathbf{x}(t)$ *and the convergence of* $\mathbf{x}(t)$ *to the origin in finite-time.*

Proof. Define the following Lyapunov function:

$$V(\mathbf{x}) = \frac{1}{2}x_1^2 + \int_{x_2^*}^{x_2}\left(s^{5/3} - x_2^{*5/3}\right)^{7/5} ds. \tag{47}$$

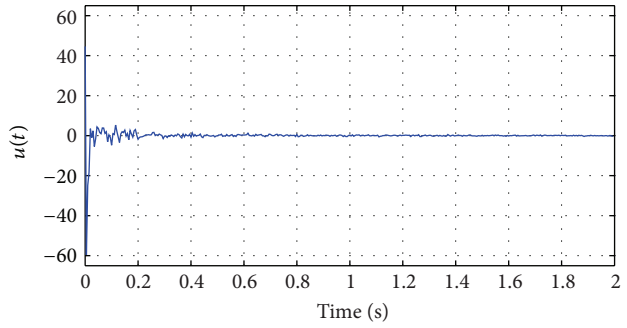

Figure 4: The applied control effort.

Fact 1. Recall that for a given dynamical system

$$d\mathbf{x} = f(\mathbf{x},t)\,dt + g(\mathbf{x},t)\,d\mathbf{w}(t). \tag{48}$$

According to the Itô differential rule $LV(\mathbf{x})$ is

$$LV(\mathbf{x}) = \frac{\partial V(\mathbf{x})}{\partial \mathbf{x}} f(\mathbf{x},t) + \frac{1}{2} Tr\left(g^T(\mathbf{x},t) \frac{\partial^2 V(\mathbf{x})}{\partial \mathbf{x}^2} g(\mathbf{x},t) \right). \tag{49}$$

So $LV(\mathbf{x})$ for the system (42) is

$$LV(\mathbf{x}) = \frac{\partial V(\mathbf{x})}{\partial x_1} x_2 + \frac{\partial V(\mathbf{x})}{\partial x_2} (f(\mathbf{x},t) + u) + \frac{1}{2} \frac{\partial^2 V(\mathbf{x})}{\partial x_2^2} g^2(\mathbf{x},t). \tag{50}$$

The partial derivative of V respect to x_1 is

$$\frac{\partial V(\mathbf{x})}{\partial x_1} = x_1 + \frac{\partial}{\partial x_1} \int_{x_2^*}^{x_2} \left(s^{5/3} - x_2^{*5/3} \right)^{7/5} ds. \tag{51}$$

Fact 2. From the elementary calculus, we get

$$\frac{d}{d\mathbf{x}} \left(\int_a^{g(\mathbf{x})} f(\mathbf{x},z)\,dz \right) = \int_a^{g(\mathbf{x})} \frac{\partial f(\mathbf{x},z)}{\partial \mathbf{x}} dz + \frac{\partial g(\mathbf{x})}{\partial x} f(\mathbf{x},z)\Big|_{z=g(\mathbf{x})}. \tag{52}$$

Using Fact 2, (49) is rewritten as

$$\frac{\partial V(\mathbf{x})}{\partial x_1} = x_1 + \int_{x_2^*}^{x_2} \frac{\partial}{\partial x_1} \left(s^{5/3} - x_2^{*5/3} \right)^{7/5} ds - \frac{\partial x_2^*}{\partial x_1} \left(s^{5/3} - x_2^{*5/3} \right)^{7/5} \Big|_{s=x_2^*}. \tag{53}$$

It follows with the fact that $(\partial x_2^*/\partial x_1)(s^{5/3} - x_2^{*5/3})^{7/5}|_{s=x_2^*} = 0$ that

$$\frac{\partial V(\mathbf{x})}{\partial x_1} = x_1 + \int_{x_2^*}^{x_2} \frac{7}{5} \left(s^{5/3} - x_2^{*5/3} \right)^{2/5} \times \left(-\frac{5}{3} x_2^{*2/3} \right) \frac{\partial x_2^*}{\partial x_1} ds. \tag{54}$$

Recall that

$$x_2^{*2/3} \frac{\partial x_2^*}{\partial x_1} = \left(-2x_1^{3/5} \right)^{2/3} \left(-\frac{6}{5} x_1^{-2/5} \right) = -\frac{6}{5} (4)^{1/3}; \tag{55}$$

we obtain

$$\frac{\partial V(\mathbf{x})}{\partial x_1} = x_1 + \frac{14}{5} (4)^{1/3} \int_{x_2^*}^{x_2} \left(s^{5/3} - x_2^{*5/3} \right)^{2/5} ds. \tag{56}$$

The partial derivative of $V(\mathbf{x})$ with respect to x_2 is

$$\frac{\partial V(\mathbf{x})}{\partial x_2} = \left(x_2^{5/3} - x_2^{*5/3} \right)^{7/5} = \xi_2^{7/5} \tag{57}$$

and the second derivative with respect to x_2 is

$$\frac{\partial^2 V(\mathbf{x})}{\partial x_2^2} = \frac{7}{3} \xi_2^{2/5} x_2^{2/3}. \tag{58}$$

So we have

$$LV(\mathbf{x}) = \left(x_1 + \frac{14}{5} (4)^{1/3} \int_{x_2^*}^{x_2} \left(s^{5/3} - x_2^{*5/3} \right)^{2/5} ds \right) x_2 + x_2^{7/5} (f(\mathbf{x}) + u) + \frac{7}{6} x_2^{2/5} x_2^{2/3} g^2(\mathbf{x}). \tag{59}$$

Define the following variables:

$$\xi_1 := x_1, \qquad \xi_2 := x_2^{5/3} - x_2^{*5/3}, \quad x_2^* := -2x_1^{3/5}. \tag{60}$$

Therefore, one yields:

$$LV = \left(\xi_1 - \frac{7}{5} \int_{x_2^*}^{x_2} \left(s^{5/3} - x_2^{*5/3} \right)^{2/5} ds \right) x_2 + \xi_2^{7/5} (f(\mathbf{x}) + u) + \frac{7}{3} g(\mathbf{x})^2 x_2^{2/3} \left(x_2^{5/3} - x_2^{*5/3} \right)^{2/5}. \tag{61}$$

Let $u := u_d + u_s$; the deterministic term is

$$u_d = -\beta(x_1,x_2) \left(x_2^{5/3} + 0.15x_1 \right)^{1/5}, \tag{62}$$

where $\beta(x_1,x_2) > 0$ is a C^1 function. Particularly, u_d and u_s provide the deterministic and stochastic parts of (44), respectively. Substituting (62) into the right-hand side of (61) gives

$$LV \le -\left(\xi_1^{8/5} + \xi_2^{8/5} \right) + \xi_2^{7/5} u_s + \frac{7}{3} g(\mathbf{x})^2 x_2^{2/3} \xi_2^{2/5}. \tag{63}$$

Assume that

$$|g(\mathbf{x},t)|^2 \le \varpi(x_1,x_2) \left(|\xi_1|^{6/5} + |\xi_2|^{6/5} \right), \tag{64}$$

where $\varpi(x_1,x_2) > 0$ is a C^1 function. From the aforementioned assumption and Young's inequality, we get

$$\begin{aligned} LV &\le -\left(\xi_1^{8/5} + \xi_2^{8/5} \right) + \xi_2^{7/5} u_s + \frac{7}{3} \varpi(x_1,x_2) \left(|\xi_1|^{6/5} + |\xi_2|^{6/5} \right) x_2^{2/3} \xi_2^{2/5} \\ &\le -\left(\xi_1^{8/5} + \xi_2^{8/5} \right) + \frac{1}{(4/3)\,\delta^{4/3}} \xi_1^{8/5} + \xi_2^{7/5} \left(u_s + \left[\frac{7}{3} \varpi(x_1,x_2) + \frac{\delta^4}{4} x_2^{8/3} \right] \xi_2^{1/5} \right), \end{aligned} \tag{65}$$

where $\delta \in (0,1)$. Let u_s be

$$u_s = -\left[\frac{7}{3}\varpi(x_1,x_2) + \frac{\delta^4}{4}x_2^{8/3}\right]\xi_2^{1/5}. \tag{66}$$

With the similar arguments as above, we have

$$LV \le -(1-\delta)\left(\xi_1^{8/5} + \xi_2^{8/5}\right). \tag{67}$$

It follows from Proposition 2 and Lemma 2.3 in [13] that

$$LV \le -(1-\delta)\left(\xi_1^{8/5} + \xi_2^{8/5}\right) \le -\rho V^{4/5} \qquad \rho \in (0,0.5). \tag{68}$$

This shows that the origin of the system is globally stochasticly finite-time stable. □

4.1. Numerical Simulation. In this section, the performance of the proposed control schemes is evaluated via a numerical example. Consider the following dynamical system:

$$\begin{aligned} dx_1 &= x_2 dt, \\ dx_2 &= u dt + x_1 dw, \end{aligned} \tag{69}$$

where $w \approx N(0, 0.05)$. Let $\beta(x_1,x_2) = 0.4$ and $\sigma = 0.8$. Initial condition is selected as $x_1(0) = 1$ and $x_2(0) = -1$. A lower bound for $\varpi(x_1,x_2)$ is

$$\varpi(x_1,x_2) \ge \frac{|g(\mathbf{x})|^2}{|\xi_1|^{6/5} + |\xi_2|^{6/5}}. \tag{70}$$

Therefore, we can choose $\varpi(x_1,x_2)$ as

$$\varpi(x_1,x_2) = b\frac{|g(\mathbf{x})|^2}{|\xi_1|^{6/5} + |\xi_2|^{6/5}}, \tag{71}$$

where $b = 1.1$. The control law obtained from the results in Theorem 11 is

$$\begin{aligned} u = & -\beta(x_1,x_2)\left(x_2^{5/3} + 0.15x_1\right)^{1/5} \\ & -\left[\frac{7}{3}\varpi(x_1,x_2) + \frac{\delta^4}{4}x_2^{8/3}\right]\xi_2^{1/5}, \end{aligned} \tag{72}$$

where

$$\xi_1 = x_1, \qquad \xi_2 = x_2^{5/3} - x_2^{*5/3}, \quad x_2^* = -2x_1^{3/5}. \tag{73}$$

Numerical simulations are implemented in MATLAB with the step size 0.001. Figures 5 and 6 illustrate the effectiveness of simulation results using the control law (70). The state trajectories are shown in Figure 5. The control input is depicted in Figure 6. Obviously, the control signal (70) is not smooth although it gives a finite-time convergence.

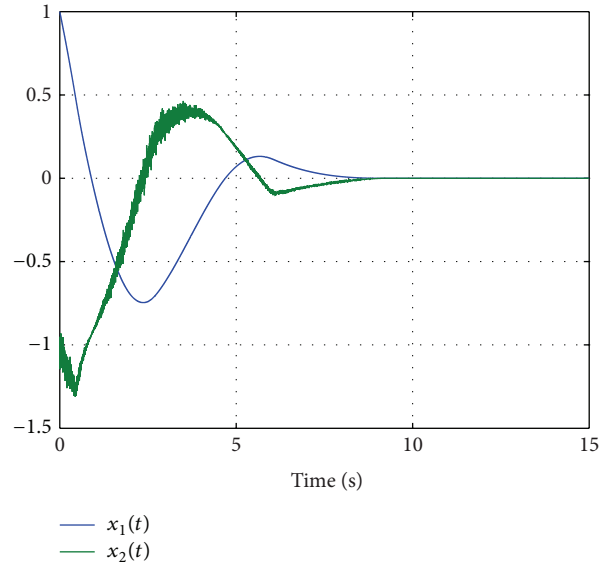

Figure 5: The state trajectories $x(t)$ due to the control scheme.

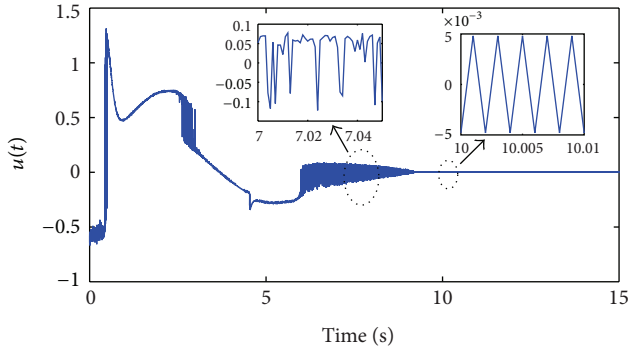

Figure 6: Input control $u(t)$ due to the control scheme.

5. Conclusions

Two guidance laws were proposed in stochastic setting. First, an adaptive guidance was presented to achieve target interception under measurement noise. The effectiveness of this result was evaluated using numerical simulations. Although this guidance law provided the effective robustness, it did not guarantee the finite-time convergence for the guidance system which is preferably required. Next, a robust control method was proposed to stabilize both the LOS angle and its angular velocity at the origin in finite-time under measurement noise. Simulation results demonstrated that the second guidance approach provided the finite-time convergence, but the signal input was not as smooth as the one in the first method. So this showed that balance between these approaches was needed.

Conflict of Interests

The authors declare that there is no conflict of interests regarding the publication of this paper.

References

[1] H. Deng and M. Krstić, "Stochastic stabilization part I: a backstepping design," *Systems and Control Letters*, vol. 32, no. 3, pp. 143–150, 1997.

[2] H. Deng and M. Krstić, "Output-feedback stochastic nonlinear stabilization," *IEEE Transactions on Automatic Control*, vol. 44, no. 2, pp. 328–333, 1999.

[3] S. Battilotti, "Lyapunov-based design of iISS feedforward systems with uncertainty and noisy measurements," *SIAM Journal on Control and Optimization*, vol. 46, no. 1, pp. 84–115, 2007.

[4] Z.-J. Wu, X.-J. Xie, and S.-Y. Zhang, "Adaptive backstepping controller design using stochastic small-gain theorem," *Automatica*, vol. 43, no. 4, pp. 608–620, 2007.

[5] J. Hu, Z. Wang, B. Shen, and H. Gao, "Gain-constrained recursive filtering with stochastic nonlinearities and probabilistic sensor delays," *IEEE Transaction on Signal Processing*, vol. 61, pp. 1230–1238, 2013.

[6] X. Mu and H. Liu, "Stabilization for a class of stochastic nonlinear systems via output feedback," *IEEE Transactions on Automatic Control*, vol. 53, no. 1, pp. 360–367, 2008.

[7] Z. Wang, D. W. C. Ho, H. Dong, and H. Gao, "Robust H∞ finite-horizon control for a class of stochastic nonlinear time-varying systems subject to sensor and actuator saturations," *IEEE Transactions on Automatic Control*, vol. 55, no. 7, pp. 1716–1722, 2010.

[8] Z. Wang, J. Lam, and X. Liu, "Stabilization of a class of stochastic nonlinear time-delay systems," *Journal of Nonlinear Dynamics and Systems Theory*, vol. 4, pp. 357–368, 2004.

[9] Z. Wu, M. Cui, P. Shi, and H. R. Karimi, "Stability of stochastic nonlinear systems with state-dependent switching," *IEEE Transaction on Automatic Control*, vol. 58, pp. 1904–1918, 2013.

[10] Y. Yin, P. Shi, and F. Liu, "Gain-scheduled PI tracking control on stochastic nonlinear systems with partially known transition probabilities," *Journal of the Franklin Institute*, vol. 348, no. 4, pp. 685–702, 2011.

[11] E. Moulay and W. Perruquetti, "Finite time stability and stabilization of a class of continuous systems," *Journal of Mathematical Analysis and Applications*, vol. 323, no. 2, pp. 1430–1443, 2006.

[12] S. P. Bhat and D. S. Bernstein, "Finite-time stability of continuous autonomous systems," *SIAM Journal on Control and Optimization*, vol. 38, no. 3, pp. 751–766, 2000.

[13] X. Huang, W. Lin, and B. Yang, "Global finite-time stabilization of a class of uncertain nonlinear systems," *Automatica*, vol. 41, no. 5, pp. 881–888, 2005.

[14] Y. Orlov, "Finite time stability and robust control synthesis of uncertain switched systems," *SIAM Journal on Control and Optimization*, vol. 43, no. 4, pp. 1253–1271, 2005.

[15] W. Chen and L. C. Jiao, "Finite-time stability theorem of stochastic nonlinear systems," *Automatica*, vol. 46, no. 12, pp. 2105–2108, 2010.

[16] D. Zhou, S. Sun, and K. L. Teo, "Guidance laws with finite time convergence," *Journal of Guidance, Control, and Dynamics*, vol. 32, no. 6, pp. 1838–1846, 2009.

[17] R. Z. Khas'minskii, *Stochastic Stability of Differential Equations*, S & N International, Rockville, Md, USA, 1980.

[18] H. Gilsing and T. Shardlow, "SDELab: a package for solving stochastic differential equations in MATLAB," *Journal of Computational and Applied Mathematics*, vol. 205, no. 2, pp. 1002–1018, 2007.

[19] S. Rubenthaler, "Numerical simulation of the solution of a stochastic differential equation driven by a Lévy process," *Stochastic Processes and Their Applications*, vol. 103, no. 2, pp. 311–349, 2003.

[20] S. Sun, D. Zhou, and W.-T. Hou, "A guidance law with finite time convergence accounting for autopilot lag," *Aerospace Science and Technology*, vol. 25, pp. 132–137, 2013.

[21] Y. Zhang, M. Sun, and Z. Chen, "Finite-time convergent guidance law with impact angle constraint based on sliding-mode control," *Nonlinear Dynamics*, vol. 70, no. 1, pp. 619–625, 2012.

Hindawi Publishing Corporation
Mathematical Problems in Engineering
Volume 2013, Article ID 749782, 9 pages
http://dx.doi.org/10.1155/2013/749782

Research Article

Stability Analysis of State Saturation 2D Discrete Time-Delay Systems Based on F-M Model

Dongyan Chen and Hui Yu

Department of Applied Mathematics, Harbin University of Science and Technology, Harbin 150080, China

Correspondence should be addressed to Hui Yu; hyu_hust@163.com

Received 25 September 2013; Accepted 13 November 2013

Academic Editor: Hongli Dong

The problem of stability analysis is investigated for a class of state saturation two-dimensional (2D) discrete time-delay systems described by the Fornasini-Marchesini (F-M) model. The delay is allowed to be a bounded time-varying function. By constructing the delay-dependent 2D discrete Lyapunov functional and introducing a nonnegative scalar β, a sufficient condition is proposed to guarantee the global asymptotic stability of the addressed systems. Subsequently, the criterion is converted into the linear matrix inequalities (LMIs) which can be easily tested by using the standard numerical software. Finally, two numerical examples are given to show the effectiveness of the proposed stability criterion.

1. Introduction

Over the past decades, the two-dimensional (2D) systems have received considerable attention due to their extensive applications [1]. The 2D discrete-time systems have been successfully applied to many practical areas such as signal processing, linear image processing, multidimensional digital filtering, seismographic data processing, water stream heating and thermal processes. To mention a few, the problem of linear image processing has been studied in [2] for 2D discrete systems based on the Roesser model (R model). Aiming at the design of the digital filter, the 2D discrete systems based on the Fornasini-Marchesini model (F-M model) have been discussed in [3]. Recently, the modeling, calculation, and stability of 2D discrete systems have been widely studied and a large amount of results on these topics have been published; see, for example, [4–9].

Saturation, as a common and typical nonlinear constraint for practical control systems, is often encountered in various industrial systems. The phenomena of saturations if not properly handled will inevitably affect the implementations of the designed control schemes and may lead to the occurrence of the zero-input limit cycles [10–13]. Dynamical systems with saturation nonlinearities appear commonly in networks and 2D digital filter [14, 15]. When designing the 2D digital filter by using fixed point arithmetic, saturations are introduced due to the overflow and quantization. Recently, many important results on stability analysis of 2D discrete F-M systems with state saturation have been reported in recent literature; see, for example, [16–21]. To be specific, by using the Lyapunov method and employing the property of matrix norm, some sufficient conditions have been presented in [16, 17] to guarantee the global asymptotic stability of the related systems. In [18], an internally stable condition has been given for the design of 2D filters. By introducing a nonnegative scalar, in [19, 20], the criteria based on linear matrix inequality (LMI) have been proposed to ensure the global asymptotic stability of F-M model. Recently, sufficient conditions have been derived in [21] to guarantee the global asymptotic stability of the addressed F-M systems with state saturation nonlinearities.

As well known, the time delays occur in many practical engineering systems [22–24]. The occurrence of the time delays would yield the instability of the controlled systems in some cases. So far, a great number of results have been reported; see, for example, [25–29]. In particular, considerable research attention has been devoted to the problems of stability analysis of 2D discrete time-delay systems. To be specific, by constructing an appropriate Lyapunov function and a scalar β, sufficient conditions have been proposed

in [26] for state saturation 2D discrete time-delay systems based on the R model. In [27], the state estimation problem has been investigated for 2D complex networks with randomly occurring nonlinearities and probabilistic sensor delays. Accordingly, some sufficient conditions have been established such that the resulted estimation error dynamics are globally asymptotically stable in the mean square sense. To be specific, the problems of global asymptotic stability have been given in [30, 31] for 2D discrete F-M systems with state saturation and constant time delays. However, to the best of author's knowledge, there has not been much work undertaken on the global asymptotic stability for state saturation 2D discrete time-varying delay systems based on F-M model.

In this paper, we aim to investigate the problem of global asymptotic stability for 2D discrete F-M systems with state saturation and time delays. Here, the delays are assumed to be time varying with known lower and upper bounds. By constructing a delay-dependent 2D discrete Lyapunov functional and introducing a nonnegative scalar β based on a row diagonally dominant matrix, a sufficient condition is proposed to guarantee the global asymptotic stability of the addressed systems. Subsequently, the problem of global asymptotic stability is converted into the problem of feasibility by solving the LMIs. Finally, two numerical examples are given to show the effectiveness of the proposed criterion. The main contribution of this paper lies in that new stability criterion is given for state saturation 2D discrete F-M systems with time-varying delays.

Notations. The fundamental notations used in the paper are given as follows: I_p and 0 denote the identity matrix and zero matrix with appropriate dimensions. For a matrix A, A^T stands for transpose of the matrix A. $A > 0$ means that A is positive definite symmetric matrix.

2. Problem Formulation and Preliminaries

In this paper, we consider the following 2D discrete F-M system with state saturation and time-varying delays:

$$\begin{aligned} x(k+1,l+1) &= f\left(y(k,l)\right), \\ y(k,l) &= \left[y_1(k,l), y_2(k,l), \ldots, y_n(k,l)\right]^T \\ &= A\begin{bmatrix} x(k,l+1) \\ x(k+1,l) \end{bmatrix} + A_d\begin{bmatrix} x\left(k-d_h(k),l+1\right) \\ x\left(k+1,l-d_v(l)\right) \end{bmatrix} \\ &= A_{11}x(k,l+1) + A_{12}x(k+1,l) \\ &\quad + A_{21}x\left(k-d_h(k),l+1\right) \\ &\quad + A_{22}x\left(k+1,l-d_v(l)\right), \end{aligned} \tag{1}$$

where $x(k,l)$ is the n-dimensional state vector and (k,l) is the 2-dimensional time variable along the vertical and horizontal directions satisfying $k \geq 0$, $l \geq 0$. $A = [A_{11}, A_{12}] \in R^{n\times 2n}$, $A_d = [A_{21}, A_{22}] \in R^{n\times 2n}$, $d_h(k)$ and $d_v(l)$ are time-varying delays along the vertical and horizontal directions, respectively. We assume $d_h(k)$ and $d_v(l)$ satisfying:

$$h_m \leq d_h(k) \leq h_M, \qquad v_m \leq d_v(l) \leq v_M, \tag{2}$$

where h_m and h_M denote the lower and upper bounds of the delay $d_h(k)$ along the horizontal directions, v_m and v_M denote the lower and upper bounds of the delay $d_v(l)$ along the vertical directions. Throughout this paper, the superscript T to any vector (or matrix) stands for the transpose of that vector (or matrix).

The saturation nonlinearity $f(\cdot)$ is given by

$$f\left(y(k,l)\right) = \left[f_1\left(y_1(k,l)\right), f_2\left(y_2(k,l)\right), \ldots, f_n\left(y_n(k,l)\right)\right]^T, \tag{3}$$

with

$$f_i\left(y_i(k,l)\right) = \begin{cases} 1, & y_i(k,l) > 1, \\ y_i(k,l), & \left|y_i(k,l)\right| \leq 1, \\ -1, & y_i(k,l) < -1, \end{cases} \quad (i = 1,2,\ldots,n). \tag{4}$$

The system (1) has finite initial conditions $x(k,0)$ and $x(0,l)$ with fixed yet nonzero values for $-h_M \leq k \leq K$ and $-v_M \leq l \leq L$, and

$$x(k,0) = 0, \quad k \geq K; \qquad x(0,l) = 0, \quad l \geq L, \tag{5}$$

where K and L are positive integers.

To proceed, we introduce the following definitions which will be used in the subsequent derivations.

Definition 1. The origin $x = 0$ of the 2D discrete time-delay system is said to be stable (in the sense of Lyapunov) if for every $\varepsilon > 0$ there exists a $\delta = \delta(\varepsilon) > 0$ such that

$$\|x(k,l)\| < \varepsilon, \tag{6}$$

for all $k \geq 0$, $l \geq 0$, whenever $\|x(k,0)\| < \delta$ $(-h_M \leq k \leq K)$ and $\|x(0,l)\| < \delta$ $(-v_M \leq l \leq L)$, where K and L are positive integers and $\|\cdot\|$ denotes any of the equivalent norms on R^n.

Definition 2 (see [21]). The origin $x = 0$ of the 2D system (1) is said to be globally asymptotically stable if the following conditions are simultaneously satisfied:

(1) system (1) is stable;

(2) every solution of system (1) tends to the origin as $k+l \to \infty$; that is,

$$\lim_{k\to\infty \text{ or } l\to\infty} x(k,l) = \lim_{k+l\to\infty} x(k,l) = 0. \tag{7}$$

Definition 3 (see [32]). The matrix M is said to be row diagonally dominant if

$$|m_{ii}| \geq \sum_{j=1, j\neq i}^{n} |m_{ij}|, \quad i \in [1, n]. \tag{8}$$

Definition 4. For a 2D function $V(k,l) = V^h(k,l) + V^v(k,l)$, denote its difference $\Delta V(k,l)$ as

$$\Delta V(k,l) = \Delta V^h(k,l) + \Delta V^v(k,l), \tag{9}$$

where

$$\begin{aligned} \Delta V^h(k,l) &= V^h(k+1,l+1) - V^h(k,l+1), \\ \Delta V^v(k,l) &= V^v(k+1,l+1) - V^v(k+1,l). \end{aligned} \tag{10}$$

3. Main Results

In this section, we aim to investigate the problem of stability analysis for the 2D discrete F-M system with state saturation and time-varying delays. By resorting to the LMI technique, a sufficient condition is given to ensure the global asymptotic stability of the addressed system.

Theorem 5. *The origin $x = 0$ of 2D discrete system* (1) *is globally asymptotically stable if there exist matrices P, Q, and M, where $P = P_1 + P_2$ and $Q = Q_1 + Q_2$ with $P_1 = [p_{ij}^1] \in R^{n\times n}$, $P_2 = [p_{ij}^2] \in R^{n\times n}$, $Q_1 = [q_{ij}^1] \in R^{n\times n}$, and $Q_2 = [q_{ij}^2] \in R^{n\times n}$ being symmetric positive definite matrices and $M = [m_{ij}] \in R^{n\times n}$ is row diagonally dominant with nonnegative diagonal elements, satisfying the following matrix inequality:*

$$\begin{bmatrix} \Pi_1 & M^T A_{11} & M^T A_{12} & M^T A_{21} & M^T A_{22} \\ * & \Pi_2 & 0 & 0 & 0 \\ * & * & \Pi_3 & 0 & 0 \\ * & * & * & -Q_1 & 0 \\ * & * & * & * & -Q_2 \end{bmatrix} < 0, \tag{11}$$

with

$$\begin{aligned} \Pi_1 &= P_1 + P_2 - \left(M + M^T\right), \\ \Pi_2 &= Q_1 - P_1 + \left(h_M - h_m\right) Q_1, \\ \Pi_3 &= Q_2 - P_2 + \left(\nu_M - \nu_m\right) Q_2. \end{aligned} \tag{12}$$

Proof. In order to prove the global asymptotic stability of the 2D discrete F-M system (1), we construct the following Lyapunov functional as in [26]:

$$V(k,l) = \sum_{i=1}^{3} V_i(k,l), \tag{13}$$

where

$$\begin{aligned} V_1(k,l) &= V_1^h(k,l) + V_1^v(k,l) \\ &= x^T(k,l) P_1 x(k,l) + x^T(k,l) P_2 x(k,l), \\ V_2(k,l) &= V_2^h(k,l) + V_2^v(k,l) \\ &= \sum_{i=k-d_h(k)}^{k-1} x^T(i,l) Q_1 x(i,l) \\ &\quad + \sum_{j=l-d_v(l)}^{l-1} x^T(k,j) Q_2 x(k,j), \\ V_3(k,l) &= V_3^h(k,l) + V_3^v(k,l) \\ &= \sum_{j=-h_M+1}^{-h_m} \sum_{i=k+j}^{k-1} x^T(i,l) Q_1 x(i,l) \\ &\quad + \sum_{i=-\nu_M+1}^{-\nu_m} \sum_{j=l+i}^{l-1} x^T(k,j) Q_2 x(k,j) \end{aligned} \tag{14}$$

with $P_1 > 0$, $P_2 > 0$, $Q_1 > 0$, and $Q_2 > 0$ being matrices to be determined.

According to Definition 4, the corresponding difference of $\Delta V(k,l)$ along the trajectory of system (1) can be calculated as follows:

$$\Delta V(k,l) = \sum_{i=1}^{3} \Delta V_i(k,l), \tag{15}$$

with

$$\begin{aligned} \Delta V_1(k,l) &= V_1(k+1,l+1) - x^T(k,l+1) P_1 x(k,l+1) \\ &\quad - x^T(k+1,l) P_2 x(k+1,l), \\ \Delta V_2(k,l) &= \sum_{i=k+1-d_h(k+1)}^{k} x^T(i,l+1) Q_1 x(i,l+1) \end{aligned}$$

$$
\begin{aligned}
&- \sum_{i=k-d_h(k)}^{k-1} x^T(i,l+1)\,Q_1 x(i,l+1) \\
&+ \sum_{j=l+1-d_v(l+1)}^{l} x^T(k+1,j)\,Q_2 x(k+1,j) \\
&- \sum_{j=l-d_v(l)}^{l-1} x^T(k+1,j)\,Q_2 x(k+1,j), \\
\Delta V_3(k,l) = &\sum_{j=-h_M+1}^{-h_m} \sum_{i=k+j+1}^{k} x^T(i,l+1)\,Q_1 x(i,l+1) \\
&- \sum_{j=-h_M+1}^{-h_m} \sum_{i=k+j}^{k-1} x^T(i,l+1)\,Q_1 x(i,l+1) \\
&+ \sum_{i=-v_M+1}^{-v_m} \sum_{j=l+i+1}^{l} x^T(k+1,j)\,Q_2 x(k+1,j) \\
&- \sum_{i=-v_M+1}^{-v_m} \sum_{j=l+i}^{l-1} x^T(k+1,j)\,Q_2 x(k+1,j).
\end{aligned} \tag{16}
$$

Noting (13)–(15), it can be derived that

$$
\begin{aligned}
\Delta V_1(k,l) = {} & x^T(k+1,l+1)\,P_1 x(k+1,l+1) \\
&+ x^T(k+1,l+1)\,P_2 x(k+1,l+1) \\
&- x^T(k,l+1)\,P_1 x(k,l+1) \\
&- x^T(k+1,l)\,P_2 x(k+1,l), \\
\Delta V_2(k,l) = {} & x^T(k,l+1)\,Q_1 x(k,l+1) \\
&- x^T(k-d_h(k),l+1)\,Q_1 x(k-d_h(k),l+1) \\
&+ \sum_{i=k+1-d_h(k+1)}^{k-1} x^T(i,l+1)\,Q_1 x(i,l+1) \\
&- \sum_{i=k+1-d_h(k)}^{k-1} x^T(i,l+1)\,Q_1 x(i,l+1) \\
&+ x^T(k+1,l)\,Q_2 x(k+1,l) \\
&- x^T(k+1,l-d_v(l))\,Q_2 x(k+1,l-d_v(l)) \\
&+ \sum_{j=l+1-d_v(l+1)}^{l} x^T(k+1,j)\,Q_2 x(k+1,j) \\
&- \sum_{j=l+1-d_v(l)}^{l-1} x^T(k+1,j)\,Q_2 x(k+1,j)
\end{aligned}
$$

$$
\begin{aligned}
&\le \sum_{i=k+1-h_M}^{k-1} x^T(i,l+1)\,Q_1 x(i,l+1) \\
&- \sum_{i=k+1-h_m}^{k-1} x^T(i,l+1)\,Q_1 x(i,l+1) \\
&+ \sum_{j=l+1-v_M}^{l-1} x^T(k+1,j)\,Q_2 x(k+1,j) \\
&- \sum_{j=l+1-v_m}^{l-1} x^T(k+1,j)\,Q_2 x(k+1,j) \\
&+ x^T(k,l+1)\,Q_1 x(k,l+1) \\
&- x^T(k-d_h(k),l+1)\,Q_1 x(k-d_h(k),l+1) \\
&+ x^T(k+1,l)\,Q_2 x(k+1,l) \\
&- x^T(k+1,l-d_v(l))\,Q_2 x(k+1,l-d_v(l)) \\
&= \sum_{i=k+1-h_M}^{k-h_m} x^T(i,l+1)\,Q_1 x(i,l+1) \\
&+ \sum_{j=l+1-v_M}^{l-v_m} x^T(k+1,j)\,Q_2 x(k+1,j) \\
&+ x^T(k,l+1)\,Q_1 x(k,l+1) \\
&- x^T(k-d_h(k),l+1)\,Q_1 x(k-d_h(k),l+1) \\
&+ x^T(k+1,l)\,Q_2 x(k+1,l) \\
&- x^T(k+1,l-d_v(l))\,Q_2 x(k+1,l-d_v(l)) \\
\Delta V_3(k,l) = {} & (h_M-h_m)\,x^T(k,l+1)\,Q_1 x(k,l+1) \\
&- \sum_{i=k+1-h_M}^{k-h_m} x^T(i,l+1)\,Q_1 x(i,l+1) \\
&+ (v_M-v_m)\,x^T(k+1,l)\,Q_2 x(k+1,l) \\
&- \sum_{j=l+1-v_M}^{l-v_m} x^T(k+1,j)\,Q_2 x(k+1,j).
\end{aligned} \tag{17}
$$

Denoting

$$
\begin{aligned}
\varphi(k,l) = {} & [f(y(k,l)), x(k,l+1), x(k+1,l), \\
& x(k-d_h(k),l+1), x(k+1,l-d_v(l))]^T,
\end{aligned} \tag{18}
$$

we have

$$
\Delta V(k,l) \le \varphi^T(k,l)\,\Theta\varphi(k,l), \tag{19}
$$

where

$$\Theta = \begin{bmatrix} P_1 + P_2 & 0 & 0 & 0 & 0 \\ * & (h_M - h_m + 1) Q_1 - P_1 & 0 & 0 & 0 \\ * & * & (v_M - v_m + 1) Q_2 - P_2 & 0 & 0 \\ * & * & * & -Q_1 & 0 \\ * & * & * & * & -Q_2 \end{bmatrix}. \tag{20}$$

Now, construct the following parameter β:

$$\begin{aligned} \beta &= 2\sum_{i=1}^{n} \left[y_i(k,l) - f_i(y_i(k,l)) \right] \\ &\quad \times \left[m_{ii} f_i(y_i(k,l)) + \sum_{j=1, j\neq i}^{n} m_{ij} f_j\left(y_j(k,l)\right) \right] \\ &= y^T(k,l) M f(y(k,l)) + f^T(y(k,l)) M^T y(k,l) \\ &\quad - f^T(y(k,l)) \left(M + M^T\right) f(y(k,l)). \end{aligned} \tag{21}$$

Let

$$\begin{aligned} \alpha_i = & \left[y_i(k,l) - f_i(y_i(k,l)) \right] \\ & \times \left[m_{ii} f_i(y_i(k,l)) + \sum_{j=1, j\neq i}^{n} m_{ij} f_j\left(y_j(k,l)\right) \right]. \end{aligned} \tag{22}$$

The saturation region can be divided into two regions, and we have

$$\begin{aligned} f_i(y_i(k,l)) &= 1, \\ y_i(k,l) - f_i(y_i(k,l)) &> 0, \text{ in Region 1}, \\ f_i(y_i(k,l)) &= -1, \\ y_i(k,l) - f_i(y_i(k,l)) &< 0, \text{ in Region 2}. \end{aligned} \tag{23}$$

Thus, we obtain

$$\alpha_i = \begin{cases} (y_i(k,l) - 1) \left(m_{ii} + \sum_{j=1, j\neq i}^{n} m_{ij} f_j\left(y_j(k,l)\right) \right), \\ \qquad \text{in Region 1}, \\ (y_i(k,l) + 1) \left(-m_{ii} + \sum_{j=1, j\neq i}^{n} m_{ij} f_j\left(y_j(k,l)\right) \right), \\ \qquad \text{in Region 2}. \end{cases} \tag{24}$$

Subsequently, due to the property of row diagonally dominant matrix M, we have $\alpha_i \geq 0$. Furthermore, note that β is the sum of nonnegative scalars, and hence $\beta \geq 0$. Therefore,

$$\Delta V \leq \varphi^T(k,l) W \varphi(k,l) - \beta, \tag{25}$$

where

$$W = \begin{bmatrix} \Pi_1 & M^T A_{11} & M^T A_{12} & M^T A_{21} & M^T A_{22} \\ * & \Pi_2 & 0 & 0 & 0 \\ * & * & \Pi_3 & 0 & 0 \\ * & * & * & -Q_1 & 0 \\ * & * & * & * & -Q_2 \end{bmatrix}. \tag{26}$$

If $W < 0$, then $\Delta V(k,l) < 0$; that is

$$\begin{aligned} & V^h(k+1, l+1) + V^v(k+1, l+1) \\ & \leq V^h(k, l+1) + V^v(k+1, l). \end{aligned} \tag{27}$$

Hence, for any nonnegative integer $d \geq \max\{K, L\}$, we have

$$\begin{aligned} \sum_{k+l=d+1} V(k,l) &= V(1,d) + V(2,d-1) + \cdots + V(d,1) \\ &\leq V^h(0,d) + V^v(1,d-1) + V^h(1,d-1) \\ &\quad + V^v(2,d-2) + \cdots + V^h(d-1,1) \\ &\quad + V^v(d,0) \\ &= \sum_{k+l=d} V(k,l). \end{aligned} \tag{28}$$

It is clear that the sum of the Lyapunov functional is a decreasing function along the state trajectories of system (1). Then, noting the initial condition $x(0,d) = x(d,0) = 0$, we have

$$\lim_{k\to\infty \text{ or } l\to\infty} x(k,l) = \lim_{k+l\to\infty} x(k,l) = 0. \tag{29}$$

Summarizing the above discussions, it can be shown that (11) is a sufficient condition which ensures the global asymptotic stability of system (1). This completes the proof of Theorem 5. □

As special cases, if there is no time delay in system (1), that is, $A_{21} = 0$ and $A_{22} = 0$, or the time delays are constant, then we can have the following corollaries.

Corollary 6. *Consider the system* (1) *without time delay. If there exist matrices P and M, with* $P = P_1 + P_2$, $P_1 = [p_{ij}^1] \in R^{n\times n}$, *and* $P_2 = [p_{ij}^2] \in R^{n\times n}$ *being symmetric positive definite matrices and* $M = [m_{ij}] \in R^{n\times n}$ *is row diagonally dominant*

with nonnegative diagonal elements, satisfying the following matrix inequality:

$$\begin{bmatrix} P - \left(M + M^T\right) & M^T A_{11} & M^T A_{12} \\ * & -P_1 & 0 \\ * & 0 & -P_2 \end{bmatrix} < 0 \qquad (30)$$

then the origin $x = 0$ of 2D discrete system (1) *without time delay is globally asymptotically stable.*

Corollary 7. *Consider the constant time delay $d_h(k) = d_h$, $d_v(l) = d_v$. If there exist matrices P, Q, and M, where $P = P_1 + P_2$ and $Q = Q_1 + Q_2$, with $P_1 = [p_{ij}^1] \in R^{n\times n}$, $P_2 = [p_{ij}^2] \in R^{n\times n}$, $Q_1 = [q_{ij}^1] \in R^{n\times n}$, and $Q_2 = [q_{ij}^2] \in R^{n\times n}$ being symmetric positive definite matrices and $M = [m_{ij}] \in R^{n\times n}$ is row diagonally dominant with nonnegative diagonal elements, satisfying the following matrix inequality:*

$$\begin{bmatrix} P_1 + P_2 - \left(M + M^T\right) & M^T A_{11} & M^T A_{12} & M^T A_{21} & M^T A_{22} \\ * & Q_1 - P_1 & 0 & 0 & 0 \\ * & * & Q_2 - P_2 & 0 & 0 \\ * & * & * & -Q_1 & 0 \\ * & * & * & * & -Q_2 \end{bmatrix} < 0, \qquad (31)$$

then the origin $x = 0$ of 2D discrete system (1) *with constant time delay is globally asymptotically stable.*

Remark 8. Note that the problem of global asymptotic stability has been investigated in [33] for state saturation 2D discrete system without time delay. Accordingly, a stability criterion has been derived in [33] but a positive diagonally matrix is needed to be searched. It can be easily seen that the stability condition in [33] is a special case of (30) in Corollary 6. Therefore, the stability condition proposed in this paper is less conservative than the one in [33]. Meanwhile, note that a stability condition has been proposed in [21] where an unknown matrix G must be given firstly. The values of G must take specific values. Compared with the results in [21], we only need to find matrix M. It concludes that the stability condition in [21] is more conservative than our result.

Remark 9. It is worth mentioning that the delay-fractioning approach has been employed in [34, 35] to reduce the conservativeness of the time delay. It has been shown that the developed approach performs well when dealing with the time delay compared with other methods. Accordingly, some effective SMC/SMO schemes based on the delay-fractioning idea have been proposed for discrete time-delay nonlinear stochastic systems with randomly occurring incomplete information. Motivated by the results in [34, 35], we are now researching into the stability criterion based on the delay-fractioning approach for the state saturation 2D discrete time-delay systems. The corresponding results will appear in the near future. Moreover, note that the recursive filters have been designed in [36–38] for time-varying networked nonlinear systems with missing measurements. It is also interesting to consider the analysis and synthesis of 2D discrete nonlinear systems with state saturations and missing measurements.

Remark 10. It is worth noting that the conditions in Theorem 5 are not strict LMI due to the fact that the matrix $M = [m_{ij}] \in R^{n\times n}$ is row diagonally dominant with nonnegative diagonal elements. Hence, the results of Theorem 5 and Corollary 6 are not convex which lead to the computational difficulties. In the following, an alternative approach is developed to deal with the nonconvex problem.

Let e_l be n-dimensional column vectors in which the lth element is 1 and other elements are 0. Let Y_l be the set of n-dimensional column vectors in which the lth element is -1 and other elements are either 1 or -1 and $Y_{ls} \in Y_l$ ($s \in [1, 2^{n-1}]$). Then, the condition where matrix $M = [m_{ij}] \in R^{n\times n}$ is row diagonally dominant and the diagonal is composed of nonnegative elements can be equivalently converted into the following LMIs:

$$e_l^T M Y_{ls} < 0, \quad l = 1, 2, \ldots, m+n;\ s \in \left[1, 2^{m+n-1}\right]. \qquad (32)$$

Together with (11) and (32), we can see that the proposed stability condition is a convex one and then can be easily solved by using the standard numerical software.

4. Numerical Examples

In this section, two numerical examples are given here to illustrate the effectiveness of the main results.

Example 1. Consider the state saturation 2D discrete time-delay system (1) with

$$A_{11} = \begin{bmatrix} 1.678 & 0.2853 & -0.2432 & -0.1246 \\ -0.84 & 0.23 & -0.1 & 1.45 \\ 0.4 & 0.0217 & 0.1785 & 0.1662 \\ 0.0245 & -0.00884 & 0.0321 & -0.2428 \end{bmatrix},$$

$$A_{12} = \begin{bmatrix} -0.495 & -0.687 & -0.030 & -0.3013 \\ -0.1630 & -0.4817 & -0.993 & 0.1814 \\ 0.2842 & 0.1790 & -0.5551 & 0.0799 \\ -0.2112 & 0.1887 & 0.0895 & 0.5604 \end{bmatrix},$$

$$A_{21} = \begin{bmatrix} -9.987 & -0.2 & 0 & 0 \\ 0 & -0.15 & 0 & -0.1 \\ 0 & 0 & -0.78 & 0 \\ -0.23 & 0 & 0 & -0.98 \end{bmatrix},$$

$$A_{22} = \begin{bmatrix} 5.763 & -0.067 & 0 & 0.04 \\ -2.314 & 0.342 & 0.098 & -5.78 \\ 4.56 & 0.001 & -0.98 & 0.231 \\ 0.23 & -0.76 & 0.043 & 8.6 \end{bmatrix}. \tag{33}$$

The lower and upper bounds are given by $h_M = 3$, $h_m = 1$, $\nu_M = 4$, and $\nu_m = 2$.

Solving the inequalities (11) and (32) in the Matlab environment, we can obtain

$$P_1 = \begin{bmatrix} 3.0067 & -0.0360 & -0.0043 & 0.0125 \\ -0.0360 & 3.1420 & 0.1635 & 0.2573 \\ -0.0043 & 0.1635 & 2.9443 & 0.1253 \\ 0.0125 & 0.2573 & 0.1253 & 2.9694 \end{bmatrix},$$

$$P_2 = \begin{bmatrix} 2.9848 & -0.0225 & -0.0006 & 0.0463 \\ -0.0225 & 3.1494 & 0.1757 & 0.2382 \\ -0.0006 & 0.1757 & 3.0049 & 0.0990 \\ 0.0463 & 0.2382 & 0.0990 & 2.9051 \end{bmatrix},$$

$$Q_1 = \begin{bmatrix} 0.5521 & -0.0048 & -0.0017 & 0.0417 \\ -0.0048 & 0.6168 & 0.0461 & 0.0573 \\ -0.0017 & 0.0461 & 0.5631 & 0.0356 \\ 0.0417 & 0.0573 & 0.0356 & 0.4917 \end{bmatrix}, \tag{34}$$

$$Q_2 = \begin{bmatrix} 0.5676 & -0.0144 & -0.0043 & 0.0175 \\ -0.0144 & 0.6115 & 0.0374 & 0.0709 \\ -0.0043 & 0.0374 & 0.5198 & 0.0545 \\ 0.0175 & 0.0709 & 0.0545 & 0.5376 \end{bmatrix},$$

$$M = \begin{bmatrix} 0.2812 & 0.0241 & -0.0475 & -0.0020 \\ 0.0353 & 0.6877 & 0.0609 & 0.2516 \\ -0.0769 & 0.0654 & 0.7074 & 0.0128 \\ 0.0027 & 0.1886 & -0.0018 & 0.5205 \end{bmatrix}.$$

Then, we can see that there exist the required matrices P_1, P_2, Q_1, Q_2, and M satisfying LMIs (11) and (32). As such, according to Theorem 5, the origin $x = 0$ of system (1) is globally asymptotically stable which confirms the feasibility of the proposed main results.

Example 2. Consider a 2D system described by (1) without time delay. The system parameters are given as

$$A_{11} = \begin{bmatrix} 1.2 & -2.8 \\ 0.1 & 0 \end{bmatrix},$$

$$A_{12} = \begin{bmatrix} 0 & 0.01 \\ 0 & 0.02 \end{bmatrix}. \tag{35}$$

By using the Matlab LMI Toolbox, it can be easily verified that the following feasible solutions can be obtained

$$P_1 = \begin{bmatrix} 1421.7 & -203.9 \\ -203.9 & 1698.1 \end{bmatrix}, \quad P_2 = \begin{bmatrix} 1321 & 25 \\ 25 & 1167.5 \end{bmatrix},$$
$$M = \begin{bmatrix} 434.848 & -11.3033 \\ -9.1992 & 818.5481 \end{bmatrix}. \tag{36}$$

That is, there exist the required matrices P_1, P_2, and M satisfying LMI (30). According to Corollary 6, the origin of system (1) is globally asymptotically stable which confirms the effectiveness of the presented results. However, it can be tested that the conditions in [33] are infeasible. Therefore, the result in our paper is less conservative than the one in [33].

5. Conclusions

In this paper, we have discussed the problem of global asymptotic stability for 2D discrete F-M systems with state saturation and time-varying delays. By constructing the 2D discrete-time Lyapunov functional, a new stability criterion has been established to ensure that the addressed system is globally asymptotically stable. The proposed stability criterion is in terms of the LMIs which can be easily tested by using the Matlab matrix toolbox. Two numerical examples have been given to demonstrate the feasibility of the proposed stability condition. It is worth mentioning that the construction of the scalar β has taken full effects from time delays with hope to reduce the conservativeness. One of the future research topics would be the extension of the proposed main results to more general state saturation 2D discrete systems as in [39–41] with network-induced phenomena.

Acknowledgments

This work was supported in part by the Science Research Project of Abroad Scholars of Educational Commission of Heilongjiang Province under Grant 1152hq09 and the National Natural Science Foundation of China under Grants 11271103 and 11301118.

References

[1] C. E. de Souza, L. Xie, and D. F. Coutinho, "Robust filtering for 2-D discrete-time linear systems with convex-bounded parameter uncertainty," *Automatica*, vol. 46, no. 4, pp. 673–681, 2010.

[2] R. P. Roesser, "A discrete state-space model for linear image processing," *IEEE Transactions on Automatic Control*, vol. 20, no. 1, pp. 1–10, 1975.

[3] E. Fornasini and G. Marchesini, "State-space realization theory of two-dimensional filters," *IEEE Transactions on Automatic Control*, vol. 21, no. 4, pp. 484–492, 1976.

[4] N. G. El-Agizi and M. M. Fahmy, "Two-dimensional digital filters with no overflow oscillations," *IEEE Transactions on Acoustics, Speech and Signal Processing*, vol. 27, no. 5, pp. 465–469, 1979.

[5] H. Gao, J. Lam, S. Xu, and C. Wang, "Stability and stabilization of uncertain 2-D discrete systems with stochastic perturbation,"

Multidimensional Systems and Signal Processing, vol. 16, no. 1, pp. 85–106, 2005.

[6] H. Gao, J. Lam, C. Wang, and S. Xu, "H_∞ model reduction for uncertain two-dimensional discrete systems," *Optimal Control Applications & Methods*, vol. 26, no. 4, pp. 199–227, 2005.

[7] P. Agathoklis, "Lower bounds for the stability margin of discrete two-dimensional systems based on the two-dimensional Lyapunov equation," *IEEE Transactions on Circuits and Systems*, vol. 35, no. 6, pp. 745–749, 1988.

[8] M. G. B. Sumanasena and P. H. Bauer, "Realization using the Fornasini-Marchesini model for implementations in distributed grid sensor networks," *IEEE Transactions on Circuits and Systems I: Regular Papers*, vol. 58, no. 11, pp. 2708–2717, 2011.

[9] X. Li and H. Gao, "Robust finite frequency H_∞ filtering for uncertain 2-D systems: the FM model case," *Automatica*, vol. 49, no. 8, pp. 2446–2452, 2013.

[10] T. A. C. M. Claasen, W. F. G. Mecklenbräuker, and J. B. H. Peek, "Effects of quantization and overflow in recursive digital filters," *IEEE Transactions on Acoustics, Speech and Signal Processing*, vol. 24, no. 6, pp. 517–529, 1976.

[11] D. Chen, S. Li, and Y. Shi, "The practical stabilization for a class of networked systems with actuator saturation and input additive disturbances," *Mathematical Problems in Engineering*, vol. 2012, Article ID 326876, 19 pages, 2012.

[12] J. Hu, Z. Wang, H. Gao, and L. K. Stergioulas, "Probability-guaranteed H_∞ finite-horizon filtering for a class of nonlinear time-varying systems with sensor saturations," *Systems & Control Letters*, vol. 61, no. 4, pp. 477–484, 2012.

[13] Z. Wang, B. Shen, and X. Liu, "H_∞ filtering with randomly occurring sensor saturations and missing measurements," *Automatica*, vol. 48, no. 3, pp. 556–562, 2012.

[14] H. Kar and V. Singh, "Stability analysis of 2-D digital filters with saturation arithmetic: an LMI approach," *IEEE Transactions on Signal Processing*, vol. 53, no. 6, pp. 2267–2271, 2005.

[15] V. Singh, "Robust stability of 2-D digital filters employing saturation," *IEEE Signal Processing Letters*, vol. 12, no. 2, pp. 142–145, 2005.

[16] D. R. Liu and A. N. Michel, "Stability analysis of state-space realizations for two-dimensional filters with overflow nonlinearities," *IEEE Transactions on Circuits and Systems I: Fundamental Theory and Applications*, vol. 41, no. 2, pp. 127–137, 1994.

[17] D. Liu, "Lyapunov stability of two-dimensional digital filters with overflow nonlinearities," *IEEE Transactions on Circuits and Systems I: Fundamental Theory and Applications*, vol. 45, no. 5, pp. 574–577, 1998.

[18] E. Fornasini and G. Marchesini, "On the internal stability of two-dimensional filters," *IEEE Transactions on Automatic Control*, vol. 24, no. 1, pp. 129–130, 1979.

[19] H. Kar and V. Singh, "Stability analysis of 2-D digital filters described by the Fornasini-Marchesini second model using overflow nonlinearities," *IEEE Transactions on Circuits and Systems I: Fundamental Theory and Applications*, vol. 48, no. 5, pp. 612–617, 2001.

[20] H. Kar and V. Singh, "Stability analysis of 1-D and 2-D fixed-point state-space digital filters using any combination of overflow and quantization nonlinearities," *IEEE Transactions on Signal Processing*, vol. 49, no. 5, pp. 1097–1105, 2001.

[21] V. Singh, "Stability analysis of 2-D discrete systems described by the Fornasini-Marchesini second model with state saturation," *IEEE Transactions on Circuits and Systems II : Express Briefs*, vol. 55, no. 8, pp. 793–796, 2008.

[22] Z. Wang, Y. Liu, and X. Liu, "Exponential stabilization of a class of stochastic system with Markovian jump parameters and mode-dependent mixed time-delays," *IEEE Transactions on Automatic Control*, vol. 55, no. 7, pp. 1656–1662, 2010.

[23] H. Dong, Z. Wang, and H. Gao, "Distributed H_∞ filtering for a class of Markovian jump nonlinear time-delay systems overlossy sensor networks," *IEEE Transactions on Industrial Electronics*, vol. 60, no. 10, pp. 4665–4672, 2013.

[24] J. Hu, Z. Wang, H. Gao, and L. K. Stergioulas, "Robust H_∞ sliding mode control for discrete time-delay systems with stochastic nonlinearities," *Journal of the Franklin Institute*, vol. 349, no. 4, pp. 1459–1479, 2012.

[25] B. Shen, S. X. Ding, and Z. Wang, "Finite-horizon H_∞ fault estimation for linear discrete time-varying systems with delayed measurements," *Automatica*, vol. 49, no. 1, pp. 293–296, 2013.

[26] S.-F. Chen, "Delay-dependent stability for 2D systems with time-varying delay subject to state saturation in the Roesser model," *Applied Mathematics and Computation*, vol. 216, no. 9, pp. 2613–2622, 2010.

[27] J. Liang, Z. Wang, and X. Liu, "State estimation for two-dimensional complex networks with randomly occurring nonlinearities and randomly varying sensor delays," *International Journal of Robust and Nonlinear Control*.

[28] J. Hu, Z. Wang, B. Shen, and H. Gao, "Gain-constrained recursive filtering with stochastic nonlinearities and probabilistic sensor delays," *IEEE Transactions on Signal Processing*, vol. 61, no. 5, pp. 1230–1238, 2013.

[29] Z. Wang, B. Shen, H. Shu, and G. Wei, "Quantized H_∞ control for nonlinear stochastic time-delay systems with missing measurements," *IEEE Transactions on Automatic Control*, vol. 57, no. 6, pp. 1431–1444, 2012.

[30] S.-F. Chen, "Stability analysis of 2-D state-delayed systems with saturation nonlinearities," in *Proceedings of the 7th Asian Control Conference (ASCC '09)*, pp. 412–417, Hong Kong, China, August 2009.

[31] A. Dey and H. Kar, "An LMI based criterion for the global asymptotic stability of 2-D discrete state-delayed systems with saturation nonlinearities," *Digital Signal Processing*, vol. 22, no. 4, pp. 633–639, 2012.

[32] H. Fang and Z. Lin, "Stability analysis for linear systems under state constraints," *IEEE Transactions on Automatic Control*, vol. 49, no. 6, pp. 950–955, 2004.

[33] T. Hinamoto, "Stability of 2-D discrete systems described by the Fornasini-Marchesini second model," *IEEE Transactions on Circuits and Systems I: Fundamental Theory and Applications*, vol. 44, no. 3, pp. 254–257, 1997.

[34] J. Hu, Z. Wang, Y. Niu, and L. K. Stergioulas, "H_∞ sliding mode observer design for a class of nonlinear discrete time-delay systems: a delay-fractioning approach," *International Journal of Robust and Nonlinear Control*, vol. 22, no. 16, pp. 1806–1826, 2012.

[35] J. Hu, Z. Wang, H. Gao, and L. K. Stergioulas, "Robust sliding mode control for discrete stochastic systems with mixed time delays, randomly occurring uncertainties, and randomly occurring nonlinearities," *IEEE Transactions on Industrial Electronics*, vol. 59, no. 7, pp. 3008–3015, 2012.

[36] J. Hu, Z. Wang, H. Gao, and L. K. Stergioulas, "Extended Kalman filtering with stochastic nonlinearities and multiple missing measurements," *Automatica*, vol. 48, no. 9, pp. 2007–2015, 2012.

[37] H. Dong, Z. Wang, and H. Gao, "Distributed filtering for a class of time-varying systems over sensor networks with quantization

errors and successive packet dropouts," *IEEE Transactions on Signal Processing*, vol. 60, no. 6, pp. 3164–3173, 2012.

[38] J. Hu, Z. Wang, and H. Gao, "Recursive filtering with random parameter matrices, multiple fading measurements and correlated noises," *Automatica*, vol. 49, no. 11, pp. 3440–3448, 2013.

[39] Z. Wang, D. Ding, H. Dong, and H. Shu, "H_∞ consensus control for multi-agent systems with missing measurements: the finite-horizon case," *Systems and Control Letters*, vol. 62, no. 10, pp. 827–836, 2013.

[40] J. Hu, Z. Wang, B. Shen, and H. Gao, "Quantised recursive filtering for a class of nonlinear systems with multiplicative noises and missing measurements," *International Journal of Control*, vol. 86, no. 4, pp. 650–663, 2013.

[41] Z. Wang, H. Dong, B. Shen, and H. Gao, "Finite-horizon H_∞ filtering with missing measurements and quantization effects," *IEEE Transactions on Automatic Control*, vol. 58, no. 7, pp. 1707–1718, 2013.

Hindawi Publishing Corporation
Mathematical Problems in Engineering
Volume 2013, Article ID 675381, 8 pages
http://dx.doi.org/10.1155/2013/675381

Research Article

Load Distribution of Evolutionary Algorithm for Complex-Process Optimization Based on Differential Evolutionary Strategy in Hot Rolling Process

Xu Yang,[1,2] Chang-bin Hu,[3] Kai-xiang Peng,[1] and Chao-nan Tong[1]

[1] *Key Laboratory of Advanced Control of Iron and Steel Process, School of Automation and Electrical Engineering, University of Science and Technology Beijing, Beijing 100083, China*
[2] *Institute for Automatic Control and Complex Systems, University of Duisburg-Essen, Duisburg 47057, Germany*
[3] *Beijing Power Electronics and Motor Drives Engineering Research Center, College of Mechanical and Electrical Engineering, North China University of Technology, Beijing 100144, China*

Correspondence should be addressed to Xu Yang; ustb.yangxu@gmail.com

Received 5 September 2013; Revised 21 October 2013; Accepted 31 October 2013

Academic Editor: Xiao He

Based on the hot rolling process, a load distribution optimization model is established, which includes rolling force model, thickness distribution model, and temperature model. The rolling force ratio distribution and good strip shape are integrated as two indicators of objective function in the optimization model. Then, the evolutionary algorithm for complex-process optimization (EACOP) is introduced in the following optimization algorithm. Due to its flexible framework structure on search mechanism, the EACOP is improved within differential evolutionary strategy, for better coverage speed and search efficiency. At last, the experimental and simulation result shows that evolutionary algorithm for complex-process optimization based on differential evolutionary strategy (DEACOP) is the organism including local search and global search. The comparison with experience distribution and EACOP shows that DEACOP is able to use fewer adjustable parameters and more efficient population differential strategy during solution searching; meanwhile it still can get feasible mathematical solution for actual load distribution problems in hot rolling process.

1. Introduction

With the increasing demand for improving the product quality and control accuracy in hot rolling process, the rolling scheduling problem has become an important issue in the steel industry. According to the principle that nominal motor power should be greater than rolling power, the main purpose of hot rolling scheduling problem consists in determining the final thickness for every rolling pass to set other process parameters [1], such as rolling force and bending force. The key point and object of hot rolling shape/gauge control is the shape control of roll gap, in the sense that the load distribution is the basis of strip shape control. Although the classic load distribution is simple and reasonable, it cannot achieve the most optimal setting to shape control [1, 2].

The hot rolling process has been optimized with rolling theory or heuristics algorithms [3–5]. For example, a differential evolution algorithm with space-adaptive idea is applied to several hot strip mills for the optimal design of scheduling. This algorithm expands or shrinks the search space by certain rules and realizes the automatic search for the suitable space and improves the convergence rate and accuracy [3]. An intelligent method named variable metric hybrid genetic algorithm was introduced to optimize hot strip mills [4]. A genetic algorithm-based optimization was coded and operated for 1370 mm tandem cold rolling schedule. It seems that the performance of the optimal rolling schedule is satisfactory and promising [5]. Although the above load distribution is reasonable, it often requires more adjustable parameters during the search for optimal solution, thereby making influence on coverage speed and search efficiency.

Thus, the major objective pursued in this paper is to formulate a better solution on the rolling scheduling optimization. Based on the evolutionary algorithm for complex-process optimization (EACOP) [6–8], we improve

this algorithm within differential evolutionary strategy and utilize it to optimize load distribution of hot rolling. The DEACOP has the flexible structure which is similar to scatter search and employs some elements of scatter search [9] and path relinking [10]. Besides, it makes use of a smaller number of tuning parameters and differential evolutionary strategy among the population members with new strategies. Firstly, according to model's characteristics of load distribution, initial diverse population strategy will be improved with the consideration of latin hypercube uniform sampling. Secondly, differential evolutionary strategy will be presented to replace the original linear combination. Thirdly, a population-update method is introduced to modify the balance between intensification and diversification. Finally, a search intensification strategy called the "go-beyond" to in-depth search is established for enhancement of the efficiency of the local optimal solution. This differential evolutionary strategy can generate broader area around the population members and get better intensification and diversification of population members by the go-beyond strategy.

Based on experimental simulation by actual data in hot rolling process, simulation result shows that the application of DEACOP optimizes the gauge reduction for each rolling pass and gives full play to the upstream rolling mill equipment's ability. Meanwhile, DEACOP algorithm regulates crown index of the downstream mills, so it can further improve the efficiency of plate-shaped regulating.

2. The Gauge and Shape Model

2.1. System Description. In order to determine rolling force of each stand, as well as the other settings, the key point of load distribution is that the exit thickness of each stand should be distributed reasonably. Thus, in this section the optimal load distribution with the consideration of overall performance on shape and gauge is proposed. The optimal load distribution of finishing mill group can be divided into three stages [11–13].

The first phase requires that the 1st stand's reduction should be left some room, as the steel billet's thickness may fluctuate when steel billet goes into rolling mill.

In the second phase, the 2nd and 3rd stands should make full use of equipment power, therefore making the amount of the reduction as large as possible.

In the third phase, the rolling force in the last stage should gradually decrease from the 4th to the last stand, so that the accuracy and performance of the shape and gauge can be synthesized properly. Meanwhile, the relative crown of the last four stands should be equal.

With the consideration of those steps, the objective function is derived as follows, which constructs with the desire of above three stages with DEACOP optimizes load distribution:

$$G = \omega_1\left(P_1 - K_1P_2\right)^2 + \omega_2\left(P_2 - K_2P_3\right)^2 + \omega_3\sum_{i=4}^{7}\left(\frac{\mathrm{CR}_i}{h_i} - \frac{\mathrm{CR}_n}{h_n} \pm \Delta_i\right)^2, \tag{1}$$

where P_i is the rolling force of the ith stand, CR_i and h_i separately represent exit crown and thickness of the ith stand, ω_i denotes weighted coefficient, and Δ_i is the compensation coefficient, which maintain the equality of relative crown from the 4th to the last stand. From the view of engineering, some related variables of rolling process can be restricted, such as $h_{i+1} < h_i$, $0 \le P_i \le P_{\max}$.K_1 and K_2 denote the proportional coefficient about rolling force and both coefficients are changed according to technological condition, where K_1 is set as 0.9 and K_2 is set as 1 in this paper. Apart from the above constraints, the Shohet discriminant [1] about sheet deformation is also necessary. Since the rolling process of hot strip mill is different from the cold rolling, to some extent, Shohet discriminant may relax the requirement of relative crown:

$$-80\left(\frac{h}{B}\right)^{\alpha} < \left(\frac{C_H}{H} - \frac{C_h}{h}\right) < 40\left(\frac{h}{B}\right)^{\alpha}, \tag{2}$$

where H, h denote the entry and exit strip thickness, C_H/H and C_h/h separately stand for relative crown of entry and exit, B is the strip width, and $\alpha = 2$ or 1.86.

The main purpose of load distribution system is seeking a set of data h_i, which not only meets the Shohet equation, but also can fulfill those technological conditions. Meanwhile, in order to get the minimum value of objective function, the rolling force model, thickness distribution model, and the temperature model have to be established.

2.2. Rolling Force Model. According to [1], the classic rolling force equation can be expressed as follows:

$$P_i = 1.15Bl_c'Q_P\sigma, \tag{3}$$

$$Q_P = 0.8049 - 0.3393\varepsilon + \left(0.2488 + 0.0393\varepsilon + 0.0732\varepsilon^2\right)\frac{l_c}{h_m}, \tag{4}$$

$$\sigma = \sigma_0\exp\left(a_1T + a_2\right)\left(\frac{u}{10}\right)^{(a_3T+a_4)} \times \left[a_6\left(\frac{e}{0.4}\right)^{a_5} - \left(a_6 - 1\right)\left(\frac{e}{0.4}\right)\right], \tag{5}$$

where the subscript i denotes the rolling pass number, B is the strip width, and l_c' denotes the horizontal projection length of contact arc between roll and workpiece. $l_c' = \sqrt{R'\Delta h}$, $R' = R(1 + (16(1-\nu^2)/\pi E)(P_i/B\Delta h))$, where R is roller radius, R' is roller radius after deformation [12], Δh is the reduction for every rolling pass, ν is Poisson's ratio, and E is Young's modulus. Relative deformation degree and average thickness are denoted as ε and h_m in (4). Deformation resistance introduces (5), where $T = (t + 273)/1000$ and t is rolling temperature. $\varepsilon = \ln(h_{i-1}/h_i)$ and $u = (v_i\varepsilon/l_c')$ separately stand for deformation degree and rate about workpiece.

2.3. Thickness Distribution Model. Consider the following:

$$h_i' = H_0 \exp\left\{\frac{K_{H2} - \sqrt{K_{H2}^2 + 4K_{H1}\phi_i a_n}}{2K_{H1}}\right\}, \quad (6)$$

$$a_n = K_{H1}\left(\ln\frac{H_0}{h_n}\right)^2 + K_{H2}\ln\left(\frac{H_0}{h_n}\right), \quad (7)$$

where h_i' is the experiential thickness value, K_{H1}, K_{H2} denote the site statistics coefficient, ϕ_i is cumulative energy distribution coefficient, H_0 is initial thickness when workpieces go into the first finishing mill, and $h_n$is exit thickness when workpieces go through the last stand.

2.4. Temperature Model. Temperature is an important factor in hot rolling, which can directly impact on the rolling force value of each pass. Equation (8) expresses temperature drop model from roughing exit to finishing entrance, while the next equation denotes slab temperature drop caused by going through finishing mill:

$$T_{F0} = 100\left[\frac{6\varepsilon\delta}{100\gamma c H_0}\tau + \left(\frac{T_{\mathrm{RC}}}{100}\right)^{-3}\right]^{-1/3}, \quad (8)$$

$$T_i = T_w + (T_{F0} - T_w)\exp\left(-K_a\frac{\sum_{j=1}^{i} L_j}{h_n v_n}\right). \quad (9)$$

T_{F0} means entry temperature when slab goes into the first finishing mill. ε is blackness, δ is Boltzmann constant, γ is density, c is specific heat capacity, and τ is the time when strip is transferred from the exit of roughing mill to the entrance of the finishing mill. T_{RC} is steel temperature after strip going through roughing mill.

The exit temperature of each finishing mill is denoted as T_i. T_w is water spray temperature between mills. K_a is cooling coefficient, the interstand distance (L_j) is indicated, and $h_n v_n$ is the product that multiplies exit thickness by rolling speed.

3. Evolutionary Algorithm for Complex-Process Optimization

In this section, the evolutionary algorithm for complex-process optimization based on differential evolutionary strategy (DEACOP) is proposed to solve load distribution problem of the hot rolling scheduling. The DEACOP is innovative strategy embedded in various submethods within the flexible. This algorithm improves path relinking to generate a new combination method which considers a broader area around the population members. Meanwhile DEACOP improves the balance between intensification and diversification with a population-update method. The above strategies can escape from suboptimal solutions and advance the search efficiency. The algorithm consists of five parts: (1) building the initial population, (2) determining similarity solution, (3) differential evolutionary strategy, (4) population update, and (5) deep search feasible solutions. Its principle is to deeply explore new population members near individuals with minimum fitness. The optimization process will be repeatedly executed unless the stop conditions were met.

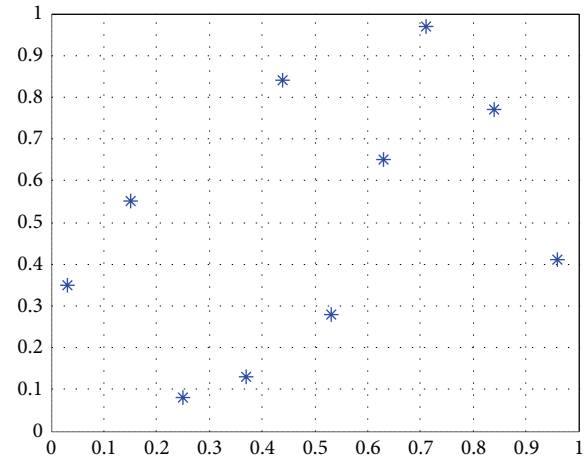

Figure 1: LHS ($H = 10, N = 2$).

3.1. Building the Initial Population. In this subsection a latin hypercube uniform sampling (LHS) is first used to generate the initial population. To illustrate how LHS works, during the following description we will explain the building process of LHS. N is variable dimension that is set as 2; sampling size H is 10. The distribution procedure of LHS is as follows.

3.1.1. LHS Algorithm

(1) Each side of the test area was divided equally into 10 parts, so test area was divided into 10^2 small areas.

(2) (1, 2, ..., 10) is randomly ordered to (7, 5, 6, 9, 2, 4, 1, 8, 10, 3) and (7, 9, 3, 8, 6, 2, 4, 10, 5, 1). They are arranged in a matrix as follows:

$$A = \begin{bmatrix} 7 & 5 & 6 & 9 & 2 & 4 & 1 & 8 & 10 & 3 \\ 7 & 9 & 3 & 8 & 6 & 2 & 4 & 10 & 5 & 1 \end{bmatrix}^T. \quad (10)$$

Column of the matrix, such as (7,7), (5,9), (6,3) ... (3,1), is fixed on 10 rectangles.

(3) A sample was randomly selected in each small rectangle, and then sampling group was composed of 10 samples. The result about LHS works is shown in Figure 1.

Through LHS procedure, an initial set Pop of Psize diverse vectors is generated, whose size is set as 10 × Nvar (Nvar is defined as a number of variables which need to be optimized). Meanwhile high-quality solution set *Pop1* is composed in terms of better fitness. Its number is $b1$. Diversity set *Pop2* (its size is $b2$) includes individual selected randomly from the remaining $m-b1$ vectors in Pop. According to the above completion strategy, the population size is $b = b1+b2$. McKay et al. [14] pointed out that the total average received LHS than a simple random sampling mean has smaller total variance.

```
for i = 1 to b
    for j = i to b
        if d(x_i, x_j) = ||x_i − x_j|| ≤ dist  then one of two solutions will be replaced with random solution within the search space.
        else
            until the end of the loop
        endif
    endfor
endfor
```

Algorithm 1: Check for solutions similarity algorithm.

3.2. Check for Similarity Solution. The purpose of similarity determining is to help escape from (possible) local optimal area. Algorithm 1 checks for duplicity with Euclid distance in the population before performing the next subsection (combination method). If the Euclidean distance between the two solutions is less than set value *dist*, then one of two solutions will be replaced with random solution within the search space. Otherwise, reserve two solutions and continue to the next judge.

3.3. Differential Evolutionary Strategy of Population. In the traditional EACOP, the reference set was usually based on linear combination method, which has advantage in some aspects. Unfortunately, there is difficult to solutions of complex issue. Thus, an improved differential variation method was introduced as follows:

$$M_i^{t+1} = X_i^t + F\left(\left(X_{r1}^t - X_i^t\right) + \left(X_{r2}^t - X_{r3}^t\right)\right), \quad (11)$$

where M_i^{t+1} is individual set after variation, X_{r1}^t is the current best individual populations, and F is scaling factor. $(X_{r1}^t - X_i^t)$ item was used in this strategy in order to increase the algorithm coverage speed. Meanwhile $(X_{r2}^t - X_{r3}^t)$ was introduced as disturbance, which can make difference for each variation individual, therefore maintaining the population diversity.

Besides, the crossover strategy is used for better evolutionary effects. After the crossover operation on X_i^t and M_i^{t+1}, thereby generating the new individual C_{ij}^{t+1}. The crossover strategy equation can be expressed as follows:

$$C_{ij}^{t+1} = \begin{cases} M_{ij}^{t+1}, & \text{rand} \le \text{CR} \\ X_{ij}^t, & \text{rand} > \text{CR} \end{cases} \quad j = 1, 2, \ldots, n, \quad (12)$$

where CR can be defined as crossover probability factor between 0 and 1 and rand is uniform random number in the same interval.

3.4. Population Update. As described in the combination method, we incorporate each member of the reference set with the rest $b - 1$ members, resulting in $b - 1$ new solution. Best quality solutions among new solutions were chosen and compared with their parent, if their value is better than the parent, and then the latter is replaced in the population. The principle of population regeneration is that new solutions are generated along with the path formed by the parent superrectangular.

3.5. Deep Search Feasible Solutions. By the previous steps, the new population members are surrounded by hyperrectangle in accordance with update strategy. For enhancing the search intensification to exploit better feasible solutions, the evolutionary algorithm has implemented *go-beyond* strategy which consists in exploiting promising directions. *Go-beyond* strategy (Figure 2) means that new solution is created in the light of direction defined by the child and its parent (Algorithm 3).

Deep search step is shown as follows: firstly, create a new solution x_{child} in hyperrectangle which is generated by a pair of solutions (x_i, x_j) and estimate if fitness value $f(x_{\text{child}})$ outperforms parent fitness value $f(x_i \text{ or } x_j)$ (x_i, x_j is selected after deciding which of them is combined with other $b - 1$ population individuals). If $f(x_{\text{child}}) > f(x_i \text{ or } x_j)$, new solution x_{Nchild} is created according to *go-beyond* strategy over again. Now once more the program determines if $f(x_{N\text{child}})$ is greater than $f(x_{\text{child}})$; if the result holds, determine update solution $x_{NN\text{child}}$ with *go-beyond* strategy again. In the end, last subsection D is introduced to make $x_{NN\text{child}}$ replace one of x_i or x_j.

3.6. Optimization Process of DEACOP. According to description about above five parts subsection, all of subsections will be integrated to build an evolutionary algorithm. Optimization steps of DEACOP are shown as follows.

Step 1. Set initial parameters that include variable dimension vars, P_{size}diverse vectors of the initial set (normally $P_{\text{size}} = 10 \times$ vars), the number of high-quality solution *b1*, and random set size *b2*. Initial population whose size b is the sum of *b1* and *b2*. To escape from suboptimal solution, the number of consecutive iterations T_{stick} is defined as a vector. $T_{\text{stick}} = [T_1, T_2, \ldots, T_b] = [0, 0, \ldots, 0]$. T_{change} is denoted as logo whether get suboptimal solution.

Step 2. This step uses a latin hypercube uniform sampling to generate initial set of diverse solutions. But the set should meet constraint condition about optimization problem.

Step 3. Check for similarity solutions. This step uses Algorithm 2 to test the diversity of population.

Step 4. Make differential evolutionary computation in reference to the actual individuals of concentration.

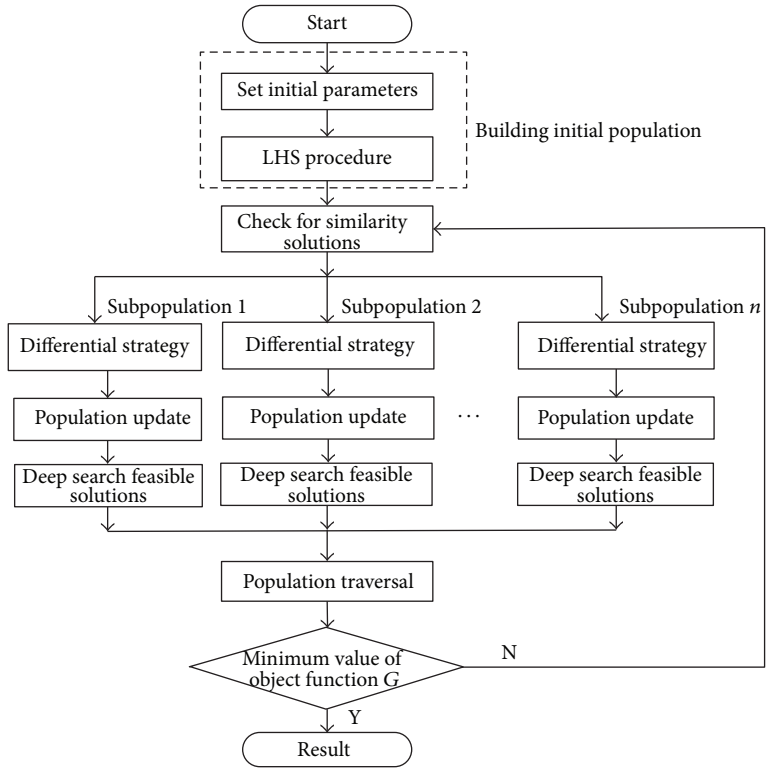

Figure 2: The flow chart of DEACOP.

if $f(x_{\text{new}}) < f(x_{\text{parent}})$
$x_{\text{parent}} = x_{\text{new}}$
endif

Algorithm 2: Population-update algorithm.

Step 5. Associate population-update strategy with *go-beyond* strategy. If the quality of child x_{child} that is generated with combination method outperforms its parent x_i, then *go-beyond* strategy is used to further exploit solution intensification. Otherwise, *go-beyond* strategy is not performed.

Step 6. Escape from suboptimal solution. If the parent x_i is replaced by the child, then the number of consecutive iterations T_i is reset as 0; otherwise $T_i = T_i + 1$, and estimate whether $T_i \geq T_{\text{change}}$. If the result is affirmative, x_i will be substituted by the random one of the remaining $P_{\text{size}} - b$ members.

Step 7. Repeatedly perform Step 4–Step 6 until all members of population come through this process.

Step 8. Until stopping criterion is met, go into Step 3.

In order to clarify this algorithm procedure, a flow chart was shown in Figure 2.

Table 1: Set parameters for optimization.

Model parameters	Value	DEACOP parameters	Value
B/mm	1520	$b1$	10
H_0/mm	35.3	$b2$	10
h_n/mm	5.9	P_{size}	70
T_{RC}/°C	1061	T_{change}	20
CR_n/mm	0.016	r	10^{-4}
n	7	ITTM	150

4. DEACOP Application and Results Analysis

4.1. Set Initial Parameters and Optimization Steps. In order to validate the effectiveness of DEACOP optimization for load distribution of the hot rolling, Q235 Steel was used for simulation experiments. The parameters load distribution was listed in Table 1, including the width of strip steel B, initial thickness of workpiece H_0, finish product thickness h_n, exit temperature of roughing mill T_{RC}, objective crown CR_n, and the number of stands n. Moreover, parameters in DEACOP include the number of population b (including the number of high-quality solutions $b1$ and the number of random solutions $b2$), the size of initial set P_{size}, the number of dropping into suboptimal region T_{change}, radius of suboptimal region r, and iteration times of optimization ITTM.

Table 2: Comparison of rolling force distribution.

Methods	Variables (/KN)						
	P_1	P_2	P_3	P_4	P_5	P_6	P_7
Classic	22438.8	20054.3	24530.9	17842.8	12593.2	12170	8941.5
EACOP	20356.8	22629.6	22048.6	17446.9	15130.7	12136.4	9184.9
DEACOP	21845.7	23648.4	23646.4	15963.3	13472.2	9813.8	9148.4

Table 3: Relative crown of each stand.

Methods	Variables ($\times 10^3$)						
	CR_1/H_1	CR_2/H_2	CR_3/H_3	CR_4/H_4	CR_5/H_5	CR_6/H_6	CR_7/H_7
Classic	1.4	1.7	3	3.1	2.6	2.9	2.8
EACOP	1.2	1.9	2.6	2.9	3.1	2.9	2.8
DEACOP	1.2	1.9	2.6	2.9	2.9	2.8	2.8

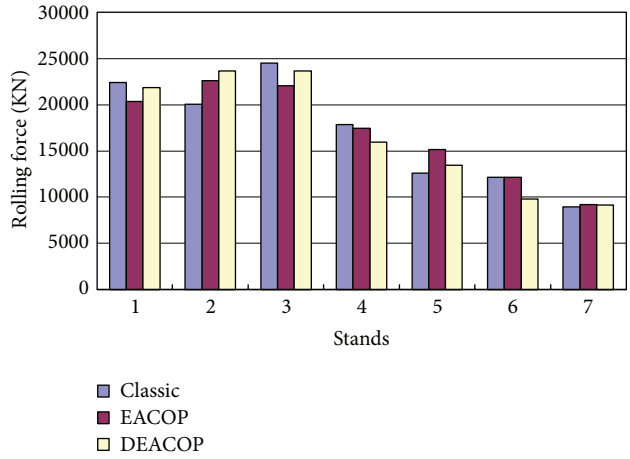

Figure 3: Comparison of rolling force distribution.

The process of DEACOP algorithm optimization for load distribution of the hot rolling is shown as follows.

Step 1. The load distribution model considering flatness is established based on the actual production process parameters.

Step 2. First of all, thickness value h_i' can be obtained according to experiential load distribution (6). Variables optimized are determined as Δoh_i, so exit thickness optimized is denoted as $h_i = h_i' + \Delta oh_i$.

Step 3. Use DEACOP to optimize mathematic model of load distribution. According to constraint condition of modeling details, the process parameters which are calculated by optimizing variable must satisfy actual production requirements.

Step 4. Until stopping criterion is met, go back to Step 3.

4.2. Simulation and Discussion. In this part, we have considered three methods for optimizing load distribution, including, experience distribution, EACOP, and DEACOP. Meanwhile, the results generated through those algorithms were compared and analyzed. Under constraints conduction and objective function, as we can notice that top three stands' reduction must be as large as possible. For the desire of rolling force, the first stand rolling force P_1 is expected as 90% of the second stand rolling force P_2, and P_2 should be equal to the third stand rolling force P_3. In addition, the purpose of optimization should guarantee integrated performance of shape and gauge control system, so the object function desires that rolling force of the last four stands should be descended one by one, and relative crown remains consistent as far as possible. The calculation results about rolling force distribution as well as relative crown of each stand were simulated separately by Matlab Platform, and the results are shown in Tables 2 and 3.

According to reference with the constraints conduction and objective function in actual rolling process, Figure 3 shows optimization effect of rolling force. For top three stands, all the results optimized by DEACOP are greater than those optimized by EACOP and classic optimization. As for the empirical distribution, the conclusion cannot meet the characteristics of objective optimization function because P_1 and P_2 are not equal. Meanwhile, the last four rolling forces which empirical distribution configure cannot be in accord with objective function neither, while rolling force allocated by DEACOP and EACOP is in line with in turn reduced law. Besides, as we can see from Table 4, the relative crown of the last four mill stands almost maintains the same by DEACOP algorithm, which perfectly meets the demand on rolling schedule that the relative crown of the last four stands should be equal.

The thickness distribution of every stand is shown in Table 4. Since the values of DEACOP optimization fully meet the requirements of objective function based on gauge control system, a similar experiment was made to verify its better results in strip shape optimization curve; the data of DEACOP in Table 4 was curved with the consideration of Shohet discriminant criterion, which is useful to determine whether shape has met requirements. As shown in Figure 4, the relative crown difference between entrances and exits which is optimized by DEACOP does not exceed the scope

for $i = 1$ *to* b
  $Expl = 0$
  $A_{\text{change}} = 1$
  for $j = 1$ *to* 2
    $x_{\text{parent}} = x_i$ or x_j
    if $f(x_{\text{child}}) < f(x_{\text{parent}})$

$$\text{The hyper-rectangle direction defined by } x_{\text{parent}} \text{ and } x_{\text{child}} \text{ is } [a, b] = \left[x_{\text{child}} - \frac{x_{\text{parent}} - x_{\text{child}}}{A_{\text{change}}}, x_{\text{child}} \right]$$

      $x_{\text{parent}} = x_{\text{child}}$
      $x_{\text{child}} = x_{N\text{child}}$
      $A_{\text{change}} = A_{\text{change}}/2$
    endif
  endfor
endfor

Algorithm 3: Go-beyond strategy algorithm.

Table 4: Thickness distribution of each stand.

Methods	Variables (/mm)						
	h_1	h_2	h_3	h_4	h_5	h_6	h_7
Classic	24.9662	18.3946	12.7358	9.7047	8.0254	6.718	5.9
EACOP	25.8395	18.2928	13.1485	10.0799	8.04719	6.7393	5.9
DEACOP	25.2135	17.3832	12.1914	9.5458	7.797	6.7361	5.9

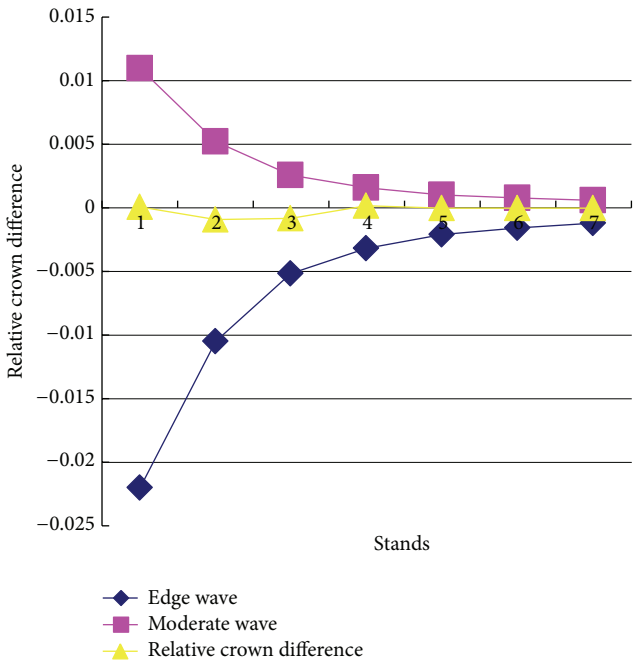

Figure 4: Judgment with Shohet formula.

of moderate wave and edge wave and has a larger margin. Conclusions show that Shohet discriminant verifies the reliability of the experimental results.

5. Conclusions

In this paper, The DEACOP which has a flexible frame structure embedding in various submethods has been introduced. This algorithm was presented to optimize the rolling schedule and show its superior ability of global searching. Moreover, it can not only escape from suboptimal solutions, but also advance the search efficiency.

According to the experimental results within actual data in hot rolling process, the DEACOP still can get feasible and better mathematical solution and validate the real-time application even by fewer adjustable parameters, which is more suitable for the actual load distribution problems. With this algorithm, the optimized rolling schedule can make full use of the upstream finishing mill equipment which controls top three stands' reduction and improves the total rolling consumption. The rolling force of the last four stands which control exit thickness can be used as an important means of shape control. Therefore, the improvement of efficiency in plate-shaped regulating by DEACOP is recommended as an important issue for further investigation.

Acknowledgments

The authors gratefully acknowledge the support by the National Natural Science Foundation of China (61074085, 51205018), China Postdoctoral Science Foundation Funded Project (2012M510321), and Fundamental Research Funds

for the Central Universities (FRF-TP-12-104A, FRF-SD-12-008B). The authors heartily appreciate the data support from Ansteel Company in Liaoning Province, China. Meanwhile, great thanks also go to former researchers for their excellent work, which gives great help for our academic study.

References

[1] Y. K. Sun, *The Model and Control of Cold and Hot Strip Mill*, Metallurgical Industry Press, Beijing, China, 2010.

[2] Y. Wang, J. Liu, and Y. Sun, "Immune genetic algorithms (IGA) based scheduling optimization for finisher," *Journal of University of Science and Technology Beijing*, vol. 24, no. 3, p. 339, 2002.

[3] F. Yao, W.-D. Yang, M. Zhang, and Z.-D. Li, "Improved space-adaptive-based differential evolution algorithm," *Control Theory and Applications*, vol. 27, no. 1, pp. 32–38, 2010.

[4] H.-J. Li, G.-D. Wang, J.-Z. Xu, and X.-H. Liu, "Optimization of draft schedules with variable metric hybrid genetic algorithm during hot strip rolling," *Journal of Iron and Steel Research*, vol. 19, no. 8, pp. 33–36, 2007.

[5] J.-M. Yang, H.-J. Che, F.-P. Dou, and T. Zhou, "Genetic algorithm-based optimization used in rolling schedule," *Journal of Iron and Steel Research International*, vol. 15, no. 2, pp. 18–22, 2008.

[6] J. A. Egea, R. Martí, and J. R. Banga, "An evolutionary method for complex-process optimization," *Computers and Operations Research*, vol. 37, no. 2, pp. 315–324, 2010.

[7] J.-T. Tsai, J.-H. Chou, and W.-H. Ho, "Improved quantum-inspired evolutionary algorithm for engineering design optimization," *Mathematical Problems in Engineering*, vol. 2012, Article ID 836597, 27 pages, 2012.

[8] J.-Y. Wu, "Solving constrained global optimization problems by using hybrid evolutionary computing and artificial life approaches," *Mathematical Problems in Engineering*, vol. 2012, Article ID 841410, 36 pages, 2012.

[9] M. Laguna and R. Marti, *Scatter Search: Methodology and Implementations in C*, Kluwer Academic Publishers, Boston, Mass, USA, 2003.

[10] F. Glover, M. Laguna, and R. Marti, "Scatter search and path relinking: foundations and advanced designs," in *New Optimization Techniques in Engineering*, G. C. Onwubolu and B. V. Babu, Eds., Springer, Berlin, Germany, 2004.

[11] H.-D. Yang and J.-Q. E, "An adaptive chaos immune optimization algorithm with mutative scale and its application," *Control Theory and Applications*, vol. 26, no. 10, pp. 1069–1074, 2009.

[12] X. Yang and C. N. Tong, "Coupling dynamic model and control of chatter in cold rolling," *Journal of Dynamic Systems, Measurement and Control-Transactions of the ASME*, vol. 134, no. 4, Article ID 041001, 8 pages, 2012.

[13] V. B. Ginzburg, *Flat-Rolled Steel Processes. Advanced Technologies*, CRC Press, New York, NY, USA, 2009.

[14] M. D. McKay, R. J. Beckman, and W. J. Conover, "A comparison of three methods for selecting values of input variables in the analysis of output from a computer code," *Technometrics*, vol. 21, no. 2, pp. 239–245, 1979.

Hindawi Publishing Corporation
Mathematical Problems in Engineering
Volume 2013, Article ID 808901, 6 pages
http://dx.doi.org/10.1155/2013/808901

Research Article

Study of Evolution Model of China Education and Research Network

Guoyong Mao[1,2] and Ning Zhang[3]

[1] *Department of Electronic Information and Electric Engineering, Changzhou Institute of Technology, Changzhou 213002, China*
[2] *German Research School for Simulation Science, 52062 Aachen, Germany*
[3] *Business School, University of Shanghai for Science and Technology, Shanghai 200093, China*

Correspondence should be addressed to Guoyong Mao; gymao@mail.shu.edu.cn

Received 2 September 2013; Revised 18 November 2013; Accepted 18 November 2013

Academic Editor: Zidong Wang

By searching the hyperlinks with domain name ".edu.cn" which constitutes the China Education and Research Network, we build a complex directed network containing 366,422 web pages containing 540,755 URLs. These URLs constitute a complex directed network through self-organization. By analyzing the topology of China Education and Research Network, we found that it is different from the common Internet in several aspects. Most of the vertices have incoming links, a few vertices have outgoing links, and very few vertices have both incoming and outgoing links. The vertex distribution has a power-law tail. A large proportion of newly added edges always connect with those pages selected from one subnetwork that they belong to, instead of connecting with the pages selected from the whole network. According to these features, we presented the evolution model of this complex directed network. The results indicate that this model reflects some main characteristics of China Education and Research Network.

1. Introduction

The research on complex networks is developing at a brisk pace, and significant achievements have been made in recent years; among them is the introduction of scale-free network and related models [1–4], as it makes big progress in revealing the characteristics of dynamic evolution of complex networks. Theoretical and empirical research on complex network has been carried out with some important achievements [5–9].

China Education and Research Network (CERNET) was established since 1995. More than 1000 universities and research institutes have been connected to this network so far. It has 36 regional network centers and main nodes, which are distributed among different provinces of China. As of now this network has host machines more than 1,200,000 and has become the second largest internet in China. However, compared with the large number of researches that has been done on the general Internet [10–13], only a few work is on CERNET can be found. From these studies we found that the features of CERNET are different from those of the general Internet, especially in the structure and formation mechanism [14, 15]. Hence, the study on CERNET is quite important.

We have been working on CERNET since 2005 and trying to establish the evolution model of CERNET for analysis and prediction purposes [14–16]. However, due mainly to the large scale of CERNET and lack of computing power, it took quite a long time to adjust the parameters to modify the model at that time. Therefore, the model we got is relatively simple which cannot well reflect the main features of CERNET [16]. For example, the average shortest path length of the simulation model is only about 2.8, far from 8.95 of the real network [17].

In this paper, the CERNET we analyze is a virtual network made up of web pages where ".edu.cn" is included in the addresses of all these pages. In this network, all web pages are nodes, and all the hyperlinks in these pages that link to other pages are the directed edges. This directed complex network has 366,422 nodes and 540,755 edges. We analyze the features of this network and extract the evolution model using empirical methods to reveal the formation mechanism of CERNET.

The remainder of the paper is organized as follows. Topological structure of CERNET is analyzed in Section 2, and the evolution model of CERNET and comparison between the real and simulated networks are described in Section 3, before giving conclusion and future work in Section 4.

2. Topological Structure of CERNET

There are several features that can be used to characterize a network, for example, the degree distribution, the average shortest path length, and the clustering coefficients. Among them the degree distribution is considered to be the most important [2].

From graph theory we know that the number of edges connected to one node is the degree of this node. For directed graph, the outdegree is the number of output edges and the indegree the number of input edges. Using the data we collect, we setup a database of CERNET and get the $P_{\text{out}}(k)$ and $P_{\text{in}}(k)$, where $P_{\text{out}}(k)$ is the probability that one page has k output pages and $P_{\text{in}}(k)$ is the probability that one page has k input pages. The formulas we use to calculate the output and input probability of node i are listed in (1) and (2), respectively, where M_{out} is the maximum outdegree of the network and M_{in} the maximum indegree of the network:

$$P_{\text{out}}(k_i) = \frac{(k_i)}{\sum_{j=1}^{M_{\text{out}}}(k_j)}, \tag{1}$$

$$P_{\text{in}}(k_i) = \frac{(k_i)}{\sum_{j=1}^{M_{\text{in}}}(k_j)}. \tag{2}$$

We plot the double logarithmic curves of $P_{\text{out}}(k)$ and $P_{\text{in}}(k)$ that change as a function of k, as shown in Figures 1 and 2, respectively. Linear-regression analysis is done on the linearized data, as shown in the straight red lines in these figures. From Figure 1 we see that the tail of outdegree distribution of CERNET follows the power law distribution, $P_{\text{out}}(k) \sim k^{-r_{\text{out}}}$, where $r_{\text{out}} = 2.48$. From Figure 2 we see that the indegree distribution generally follows the power law distribution, but the tail is not very smooth, $P_{\text{in}}(k) \sim k^{-r_{\text{in}}}$, where $r_{\text{in}} = 2.40$, which differs greatly with the Poisson distribution predicted using the traditional theory of random graph.

We make statistical analysis of these data and get the accumulated frequency of degree and the corresponding ratio of the degree to total degree in CERNET, as shown in Table 1. From Table 1 we can see that a large amount of pages have small connections, a few pages have a medium number of connections, while a tiny minority of notable pages have a large number of connections. This phenomenon is similar to the research result made by Albert et al. [1].

This virtual network of CERNET is made up of subsets of web pages of different universities. The number of web pages of each subset is determined by the corresponding universities; the addition and deletion of pages totally depended on the university that these pages belong to. However, we find that though the number of pages is different for different universities they do share some similar features. For example, the proportion of pages that have output links to the total number of pages is less than 25% in every university, while the proportion of pages that have input links to the total number of pages is usually bigger than 85%. Only a very small number of pages have both output links and input links. Hence, if each university is treated as a subnetwork, then in each network most nodes only have input edges, a few nodes only have output edges, and the number of nodes with both

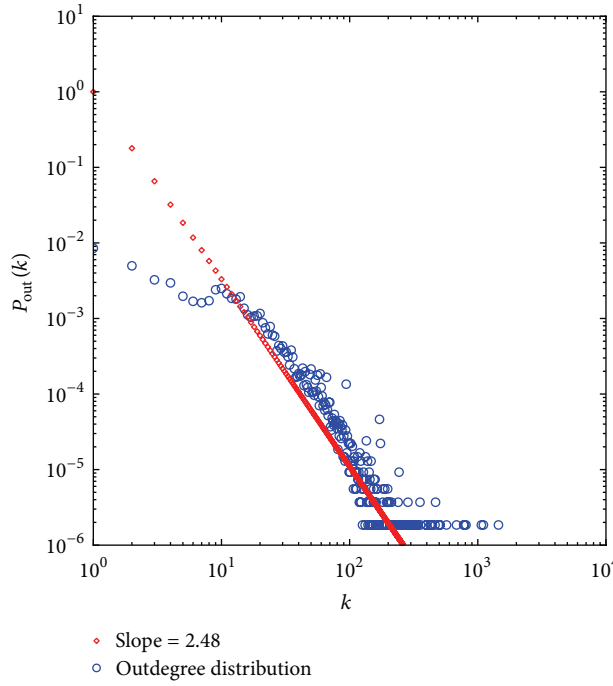

Figure 1: Distribution of outdegree of real data.

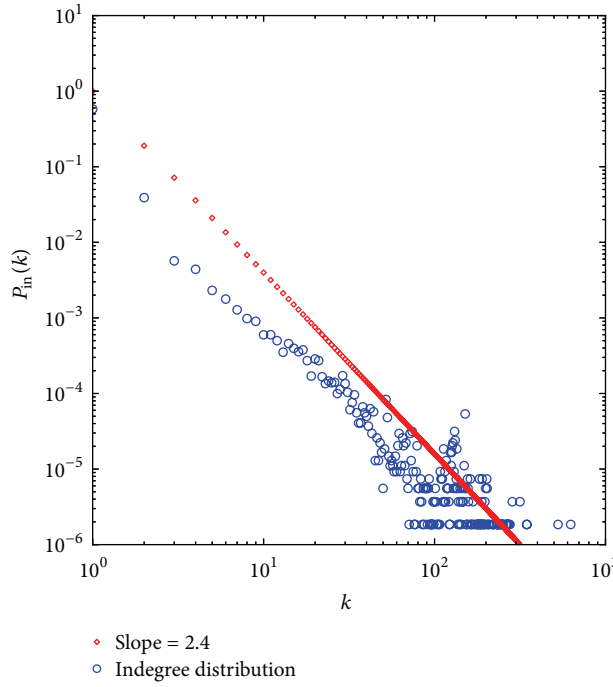

Figure 2: Distribution of indegree of real data.

Table 1: The accumulated frequency and percentage of degree in CERNET.

Outdegree	Accumulated frequency	Ratio to total outdegree (%)	Indegree	Accumulated frequency	Ratio to total indegree (%)
1~50	30463	93.7	1~5	341535	98.0
51~300	32478	6.2	6~199	348477	1.9
301~1449	32510	0.1	201~626	348491	0.1

Table 2: Degree and link features in some universities.

Name of university	Number of web pages	Number of outdegrees	Number of indegrees	Ratio of pages with output edge to total number of pages (%)	Ratio of pages with input edge to total number of pages (%)
CIM	9576	14532	13515	0.15	0.87
SHUFE	9151	13546	12620	0.12	0.93
ZJU	11537	20586	18943	0.085	0.973
CQU	864	1403	1326	0.075	0.987
NBU	1985	2995	2785	0.159	0.908
SHU	15035	19443	18522	0.096	0.939
SUDA	13643	20197	18051	0.071	0.964
CUMT	9371	18089	12293	0.134	0.914
SHISU	10733	13734	12941	0.089	0.933
ECUN	13707	19890	17379	0.068	0.959
SHSMU	3663	6335	5730	0.114	0.916
CUN	6120	7020	6762	0.18	0.84

input edges and output edges is rare. From these features we know that each university connects to other universities through a small number of pages, as shown in Table 2.

3. The Evolution Model of CERNET

Using the mechanism of growth and preferential attachment, the scale-free model proposed by Barabasi et al. can to some degree disclose the nature of many complicated phenomena in the practical world. However, this model cannot be applied to CERNET. For example, every newly attached node has output edges in this scale-free model, but for the directed network of CERNET a larger amount of newly attached nodes have only one input edge; that is, these nodes have zero outdegree. Also in this model, the preferential attachment of newly added nodes will search the whole network for the best node to connect to, while in CERNET the newly added pages will generally choose some pages in the same university to connect to. Only occasionally, the newly added pages will choose pages in other universities, but these pages will not search the whole CERNET for the best pages to connect to. From these features of CERNET, we propose the evolution model of CERNET, as follows.

(i) The CERNET starts from m_0 nodes and e_0 edges. The m_0 nodes are randomly divided into l subsets. There are $m_{01}, m_{02}, \ldots$, and m_{0l} nodes and $e_{01}, e_{02}, \ldots$, and e_{0l} edges in each subset, respectively, where $\sum_{i=1}^{l} m_{0i} = m_0$, and $\sum_{i=1}^{l} e_{0i} = e_0$.

(ii) At each moment, a new node will randomly be added into one of the subsets of the network. There are 5 cases for the edges that are added together with the new node:

(1) the new node has only one input edge;
(2) the new node has only m output edges;
(3) the new node has one input edge and one output edge;
(4) the new node has one input edge and $m - 1$ output edges;
(5) the new node has one output edge and $m - 1$ input edges,

where $m \leq (m_{0\min})$ and $m_{0\min}$ is the minimum initial number of nodes among l subsets and $m_{0\min} = \min(m01, m02, \ldots, m0l)$.

(iii) When the new node with one input edge is added to the network with probability α, this node will randomly choose a subset and let itself be connected by a preferentially selected node in this subset. Let $\prod_{\text{out}}(i)$ denote the probability of node i to be selected as the source node; then $\prod_{\text{out}}(i)$ is determined by k_{out}^{i}, the outdegree of i.

(iv) When the new node with m output edges is added to the network, there are 2 cases we should consider. The probabilities of the two cases are β_1 and β_2, respectively.

(1) For the first case, the new node will randomly choose a subset and let itself connect to a preferentially selected node in this subset. Let $\prod_{\text{in}}(i)$ denote the probability of node i be selected as the target node; then $\prod_{\text{in}}(i)$ is determined by k_{in}^i, the indegree of i. For the rest of the $m-1$ output edges, at each moment only one edge randomly chooses a subset which has not been connected by the new node and connects itself to a preferentially selected node in this subset, till all $m-1$ output edges are processed.

(2) For the second case, the new node will still randomly choose a subset, but this time this node will preferentially choose $m-1$ nodes in this subset and let itself be connected. Let $\prod_{\text{in}}(i)$ denote the probability of node i be selected as the target node; then $\prod_{\text{in}}(i)$ is determined by k_{in}^i, the indegree of i. For the rest of the edges that this new node carries, it will randomly pick a subset which has not been connected by this new node and connect itself to a preferentially selected node in this subset.

(v) When the new node with one input edge and one output edge is added to the network, there are also 2 cases we should consider. The probabilities of the two cases are γ_1 and γ_2, respectively.

(1) For the first case, the new node will randomly choose a subset and let itself be connected by a preferentially selected node in this subset. The probability of node i to be selected as the source node is determined by k_{out}^i, the outdegree of i. The output edge of the new node will randomly select a subset which has not been connected by the new node and connect itself to a preferentially selected node. The probability of a node i to be selected as the target node is determined by k_{in}^i, the indegree of i.

(2) For the second case, the new node will randomly choose a subset and let itself be connected by a preferentially selected node in this subset. The probability of node i to be selected as the source node is determined by k_{out}^i, the outdegree of i. For the output edge that this new node carries, it will still pick a node in the same subset and connect itself to a preferentially selected node which has not been connected by the input edge of the new node. The probability of a node i to be selected as the target node is determined by k_{in}^i, the indegree of i.

(vi) When the new node with 1 input edge and $m-1$ output edges is added to the network with probability δ, this node will randomly choose a subset and let itself be connected by a preferentially selected node in this subset. The probability of node i to be selected as the source node is determined by k_{out}^i, the outdegree of i. For the rest of the $m-1$ output edges, at each moment only one edge randomly chooses a subset which has not been connected by the new node and connects itself to a preferentially selected node in this subset, till all the $m-1$ output edges are processed. The probability of node i to be selected as the target node is determined by k_{in}^i, the indegree of i.

(vii) When the new node with 1 output edge and $m-1$ input edges is added to the network with probability ζ, this node will randomly choose a subset and connect itself to a preferentially selected node in this subset. The probability of node i to be selected as the target node is determined by k_{in}^i, the indegree of i. For the rest of the $m-1$ input edges, at each time only one edge randomly chooses a subset which has not been connected by the new node and lets itself be connected to a preferentially selected node in this subset, till all $m-1$ input edges are processed. The probability of node i to be selected as the source node is determined by k_{out}^i, the outdegree of i.

The definitions of $\prod_{\text{in}}(i)$ and $\prod_{\text{out}}(i)$ are listed in (3) and (4), respectively. The relation between different probabilities is listed in (5). We have the following equations:

$$\prod_{\text{in}}(i) = \frac{k_{\text{in}}^i}{\sum_{j=1}^{n_l}\left(k_{\text{in}}^j\right)}, \tag{3}$$

$$\prod_{\text{out}}(i) = \frac{k_{\text{out}}^i}{\sum_{j=1}^{n_l}\left(k_{\text{out}}^j\right)}, \tag{4}$$

$$\alpha + \beta_1 + \beta_2 + \gamma_1 + \gamma_2 + \delta + \zeta = 1. \tag{5}$$

In (3) and (4), n_l is the number of nodes of the subset that has new edges connected to it. The denominator of (3) is the sum of indegree of the same subset and the denominator of (4) is the sum of outdegree in this subset.

After t moments, we get a directed random network with N nodes and V edges, where $N = m_0 + t$, and

$$\begin{aligned} V = {} & e_0 + \alpha * t + (\beta_1 + \beta_2) * m * t \\ & + (\gamma_1 + \gamma_2) * 2t + (\delta + \zeta) * m * t. \end{aligned} \tag{6}$$

From the analysis of CERNET we set $\alpha = 0.60$, $\beta_1 = 0.2$, $\beta_2 = 0.12$, $\gamma_1 = 0.04$, $\gamma_2 = 0.02$, $\delta = 0.01$, and $\zeta = 0.01$. When $m_0 = 12$, $m = 3$, and $l = 3$, we get the distribution of outdegree and indegree of this simulated model. The outdegree and indegree distributions are illustrated in Figures 3 and 4, respectively. Figures 5 and 6 illustrate the comparison between the simulated data and the real data. From the comparison of outdegree distribution we can see that the slope of the simulated data is 2.48, the same as that of the real data, but the beginning part of the simulated data cannot

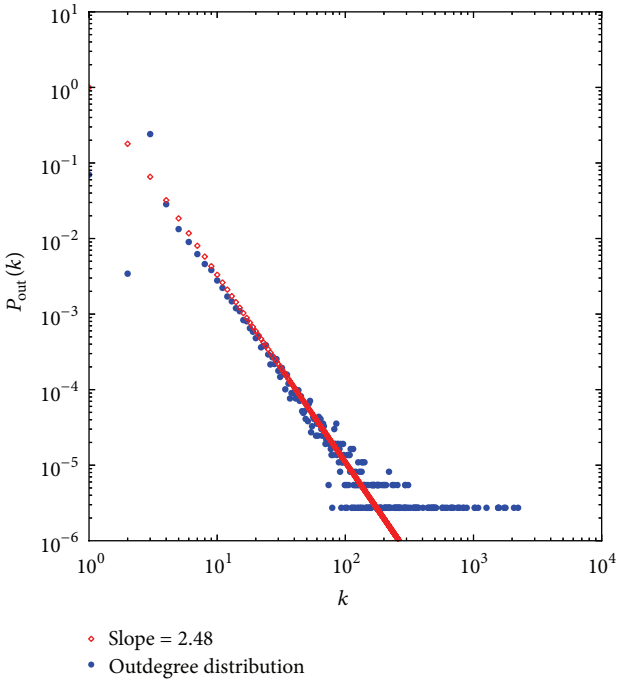

Figure 3: Distribution of outdegree of simulated data.

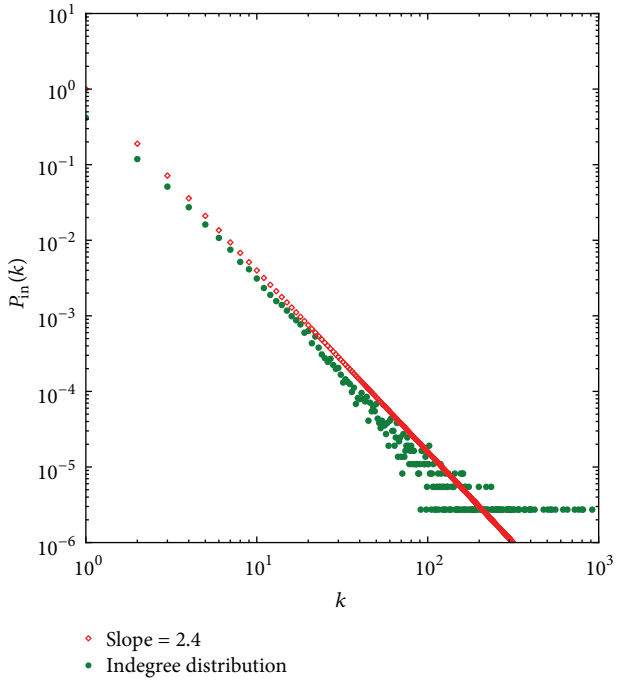

Figure 4: Distribution of indegree of simulated data.

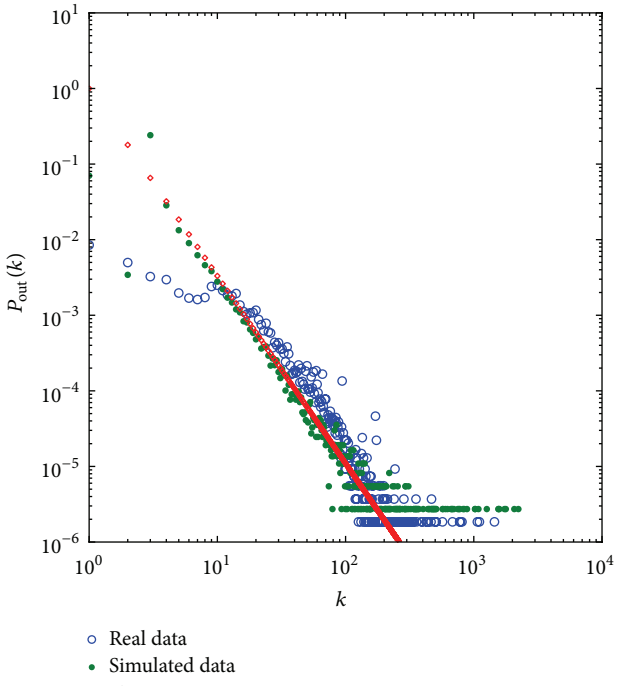

Figure 5: Comparison of outdegree distribution.

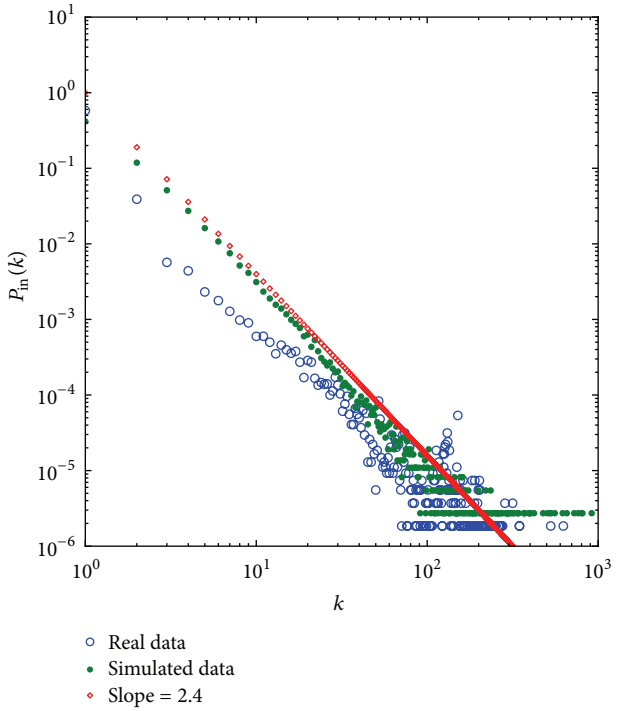

Figure 6: Comparison of indegree distribution.

fully reflect the statistical result of the real data. From the comparison of indegree distribution we see that the slope of simulated data is 2.40, the same as that of the real data, but the beginning part of the simulated data cannot fully reflect the statistical result of the real data. The tail is smoother than that of the real data. The slope is 2.40, the same as the real data.

4. Conclusions

From the figures of degree distribution, we can see that the simulated network can partly reflect the characteristic of CERNET. The degree distribution of the simulated network matches much better the real network than that in model [16].

We also compared other features of the simulated and the real networks. For example, the average shortest path length for the real network is 8.95, while for the simulated network, it is 7.81, which is much closer than that of the model listed in [16].

The main contribution of this paper is the evolution model of the CERNET. The result shows that the simulated model can partly disclose the property of this network. However, the model introduced in this paper is only the ideal model, which means that only the main features of the real network are considered. With the help of the fast growing computing power, we intend to adjust this model so that it can be used in the analysis of the ever increasing large scale complex networks.

Acknowledgments

The authors are grateful to colleagues in the German Research School for Simulation Science for their constructive suggestions. The authors are also grateful to the reviewers for their valuable comments and suggestions to improve the presentation of this paper. This work is supported by the National Natural Science Foundation of China under Grant no. 70971089, Shanghai Leading Academic Discipline Project under Grant no. XTKX2012, and Jiangsu Overseas Research and Training Programs for University Prominent Young and Middle-Aged Teachers and Presidents.

References

[1] R. Albert, H. Jeong, and A.-L. Barabási, "Diameter of the world-wide web," *Nature*, vol. 401, no. 6749, pp. 130–131, 1999.

[2] A.-L. Barabási and R. Albert, "Emergence of scaling in random networks," *Science*, vol. 286, no. 5439, pp. 509–512, 1999.

[3] A.-L. Barabási, R. Albert, and H. Jeong, "Mean-field theory for scale-free random networks," *Physica A*, vol. 272, no. 1-2, pp. 173–187, 1999.

[4] R. Albert and A.-L. Barabási, "Statistical mechanics of complex networks," *Reviews of Modern Physics*, vol. 74, no. 1, pp. 47–97, 2002.

[5] X. Li and G. Chen, "A local-world evolving network model," *Physica A*, vol. 328, no. 1-2, pp. 274–286, 2003.

[6] Q. Chen and D. Shi, "The modeling of scale-free networks," *Physica A*, vol. 335, no. 1-2, pp. 240–248, 2004.

[7] H. Che and J. Gu, "Scale-free networks and their signicance for systems science," *Systems Engineering-Theory & Practice*, vol. 24, pp. 11–16, 2004.

[8] J. Wu and Z. Di, "Complex networks in statistical physics," *Progress in Physics*, vol. 24, pp. 18–46, 2003.

[9] A. Lancichinetti and S. Fortunato, "Consensus clustering in complex networks," *Scientific Reports*, vol. 2, no. 336, 2012.

[10] X. Wang and D. Loguinov, "Wealth-based evolution model for the internet AS-level topology," in *Proceedings of the 25th IEEE International Conference on Computer Communications (INFOCOM '06)*, pp. 1–11, Barcelona, Spain, April 2006.

[11] S. Zhou, "Understanding the evolution dynamics of internet topology," *Physical Review E*, vol. 74, no. 1, Article ID 016124, 11 pages, 2006.

[12] A. Dhamdhere and C. Dovrolis, "Ten years in the evolution of the internet ecosystem," in *Proceedings of the 8th ACM SIGCOMM Conference on Internet Measurement (IMC '08)*, pp. 183–196, ACM, Vouliagmeni, Greece, October 2008.

[13] L. Šubelj and M. bajec, "Model of complex networks based on citation dynamics," in *Proceedings of the 22nd International Conference on World Wide Web Companion (WWW '13)*, pp. 527–530, Rio de Janeiro, Brazil, May 2013.

[14] N. Zhang, "Analysis of China education network structure," *Computer Engineering*, vol. 33, no. 17, pp. 140–142, 2007.

[15] L. Su, N. Zhang, and L. Ma, "Comparative studies on the topological structure of China education network," *Journal of University of Shanghai for Science and Technology*, vol. 30, no. 3, pp. 297–299, 2008.

[16] N. Zhang, "Complex network demonstration—China education network," *Journal of Systems Engineering*, vol. 21, no. 4, pp. 337–340, 2006.

[17] X. Ni, N. Zhang, and M. Wang, "Parallel algorithms (MPI) on solving the shortest-path problem of china educational network," *Computer Engineering and Applications*, vol. 15, pp. 135–137, 2006.

Hindawi Publishing Corporation
Mathematical Problems in Engineering
Volume 2013, Article ID 131063, 19 pages
http://dx.doi.org/10.1155/2013/131063

Research Article

Wiretap Channel with Action-Dependent States and Rate-Limited Feedback

Xinxing Yin, Xiao Chen, and Zhi Xue

Department of Electrical Engineering, Shanghai Jiao Tong University, Shanghai 200240, China

Correspondence should be addressed to Xinxing Yin; yinxinxing@sjtu.edu.cn

Received 5 September 2013; Revised 1 November 2013; Accepted 2 November 2013

Academic Editor: Hamid Reza Karimi

We introduce the wiretap channel with action-dependent states and rate-limited feedback. In the new model, the state sequence is dependent on the action sequence which is selected according to the message, and a secure rate-limited feedback link is shared between the transmitter and the receiver. We obtain the capacity-equivocation region and secrecy capacity of such a channel both for the case where the channel inputs depend noncausally on the state sequence and the case where they are restricted to causal dependence. We construct the capacity-achieving coding schemes utilizing Wyner's random binning, Gel'fand and Pinsker's coding technique, and rate splitting. Furthermore, we compare our results with the existing approaches without feedback, with noiseless feedback, and without action-dependent states. The simulation results show that the secrecy capacity of our model is bigger than that of the first two existed approaches. Besides, it is also shown that, by taking actions to affect the channel states, we guarantee the data integrity of the message transmitted in the two-stage communication systems although the tolerable overhead of transmission time is brought.

1. Introduction

The framework of channels with action-dependent states was first introduced by Weissman [1] to model scenarios in which transmission took place in two successive phases. In the first phase, a message-dependent action sequence was selected by the encoder. The action sequence affected the formation of the channel states. In the second phase, the transmitter began to send the message to the receiver in the presence of the action-dependent states. In [1], the capacity of such a channel both for the case where the channel inputs were allowed to depend noncausally on the channel states and the case where they were restricted to causal dependence was obtained. After the publication of Weissman's work, a number of extensions of the results in [1] have been reported; see [2–6].

However, the above scenarios considered no security constraints which are essential in many communication systems. For instance, the broadcast nature of wireless networks gives rise to the hidden danger of information leakage to the malicious receiver when broadcasting sensitive data and acquiring channel state information. The secure communication for the wiretap channel was first studied by Wyner [7]. In his model, the transmitter aimed to send a confidential message to the receiver through a noisy discrete memoryless channel (DMC) and keep the wiretapper as ignorant of the message as possible. The wiretapper observed a degraded version of the legitimate receiver's observation through another DMC. Equivocation was introduced in [7] to measure wiretapper's uncertainty of the confidential message. Wyner characterized the secrecy capacity, that is, the best transmission rate under perfect secrecy, as the difference between the capacity of the main channel and the wiretap channel. This model was further explored by many researchers; see [8–14]. Among them, Dai et al. studied the wiretap channel with action-dependent states [13] and gave the lower and upper bounds on the *capacity-equivocation region*. The *capacity-equivocation region* is the set of all the achievable rate pairs (R, R_e), where R and R_e are the rates of the confidential message and wiretapper's equivocation about the message.

Note that the action-dependent channel models [1–6] as well as the wiretap channel models [7–14] only dealt with one-way communication. However, many systems involve two-way communication. For example, feedback links are usually seen in satellite communication, telephone connections, and

wireless sensor networks. To investigate the effects of the feedback on secrecy capacity, Ahlswede and Cai first studied the wiretap channel with noiseless causal feedback [15], where the channel output symbol is fed back to the transmitter and used as a secret key. Then, Ardestanizadeh et al. studied the problem of secure communication over a wiretap channel with a rate-limited feedback link [16]. The main contribution of [16] was that the upper and lower bounds on the secrecy capacity were obtained as a function of the secure feedback rate R_f. Moreover, the recursive argument was introduced to find the single-letter characterization of the upper bound and claimed to be a powerful tool for similar problems [16]. Besides, Yin et al. [17] studied the discrete memoryless broadcast channels with noiseless feedback based on [15, 16]. The channel model in [17] did not consider channel state information. Recently, Dai et al. studied the wiretap channel with action-dependent states and noiseless feedback [18]. In Dai's model, similar to [15], the output symbol received at the receiver was fed back securely to the transmitter and used as a shared key between the transmitter and the receiver. However, in [15, 18], only part of the feedback contributed to the secure communication and the wiretapper was provided a chance to get the secret message by guessing the legitimate receiver's channel output with its own channel observation. Then, it is natural to ask whether the feedback can be used more efficiently and securely.

Inspired by [16, 18], this paper studies a new model, that is, wiretap channel with action-dependent states and rate-limited feedback; see Figure 1. In the model, the feedback is independent of the channel output and sent to the transmitter through a secure feedback link of rate R_f. The formation of the channel states is affected by the message-dependent action sequence. This model can provide insights into the value of two-way two-phase interactions in communication systems. Note that since the feedback symbol is independent of the channel output, the wiretapper attempt to get the secret key by guessing the legitimate receiver's channel output is in vain. The contributions of this work are summarized as follows.

(i) The capacity-equivocation region of the channel model in Figure 1 is obtained both for the case where the inputs of the main channel depend noncausally on the channel states and the case where they depend causally on the channel states. The capacity-equivocation region is presented in Section 2. Besides, the secrecy capacity of the channel model in Figure 1 is also got. We calculate the secrecy capacity of a binary example in Section 3.

(ii) To achieve the secrecy capacity, we construct several coding schemes and evaluate their reliability and security using the techniques of Wyner's random binning, Gel'fand and Pinsker's coding, and rate splitting. The coding schemes are presented in the Appendices.

(iii) The rate-limited feedback is added in our model. The secrecy capacity of our approach is bigger than that of the model without feedback. This indicates that feedback is useful for increasing the secrecy capacity. The corresponding simulation is presented in Section 3.

(iv) The capacity-equivocation region of the wiretap channel with action-dependent states and noiseless feedback [18] is included in our results by setting the feedback rate to be a specific value. We find that the secrecy capacity of our model is bigger than that of [18]. Specifically, when the wiretap channel is in the "best" condition, it is unable to transmit message securely using the approach in [18], while our approach can still work. Section 3 discusses the result in detail.

(v) The (degraded) wiretap channel with secure rate-limited feedback [16] is a special case of our model. The secrecy capacity of [16] can be obtained from our results without considering the action-dependent states. Our approach can guarantee data integrity in the two-stage systems. However, data integrity cannot be guaranteed by using the approach in [16] where no actions were taken. This result is illustrated in Section 3.

The remainder of the paper is organized as follows. Section 2 presents our new model and two theorems. Section 3 gives the secrecy capacity of our model and compares it with the existing channel models through simulation. We conclude in Section 4 with a summary of the whole work and some future directions.

2. Channel Models and Main Results

In this section, the notations of characters and variables are given in Section 2.1. The channel model is described in Section 2.2. The main results, that is, the capacity-equivocation region of the model in Figure 1 with causal and noncausal states, are presented in Section 2.3.

2.1. Notations. Throughout this paper, we use calligraphic letters, for example, $\mathcal{X}$, $\mathcal{Y}$, to denote the finite sets and $\|\mathcal{X}\|$ to denote the cardinality of the set $\mathcal{X}$. Uppercase letters, for example, X, Y, are used to denote random variables taking values from finite sets, for example, $\mathcal{X}$, $\mathcal{Y}$. The value of a random variable X is denoted by the lowercase letter x. We use Z_i^j to denote the $(j-i+1)$-vectors $(Z_i, Z_{i+1}, \ldots, Z_j)$ of random variables for $1 \le i \le j$, and we will always drop the subscript when $i = 1$. Moreover, we use $X \sim p(x)$ to denote the probability mass function of the random variable X. For $X \sim p(x)$ and $0 \le \epsilon \le 1$, the set of the typical N-sequences x^N is defined as $\mathcal{T}_X^N(\epsilon) = \{x^N : |\pi(x \mid x^N) - p(x)| \le \epsilon p(x) \text{ for all } x \in \mathcal{X}\}$, where $\pi(x \mid x^N)$ denotes the frequency of occurrences of letter x in the sequence x^N. (For more details about typical sequences, please refer to [19, Chap. 2].) The set of the conditional typical sequences, for example, $\mathcal{T}_{Y|X}^N(\epsilon)$, follows similarly. In this paper, it is assumed that the base of the log function is 2.

2.2. Wiretap Channel with Action-Dependent States and Rate-Limited Feedback. We consider the wiretap channel with

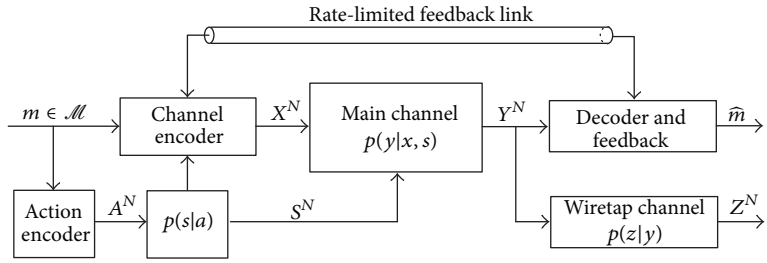

Figure 1: Wiretap channel with action-dependent states and rate-limited feedback.

action-dependent states and rate-limited feedback, as shown in Figure 1. The transmitter aims to convey a confidential message M which is uniformly distributed over $\mathscr{M}$ to the legitimate receiver whose observation is $Y^N \in \mathscr{Y}^N$. The confidential message should be kept secret from the wiretapper as much as possible. We use equivocation at the wiretapper to characterize the secrecy of the confidential message. Given the message M, an action sequence $A^N(M) \in \mathscr{A}^N$ is selected. The channel state sequence $S^N \in \mathscr{S}^N$ is generated in response to the action sequence and accessible to the channel encoder. To enhance the secrecy of the communication, the receiver feeds back symbols $K \in \mathscr{K}$ to the encoder over a feedback link of rate R_f. The feedback symbol is assumed to be independent of the channel output Y^N and kept secret from the wiretapper. Then, the input sequence of the main channel $X^N \in \mathscr{X}^N$ is generated based on the message M, the channel state sequence S^N, and the feedback symbol K. The output sequence of the main channel Y^N is distributed as $p(y^N \mid s^N, x^N) = \prod_{i=1}^N p(y_i \mid s_i, x_i)$. With the received Y^N, the decoder outputs the decoded message $\widehat{M} \in \mathscr{M}$. The wiretap channel is also a DMC with transition probability $p(z^N \mid y^N) = \prod_{i=1}^N p(z_i \mid y_i)$, where $Z^N \in \mathscr{Z}^N$ is the observation of the wiretapper. Note that the wiretap channel is assumed to be degraded from the main channel; that is, $X \to Y \to Z$ form a Markov chain. More precisely, we define the $(2^{NR}, 2^{NR_f}, N)$ code in Definition 1.

Definition 1. The $(2^{NR}, 2^{NR_f}, N)$ code for the wiretap channel with action-dependent states and rate-limited feedback is defined as follows.

(i) The feedback alphabet $\mathscr{K}$ satisfies $\lim_{N\to\infty} (\log \|\mathscr{K}\|/N) \le R_f$. The feedback symbol is generated independently of the channel output symbols and uniformly distributed over $\mathscr{K}$.

(ii) The message M is uniformly distributed over $\mathscr{M}$. The action sequence $A^N(M) \in \mathscr{A}^N$ is selected from a deterministic mapping $g : \mathscr{M} \to \mathscr{A}^N$. The state sequence is generated as the output of a memoryless channel $p(s^N \mid a^N) = \prod_{i=1}^N p(s_i \mid a_i)$ whose input is A^N.

(iii) The stochastic channel encoder φ is specified by a matrix of conditional probability distributions $\varphi(x^N \mid m, s^N, k^N)$, where $m \in \mathscr{M}$, $s^N \in \mathscr{S}^N$, $k^N \in \mathscr{K}^N$, and $\sum_{x^N} \varphi(x^N \mid m, s^N, k^N) = 1$. Note that $\varphi(x^N \mid m, s^N, k^N)$ is the probability that the message m, the state sequence s^N, and the feedback k^N are encoded as the channel input x^N. When the state sequence s^N is known causally to the channel encoder, the channel encoder at time i is $\varphi_i(x_i \mid m, s^i, k_i)$, where x_i is the output of the channel encoder at time i, k_i is the feedback symbol at time i, and $s^i = (s_1, s_2, \ldots, s_i)$ is the channel states before time i. When the channel encoder knows the state sequence s^N in a noncausal manner, the channel encoder at time i is $\varphi_i(x_i \mid m, s^N, k_i)$. For the causal manner, Shannon strategy will be used in the encoding scheme (see Appendix A). For the noncausal manner, Gel'fand and Pinsker's coding technique [20] will be used (see Appendix C).

(iv) The decoder is a mapping $\psi : \mathscr{Y}^N \to \mathscr{M}$. The input of the decoder is Y^N and the output is $\widehat{M}$. The decoding error probability is defined as $P_e = \Pr\{\psi(Y^N) \ne M\}$.

(v) The equivocation of the message at the wiretapper is defined as

$$\Delta = \frac{1}{N} H\left(M \mid Z^N\right). \tag{1}$$

Definition 2. A rate pair (R, R_e) is said to be achievable for the model in Figure 1 if there exists a $(2^{NR}, 2^{NR_f}, N)$ code defined in Definition 1, such that

$$\begin{aligned} \lim_{N\to\infty} \frac{\log \|\mathscr{M}\|}{N} &= R; \\ \lim_{N\to\infty} \frac{\log \|\mathscr{K}\|}{N} &\le R_f; \\ \lim_{N\to\infty} \Delta &\ge R_e; \\ P_e &\le \epsilon, \end{aligned} \tag{2}$$

where ϵ is an arbitrary small positive real number and R, R_e are the rates of the message and equivocation. The capacity-equivocation region is defined as the convex closure of all achievable rate pairs (R, R_e).

Definition 3. The secrecy capacity is defined as the maximum rate at which the confidential message can be sent to the

receiver in perfect secrecy; that is, $H(M) = H(M \mid Z^N)$. The secrecy capacity is

$$C_s = \max_{(R,R_e=R)\in\mathscr{R}} R, \tag{3}$$

where $\mathscr{R}$ is the capacity-equivocation region.

The capacity-equivocation regions of the model in Figure 1 with causal and noncausal channel states are shown in Theorems 4 and 5, respectively; see Section 2.3.

2.3. Main Results

Theorem 4. *For the wiretap channel with causal action-dependent states and rate-limited feedback, the capacity-equivocation region is the set*

$$\begin{aligned}\mathscr{R}_c = \Big\{ (R, R_e) : 0 \le R_e \le R; R \le I(U;Y); R_e \le I(U;Y) \\ -I(U;Z) + R_f; R_e \le H(A \mid Z) \Big\},\end{aligned} \tag{4}$$

where $(A,U) \to (X,S) \to Y \to Z$ form a Markov chain and R_f is the rate of the feedback link.

Comments. (i) The proof of Theorem 4 is given in Appendices A and B. In Appendix A, a coding scheme is provided to show the achievability of the rate pair in $\mathscr{R}_c$. The proof of the converse part is shown in Appendix B. (ii) The set $\mathscr{R}_c$ is convex, and the proof is similar to that of [8, lemma 5]. (iii) To exhaust $\mathscr{R}_c$, it is enough to restrict $\mathscr{U}$ to satisfy $\|\mathscr{U}\| \le \|\mathscr{A}\|\|\mathscr{X}\|\|\mathscr{S}\| + 1$. It can be easily proved by using the *support lemma* [21, page 310].

Theorem 5. *For the wiretap channel with noncausal action-dependent states and rate-limited feedback, the capacity-equivocation region is the set*

$$\begin{aligned}\mathscr{R}_n = \big\{ (R, R_e) : 0 \le R_e \le R; R \le I(U;Y) - I(U;S \mid A); \\ R_e \le I(U;Y) - I(U;Z) + R_f; \\ R_e \le H(A \mid Z) \big\},\end{aligned} \tag{5}$$

where $(A,U) \to (X,S) \to Y \to Z$ form a Markov chain and R_f is the rate of the feedback link.

Comments. (i) The proof of Theorem 5 is given in Appendices C and D. In Appendix C, a coding scheme is provided to show the achievability of the rate pair in $\mathscr{R}_n$. The proof of the converse part is shown in Appendix D. (ii) The set $\mathscr{R}_n$ is convex, and the proof is similar to that of [8, lemma 5]. (iii) To exhaust $\mathscr{R}_n$, it is enough to restrict $\mathscr{U}$ to satisfy $\|\mathscr{U}\| \le \|\mathscr{A}\|\|\mathscr{X}\|\|\mathscr{S}\| + 2$. It can be easily proved by using the *support lemma* [21, page 310].

3. Discussion and Simulation

In this section, we first calculate the secrecy capacity of our model and show how the secrecy capacities of several existing channel models are derived from our results. Then, to better illustrate how our approach improves the existing results, we consider a binary symmetric channel with causal action-dependent states and rate-limited feedback. We try to compare the secrecy capacities of our model and the existing channel models through simulation.

3.1. Discussion. According to the definition in (3), the secrecy capacity of wiretap channel with causal action-dependent states and rate-limited feedback is

$$\begin{aligned}C_{\mathrm{sc}}(R_f) &= \max_{(R,R_e=R)\in\mathscr{R}_c} R \\ &= \max \min \big\{ I(U;Y), I(U;Y) - I(U;Z) \\ &\qquad + R_f, H(A \mid Z) \big\}.\end{aligned} \tag{6}$$

We see that the secrecy capacity is a function of the feedback rate R_f. By setting $R_f = H(Y \mid UZ)$,

$$\begin{aligned}&I(U;Y) - I(U;Z) + R_f \\ &\quad = I(U;Y) - I(U;Z) + H(Y \mid UZ) \\ &\quad = H(U \mid Z) - H(U \mid Y) + H(Y \mid UZ) \\ &\quad = H(U \mid Z) - H(U \mid YZ) + H(Y \mid UZ),\end{aligned} \tag{7}$$

$$\begin{aligned}&I(U;Y) - I(U;Z) + R_f \\ &\quad = I(U;Y \mid Z) + H(Y \mid UZ) \\ &\quad = H(Y \mid Z) - H(Y \mid UZ) + H(Y \mid UZ) \\ &\quad = H(Y \mid Z),\end{aligned} \tag{8}$$

where (7) is from the Markov chain $U \to Y \to Z$. Substituting (8) into (6), we have

$$\begin{aligned}C_{\mathrm{sc}} &= \max_{(R,R_e=R)\in\mathscr{R}_c} R \\ &= \max \min \{ I(U;Y), H(Y \mid Z), H(A \mid Z) \},\end{aligned} \tag{9}$$

which is the secrecy capacity of the causal case in [18].

Similarly, according to the definition in (3), the secrecy capacity of wiretap channel with noncausal action-dependent states and rate-limited feedback is

$$\begin{aligned}C_{\mathrm{sn}}(R_f) &= \max_{(R,R_e=R)\in\mathscr{R}_n} R \\ &= \max \min \big\{ I(U;Y) - I(U;S \mid A), I(U;Y) \\ &\qquad - I(U;Z) + R_f, H(A \mid Z) \big\}.\end{aligned} \tag{10}$$

By setting $R_f = H(Y \mid UZ)$, (10) turns into

$$\begin{aligned}C_{\mathrm{sn}} = \max \min \{ &I(U;Y) - I(U;S \mid A), \\ &H(Y \mid Z), H(A \mid Z) \},\end{aligned} \tag{11}$$

which is the secrecy capacity of the noncausal case in [18].

We should emphasize that the feedback in [18] comes from the output of the main channel and is used as a shared key between the transmitter and receiver. This kind of feedback mechanism gives rise to potential danger of revealing the key to the wiretapper since the wiretapper can guess the output of the main channel indirectly to get the key. Our approach avoids this potential danger of information leakage by constructing a feedback link and generating the feedback independently of the main channel's output.

In addition, without considering the causal or noncausal action-dependent states in the model of Figure 1, the secrecy capacity turns into $C'_{sc}(R_f) = \max \min\{I(U;Y), I(U;Y) - I(U;Z) + R_f\}$ which coincides with the secrecy capacity of the (degraded) wiretap channel with rate-limited feedback [16].

To better illustrate how our approach improves these models, such as channel without feedback, with noiseless feedback [18], and without actions [16], we present the simulation in the following subsection.

3.2. Simulation and Comparison. In the example, we consider a binary symmetric channel with causal action-dependent states and rate-limited feedback. The channel model is shown in Figure 2. Let the main channel be a binary symmetric channel (BSC), and let its crossover probability be affected by the channel states. The wiretap channel is also assumed to be a BSC with crossover probability q. In a more accurate way, define

$$p(y \mid x, s = i) = \begin{cases} (1-p)(1-i) + pi, & \text{if } y = x, \\ (1-p)\, i + p(1-i), & \text{otherwise,} \end{cases}$$
$$p(z \mid y) = \begin{cases} 1-q, & \text{if } z = y, \\ q, & \text{otherwise,} \end{cases} \tag{12}$$

where $i \in \{0, 1\}$, $0 \le p \le 1$, and $0 \le q \le 1$.

To simplify the math, let the channel from the action to the channel states be a BSC with crossover probability equal to 1.0; that is, the channel states are totally determined by the action sequence. Similar to the arguments in [1, 13, 18], the maximum values of $I(U;Y)$, $H(A \mid Z)$, and $I(U;Y) - I(U;Z)$ are achieved when $g : \mathcal{U} \to \mathcal{A}$ and $f : \mathcal{U} \times \mathcal{S} \to \mathcal{X}$ are deterministic mappings. This implies that $H(A \mid Z) = H(U \mid Z)$. We choose g and f as

$$g(u = i) = i,$$
$$f(u = i, s = j) = i + j \pmod 2, \tag{13}$$

where $i, j \in \{0, 1\}$. Let $U \sim \text{Bernoulli}(\alpha)$, where $0 \le \alpha \le 1$. Then, the joint distribution $p(a, s, u, x, y, z) = p(z \mid y)p(y \mid x, s)p(x \mid u, s)p(s \mid a)p(a \mid u)p(u)$ can be calculated. Since

$$p(u, y) = \sum_{a,s,x,z} p(a, s, u, x, y, z),$$
$$p(u, z) = \sum_{a,s,x,y} p(a, s, u, x, y, z), \tag{14}$$

by taking some mathematical calculation, we can get

$$C_{sc}(R_f) = \max_{p(u)} \min \{I(U;Y), I(U;Y) - I(U;Z) + R_f, H(A \mid Z)\}$$
$$= \min \{1 - h(p), h(p * q) - h(p) + R_f, h(p * q)\}, \tag{15}$$

where $p * q = p + q - 2pq$ and $h(p)$ is the binary entropy function; that is, $h(p) = -p \log p - (1-p)\log(1-p)$. The calculation of the above $C_{sc}(R_f)$ is based on the *information theoretic methods* which involve the knowledge of *Information Theory* and *Probability Theory*. They are standard techniques, so it is not difficult to obtain the result of formula (15). The computation complexity of the calculation process is low. Similar arguments for calculating secrecy capacity can be seen in [1, 18]. Figure 3 shows that C_{sc} starts from $h(p * q) - h(p)$ and increases linearly with R_f until it gets saturated at $\min\{1 - h(p), h(p * q)\}$ for feedback rate $R_f \ge \min\{1 - h(p * q), h(p)\}$.

When $R_f \ge \min\{1 - h(p * q), h(p)\}$ and p is fixed, the value of C_{sc} changing with q is shown in Figure 4. It can be seen from Figure 4 that when the crossover probability of the main channel is $p = 0.5$, the secrecy capacity is equal to 0. This result is straightforward since the legitimate receiver cannot correctly decode the message when the main channel is in the "poorest" condition. When the main channel condition gets better, that is, p increases from 0.5 to 1.0, the maximum value of C_{sc} increases. The secrecy capacity reaches $1 - h(q)$ when the crossover probability of the main channel $p = 1.0$. This is because when the main channel is noiseless, the input of main channel is the same as receiver's observation. This implies that the input of the main channel can be seen as the input of the wiretap channel.

When no feedback is imposed, that is, $R_f = 0$, Figure 5 shows the secrecy capacity C_{sc} changing with p when q is fixed. As can be seen from Figure 5, when the quality of the wiretap channel gets better, that is, q increases from 0.5 to 1.0, the secrecy capacity decreases. This warns the transmitter to pay attention to the trade-off between the transmission rate and confidentiality. When the wiretap channel is noiseless ($q = 1.0$), the secrecy capacity C_{sc} is zero no matter how good the quality of the main channel is. It results from the fact that the wiretapper has the same observation as the receiver. Note that when the crossover probability of the wiretap channel is $q = 0.5$, the secrecy capacity is $C_{sc} = 1 - h(p)$ which is the capacity of the main channel. This is because no information leakage emerges when the wiretap channel is in the "poorest" condition.

The comparison among our approach, the model without feedback, the model with dependent noiseless feedback [18], and the model without taking actions [16] is presented as follows.

3.2.1. Feedback versus No Feedback. The comparison on the secrecy capacity between the channel with feedback and the channel without feedback is shown in Figures 6 and 7. It

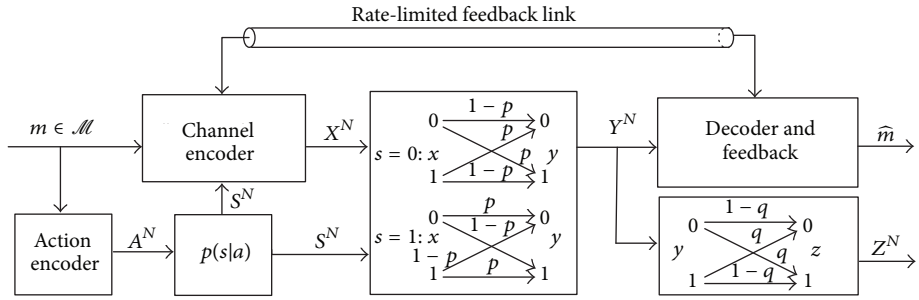

Figure 2: Binary symmetric channel with causal action-dependent states and rate-limited feedback.

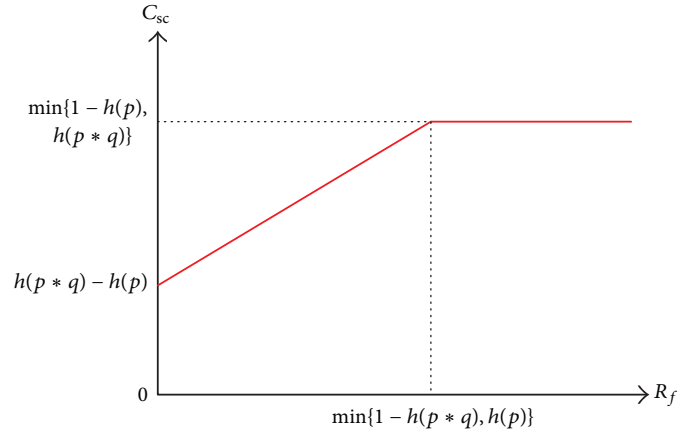

Figure 3: The secrecy capacity of the degraded binary symmetric wiretap channel with causal action-dependent states and rate-limited feedback.

can be seen from Figure 6 that the secrecy capacity of the model without feedback is covered by that with feedback. This indicates that the secrecy capacity of our approach is bigger than the channel model without feedback, and feedback can increase the secrecy capacity. To see it more clearly, we pick out four cross sections shown in Figure 7. In the lower right subgraph of Figure 7 where the wiretap channel is noiseless (i.e., $q = 1.0$), the secrecy capacity for the channel with and without feedback is a positive value and zero, respectively. This implies the fact that when the wiretap channel is noiseless and no feedback is imposed, no information can be securely transmitted to the receiver. Luckily, by introducing feedback, our approach makes it possible to transmit the message securely even if the wiretap channel is in the "best" condition.

3.2.2. Independent Feedback versus Dependent Feedback. Figures 8 and 9 present the secrecy capacities of our approach (with independent feedback) and the model [18] (with dependent feedback). In Figure 8, we can see that the secrecy capacity of our approach covers the secrecy capacity of [18]. To see it more clearly, we also choose four cross-sections shown in Figure 9. In general, the secrecy capacity of our approach is bigger than the model with noiseless feedback [18]. Concretely, one has the following.

(i) According to the results shown in [18], the secrecy capacity of the binary channel with causal channel states and noiseless feedback is $C_{\text{dai}} = \min\{1 - h(p), \min\{h(p * q), h(q)\}\}$. It is easy to see that $C_{\text{dai}} \leq C_{\text{sc}}(R_f)$ when $R_f \geq \min\{1 - h(p * q), h(p)\}$. The difference between C_{dai} and $C_{\text{sc}}(R_f)$ is that there exists $h(q)$ in the expression of C_{dai}. Note that $h(q)$ is brought by $H(Y \mid Z)$ which is the wiretapper's uncertainty of the output of the main channel.

(ii) As can be seen from Figure 9, the maximum secrecy capacity gap between our approach and [18] is enlarged with the increase of q, and so does the range of variation of the main channel's transition probability when $C_{\text{sc}}(R_f) \geq C_{\text{dai}}$. This indicates that when the quality of the wiretap channel becomes better (i.e., q increases from 0.5 to 1.0), the number of the main channels, in which our approach brings about bigger secrecy capacities than those in [18], increases.

(iii) In Figures 8 and 9, we also see that when q increases (from 0.5 to 1.0), the maximum value of secrecy capacity in our approach and the model with noiseless feedback [18] decreases. This results from the fact that when q varies from 0.5 to 1.0, the condition of the wiretap channel gets better so that the wiretapper is more able to obtain the confidential message.

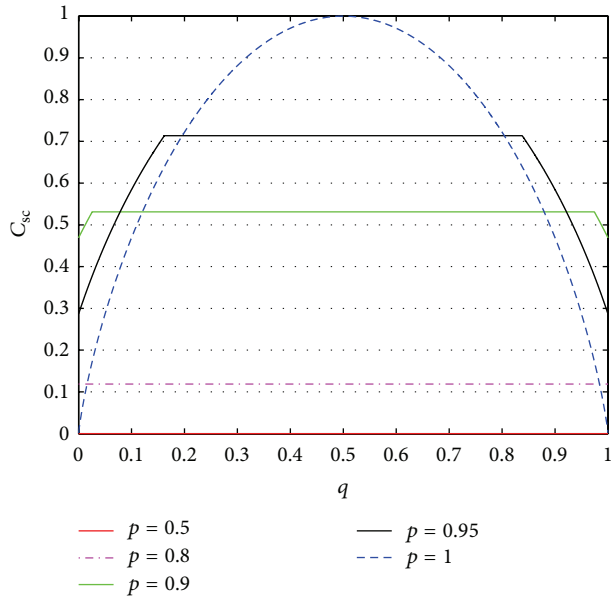

FIGURE 4: The secrecy capacity of the BSC example with feedback rate $R_f \geq \min\{1 - h(p * q), h(p)\}$.

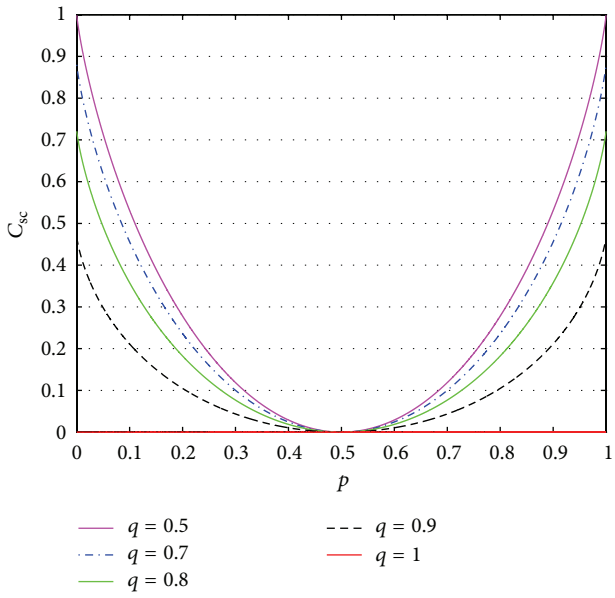

FIGURE 5: The secrecy capacity of the BSC example with feedback rate $R_f = 0$.

(iv) In the lower right subgraph of Figure 9 where $q = 1$ (i.e., the wiretap channel is noiseless), the secrecy capacity of the model with noiseless feedback [18] is zero. This indicates that it is unable to transmit the message securely over the channel. However, the secrecy capacity of our approach is positive. This means that the transmitter can still send the message securely although the wiretapper is more "powerful" than the legitimate receiver.

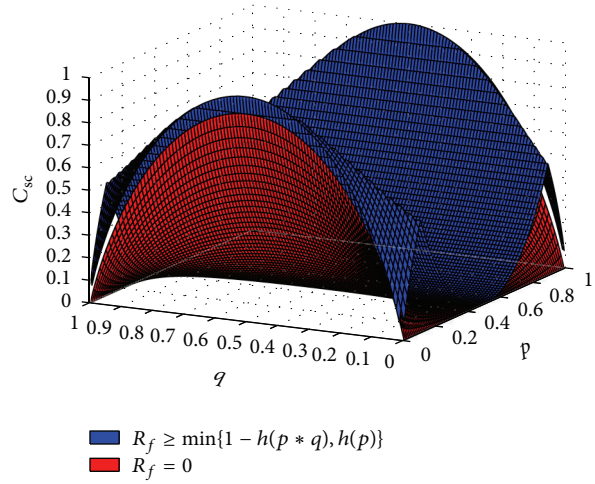

FIGURE 6: With feedback versus without feedback (i).

We can also explain the results from the aspect of feedback. In the channel model with noiseless feedback [18], the feedback is dependent on the output of the main channel and used as a shared key between the transmitter and the receiver. This enables the wiretapper to get the key and, further, the confidential message by guessing the output of the main channel indirectly. However, in our model, since the feedback is independent of the channel output, the wiretapper tries in vain to get the key through guessing the channel output. Therefore, our approach makes the system more secure.

3.2.3. Actions versus No Actions. We consider six representative cases to evaluate the secrecy capacities of our model and the model without actions [16].

Case 1 ($p = 0.99, q = 0.65$). The main channel is almost "perfect," while the wiretap channel is in the "poorest" condition.

Case 2 ($p = 0.96, q = 0.82$). The main channel is better than the wiretap channel. They are both in "good" condition.

Case 3 ($p = 0.93, q = 0.93$). The main channel and wiretap channel share the same transition probability. They are both in "good" condition.

Case 4 ($p = 0.90, q = 0.99$). The wiretap channel is better than the main channel. They are both in "good" condition.

Case 5 ($p = 0.65, q = 0.99$). The wiretap channel is almost "perfect," while the main channel is in the "poorest" condition.

Case 6 ($p = 0.60, q = 0.60$). The main channel and wiretap channel share the same transition probability. They are both in the "poorest" condition.

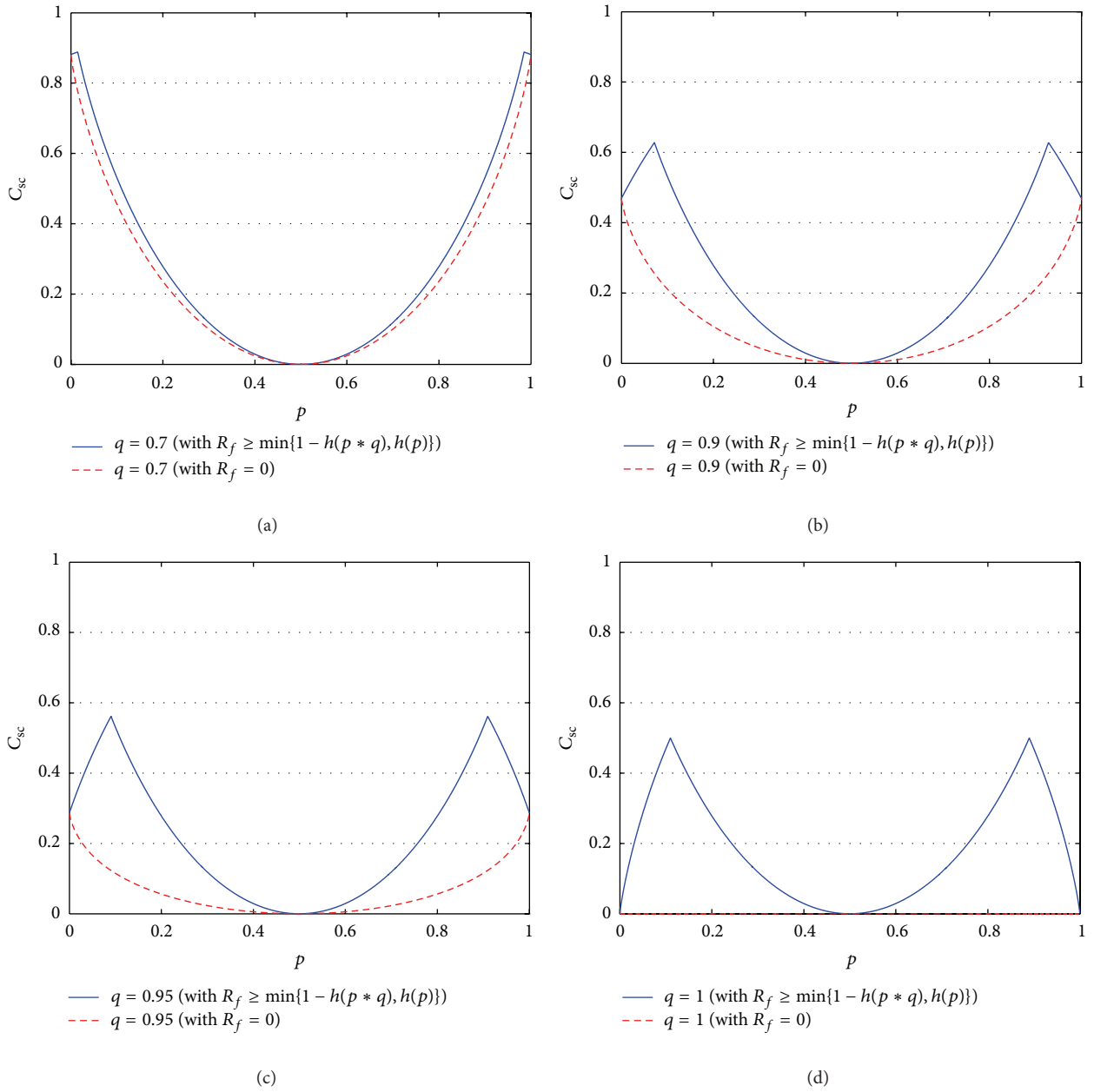

Figure 7: With feedback versus without feedback (ii).

Our model provides insights into the value of actions in the two-stage coding systems, such as recording for magnetic storage devices and coding for computer memories with defects. To better explain the value of actions, let us consider an example of writing information into a memory with defects. The memory can be seen as the main channel in our model, the location of the defects corresponds to the channel states, and writing information into the memory corresponds to transmitting information over the channel. Before writing information into the memory, suppose that neither encoder nor decoder knows the locations of the defects. In the first stage, the encoder writes into the memory for the first time. It gets a noisy version of the inputs when it reads from the memory. Then, in the second stage, the encoder rewrites at whichever memory locations it chooses before the decoder attempts to decode the information [1]. Note that, in the second stage, the encoder will have some knowledge about the memory defects according to the information written in the first stage and the noisy version it reads from the memory in that stage. The first stage can be seen as the "preparing stage" in which the encoder takes "actions" to learn about the defects (i.e., channel state).

Figure 10 shows the process of writing eight data blocks into a memory with defects by our approach and the approach in [16] where no actions were taken. As can be seen from Figure 10, without taking actions to probe the locations of the

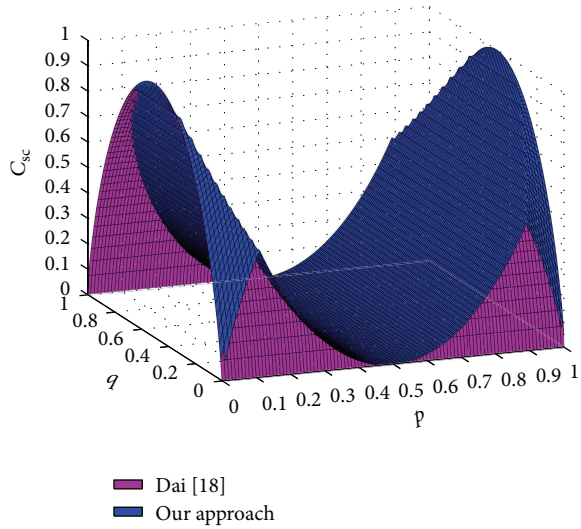

Figure 8: Independent feedback versus dependent feedback (i).

Table 1: The extra overhead of the transmission time.

Case	The extra overhead of transmission time
1	0
2	3.37%
3	13.64%
4	7.51%
5	0
6	0

defects, some data blocks are missed after they are written into the memory. It is well known that data integrity is one of the most important aspects of communication. From the above example, by introducing actions in such two-stage systems, the integrity of the transmitted data is guaranteed. Therefore, the scheme in [16] where no actions were taken is unsuitable for the two-stage systems. From this point of view, our assumption that the encoder takes actions to acquire channel state information is essential and valuable.

At the same time, the cost of taking actions is that the secrecy capacity decreases; see Figure 11. The secrecy capacity of the binary example without actions [16] is $C'_{sc}(R_f) = \min\{1 - h(p), h(p * q) - h(p) + R_f\}$. As can be seen from Figure 11, when the rate of the feedback link R_f is less than a specific value, the secrecy capacity C_{sc} of our approach is equal to the secrecy capacity C'_{sc} of the model [16]. This means no extra transmission time (or channel use) is produced by introducing "actions" when R_f is small. However, when R_f is greater than a specific value, the secrecy capacity is $C_{sc} \leq C'_{sc}$. This indicates that the "actions" bring the overhead of transmission time. Concretely, the extra overhead of the transmission time is shown in Table 1.

From Table 1, we can see that when $p = 0.96$, $q = 0.82$ (Case 2), the overhead of the transmission time shows an increase of 3.37 percent over the approach [16] where no action-dependent states were considered. When $p = 0.93$, $q = 0.93$ and $p = 0.90$, $q = 0.99$, the extra time overhead is 13.64 and 7.51 percent, respectively. In general, the extra time overhead is small. On the premise of data integrity, the amount of such extra time overhead is tolerable.

4. Conclusion

This paper studies the wiretap channel with action-dependent states and rate-limited feedback. It is a degraded channel model where the wiretap channel is degraded from the main channel. The capacity-equivocation region of such a channel both for the case where the channel inputs depend noncausally on the state sequence and the case where they are restricted to causal dependence is obtained. This paper also gets the secrecy capacities for both cases. At the same time, we construct capacity-achieving coding schemes using the methods of Wyner's random binning, Gel'fand and Pinsker's coding technique, and rate splitting. The simulation results show that using feedback can increase the secrecy capacity of the channel in Figure 1, and the secrecy capacity of our model is bigger than that of [16, 18]. Besides, we also find that taking actions to affect the channel states can ensure the data integrity of the message transmitted in the two-stage systems although the tolerable overhead of transmission time is brought.

Some potential directions that our work leaves open for future study are as follows.

(i) *Nondegraded Wiretap Channel*. In this paper, the wiretap channel is degraded from the main channel where $p(z, y \mid x, s) = p(z \mid y)p(y \mid x, s)$. This indicates that $(X, S) \to Y \to Z$ form a Markov chain. However, the degraded wiretap channel is a special case of non-degraded wiretap channel where $p(z, y \mid x, s) = p(z \mid y)p(y \mid x, s)$ does not need to hold. Without this Markov chain, the coding schemes as well as the proof of converse part will be different, and further the secrecy capacity of the non-degraded wiretap channel will be different from the current results.

(ii) *Adaptive Action*. Adaptive action means that the action sequence is generated by the message and the previous channel states, that is, $a_i(m, s^{i-1})$. Adaptive action is widely used in many applications such as information hiding, digital watermarking, and data storage in the memory. It is valuable to study the adaptive action in our model. From [22], we have already known that adaptive action is not useful in increasing the point-to-point channel capacity. We will study whether it influences the secrecy capacity of our channel model.

(iii) *Multiple Transmitters or Receivers*. Nowadays, many types of communication involves two or more transmitters (or receivers), such as the multiple-access channel (MAC), broadcast channel (BC), and multiple-input-multiple-output (MIMO) channel. By introducing action-dependent states and feedback in such channels (with an additional wiretapper), we

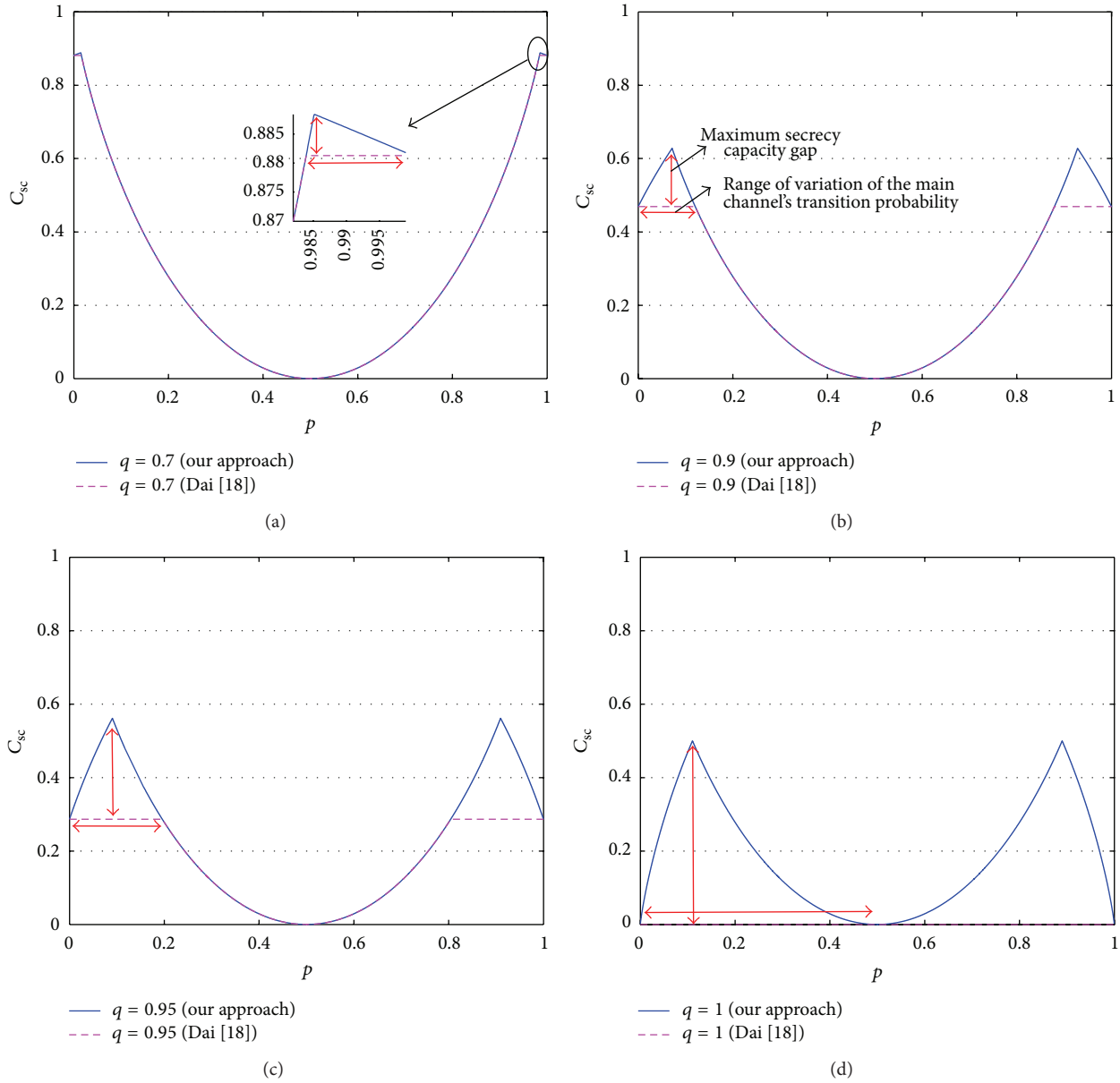

Figure 9: Independent feedback versus dependent feedback (ii).

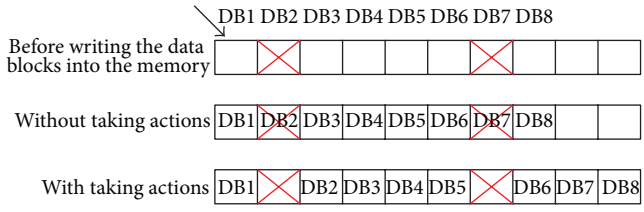

Figure 10: Writing information into a memory with defects.

can revisit their capacity-equivocation regions and secrecy capacities.

Besides, the Gaussian wiretap channel with action-dependent states and feedback is also a practical channel model that is worthy of being explored.

Appendices

A. Coding Schemes for Causal Channel State Information

This section provides the coding schemes to achieve $(R, R_e) \in \mathcal{R}_c$. Similar to the coding scheme in [18], two different coding schemes for $H(A \mid Z) \geq \min\{I(U;Y), I(U;Y) - I(U;Z) + R_f\}$ and $H(A \mid Z) \leq \min\{I(U;Y), I(U;Y) - I(U;Z) + R_f\}$ are constructed in Cases 1 and 2, respectively.

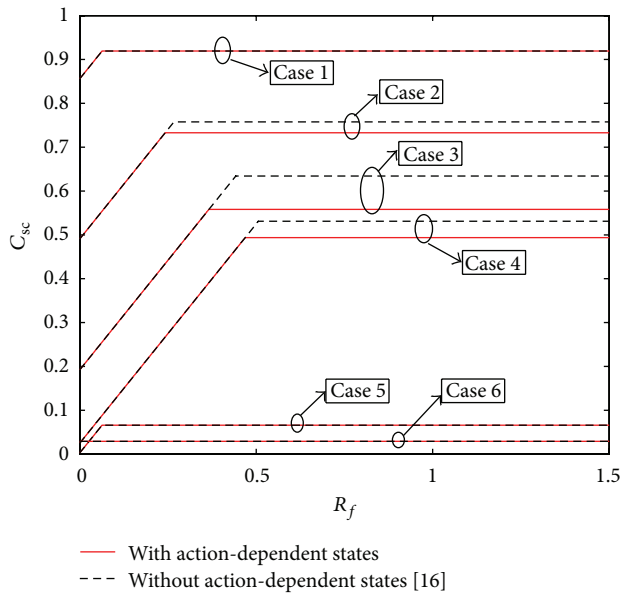

Figure 11: Actions versus no actions.

Case 1 ($H(A \mid Z) \geq \min\{I(U;Y), I(U;Y) - I(U;Z) + R_f\}$). In Case 1, we need to show that all rate pairs (R, R_e), satisfying

$$\begin{aligned} 0 \leq R_e &\leq R, \\ R &\leq I(U;Y), \\ R_e &\leq I(U;Y) - I(U;Z) + R_f, \end{aligned} \tag{A.1}$$

are achievable. It is sufficient to prove that the rate pairs $(R, R_e = \min\{I(U;Y), I(U;Y) - I(U;Z) + R_f\})$ are achievable. In the coding scheme, Wyner's random binning technique and rate splitting are used. The feedback symbol is used as a shared secret key between the transmitter and the receiver. The wiretapper is assumed to have no knowledge of the secret key.

Split the message $\mathscr{M}$ into two parts, that is, $\mathscr{M} = (\mathscr{M}_1, \mathscr{M}_2)$. The corresponding random variables M_1, M_2 are uniformly distributed over $\mathscr{M}_1 = \{1, 2, 3, \ldots, 2^{NR'}\}$ and $\mathscr{M}_2 = \{1, 2, 3, \ldots, 2^{NR'_f}\}$, where

$$\begin{aligned} 0 \leq R'_f &\leq \min\left\{I(U;Z), R_f\right\}, \\ R' &= R - R'_f > 0. \end{aligned} \tag{A.2}$$

Define three alphabets $\mathscr{J}_N$, $\mathscr{L}_N$, and $\mathscr{F}_N$ satisfying

$$\begin{aligned} \lim_{N\to\infty} \frac{1}{N} \log \|\mathscr{J}_N\| &= I(U;Z) - R'_f; \\ \lim_{N\to\infty} \frac{1}{N} \log \|\mathscr{L}_N\| &= I(U;Y) - I(U;Z); \\ \lim_{N\to\infty} \frac{1}{N} \log \|\mathscr{F}_N\| &= R'_f. \end{aligned} \tag{A.3}$$

Note that $\lim_{N\to\infty}((1/N)\log(\|\mathscr{J}_N\| \cdot \|\mathscr{L}_N\| \cdot \|\mathscr{F}_N\|)) = I(U;Y)$.

Since $R \leq I(U;Y)$, let $\mathscr{M}_1 = \mathscr{D}_N \times \mathscr{L}_N$ and $\mathscr{M}_2 = \mathscr{F}_N$, where $\mathscr{D}_N$ is an arbitrary set such that $\lim_{N\to\infty}((1/N)\log\|\mathscr{M}\|) = R$ holds and $\|\mathscr{D}_N\| \leq \|\mathscr{J}_N\|$. Define a deterministic mapping g_1 from $\mathscr{J}_N$ into $\mathscr{D}_N$, which partitions $\mathscr{J}_N$ into subsets of size $\|\mathscr{J}_N\|/\|\mathscr{D}_N\|$. The codebook is constructed as follows.

Codebook Generation and Encoding. Generate $2^{NR'}$ independent and identically distributed (i.i.d) action sequences $a^N(m_1)$ according to $p(a^N) = \prod_{i=1}^N p(a_i)$, where $m_1 \in \mathscr{M}_1$. The channel state sequence s^N is generated through the discrete memoryless channel $p(s^N \mid a^N) = \prod_{i=1}^N p(s_i \mid a_i)$.

The feedback link is shared between the transmitter and the legitimate receiver. It is assumed that a secret key $k \in \{1, 2, 3, \ldots, 2^{NR'_f}\}$ is transmitted through the feedback link. Let the corresponding random variable K be independent of M and uniformly distributed over $\{1, 2, 3, \ldots, 2^{NR'_f}\}$.

For each $a^N(m_1)$, generate $2^{N(I(U;Y)-R')}$ independent and identically distributed (i.i.d) sequences u^N according to $p(u^N \mid a^N) = \prod_{i=1}^N p(u_i \mid a_i)$. Put these sequences into $2^{NR'_f}$ bins so that each bin contains $\|\mathscr{J}_N\|/\|\mathscr{D}_N\|$ sequences $u^N(m_1, t_b, t_u)$, where the bin index $t_b \in \{1, 2, 3, \ldots, 2^{NR'_f}\}$ and the sequence index $t_u \in \{1, 2, \ldots, \|\mathscr{J}_N\|/\|\mathscr{D}_N\|\}$.

Suppose that $k \in \{1, 2, 3, \ldots, 2^{NR'_f}\}$ is the shared secret key between the transmitter and the receiver during one transmission. To send message $(m_1, m_2) = (d, l, m_2)$ with the action sequence $a^N(m_1)$ and the state sequence s^N, where $d \in \mathscr{D}_N$, $l \in \mathscr{L}_N$, and $m_2 \in \mathscr{M}_2$, randomly choose a sequence $u^N(m_1, t_b, t_u)$ from the bin indexed by $t_b = m_2 \oplus k$. Here $\oplus$ is modulo addition over $\mathscr{F}_N$. Then, the input sequence of the main channel is generated by $p(x^N \mid u^N, s^N) = \prod_{i=1}^N p(x_i \mid u_i, s_i)$.

Decoding. When observing the channel output y^N, the receiver tries to find a sequence $u^N(\widehat{m}_1, \widehat{t}_b, \widehat{t}_u)$ such that $(u^N(\widehat{m}_1, \widehat{t}_b, \widehat{t}_u), y^N) \in T_{UY}^N$. Then, the decoder outputs $(\widehat{m}_1, \widehat{t}_b \ominus k)$, where $\ominus$ is modulo subtraction over $\mathscr{F}_N$. If no such $(\widehat{m}_1, \widehat{t}_b, \widehat{t}_u)$ exists, take $(\widehat{m}_1, \widehat{t}_b, \widehat{t}_u) = (1, 1, 1)$.

Analysis of Error Probability. By using similar arguments in [1], it is easy to show that the legitimate receiver can decode the message with vanishing probability of decoding error. The details for proving $P_e \leq \epsilon$ are omitted.

Analysis of Equivocation. We focus on calculating wiretapper's equivocation of the message, that is, the uncertainty about the message given wiretapper's observation. To serve the analysis of equivocation, the fact that M_2 is independent of $M_2 \oplus K$ will be shown firstly. Using similar derivation in [18], we start with the definition of mutual independence

$$\begin{aligned} &p\left(M_2 \oplus K = k', M_2 = m_2\right) \\ &\quad = p\left(K = k' \ominus m_2, M_2 = m_2\right) \\ &\quad =^{(a1)} p\left(K = k' \ominus m_2\right) p\left(M_2 = m_2\right) \end{aligned}$$

$$
\begin{aligned}
&=^{(a2)} \frac{1}{\left\|\mathscr{F}_N\right\|} \cdot \frac{1}{\left\|\mathscr{F}_N\right\|}, \\
&p\left(M_2 \oplus K = k'\right) \\
&\quad = \sum_k p\left(M_2 \oplus K = k' \mid K = k\right) p\left(K = k\right) \\
&\quad =^{(a3)} \sum_k p\left(M_2 \oplus K = k' \mid K = k\right) \frac{1}{\left\|\mathscr{F}_N\right\|} \\
&\quad = \frac{1}{\left\|\mathscr{F}_N\right\|} \sum_k p\left(M_2 \oplus K = k' \mid K = k\right) \\
&\quad = \frac{1}{\left\|\mathscr{F}_N\right\|} \sum_k p\left(M_2 = k' \ominus k \mid K = k\right) \\
&\quad =^{(a4)} \frac{1}{\left\|\mathscr{F}_N\right\|} \sum_k p\left(M_2 = k' \ominus k\right) \\
&\quad = \frac{1}{\left\|\mathscr{F}_N\right\|},
\end{aligned}
\tag{A.4}
$$

where $(a1)$ and $(a4)$ follow from the fact that M_2 is independent of K and $(a2)$ and $(a3)$ follow from the fact that M_2 and K are both uniformly distributed over $\mathscr{F}_N$. According to (A.4),

$$
\begin{aligned}
&p\left(M_2 \oplus K = k', M_2 = m_2\right) \\
&\quad = p\left(M_2 \oplus K = k'\right) p\left(M_2 = m_2\right).
\end{aligned}
\tag{A.5}
$$

Therefore, M_2 is independent of $M_2 \oplus K$.

Utilizing the above fact,

$$
\begin{aligned}
H\left(M \mid Z^N\right) &= H\left(M_1, M_2 \mid Z^N\right) \\
&= H\left(M_1 \mid Z^N\right) + H\left(M_2 \mid Z^N, M_1\right) \\
&\geq H\left(M_1 \mid Z^N\right) + H\left(M_2 \mid Z^N, M_1, K \oplus M_2\right) \\
&=^{(a5)} H\left(M_1 \mid Z^N\right) + H\left(M_2 \mid K \oplus M_2\right) \\
&=^{(a6)} H\left(M_1 \mid Z^N\right) + H\left(M_2\right) \\
&=^{(a7)} H\left(M_1 \mid Z^N\right) + NR'_f,
\end{aligned}
\tag{A.6}
$$

where $(a5)$ follows from the Markov chain $M_2 \rightarrow M_2 \oplus K \rightarrow (Z^N, M_1)$, $(a6)$ follows from the fact that M_2 is independent of $M_2 \oplus K$, and $(a7)$ follows from the fact that M_2 is uniformly distributed over $\{1, 2, 3, \ldots, 2^{NR'_f}\}$. To bound $H(M_1 \mid Z^N)$ in (A.6), Csiszar's method for analyzing equivocation [8] is used:

$$
\begin{aligned}
&H\left(M_1 \mid Z^N\right) \\
&\quad = H\left(M_1, Z^N\right) - H\left(Z^N\right) \\
&\quad = H\left(M_1, Z^N, U^N\right) - H\left(U^N \mid M_1, Z^N\right) - H\left(Z^N\right) \\
&\quad = H\left(M_1, U^N\right) + H\left(Z^N \mid M_1, U^N\right) \\
&\qquad - H\left(U^N \mid M_1, Z^N\right) - H\left(Z^N\right) \\
&\quad \geq H\left(U^N\right) + H\left(Z^N \mid M_1, U^N\right) - H\left(U^N \mid M_1, Z^N\right) \\
&\qquad - H\left(Z^N\right) \\
&\quad \geq H\left(U^N\right) - H\left(U^N \mid Y^N\right) + H\left(Z^N \mid M_1, U^N\right) \\
&\qquad - H\left(U^N \mid M_1, Z^N\right) - H\left(Z^N\right) \\
&\quad = I\left(U^N; Y^N\right) + H\left(Z^N \mid M_1, U^N\right) \\
&\qquad - H\left(U^N \mid M_1, Z^N\right) - H\left(Z^N\right) \\
&\quad =^{(a8)} I\left(U^N; Y^N\right) + H\left(Z^N \mid U^N\right) \\
&\qquad - H\left(U^N \mid M_1, Z^N\right) - H\left(Z^N\right) \\
&\quad =^{(a9)} NI\left(U; Y\right) + NH\left(Z \mid U\right) \\
&\qquad - H\left(U^N \mid M_1, Z^N\right) - H\left(Z^N\right) \\
&\quad \geq^{(a10)} NI\left(U; Y\right) + NH\left(Z \mid U\right) \\
&\qquad - H\left(U^N \mid M_1, Z^N\right) - NH\left(Z\right) \\
&\quad \geq^{(a11)} NI\left(U; Y\right) - NI\left(U; Z\right) - N\epsilon_2.
\end{aligned}
\tag{A.7}
$$

In the above derivations, $(a8)$ follows from the fact that $M_1 \rightarrow U^N \rightarrow Z^N$ is a Markov chain. $(a9)$ follows from the fact that S^N, U^N and X^N are i.i.d generated and both the main channel and wiretap channel are discrete memoryless. $(a10)$ follows from the fact that $H(Z^N) = \sum_{i=1}^N H(Z_i \mid Z^{i-1}) \leq NH(Z)$, where Z is regarded as the general random variable of Z_i. To verify $(a11)$, note the fact that given the message $m_1 = (d, l)$, the number of U^N is

$$
\begin{aligned}
2^{N(I(U;Y)-R')} &= \frac{2^{NI(U;Y)}}{2^{NR'}} \\
&= \frac{\left\|\mathscr{J}_N\right\| \cdot \left\|\mathscr{L}_N\right\| \cdot \left\|\mathscr{F}_N\right\|}{\left\|\mathscr{M}_1\right\|} \\
&= \frac{\left\|\mathscr{J}_N\right\| \cdot \left\|\mathscr{L}_N\right\| \cdot \left\|\mathscr{F}_N\right\|}{\left\|\mathscr{D}_N\right\| \cdot \left\|\mathscr{L}_N\right\|}
\end{aligned}
$$

$$
\begin{aligned}
&= \frac{\left\|\mathcal{J}_N\right\| \cdot \left\|\mathcal{F}_N\right\|}{\left\|\mathcal{D}_N\right\|} \\
&\leq \left\|\mathcal{J}_N\right\| \cdot \left\|\mathcal{F}_N\right\| \\
&= 2^{N(I(U;Z)-R_f')} \cdot 2^{NR_f'} \\
&= 2^{NI(U;Z)}.
\end{aligned} \tag{A.8}
$$

By applying the standard channel coding theorem [23, Theorem 7.7.1], the wiretapper can decode U^N with vanishing decoding error probability. Then, utilizing Fano's inequality, we get $H(U^N \mid M_1, Z^N) \leq N\epsilon_2$, where $\epsilon_2 \to 0$ when $N \to \infty$. (A.7) is verified.

Using the definition of equivocation and substituting (A.7) into (A.6),

$$
\begin{aligned}
\lim_{N\to\infty} \Delta &= \lim_{N\to\infty} \frac{H\left(M \mid Z^N\right)}{N} \\
&\geq \lim_{N\to\infty} \left(\frac{H\left(M_1 \mid Z^N\right)}{N} + R_f' \right) \\
&\geq \lim_{N\to\infty} \left(\frac{NI(U;Y) - NI(U;Z) - N\epsilon_2}{N} + R_f' \right) \\
&= I(U;Y) - I(U;Z) + R_f' \\
&\geq R_e.
\end{aligned} \tag{A.9}
$$

This completes the achievability proof of Case 1.

Case 2 ($H(A \mid Z) \leq \min\{I(U;Y), I(U;Y) - I(U;Z) + R_f\}$). In Case 2, we show that all rate pairs (R, R_e), satisfying

$$
\begin{aligned}
0 \leq R_e &\leq R, \\
R &\leq I(U;Y), \\
R_e &\leq H(A \mid Z),
\end{aligned} \tag{A.10}
$$

are achievable. It is sufficient to prove that the rate pairs $(R, R_e = \min\{I(U;Y), H(A \mid Z)\})$ are achievable. The coding scheme is similar to [18].

Codebook Generation and Encoding. Generate 2^{NR} action sequences $a^N(m)$ according to $p(a^N) = \prod_{i=1}^N p(a_i)$, where $m \in \{1, 2, \ldots, 2^{NR}\}$. The state s^N is generated in response to $a^N(m)$ according to $p(s^N \mid a^N) = \prod_{i=1}^N p(s_i \mid a_i)$. Generate 2^{NR} i.i.d sequences $u^N(m)$ according to $p(u^N \mid a^N) = \prod_{i=1}^N p(u_i \mid a_i)$. To send message m with the action sequence $a^N(m)$ and the state sequence s^N, find the sequence $u^N(m)$. Then, the input sequence of the main channel is generated by $p(x^N \mid u^N, s^N) = \prod_{i=1}^N p(x_i \mid u_i, s_i)$.

Decoding. When observing the channel output y^N, the receiver tries to find a sequence $u^N(\widehat{m})$ such that $(u^N(\widehat{m}), y^N) \in T_{UY}^N(\epsilon_1')$. Then, the decoder outputs $\widehat{m}$. If no such $\widehat{m}$ exists, take $\widehat{m} = 1$.

Analysis of Error Probability. By using similar arguments in [1], it is easy to show that the legitimate receiver can decode the message with vanishing probability of decoding error. The details for proving $P_e \leq \epsilon$ are omitted.

Analysis of Equivocation. We focus on calculating wiretapper's equivocation of the the message, that is, the uncertainty about the message given wiretapper's observation. The method for calculating the equivocation in [13] is utilized in this case:

$$
\begin{aligned}
\lim_{N\to\infty} \Delta &= \lim_{N\to\infty} \frac{H\left(M \mid Z^N\right)}{N} \\
&=^{(a12)} \lim_{N\to\infty} \frac{H\left(A^N \mid Z^N\right)}{N} \\
&=^{(a13)} \lim_{N\to\infty} \frac{NH(A \mid Z)}{N} \\
&= H(A \mid Z) \\
&\geq R_e,
\end{aligned} \tag{A.11}
$$

where $(a12)$ follows from the fact that the action sequence $a^N(m)$ is a determination function of the message m and $(a13)$ follows from the fact that A^N and X^N are i.i.d generated and both the main channel and wiretap channel are discrete memoryless. This completes the achievability proof of Case 2.

The achievability proof of Theorem 4 is completed.

B. Proof of the Converse Part of Theorem 4

In this section, we show that all achievable rate pairs (R, R_e) for the channel model in Figure 1 with causal states are contained in $\mathcal{R}_c$. Concretely, for any rate pair (R, R_e), feedback alphabet $\mathcal{K}$, and decoding error probability P_e satisfying

$$
R = \lim_{N\to\infty} \frac{\log \|\mathcal{M}\|}{N}, \tag{B.1}
$$

$$
\lim_{N\to\infty} \frac{\log \|\mathcal{K}\|}{N} \leq R_f, \tag{B.2}
$$

$$
R_e \leq \lim_{N\to\infty} \Delta, \tag{B.3}
$$

$$
P_e \leq \epsilon, \tag{B.4}
$$

there exist random variables $(A, U) \to (X, S) \to Y \to Z$ such that

$$
0 \leq R_e \leq R, \tag{B.5}
$$

$$
R \leq I(U;Y), \tag{B.6}
$$

$$
R_e \leq I(U;Y) - I(U;Z) + R_f, \tag{B.7}
$$

$$
R_e \leq H(A \mid Z). \tag{B.8}
$$

The four inequalities (B.5), (B.6), (B.7), and (B.8) will be proved successively.

One has consider condition (B.5) first.

$$\begin{aligned} R_e &\le \lim_{N\to\infty} \Delta \\ &= \lim_{N\to\infty} \frac{H\left(M \mid Z^N\right)}{N} \\ &\le \lim_{N\to\infty} \frac{H(M)}{N} \\ &=^{(b1)} R, \end{aligned} \tag{B.9}$$

where $(b1)$ is from (B.1). Condition (B.5) is proved.

To prove condition (B.6), we consider

$$\begin{aligned} \frac{1}{N}H(M) &= \frac{1}{N}I\left(M;Y^N\right) + \frac{1}{N}H\left(M \mid Y^N\right) \\ &\le^{(b2)} \frac{1}{N}I\left(M;Y^N\right) + \frac{1}{N}\eta\left(P_e\right) \\ &= \frac{1}{N}\sum_{i=1}^{N} I\left(M;Y_i \mid Y^{i-1}\right) + \frac{1}{N}\eta\left(P_e\right) \\ &\le \frac{1}{N}\sum_{i=1}^{N} I\left(M,Y^{i-1},S^{i-1};Y_i\right) + \frac{1}{N}\eta\left(P_e\right) \\ &\le^{(b3)} \frac{1}{N}\sum_{i=1}^{N} I\left(U_i;Y_i\right) + \frac{1}{N}\eta\left(P_e\right). \end{aligned} \tag{B.10}$$

Inequality $(b2)$ is from Fano's inequality. To be more accurate, $\eta(P_e) = h(P_e) + P_e \log(\|M\| - 1)$, where $h(P_e)$ is the binary entropy function; that is, $h(P_e) = -P_e \log P_e - (1 - P_e)\log(1 - P_e)$. Note that $\eta(P_e) \to 0$ when P_e approaches zero. $(b3)$ is from defining $U_i = (M, Y^{i-1}, S^{i-1})$. According to (B.1) and (B.10), it is easy to see that

$$\begin{aligned} R &= \lim_{N\to\infty} \frac{\log\|\mathscr{M}\|}{N} \\ &=^{(b4)} \lim_{N\to\infty} \frac{1}{N}H(M) \\ &\le \lim_{N\to\infty} \frac{1}{N}\sum_{i=1}^{N} I\left(U_i;Y_i\right) + \frac{1}{N}\eta\left(P_e\right), \end{aligned} \tag{B.11}$$

where $(b4)$ follows from the fact that M is uniformly distributed over $\{1, 2, \ldots, \|\mathscr{M}\|\}$.

To prove condition (B.7), the recursive argument lemma [16] will be exploited. Therefore, we present the lemma below. The detailed proof of the lemma is shown in [16].

Recursive Argument Lemma [16]. For each $j = 1, 2, \ldots, N$, the following inequality holds:

$$\begin{aligned} &H\left(K^j \mid Z^j\right) + I\left(M, X^j; Y^j \mid K^j, Z^j\right) \\ &\quad\le H\left(K^{j-1} \mid Z^{j-1}\right) + I\left(M, X^{j-1}; Y^{j-1} \mid K^{j-1}, Z^{j-1}\right) \\ &\qquad + I\left(X_j;Y_j \mid Z_j\right) + H\left(K_j \mid M, X^{j-1}, K^{j-1}, Z^{j-1}\right), \end{aligned} \tag{B.12}$$

where K, X, Y, and Z are the the feedback random variable, the input of the main channel, the input of the wiretap channel, and the output of the wiretap channel. (Actually, [16] gave the lemma under a more relaxed condition that the wiretap channel did not need to be physically degraded.)

Then, we prove condition (B.7) as follows:

$$\begin{aligned} R_e &\le \lim_{N\to\infty} \Delta \\ &= \lim_{N\to\infty} \frac{1}{N}H\left(M \mid Z^N\right) \\ &= \lim_{N\to\infty} \frac{1}{N}\left(I\left(M;Y^N,K^N \mid Z^N\right)\right. \\ &\qquad \left. + H\left(M \mid Y^N, Z^N, K^N\right)\right) \\ &\le \lim_{N\to\infty} \frac{1}{N}\left(I\left(M;Y^N,K^N \mid Z^N\right) + H\left(M \mid Y^N\right)\right) \\ &\le^{(b5)} \lim_{N\to\infty} \frac{1}{N}\left(I\left(M;Y^N,K^N \mid Z^N\right) + \eta\left(P_e\right)\right) \\ &= \lim_{N\to\infty} \frac{1}{N}\left(I\left(M;K^N \mid Z^N\right)\right. \\ &\qquad \left. + I\left(M;Y^N \mid K^N, Z^N\right) + \eta\left(P_e\right)\right) \\ &\le \lim_{N\to\infty} \frac{1}{N}\left(H\left(K^N \mid Z^N\right)\right. \\ &\qquad \left. + I\left(M,U^N;Y^N \mid K^N, Z^N\right) + \eta\left(P_e\right)\right), \end{aligned} \tag{B.13}$$

where $(b5)$ follows from Fano's inequality. By applying the lemma recursively, the two terms in (B.13) can be single letterized as follows:

$$\begin{aligned} &H\left(K^N \mid Z^N\right) + I\left(M,U^N;Y^N \mid K^N, Z^N\right) \\ &\quad\le H\left(K^{N-1} \mid Z^{N-1}\right) + I\left(M,U^{N-1};Y^{N-1} \mid K^{N-1}, Z^{N-1}\right) \\ &\qquad + I\left(U_N;Y_N \mid Z_N\right) + H\left(K_N \mid M, U^{N-1}, K^{N-1}, Z^{N-1}\right) \\ &\quad\le H\left(K^{N-1} \mid Z^{N-1}\right) + I\left(M,U^{N-1};Y^{N-1} \mid K^{N-1}, Z^{N-1}\right) \\ &\qquad + I\left(U_N;Y_N \mid Z_N\right) + H\left(K_N\right) \\ &\quad\le H\left(K^{N-2} \mid Z^{N-2}\right) + I\left(M,U^{N-2};Y^{N-2} \mid K^{N-2}, Z^{N-2}\right) \\ &\qquad + I\left(U_{N-1};Y_{N-1} \mid Z_{N-1}\right) + H\left(K_{N-1}\right) \\ &\qquad + I\left(U_N;Y_N \mid Z_N\right) + H\left(K_N\right) \\ &\quad\le \sum_{i=1}^{N} \left(I\left(U_i;Y_i \mid Z_i\right) + H\left(K_i\right)\right) \\ &\quad\le \sum_{i=1}^{N} \left(I\left(U_i;Y_i \mid Z_i\right) + R_f\right). \end{aligned} \tag{B.14}$$

Substituting (B.14) into (B.13), we get

$$R_e \le \lim_{N\to\infty} \frac{1}{N}\left(\sum_{i=1}^{N}\left(I\left(U_i;Y_i \mid Z_i\right)+R_f\right)+\eta\left(P_e\right)\right). \tag{B.15}$$

To prove (B.8), consider

$$\begin{aligned} R_e &\le \lim_{N\to\infty}\Delta \\ &= \lim_{N\to\infty}\frac{1}{N}H\left(M \mid Z^N\right) \\ &=^{(b6)} \lim_{N\to\infty}\frac{1}{N}H\left(A^N \mid Z^N\right) \\ &= \lim_{N\to\infty}\frac{1}{N}\sum_{i=1}^{N}H\left(A_i \mid A^{i-1}, Z^N\right) \\ &\le \lim_{N\to\infty}\frac{1}{N}\sum_{i=1}^{N}H\left(A_i \mid Z_i\right), \end{aligned} \tag{B.16}$$

where $(b6)$ follows from the fact that the action sequence a^N is a deterministic function of the message m.

To serve the single-letter characterization, let us introduce a time-sharing random variable Q independent of M, A^N, S^N, U^N, X^N, Y^N, and Z^N and uniformly distributed over $\{1,2,\ldots,N\}$. Set

$$\begin{aligned} U &= \left(M, Y^{Q-1}, S^{Q-1}, Q\right), \\ A &= A_Q, \qquad S = S_Q, \qquad X = X_Q, \\ Y &= Y_Q, \qquad Z = Z_Q. \end{aligned} \tag{B.17}$$

It is straightforward to see that $(A,U) \to (X,S) \to Y \to Z$ and $U \to Y \to Z$ form Markov chains. Then, it is easy to get

$$\begin{aligned} I\left(U;Y \mid Z\right) &= H\left(U \mid Z\right) - H\left(U \mid YZ\right) \\ &= H\left(U\right) - H\left(U \mid YZ\right) - \left(H\left(U\right) - H\left(U \mid Z\right)\right) \\ &=^{(b7)} H\left(U\right) - H\left(U \mid Y\right) - \left(H\left(U\right) - H\left(U \mid Z\right)\right) \\ &= I\left(U;Y\right) - I\left(U;Z\right), \end{aligned} \tag{B.18}$$

where $(b7)$ follows from the Markov chain $U \to Y \to Z$. After using the standard time sharing argument [19, Section 5.4], utilizing (B.18), and letting $P_e \to 0$, (B.11), (B.15), and (B.16) are simplified into (B.6), (B.7), and (B.8), respectively.

This completes the proof of the converse part of Theorem 4.

C. Coding Schemes for Noncausal Channel State Information

This section provides two different coding schemes for $H(A \mid Z) \ge \min\{I(U;Y) - I(U;S \mid A), I(U;Y) - I(U;Z) + R_f\}$ and $H(A \mid Z) \le \min\{I(U;Y) - I(U;S \mid A), I(U;Y) - I(U;Z) + R_f\}$ in Cases 1 and 2, respectively.

Case 1 ($H(A \mid Z) \ge \min\{I(U;Y) - I(U;S \mid A), I(U;Y) - I(U;Z) + R_f\}$). In this case, we need to prove that all rate pairs (R, R_e), satisfying

$$\begin{aligned} 0 &\le R_e \le R, \\ R &\le I\left(U;Y\right) - I\left(U;S \mid A\right), \\ R_e &\le I\left(U;Y\right) - I\left(U;Z\right) + R_f, \end{aligned} \tag{C.1}$$

are achievable. It is sufficient to prove the rate pairs $(R, R_e = \min\{I(U;Y) - I(U;S \mid A), I(U;Y) - I(U;Z) + R_f\})$ are achievable. In the following coding scheme, Gel'fand and Pinsker's coding technique [20] and rate splitting are used. The feedback symbol is used as a shared secret key between the transmitter and the receiver. The wiretapper has no knowledge of the secret key.

Define

$$\begin{aligned} R' &= I\left(U;Y\right) - I\left(U;Z\right); \\ R'_f &= R - R'. \end{aligned} \tag{C.2}$$

Split the message $\mathscr{M}$ into two parts, that is, $\mathscr{M} = (\mathscr{M}_1, \mathscr{M}_2)$. The corresponding random variables M_1, M_2 are uniformly distributed over $\mathscr{M}_1 = \{1,2,3,\ldots,2^{NR'}\}$ and $\mathscr{M}_2 = \{1,2,3,\ldots,2^{NR'_f}\}$. Since

$$\begin{aligned} R &\le C_{\text{sn}}\left(R_f\right) \\ &= \min\left\{I\left(U;Y\right) - I\left(U;S \mid A\right), I\left(U;Y\right)\right. \\ &\qquad \left. -I\left(U;Z\right) + R_f, H\left(A \mid Z\right)\right\} \\ &= \min\left\{I\left(U;Y\right) - I\left(U;S \mid A\right), I\left(U;Y\right) - I\left(U;Z\right) + R_f\right\}, \end{aligned} \tag{C.3}$$

it is easy to get

$$\begin{aligned} R'_f &= R - R' \\ &\le \min\left\{I\left(U;Y\right) - I\left(U;S \mid A\right), I\left(U;Y\right) - I\left(U;Z\right) + R_f\right\} \\ &\quad - \left(I\left(U;Y\right) - I\left(U;Z\right)\right) \\ &= \min\left\{I\left(U;Z\right) - I\left(U;S \mid A\right), R_f\right\}. \end{aligned} \tag{C.4}$$

Codebook Generation and Encoding. Let $R = I(U;Y) - I(U;S \mid A) - \tau_1$, where τ_1 is a fixed positive number. Generate $2^{NR'}$ i.i.d action sequences $a^N(m_1)$ according to $p(a^N) = \prod_{i=1}^{N} p(a_i)$ where $m_1 \in \mathscr{M}_1$. The channel state sequence s^N is generated through the discrete memoryless channel $p(s^N \mid a^N) = \prod_{i=1}^{N} p(s_i \mid a_i)$.

The feedback link is shared between the transmitter and the legitimate receiver. It is assumed that a secret key $k \in \{1,2,3,\ldots,2^{NR'_f}\}$ is transmitted through the feedback link and the wiretapper has no knowledge about the secret key. Let the corresponding random variable K be independent of M and uniformly distributed over $\{1,2,3,\ldots,2^{NR'_f}\}$.

For each $a^N(m_1)$, generate $2^{N(I(U;Y)-R'-\epsilon)}$ i.i.d sequences u^N according to $p(u^N \mid a^N) = \prod_{i=1}^N p(u_i \mid a_i)$, where $\epsilon \to 0$ as $N \to \infty$. Note that

$$\begin{aligned} 2^{N(I(U;Y)-R'-\epsilon)} &= 2^{N(I(U;Y)-R+R'_f-\epsilon)} \\ &= 2^{N(I(U;S|A)+\tau_1+R'_f-\epsilon)}. \end{aligned} \tag{C.5}$$

Then, put these sequences into $2^{NR'_f}$ bins so that each bin contains $2^{N(I(U;S\mid A)+\tau_1-\epsilon)}$ sequences $u^N(m_1, t_b, t_u)$, where the bin index $t_b \in \{1, 2, 3, \ldots, 2^{NR'_f}\}$ and the sequence index $t_u \in \{1, 2, 3, \ldots, 2^{N(I(U;S\mid A)+\tau_1-\epsilon)}\}$.

Suppose that $k \in \{1, 2, 3, \ldots, 2^{NR'_f}\}$ is the shared secret key between the transmitter and the receiver during one transmission. To send message $m = (m_1, m_2)$ with the action sequence $a^N(m_1)$ and the state sequence s^N, where $m_1 \in \mathcal{M}_1$, $m_2 \in \mathcal{M}_2$, the transmitter tries to find a sequence $u^N(m_1, t_b, t_u)$ from the bin indexed by $t_b = m_2 \oplus k$ such that $(u^N(m_1, t_b, t_u), s^N, a^N(m_1)) \in T^N_{US|A}$. Here, $\oplus$ is modulo addition over $\{1, 2, 3, \ldots, 2^{NR'_f}\}$. If no such sequence exists in that bin, take $t_u = 1$. (In fact, at least one such sequence will exist because there are more than $2^{NI(U;S\mid A)} u^N(m_1, t_b, t_u)$ in each bin.) Then, The input sequence of the main channel is generated by $p(x^N \mid u^N, s^N) = \prod_{i=1}^N p(x_i \mid u_i, s_i)$.

Decoding. When observing the channel output y^N, the receiver tries to find a sequence $u^N(\widehat{m}_1, \widehat{t}_b, \widehat{t}_u)$ such that $(u^N(\widehat{m}_1, \widehat{t}_b, \widehat{t}_u), y^N) \in T^N_{UY}$. Then, the decoder outputs $(\widehat{m}_1, \widehat{t}_b \ominus k)$, where $\ominus$ is modulo subtraction over $\{1, 2, 3, \ldots, 2^{NR'_f}\}$. If no such $(\widehat{m}_1, \widehat{t}_b, \widehat{t}_u)$ exists, take $(\widehat{m}_1, \widehat{t}_b, \widehat{t}_u) = (1, 1, 1)$.

Analysis of Error Probability. By using similar arguments in [1], it is easy to show that the legitimate receiver can decode the message with vanishing decoding error probability. Note that since Gel'fand and Pinsker's coding technique is used for the noncausal case, particular attention should be paid to the encoding error probability when calculating the whole error probability. The details for proving $P_e \le \epsilon$ are omitted.

Analysis of Equivocation. We focus on calculating wiretapper's equivocation of the message, that is, the uncertainty about the message given wiretapper's observation.

Using the same derivation in (A.6), we have

$$H\left(M \mid Z^N\right) \ge H\left(M_1 \mid Z^N\right) + NR'_f. \tag{C.6}$$

The first term in (C.6) is calculated by applying Csiszar's method for analyzing equivocation [8]:

$$\begin{aligned} &H\left(M_1 \mid Z^N\right) \\ &\quad = H\left(M_1, Z^N\right) - H\left(Z^N\right) \\ &\quad = H\left(M_1, Z^N, U^N\right) - H\left(U^N \mid M_1, Z^N\right) - H\left(Z^N\right) \\ &\quad = H\left(M_1, U^N\right) + H\left(Z^N \mid M_1, U^N\right) \\ &\qquad - H\left(U^N \mid M_1, Z^N\right) - H\left(Z^N\right) \\ &\quad \ge H\left(U^N\right) + H\left(Z^N \mid M_1, U^N\right) \\ &\qquad - H\left(U^N \mid M_1, Z^N\right) - H\left(Z^N\right) \\ &\quad \ge H\left(U^N\right) - H\left(U^N \mid Y^N\right) + H\left(Z^N \mid M_1, U^N\right) \\ &\qquad - H\left(U^N \mid M_1, Z^N\right) - H\left(Z^N\right) \\ &\quad = I\left(U^N; Y^N\right) + H\left(Z^N \mid M_1, U^N\right) \\ &\qquad - H\left(U^N \mid M_1, Z^N\right) - H\left(Z^N\right) \\ &\quad =^{(c1)} I\left(U^N; Y^N\right) + H\left(Z^N \mid U^N\right) \\ &\qquad - H\left(U^N \mid M_1, Z^N\right) - H\left(Z^N\right) \\ &\quad =^{(c2)} NI\left(U; Y\right) + NH\left(Z \mid U\right) \\ &\qquad - H\left(U^N \mid M_1, Z^N\right) - H\left(Z^N\right) \\ &\quad \ge^{(c3)} NI\left(U; Y\right) + NH\left(Z \mid U\right) \\ &\qquad - H\left(U^N \mid M_1, Z^N\right) - NH\left(Z\right) \\ &\quad \ge^{(c4)} NI\left(U; Y\right) - NI\left(U; Z\right) - N\epsilon_3. \end{aligned} \tag{C.7}$$

In the above derivations, $(c1)$ follows from the fact that $M_1 \to U^N \to Z^N$ is a Markov chain. $(c2)$ follows from the fact that S^N, U^N, and X^N are i.i.d generated and both the main channel and wiretap channel are discrete memoryless. $(c3)$ follows from $H(Z^N) = \sum_{i=1}^N H(Z_i \mid Z^{i-1}) \le NH(Z)$, where Z is regarded as the general random variable of Z_i. To verify $(c4)$, note the fact that given the message m_1, the number of U^N is

$$\begin{aligned} 2^{N(I(U;Y)-R'-\epsilon)} &= 2^{N[I(U;Y)-(I(U;Y)-I(U;Z))-\epsilon]} \\ &= 2^{N(I(U;Z)-\epsilon)} \le 2^{NI(U;Z)}. \end{aligned} \tag{C.8}$$

By applying the standard channel coding theorem [23, theorem 7.7.1], the wiretapper can decode U^N with vanishing decoding error probability. Then, utilizing Fano's inequality, we get $H(U^N \mid M_1, Z^N) \le N\epsilon_3$, where $\epsilon_2 \to 0$ when $N \to \infty$. (C.7) is verified.

Substituting (C.7) into (C.6) and using the same derivation in (A.9), the achievability proof of Case 1 is completed.

Case 2 ($H(A \mid Z) \le \min\{I(U;Y) - I(U;S \mid A), I(U;Y) - I(U;Z) + R_f\}$). In this case, we show that all rate pairs (R, R_e), satisfying

$$0 \le R_e \le R,$$
$$R \le I(U;Y) - I(U;S \mid A), \tag{C.9}$$
$$R_e \le H(A \mid Z),$$

are achievable. It is sufficient to prove that the rate pairs $(R, R_e = \min\{I(U;Y) - I(U;S \mid A), H(A \mid Z)\})$ are achievable. Gel'fand and Pinsker's coding technique is used. The proof is similar to that in [18].

Codebook Generation and Encoding. Let $R = I(U;Y) - I(U;S \mid A) - \tau_2$, where τ_2 is a fixed positive number. M is uniformly distributed over $\mathscr{M} = \{1, 2, 3, \ldots, 2^{NR}\}$. Generate 2^{NR} action sequences $a^N(m)$ according to $p(a^N) = \prod_{i=1}^{N} p(a_i)$, where $m \in \mathscr{M}$. The channel state sequence s^N is generated through the discrete memoryless channel $p(s^N \mid a^N) = \prod_{i=1}^{N} p(s_i \mid a_i)$. For each $a^N(m)$, generate $2^{N(I(U;Y)-R-\epsilon)} = 2^{N(I(U;S \mid A)+\tau_2-\epsilon)}$ i.i.d sequences $u^N(m,t)$ according to $p(u^N \mid a^N) = \prod_{i=1}^{N} p(u_i \mid a_i)$, where $t \in \{1, 2, 3, \ldots, 2^{N(I(U;S \mid A)+\tau_2-\epsilon)}\}$.

To send message m with the action sequence $a^N(m)$ and the state sequence s^N, the transmitter chooses a sequence $u^N(m,t)$ such that $(u^N(m,t), s^N, a^N(m)) \in T^N_{US \mid A}$. If no such sequence exists, take $t = 1$. Then, the input sequence of the main channel is generated by $p(x^N \mid u^N, s^N) = \prod_{i=1}^{N} p(x_i \mid u_i, s_i)$.

Decoding. When observing the channel output y^N, the receiver tries to find a sequence $u^N(\widehat{m}, \widehat{t})$ such that $(u^N(\widehat{m}, \widehat{t}), y^N) \in T^N_{UY}$. Then, the decoder outputs $\widehat{m}$. If no such $\widehat{m}$ exists, take $\widehat{m} = 1$.

Analysis of Error Probability. By using similar arguments in [1], it is easy to show that the legitimate receiver can decode the message with vanishing decoding error probability. Note that since Gel'fand and Pinsker's coding technique is used for the noncausal case, particular attention should be paid to the encoding error probability when calculating the whole error probability. The details for proving $P_e \le \epsilon$ are omitted.

The *analysis of equivocation* is the same as (A.11). The achievability proof of Case 2 is finished.

The achievability proof of Theorem 5 is completed.

D. Proof of the Converse Part of Theorem 5

This section proves that all achievable rate pairs (R, R_e) for the channel model in Figure 1 with noncausal states are contained in $\mathscr{R}_n$. Concretely, we need to show that, for any rate pair (R, R_e), feedback alphabet $\mathscr{K}$, and decoding error probability P_e satisfying (2), there exist random variables $(A, U) \to (X, S) \to Y \to Z$ such that

$$0 \le R_e \le R, \tag{D.1}$$
$$R \le I(U;Y) - I(U;S \mid A), \tag{D.2}$$
$$R_e \le I(U;Y) - I(U;Z) + R_f, \tag{D.3}$$
$$R_e \le H(A \mid Z). \tag{D.4}$$

The four inequalities (D.1), (D.2), (D.3), and (D.4) are proved as follows.

(D.1), (D.3), and (D.4) can be proved using the same derivations in (B.9), (B.15), and (B.16), respectively, except for the identification of the auxiliary random variable U. Therefore, we focus on proving (D.2) and giving the identification of the auxiliary random variable U.

A lemma in [13] is presented first.

Lemma 6 (see [13]). *One has*

$$\sum_{i=1}^{N} I\left(S_{i+1}^N, A^N; Y_i \mid M, Y^{i-1}\right) = \sum_{i=1}^{N} I\left(S_i; Y^{i-1} \mid M, S_{i+1}^N, A^N\right). \tag{D.5}$$

Proof. One has

$$\begin{aligned}
&\sum_{i=1}^{N} I\left(S_{i+1}^N, A^N; Y_i \mid M, Y^{i-1}\right) \\
&\quad =^{(d1)} \sum_{i=1}^{N} I\left(S_{i+1}^N, A^N; Y_i \mid M, Y^{i-1}, A^N\right) \\
&\quad = \sum_{i=1}^{N} I\left(S_{i+1}^N; Y_i \mid M, Y^{i-1}, A^N\right) \\
&\quad = \sum_{i=1}^{N} \sum_{j=i+1}^{N} I\left(S_j; Y_i \mid M, S_{j+1}^N, Y^{i-1}, A^N\right) \\
&\quad = \sum_{j=1}^{N} \sum_{i=j+1}^{N} I\left(S_i; Y_j \mid M, S_{i+1}^N, Y^{j-1}, A^N\right) \\
&\quad = \sum_{i=1}^{N} \sum_{j=1}^{i-1} I\left(S_i; Y_j \mid M, S_{i+1}^N, Y^{j-1}, A^N\right) \\
&\quad = \sum_{i=1}^{N} I\left(S_i; Y^{i-1} \mid M, S_{i+1}^N, A^N\right),
\end{aligned} \tag{D.6}$$

where $(d1)$ follows from the fact that the action sequence is a deterministic function of the transmitted message.

Since the transmission rate is

$$R = \lim_{N \to \infty} \frac{1}{N} \log \|\mathscr{M}\| = \lim_{N \to \infty} \frac{1}{N} H(M), \tag{D.7}$$

let us consider

$$\begin{aligned}
&\frac{1}{N} H(M) \\
&\quad = \frac{1}{N} I\left(M; Y^N\right) + \frac{1}{N} H\left(M \mid Y^N\right) \\
&\quad \le^{(d2)} \frac{1}{N} I\left(M; Y^N\right) + \frac{1}{N} \eta(P_e)
\end{aligned}$$

$$
\begin{aligned}
&= \frac{1}{N}\sum_{i=1}^{N} I\left(M; Y_i \mid Y^{i-1}\right) + \frac{1}{N}\eta\left(P_e\right) \\
&\leq \frac{1}{N}\sum_{i=1}^{N} I\left(M, Y^{i-1}; Y_i\right) + \frac{1}{N}\eta\left(P_e\right) \\
&= \frac{1}{N}\sum_{i=1}^{N} \left[I\left(M, Y^{i-1}, S_{i+1}^{N}, A^{N}; Y_i\right)\right. \\
&\qquad \left. - I\left(S_{i+1}^{N}, A^{N}; Y_i \mid M, Y^{i-1}\right)\right] + \frac{1}{N}\eta\left(P_e\right) \\
&=^{(d3)} \frac{1}{N}\sum_{i=1}^{N} \left[I\left(M, Y^{i-1}, S_{i+1}^{N}, A^{N}; Y_i\right)\right. \\
&\qquad \left. - I\left(S_i; Y^{i-1} \mid M, S_{i+1}^{N}, A^{N}\right)\right] + \frac{1}{N}\eta\left(P_e\right) \\
&= \frac{1}{N}\sum_{i=1}^{N} \left[I\left(M, Y^{i-1}, S_{i+1}^{N}, A^{N}; Y_i\right)\right. \\
&\qquad \left. - I\left(S_i; Y^{i-1} \mid M, S_{i+1}^{N}, A^{N}, A_i\right)\right] + \frac{1}{N}\eta\left(P_e\right) \\
&= \frac{1}{N}\sum_{i=1}^{N} \left[I\left(M, Y^{i-1}, S_{i+1}^{N}, A^{N}; Y_i\right)\right. \\
&\qquad - I\left(S_i; M, Y^{i-1}, S_{i+1}^{N}, A^{N} \mid A_i\right) \\
&\qquad \left. + I\left(S_i; M, S_{i+1}^{N}, A^{N} \mid A_i\right)\right] + \frac{1}{N}\eta\left(P_e\right) \\
&= \frac{1}{N}\sum_{i=1}^{N} \left[I\left(M, Y^{i-1}, S_{i+1}^{N}, A^{N}; Y_i\right)\right. \\
&\qquad - I\left(S_i; M, Y^{i-1}, S_{i+1}^{N}, A^{N} \mid A_i\right) \\
&\qquad \left. + I\left(S_i; M, S_{i+1}^{N}, A^{i-1}, A_{i+1}^{N} \mid A_i\right)\right] + \frac{1}{N}\eta\left(P_e\right) \\
&=^{(d4)} \frac{1}{N}\sum_{i=1}^{N} \left[I\left(M, Y^{i-1}, S_{i+1}^{N}, A^{N}; Y_i\right)\right. \\
&\qquad \left. - I\left(S_i; M, Y^{i-1}, S_{i+1}^{N}, A^{N} \mid A_i\right)\right] + \frac{1}{N}\eta\left(P_e\right) \\
&=^{(d5)} \frac{1}{N}\sum_{i=1}^{N} \left[I\left(U_i; Y_i\right) - I\left(S_i; U_i \mid A_i\right)\right] + \frac{1}{N}\eta\left(P_e\right),
\end{aligned}
\tag{D.8}
$$

where $(d2)$ follows from Fano's inequality, $(d3)$ is from Lemma 6, $(d4)$ follows from the fact that $S_i \rightarrow A_i \rightarrow (M, S_{i+1}^{N}, A^{i-1}, A_{i+1}^{N})$ form a Markov chain, and $(d5)$ follows from defining $U_i = (M, Y^{i-1}, S_{i+1}^{N}, A^{N})$. Substituting (D.8) into (D.7),

$$
\begin{aligned}
R &= \lim_{N\to\infty} \frac{1}{N} H\left(M\right) \\
&\leq \lim_{N\to\infty} \frac{1}{N}\sum_{i=1}^{N} \left[I\left(U_i; Y_i\right) - I\left(S_i; U_i \mid A_i\right)\right].
\end{aligned}
\tag{D.9}
$$

To serve the single-letter characterization, let us introduce a time-sharing random variable Q independent of M, A^N, S^N, U^N, X^N, Y^N, and Z^N and uniformly distributed over $\{1, 2, \ldots, N\}$. Set

$$
\begin{aligned}
U &= \left(M, Y^{Q-1}, S_{Q+1}^{N}, A^{N}, Q\right), \\
A &= A_Q, \qquad S = S_Q, \qquad X = X_Q, \\
Y &= Y_Q, \qquad Z = Z_Q.
\end{aligned}
\tag{D.10}
$$

It is straightforward to see that $(A, U) \rightarrow (X, S) \rightarrow Y \rightarrow Z$ form a Markov chain. Applying the standard time-sharing argument [19, Section 5.4] to (D.9), we can easily get (D.2).

This completes the proof of the converse part of Theorem 5. □

Conflict of Interests

The authors declare that there is no conflict of interests regarding the publication of this paper.

Acknowledgments

This work was supported in part by the National Natural Science Foundation of China under Grants no. 61171173, 60932003, and 61271220. The authors also would like to thank the anonymous reviewers for helpful comments.

References

[1] T. Weissman, "Capacity of channels with action-dependent states," *IEEE Transactions on Information Theory*, vol. 56, no. 11, pp. 5396–5411, 2010.

[2] B. Ahmadi and O. Simeone, "On channels with action-dependent states," in *Proceedings of the IEEE Information Theory Workshop (ITW '12)*, Lausanne, Switzerland, September 2012.

[3] Y. Steinberg and T. Weissman, "The degraded broadcast channel with action-dependent states," in *Proceedings of the IEEE International Symposium on Information Theory (ISIT '12)*, Boston, Mass, USA, July 2012.

[4] H. Asnani, H. Permuter, and T. Weissman, "Probing capacity," *IEEE Transactions on Information Theory*, vol. 57, no. 11, pp. 7317–7332, 2011.

[5] K. Kittichokechai, T. J. Oechtering, and M. Skoglund, "Coding With action-dependent side information and additional reconstruction requirements," Submitted to *IEEE Transactions on Information Theory*, http://arxiv.org/abs/1202.1484v1.

[6] C. Choudhuri and U. Mitra, "Action dependent strictly causal state communication," in *Proceedings of the IEEE International Symposium on Information Theory (ISIT '12)*, Cambridge, Mass, USA, July 2012.

[7] A. D. Wyner, "The wire-tap channel," *The Bell System Technical Journal*, vol. 54, no. 8, pp. 1355–1387, 1975.

[8] I. Csiszár and J. Körner, "Broadcast channels with confidential messages," *IEEE Transactions on Information Theory*, vol. 24, no. 3, pp. 339–348, 1978.

[9] A. Khisti, G. Wornell, A. Wiesel, and Y. Eldar, "On the Gaussian MIMO wiretap channel," in *Proceedings of the IEEE International Symposium on Information Theory (ISIT '07)*, pp. 2471–2475, Nice, France, June 2007.

[10] S. Shafiee, N. Liu, and S. Ulukus, "Towards the secrecy capacity of the Gaussian MIMO wire-tap channel: the 2-2-1 channel," *IEEE Transactions on Information Theory*, vol. 55, no. 9, pp. 4033–4039, 2009.

[11] F. Oggier and B. Hassibi, "The secrecy capacity of the MIMO wiretap channel," *IEEE Transactions on Information Theory*, vol. 57, no. 8, pp. 4961–4972, 2011.

[12] B. Dai and Y. Luo, "Some new results on the wiretap channel with side information," *Entropy*, vol. 14, no. 9, pp. 1671–1702, 2012.

[13] B. Dai, A. J. H. Vinck, Y. Luo, and X. Tang, "Wiretap channel with action-dependent channel state information," *Entropy*, vol. 15, no. 2, pp. 445–473, 2013.

[14] E. Ekrem and S. Ulukus, "Multi-receiver wiretap channel with public and confidential messages," *IEEE Transactions on Information Theory*, vol. 59, no. 4, pp. 2165–2177, 2013.

[15] R. Ahlswede and N. Cai, "Transmission, identification and common randomness capacities for wire-tape channels with secure feedback from the decoder," in *General Theory of Information Transfer and Combinatorics*, vol. 4123 of *Lecture Notes in Computer Science*, pp. 258–275, Springer, Berlin, Germany, 2006.

[16] E. Ardestanizadeh, M. Franceschetti, T. Javidi, and Y.-H. Kim, "Wiretap channel with secure rate-limited feedback," *IEEE Transactions on Information Theory*, vol. 55, no. 12, pp. 5353–5361, 2009.

[17] X. Yin, Z. Xue, and B. Dai, "Capacity-equivocation regions of the DMBCs with noiseless feedback," *Mathematical Problems in Engineering*, vol. 2013, Article ID 102069, 13 pages, 2013.

[18] B. Dai, A. J. H. Vinck, and Y. Luo, "Wiretap channel in the presence of action-dependent states and noiseless feedback," *Journal of Applied Mathematics*, vol. 2013, Article ID 423619, 17 pages, 2013.

[19] A. El Gamal and Y.-H. Kim, *Network Information Theory*, Cambridge University Press, Cambridge, UK, 2011.

[20] S. I. Gel'fand and M. S. Pinsker, "Coding for channel with random parameters," *Problems of Control and Information Theory*, vol. 9, no. 1, pp. 19–31, 1980.

[21] I. Csiszár and J. Körner, *Information Theory*, Probability and Mathematical Statistics, Academic Press, london, UK, 1981.

[22] C. Choudhuri and U. Mitra, "How useful is adaptive action?" in *Proceedings of the Global Communications Conference (GLOBECOM '12)*, Anaheim, Calif, USA, December 2012.

[23] T. M. Cover and J. A. Thomas, *Elements of Information Theory*, John Wiley & Sons, New York, NY, USA, 1991.

Hindawi Publishing Corporation
Mathematical Problems in Engineering
Volume 2013, Article ID 874085, 18 pages
http://dx.doi.org/10.1155/2013/874085

Research Article

H_∞ Control of Pairwise Distributable Large-Scale TS Fuzzy Systems

Anna Filasová and Dušan Krokavec

Department of Cybernetics and Artificial Intelligence, Faculty of Electrical Engineering and Informatics, Technical University of Košice, Letná 9, 042 00 Košice, Slovakia

Correspondence should be addressed to Dušan Krokavec; dusan.krokavec@tuke.sk

Received 12 July 2013; Revised 1 October 2013; Accepted 3 October 2013

Academic Editor: Hongli Dong

The paper presents new conditions suitable in design of the stabilizing state controller for a class of continuous-time nonlinear systems, which are representable by pairwise distributable Takagi-Sugeno models. Taking into account the affine properties of the TS model structure and applying the pairwise subsystems fuzzy control scheme relating to the parallel distributed output compensators, the extended bounded real lemma form and the sufficient design conditions for pairwise decentralized control are outlined in terms of linear matrix inequalities. The proposed procedure decouples the Lyapunov matrix and the system parameter matrices in the LMIs and, using free tuning parameter, provides the way to obtain global stability of such large-scale TS systems and optimizes subsystems interaction H_∞ norm bounds.

1. Introduction

A number of problems that arise in state control can be reduced to a handful of standard convex and quasiconvex problems that involve matrix inequalities (LMI). It is known that the optimal solution can be computed by using the interior point methods [1], which converge in polynomial time with respect to the problem size. Thus, efficient interior point algorithms have recently been developed and further development of algorithms for these standard problems is an area of active research. For this approach, the stability conditions may be expressed in terms of LMIs, which have a notable practical interest due to the existence of numerical solvers. Some progress review in this field can be found, for example, in [2, 3] and the references therein.

Based on the concept of quadratic stability, the control design problems, in respect of the H_∞ norm of the closed-loop system transfer matrix, are transferred into a standard LMI optimization task, which includes bounded real lemma (BRL) formulation. The first version of BRL presented simple condition under which a transfer function was contractive on the imaginary axis of the complex variable plain. Using this formulation, it was possible to determine the H_∞ norm of a transfer function, and the BRL has become a significant element to show and prove that the existence of feedback controllers, resulting in a closed-loop transfer matrix having the H_∞ norm less than a given upper bound, is equivalent to the existence of a solution of certain LMIs. Motivated by the underlying ideas, the technique for BRL representation was extended to state feedback control design and stayed preferable for systems with time-varying parameters [4–6]. When used in robust analysis of linear systems with polytopic uncertainties, as the number of polytops increases, the solution turned out to be very conservative. To reduce conservatism inherent in such use of quadratic methods, the equivalent LMI representations of BRL for continuous-time as well as discrete-time uncertain systems were introduced [7–10]. Moreover, exploiting the sector nonlinearity approach to obtain Takagi-Sugeno (TS) models from the nonlinear system equations [11], suitable BRLs as well as enhanced BRL representation guaranteeing quadratic performances for the closed-loop nonlinear systems are exploited in H_∞ fuzzy control [12–14].

In last years, modern control methods have found their way into design of interconnected systems and led to a wide variety of new concepts and results. In particular, paradigms of LMIs and H_∞ norm have appeared to be very attractive due to their promise of handling systems with relative high dimensions, and design of partly decentralized schemes substantially minimized the information exchange between subsystems of a large scale system. With respect to the existing structure of interconnections in a large-scale system, it is generally impossible to stabilize all subsystems and the whole system simultaneously by using decentralized controllers, since the stability of interconnected systems is not only dependent on the stability degree of subsystems but is also closely dependent on the interconnections [15–17]. Analogous principles were applied in decentralized fuzzy control [18].

Considering the decomposition-based control strategy [19] and including into design step the effects of subsystem pairs interconnections [20], a pairwise decentralized control problem was proposed for linear large-scale systems in [21] and for linear large-scale systems with polytopic uncertainties in [22], respectively. Introducing the results as a pairwise partially decentralized control, in [21] there were formulated design conditions for a linear control, while the design conditions given in [22] reflect the robust linear control design task, both solved in the frames of LMI representations. Since the feedback control for TS models is the so-called parallel distributed compensation (PDC) control, the above results have to be significantly reformulated considering the pairwise distributable large-scale TS fuzzy systems.

Inspired by the enhanced design conditions proposed in [13] in designing the optimal control of TS systems with quadratic optimality criterion, the paper is devoted to studying the partially decentralized control problems from the above given viewpoint for pairwise distributable large-scale TS fuzzy systems. Sufficient stability conditions are stated now as a set of LMIs to encompass the quadratic stability case in respect of the H_∞ approach. Used structures in the presented forms enable us potentially to design systems with an embedded reconfigurable control structure property [21]. To the best of the authors' knowledge, the paper presents a new formulation of the control principle of pairwise distributable large-scale TS fuzzy systems, newly defines the conditions of existence of solutions for the fuzzy control scheme relating to PDCs in such distributable structure, and offers the possibility of new ways to solve the problem of control law synthesis for TS fuzzy systems with a large number of membership functions.

The paper is organized as follows. In Section 2, the basis preliminaries, concerning the TS models and the H_∞ norm problems, are presented with results on BRL and enhanced BRL for TS systems. Formulating the pairwise distributable large-scale TS fuzzy systems structure in Section 3 and continuing with this formalism in Section 4, the equivalent TS BRL design methods are outlined to possess the sufficient conditions for the pairwise decentralized control of given class of TS large-scale systems. Finally, the example is given in Section 5, to illustrate the feasibility and properties of the proposed method and some concluding remarks are stated in Section 6.

Throughout the paper, the following notations are used: $\mathbf{x}^T$, $\mathbf{X}^T$ denote the transposes of the vector $\mathbf{x}$ and matrix $\mathbf{X}$, respectively, diag$[\mathbf{X}_i]$, $i = 1, 2, \ldots, p$ denotes a block diagonal matrix with p blocks, blk$[\mathbf{X}_{il}]$, $i, l = 1, 2, \ldots, p$ entails a row- and column-wise partitioned matrix, broken into blocks by partitioning its rows and columns into p collection of row-groups and p collection of column-groups, for a square matrix, $\mathbf{X} < 0$ means that $\mathbf{X}$ is a symmetric negative definite matrix, the symbol $\mathbf{I}_n$ indicates the nth order unit matrix, $\mathbb{R}$ denotes the set of real numbers, and $\mathbb{R}^{n\times r}$ refers to the set of $n \times r$ real matrices.

2. Preliminaries

2.1. System Model. The class of TS systems, considered in the paper, is formed as follows:

$$\dot{\mathbf{q}}(t) = \sum_{j=1}^{s} h_j(\boldsymbol{\theta}(t)) \left(\mathbf{A}_j \mathbf{q}(t) + \mathbf{B}_j \mathbf{u}(t)\right), \tag{1}$$

$$\mathbf{y}(t) = \mathbf{C}\mathbf{q}(t), \tag{2}$$

where $\mathbf{q}(t) \in \mathbb{R}^n$, $\mathbf{u}(t) \in \mathbb{R}^r$, and $\mathbf{y}(t) \in \mathbb{R}^m$ are vectors of the state, input, and measurable output variables, respectively, matrices $\mathbf{A}_j \in \mathbb{R}^{n\times n}$, $\mathbf{B}_j \in \mathbb{R}^{n\times r}$, and $\mathbf{C} \in \mathbb{R}^{m\times n}$ are real matrices, $t \in \mathbb{R}$ is the time variable, and $\mu_j(\boldsymbol{\theta}(t))$ is the weight for jth fuzzy rule. Satisfying the following, by definition, the property

$$0 \le \mu_j(\boldsymbol{\theta}(t)) \le 1, \quad \sum_{j=1}^{s} \mu_j(\boldsymbol{\theta}(t)) = 1 \quad \forall j \in \langle 1, 2, \ldots, s\rangle,$$
$$\boldsymbol{\theta}(t) = [\theta_1(t) \;\; \theta_2(t) \;\; \cdots \;\; \theta_v(t)] \tag{3}$$

is the vector of the premise variables, where s, v are the numbers of fuzzy rules and premise variables, respectively. It is supposed next that all premise variables are measurable and independent on $\mathbf{u}(t)$ (more details can be found, e.g., in [11, 13]).

2.2. LMI Formulations for H_∞ Performance. Let the TS systems model (1), (2) be considered (in this subsection only) in the next extended form

$$\dot{\mathbf{q}}(t) = \sum_{j=1}^{s} \mu_j(\boldsymbol{\theta}(t)) \left(\mathbf{A}_j \mathbf{q}(t) + \mathbf{B}_j \mathbf{u}(t) + \mathbf{G}_j \mathbf{w}(t)\right), \tag{4}$$

$$\mathbf{y}(t) = \mathbf{C}\mathbf{q}(t) + \mathbf{D}\mathbf{w}(t), \tag{5}$$

where $\mathbf{G}_j \in \mathbb{R}^{n\times r}$, $\mathbf{D} \in \mathbb{R}^{m\times r}$, and $w(t) \in \mathbb{R}^r$ is the disturbance input that belongs to $L_2\langle 0, +\infty)$ and, using the same set of membership functions, the fuzzy state control law is defined as

$$\mathbf{u}(t) = -\sum_{g=1}^{s} \mu_g(\boldsymbol{\theta}(t)) \mathbf{K}_g \mathbf{q}(t). \tag{6}$$

Evidently, the closed-loop system state variable dynamics is described by the next equation

$$\dot{\mathbf{q}}(t) = \sum_{j=1}^{s}\sum_{g=1}^{s}\mu_j(\boldsymbol{\theta}(t))\,\mu_g(\boldsymbol{\theta}(t))\left(\mathbf{H}_{jg}\mathbf{q}(t) + \mathbf{G}_j\mathbf{w}(t)\right) \quad (7)$$

and also, owing to the symmetry in summations, by the symmetric equation

$$\dot{\mathbf{q}}(t) = \sum_{j=1}^{s}\sum_{g=1}^{s}\mu_j(\boldsymbol{\theta}(t))\,\mu_g(\boldsymbol{\theta}(t))\left(\mathbf{H}_{gj}\mathbf{q}(t) + \mathbf{G}_g\mathbf{w}(t)\right), \quad (8)$$

where

$$\mathbf{H}_{jg} = \mathbf{A}_j - \mathbf{B}_j\mathbf{K}_g, \qquad \mathbf{H}_{gj} = \mathbf{A}_g - \mathbf{B}_g\mathbf{K}_j. \quad (9)$$

Thus, adding (8), (9) gives

$$2\dot{\mathbf{q}}(t) = \sum_{j=1}^{s}\sum_{g=1}^{s}\mu_j(\boldsymbol{\theta}(t))\,\mu_g(\boldsymbol{\theta}(t)) \times\left(\left(\mathbf{H}_{jg} + \mathbf{H}_{gj}\right)\mathbf{q}(t) + \left(\mathbf{G}_j + \mathbf{G}_g\right)\mathbf{w}(t)\right). \quad (10)$$

Rearranging the computation, (10) can be written as

$$\begin{aligned}2\dot{\mathbf{q}}(t) = {}& \sum_{j=1}^{s}\mu_j(\boldsymbol{\theta}(t))\,\mu_j(\boldsymbol{\theta}(t)) \times\left(\left(\mathbf{H}_{jj} + \mathbf{H}_{jj}\right)\mathbf{q}(t) + \left(\mathbf{G}_j + \mathbf{G}_j\right)\mathbf{w}(t)\right) \\ & + 2\sum_{j=1}^{s-1}\sum_{g=j+1}^{s}\mu_j(\boldsymbol{\theta}(t))\,\mu_g(\boldsymbol{\theta}(t)) \times\left(\left(\mathbf{H}_{jg} + \mathbf{H}_{gj}\right)\mathbf{q}(t) + \left(\mathbf{G}_j + \mathbf{G}_g\right)\mathbf{w}(t)\right),\end{aligned} \quad (11)$$

$$\begin{aligned}\dot{\mathbf{q}}(t) = {}& \sum_{j=1}^{s}\mu_j(\boldsymbol{\theta}(t))\,\mu_j(\boldsymbol{\theta}(t)) \times\left(\mathbf{H}_{jj}\mathbf{q}(t) + \mathbf{G}_j\mathbf{w}(t)\right) \\ & + 2\sum_{j=1}^{s-1}\sum_{g=j+1}^{s}\mu_j(\boldsymbol{\theta}(t))\,\mu_g(\boldsymbol{\theta}(t)) \times\left(\frac{\mathbf{H}_{jg} + \mathbf{H}_{gj}}{2}\mathbf{q}(t) + \frac{\mathbf{G}_j + \mathbf{G}_g}{2}\mathbf{w}(t)\right),\end{aligned} \quad (12)$$

respectively.

Considering this, the next lemmas can be introduced.

Lemma 1 (bounded real lemma). *The closed-loop system* (7), (5) *is stable with the performance* $\sum_{j=1}^{s}\sum_{g=1}^{s}\mu_j(\boldsymbol{\theta}(t))\mu_g(\boldsymbol{\theta}(t))\left\|\mathbf{C}(s\mathbf{I} - \mathbf{H}_{jg})^{-1}\mathbf{G}_j + \mathbf{D}\right\|_\infty^2 \le \gamma$ *if there exist a positive definite matrix* $\mathbf{X} \in \mathbb{R}^{n\times n}$ *and a positive scalar* $\gamma \in \mathbb{R}$ *such that*

$$\mathbf{X} = \mathbf{X}^T > 0, \qquad \gamma > 0, \quad (13)$$

$$\begin{bmatrix}\mathbf{H}_{jj}\mathbf{X} + \mathbf{X}\mathbf{H}_{jj}^T & \mathbf{G}_j & \mathbf{X}\mathbf{C}^T \\ * & -\gamma\mathbf{I}_r & \mathbf{D}^T \\ * & * & -\mathbf{I}_m\end{bmatrix} < 0, \quad (14)$$

$$\begin{bmatrix}\dfrac{\mathbf{H}_{jg} + \mathbf{H}_{gj}}{2}\mathbf{X} + \mathbf{X}\dfrac{\left(\mathbf{H}_{jg} + \mathbf{H}_{gj}\right)^T}{2} & \dfrac{\mathbf{G}_j + \mathbf{G}_g}{2} & \mathbf{X}\mathbf{C}^T \\ * & -\gamma\mathbf{I}_r & \mathbf{D}^T \\ * & * & -\mathbf{I}_m\end{bmatrix} < 0, \quad (15)$$

for all $j \in \langle 1, 2, \ldots s\rangle$, *and* $j < g \le s$, $j, g \in \langle 1, 2, \ldots s\rangle$, *respectively, where* $\mathbf{I}_r \in \mathbb{R}^{r\times r}$, $\mathbf{I}_m \in \mathbb{R}^{m\times m}$ *are identity matrices and* $\sqrt{\gamma}$ *is an upper bound of* H_∞ *norm of the disturbance transfer matrix function.*

Here and hereafter, $*$ *denotes the symmetric item in a symmetric matrix.*

Proof. Defining Lyapunov function as

$$v(\mathbf{q}(t)) = \mathbf{q}^T(t)\,\mathbf{P}\mathbf{q}(t) + 3\int_0^t\left(\mathbf{y}^T(\tau)\,\mathbf{y}(\tau) - \gamma\mathbf{w}^T(\tau)\,\mathbf{w}(\tau)\right)d\tau > 0, \quad (16)$$

where $\mathbf{P} = \mathbf{P}^T > 0$, $\mathbf{P} \in \mathbb{R}^{n\times n}$, $\gamma > 0$, $\gamma \in \mathbb{R}$ and evaluating the derivative of $v(\mathbf{q}(t))$ with respect to t along a system trajectory, then it yields

$$\dot{v}(\mathbf{q}(t)) = \dot{\mathbf{q}}^T(t)\,\mathbf{P}\mathbf{q}(t) + \mathbf{q}^T(t)\,\mathbf{P}\dot{\mathbf{q}}(t) + 3\left(\mathbf{y}^T(t)\,\mathbf{y}(t) - \gamma\mathbf{w}^T(t)\,\mathbf{w}(t)\right) < 0. \quad (17)$$

Substituting (5) and (12) in (17), the next inequality is obtained:

$$\begin{aligned}&\dot{v}(\mathbf{q}(t)) \\ &= \sum_{j=1}^{s}\mu_j(\boldsymbol{\theta}(t))\,\mu_j(\boldsymbol{\theta}(t)) \\ &\quad\times\left\{\begin{array}{l}\left(\mathbf{H}_{jj}\mathbf{q}(t) + \mathbf{G}_j\mathbf{w}(t)\right)^T\mathbf{P}\mathbf{q}(t) \\ \quad+\mathbf{q}^T(t)\,\mathbf{P}\left(\mathbf{H}_{jj}\mathbf{q}(t) + \mathbf{G}_j\mathbf{w}(t)\right) \\ \quad+(\mathbf{C}\mathbf{q}(t) + \mathbf{D}\mathbf{w}(t))^T(\mathbf{C}\mathbf{q}(t) + \mathbf{D}\mathbf{w}(t)) \\ \quad-\gamma\mathbf{w}^T(t)\,\mathbf{w}(t)\end{array}\right\}\end{aligned}$$

$$
\begin{aligned}
&+2\sum_{j=1}^{s-1}\sum_{g=j+1}^{s}\mu_j(\boldsymbol{\theta}(t))\,\mu_g(\boldsymbol{\theta}(t))\\
&\times\left\{\begin{array}{l}
\left(\dfrac{\mathbf{H}_{jg}+\mathbf{H}_{gj}}{2}\mathbf{q}(t)+\dfrac{\mathbf{G}_j+\mathbf{G}_g}{2}\mathbf{w}(t)\right)^T\mathbf{P}\mathbf{q}(t)\\
+\mathbf{q}^T(t)\,\mathbf{P}\left(\dfrac{\mathbf{H}_{jg}+\mathbf{H}_{gj}}{2}\mathbf{q}(t)+\dfrac{\mathbf{G}_j+\mathbf{G}_g}{2}\mathbf{w}(t)\right)\\
+(\mathbf{C}\mathbf{q}(t)+\mathbf{D}\mathbf{w}(t))^T(\mathbf{C}\mathbf{q}(t)+\mathbf{D}\mathbf{w}(t))\\
-\gamma\mathbf{w}^T(t)\,\mathbf{w}(t)
\end{array}\right\}\\
&<0
\end{aligned}
\tag{18}
$$

and with the notation

$$
\mathbf{q}_w^T(t)=\left[\mathbf{q}^T(t)\quad\mathbf{w}^T(t)\right],
\tag{19}
$$

it yields

$$
\begin{aligned}
\dot{v}(\mathbf{q}(t))=&\sum_{j=1}^{s}\mu_j(\boldsymbol{\theta}(t))\,\mu_j(\boldsymbol{\theta}(t))\,\mathbf{q}_w^T(t)\\
&\times\left(\mathbf{R}_{jj}+\mathbf{Q}\right)\mathbf{q}_w(t)\\
&+2\sum_{j=1}^{s-1}\sum_{g=j+1}^{s}\mu_j(\boldsymbol{\theta}(t))\,\mu_g(\boldsymbol{\theta}(t))\\
&\times\mathbf{q}_w^T(t)\left(\mathbf{R}_{jg}+\mathbf{Q}\right)\mathbf{q}_w(t)<0,
\end{aligned}
\tag{20}
$$

where

$$
\mathbf{R}_{jj}=\begin{bmatrix}\mathbf{P}\mathbf{H}_{jj}+\mathbf{H}_{jj}^T\mathbf{P} & \mathbf{P}\mathbf{G}_j\\ * & -\gamma\mathbf{I}_r\end{bmatrix},\qquad \mathbf{Q}=\begin{bmatrix}\mathbf{C}^T\\ \mathbf{D}^T\end{bmatrix}\begin{bmatrix}\mathbf{C} & \mathbf{D}\end{bmatrix},
$$

$$
\mathbf{R}_{jg}=\begin{bmatrix}\mathbf{P}\dfrac{\mathbf{H}_{jg}+\mathbf{H}_{gj}}{2}+\dfrac{\left(\mathbf{H}_{jg}+\mathbf{H}_{gj}\right)^T}{2}\mathbf{P} & \mathbf{P}\dfrac{\mathbf{G}_j+\mathbf{G}_g}{2}\\ * & -\gamma\mathbf{I}_r\end{bmatrix}.
\tag{21}
$$

Since (20) implies

$$
\mathbf{R}_{jj}+\mathbf{Q}<0,\qquad \mathbf{R}_{jg}+\mathbf{Q}<0,
\tag{22}
$$

for all $j\in\langle 1,2,\ldots,s\rangle$ and $j<g\le s$, $i,j\in\langle 1,2,\ldots,s\rangle$, respectively, then using the Schur complement property, (22) can be written as

$$
\begin{bmatrix}\mathbf{P}\mathbf{H}_{jj}+\mathbf{H}_{jj}^T\mathbf{P} & \mathbf{P}\mathbf{G}_j & \mathbf{C}^T\\ * & -\gamma\mathbf{I}_r & \mathbf{D}^T\\ * & * & -\mathbf{I}_m\end{bmatrix}<0,
$$

$$
\begin{bmatrix}\mathbf{P}\dfrac{\mathbf{H}_{jg}+\mathbf{H}_{gj}}{2}+\dfrac{\left(\mathbf{H}_{jg}+\mathbf{H}_{gj}\right)^T}{2}\mathbf{P} & \mathbf{P}\dfrac{\mathbf{G}_j+\mathbf{G}_g}{2} & \mathbf{C}^T\\ * & -\gamma\mathbf{I}_r & \mathbf{D}^T\\ * & * & -\mathbf{I}_m\end{bmatrix}<0.
\tag{23}
$$

Defining the transform matrix $\mathbf{L}$ as

$$
\mathbf{L}=\operatorname{diag}\left[\mathbf{P}^{-1}\quad\mathbf{I}_r\quad\mathbf{I}_m\right],
\tag{24}
$$

premultiplying the left-hand side and the right-hand side of (23) by $\mathbf{L}$, gives

$$
\begin{bmatrix}\mathbf{H}_{jj}\mathbf{P}^{-1}+\mathbf{P}^{-1}\mathbf{H}_{jj}^T & \mathbf{G}_j & \mathbf{P}^{-1}\mathbf{C}^T\\ * & -\gamma\mathbf{I}_r & \mathbf{D}^T\\ * & * & -\mathbf{I}_m\end{bmatrix}<0,
\tag{25}
$$

$$
\begin{bmatrix}\dfrac{\mathbf{H}_{jg}+\mathbf{H}_{gj}}{2}\mathbf{P}^{-1}+\mathbf{P}^{-1}\dfrac{\left(\mathbf{H}_{jg}+\mathbf{H}_{gj}\right)^T}{2} & \dfrac{\mathbf{G}_j+\mathbf{G}_g}{2} & \mathbf{P}^{-1}\mathbf{C}^T\\ * & -\gamma\mathbf{I}_r & \mathbf{D}^T\\ * & * & -\mathbf{I}_m\end{bmatrix}<0.
\tag{26}
$$

Thus, using the substitution $\mathbf{X}=\mathbf{P}^{-1}$ then (25) and (26) imply (14) and (15), respectively. This concludes the proof. □

Remark 2. Another form of bounded real lemma can be obtained using Lyapunov function of the form

$$
\begin{aligned}
v(\mathbf{q}(t))=&\,\mathbf{q}^T(t)\,\mathbf{P}\mathbf{q}(t)\\
&+3\gamma^{-1}\int_0^t\left(\mathbf{y}^T(\tau)\,\mathbf{y}(\tau)-\gamma^2\mathbf{w}^T(\tau)\,\mathbf{w}(\tau)\right)d\tau>0,
\end{aligned}
\tag{27}
$$

(compare, e.g., [6, 12, 13, 18]), but the BRL forms implying from (27) result, in general, the higher H_∞ norm upper bound γ then using the presented conditions (14), (15).

Lemma 3 (enhanced bounded real lemma). *The closed-loop system* (7), (5) *is stable with the performance* $\sum_{j=1}^{s}\sum_{g=1}^{s}\mu_j(\boldsymbol{\theta}(t))\mu_g(\boldsymbol{\theta}(t))\|\mathbf{C}(s\mathbf{I}-\mathbf{H}_{jg})^{-1}\mathbf{G}_j+\mathbf{D}\|_\infty^2\le\gamma$ *if for given* $\delta>0$, $\delta\in\mathbb{R}$, *there exist positive definite matrices* $\mathbf{V},\mathbf{T}\in\mathbb{R}^{n\times n}$ *and a positive scalar* $\gamma\in\mathbb{R}$ *such that*

$$\mathbf{V} = \mathbf{V}^T > 0, \qquad \gamma > 0, \tag{28}$$

$$\begin{bmatrix} \mathbf{H}_{jj}\mathbf{V} + \mathbf{V}\mathbf{H}_{jj}^T & \mathbf{G}_j & \mathbf{T} - \delta\mathbf{V} + \mathbf{V}\mathbf{H}_{jj}^T & \mathbf{V}\mathbf{C}^T \\ * & -\gamma\mathbf{I}_r & \mathbf{G}_j^T & \mathbf{D}^T \\ * & * & -2\delta\mathbf{V} & \mathbf{0} \\ * & * & * & -\mathbf{I}_m \end{bmatrix} < 0, \tag{29}$$

$$\begin{bmatrix} \dfrac{\mathbf{H}_{jg} + \mathbf{H}_{gj}}{2}\mathbf{V} + \mathbf{V}\dfrac{\left(\mathbf{H}_{jg} + \mathbf{H}_{gj}\right)^T}{2} & \dfrac{\mathbf{G}_j + \mathbf{G}_g}{2} & \mathbf{T} - \delta\mathbf{V} + \mathbf{V}\dfrac{\left(\mathbf{H}_{jg} + \mathbf{H}_{gj}\right)^T}{2} & \mathbf{V}\mathbf{C}^T \\ * & -\gamma\mathbf{I}_r & \dfrac{\left(\mathbf{G}_j + \mathbf{G}_g\right)^T}{2} & \mathbf{D}^T \\ * & * & -2\delta\mathbf{V} & \mathbf{0} \\ * & * & * & -\mathbf{I}_m \end{bmatrix} < 0, \tag{30}$$

for all $j \in \langle 1, 2, \ldots, s\rangle$ *and* $j < g \le s$, $j, g \in \langle 1, 2, \ldots, s\rangle$, *respectively.*

Proof. Since (12) implies

$$\begin{aligned} &\sum_{j=1}^{s} \mu_j(\boldsymbol{\theta}(t))\,\mu_j(\boldsymbol{\theta}(t))\left(\mathbf{H}_{jj}\mathbf{q}(t) + \mathbf{G}_j\mathbf{w}(t)\right) \\ &\quad + 2\sum_{j=1}^{s-1}\sum_{g=j+1}^{s} \mu_j(\boldsymbol{\theta}(t))\,\mu_g(\boldsymbol{\theta}(t)) \\ &\quad \times \left(\frac{\mathbf{H}_{jg} + \mathbf{H}_{gj}}{2}\mathbf{q}(t) + \frac{\mathbf{G}_j + \mathbf{G}_g}{2}\mathbf{w}(t)\right) - \dot{\mathbf{q}}(t) \\ &\quad = \mathbf{0}, \end{aligned} \tag{31}$$

then, with arbitrary regular symmetric square matrices $\mathbf{S}_1, \mathbf{S}_2 \in \mathbb{R}^{n\times n}$, it yields

$$\left(\mathbf{q}^T(t)\,\mathbf{S}_1 + \dot{\mathbf{q}}^T(t)\,\mathbf{S}_2\right)\left(\begin{array}{l} \displaystyle\sum_{j=1}^{s} \mu_j(\boldsymbol{\theta}(t))\,\mu_j(\boldsymbol{\theta}(t))\left(\mathbf{H}_{jj}\mathbf{q}(t) + \mathbf{G}_j\mathbf{w}(t)\right) \\ \quad \displaystyle +2\sum_{j=1}^{s-1}\sum_{g=j+1}^{s} \mu_j(\boldsymbol{\theta}(t))\,\mu_g(\boldsymbol{\theta}(t))\left(\frac{\mathbf{H}_{jg} + \mathbf{H}_{gj}}{2}\mathbf{q}(t) + \frac{\mathbf{G}_j + \mathbf{G}_g}{2}\mathbf{w}(t)\right) - \dot{\mathbf{q}}(t) \end{array}\right) = \mathbf{0}. \tag{32}$$

Thus, adding (32), as well as its transposition to (17), and substituting (5) into (17) give

$$\begin{aligned} 0 > {} & \dot{v}(\mathbf{q}(t)) \\ = {} & \dot{\mathbf{q}}^T(t)\,\mathbf{P}\mathbf{q}(t) + \mathbf{q}^T(t)\,\mathbf{P}\dot{\mathbf{q}}(t) \\ & + 3(\mathbf{C}\mathbf{q}(t) + \mathbf{D}\mathbf{w}(t))^T(\mathbf{C}\mathbf{q}(t) + \mathbf{D}\mathbf{w}(t)) \\ & - 3\gamma\mathbf{w}^T(t)\,\mathbf{w}(t) \\ & + 2\left(\mathbf{q}^T(t)\,\mathbf{S}_1 + \dot{\mathbf{q}}^T(t)\,\mathbf{S}_2\right) \\ & \times \left(\sum_{j=1}^{s} \mu_j(\boldsymbol{\theta}(t))\,\mu_j(\boldsymbol{\theta}(t))\right. \\ & \qquad \left. \times \left(\mathbf{H}_{jj}\mathbf{q}(t) + \mathbf{G}_j\mathbf{w}(t)\right) - \dot{\mathbf{q}}(t)\right) \\ & + 4\left(\mathbf{q}^T(t)\,\mathbf{S}_1 + \dot{\mathbf{q}}^T(t)\,\mathbf{S}_2\right) \\ & \times \sum_{j=1}^{s-1}\sum_{g=j+1}^{s} \mu_j(\boldsymbol{\theta}(t))\,\mu_g(\boldsymbol{\theta}(t)) \\ & \qquad \times \left(\frac{\mathbf{H}_{jg} + \mathbf{H}_{gj}}{2}\mathbf{q}(t) + \frac{\mathbf{G}_j + \mathbf{G}_g}{2}\mathbf{w}(t)\right), \end{aligned} \tag{33}$$

and using the notation

$$\mathbf{q}_w^{\diamond T}(t) = \left[\mathbf{q}^T(t) \quad \mathbf{w}^T(t) \quad \dot{\mathbf{q}}^T(t)\right] \tag{34}$$

can be obtained the following:

$$\begin{aligned}\dot{v}(\mathbf{q}(t)) = &\sum_{j=1}^{s}\mu_j(\boldsymbol{\theta}(t))\,\mu_j(\boldsymbol{\theta}(t)) \\ &\times \mathbf{q}_w^{\diamond T}(t)\left(\mathbf{R}_{jj}^{\diamond}+\mathbf{Q}^{\diamond}\right)\mathbf{q}_w^{\diamond}(t) \\ &+2\sum_{j=1}^{s-1}\sum_{g=j+1}^{s}\mu_j(\boldsymbol{\theta}(t))\,\mu_g(\boldsymbol{\theta}(t)) \\ &\times \mathbf{q}_w^{\diamond T}(t)\left(\mathbf{R}_{jg}^{\diamond}+\mathbf{Q}^{\diamond}\right)\mathbf{q}_w^{\diamond}(t) < 0,\end{aligned} \tag{35}$$

where

$$\begin{aligned}\mathbf{R}_{jj}^{\diamond} &= \begin{bmatrix}\mathbf{S}_1\mathbf{H}_{jj}+\mathbf{H}_{jj}^T\mathbf{S}_1 & \mathbf{S}_1\mathbf{G}_j & \mathbf{P}-\mathbf{S}_1+\mathbf{H}_{jj}^T\mathbf{S}_2 \\ * & -\gamma\mathbf{I}_r & \mathbf{G}_j^T\mathbf{S}_2 \\ * & * & -2\mathbf{S}_2\end{bmatrix}, \\ \mathbf{R}_{jg}^{\diamond} &= \begin{bmatrix}\mathbf{S}_1\dfrac{\mathbf{H}_{jg}+\mathbf{H}_{gj}}{2}+\dfrac{\left(\mathbf{H}_{jg}+\mathbf{H}_{gj}\right)^T}{2}\mathbf{S}_1 & \mathbf{S}_1\dfrac{\mathbf{G}_j+\mathbf{G}_g}{2} & \mathbf{P}-\mathbf{S}_1+\dfrac{\left(\mathbf{H}_{jg}+\mathbf{H}_{gj}\right)^T}{2}\mathbf{S}_2 \\ * & -\gamma\mathbf{I}_r & \dfrac{\left(\mathbf{G}_j+\mathbf{G}_g\right)^T}{2}\mathbf{S}_2 \\ * & * & -2\mathbf{S}_2\end{bmatrix}, \\ \mathbf{Q}^{\diamond} &= \begin{bmatrix}\mathbf{C}^T \\ \mathbf{D}^T \\ \mathbf{0}\end{bmatrix}\begin{bmatrix}\mathbf{C} & \mathbf{D} & \mathbf{0}\end{bmatrix}.\end{aligned} \tag{36}$$

Since (35) implies

$$\mathbf{R}_{jj}^{\diamond}+\mathbf{Q}^{\diamond} < 0, \qquad \mathbf{R}_{jg}^{\diamond}+\mathbf{Q}^{\diamond} < 0, \tag{37}$$

for all $j \in \langle 1,2,\ldots,s\rangle$ and $j < g \le s$, $i,j \in \langle 1,2,\ldots,s\rangle$, respectively, using the Schur complement property, (37) can be written as

$$\begin{bmatrix}\mathbf{S}_1\mathbf{H}_{jj}+\mathbf{H}_{jj}^T\mathbf{S}_1 & \mathbf{S}_1\mathbf{G}_j & \mathbf{P}-\mathbf{S}_1+\mathbf{H}_{jj}^T\mathbf{S}_2 & \mathbf{C}^T \\ * & -\gamma\mathbf{I}_r & \mathbf{G}_j^T\mathbf{S}_2 & \mathbf{D}^T \\ * & * & -2\mathbf{S}_2 & \mathbf{0} \\ * & * & * & -\mathbf{I}_m\end{bmatrix},$$

$$\begin{bmatrix}\mathbf{S}_1\dfrac{\mathbf{H}_{jg}+\mathbf{H}_{gj}}{2}+\dfrac{\left(\mathbf{H}_{jg}+\mathbf{H}_{gj}\right)^T}{2}\mathbf{S}_1 & \mathbf{S}_1\dfrac{\mathbf{G}_j+\mathbf{G}_g}{2} & \mathbf{P}-\mathbf{S}_1+\dfrac{\left(\mathbf{H}_{jg}+\mathbf{H}_{gj}\right)^T}{2}\mathbf{S}_2 & \mathbf{C}^T \\ * & -\gamma\mathbf{I}_r & \dfrac{\left(\mathbf{G}_j+\mathbf{G}_g\right)^T}{2}\mathbf{S}_2 & \mathbf{D}^T \\ * & * & -2\mathbf{S}_2 & \mathbf{0} \\ * & * & * & -\mathbf{I}_m\end{bmatrix}. \tag{38}$$

Since $\mathbf{S}_1$, $\mathbf{S}_2$ are supposed to be regular and symmetric, the transform matrix $\mathbf{L}^{\diamond}$ can be defined as

$$\mathbf{L}^{\diamond} = \operatorname{diag}\left[\mathbf{S}_1^{-1} \quad \mathbf{I}_r \quad \mathbf{S}_2^{-1} \quad \mathbf{I}_m\right], \tag{39}$$

and pre-multiplying the left-hand and the right-hand side of (38) by $\mathbf{L}^{\diamond}$ gives

$$\begin{bmatrix}\mathbf{H}_{jj}\mathbf{S}_1^{-1}+\mathbf{S}_1^{-1}\mathbf{H}_{jj}^T & \mathbf{G}_j & \mathbf{T}-\mathbf{S}_2^{-1}+\mathbf{S}_1^{-1}\mathbf{H}_{jj}^T & \mathbf{S}_1^{-1}\mathbf{C}^T \\ * & -\gamma\mathbf{I}_r & \mathbf{G}_j^T & \mathbf{D}^T \\ * & * & -2\mathbf{S}_2^{-1} & \mathbf{0} \\ * & * & * & -\mathbf{I}_m\end{bmatrix}, \tag{40}$$

$$\begin{bmatrix}\boldsymbol{\Pi}_{jg} & \dfrac{\mathbf{G}_j+\mathbf{G}_g}{2} & \mathbf{T}-\mathbf{S}_2^{-1}+\mathbf{S}_1^{-1}\dfrac{\left(\mathbf{H}_{jg}+\mathbf{H}_{gj}\right)^T}{2} & \mathbf{S}_1^{-1}\mathbf{C}^T \\ * & -\gamma\mathbf{I}_r & \dfrac{\left(\mathbf{G}_j+\mathbf{G}_g\right)^T}{2} & \mathbf{D}^T \\ * & * & -2\mathbf{S}_2^{-1} & \mathbf{0} \\ * & * & * & -\mathbf{I}_m\end{bmatrix}, \tag{41}$$

$$\mathbf{T} = \mathbf{S}_1^{-1}\mathbf{P}\mathbf{S}_2^{-1}, \qquad \boldsymbol{\Pi}_{jg} = \frac{\mathbf{H}_{jg}+\mathbf{H}_{gj}}{2}\mathbf{S}_1^{-1}+\mathbf{S}_1^{-1}\frac{\left(\mathbf{H}_{jg}+\mathbf{H}_{gj}\right)^T}{2}. \tag{42}$$

Thus, using the notation

$$\mathbf{S}_2^{-1} = \delta\mathbf{V}, \qquad \mathbf{S}_1^{-1} = \mathbf{V}, \tag{43}$$

(40), (41) imply (29), (30). This concludes the proof. □

This enhanced form of the bounded real lemma eliminates products of a Lyapunov matrix $\mathbf{T}$ and the system matrix parameters $\mathbf{A}_j$, $\mathbf{B}_j$, $\mathbf{C}$, and $\mathbf{D}$ in the LMI stability conditions. When used in the synthesis of controllers or observers for TS systems (that are, evidently, the systems with polytopic uncertainties), the enhanced form of BRL gives solutions that are less conservative than ones given by the standard form of BRL. In that sense, the enhanced form of BRL can be preferred in TS systems analysis and design [13] giving less conservative equivalency to the synthesis based on the parameter dependent Lyapunov functions principle [4].

3. Pairwise Distributed Principle in Control Design

The main property of the pairwise distributable structure of TS large-scale systems is given by the next two lemmas.

Lemma 4. *Let the system* (1), (2) *is structured in p subsystems in such way that, for $j = 1, 2, \ldots, s$, $r \geq 3$, $i, l = 1, 2, \ldots, p$,*

$$\mathbf{A}_j = blk\left[\mathbf{A}_{jil}\right], \qquad \mathbf{C} = blk\left[\mathbf{C}_{il}\right], \qquad \mathbf{B}_j = \operatorname{diag}\left[\mathbf{B}_{ji}\right], \qquad \mathbf{D} = \mathbf{0}, \tag{44}$$

$$\dot{\mathbf{q}}_h(t) = \sum_{j=1}^{s} \mu_j(\boldsymbol{\theta}(t)) \times \left(\mathbf{A}_{jhh}\mathbf{q}_h(t) + \sum_{l=1, l\neq h}^{p} \left(\mathbf{A}_{jhl}\mathbf{q}_l(t) + \mathbf{B}_{jh}\mathbf{u}_h(t)\right)\right), \tag{45}$$

$$\mathbf{y}_h(t) = \mathbf{C}_{hh}\mathbf{q}_h(t) + \sum_{l=1, l\neq h}^{p} \mathbf{C}_{hl}\mathbf{q}_l(t), \tag{46}$$

where $\mathbf{q}_h(t) \in \mathbb{R}^{n_h}$, $\mathbf{u}_h(t) \in \mathbb{R}^{r_h}$, $\mathbf{y}_h(t) \in \mathbb{R}^{m_h}$, $\mathbf{A}_{jhl} \in \mathbb{R}^{n_h \times n_l}$, $\mathbf{B}_{jh} \in \mathbb{R}^{r_h \times n_h}$, and $\mathbf{C}_{hl} \in \mathbb{R}^{m_h \times n_h}$, respectively, and $n = \sum_{h=1}^{p} n_h$, $r = \sum_{h=1}^{p} r_h$, and $m = \sum_{h=1}^{p} m_h$.

Then the hkth unforced subsystem pair in unforced system (1), (2), *and* (44) *is stable if there exists a set of symmetric matrices*

$$\mathbf{P}_{hk}^{\circ} = \begin{bmatrix} \mathbf{P}_h^k & \mathbf{P}_{hk} \\ \mathbf{P}_{kh} & \mathbf{P}_k^h \end{bmatrix}, \quad h = 1, 2, \ldots, p-1, \quad k = h+1, h+2, \ldots, p, \tag{47}$$

such that

$$\sum_{h=1}^{p-1}\sum_{k=h+1}^{p} \left(\dot{\mathbf{q}}_{hk}^T(t) \begin{bmatrix} \mathbf{P}_h^k & \mathbf{P}_{hk} \\ \mathbf{P}_{kh} & \mathbf{P}_k^h \end{bmatrix} \mathbf{q}_{hk}(t) + \mathbf{q}_{hk}^T(t) \begin{bmatrix} \mathbf{P}_h^k & \mathbf{P}_{hk} \\ \mathbf{P}_{kh} & \mathbf{P}_k^h \end{bmatrix} \dot{\mathbf{q}}_{hk}(t)\right) < 0, \tag{48}$$

where

$$\mathbf{q}_{hk}^T(t) = \left[\mathbf{q}_h^T(t) \;\; \mathbf{q}_k^T(t)\right], \tag{49}$$

$$\dot{\mathbf{q}}_{hk}(t) = \sum_{j=1}^{s} \mu_j(\boldsymbol{\theta}(t)) \times \left(\begin{bmatrix} \mathbf{A}_{jhh} & \mathbf{A}_{jhk} \\ \mathbf{A}_{jkh} & \mathbf{A}_{jkk} \end{bmatrix} \mathbf{q}_{hk}(t) + \sum_{\substack{l=1 \\ l\neq h,k}}^{p} \begin{bmatrix} \mathbf{A}_{jhl} \\ \mathbf{A}_{jkl} \end{bmatrix} \mathbf{q}_l(t)\right). \tag{50}$$

Proof. Defining Lyapunov function as

$$v(\mathbf{q}(t)) = \mathbf{q}^T(t)\mathbf{P}\mathbf{q}(t) > 0, \tag{51}$$

where $\mathbf{P} = \mathbf{P}^T > 0$, $\mathbf{P} \in \mathbb{R}^{n\times n}$, then the time derivative of $v(\mathbf{q}(i))$ along a solution of the system (1), (2) is

$$\dot{v}(\mathbf{q}(t)) = \dot{\mathbf{q}}^T(t)\mathbf{P}\mathbf{q}(t) + \mathbf{q}^T(t)\mathbf{P}\dot{\mathbf{q}}(t) < 0. \tag{52}$$

Considering $\mathbf{P}$ of the next form

$$\mathbf{P} = \begin{bmatrix} \mathbf{P}_{11} & \mathbf{P}_{12} & \cdots & \mathbf{P}_{1p} \\ \mathbf{P}_{21} & \mathbf{P}_{22} & \cdots & \mathbf{P}_{2p} \\ \vdots & \vdots & \ddots & \vdots \\ \mathbf{P}_{p1} & \mathbf{P}_{p2} & \cdots & \mathbf{P}_{pp} \end{bmatrix}, \qquad \mathbf{P}_{hh} = \sum_{\substack{l=1 \\ l\neq h}}^{p} \mathbf{P}_h^l, \quad h = 1, 2, \ldots\ p, \tag{53}$$

then the next separation is possible

$$\mathbf{P} = \left\{ \left(\begin{bmatrix} \mathbf{P}_1^2 & \mathbf{P}_{12} & \mathbf{0} & \ldots & \mathbf{0} \\ \mathbf{P}_{21} & \mathbf{P}_2^1 & \mathbf{0} & \ldots & \mathbf{0} \\ & & & \vdots & \\ \mathbf{0} & \mathbf{0} & \mathbf{0} & \ldots & \mathbf{0} \end{bmatrix} + \cdots + \begin{bmatrix} \mathbf{P}_1^p & \mathbf{0} & \ldots & \mathbf{0} & \mathbf{P}_{1p} \\ \mathbf{0} & \mathbf{0} & \ldots & \mathbf{0} & \mathbf{0} \\ & & \vdots & & \\ \mathbf{P}_{p1} & \mathbf{0} & \ldots & \mathbf{0} & \mathbf{P}_p^1 \end{bmatrix} \right) + \cdots + \begin{bmatrix} \mathbf{0} & \ldots & \mathbf{0} & \mathbf{0} & \mathbf{0} \\ & & \vdots & & \\ \mathbf{0} & \ldots & \mathbf{0} & \mathbf{P}_{p-1}^p & \mathbf{P}_{p-1,p} \\ \mathbf{0} & \ldots & \mathbf{0} & \mathbf{P}_{p,p-1} & \mathbf{P}_p^{p-1} \end{bmatrix} \right\}. \tag{54}$$

Using (49) and writing (45) as

$$\dot{\mathbf{q}}_{hk}(t) = \sum_{j=1}^{s} \mu_j(\boldsymbol{\theta}(t)) \times \left(\begin{bmatrix} \mathbf{A}_{jhh} & \mathbf{A}_{jhk} \\ \mathbf{A}_{jkh} & \mathbf{A}_{jkk} \end{bmatrix} \mathbf{q}_{hk}(t) + \sum_{\substack{l=1 \\ l\neq h,k}}^{p} \begin{bmatrix} \mathbf{A}_{jhl} \\ \mathbf{A}_{jkl} \end{bmatrix} \mathbf{q}_l(t) + \begin{bmatrix} \mathbf{B}_{jh} & \mathbf{0} \\ \mathbf{0} & \mathbf{B}_{jk} \end{bmatrix} \begin{bmatrix} \mathbf{u}_h(t) \\ \mathbf{u}_k(t) \end{bmatrix} \right) \tag{55}$$

and considering that for an unforced regime $\mathbf{u}_l(t) = \mathbf{0}$, $l = 1, 2, \dots p$, then (55) implies (50). Subsequently, (1), (52), and (54) give

$$\sum_{j=1}^{s} \mu_j(\boldsymbol{\theta}(t)) \sum_{h=1}^{p-1} \sum_{k=h+1}^{p} \left(\begin{array}{l} \dot{\mathbf{q}}_{hk}^T(t) \begin{bmatrix} \mathbf{P}_h^k & \mathbf{P}_{hk} \\ \mathbf{P}_{kh} & \mathbf{P}_k^h \end{bmatrix} \mathbf{q}_{hk}(t) \\ \\ + \mathbf{q}_{hk}^T(t) \begin{bmatrix} \mathbf{P}_h^k & \mathbf{P}_{hk} \\ \mathbf{P}_{kh} & \mathbf{P}_k^h \end{bmatrix} \dot{\mathbf{q}}_{hk}(t) \end{array} \right) < 0, \tag{56}$$

and the inequality (56) implies (48). This concludes the proof. □

Lemma 5. *System* (1), (2), (44) *with the pairwise distributed control takes the form*

$$\dot{\mathbf{q}}_{hk}(t) = \sum_{j=1}^{s} \sum_{g=1}^{s} \mu_j(\boldsymbol{\theta}(t)) \mu_g(\boldsymbol{\theta}(t)) \times \left(\left(\mathbf{A}_{jhk}^{\circ} - \mathbf{B}_{jhk}^{\circ} \mathbf{K}_{ghk}^{\circ} \right) \mathbf{q}_{hk}(t) + \boldsymbol{\omega}_{jghk}^{\circ}(t) \right), \tag{57}$$

$$\mathbf{y}_{hk}(t) = \mathbf{C}_{hk}^{\circ} \mathbf{q}_{hk}(t) + \sum_{\substack{l=1 \\ l \neq h,k}}^{p} \mathbf{C}_{hk}^{l\circ} \mathbf{q}_l(t) + \mathbf{0}\boldsymbol{\omega}_{hk}(t), \tag{58}$$

where

$$\mathbf{A}_{jhk}^{\circ} = \begin{bmatrix} \mathbf{A}_{jhh} & \mathbf{A}_{jhk} \\ \mathbf{A}_{jkh} & \mathbf{A}_{jkk} \end{bmatrix}, \qquad \mathbf{B}_{jhk}^{\circ} = \begin{bmatrix} \mathbf{B}_{jh} & \mathbf{0} \\ \mathbf{0} & \mathbf{B}_{jk} \end{bmatrix}, \qquad \mathbf{K}_{ghk}^{\circ} \begin{bmatrix} \mathbf{K}_{gh}^k & \mathbf{K}_{ghk} \\ \mathbf{K}_{gkh} & \mathbf{K}_{gk}^h \end{bmatrix}, \tag{59}$$

$$\boldsymbol{\omega}_{jghk}^{\circ}(t) = \sum_{\substack{l=1 \\ l \neq h,k}}^{p} \mathbf{A}_{jhk}^{l\circ} \mathbf{q}_l(t) + \mathbf{B}_{jhk}^{\circ} \boldsymbol{\omega}_{ghk}(t), \tag{60}$$

$$\mathbf{A}_{jhk}^{l\circ} = \begin{bmatrix} \mathbf{A}_{jhl} \\ \mathbf{A}_{jkl} \end{bmatrix}, \qquad \boldsymbol{\omega}_{ghk}(t) = \sum_{\substack{l=1 \\ l \neq h,k}}^{p} \begin{bmatrix} \mathbf{u}_{gh}^l(t) \\ \mathbf{u}_{gk}^l(t) \end{bmatrix}, \qquad \mathbf{u}_{gh}^l(t) = \begin{bmatrix} \mathbf{K}_{gh}^l & \mathbf{K}_{ghl} \end{bmatrix} \begin{bmatrix} \mathbf{q}_h(t) \\ \mathbf{q}_l(t) \end{bmatrix}, \tag{61}$$

$$\mathbf{C}_{hk}^{\circ} = \begin{bmatrix} \mathbf{C}_h^k & \mathbf{C}_{hk} \\ \mathbf{C}_{kh} & \mathbf{C}_k^h \end{bmatrix}, \qquad \mathbf{C}_{hk}^{l\circ} = \begin{bmatrix} \mathbf{C}_{hl} \\ \mathbf{C}_{kl} \end{bmatrix}, \qquad \mathbf{C}_{hh} = \sum_{\substack{l=1 \\ l \neq h}}^{p} \mathbf{C}_h^l. \tag{62}$$

Proof. Considering in (6) the same structure of $\mathbf{K}_g$, $g = 1, 2, \dots s$, as is defined for $\mathbf{P}$ in (53), that is,

$$\mathbf{K}_g = \begin{bmatrix} \mathbf{K}_{g11} & \mathbf{K}_{g12} & \dots & \mathbf{K}_{g1p} \\ \mathbf{K}_{g21} & \mathbf{K}_{g22} & \dots & \mathbf{K}_{g2p} \\ & & \vdots & \\ \mathbf{K}_{gp1} & \mathbf{K}_{gp2} & \dots & \mathbf{K}_{gpp} \end{bmatrix}, \qquad \mathbf{K}_{ghh} = \sum_{\substack{l=1 \\ l \neq h}}^{p} \mathbf{K}_{gh}^l, \tag{63}$$

then the control law $\mathbf{u}_h(t)$ takes the form

$$\mathbf{u}_h(t) = -\sum_{g=1}^{s} \mu_g(\boldsymbol{\theta}(t)) \left(\mathbf{K}_{ghh} \mathbf{q}_h(t) + \sum_{\substack{l=1 \\ l \neq h}}^{p} \mathbf{K}_{ghl} \mathbf{q}_l(t) \right), \tag{64}$$

where $\mathbf{K}_{ghl}(t)$, $h, l = 1, 2, \dots, p$, are non-zero gain matrices.

Exploiting the main diagonal block property (63), then

$$\begin{aligned} \mathbf{u}_h(t) &= -\sum_{g=1}^{s} \mu_g(\boldsymbol{\theta}(t)) \times \sum_{\substack{l=1 \\ l \neq h}}^{p} \begin{bmatrix} \mathbf{K}_{gh}^l & \mathbf{K}_{ghl} \end{bmatrix} \begin{bmatrix} \mathbf{q}_h(t) \\ \mathbf{q}_l(t) \end{bmatrix} \\ &= -\sum_{g=1}^{s} \mu_g(\boldsymbol{\theta}(t)) \left(\begin{bmatrix} \mathbf{K}_{gh}^k & \mathbf{K}_{ghk} \end{bmatrix} \begin{bmatrix} \mathbf{q}_h(t) \\ \mathbf{q}_k(t) \end{bmatrix} + \sum_{\substack{l=1 \\ l \neq h,k}}^{p} \begin{bmatrix} \mathbf{K}_{gh}^l & \mathbf{K}_{ghl} \end{bmatrix} \begin{bmatrix} \mathbf{q}_h(t) \\ \mathbf{q}_l(t) \end{bmatrix} \right) \\ &= -\sum_{g=1}^{s} \mu_g(\boldsymbol{\theta}(t)) \left(\mathbf{u}_{gh}^k(t) + \sum_{\substack{l=1 \\ l \neq h,k}}^{p} \mathbf{u}_{gh}^l(t) \right), \end{aligned} \tag{65}$$

where for $l = 1, 2, \dots, p$, $l \neq h, k$,

$$\mathbf{u}_{gh}^l(t) = \begin{bmatrix} \mathbf{K}_{gh}^l & \mathbf{K}_{ghl} \end{bmatrix} \begin{bmatrix} \mathbf{q}_h(t) \\ \mathbf{q}_l(t) \end{bmatrix}. \tag{66}$$

Defining for $h = 1, 2, \dots, p-1$, $k = h+1, h+2, \dots, p$ and with respect to the notations (59) that

$$\begin{bmatrix} \mathbf{u}_{gh}^k(t) \\ \mathbf{u}_{gk}^h(t) \end{bmatrix} = \begin{bmatrix} \mathbf{K}_{gh}^k & \mathbf{K}_{ghk} \\ \mathbf{K}_{gkh} & \mathbf{K}_{gk}^h \end{bmatrix} \begin{bmatrix} \mathbf{q}_h(t) \\ \mathbf{q}_k(t) \end{bmatrix} = \mathbf{K}_{ghk}^{\circ} \begin{bmatrix} \mathbf{q}_h(t) \\ \mathbf{q}_k(t) \end{bmatrix} \tag{67}$$

and combining (64) for h and k, is obtained the following:

$$\begin{bmatrix}\mathbf{u}_h(t)\\ \mathbf{u}_k(t)\end{bmatrix} = -\sum_{g=1}^{s}\mu_g(\boldsymbol{\theta}(t)) \times\left(\begin{bmatrix}\mathbf{K}_{gh}^{k} & \mathbf{K}_{gkh}\\ \mathbf{K}_{ghk} & \mathbf{K}_{gk}^{h}\end{bmatrix}\begin{bmatrix}\mathbf{q}_h(t)\\ \mathbf{q}_k(t)\end{bmatrix} - \begin{bmatrix}\sum_{\substack{l=1\\ l\neq h,k}}^{p}\begin{bmatrix}\mathbf{K}_{gh}^{l} & \mathbf{K}_{ghl}\end{bmatrix}\begin{bmatrix}\mathbf{q}_h(t)\\ \mathbf{q}_l(t)\end{bmatrix}\\ \sum_{\substack{l=1\\ l\neq h,k}}^{p}\begin{bmatrix}\mathbf{K}_{gk}^{l} & \mathbf{K}_{gkl}\end{bmatrix}\begin{bmatrix}\mathbf{q}_k(t)\\ \mathbf{q}_l(t)\end{bmatrix}\end{bmatrix}\right), \tag{68}$$

$$\begin{bmatrix}\mathbf{u}_h(t)\\ \mathbf{u}_k(t)\end{bmatrix} = -\sum_{g=1}^{s}\mu_g(\boldsymbol{\theta}(t)) \times\left(\begin{bmatrix}\mathbf{u}_{gh}^{k}(t)\\ \mathbf{u}_{gk}^{h}(t)\end{bmatrix} + \sum_{\substack{l=1\\ l\neq h,k}}^{p}\begin{bmatrix}\mathbf{u}_{gh}^{l}(t)\\ \mathbf{u}_{gk}^{l}(t)\end{bmatrix}\right), \tag{69}$$

respectively. Then, substituting (69) in (55) gives

$$\dot{\mathbf{q}}_{hk}(t) = \sum_{j=1}^{s}\sum_{g=1}^{s}\mu_j(\boldsymbol{\theta}(t))\,\mu_g(\boldsymbol{\theta}(t))\left(\mathbf{A}_{jghkc}^{\circ}\mathbf{q}_{hk}(t) + \boldsymbol{\omega}_{jghk}^{\circ}(t)\right), \tag{70}$$

where

$$\mathbf{A}_{jghkc}^{\circ} = \begin{bmatrix}\mathbf{A}_{jhh} & \mathbf{A}_{jhk}\\ \mathbf{A}_{jkh} & \mathbf{A}_{jkk}\end{bmatrix} - \begin{bmatrix}\mathbf{B}_{jh} & \mathbf{0}\\ \mathbf{0} & \mathbf{B}_{jk}\end{bmatrix}\begin{bmatrix}\mathbf{K}_{gh}^{k} & \mathbf{K}_{ghk}\\ \mathbf{K}_{gkh} & \mathbf{K}_{gk}^{h}\end{bmatrix}, \tag{71}$$

$$\boldsymbol{\omega}_{jghk}^{\circ}(t) = \sum_{\substack{l=1\\ l\neq h,k}}^{p}\begin{bmatrix}\mathbf{B}_{jh}\mathbf{u}_{gh}^{l}(t) + \mathbf{A}_{jhl}\mathbf{q}_l(t)\\ \mathbf{B}_{jk}\mathbf{u}_{gk}^{l}(t) + \mathbf{A}_{jkl}\mathbf{q}_l(t)\end{bmatrix}. \tag{72}$$

Using (59) and denoting

$$\mathbf{A}_{jghkj}^{\circ} = \mathbf{A}_{jhk}^{\circ} - \mathbf{B}_{jhk}^{\circ}\mathbf{K}_{ghk}^{\circ}, \tag{73}$$

then (71) implies (57).

Rewriting (72) in the form

$$\boldsymbol{\omega}_{jghk}^{\circ}(t) = \sum_{\substack{l=1\\ l\neq h,k}}^{p}\left(\mathbf{B}_{jhk}^{\circ}\begin{bmatrix}\mathbf{u}_{gh}^{l}(t)\\ \mathbf{u}_{gk}^{l}(t)\end{bmatrix} + \begin{bmatrix}\mathbf{A}_{jhl}\\ \mathbf{A}_{jkl}\end{bmatrix}\mathbf{q}_l(t)\right) \tag{74}$$

and using (61), then (74) implies (60).

Finally, using (62), it can be written as

$$\mathbf{y}(t) = \sum_{h=1}^{p-1}\sum_{k=h+1}^{p}\left(\mathbf{C}_{hk}^{\circ}\mathbf{q}_{hk}(t) + \sum_{l=1,l\neq h}^{p}\mathbf{C}_{h}^{l}\mathbf{q}_l(t)\right), \tag{75}$$

$$\mathbf{y}_{hk}(t) = \mathbf{C}_{hk}^{\circ}\mathbf{q}_{hk}(t) + \sum_{l=1,l\neq h}^{p}\mathbf{C}_{hk}^{l\circ}\mathbf{q}_l(t), \tag{76}$$

and (76) implies (58). This concludes the proof. □

4. Pairwise Control Law Parameter Design

The design conditions, formulated as the set of LMIs, imply from the next theorems.

Theorem 6. *Controlled subsystem pair* (57), (58) *in the system* (1), (3) *is stable with performances* $\sum_{j=1}^{s}\sum_{g=1}^{s}\mu_j(\boldsymbol{\theta}(t))\mu_g(\boldsymbol{\theta}(t))\left\|\mathbf{C}_{hk}^{\circ}(s\mathbf{I}-\mathbf{H}_{jghk}^{\circ})^{-1}\mathbf{B}_{jhk}^{\circ}+\mathbf{D}_{jhk}^{\circ}\right\|_{\infty}^{2} \leq \gamma_{hk}$, *if there exist a symmetric positive definite matrix* $\mathbf{X}_{hk}^{\circ} \in \mathbb{R}^{(n_h+n_k)\times(n_h+n_k)}$, *matrices* $\mathbf{Y}_{jhk}^{\circ} \in \mathbb{R}^{(r_h+r_k)\times(n_h+n_k)}$, *and positive scalars* $\gamma_{hk}, \varepsilon_{hkl} \in \mathbb{R}$ *such that*

$$\mathbf{X}_{hk}^{\circ} = \mathbf{X}_{hk}^{\circ T} > 0, \quad \varepsilon_{hkl} > 0, \quad \gamma_{hk} > 0, \tag{77}$$

for $h, l = 1, \ldots, p$, $l \neq h, k$, $h < k \leq p$,

$$\begin{bmatrix}\boldsymbol{\Phi}_{jjhk}^{\circ} & \mathbf{A}_{jhk}^{1\circ} & \cdots & \mathbf{A}_{jhk}^{p\circ} & \mathbf{B}_{jhk}^{\circ} & \mathbf{X}_{hk}^{\circ}\mathbf{C}_{hk}^{\circ T}\\ * & -\varepsilon_{hk1}\mathbf{I}_{n_1} & \cdots & \mathbf{0} & \mathbf{0} & \mathbf{C}_{hk}^{1\circ T}\\ \vdots & \vdots & \ddots & \vdots & \vdots & \vdots\\ * & * & \cdots & -\varepsilon_{hkp}\mathbf{I}_{n_p} & \mathbf{0} & \mathbf{C}_{hk}^{p\circ T}\\ * & * & \cdots & * & -\gamma_{hk}\mathbf{I}_{(r_h+r_k)} & \mathbf{0}\\ * & * & \cdots & * & * & -\mathbf{I}_{(m_h+m_k)}\end{bmatrix} < 0, \tag{78}$$

for $j = 1, 2, \ldots, s$, $h = 1, 2, \ldots, p-1$, $k = h+1, h+2, \ldots, p$, $l = 1, 2, \ldots, p$, $l \neq h, k$,

$$\begin{bmatrix}\boldsymbol{\Phi}_{jghk}^{\circ} & \dfrac{\mathbf{A}_{jhk}^{1\circ}+\mathbf{A}_{ghk}^{1\circ}}{2} & \cdots & \dfrac{\mathbf{A}_{jhk}^{p\circ}+\mathbf{A}_{ghk}^{p\circ}}{2} & \dfrac{\mathbf{B}_{jhk}^{\circ}+\mathbf{B}_{ghk}^{\circ}}{2} & \mathbf{X}_{hk}^{\circ}\mathbf{C}_{hk}^{\circ T}\\ * & -\varepsilon_{hk1}\mathbf{I}_{n_1} & \cdots & \mathbf{0} & \mathbf{0} & \mathbf{C}_{hk}^{1\circ T}\\ \vdots & \vdots & \ddots & \vdots & \vdots & \vdots\\ * & * & \cdots & -\varepsilon_{hkp}\mathbf{I}_{n_p} & \mathbf{0} & \mathbf{C}_{hk}^{p\circ T}\\ * & * & \cdots & * & -\gamma_{hk}\mathbf{I}_{(r_h+r_k)} & \mathbf{0}\\ * & * & \cdots & * & * & -\mathbf{I}_{(m_h+m_k)}\end{bmatrix} < 0, \tag{79}$$

for $j = 1, 2, \dots\ s-1$, $j = 2, 3, \dots\ s$, $h = 1, 2, \dots\ p-1$, $k = h+1, h+2, \dots\ p$, $l = 1, 2, \dots\ p$, $l \neq h, k$, $j < g \leq s$, *with* $\mathbf{A}^{\circ}_{jhk}$, $\mathbf{B}^{\circ}_{jhk}$, $\mathbf{A}^{l\circ}_{jhk}$, $\mathbf{C}^{\circ}_{hk}$, *and* $\mathbf{C}^{l\circ}_{hk}$ *defined in* (59), (61), *and* (62), *respectively,*

$$\begin{aligned}
\boldsymbol{\Phi}^{\circ}_{jjhk} &= \mathbf{A}^{\circ}_{jhk}\mathbf{X}^{\circ}_{hk} + \mathbf{X}^{\circ}_{hk}\mathbf{A}^{\circ T}_{jhk} - \mathbf{B}^{\circ}_{jhk}\mathbf{Y}^{\circ T}_{jhk} - \mathbf{Y}^{\circ T}_{jhk}\mathbf{B}^{\circ T}_{jhk},\\
\boldsymbol{\Phi}^{\circ}_{jghk} &= \frac{\mathbf{A}^{\circ}_{jhk} + \mathbf{A}^{\circ}_{ghk}}{2}\mathbf{X}^{\circ}_{hk} + \mathbf{X}^{\circ}_{hk}\frac{\left(\mathbf{A}^{\circ}_{jhk} + \mathbf{A}^{\circ}_{ghk}\right)^{T}}{2}\\
&\quad - \frac{\mathbf{B}^{\circ}_{jhk}\mathbf{Y}^{\circ}_{ghk} + \mathbf{B}^{\circ}_{ghk}\mathbf{Y}^{\circ}_{jhk}}{2}\\
&\quad - \frac{\left(\mathbf{B}^{\circ}_{jhk}\mathbf{Y}^{\circ}_{ghk} + \mathbf{B}^{\circ}_{ghk}\mathbf{Y}^{\circ}_{jhk}\right)^{T}}{2},
\end{aligned} \tag{80}$$

and where, for given h, k, $\mathbf{A}^{h\circ}_{jhk}$, $\mathbf{A}^{k\circ}_{jhk}$, *and* $\mathbf{C}^{h\circ}_{hk}$, $\mathbf{C}^{k\circ}_{hk}$ *are not included into the structure of* (78).

When the above conditions hold, the gain matrices $\mathbf{K}^{\circ}_{jhk}$ *are given by*

$$\mathbf{K}^{\circ}_{jhk} = \mathbf{Y}^{\circ}_{jhk}\mathbf{X}^{\circ -1}_{hk}. \tag{81}$$

Proof. Considering $\sum_{j=1}^{s}\sum_{g=1}^{s}\mu_j(\boldsymbol{\theta}(t))\mu_g(\boldsymbol{\theta}(t))\boldsymbol{\omega}^{\circ}_{jghk}(t)$, with $\boldsymbol{\omega}^{\circ}_{jghk}(t)$ given in (60), as a generalized disturbance acting on the subsystem pair (57), (58), and introducing the notations

$$\begin{aligned}
\mathbf{G}^{\circ}_{jhk} &= \left[\left\{\mathbf{A}^{l\circ}_{jhk}\right\}^{p}_{l=1,l\neq h,k} \quad \mathbf{B}^{\circ}_{jhk}\right],\\
\boldsymbol{\omega}^{\circ T}_{hk} &= \left[\left\{\mathbf{q}^{T}_{l}\right\}^{p}_{l=1,l\neq h,k} \quad \boldsymbol{\omega}^{T}_{hk}(t)\right],
\end{aligned} \tag{82}$$

(57) takes the form

$$\begin{aligned}
\dot{\mathbf{q}}_{hk}(t) = \sum_{j=1}^{s}\sum_{g=1}^{s}&\mu_j(\boldsymbol{\theta}(t))\,\mu_g(\boldsymbol{\theta}(t))\\
&\times\left(\left(\mathbf{A}^{\circ}_{jhk} - \mathbf{B}^{\circ}_{jhk}\mathbf{K}^{\circ}_{ghk}\right)\mathbf{q}_{hk}(t) + \mathbf{G}^{\circ}_{jhk}\boldsymbol{\omega}^{\circ}_{hk}(t)\right).
\end{aligned} \tag{83}$$

Analogously, (58) can be rewritten as

$$\mathbf{y}_{hk}(t) = \mathbf{C}^{\circ}_{hk}\mathbf{q}_{hk}(t) + \mathbf{D}^{\circ}_{hk}\boldsymbol{\omega}^{l\circ}_{hk}, \tag{84}$$

where

$$\mathbf{D}^{\circ}_{hk} = \left[\left\{\mathbf{C}^{l\circ}_{hk}\right\}^{p}_{l=1,l\neq h,k} \quad \mathbf{0}\right]. \tag{85}$$

Since (56) also gives

$$\begin{aligned}
&\sum_{j=1}^{s}\sum_{g=1}^{s}\mu_j(\boldsymbol{\theta}(t))\,\mu_g(\boldsymbol{\theta}(t))\\
&\quad\times\sum_{h=1}^{p-1}\sum_{k=h+1}^{p}\left(\dot{\mathbf{q}}^{T}_{hk}(t)\,\mathbf{P}^{\circ}_{hk}\mathbf{q}_{hk}(t) + \mathbf{q}^{T}_{hk}(t)\,\mathbf{P}^{\circ}_{hk}\dot{\mathbf{q}}_{hk}(t)\right) < 0,
\end{aligned} \tag{86}$$

defining the matrices

$$\boldsymbol{\Gamma}^{\circ}_{hk} = \operatorname{diag}\left[\left\{\varepsilon_{hkl}\mathbf{I}_{n_l}\right\}^{p}_{l=1,l\neq h,k} \quad \gamma_{hk}\mathbf{I}_{(r_h+r_k)}\right], \tag{87}$$

(18) gives

$$\begin{aligned}
0 > \dot{v}\left(\mathbf{q}_{hk}(t)\right) = \sum_{j=1}^{s}\sum_{h=1}^{p-1}\sum_{k=h+1}^{p}\mu_j\mu_j \times &\left\{\begin{array}{l}
\left(\mathbf{C}^{\circ}_{hk}\mathbf{q}_{hk}(t) + \mathbf{D}^{\circ}_{hk}\boldsymbol{\omega}^{\circ}_{hk}(t)\right)^{T}\left(\mathbf{C}^{\circ}_{hk}\mathbf{q}_{hk}(t) + \mathbf{D}^{\circ}_{hk}\boldsymbol{\omega}^{\circ}_{hk}(t)\right)\\
-\boldsymbol{\omega}^{\circ T}_{hk}(t)\,\boldsymbol{\Gamma}^{\circ}_{hk}\boldsymbol{\omega}^{\circ}_{hk}(t)\\
+\mathbf{q}^{T}_{hk}(t)\,\mathbf{P}^{\circ}_{hk}\left(\mathbf{H}^{\circ}_{jjhk}\mathbf{q}_{hk}(t) + \mathbf{G}^{\circ}_{jhk}\boldsymbol{\omega}^{\circ}_{hk}(t)\right)\\
+\left(\mathbf{H}^{\circ}_{jjhk}\mathbf{q}_{hk}(t) + \mathbf{G}^{\circ}_{jhk}\boldsymbol{\omega}^{\circ}_{hk}(t)\right)^{T}\mathbf{P}^{\circ}_{hk}\mathbf{q}_{hk}(t)
\end{array}\right\}\\
+ 2\sum_{j=1}^{s-1}\sum_{g=j+1}^{s}\sum_{h=1}^{p-1}\sum_{k=h+1}^{p}\mu_j\mu_g &\left\{\begin{array}{l}
\left(\mathbf{C}^{\circ}_{hk}\mathbf{q}_{hk}(t) + \mathbf{D}^{\circ}_{hk}\boldsymbol{\omega}^{\circ}_{hk}(t)\right)^{T}\left(\mathbf{C}^{\circ}_{hk}\mathbf{q}_{hk}(t) + \mathbf{D}^{\circ}_{hk}\boldsymbol{\omega}^{\circ}_{hk}(t)\right)\\
-\boldsymbol{\omega}^{\circ T}_{hk}(t)\,\boldsymbol{\Gamma}^{\circ}_{hk}\boldsymbol{\omega}^{\circ}_{hk}(t)\\
+\mathbf{q}^{T}_{hk}(t)\,\mathbf{P}^{\circ}_{hk}\left(\dfrac{\mathbf{H}^{\circ}_{jghk} + \mathbf{H}^{\circ}_{gjhk}}{2}\mathbf{q}_{hk}(t) + \dfrac{\mathbf{G}^{\circ}_{jhk} + \mathbf{G}^{\circ}_{ghk}}{2}\boldsymbol{\omega}^{\circ}_{hk}(t)\right)\\
+\left(\dfrac{\mathbf{H}^{\circ}_{jghk} + \mathbf{H}^{\circ}_{gjhk}}{2}\mathbf{q}_{hk}(t) + \dfrac{\mathbf{G}^{\circ}_{jhk} + \mathbf{G}^{\circ}_{ghk}}{2}\boldsymbol{\omega}^{\circ}_{hk}(t)\right)^{T}\mathbf{P}^{\circ}_{hk}\mathbf{q}_{hk}(t)
\end{array}\right\},
\end{aligned} \tag{88}$$

where, for simplicity, the argument of membership functions was omitted.

Therefore, inserting appropriate into (14), (15), it is obtained the following:

$$\begin{bmatrix} \boldsymbol{\Psi}^{\circ}_{jjhk} & \mathbf{A}^{1\circ}_{jhk} & \cdots & \mathbf{A}^{p\circ}_{jhk} & \mathbf{B}^{\circ}_{jhk} & \mathbf{X}^{\circ}_{hk}\mathbf{C}^{\circ T}_{hk} \\ * & -\varepsilon_{hk1}\mathbf{I}_{n_1} & \cdots & \mathbf{0} & \mathbf{0} & \mathbf{C}^{1\circ T}_{hk} \\ \vdots & \vdots & \ddots & \vdots & \vdots & \vdots \\ * & * & \cdots & -\varepsilon_{hkp}\mathbf{I}_{n_p} & \mathbf{0} & \mathbf{C}^{p\circ T}_{hk} \\ * & * & \cdots & * & -\gamma_{hk}\mathbf{I}_{(r_h+r_k)} & \mathbf{0} \\ * & * & \cdots & * & * & -\mathbf{I}_{(m_h+m_k)} \end{bmatrix} < 0,$$

$$\begin{bmatrix} \boldsymbol{\Psi}^{\circ}_{jghk} & \dfrac{\mathbf{A}^{1\circ}_{jhk}+\mathbf{A}^{1\circ}_{ghk}}{2} & \cdots & \dfrac{\mathbf{A}^{p\circ}_{jhk}+\mathbf{A}^{p\circ}_{ghk}}{2} & \dfrac{\mathbf{B}^{\circ}_{jhk}+\mathbf{B}^{\circ}_{ghk}}{2} & \mathbf{X}^{\circ}_{hk}\mathbf{C}^{\circ T}_{hk} \\ * & -\varepsilon_{hk1}\mathbf{I}_{n_1} & \cdots & \mathbf{0} & \mathbf{0} & \mathbf{C}^{1\circ T}_{hk} \\ \vdots & \vdots & \ddots & \vdots & \vdots & \vdots \\ * & * & \cdots & -\varepsilon_{hkp}\mathbf{I}_{n_p} & \mathbf{0} & \mathbf{C}^{p\circ T}_{hk} \\ * & * & \cdots & * & -\gamma_{hk}\mathbf{I}_{(r_h+r_k)} & \mathbf{0} \\ * & * & \cdots & * & * & -\mathbf{I}_{(m_h+m_k)} \end{bmatrix} < 0, \tag{89}$$

where

$$\begin{aligned} \boldsymbol{\Psi}^{\circ}_{jjhk} &= \mathbf{A}^{\circ}_{jhk}\mathbf{X}^{\circ}_{hk} + \mathbf{X}^{\circ}_{hk}\mathbf{A}^{\circ T}_{jhk} - \mathbf{B}^{\circ}_{jhk}\mathbf{K}^{\circ T}_{jhk}\mathbf{X}^{\circ}_{hk} - \mathbf{X}^{\circ}_{hk}\mathbf{K}^{\circ T}_{jhk}\mathbf{B}^{\circ T}_{jhk}, \\ \boldsymbol{\Psi}^{\circ}_{jghk} &= \frac{\mathbf{A}^{\circ}_{jhk}+\mathbf{A}^{\circ}_{ghk}}{2}\mathbf{X}^{\circ}_{hk} + \mathbf{X}^{\circ}_{hk}\frac{\left(\mathbf{A}^{\circ}_{jhk}+\mathbf{A}^{\circ}_{ghk}\right)^{T}}{2} \\ &\quad - \frac{\mathbf{B}^{\circ}_{jhk}\mathbf{K}^{\circ}_{ghk}+\mathbf{B}^{\circ}_{ghk}\mathbf{K}^{\circ}_{jhk}}{2}\mathbf{X}^{\circ}_{hk} \\ &\quad - \mathbf{X}^{\circ}_{hk}\frac{\left(\mathbf{B}^{\circ}_{jhk}\mathbf{K}^{\circ}_{ghk}+\mathbf{B}^{\circ}_{ghk}\mathbf{K}^{\circ}_{jhk}\right)^{T}}{2}. \end{aligned} \tag{90}$$

Thus, with the substitutions

$$\mathbf{Y}^{\circ}_{jhk} = \mathbf{K}^{\circ}_{jhk}\mathbf{X}^{\circ}_{hk}, \qquad \mathbf{Y}^{\circ}_{ghk} = \mathbf{K}^{\circ}_{ghk}\mathbf{X}^{\circ}_{hk}, \tag{91}$$

(89)-(90) imply (78)-(79). This concludes the proof. □

Theorem 7. *Controlled subsystem pair* (57), (58) *in the system* (1), (3) *is stable with performances* $\sum_{j=1}^{s}\sum_{g=1}^{s}\mu_j(\boldsymbol{\theta}(t))\mu_g(\boldsymbol{\theta}(t))\|\mathbf{C}^{\circ}_{hk}(s\mathbf{I}-\mathbf{H}^{\circ}_{jghk})^{-1}\mathbf{B}^{\circ}_{jhk}+\mathbf{D}^{\circ}_{jhk}\|^2_{\infty} \le \gamma_{hk}$, *if for given* $\delta > 0$, $\delta \in \mathbb{R}$ *there exist symmetric positive definite matrices* $\mathbf{V}^{\circ}_{hk}, \mathbf{T}^{\circ}_{hk} \in \mathbb{R}^{(n_h+n_k)\times(n_h+n_k)}$, *matrices* $\mathbf{W}^{\circ}_{jhk} \in \mathbb{R}^{(r_h+r_k)\times(n_h+n_k)}$, *and positive scalars* $\gamma_{hk}, \varepsilon_{hkl} \in \mathbb{R}$ *such that*

$$\begin{aligned} &\mathbf{V}^{\circ}_{hk} = \mathbf{V}^{\circ T}_{hk} > 0, \qquad \mathbf{T}^{\circ}_{hk} = \mathbf{T}^{\circ T}_{hk} > 0, \\ &\varepsilon_{hkl} > 0, \qquad \gamma_{hk} > 0, \end{aligned} \tag{92}$$

for $h, l = 1, \ldots, p$, $l \neq h, k$, $h < k \le p$,

$$\begin{bmatrix} \boldsymbol{\Sigma}^{\circ}_{jjhk} & \mathbf{A}^{1\circ}_{jhk} & \cdots & \mathbf{A}^{p\circ}_{jhk} & \mathbf{B}^{\circ}_{jhk} & \boldsymbol{\Gamma}^{\circ}_{jjhk} & \mathbf{V}^{\circ}_{hk}\mathbf{C}^{\circ T}_{hk} \\ * & -\varepsilon_{hk1}\mathbf{I}_{n_1} & \cdots & \mathbf{0} & \mathbf{0} & \mathbf{A}^{1\circ T}_{jhk} & \mathbf{C}^{1\circ T}_{hk} \\ \vdots & \vdots & \ddots & \vdots & \vdots & \vdots & \vdots \\ * & * & \cdots & -\varepsilon_{hkp}\mathbf{I}_{n_p} & \mathbf{0} & \mathbf{A}^{p\circ T}_{jhk} & \mathbf{C}^{p\circ T}_{hk} \\ * & * & \cdots & * & -\gamma_{hk}\mathbf{I}_{(r_h+r_k)} & \mathbf{B}^{\circ T}_{jhk} & \mathbf{0} \\ * & * & \cdots & * & * & -2\delta\mathbf{V}^{\circ}_{hk} & \mathbf{0} \\ * & * & \cdots & * & * & * & -\mathbf{I}_{(m_h+m_k)} \end{bmatrix} < 0, \tag{93}$$

for $j = 1, 2, \ldots, s$, $h = 1, 2, \ldots, p-1$, $k = h+1, h+2, \ldots, p$, $l = 1, 2, \ldots, p$, $l \neq h, k$,

$$\begin{bmatrix} \boldsymbol{\Sigma}^{\circ}_{jghk} & \dfrac{\mathbf{A}^{1\circ}_{jhk} + \mathbf{A}^{1\circ}_{ghk}}{2} & \cdots & \dfrac{\mathbf{A}^{p\circ}_{jhk} + \mathbf{A}^{p\circ}_{ghk}}{2} & \dfrac{\mathbf{B}^{\circ}_{jhk} + \mathbf{B}^{\circ}_{ghk}}{2} & \boldsymbol{\Gamma}^{\circ}_{jghk} & \mathbf{V}^{\circ}_{hk}\mathbf{C}^{\circ T}_{hk} \\ * & -\varepsilon_{hk1}\mathbf{I}_{n_1} & \cdots & \mathbf{0} & \mathbf{0} & \dfrac{\left(\mathbf{A}^{1\circ}_{jhk} + \mathbf{A}^{1\circ}_{ghk}\right)^T}{2} & \mathbf{C}^{1\circ T}_{hk} \\ \vdots & \vdots & \ddots & \vdots & \vdots & \vdots & \vdots \\ * & * & \cdots & -\varepsilon_{hkp}\mathbf{I}_{n_p} & \mathbf{0} & \dfrac{\left(\mathbf{A}^{p\circ}_{jhk} + \mathbf{A}^{p\circ}_{ghk}\right)^T}{2} & \mathbf{C}^{p\circ T}_{hk} \\ * & * & \cdots & * & -\gamma_{hk}\mathbf{I}_{(r_h+r_k)} & \dfrac{\left(\mathbf{B}^{\circ}_{jhk} + \mathbf{B}^{\circ}_{jhk}\right)^T}{2} & \mathbf{0} \\ * & * & \cdots & * & * & -2\delta\mathbf{V}^{\circ}_{hk} & \mathbf{0} \\ * & * & \cdots & * & * & * & -\mathbf{I}_{(m_h+m_k)} \end{bmatrix} < 0, \tag{94}$$

for $j = 1, 2, \ldots, s-1$, $j = 2, 3, \ldots, s$, $h = 1, 2, \ldots, p-1$, $k = h+1, h+2, \ldots, p$, $l = 1, 2, \ldots, p$, $l \neq h, k$, $j < g \leq s$, *with* $\mathbf{A}^{\circ}_{jhk}$, $\mathbf{B}^{\circ}_{jhk}$, $\mathbf{A}^{l\circ}_{jhk}$, $\mathbf{C}^{\circ}_{hk}$, *and* $\mathbf{C}^{l\circ}_{hk}$ *defined in* (59), (61), *and* (62), *respectively, and with*

$$\boldsymbol{\Sigma}^{\circ}_{jjhk} = \mathbf{A}^{\circ}_{jhk}\mathbf{V}^{\circ}_{hk} + \mathbf{V}^{\circ}_{hk}\mathbf{A}^{\circ T}_{jhk} - \mathbf{B}^{\circ}_{jhk}\mathbf{W}^{\circ}_{jhk} - \mathbf{W}^{\circ T}_{jhk}\mathbf{B}^{\circ T}_{jhk}, \tag{95}$$

$$\begin{aligned} \boldsymbol{\Sigma}^{\circ}_{jghk} = {} & \frac{\mathbf{A}^{\circ}_{jhk} + \mathbf{A}^{\circ}_{ghk}}{2}\mathbf{V}^{\circ}_{hk} + \mathbf{V}^{\circ}_{hk}\frac{\left(\mathbf{A}^{\circ}_{jhk} + \mathbf{A}^{\circ}_{ghk}\right)^T}{2} \\ & - \frac{\mathbf{B}^{\circ}_{jhk}\mathbf{W}^{\circ}_{ghk} + \mathbf{B}^{\circ}_{ghk}\mathbf{W}^{\circ}_{jhk}}{2} \\ & - \frac{\left(\mathbf{B}^{\circ}_{jhk}\mathbf{W}^{\circ}_{ghk} + \mathbf{B}^{\circ}_{ghk}\mathbf{W}^{\circ}_{jhk}\right)^T}{2}, \end{aligned} \tag{96}$$

$$\boldsymbol{\Gamma}^{\circ}_{jjhk} = \mathbf{T}^{\circ}_{hk} - \delta\mathbf{V}^{\circ}_{hk} + \mathbf{V}^{\circ}_{hk}\mathbf{A}^{T}_{jhk} - \mathbf{W}^{\circ T}_{jhk}\mathbf{B}^{\circ T}_{jhk}, \tag{97}$$

$$\begin{aligned} \boldsymbol{\Gamma}^{\circ}_{jghk} = {} & \mathbf{T}^{\circ}_{hk} - \delta\mathbf{V}^{\circ}_{hk} + \mathbf{V}^{\circ}_{hk}\frac{\mathbf{A}^{\circ T}_{jhk} + \mathbf{A}^{\circ T}_{ghk}}{2} \\ & - \frac{\mathbf{W}^{\circ T}_{ghk}\mathbf{B}^{\circ T}_{jhk} + \mathbf{W}^{\circ T}_{jhk}\mathbf{B}^{\circ T}_{ghk}}{2}, \end{aligned} \tag{98}$$

where, for given h, k, $\mathbf{A}^{h\circ}_{jhk}$, $\mathbf{A}^{k\circ}_{jhk}$, *and* $\mathbf{C}^{h\circ}_{hk}$, $\mathbf{C}^{k\circ}_{hk}$ *are not included into the structure of* (78).

When the above conditions hold, the gain matrices $\mathbf{K}^{\circ}_{jhk}$ *are given by*

$$\mathbf{K}^{\circ}_{jhk} = \mathbf{W}^{\circ}_{jhk}\mathbf{V}^{\circ -1}_{hk}. \tag{99}$$

Proof. Using the above given notations, (33) gives

$$\begin{aligned} 0 > \dot{v}\left(\mathbf{q}_{hk}(t)\right) = {} & \sum_{j=1}^{s}\sum_{h=1}^{p-1}\sum_{k=h+1}^{p}\mu_j\mu_j \left\{ \begin{array}{l} \dot{\mathbf{q}}^T_{hk}(t)\,\mathbf{P}_{hk}\mathbf{q}_{hk}(t) + \mathbf{q}^T_{hk}(t)\,\mathbf{P}_{hk}\dot{\mathbf{q}}_{hk}(t) \\ \quad +3\left(\mathbf{C}^{\circ}_{hk}\mathbf{q}_{hk}(t) + \mathbf{D}^{\circ}_{hk}\boldsymbol{\omega}^{\circ}_{hk}(t)\right)^T\left(\mathbf{C}^{\circ}_{hk}\mathbf{q}_{hk}(t) + \mathbf{D}^{\circ}_{hk}\boldsymbol{\omega}^{\circ}_{hk}(t)\right) \\ \quad -3\gamma\boldsymbol{\omega}^{\circ T}_{hk}(t)\,\boldsymbol{\omega}^{\circ}_{hk}(t) \\ \quad +2\left(\mathbf{q}^T_{hk}(t)\,\mathbf{S}^{\circ}_1 + \dot{\mathbf{q}}^T_{hk}(t)\,\mathbf{S}^{\circ}_2\right)\left\{ \begin{array}{c} \mathbf{H}^{\circ}_{jjhk}\mathbf{q}_{hk}(t) + \mathbf{G}^{\circ}_{jhk}\boldsymbol{\omega}^{\circ}_{hk}(t) \\ -\dot{\mathbf{q}}_{hk}(t) \end{array} \right\} \end{array} \right\} \\ & + 4\sum_{j=1}^{s-1}\sum_{g=j+1}^{s}\sum_{h=1}^{p-1}\sum_{k=h+1}^{p}\mu_j\mu_g\left(\mathbf{q}^T_{hk}(t)\,\mathbf{S}^{\circ}_1 + \dot{\mathbf{q}}^T_{hk}(t)\,\mathbf{S}^{\circ}_2\right)\left\{ \begin{array}{c} \dfrac{\mathbf{H}_{jghk} + \mathbf{H}_{gjhk}}{2}\mathbf{q}_{hk}(t) \\ +\dfrac{\mathbf{G}_{jhk} + \mathbf{G}_{ghk}}{2}\boldsymbol{\omega}^{\circ}_{hk}(t) \end{array} \right\}, \end{aligned} \tag{100}$$

and so (29), (30) take the forms

$$\begin{bmatrix} \Xi^{\circ}_{jjhk} & \mathbf{A}^{1\circ}_{jhk} & \cdots & \mathbf{A}^{p\circ}_{jhk} & \mathbf{B}^{\circ}_{jhk} & \Upsilon^{\circ}_{jjhk} & \mathbf{X}^{\circ}_{hk}\mathbf{C}^{\circ T}_{hk} \\ * & -\varepsilon_{hk1}\mathbf{I}_{n_1} & \cdots & \mathbf{0} & \mathbf{0} & \mathbf{A}^{1\circ T}_{jhk} & \mathbf{C}^{1\circ T}_{hk} \\ \vdots & \vdots & \ddots & \vdots & \vdots & \vdots & \vdots \\ * & * & \cdots & -\varepsilon_{hkp}\mathbf{I}_{n_p} & \mathbf{0} & \mathbf{A}^{p\circ T}_{jhk} & \mathbf{C}^{p\circ T}_{hk} \\ * & * & \cdots & * & -\gamma_{hk}\mathbf{I}_{(r_h+r_k)} & \mathbf{B}^{\circ T}_{jhk} & \mathbf{0} \\ * & * & \cdots & * & * & -2\delta\mathbf{V}^{\circ}_{hk} & \mathbf{0} \\ * & * & \cdots & * & * & * & -\mathbf{I}_{(m_h+m_k)} \end{bmatrix} < 0,$$

$$\begin{bmatrix} \Xi^{\circ}_{jghk} & \dfrac{\mathbf{A}^{1\circ}_{jhk}+\mathbf{A}^{1\circ}_{ghk}}{2} & \cdots & \dfrac{\mathbf{A}^{p\circ}_{jhk}+\mathbf{A}^{p\circ}_{ghk}}{2} & \dfrac{\mathbf{B}^{\circ}_{jhk}+\mathbf{B}^{\circ}_{ghk}}{2} & \Upsilon^{\circ}_{jghk} & \mathbf{V}^{\circ}_{hk}\mathbf{C}^{\circ T}_{hk} \\ * & -\varepsilon_{hk1}\mathbf{I}_{n_1} & \cdots & \mathbf{0} & \mathbf{0} & \dfrac{\left(\mathbf{A}^{1\circ}_{jhk}+\mathbf{A}^{1\circ}_{ghk}\right)^T}{2} & \mathbf{C}^{1\circ T}_{hk} \\ \vdots & \vdots & \ddots & \vdots & \vdots & \vdots & \vdots \\ * & * & \cdots & -\varepsilon_{hkp}\mathbf{I}_{n_p} & \mathbf{0} & \dfrac{\left(\mathbf{A}^{p\circ}_{jhk}+\mathbf{A}^{p\circ}_{ghk}\right)^T}{2} & \mathbf{C}^{p\circ T}_{hk} \\ * & * & \cdots & * & -\gamma_{hk}\mathbf{I}_{(r_h+r_k)} & \dfrac{\left(\mathbf{B}^{\circ}_{jhk}+\mathbf{B}^{\circ}_{jhk}\right)^T}{2} & \mathbf{0} \\ * & * & \cdots & * & * & -2\delta\mathbf{V}^{\circ}_{hk} & \mathbf{0} \\ * & * & \cdots & * & * & * & -\mathbf{I}_{(m_h+m_k)} \end{bmatrix} < 0, \tag{101}$$

respectively, where

$$\Xi^{\circ}_{jjhk} = \mathbf{A}^{\circ}_{jhk}\mathbf{V}^{\circ}_{hk} + \mathbf{V}^{\circ}_{hk}\mathbf{A}^{\circ T}_{jhk} - \mathbf{B}^{\circ}_{jhk}\mathbf{K}^{\circ}_{jhk}\mathbf{V}^{\circ}_{hk} - \mathbf{V}^{\circ}_{hk}\mathbf{K}^{\circ T}_{jhk}\mathbf{B}^{\circ T}_{jhk}, \tag{102}$$

$$\begin{aligned} \Xi^{\circ}_{jghk} = {} & \frac{\mathbf{A}^{\circ}_{jhk}+\mathbf{A}^{\circ}_{ghk}}{2}\mathbf{V}^{\circ}_{hk} + \mathbf{V}^{\circ}_{hk}\frac{\left(\mathbf{A}^{\circ}_{jhk}+\mathbf{A}^{\circ}_{ghk}\right)^T}{2} \\ & - \frac{\mathbf{B}^{\circ}_{jhk}\mathbf{K}^{\circ}_{ghk}+\mathbf{B}^{\circ}_{ghk}\mathbf{K}^{\circ}_{jhk}}{2}\mathbf{V}^{\circ}_{hk} \\ & - \mathbf{V}^{\circ}_{hk}\frac{\left(\mathbf{B}^{\circ}_{jhk}\mathbf{K}^{\circ}_{ghk}+\mathbf{B}^{\circ}_{ghk}\mathbf{K}^{\circ}_{jhk}\right)^T}{2}, \end{aligned} \tag{103}$$

$$\Upsilon^{\circ}_{jjhk} = \mathbf{T}^{\circ}_{hk} - \delta\mathbf{V}^{\circ}_{hk} + \mathbf{V}^{\circ}_{hk}\mathbf{A}^{T}_{jhk} - \mathbf{V}^{\circ}_{hk}\mathbf{K}^{\circ T}_{jhk}\mathbf{B}^{\circ T}_{jhk}, \tag{104}$$

$$\begin{aligned} \Upsilon^{\circ}_{jghk} = {} & \mathbf{T}^{\circ}_{hk} - \delta\mathbf{V}^{\circ}_{hk} + \mathbf{V}^{\circ}_{hk}\frac{\mathbf{A}^{\circ T}_{jhk}+\mathbf{A}^{\circ T}_{ghk}}{2} \\ & - \mathbf{V}^{\circ}_{hk}\frac{\mathbf{K}^{\circ T}_{ghk}\mathbf{B}^{\circ T}_{jhk}+\mathbf{K}^{\circ T}_{jhk}\mathbf{B}^{\circ T}_{ghk}}{2}. \end{aligned} \tag{105}$$

Therefore, with the substitutions

$$\mathbf{W}^{\circ}_{jhk} = \mathbf{K}^{\circ}_{jhk}\mathbf{V}^{\circ}_{hk}, \qquad \mathbf{W}^{\circ}_{ghk} = \mathbf{K}^{\circ}_{ghk}\mathbf{V}^{\circ}_{hk}, \tag{106}$$

(101)–(105) imply (93)–(98). This concludes the proof. □

To bet both of these theorems in the context of the control design for systems specified by TS models, it is necessary to make some remarks.

Although both theorems solve the same problem, the role of Theorem 6 is primarily methodological and in particular shows that the design problem of pairwise distributable control of large-scale TS systems can be formulated in the terms of H_∞ approach. Because it is based on the default structure of BRL, the Lyapunov matrices $\mathbf{X}^{\circ}_{hk}$ and the subsystem dynamic matrices $\mathbf{A}^{\circ}_{jhk}$ form bound pairs with regard to the operation of multiplication. Consequently, when using the design conditions proposed in Theorem 6 and the LMI task is feasible, the obtained solution is very conservative.

Under the conditions defined by Theorem 7, the set of subsystem matrices $\mathbf{A}^{\circ}_{jhk}$ are decoupled from the set of Lyapunov matrices $\mathbf{T}^{\circ}_{hk}$ by using the set of slack matrix variables $\mathbf{V}^{\circ}_{hk}$. This enables the design conditions in respect of natural affine properties of TS models and, compared with the result by Theorem 6, a less conservative solution. In addition, by tuning parameter δ, the stability conditions setting of the whole system can be modified. Less conservatism in this case also means that the linear control of certain subsystem pair can be used instead of the nonlinear TS fuzzy control algorithm (see Section 5).

These theorems, which could be potentially considered as equivalent, give generally different solutions, except for the special case when for a pair h, k by chance is $\delta = 1$ and $\mathbf{V}^{\circ}_{hk} = \mathbf{T}^{\circ}_{hk} = \mathbf{X}^{\circ}_{hk}$.

In terms of computational complexity, if there is, for example, only one nonlinear sector in each block of the matrix $\mathbf{A}$ and every sector is described only by a pair of sector functions, the number of fuzzy rules is $s = 2^{p^2}$ to formulate the global control design and $s = 2^{2p}$ if pairwise distributed control principle is preferred. This can play a major role due to boundaries of LMI solvers. Moreover, as mentioned above, the proposed method can reduce this number in some subsystem pair structures.

On the other hand, although the pairwise subsystem control principle brings more complex control gain, the use of the state control laws does not substantially modify the computational complexity in dependency on the dimensionality of global state vector parts in the control algorithms.

5. Illustrative Example

To demonstrate properties of this approach, a system with four inputs and four outputs is used in the example. The parameters of (1)–(3) are [22]

$$\mathbf{A} = \begin{bmatrix} -3 & 1 & 2 & -1 & 4 & 0 \\ -1 & -2 & 1 & 1 & 5 & 2 \\ 1 & -1 & 1 & -a_j & -2 & 4 \\ 1 & -2 & -2 & 2 & 1 & 2 \\ 3 & -1 & -2 & 0 & 1 & 5 \\ 0 & 0 & -1 & 3 & -2 & -4 \end{bmatrix},$$

$$\mathbf{C}^T = \begin{bmatrix} 3 & 0 & 2 & 0 \\ 1 & 6 & -1 & 0 \\ 1 & 6 & -1 & 0 \\ 2 & 1 & 3 & 1 \\ 1 & 0 & 0 & 3 \\ 1 & 0 & 0 & 3 \end{bmatrix}, \qquad \mathbf{B} = \begin{bmatrix} 1 & & & \\ & 2 & & \\ & 1 & & \\ & & 2 & \\ & & & 1 \\ & & & 2 \end{bmatrix},$$

$$a_1 = 0.8, \qquad a_2 = 1.2,$$

$$\mu_1(\vartheta(t)) = \frac{a_1 - q_1(t)}{a_1 - a_2}, \qquad \mu_2(\vartheta(t)) = 1 - \mu_1(\vartheta(t)),$$

$$\vartheta(t) = q_1(t). \tag{107}$$

To solve this problem, the next pairs grupping were done

$$\mathbf{A}^{\circ}_{\bullet 12} = \begin{bmatrix} -3 & 1 & 2 \\ -1 & -2 & 1 \\ 1 & -1 & 1 \end{bmatrix}, \quad \mathbf{A}^{3\circ}_{112} = \begin{bmatrix} -1.0 \\ 1.0 \\ -0.8 \end{bmatrix},$$

$$\mathbf{A}^{3\circ}_{212} = \begin{bmatrix} -1.0 \\ 1.0 \\ -1.2 \end{bmatrix}, \quad \mathbf{A}^{4\circ}_{\bullet 12} = \begin{bmatrix} 4 & 0 \\ 5 & 2 \\ -2 & 4 \end{bmatrix},$$

$$\mathbf{A}^{\circ}_{\bullet 13} = \begin{bmatrix} -3 & -1 \\ 1 & 2 \end{bmatrix}, \quad \mathbf{A}^{2\circ}_{\bullet 13} = \begin{bmatrix} 1 & 2 \\ -2 & -2 \end{bmatrix},$$

$$\mathbf{A}^{4\circ}_{\bullet 13} = \begin{bmatrix} 4 & 0 \\ 1 & 2 \end{bmatrix},$$

$$\mathbf{A}^{\circ}_{\bullet 14} = \begin{bmatrix} -3 & 4 & 0 \\ 3 & 2 & 5 \\ 0 & 5 & -4 \end{bmatrix}, \qquad \mathbf{A}^{2\circ}_{\bullet 14} = \begin{bmatrix} 1 & 2 \\ -1 & -2 \\ 0 & -1 \end{bmatrix},$$

$$\mathbf{A}^{3\circ}_{\bullet 14} = \begin{bmatrix} -1 \\ 0 \\ 3 \end{bmatrix}, \qquad \mathbf{A}^{1\circ}_{\bullet 23} = \begin{bmatrix} -1 \\ 1 \\ 1 \end{bmatrix},$$

$$\mathbf{A}^{\circ}_{123} = \begin{bmatrix} -2 & 1 & 1.0 \\ -1 & 1 & -0.8 \\ -2 & -2 & 2.0 \end{bmatrix}, \qquad \mathbf{A}^{\circ}_{223} = \begin{bmatrix} -2 & 1 & 1.0 \\ -1 & 1 & -1.2 \\ -2 & -2 & 2.0 \end{bmatrix},$$

$$\mathbf{A}^{4\circ}_{\bullet 23} = \begin{bmatrix} 5 & 2 \\ -2 & 4 \\ 1 & 2 \end{bmatrix},$$

$$\mathbf{A}^{\circ}_{\bullet 24} = \begin{bmatrix} -2 & 1 & 5 & 2 \\ -1 & 1 & -2 & 4 \\ -1 & -2 & 1 & 5 \\ 0 & -1 & -2 & -4 \end{bmatrix}, \qquad \mathbf{A}^{1\circ}_{\bullet 24} = \begin{bmatrix} -1 \\ 1 \\ 3 \\ 0 \end{bmatrix},$$

$$\mathbf{A}^{3\circ}_{124} = \begin{bmatrix} 1 \\ -0.8 \\ 0 \\ 3 \end{bmatrix}, \qquad \mathbf{A}^{3\circ}_{224} = \begin{bmatrix} 1 \\ -1.2 \\ 0 \\ 3 \end{bmatrix},$$

$$\mathbf{A}^{\circ}_{\bullet 34} = \begin{bmatrix} 2 & 1 & 2 \\ 0 & 1 & 5 \\ 3 & -2 & -4 \end{bmatrix}, \quad \mathbf{A}^{1\circ}_{\bullet 34} = \begin{bmatrix} 1 \\ 3 \\ 0 \end{bmatrix}, \quad \mathbf{A}^{2\circ}_{\bullet 34} = \begin{bmatrix} -2 & -2 \\ -1 & -2 \\ 0 & -1 \end{bmatrix},$$

$$\mathbf{B}_{\bullet 12} = \begin{bmatrix} 1 & 0 \\ 0 & 2 \\ 0 & 1 \end{bmatrix}, \quad \mathbf{B}_{\bullet 13} = \begin{bmatrix} 1 & 0 \\ 0 & 2 \end{bmatrix}, \quad \mathbf{B}_{\bullet 14} = \begin{bmatrix} 1 & 0 \\ 0 & 1 \\ 0 & 2 \end{bmatrix},$$

$$\mathbf{B}_{\bullet 23} = \begin{bmatrix} 2 & 0 \\ 1 & 0 \\ 0 & 2 \end{bmatrix}, \quad \mathbf{B}_{\bullet 24} = \begin{bmatrix} 2 & 0 \\ 1 & 0 \\ 0 & 1 \\ 0 & 2 \end{bmatrix}, \quad \mathbf{B}_{\bullet 34} = \begin{bmatrix} 2 & 0 \\ 0 & 1 \\ 0 & 2 \end{bmatrix},$$

$$\mathbf{C}^{\circ}_{\bullet 12} = \begin{bmatrix} 1 & 1 & 1 \\ 0 & 2 & 2 \end{bmatrix}, \quad \mathbf{C}^{3\circ}_{\bullet 12} = \begin{bmatrix} 1 \\ 2 \end{bmatrix}, \quad \mathbf{C}^{4\circ}_{\bullet 12} = \begin{bmatrix} 1 & 1 \\ 0 & 0 \end{bmatrix},$$

$$\mathbf{C}^{\circ}_{\bullet 13} = \begin{bmatrix} 1 & 2 \\ 2 & 1 \end{bmatrix}, \quad \mathbf{C}^{2\circ}_{\bullet 13} = \begin{bmatrix} 1 & 1 \\ -1 & -1 \end{bmatrix}, \quad \mathbf{C}^{4\circ}_{\bullet 13} = \begin{bmatrix} 1 & 1 \\ 0 & 0 \end{bmatrix},$$

$$\mathbf{C}^{\circ}_{\bullet 14} = \begin{bmatrix} 1 & 1 & 1 \\ 0 & 1 & 1 \end{bmatrix}, \quad \mathbf{C}^{2\circ}_{\bullet 14} = \begin{bmatrix} 1 & 1 \\ 0 & 0 \end{bmatrix}, \quad \mathbf{C}^{3\circ}_{\bullet 14} = \begin{bmatrix} 2 \\ 1 \end{bmatrix},$$

$$\mathbf{C}^{\circ}_{\bullet 23} = \begin{bmatrix} 2 & 2 & 1 \\ -1 & -1 & 1 \end{bmatrix}, \quad \mathbf{C}^{1\circ}_{\bullet 23} = \begin{bmatrix} 0 \\ 2 \end{bmatrix}, \quad \mathbf{C}^{4\circ}_{\bullet 23} = \begin{bmatrix} 0 & 0 \\ 0 & 0 \end{bmatrix},$$

$$\mathbf{C}^{\circ}_{\bullet 24} = \begin{bmatrix} 2 & 2 & 0 & 0 \\ 0 & 0 & 1 & 1 \end{bmatrix}, \quad \mathbf{C}^{1\circ}_{\bullet 24} = \begin{bmatrix} 0 \\ 0 \end{bmatrix}, \quad \mathbf{C}^{3\circ}_{\bullet 24} = \begin{bmatrix} 1 \\ 1 \end{bmatrix},$$

$$\mathbf{C}^{\circ}_{\bullet 34} = \begin{bmatrix} 1 & 0 & 0 \\ 1 & 1 & 1 \end{bmatrix}, \quad \mathbf{C}^{1\circ}_{\bullet 34} = \begin{bmatrix} 2 \\ 0 \end{bmatrix}, \quad \mathbf{C}^{2\circ}_{\bullet 34} = \begin{bmatrix} -1 & -1 \\ 0 & 0 \end{bmatrix}, \tag{108}$$

where $\bullet hk$ denotes that the matrix parameters with this subscript are independent of the fuzzy rules. That means that in the pairwise partially decentralized control structure of this example, the control loop pairs 13, 14, and 34 will be surely fuzzy independent.

Solving for given tuning parameter δ, for example, with respect to $\mathbf{V}_{23}^{\circ}$, $\mathbf{T}_{23}^{\circ}$, $\mathbf{W}_{123}^{\circ}$, $\mathbf{W}_{223}^{\circ}$, ε_{231}, ε_{234}, and γ_{23}, it means writing (92)–(98) as

$$\mathbf{V}_{23}^{\circ} = \mathbf{V}_{23}^{\circ T} > 0, \qquad \mathbf{T}_{23}^{\circ} = \mathbf{T}_{23}^{\circ T} > 0,$$

$$\varepsilon_{231} > 0, \qquad \varepsilon_{234} > 0, \qquad \gamma_{23} > 0,$$

$$\begin{bmatrix} \boldsymbol{\Sigma}_{jg23}^{\circ} & \mathbf{A}_{\bullet 23}^{1\circ} & \mathbf{A}_{\bullet 23}^{4\circ} & \mathbf{B}_{\bullet 23}^{\circ} & \boldsymbol{\Gamma}_{jg23}^{\circ} & \mathbf{V}_{23}^{\circ}\mathbf{C}_{\bullet 23}^{\circ T} \\ * & -\varepsilon_{231} & \mathbf{0} & \mathbf{0} & \mathbf{A}_{\bullet 23}^{1\circ T} & \mathbf{C}_{\bullet 23}^{1\circ T} \\ * & * & -\varepsilon_{234} & \mathbf{0} & \mathbf{A}_{\bullet 23}^{4\circ T} & \mathbf{C}_{\bullet 23}^{4\circ T} \\ * & * & * & -\gamma_{23}\mathbf{I}_2 & \mathbf{B}_{\bullet 23}^{\circ T} & \mathbf{0} \\ * & * & * & * & -2\delta\mathbf{Z}_{23}^{\circ} & \mathbf{0} \\ * & * & * & * & * & -\mathbf{I}_2 \end{bmatrix} < 0,$$

$$\boldsymbol{\Sigma}_{jj23}^{\circ} = \mathbf{V}_{23}^{\circ}\mathbf{A}_{j23}^{\circ T} + \mathbf{A}_{j23}^{\circ}\mathbf{V}_{23}^{\circ} - \mathbf{B}_{\bullet 23}^{\circ}\mathbf{W}_{j23}^{\circ} - \mathbf{W}_{j23}^{\circ T}\mathbf{B}_{\bullet 23}^{\circ T}, \qquad j = 1, 2,$$

$$\boldsymbol{\Sigma}_{jg23}^{\circ} = \frac{\mathbf{A}_{j23}^{\circ} + \mathbf{A}_{g23}^{\circ}}{2}\mathbf{V}_{23}^{\circ} + \mathbf{V}_{23}^{\circ}\frac{\left(\mathbf{A}_{j23}^{\circ} + \mathbf{A}_{g23}^{\circ}\right)^{T}}{2} - \frac{\mathbf{B}_{\bullet 23}^{\circ}\mathbf{W}_{g23}^{\circ} + \mathbf{B}_{\bullet 23}^{\circ}\mathbf{W}_{j23}^{\circ}}{2} - \frac{\left(\mathbf{B}_{\bullet 23}^{\circ}\mathbf{W}_{g23}^{\circ} + \mathbf{B}_{\bullet 23}^{\circ}\mathbf{W}_{j23}^{\circ}\right)^{T}}{2}, \qquad j = 1, \quad g = 2,$$

$$\boldsymbol{\Gamma}_{jj23}^{\circ} = \mathbf{T}_{23}^{\circ} - \delta\mathbf{V}_{23}^{\circ} + \mathbf{V}_{23}^{\circ}\mathbf{A}_{j23}^{\circ T} - \mathbf{W}_{23}^{\circ T}\mathbf{B}_{\bullet 23}^{\circ T}, \qquad j = 1, 2,$$

$$\boldsymbol{\Gamma}_{jg23}^{\circ} = \mathbf{T}_{23}^{\circ} - \delta\mathbf{V}_{23}^{\circ} + \mathbf{V}_{23}^{\circ}\frac{\mathbf{A}_{j23}^{\circ T} + \mathbf{A}_{g23}^{\circ T}}{2} - \frac{\mathbf{W}_{g23}^{\circ T}\mathbf{B}_{\bullet 23}^{\circ T} + \mathbf{W}_{j23}^{\circ T}\mathbf{B}_{\bullet 23}^{\circ T}}{2}, \qquad j = 1, \quad g = 2, \tag{109}$$

and using SeDuMi package for Matlab [23], the feasible task for subsystem 23 and $\delta = 10$ yields the parameters

$$\varepsilon_{231} = 58.0063, \quad \varepsilon_{234} = 70.1966, \quad \gamma_{23} = 32.4549,$$

$$\mathbf{T}_{23}^{\circ} = \begin{bmatrix} 27.9470 & 10.1742 & -4.8315 \\ 10.1742 & 8.0186 & 3.1112 \\ -4.8315 & 3.1112 & 38.0154 \end{bmatrix},$$

$$\mathbf{W}_{j23}^{\circ} = \begin{bmatrix} 7.5666 & 4.4717 & 0.6808 \\ -1.9191 & -0.3955 & 13.6818 \end{bmatrix},$$

$$\mathbf{V}_{23}^{\circ} = \begin{bmatrix} 1.2004 & 0.2170 & -0.5773 \\ 0.2170 & 0.3793 & 0.2991 \\ -0.5773 & 0.2991 & 2.2580 \end{bmatrix},$$

$$\mathbf{K}_{\diamond 23}^{\circ} = \begin{bmatrix} 4.9482 & 8.6232 & 0.4245 \\ 4.3630 & -10.2695 & 8.5351 \end{bmatrix}, \tag{110}$$

where $\mathbf{K}_{\diamond 23}^{\circ}$ means that $\mathbf{K}_{j23}^{\circ}$ were computed equally to $g = 1, 2$.

By the same way, solving the rest LMIs, the gain matrix set is computed as

$$\mathbf{K}_{112}^{\circ} = \begin{bmatrix} 7.9346 & -2.8080 & 12.4851 \\ 0.7258 & 5.3963 & 6.0160 \end{bmatrix},$$

$$\mathbf{K}_{212}^{\circ} = \begin{bmatrix} 7.8740 & -2.8497 & 12.3828 \\ 0.7250 & 5.4268 & 6.0364 \end{bmatrix},$$

$$\mathbf{K}_{\bullet 14}^{\circ} = \begin{bmatrix} 4.0106 & 5.9223 & 1.4848 \\ 2.0249 & 4.1941 & 3.8514 \end{bmatrix},$$

$$\mathbf{K}_{\diamond 34}^{\circ} = \begin{bmatrix} 5.4294 & 1.1356 & 1.5393 \\ 2.0320 & 4.0784 & 3.0034 \end{bmatrix},$$

$$\mathbf{K}_{\bullet 13}^{\circ} = \begin{bmatrix} 6.2603 & 2.7947 \\ 2.0298 & 5.8502 \end{bmatrix},$$

$$\mathbf{K}_{\diamond 24}^{\circ} = \begin{bmatrix} 0.8349 & 2.2731 & 0.5904 & 1.1688 \\ -0.0995 & -0.1542 & 2.2100 & 1.8754 \end{bmatrix}. \tag{111}$$

$$\gamma_{12} = 22.9891, \qquad \gamma_{13} = 9.5395,$$

$$\gamma_{14} = 9.4173, \qquad \gamma_{24} = 9.5641,$$

$$\gamma_{34} = 11.0660.$$

The results imply that in this example only the control of the subsystem pair 1, 2 has to be realized in a TS fuzzy structure and all other pairs controls can be realized in constant linear pairwise control structure.

Generalizing, with respect the results presented in [13], the design methods based on the enhanced principle tend to produce for TS models the same control gain matrices which radically reduce the control structure, since such results mean very often stabilizing linear control laws for the nonlinear system or, as here, for its pair parts.

It is possible to verify—routinely—that the resulting closed-loop large-scale system will be stable if the tuning parameter is chosen as $\delta = 10$. Moreover, this example implies that with $\delta \leq 5$ such pairwise distributed TS fuzzy control structure ensures all stable closed-loop pairs but does not ensure the stability of the whole closed-loop system. That means that using this design principle, the stability of all closed-loop subsystem pairs does not mean automatically the stability of the whole TS large-scale closed-loop system. Note that the control laws are given in the partly autonomous structure (68), (69), which ensures now that every closed-loop subsystem pair is stable and designed for $\delta = 10$, and the large-scale closed-loop system will be stable too.

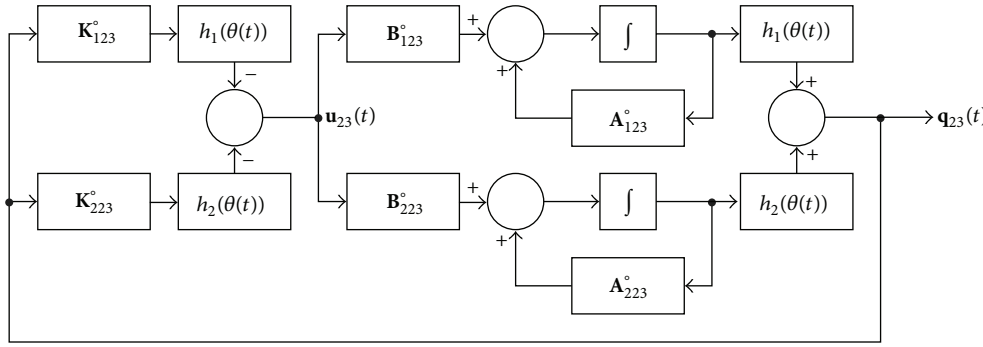

Figure 1: The general closed-loop structure for control of the subsystems pair (23) in the autonomous regime.

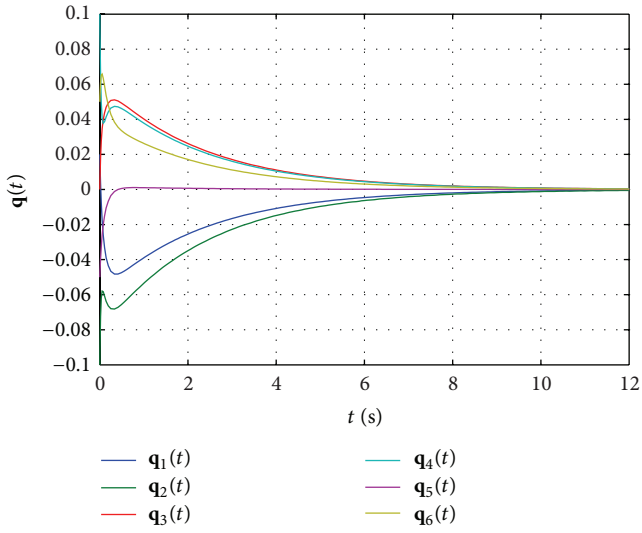

Figure 2: State response of the global closed-loop TS system in the autonomous regime.

The block diagram on Figure 1 describes how the control of the subsystems pair (23) is, in general, implemented. This specific subsystem pair in the example is the only one that is controlled by the fuzzy PDC controller. As stated earlier, $\mathbf{B}^{\circ}_{123} = \mathbf{B}^{\circ}_{223} = \mathbf{B}^{\circ}_{23}$, while, for example, $\mathbf{q}_2(t)$ of the global TS system can be obtained as the sum of the second component of vector $\mathbf{q}_{12}(t)$ and the first components of vectors $\mathbf{q}_{23}(t)$ and $\mathbf{q}_{24}(t)$. It is assumed, of course, that bonds to create $\mathbf{A}^{\circ}_{123}$, $\mathbf{A}^{\circ}_{223}$, and $\mathbf{B}^{\circ}_{23}$ structures can be realized.

Using autonomous control regime, defined by (68), (69), the illustrative simulations were realized under the initial condition

$$\mathbf{q}^{T}(0) = \begin{bmatrix} 0.02 & -0.10 & 0.00 & 0.10 & -0.05 & 0.05 \end{bmatrix}. \tag{112}$$

Figure 2 gives the global closed-loop TS system state response in the used simulation conditions.

For comparison, an equivalent set of gain matrices for the centralized fuzzy control can be constructed using above obtained results, where, for the control law (6),

$$\mathbf{K}_1 = \begin{bmatrix} \mathbf{18.2055} & -2.8080 & 12.4851 & 2.7947 & 5.9223 & 1.4848 \\ 0.7258 & \mathbf{13.4370} & \mathbf{20.2510} & 0.4245 & -1.1914 & 1.7646 \\ 2.0298 & 4.3630 & -10.2695 & \mathbf{19.8147} & 1.1356 & 1.5393 \\ 2.0249 & 1.5018 & -5.8333 & 2.0320 & \mathbf{19.8317} & \mathbf{10.8627} \end{bmatrix},$$

$$\mathbf{K}_2 = \begin{bmatrix} \mathbf{18.1449} & -2.8497 & 12.3828 & 2.7947 & 5.9223 & 1.4848 \\ 0.7250 & \mathbf{13.4675} & \mathbf{20.2714} & 0.4245 & -1.1914 & 1.7646 \\ 2.0298 & 4.3630 & -10.2695 & \mathbf{19.8147} & 1.1356 & 1.5393 \\ 2.0249 & 1.5018 & -5.8333 & 2.0320 & \mathbf{19.8317} & \mathbf{10.8627} \end{bmatrix}, \tag{113}$$

and the resulting closed-loop eigenvalue spectrums are stable, where

$$\rho\left(\mathbf{A}_1 - \mathbf{B}\mathbf{K}_1\right) = \{-0.3278, -8.1143, -18.2169, -35.0038, -41.2029, -48.6512\},$$
$$\rho\left(\mathbf{A}_2 - \mathbf{B}\mathbf{K}_2\right) = \{-0.3267, -8.1208, -18.1581, -35.0064, -41.1984, -48.7273\}. \tag{114}$$

Note that the structure of the matrices $\mathbf{K}_g$, $g = 1, 2$ evidently implies that the control laws are block diagonal dominant.

6. Concluding Remarks

The main difficulty of solving the decentralized control problem comes from the fact that the feedback gain is subject to structural constraints. At the beginning the study of large scale system theory, there was prevailing idea that a large of scale system is decentrally stabilizable under controllability condition by strengthening the stability degree of subsystems. But, because of the existence of decentralized fixed modes, some large scale systems can not be decentrally stabilized at all. In this paper, the idea to stabilize all subsystems and the whole system simultaneously by using decentralized controllers is replaced by another one, to stabilize all subsystems pairs and the whole system simultaneously by using partly pairwise decentralized control. In this sense the final scope of the paper is the design conditions for pairwise control of one class of pairwise-distributable continuous time TS large-scale systems. It is shown, based on the equivalent BRL formulations, how to expand the Lyapunov condition for pairwise TS control by using slack matrix variables in LMIs. As mentioned above, such matrix inequalities are linear with respect to the subsystem pairs variables and do not involve any product of the matrices, obtained by the Lyapunov matrix block separation and the subsystem pairs matrices. This enables us to derive a sufficient design condition for control with quadratic performances, optimizing subsystems interaction H_∞ norm bounds.

The method generally requires to solve, but separate, a larger number of linear matrix inequalities, and so more computational efforts are needed to provide design control parameters. However, used design conditions are less restrictive and are more close to necessity conditions in the sense of [24]. It is a very useful extension to TS system control performance synthesis problem. Numerical example demonstrates the principle effectiveness, although some computational complexity is increased.

Acknowledgments

The work presented in this paper was supported by VEGA, the Grant Agency of Ministry of Education and the Academy of Science of the Slovak Republic under Grant no. 1/0256/11. This support is very gratefully acknowledged.

References

[1] Y. Nesterov and A. Nemirovsky, *Interior Point Polynomial Methods in Convex Programming. Theory and Applications*, SIAM, Philadelphia, Pa, USA, 1994.

[2] S. Boyd, L. El Ghaoui, E. Feron, and V. Balakrishnan, *Linear Matrix Inequalities in System and Control Theory*, vol. 15 of *SIAM Studies in Applied Mathematics*, SIAM, Philadelphia, Pa, USA, 1994.

[3] G. Pipeleers, B. Demeulenaere, J. Swevers, and L. Vandenberghe, "Extended LMI characterizations for stability and performance of linear systems," *Systems & Control Letters*, vol. 58, no. 7, pp. 510–518, 2009.

[4] E. Feron, P. Apkarian, and P. Gahinet, "Analysis and synthesis of robust control systems via parameter-dependent Lyapunov functions," *IEEE Transactions on Automatic Control*, vol. 41, no. 7, pp. 1041–1046, 1996.

[5] V. Veselý and D. Rosinová, "Robust output model predictive control design: bmi approach," *International Journal of Innovative Computing, Information and Control*, vol. 5, no. 4, pp. 1115–1123, 2009.

[6] T. Bakka and H. R. Karimi, "Robust $\mathscr{H}_\infty$ dynamic output feedback control synthesis with pole placement constraints for offshore wind turbine systems," *Mathematical Problems in Engineering*, vol. 2012, Article ID 616507, 18 pages, 2012.

[7] Y. Jia, "Alternative proofs for improved LMI representations for the analysis and the design of continuous-time systems with polytopic type uncertainty: a predictive approach," *IEEE Transactions on Automatic Control*, vol. 48, no. 8, pp. 1413–1416, 2003.

[8] Y. He, M. Wu, and J.-H. She, "Improved bounded-real-lemma representation and H_∞ control of systems with polytopic uncertainties," *IEEE Transactions on Circuits and Systems II*, vol. 52, no. 7, pp. 380–383, 2005.

[9] A. T. Wu and G. R. Duan, "Enhanced LMI representations for H_2 performance of polytopic uncertain systems: continuous-time case," *International Journal of Automation and Computing*, vol. 3, no. 3, pp. 304–308, 2006.

[10] W. Xie, "An equivalent LMI representation of bounded real lemma for continuous-time systems," *Journal of Inequalities and Applications*, vol. 2008, Article ID 672905, 8 pages, 2008.

[11] K. Tanaka and H. O. Wang, *Fuzzy Control Systems Design and Analysis. A Linear Matrix Inequality Approach*, John Wiley & Sons, New York, NY, USA, 2001.

[12] S.-K. Hong and R. Langari, "Synthesis of an LMI-based fuzzy control system with guaranteed optimal H_∞ performance," in *Proceedings of the IEEE International Conference on Fuzzy Systems*, pp. 422–427, Anchorage, Alaska, USA, May 1998.

[13] D. Krokavec and A. Filasová, "Optimal fuzzy control for a class of nonlinear systems," *Mathematical Problems in Engineering*, vol. 2012, Article ID 481942, 29 pages, 2012.

[14] D. Krokavec and A. Filasová, "Stabilizing fuzzy output control for a class of nonlinear systems," *Advances in Fuzzy Systems*, vol. 2013, Article ID 294971, 9 pages, 2013.

[15] J. Lunze, *Feedback Control of Large-Scale Systems*, Prentice Hall, London, UK, 1992.

[16] M. Jamshidi, *Large-Scale Systems: Modeling, Control and Fuzzy Logic*, Prentice Hall, Upper Saddle River, NJ, USA, 1997.

[17] Z. Duan, J.-Z. Wang, and L. Huang, "Special decentralized control problems and effectiveness of parameter-dependent Lyapunov function method," in *Proceedings of the American Control Conference (ACC '05)*, pp. 1697–1702, Portland, Ore, USA, June 2005.

[18] C.-X. Dou, Z.-S. Duan, X.-B. Jia et al., "Delay-dependent robust stabilization for nonlinear large systems via decentralized fuzzy control," *Mathematical Problems in Engineering*, vol. 2011, Article ID 605794, 20 pages, 2011.

[19] A. I. Zečević and D. D. Šiljak, "A decomposition-based control strategy for large, sparse dynamic systems," *Mathematical Problems in Engineering*, vol. 2005, no. 1, pp. 33–48, 2005.

[20] A. P. Leros, "LSS linear regulator problem: a partially decentralized approach," *International Journal of Control*, vol. 49, no. 4, pp. 1377–1399, 1989.

[21] A. Filasová and D. Krokavec, "Pairwise control principle in large-scale systems," *Archives of Control Sciences*, vol. 21(57), no. 3, pp. 227–242, 2011.

[22] A. Filasová and D. Krokavec, "H1 subsystem pairwise distributed control of uncertain linear systems," in *Proceedings of the 7th IFAC Symposium on Robust Control Design (ROCOND '12)*, pp. 430–435, Aalborg, Denmark, 2012.

[23] D. Peaucelle, D. Henrion, V. Labit, and K. Taitz, *User's Guide for SeDuMi Interface 1.04*, LAAS-CNRS, Toulouse, France, 1994.

[24] A. Sala and C. Ariño, "Asymptotically necessary and sufficient conditions for stability and performance in fuzzy control: applications of Polya's theorem," *Fuzzy Sets and Systems*, vol. 158, no. 24, pp. 2671–2686, 2007.

Hindawi Publishing Corporation
Mathematical Problems in Engineering
Volume 2013, Article ID 818401, 10 pages
http://dx.doi.org/10.1155/2013/818401

Research Article

Impulsive Vaccination SEIR Model with Nonlinear Incidence Rate and Time Delay

Dongmei Li, Chunyu Gui, and Xuefeng Luo

Department of Applied Mathematics, Harbin University of Science and Technology, Harbin 150080, China

Correspondence should be addressed to Dongmei Li; dmli_2013@126.com

Received 12 July 2013; Revised 22 October 2013; Accepted 30 October 2013

Academic Editor: Jun Hu

This paper aims to discuss the delay epidemic model with vertical transmission, constant input, and nonlinear incidence. Some sufficient conditions are given to guarantee the existence and global attractiveness of the infection-free periodic solution and the uniform persistence of the addressed model with time delay. Finally, a numerical example is given to demonstrate the effectiveness of the proposed results.

1. Introduction

Vaccination has been widely used as a method of disease control; inoculate is an effective approach according to the characteristics of the disease which takes the defense in advance. The implementation of inoculate is not continuous but cyclical. As early as in the 1960s, the principle of the stability has been given in [1] for the impulsive differential equation. Subsequently, a better definition of stability has been proposed in [2] for the impulsive differential equation. Motivated by the above work, the attention has been made on the application of the pulse immunization in the infectious disease model. For example, the study has been reported in [3] where the research has been made about inoculating the pulse vaccination for the people who are easily infected. The researchers have realized that the pulse vaccination strategies can eliminate the positive role to measles; see for example [3, 4]. Moreover, the SIV infection model has been studied in [5]. The inoculation ratio and the inoculation interval time to eliminate the influence of the disease have been pointed out. Accordingly, a huge amount of results has appeared concerning the pulse model to study epidemics of infectious diseases; see for example [6, 7].

On the other hand, the pulse SEIR epidemic model with the incubation period has been established in [8]. The qualitative analysis has been given that the local asymptotic stability of infection-free periodic solution is globally stable. Note that the existence of time delay would degrade the desired performance or even result in the instability [9–12]. As such, a new class of models with vertical transmission delay pulse infectious disease has been given in [7]. By using the impulsive differential inequality, the sufficient conditions have been presented to guarantee the global attractability of infection-free periodic solution and uniform persistence of the disease. Subsequently, the disease delay pulse models with multiple infectious diseases have been addressed in [13] and the SIR pulse vaccination infectious disease model with time delay has been discussed in [14]. By constructing an appropriate Lyapunov function, the global attractability of the unique positive periodic solution has been discussed in [15] for the pulse predator-prey system with distributed delay and proliferated. Also, by using the comparison principle of impulsive differential equations, the influence from the time delay, the pulse vaccination, and the other factors on the nature of the model has been tackled in [16, 17].

An impulsive vaccination SEIR epidemic model with saturation infectious and constant input has been studied in [18], and the sufficient conditions have been established to ensure the stability and the persistence of the disease-free periodic solution. In [19], the SEIRS pulse infectious disease model with saturated incidence has been investigated. Sufficient conditions of infection-free periodic solution and disease-lasting conclusion have been obtained. Also, it has been shown that the size of the pulse cycle is an important factor affecting the disease extinction. The SIR epidemic model with nonlinear incidence rate and two class infectious diseases

containing the pulse effect has been studied in [20]. Sufficient conditions of the global attractability of the disease-free periodic solutions have been given. It has confirmed that the system is uniformly persistent under a certain condition. Meanwhile, the time delay, pulse vaccination, and nonlinear incidence play important roles in the nature of the model. The conditions have been proposed to control two kinds of diseases. In [21], the pulse vaccination SIQRS epidemic model with constant input and saturated incidence rate has been addressed. However, it is worth mentioning that the unified model with vertical transmission, constant input, and nonlinear incidence has not been investigated.

In this paper, the cases of constant population input and vertical transmission are considered. Patients who contact susceptible people with saturated incidence way are taken into account. A new impulsive vaccination SEIR epidemic model with time delay and nonlinear incidence rate is established. The sufficient condition is given to guarantee the stability of the disease-free periodic solution and the persistence of the model. Compared to existing results, the main contributions lie in the following aspects: (i) the nonlinear incidence rate is considered in the model to describe the spread of the disease which is more close to reality; (ii) all kinds of infectious diseases have the incubation period, and therefore it is necessary to deal with the phenomenon of time delay; (iii) a unified pulse SEIR epidemic model including the nonlinear contract rate, vertical transmission, and time delays is established. As discussed in [22–24], the study of the pulse epidemic model conducted in this paper has analyzed the trend of the disease in the theoretical aspect which will contribute to making the strategy of the disease prevention.

2. Model Establishment

We consider an SEIR model by assuming that the input term has a constant population, a nonlinear occurrence rate as $\beta S(t)I(t)/(1+mI^h(t))$, and the number of sick of which the sick people who birth to the newborn are $q\mu I(t)$, the time needed which the lurker transfer into the infected people is τ, so after a time τ, the number of survived lurker which into the infected person is

$$\frac{\beta S(t-\tau)I(t-\tau)}{1+mI^h(t-\tau)}e^{-\mu\tau}+q\mu I(t-\tau)e^{-\mu\tau}. \tag{1}$$

The effective coverage of the pulse vaccination needle for the newborn that is not infected is denoted by θ; the vaccination cycle is T. Now we can obtain the following impulsive differential equation model:

$$\begin{aligned}
S'(t) &= A-\frac{\beta S(t)I(t)}{1+mI^h(t)}-\mu S(t)-q\mu I(t),\\
E'(t) &= \frac{\beta S(t)I(t)}{1+mI^h(t)}-\frac{\beta S(t-\tau)I(t-\tau)}{1+mI^h(t-\tau)}e^{-\mu\tau}+q\mu I(t)\\
&\quad -q\mu I(t-\tau)e^{-\mu\tau}-\mu E(t),\\
I'(t) &= \frac{\beta S(t-\tau)I(t-\tau)}{1+mI^h(t-\tau)}e^{-\mu\tau}+q\mu I(t-\tau)e^{-\mu\tau}\\
&\quad -(\mu+\gamma+\alpha)I(t),\\
R'(t) &= \gamma I(t)-\mu R(t), \qquad t\neq nT,\\
S(t^+) &= S(t)-\theta\mu(S(t)+E(t)+R(t))-\theta p\mu I(t),\\
E(t^+) &= E(t),\\
I(t^+) &= I(t),\\
R(t^+) &= R(t)+\theta\mu(S(t)+E(t)+R(t))+\theta p\mu I(t), \qquad t=nT.
\end{aligned} \tag{2}$$

Here, $S(t)$, $E(t)$, $I(t)$, and $R(t)$ represent susceptible, lurker, disease, and cure at time t, respectively; μ represents the birth rate (the birth rate is equal to death rate); β represents the effective contact number; α is the mortality due to illness; γ denotes the cure rate; q $(0<q<1)$ represents the infected people who give birth to the newborn and who are vertically infected into "the kind of latent" at time t; $p=1-q$ is the proportion of infected people who gave birth to newborn who are not vertically infected at time t; θ $(0<\theta<1)$ denotes the succeeded vaccination proportion of newborn for all those who are not infected; A represents input number of the population of constant; τ denotes the time of lurker who become infected people; T is the pulse vaccination cycle; h, m, A, μ, β, and γ are positive constants. In this paper, we consider the property of the model under $S(t)\geq 0$, $E(t)\geq 0$, $I(t)\geq 0$, and $R(t)\geq 0$, and the initial conditions are given as follows:

$$\begin{aligned}
&(\varphi_1(s),\varphi_2(s),\varphi_3(s),\varphi_4(s))\in C\left([-\tau,0],R_+^4\right),\\
&\varphi_i(0)>0 \quad (i=1,2,3,4).
\end{aligned} \tag{3}$$

Letting $N(t)=S(t)+E(t)+I(t)+R(t)$ and according to (2), we have

$$\begin{aligned}
N'(t) &= S'(t)+E'(t)+I'(t)+R'(t)\\
&= A-\mu N(t)-\alpha I(t).
\end{aligned} \tag{4}$$

So (2) can be transformed into the following form:

$$\begin{aligned}
S'(t) &= A-\frac{\beta S(t)I(t)}{1+mI^h(t)}-\mu S(t)-q\mu I(t),\\
E'(t) &= \frac{\beta S(t)I(t)}{1+mI^h(t)}-\frac{\beta S(t-\tau)I(t-\tau)}{1+mI^h(t-\tau)}e^{-\mu\tau}+q\mu I(t)\\
&\quad -q\mu I(t-\tau)e^{-\mu\tau}-\mu E(t),\\
I'(t) &= \frac{\beta S(t-\tau)I(t-\tau)}{1+mI^h(t-\tau)}e^{-\mu\tau}+q\mu I(t-\tau)e^{-\mu\tau}\\
&\quad -(\mu+\gamma+\alpha)I(t),\\
N'(t) &= A-\mu N(t)-\alpha I(t), \qquad t\neq nT,\\
S(t^+) &= S(t)-\theta\mu N(t)+\theta\mu qI(t),\\
E(t^+) &= E(t),\\
I(t^+) &= I(t),\\
N(t^+) &= N(t), \qquad t=nT.
\end{aligned} \tag{5}$$

Noticing $N'(t) \le A - \mu N(t)$ and by the comparison principle, we have $N'(t) \le (A/\mu) + e^{-\mu t}(N(0) - (A/\mu))$ and then we have $\lim_{t\to\infty} N(t) \le (A/\mu)$. Then, all solutions $(S(t), E(t), I(t),$ and $N(t))$ of model (5) eventually enter and remain in the domain $\Omega = \{(S, E, I, N) \in R_+^4 : N \le A/\mu\}$. Therefore, Ω is the positive invariant set of (5).

To proceed, we introduce the following two lemmas which will play important roles in the remaining parts of this paper.

Lemma 1 (see [25]). *Consider the following differential equations with delay:*

$$\begin{aligned} w'(t) &\le (\ge)\, p(t)\, w(t) + q(t), \quad t \ne t_k, \\ w\left(t_k^+\right) &\le (\ge)\, d_k w\left(t_k\right) + b_k, \quad t = t_k,\ k \in N, \end{aligned} \tag{6}$$

where $p(t), q(t) \in C[R_+, R]$, $d_k \ge 0$, and b_k are constants. Assume that

(i) *the sequence $\{t_k\}$ satisfies $0 \le t_1 < t_2$ and $\lim_{t\to\infty} t_k = \infty$;*

(ii) *$w \in PC'[R_+, R]$ and $w(t)$ are left continuous at t_k ($k \in N$), then*

$$\begin{aligned} w(t) \le (\ge)\, & w\left(t_0\right) \prod_{t_0<t_k<t} d_k \exp\left(\int_{t_0}^{t} p(s)\, ds\right) \\ & + \sum_{t_0<t_k<t} \left(\prod_{t_k<t_j<t} d_j \exp\left(\int_{t_k}^{t} p(s)\, ds\right)\right) b_k \\ & + \int_{t_0}^{t} \prod_{s<t_k<t} d_k \exp\left(\int_{s}^{t} p(\theta)\, d\theta\right) q(s)\, ds, \quad t \ge t_0. \end{aligned} \tag{7}$$

Lemma 2 (see [26]). *Considering the following differential equations with delay:*

$$x'(t) = r_1 x(t-\tau) - r_2 x(t), \tag{8}$$

where r_1, r_2, and τ are positive constants, and $x(t) > 0$, one has the following

(i) *if $r_1 < r_2$, then $\lim_{t\to\infty} x(t) = 0$,*

(ii) *if $r_1 > r_2$, then $\lim_{t\to\infty} x(t) = +\infty$,*

for all $t \in [-\tau, 0]$.

3. Main Results

In this section, for model (2), we aim to propose the sufficient conditions to guarantee the existence of the disease-free periodic solutions, the global stability of disease-free periodic solution, and the uniform persistence of the considered model.

3.1. Existence of the Disease-Free Periodic Solutions. Firstly, the analysis result is given to ensure the existence of the disease-free periodic solutions.

Theorem 3. *If $\theta\mu/(1 - e^{-\mu T}) < 1$, (10) has a unique and positive periodic solution $(S^*(t), N^*(t))$. Moreover (5) has a unique disease-free periodic solution $(S^*(t), 0, 0, N^*(t))$.*

Proof. The existence of the disease-free periodic solution means that the number of sick people is zero, that is $I(t) = 0$ for all $t \ge 0$. Thus (5) is transformed into

$$\begin{aligned} S'(t) &= A - \mu S(t), \\ E'(t) &= -\mu E(t), \\ N'(t) &= A - \mu N(t), \\ & t \ne nT, \\ S\left(t^+\right) &= S(t) - \theta\mu N(t), \\ E\left(t^+\right) &= E(t), \\ N\left(t^+\right) &= N(t), \\ & t = nT. \end{aligned} \tag{9}$$

Noticing that $E(t)$ only appears in the second equation of (9), so we only need to consider the first and third equations of (9),

$$\begin{aligned} S'(t) &= A - \mu S(t), \\ N'(t) &= A - \mu N(t), \\ & t \ne nT, \\ S\left(t^+\right) &= S(t) - \theta\mu N(t), \\ N\left(t^+\right) &= N(t), \\ & t = nT. \end{aligned} \tag{10}$$

Let $N(nT)$ and $S(nT)$ represent the initial value of $N(t)$ and $S(t)$, at the time $t = nT$, respectively. For brevity, denote $N_n = N(nT)$, $S_n = S(nT)$. Then, we can be integral in the pulse interval $[nT, (n+1)T]$, respectively, and for the total population and infected people, and we have

$$\begin{aligned} S(t) &= \frac{A}{\mu} - \left(\frac{A}{\mu} - S(nT)\right) e^{-\mu(t-nT)}, \\ N(t) &= \frac{A}{\mu} - \left(\frac{A}{\mu} - N(nT)\right) e^{-\mu(t-nT)}. \end{aligned} \tag{11}$$

According to (11), we have the following stroboscopic map:

$$\begin{pmatrix} S_{n+1} \\ N_{n+1} \end{pmatrix} = \begin{pmatrix} e^{-\mu T} & -\theta\mu \\ 0 & e^{-\mu T} \end{pmatrix} \begin{pmatrix} S_n \\ N_n \end{pmatrix} + \begin{pmatrix} \frac{A}{\mu}\left(1 - e^{-\mu T}\right) \\ \frac{A}{\mu}\left(1 - e^{-\mu T}\right) \end{pmatrix}. \tag{12}$$

The Jacobi matrix of (12) is

$$J = \begin{pmatrix} e^{-\mu T} & -\theta\mu e^{-\mu T} \\ 0 & e^{-\mu T} \end{pmatrix}. \tag{13}$$

The matrix J has the characteristic roots $\lambda_1 = \lambda_2 = e^{-\mu T}$ with $|\lambda_i| = e^{-\mu t} < 1$ $(i = 1, 2)$. If $\theta\mu/(1 - e^{-\mu T}) < 1$, that is, $(A/\mu) - (\theta A/(1 - e^{-\mu T})) > 0$, then map (12) has a unique and positive fixed point (S^*, N^*) with $S^* = (A/\mu) - (\theta A/(1 - e^{-\mu T}))$, $N^* = A/\mu$. Therefore, the periodic solution of (10) is

$$S^*(t) = \begin{cases} \dfrac{A}{\mu} - \dfrac{\theta A}{1 - e^{-\mu T}} e^{-\mu(t - nT)}, & t \neq nT, \\ \dfrac{A}{\mu} - \dfrac{\theta A}{1 - e^{-\mu T}}, & t = nT, \end{cases} \qquad N^*(t) = \frac{A}{\mu}. \tag{14}$$

By using the second and fifth equations of (9), we have $\lim_{t \to \infty} E^*(t) = 0$. Thus the proof of this theorem is complete. □

3.2. Global Stability of Disease-Free Periodic Solution. In this subsection, the global stability of the disease-free periodic solution is discussed and the sufficient condition is given accordingly.

Theorem 4. *If $R_1 = \max\{R_1, \theta\mu/(1 - e^{-\mu t})\} < 1$, then the disease-free periodic solution $(S^*(t), 0, 0, A/\mu)$ of (9) is globally attractive, where*

$$R_1 = \frac{\beta\left((A/\mu) - \left(\theta\mu A/\left(\mu + \alpha\right)\left(1 - e^{-\mu T}\right)\right)\right) + q\mu}{e^{\mu\tau}\left(\gamma + \alpha + \mu\right)}. \tag{15}$$

Proof. By the first and fifth equations of (5) and $N'(t) \geq A - (\mu + \alpha)N(t)$, we have $N(t) \geq A/(\mu + \alpha)$, and then we have

$$\begin{aligned} S'(t) &\leq A - \mu S(t), \quad t \neq nT,\ n \in N \\ S\left(t^+\right) &\leq S(t) - \frac{\theta\mu A}{\mu + \alpha}, \quad t = nT,\ n \in N. \end{aligned} \tag{16}$$

By Lemma 1, we obtain

$$\begin{aligned} S(t) &\leq S\left(0^+\right) \prod_{0<nT<t} e^{\int_0^t -\mu\, ds} + \sum_{0<nT<t} e^{\int_{nT}^t -\mu\, ds} \cdot \left(-\frac{\theta\mu A}{\mu + \alpha}\right) \\ &\quad + \int_0^t \prod_{s<nT<t} e^{\int_s^t -\mu\, d\theta} \cdot A\, ds \\ &\leq S\left(0^+\right) e^{-\mu t} + \left(-\frac{\theta\mu A}{\mu + \alpha}\right) e^{-\mu t} \frac{e^{\mu T}\left(1 - e^{\mu[t/T]T}\right)}{1 - e^{\mu T}} + \overline{\Delta}, \end{aligned} \tag{17}$$

where

$$\begin{aligned} \overline{\Delta} &= \int_0^t \prod_{s<nT<t} e^{\int_s^t -\mu\, d\theta} \cdot A\, ds \\ &= \frac{A}{\mu} e^{-\mu t} \int_0^t \prod_{s<nT<t} e^{\mu s} d\mu s \\ &= \frac{A}{\mu} e^{-\mu t} \int_0^{t/T} \prod_{\xi<n<t/T} e^{\mu T\xi} d\mu T\xi \\ &= \frac{A}{\mu} e^{-\mu t} \left[\int_0^1 \prod_{\xi<n<t/T} e^{\mu T\xi} d\mu T\xi + \int_1^2 \prod_{\xi<n<t/T} e^{\mu T\xi} d\mu T\xi \right. \\ &\qquad \left. + \cdots + \int_{[t/T]}^{t/T} \prod_{\xi<n<t/T} e^{\mu T\xi} d\mu T\xi \right] \\ &= \frac{A}{\mu} e^{-\mu t} \left[\frac{\left(e^{\mu T} - 1\right)\left(1 - e^{\mu T[t/T]}\right)}{1 - e^{\mu T}} + e^{\mu t} - e^{\mu T[t/T]} \right] \\ &= \frac{A}{\mu} - \frac{A}{\mu} e^{-\mu t}. \end{aligned} \tag{18}$$

So

$$\begin{aligned} S(t) &\leq S\left(0^+\right) e^{-\mu t} + \left(-\frac{\theta\mu A}{\mu + \alpha}\right) e^{-\mu t} \frac{e^{\mu T}\left(1 - e^{\mu[t/T]T}\right)}{1 - e^{\mu T}} \\ &\quad + \frac{A}{\mu} - \frac{A}{\mu} e^{-\mu t} \\ &\leq e^{-\mu t}\left[S\left(0^+\right) - \frac{A}{\mu} + \frac{\theta\mu A}{\left(\mu + \alpha\right)\left(1 - e^{-\mu T}\right)}\right] \\ &\quad + \frac{A}{\mu} + \frac{\theta\mu A e^{\mu T([t/T]+1-(t/T))}}{\left(\mu + \alpha\right)\left(e^{\mu T} - 1\right)} \\ &\leq e^{-\mu t}\left[S\left(0^+\right) - \frac{A}{\mu} + \frac{\theta\mu A}{\left(\mu + \alpha\right)\left(1 - e^{-\mu T}\right)}\right] \\ &\quad + \frac{A}{\mu} - \frac{\theta\mu A}{\left(\mu + \alpha\right)\left(1 - e^{-\mu T}\right)}, \end{aligned} \tag{19}$$

that is,

$$\limsup_{t \to \infty} S(t) \leq \frac{A}{\mu} - \frac{\mu\theta A}{\left(\mu + \alpha\right)\left(1 - e^{-\mu T}\right)}. \tag{20}$$

Noticing $\theta\mu/(1 - e^{-\mu T}) < 1$, we have $\theta\mu/(1 - e^{-\mu T}) \cdot \mu/(\mu + \alpha) < 1$. Moreover, we obtain $(A/\mu) - (\mu\theta A/(\mu + \alpha)(1 - e^{-\mu T})) > 0$. Then, for all $\varepsilon > 0$, there exists $n_1 \in N$ such that

$$S(t) \leq \frac{A}{\mu} - \frac{\mu\theta A}{\left(\mu + \alpha\right)\left(1 - e^{-\mu T}\right)} + \varepsilon \triangleq \eta \tag{21}$$

for all $t \geq n_1 T$.

Subsequently, it follows from (21) and the third equation of (5) that

$$\begin{aligned} I'(t) &\le \frac{\beta\eta I(t-\tau)}{1+mI^h(t-\tau)}e^{-\mu\tau} \\ &\quad + q\mu I(t-\tau)e^{-\mu\tau} - (\mu+\alpha+\gamma)I(t) \\ &\le \beta\eta I(t-\tau)e^{-\mu\tau} + q\mu I(t-\tau)e^{-\mu\tau} - (\mu+\alpha+\gamma)I(t) \\ &= e^{-\mu\tau}(\beta\eta+q\mu)I(t-\tau) - (\mu+\alpha+\gamma)I(t) \end{aligned} \tag{22}$$

for $\forall t > n_1T + \tau$.

Consider the comparison system of (22)

$$z'(t) = e^{-\mu\tau}(\beta\eta+q\mu)z(t-\tau) - (\mu+\alpha+\gamma)z(t). \tag{23}$$

Due to $R_1 < 1+\varepsilon$, the following inequalities hold:

$$\begin{aligned} &e^{-\mu\tau}\left[\beta\left(\frac{A}{\mu} - \frac{\theta\mu A}{(\mu+\alpha)(1-e^{-\mu T})} + \varepsilon\right) + q\mu\right] \\ &\quad - (\gamma+\alpha+\mu) < 0, \\ &\quad e^{-\mu\tau}(\beta\eta+q\mu) < (\gamma+\alpha+\mu) \end{aligned} \tag{24}$$

for $\forall\varepsilon > 0$. By Lemma 2, we have $\lim_{t\to\infty} z(t) = 0$. Note that $I(s) = z(s) = \varphi_2(s) > 0$ for all $s \in [-\tau, 0]$. Then, according to the comparison theorem of differential equation, one gets $\lim_{t\to\infty} I(t) = 0$.

Without loss of generality, assuming that there exists $t_0 > 0$, we have $0 < I(t) < \varepsilon < A/\alpha$ for all $t \ge t_0$. By the first and the fifth equations of (5), we have

$$\begin{aligned} S'(t) &\ge (A - q\mu\varepsilon) - (\beta\varepsilon+\mu)S(t), \quad t \ne nT,\ n \in N, \\ S(t^+) &\ge S(t) - \theta A, \quad t = nT,\ n \in N. \end{aligned} \tag{25}$$

Considering the comparison systems of (25),

$$\begin{aligned} z_1'(t) &= (A - q\mu\varepsilon) - (\beta\varepsilon+\mu)z_1(t), \\ &\qquad t \ne nT,\ n \in N, \\ z_1(t^+) &= z_1(t) - \theta A, \quad t = nT,\ n \in N, \\ z_1(0^+) &= S(0^+) \end{aligned} \tag{26}$$

when $nT < t \le (n+1)T$, we obtain

$$z_1^*(t) = \begin{cases} \dfrac{A - q\mu\varepsilon}{\beta\varepsilon+\mu} - \dfrac{\theta A}{1-e^{-(\beta\varepsilon+\mu)T}}e^{-(\beta\varepsilon+\mu)(t-nT)}, & t \ne nT \\ \dfrac{A - q\mu\varepsilon}{\beta\varepsilon+\mu} - \dfrac{\theta A}{1-e^{-(\beta\varepsilon+\mu)T}}, & t = nT, \end{cases} \tag{27}$$

where

$$\lim_{\varepsilon\to 0} z_1^*(t) = S^*(t). \tag{28}$$

By the comparison theorem of impulsive differential equation, for $\forall\varepsilon_1 > 0$, there exists $T_1 > t_0$, when $t > T_1$, and we obtain

$$S(t) > z_1^*(t) - \varepsilon_1 \tag{29}$$

for all $t > T_1$. As $A - \mu N - \alpha\varepsilon \le N'(t)$, $t \ge t_0$, $N(t) \ge (A - \alpha\varepsilon)/\mu > 0$. Then due to the first and the fifth equations of (5), we obtain

$$\begin{aligned} S'(t) &\le A - \mu S(t), \quad t \ne nT,\ n \in N, \\ S(t^+) &\le S(t) - \theta A + (\alpha+\mu q)\theta\varepsilon, \quad t = nT,\ n \in N. \end{aligned} \tag{30}$$

Considering the comparison systems of (30),

$$\begin{aligned} z_2'(t) &= A - \mu z_2(t), \quad t \ne nT,\ n \in N, \\ z_2(t^+) &= z_2(t) - \theta A + (\alpha+\mu q)\theta\varepsilon, \quad t = nT,\ n \in N, \\ z_2(0^+) &= S(0^+), \end{aligned} \tag{31}$$

we have

$$z_2^*(t) = \begin{cases} \dfrac{A}{\mu} - \dfrac{\theta A - (\alpha+\mu q)\theta\varepsilon}{1-e^{-\mu T}}e^{-\mu(t-nT)}, & t \ne nT \\ \dfrac{A}{\mu} - \dfrac{\theta A - (\alpha+\mu q)\theta\varepsilon}{1-e^{-\mu T}}, & t = nT \end{cases} \tag{32}$$

when $nT < t \le (n+1)T$.

Similarly, for $\forall\varepsilon_1 > 0$, there exists $T_2 > t_0$ such that

$$S(t) < \overline{z_2}(t) + \varepsilon_1 \tag{33}$$

for $t > T_2$. Denote $\overline{T} = \max\{T_1, T_2\}$. When $t > \overline{T}$, let $\varepsilon_1 \to 0$. Then it follows from (29) and (33) that $S^*(t) - \varepsilon_1 < S(t) < S^*(t) + \varepsilon_1$, that is,

$$\lim_{t\to\infty} S(t) = S^*(t). \tag{34}$$

By substituting $I(t) = 0$ into (5), we have $\lim_{t\to\infty} E(t) = 0$, $\lim_{t\to\infty} N(t) = A/\mu$. Then, the proof of this theorem is complete. □

3.3. Uniform Persistence of the Model. In this subsection, the definition of the uniform persistence is first given. Then the sufficient condition is proposed to ensure the uniform persistence of the addressed model.

Definition 5. If there exists a compact set $D \subset \Omega$, such that (2) at any periodic solution enters into D and finally remains D under the initial condition of (3), then (2) is uniformly persistent.

According to the above definition, we aim to present the analysis result about the uniform persistence for model (2).

Theorem 6. *If* $R_2 = \min\{R_2, R_3, R_4\} > 1$ *then the* (2) *is uniformly persistent, where*

$$R_2 = \frac{(A+q\mu)\left(1-e^{-\mu T}\right)+\theta A(\mu+\beta)-\left(1+m\delta^h\right)(\alpha+\gamma+\xi)}{q\mu\left(1-e^{-\mu T}\right)+\theta A\beta},$$
$$R_3 = \frac{(1-q)\left(1-e^{-(\delta\beta+\mu)T}\right)}{(\delta\beta+\mu)\theta},$$
$$\delta = \frac{A}{\mu}, \qquad \xi = \mu\left(1-qe^{-\mu\tau}\right). \tag{35}$$

Proof. It follows from Ω that, we obtain $N(t) \le A/\mu = \delta$, then the solutions of (2) have upper bound. So we only need to consider the lower bound solution of (2).

First, we show the existence of a lower bound for $I(t)$. The third equation of (2) transforms the form as follows:

$$I'(t) = \left[\frac{\beta S(t)}{1+mI^h(t)}e^{-\mu\tau} - (\alpha+\gamma+\xi)\right] I(t) - e^{-\mu\tau}\frac{d}{dt}\int_{t-\tau}^{t}\left(\frac{\beta S(\theta)}{1+mI^h(\theta)}+q\mu\right) I(\theta)\,d\theta. \tag{36}$$

Construct $V(t) = I(t) + e^{-\mu\tau}\int_{t-\tau}^{t}((\beta S(\theta)/(1+mI^h(\theta))) + q\mu)I(\theta)d\theta$. So $V(t)$ is a bounded function. Along the solution of (2), we have

$$\begin{aligned} V'(t) &= I'(t) + e^{-\mu\tau}\frac{d}{dt}\int_{t-\tau}^{t}\left(\frac{\beta S(\theta)}{1+mI^h(\theta)}+q\mu\right) I(\theta)\,d\theta \\ &= (\alpha+\gamma+\xi)\left[\frac{\beta S(t)}{1+mI^h(t)}e^{-\mu\tau}\cdot\frac{1}{\alpha+\gamma+\xi}-1\right] I(t). \end{aligned} \tag{37}$$

By $R_2 > 1$, there exists $m_2^* = R_2 - 1 > 0$ satisfying

$$m_2^* = \frac{\beta e^{-\mu\tau}A\left[1-e^{-\mu T}-\theta\mu\right]-\left(1+m\delta^h\right)(\alpha+\gamma+\xi)}{\left[\left(1-e^{-\mu T}\right)q\mu+\theta A\beta\right]\beta e^{-\mu\tau}} > 0. \tag{38}$$

Then, we have

$$\frac{\beta e^{-\mu\tau}}{(1+m\delta^h)(\alpha+\gamma+\xi)}\left[\frac{A-q\mu m_2^*}{\beta m_2^*+\mu}-\frac{\theta A}{1-e^{-\mu T}}\right] = 1. \tag{39}$$

Subsequently, there exists $\varepsilon_1 > 0$, such that

$$\frac{\beta e^{-\mu\tau}}{(1+m\delta^h)(\alpha+\gamma+\xi)}\left[\frac{A-q\mu m_2^*}{\beta m_2^*+\mu}-\frac{\theta A}{1-e^{-(\beta m_2^*+\mu)T}}-\varepsilon_1\right] > 1. \tag{40}$$

So

$$\frac{\beta e^{-\mu\tau}}{(1+m\delta^h)(\alpha+\gamma+\xi)}\Delta > 1, \tag{41}$$

where

$$\Delta = \frac{A-q\mu m_2^*}{\beta m_2^*+\mu}-\frac{\theta A}{1-e^{-(\beta m_2^*+\mu)T}}-\varepsilon_1. \tag{42}$$

Now we prove that $I(t) \le m_2^*$ is not true. Otherwise, assume that there exists $t_0 > 0$, and when $t > t_0$, there is $I(t) < m_2^*$. By using the first and the fifth equations of (2), we have

$$\begin{aligned} S'(t) &\ge (A-q\mu m_2^*) - (\beta m_2^*+\mu)S(t), \\ &\qquad t \ne nT,\ n \in N, \\ S(t) &\ge S(t) - \theta A, \quad t = nT,\ n \in N. \end{aligned} \tag{43}$$

By Lemma 1, there exists $T_1 \ge t_0 + \tau$, and we have

$$S(t) > \frac{A-q\mu m_2^*}{\beta m_2^*+\mu}-\frac{\theta A}{1-e^{-(\beta m_2^*+\mu)T}}-\varepsilon_1 \triangleq \Delta \tag{44}$$

for $t > T_1$. Together with (37) and (44), one gets

$$V'(t) > (\gamma+\xi)\left[\frac{\beta e^{-\mu\tau}}{(1+m\delta^h)(\alpha+\gamma+\xi)}\cdot\Delta-1\right] I(t). \tag{45}$$

Denote $I^l = \min_{t\in[T_1,T_1+\tau]} I(t)$. Then $t \ge T_1 > t_0$, that is, $I(t) \ge I^l$. Otherwise there exists $T_2 > 0$, such that $t \in [T_1, T_1+\tau+T_2]$. Then there are $I(t) \ge I^l$, $I(T_1+\tau+T_2) = I^l$, and $I'(T_1+\tau+T_2) \le 0$. It follows from the second equation of (2) and (41) that

$$\begin{aligned} &I'(T_1+\tau+T_2) \\ &\quad \ge (\alpha+\gamma+\xi)\left[\frac{\beta e^{-\mu\tau}}{(1+m\delta^h)(\alpha+\gamma+\xi)}\Delta-1\right] I^l > 0, \end{aligned} \tag{46}$$

which is a contradiction. So, for $t \ge T_1$, according to (36), $I(t) \ge I^l$, $V'(t) > 0$, that is $\lim_{t\to\infty} V(t) = +\infty$. This is, a contradiction of which $V(t)$ is bounded. So when $t > t_0$, $I(t) < m_2^*$ is not tenable.

Two cases to prove are given as follows.

Case 1. If, for t which is sufficiently large, $I(t) \ge m_2^*$, hence the statements are proved.

Case 2. If $I(t)$ is shocked near m_2^*, let $m_2 = \min\{m_2^*/2, m_2^* e^{-(\alpha+\gamma+\mu)\tau}\}$. There exists two constants: $\bar{t}$ and ϖ satisfying $I(\bar{t}) = I(\bar{t}+\varpi) = m_2^*$, and when $\bar{t} < t < \bar{t}+\varpi$, there is $I(t) < m_2^*$. Because $I(t)$ is a continuous and bounded function which is not affected by pulse, then $I(t)$is uniformly continuous. So, there exists $0 < T_3 < \tau$ (T_3 depends on the selection of $\bar{t}$), met for all $\bar{t} < t < \bar{t}+T_3$, and there is $I(t) > m_2^*/2$. If $\varpi < T_3$. The conclusion was established. If $T_3 < \varpi < \tau$, then, by the second equation of (5) that we have when $\bar{t} < t < \bar{t}+\varpi$, $I'(t) \ge -(\alpha+\gamma+\mu)I(t)$; again by $I(\bar{t}) = m_2^*$, there is $I(t) \ge m_2^* e^{-(\alpha+\gamma+\mu)\tau}$, and obviously $I(t) \ge m_2$ is established. Similarly, if $\varpi \ge \tau$, then, by the second equation of (5), when $\bar{t} < t < \bar{t}+\tau$, $I(t) \ge m_2$. Then proof is as follows, when

$\bar{t}+\tau \le t \le \bar{t}+\varpi$, and there is still $I(t) \ge m_2$. If not, there exists $\overline{T} \ge 0$, when $\bar{t} \le t \le \bar{t}+\tau+\overline{T}$, and there are $I(t) \ge m_2$, $I(\bar{t}+\tau+\overline{T}) = m_2$, and $I'(\bar{t}+\tau+\overline{T}) \le 0$. It follows from the second equation of (2) that

$$I'\left(\bar{t}+\tau+\overline{T}\right) \ge \left[\frac{\beta e^{-\mu\tau}}{\left(1+m\delta^h\right)\left(\alpha+\gamma+\xi\right)}\Delta - 1\right] m_2 > 0. \tag{47}$$

It is a contradiction. So when $\bar{t} < t < \bar{t}+\varpi$, there is $I(t) \ge m_2$.

Above all, any positive periodic solution of (2) which for sufficiently large t, it can be concluded that $I(t) \ge m_2$.

It follows from the first and the fifth equations of (2) that

$$\begin{aligned} S'(t) &\ge (1-q)A - (\delta\beta+\mu)S(t), \quad t \ne nT,\ n \in N, \\ S\left(t^+\right) &\ge S(t) - \theta A, \quad t = nT,\ n \in N. \end{aligned} \tag{48}$$

It follows from Lemma 1 that

$$\begin{aligned} S(t) \ge e^{-(\delta\beta+\mu)t}&\left[S\left(0^+\right) - \frac{(1-q)A}{\delta\beta+\mu} + \frac{\theta A}{1-e^{-(\delta\beta+\mu)T}}\right] \\ &+ \frac{(1-q)A}{\delta\beta+\mu} - \frac{\theta A e^{(\delta\beta+\mu)(T[t/T]+T-t)}}{e^{(\delta\beta+\mu)T}-1}. \end{aligned} \tag{49}$$

Since $0 < T[t/T] + T - t < T$, so

$$\begin{aligned} S(t) \ge e^{-(\delta\beta+\mu)t}&\left[S\left(0^+\right) - \frac{(1-q)A}{\delta\beta+\mu} + \frac{\theta A}{1-e^{-(\delta\beta+\mu)T}}\right] \\ &+ \frac{(1-q)A}{\delta\beta+\mu} - \frac{\theta A}{1-e^{-(\delta\beta+\mu)T}}. \end{aligned} \tag{50}$$

Thus $\lim_{t\to\infty} S(t) \ge A[((1-q)/(\delta\beta+\mu)) - (\theta/(1-e^{-(\delta\beta+\mu)T}))]$; it follows from $R_3 > 1$ that $((1-q)/(\delta\beta+\mu)) - (\theta/(1-e^{-(\delta\beta+\mu)T})) > 0$, that is; for $\forall\varepsilon > 0$, there exists $T_4 > 0$, when $t > T_4$, and there is

$$S(t) \ge A\left[\frac{1-q}{\delta\beta+\mu} - \frac{\theta}{1-e^{-(\delta\beta+\mu)T}}\right] - \varepsilon \triangleq m_1. \tag{51}$$

Because of the second equation of (2)

$$\begin{aligned} E(t) &= \int_{t-\tau}^{t} \frac{\beta S(u) I(u)}{1+mI^h(u)} e^{-\mu(t-u)} du + \int_{t-\tau}^{t} q\mu I(u) e^{-\mu(t-u)} du \\ &\ge \left(\frac{\beta m_1 m_2}{\mu\left(1+m\delta^h\right)} + q m_2\right)\left(1-e^{-\mu\tau}\right) \triangleq m_3. \end{aligned} \tag{52}$$

Subsequently, it follows from the fourth equation of (2) that

$$R'(t) \ge r m_2 - \mu R(t). \tag{53}$$

Similarly, there is $R(t) \ge r m_2/\mu \triangleq m_4$ satisfying

$$\begin{aligned} \overline{D} = \{(S,E,I,R) \mid\ & m_1 \le S(t) \le \delta, m_2 \le I(t) \le \delta, \\ & m_3 \le E(t) \le \delta, m_4 \le R(t) \le \delta\}. \end{aligned} \tag{54}$$

Then, $\overline{D}$ is a bounded compact set, nontrivial for any cycle solution of (2) to enter and stay in $\overline{D}$ inside. Hence, it completes the proof of this theorem. □

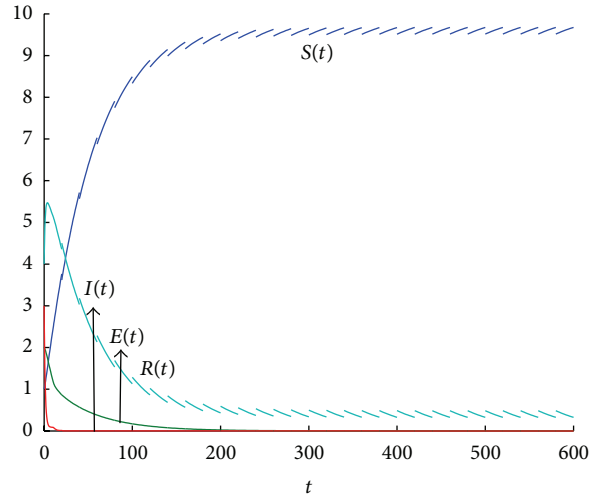

Figure 1: The global attractability of disease-free periodic solution.

Remark 7. Up till now, we investigate the delay epidemic model with vertical transmission, constant input and nonlinear incidence. The sufficient conditions are given to guarantee the existence of the disease-free periodic solutions, the global stability of disease-free periodic solution, and the uniform persistence of the considered model. It is worth mentioning that, according to the statistics of the suspected patients and patients and using the data identification approach, the parameters in the model can be determined when the disease outbreaks. Subsequently, the illness trend of the epidemic can be predicted. Hence, we can make the reasonable control measures. One of the future research directions would be to apply the developed results to make the control strategy by properly considering the real information on the epidemic data.

4. A Numerical Simulation

For comparisons, we consider the following five cases.

Case 1. Let the parameters be specified as certain fixed values in (2): $A = 0.2$, $\mu = 0.02$, $\beta = 0.05$, $q = 0.8$, $\gamma = 0.5$, $\alpha = 0.3$, $\theta = 0.8$, $\tau = 10$, $T = 20$, and $m = h = 1$; then the result $R_1 = \max\{0.5137, 0.04853\} < 1$ is obtained after calculation. By Theorem 4, we know that the disease-free periodic solution of (2) is globally attractive. Setting the initial value $S(0) = 1$, $E(0) = 2$, $I(0) = 3$, and $R(0) = 4$, the numerical simulation of the diagram is shown in Figure 1.

Case 2. Take the following parameters: $\tau = 1$, $\alpha = 0.01$, $A = 0.5$, $\beta = 0.12$, $\mu = 0.1$, $q = 0.8$, $m = 0.02$, $h = 0.8$, $\gamma = 0.06$, $T = 10$, $p = 1-q$, and $\theta = 0.1$; we calculate that $R_2 = \min\{5.2830, 2.8545\} > 1$. By Theorem 6, (2) is uniform persistence. Letting the initial $S(0) = 0.5$, $E(0) = 1$, $I(0) = 1.5$, $R(0) = 2$, the numerical simulation of (2) is shown in Figure 2.

Case 3. The parameter of (2) is the same as that in Figure 1 except for parameter β. Taking $\beta = 0.08$, we have

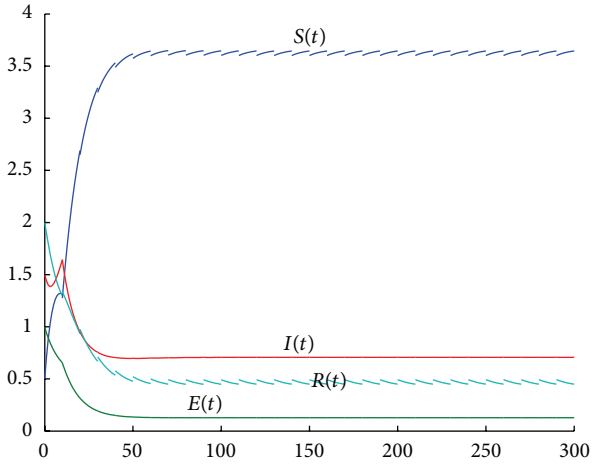

Figure 2: The uniform persistence of disease when $\beta = 0.12, q = 0.8$, and $\theta = 0.1$.

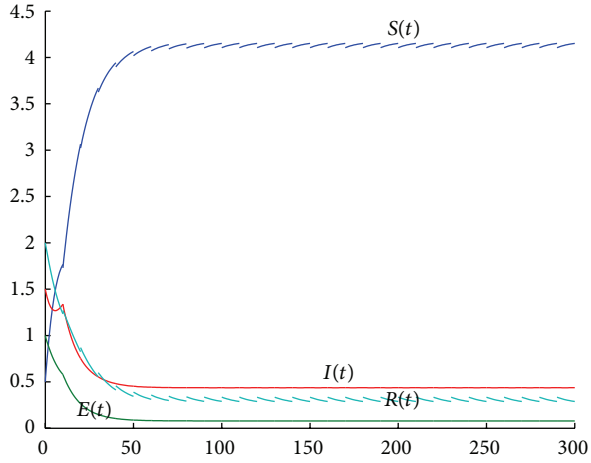

Figure 3: The uniform persistence of disease when $\beta = 0.08$.

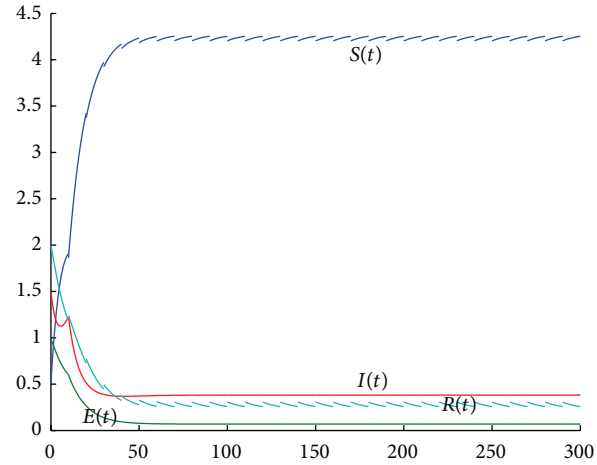

Figure 4: The uniform persistence of disease when $q = 0.1$.

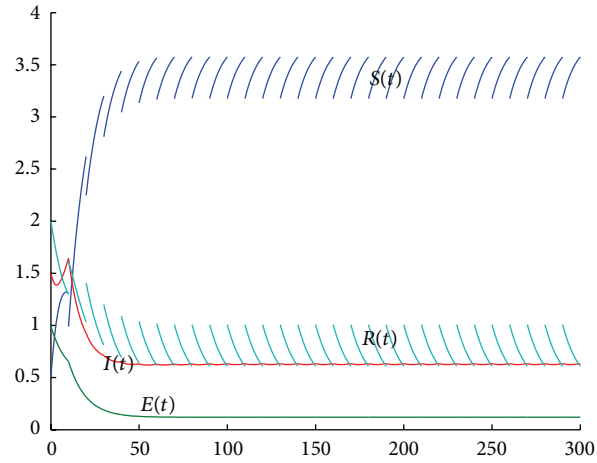

Figure 5: The uniform persistence of disease when $\theta = 0.9$.

$R_2 = \min\{5.4400, 3.9730\} > 1$. Then, by Theorem 6, (2) is of uniform persistence. The corresponding numerical simulation of (2) is shown in Figure 3.

Case 4. If the parameter of (2) is the same as in Figure 1 except q. Taking $q = 0.1$, we obtain $R_2 = \min\{20.1653, 12.8454\} > 1$. By Theorem 6, (2) is of uniform persistence. Accordingly, the simulation of (2) is shown in Figure 4.

Case 5. If the parameter of (2) is the same as in Figure 1 except θ. Taking $\theta = 0.9$, we have $R_2 = \min\{4.9835, 1.2496\} > 1$. By Theorem 6, (2) is of uniform persistence. The numerical simulation of (2) is shown in Figure 5.

It can be seen that $I(t)$ is more influenced by the change of β, p but is less influenced by the change of θ.

By Figures 2 and 3, we can see that when the contact rate is smaller, the numbers of lurker and infective are reduced, but the numbers of susceptible and removed accordingly changed much. Also, there is a proportional relationship between the size of the extent of epidemic and the contact rate. By comparing Figures 2 and 4, when the vertical transmission rate is bigger, the number of infective is increased by controlling the vertical transmission rate of infected newborn. Moreover, by comparing Figures 2 and 5, the increase of vaccination rate has a certain effect for the control of the disease, but it is not obvious. Therefore, if we reduce the extent of the epidemic, the measure of one is reducing the contact rate and vertical transmission rate. From the simulation the feasibility and usefulness of the proposed main results are confirmed.

5. Conclusions

In this paper, we have discussed the SEIR model with the pulse vaccination, the constant input item of population, and the vertical transmission. By employing the impulsive differential inequality and the stroboscopic map, the existence conditions of the disease-free periodic solution of the model have been given. Also, the sufficient conditions of globally attractive and uniform persistence have been proposed. Finally, a numerical example has been given to illustrate the

validity of the proposed results. One of our future research interests is to extend the main results of the analysis and synthesis of gene regulatory networks or complex dynamical systems as discussed in [27–32].

Acknowledgments

This work was supported in part by the National Natural Science Foundation of Heilongjiang Province under Grant no. A200502 and the Foundation of Educational Commission of Heilongjiang Province under Grant no. 12521099.

References

[1] V. D. Mil'man and A. D. Myškis, "On the stability of motion in the presence of impulses," *Sibirskii Matematicheskii Journal*, vol. 1, no. 2, pp. 233–237, 1960 (Russian).

[2] A. N. Perestyuk and A. M. Samoilenko, "Stability of solutions of differential equations with impulse effect," *Different Equation*, vol. 13, no. 1, pp. 1981–1992, 1977.

[3] Z. Agur, L. Cojocaru, G. Mazor, R. M. Anderson, and Y. L. Danon, "Pulse mass measles vaccination across age cohorts," *Proceedings of the National Academy of Sciences of the United States of America*, vol. 90, no. 24, pp. 11698–11702, 1993.

[4] S. Gao, L. Chen, and Z. Teng, "Impulsive vaccination of an SEIRS model with time delay and varying total population size," *Bulletin of Mathematical Biology*, vol. 69, no. 2, pp. 731–745, 2007.

[5] H. Liu, J. Yu, and G. Zhu, "Global asymptotic stable eradication for the SIV epidemic model with impulsive vaccination and infection-age," *Journal of Systems Science & Complexity*, vol. 19, no. 3, pp. 393–402, 2006.

[6] A. d'Onofrio, "Mixed pulse vaccination strategy in epidemic model with realistically distributed infectious and latent times," *Applied Mathematics and Computation*, vol. 151, no. 1, pp. 181–187, 2004.

[7] X.-Z. Meng, L.-S. Chen, and Z.-T. Song, "Global dynamics behaviors for new delay SEIR epidemic disease model with vertical transmission and pulse vaccination," *Applied Mathematics and Mechanics (English Edition)*, vol. 28, no. 9, pp. 1259–1271, 2007.

[8] A. d'Onofrio, "Stability properties of pulse vaccination strategy in SEIR epidemic model," *Mathematical Biosciences*, vol. 179, no. 1, pp. 57–72, 2002.

[9] J. Hu, Z. Wang, B. Shen, and H. Gao, "Gain-constrained recursive filtering with stochastic nonlinearities and probabilistic sensor delays," *IEEE Transactions on Signal Processing*, vol. 61, no. 5, pp. 1230–1238, 2013.

[10] J. Hu, Z. Wang, H. Gao, and L. K. Stergioulas, "Robust sliding mode control for discrete stochastic systems with mixed time delays, randomly occurring uncertainties, and randomly occurring nonlinearities," *IEEE Transactions on Industrial Electronics*, vol. 59, no. 7, pp. 3008–3015, 2012.

[11] J. Hu, Z. Wang, Y. Niu, and L. K. Stergioulas, "H_∞ sliding mode observer design for a class of nonlinear discrete time-delay systems: a delay-fractioning approach," *International Journal of Robust and Nonlinear Control*, vol. 22, no. 16, pp. 1806–1826, 2012.

[12] J. Hu, Z. Wang, H. Gao, and L. K. Stergioulas, "Robust H_∞ sliding mode control for discrete time-delay systems with stochastic nonlinearities," *Journal of the Franklin Institute*, vol. 349, no. 4, pp. 1459–1479, 2012.

[13] X.-B. Zhang, H.-F. Huo, X.-K. Sun, and Q. Fu, "The differential susceptibility SIR epidemic model with time delay and pulse vaccination," *Journal of Applied Mathematics and Computing*, vol. 34, no. 1-2, pp. 287–298, 2010.

[14] Y. Du and R. Xu, "A delayed SIR epidemic model with nonlinear incidence rate and pulse vaccination," *Journal of Applied Mathematics & Informatics*, vol. 28, no. 5-6, pp. 1089–1099, 2010.

[15] Z. Zhao, Z. Li, and L. Chen, "Existence and global stability of periodic solution for impulsive predator-prey model with diffusion and distributed delay," *Journal of Applied Mathematics and Computing*, vol. 33, no. 1-2, pp. 389–410, 2010.

[16] C. Huang and X. An, "An impulsive vaccination SEIRS epidemic model with multi-delay a nonlinear incidence rate," *Journal of Lanzhou University of Technology*, vol. 37, no. 1, pp. 121–125, 2011.

[17] Y. Du and R. Xu, "Pulse vaccination of a SEIRS epidemic model with time delays a nonlinear incidence rate," *Journal of Beihua University (Natural Science)*, vol. 12, no. 3, pp. 258–264, 2011.

[18] S. J. Gao and Z. D. Teng, "Impulsive vaccination of an SIRS model with saturation infectious force and constant recruitment," *Journal of Biomathematics*, vol. 23, no. 2, pp. 209–217, 2008.

[19] C. Wei and L. Chen, "A delayed epidemic model with pulse vaccination," *Discrete Dynamics in Nature and Society*, vol. 2008, Article ID 746951, 12 pages, 2008.

[20] X. Meng, Z. Li, and X. Wang, "Dynamics of a novel nonlinear SIR model with double epidemic hypothesis and impulsive effects," *Nonlinear Dynamics*, vol. 59, no. 3, pp. 503–513, 2010.

[21] W. J. Xu, "The SIQRS epidemic model of impulsive vaccination with constant input and saturation incidence rate," *Journal of Systems Science and Mathematical Sciences*, vol. 30, no. 1, pp. 43–52, 2010.

[22] X.-Z. Meng, L.-S. Chen, and Z.-T. Song, "Global dynamics behaviors for new delay SEIR epidemic disease model with vertical transmission and pulse vaccination," *Applied Mathematics and Mechanics (English Edition)*, vol. 28, no. 9, pp. 1259–1271, 2007.

[23] Y. Z. Pei, S. Y. Liu, C. G. Li, and S. J. Gao, "A pulse vaccination epidemic model with multi-delay and vertical transmission," *Chinese Annals of Mathematics A*, vol. 30, no. 5, pp. 669–676, 2009.

[24] J. Zhu, W. Li, and L. Zhu, "An SIR epidemic model with birth pulse and pulse vaccination," *Journal of Biomathematics*, vol. 26, no. 3, pp. 490–496, 2011.

[25] V. Lakshmikantham, D. D. Baĭnov, and P. S. Simeonov, *Theory of Impulsive Differential Equations*, World Scientific Publishing, River Edge, NJ, USA, 1989.

[26] K. Yang, *Delay Differential Equations with Applications in Population Dynamics*, Academic Press, San Diego, Calif, USA, 1993.

[27] J. Hu, Z. Wang, H. Gao, and L. K. Stergioulas, "Extended Kalman filtering with stochastic nonlinearities and multiple missing measurements," *Automatica*, vol. 48, no. 9, pp. 2007–2015, 2012.

[28] Z. Wang, H. Wu, J. Liang, and X. Liu, "On modeling and state estimation for genetic regulatory networks with polytopic uncertainties," *IEEE Transactions on NanoBioscience*, vol. 12, no. 1, pp. 13–20, 2013.

[29] J. Hu, Z. Wang, H. Gao, and L. K. Stergioulas, "Probability-guaranteed H_∞ finite-horizon filtering for a class of nonlinear time-varying systems with sensor saturations," *Systems & Control Letters*, vol. 61, no. 4, pp. 477–484, 2012.

[30] Z. Wang, Y. Wang, and Y. Liu, "Global synchronization for discrete-time stochastic complex networks with randomly occurred nonlinearities and mixed time delays," *IEEE Transactions on Neural Networks*, vol. 21, no. 1, pp. 11–25, 2010.

[31] J. Hu, Z. Wang, B. Shen, and H. Gao, "Quantised recursive filtering for a class of nonlinear systems with multiplicative noises and missing measurements," *International Journal of Control*, vol. 86, no. 4, pp. 650–663, 2013.

[32] Z. Wang, X. Liu, Y. Liu, J. Liang, and V. Vinciotti, "An extended kalman filtering approach to modeling nonlinear dynamic gene regulatory networks via short gene expression time series," *IEEE/ACM Transactions on Computational Biology and Bioinformatics*, vol. 6, no. 3, pp. 410–419, 2009.

Hindawi Publishing Corporation
Mathematical Problems in Engineering
Volume 2013, Article ID 458047, 7 pages
http://dx.doi.org/10.1155/2013/458047

Research Article

The Method of Lyapunov Function and Exponential Stability of Impulsive Delay Systems with Delayed Impulses

Pei Cheng,[1] Feiqi Deng,[2] and Lianglong Wang[1]

[1] *School of Mathematical Sciences, Anhui University, Hefei 230601, China*
[2] *Systems Engineering Institute, South China University of Technology, Guangzhou 510640, China*

Correspondence should be addressed to Pei Cheng; chengpei_pi@163.com

Received 4 September 2013; Revised 5 November 2013; Accepted 5 November 2013

Academic Editor: Bo Shen

This paper investigates the exponential stability of general impulsive delay systems with delayed impulses. By using the Lyapunov function method, some Lyapunov-based sufficient conditions for exponential stability are derived, which are more convenient to be applied than those Razumikhin-type conditions in the literature. Their applications to linear impulsive systems with time-varying delays are also proposed, and a set of sufficient conditions for exponential stability is provided in terms of matrix inequalities. Meanwhile, two examples are discussed to illustrate the effectiveness and advantages of the results obtained.

1. Introduction

Impulsive dynamical systems have received considerable attention during the recent decades since they provide a natural framework for mathematical modeling of many real-world evolutionary processes where the states undergo abrupt changes at certain instants (see, e.g., [1–4]). On the other hand, time delays often appear in practical systems and may poorly affect the performance of a system. Stability and stabilization of such systems are of both theoretical and practical importance. Therefore, the study of time-delay systems has attracted great attention over the past few years (see, e.g., [5–10]). An area of particular interest has been the stability analysis and stabilization of impulsive delay systems (IDSs), and there is extensive literature on this field (see, e.g., [11–26]). For instance, in [11–14], the robust stability for uncertain impulsive system with time-delay was studied, and the linear matrix inequalities approach to the stability was presented. In [15–26], the Lyapunov function or Lyapunov functional coupled with the Razumikhin techniques was suggested for the exponential stability and asymptotical stability of IDSs.

In the previous works on stability and stabilization of IDSs, the impulses are assumed to take the form of $\Delta x(t_k) = I_k(t_k, x(t_k^-))$, which indicates that the state "jump" at impulse times t_k is only related to the present state variables (see, e.g., [18–26]). But, in most cases, it is more applicable that the state variables on the impulses are also related to the past states. For example, in the transmission of the impulse information, input delays are often encountered. So, compared with the nondelayed impulses described above, it is much more meaningful to model the impulses as

$$\Delta x\left(t_k\right) = I_k\left(t_k, x\left(t_k^-\right)\right) + J_k\left(t_k, x_{t_k^-}\right). \tag{1}$$

In fact, there have been several attempts in the literature to study the stability and control problems of a particular class of delayed impulsive systems [27, 28]. For example, Lian et al. [27] investigated the optimal control problem of linear continuous-time systems possessing delayed discrete-time controllers in networked control systems. For nonlinear impulsive systems, Khadra et al. [28] studied the impulsive synchronization problem coupled by linear delayed impulses. By using the Razumikhin techniques, some sufficient conditions for asymptotic stability and exponential stability of general IDS-DI were established in [29–32], and sufficient conditions for exponential stability of impulsive stochastic functional differential systems with delayed impulses were obtained in [33].

In this paper, we will further investigate the stability of IDS-DI. By using the Lyapunov functions, some sufficient conditions ensuring exponential stability of IDS-DI are derived, which are more convenient to be applied than those Razumikhin-type conditions in [31, 32]. Their applications to linear impulsive systems with time-varying delays are also proposed, and a set of sufficient conditions for exponential stability are derived in terms of matrix inequalities.

2. Preliminaries

Let $\mathbb{R}$ denote the set of real numbers, $\mathbb{R}_+$ the set of nonnegative real numbers, $\mathbb{Z}_+$ the set of positive integers, and $\mathbb{R}^n$ the n-dimensional real space equipped with the Euclidean norm $|\cdot|$. Let $\tau > 0$, and let $PC([-\tau, 0]; \mathbb{R}^n) = \{\varphi : [-\tau, 0] \to \mathbb{R}^n \mid \varphi(t^+) = \varphi(t)$ for all $t \in [-\tau, 0)$, $\varphi(t^-)$ exists and $\varphi(t^-) = \varphi(t)$ for all but at most a finite number of points $t \in (-\tau, 0]\}$ be with the norm $\|\varphi\| = \sup_{-\tau \leqslant \theta \leqslant 0} |\varphi(\theta)|$, where $\varphi(t^+)$ and $\varphi(t^-)$ denote the right-hand and left-hand limits of function $\varphi(t)$ at t respectively.

Consider the IDS-DI described by the state equations

$$\begin{aligned} \dot{x}(t) &= f(t, x_t), \quad t \neq t_k,\ t \geqslant t_0, \\ \Delta x(t_k) &= I_k\left(t_k, x\left(t_k^-\right)\right) + J_k\left(t_k, x_{t_k^-}\right), \quad k \in \mathbb{Z}_+, \\ x_{t_0} &= \phi(s), \quad s \in [-\tau, 0], \end{aligned} \tag{2}$$

where $x \in \mathbb{R}^n$, $f : \mathbb{R}_+ \times \mathbb{C} \to \mathbb{R}^n$, $I_k : \mathbb{R}_+ \times \mathbb{R}^n \to \mathbb{R}^n$, $J_k : \mathbb{R}_+ \times \mathbb{C} \to \mathbb{R}^n$, $\phi \in PC([-\tau, 0]; \mathbb{R}^n)$, and $\mathbb{C}$ is an open set in $PC([-\tau, 0]; \mathbb{R}^n)$. The fixed moments of impulse times $\{t_k, k \in \mathbb{Z}_+\}$ satisfy $0 \leqslant t_0 < t_1 < \cdots < t_k < \cdots$ and $t_k \to \infty$ (as $k \to \infty$) and $\Delta x(t_k) = x(t_k) - x(t_k^-)$; $x_t, x_{t^-} \in PC([-\tau, 0]; \mathbb{R}^n)$ are defined as $x_t = x(t + \theta)$ and $x_{t^-} = x(t^- + \theta)$ for $\theta \in [-\tau, 0]$ respectively.

Throughout this paper, we assume that f, I_k, and J_k, $k \in \mathbb{Z}_+$, satisfy the necessary conditions for the global existence and uniqueness of solutions for all $t \geqslant t_0$ (refer to [3, 34, 35]). Then, for any $\phi \in PC([-\tau, 0]; \mathbb{R}^n)$, there exists a unique function satisfying system (2) denoted by $x(t; t_0, \phi)$, which is continuous on the right-hand side and limitable on the left-hand side. Moreover, we assume that $f(t, 0) \equiv 0$, $I_k(t_k, 0) \equiv 0$, and $J_k(t_k, 0) \equiv 0$, $k \in \mathbb{Z}_+$, which implies that $x(t) \equiv 0$ is a solution of (2), which is called the trivial solution.

At the end of this section, let us introduce the following definitions.

Definition 1. A function $V : [t_0 - \tau, \infty) \times \mathbb{R}^n \to \mathbb{R}_+$ belongs to class v_0 if the following are satisfied.

(i) V is continuous on each of the sets $[t_{k-1}, t_k) \times \mathbb{R}^n$, and for each $x, y \in \mathbb{R}^n$, $t \in [t_{k-1}, t_k)$, $k \in \mathbb{Z}_+$, $\lim_{(t,y) \to (t_k^-, x)} V(t, y) = V(t_k^-, x)$ exists.

(ii) $V(t, x)$ is locally Lipschitz in $x \in \mathbb{R}^n$, and $V(t, 0) \equiv 0$ for all $t \geqslant t_0$.

Definition 2. Given a function $V \in v_0$, the upper right-hand Dini derivative of V with respect to system (2) is defined by

$$\begin{aligned} &D^+V(t, \psi(0)) \\ &= \limsup_{h \to 0^+} \frac{1}{h} \left[V(t + h, \psi(0) + hf(t, \psi)) - V(t, \psi(0))\right] \end{aligned} \tag{3}$$

for $(t, \psi) \in [t_0, \infty) \times PC([-\tau, 0]; \mathbb{R}^n)$.

Definition 3. The trivial solution of system (2) or, simply, system (2) is said to be exponentially stable if there is a pair of positive constants λ, C such that, for any initial data $x_{t_0} = \phi \in PC([-\tau, 0]; \mathbb{R}^n)$, the solution $x(t; t_0, \phi)$ satisfies

$$\left|x(t; t_0, \phi)\right| \leqslant C \|\phi\| e^{-\lambda(t - t_0)}, \quad t \geqslant t_0. \tag{4}$$

3. Main Results

In this section, we will analyze the exponential stability of system (2) by employing the Lyapunov functions.

Theorem 4. *Assume that $V \in v_0$ and there exist constants $p > 0$, $c_1 > 0$, $c_2 > 0$, $\eta_2 \geqslant 0$, $d_{1k} > 0$, $d_{2k} \geqslant 0$, $k \in \mathbb{Z}_+$, η_1, and δ such that*

(i) $c_1|x|^p \leqslant V(t, x) \leqslant c_2|x|^p$ *for all* $(t, x) \in [t_0 - \tau, \infty) \times \mathbb{R}^n$;

(ii) $V(t_k, \varphi(0) + I_k(t_k, \varphi(0)) + J_k(t_k, \varphi)) \leqslant d_{1k} V(t_k^-, \varphi(0)) + d_{2k} \sup_{\theta \in [-\tau, 0]} V(t_k^- + \theta, \varphi(\theta))$ *for all* $\varphi \in PC([-\tau, 0]; \mathbb{R}^n)$, $k \in \mathbb{Z}_+$;

(iii) $D^+V(t, \varphi) \leqslant \eta_1 V(t, \varphi(0)) + \eta_2 \sup_{\theta \in [-\tau, 0]} V(t + \theta, \varphi(\theta))$ *for all* $\varphi \in PC([-\tau, 0]; \mathbb{R}^n)$ *and* $t \geqslant t_0$, $t \neq t_k$, $k \in \mathbb{Z}_+$;

(iv) $\ln(d_{1k} + d_{2k} \max_{\theta \in [-\tau, 0]} e^{\eta_1 \theta}) \leqslant \delta(t_k - t_{k-1})$ *for each* $k \in \mathbb{Z}_+$;

(v) $\delta + \eta_1 + \gamma\eta_2 < 0$, *where* $\gamma = \sup_{k \in \mathbb{Z}_+} \{e^{\delta(t_k - t_{k-1})}, 1/e^{\delta(t_k - t_{k-1})}\}$.

Then, system (2) *is exponentially stable, and the convergence rate should not be greater than λ/p, where λ is the unique positive solution of $\lambda + \delta + \eta_1 + \gamma\eta_2 e^{\lambda\tau} = 0$.*

Proof. Fix any initial data $\phi \in PC([-\tau, 0]; \mathbb{R}^n)$, and write $x(t; t_0, \phi) = x(t)$ and $V(t, x(t)) = V(t)$ simply. Set $W(t) = e^{-\eta_1(t - t_0)} V(t)$, $t \in [t_0 - \tau, \infty)$. For each $k \in \mathbb{Z}_+$, by condition (ii), we have

$$\begin{aligned} W(t_k) &= e^{-\eta_1(t_k - t_0)} V(t_k) \\ &\leqslant e^{-\eta_1(t_k - t_0)} \left[d_{1k} V(t_k^-) + d_{2k} \sup_{\theta \in [-\tau, 0]} V(t_k^- + \theta)\right] \\ &\leqslant d_{1k} e^{-\eta_1(t_k - t_0)} V(t_k^-) \\ &\quad + \alpha d_{2k} \sup_{\theta \in [-\tau, 0]} \left(V(t_k^- + \theta) e^{-\eta_1(t_k + \theta - t_0)}\right) \\ &= d_{1k} W(t_k^-) + \alpha d_{2k} \sup_{\theta \in [-\tau, 0]} W(t_k^- + \theta), \end{aligned} \tag{5}$$

where $\alpha = \max_{\theta \in [-\tau, 0]} e^{\eta_1 \theta}$.

On the other hand, by condition (iii), we know that, for any $t \neq t_k$, $k \in \mathbb{Z}_+$,

$$\begin{aligned} D^+W(t) &= e^{-\eta_1(t-t_0)}\left[-\eta_1 V(t) + D^+V(t)\right] \\ &\leqslant \eta_2 e^{-\eta_1(t-t_0)} \sup_{\theta\in[-\tau,0]} V(t+\theta). \end{aligned} \tag{6}$$

For $t \in [t_0, t_1)$, integrating inequality (6) from t_0 to t, we obtain

$$W(t) \leqslant W(t_0) + \int_{t_0}^{t} \eta_2 e^{-\eta_1(s-t_0)} \sup_{\theta\in[-\tau,0]} V(s+\theta)\, ds. \tag{7}$$

This implies that

$$W(t_1^-) \leqslant W(t_0) + \int_{t_0}^{t_1} \eta_2 e^{-\eta_1(s-t_0)} \sup_{\theta\in[-\tau,0]} V(s+\theta)\, ds. \tag{8}$$

For $t \in [t_1, t_2)$, by the same method, together with (5) and (8), we have

$$\begin{aligned} W(t) &\leqslant W(t_1) + \int_{t_1}^{t} \eta_2 e^{-\eta_1(s-t_0)} \sup_{\theta\in[-\tau,0]} V(s+\theta)\, ds \\ &\leqslant d_{11} W(t_1^-) + \alpha d_{21} \sup_{\theta\in[-\tau,0]} W(t_1^- + \theta) \\ &\quad + \int_{t_1}^{t} \eta_2 e^{-\eta_1(s-t_0)} \sup_{\theta\in[-\tau,0]} V(s+\theta)\, ds \\ &\leqslant d_{11}\left[W(t_0) + \int_{t_0}^{t_1} \eta_2 e^{-\eta_1(s-t_0)} \sup_{\theta\in[-\tau,0]} V(s+\theta)\, ds\right] \\ &\quad + \alpha d_{21}\left[W(t_0) + \sup_{\theta\in[-\tau,0]} \int_{t_0}^{t_1+\theta} \eta_2 e^{-\eta_1(s-t_0)} \times \sup_{\theta\in[-\tau,0]} V(s+\theta)\, ds\right] \\ &\quad + \int_{t_1}^{t} \eta_2 e^{-\eta_1(s-t_0)} \sup_{\theta\in[-\tau,0]} V(s+\theta)\, ds \\ &\leqslant (d_{11} + \alpha d_{21}) W(t_0) \\ &\quad + (d_{11} + \alpha d_{21}) \int_{t_0}^{t_1} \eta_2 e^{-\eta_1(s-t_0)} \sup_{\theta\in[-\tau,0]} V(s+\theta)\, ds \\ &\quad + \int_{t_1}^{t} \eta_2 e^{-\eta_1(s-t_0)} \sup_{\theta\in[-\tau,0]} V(s+\theta)\, ds. \end{aligned} \tag{9}$$

By induction, we have, for $t \in [t_{k-1}, t_k)$, $k \in \mathbb{Z}_+$,

$$\begin{aligned} W(t) &\leqslant W(t_0) \prod_{t_0<t_i\leqslant t} (d_{1i} + \alpha d_{2i}) \\ &\quad + \int_{t_0}^{t} \prod_{s<t_i\leqslant t} (d_{1i} + \alpha d_{2i})\, \eta_2 e^{-\eta_1(s-t_0)} \sup_{\theta\in[-\tau,0]} V(s+\theta)\, ds. \end{aligned} \tag{10}$$

Thus, for $t > t_0$, we get

$$\begin{aligned} V(t) &\leqslant V(t_0) e^{\eta_1(t-t_0)} \prod_{t_0<t_i\leqslant t} (d_{1i} + \alpha d_{2i}) \\ &\quad + \int_{t_0}^{t} \prod_{s<t_i\leqslant t} (d_{1i} + \alpha d_{2i})\, \eta_2 e^{\eta_1(t-s)} \sup_{\theta\in[-\tau,0]} V(s+\theta)\, ds. \end{aligned} \tag{11}$$

Let $t_{j_1}, t_{j_2}, \ldots, t_{j_m}$ be impulse points in $(s, t]$, $t > s$. In view of condition (iv), we get

$$\begin{aligned} &\prod_{s<t_i\leqslant t} (d_{1i} + \alpha d_{2i}) \\ &\quad = \left(d_{1j_1} + \alpha d_{2j_1}\right)\left(d_{1j_2} + \alpha d_{2j_2}\right)\cdots\left(d_{1j_m} + \alpha d_{2j_m}\right) \\ &\quad \leqslant e^{\delta(t_{j_1} - t_{j_1-1})} e^{\delta(t_{j_2} - t_{j_1})} \cdots e^{\delta(t_{j_m} - t_{j_{m-1}})} = e^{\delta(t_{j_m} - t_{j_1-1})} \\ &\quad = e^{\delta(t-s)} e^{\delta(t_{j_m} - t)} e^{\delta(s - t_{j_1-1})} \leqslant \gamma e^{\delta(t-s)}, \end{aligned} \tag{12}$$

where t_{j_1-1} is the first impulsive point before t_{j_1} and satisfies $t_{j_1-1} < s$. Submitting this into inequality (11), then, for $t > t_0$,

$$\begin{aligned} V(t) &\leqslant \gamma e^{(\eta_1+\delta)(t-t_0)} V(t_0) \\ &\quad + \int_{t_0}^{t} \gamma\eta_2 e^{(\eta_1+\delta)(t-s)} \sup_{\theta\in[-\tau,0]} V(s+\theta)\, ds. \end{aligned} \tag{13}$$

Let $\Phi(\lambda) = \lambda + \eta_1 + \delta + \gamma\eta_2 e^{\lambda\tau}$. Then, condition (v) implies $\Phi(0) < 0$. Moreover, $\Phi(+\infty) = +\infty$, and $\Phi'(\lambda) = 1 + \tau\gamma\eta_2 e^{\lambda\tau} > 0$. Hence, $\Phi(\lambda) = 0$ has a unique positive solution λ. Next, we claim that

$$V(t) \leqslant \gamma \sup_{\theta\in[-\tau,0]} V(t_0+\theta)\, e^{-\lambda(t-t_0)}, \quad t \geqslant t_0 - \tau. \tag{14}$$

Obviously,

$$\begin{aligned} V(t) \leqslant \sup_{\theta\in[-\tau,0]} V(t_0+\theta) \leqslant \gamma \sup_{\theta\in[-\tau,0]} V(t_0+\theta)\, e^{-\lambda(t-t_0)}, \\ t \in [t_0 - \tau, t_0]. \end{aligned} \tag{15}$$

So we only need to prove (14) for $t > t_0$. Suppose not; then there exists a $t^* \in (t_0, +\infty)$ such that

$$V(t^*) > \gamma \sup_{\theta\in[-\tau,0]} V(t_0+\theta)\, e^{-\lambda(t^*-t_0)}, \tag{16}$$

$$V(t) \leqslant \gamma \sup_{\theta\in[-\tau,0]} V(t_0+\theta)\, e^{-\lambda(t-t_0)}, \quad t \in [t_0 - \tau, t^*). \tag{17}$$

Thus, from (13), (17), and $\Phi(\lambda) = 0$, we see that

$$\begin{aligned} V(t^*) &\leqslant \gamma \sup_{\theta\in[-\tau,0]} V(t_0+\theta)\, e^{(\eta_1+\delta)(t^*-t_0)} \\ &\quad + \gamma \int_{t_0}^{t^*} \eta_2 e^{(\eta_1+\delta)(t^*-s)} \sup_{\theta\in[-\tau,0]} V(s+\theta)\, ds \\ &\leqslant \gamma \sup_{\theta\in[-\tau,0]} V(t_0+\theta)\, e^{(\eta_1+\delta)(t^*-t_0)} \\ &\quad + \gamma \int_{t_0}^{t^*} \gamma\eta_2 e^{\lambda\tau} e^{(\eta_1+\delta)(t^*-s)} e^{-\lambda(s-t_0)} \sup_{\theta\in[-\tau,0]} V(t_0+\theta)\, ds \\ &= \gamma \sup_{\theta\in[-\tau,0]} V(t_0+\theta)\, e^{-\lambda(t^*-t_0)}, \end{aligned} \tag{18}$$

which is a contradiction. Therefore, (14) holds.

Then, it follows from (14) and condition (i) that

$$\begin{aligned} c_1|x(t)|^p \leqslant V(t) &\leqslant \gamma \sup_{\theta\in[-\tau,0]} V(t_0+\theta)\, e^{-\lambda(t-t_0)} \\ &\leqslant \gamma c_2 \|\phi\|^p e^{-\lambda(t-t_0)}, \quad t \geqslant t_0, \end{aligned} \tag{19}$$

which implies that

$$|x(t)| \leqslant C\|\phi\|\, e^{(-\lambda/p)(t-t_0)}, \quad t \geqslant t_0, \tag{20}$$

where $C = (\gamma c_2/c_1)^{1/p}$. This completes the proof. □

Remark 5. The parameters d_{1k} and d_{2k} in condition (ii) describe the influence of impulses on the stability of the underlying continuous systems. Conditions (iv) and (v) in Theorem 4 show that the system will be stable if the impulses frequency and amplitude are suitably related to the increase or decrease of the continuous flows.

Remark 6. It is well known that the Razumikhin techniques are very effective in the study of stability problems for ordinary and functional differential systems. However, when we use the Razumikhin techniques, we need to choose an appropriate minimal class of functionals relative to which the derivative of the Lyapunov function or Lyapunov functional is estimated, which is not entirely convenient. In this sense, Theorem 4 is more convenient to be applied than those Razumikhin-type theorems in [31, 32].

Let $J_k \equiv 0$ in system (2); then we have the following IDS (see, e.g., [19–24]):

$$\begin{aligned} \dot{x}(t) &= f(x_t, t), \quad t \neq t_k, t \geqslant t_0, \\ \Delta x(t_k) &= I_k(x(t_k^-), t_k), \quad k \in \mathbb{Z}_+, \\ x_{t_0} &= \phi(s), \quad s \in [-\tau, 0]. \end{aligned} \tag{21}$$

For system (21), we have the following results by Theorem 4.

Theorem 7. *Assume that $V \in v_0$ and there exist constants $p > 0$, $c_1 > 0$, $c_2 > 0$, $\eta_2 \geqslant 0$, $d_k > 0$, $k \in \mathbb{Z}_+$, η_1, and δ such that*

(i) $c_1|x|^p \leqslant V(t,x) \leqslant c_2|x|^p$ *for all* $(t,x) \in [t_0-\tau, \infty)\times\mathbb{R}^n$;

(ii) $V(t_k, \varphi(0)) + I_k(t_k, \varphi(0)) \leqslant d_k V(t_k^-, \varphi(0))$ *for all* $\varphi \in PC([-\tau, 0]; \mathbb{R}^n)$, $k \in \mathbb{Z}_+$;

(iii) $D^+V(t,\varphi) \leqslant \eta_1 V(t, \varphi(0)) + \eta_2 \sup_{\theta\in[-\tau,0]} V(t+\theta, \varphi(\theta))$ *for all* $\varphi \in PC([-\tau, 0]; \mathbb{R}^n)$ *and* $t \geqslant t_0$, $t \neq t_k$, $k \in \mathbb{Z}_+$;

(iv) $\ln d_k \leqslant \delta(t_k - t_{k-1})$ *for each* $k \in \mathbb{Z}_+$;

(v) $\delta + \eta_1 + \gamma\eta_2 < 0$, *where* $\gamma = \sup_{k\in\mathbb{Z}_+}\{e^{\delta(t_k-t_{k-1})}, 1/e^{\delta(t_k-t_{k-1})}\}$.

Then, system (21) *is exponentially stable for any time delay* $\tau \in (0, \infty)$, *and the convergence rate should not be greater than* λ/p, *where* λ *is the unique positive solution of* $\lambda + \delta + \eta_1 + \gamma\eta_2 e^{\lambda\tau} = 0$.

In particular, if one takes $d_k \equiv d$ *for all* $k \in \mathbb{Z}_+$, *then suppose the impulsive instances* t_k *satisfy*

$$\Delta_{\sup} = \sup_{k\in\mathbb{Z}_+}\{t_k - t_{k-1}\} < \infty, \qquad \Delta_{\inf} = \inf_{k\in\mathbb{Z}_+}\{t_k - t_{k-1}\} > 0. \tag{22}$$

For system (21), Theorem 7 yields the following result.

Theorem 8. *Assume that $V \in v_0$ and there exist constants $p > 0$, $c_1 > 0$, $c_2 > 0$, $d > 0$, $\varrho > 0$, $\eta_2 \geqslant 0$, and η_1 such that*

(i) $c_1|x|^p \leqslant V(t,x) \leqslant c_2|x|^p$ *for all* $(t,x) \in [t_0-\tau, \infty)\times\mathbb{R}^n$;

(ii) $V(t_k, \varphi(0)) + I_k(t_k, \varphi(0)) \leqslant dV(t_k^-, \varphi(0))$ *for all* $\varphi \in PC([-\tau, 0]; \mathbb{R}^n)$, $k \in \mathbb{Z}_+$;

(iii) $D^+V(t,\varphi) \leqslant \eta_1 V(t, \varphi(0)) + \eta_2 \sup_{\theta\in[-\tau,0]} V(t+\theta, \varphi(\theta))$ *for all* $\varphi \in PC([-\tau, 0]; \mathbb{R}^n)$ *and* $t \geqslant t_0$, $t \neq t_k$, $k \in \mathbb{Z}_+$;

(iv) $\eta_1 + \eta_2 g(d) + \ln d/\varrho < 0$, *where* $g(d) = d^{\Delta_{\sup}/\varrho}$ *if* $d > 1$; $g(d) = 1$ *if* $d = 1$; $g(d) = 1/d^{\Delta_{\inf}/\varrho}$ *if* $d < 1$.

Then, for any $\tau \in (0, \infty)$, *when* $d > 1$, *system* (21) *is exponentially stable with impulse time sequences that satisfy* $\Delta_{\inf} \geqslant \varrho$; *when* $d = 1$, *system* (21) *is exponentially stable with any impulse time sequences; when* $d < 1$, *system* (21) *is exponentially stable with impulse time sequences that satisfy* $\Delta_{\sup} \leqslant \varrho$.

Proof. We just need to apply Theorem 7 with $\delta = \ln d/\varrho$ and $\gamma = g(d)$. □

Remark 9. When $d > 1$, the Lyapunov function V may jump up along the state trajectories of system (21) at impulse times t_k. Thus, the impulses may be viewed as disturbances; that is, they potentially destroy the stability of continuous system. In this case, it is required that the impulses do not occur too frequently.

Remark 10. When $d < 1$, the Lyapunov function V may jump down along the state trajectories of system (21) at impulse times t_k. Thus, the impulses may be treated as a stabilizing factor; that is, they may be used to stabilize an unstable continuous system. In this case, the impulses must take place frequently enough, and their amplitude must be suitably related to the growth rate of V.

Remark 11. When $d = 1$, both the continuous dynamics and the discrete dynamics are stable, so the system can preserve exponential stability regardless of how often or how seldom impulses occur.

4. Applications and Example

Consider the following linear impulsive systems with time-varying delays:

$$\begin{aligned} \dot{x}(t) &= Ax(t) + Bx(t - r(t)), \quad t \neq t_k, t \geqslant t_0, \\ \Delta x(t_k) &= x(t_k) - x(t_k^-) = C_k x(t_k^-) + D_k x(t_k^- - r(t_k)), \\ & \qquad k \in \mathbb{Z}_+, \\ x_{t_0} &= \phi(s), \quad s \in [-\tau, 0], \end{aligned} \tag{23}$$

where $x(t) \in \mathbb{R}^n$ is the system state vector, A, B, C_k, and D_k are $n \times n$ matrices, and $r : \mathbb{R}_+ \to [0, \tau]$ with $\tau < \infty$ is the time-varying delay.

Theorem 12. *Assume that there exist a matrix $P > 0$ and several constants $d_1 > 0$, $d_2 \geqslant 0$, $\eta_2 \geqslant 0$, and η_1 such that*

(i) *the following matrix inequalities hold:*

$$\begin{bmatrix} -d_1 P & 0 & (I + C_k)^T P \\ * & -d_2 P & D_k^T P \\ * & * & -P \end{bmatrix} \leqslant 0, \tag{24}$$

$$\begin{bmatrix} PA + A^T P - \eta_1 P & PB \\ * & -\eta_2 P \end{bmatrix} \leqslant 0; \tag{25}$$

(ii) $\ln(d_1 + d_2 \max_{\theta \in [-\tau, 0]} e^{\eta_1 \theta}) \leqslant \delta(t_k - t_{k-1})$;

(iii) $\delta + \eta_1 + \eta_2 \gamma < 0$, *where* $\gamma = \sup_{k \in \mathbb{Z}_+} \{e^{\delta(t_k - t_{k-1})}, 1/e^{\delta(t_k - t_{k-1})}\}$.

Then, system (23) *is exponentially stable, and the convergence rate should not be greater than $\lambda/2$, where λ is the unique positive solution of $\lambda + \delta + \eta_1 + \gamma \eta_2 e^{\lambda \tau} = 0$.*

Proof. Let $V(t, x) = x^T P x$, $I_k(t_k, x(t_k^-)) = C_k x(t_k^-)$, and $J_k(t_k, x_{t_k^-}) = D_k x(t_k^- - r(t_k))$. Then, (24) combined with Schur complement yields

$$\begin{bmatrix} -d_1 P & 0 \\ 0 & -d_2 P \end{bmatrix} + \begin{bmatrix} I + C_k & D_k \end{bmatrix}^T P \begin{bmatrix} I + C_k & D_k \end{bmatrix} \leqslant 0. \tag{26}$$

Thus, for $\varphi \in PC([-\tau, 0]; \mathbb{R}^n)$, $t = t_k$, $k \in \mathbb{Z}_+$, using the second equation of (23), we get

$$\begin{aligned} & V(t_k, \varphi(0) + I_k(t_k, \varphi(0)) + J_k(t_k, \varphi)) \\ &= \begin{bmatrix} \varphi(0) \\ \varphi(-r(t_k)) \end{bmatrix}^T \begin{bmatrix} I + C_k & D_k \end{bmatrix}^T P \begin{bmatrix} I + C_k & D_k \end{bmatrix} \\ &\quad \times \begin{bmatrix} \varphi(0) \\ \varphi(-r(t_k)) \end{bmatrix} \\ &\leqslant \begin{bmatrix} \varphi(0) \\ \varphi(-r(t_k)) \end{bmatrix}^T \begin{bmatrix} d_1 P & 0 \\ 0 & d_2 P \end{bmatrix} \begin{bmatrix} \varphi(0) \\ \varphi(-r(t_k)) \end{bmatrix} \\ &\leqslant d_1 V(t_k^-, \varphi(0)) + d_2 \sup_{\theta \in [-\tau, 0]} V(t_k^- + \theta, \varphi(\theta)). \end{aligned} \tag{27}$$

In view of (25), for $\varphi \in PC([-\tau, 0]; \mathbb{R}^n)$ and $t \neq t_k$, $k \in \mathbb{Z}_+$, we have

$$\begin{aligned} D^+ V(t, \varphi) &= \begin{bmatrix} \varphi(0) \\ \varphi(-r(t)) \end{bmatrix}^T \begin{bmatrix} PA + A^T P & PB \\ * & 0 \end{bmatrix} \begin{bmatrix} \varphi(0) \\ \varphi(-r(t)) \end{bmatrix} \\ &\leqslant \begin{bmatrix} \varphi(0) \\ \varphi(-r(t)) \end{bmatrix}^T \begin{bmatrix} \eta_1 P & 0 \\ * & \eta_2 P \end{bmatrix} \begin{bmatrix} \varphi(0) \\ \varphi(-r(t)) \end{bmatrix} \\ &\leqslant \eta_1 V(t, \varphi(0)) + \eta_2 \sup_{\theta \in [-\tau, 0]} V(t + \theta, \varphi(\theta)). \end{aligned} \tag{28}$$

Consequently, the conclusion follows from Theorem 4 immediately, and the proof is complete. □

Consider the special case $D_k \equiv 0$; from Theorem 7 and using the similar method in the proof of Theorem 12, we can obtain the following results.

Theorem 13. *Let $D_k \equiv 0$, $\Delta_{\sup} = \sup_{k \in \mathbb{Z}_+} \{t_k - t_{k-1}\} < \infty$, and $\Delta_{\inf} = \inf_{k \in \mathbb{Z}_+} \{t_k - t_{k-1}\} > 0$. Assume that there exist a matrix $P > 0$ and several constants $d > 0$, $\varrho > 0$, $\eta_2 \geqslant 0$, and η_1 such that*

(i) *the following matrix inequalities hold:*

$$\begin{aligned} & (I + C_k)^T P (I + C_k) \leqslant dP, \\ & \begin{bmatrix} PA + A^T P - \eta_1 P & PB \\ * & -\eta_2 P \end{bmatrix} \leqslant 0; \end{aligned} \tag{29}$$

(ii) $\eta_1 + \eta_2 g(d) + \ln d/\varrho < 0$, *where* $g(d) = d^{\Delta_{\sup}/\varrho}$ *if* $d > 1$; $g(d) = 1$ *if* $d = 1$; $g(d) = 1/d^{\Delta_{\inf}/\varrho}$ *if* $d < 1$.

Then, for any $\tau \in (0, \infty)$, when $d > 1$, system (23) *is exponentially stable with impulse time sequences that satisfy $\Delta_{\inf} \geqslant \varrho$; when $d = 1$, system* (23) *is exponentially stable with any impulse time sequences; when $d < 1$, system* (23) *is exponentially stable with impulse time sequences that satisfy $\Delta_{\sup} \leqslant \varrho$.*

Example 14. Consider the following first-order impulsive delayed neural network:

$$\dot{x}(t) = -ax(t) + b_0 f(x(t)) + b_1 f(x(t-\tau)), \quad t \neq t_k, t \geqslant t_0,$$
$$\Delta x(t_k) = cx(t_k^-) + dx(t_k^- - \tau), \quad k \in \mathbb{Z}_+, \tag{30}$$

where $a = 2.5$, $b_0 = -1.5$, $b_1 = 0.5$, $c = 0.2$, $d = 0.1$, and $\tau = 0.05$. $f(x) = \tanh(x)$, and $t_k = \sigma k$, $k \in \mathbb{Z}_+$, $\sigma > 0$, is a constant. It is easy to see that system without impulses is exponentially stable and the impulses are destabilizing since $c, d > 0$. Choose $V(t,x) = x^2/2$; then we obtain that conditions (i) and (ii) of Theorem 4 hold with $c_1 = c_2 = 1/2$, $p = 2$, $d_{1k} = (1+c)(1+c+d) = 1.56$, and $d_{2k} = d(1+c+d) = 0.13$.

For $t \neq t_k$, by simple calculation, we have

$$\begin{aligned} D^+V(t,x(t)) &= -ax^2(t) + b_0 x(t) f(x(t)) \\ &\quad + b_1 x(t) f(x(t-\tau)) \\ &\leqslant -\left(a + b_0 - \frac{1}{2}b_1\right)x^2(t) + \frac{1}{2}b_1 x^2(t-\tau) \\ &= -(2a + 2b_0 - b_1)V(t,x(t)) \\ &\quad + b_1 V(t,x(t-\tau)), \end{aligned} \tag{31}$$

which implies that condition (iii) of Theorem 4 holds with $\eta_1 = -(2a + 2b_0 - b_1) = -1.5$ and $\eta_2 = b_1 = 0.5$. Note that $t_k = \sigma k$, so we can take $\delta = \ln(d_{1k} + d_{2k}e^{-\eta_1\tau})/(t_k - t_{k-1}) = \ln(1.56 + 0.13e^{0.075})/\sigma$ and $\gamma = d_{1k} + d_{2k}e^{-\eta_1\tau} = 1.56 + 0.13e^{0.075}$. Then, by Theorem 4, system (30) is exponentially stable over any impulse time sequences satisfying $t_k - t_{k-1} \geqslant \sigma > \ln(1.56+0.13e^{0.075})/[1.5-0.5(1.56+0.13e^{0.075})] = 0.4298$.

Remark 15. Since the system without impulses is exponentially stable and the impulses are destabilizing, the existing results in [29, 32] cannot be applied to (30). The Razumikhin-type theorem in [31] is also not convenient to be applied to this system since it is not easy to find an appropriate constant $q > 1$ to satisfy the Razumikhin-type condition.

Example 16. Consider system (23) with the following parameters:

$$A = \begin{bmatrix} 2 & 1 \\ 0.8 & 2 \end{bmatrix}, \qquad B = \begin{bmatrix} 1 & -0.2 \\ 0.3 & 1 \end{bmatrix},$$
$$C_k \equiv \begin{bmatrix} -0.3 & 0 \\ 0 & -0.3 \end{bmatrix}, \qquad D_k \equiv \begin{bmatrix} 0.2 & 0 \\ 0 & 0.2 \end{bmatrix}, \quad k \in \mathbb{Z}_+, \tag{32}$$

and $r(t) = 8 + 0.02[\sin(t)]$, where $[\cdot]$ denotes the integer function. Let $\tau = 8.2$, $d_1 = 0.49$, $d_2 = 0.04$, $\eta_1 = 7$, $\eta_2 = 1$, $\gamma = 0.53$, $\delta = -7.9360$, and $t_k - t_{k-1} \leqslant 0.08$. It is easy to verify that

$$\eta_1 + \eta_2\gamma + \delta = -0.4060 < 0,$$
$$\ln\left(d_1 + d_2 \max_{\theta\in[-\tau,0]} e^{\eta_1\theta}\right) = \ln 0.53 = -0.6349 < -7.9360 \times 0.08 \leqslant \delta(t_k - t_{k-1}). \tag{33}$$

Solving the linear matrix inequalities (24) and (25) in Theorem 12, we obtain the following feasible solution $P = \begin{bmatrix} 0.3507 & 0.0332 \\ 0.0332 & 0.3076 \end{bmatrix}$. Then, by Theorem 12, we know the given system is exponentially stable.

Remark 17. In Example 16, the impulses are used to stabilize an unstable system. In this case, the impulses must be frequent enough, and their amplitude must be suitably related to the growth rate of the continuous flow.

5. Conclusions

This paper has studied the exponential stability of impulsive delay systems in which the state variables on the impulses are related to the time delay. By using the Lyapunov function method, some criteria on the exponential stability are established. Moreover, the stability criteria obtained are applied to linear impulsive systems with time-varying delays, and a set of sufficient conditions for exponential stability is provided in terms of matrix inequalities. The obtained results improve and complement some recent works. Two examples have been given to illustrate the effectiveness and advantages of the results obtained.

Conflict of Interests

The authors declare that there is no conflict of interests regarding the publication of this paper.

Acknowledgments

This work was supported by the National Natural Science Foundation of China (61273126, 11226247, and 11301004), the Anhui Provincial Nature Science Foundation (1308085QA15, 1308085MA01), the Key Natural Science Foundation (KJ2009A49), the Foundation of Anhui Education Bureau (KJ2012A019), and the 211 Project of Anhui University (32030018 and 33010205).

References

[1] V. Lakshmikantham, D. D. Baĭnov, and P. S. Simeonov, *Theory of Impulsive Differential Equations*, vol. 6 of *Series in Modern Applied Mathematics*, World Scientific, Singapore, 1989.

[2] K. Gopalsamy and B. G. Zhang, "On delay differential equations with impulses," *Journal of Mathematical Analysis and Applications*, vol. 139, no. 1, pp. 110–122, 1989.

[3] G. Ballinger and X. Liu, "Existence, uniqueness and boundedness results for impulsive delay differential equations," *Applicable Analysis*, vol. 74, no. 1-2, pp. 71–93, 2000.

[4] W. M. Haddad, V. Chellaboina, and S. G. Nersesov, *Impulsive and Hybrid Dynamical Systems: Stability, Dissipativity, and Control*, Princeton Series in Applied Mathematics, Princeton University Press, Princeton, NJ, USA, 2006.

[5] W. Chen and W. Zheng, "On improved robust stabilization of uncertain systems with unknown input delay," *Automatica*, vol. 42, no. 6, pp. 1067–1072, 2006.

[6] E. Fridman and U. Shaked, "An improved stabilization method for linear time-delay systems," *IEEE Transactions on Automatic Control*, vol. 47, no. 11, pp. 1931–1937, 2002.

[7] S. Xu and T. Chen, "Robust H_∞ control for uncertain stochastic systems with state delay," *IEEE Transactions on Automatic Control*, vol. 47, no. 12, pp. 2089–2094, 2002.

[8] D. Yue, "Robust stabilization of uncertain systems with unknown input delay," *Automatica*, vol. 40, no. 2, pp. 331–336, 2004.

[9] L. Huang and X. Mao, "Robust delayed-state-feedback stabilization of uncertain stochastic systems," *Automatica*, vol. 45, no. 5, pp. 1332–1339, 2009.

[10] D. Wang, P. Shi, J. Wang, and W. Wang, "Delay-dependent exponential H_∞ filtering for discrete-time switched delay systems," *International Journal of Robust and Nonlinear Control*, vol. 22, no. 13, pp. 1522–1536, 2012.

[11] W. Chen and W. Zheng, "Robust stability and H_∞-control of uncertain impulsive systems with time-delay," *Automatica*, vol. 45, no. 1, pp. 109–117, 2009.

[12] G. Zong, S. Xu, and Y. Wu, "Robust H_∞ stabilization for uncertain switched impulsive control systems with state delay: an LMI approach," *Nonlinear Analysis: Hybrid Systems*, vol. 2, no. 4, pp. 1287–1300, 2008.

[13] B. Liu, K. L. Teo, and X. Liu, "Robust exponential stabilization for large-scale uncertain impulsive systems with coupling time-delays," *Nonlinear Analysis: Theory, Methods & Applications*, vol. 68, no. 5, pp. 1169–1183, 2008.

[14] X. Liu, S. Zhong, and X. Ding, "Robust exponential stability of impulsive switched systems with switching delays: a Razumikhin approach," *Communications in Nonlinear Science and Numerical Simulation*, vol. 17, no. 4, pp. 1805–1812, 2012.

[15] A. Anokhin, L. Berezansky, and E. Braverman, "Exponential stability of linear delay impulsive differential equations," *Journal of Mathematical Analysis and Applications*, vol. 193, no. 3, pp. 923–941, 1995.

[16] Z. Luo and J. Shen, "Stability and boundedness for impulsive functional differential equations with infinite delays," *Nonlinear Analysis: Theory, Methods & Applications*, vol. 46, no. 4, pp. 475–493, 2001.

[17] I. M. Stamova and G. T. Stamov, "Lyapunov-Razumikhin method for impulsive functional differential equations and applications to the population dynamics," *Journal of Computational and Applied Mathematics*, vol. 130, no. 1-2, pp. 163–171, 2001.

[18] Z. Luo and J. Shen, "Impulsive stabilization of functional differential equations with infinite delays," *Applied Mathematics Letters*, vol. 16, no. 5, pp. 695–701, 2003.

[19] Y. Zhang and J. Sun, "Stability of impulsive infinite delay differential equations," *Applied Mathematics Letters*, vol. 19, no. 10, pp. 1100–1106, 2006.

[20] Z. Chen and X. Fu, "New Razumikhin-type theorems on the stability for impulsive functional differential systems," *Nonlinear Analysis: Theory, Methods & Applications*, vol. 66, no. 9, pp. 2040–2052, 2007.

[21] A. Weng and J. Sun, "Impulsive stabilization of second-order delay differential equations," *Nonlinear Analysis: Real World Applications*, vol. 8, no. 5, pp. 1410–1420, 2007.

[22] X. Fu and X. Li, "Razumikhin-type theorems on exponential stability of impulsive infinite delay differential systems," *Journal of Computational and Applied Mathematics*, vol. 224, no. 1, pp. 1–10, 2009.

[23] Z. Luo and J. Shen, "Stability of impulsive functional differential equations via the Liapunov functional," *Applied Mathematics Letters*, vol. 22, no. 2, pp. 163–169, 2009.

[24] S. Peng and L. Yang, "Global exponential stability of impulsive functional differential equations via Razumikhin technique," *Abstract and Applied Analysis*, vol. 2010, Article ID 987372, 11 pages, 2010.

[25] X. Li, "Uniform asymptotic stability and global stabiliy of impulsive infinite delay differential equations," *Nonlinear Analysis: Theory, Methods & Applications*, vol. 70, no. 5, pp. 1975–1983, 2009.

[26] X. Li, "New results on global exponential stabilization of impulsive functional differential equations with infinite delays or finite delays," *Nonlinear Analysis: Real World Applications*, vol. 11, no. 5, pp. 4194–4201, 2010.

[27] F. Lian, J. Moyne, and D. Tilbury, "Modelling and optimal controller design of networked control systems with multiple delays," *International Journal of Control*, vol. 76, no. 6, pp. 591–606, 2003.

[28] A. Khadra, X. Liu, and X. Shen, "Analyzing the robustness of impulsive synchronization coupled by linear delayed impulses," *IEEE Transactions on Automatic Control*, vol. 54, no. 4, pp. 923–928, 2009.

[29] Y. Zhang and J. Sun, "Stability of impulsive functional differential equations," *Nonlinear Analysis: Theory, Methods & Applications*, vol. 68, no. 12, pp. 3665–3678, 2008.

[30] W. Chen and W. Zheng, "Exponential stability of nonlinear time-delay systems with delayed impulse effects," *Automatica*, vol. 47, no. 5, pp. 1075–1083, 2011.

[31] P. Cheng, Z. Wu, and L. Wang, "New results on global exponential stability of impulsive functional differential systems with delayed impulses," *Abstract and Applied Analysis*, vol. 2012, Article ID 376464, 13 pages, 2012.

[32] D. Lin, X. Li, and D. O'Regan, "Stability analysis of generalized impulsive functional differential equations," *Mathematical and Computer Modelling*, vol. 55, no. 5-6, pp. 1682–1690, 2012.

[33] F. Yao, F. Deng, and P. Cheng, "Exponential stability of impulsive stochastic functional differential systems with delayed impulses," *Abstract and Applied Analysis*, vol. 2013, Article ID 548712, 8 pages, 2013.

[34] X. Liu and G. Ballinger, "Uniform asymptotic stability of impulsive delay differential equations," *Computers & Mathematics with Applications*, vol. 41, no. 7-8, pp. 903–915, 2001.

[35] Q. Wang and X. Liu, "Exponential stability for impulsive delay differential equations by Razumikhin method," *Journal of Mathematical Analysis and Applications*, vol. 309, no. 2, pp. 462–473, 2005.

Hindawi Publishing Corporation
Mathematical Problems in Engineering
Volume 2013, Article ID 963089, 13 pages
http://dx.doi.org/10.1155/2013/963089

Research Article

LMI-Based Model Predictive Control for a Class of Constrained Uncertain Fuzzy Markov Jump Systems

Ting Yang[1,2] and Hamid Reza Karimi[3]

[1] *Research Center of Intelligent Control and Systems, Harbin Institute of Technology, Harbin, Heilongjiang 150080, China*
[2] *Department of Mechanical and Aerospace Engineering, North Carolina State University, Raleigh, NC 27606, USA*
[3] *Department of Engineering, Faculty of Engineering and Science, University of Agder, 4898 Grimstad, Norway*

Correspondence should be addressed to Ting Yang; tingtingyang162@gmail.com

Received 8 August 2013; Accepted 27 September 2013

Academic Editor: Jun Hu

An extended model predictive control algorithm is proposed to address constrained robust model predictive control. New upper bounds on arbitrarily long time intervals are derived by introducing two external parameters, which can relax the requirements for the increments of the Lyapunov function. The main merit of this new approach compared to other well-known techniques is the reduced conservativeness. The proposed method is proved to be effective for a class of uncertain fuzzy Markov jump systems with partially unknown transition probabilities. A single pendulum example is given to illustrate the advantages and effectiveness of the proposed controller design method.

1. Introduction

Model predictive control (MPC), a powerful strategy for dealing with input and state constraints for a control system, has first attracted notable attention in industrial applications [1]. Since stability analysis approach for MPC was proposed, many significant advances in understanding MPC from a control theoretician's viewpoint have then been acquired [2–4]. Meanwhile, the MPC formulation for constrained linear systems has been naturally extended to not only nonlinear systems [5–7] but also some more complex systems, for example, stochastic systems [8, 9], time-delay systems [10], hybrid systems [11], uncertain systems [12], and so on. By employing the idea of control structure optimization, for example, distributed MPC [13], centralized MPC, and coordinated MPC, the theory of MPC has been further refined. As is well known, for a long time, efficient setting of the large set of tunable parameters has been a hard problem for MPC. Fortunately, many available methods have already been developed (see [14] and the references therein for more details). Nowadays, many scholars tend to develop "fast MPC" in order to ease the huge online computational burden [15–17]. However, it should be noticed that MPC algorithm may perform very poorly when model mismatch occurs in spite of the inherent robustness provided by the feedback strategy based on the plant measurement at the next sampling time.

Therefore, in the past decades, the issues of MPC algorithm for uncertain systems have been addressed much in the literature. A robust constrained MPC scheme considering two classes of system uncertainty, that is, polytopic paradigm and structured feedback uncertainty, has been analyzed by means of linear matrix inequalities (LMIs) by Kothare et al. [18]. As opposed to a single linear static state-feedback law in [18], Bloemen et al. [19] divided the input sequence into two parts, the first H_S inputs being computed by finite MPC method and the other inputs being calculated based on linear static state-feedback law. Because H_S was variable, the

end-point state-weighting matrix and the invariant ellipsoid were transformed into variables in the online optimization, and thus this algorithm achieved the trade-off between feasibility and performance. This work has been improved by applying parameter-dependent Lyapunov function [20–22]. In [23–25], an efficient robust constrained MPC with a time-varying terminal constraint set was developed. The proposed algorithm can obtain a perfect control schema achieving lower online computation and larger stabilizable set of states while retaining the unconstrained optimal performance as much as possible. It is worth mentioning that in order to analyze the stability of the system and obtain an upper bound of cost function, the optimal cost function has been qualified as a constraint on the increments of Lyapunov function [26]. However, this constraint is too strict, since to guarantee the system stability, the increments of Lyapunov function are only required to be negative. Motivated by this, in the present paper, a modified MPC scheme in which two extra parameters are introduced is proposed based on the characteristics of convergent series in order to reduce the conservativeness.

Many real systems, such as solar thermal receivers, economic systems, and networked control systems, may experience random abrupt changes in system inputs, internal variables, and other system parameters. Uncertainties like these are best represented via stochastic models [27–29], such as fuzzy Markov jump system (MJS) in which the subsystems are modeled as fuzzy systems. Based on the approximation property of the fuzzy logic systems [30–32], fuzzy MJSs are developed for the nonlinear control systems with abrupt changes in their structure and parameters.

In this paper, the problem of MPC controller design for a class of uncertain fuzzy MJSs with partially unknown transition probabilities is addressed. This kind of system fits into a very wide range of practical dynamic systems combining nonlinear behaviors with changes or uncertainties of structure or parameters. Meanwhile, constraints, such as energy limitation, levels in tanks, flows in piping, and maximum of pH value, can be systematically included during the controller design process. The system concerned is much more complex than fuzzy systems with uncertainties or MJSs with partially unknown transition probabilities [33, 34], because here the uncertainties will consist of four levels (the system parameter uncertainty, the membership degree uncertainty, the mode uncertainty, and the transition probability uncertainty) and they are not mutually independent. Therefore, although the formulation seems similar, the results for fuzzy systems with uncertainties or MJSs with partially unknown transition probabilities cannot be directly used in this scenario. A comparison with the method in [20] (modified in [22]) is carried out by simulation on a single pendulum control problem. Due to LMIs' prevalence in convex optimization problems, especially for the cases with high order matrices, and the availability of reliable general commercial solvers, the LMI algorithm is employed to deal with the underlying optimization problems in this study. The remainder of this paper is organized as follows. The mathematical model of the concerned system is formulated and some preliminaries are given in Section 2. Section 3 is devoted to deriving the results for the controller design. Numerical examples are provided in Section 4 and this paper is concluded in Section 5.

Notation. The notation used throughout the paper is fairly standard. The superscript "T" stands for matrix transposition. $\mathbb{R}^n$ denotes the n-dimensional Euclidean space. The notation $P > 0$ (≥ 0) means that P is real symmetric and positive (semipositive) definite and $A > B$ ($\geq B$) means $A - B > 0$ (≥ 0). In symmetric block matrices or complex matrix expressions, we use an asterisk ($*$) to represent a term that is induced by symmetry and diag$\{\cdots\}$ stands for a block-diagonal matrix. I and 0 represent identity matrix and zero matrix, respectively. Matrices, if their dimensions are not explicitly stated, are assumed to be compatible for algebraic operations. $\|\cdot\|_2$ stands for the usual Euclidean norm.

2. Problem Formulation and Preliminaries

2.1. Uncertain Fuzzy MJSs with Partially Unknown Transition Probabilities. Consider the following time-varying discrete-time fuzzy Markov jump system. For each mode r_k, the fuzzy model is composed of s plant rules that can be represented as follows.

Plant Rule i. If $\theta_1(k)$ is F_1^i,..., and $\theta_d(k)$ is F_d^i, then

$$\begin{aligned} x(k+1) &= A_i(r_k,k)\,x(k) + B_i(r_k,k)\,u(k), \\ y(k) &= C_i(r_k,k)\,x(k), \quad i = 1,2,\ldots,s, \end{aligned} \tag{1}$$

where $x(k) \in \mathbb{R}^n$ is the state vector, $u(k) \in \mathbb{R}^m$ is the control input, $y(k) \in \mathbb{R}^q$ is the system output, $\theta \triangleq [\theta_1, \ldots, \theta_d]^T$ is the premise variable vector, d is the number of premise variables, and $\{F_j^i,\ i \in \mathbb{S},\ j \in \{1,2,\ldots,d\}\}$ is a fuzzy set. For simplicity, we denote $\{1,2,\ldots,s\}$ by $\mathbb{S}$. The Markov chain $\{r_k, k \geq 0\}$, taking values in a finite set $\mathcal{S} \triangleq \{1,\ldots,N\}$, governs switching among different system modes. The system matrices of the r_k mode are denoted by $[A_i(r_k,k)\ \ B_i(r_k,k)\ \ C_i(r_k,k)] \in \Omega(r_k,i)$ and the set $\Omega(r_k,i)$ is a set of polytopes

$$\begin{aligned} \Omega(r_k,i) \triangleq \mathrm{Co}\{&[A_{i1}(r_k),\ldots,C_{i1}(r_k)], \\ &[A_{i2}(r_k),\ldots,C_{i2}(r_k)] \\ &,\ldots,[A_{iL}(r_k),\ldots,C_{iL}(r_k)]\}, \end{aligned} \tag{2}$$

where Co denotes the convex hull. In other words, if $[A_i(r_k,k)\ \ B_i(r_k,k)\ \ C_i(r_k,k)] \in \Omega(r_k,i)$, then for some nonnegative $\lambda_j(i,r_k,k)$, $j \in [1,L]$ summing to one, the following holds:

$$\begin{aligned} &[A_i(r_k,k)\ \ B_i(r_k,k)\ \ C_i(r_k,k)] \\ &\quad = \sum_{j=1}^{L} \lambda_j(i,r_k,k)\,[A_{ij}(r_k)\ \ B_{ij}(r_k)\ \ C_{ij}(r_k)]. \end{aligned} \tag{3}$$

For the sake of simplicity, we denote $\{1,2,\ldots,L\}$ by $\mathbb{L}$ and $A_i(r_k,k), B_i(r_k,k), C_i(r_k,k)$, and $\lambda_j(i,r_k,k)$ by $A_{ir_k}^k, B_{ir_k}^k, C_{ir_k}^k$, and $\lambda_{ijr_k}^k$, respectively.

As commonly done in the literature, it is assumed that the premise variable vector θ does not depend on the control variables and the disturbance. The center-average defuzzification method is used as follows:

$$h_i\left[\theta\left(k\right)\right] = \frac{\prod_{j=1}^{d}\mu_{ij}\left[\theta_j\left(k\right)\right]}{\sum_{l=1}^{s}\prod_{j=1}^{d}\mu_{lj}\left[\theta_j\left(k\right)\right]} \geq 0, \quad i \in \mathbb{S},$$
$$\sum_{i=1}^{s} h_i\left[\theta\left(k\right)\right] = 1, \tag{4}$$

where $\mu_{ij}[\theta_j(k)]$ is the grade of membership of $\theta_j(k)$ in F_j^i. In what follows, we use the following notation for simplicity: $h_i^{k+l} = h_i[\theta(k+l)]$.

A more compact presentation of system (1) is given by

$$\Sigma : x\left(k+1\right) = \sum_{i=1}^{s} h_i^k\left(A_{ir_k}^k x\left(k\right) + B_{ir_k}^k u\left(k\right)\right)$$
$$y\left(k\right) = \sum_{i=1}^{s} h_i^k C_{ir_k}^k x\left(k\right), \quad r_k \in \mathcal{I}. \tag{5}$$

The process $\{r_k, k \geq 0\}$ is described by a discrete-time homogeneous Markov chain, which takes values in the finite set $\mathcal{I}$ with mode transition probabilities

$$\Pr\left(r_{k+1} = j \mid r_k = i\right) = \pi_{ij}, \tag{6}$$

where $\pi_{ij} \geq 0$, $\forall(i, j) \in \mathcal{I}\times\mathcal{I}$, and $\sum_{j=1}^{N}\pi_{ij} = 1$. For example, the transition probability matrix (TPM) can be given by

$$\Pi = \begin{bmatrix} \pi_{11} & \widehat{\pi}_{12} & \cdots & \widehat{\pi}_{1N} \\ \widehat{\pi}_{21} & \pi_{22} & \cdots & \pi_{2N} \\ \vdots & \vdots & \ddots & \vdots \\ \widehat{\pi}_{N1} & \pi_{N2} & \cdots & \widehat{\pi}_{NN} \end{bmatrix}. \tag{7}$$

The transition probabilities described above are considered to be partially available and can be divided into two parts as

$$\mathcal{I}_{\mathcal{K}}^{(i)} \triangleq \left\{j : \pi_{ij} \text{ is known}\right\}, \qquad \mathcal{I}_{\mathcal{UK}}^{(i)} \triangleq \left\{j : \widehat{\pi}_{ij} \text{ is unknown}\right\}. \tag{8}$$

In addition, if $\mathcal{I}_{\mathcal{K}}^{(i)} \neq \emptyset$, $\mathcal{I}_{\mathcal{K}}^{(i)}$ is further described as

$$\mathcal{I}_{\mathcal{K}}^{(i)} = \left\{\mathcal{K}_1, \mathcal{K}_2, \ldots, \mathcal{K}_{z_i}\right\}, \quad z_i \in \{1, 2, \ldots, N-2\}, \tag{9}$$

where $\mathcal{K}_s \in \mathbb{N}^+, s \in \{1, 2, \ldots, z_i\}$, represents the index of the sth known element in the ith row of matrix Π. And we denote

$$\pi_{\mathcal{K}}\left(i\right) \triangleq \sum_{j\in\mathcal{I}_{\mathcal{K}}^{(i)}} \pi_{ij}. \tag{10}$$

The following fuzzy control law is chosen:

$$u\left(k\right) = \sum_{p=1}^{s} h_p^k F_p\left(r_k\right) x\left(k\right), \quad r_k \in \mathcal{I}. \tag{11}$$

Under the control law, the closed-loop system of Σ is given by

$$\Sigma^C : x\left(k+1\right) = \sum_{p=1}^{s}\sum_{q=1}^{s} h_p^k h_q^k A_{pqr_k}^k x\left(k\right),$$
$$y\left(k\right) = \sum_{p=1}^{s} h_p^k C_{pr_k}^k x\left(k\right), \quad r_k \in \mathcal{I}, \tag{12}$$

where $A_{pqr_k}^k = A_{pq}(r_k, k) \triangleq A_{pr_k}^k + B_{pr_k}^k F_q(r_k)$.

For the fuzzy MJS, the following definition will be adopted in the rest of this paper.

Definition 1. The fuzzy MJS in (12) is said to be stochastically stable, if for any initial condition $x(0) = x_0, r_0 \in \mathcal{I}$, the following inequality holds:

$$\lim_{N\to\infty} E\left\{\sum_{k=0}^{N}\left\|x\left(k, x_0, r_0\right)\right\|_2^2\right\} < \infty, \tag{13}$$

where $E\{\cdot\}$ stands for the mathematical expectation.

The objective of this paper is to design a state-feedback model predictive controller such that the closed-loop system (12) is stochastically stable.

2.2. Model Predictive Control. Model predictive control (MPC) makes use of a receding horizon principle, which means that at each sampling time k, an optimization algorithm will be applied to compute a sequence of future control signals. The used performance index depends on the predicted future states of the plant $x(k+i \mid k), i \geq 0$, which can be calculated through the newly obtained measurements $x(k)$ and the predictive model. Here, we use $x(k+i \mid k)$, $y(k+i \mid k)$ as the state and output, respectively, of the plant at time $k+i$ predicted by utilizing the measurements at time k; $u(k+i \mid k)$ represents the control action moves at time $k+i$ computed by the optimization problem (14); P is the prediction horizon and M is the control horizon. In what follows, let $\mathbb{P}$ and $\mathbb{M}$ represent $\{0, 1, \ldots, P\}$ and $\{0, 1, \ldots, M\}$, respectively.

In this section, the problem formulation for MPC using the model (12) is discussed. The goal is to find an input sequence $\{u(k \mid k), u(k+1 \mid k), \ldots, u(k+M-1 \mid k)\}$ at each sampling time k which minimizes the following performance index $J(k)$:

$$\min_{u(k+i|k),\, i\in\mathbb{M}} J\left(k\right), \tag{14}$$

where

$$J\left(k\right) \triangleq E\left\{\sum_{i=0}^{P} x(k+i \mid k)^T Q x\left(k+i \mid k\right) + \sum_{j=0}^{M} u(k+j \mid k)^T R u\left(k+j \mid k\right)\right\}, \tag{15}$$

and then it can be replaced by

$$\min_{u(k+i|k),\, i\in\mathbb{M}} \max_{\left[A_{jr_k}^{k+i} \;\; B_{jr_k}^{k+i} \;\; C_{jr_k}^{k+i}\right]\in\Omega(r_k,j),\, i\in\mathbb{P},\, j\in\mathbb{S}} J(k). \tag{16}$$

The matrices $Q > 0$ and $R > 0$ are symmetric weighting matrices. In particular, we will consider the case where $P = M$, which means that the control horizon is equal to the prediction horizon. The input and output constraints focused on in this paper are Euclidean norm bounds and componentwise peak bounds, given, respectively, as

$$\begin{aligned} &\|u(k+i \mid k)\|_2 \le u_{\max}, \quad k \ge 0,\ i \in \mathbb{M}, \\ &\left|u_j(k+i \mid k)\right| \le u_{j,\max}, \quad k \ge 0,\ i \in \mathbb{M},\ j = 1, 2, \ldots, m, \\ &\left\|y(k+i \mid k)\right\|_2 \le y_{\max}, \quad k \ge 0,\ i \in \mathbb{M}. \end{aligned} \tag{17}$$

3. Model Predictive Control Using Linear Matrix Inequalities

In this section, the problem is solved by deriving an upper bound on the objective function $J(k)$ based on the state-feedback control law $u(k+i \mid k) = \sum_{p=1}^{s} h_p^k F_p(r_k) x(k+i \mid k)$, $i \in \mathbb{P}$. Therefore, via minimizing this upper bound at each sampling time k, we will obtain the sequence of control input signals.

3.1. Derivation of the Upper Bound. In this paper, the following objective function $J(k)$ is considered:

$$\min_{u(k+i|k),\, i\in\mathbb{P}} \max_{\left[A_{jr_k}^{k+i} \;\; B_{jr_k}^{k+i} \;\; C_{jr_k}^{k+i}\right]\in\Omega(r_k,j),\, i\in\mathbb{P},\, j\in\mathbb{S}} J(k), \tag{18}$$

where

$$\begin{aligned} J(k) \triangleq E\Bigg\{\sum_{i=0}^{P} \Big[&x(k+i \mid k)^T Q x(k+i \mid k) \\ &+ u(k+i \mid k)^T R u(k+i \mid k)\Big]\Bigg\}. \end{aligned} \tag{19}$$

Consider a parameter-dependent function

$$\begin{aligned} V(x(k+i \mid k)) \triangleq\ & x(k+i \mid k)^T \left(\sum_{j=1}^{s}\sum_{l=1}^{L} h_j^{k+i} \lambda_{jlr_{k+i}}^{k+i} \mathscr{P}_{jl}(r_{k+i})\right) \\ &\times x(k+i \mid k), \quad k \ge 0,\ i \in \mathbb{P}, \end{aligned} \tag{20}$$

where $\mathscr{P}_{jl}(r_{k+i}) > 0$, $V(x(0)) = 0$, and $x(k \mid k) = x(k)$ is the system state. Assume that there exists a convergent series a_k, $\sum_{k=1}^{\infty} a_k = b < \infty$ such that, at each sampling time k, the following inequality holds for all $x(k+i \mid k), u(k+i \mid k), i \in \mathbb{P}$ satisfying (12): $\forall \left[A_{ir_k}^{k+i} \;\; B_{ir_k}^{k+i} \;\; C_{ir_k}^{k+i}\right] \in \Omega(r_k, i), i \in \mathbb{P}, r_k \in \mathscr{F}$,

$$\begin{aligned} &E\{V(x(k+i+1 \mid k)) - V(x(k+i \mid k))\} \\ &\le E\Big\{-\beta\Big(x(k+i \mid k)^T Q x(k+i \mid k) \\ &\qquad + u(k+i \mid k)^T R u(k+i \mid k) - a_{k+i}\Big)\Big\}, \\ &\qquad 0 < \beta \le 1. \end{aligned} \tag{21}$$

Summing (21) from $i = 0$ to $i = P$, we get

$$E\{V(x(k+P \mid k)) - V(x(k \mid k))\} \le -\beta(J(k) - S(k)), \tag{22}$$

where $S(k) = \sum_{i=0}^{P} a_{k+i}$. Thus

$$\begin{aligned} &\max_{\left[A_{jr_k}^{k+i} \;\; B_{jr_k}^{k+i} \;\; C_{jr_k}^{k+i}\right]\in\Omega(r_k,j),\, i\in\mathbb{P},\, j\in\mathbb{S}} J(k) \\ &\le E\left\{\frac{1}{\beta}\left(V(x(k \mid k)) - V(x(k+P \mid k))\right) + S(k)\right\} \\ &\le E\left\{\frac{1}{\beta} V(x(k \mid k)) + b\right\}. \end{aligned} \tag{23}$$

Specially, when $P = M = \infty$, we will have $x(\infty \mid k) = 0$ for the robust performance objective function to be finite and hence $V(x(\infty, k)) = 0$. Summing (21) from $i = 0$ to $i = \infty$, we get

$$E\{-V(x(k \mid k))\} \le -\beta(J(k) - b). \tag{24}$$

Thus

$$\begin{aligned} &\max_{\left[A_{jr_k}^{k+i} \;\; B_{jr_k}^{k+i} \;\; C_{jr_k}^{k+i}\right]\in\Omega(r_k,j),\, i\in\mathbb{P},\, j\in\mathbb{S}} J(k) \\ &\qquad \le E\left\{\frac{1}{\beta} V(x(k \mid k)) + b\right\}. \end{aligned} \tag{25}$$

Set

$$a_{k+i} = x(k+i \mid k)^T c_{k+i} I x(k+i \mid k), \tag{26}$$

where $\sum_{k=1}^{\infty} c_k = d$. For the robust performance objective function to be finite, we will have $x(k+i \mid k) \in \left[X_{\min} \;\; X_{\max}\right]$ and $x(k+i \mid k) \le X_{\max}$; hence, $a_{k+i} \le X_{\max}^T c_{k+i} I X_{\max}$, and then $\sum_{k=1}^{\infty} a_k < X_{\max}^T \sum_{k=1}^{\infty} c_k I X_{\max} = X_{\max}^T d I X_{\max}$. Therefore, (21) can be written as

$$\begin{aligned} &E\{V(x(k+i+1 \mid k)) - V(x(k+i \mid k))\} \\ &\le E\Big\{-\beta\Big[x(k+i \mid k)^T Q x(k+i \mid k) \\ &\qquad + u(k+i \mid k)^T R u(k+i \mid k)\Big] \\ &\qquad + \beta x(k+i \mid k)^T c_{k+i} I x(k+i \mid k)\Big\}. \end{aligned} \tag{27}$$

In order to guarantee the increment $\Delta V(k) \leq 0$, $c_k I < Q$ is required. This gives an upper bound on the robust performance objective. Thus the goal of our robust MPC algorithm has been redefined to deduce, at each time step k, a state-feedback control law $u(k+i \mid k) = \sum_{p=1}^{s} h_p^{k+i} F_p(r_k) x(k+i \mid k)$ to minimize this upper bound $E\{(1/\beta)V(x(k \mid k)) + b\}$, that is to say, $E\{V(x(k \mid k))\}$.

3.2. Minimization of the Upper Bound without Constraints

Theorem 2. *Consider the closed-loop uncertain system* (12) *with the polytopic uncertainty set* $\Omega(r_k, i), r_k \in \mathcal{I}, i \in \mathbb{S}$. *Let* $x(k) = x(k \mid k)$ *be the state measured at sampling time* k. *Assume that there are no constraints on the control input and plant output. Then the state-feedback matrix* $F_p(r_{k+i})$ *in the control law* $u(k+i \mid k) = \sum_{p=1}^{s} h_p^{k+i} F_p(r_{k+i}) x(k+ik), i \in \mathbb{P}$, *that minimizes the upper bound* $E\{(1/\beta)V(x(k \mid k)) + b\}$ *on the robust performance objective function at sampling time* k *is given by*

$$F_p(r_{k+i}) = Y_p(r_{k+i}) G^{-1}, \tag{28}$$

where $G > 0$ *and* $Y_p(r_{k+i})$ *are obtained from the solution (if it exists) to the following linear objective minimization problem:*

$$\begin{aligned}
&\min_{\gamma, \mathcal{Q}, G, Y} \quad \gamma \\
&\text{subject to} \quad \begin{bmatrix} 1 & x(k \mid k)^T \\ x(k \mid k) & \mathcal{Q}_{pj}(r_k) \end{bmatrix} \geq 0, \quad \forall i \in \mathbb{P}, \\
&\qquad\qquad p \in \mathbb{S},\ j \in \mathbb{L},\ r_k \in \mathcal{I}, \\
&\begin{bmatrix} G + G^T - \mathcal{Q}_{pj}(r_{k+i}) & * & * & * \\ \widehat{M}_{pqfo}(r_{k+i}) & N_{wv} & * & * \\ \beta^{1/2}(Q - \widehat{c}_{k+i} I)^{1/2} G & 0 & \gamma I & * \\ \beta^{1/2} R^{1/2} Y_p(r_{k+i}) & 0 & 0 & \gamma I \end{bmatrix} \geq 0, \quad \forall i \in \mathbb{P}, \\
&p \geq q,\ w \in \mathbb{S},\ j, v, f \geq o \in \mathbb{L},\ r_{k+i} \in \mathcal{I},\ g \in \mathcal{I}_{\mathcal{U}\mathcal{K}}^{(r_{k+i})},
\end{aligned} \tag{29}$$

with

$$\begin{aligned}
\widehat{M}_{pqfo}(r_{k+i}) \triangleq\ & \Big[\sqrt{\pi_{r_{k+i}\mathcal{K}_1}} \widehat{E}_{pqfo}(r_{k+i}), \ldots, \\
& \sqrt{\pi_{r_{k+i}\mathcal{K}_{z_{r_{k+i}}}}} \widehat{E}_{pqfo}(r_{k+i}), \\
& \sqrt{1 - \pi_{\mathcal{K}}(r_{k+i})} \widehat{E}_{pqfo}(r_{k+i}) \Big]^T, \\
N_{wv} \triangleq\ & \operatorname{diag} \Big\{ \mathcal{Q}_{wv}(\mathcal{K}_1), \mathcal{Q}_{wv}(\mathcal{K}_2), \ldots, \\
& \mathcal{Q}_{wv}\left(\mathcal{K}_{z_{r_{k+i}}}\right), \mathcal{Q}_{wv}\left(\mathcal{K}_g\right) \Big\}, \\
& \sum_{k=1}^{\infty} \widehat{c}_k < \infty, \quad \widehat{c}_k I < Q, \\
\widehat{E}_{pqfo}(r_{k+i}) \triangleq\ & \big(A_{pfr_{k+i}} G + B_{pfr_{k+i}} Y_q(r_{k+i}) \\
& + A_{qor_{k+i}} G + B_{qor_{k+i}} Y_p(r_{k+i}) \big) \\
& \times 2^{-1}, \quad \mathcal{Q}_{pj}(r_k) > 0.
\end{aligned} \tag{30}$$

Proof. Minimization of the upper bound means minimizing $V(x(k \mid k))$ which is equivalent to

$$\begin{aligned}
&\min_{\gamma, \mathcal{P}} \quad \gamma \\
&\text{subject to} \quad x(k \mid k)^T \left(\sum_{p=1}^{s} \sum_{j=1}^{L} h_p^k \lambda_{pjr_k}^k \mathcal{P}_{pj}(r_k) \right) \\
&\qquad\qquad \times x(k \mid k) \leq \gamma.
\end{aligned} \tag{31}$$

Defining $\mathcal{Q}_{pj}(r_k) \triangleq \gamma \mathcal{P}_{pj}^{-1}(r_k) > 0$ and using Schur complements, this is equivalent to

$$\begin{aligned}
&\min_{\gamma, \mathcal{Q}} \quad \gamma \\
&\text{subject to} \quad \begin{bmatrix} 1 & x(k \mid k)^T \\ x(k \mid k) & \mathcal{Q}_{pj}(r_k) \end{bmatrix} \geq 0, \quad \forall i \in \mathbb{P}, \\
&\qquad\qquad p \in \mathbb{S},\ j \in \mathbb{L},\ r_k \in \mathcal{I}.
\end{aligned} \tag{32}$$

The parameter-dependent function V is required to satisfy (27). By substituting

$$u(k+i \mid k) = \sum_{p=1}^{s} h_p^{k+i} F_p(r_k) x(k+i \mid k), \quad i \in \mathbb{P}, \tag{33}$$

and the state-space equations in (12), inequality (27) becomes

$$\begin{aligned}
E \Bigg\{ & x(k+i \mid k)^T \sum_{p=1}^{s} \sum_{q=1}^{s} \sum_{m=1}^{s} \sum_{n=1}^{s} \sum_{w=1}^{s} \sum_{v=1}^{L} \sum_{j=1}^{L} h_p^{k+i} h_q^{k+i} h_m^{k+i} h_n^{k+i} h_w^{k+i+1} \lambda_{wvr_{k+i+1}}^{k+i+1} \lambda_{pjr_{k+i}}^{k+i} \\
& \times \Big\{ A_{pqr_{k+i}}^T \cdot \mathcal{P}_{wv}(r_{k+i+1}) A_{mnr_{k+i}} - \mathcal{P}_{pj}(r_{k+i})
\end{aligned}$$

$$
\begin{aligned}
&+\beta F_p(r_{k+i})^T R F_q(r_{k+i}) + \beta Q - \beta \widehat{c}_{k+i} I \Big\} \\
&\times x(k+i \mid k) \Bigg\} \\
= x(k+i \mid k)^T &\sum_{p=1}^{s}\sum_{q=1}^{s}\sum_{m=1}^{s}\sum_{n=1}^{s}\sum_{w=1}^{s}\sum_{v=1}^{L}\sum_{j=1}^{L}\sum_{r_{k+i+1}=1}^{N} h_p^{k+i} h_q^{k+i} h_m^{k+i} h_n^{k+i} h_w^{k+i+1} \lambda_{wvr_{k+i+1}}^{k+i+1} \lambda_{pjr_{k+i}}^{k+i} \\
&\times \Big\{ A_{pqr_{k+i}}^T \cdot \pi_{r_{k+i} r_{k+i+1}} \mathscr{P}_{wv}(r_{k+i+1}) A_{mnr_{k+i}} \\
&- \mathscr{P}_{pj}(r_{k+i}) + \beta F_p(r_{k+i})^T R F_q(r_{k+i}) \\
&+\beta Q - \beta \widehat{c}_{k+i} I \Big\} x(k+i \mid k) \le 0.
\end{aligned} \tag{34}
$$

This is equivalent to

$$
\begin{aligned}
&\sum_{p=1}^{s}\sum_{q=1}^{s}\sum_{m=1}^{s}\sum_{n=1}^{s}\sum_{w=1}^{s}\sum_{v=1}^{L}\sum_{j=1}^{L}\sum_{r_{k+i+1}=1}^{N} h_p^{k+i} h_q^{k+i} h_m^{k+i} h_n^{k+i} h_w^{k+i+1} \lambda_{wvr_{k+i+1}}^{k+i+1} \lambda_{pjr_{k+i}}^{k+i} \\
&\times \Big\{ A_{pqr_{k+i}}^T \cdot \pi_{r_{k+i} r_{k+i+1}} \mathscr{P}_{wv}(r_{k+i+1}) A_{mnr_{k+i}} \\
&- \mathscr{P}_{pj}(r_{k+i}) + \beta F_p(r_{k+i})^T R F_q(r_{k+i}) \\
&+\beta Q - \beta \widehat{c}_{k+i} I \Big\} \\
= &\sum_{p=1}^{s}\sum_{q=1}^{s}\sum_{m=1}^{s}\sum_{n=1}^{s}\sum_{w=1}^{s}\sum_{v=1}^{L}\sum_{j=1}^{L}\sum_{r_{k+i+1}=1}^{N} \frac{1}{4} h_p^{k+i} h_q^{k+i} h_m^{k+i} h_n^{k+i} h_w^{k+i+1} \lambda_{wvr_{k+i+1}}^{k+i+1} \lambda_{pjr_{k+i}}^{k+i} \\
&\times \Big\{ \left(A_{pqr_{k+i}}^T + A_{qpr_{k+i}}^T \right) \cdot \pi_{r_{k+i} r_{k+i+1}} \mathscr{P}_{wv}(r_{k+i+1}) \\
&\times \left(A_{mnr_{k+i}} + A_{nmr_{k+i}} \right) - 4\mathscr{P}_{pj}(r_{k+i}) \\
&+4\beta F_p(r_{k+i})^T R F_q(r_{k+i}) + 4\beta Q - 4\beta \widehat{c}_{k+i} I \Big\} \\
= &\sum_{p=1}^{s}\sum_{q=1}^{s}\sum_{m=1}^{s}\sum_{n=1}^{s}\sum_{w=1}^{s}\sum_{v=1}^{L}\sum_{j=1}^{L}\sum_{r_{k+i+1}=1}^{N} \frac{1}{8} h_p^{k+i} h_q^{k+i} h_m^{k+i} h_n^{k+i} h_w^{k+i+1} \lambda_{wvr_{k+i+1}}^{k+i+1} \lambda_{pjr_{k+i}}^{k+i} \\
&\times \Big\{ \left(A_{pqr_{k+i}}^T + A_{qpr_{k+i}}^T \right) \cdot \pi_{r_{k+i} r_{k+i+1}} \mathscr{P}_{wv}(r_{k+i+1}) \\
&\times \left(A_{mnr_{k+i}} + A_{nmr_{k+i}} \right) + \left(A_{mnr_{k+i}}^T + A_{nmr_{k+i}}^T \right) \\
&\times \mathscr{P}_{wv}(r_{k+i+1}) \left(A_{pqr_{k+i}} + A_{qpr_{k+i}} \right) \\
&- 8\mathscr{P}_{pj}(r_{k+i}) + 4\beta F_p(r_{k+i})^T R F_q(r_{k+i}) \\
&+ 4\beta F_q(r_{k+i})^T R F_p(r_{k+i}) + 8\beta Q - 8\beta \widehat{c}_{k+i} I \Big\} \\
\le &\sum_{p=1}^{s}\sum_{q=1}^{s}\sum_{m=1}^{s}\sum_{n=1}^{s}\sum_{w=1}^{s}\sum_{v=1}^{L}\sum_{j=1}^{L}\sum_{r_{k+i+1}=1}^{N} \frac{1}{8} h_p^{k+i} h_q^{k+i} h_m^{k+i} h_n^{k+i} h_w^{k+i+1} \lambda_{wvr_{k+i+1}}^{k+i+1} \lambda_{pjr_{k+i}}^{k+i} \\
&\times \Big\{ \left(A_{pqr_{k+i}}^T + A_{qpr_{k+i}}^T \right) \cdot \pi_{r_{k+i} r_{k+i+1}} \mathscr{P}_{wv}(r_{k+i+1})
\end{aligned}
$$

$$\times \left(A_{pqr_{k+i}} + A_{qpr_{k+i}}\right) + \left(A^T_{mnr_{k+i}} + A^T_{nmr_{k+i}}\right)$$
$$\times \mathscr{P}_{wv}\left(r_{k+i+1}\right)\left(A_{mnr_{k+i}} + A_{nmr_{k+i}}\right)$$
$$- 8\mathscr{P}_{pj}\left(r_{k+i}\right) + 4\beta F_p(r_{k+i})^T RF_p\left(r_{k+i}\right)$$
$$+4\beta F_q(r_{k+i})^T RF_q\left(r_{k+i}\right) + 8\beta Q - 8\beta\widehat{c}_{k+i}I\Big\}$$

$$= \sum_{p=1}^{s}\sum_{q=1}^{s}\sum_{m=1}^{s}\sum_{n=1}^{s}\sum_{w=1}^{s}\sum_{v=1}^{L}\sum_{j=1}^{L}\sum_{r_{k+i+1}=1}^{N}\frac{1}{4}h_p^{k+i}h_q^{k+i}h_m^{k+i}h_n^{k+i}h_w^{k+i+1}\lambda^{k+i+1}_{wvr_{k+i+1}}\lambda^{k+i}_{pjr_{k+i}}$$
$$\times \Big\{\left(A^T_{pqr_{k+i}} + A^T_{qpr_{k+i}}\right)\cdot \pi_{r_{k+i}r_{k+i+1}}\mathscr{P}_{wv}\left(r_{k+i+1}\right)$$
$$\times \left(A_{pqr_{k+i}} + A_{qpr_{k+i}}\right) - 4\mathscr{P}_{pj}\left(r_{k+i}\right)$$
$$+ 4\beta F_p(r_{k+i})^T RF_p\left(r_{k+i}\right) + 4\beta Q - 4\beta\widehat{c}_{k+i}I\Big\}$$

$$= \sum_{p=1}^{s}\sum_{q=1}^{s}\sum_{m=1}^{s}\sum_{n=1}^{s}\sum_{w=1}^{s}\sum_{v=1}^{L}\sum_{j=1}^{L}\frac{1}{4}h_p^{k+i}h_q^{k+i}h_m^{k+i}h_n^{k+i}h_w^{k+i+1}\lambda^{k+i+1}_{wvr_{k+i+1}}\lambda^{k+i}_{pjr_{k+i}}$$
$$\times \Big\{\left(A^T_{pqr_{k+i}} + A^T_{qpr_{k+i}}\right)$$
$$\cdot \left[\sum_{g\in\mathscr{F}_{\mathscr{K}}^{(r_{k+i})}}\pi_{r_{k+i}g}\mathscr{P}_{wv}(g) + \sum_{l\in\mathscr{F}_{\mathscr{U}\mathscr{K}}^{(r_{k+i})}}\widehat{\pi}_{r_{k+i}l}\mathscr{P}_{wv}(l)\right]$$
$$\times \left(A_{pqr_{k+i}} + A_{qpr_{k+i}}\right) - 4\mathscr{P}_{pj}\left(r_{k+i}\right)$$
$$+4\beta F_p(r_{k+i})^T RF_p\left(r_{k+i}\right) + 4\beta Q - 4\beta\widehat{c}_{k+i}I\Big\}$$

$$= \sum_{p=1}^{s}\sum_{q=1}^{s}\sum_{m=1}^{s}\sum_{n=1}^{s}\sum_{w=1}^{s}\sum_{v=1}^{L}\sum_{j=1}^{L}\frac{1}{4}h_p^{k+i}h_q^{k+i}h_m^{k+i}h_n^{k+i}h_w^{k+i+1}\lambda^{k+i+1}_{wvr_{k+i+1}}\lambda^{k+i}_{pjr_{k+i}}$$
$$\times \Bigg\{\left(A^T_{pqr_{k+i}} + A^T_{qpr_{k+i}}\right)\cdot \Bigg[\sum_{g\in\mathscr{F}_{\mathscr{K}}^{(r_{k+i})}}\pi_{r_{k+i}g}\mathscr{P}_{wv}(g)$$
$$+\left(1-\pi_{\mathscr{K}}\left(r_{k+i}\right)\right)\sum_{l\in\mathscr{F}_{\mathscr{U}\mathscr{K}}^{(r_{k+i})}}\frac{\widehat{\pi}_{r_{k+i}l}}{1-\pi_{\mathscr{K}}\left(r_{k+i}\right)}\mathscr{P}_{wv}(l)\Bigg]$$
$$\times \left(A_{pqr_{k+i}} + A_{qpr_{k+i}}\right) - 4\mathscr{P}_{pj}\left(r_{k+i}\right)$$
$$+4\beta F_p(r_{k+i})^T RF_p\left(r_{k+i}\right) + 4\beta Q - 4\beta\widehat{c}_{k+i}I\Bigg\}$$

$$= \sum_{p=1}^{s}\sum_{q=1}^{s}\sum_{m=1}^{s}\sum_{n=1}^{s}\sum_{w=1}^{s}\sum_{v=1}^{L}\sum_{j=1}^{L}\sum_{l\in\mathscr{F}_{\mathscr{U}\mathscr{K}}^{(r_{k+i})}}\frac{\widehat{\pi}_{r_{k+i}l}}{1-\pi_{\mathscr{K}}\left(r_{k+i}\right)}$$
$$\times h_p^{k+i}h_q^{k+i}h_m^{k+i}h_n^{k+i}h_w^{k+i+1}\lambda^{k+i+1}_{wvr_{k+i+1}}\lambda^{k+i}_{pjr_{k+i}}$$

$$\cdot \left\{ \frac{A_{pqr_{k+i}}^T + A_{qpr_{k+i}}^T}{2} \left[\sum_{g \in \mathcal{F}_{\mathcal{K}}^{(r_{k+i})}} \pi_{r_{k+i}g} \mathcal{P}_{wv}(g) + \left(1 - \pi_{\mathcal{K}}(r_{k+i})\right) \mathcal{P}_{wv}(l) \right] \frac{A_{pqr_{k+i}} + A_{qpr_{k+i}}}{2} - \mathcal{P}_{pj}(r_{k+i}) + \beta F_p(r_{k+i})^T \times R F_p(r_{k+i}) + \beta Q - \beta \widehat{c}_{k+i} I \right\}. \tag{35}$$

Then, (34) is satisfied for all $i \in \mathbb{P}$ if

$$\frac{A_{pqr_{k+i}}^T + A_{qpr_{k+i}}^T}{2} \left[\sum_{g \in \mathcal{F}_{\mathcal{K}}^{(r_{k+i})}} \pi_{r_{k+i}g} \mathcal{P}_{wv}(g) + \left(1 - \pi_{\mathcal{K}}(r_{k+i})\right) \mathcal{P}_{wv}(l) \right] \times \frac{A_{pqr_{k+i}} + A_{qpr_{k+i}}}{2} - \mathcal{P}_{pj}(r_{k+i}) + \beta F_p(r_{k+i})^T R F_p(r_{k+i}) + \beta Q - \beta \widehat{c}_{k+i} I \le 0, \tag{36}$$

where $\widehat{c}_k$ is the minimum term of $c_{k+i}, i \in [0 \;\; P]$. Substituting $\mathcal{P}_{pq}(r_k) = \gamma \mathcal{Q}_{pq}^{-1}(r_k), \mathcal{Q}_{pq}(r_k) > 0$, using Schur complements, and then pre- and postmultiplying the above inequality by $\mathrm{diag}\{\mathcal{Q}_{pj}(r_{k+i}), I, I, I\}$ and $\mathrm{diag}\{\mathcal{Q}_{pj}(r_{k+i}), I, I, I\}$, we can see that this is equivalent to

$$\begin{bmatrix} \mathcal{Q}_{pj}(r_{k+i}) & * & * & * \\ M_{pq}(r_{k+i}) & N_{wv} & * & * \\ \beta^{1/2}(Q - \widehat{c}_{k+i} I)^{1/2} \mathcal{Q}_{pj}(r_{k+i}) & 0 & \gamma I & * \\ \beta^{1/2} R^{1/2} F_p(r_{k+i}) \mathcal{Q}_{pj}(r_{k+i}) & 0 & 0 & \gamma I \end{bmatrix} \ge 0, \tag{37}$$

$$\forall i \in \mathbb{P}, p, q, w \in \mathbb{S}, j, \nu \in \mathbb{L}, r_{k+i} \in \mathcal{I}, g \in \mathcal{F}_{\mathcal{UK}}^{(r_{k+i})},$$

with

$$\begin{aligned} M_{pq}(r_{k+i}) &\triangleq \left[\sqrt{\pi_{r_{k+i}\mathcal{K}_1}} E_{pq}(r_{k+i}), \ldots, \sqrt{\pi_{r_{k+i}\mathcal{K}_{z_{r_{k+i}}}}} E_{pq}(r_{k+i}), \sqrt{1 - \pi_{\mathcal{K}}(r_{k+i})} E_{pq}(r_{k+i}) \right]^T, \\ N_{wv} &\triangleq \mathrm{diag}\left\{ \mathcal{Q}_{wv}(\mathcal{K}_1), \mathcal{Q}_{wv}(\mathcal{K}_2), \ldots, \mathcal{Q}_{wv}\left(\mathcal{K}_{z_{r_{k+i}}}\right), \mathcal{Q}_{wv}\left(\mathcal{K}_g\right) \right\}, \\ E_{pq}(r_{k+i}) &\triangleq \left(\left[A_{pr_{k+i}} + B_{pr_{k+i}} F_q(r_{k+i}) \right] \mathcal{Q}_{pj}(r_{k+i}) + \left[A_{qr_{k+i}} + B_{qr_{k+i}} F_p(r_{k+i}) \right] \mathcal{Q}_{pj}(r_{k+i}) \right) \times 2^{-1}. \end{aligned} \tag{38}$$

Inequality (37) is affine in $[A_p(k+i, r_k) \;\; B_p(k+i, r_k)]$. Following the logic of de Oliveira, Bernussou and Geromel [35], and Cuzzola et al. [20], (37) is satisfied for all

$$\begin{aligned} \begin{bmatrix} A_{pr_k}^{k+i} & B_{pr_k}^{k+i} \end{bmatrix} &\in \Omega_p(r_k) \\ &= \mathrm{Co}\left\{ [A_{p1}(r_k) \;\; B_{p1}(r_k)], [A_{p2}(r_k) \;\; B_{p2}(r_k)], \ldots, [A_{pL}(r_k) \;\; B_{pL}(r_k)] \right\}, \end{aligned} \tag{39}$$

if and only if there exist $G > 0, Y_p(r_k) = F_p(r_k)G$, and a positive γ such that

$$\begin{bmatrix} G + G^T - \mathcal{Q}_{pj}(r_{k+i}) & * & * & * \\ \widehat{M}_{pqfo}(r_{k+i}) & N_{wv} & * & * \\ \beta^{1/2}(Q - \widehat{c}_{k+i} I)^{1/2} G & 0 & \gamma I & * \\ \beta^{1/2} R^{1/2} Y_p(r_{k+i}) & 0 & 0 & \gamma I \end{bmatrix} \ge 0, \tag{40}$$

$$\forall i \in \mathbb{P}, \; p \ge q, w \in \mathbb{S}, j, \nu, f \ge o \in \mathbb{L}, \; r_{k+i} \in \mathcal{I}, g \in \mathcal{F}_{\mathcal{UK}}^{(r_{k+i})},$$

with

$$\begin{aligned}\widehat{M}_{pqfo}(r_{k+i}) \triangleq & \left[\sqrt{\pi_{r_{k+i}\mathscr{K}_1}}\widehat{E}_{pqfo}(r_{k+i}),\ldots,\right.\\ & \sqrt{\pi_{r_{k+i}\mathscr{K}_{z_{r_{k+i}}}}}\widehat{E}_{pqfo}(r_{k+i}),\\ & \left.\sqrt{1-\pi_{\mathscr{K}}(r_{k+i})}\widehat{E}_{pqfo}(r_{k+i})\right]^T,\\ N_{wv} \triangleq & \operatorname{diag}\left\{\mathcal{Q}_{wv}(\mathscr{K}_1),\mathcal{Q}_{wv}(\mathscr{K}_2),\ldots,\right.\\ & \left.\mathcal{Q}_{wv}\left(\mathscr{K}_{z_{r_{k+i}}}\right),\mathcal{Q}_{wv}\left(\mathscr{K}_g\right)\right\},\\ \widehat{E}_{pqfo}(r_{k+i}) \triangleq & \left(A_{pfr_{k+i}}G+B_{pfr_{k+i}}Y_q(r_{k+i})\right.\\ & \left.+A_{qor_{k+i}}G+B_{qor_{k+i}}Y_p(r_{k+i})\right)\\ & \times 2^{-1}.\end{aligned} \tag{41}$$

The feedback matrix is then given by $F_p(r_{k+i}) = Y_p(r_{k+i})G^{-1}$. □

Remark 3. Based on the above analysis, we can see that the choice of control horizon M can amount to the choice of series $\widehat{c}_k$. That is, given a constant control horizon M, we can construct some infinite convergent series whose corresponding series $\widehat{c}_k$ possess some properties, such as $\widehat{c}_k = 1/(k+1)^2$. Therefore, we will discuss neither the control horizon M nor the predictive horizon P which is supposed to be equal to M.

Remark 4. In particular, when the control horizon $M = \infty$, the conditions for the above derivation can be satisfied if and only if the series $\widehat{c}_k = 0, k \geq 0$. Then it follows that the method is equivalent to the approach in [20] (modified in [22]).

3.3. Minimization of the Upper Bound with Input and Output Constraints

Theorem 5. *Consider the closed-loop uncertain system* (12) *with the polytopic uncertainty set* $\Omega(r_k, p), p \in \mathbb{S}, r_k \in \mathscr{I}$. *Let* $x(k) = x(k \mid k)$ *be the state measured at sampling time* k, *and* $\mathcal{Q}_{pj}(r_k) > 0$, *for all* $p \in \mathbb{S}, j \in \mathbb{L}, r_k \in \mathscr{I}$. *The constraints on the control input and plant output in the form of* (17) *can be transferred into problems expressed by the following linear matrix inequalities, respectively:*

$$\begin{bmatrix} u_{\max}^2 I & Y_p(r_{k+i}) \\ Y_p^T(r_{k+i}) & G+G^T-\mathcal{Q}_{pj}(r_{k+i}) \end{bmatrix} \geq 0, \quad \forall p \in \mathbb{S},\ j \in \mathbb{L},\ r_{k+i} \in \mathscr{I}, \tag{42}$$

$$\begin{bmatrix} X & Y_p(r_{k+i}) \\ Y_p^T(r_k+i) & G+G^T-\mathcal{Q}_{pj}(r_{k+i}) \end{bmatrix} \geq 0, \quad \forall p \in \mathbb{S},\ j \in \mathbb{L},\ r_{k+i} \in \mathscr{I}, \tag{43}$$

with $X_{dd} \leq u_{d,\max}^2, d = 1, 2, \ldots, m$,

$$\begin{bmatrix} G+G^T-\mathcal{Q}_{pj}(r_{k+i}) & * \\ C_{pjr_{k+i}}\left(A_{pjr_{k+i}}G+B_{pjr_{k+i}}Y_q(r_{k+i})\right) & y_{\max}^2 I \end{bmatrix} \geq 0, \quad \forall p, q \in \mathbb{S},\ j \in \mathbb{L},\ r_{k+i} \in \mathscr{I}. \tag{44}$$

Proof. Following [36], we have

$$\begin{aligned}&\max_{i\geq 0}\|u(k+i \mid k)\|_2^2\\ &= \max_{i\geq 0}\left\|\sum_{p=1}^{s}h_p^{k+i}F_p(r_{k+i})\,x(k+i \mid k)\right\|_2^2\\ &= \max_{i\geq 0}\left\|\sum_{p=1}^{s}h_p^{k+i}Y_p(r_{k+i})G^{-1}x(k+i \mid k)\right\|_2^2\\ &\leq \max_{z\in\xi}\left\|\sum_{p=1}^{s}h_p^{k+i}Y_p(r_{k+i})G^{-1}z\right\|_2^2\\ &= \overline{\sigma}_{z\in\xi}\left(\sum_{p=1}^{s}\sum_{q=1}^{s}h_p^{k+i}h_q^{k+i}z^TG^{-T}\right.\\ &\qquad\left.\times Y_p^T(r_{k+i})Y_q(r_{k+i})G^{-1}z\right)\\ &= \overline{\sigma}_{z\in\xi}\left(\sum_{p=1}^{s}\sum_{q=1}^{s}\frac{1}{2}h_p^{k+i}h_q^{k+i}z^TG^{-T}\right.\\ &\qquad\times\left[Y_p^T(r_{k+i})Y_q(r_{k+i})\right.\\ &\qquad\left.\left.+Y_q^T(r_{k+i})Y_p(r_{k+i})\right]G^{-1}z\right)\\ &\leq \overline{\sigma}_{z\in\xi}\left(\sum_{p=1}^{s}h_p^{k+i}z^TG^{-T}Y_p^T(r_{k+i})Y_p(r_{k+i})G^{-1}z\right)\\ &= \overline{\sigma}_{z\in\xi}\left(\sum_{p=1}^{s}\sum_{j=1}^{L}h_p^{k+i}\lambda_{pjr_{k+i}}^{k+i}\,z^T\mathcal{Q}_{pj}^{-1/2}\mathcal{Q}_{pj}^{1/2}G^{-T}Y_p^T(r_{k+i})\right.\\ &\qquad\left.\times Y_p(r_{k+i})G^{-1}\mathcal{Q}_{pj}^{1/2}\mathcal{Q}_{pj}^{-1/2}z\right)\\ &\leq \overline{\sigma}\left(\mathcal{Q}_{pj}^{1/2}G^{-T}Y_p^T(r_{k+i})Y_p(r_{k+i})G^{-1}\mathcal{Q}_{pj}^{1/2}\right).\end{aligned} \tag{45}$$

By virtue of Schur complements, we have $\|u(k+i \mid k)\|_2 \leq u_{\max}, k, i \geq 0$, if

$$\begin{bmatrix} u_{\max}^2 I & Y_p(r_{k+i}) \\ Y_p^T(r_{k+i}) & G\mathcal{Q}_{pj}G^T \end{bmatrix} \geq 0, \quad \forall p \in \mathbb{S},\ j \in \mathbb{L},\ r_{k+i} \in \mathscr{I}. \tag{46}$$

Using the similar logic in [35], (46) is proved equivalent to (42). The proof of (43)-(44), which can be achieved by an analogous argument, is omitted for the sake of brevity. □

Remark 6. The obtained theorems can be easily reduced to simple situations, for example, fuzzy systems with uncertainties and Markov jump systems, and can be solved via commercial solvers such as LMITOOL, YALMIP, and GloptiPoly.

4. Numerical Simulation

In this section, we present a numerical example that clearly illustrates the improvement obtained with Theorem 2. We will compare under different situations the improved method with the approach in [20] (modified in [22]) which can be seen as $\widehat{c}_k = 0, k > 0$ and $\beta = 1$. Consider the single pendulum system:

$$\begin{aligned} \dot{x}_1(t) &= x_2(t), \\ \dot{x}_2(t) &= -c_{1,l}\sin\left(x_1(t)\right) + c_{2,l}x_2(t) + u(t) + 0.1w(t), \end{aligned} \tag{47}$$

where $x_1(t)$ is the angular displacement, $x_2(t)$ is the angular velocity, $u(t)$ is the control torque, $w(t)$ is the disturbance, and $c_{1,l}$ and $c_{2,l}$ are jump parameters with values $c_{1,1} = 1, c_{1,2} = 2$, $c_{1,3} = 0.5$, $c_{2,1} = 1$, $c_{2,2} = 0.5$, and $c_{2,3} = 2$. The angular displacement $x_1(t)$ is assumed to vary in the intervals $[-\pi/2, \pi/2]$. This system can be represented as the following discrete-time fuzzy model with partly unknown transition probabilities:

$$\Pi = \begin{bmatrix} * & 0.4 & * \\ 0.9 & * & * \\ 0.25 & 0.4 & 0.35 \end{bmatrix}. \tag{48}$$

Set $x(k) = \left[x_1(k) \;\; x_2(k)\right]^T$, and choose the membership functions as

$$\begin{aligned} h_1\left(x_1(k)\right) &= \frac{4x_1^2(k)}{\pi^2}, \\ h_2\left(x_1(k)\right) &= 1 - h_1\left(x_1(k)\right). \end{aligned} \tag{49}$$

For the sake of simplicity, we use two T-S fuzzy rules to approximate this system.

Plant Rule 1. If $x_1(k)$ is about $\pi/2$, then

$$\begin{aligned} x(k+1) &= A_1\left(r_k\right)x(k) + B_1\left(r_k\right)u(k), \\ y(k) &= C_1\left(r_k\right)x(k). \end{aligned} \tag{50}$$

Plant Rule 2. If $x_1(k)$ is about $-\pi/2$, then

$$\begin{aligned} x(k+1) &= A_2\left(r_k\right)x(k) + B_2\left(r_k\right)u(k), \\ y(k) &= C_2\left(r_k\right)x(k). \end{aligned} \tag{51}$$

where

$$\begin{aligned} &A_l\left(r_k\right) \in \Omega\left(l, r_k\right), \qquad B_l\left(r_k\right) = \left[0 \;\; T\right]^T, \\ &C_l\left(r_k\right) = \left[1 \;\; 1\right], \quad l = 1, 2, \; r_k = 1, 2, 3, \\ &\Omega(1,1) = \left\{\begin{bmatrix} 1 & T \\ -0.4530T & 1 + 0.7116T \end{bmatrix}, \right. \\ &\qquad \left. \begin{bmatrix} 1 + 0.2T & T \\ -0.3530T & 1 + 0.7116T \end{bmatrix}\right\}, \\ &\Omega(2,1) = \left\{\begin{bmatrix} 1 & T \\ -T & 1 + T \end{bmatrix}, \begin{bmatrix} 1 + 0.2T & T \\ -0.9T & 1 + T \end{bmatrix}\right\}, \\ &\Omega(1,2) = \left\{\begin{bmatrix} 1 & T \\ -0.9060T & 1 + 0.0768T \end{bmatrix}, \right. \\ &\qquad \left. \begin{bmatrix} 1 + 0.2T & T \\ -0.8060T & 1 + 0.0768T \end{bmatrix}\right\}, \\ &\Omega(2,2) = \left\{\begin{bmatrix} 1 & T \\ -2T & 1 + 0.5T \end{bmatrix}, \right. \\ &\qquad \left. \begin{bmatrix} 1 + 0.2T & T \\ -1.9T & 1 + 0.5T \end{bmatrix}\right\}, \\ &\Omega(1,3) = \left\{\begin{bmatrix} 1 & T \\ -0.2265T & 1 + 1.8558T \end{bmatrix}, \right. \\ &\qquad \left. \begin{bmatrix} 1 + 0.2T & T \\ -0.1265T & 1 + 1.8558T \end{bmatrix}\right\}, \\ &\Omega(2,3) = \left\{\begin{bmatrix} 1 & T \\ -0.5T & 1 + 2T \end{bmatrix}, \right. \\ &\qquad \left. \begin{bmatrix} 1 + 0.2T & T \\ -0.4T & 1 + 2T \end{bmatrix}\right\}. \end{aligned} \tag{52}$$

Our purpose here is to illustrate the advantages of the proposed method by comparing the optimal parameter γ for different situations. First of all, supposing $\widehat{c}_k = 1/(k+1)^2$, $\beta = 0.5$, and the initial states $x(0) = [3\pi/8; 0.5]$, the steady-state responses of the closed-loop fuzzy MJS with input constraints $\|u(k+i \mid k)\|_2 \le 3, k > 0, i \in \mathbb{M}$, are shown in Figure 1. Meanwhile, the optimal results of γ compared for different initial conditions are shown in Table 1. One may note that the average values of γ become much smaller when the additional parameters $\widehat{c}_k$ and β are introduced. Then, assuming initial states $x(0) = [\pi/4; 0.5]$, $\beta = 0.5$, we can obtain the corresponding values of γ for different $\widehat{c}_k$ listed in Table 2. In the same way, by assuming initial states $x(0) = [\pi/4; 0.5]$, $\widehat{c}_k = 1/(k+1)^2$, the information about γ for different values of β is given in Table 3. It is easy to observe from Tables 2 and 3 that the optimal performance is closely related to the two parameters.

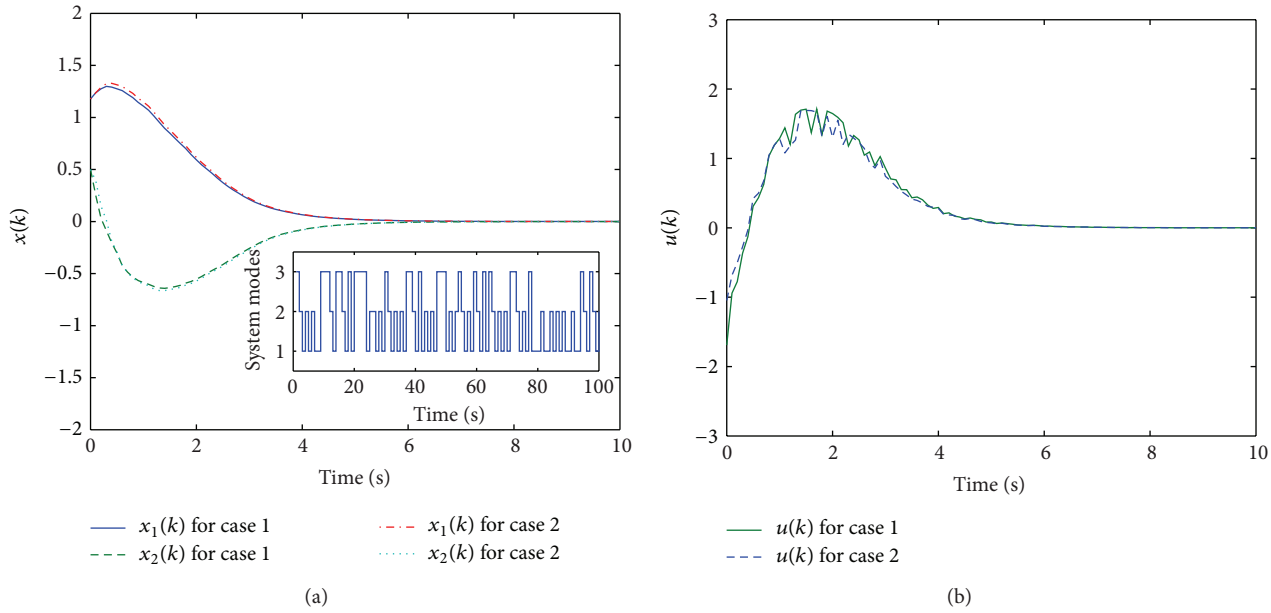

Figure 1: (a) State response of MJS system with $x(0) = [3\pi/8; 0.5]$ and $\widehat{c}_k = 1/(k+1)^2$, and $\beta = 0.5$ for case 1, $\widehat{c}_k = 0$, $\beta = 1$ for case 2. (b) Input signals obtained based on Theorem 2.

Table 1: The value of γ for different initial conditions with constraints.

Initial condition	Average value of γ with $\widehat{c}_k = 1/(k+1)^2, k > 0, \beta = 0.5$	Average value of γ with $\widehat{c}_k = 0, k > 0, \beta = 1$
$[\pi/16; 1]$	0.5895	1.2517
$[\pi/4; 1]$	3.1578	6.8014
$[\pi/8; 0.5]$	0.2619	0.5568
$[\pi/4; 0.5]$	1.0452	2.2344
$[3\pi/8; 0.5]$	2.8360	6.1012

Table 2: The value of γ for different $\widehat{c}_k, k > 0$ with constraints.

Parameter $\widehat{c}_k$	$\widehat{c}_k = 1/(k+1)^{1.1}$	$\widehat{c}_k = 1/(k+1)^{1.5}$	$\widehat{c}_k = 1/(k+1)^2$	$\widehat{c}_k = 1/(k+1)^{2.5}$	$\widehat{c}_k = 1/(k+1)^3$
Average value of γ with $x(0) = [\pi/4; 0.5], \beta = 0.5$	0.9066	0.9924	1.0452	1.2189	1.2220

Table 3: The value of γ for different β with constraints.

Parameter β	$\beta = 0.1$	$\beta = 0.3$	$\beta = 0.5$	$\beta = 0.7$	$\beta = 0.9$
Average value of γ with $x(0) = [\pi/4; 0.5], \widehat{c}_k = 1/(k+1)^2$	0.2508	0.6271	1.0452	1.5800	1.8782

5. Conclusion

In this paper, the problem of controller design based on MPC algorithm for uncertain systems is discussed. A relaxed scheme which has less conservativeness than traditional approaches is derived through introducing two additional parameters. Based on this scheme, a new set of criteria for model predictive controller design is obtained based on the fuzzy Markov jump system with partially unknown TPMs in an arbitrarily large horizon. A practical example is presented to show the effectiveness and applicability of the developed method. It is expected that the methods and ideas behind the paper could be extended to other systems or issues, such as filter design for the underlying system.

Conflict of Interests

The authors declare that there is no conflict of interests regarding the publication of this paper.

References

[1] E. F. Camacho, *Model Predictive Control*, Springer, New York, NY, USA, 1998.

[2] E. G. Gilbert and K. T. Tan, "Linear systems with state and control constraints: the theory and application of maximal output admissible sets," *IEEE Transactions on Automatic Control*, vol. 36, no. 9, pp. 1008–1020, 1991.

[3] S. S. Keerthi and E. G. Gilbert, "Optimal infinite-horizon feedback laws for a general class of constrained discrete-time systems: stability and moving-horizon approximations," *Journal of Optimization Theory and Applications*, vol. 57, no. 2, pp. 265–293, 1988.

[4] J. B. Rawlings and K. R. Muske, "The stability of constrained receding horizon control," *IEEE Transactions on Automatic Control*, vol. 38, no. 10, pp. 1512–1516, 1993.

[5] G. Franzè, "A nonlinear sum-of-squares model predictive control approach," *IEEE Transactions on Automatic Control*, vol. 55, no. 6, pp. 1466–1471, 2010.

[6] S. L. de Oliveira Kothare and M. Morari, "Contractive model predictive control for constrained nonlinear systems," *IEEE Transactions on Automatic Control*, vol. 45, no. 6, pp. 1053–1071, 2000.

[7] L. Magni and R. Scattolini, "Stabilizing model predictive control of nonlinear continuous time systems," *Annual Reviews in Control*, vol. 28, no. 1, pp. 1–11, 2004.

[8] P. Mhaskar, N. H. El-Farra, and P. D. Christofides, "Robust predictive control of switched systems: satisfying uncertain schedules subject to state and control constraints," *International Journal of Adaptive Control and Signal Processing*, vol. 22, no. 2, pp. 161–179, 2008.

[9] J. Hu, Z. Wang, H. Gao, and L. K. Stergioulas, "Extended Kalman filtering with stochastic nonlinearities and multiple missing measurements," *Automatica*, vol. 48, no. 9, pp. 2007–2015, 2012.

[10] G. Huang and S. Wang, "Use of uncertainty polytope to describe constraint processes with uncertain time-delay for robust model predictive control applications," *ISA Transactions*, vol. 48, no. 4, pp. 503–511, 2009.

[11] E. F. Camacho, D. R. Ramirez, D. Limon et al., "Model predictive control techniques for hybrid systems," *Annual Reviews in Control*, vol. 34, no. 1, pp. 21–31, 2010.

[12] J. Hu, Z. Wang, H. Gao, and L. K. Stergioulas, "Probability-guaranteed H_∞ finite-horizon filtering for a class of nonlinear time-varying systems with sensor saturations," *Systems & Control Letters*, vol. 61, no. 4, pp. 477–484, 2012.

[13] W. Al-Gherwi, H. Budman, and A. Elkamel, "Robust distributed model predictive control: a review and recent developments," *Canadian Journal of Chemical Engineering*, vol. 89, no. 5, pp. 1176–1190, 2011.

[14] J. L. Garriga and M. Soroush, "Model predictive control tuning methods: a review," *Industrial and Engineering Chemistry Research*, vol. 49, no. 8, pp. 3505–3515, 2010.

[15] H. J. Ferreau, H. G. Bock, and M. Diehl, "An online active set strategy to overcome the limitations of explicit MPC," *International Journal of Robust and Nonlinear Control*, vol. 18, no. 8, pp. 816–830, 2008.

[16] G. Pannocchia, J. B. Rawlings, and S. J. Wright, "Fast, large-scale model predictive control by partial enumeration," *Automatica*, vol. 43, no. 5, pp. 852–860, 2007.

[17] Y. Wang and S. Boyd, "Fast model predictive control using on-line optimization," *IEEE Transactions on Control System Technology*, vol. 18, no. 2, pp. 267–278, 2010.

[18] M. V. Kothare, V. Balakrishnan, and M. Morari, "Robust constrained model predictive control using linear matrix inequalities," *Automatica*, vol. 32, no. 10, pp. 1361–1379, 1996.

[19] H. H. J. Bloemen, T. J. J. van den Boom, and H. B. Verbruggen, "Optimizing the end-point state-weighting matrix in model-based predictive control," *Automatica*, vol. 38, no. 6, pp. 1061–1068, 2002.

[20] F. A. Cuzzola, J. C. Geromel, and M. Morari, "An improved approach for constrained robust model predictive control," *Automatica*, vol. 38, no. 8, pp. 1183–1189, 2002.

[21] B. C. Ding, Y. G. Xi, and S. Y. Li, "A synthesis approach of on-line constrained robust model predictive control," *Automatica*, vol. 40, no. 1, pp. 163–167, 2004.

[22] W.-J. Mao, "Robust stabilization of uncertain time-varying discrete systems and comments on: 'An improved approach for constrained robust model predictive control'," *Automatica*, vol. 39, no. 6, pp. 1109–1112, 2003.

[23] B. Pluymers, J. A. K. Suykens, and B. De Moor, "Min-max feedback MPC using a time-varying terminal constraint set and comments on: 'Efficient robust constrained model predictive control with a time varying terminal constraint set'," *Systems & Control Letters*, vol. 54, no. 12, pp. 1143–1148, 2005.

[24] Z. Y. Wan, B. Pluymers, M. V. Kothare, and B. de Moor, "Comments on 'Efficient robust constrained model predictive control with a time varying terminal constraint set'," *Systems & Control Letters*, vol. 55, no. 7, pp. 618–621, 2006.

[25] Z. Y. Wan and M. V. Kothare, "Efficient robust constrained model predictive control with a time varying terminal constraint set," *Systems & Control Letters*, vol. 48, no. 5, pp. 375–383, 2003.

[26] J. H. Lee, "Model predictive control: review of the three decades of development," *International Journal of Control, Automation, and Systems*, vol. 9, no. 3, pp. 415–424, 2011.

[27] L. Blackmore, M. Ono, A. Bektassov, and B. C. Williams, "A probabilistic particle-control approximation of chance-constrained stochastic predictive control," *IEEE Transactions on Robotics*, vol. 26, no. 3, pp. 502–517, 2010.

[28] J. Hu, Z. Wang, H. Gao, and L. K. Stergioulas, "Robust sliding mode control for discrete stochastic systems with mixed time-delays, randomly occurring uncertainties and randomly occurring nonlinearities," *IEEE Transactions on Industrial Electronics*, vol. 59, no. 7, pp. 3008–3015, 2012.

[29] J. Hu, Z. Wang, B. Shen, and H. Gao, "Gain-constrained recursive filtering with stochastic nonlinearities and probabilistic sensor delays," *IEEE Transactions on Signal Processing*, vol. 61, no. 5, pp. 1230–1238, 2013.

[30] S. Mollov, T. van den Boom, F. Cuesta et al., "Robust stability constraints for fuzzy model predictive control," *IEEE Transactions on Fuzzy Systems*, vol. 10, no. 1, pp. 50–64, 2002.

[31] L. Wu, X. Su, P. Shi, and J. Qiu, "Model approximation for discrete-time state-delay systems in the T-S fuzzy framework," *IEEE Transactions on Fuzzy Systems*, vol. 19, no. 2, pp. 366–378, 2011.

[32] Y. Xia, H. Yang, P. Shi, and M. Fu, "Constrained infinite-horizon model predictive control for fuzzy discrete-time systems," *IEEE Transactions on Fuzzy Systems*, vol. 18, no. 2, pp. 429–436, 2010.

[33] L. Zhang and E.-K. Boukas, "Stability and stabilization of Markovian jump linear systems with partly unknown transition probabilities," *Automatica*, vol. 45, no. 2, pp. 463–468, 2009.

[34] L. Zhang, E.-K. Boukas, and J. Lam, "Analysis and synthesis of Markov jump linear systems with time-varying delays and partially known transition probabilities," *IEEE Transactions on Automatic Control*, vol. 53, no. 10, pp. 2458–2464, 2008.

[35] M. C. de Oliveira, J. Bernussou, and J. C. Geromel, "A new discrete-time robust stability condition," *Systems & Control Letters*, vol. 37, no. 4, pp. 261–265, 1999.

[36] S. Boyd, L. El Ghaoui, E. Feron, and V. Balakrishnan, *Linear Matrix Inequalities in System and Control Theory*, vol. 15, Society for Industrial and Applied Mathematics (SIAM), Philadelphia, Pa, USA, 1994.

Hindawi Publishing Corporation
Mathematical Problems in Engineering
Volume 2013, Article ID 920796, 10 pages
http://dx.doi.org/10.1155/2013/920796

Research Article

Adaptive Finite-Time Control for a Flexible Hypersonic Vehicle with Actuator Fault

Jie Wang,[1] Qun Zong,[1] Xiao He,[2] and Hamid Reza Karimi[3]

[1] *Department of Electrical Engineering and Automation, Tianjin University, Tianjin 300072, China*
[2] *Department of Automation, Tsinghua University, Beijing 100084, China*
[3] *Department of Engineering, Faculty of Engineering and Science, University of Agder, N-4898 Grimstad, Norway*

Correspondence should be addressed to Xiao He; hexiao@tsinghua.edu.cn

Received 6 September 2013; Accepted 3 October 2013

Academic Editor: Hongli Dong

The problem of robust fault-tolerant tracking control is investigated. Simulation on the longitudinal model of a flexible air-breathing hypersonic vehicle (FAHV) with actuator faults and uncertainties is conducted. In order to guarantee that the velocity and altitude track their desired commands in finite time with the partial loss of actuator effectiveness, an adaptive fault-tolerant control strategy is presented based on practical finite-time sliding mode method. The adaptive update laws are used to estimate the upper bound of uncertainties and the minimum value of actuator efficiency factor. Finally, simulation results show that the proposed control strategy is effective in rejecting uncertainties even in the presence of actuator faults.

1. Introduction

Air-breathing hypersonic vehicles (AHVs) are intended to be a reliable and cost-effective technology for access to space. Because the slender geometries and light structures cause significant flexible effects and strong coupling between propulsive and aerodynamic forces resulting from the integration of the scramjet engine, AHVs are confronting many complex problems and challenges, involving many different research areas, such as aerodynamics, thermal protection, and communication, and many problems of these fields have been reported [1–3]. Meanwhile, flight control design for AHVs is a hot topic and a challenging task [4, 5].

During the last decades, a kind of flexible hypersonic vehicle model including flexible dynamics has been developed in [6, 7]. Based on this model, there have been several papers discussing the challenges associated with the control of air-breathing hypersonic vehicle (AHV) [8, 9] and many control methods have been employed in the flight control system. In [10], a linear quadratic regulator (LQR) was presented for a linearized FAHV model. In [11–13], sequential loop closure controller was designed for the FAHV based on adaptive dynamic inversion together with backstepping structure. In [14, 15], approximate feedback linearization based on dynamic inversion method was adopted to design controller for the FAHV. In [16, 17], a nonlinear tracking controller was constructed by using a minimax LQR control approach, which provides robust stability and excellent tracking performance with parameter uncertainties.

The approaches mentioned above do not specifically consider possible actuator faults, which deteriorate the control performance, affect stability, and security of the AHVs, and sometimes even lead to catastrophic accidents. Consequently, it is essential that the actuator faults must be taken into account in the controller design. In the current papers, some fault-tolerant control schemes for AHVs have attracted more and more research attention and gained fruitful results, which can be reported in [18–21]. In [18–20], the results mainly concentrate on the reentry attitude control of the AHV. Meanwhile, the fault tolerant control strategies for the longitudinal model of the AHVs are studied. In [21], an observer-based fault-tolerant control approach using both robust control and LMI techniques is designed for a linearized longitudinal AHV model in the presence of parameter uncertainties and actuator faults, but this method was effective only in the neighborhood of the operating point. On the other hand, nonlinear fault-tolerant control design methods have been devoted to the longitudinal AHV

model. A finite-time integral sliding mode control method was proposed in [22], which could achieve superior velocity and altitude tracking performance with actuator fault. In [23], the longitudinal AHV model with unknown parameters and uncertain actuator faults is formatted into a parametric strict-feedback form, and then an adaptive fault-tolerant control scheme based on a combination of back-stepping control and dynamic surface control techniques is applied to make the velocity and altitude track the desired value.

However, the aforesaid methods only consider the rigid body of AHVs without flexible effects. A fault-tolerant control scheme for the FAHV was presented in [24], according to the model obtained by approximate linearization in given flight conditions. So, this scheme may not obtain good control performances when flight dynamics undergo great parameter perturbations. To the best of our knowledge, although considerable effort has been made on the control design for the AHVs, the important issue of fault-tolerant control of the FAHV dynamical system has not been fully investigated yet, which remains challenging and motivates us to do this study.

As a typical robust control method, sliding mode control (SMC) scheme is regarded as an effective method to cope with external disturbances and parametric uncertainties [25]. Recently, the SMC method has been widely applied for the fault tolerant control of aircraft system, spacecraft, and so on. In [26], a fault-tolerant sliding mode controller was presented for an aircraft system, which requires the message of the effectiveness factor, while it may be difficult and expensive to obtain the actuator faults online. In [27], a finite-time convergent SMC scheme is developed to solve the problem of fault-tolerant control for a rigid spacecraft. The drawback of this method is that the message of the lower bound of the effectiveness factor and the upper bound of system uncertainties needs to be known in prior.

The aforementioned references could achieve desired performance through the SMC methodology affected by actuator faults. Although the traditional SMC can guarantee the stability of the system, it adopts a linear switching function. Then the system states and the errors converge to an equilibrium point asymptotically in infinite time. In other words, it means that finite-time convergence is not ensured. Motivated by the above discussions, we propose a novel adaptive sliding mode control scheme for the longitudinal model of the FAHV with uncertainties and actuator faults in this paper. As compared with the existing results, the main contributions are as follows. Firstly, the design method of sliding mode surface based on homogeneous geometry could assure practical finite-time converged tracking of the desired command. Secondly, the upper bounds of aerodynamic uncertainties and the minimum value of actuator efficiency factor are not required in prior. The adaptive law is designed to adjust the control gains dynamically so as to ensure the establishment of sliding mode motion, and the robustness against uncertainties is ensured at the same time. After the uncertainties and actuator faults are compensated using adaptive sliding mode control scheme, the stability of the closed-loop system can be maintained.

The rest of this paper is organized as follows. In Section 2 the FAHV model is introduced and control objective is stated. Section 3 designs the sliding mode surface and the corresponding adaptive finite-time fault tolerant controller was proposed with actuator fault. Simulation results are discussed in Section 4 and the conclusions are provided in Section 5.

2. Problem Statement

The considered FAHV model is derived from [6, 28], and the longitudinal equations of motion of the FAHV are given by

$$\begin{aligned}
\dot{V} &= \frac{(T\cos\alpha - D)}{m} - g\sin\gamma,\\
\dot{\gamma} &= \frac{(L + T\sin\alpha)}{mV} - \frac{g\cos\gamma}{V},\\
\dot{h} &= V\sin\gamma,\\
\dot{\alpha} &= Q - \dot{\gamma},\\
\dot{Q} &= \frac{M_{yy}}{I_{yy}},\\
\ddot{\eta}_i &= -2\varsigma_m\omega_{m,i}\dot{\eta}_i - \omega_{m,i}^2\eta_i + N_i, \qquad i = 1, 2, 3,
\end{aligned} \tag{1}$$

where $x = [V, \gamma, h, \alpha, Q]^T$ is a vector of rigid-body state, which includes the vehicle speed, flight path angle, altitude, angel of attack, and pitch rate, respectively; η_i, $\omega_{m,i}$, and ς_m are the generalized flexible coordinate, natural frequencies, and damping coefficients of the ith elastic mode. The readers may refer to [7] for a full description of the variables in this model.

Because of coupling in aerodynamic forces of the FAHV model (1), some simplifications must be carried out for the purpose of feedback linearization. The simplification of the model is necessary because we want to obtain a linearized model, and the same simplified process can be found in [29]. An input-output linearization model is developed by repeated differentiation of the outputs V and h as follows:

$$\ddot{V} = f_V + b_{11}\phi_c + b_{12}\delta_e, \tag{2}$$

$$h^{(4)} = f_h + b_{21}\phi_c + b_{22}\delta_e, \tag{3}$$

where ϕ_c and δ_e are control inputs and the specific expressions of f_V, f_h, b_{11}, b_{12}, b_{21}, and b_{22} are presented in [29, equation (17)].

Compared with [29], the main propose of this study is discussing the fault tolerant controller design for the FAHV to follow a given desired output reference signals $y_d = [V_d, h_d]^T$ in the presence of partial loss of actuator effectiveness.

3. Adaptive Finite-Time Fault-Tolerant Controller Design

The specific controller design step includes two parts: sliding mode surface design and sliding mode control design, which can be described as follows.

3.1. Sliding Mode Surface Design. Define tracking error variable as follows:

$$e_V = V - V_d, \tag{4}$$

$$e_h = h - h_d. \tag{5}$$

Differentiating (4) and (5) three times, and four times respectively, results in

$$\ddot{e}_V = f_V - \dddot{V}_d + b_{11}\phi_c + b_{12}\delta_e, \tag{6}$$

$$e_h^{(4)} = f_h - h_d^{(4)} + b_{21}\phi_c + b_{22}\delta_e. \tag{7}$$

Equations (6)-(7) can be expressed in matrix form:

$$\begin{bmatrix} \ddot{e}_V \\ e_h^{(4)} \end{bmatrix} = \underbrace{\begin{bmatrix} f_V - \dddot{V}_d \\ f_h - h_d^{(4)} \end{bmatrix}}_{F=\left[F_1,F_2\right]^T} + \underbrace{\begin{bmatrix} b_{11} & b_{12} \\ b_{21} & b_{22} \end{bmatrix}}_{B} \underbrace{\begin{bmatrix} \phi_c \\ \delta_e \end{bmatrix}}_{u} + \underbrace{\begin{bmatrix} \Delta F_1 \\ \Delta F_2 \end{bmatrix}}_{\Delta F=\left[\Delta F_1,\Delta F_2\right]^T}. \tag{8}$$

Note that the additional item ΔF is introduced to represent the flexible effects and coupled uncertainties described in [29, equation (14)].

Introduce new control variable:

$$U = \begin{bmatrix} U_1 \\ U_2 \end{bmatrix} = \begin{bmatrix} b_{11} & b_{12} \\ b_{21} & b_{22} \end{bmatrix} \begin{bmatrix} \phi_c \\ \delta_e \end{bmatrix}. \tag{9}$$

Then (8)-(9) can be rewritten as

$$\begin{bmatrix} \ddot{e}_V \\ e_h^{(4)} \end{bmatrix} = \begin{bmatrix} F_1 \\ F_2 \end{bmatrix} + \begin{bmatrix} U_1 \\ U_2 \end{bmatrix} + \begin{bmatrix} \Delta F_1 \\ \Delta F_2 \end{bmatrix}. \tag{10}$$

Assumption 1. The uncertainties discussed in the research are bounded $\|\Delta F\| \le \upsilon$, but the value υ is unknown in advance.

Assumption 2. The matrix B denoted in (8) is nonsingular over the entire flight envelope given in [12], so Assumption 1 is reasonable to be assumed.

Now, according to the definition of HOSM [30, 31], our objective is to design controller which makes the e_V, e_h and their derivatives converge to the neighborhood of origin.

Design sliding mode surface as follows:

$$s_V = \ddot{e}_V + \int_0^t \underbrace{\lambda_{1V}\left|e_V\right|^{a_{1V}} \operatorname{sign}\left(e_V\right) + \lambda_{2V}\left|\dot{e}_V\right|^{a_{2V}} \operatorname{sign}\left(\dot{e}_V\right) + \lambda_{3V}\left|\ddot{e}_V\right|^{a_{3V}} \operatorname{sign}\left(\ddot{e}_V\right)}_{G_V}, \tag{11}$$

$$s_h = \dddot{e}_h + \int_0^t \underbrace{\lambda_{1h}\left|e_h\right|^{a_{1h}} \operatorname{sign}\left(e_h\right) + \lambda_{2h}\left|\dot{e}_h\right|^{a_{2h}} \operatorname{sign}\left(\dot{e}_h\right) + \lambda_{3h}\left|\ddot{e}_h\right|^{a_{3h}} \operatorname{sign}\left(\ddot{e}_h\right) + \lambda_{4h}\left|\dddot{e}_h\right|^{a_{4h}} \operatorname{sign}\left(\dddot{e}_h\right)}_{G_h} ds. \tag{12}$$

The parameters λ_{iV} $(i = 1, 2, 3)$ and λ_{jh} $(j = 1, 2, 3, 4)$ are some positive constants such that $\lambda_{3V}s^2 + \lambda_{2V}s + \lambda_{1V}$ and $\lambda_{4h}s^3 + \lambda_{3h}s^2 + \lambda_{2h}s + \lambda_{1h}$ are Hurwitz polynomial. The parameters a_{iV} $(i = 1, 2, 3)$ and a_{jh} $(j = 1, 2, 3, 4)$ are determined by

$$\begin{aligned} a_{(i-1)V} &= \frac{a_{iV}a_{(i+1)V}}{2a_{(i+1)V} - a_{iV}}, \quad i \in \{2, 3\}, \\ a_{(j-1)h} &= \frac{a_{jh}a_{(j+1)h}}{2a_{(j+1)h} - a_{jh}}, \quad j \in \{2, 3, 4\} \end{aligned} \tag{13}$$

with $a_{4V} = a_{5h} = 1$, $a_{3V} \in (1 - \varepsilon_V, 1)$, and $a_{4h} \in (1 - \varepsilon_h, 1)$, where $\varepsilon_V \in (0, 1)$, $\varepsilon_h \in (0, 1)$.

Based on the homogeneity theory provided in [32], it is easily shown that e_V, $\dot{e}_V$, $\ddot{e}_V$ and e_h, $\dot{e}_h$, $\ddot{e}_h$, $\dddot{e}_h$ will converge to the neighborhood of origin in finite time if it is satisfied that s_V, s_h converge to the neighborhood of origin in finite time.

3.2. Adaptive Sliding Mode Controller Design. Now, let us consider the situation in which the actuator experiences partial loss of effectiveness fault. Then, differentiating (11) and (12), we obtain

$$\begin{bmatrix} \dot{s}_V \\ \dot{s}_h \end{bmatrix} = \begin{bmatrix} F_1 \\ F_2 \end{bmatrix} + \underbrace{\begin{bmatrix} G_V \\ G_h \end{bmatrix}}_{G=\left[G_V,G_h\right]^T} + \underbrace{\begin{bmatrix} E_1 & 0 \\ 0 & E_2 \end{bmatrix}}_{E} \begin{bmatrix} U_1 \\ U_2 \end{bmatrix} + \begin{bmatrix} \Delta F_1 \\ \Delta F_2 \end{bmatrix}, \tag{14}$$

where $E = \operatorname{diag}(E_1, E_2) \in R^{2\times 2}$ is a matrix characterizing the health condition of the actuators with $0 \le E_i \le 1$ $(i = 1, 2)$. Note that the case $E_i = 1$ means that the ith actuator is totally healthy, the case $E_i = 0$ implies that the ith actuator completely fails, and the case $0 < E_i < 1$ corresponds to the case in which the ith actuator partially loses its effectiveness, but it still has effect all the time. In this sense, the matrix E becomes uncertain and even time varying but remains positive definite. In this study, an assumption $0 < E_i \le 1$ is given.

The control objective is to design the control inputs for ϕ_c and δ_e such that all of the closed-loop signals are bounded and the velocity V and altitude h track desired command trajectories V_d and h_d in the presence of flexible uncertainties and loss of effective actuator faults. That is to say, the velocity sliding mode surface s_V and altitude sliding mode surface s_h converge to an arbitrary small set containing the origin

in finite time T_0, which is $\|s_V\| \le \delta_V$ and $\|s_h\| \le \delta_h$ for $t \ge T_0$, where δ_V and δ_h are arbitrary small positive constant numbers.

Let $E_{\min} = \min_{i=1,2} E_i$ and denote $\mu = 1 - E_{\min}$ and then $\mu < 1$. Selecting $\theta = 1/(1-\mu)$, then the main result of the paper is formulated in the following theorem.

Theorem 3. *Consider the nonlinear sliding mode dynamic system* (14) *with Assumptions 1 and 2, if the control* $U = [U_1, U_2]^T$ *is designed as*

$$U = -F - G - k \cdot \operatorname{sig}^{\tau}(s) - \widehat{\sigma}\frac{s}{\|s\|} - \widehat{\upsilon}\frac{s}{\|s\|}, \tag{15}$$

with the adaptive gains

$$\widehat{\sigma} = -\psi + \widehat{\theta}\psi, \qquad \psi = \|F\| + \|G\| + \left\|k \cdot \operatorname{sig}^{\tau}(s)\right\| + \widehat{\upsilon}, \tag{16}$$

$$\dot{\widehat{\theta}} = p_0\left(-\varepsilon_0\widehat{\theta} + \psi\|s\|\right), \tag{17}$$

$$\dot{\widehat{\upsilon}} = p_1\left(-\varepsilon_1\widehat{\upsilon} + \|s\|\right), \tag{18}$$

where $s = [s_V, s_h]^T$, $k = [k_V, k_h]^T$, and $0 < \tau < 1$, and define the function $\operatorname{sig}^{\tau}(\cdot) = \operatorname{sign}(\cdot)|\cdot|^{\tau}$, p_0, p_1, ε_0 and ε_1 are positive control constants, and the initial values $\widehat{\sigma}(0)$, $\widehat{\upsilon}(0)$ are chosen as positive constants. Then, the system trajectory will converge to the neighborhood of $s_V = s_h = 0$ in finite time despite of the uncertainties ΔF and actuator faults E.

Proof. The stability analysis of system (14) is performed via constructing the following Lyapunov function:

$$W = \frac{1}{2}\left(s^T s + \frac{1-\mu}{p_0}\left(\theta - \widehat{\theta}\right)^2 + \frac{1}{p_1}(\upsilon - \widehat{\upsilon})^2\right), \tag{19}$$

where $\widetilde{\sigma} = \sigma - \widehat{\sigma}$ and $\widetilde{\upsilon} = \upsilon - \widehat{\upsilon}$. The derivative of (19) is presented

$$\begin{aligned}
\dot{W} &= s^T\dot{s} - \frac{1-\mu}{p_0}\widetilde{\theta}\dot{\widehat{\theta}} - \frac{1}{p_1}\widetilde{\upsilon}\dot{\widehat{\upsilon}} \\
&= s^T(F + G + EU + \Delta F) - \frac{1-\mu}{p_0}\widetilde{\theta}\dot{\widehat{\theta}} - \frac{1}{p_1}\widetilde{\upsilon}\dot{\widehat{\upsilon}} \\
&= s^T\left(F + G + U - \underbrace{(I-E)}_{\Delta E}U + \Delta F\right) - \frac{1-\mu}{p_0}\widetilde{\theta}\dot{\widehat{\theta}} - \frac{1}{p_1}\widetilde{\upsilon}\dot{\widehat{\upsilon}} \\
&= s^T\left(-k \cdot \operatorname{sig}^{\tau}(s) - \widehat{\sigma}\frac{s}{\|s\|} - \widehat{\upsilon}\frac{s}{\|s\|} - \underbrace{(I-\mathrm{E})}_{\Delta E}U + \Delta F\right) \\
&\quad - \frac{1-\mu}{p_0}\widetilde{\theta}\dot{\widehat{\theta}} - \frac{1}{p_1}\widetilde{\upsilon}\dot{\widehat{\upsilon}} \\
&\le -k_V|s_V|^{\tau+1} - k_h|s_h|^{\tau+1} \\
&\quad + s^T\left(-\widehat{\sigma}\frac{s}{\|s\|} - \widehat{\upsilon}\frac{s}{\|s\|} - \Delta EU + \Delta F\right) - \frac{1-\mu}{p_0}\widetilde{\theta}\dot{\widehat{\theta}} - \frac{1}{p_1}\widetilde{\upsilon}\dot{\widehat{\upsilon}} \\
&\le -k_V|s_V|^{\tau+1} - k_h|s_h|^{\tau+1} + s^T\left(-\widehat{\sigma}\frac{s}{\|s\|} - \Delta EU\right) \\
&\quad - \frac{1-\mu}{p_0}\widetilde{\theta}\dot{\widehat{\theta}} + s^T\left(\Delta F - \widehat{\upsilon}\frac{s}{\|s\|}\right) - \frac{1}{p_1}\widetilde{\upsilon}\dot{\widehat{\upsilon}} \\
&\le -k_V|s_V|^{\tau+1} - k_h|s_h|^{\tau+1} + s^T\left(-\widehat{\sigma}\frac{s}{\|s\|} - \Delta EU\right) \\
&\quad - \frac{1-\mu}{p_0}\widetilde{\theta}\dot{\widehat{\theta}} + s^T\left(\Delta F - \upsilon\frac{s}{\|s\|}\right) + \widetilde{\upsilon}\|s\| - \frac{1}{p_1}\widetilde{\upsilon}\dot{\widehat{\upsilon}}.
\end{aligned} \tag{20}$$

In view of Assumption 1 and adaptive update laws (18), inequality (20) can be rewritten as

$$\begin{aligned}
\dot{W} &\le -k_V|s_V|^{\tau+1} - k_h|s_h|^{\tau+1} + s^T\left(-\widehat{\sigma}\frac{s}{\|s\|} - \Delta EU\right) \\
&\quad - \frac{1-\mu}{p_0}\widetilde{\theta}\dot{\widehat{\theta}} + \varepsilon_1\widetilde{\upsilon}\widehat{\upsilon} \\
&\le -k_V|s_V|^{\tau+1} - k_h|s_h|^{\tau+1} - \widehat{\sigma}\|s\| - s^T\Delta EU \\
&\quad - \frac{1-\mu}{p_0}\widetilde{\theta}\dot{\widehat{\theta}} + \varepsilon_1\widetilde{\upsilon}\widehat{\upsilon} \\
&\le -k_V|s_V|^{\tau+1} - k_h|s_h|^{\tau+1} - \widehat{\sigma}\|s\| \\
&\quad + \|\Delta E\| \cdot s^T \cdot \left(\|F\| + \|G\| + \left\|k \cdot \operatorname{sig}^{\tau}(s)\right\| + \widehat{\sigma} + \widehat{\upsilon}\right) \\
&\quad - \frac{1-\mu}{p_0}\widetilde{\theta}\dot{\widehat{\theta}} + \varepsilon_1\widetilde{\upsilon}\widehat{\upsilon}.
\end{aligned} \tag{21}$$

According to (16), inequality (21) can be rewritten as

$$\begin{aligned}
\dot{W} &\le -k_V|s_V|^{\tau+1} - k_h|s_h|^{\tau+1} + \left(1 - \widehat{\theta}\right)\psi\|s\| + \mu \cdot \widehat{\theta} \cdot \psi\|s\| \\
&\quad - \frac{1-\mu}{p_0}\widetilde{\theta}\dot{\widehat{\theta}} + \varepsilon_1\widetilde{\upsilon}\widehat{\upsilon} \\
&\le -k_V|s_V|^{\tau+1} - k_h|s_h|^{\tau+1} + \left(1 - (1-\mu)\widehat{\theta}\right)\psi\|s\| \\
&\quad - \frac{1-\mu}{p_0}\widetilde{\theta}\dot{\widehat{\theta}} + \varepsilon_1\widetilde{\upsilon}\widehat{\upsilon} \\
&\le -k_V|s_V|^{\tau+1} - k_h|s_h|^{\tau+1} \\
&\quad + \left((1-\mu)\theta - (1-\mu)\widehat{\theta}\right)\psi\|s\| - \frac{1-\mu}{p_0}\widetilde{\theta}\dot{\widehat{\theta}} + \varepsilon_1\widetilde{\upsilon}\widehat{\upsilon} \\
&\le -k_V|s_V|^{\tau+1} - k_h|s_h|^{\tau+1} + (1-\mu)\widetilde{\theta}\psi\|s\| \\
&\quad - \frac{1-\mu}{p_0}\widetilde{\theta}\dot{\widehat{\theta}} + \varepsilon_1\widetilde{\upsilon}\widehat{\upsilon}.
\end{aligned} \tag{22}$$

According to the adaptive update laws defined in (17), the inequality (22) can be rewritten as

$$\dot{W} \le -k\left(|s_V|^{\tau+1} + |s_h|^{\tau+1}\right) + (1-\mu)\,\varepsilon_0\tilde{\theta}\hat{\theta} + \varepsilon_1\tilde{v}\hat{v}, \tag{23}$$

where $k = \min_{i=V,h} k_i$. In view of Lemma 3.1 in [33], inequality (23) can be written as

$$\begin{aligned}\dot{W} &\le -k\left(|s_V|^2 + |s_h|^2\right)^{(\tau+1)/2} + (1-\mu)\,\varepsilon_0\tilde{\theta}\hat{\theta} + \varepsilon_1\tilde{v}\hat{v} \\ &\le -k\left(\frac{1}{2}|s_V|^2 + |s_h|^2\right)^{(\tau+1)/2} + (1-\mu)\,\varepsilon_0\tilde{\theta}\hat{\theta} + \varepsilon_1\tilde{v}\hat{v}.\end{aligned} \tag{24}$$

Inspired by [33] for any positive numbers $\delta_0 > 0.5$ and $\delta_1 > 0.5$, inequality (24) can be rewritten as

$$\begin{aligned}\dot{W} \le\ & -k\left(\frac{1}{2}s^T s\right)^{(\tau+1)/2} - \left(\frac{(1-\mu)\,\varepsilon_0\,(2\delta_0-1)}{2\delta_0}\tilde{\theta}^2\right)^{(\tau+1)/2} \\ & - \left(\frac{\varepsilon_1\,(2\delta_1-1)}{2\delta_1}\tilde{v}^2\right)^{(\tau+1)/2} \\ & + \left(\frac{(1-\mu)\,\varepsilon_0\,(2\delta_0-1)}{2\delta_0}\tilde{\theta}^2\right)^{(\tau+1)/2} \\ & + \left(\frac{\varepsilon_1\,(2\delta_1-1)}{2\delta_1}\tilde{v}^2\right)^{(\tau+1)/2} + (1-\mu)\,\varepsilon_0\tilde{\theta}\hat{\theta} + \varepsilon_1\tilde{v}\hat{v}.\end{aligned} \tag{25}$$

denote

$$p_0 = \frac{\delta_0 k^{2/(\tau+1)}}{\varepsilon_0\,(2\delta_0-1)}, \qquad p_1 = \frac{\delta_1 k^{2/(\tau+1)}}{\varepsilon_1\,(2\delta_1-1)}. \tag{26}$$

Then, inequality (25) can be rewritten as

$$\begin{aligned}\dot{W} \le -k\Bigg[& \left(\frac{1}{2}s^T s\right)^{(\tau+1)/2} + \left(\frac{(1-\mu)}{2p_0}\tilde{\theta}^2\right)^{(\tau+1)/2} \\ & + \left(\frac{1}{2p_1}\tilde{v}^2\right)^{(\tau+1)/2}\Bigg] \\ & + \left(\frac{(1-\mu)\,\varepsilon_0\,(2\delta_0-1)}{2\delta_0}\tilde{\theta}^2\right)^{(\tau+1)/2} \\ & + \left(\frac{\varepsilon_1\,(2\delta_1-1)}{2\delta_1}\tilde{v}^2\right)^{(\tau+1)/2} + (1-\mu)\,\varepsilon_0\tilde{\theta}\hat{\theta} + \varepsilon_1\tilde{v}\hat{v}.\end{aligned} \tag{27}$$

According to Lemma 3.2 in [33], when $\delta_0 > 0.5$, $\delta_1 > 0.5$, and $0.5 < 0.5(\tau+1) < 1$, the time derivative of the Lyapunov function $\dot{W}$ becomes

$$\begin{aligned}\dot{W} \le\ & -k\left[\left(\frac{1}{2}s^T s\right) + \left(\frac{(1-\mu)}{2p_0}\tilde{\theta}^2\right) + \left(\frac{1}{2p_1}\tilde{v}^2\right)\right]^{(\tau+1)/2} \\ & + \left(\frac{(1-\mu)\,\varepsilon_0\,(2\delta_0-1)}{2\delta_0}\tilde{\theta}^2\right)^{(\tau+1)/2} \\ & + \left(\frac{\varepsilon_1\,(2\delta_1-1)}{2\delta_1}\tilde{v}^2\right)^{(\tau+1)/2} \\ & + (1-\mu)\,\varepsilon_0\tilde{\theta}\hat{\theta} + \varepsilon_1\tilde{v}\hat{v} \\ \le\ & -kW^{(\tau+1)/2} + \left(\frac{(1-\mu)\,\varepsilon_0\,(2\delta_0-1)}{2\delta_0}\tilde{\theta}^2\right)^{(\tau+1)/2} \\ & + \left(\frac{\varepsilon_1\,(2\delta_1-1)}{2\delta_1}\tilde{v}^2\right)^{(\tau+1)/2} + (1-\mu)\,\varepsilon_0\tilde{\theta}\hat{\theta} + \varepsilon_1\tilde{v}\hat{v}.\end{aligned} \tag{28}$$

Note that, for any positive constants $\delta_0 > 0.5$ and $\delta_1 > 0.5$, the following inequality holds:

$$\begin{aligned}\varepsilon_1\tilde{v}\hat{v} &= \varepsilon_1\left(-\tilde{v}^2 + \tilde{v}v\right) \\ &\le \varepsilon_1\left(-\tilde{v}^2 + \frac{1}{2\delta_1}\tilde{v}^2 + \frac{\delta_1}{2}v^2\right) \\ &\le \frac{-\varepsilon_1\,(2\delta_1-1)}{2\delta_1}\tilde{v}^2 + \frac{\varepsilon_1\delta_1}{2}v^2.\end{aligned} \tag{29}$$

Similarly $(1-\mu)\varepsilon_0\tilde{\theta}\hat{\theta}$ satisfies the following inequality:

$$(1-\mu)\,\varepsilon_0\tilde{\theta}\hat{\theta} \le \frac{-\varepsilon_0\,(1-\mu)\,(2\delta_0-1)}{2\delta_0}\tilde{\theta}^2 + \frac{\varepsilon_0\,(1-\mu)\,\delta_0}{2}\theta^2. \tag{30}$$

According to inequality (29), if $(\varepsilon_1(2\delta_1-1)/2\delta_1)\tilde{v}^2 > 1$, we obtain

$$\begin{aligned}&\left(\frac{\varepsilon_1\,(2\delta_1-1)}{2\delta_1}\tilde{v}^2\right)^{(\tau+1)/2} + \varepsilon_1\tilde{v}\hat{v} \\ &\qquad \le \frac{\varepsilon_1\,(2\delta_1-1)}{2\delta_1}\tilde{v}^2 + \varepsilon_1\tilde{v}\hat{v} \le \frac{\varepsilon_1\delta_1}{2}v^2.\end{aligned} \tag{31}$$

If $(\varepsilon_1(2\delta_1-1)/2\delta)\tilde{v}^2 \le 1$, we have

$$\begin{aligned}&\left(\frac{\varepsilon_1\,(2\delta_1-1)}{2\delta_1}\tilde{v}^2\right)^{(\tau+1)/2}\Bigg|_{(\varepsilon_1(2\delta_1-1)/2\delta_1)\tilde{v}^2\le 1} \\ &\qquad < \left(\frac{\varepsilon_1\,(2\delta_1-1)}{2\delta_1}\tilde{v}^2\right)^{(\tau+1)/2}\Bigg|_{(\varepsilon_1(2\delta_1-1)/2\delta_1)\tilde{v}^2>1}.\end{aligned} \tag{32}$$

Therefore, combining (31) and (32) yields

$$\left(\frac{\varepsilon_1\,(2\delta_1-1)}{2\delta_1}\tilde{v}^2\right)^{(\tau+1)/2} + \varepsilon_1\tilde{v}\hat{v} \le \frac{\varepsilon_1\delta_1}{2}v^2. \tag{33}$$

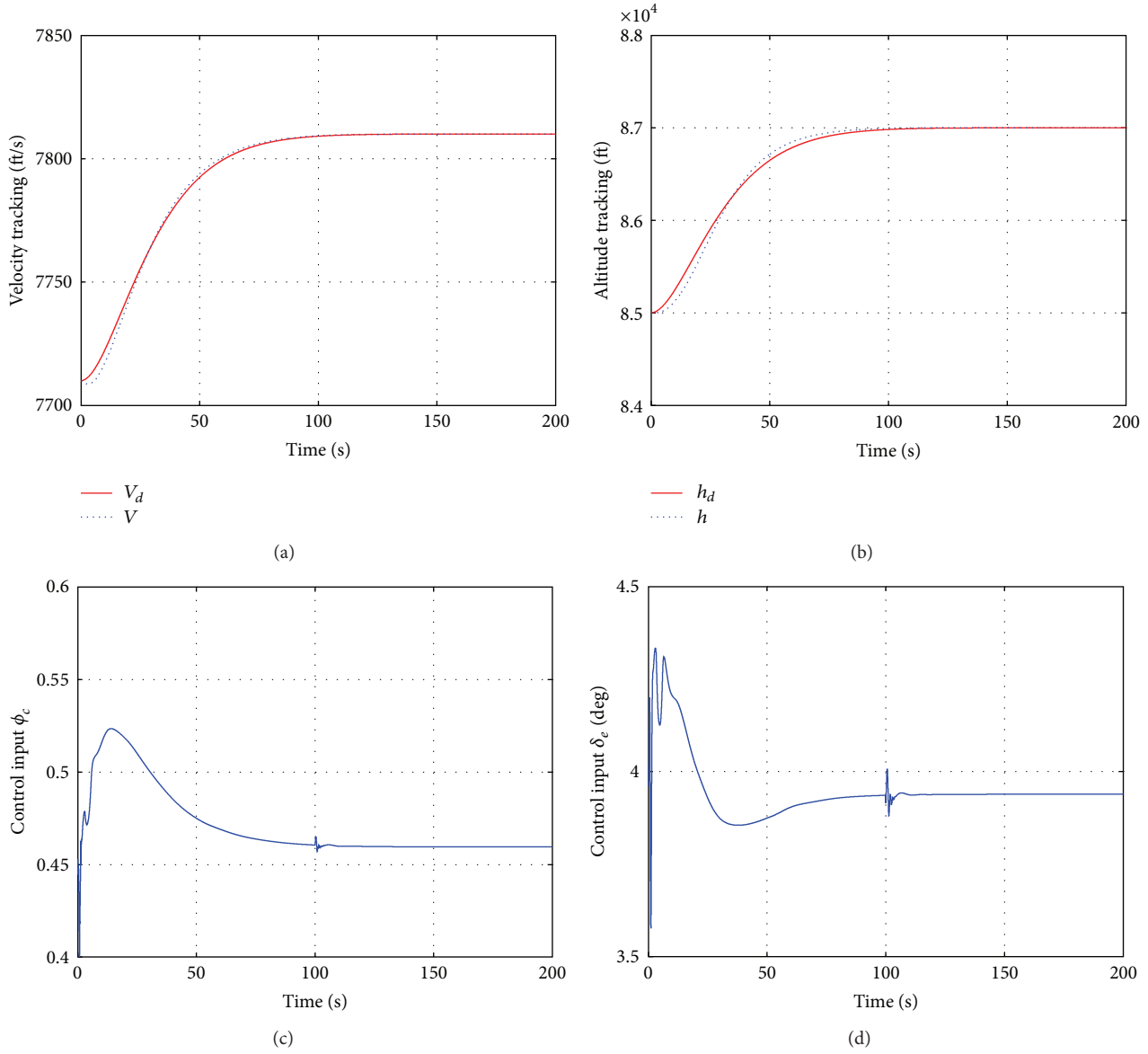

FIGURE 1: Regulated outputs and control inputs with actuator faults.

Similar to (33), the following inequality can be obtained:

$$\left(\frac{(1-\mu)\,\varepsilon_0\,(2\delta_0-1)}{2\delta_0}\widetilde{\theta}^2\right)^{(\tau+1)/2} + (1-\mu)\,\varepsilon_0\widetilde{\theta}\widehat{\theta} \leq \frac{(1-\mu)\,\varepsilon_0\delta_0}{2}\theta^2. \tag{34}$$

Thus, from (28)–(34), the derivative of the Lyapunov function (28) becomes

$$\dot{W} \leq -kW^{(\tau+1)/2} + \mu_0, \tag{35}$$

where

$$\mu_0 = \frac{\varepsilon_1\delta_1}{2}\upsilon^2 + \frac{(1-\mu)\,\varepsilon_0\delta_0}{2}\theta^2. \tag{36}$$

According to Lemma 3.6 in [33], the decrease of W can drive the sliding mode surfaces s_V and s_h to converge to a neighborhood of the sliding surface in finite time. Furthermore, selecting $0 < \beta \leq 1$, inequality (35) can be expressed as

$$\dot{W} \leq -\beta kW^{(\tau+1)/2} - (1-\beta)\,kW^{(\tau+1)/2} + \mu_0. \tag{37}$$

If $-(1-\beta)kW^{(\tau+1)/2} + \mu_0 < 0$, then $\dot{W} \leq -\beta kW^{(\tau+1)/2}$. Based on the conclusion from [30], the decrease of W drives the trajectories of the closed-loop system into $W^{(\tau+1)/2} \leq \mu_0/(1-\beta)k$. Therefore, the trajectories of the closed-loop system is bounded in finite time as

$$\lim_{\beta\to\beta_0} s(t) \in \left(\|s\| \leq \underbrace{\left(\frac{\mu_0}{(1-\beta_0)k}\right)^{1/(\tau+1)}}_{\varepsilon}\right), \tag{38}$$

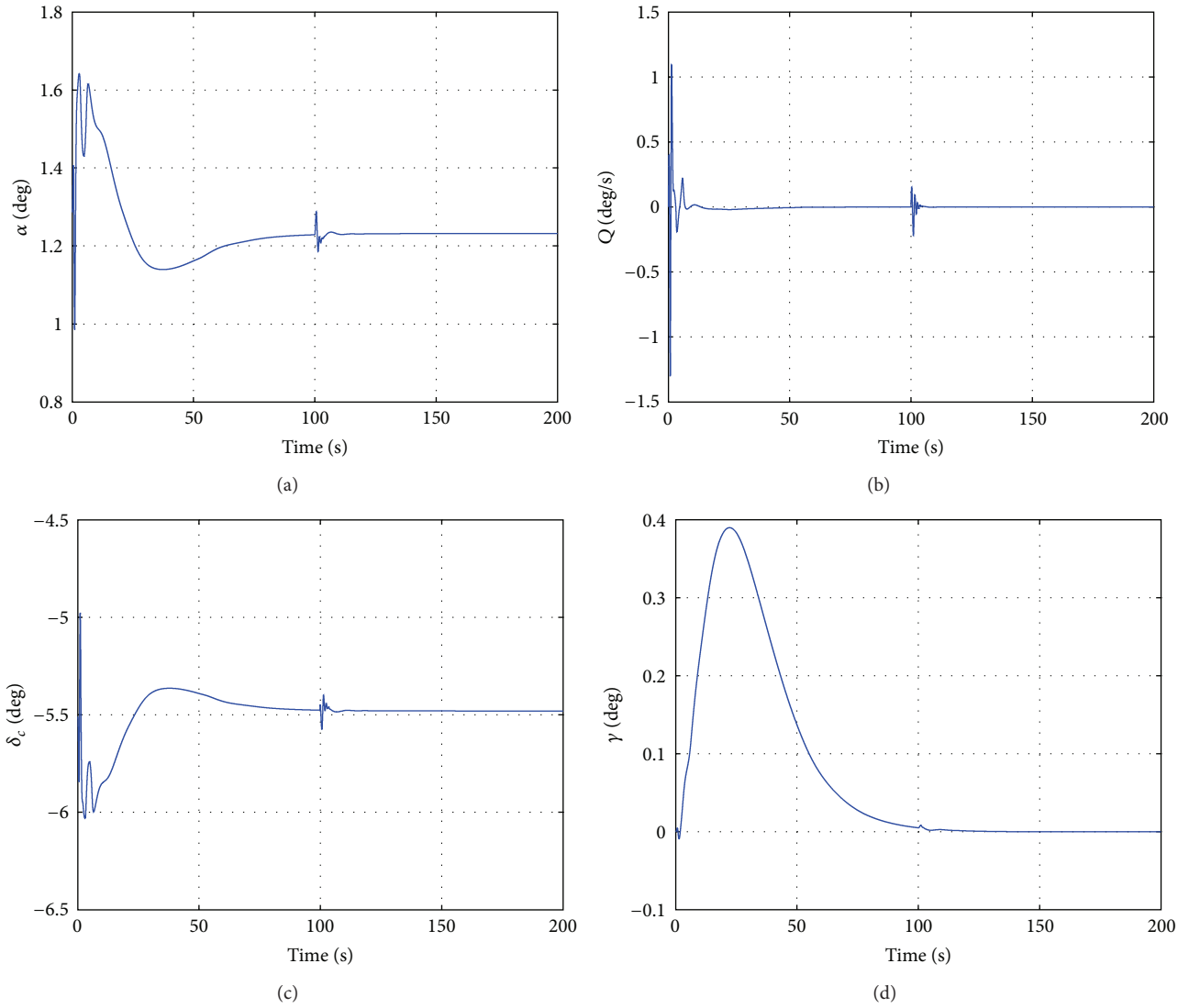

Figure 2: Other flight states with actuator faults.

where $0 < \beta_0 < 1$ and ε is a small set containing the origin of the closed-loop system. And the time needed to reach (38) is bound as

$$T \leq \frac{2W(0)^{(1-\tau)/2}}{k\beta_0(1-\tau)}, \tag{39}$$

where $W(0)$ is the initial value of W. After that, the control objective that the e_V, $\dot{e}_V$, $\ddot{e}_V$ and e_h, $\dot{e}_h$, $\ddot{e}_h$, $\dddot{e}_h$ converge to the neighborhood of origin is established.

When the control $U = [U_1, U_2]^T$ is designed via (9), according to Assumption 2 the actual control variable is calculated as

$$\begin{bmatrix} \phi_c \\ \delta_e \end{bmatrix} = \begin{bmatrix} b_{11} & b_{12} \\ b_{21} & b_{22} \end{bmatrix}^{-1} \begin{bmatrix} U_1 \\ U_2 \end{bmatrix}. \tag{40}$$

It is evident from (40) that the finite-time convergent performance of the proposed adaptive fault tolerant controller can be obtained without the knowledge of the minimum value of actuator effectiveness factor. Meanwhile, the upper bound of uncertainties does not need to be known in advance. □

4. Simulation

To illustrate the efficiency of controller designed previously, a climbing maneuver with longitudinal acceleration for a 100 ft/s velocity change and a 1000 ft altitude change is considered. Simulation studies have been done on the full nonlinear flexible hypersonic vehicle defined in (1). The reference commands have been generated by filtering step reference commands by a second-order prefilter with natural frequency $\omega_f = 0.06$ rad/s and damping ratio $\zeta_f = 0.95$.

The initial trim condition is selected as $V = 7710$ ft/s and $h = 85000$ ft. Simulation parameters are provided in Table 1.

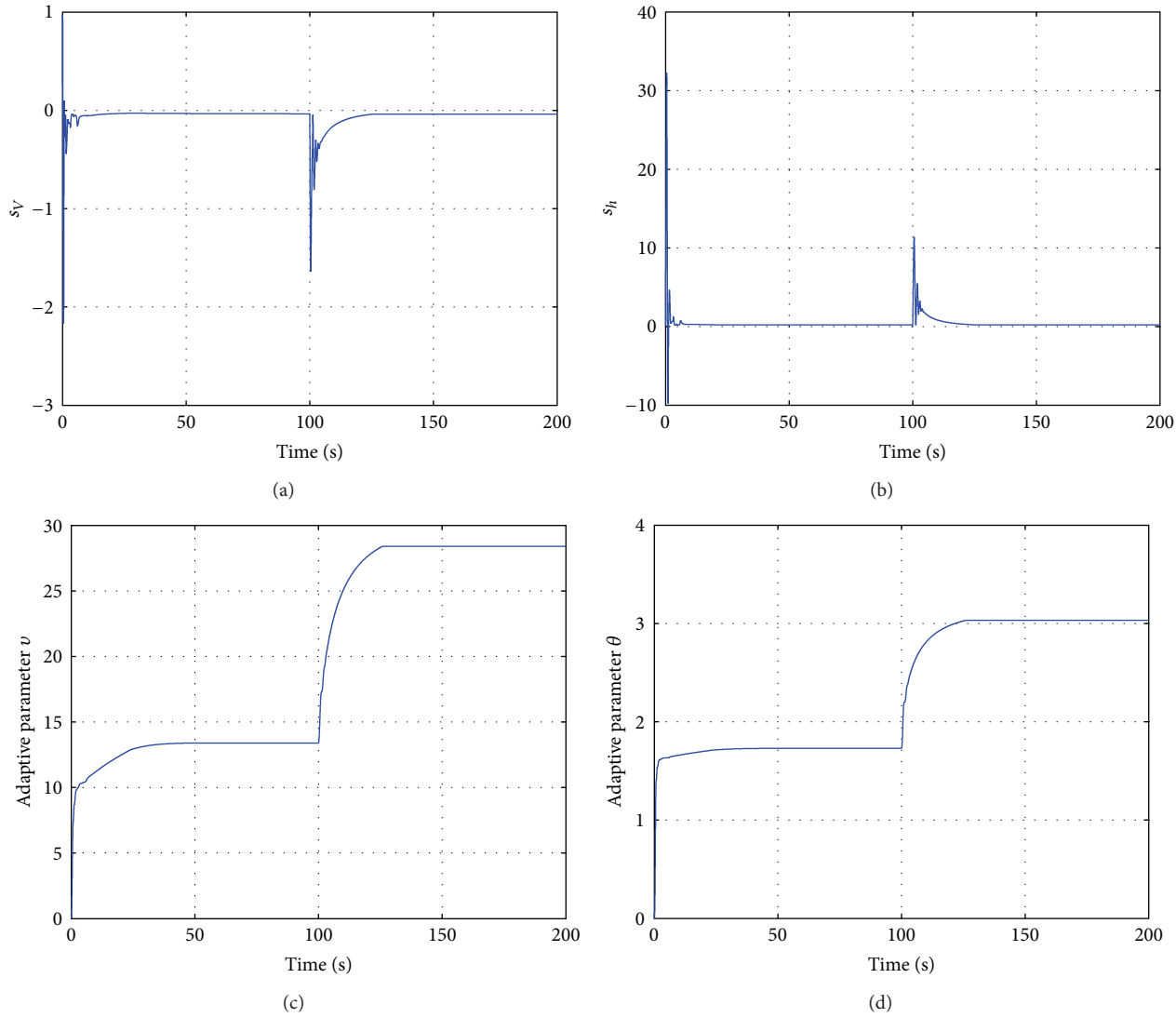

FIGURE 3: Sliding mode surface and adaptive parameters $\widehat{\upsilon}$ and $\widehat{\theta}$ with actuator faults.

TABLE 1: Simulation parameters setting.

Items	Values	Items	Values	Items	Values
λ_{1V}	10	λ_{4h}	10	a_{3h}	3/5
λ_{2V}	15	a_{1V}	1/2	a_{4h}	3/4
λ_{3V}	15	a_{2V}	3/5	τ	0.7
λ_{1h}	15	a_{3V}	3/4	k_V	10
λ_{2h}	25	a_{1h}	3/7	k_h	10
λ_{3h}	20	a_{2h}	1/2		

It is assumed that actuator faults are chosen as

$$E_1 = 0.7, \quad t \geq 100,$$
$$E_2 = 0.7, \quad t \geq 100. \tag{41}$$

The simulation results are provided in Figures 1–4. Figure 1 denotes the response to the 100 ft/s step velocity and 1000 ft step altitude. It has been observed that the velocity and altitude converge to the desired value. The control inputs of ϕ_c and δ_e could be seen in bottom plots of Figure 1.

Figure 2 shows the performance of the angle of attack α and the pitch rate Q at the top, as well as the canard deflection δ_c and the flight path angle γ at the bottom.

The velocity and altitude sliding mode surfaces s_V, s_h are shown in Figure 3, which are oscillation with small magnitudes when actuator fault occurred. The convergent performance verifies the effectiveness of the proposed control strategy. The adaptive parameters $\widehat{\upsilon}$ and $\widehat{\theta}$ in control laws of (15)–(18) could be seen in bottom plots of Figure 3, where the convergence of $\widehat{\upsilon}$ is confirmed. From the simulation results in Figure 3, the approximate equation $\widehat{\theta} \approx 3$ can be obtained. According to the relationship based on equation $\theta = 1/(1-\mu)$, we can solve that $\widehat{\mu} = 0.67$ and denote the estimated error as

$$e_\mu = \mu - \widehat{\mu} \approx 0.7 - 0.67 = 0.03. \tag{42}$$

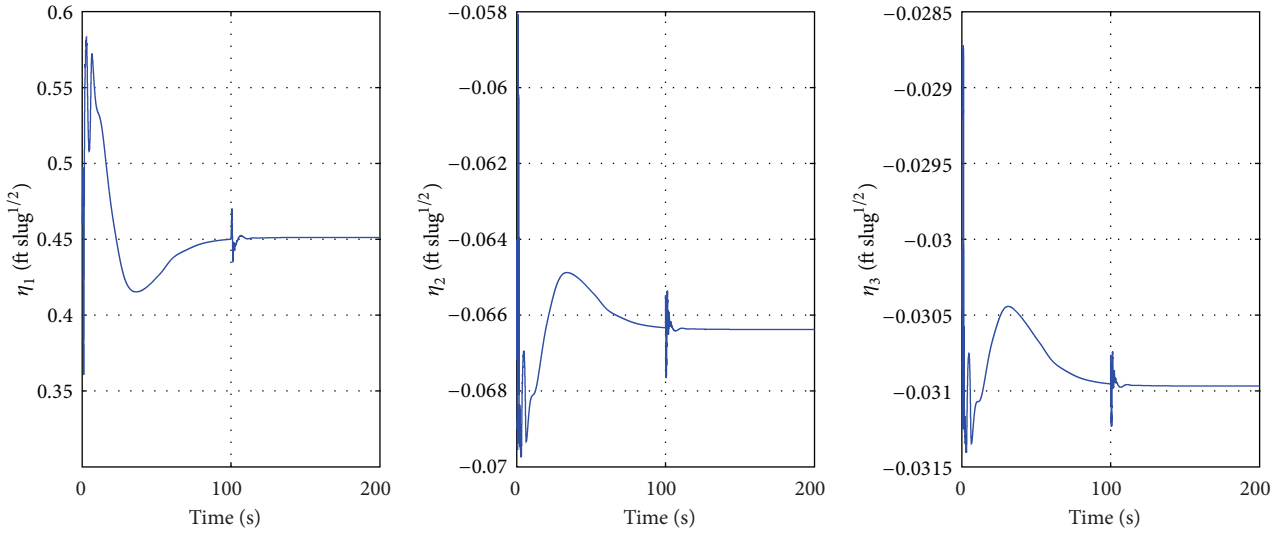

Figure 4: The dynamic response curves of flexile modes with actuator faults.

The value of e_μ in our research is in tolerance. Meanwhile, the stability of flexible states is depicted by Figure 4. And it can be seen that the flexible states η_1, η_2, and η_3 converge to constant values, respectively.

In summary, the simulation results demonstrate that, although there are actuator faults and uncertainties in the system, the good tracking performance and satisfactory system responses can be guaranteed.

5. Conclusions and Future Work

In this paper, an effective method has been proposed for linearizing the nonlinear model of the FAHV via feedback, which simplifies the complexity of the controller design process. Furthermore, an adaptive fault-tolerant control scheme based on finite-time sliding mode control technique has been brought forward for the FAHV without any information about the upper bound of uncertainties or the minimum value of actuator effectiveness. Simulation results have been presented to evaluate the validity of the proposed control scheme and to show its robustness to uncertainties and the loss of actuator effectiveness.

Further research work includes two aspects. Firstly, only the loss-of-effectiveness fault has been investigated in this paper; other types of actuator faults such as float failure and actuator faults in FAHV with unknown structure are worth being dealt with. Furthermore, the FAHV model considered in this paper is highly nonlinear and strongly coupled, and a more general active FTC scheme as adaptive fault diagnosis observer in [34, 35] should be investigated in our future study.

Conflict of Interests

The authors declare that there is no conflict of interests regarding the publication of this paper.

Acknowledgments

This research was supported in part by National Natural Science Foundation of China (nos. 91016018, 61004073, and 61203119), the Foundation for Key Program of Ministry of Education, China (no. 311012), the Key Program for Basic Research of Tianjin (no. 11JCZDJC25100), and the Key Program of Tianjin Natural Science (no. 12JCZDJC30300), and Aeronautical Science Foundation of China (no. 20125848004) supported by Science and Technology on Aircraft Control Laboratory.

References

[1] A. Mehrsai, H. R. Karimi, and K. D. Thoben, "Integration of supply networks for customization with modularity in cloud and make-to-upgrade strategy," *Systems Science and Control Engineering*, vol. 1, no. 1, pp. 28–42, 2013.

[2] S. R. Desai and R. Prasad, "A new approach to order reduction using stability equation and big bang big crunch optimization," *Systems Science and Control Engineering*, vol. 1, no. 1, pp. 20–27, 2013.

[3] Y. Chen and K. A. Hoo, "Stability analysis for closed-loop management of a reservoir based on identification of reduced-order nonlinear model," *Systems Science and Control Engineering*, vol. 1, no. 1, pp. 12–19, 2013.

[4] B. Fidan, M. Mirmirani, and P. A. Ioannou, "Flight dynamics and control of air-breathing hypersonic vehicles: review and new direction," in *Proceedings of the 12th AIAA International Space Planes and Hypersonic Systems and Technologies*, pp. 2003–7081, Norfolk, UK, December 2003.

[5] M. A. Bolender and D. B. Doman, "Nonlinear longitudinal dynamical model of an air-breathing hypersonic vehicle," *Journal of Spacecraft and Rockets*, vol. 44, no. 2, pp. 374–387, 2007.

[6] T. Williams, M. A. Bolender, D. B. Doman, and O. Morataya, "An aerothermal flexible mode analysis of a hypersonic vehicle,"

in *Proceesings of the Atmospheric Flight Mechanics Conference*, pp. 1391–1412, August 2006.

[7] D. O. Sigthorsson and A. Serrani, "Development of linear parameter-varying models of hypersonic air-breathing vehicles," in *Proceedings of the AIAA Guidance, Navigation, and Control Conference and Exhibit*, Chicago, Ill, USA, August 2009.

[8] M. Kuipers, M. Mirmirani, P. Ioannou, and Y. Huo, "Adaptive control of an aeroelastic airbreathing hypersonic cruise vehicle," in *Proceedings of the AIAA Guidance, Navigation, and Control Conference*, pp. 235–246, Hilton Head, SC, USA, August 2007.

[9] H. B. Duan and P. Li, "Progress in control approaches for hypersonic vehicle," *Science China*, vol. 55, no. 10, pp. 2965–2970, 2012.

[10] K. P. Groves, D. O. Sigthorsson, A. Serrani, S. Yurkovich, M. A. Bolender, and D. B. Doman, "Reference command tracking for a linearized model of an air-breathing hypersonic vehicle," in *Proceedings of the AIAA Guidance, Navigation, and Control Conference*, pp. 2901–2914, August 2005.

[11] L. Fiorentini, A. Serrani, M. A. Bolender, and D. B. Doman, "Robust nonlinear sequential loop closure control design for an air-breathing hypersonic vehicle model," in *Proceedings of the American Control Conference (ACC '08)*, pp. 3458–3463, Seattle, Wash, USA, June 2008.

[12] L. Fiorentini, A. Serrani, M. A. Bolender, and D. B. Doman, "Nonlinear robust adaptive control of flexible air-breathing hypersonic vehicles," *Journal of Guidance, Control, and Dynamics*, vol. 32, no. 2, pp. 401–416, 2009.

[13] L. Fiorentini, *Nonlinear Adaptive Controller Design for Air-breathing Hypersonic Vehicles [M.S. thesis]*, Ohio State University, 2010.

[14] J. T. Parker, A. Serrani, S. Yurkovich, M. A. Bolender, and D. B. Doman, "Approximate feedback linearization of an air-breathing hypersonic vehicle," in *Proceedings of the AIAA Guidance, Navigation, and Control Conference*, pp. 3633–3648, usa, August 2006.

[15] J. T. Parker, A. Serrani, S. Yurkovich, M. A. Bolender, and D. B. Doman, "Control-oriented modeling of an air-breathing hypersonic vehicle," *Journal of Guidance, Control, and Dynamics*, vol. 30, no. 3, pp. 856–869, 2007.

[16] O. U. Rehman, B. Fidan, and I. Petersen, "Uncertainty modeling for robust minimax LQR control of hypersonic flight vehicles," in *Proceedings of the AIAA Guidance, Navigation, and Control Conference and Exhibit*, October 2009.

[17] O. U. Rehman, I. R. Petersen, and B. Fidan, "Robust nonlinear control of a nonlinear uncertain system with input coupling and its application to hypersonic flight vehicles," in *Proceedings of the IEEE International Conference on Control Applications, CCA 2010*, pp. 1451–1457, Yokohama, Japan, September 2010.

[18] Z. Gao, B. Jiang, R. Qi, and Y. Xu, "Robust reliable control for a near space vehicle with parametric uncertainties and actuator faults," *International Journal of Systems Science*, vol. 42, no. 12, pp. 2113–2124, 2011.

[19] Z. Gao, B. Jiang, P. Shi, M. Qian, and J. Lin, "Active fault tolerant control design for reusable launch vehicle using adaptive sliding mode technique," *Journal of the Franklin Institute*, vol. 349, no. 4, pp. 1543–1560, 2012.

[20] Z. F. Gao and B. Jiang, "Active fault tolerant control design for near-space vehicle attitude dynamic with actuator faults," *Proceedings of the IMechE I*, vol. 225, no. 3, pp. 413–422, 2012.

[21] Z. Gao, B. Jiang, P. Shi, J. Liu, and Y. Xu, "Passive fault-tolerant control design for near-space hypersonic vehicle dynamical system," *Circuits, Systems, and Signal Processing*, vol. 31, no. 2, pp. 565–581, 2012.

[22] H. Li, L. Wu, Y. Si, H. Gao, and X. Hu, "Multi-objective fault-tolerant output tracking control of a flexible air-breathing hypersonic vehicle," *Proceedings of the Institution of Mechanical Engineers I*, vol. 224, no. 6, pp. 647–667, 2010.

[23] R. Y. Qi, Y. H. Huang, and B. Jiang, "Adaptive back-stepping control for a hypersonic vehicle with uncertain parameters and actuator faults," *Proceedings of the IMechE I*, vol. 227, no. 1, pp. 51–61, 2013.

[24] S. H. Li, H. B. Sun, and C. Y. Sun, "Robust adaptive integral sliding mode fault-tolerant control for airbreathing hypersonic vehicles," *Proceedings of the IMechE I*, vol. 226, no. 10, pp. 1344–1355, 2012.

[25] V. I. Utkin, "Variable structure systems with sliding modes," *IEEE Transactions on Automatic Control*, vol. 22, no. 2, pp. 212–222, 1977.

[26] H. Alwi, C. Edwards, O. Stroosma, and J. A. Mulder, "Fault tolerant sliding mode control design with piloted simulator evaluation," *Journal of Guidance, Control, and Dynamics*, vol. 31, no. 5, pp. 1186–1201, 2008.

[27] Q. L. Hu and B. Xiao, "Robust finite-time control for spacecraft attitude stabilization under actuator fault," *Proceedings of the IMechE I*, vol. 226, no. 13, pp. 416–428, 2013.

[28] M. A. Bolender, "An overview on dynamics and controls modelling of hypersonic vehicles," in *Proceedings of the American Control Conference (ACC '09)*, pp. 2507–2512, St. Louis, MO, USA, June 2009.

[29] B. Tian, W. Fan, Q. Zong, J. Wang, and F. Wang, "Adaptive high order sliding mode controller design for hypersonic vehicle with flexible body dynamics," *Mathematical Problems in Engineering*, vol. 2013, Article ID 357685, 11 pages, 2013.

[30] A. Levant, "Homogeneous high-order sliding modes," in *Proceedings of the 17th IFAC World Congress*, pp. 3799–3810, Seoul, Korea, 2008.

[31] A. Levant, "Finite-time stability and high relative degrees in sliding-mode control," in *Sliding Modes After the First Decade of the 21st Century*, vol. 412 of *Lecture Notes in Control and Information Sciences*, pp. 59–92, 2012.

[32] S. P. Bhat and D. S. Bernstein, "Geometric homogeneity with applications to finite-time stability," *Mathematics of Control, Signals, and Systems*, vol. 17, no. 2, pp. 101–127, 2005.

[33] Z. Zhu, Y. Xia, and M. Fu, "Attitude stabilization of rigid spacecraft with finite-time convergence," *International Journal of Robust and Nonlinear Control*, vol. 21, no. 6, pp. 686–702, 2011.

[34] S. Yin, S. Ding, A. Haghani, and H. Hao, "A comparison study of basic data driven fault diagnosis and process monitoring methods on the benchmark Tennessee Eastman process," *Journal of Process Control*, vol. 22, no. 9, pp. 1567–1581, 2012.

[35] S. Yin, H. Luo, and S. Ding, "Real-time implementation of fault-tolerant control systems with performance optimization," *IEEE Transactions on Industrial Electronics*, vol. 61, no. 5, pp. 2402–2411, 2013.

Hindawi Publishing Corporation
Mathematical Problems in Engineering
Volume 2013, Article ID 282168, 10 pages
http://dx.doi.org/10.1155/2013/282168

Research Article

Intermittent Fault Detection for Uncertain Networked Systems

Xiao He,[1,2] Yanyan Hu,[3] and Kaixiang Peng[4]

[1] *Department of Automation, TNList, Tsinghua University, Beijing 100084, China*
[2] *School of Automation, Beijing Institute of Technology, Beijing 100081, China*
[3] *Beijing Engineering Research Center of Industrial Spectrum Imaging, School of Automation and Electrical Engineering, University of Science and Technology of Beijing, Beijing 100083, China*
[4] *Key Laboratory for Advanced Control of Iron and Steel Process, School of Automation and Electrical Engineering, University of Science and Technology of Beijing, Beijing 100083, China*

Correspondence should be addressed to Kaixiang Peng; kaixiang@ustb.edu.cn

Received 12 September 2013; Accepted 25 September 2013

Academic Editor: Hongli Dong

This paper investigates intermittent fault detection problem for a class of networked systems with multiple state delays and unknown input. Polytopic-type parameter uncertainty in the state-space model matrices is considered. A novel measurement model is employed to account for both the random measurement delays and the stochastic data missing (package dropout) phenomenon, which are typically resulted from the limited capacity of the communication networks. We aim to design an uncertainty-dependent fault detection filter such that, for all unknown input, all possible parameter uncertainties, and all incomplete measurements, the error between residual and weighted fault is made as small as possible. By converting the addressed robust fault detection problem into an alternative robust H_∞ filtering problem of a certain Markovian jumping system (MJS), a sufficient condition for the existence of the desired robust fault detection filter is derived. A residual evaluation within an incremental form is brought forward to make the whole method suitable for intermittent fault detection. A numerical example is utilized to demonstrate the effectiveness of the proposed approach.

1. Introduction

For traditional control systems with point-to-point data transmission, a variety of methods have been proposed to deal with the modeling, identification, estimation, and control problems [1–3]. During the past decades, the rapid developments in network technologies have led to more and more feedback control systems with control loops closed via digital communication channels. Compared with the traditional point-to-point wiring, in networked systems, serial communication networks are used to exchange information (reference input, plant output, control input, etc.) among control system components (sensors, controller, actuators, etc.) [4]. The use of the communication channels can reduce the costs of cables and power, simplify the installation and maintenance of the whole system, and increase the reliability, so network-based analysis and designs have many industrial applications such as in automobiles, manufacturing plants, aircrafts, and HVAC systems. However, the insertion of the communication channels raises new interesting and challenging problems such as network-induced delays or packets dropout, see [4–6] for some representative works.

With the increasing demand for higher performance, higher safety, and reliability standards, fault detection and isolation (FDI) has been an active field of research over the past decades [7, 8]. The main purpose of fault detection is to construct a residual signal which can then be compared with a predefined threshold. When the residual exceeds the threshold, the fault is detected and an alarm is generated. Among different approaches for residual generation, the model-based approaches to FDI problems for dynamic systems have received more attention. For example, in [9], the H_∞ norm of transfer function matrix from unknown input to residual has been designed to be small, while the H_∞ norm (or the smallest nonzero singular value) of transfer function matrix from fault to residual has been guaranteed to be large. In [10],

the error between residual and weighted fault has been made as small as possible, and then the FDI problem can be solved by using the H_∞ filtering approach.

Due to the popularization of the using of network cables, it is necessary and interesting to consider the FDI problem for networked systems with network-induced delays or data missing, see [11, 12] and the references therein. Since network-induced delays and data missing (dropout) phenomenon are inherently random and time-varying [13], they have been modeled in various probabilistic ways [14]. One of the attractive approaches is to use binary switching sequence viewed as a Bernoulli distributed white sequence taking on values of 0 and 1, since such a representation is very effective to describe network-induced delays [15] or data missing [16]. Very recently, in [17], the network-induced delay and data dropout problems have been investigated in an integrated way within a unified framework and the robust filtering problem with polytopic uncertainties has been thoroughly studied. Note that in all the aforementioned results, it has been assumed that the delay or missing characteristics are statistically mutually independent from transfer to transfer. In [18], the fault detection problem for systems with missing measurements has been discussed by characterizing the residual dynamics by a discrete-time MJS. In [19], the diagnosis of intermittent faults in dynamic systems modeled as discrete event systems has been considered. So far, to the best of the authors' knowledge, the robust intermittent fault detection problems in the presence of parameter uncertainty for networked systems with simultaneous measurement delays and data missing have not been fully investigated, which constitutes the main focus of this paper.

In this paper, intermittent fault detection problem for a class of uncertain networked systems with multiple state delays and incomplete measurement is investigated. A sequence varying in a Markov fashion is employed in the measurement model so that both the measurement delays and data missing can be simultaneously represented. Polytopic-type parameter uncertainty in state-space model matrices is considered. After augmenting the state, the addressed robust fault detection problem is converted to an equivalent robust H_∞ filtering problem for a certain Markovian jumping system (MJS), and a sufficient condition for the existence of the desired robust fault detection filter is brought forward. By introducing the new residual evaluation function within an incremental form, the proposed method can detect the possible intermittent fault.

Notation. The notations used throughout the paper are fairly standard. $\mathbb{R}^n$ and $\mathbb{R}^{n\times m}$ denote, respectively, the n-dimensional Euclidean space and the set of all $n \times m$ real matrices. $P > 0$ means that P is real symmetric and positive definite. The subscript "T" denotes the matrix transpose. $\Pr\{\cdot\}$ represents the occurrence probability of the event "$\cdot$", and when x and y are both stochastic variables, $\mathbb{E}\{x\}$ stands for the mathematical expectation of x. $l_2[0,\infty)$ is the space of all square-summable vector functions over $[0,\infty)$, with $\|x\|$ being the standard l_2 norm of x, that is, $\|x\| = (x^T x)^{1/2}$. $\mathbf{RH}_\infty$ is the set of proper and stable rational functions with real coefficients. In symmetric block matrices, we use "$*$" to represent a term that is induced by symmetry, and $\mathrm{diag}\{\cdots\}$ stands for a block-diagonal matrix. Matrices, if their dimensions are not explicitly stated, are assumed to be compatible for algebraic operations and, sometimes, the arguments of a function will be omitted in the analysis when no confusion can arise.

2. Problem Formulation and Preliminaries

Consider the following class of discrete-time linear networked systems with multiple delays in the state:

$$\begin{aligned} x_{k+1} &= A_0 x_k + \sum_{i=1}^{q} A_i x_{k-i} + B_w w_k + B_f f_k, \\ y_k &= \delta(\tau_k, 0) C_0 x_k + \sum_{i=1}^{q} \delta(\tau_k, i) C_i x_{k-i} + D w_k, \\ x_k &= \varphi_k, \quad k = -q, -q+1, \ldots, 0, \end{aligned} \tag{1}$$

where $x_k \in \mathbb{R}^n$ stands for the state vector, $w_k \in \mathbb{R}^p$ is the unknown input belonging to $l_2[0,\infty)$, and $f_k \in \mathbb{R}^l$ is the fault to be detected. $1 \le i \le q$ ($q \ge 1$) are integer time delays. $y_k \in \mathbb{R}^m$ is the measured output vector, which may contain random communication delays and stochastic data missing induced by the limited capacity of the communication networks. All system matrices in (1) are assumed to have appropriate dimensions. φ_k is a given real initial sequence on $[-q, 0]$, and $\delta(\cdot,\cdot)$ stands for the Kronecker delta; that is,

$$\delta(j,l) = \begin{cases} 0, & \text{if } j \neq l, \\ 1, & \text{if } j = l. \end{cases} \tag{2}$$

Furthermore, τ_k is a stochastic variable whose role is to determine, at time k, the size of the occurred delay as well as the possibility of data missing. In this paper, $\{\tau_k\}$ is assumed to be a discrete-time homogeneous Markov chain taking values in the following finite state space:

$$\Xi = \{-1, 0, \ldots, q\} \tag{3}$$

and stationary transition probability matrix $\Lambda = [\lambda_{ij}]$, where

$$\lambda_{ij} = \Pr\{\tau_{k+1} = j \mid \tau_k = i\}. \tag{4}$$

Remark 1. The assumption that the switching between difference modes abides by a Markovian chain seems realistic since, in network-based signal transmissions, time delays and data dropouts typically occur in a *batch* mode, and the status of the network varies slower than the sampling period and the characteristics of the network at a certain time is usually dependent on the superior time instant. The transition from one mode to another may obey certain probability distribution, and our "Markov jumping" assumption of $\{\tau_k\}$ describes this phenomenon properly.

Remark 2. In our measurement model, the event $\{\tau_k = 0\}$ means that the measurements are ideally transmitted over the network without any delays or data missing, the event $\{\tau_k = i\}$

($1 \le i \le q$) corresponds to the case that the i-step measurement delay occurs. Without loss of generality and for the convenience in denoting the transition probability matrix, we set the state in the state space of the Markov chain corresponding to the measurement missing situation to -1, so $\{\tau_k = -1\}$ means that the measurements are missing and y_k consists of pure noise only.

In this paper, we are interested in the problem of robust fault detection for uncertain system described by (1) with incomplete measurements. The system matrices $A_0, A_1, \ldots, A_q, B_w, B_f, C_0, C_1, \ldots, C_q, D$ are assumed to be uncertain but belong to a known convex compact set of polytopic type,that is,

$$\Omega := \left(A_0, A_1, \ldots, A_q, B_w, B_f, C_0, C_1, \ldots, C_q, D\right) \in \Theta, \quad (5)$$

where Θ is a given convex bounded polyhedral domain described by ν vertices as follows:

$$\Theta := \left\{\Omega \mid \Omega = \sum_{r=1}^{\nu} \alpha_r \Omega_r;\ \sum_{r=1}^{\nu} \alpha_r = 1, \alpha_r \ge 0\right\}, \quad (6)$$

where $\Omega_r := (A_{0r}, A_{1r}, \ldots, A_{qr}, B_{wr}, B_{fr}, C_{0r}, C_{1r}, \ldots, C_{qr}, D_r)$, $r = 1, \ldots, \nu$, denotes the rth vertex of the polytope.

Consider a full-order fault detection filter of the following form:

$$\begin{aligned} \widetilde{x}_{k+1} &= G(\tau_k)\,\widetilde{x}_k + K(\tau_k)\,y_k, \\ r_k &= L(\tau_k)\,\widetilde{x}_k, \end{aligned} \quad (7)$$

where $\widetilde{x}_k \in \mathbb{R}^n$ is the filter state vector and $r_k \in \mathbb{R}^l$ is the so-called residual that is compatible with the fault vector f_k. For $\tau_k = i \in \Xi$, we denote matrices $G(\tau_k)$, $K(\tau_k)$, and $L(\tau_k)$ as $G_i = G(\tau_k = i)$, $K_i = K(\tau_k = i)$, and $L_i = L(\tau_k = i)$. Our main aim is to make the error between residual r_k and fault signal f_k as small as possible.

For the purpose of fault detection, it is not necessary to estimate the fault f_k. Sometimes one is more interested in the fault signal of a certain frequency interval, which can be formulated as the weighted fault as follows:

$$\widehat{f}(z) = T_f(z)\, f(z), \quad (8)$$

where $T_f(z) \in \mathbf{RH}_\infty$ is a prescribed weighting matrix.

Remark 3. Similar to [10], the introduction of a suitable weighting matrix $T_f(z)$ can limit the frequency interval of interest, and the system performance can then be improved. In fact, the use of weighted fault $\widehat{f}(z)$ is more general than using the original fault $f(z)$, because if we impose $T_f(z) = I$, we can obtain $\widehat{f}(z) = f(z)$.

Suppose a minimal realization of $\widehat{f}(z) = T_f(z)f(z)$ is

$$\begin{aligned} \widehat{x}_{k+1} &= A_t \widehat{x}_k + B_t f_k, \\ \widehat{f}_k &= C_t \widehat{x}_k + D_t f_k, \end{aligned} \quad (9)$$

where $\widehat{x}_k \in \mathbb{R}^{\widehat{n}}$ is the weighted fault state, $f_k \in \mathbb{R}^l$ is the original fault, and $\widehat{f}_k \in \mathbb{R}^l$ is the weighted fault. A_t, B_t, C_t, and D_t are assumed to be known real constant matrices with appropriate dimensions.

By defining

$$\begin{aligned} \zeta_k &= \left[w_k^T \ f_k^T\right]^T, \qquad \widetilde{r}_k = r_k - \widehat{f}_k, \\ \overline{x}_k &= \left[x_{k-1}^T \ \cdots \ x_{k-q}^T\right]^T, \qquad \eta_k = \left[x_k^T \ \overline{x}_k^T \ \widetilde{x}_k^T \ \widehat{x}_k^T\right]^T \end{aligned} \quad (10)$$

and again, denoting matrices $\widetilde{A}(\tau_k)$, $\widetilde{B}(\tau_k)$, $\widetilde{C}(\tau_k)$ and $\widetilde{D}(\tau_k)$ as $\widetilde{A}_i = \widetilde{A}(\tau_k = i)$, $\widetilde{B}_i = \widetilde{B}(\tau_k = i)$, $\widetilde{C}_i = \widetilde{C}(\tau_k = i)$, and $\widetilde{D}_i = \widetilde{D}(\tau_k = i)$, we have the overall fault detection dynamics governed by the following system:

$$\begin{aligned} \eta_{k+1} &= \widetilde{A}_i \eta_k + \widetilde{B}_i \zeta_k, \\ \widetilde{r}_k &= \widetilde{C}_i \eta_k + \widetilde{D}_i \zeta_k, \end{aligned} \quad (11)$$

where

$$\begin{aligned} \widetilde{A}_i &= \begin{bmatrix} \widehat{A}_i & 0 \\ 0 & A_t \end{bmatrix}, \qquad \widetilde{B}_i = \begin{bmatrix} \widehat{B}_i \\ \widehat{B}_t \end{bmatrix}, \\ \widetilde{C}_i &= \begin{bmatrix} \widehat{C}_i & -C_t \end{bmatrix}, \qquad \widetilde{D}_i = \begin{bmatrix} 0 & -D_t \end{bmatrix}, \\ \widehat{A}_i &= \begin{bmatrix} A_0 & A_d & 0 \\ \widehat{A}_{21} & \widehat{A}_{22} & 0 \\ \delta(i,0)\,K_0 C_0 & K_i C_i e_i & G_i \end{bmatrix}, \\ \widehat{B}_i &= \begin{bmatrix} B_w & B_f \\ 0_{qn\times p} & 0_{qn\times l} \\ K_i D & 0 \end{bmatrix}, \qquad \widehat{B}_t = \begin{bmatrix} 0 & B_t \end{bmatrix}, \\ \widehat{A}_{21} &= \begin{bmatrix} I_n \\ 0_{(q-1)n\times n} \end{bmatrix}, \qquad \widehat{A}_{22} = \begin{bmatrix} 0 & 0 \\ I_{(q-1)n\times(q-1)n} & 0 \end{bmatrix}, \\ A_d &= \begin{bmatrix} A_1 & \cdots & A_q \end{bmatrix}, \\ e_i &= \begin{bmatrix} \delta(i,1)\, I_{n\times n} & \cdots & \delta(i,q)\, I_{n\times n} \end{bmatrix}, \\ \widehat{C}_i &= \begin{bmatrix} 0_{l\times n} & 0_{l\times qn} & L_i \end{bmatrix}, \qquad \widehat{D}_i := \widetilde{D}_i. \end{aligned} \quad (12)$$

After the above manipulations, the admissible sensor delays and data missing can be reformulated as the jumping parameters of a Markovian jumping system (11) with the same transition probability matrix Λ.

The matrices $\widetilde{A}_i$, $\widetilde{B}_i$, $\widetilde{C}_i$, and $\widetilde{D}_i$, $i \in \Xi$, are uncertain, but they belong to prescribed matrix polytopes $\widetilde{\Omega}_i := (\widetilde{A}_i, \widetilde{B}_i, \widetilde{C}_i, \widetilde{D}_i,) \in \widetilde{\Theta}_i$, where $\widetilde{\Theta}_i$ are given convex bounded polyhedral domain described by ν vertices as follows:

$$\widetilde{\Theta}_i := \left\{\widetilde{\Omega}_i \mid \widetilde{\Omega}_i = \sum_{r=1}^{\nu} \alpha_r \widetilde{\Omega}_{ir};\ \sum_{r=1}^{\nu} \alpha_r = 1,\ \alpha_r \ge 0\right\}, \quad (13)$$

and $\widetilde{\Omega}_{ir} = (\widetilde{A}_{ir}, \widetilde{B}_{ir}, \widetilde{C}_{ir}, \widetilde{D}_{ir})$ denotes the rth vertices of the polytopes, where

$$\widetilde{A}_{ir} = \begin{bmatrix} \widehat{A}_{ir} & 0 \\ 0 & A_t \end{bmatrix}, \qquad \widetilde{B}_{ir} = \begin{bmatrix} \widehat{B}_{ir} \\ \widehat{B}_t \end{bmatrix},$$

$$\widetilde{C}_{ir} = \begin{bmatrix} \widehat{C}_i & -C_t \end{bmatrix} = \widetilde{C}_i,$$

$$\widetilde{D}_{ir} = \begin{bmatrix} 0 & -D_t \end{bmatrix} = \widehat{D}_{ir},$$

$$\widehat{A}_{ir} = \begin{bmatrix} A_{0r} & A_{dr} & 0 \\ \widehat{A}_{21} & \widehat{A}_{22} & 0 \\ \delta(i,0) K_0 C_{0r} & K_i C_{ir} e_i & G_i \end{bmatrix}, \tag{14}$$

$$\widehat{B}_{ir} = \begin{bmatrix} B_{wr} & B_{fr} \\ 0_{qn\times p} & 0_{qn\times l} \\ K_i D_r & 0 \end{bmatrix},$$

$$A_{dr} = \begin{bmatrix} A_{1r} & \cdots & A_{qr} \end{bmatrix}.$$

Matrices $\widehat{A}_{21}$, $\widehat{A}_{22}$, e_i, $\widehat{B}_t$, $\widetilde{C}_i$, $\widehat{C}_i$, $\widetilde{D}_i$, and $\widehat{D}_i$ are the same as defined in (12). Note that from (14), matrices $\widetilde{A}_{ir}$, $\widetilde{B}_{ir}$, $\widetilde{C}_{ir}$, and $\widetilde{D}_{ir}$ are affinely dependent on the matrices $A_{0r}, A_{1r}, \ldots, A_{qr}, B_{wr}, B_{fr}, C_{0r}, C_{1r}, \ldots, C_{qr}, D_r$, then for any $i \in \Xi$, the uncertainty polytopes (13) have the same number of vertices v, as well as the same combination coefficients α_r with (6), but different vertices for different Markovian model i.

Recall the following definition of mean square stability for MJSs.

Definition 4 (see [20]). System (11) with $\zeta_k = 0$ is said to be mean square stable if

$$\mathbb{E}\left\{\|\eta_k\|^2\right\} \longrightarrow 0, \quad \text{as } k \longrightarrow \infty \tag{15}$$

for any initial condition η_0 and initial distribution $\tau_0 \in \Xi$.

We further introduce the following definition.

Definition 5. System (11) with uncertain $\widetilde{\Omega}_i \in \widetilde{\Theta}_i$, $i \in \Xi$ (resp., $\Lambda \in \Pi$) is robust mean square stable if (11) is mean square stable for every $\widetilde{\Omega}_i \in \widetilde{\Theta}_i$, $i \in \Xi$ (resp., $\Lambda \in \Pi$).

Assumption 6. System (1) with $w_k = 0$ and $f_k = 0$ is assumed to be robust mean square stable.

With Definition 5, we can transform the robust fault detection filter design problem of system (1) to a robust H_∞ filtering problem for MJS (11). What we need to do here is to find the filter parameters G_i, K_i and L_i ($i \in \Xi$) such that the augmented fault detection dynamics (11) is robust mean square stable and the infimum of γ is made small in the feasibility of the following:

$$\sup_{\zeta_k \neq 0} \frac{\mathbb{E}\left\{\|\widetilde{r}_k\|^2\right\}}{\|\zeta_k\|^2} < \gamma^2, \quad \gamma > 0. \tag{16}$$

We further adopt a residual evaluation stage including an incremental evaluation function $J(k)$ and a threshold J_{th} of the following form:

$$J^L(k) = \left\{ \sum_{h=k-L}^{k} r_h^T r_h \right\}^{1/2}, \tag{17}$$

$$J_{\text{th}}^L = \sup_{w_k \in l_2, f_k = 0} \mathbb{E}\left\{J^L(k)\right\}, \tag{18}$$

where $r_{1-L} = r_{2-L} = \cdots = r_{-1} = r_0 = 0$ and L denotes the length of time window for evaluation function.

Based on (17), the occurrence of faults can be detected by comparing $J(k)$ with J_{th} according to the following rule:

$$\begin{aligned} &J^L(k) > J_{\text{th}}^L \Longrightarrow \text{with faults} \Longrightarrow \text{alarm}, \\ &J^L(k) \leq J_{\text{th}}^L \Longrightarrow \text{no faults} \Longrightarrow \text{do nothing}. \end{aligned} \tag{19}$$

Remark 7. By introducing the residual evaluation function with an incremental form (17), one can detect the possible intermittent fault for an uncertain networked system by analyzing the residual signal once it is generated by the fault detection filter (7). The reason is that the residual evaluation signal (11) is decreased to a small value over time once the fault disappears. This nature makes the proposed method in this paper be used for intermittent fault detection.

3. Fault Detection Filter Design

In this section, we shall discuss the robust fault detection filter design problem of system (1), under the existence of parameter uncertainty (13). We introduce the following lemma which is useful in deriving our main results in the sequel.

Lemma 8. *Consider system* (1) *with system uncertainty* (5)*, for a given fault detection filter of the form* (7)*, the augmented dynamic* (11) *is robust mean square stable and satisfies the constraint* (16)*, if there exist matrices* $P_{ir} \in \mathbb{R}^{(q+2)n}$, $i \in \Xi$, $r = 1, \ldots, v$, $P_t \in \mathbb{R}^{\tilde{n}}$, *and* $Q_i \in \mathbb{R}^{(q+2)n}$ *such that the following LMIs*

$$\begin{bmatrix} -P_{ir} & \widehat{A}_{ir}^T Q_i^T & 0 & \widehat{C}_i^T & 0 & 0 \\ * & -Q_i - Q_i^T + \mathscr{P}_r^T \mathscr{S}_i & Q_i \widehat{B}_{ir} & 0 & 0 & 0 \\ * & * & -\gamma^2 I & \widehat{D}_i^T & 0 & \widehat{B}_t^T P_t \\ * & * & * & -I & -C_t & 0 \\ * & * & * & * & -P_t & A_t^T P_t \\ * & * & * & * & * & -P_t \end{bmatrix} < 0 \tag{20}$$

hold for all $i \in \Xi$, $r = 1, \ldots, v$, *where* $\widehat{A}_{ir}$, $\widehat{B}_{ir}$, $\widehat{C}_i$, *and* $\widehat{D}_i$ *are defined in* (14), $\widehat{B}_t$ *is defined in* (12), A_t, B_t, C_t, D_t *are defined in* (9) *and,*

$$\begin{aligned} \mathscr{P}_r &= \begin{bmatrix} P_{(-1)r} & \cdots & P_{qr} \end{bmatrix}^T, \\ \mathscr{S}_i &= \begin{bmatrix} \lambda_{i(-1)} I_{(q+2)n} & \cdots & \lambda_{iq} I_{(q+2)n} \end{bmatrix}^T. \end{aligned} \tag{21}$$

Proof. Considering the structure of $\widetilde{A}_i$, $\widetilde{B}_i$, $\widetilde{C}_i$, and $\widetilde{D}_i$, and imposing

$$\widetilde{P}_i = \begin{bmatrix} P_i & 0 \\ 0 & P_t \end{bmatrix} \tag{22}$$

for all $i \in \Xi$, it can be concluded from the bounded real Lemma in [21] that a sufficient condition is that there exist matrices $P_i \in \mathbb{R}^{(q+2)n}$, $i \in \Xi$, $P_t \in \mathbb{R}^{\widehat{n}}$ such that the following LMIs

$$\begin{bmatrix} -P_i & \widehat{A}_i^T \mathscr{P}^T \mathcal{S}_i & 0 & \widehat{C}_i^T & 0 & 0 \\ * & -\mathscr{P}^T \mathcal{S}_i & \mathscr{P}^T \mathcal{S}_i \widehat{B}_i & 0 & 0 & 0 \\ * & * & -\gamma^2 I & \widehat{D}_i^T & 0 & \widehat{B}_t^T P_t \\ * & * & * & -I & -C_t & 0 \\ * & * & * & * & -P_t & A_t^T P_t \\ * & * & * & * & * & -P_t \end{bmatrix} < 0 \tag{23}$$

hold for any $i \in \Xi$, where $\widehat{A}_i$, $\widehat{B}_i$, $\widehat{C}_i$, $\widehat{D}_i$, and $\widehat{B}_t$ are defined in (12), A_t, B_t, C_t, and D_t are defined in (9), $\mathcal{S}_i$ is the same defined in (21) and

$$\mathscr{P} = \begin{bmatrix} P_{(-1)} & \cdots & P_q \end{bmatrix}^T. \tag{24}$$

Following the steps as the proof of Theorem 1 in [22], it can be shown that LMIs (23) are feasible if and only if there exist matrices $P_i \in \mathbb{R}^{(q+2)n}$, $Q_i \in \mathbb{R}^{(q+2)n}$, $i \in \Xi$, and $P_t \in \mathbb{R}^{\widehat{n}}$ satisfying

$$\begin{bmatrix} -P_i & \widehat{A}_i^T Q_i^T & 0 & \widehat{C}_i^T & 0 & 0 \\ * & -Q_i - Q_i^T + \mathscr{P}^T \mathcal{S}_i & Q_i \widehat{B}_i & 0 & 0 & 0 \\ * & * & -\gamma^2 I & \widehat{D}_i^T & 0 & \widehat{B}_t^T P_t \\ * & * & * & -I & -C_t & 0 \\ * & * & * & * & -P_t & A_t^T P_t \\ * & * & * & * & * & -P_t \end{bmatrix} < 0. \tag{25}$$

We are now in the position to prove that for system (1) with uncertainty (13), (20) ensures the robust mean square stable as well as the constraint (16) of the augmented dynamic (11). For an arbitrary fixed uncertain system with system matrices Ω, one can always find a set of coefficients $\alpha_r \geq 0$, $r = 1, \ldots, v$, such that both (6) and (13) hold. Note that LMIs (20) are affine in the matrices P_{ir}, $\widehat{A}_{ir}$, $\widehat{B}_{ir}$, $\widehat{C}_i$, and $\widehat{D}_i$, multiplying suitable inequalities of (20) by appropriate scalars α_r and summing up, it can be readily shown that (25) holds for every $\widetilde{\Omega}_i$ with a matrix $P_i(\alpha) = \sum_{r=1}^{v} \alpha_r P_{ir}$, $i = -1, \ldots, q$. By using the Bounded Real Lemma in [21], it follows that system (1) is robust mean square stable and (16) is satisfied. This concludes the proof. □

Next, we give the robust fault detection filter design result for system (1) with system uncertainty (13).

Theorem 9. *Consider system* (1) *with uncertain matrices* (13), *let* $\gamma > 0$ *be a given scalar, there exists an admissible full-order robust fault detection filter of the form* (7) *ensuring that the overall augmented dynamics* (11) *is robust mean square stable and the constraint* (16) *is satisfied, if there exist matrices* $0 < X_{ir}^T = X_{ir} \in \mathbb{R}^{(q+2)n \times (q+2)n}$, $S_i \in \mathbb{R}^{n \times n}$, $Z_i \in \mathbb{R}^{n \times n}$, $Y_i \in \mathbb{R}^{n \times n}$, $\overline{G}_i \in \mathbb{R}^{n \times n}$, $\overline{K}_i \in \mathbb{R}^{n \times m}$, $\overline{L}_i \in \mathbb{R}^{l \times n}$, $M_i \in \mathbb{R}^{qn \times qn}$, $i = -1, \ldots, q$, $r = 1, \ldots, v$, *and* $0 < P_t^T = P_t \in \mathbb{R}^{\widehat{n} \times \widehat{n}}$, *such that the following LMIs*

$$\begin{bmatrix} -X_{ir} & \Phi_{12} & 0 & \Phi_{14} & 0 & 0 \\ * & \Phi_{22} & \Phi_{23} & 0 & 0 & 0 \\ * & * & -\gamma^2 I & \widehat{D}_{ir}^T & 0 & \widehat{B}_t^T P_t \\ * & * & * & -I & -C_t & 0 \\ * & * & * & * & -P_t & A_t^T P_t \\ * & * & * & * & * & -P_t \end{bmatrix} < 0 \tag{26}$$

hold for $i = -1, \ldots, q$ *and* $r = 1, \ldots, v$, *where*

$$\Phi_{12} = \begin{bmatrix} A_{0r}^T Z_i^T & \begin{bmatrix} I_{n \times n} & 0_{n \times (q-1)n} \end{bmatrix} M_i^T & A_{0r}^T Y_i^T + \delta(i,0) C_{0r}^T \overline{K}_0^T + \overline{G}_i^T \\ A_{dr}^T Z_i^T & \begin{bmatrix} 0_{(q-1)n \times n} & I_{(q-1)n \times (q-1)n} \\ 0_{n \times n} & 0_{n \times (q-1)n} \end{bmatrix} M_i^T & A_{dr}^T Y_i^T + e_i^T C_{ir}^T \overline{K}_i^T \\ A_{0r}^T Z_i^T & \begin{bmatrix} I_{n \times n} & 0_{n \times (q-1)n} \end{bmatrix} M_i^T & A_{0r}^T Y_i^T + \delta(i,0) C_{0r}^T \overline{K}_0^T \end{bmatrix},$$

$$\Phi_{14} = \begin{bmatrix} \overline{L}_i^T \\ 0 \\ 0 \end{bmatrix}, \qquad \Phi_{22} := -\begin{bmatrix} Z_i + Z_i^T & 0 & Z_i + Y_i^T + S_i^T \\ * & M_i + M_i^T & 0 \\ * & * & Y_i + Y_i^T \end{bmatrix} + \mathcal{X}_r^T \mathcal{S}_i,$$

$$\Phi_{23} = \begin{bmatrix} Z_i B_{wr} & Z_i B_{fr} \\ 0 & 0 \\ Y_i B_{wr} + \overline{K}_i D_r & Y_i B_{fr} \end{bmatrix}, \qquad \mathcal{X}_r = \left[X_{(-1)r} \ \cdots \ X_{qr} \right]^T, \tag{27}$$

$\widehat{D}_{ir}$ is defined in (14) *and $\mathcal{S}_i$ is the same in* (21)*. Moreover, if* (26) *is feasible, the parameters of the desired robust fault detection filter can be given by*

$$G_i = V_i^{-1} \overline{G}_i S_i^{-1} V_i, \qquad K_i = V_i^{-1} \overline{K}_i, \qquad L_i = \overline{L}_i S_i^{-1} V_i, \tag{28}$$

where $V_i \in \mathbb{R}^{n \times n}$ is any invertible matrix (e.g., V_i could be set as I).

Proof. Considering (20), Let $U_i \in \mathbb{R}^{n \times n}$ and $V_i \in \mathbb{R}^{n \times n}$ be two nonsingular matrices, and set

$$Q_i^T = \begin{bmatrix} Y_i^T & 0 & Q_{31i}^T \\ 0 & M_i^T & 0 \\ V_i^T & 0 & Q_{33i}^T \end{bmatrix}. \tag{29}$$

Introducing the followind new matrices:

$$\overline{Q}_i^T = \begin{bmatrix} Z_i^{-T} & 0 & \overline{Q}_{31i}^T \\ 0 & I & 0 \\ U_i^T & 0 & \overline{Q}_{33i}^T \end{bmatrix}, \tag{30}$$

where the entries Q_{31i}^T, Q_{33i}^T, $\overline{Q}_{31i}^T$, and $\overline{Q}_{33i}^T$ are uniquely determined from the following relation:

$$\begin{bmatrix} Y_i^T & Q_{31i}^T \\ V_i^T & Q_{33i}^T \end{bmatrix} \begin{bmatrix} Z_i^{-T} & \overline{Q}_{31i}^T \\ U_i^T & \overline{Q}_{33i}^T \end{bmatrix} = \begin{bmatrix} Z_i^{-T} & \overline{Q}_{31i}^T \\ U_i^T & \overline{Q}_{33i}^T \end{bmatrix} \begin{bmatrix} Y_i^T & Q_{31i}^T \\ V_i^T & Q_{33i}^T \end{bmatrix} = I, \tag{31}$$

we further have the following relation

$$Q_i^T \overline{Q}_i^T = \overline{Q}_i^T Q_i^T = \begin{bmatrix} I & 0 & 0 \\ 0 & M_i^T & 0 \\ 0 & 0 & I \end{bmatrix}. \tag{32}$$

By defining

$$T_i = \begin{bmatrix} Z_i^T & 0 & Y_i^T \\ 0 & I & 0 \\ 0 & 0 & V_i^T \end{bmatrix}, \tag{33}$$

we obtain

$$T_i^T \overline{Q}_i \widehat{A}_{ir}^T Q_i^T \overline{Q}_i^T T_i = \begin{bmatrix} A_{0r}^T Z_i^T & \left[I_{n \times n} \ \ 0_{n \times (q-1)n} \right] M_i^T & A_{0r}^T Y_i^T + \delta(i,0) C_{0r}^T K_0^T V_0^T + Z_i U_i G_i^T V_i^T \\ A_{dr}^T Z_i^T & \begin{bmatrix} 0_{(q-1)n \times n} & I_{(q-1)n \times (q-1)n} \\ 0_{n \times n} & 0_{n \times (q-1)n} \end{bmatrix} M_i^T & A_{dr}^T Y_i^T + e_i^T C_{ir}^T K_i^T V_i^T \\ A_{0r}^T Z_i^T & \left[I_{n \times n} \ \ 0_{n \times (q-1)n} \right] M_i^T & A_{0r}^T Y_i^T + \delta(i,0) C_{0r}^T K_0^T V_0^T \end{bmatrix},$$

$$T_i^T \overline{Q}_i \widehat{C}_i^T = \begin{bmatrix} Z_i U_i L_i^T \\ 0 \\ 0 \end{bmatrix}, \qquad T_i^T \overline{Q}_i \left(Q_i + Q_i^T \right) \overline{Q}_i^T T_i = \begin{bmatrix} Z_i + Z_i^T & 0 & Z_i + Y_i^T + S_i^T \\ * & M_i + M_i^T & 0 \\ * & * & Y_i + Y_i^T \end{bmatrix}, \tag{34}$$

$$T_i^T \overline{Q}_i Q_i \widehat{B}_{ir} = \begin{bmatrix} Z_i B_{wr} & Z_i B_{fr} \\ 0 & 0 \\ Y_i B_{wr} + V_i K_i D_r & Y_i B_{fr} \end{bmatrix}.$$

Performing congruence transformations to (20) by $\mathrm{diag}\{\overline{Q}_i^T T_i, \overline{Q}_i^T T_i, I, I, I, I\}$, define

$$X_{ir} = T_i^T \overline{Q}_i P_{ir} \overline{Q}_i^T T_i, \qquad \overline{G}_i = V_i G_i U_i^T Z_i^T,$$

$$\overline{K}_i = V_i K_i, \qquad \overline{L}_i = L_i U_i^T Z_i^T, \qquad S_i = V_i U_i^T Z_i^T, \tag{35}$$

then, it can be easily shown that LMIs (26) together with the additional constraints (29) and (30) are equivalent to LMIs

in (20). Hence, if there exist matrices $X_{ir} > 0$, S_i, Z_i, Y_i, $\overline{G}_i$, $\overline{K}_i$, $\overline{L}_i$, M_i, $i = -1, \ldots, q$, and $P_t > 0$ such that LMIs (20) are feasible, the overall fault detection dynamic (11) is robust mean square stable and the constraint (16) is satisfied.

Furthermore, from LMIs (26), we have for $i = -1, \ldots, q$,

$$\begin{bmatrix} Z_i + Z_i^T & 0 & Z_i + Y_i^T + S_i^T \\ * & M_i + M_i^T & 0 \\ * & * & Y_i + Y_i^T \end{bmatrix} > 0. \tag{36}$$

This indicates that Z_i and Y_i are nonsingular and

$$\begin{aligned} &\begin{bmatrix} I & 0 & -I \end{bmatrix} \begin{bmatrix} Z_i + Z_i^T & 0 & Z_i + Y_i^T + S_i^T \\ * & M_i + M_i^T & 0 \\ * & * & Y_i + Y_i^T \end{bmatrix} \begin{bmatrix} I \\ 0 \\ -I \end{bmatrix} \\ &= -S_i - S_i^T > 0, \end{aligned} \tag{37}$$

which implies that S_i is nonsingular and also ensures the existence of parameter matrices G_i, K_i, and L_i in (28). The proof is completed. □

Remark 10. In Theorem 9, uncertainty-dependent robust fault detection filter design result is provided, which reduces the conservatism than the uncertainty-independent results. If we impose

$$X_{ir} = X_i, \quad i = -1, \ldots, q, \quad r = 1, \ldots, v, \tag{38}$$

to (26), the uncertainty-independent result can be recovered.

Remark 11. In most cases, we can know the size of the measurement delay or whether the data is missing at a certain time by using the time-stamp at the system node [5], and therefore the jumping parameters of the transformed MJS are accessible. In this sense, Theorem 9 provides us with network-status-dependent fault detection filter design methods. On the other hand, if the network status is not accessible; that is, the jumping parameters of the transformed MJS are unavailable, a network-status-independent result can be easily obtained by imposing

$$\begin{aligned} S_i = S, \qquad \overline{G}_i = \overline{G}, \\ \overline{K}_i = \overline{K}, \quad \overline{L}_i = \overline{L}, \quad i = -1, \ldots, q, \end{aligned} \tag{39}$$

in Theorem 9.

Note that (26) are LMIs over both the matrix variables and the prescribed scalar γ^2. This implies that (i) the robust full-order fault detection filter can be obtained from the solution of convex optimization problems in terms of LMIs, which can be solved via efficient interior-point algorithms [23]; (ii) the scalar γ^2 can be included as one of the optimization variables for LMIs (20), which makes it possible to obtain the minimum noise attenuation level bound for the fault detection dynamics (11). Then, the uncertainty-dependent suboptimal robust fault detection filter can be readily found by solving the following convex optimization problem.

Problem 12. Consider the parameter uncertainty (5), the sub-optimal robust fault detection filter for networked systems (1) with multiple state-delays and unknown inputs based on the idea of uncertainty dependence and network status dependence can be brought forward as follows:

$$\min_{\substack{X_{ir}>0, S_i, Z_i, Y_i, M_i, \overline{G}_i, \overline{K}_i, \overline{L}_i, \\ P_t>0, i=-1,\ldots,q, r=1,\ldots,v}} \gamma^2, \quad \text{s.t. (26)}. \tag{40}$$

For the problems mentioned above, the parameters of the sub-optimal robust fault detection filter can be determined by (28), and the sub-optimal robust H_∞ attenuation level for fault detection dynamics is given by $\gamma^* = \sqrt{\gamma_{\text{opt}}^2}$, where γ_{opt}^2 are the sub-optimal solution of the corresponding convex optimization problems.

Here is a summary of the whole fault detection method for system (1).

Step 1. Determine the vertex of uncertain parameters of (1).

Step 2. Calculate the parameters of fault detection filter using Theorem 9.

Step 3. Get a appropriate threshold from experiments for a specific noise type.

Step 4. Generate a real-time residual signal from the fault detection filter designed in Step 2.

Step 5. Compare the evaluation function with the threshold and use the logic (19) to alarm a fault.

Remark 13. In the present work, a model-based approach is considered since there is a mathematical model for the system plant. However, when there is no such a model and only input and output data can be obtained in many complex systems, data-driven methods may work better than the model based ones since there is a leakage of prior information of system dynamics. Please see [24, 25] for typical data-driven fault detection methods.

4. A Numerical Example

To illustrate the effectiveness of the proposed method, we provide a numerical examples in this section. Consider system (1) with the following uncertain system parameters:

$$\begin{aligned} A_0 &= \begin{bmatrix} 0 & 0.5 \\ 0.2 & \theta \end{bmatrix}, \qquad A_1 = \begin{bmatrix} 0.2 & 0 \\ 0.7 & 0.1 \end{bmatrix}, \\ B_w &= \begin{bmatrix} 0.5 \\ 0.3 \end{bmatrix}, \qquad B_f = \begin{bmatrix} -1 \\ 2 \end{bmatrix}, \\ C_0 &= C_1 = \begin{bmatrix} 0.2 & 0 \\ 0 & 0.5 \end{bmatrix}, \qquad D = \begin{bmatrix} 0.2 \\ -0.1 \end{bmatrix}, \end{aligned} \tag{41}$$

where θ is an uncertain real parameter satisfying $0.1 \le \theta \le 0.3$. The initial state values φ_k are set to be $\varphi_{-1} = \varphi_0 = 0$.

Let $q = 1$, so the state-space of the Markov chain $\{\tau_k\}$ is $\Xi = \{-1, 0, 1\}$. The transition probability matrix is given by

$$\Lambda := \begin{bmatrix} \lambda_{-1,-1} & \lambda_{-1,0} & \lambda_{-1,1} \\ \lambda_{0,-1} & \lambda_{0,0} & \lambda_{0,1} \\ \lambda_{1,-1} & \lambda_{1,0} & \lambda_{1,1} \end{bmatrix} = \begin{bmatrix} 0.7 & 0.2 & 0.1 \\ 0.3 & 0.4 & 0.3 \\ 0.2 & 0.3 & 0.5 \end{bmatrix}, \quad (42)$$

and the initial mode is set to be $\tau_0 = 0$. For $k = 0, 1, \ldots, 300$, the unknown input w_k is supposed to be a random noise uniformly distributed over $[-0.5, 0.5]$, and the fault signal f_k is of the following intermittent form:

$$f_k = \begin{cases} 1, & \text{for } k = 200s + 101, \ldots, 200s + 200 \ \ (s = 0, 1, 2), \\ 0, & \text{others.} \end{cases} \quad (43)$$

The weighting matrix is supposed to be $T_f(z) = (0.5z)/(z - 0.5)$, with the following state space realization:

$$\begin{aligned} \widehat{x}_{k+1} &= 0.5\widehat{x}_k + 0.25 f_k, \\ \widehat{f}_k &= \widehat{x}_k + 0.5 f_k, \\ \widehat{x}_0 &= 0, \end{aligned} \quad (44)$$

where f_k and $\widehat{f}_k$ are shown in Figure 1.

With the predefined parameters, from Theorem 9, Problem 12 can be solved by using the Matlab LMI toolbox [23]. As a result, the minimum noise attenuation level bound of the fault detection dynamic is $\gamma_{\text{opt}} = 1.0012$, and the parameters of the sub-optimal fault detection filter in different modes are given by

$$\begin{aligned} G_{-1} &= \begin{bmatrix} 0.1311 & 1.3402 \\ 0.1620 & 0.6100 \end{bmatrix}, \quad K_{-1} = \begin{bmatrix} 4.3089 & 8.6222 \\ 21.7929 & 43.5879 \end{bmatrix}, \\ L_{-1} &= \begin{bmatrix} -0.7029 & 0.0724 \end{bmatrix}, \quad G_0 = \begin{bmatrix} 0.0315 & 0.4950 \\ -0.0373 & 0.2187 \end{bmatrix}, \\ K_0 &= \begin{bmatrix} -0.0002 & -0.0025 \\ -0.0005 & -0.0006 \end{bmatrix}, \quad L_0 = \begin{bmatrix} -0.1088 & -0.0396 \end{bmatrix}, \\ G_1 &= \begin{bmatrix} -0.1343 & 0.8207 \\ -0.0807 & 0.3832 \end{bmatrix}, \quad K_1 = \begin{bmatrix} -0.0014 & -0.0001 \\ -0.0018 & -0.0002 \end{bmatrix}, \\ L_1 &= \begin{bmatrix} -0.6086 & 0.2436 \end{bmatrix}. \end{aligned} \quad (45)$$

If we impose the uncertainty-independent and network-status-independent method indicated in Remarks 10 and 11, a fault detection filter with $\gamma_{\text{opt}} = 1.0082$ can be obtained.

Next, we consider the time-domain simulation using the obtained fault detection filter. we arbitrarily choose $\theta = 0.15$. Figure 2 shows the measurement mode with random delays and stochastic missing phenomenon. $\tau_k = -1, 0, 1$,means that the measurement is missing, transmitted over the network ideally, and with one-step delay, respectively.

Figure 3 shows the generated residual signal r_k, and the evolution of $J^L(k)$ is presented in Figure 4, where we choose

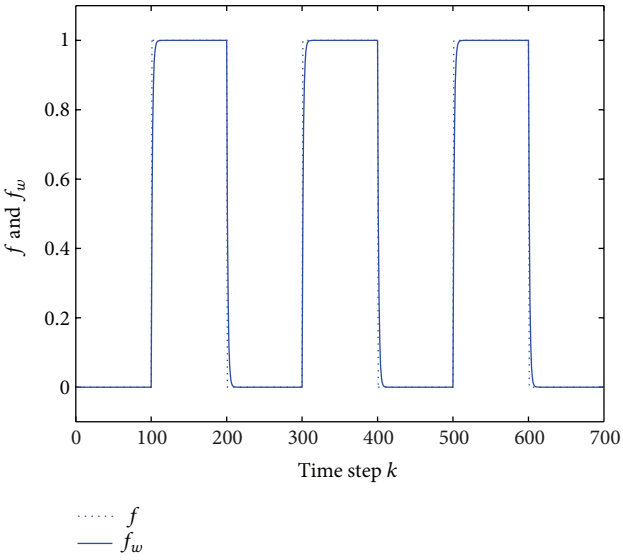

Figure 1: Fault f_k and weighting fault $\widehat{f}_k(f_w)$.

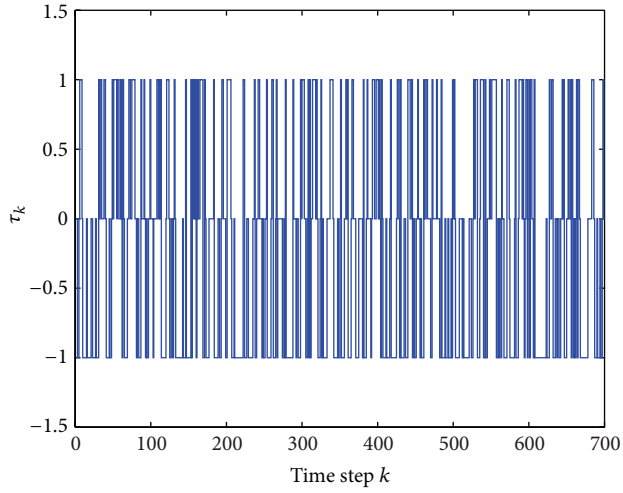

Figure 2: Measurement mode over network.

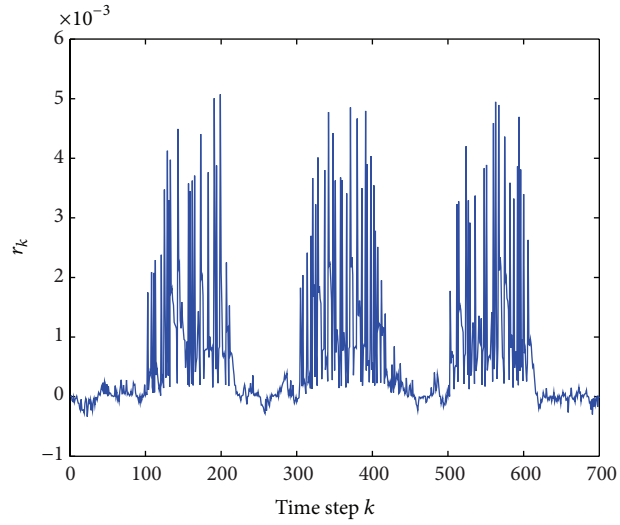

Figure 3: Residual signal r_k.

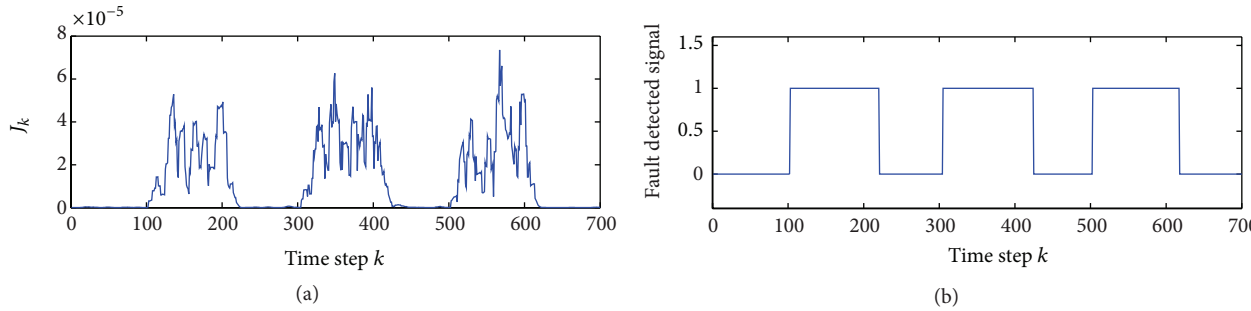

Figure 4: Evolution of $J^L(k)$.

the length of time window $L = 8$. After 400 times of simulations, we get a threshold $J_{\text{th}}^L = 1.5215 \times 10^{-6}$. Figure 4 shows the real-time fault detection result:

$$\begin{aligned}
&4.9199 \times 10^{-8} = J(102) < J_{\text{th}}^L < J(103) = 3.1041 \times 10^{-6},\\
&1.9392 \times 10^{-6} = J(220) < J_{\text{th}}^L < J(221) = 1.4006 \times 10^{-6},\\
&9.1655 \times 10^{-8} = J(304) < J_{\text{th}}^L < J(305) = 3.4154 \times 10^{-6},\\
&2.5346 \times 10^{-6} = J(424) < J_{\text{th}}^L < J(425) = 6.0104 \times 10^{-7},\\
&8.1835 \times 10^{-8} = J(502) < J_{\text{th}}^L < J(503) = 3.2139 \times 10^{-6},\\
&1.9241 \times 10^{-6} = J(617) < J_{\text{th}}^L < J(618) = 1.1692 \times 10^{-6}.
\end{aligned} \tag{46}$$

From above inequations, we can observe the fault occurrence can be detected after 3, 5, 3 steps, while the disappearance of fault can be detected after 21, 25, 18 steps, respectively.

Remark 14. After introducing a novel residual evaluation function of the incremental type (17), one can detect not only the occurrence of a fault but also its disappearance. It can be observed from Figure 4 that the disappearance of the fault usually needs longer time to detect than the occurrence of faults. This is because the mathematical model of the system is based on the plant without the faults. This is of engineering significance and the proposed method in this paper can be applied to detect intermittent faults in many practical industrial processes.

Remark 15. The length of time window for evaluation function L in (17) is also a factor that can affect the fault detection performance. Longer L can reduce the missing alarm rate and false alarm rate; however, it costs longer detection time. Short L can provide a rapid fault detection but this results in larger missing alarm rate and false alarm rate.

5. Conclusions

In this paper, the robust intermittent fault detection problem has been investigated for a class of discrete-time uncertain networked systems with state delays and incomplete measurements. The random delay and stochastic missing phenomenon in the measurements have been simultaneously investigated. Polytopic-type parameter uncertainty in the state-space model matrices has been considered. By augmenting the states, the addressed robust fault detection problem has been converted to an auxiliary robust H_∞ filtering problem for a certain Markovian jumping system (MJS). A sufficient condition for the design of the desired robust fault detection filter has been established. A numerical example has been introduced to illustrate the effectiveness of the proposed methodology.

Acknowledgments

This work was supported in part by the National Natural Science Foundation of China under Grant 61074084 and 61074085 and an open Grant of the Key Laboratory of Hydro-Science and Engineering in Chongqing Jiaotong University under Grant SLK2010.

References

[1] S. Elmadssia, K. Saadaoui, and M. Benrejeb, "New delay-dependent stability conditions for linear systems with delay," *Systems Science and Control Engineering*, vol. 1, no. 1, pp. 2–11, 2013.

[2] Y. Chen and K. A. Hoo, "Stability analysis for closed-loop management of a reservoir based on identification of reduced-order nonlinear model," *Systems Science and Control Engineering*, vol. 1, no. 1, pp. 12–19, 2013.

[3] M. Darouach and M. Chadli, "Admissibility and control of switched discrete-time singular systems," *Systems Science and Control Engineering*, vol. 1, no. 1, pp. 43–51, 2013.

[4] W. Zhang, M. S. Branicky, and S. M. Phillips, "Stability of networked control systems," *IEEE Control Systems Magazine*, vol. 21, no. 1, pp. 84–99, 2001.

[5] J. Nilsson, *Real-time control systems with delays [Ph.D. dissertation]*, Department Automatic Control, Lund Institute of Technology, Lund, Sweden, 1998.

[6] D. Yue, E. Tian, and Q.-L. Han, "A delay system method for designing event-triggered controllers of networked control systems," *IEEE Transactions on Automatic Control*, vol. 58, no. 2, pp. 475–481, 2013.

[7] P. M. Frank, S. X. Ding, and B. Koppen-Seliger, "Current developments in the theory of FDI," in *Proceedings of the 4th IFAC Symposium Fault Detection Supervision Safety Technical Processes*, Proceedings of SAFEPRO-CESS, pp. 16–27, Budapest, Hungary, 2000.

[8] M. Kinnaert, "Fault diagnosis based on analytical models for linear and nonlinear systems," in *Proceedings of the 15th International Workshop on Principles of Diagnosis*, Proceedings of SAFEPROCESS, pp. 37–50, Washington, DC, USA, 2003.

[9] S. X. Ding, T. Jeinsch, P. M. Frank, and E. L. Ding, "A unified approach to the optimization of fault detection systems," *International Journal of Adaptive Control and Signal Processing*, vol. 14, no. 7, pp. 725–745, 2000.

[10] M. Zhong, H. Ye, P. Shi, and G. Wang, "Fault detection for markovian jump systems," *IEE Proceedings Control Theory and Applications*, vol. 152, no. 4, pp. 397–402, 2005.

[11] H. Fang, H. Ye, and M. Zhong, "Fault diagnosis of networked control systems (MED '09)," in *Mediterranean Conference on Control and Automation*, Proceedings of SAFEPROCESS, pp. 1–12, Beijing, China, June 2006.

[12] M. Nader and K. Khashayar, "Actuator fault detection and isolation for a network of unmanned vehicles," *IEEE Transactions on Automatic Control*, vol. 54, no. 4, pp. 835–840, 2009.

[13] R. Luck and A. Ray, "An observer-based compensator for distributed delays," *Automatica*, vol. 26, no. 5, pp. 903–908, 1990.

[14] L. Zhang, Y. Shi, T. Chen, and B. Huang, "A new method for stabilization of networked control systems with random delays," *IEEE Transactions on Automatic Control*, vol. 50, no. 8, pp. 1177–1181, 2005.

[15] F. Yang, Z. Wang, Y. S. Hung, and M. Gani, "H_∞ control for networked systems with random communication delays," *IEEE Transactions on Automatic Control*, vol. 51, no. 3, pp. 511–518, 2006.

[16] Z. Wang, D. W. C. Ho, and X. Liu, "Variance-constrained filtering for uncertain stochastic systems with missing measurements," *IEEE Transactions on Automatic Control*, vol. 48, no. 7, pp. 1254–1258, 2003.

[17] X. He, Z. Wang, and D. Zhou, "Robust H_∞ filtering for networked systems with multiple state-delays," *International Journal of Control*, vol. 80, no. 8, pp. 1217–1232, 2007.

[18] P. Zhang, S. X. Ding, P. M. Frank, and M. Sader, "Fault detection of networked control systems with missing measurements," in *Proceedings of Asian Control Conference*, pp. 1258–1263, Melbourne, Australia, 2004.

[19] O. Contant, S. Lafortune, and D. Teneketzis, "Diagnosis of intermittent faults," *Discrete Event Dynamic Systems: Theory and Applications*, vol. 14, no. 2, pp. 171–202, 2004.

[20] O. L. V. Costa and M. D. Fragoso, "Stability results for discrete-time linear systems with Markovian jumping parameters," *Journal of Mathematical Analysis and Applications*, vol. 179, no. 1, pp. 154–178, 1993.

[21] O. L. V. Costa and R. P. Marques, "Mixed H_2/H_∞-control of discrete-time Markovian jump linear systems," *IEEE Transactions on Automatic Control*, vol. 43, no. 1, pp. 95–100, 1998.

[22] M. C. de Oliveira, J. C. Geromel, and J. Bernussou, "Extended H_2 and H_∞ norm characterizations and controller parametrizations for discrete-time systems," *International Journal of Control*, vol. 75, no. 9, pp. 666–679, 2002.

[23] S. Boyd, L. El Ghaoui, E. Feron, and V. Balakrishnan, *Linear Matrix Inequalities in System and Control Theory*, vol. 15 of *SIAM Studies in Applied Mathematics*, Society for Industrial and Applied Mathematics (SIAM), Philadelphia, PA, USA, 1994.

[24] S. Yin, H. Luo, and S. X. Ding, "Real-time implementation of fault tolerant control system with performance optimization," *IEEE Transactions on Industrial Electronics*, 2013.

[25] S. Yin, S. X. Ding, A. Gaghani, H. Hao, and P. Zhang, "A comparison study of basic data-driven fault diagnosis and process monitoring methods on the benchmark Tennessee Eastman process," *Journal of Process Control*, vol. 22, no. 9, pp. 1567–1581, 2012.

Hindawi Publishing Corporation
Mathematical Problems in Engineering
Volume 2013, Article ID 916040, 9 pages
http://dx.doi.org/10.1155/2013/916040

Research Article

Self-Triggered Model Predictive Control Using Optimization with Prediction Horizon One

Koichi Kobayashi and Kunihiko Hiraishi

School of Information Science, Japan Advanced Institute of Science and Technology, Ishikawa 923-1292, Japan

Correspondence should be addressed to Koichi Kobayashi; k-kobaya@jaist.ac.jp

Received 1 August 2013; Revised 12 October 2013; Accepted 13 October 2013

Academic Editor: Bo Shen

Self-triggered control is a control method that the control input and the sampling period are computed simultaneously in sampled-data control systems and is extensively studied in the field of control theory of networked systems and cyber-physical systems. In this paper, a new approach for self-triggered control is proposed from the viewpoint of model predictive control (MPC). First, the difficulty of self-triggered MPC is explained. To overcome this difficulty, two problems, that is, (i) the one-step input-constrained problem and (ii) the N-step input-constrained problem are newly formulated. By repeatedly solving either problem in each sampling period, the control input and the sampling period can be obtained, that is, self-triggered MPC can be realized. Next, an iterative solution method for the latter problem and an approximate solution method for the former problem are proposed. Finally, the effectiveness of the proposed approach is shown by numerical examples.

1. Introduction

In recent years, analysis and synthesis of networked control systems (NCSs) have been extensively studied [1, 2]. An NCS is a control system in which plants, sensors, controllers, and actuators are connected through communication networks. In distributed control systems, subsystems are frequently connected via communication networks, and it is important to consider analysis and synthesis of distributed control systems from the viewpoint of NCSs. In the design of NCSs, several technical issues such as packet losses, transmission delays, and communication constraints are included. However, it is difficult to consider these issues in a unified way, and it is suitable to discuss an individual problem. From this viewpoint, several results have been obtained so far (see, e.g., [3–6]).

In this paper, the periodic paradigm is focused as one of the technical issues in NCSs. The periodic paradigm is that the controller is periodically executed at a given unit of time. The period is chosen based on CPU processing time, communication bandwidth, and so on. However, in NCSs, communication should occur, when there exists important information, which must be transmitted from the controller to the actuator and/or from the sensor to the controller. In this sense, the periodic paradigm is not necessarily suitable, and it is important to consider a new approach for the design of NCSs. One of the methods to overcome this drawback of the periodic paradigm, self-triggered control has been proposed so far (see, e.g., [7–12]). Also in the field of cyber-physical systems, this control method is focused. In self-triggered control, the next sampling time at which the control input is recomputed is computed. That is, both the sampling period and the control input are computed simultaneously. In many existing works, first, the continuous-time controller is obtained, and after that, the sampling period such that stability is preserved is computed. However, few results on optimal control have been obtained so far. From the viewpoint of optimal control, for example, a design method based one-step finite horizon boundary has been recently proposed in [13, 14]. In this method, the first sampling period such that the optimal value of the cost function is improved, is computed under the constraint that other sampling periods are given as a constant. However, a nonlinear equation must be solved. Furthermore, input constraints cannot be considered in this method. In [10], the authors have proposed self-triggered model predictive control using Taylor series expansions. In this method, the control input and the sampling period are computed by solving a quadratic programming (QP)

problem, but the convexity of the obtained QP problem has not been guaranteed.

In this paper, we propose two methods for self-triggered model predictive control (MPC) using optimization with horizon one. First, the optimal control problem with horizon one is formulated. However, in constrained systems, one-step prediction may be insufficient, and a longer time interval, in which the input constraint is imposed, is required. Focusing on this fact, another problem in which the time interval with input constraints is enlarged is also formulated. In the former problem, the first sampling period and the first control input are optimized. In the latter problem, the first sampling period and the control input sequence are optimized. Next, an iterative solution method for the latter problem and an approximate solution method for the former problem are proposed. In the iterative solution method, a QP problem is repeatedly solved. In the approximate solution method, the problem is approximated by one QP problem. The obtained QP problem is in general not convex, and we discuss the convexity. By solving either problem according to the receding horizon policy, self-triggered MPC can be realized. Finally, the effectiveness of the proposed approach is shown by a numerical example. The proposed approach provides us a basic result for self-triggered optimal control.

Notation. Let $\mathscr{R}$ denote the set of real numbers. Let I_n, $0_{m\times n}$ denote the $n \times n$ identity matrix, the $m \times n$ zero matrix, respectively. For simplicity, we sometimes use the symbol 0 instead of $0_{m\times n}$, and the symbol I instead of I_n.

2. Self-Triggered Model Predictive Control

Consider the following continuous-time linear system:

$$\dot{x}(t) = Ax(t) + Bu(t), \tag{1}$$

where $x \in \mathscr{R}^n$ is the state, and $u \in [u_{\min}, u_{\max}] \subseteq \mathscr{R}^m$ is the control input with the input constraint. The vectors $u_{\min}$, $u_{\max} \in \mathscr{R}^m$ are a given constant vector. Let t_k, $k = 0, 1, \ldots$ denote the sampling time. The sampling period is defined by $h_k := t_{k+1} - t_k$, which is a nonnegative scalar. Assume that the control input is piecewise constant, that is, the control input is given by

$$u(t) = u(t_k), \quad t \in [t_k, t_{k+1}). \tag{2}$$

Hereafter, we denote $u(t_k)$ as u_k. In addition, assume that a pair (A, B) is controllable.

First, for the system (1), the self-triggered optimal control problem is formulated as follows.

Problem 1 (self-triggered optimal control problem). Suppose that for the system (1), the initial time t_0, the initial state $x(t_0) = x_0$, the final time t_f, and the final step f are given. Then, find both a control input sequence $u_0, u_1, \ldots, u_{f-1}$ and a sampling period sequence $h_0, h_1, \ldots, h_{f-1}$ minimizing the following cost function:

$$J = \int_{t_0}^{t_f} \left\{ x^T(t) Q x(t) + u^T(t) R u(t) \right\} dt, \tag{3}$$

under the following two constraints:

$$\begin{aligned} h_{\min} &\le h_k \le h_{\max}, \\ u_{\min} &\le u_k \le u_{\max}, \\ h_0 + h_1 + \cdots + h_{f-1} &= t_f, \end{aligned} \tag{4}$$

where Q is positive semidefinite, R is positive definite, and $h_{\min}$, $h_{\max} \ge 0$ are a given constant.

Next, we present a procedure of MPC based on the self-triggered strategy.

Procedure of Self-Triggered MPC

Step 1. Set $t_0 = 0$, and give the initial state $x(0) = x_0$.

Step 2. Solve Problem 1.

Step 3. Apply only $u(t)$, $t \in [t_0, t_0 + h_0)$ to the plant.

Step 4. Compute the predicated state $\hat{x}(t_0 + h_0)$ by using $x(t_0)$, u_0, and h_0.

Step 5. Solve Problem 1 by using $\hat{x}(t_0 + h_0)$ as x_0.

Step 6. Wait until time $t_0 + h_0$.

Step 7. Update $t_0 := t_0 + h_0$, measure $x(t_0)$, and return to Step 3.

Note here that in this procedure, the timing (i.e., the sampling time) to measure the state and to recompute the control input is computed. In this sense, self-triggered control is realized.

In the above procedure, Problem 1 must be solved repeatedly. However, Problem 1 is in general reduced to a nonlinear programming problem, and it is difficult to solve this problem. Then, it is important to compute a suboptimal and approximate solution for Problem 1. To compute a suboptimal and approximate solution, two problems, which are solved in Steps 2 and 5 instead of Problem 1, will be formulated in the next section.

3. Problem Formulation

In self-triggered MPC, only $u(t)$, $t \in [t_0, t_0 + h_0)$ is applied to the plant. Hence, it is important to consider the problem of finding suitable h_0 and u_0. By solving this problem repeatedly, we can continue to obtain the control input. Thus, a sampling period sequence $h_0, h_1, \ldots, h_{f-1}$ is approximated as follows: (i) only h_0 is a decision variable (i.e., the other sampling periods are given in advance), (ii) $h_1 = h_2 = \cdots = h_{f-1}$ holds. In addition, the time interval $[t_0, t_f)$ in Problem 1 is enlarged to $[t_1, \infty)$. Here, we consider the following two optimal control problems with prediction horizon one.

(i) One-step input-constrained problem.

(ii) N-step input-constrained problem.

In the former problem, the constraint is imposed for only u_0. In the latter problem, the constraint is imposed for $u_0, u_1, \ldots, u_{N-1}$, where $N \leq f$ is given in advance.

Before these problems are formally given, some preparations are given. In the time interval $[t_1, t_f)$, suppose that $h_1 = h_2 = \cdots = h_{f-1} = h$ is satisfied, where h is a given constant (see also Remark 4). In addition, the input constraint $u_{\min} \leq u_k \leq u_{\max}$, $k = 1, 2, \ldots, f-1$ is ignored. Then, the optimal value of the cost function $J = \int_{t_1}^{\infty} \{x^T(t)Qx(t) + u^T(t)Ru(t)\}dt$ can be derived as $x^T(t_1)P(h)x(t_1)$, where $P(h)$ is a symmetric positive definite matrix, which is a solution of the following discrete-time algebraic Riccati equation:

$$\begin{aligned} &\widetilde{A}^T(h)\,P(h)\,\widetilde{A}(h) - P(h) \\ &\quad - \left(\widetilde{A}^T(h)\,P(h)\,\widetilde{B}(h) + \widetilde{S}(h)\right) \\ &\quad \times \left(\widetilde{B}^T(h)\,P(h)\,\widetilde{B}(h) + \widetilde{R}(h)\right)^{-1} \\ &\quad \times \left(\widetilde{B}^T(h)\,P(h)\,\widetilde{A}(h) + \widetilde{S}^T(h)\right) + \widetilde{Q}(h) = 0, \end{aligned} \tag{5}$$

where

$$\begin{aligned} \widetilde{A}(h) &:= e^{Ah}, \\ \widetilde{B}(h) &:= \int_0^h e^{A\tau}d\tau B, \end{aligned} \tag{6}$$

$$\begin{bmatrix} \widetilde{Q}(h) & \widetilde{S}(h) \\ \widetilde{S}^T(h) & \widetilde{R}(h) \end{bmatrix} := \int_0^h e^{F^T t} \begin{bmatrix} Q & 0 \\ 0 & R \end{bmatrix} e^{Ft}dt, \tag{7}$$

$$F := \begin{bmatrix} A & B \\ 0 & 0 \end{bmatrix}.$$

Under the above preparation, we formulate the one-step input-constrained problem as follows.

Problem 2 (one-step input-constrained problem). Suppose that for the system (1), the initial time t_0, the initial state $x(t_0) = x_0$, and $h_1 = h_2 = \cdots = h$ are given. Then, find both a control input u_0 and a sampling period h_0 minimizing the following cost function:

$$\begin{aligned} J = &\int_{t_0}^{t_1} \left\{x^T(t)\,Qx(t) + u^T(t)\,Ru(t)\right\} dt \\ &+ x^T(t_1)\,P(h)\,x(t_1) \end{aligned} \tag{8}$$

under the following two constraints:

$$\begin{aligned} h \leq h_0 \leq h_{\max}, \\ u_{\min} \leq u_0 \leq u_{\max}, \end{aligned} \tag{9}$$

where $h_{\max} \geq 0$ is a given constant.

In [13, 14], a related problem has been discussed, but in these existing results, the above two constraints cannot be imposed. In [10], the authors have considered a more complicated problem with delay compensation. In this paper, the above simplified problem is considered for analyzing the convexity.

In constrained systems, when control is started, the control input is frequently saturated. It is important to determine the time interval of input saturation. Then, one-step prediction may be insufficient, and a longer time interval in which the input constraint is imposed is required. From this viewpoint, another problem, that is, the N-step input-constrained problem is formulated.

First, suppose that the input constraint is imposed in the time interval $[t_0, t_0 + h_0 + h(N-1))$, where $N \geq 1$ is a given integer. In addition, suppose that no input constraint is imposed in the time interval $[t_0 + h_0 + h(N-1), \infty)$, then, consider the following cost function:

$$\begin{aligned} J &= J_1 + J_2 + J_3, \\ J_1 &= \int_{t_0}^{t_0+h_0} \left\{x^T(t)\,Qx(t) + u^T(t)\,Ru(t)\right\} dt, \\ J_2 &= \int_{t_0+h_0}^{t_0+h_0+h(N-1)} \left\{x^T(t)\,Qx(t) + u^T(t)\,Ru(t)\right\} dt, \\ J_3 &= \int_{t_0+h_0+h(N-1)}^{\infty} \left\{x^T(t)\,Qx(t) + u^T(t)\,Ru(t)\right\} dt \\ &= x^T\left(t_0 + h_0 + h(N-1)\right) \\ &\quad \times P(h)\,x\left(t_0 + h_0 + h(N-1)\right). \end{aligned} \tag{10}$$

The optimal value of J_3 can be characterized by $x(t_0 + h_0 + h(N-1))$, because no input constraint is imposed in the time interval $[t_0 + h_0 + h(N-1), \infty)$.

Under the above preparation, consider the following N-step input-constrained problem.

Problem 3 (N-step input-constrained problem). Suppose that for the system (1), the initial time t_0, the initial state $x(t_0) = x_0$, $h_1 = h_2 = \cdots = h$, $N \geq 1$, and $\gamma \geq 1$ are given. Then, find a control input sequence $u_0, u_1, \ldots, u_{T-1}$ maximizing a sampling period h_0 under the following constraints:

$$\begin{aligned} h \leq h_0 \leq h_{\max}, \\ u_{\min} \leq u_k \leq u_{\max}, \quad k = 0, 1, \ldots, N-1, \end{aligned} \tag{11}$$

$$J^*_{h_0} \leq \gamma J^*_h, \tag{12}$$

where $h_{\max} \geq 0$ is a given constant, and $J^*_{h_0}$ is the optimal value of the cost function of (10), J^*_h is the optimal value of the cost function of (10) under $h_0 = h$.

In Problem 3, control performance can be adjusted by suitably giving γ. We remark that in this problem, h_0 is maximized under certain constraints. Furthermore, in this problem, a control input sequence is computed, but only the first one (h_0) is computed on sampling periods. In this sense, this problem is regarded as a kind of the optimal control problem with prediction horizon one.

Hereafter, in Section 4, an iterative solution method for the N-step input-constrained problem (Problem 3) will be proposed. In Section 5, an approximate solution method for the one-step input-constrained problem (Problem 2) will be proposed.

Remark 4. The parameter h in Problems 2 and 3 is chosen based on the computation time for solving the problem and the dynamics of a given plant. If computation of the problem is not finished until time $t_0 + h_0 \in [t_0 + h, t_0 + h_{\max}]$, then the next control input cannot be applied to the plant. See also the procedure of self-triggered MPC in Section 2.

4. Iterative Solution Method for N-Step Input-Constrained Problem

First, for a fixed h_0, consider deriving $J^*_{h_0}$. The value of J^*_h can be derived by a similar method. The value of $J^*_{h_0}$ is given by the optimal value of the following optimal control problem.

Problem 5. Suppose that for the system (1), the initial time t_0, the initial state $x(t_0) = x_0$, h_0 and $h_1 = h_2 = \cdots = h$, $N \geq 1$ are given. Then, find a control input sequence $u_0, u_1, \ldots, u_{N-1}$ minimizing the cost function (10) under the input constraint (11).

From the conventional result on sampled-data control theory, Problem 5 can be equivalently rewritten as the following optimal control problem of time-varying discrete-time linear systems with the input constraint (11).

Problem 6. Suppose that the initial time t_0, the initial state $x(0) = x_0$, h_0, and $h_1 = h_2 = \cdots = h$, $N \geq 1$ are given. Consider the following discrete-time linear system:

$$\begin{aligned} x_1 &= \widetilde{A}(h_0)\, x_0 + \widetilde{B}(h_0)\, u_0, \\ x_{k+1} &= \widetilde{A}(h)\, x_k + \widetilde{B}(h)\, u_k, \quad k \geq 1, \end{aligned} \tag{13}$$

where $x_k := x(t_k)$. Then, find a control input sequence $u_0, u_1, \ldots, u_{N-1}$ minimizing the cost function (10), that is,

$$\begin{aligned} J = {} & \begin{bmatrix} x_0 \\ u_0 \end{bmatrix}^T \begin{bmatrix} \widetilde{Q}(h_0) & \widetilde{S}(h_0) \\ \widetilde{S}^T(h_0) & \widetilde{R}(h_0) \end{bmatrix} \begin{bmatrix} x_0 \\ u_0 \end{bmatrix} \\ & + \sum_{k=1}^{N-1} \begin{bmatrix} x_k \\ u_k \end{bmatrix}^T \begin{bmatrix} \widetilde{Q}(h) & \widetilde{S}(h) \\ \widetilde{S}^T(h) & \widetilde{R}(h) \end{bmatrix} \begin{bmatrix} x_k \\ u_k \end{bmatrix} \\ & + x_N^T P(h)\, x_N \end{aligned} \tag{14}$$

under the input constraint (11).

Next, consider reducing Problem 6 to a QP problem. Define $\overline{x} := [x_0^T \;\; x_1^T \;\; \cdots \;\; x_N^T]^T$ and $\overline{u} := [u_0^T \;\; u_1^T \;\; \cdots \;\; u_{N-1}^T]^T$. Then, we can obtain $\overline{x} = \overline{A}x_0 + \overline{B}\overline{u}$, where

$$\begin{aligned} \overline{A} &= \begin{bmatrix} I \\ \widetilde{A}(h_0) \\ \widetilde{A}(h)\,\widetilde{A}(h_0) \\ \widetilde{A}^2(h)\,\widetilde{A}(h_0) \\ \vdots \\ \widetilde{A}^{N-1}(h)\,\widetilde{A}(h_0) \end{bmatrix}, \\ \overline{B} &= \begin{bmatrix} 0 & 0 & \cdots & 0 \\ \widetilde{B}(h_0) & 0 & \cdots & \vdots \\ \widetilde{A}(h)\,\widetilde{B}(h_0) & \widetilde{B}(h) & \cdots & \vdots \\ \widetilde{A}^2(h)\,\widetilde{B}(h_0) & \widetilde{A}(h)\,\widetilde{B}(h) & \cdots & \vdots \\ \vdots & \vdots & \cdots & 0 \\ \widetilde{A}^{N-1}(h)\,\widetilde{B}(h_0) & \widetilde{A}^{N-2}(h)\,\widetilde{B}(h) & \cdots & \widetilde{B}(h) \end{bmatrix}. \end{aligned} \tag{15}$$

In addition, we define

$$\begin{aligned} \overline{Q} &:= \text{block-diag}\left(\widetilde{Q}(h_0), \widetilde{Q}(h), \ldots, \widetilde{Q}(h), P(h)\right), \\ \overline{S} &:= \begin{bmatrix} \text{block-diag}\left(\widetilde{S}(h_0), \widetilde{S}(h), \ldots, \widetilde{S}(h)\right) \\ 0_{n\times(N-1)m} \end{bmatrix}, \\ \overline{R} &:= \text{block-diag}\left(\widetilde{R}(h_0), \widetilde{R}(h), \ldots, \widetilde{R}(h)\right). \end{aligned} \tag{16}$$

Then, the cost function (14) can be rewritten as follows:

$$\begin{aligned} J &= \overline{x}^T \overline{Q}\overline{x} + 2\overline{x}^T \overline{S}\overline{u} + \overline{u}^T \overline{R}\overline{u} \\ &= \overline{u}^T L_2 \overline{u} + L_1 \overline{u} + L_0, \end{aligned} \tag{17}$$

where

$$\begin{aligned} L_2 &= \overline{R} + \overline{B}^T \overline{S} + \overline{S}^T \overline{B} + \overline{B}^T \overline{Q} \overline{B}, \\ L_1 &= 2x_0^T \overline{A}^T \left(\overline{S} + \overline{Q}\overline{B}\right), \\ L_0 &= x_0^T \overline{A}^T \overline{Q}\overline{A} x_0. \end{aligned} \tag{18}$$

Finally, $\overline{u}_{\min} := [u_{\min}^T \;\; u_{\min}^T \;\; \cdots \;\; u_{\min}^T]^T$ and $\overline{u}_{\max} := [u_{\max}^T \;\; u_{\max}^T \;\; \cdots \;\; u_{\max}^T]^T$ are also defined.

Under the above preparation, Problem 6 is equivalent to the following QP problem.

Problem A. Consider

$$\begin{aligned} &\text{find} && u_0, u_1, \ldots, u_{N-1}, \\ &\min && \overline{u}^T L_2 \overline{u} + L_1 \overline{u} + L_0, \\ &\text{subject to} && \overline{u}_{\min} \leq \overline{u} \leq \overline{u}_{\max}. \end{aligned} \tag{19}$$

A QP problem can be solved by using a suitable solver such as MATLAB and IBM ILOG CPLEX [15].

Third, by using the obtained QP problem, we propose an algorithm for solving Problem 3.

Algorithm 7. Step 1. Derive J_h^* by solving Problem A with $h_0 = h$.

Step 2. Set $a = h$ and $b = h_{\max}$, and give a sufficiently small positive real number ε.

Step 3. Set $h_0 = (a + b)/2$.

Step 4. Derive $J_{h_0}^*$ by solving Problem A.

Step 5. If $J_{h_0}^* \le \gamma J_h^*$ in Problem 3 is satisfied, then set $a = h_0$, otherwise set $b = h_0$.

Step 6. If $|a-b| < \varepsilon$ is satisfied, then the optimal h_0 in Problem 3 is derived as a, and the optimal control input sequence is also derived. Otherwise go to Step 3.

In a numerical example (Section 6.1), we will discuss the computation time of Algorithm 7.

Finally, we discuss the stabilization issue. For Problem 6, consider imposing the constraint $V(x_{k+1}) \le \rho V(x_k)$, where $V(x)$ is a given nonnegative function, and $\rho \in [0, 1)$ is a given constant. If $V(x)$ is restricted to $V(x) = \|Px\|_\infty$, where $P \in \mathscr{R}^{n\times n}$ and $\|\cdot\|_\infty$ is an infinity matrix norm, then the constraint $V(x_{k+1}) \le \rho V(x_k)$ can be transformed into a set of linear inequalities (see, e.g., [16]), and can be embedded in Problem A. Then, the closed-loop system in which the control input derived by Algorithm 7 is applied is asymptotically stable. See, for example, [17, 18] for further details.

5. Approximate Solution Method for One-Step Input-Constrained Problem

In this section, first we derive a solution method for the one-step input-constrained problem (Problem 2). In the proposed solution method, Problem 2 is approximately reduced to a quadratic programming (QP) problem, but the convexity is not guaranteed. Next, we discuss the convexity.

5.1. Proposed Solution Method. First, noting that the control input is piecewise constant, from (7), the cost function of (8) can be equivalently rewritten as

$$J = \begin{bmatrix} x_0 \\ u_0 \end{bmatrix}^T \begin{bmatrix} \widetilde{Q}(h_0) & \widetilde{S}(h_0) \\ \widetilde{S}^T(h_0) & \widetilde{R}(h_0) \end{bmatrix} \begin{bmatrix} x_0 \\ u_0 \end{bmatrix} + x_1^T P(h) x_1, \tag{20}$$

$$x_1 = e^{Ah_0} x_0 + \int_0^{h_0} e^{A\tau} d\tau B u_0. \tag{21}$$

We focus on the weight matrices. By using Taylor series expansions, we can obtain the following relation:

$$e^{F^T t} \begin{bmatrix} Q & 0 \\ 0 & R \end{bmatrix} e^{Ft} = \Phi_0 + \Phi_1 t + \Phi_2 t^2 + \cdots, \tag{22}$$

where

$$\Phi_0 = \begin{bmatrix} Q & 0 \\ 0 & R \end{bmatrix},$$

$$\Phi_1 = \begin{bmatrix} QA + A^TQ & QB \\ B^TQ & 0 \end{bmatrix},$$

$$\Phi_2 = \begin{bmatrix} \Phi_{2,11} & A^TQB + \frac{1}{2}QAB \\ B^TQA + \frac{1}{2}B^TA^TQ & B^TQB \end{bmatrix}, \tag{23}$$

$$\Phi_{2,11} = A^TQA + \frac{1}{2}\left(QA^2 + \left(A^2\right)^TQ\right).$$

Then, the weight matrices of (7) can be rewritten as

$$\begin{bmatrix} \widetilde{Q}(h_0) & \widetilde{S}(h_0) \\ \widetilde{S}^T(h_0) & \widetilde{R}(h_0) \end{bmatrix} = \Phi_0 h_0 + \frac{1}{2}\Phi_1 h_0^2 + \cdots. \tag{24}$$

Next, we focus on the term $x_1^T P(h) x_1$. From x_1 of (21), $x_1^T P(h) x_1$ can be rewritten as

$$x_1^T P(h) x_1 = \begin{bmatrix} x_0 \\ u_0 \end{bmatrix}^T \begin{bmatrix} \Psi_{11} & \Psi_{12} \\ \Psi_{12}^T & \Psi_{22} \end{bmatrix} \begin{bmatrix} x_0 \\ u_0 \end{bmatrix}, \tag{25}$$

where

$$\Psi_{11} = e^{A^Th_0} P(h) e^{Ah_0},$$

$$\Psi_{12} = e^{A^Th_0} P(h) \left(e^{Ah_0} - I\right) A^{-1} B, \tag{26}$$

$$\Psi_{22} = B^T\left(A^{-1}\right)^T \left(e^{A^Th_0} - I\right) P(h) \left(e^{Ah_0} - I\right) A^{-1} B.$$

We use Taylor series expansions for e^{Ah_0}. Then, we can obtain

$$\begin{aligned} \Psi_{11} &= P(h) + \left(P(h)A + A^TP(h)\right)h_0 \\ &\quad + \left(A^TP(h)A + \frac{1}{2}P(h)A^2 + \frac{1}{2}\left(A^2\right)^TP(h)\right)h_0^2 \\ &\quad + \cdots, \\ \Psi_{12} &= P(h)Ah_0 + \left(A^TP(h)B + \frac{1}{2}P(h)AB\right)h_0^2 + \cdots, \\ \Psi_{22} &= B^TP(h)Bh_0^2 + \cdots. \end{aligned} \tag{27}$$

From these results, the cost function can be expressed as follows:

$$J = \begin{bmatrix} x_0 \\ u_0 \end{bmatrix}^T \left(\Gamma_0 + \Gamma_1 h_0 + \Gamma_2 h_0^2 + \cdots\right) \begin{bmatrix} x_0 \\ u_0 \end{bmatrix}, \tag{28}$$

where

$$\Gamma_0 = \begin{bmatrix} P(h) & 0 \\ 0 & 0 \end{bmatrix},$$

$$\Gamma_1 = \begin{bmatrix} \Gamma_{1,11} & P(h)B \\ B^T P(h) & R \end{bmatrix},$$

$$\Gamma_2 = \begin{bmatrix} \Gamma_{2,11} & \Gamma_{2,12} \\ \Gamma_{2,12}^T & B^T P(h) B \end{bmatrix},$$

$$\Gamma_{1,11} = P(h)A + A^T P(h) + Q,$$

$$\Gamma_{2,11} = \frac{1}{2}\left(QA + A^T Q + P(h)A^2 + \left(A^2\right)^T P(h)\right) + A^T P(h) A,$$

$$\Gamma_{2,12} = A^T P(h) B + \frac{1}{2}\left(P(h)AB + QB\right). \tag{29}$$

In this paper, the second-order truncated Taylor series is used. Furthermore, the term $u_0^T(h_0R)u_0$ appeared in (28) is approximated as follows:

$$u_0^T(h_0R)u_0 \approx u_0^T\left(h_0^2R'\right)u_0, \tag{30}$$

where $R' := R/((h_{\max}+h)/2)$. Then, we consider the following cost function J_a:

$$J \approx J_a = \begin{bmatrix} x_0 \\ u_0 \end{bmatrix}^T \left(\Gamma_0 + \Gamma_1' h_0 + \Gamma_2' h_0^2\right) \begin{bmatrix} x_0 \\ u_0 \end{bmatrix}, \tag{31}$$

where

$$\Gamma_1' = \begin{bmatrix} \Gamma_{1,11} & P(h)B \\ B^T P(h) & 0 \end{bmatrix},$$

$$\Gamma_2' = \begin{bmatrix} \Gamma_{2,11} & \Gamma_{2,12} \\ \Gamma_{2,12}^T & R' + B^T P(h) B \end{bmatrix}. \tag{32}$$

Under these preparations, we can obtain the following theorem.

Theorem 8. *The one-step input-constrained problem of Problem 2 is approximately reduced to the following QP problem.*

Problem B. Consider

$$\begin{aligned} &\text{find} && v_0, h_0, \\ &\min && \begin{bmatrix} v_0 \\ h_0 \end{bmatrix}^T M_2 \begin{bmatrix} v_0 \\ h_0 \end{bmatrix} + M_1 \begin{bmatrix} v_0 \\ h_0 \end{bmatrix} + M_0, \\ &\text{subject to} && h \le h_0 \le h_{\max}, \\ & && u_{\min} h_0 \le v_0 \le u_{\max} h_0, \end{aligned} \tag{33}$$

where $v_0 := h_0 u_0$, and

$$M_2 = \begin{bmatrix} R' + B^T P(h) B & \Gamma_{2,12}^T x_0 \\ x_0^T \Gamma_{2,12} & x_0^T \Gamma_{2,11} x_0 \end{bmatrix},$$

$$M_1 = \begin{bmatrix} 2x_0^T P(h) B & x_0^T \Gamma_{1,11} x_0 \end{bmatrix},$$

$$M_0 = x_0^T P(h) x_0. \tag{34}$$

Proof. By rewriting J_a of (31), the cost function in Problem B is derived. In addition, by using v_0, h_0, the input constraint $u_{\min} \le u_0 \le u_{\max}$ in Problem 2 is equivalent to $u_{\min}h_0 \le v_0 \le u_{\max}h_0$, which is a linear inequality constraint. □

By solving Problem B, we can obtain suboptimal $u_0 (= v_0/h_0)$ and h_0. Problem B is a QP problem, but the cost function is in general nonconvex. A local optimal solution can be derived by using a suitable solver, for example, MATLAB.

Remark 9. In Theorem 8, the accuracy of approximations is not considered. Several existing results on analysis of the truncation error in Taylor series have been obtained so far. In addition, by suitably setting R' in (30), the approximation of (30) can be regarded as an over-approximation of $u_0^T(h_0R)u_0$. Using the above discussion, the upper bound of the optimal value in Problem 2 can be evaluated by solving Problem B.

5.2. Discussion on Convexity. The cost function in Problem B is in general nonconvex. In other words, the matrix M_2 is not a positive definite matrix generally. In this subsection, we clarify the reason why M_2 is not positive definite.

The matrix M_2 can be rewritten as

$$M_2 = \begin{bmatrix} I & 0 \\ 0 & x_0 \end{bmatrix}^T N_2 \begin{bmatrix} I & 0 \\ 0 & x_0 \end{bmatrix}, \tag{35}$$

where

$$N_2 = N_2' - \frac{1}{2} C^T P^{-1}(h) C,$$

$$N_2' = \begin{bmatrix} R' & 0 \\ 0 & 0 \end{bmatrix} + \frac{1}{2}\begin{bmatrix} B & A \end{bmatrix}^T P(h) \begin{bmatrix} B & A \end{bmatrix} + \frac{1}{2} D^T D,$$

$$C = \begin{bmatrix} 0 & A^T P(h) + Q \end{bmatrix},$$

$$D = \left[P^{1/2}(h) B \quad P^{-1/2}(h)\left(P(h)A + A^T P(h) + Q\right)\right]. \tag{36}$$

Since $P(h)$ is positive definite, N_2' is also positive definite. However, it is obvious that $-(1/2)C^T P^{-1}(h) C$ is not positive definite. Therefore, M_2 is not a positive definite matrix generally.

Consider approximating the cost function in Problem B, that is, J_a in (31) by a convex function. We define the following positive definite matrix:

$$M_2' := \begin{bmatrix} I & 0 \\ 0 & x_0 \end{bmatrix}^T N_2' \begin{bmatrix} I & 0 \\ 0 & x_0 \end{bmatrix}, \tag{37}$$

and we rewrite J_a in (31). Then, we can obtain

$$J_a = \begin{bmatrix} v_0 \\ h_0 \end{bmatrix}^T M_2' \begin{bmatrix} v_0 \\ h_0 \end{bmatrix} + M_1 \begin{bmatrix} v_0 \\ h_0 \end{bmatrix} + M_0 + \alpha h_0^2,$$

$$\alpha = -\frac{1}{2} x_0^T \left(A^T P(h) + Q\right)^T \times P^{-1}(h)\left(A^T P(h) + Q\right) x_0. \tag{38}$$

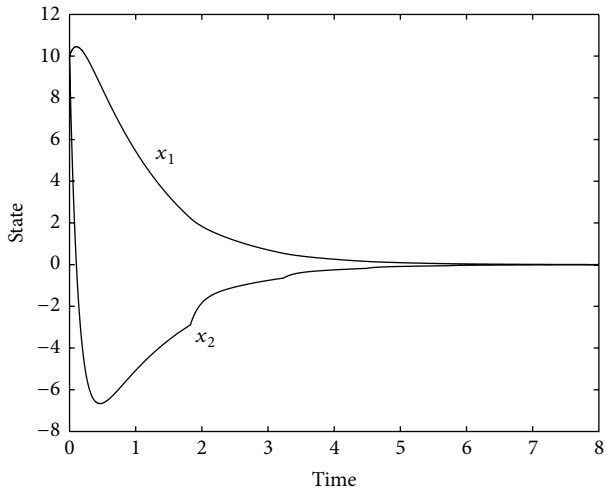

Figure 1: State trajectory.

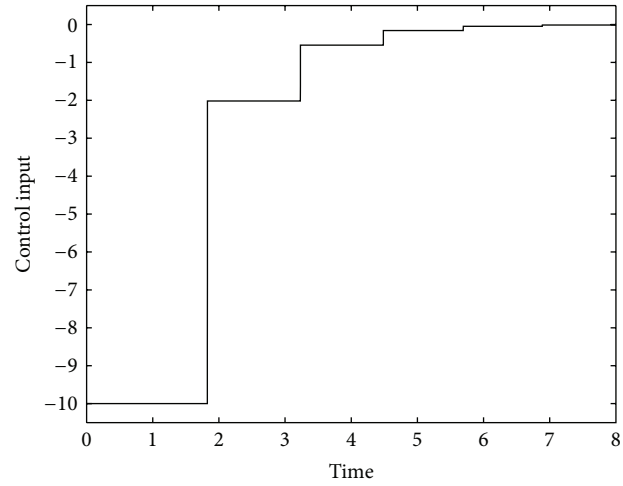

Figure 2: Control input.

By approximating the negative term αh_0^2 to a linear term, Problem B can be in general reduced to a convex QP problem. Noting that $h \le h_0 \le h_{\max}$, we can make a two-dimensional graph on h_0 and αh_0^2. Using the two-dimensional graph obtained, we can evaluate whether the approximation is reasonable.

6. Numerical Examples

6.1. Iterative Solution Method. First, we show an example of the iterative solution method proposed in Section 4.

Consider the following system:

$$\dot{x}(t) = \begin{bmatrix} 0 & 1 \\ -5 & -8 \end{bmatrix} x(t) + \begin{bmatrix} 0 \\ 1 \end{bmatrix} u(t). \tag{39}$$

The input constraint is given as $u(t) \in [-10, +10]$. Parameters in Problem 3 are given as follows: $h = 0.5, \gamma = 1.001, h_{\max} = 5$, $Q = 10^3 I_n$, and $R = 1$. In Algorithm 7, we set $\varepsilon = 10^{-4}$. Then, $P(h)$ can be derived as

$$P(h) = \begin{bmatrix} 10615 & 593 \\ 593 & 575 \end{bmatrix}. \tag{40}$$

In addition, we consider two cases, that is, the case of $N = 1$ and the case of $N = 10$.

We show the computational result on self-triggered MPC with the N-step input-constrained problem of Problem 3. The initial state is given as $x_0 = [10 \quad 10]^T$, and the case of $N = 10$ is considered. Figure 1 shows the obtained state trajectory, and Figure 2 shows the control input trajectory. From these figures, we see that the sampling period is nonuniform.

Next, compare two cases. In these cases, the obtained state trajectories are almost the same. The difference between two cases is as follows. In Figures 1 and 2, that is, the case of $N = 10$, the control input at each time is shown as follows:

$$\begin{aligned}
&u(t) = -10.00, \quad t \in [0, 1.83), && h_0 = 1.83,\\
&u(t) = -1.90, \quad t \in [1.83, 3.23), && h_0 = 1.41,\\
&u(t) = -0.49, \quad t \in [3.23, 4.49), && h_0 = 1.25,\\
&u(t) = -0.14, \quad t \in [4.49, 5.69), && h_0 = 1.21,\\
&u(t) = -0.04, \quad t \in [5.69, 6.89), && h_0 = 1.20,\\
&u(t) = -0.01, \quad t \in [6.89, 8.08), && h_0 = 1.19.
\end{aligned} \tag{41}$$

In the case of $N = 1$, the control input at each time is derived as follows:

$$\begin{aligned}
&u(t) = -10.00, \quad t \in [0, 0.62), && h_0 = 0.62,\\
&u(t) = -10.00, \quad t \in [0.62, 1.66), && h_0 = 1.03,\\
&u(t) = -2.62, \quad t \in [1.66, 2.88), && h_0 = 1.22,\\
&u(t) = -0.75, \quad t \in [2.88, 4.08), && h_0 = 1.20,\\
&u(t) = -0.22, \quad t \in [4.08, 5.27), && h_0 = 1.19,\\
&u(t) = -0.06, \quad t \in [5.27, 6.47), && h_0 = 1.19,\\
&u(t) = -0.02, \quad t \in [6.47, 7.66), && h_0 = 1.19,\\
&u(t) = -0.01, \quad t \in [7.66, 8.85), && h_0 = 1.19.
\end{aligned} \tag{42}$$

From these results, we can discuss the following topic. In this example, input saturation is needed to improve the transient behavior. However, in the case of $N = 1$, the time interval of input saturation was not computed suitably. As a result, to derive the state trajectory in time interval $[0, 8]$, Problem 3 must be solved eight times. In the case of $N = 10$, Problem 3 is solved six times. Hence, it is important to choose a suitable N. We remark that in this example, the computational result in the case of $N = 20$ is the same as that in the case of $N = 10$. In this sense, $N = 10$ is one of the suitable horizons.

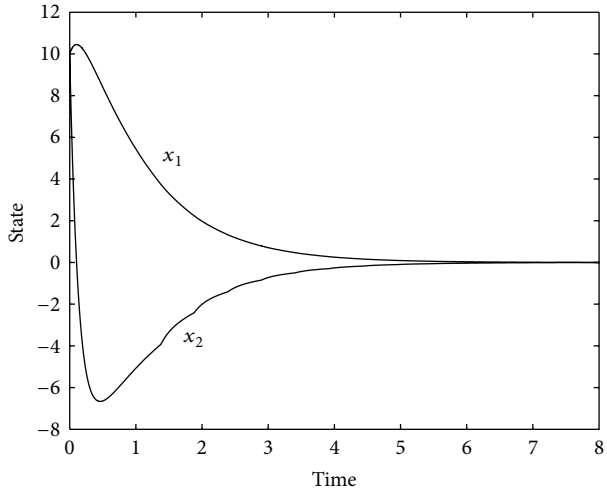

Figure 3: State trajectory.

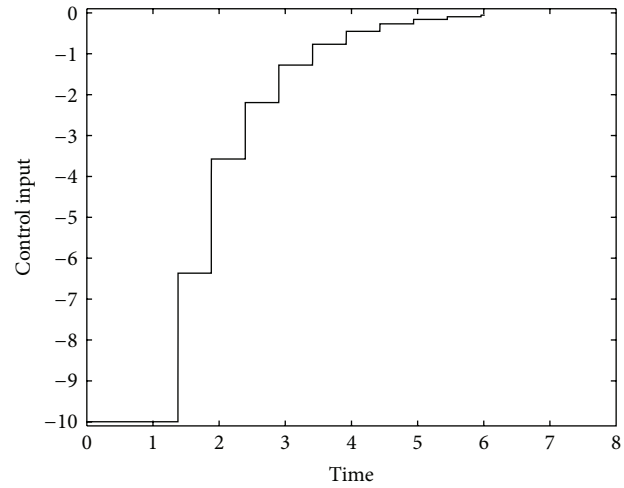

Figure 4: Control input.

In addition, we discuss the effect of changing γ in (12). In the case of $N = 10$, consider the following cases: $\gamma = 1.001, 1.005, 1.010, 1.015, 1.020$. For each case, the first h_0 is obtained as follows:

$$\begin{aligned} &\gamma = 1.001\text{: } h_0 = 1.83, \\ &\gamma = 1.005\text{: } h_0 = 2.38, \\ &\gamma = 1.010\text{: } h_0 = 2.79, \\ &\gamma = 1.015\text{: } h_0 = 3.12, \\ &\gamma = 1.020\text{: } h_0 = 3.44. \end{aligned} \tag{43}$$

From these results, we see that h_0 becomes longer by setting a larger γ. Since control performance decreases for a larger γ, it is important to consider the trade-off between γ and h_0.

Finally, we discuss the computation time for solving the N-step input-constrained problem of Problem 3. In the case of $N = 10$, Problem 3 with the different initial state is solved six times. Then, the mean computation time for solving Problem 3 was 6.51 [sec], where we used IBM ILOG CPLEX 11.0 [15] as the MIQP solver on the computer with the Intel Core2 Duo 3.0 GHz processor and the 2 GB memory. In the case of $N = 1$, Problem 3 with the different initial state is solved eight times. Then, the mean computation time was 6.22 [sec]. From these results, it is difficult at this stage to solve Problem 3 in real-time. It is significant to consider several approaches for reducing the computation time. One of the simple methods is that the number of iterations in Algorithm 7 is limited to some integer depending on the computer environment.

6.2. Approximate Solution Method. Next, we show an example of the approximate solution method proposed in Section 5.

Consider the system (39) again. The input constraint is given as $u(t) \in [-10, +10]$. Parameters in the one-step input-constrained problem of Problem 2 are given as follows: $h = 0.2$, $h_{\max} = 1$, $Q = 10^3 I_n$, and $R = 1$. Since the approximate solution method in Section 5 is derived using an approximation via Taylor series expansions, it is not desirable that the difference between h and $h_{\max}$ is large. Therefore, h and $h_{\max}$ must set carefully. Furthermore, in this example, Problem B is transformed into a convex QP problem. From $h = 0.2$ and $h_{\max} = 1$, the term αh_0^2 is approximated by αh_0.

We show the computational result on self-triggered MPC with the transformed Problem B. The initial state is given as $x_0 = [10 \quad 10]^T$. Figure 3 shows the obtained state trajectory, and Figure 4 shows the control input trajectory. The obtained control input is shown as follow:

$$\begin{aligned} &u(t) = -10.00, \quad t \in [0, 0.86), && h_0 = 0.86, \\ &u(t) = -10.00, \quad t \in [0.86, 1.38), && h_0 = 0.52, \\ &u(t) = -6.37, \quad t \in [1.38, 1.88), && h_0 = 0.50, \\ &u(t) = -3.57, \quad t \in [1.88, 2.40), && h_0 = 0.52, \\ &u(t) = -2.19, \quad t \in [2.40, 2.90), && h_0 = 0.50, \\ &u(t) = -1.28, \quad t \in [3.41, 3.92), && h_0 = 0.51, \\ &u(t) = -0.77, \quad t \in [3.92, 4.43), && h_0 = 0.51, \\ &u(t) = -0.45, \quad t \in [4.43, 4.94), && h_0 = 0.51. \end{aligned} \tag{44}$$

From these results, we see that also in this example, the sampling period is nonuniform.

Finally, we discuss the computation time for solving the transformed Problem B. The transformed Problem B with the different initial state is solved 17 times. Then, the mean computation time was 0.01 [sec], where we used IBM ILOG CPLEX 11.0 as the QP solver. Since in this example the number of decision variables is only two, computation is very fast.

7. Conclusion

In this paper, we discussed self-triggered MPC of linear systems. Since it is difficult to solve the original problem (Problem 1), two control problems (the one-step input-constrained problem of Problem 2 and the N-step input-constrained problem of Problem 3) were formulated, instead of Problem 1. For Problem 3, the iterative solution method was proposed. For Problem 2, the approximate solution method was proposed. In the latter, we also discussed the convexity. The effectiveness of these proposed method was shown by numerical examples. The proposed methods are useful as a new method of self-triggered optimal control.

In the future works, first, it is important to develop a more efficient method for solving Problem 3. Then, the continuation method [19] may be useful. Next, since the proposed method for the one-step input-constrained problem (Problem 2) is an approximate method, it is difficult at the current stage to guarantee the stability of the closed-loop system. The stabilization issue for the one-step input-constrained problem is also important as one of the future works.

Conflict of Interests

The authors declare that they have no conflict of interests.

Acknowledgment

This work was partially supported by Grant-in-Aid for Young Scientists (B) 23760387.

References

[1] C. T. Abdallah and H. G. Tanner, "Complex networked control systems: introduction to the special section," *IEEE Control Systems Magazine*, vol. 27, no. 4, pp. 30–32, 2007.

[2] P. Antsaklis and J. Baillieul, "Special issue on technology of networked control systems," *Proceedings of the IEEE*, vol. 95, no. 1, pp. 5–8, 2007.

[3] L.-S. Hu, T. Bai, P. Shi, and Z. Wu, "Sampled-data control of networked linear control systems," *Automatica*, vol. 43, no. 5, pp. 903–911, 2007.

[4] H. Ishii, "Stabilization under shared communication with message losses and its limitations," in *Proceedings of the 45th IEEE Conference on Decision and Control (CDC '06)*, pp. 4974–4979, December 2006.

[5] H. Ishii, "H^{∞} control with limited communication and message losses," *Systems & Control Letters*, vol. 57, no. 4, pp. 322–331, 2008.

[6] K. Kobayashi and K. Hiraishi, "Optimal control of a class of networked systems based on MLD framework," in *Proceedings of the 18th IFAC World Congress*, pp. 66–71, 2011.

[7] A. Anta and P. Tabuada, "Self-triggered stabilization of homogeneous control systems," in *Proceedings of the American Control Conference (ACC '08)*, pp. 4129–4134, Seattle, Wash, USA, June 2008.

[8] A. Anta and P. Tabuada, "To sample or not to sample: self-triggered control for nonlinear systems," *IEEE Transactions on Automatic Control*, vol. 55, no. 9, pp. 2030–2042, 2010.

[9] A. Camacho, P. Martí, M. Velasco et al., "Self-triggered networked control systems: an experimental case study," in *Proceedings of the International Conference on Industrial Technology (ICIT '10)*, pp. 123–128, Viña del Mar Valparaíso, Chile, March 2010.

[10] K. Kobayashi and K. Hiraishi, "Self-triggered model predictive control with delay compensation for networked control systems," in *Proceedings of the 38th Annual Conference of the IEEE Industrial Electronics Society*, pp. 3182–3187, 2012.

[11] M. Mazo Jr. and P. Tabuada, "On event-triggered and self-triggered control over sensor/actuator networks," in *Proceedings of the 47th IEEE Conference on Decision and Control (CDC '08)*, pp. 435–440, Cancún, Mexico, December 2008.

[12] X. Wang and M. D. Lemmon, "Self-triggered feedback control systems with finite-gain L_2 stability," *IEEE Transactions on Automatic Control*, vol. 54, no. 3, pp. 452–467, 2009.

[13] M. Velasco, P. Marti, J. Yepez et al., "Qualitative analysis of a one-step finite horizon boundary for event-driven controllers," in *Proceedings of the 50th IEEE Conference on Decision and Control and European Control*, pp. 1662–1667, 2011.

[14] J. Yepez, M. Velasco, P. Marti, E. X. Martin, and J. M. Fuertes, "One-step finite horizon boundary with varying control gain for event-driven networked control systems," in *Proceedings of the 37th Annual Conference of the IEEE Industrial Electronics Society*, pp. 2531–2536, 2011.

[15] IBM ILOG CPLEX Optimizer, http://www-01.ibm.com/software/commerce/optimization/cplex-optimizer/.

[16] M. Lazar, "Flexible control lyapunov functions," in *Proceedings of the American Control Conference (ACC '09)*, pp. 102–107, St. Louis, Mo, USA, June 2009.

[17] S. Di Cairano, M. Lazar, A. Bemporad, and W. P. M. H. Heemels, "A control Lyapunov approach to predictive control of hybrid systems," in *Proceedings of the 11th International Conference on Hybrid Systems: Computation and Control*, Lecture Notes in Computer Science, no. 4981, Springer, 2008.

[18] K. Kobayashi, J.-i. Imura, and K. Hiraishi, "Stabilization of finite automata with application to hybrid systems control," *Discrete Event Dynamic Systems*, vol. 21, no. 4, pp. 519–545, 2011.

[19] T. Ohtsuka, "A continuation/GMRES method for fast computation of nonlinear receding horizon control," *Automatica*, vol. 40, no. 4, pp. 563–574, 2004.

Hindawi Publishing Corporation
Mathematical Problems in Engineering
Volume 2013, Article ID 343524, 5 pages
http://dx.doi.org/10.1155/2013/343524

Research Article

Fault Diagnosis for Linear Discrete Systems Based on an Adaptive Observer

Jianwei Liu, Bin Jiang, and Ke Zhang

College of Automation Engineering, Nanjing University of Aeronautics and Astronautics, Nanjing 210016, China

Correspondence should be addressed to Bin Jiang; ebjiang@yahoo.com

Received 9 July 2013; Revised 9 September 2013; Accepted 23 September 2013

Academic Editor: Zidong Wang

This paper presents a fault diagnosis algorithm to estimate the fault for a class of linear discrete systems based on an adaptive fault estimation observer. And observer gain matrix and adaptive adjusting rule of the fault estimator are designed. Furthermore, the adaptive regulating algorithm can guarantee the first-order difference of a Lyapunov discrete function to be negative, so that the observer is ensured to be stable and fault estimation errors are convergent. Finally, simulation results of an aircraft F-16 illustrate the advantages of the theoretic results that are obtained in this paper.

1. Introduction

As the scale and complexity of modern control systems are increasing, the requirements on system reliability are also increasing. Therefore, the design and analysis of fault detection and diagnosis (FDD) algorithms have received considerable attention during the past three decades. The development of FDD has been addressed by more and more authors and fruitful results have been obtained; see [1–3].

The observer technology is one of the important methods for FDD and fault-tolerant control [4, 5]. Commonly used observer-based fault estimation methods include sliding mode observers [6], unknown input observers [7], H_∞ filtering methods [8], neural networks observers [9], and adaptive observers [10, 11]. But most of them focus on the continuous systems, and only few results have been reported on the fault estimation design in discrete-time systems. The discrete-time is widely used in practical implementations, for example, computer control systems, networked control systems, and so forth [12]. Reference [13] designed an H_∞ FD filter for a class of linear discrete-time systems in a networked environment. Reference [14] used an adaptive fault observer to deal with discrete-time systems, but it did not involve the issue of fault estimation. Reference [15] also dealt with discrete-time nonlinear systems, but its inequality functions were complex and it was difficult to get solutions. On the other hand, aircraft flight control systems are good examples for applications of fault accommodation/active reliable control, and the fault observers have been employed to detect faults [11].

In this paper, a novel discrete-time actuator fault estimation scheme is proposed to deal with abrupt actuator failures. The proposed actuator fault estimation scheme is then applied by using the Lyapunov method. Simulation results of a numerical example are also given.

The paper is organized as follows. Section 2 describes the mathematical preliminaries and problem formulation. In Section 3, concerning the theoretical results of the proposed fault diagnosis scheme, a fault estimation scheme is proposed to deal with the actuator failures of discrete-time system. In Section 4, an example of aircraft flight control system is given to illustrate the performance of the proposed scheme. The concluding remarks are given in Section 5.

2. System Description and Preliminaries

Consider a discrete-time linear system

$$\begin{aligned} x(k+1) &= Ax(k) + Bu(k) + Ef(k), \\ y(k) &= Cx(k), \end{aligned} \tag{1}$$

where $x(k) \in R^n$ is the state, $u \in R^m$ is the control input, $f(k) \in R^q$ with $q \leq m$ is the function to model the actuator faults, and $y(k) \in R^r$ is the measurable output. Matrices A, B,

C, and E are real matrices of appropriate dimensions. Matrix E is of full column rank; that is, rank $(E) = q$.

For estimating the actuator fault $f(k)$, an adaptive observer is constructed as follows:

$$\begin{aligned} \hat{x}(k+1) &= A\hat{x}(k) + Bu(k) + E\hat{f}(k) - L\left[\hat{y}(k) - y(k)\right], \\ \hat{y}(k) &= C\hat{x}(k), \end{aligned} \tag{2}$$

where $\hat{x}(k) \in R^n$ is the observer state vector, $\hat{y}(k) \in R^r$ is the observer output vector, $\hat{f}(k) \in R^q$ is the estimate of the actuator fault $f(k)$, $L \in R^{n\times r}$ is the observer gain to be designed.

Denoting that

$$\begin{aligned} e_x &= \hat{x}(k) - x(k), \qquad e_y = \hat{y}(k) - y(k), \\ e_f &= \hat{f}(k) - f(k), \end{aligned} \tag{3}$$

then the estimation error dynamics is modeled as follows:

$$\begin{aligned} e_x(k+1) &= (A - LC)e_x(k) + Ee_f(k), \\ e_y(k) &= Ce_x(k). \end{aligned} \tag{4}$$

3. Main Results

3.1. Modified Adaptive Fault Estimation Algorithm

Theorem 1. *For constant actuator fault $f(k)$, if there exist matrices $P > 0$ and $Q > 0$ and positive scalars ε and defined*

$$\Gamma = 2\left(\varepsilon EE^T + Q\right)^{-1} \tag{5}$$

such that the following condition holds:

$$\Xi = \begin{bmatrix} (A-LC)^T P(A-LC) - P & (A-LC)^T PE \\ * & E^T\left(-\Gamma^T Q\Gamma + P\right)E \end{bmatrix} < 0, \tag{6}$$

then the algorithm

$$\Delta\hat{f}(k+1) = -\varepsilon E^T\Gamma\left[e_x(k+1) - (A-LC)e_x(k)\right] \tag{7}$$

and the fault estimation

$$\hat{f}(k+1) = \hat{f}(k) + \Delta\hat{f}(k+1) = \hat{f}(0) + \sum_{i=1}^{k+1}\Delta\hat{f}(i) \tag{8}$$

can realize estimation error of both the state and fault uniformly bounded for the entire time period.

Proof. From system (4), one gets $Ee_f(k) = e_x(k+1) - (A - LC)e_x(k)$, so the algorithm (7) becomes

$$\begin{aligned} \Delta\hat{f}(k+1) &= -\varepsilon E^T\Gamma\left[e_x(k+1) - (A-LC)e_x(k)\right] \\ &= -\varepsilon E^T\Gamma Ee_f(k). \end{aligned} \tag{9}$$

Then,

$$\begin{aligned} e_f(k+1) &= \hat{f}(k+1) - f(k+1) \\ &= \hat{f}(k+1) - \hat{f}(k) + \hat{f}(k) - f(k+1). \end{aligned} \tag{10}$$

Because $f(k)$ is constant, $f(k+1) = f(k)$ and $\Delta\hat{f}(k+1) = \hat{f}(k+1) - \hat{f}(k)$; then one gets

$$e_f(k+1) = \Delta\hat{f}(k+1) + e_f(k) = \left(I - \varepsilon E^T\Gamma E\right)e_f(k). \tag{11}$$

Based on (4) and (11), we can obtain the following augmented system:

$$\begin{bmatrix} e_x(k+1) \\ e_f(k+1) \end{bmatrix} = \begin{bmatrix} A-LC & E \\ 0 & I - \varepsilon E^T\Gamma E \end{bmatrix}\begin{bmatrix} e_x(k) \\ e_f(k) \end{bmatrix}. \tag{12}$$

Consider the following Lyapunov function:

$$V(k) = e_x^T(k)Pe_x(k) + \varepsilon^{-1}e_f^T(k)e_f(k). \tag{13}$$

Then,

$$\begin{aligned} \Delta V(k) &= e_x^T(k+1)Pe_x(k+1) - e_x^T(k)Pe_x(k) \\ &\quad + \varepsilon^{-1}e_f^T(k+1)e_f(k+1) - \varepsilon^{-1}e_f^T(k)e_f(k) \\ &= e_x^T(k)\left[(A-LC)^T P(A-LC) - P\right]e_x(k) \\ &\quad + 2e_x^T(k)(A-LC)^T PEe_f(k) + e_f^T(k)E^T PEe_f(k) \\ &\quad + \varepsilon^{-1}e_f^T(k)\left(I - E^T\Gamma E\right)^T\left(I - E^T\Gamma E\right)e_f(k) \\ &\quad - \varepsilon^{-1}e_f^T(k)e_f(k) \\ &= e_x^T(k)\left[(A-LC)^T P(A-LC) - P\right]e_x(k) \\ &\quad + 2e_x^T(k)(A-LC)^T PEe_f(k) \\ &\quad + e_f^T(k)E^T\left(-\Gamma^T Q\Gamma + P\right)Ee_f(k). \end{aligned} \tag{14}$$

Denoting that $e(k) = [e_x(k)\, e_f(k)]^T$, then $\Delta V(k) = e(k)^T\Xi e(k) < 0$, and Ξ is defined as (6). □

Remark 2. The pair (A, C) is observable, and define the observe matrix $U = [C^T(CA)^T \ldots (CA^{l-1})^T]^T$. So, it gets that the rank of U is n. When C is full column rank,we have

$$\begin{aligned} \Delta\hat{f}(k+1) &= -\varepsilon E^T\Gamma\left[e_x(k+1) - (A-LC)e_x(k)\right] \\ &= -\varepsilon E^T\Gamma\left[C^{-1}e_y(k+1) - \left(AC^{-1} - L\right)e_y(k)\right]. \end{aligned} \tag{15}$$

At the first step, the online fault estimation is as follows:

$$\begin{aligned} \hat{f}(1) &= \hat{f}(0) + \Delta\hat{f}(1) \\ &= \hat{f}(0) - \varepsilon E^T\Gamma\left[C^{-1}e_y(1) - \left(AC^{-1} - L\right)e_y(0)\right]. \end{aligned} \tag{16}$$

And at the kth step, fault estimation is as (8).

If C is not full column rank, then more system outputs and observer estimations should be used to get the state estimation.

When the output $y(k)$ satisfies Lipschitz condition, define $l_{\min} = \operatorname{argmax}_l[\operatorname{rank}(U)]$, and define $F = (A - LC)^{-1}$ and $U_F = [C^T (CF)^T \cdots (CF^{l\min-1})^T]^T$; then one can get

$$\begin{aligned}\Delta\widehat{f}(k+1) &= -\varepsilon E^T \Gamma \left\{ U_F^{-1} \left[e_y(k+1)^T \ \cdots \ e_y(k+2-l\min)^T \right]^T \right. \\ &\quad - AU_F^{-1} \left[e_y(k)^T \ \cdots \ e_y(k+1-l\min)^T \right] \\ &\quad \left. + Le_y(k) \right\}. \end{aligned} \tag{17}$$

Then, fault estimation is $\widehat{f}(k+1) = \widehat{f}(k) + \Delta\widehat{f}(k+1) = \widehat{f}(0) + \sum_{i=1}^{k+1} \Delta\widehat{f}(i)$.

Remark 3. Equation (6) is a nonlinear matrix inequality about matrices Γ and Q, and it is not easy to be calculated, so let $Q = \varepsilon EE^T + \delta \operatorname{tr}(EE^T)$. And after we choose $0 < \delta < \varepsilon$, the solution can be found easily.

Remark 4. If the fault $f(k)$ is not constant but is a linear function, such as $f(k+1) = Hf(k)$, then

$$e_f(k+1) = \left(H - E^T \Gamma E\right) e_f(k). \tag{18}$$

Consider the same Lyapunov function $V(k) = e_x^T(k) P e_x(k) + \varepsilon^{-1} e_f^T(k) e_f(k)$. We can also get

$$\Xi = \begin{bmatrix} (A-LC)^T P (A-LC) - P & (A-LC)^T PE \\ * & E^T\left(-\varepsilon\Gamma^T Q\Gamma + P\right)E + \varepsilon\left(H^T H - I\right) \end{bmatrix} < 0. \tag{19}$$

The proof is smilar to that of Theorem 1 and it is omitted here for brevity.

4. Simulation Results

In this section, the fault estimation algorithm is applied to a model of the vertical dynamics of an F-16 aircraft. The model is taken from [16]. The signals and their generation in the simulations are summarized in Table 1, where size means the variance for the inputs and constant magnitude for the faults, respectively.

Table 1: Signals in the F-16 simulation study.

Signal	Not.	Meaning	Size
Inputs	u_1	Spoiler angle (0.1 deg)	1
	u_2	Forward accelerations (m/s^2)	1
	u_3	Elevator angle (deg)	1
Outputs	y_1	Relative altitude (m)	10^{-4}
	y_2	Forward speed (m/s)	10^{-6}
	y_3	Pitch angle (deg)	10^{-6}
States	x_1	Altitude (m)	10^{-4}
	x_2	Forward speed (m/s)	10^{-4}
	x_3	Pitch angle (deg)	10^{-4}
	x_4	Pitch rate (deg/s)	10^{-4}
	x_5	Vertical speed (deg/s)	10^{-4}
Faults	f_1	Spoiler angle actuator	0.5
	f_2	Forward acceleration actuator	0.1
	f_3	Elevator angle actuator	1

We have the following numerical values in (1):

$$\begin{aligned} A &= \begin{bmatrix} 1 & 0.0014 & 0.1133 & 0.0004 & -0.0997 \\ 0 & 0.9945 & -0.0171 & -0.0005 & 0.0070 \\ 0 & 0.0003 & 1 & 0.0957 & -0.0049 \\ 0 & 0.0061 & 0 & 0.9130 & -0.0966 \\ 0 & -0.0286 & 0.0002 & 0.1004 & 0.9879 \end{bmatrix}, \\ B &= \begin{bmatrix} -0.0078 & 0 & 0.0003 \\ -0.0115 & 0.0997 & 0 \\ 0.0212 & 0 & -0.0081 \\ 0.4150 & 0.0003 & -0.1589 \\ 0.1794 & -0.0014 & -0.0158 \end{bmatrix}, \\ E &= \begin{bmatrix} -0.0078 & 0 & 0.0003 \\ -0.0115 & 0.0997 & 0 \\ 0.0212 & 0 & -0.081 \\ 0.4150 & 0.0003 & -0.1589 \\ 0.1794 & -0.0014 & -0.0158 \end{bmatrix}, \\ C &= \begin{bmatrix} 1 & 0 & 0 & 0 & 0 \\ 0 & 1 & 0 & 0 & 0 \\ 0 & 0 & 1 & 0 & 0 \end{bmatrix}, \\ l_{\min} &= 2, \qquad U_F = \left[C^T \ \ (CF)^T\right]^T. \end{aligned} \tag{20}$$

By solving conditions in Theorem 1, one can obtain the following solutions after iterations: L = [0.0001 0 0; 0 0.0001 0; 0 0 0.0002; 0.0001 0.0001 0; 0 0.0001 0.0001]; $\varepsilon = 1$, $\delta = 0.1$. Then, one can take the learning rate Γ = [189923 −147.6 646.2 2443 1727.8; −147.6 100.6 1.31 −0.58 1.24; 646.2 1.31 9365 −465.8 −1.27; 2443 −0.589 −465.8 71.3 −5.26; 1727.8 1.24 −1.27 −5.26 87.5].

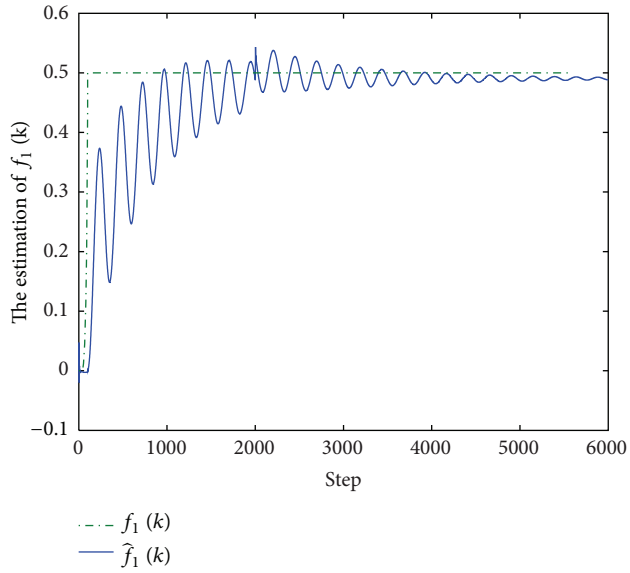

Figure 1: Estimation of the fault $f_1(k)$.

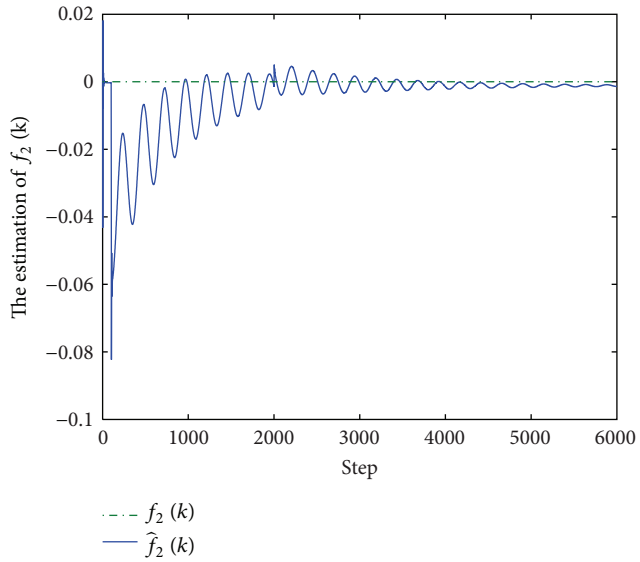

Figure 2: Estimation of the fault $f_2(k)$.

In this simulation, it is assumed that three kinds of actuator faults $f_i(k)$ are, respectively, created as

$$f_1(k) = \begin{cases} 0, & k < 100, \\ 0.5, & k > 100, \end{cases} \quad f_2(k) \text{ is free,}$$
$$f_3(k) = \begin{cases} 0, & k < 2000 \\ 1, & k > 2000 \end{cases}. \tag{21}$$

The fault $f_1(k)$ estimation result is shown in Figure 1, while Figure 2 illustrates the estimation of $f_2(k)$, and Figure 3 illustrates the estimation of $f_3(k)$.

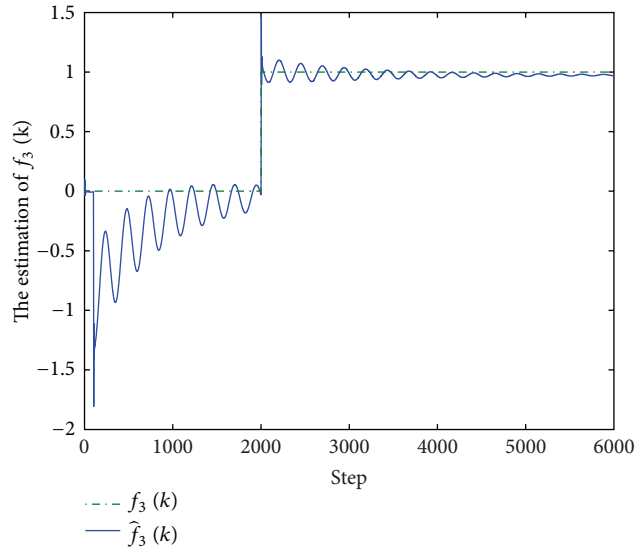

Figure 3: Estimation of the fault $f_3(k)$.

5. Conclusions

In this paper, a fault estimation algorithm is established for linear discrete systems with actuator faults. The algorithm can enhance the performance of fault estimation. And simulation results show that using the algorithm, the accuracy of fault estimation can be improved evidently. Extension of the proposed fault estimation method to more general nonlinear systems is an interesting issue, which will be investigated in our future research work.

Acknowledgments

This work is supported by the National Natural Science Foundation of China (nos. 61273171, 61304112, and 61104020), the Natural Science Foundation of Jiangsu Province (BK20131364), and the Doctoral Fund of Ministry of Education of China (no. 20113218110011).

References

[1] R. J. Patton, P. Frank, and R. Clark, *Fault Diagnosis in Dynamic Systems: Theory and Application*, Prentice-Hall, Upper Saddle River, NJ, USA, 1989.

[2] J. Chen and R. J. Patton, *Robust Model-Based Fault Diagnosis for Dynamic Systems*, Kluwer Academic, London, UK, 1999.

[3] B. Jiang, Z. H. Mao, H. Yang, and Y. Zhang, *Fault Diagnosis and Fault Accommodation for Control Systems*, National Defence Industry Press, Beijing, China, 2009.

[4] R. Marino and P. Tomei, "Adaptive observers for a class of multi-output non-linear systems," *International Journal of Adaptive Control and Signal Processing*, vol. 6, no. 4, pp. 353–365, 1992.

[5] D. Zhou, H. Ye, G. Wang, and X. Ding, "Discussion of some important issues of observer based fault diagnosis technique," *Acta Automatica Sinica*, vol. 24, no. 3, pp. 338–344, 1998.

[6] C.-F. Zhang, M. Yan, J. He, and C. Luo, "LMI-based sliding mode observers for incipient faults detection in nonlinear

system," *Journal of Applied Mathematics*, vol. 2012, Article ID 528932, 13 pages, 2012.

[7] M. Witczak, J. Korbicz, and R. I. Józefowicz, "Design of unknown input observers for non-linear stochastic systems and their application to robust fault diagnosis," *Control and Cybernetics*, vol. 42, no. 1, pp. 227–256, 2013.

[8] Y. C. Zhang, L. N. Wu, and Z. F. Wang, "An LMI approach to mixed H_-/H_∞ robust fault detection observer design," *Advanced Materials Research*, vol. 546, pp. 874–879, 2012.

[9] Q. Wu and M. Saif, "Robust fault detection and diagnosis in a class of nonlinear systems using a neural sliding mode observer," *International Journal of Systems Science*, vol. 38, no. 11, pp. 881–899, 2007.

[10] Y. Zhang and Z. Zheng, "Adaptive observer-based integrated fault diagnosis and fault-tolerant control systems against actuator faults and saturation," *Journal of Dynamic Systems, Measurement, and Control*, vol. 135, no. 4, Article ID 041008, pp. 1–13, 2013.

[11] B. Jiang, J. L. Wang, and Y. C. Soh, "An adaptive technique for robust diagnosis of faults with independent effects on system outputs," *International Journal of Control*, vol. 75, no. 11, pp. 792–802, 2002.

[12] Z. Wang, H. Guan, and C. Zheng, "Fault diagnosis observer design for discrete-time delayed complex interconnected networks with linear coupling," *Mathematical Problems in Engineering*, vol. 2012, Article ID 860489, 22 pages, 2012.

[13] X. He, Z. Wang, Y. D. Ji, and D. Zhou, "Fault detection for discrete-time systems in a networked environment," *International Journal of Systems Science*, vol. 41, no. 8, pp. 937–945, 2010.

[14] F. Caccavale and L. Villani, "An adaptive observer for fault diagnosis in nonlinear discrete-time systems," in *Proceedings of the American Control Conference (AAC '04)*, pp. 2463–2468, Boston, Mass, USA, July 2004.

[15] K. Zhang, B. Jiang, and P. Shi, "Observer-based integrated robust fault estimation and accommodation design for discrete-time systems," *International Journal of Control*, vol. 83, no. 6, pp. 1167–1181, 2010.

[16] A. Hagenblad, F. Gustafsson, and I. Klein, "A comparison of two methods for stochastic fault detection: the parity space approach and principal component analysis," in *Proceedings of the 13th IFAC Symposium on System Identification*, Rotterdam, The Netherlands, August 2003.

Hindawi Publishing Corporation
Mathematical Problems in Engineering
Volume 2013, Article ID 250683, 12 pages
http://dx.doi.org/10.1155/2013/250683

Research Article

Numerical Optimization Design of Dynamic Quantizer via Matrix Uncertainty Approach

Kenji Sawada and Seiichi Shin

Department of Mechanical Engineering and Intelligent Systems, The University of Electro-Communications, 1-5-1 Chofugaoka, Chofu, Tokyo, 182-8585, Japan

Correspondence should be addressed to Kenji Sawada; knj.sawada@uec.ac.jp

Received 12 July 2013; Accepted 12 September 2013

Academic Editor: Zidong Wang

In networked control systems, continuous-valued signals are compressed to discrete-valued signals via quantizers and then transmitted/received through communication channels. Such quantization often degrades the control performance; a quantizer must be designed that minimizes the output difference between before and after the quantizer is inserted. In terms of the broadbandization and the robustness of the networked control systems, we consider the continuous-time quantizer design problem. In particular, this paper describes a numerical optimization method for a continuous-time dynamic quantizer considering the switching speed. Using a matrix uncertainty approach of sampled-data control, we clarify that both the temporal and spatial resolution constraints can be considered in analysis and synthesis, simultaneously. Finally, for the slow switching, we compare the proposed and the existing methods through numerical examples. From the examples, a new insight is presented for the two-step design of the existing continuous-time optimal quantizer.

1. Introduction

With the rapid network technology development, the networked control systems (NCSs) have been widely studied [1–10]. One of the challenges in NCSs is quantized control. In NCSs, the continuous-valued signals are compressed and quantized to the discrete-valued signals via the quantizer of the communication channel, and such quantization often degrades the control performance. Hence, a desirable quantizer minimizes the performance error between before and after the quantizer insertion.

Motivated by this, researchers [11–14] have provided optimal dynamic quantizers for the following problem formulation in the discrete-time domain. For a given plant P, synthesize a "dynamic" quantizer Q_d such that the system Σ_Q composed of P and Q_d in Figure 1(a) "optimally" approximates the plant P in Figure 1(b) in the sense of the input-output relation. The obtained quantizer allows us to design various controllers for the plant P on the basis of the conventional control theories. Also, this framework is helpful in not only the NCS problem but also various control problems such as hybrid control, embedded system control, and on-off actuator control.

When we consider controlling a mechanical system with an on-off actuator, first the controlled object and its uncertainties are usually modeled in the continuous-time domain. Second, the model and its uncertainties are discretized to apply the above dynamic quantizer. However, the discretization sometimes results in uncertainties more complicated than those in the original model and creates undesirable complexity in robust control. The continuous-time setting quantizer is more suitable for the robust control of the quantized system than discrete-time one. Thus, our previous works [15, 16] have considered the continuous-time setting, while a number of the discrete-time settings have been studied by others [11–14]. In these works, it is assumed that the switching process of discretizing the continuous-valued signal is sufficiently quick relative to the control frequency and only the spatial determination (quantized accuracy) is considered as the quantization effect. This is

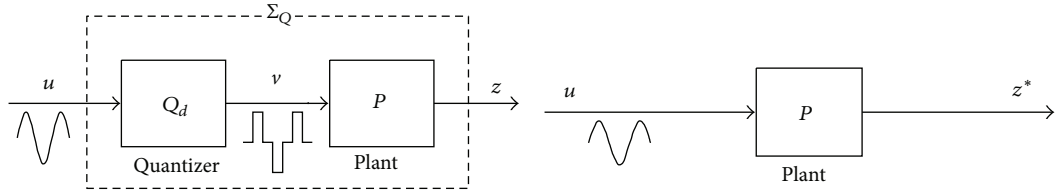

(a) Discrete-valued input system (b) Usual system

Figure 1: Two systems.

because the switching speed of the continuous-time delta-sigma modulator for wireless broadband network systems is from 1 MHz to 100 MHz [17, 18].

On the other hand, the above assumption is essentially weak in the case of the slow switching such as the mechanical systems with on-off actuators [19]. For the slow switching, we need to consider the quantization effect on both the switching speed and the spatial constraints in continuous time. For example, Ishikawa et al. proposed a two-step design of a feedback modulator [20]: (i) the control performance of the modulator is considered under only the spatial constraint, and (ii) the modulator is tuned in terms of the switching speed constraint. However, the structure of the modulator is more restricted than that of the dynamic quantizer and the obtained modulator is not always optimal. Therefore, the dynamic quantizer under temporal resolution (switching speed) and spatial resolution constraints has still to be optimally designed. The simultaneous consideration of the two constraints is the particular challenge we address in this paper.

We propose a numerical optimization method for the continuous-time dynamic quantizer under switching speed and quantized accuracy constraints. To achieve the method, this paper solves the design problem via sampled-data control framework that has so far provided various results for networked control problems [7–9]. We refer to the previous work on optimal dynamic quantizer design [11, 12] and consider the basic feedforward system in Figure 1(a). In addition to the invariant set analysis [21, 22] similarly to our previous works [13, 15, 16], this paper utilizes a matrix uncertainty approach [23, 24] that is proposed in a sampled-data control framework. Although the obtained results can be more conservative than those in the previous works on continuous-time dynamic quantizer [15, 16] from the viewpoint of the class of the exogenous input and the applicable plants, both temporal and spatial resolution constraints can be addressed in analysis and synthesis, simultaneously. For the fast switching case, the proposed conditions converge to the corresponding conditions of our previous works. Finally, for the slow switching, we compare the proposed and existing methods [15, 16] through numerical examples. In particular, a new insight is presented for the two-step design of the existing continuous-time optimal quantizer.

Notation. The set of $n \times m$ (positive) real matrices is denoted by $\mathbb{R}^{n\times m}$ ($\mathbb{R}_+^{n\times m}$). The set of $n \times m$ (positive) integer matrices is denoted by $\mathbb{N}^{n\times m}$ ($\mathbb{N}_+^{n\times m}$). We denote by $\mathscr{L}_\infty^p$ the set of piecewise-continuous functions of p-dimensional finite vectors such that ∞-norm of its functions is finite. $0_{n\times m}$ and I_m (or for simplicity of notation, 0 and I) denote the $n \times m$ zero matrix and the $m \times m$ identity matrix, respectively. For a matrix M, M^T, $\rho(M)$ and $\sigma_{\max}(M)$ denote its transpose, its spectrum radius, and its maximum singular value, respectively. For a vector x, x_i is the ith entry of x. For a symmetric matrix X, $X > 0$ ($X \geq 0$) means that X is positive (semi) definite. For a vector x and a sequence of vectors $X := \{x_1, x_2, \ldots\}$, $\|x\|$ and $\|X\|$ denote their ∞-norms, respectively. Finally, we use the "packed" notation $\left(\begin{smallmatrix} A & B \\ \hline C & D \end{smallmatrix}\right) := C(sI - A)^{-1}B + D$.

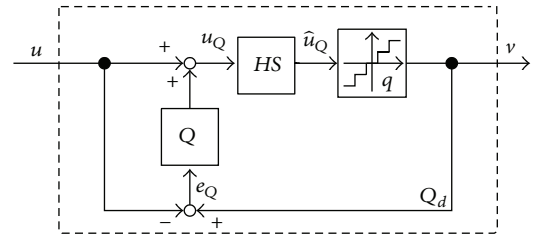

Figure 2: Continuous-time dynamic quantizer with switching speed h.

2. Problem Formulation

Consider the discrete-valued input system Σ_Q in Figure 1(a), which consists of the linear time invariant (LTI) continuous-time plant P and the quantizer $v = Q_d(u)$. The system P is given by

$$P : \begin{bmatrix} \dot{x} \\ z \end{bmatrix} = \begin{bmatrix} A & B \\ C & 0 \end{bmatrix} \begin{bmatrix} x \\ v \end{bmatrix}, \tag{1}$$

where $x \in \mathbb{R}^n$, $z \in \mathbb{R}^q$, $u \in \mathbb{R}^m$, and $v \in \mathbb{R}^m$ denote the state vector, the measured output, the exogenous input, and the quantizer output, respectively. The continuous-valued signal u is quantized into the discrete-valued signal v via the quantizer Q_d. We assume that the matrix A is Hurwitz; that is, the usual system in Figure 1(b) is stable in the continuous-time domain. The initial state is given as $x(0) = x_0$.

For the system P, consider the continuous-time dynamic quantizer $v = Q_d(u)$ with the state vector $x_Q \in \mathbb{R}^{n_Q}$ as shown in Figure 2. Its switching speed $h \in \mathbb{R}_+$ (or its temporal resolution) is determined by the operator HS, which converts

the continuous-time signal g into the low temporal resolution signal $\widehat{g}$ as follows:

$$HS : g \longrightarrow \widehat{g} : \widehat{g}(kh+\theta) = g[k], \quad g[k] = g(kh), \quad k = 0,1,2,3,\ldots, \ \theta \in [0,h). \tag{2}$$

That is, $\widehat{u}_Q = HSu_Q$. S is the ideal sampler with the sampling period h and H is the zero-order hold operator. The spatial resolution of the quantizer Q_d is expressed by the static quantizer $q : \mathbb{R}^m \to d\mathbb{N}^m$ with the quantization interval $d \in \mathbb{R}_+$, that is,

$$v = q(HSu_Q), \qquad u_Q = u + v_Q \tag{3}$$

and the continuous-time LTI filter Q is given by

$$\begin{bmatrix} \dot{x}_Q \\ v_Q \end{bmatrix} = \begin{bmatrix} A_Q & B_Q \\ C_Q & 0 \end{bmatrix} \begin{bmatrix} x_Q \\ e_Q \end{bmatrix}, \qquad e_Q := v - u. \tag{4}$$

Note that q is of the nearest-neighbor type toward $-\infty$ such as the midtread quantizer in Figure 3 ($\|q_i(\widehat{u}_{Qi}) - \widehat{u}_{Qi}\| \le d/2$ where q_i and $\widehat{u}_{Qi}$ are the ith row of q and $\widehat{u}_Q$) and the initial state is given by $x_Q(0) = 0$ for the drift free of Q_d [11, 12].

Remark 1. In synthesis, our previous works [15, 16] ignored the operator HS. In implementation, however, the continuous-time quantizer needs the switching process discretizing the continuous-valued signal. Of course, the applicable interval of switching depends on controlled objects such as narrowband or broadband networked systems and mechanical systems with on-off actuators. Therefore, it is important to consider the operator HS in synthesis.

For the system Σ_Q in Figure 1(a) with the initial state x_0 and the exogenous input $u \in \mathscr{L}_\infty^m$, $z(t, x_0, Q_d(u))$ denotes the output of z at the time t. Also, for the system in Figure 1(b) without Q_d, $z^*(t, x_0, u)$ denotes its output at the time t. Consider the following cost function:

$$J(Q_d) := \sup_{(x_0,u)\in\mathbb{R}^n\times\mathscr{L}_\infty^m} \sup_{t\in\mathbb{R}_+\cup\{0\}} \left\| z(t, x_0, Q_d(u)) - z^*(t, x_0, u) \right\|. \tag{5}$$

If the quantizer minimizes $J(Q_d)$, the system Σ_Q "optimally" approximates the usual system P in the sense of the input-output relation. In this case, we can use the existing continuous-time controller design methods for the system in Figure 1(b) without considering the quantization effect. When the controlled object and its uncertainties are modeled in the continuous-time domain, therefore, the continuous-time quantizer can introduce robust control of the continuous-time setting directly, while the discrete-time quantizer requires discretization of the whole control system. Our previous works [15, 16] proposed an optimal dynamic quantizer for the cost function $J(Q_d)$ for the fast switching case $h = 0$. That is, only the spatial deterioration has been considered.

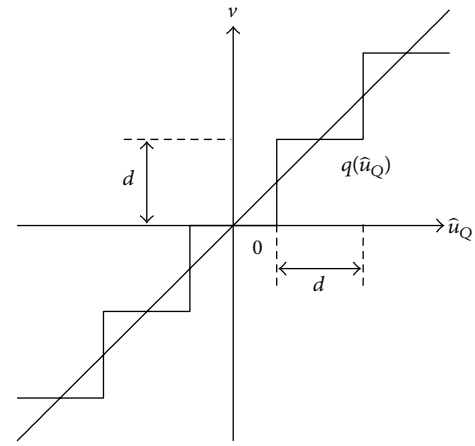

Figure 3: Midtread quantization.

On the other hand, the simultaneous consideration of the temporal and spatial resolution constraints is the problem we address in this paper. To consider the temporal resolution constraint caused by the operator HS, this paper modifies the cost function as follows:

$$J_{HS}(Q_d) := \sup_{(x_0,u)\in\mathbb{R}^n\times\mathscr{L}_\infty^m} \sup_{\theta\in[0,h)} \sup_{k\in\mathbb{N}_+\cup\{0\}} \left\| z(kh+\theta, x_0, Q_d(u)) - z^*(kh+\theta, x_0, u) \right\|. \tag{6}$$

Fixing $\theta = 0$ ignores the output error between before and after the quantizer is inserted over the kth sampling interval and leads to the cost function setting that is utilized for the discrete-time optimal dynamic quantizers [11–14]. Therefore, the optimal quantizer for $J_{HS}(Q_d)$ minimizes the output error between the systems in Figures 1(a) and 1(b) in terms of the input-output relation under the temporal and spatial resolution constraints.

Motivated by the above, our objective is to solve the following continuous-time dynamic quantizer synthesis problem **(E)**: *for the system Σ_Q composed of P and Q_d with the initial state $x_0 \in \mathbb{R}^n$ and the exogenous input $u \in \ell_\infty^m$, suppose that the quantization interval $d \in \mathbb{R}_+$, the switching speed $h \in \mathbb{R}_+$, and the performance level $\gamma \in \mathbb{R}_+$ are given. Characterize a continuous-time dynamic quantizer Q_d* (i.e., *find parameters (n_Q, A_Q, B_Q, C_Q)) achieving $J_{HS}(Q_d) \le \gamma$.*

This paper proposes continuous-time quantizers in terms of solving the problem **(E)** on the basis of invariant set analysis and the sampled-data control technique, while other researchers [11, 12, 14] have proposed the discrete-time optimal ones.

Remark 2. The cost function setting of this paper is more complicated than the existing continuous-time and discrete-time cases [11–16], so this paper considers the basic feedforward system composed of P and Q_d similar to the previous works on optimal dynamic quantizer design [11, 12].

Remark 3. The plant P is restricted to be stable because of the feedforward structure, while the existing results can address unstable plants. To remove this restriction, we need to consider a feedback system structure similar to existing ones [13–16]. This is our future task.

3. Main Result

3.1. System Expression. In this subsection, we consider the system expression for the quantizer analysis. Define the quantization error e as

$$e := q\left(\widehat{u}_Q\right) - \widehat{u}_Q = v - \widehat{u}_Q. \tag{7}$$

From the properties of the quantizer q and the operator HS,

$$e\left(kh+\theta\right) = e\left[k\right] \in \left[-\frac{d}{2}, \frac{d}{2}\right]^m, \quad k = 0, 1, 2, \ldots, \ \theta \in [0, h), \tag{8}$$

holds where $e[k] = e(kh)$. Then, one obtains

$$v\left(kh+\theta\right) = v_Q\left[k\right] + u\left[k\right] + e\left[k\right], \tag{9}$$

where $v_Q[k] = v_Q(kh)$ and $u[k] = u(kh)$ for $k = 0, 1, 2, \ldots$, $\theta \in [0, h)$. In this case, by using the sampled-data control technique, the following lemma holds.

Lemma 4. *Denote by $\widehat{x}$ the state vector of the usual system in Figure 1(b) and define the signals as follows:*

$$\xi := \left[x^T - \widehat{x}^T \ \ x_Q^T\right]^T, \qquad z_p := z - z^*. \tag{10}$$

For the cost function $J_{HS}(Q_d)$, the difference between $z(kh+\theta, x_0, Q_d(u))$ and $z^*(kh+\theta, x_0, u)$ for $k = 0, 1, 2, \ldots, \theta \in [0, h)$ is given by the following system:

$$\Sigma : \begin{cases} \xi\left[k+1\right] = \mathscr{A}\xi\left[k\right] + \mathscr{B}e\left[k\right] \\ \qquad\qquad + \begin{bmatrix} \int_0^h e^{A(h-\tau)} B\widetilde{u}\left(kh+\tau\right)\mathrm{d}\tau \\ \int_0^h e^{A_Q(h-\tau)} B_Q\widetilde{u}\left(kh+\tau\right)\mathrm{d}\tau \end{bmatrix} \\ z_p\left(kh+\theta\right) = \mathscr{C}\left(\theta\right)\xi\left[k\right] + \mathscr{D}\left(\theta\right)e\left[k\right] \\ \qquad\qquad + C\int_0^\theta e^{A(h-\tau)} B\widetilde{u}\left(kh+\tau\right)\mathrm{d}\tau, \end{cases} \tag{11}$$

where $\xi[0] = 0$, $\widetilde{u}(kh+\tau) := u[k] - u(kh+\tau)$; the matrices $\mathscr{A}$, $\mathscr{B}$, $\mathscr{C}(\theta)$, and $\mathscr{D}(\theta)$ are defined as follows:

$$\begin{aligned} \mathscr{A} &:= \begin{bmatrix} e^{Ah} & \int_0^h e^{A\tau}\mathrm{d}\tau BC_Q \\ 0 & e^{A_Q h} + \int_0^h e^{A_Q\tau}\mathrm{d}\tau B_Q C_Q \end{bmatrix}, \\ \mathscr{B} &:= \begin{bmatrix} \int_0^h e^{A\tau}\mathrm{d}\tau B \\ \int_0^h e^{A_Q\tau}\mathrm{d}\tau B_Q \end{bmatrix}, \\ \mathscr{C}\left(\theta\right) &:= \begin{bmatrix} Ce^{A\theta} & C\int_0^\theta e^{A\tau}\mathrm{d}\tau BC_Q \end{bmatrix}, \\ \mathscr{D}\left(\theta\right) &:= C\int_0^\theta e^{A\tau}\mathrm{d}\tau. \end{aligned} \tag{12}$$

Proof. See Appendix A. □

We focus on $\widetilde{u}(kh+\tau)$ of Σ. For the operator HS and the signal $u \in \mathscr{L}_\infty^m$,

$$\lim_{h\to 0} \left\|\left[\left(I - HS\right)u\right](t)\right\| \neq 0 \tag{13}$$

holds. This implies that we cannot ignore the temporal resolution constraint on the cost function $J_{HS}(Q_d)$ even if $h \to 0$. On the other hand, low-pass prefiltering rectifies this situation [25]. In fact, for the stable LTI system F,

$$\begin{aligned} &\lim_{h\to 0} \left\|\left[\left(I - HS\right)Fu\right](t)\right\| = 0, \\ &F := \left(\left(\begin{array}{c|c} A_F & B_F \\ \hline C_F & 0 \end{array}\right)\right) \end{aligned} \tag{14}$$

holds. For the evaluation of the cost function $J_{HS}(Q_d)$, then this paper utilizes

$$u = HSFr, \quad r \in \mathscr{L}_\infty^m \tag{15}$$

as the exogenous input. Note that $u \in \mathscr{L}_\infty^m$ if stable F is strictly proper and $r \in \mathscr{L}_\infty^m$. For the signal (15), $u[k] = u(kh+\theta)$ ($k = 0, 1, 2, \ldots$, $\theta \in [0, h)$) holds, so the terms of $\widetilde{u}(kh+\tau)$ in (11) are eliminated. Then, Σ is rewritten as

$$\Sigma_{HS} : \begin{cases} \xi\left[k+1\right] = \mathscr{A}\xi\left[k\right] + \mathscr{B}e\left[k\right], \\ z_p\left(kh+\theta\right) = \mathscr{C}\left(\theta\right)\xi\left[k\right] + \mathscr{D}\left(\theta\right)e\left[k\right]. \end{cases} \tag{16}$$

Also, this paper solves the following synthesis problem **(E′)**: *for the system Σ_Q composed of P and Q_d with the initial state $x_0 \in \mathbb{R}^n$ and the exogenous input $u \in \mathscr{L}_\infty^m$ in (15), suppose that the quantization interval $d \in \mathbb{R}_+$,* the *switching speed $h \in \mathbb{R}_+$, and the performance level $\gamma \in \mathbb{R}_+$ are given. Characterize a continuous-time dynamic quantizer Q_d* (i.e., *find parameters (n_Q, A_Q, B_Q, C_Q)) achieving $J_{HS}(Q_d) \leq \gamma$.*

3.2. Quantizer Analysis. The quantization error e of (16) is bounded as mentioned earlier. The reachable set and the invariant set characterize such a system with bounded input. Consider the LTI discrete-time system given by

$$\widetilde{\xi}[k+1] = \mathscr{A}\widetilde{\xi}[k] + \mathscr{B}w[k], \tag{17}$$

where $\widetilde{\xi} \in \mathbb{R}^{n_\xi}$ and $w \in \mathbb{R}^m$ denote the state vector and disturbance input, respectively. We define the reachable set and the invariant set.

Definition 5. Define the reachable set of the system (17) to be a set $\mathbb{R}_\infty$ which satisfies

$$\mathbb{R}_\infty := \left\{ \widetilde{\xi} \in \mathbb{R}^{n_\xi} \;\middle|\; \begin{array}{l} \exists k \in \mathbb{N}_+ \quad \exists w[\cdot] \in \mathbb{W}, \\ \widetilde{\xi}[k] = \sum_{i=0}^{k-1} \mathscr{A}^{k-1-i}\mathscr{B}w[i] \end{array} \right\}, \tag{18}$$

$$\mathbb{W} := \left\{ w \in \mathbb{R}^m : w^T w \le 1 \right\}.$$

Definition 6. Define the invariant set of the system (17) to be a set x which satisfies

$$\widetilde{\xi} \in x, \quad w \in \mathbb{W} \Longrightarrow \mathscr{A}\widetilde{\xi} + \mathscr{B}w \in x. \tag{19}$$

The analysis condition can be expressed in terms of matrix inequalities as summarized in the following proposition [22].

Proposition 7. *Consider the system* (17). *For a matrix* $0 < \mathscr{P} = \mathscr{P}^T \in \mathbb{R}^{n_\xi \times n_\xi}$, *the ellipsoid* $\mathbb{E}(\mathscr{P}) := \{\widetilde{\xi} \in \mathbb{R}^{n_\xi} : \widetilde{\xi}^T \mathscr{P} \widetilde{\xi} \le 1\}$ *is an invariant set if and only if there exists a scalar* $\alpha \in [0, 1 - \rho(\mathscr{A})^2]$ *satisfying*

$$\begin{bmatrix} \mathscr{A}^T\mathscr{P}\mathscr{A} - (1-\alpha)\mathscr{P} & \mathscr{A}^T\mathscr{P}\mathscr{B} \\ \mathscr{B}^T\mathscr{P}\mathscr{A} & \mathscr{B}^T\mathscr{P}\mathscr{B} - \alpha I_m \end{bmatrix} \le 0. \tag{20}$$

Note that the ellipsoidal set $\mathbb{E}(\mathscr{P})$ covers the reachable set $\mathbb{R}_\infty$ from outside. Define the set $\mathscr{E} := \{\widetilde{w} \in \mathbb{R}^m : e = (\sqrt{m}d/2)\widetilde{w}$ satisfies (7)$\}$ and rewrite the system (16) as

$$\widetilde{\Sigma}_{HS} : \begin{cases} \widetilde{\xi}[k+1] = \boldsymbol{\mathscr{A}}\widetilde{\xi}[k] + \boldsymbol{\mathscr{B}}\widetilde{w}[k], \\ \widetilde{z}_p(kh+\theta) = \boldsymbol{\mathscr{C}}(\theta)\widetilde{\xi}[k] + \boldsymbol{\mathscr{D}}(\theta)\widetilde{w}[k], \end{cases} \tag{21}$$

where $\xi = (\sqrt{m}d/2)\widetilde{\xi}$, $z_p = (\sqrt{m}d/2)\widetilde{z}_p$, $e = (\sqrt{m}d/2)\widetilde{w}$, and $\widetilde{w} \in \mathscr{E}$. The left multiplication of $\widetilde{\Sigma}_{HS}$ with $\sqrt{m}d/2$ leads to Σ_{HS}. The relation $\mathscr{E} \subseteq \mathbb{W}$ clearly holds because $e^T e \le md^2/4$ and the set $\mathbb{W}$ is an independent bounded disturbance without the relation (7). That is, the reachable set of $\widetilde{\Sigma}_{HS}$ with $\widetilde{w} \in \mathscr{E}$ is no larger than that of $\widetilde{\Sigma}_{HS}$ with the disturbance $\widetilde{w} \in \mathbb{W}$.

Then, this paper utilizes the reachable set to estimate the influences of the quantization error and the invariant set to characterize the cost function $J_{HS}(Q_d)$ by substituting $\mathscr{A} = \boldsymbol{\mathscr{A}}$ and $\mathscr{B} = \boldsymbol{\mathscr{B}}$ into (20). Move on to the matrix exponential $e^{A\theta}$ of $\boldsymbol{\mathscr{C}}(\theta)$ and $\boldsymbol{\mathscr{D}}(\theta)$ in (21), which is rewritten as

$$e^{A\theta} = I + \Omega(\theta)A, \qquad \Omega(\theta) := \int_0^\theta e^{A\tau} d\tau. \tag{22}$$

Along with this, $\widetilde{z}_p$ of (21) is also rewritten as

$$\begin{aligned} &\widetilde{z}_p(kh+\theta) \\ &\quad = \left[C + C\Omega(\theta)A \;\; C\Omega(\theta)BC_Q\right]\widetilde{\xi}[k] + C\Omega(\theta)\widetilde{w}[k] \\ &\quad = \left(\widehat{\boldsymbol{\mathscr{C}}} + C\Omega(\theta)\widehat{\boldsymbol{\mathscr{D}}}\right)\widetilde{\xi}[k] + C\Omega(\theta)\widetilde{w}[k], \\ &\qquad \widehat{\boldsymbol{\mathscr{C}}} := \left[C \;\; 0\right], \qquad \widehat{\boldsymbol{\mathscr{D}}} := \left[A \;\; BC_Q\right]. \end{aligned} \tag{23}$$

In addition, from the properties of $\mathbb{R}_\infty$ and $\mathbb{E}(\mathscr{P})$,

$$\begin{aligned} &J_{HS}(Q_d) \\ &\le \sup_{\theta\in[0,h)} \sup_{\widetilde{\xi}\in\mathbb{R}_\infty, \widetilde{w}\in\mathscr{E}} \left\| \boldsymbol{\mathscr{C}}(\theta)\widetilde{\xi} + \boldsymbol{\mathscr{D}}(\theta)\widetilde{w} \right\| \frac{\sqrt{m}d}{2} \\ &\le \sup_{\theta\in[0,h)} \sup_{\widetilde{\xi}\in\mathbb{R}_\infty, \widetilde{w}\in\mathbb{W}} \left\| \boldsymbol{\mathscr{C}}(\theta)\widetilde{\xi} + \boldsymbol{\mathscr{D}}(\theta)\widetilde{w} \right\| \frac{\sqrt{m}d}{2} \quad (\because \mathscr{E} \subseteq \mathbb{W}) \\ &\le \sup_{\theta\in[0,h)} \sup_{\widetilde{\xi}\in\mathbb{E}(\mathscr{P}), \widetilde{w}\in\mathbb{W}} \left\| \boldsymbol{\mathscr{C}}(\theta)\widetilde{\xi} + \boldsymbol{\mathscr{D}}(\theta)\widetilde{w} \right\| \frac{\sqrt{m}d}{2} \\ &\qquad\qquad (\because \mathbb{R}_\infty \subseteq \mathbb{E}(\mathscr{P})) \\ &\le \underbrace{\sup_{\theta\in[0,h)} \sup_{\widetilde{\xi}\in\mathbb{E}(\mathscr{P})} \left\| (\widehat{\boldsymbol{\mathscr{C}}} + C\Omega(\theta)\widehat{\boldsymbol{\mathscr{D}}})\widetilde{\xi} \right\|}_{\gamma_1} \frac{\sqrt{m}d}{2} \\ &\quad + \underbrace{\sup_{\theta\in[0,h)} \sup_{\widetilde{w}\in\mathbb{W}} \left\| C\Omega(\theta)\widetilde{w} \right\|}_{\gamma_2} \frac{\sqrt{m}d}{2} \end{aligned} \tag{24}$$

holds. Similarly to our previous papers [13, 15, 16], by using the $\mathscr{L}_1$ control technique in [21], we provide the sufficient conditions for computing $\gamma_1 \in \mathbb{R}_+$ and $\gamma_2 \in \mathbb{R}_+$ of (24) as follows:

$$\begin{aligned} &\begin{bmatrix} \mathscr{P} & \widehat{\boldsymbol{\mathscr{C}}}^T + \widehat{\boldsymbol{\mathscr{D}}}^T\Omega(\theta)^T C^T \\ \widehat{\boldsymbol{\mathscr{C}}} + C\Omega(\theta)\widehat{\boldsymbol{\mathscr{D}}} & \gamma_1^2 I_q \end{bmatrix} \ge 0, \\ &\Omega(\theta)^T C^T C\Omega(\theta) \le \gamma_2^2 I_n, \quad \forall\theta \in [0,h). \end{aligned} \tag{25}$$

Remark 8. For the inequalities (25) and any vectors $\widetilde{\xi} \in \mathbb{R}^n$ and $\widetilde{w} \in \mathbb{R}^m$, we have

$$\begin{aligned} &\begin{bmatrix} \widetilde{\xi}^T\mathscr{P}\widetilde{\xi} & \widetilde{\xi}^T\left(\widehat{\boldsymbol{\mathscr{C}}}^T + \widehat{\boldsymbol{\mathscr{D}}}^T\Omega(\theta)^T C^T\right) \\ \left(\widehat{\boldsymbol{\mathscr{C}}} + C\Omega(\theta)\widehat{\boldsymbol{\mathscr{D}}}\right)\widetilde{\xi} & \gamma_1^2 I_q \end{bmatrix} \ge 0 \\ &\quad \Longleftrightarrow \widetilde{\xi}^T\left(\widehat{\boldsymbol{\mathscr{C}}} + C\Omega(\theta)\widehat{\boldsymbol{\mathscr{D}}}\right)^T\left(\widehat{\boldsymbol{\mathscr{C}}} + C\Omega(\theta)\widehat{\boldsymbol{\mathscr{D}}}\right)\widetilde{\xi} \\ &\quad \le \gamma_1^2\widetilde{\xi}^T\mathscr{P}\widetilde{\xi} \quad (\because \text{Schur complement}) \end{aligned} \tag{26}$$

and $\widetilde{w}^T\Omega(\theta)^T C^T C\Omega(\theta)\widetilde{w} \le \gamma_2^2\widetilde{w}^T\widetilde{w}$. Then, we see that (24) holds if $\widetilde{\xi} \in \mathbb{E}(\mathscr{P})$ and $\widetilde{w} \in \mathbb{W}$.

The inequalities (25) are difficult to test since we need to find $\mathscr{P}$, γ_1, and γ_2 satisfying (20) and (25) for infinitely many values of $\theta \in [0, h)$. Then, using the matrix uncertainty technique [23, 24], we consider their sufficient conditions, which are easy to compute. Considering $\Omega(\theta)$ in (22) as a matrix uncertainty, we introduce the following lemma regarding the matrix exponential [26, 27].

Lemma 9. *For the matrix $\Omega(\theta)$ in (22),*

$$\sigma_{\max}(\Omega(\theta)) \le \delta(\theta) \le \delta(h), \quad \forall \theta \in [0, h), \tag{27}$$

holds where

$$\delta(\theta) := \begin{cases} \dfrac{e^{\mu(A)\theta} - 1}{\mu(A)}, & \mu(A) \neq 0, \\ \theta, & \mu(A) = 0, \end{cases}$$
$$\mu(A) := \max\left\{\lambda : \lambda \in eig\left(\frac{\left(A + A^T\right)}{2}\right)\right\}. \tag{28}$$

Proof. Since $\sigma_{\max}(e^{A\theta}) \le e^{\mu(A)\theta}$ (see [26]),

$$\sigma_{\max}(\Omega(\theta)) \le \int_0^\theta \sigma_{\max}\left(e^{A\beta}\right) d\beta \le \int_0^\theta e^{\mu(A)\beta} d\beta \tag{29}$$

holds. □

By using Lemma 9 and the S-procedure [23, 28, 29], the sufficient condition analyzing the cost function $J_{HS}(Q_d)$ of the system Σ_Q can be expressed in terms of matrix inequality as summarized in the following theorem.

Theorem 10. *Consider the system Σ_Q composed of P and Q_d with the initial state $x_0 \in \mathbb{R}^n$ and the exogenous input $u \in \mathscr{L}_\infty^m$ in (15). For the quantization interval $d \in \mathbb{R}_+$ and the switching speed $h \in \mathbb{R}_+$, the upper bound of the cost function $J_{HS}(Q_d)$ is given by*

$$J_{HS}(Q_d) \le \gamma(h)$$
$$s.t.\ \gamma(h) := \left(\gamma + \sigma_{\max}(C)\,\delta(h)\right)\frac{\sqrt{m}d}{2} \tag{30}$$

if there exist $0 < \mathcal{Q} = \mathcal{Q}^T \in \mathbb{R}^{(n+n_Q)\times(n+n_Q)}$, $0 < S = S^T \in \mathbb{R}^{n\times n}$, $\alpha_h \in [0, 1/2h - \rho(\mathscr{A})^2/2h]$ and $\gamma \in \mathbb{R}_+$ satisfying

$$\begin{bmatrix} \Phi_h\mathcal{Q} + \mathcal{Q}\Phi_h^T + 2\alpha_h\mathcal{Q} & \Gamma_h & \sqrt{h}\mathcal{Q}\Phi_h^T \\ \Gamma_h^T & -2\alpha_h I_m & \sqrt{h}\Gamma_h^T \\ \sqrt{h}\Phi_h\mathcal{Q} & \sqrt{h}\Gamma_h & -\mathcal{Q} \end{bmatrix} \le 0, \tag{31}$$

$$\begin{bmatrix} \mathcal{Q} & \mathcal{Q}\widehat{\mathscr{C}}^T & \sqrt{\delta(h)}\mathcal{Q}\widehat{\mathscr{D}}^T \\ \widehat{\mathscr{C}}\mathcal{Q} & \gamma^2 I_q - \delta(h)CSC^T & 0 \\ \sqrt{\delta(h)}\widehat{\mathscr{D}}\mathcal{Q} & 0 & S \end{bmatrix} \ge 0,$$
$$S\Omega(\theta) = \Omega(\theta)S, \quad \forall \theta \in [0, h), \tag{32}$$

where the matrices Φ_h and Γ_h are defined by

$$\Phi_h := \begin{bmatrix} \dfrac{1}{h}\displaystyle\int_0^h e^{A\tau}d\tau A & \dfrac{1}{h}\displaystyle\int_0^h e^{A\tau}d\tau BC_Q \\ 0 & \dfrac{1}{h}\displaystyle\int_0^h e^{A_Q\tau}d\tau\left(A_Q + B_QC_Q\right) \end{bmatrix}, \tag{33}$$
$$\Gamma_h := \begin{bmatrix} \dfrac{1}{h}\displaystyle\int_0^h e^{A\tau}d\tau B \\ \dfrac{1}{h}\displaystyle\int_0^h e^{A_Q\tau}d\tau B_Q \end{bmatrix}.$$

Proof. See Appendix A. □

Denote by $\widehat{\Sigma}$ the system Σ without operator HS. In this case, the system $\widehat{\Sigma}$ is given by

$$\widehat{\Sigma} : \dot{\xi}(t) = \widehat{\mathscr{A}}\xi(t) + \widehat{\mathscr{B}}e(t), \qquad z_p(t) = \widehat{\mathscr{C}}\xi(t), \tag{34}$$

where

$$\widehat{\mathscr{A}} := \begin{bmatrix} A & BC_Q \\ 0 & A_Q + B_QC_Q \end{bmatrix}, \qquad \widehat{\mathscr{B}} := \begin{bmatrix} B \\ B_Q \end{bmatrix}. \tag{35}$$

Regarding the definition of $\xi(t)$, see Lemma 4. An advantage the condition (31) over conditions (20) is that it can be used for a small h without numerical difficulty. This idea comes from [23, 24]. In the limit of $h \to 0$, $(1/h)\int_0^h e^{Ah}d\tau \to I$ and $(1/h)\int_0^h e^{A_Qh}d\tau \to I$ hold, so $\Phi_h \to \widehat{\mathscr{A}}$ and $\Gamma_h \to \widehat{\mathscr{B}}$ hold. In the same limit, from $\delta(h) \to 0$, conditions (31) and (32) converge to the analysis conditions of the continuous-time dynamic quantizer for the system $\widehat{\Sigma}$ in [15, 16]. On the other hand, for a small h, $e^{Ah} \to I$, $e^{A_Qh} \to I$, $\int_0^h e^{Ah}d\tau \to 0$ and $\int_0^h e^{A_Qh}d\tau \to 0$ hold, so $\mathscr{A}$ and $\mathscr{B}$ ($\widehat{\mathscr{A}}$ and $\widehat{\mathscr{B}}$) are close to identity and zero matrices, respectively, and the left side of (20) is close to zero.

In numerical computation, it is appropriate to fix the structure of S such that $S\Omega(\theta) = \Omega(\theta)S$ holds. For example, we can set $S = s_\theta I_n$, $s_\theta \in \mathbb{R}_+$ and this setting leads to the following optimization problem **(Aop)**:

$$\min_{\mathcal{Q}=\mathcal{Q}^T>0, S=s_\theta I_n>0, 1/2h-\rho(\mathscr{A})^2/2h\ge\alpha_h\ge0, \gamma>0} \gamma^2$$
$$\text{s.t. (31) and (32)}. \tag{36}$$

When scalar α_h is fixed, the conditions in Theorem 10 are linear matrix inequalities (LMIs) in terms of the other variables. Using standard LMI software and the line search of α_h, we can obtain an upper bound of $J_{HS}(Q_d)$.

3.3. Quantizer Synthesis. The problem **(Aop)** suggests that the quantizer synthesis problem $(\mathbf{E}')$ is reduced to the following nonconvex optimization problem **(OP)**:

$$\min_{\mathcal{Q}=\mathcal{Q}^T>0, S=s_\theta I_n>0, A_Q, B_Q, C_Q, 1/2h-\rho(\mathscr{A})^2/2h\ge\alpha_h\ge0, \gamma>0} \gamma^2$$
$$\text{s.t. (31) and (32)}. \tag{37}$$

That is, if **(OP)** is feasible, $(\mathbf{E}')$ is feasible.

From the matrix product such as $(1/h)\int_0^h e^{A_Q h}\mathrm{d}\tau$ and $A_Q+B_QC_Q$ in (31), the synthesis condition is difficult to derive from Theorem 10 unlike the continuous-time case without the operator HS in [15, 16]. Thus, we fixed the parameters as follows:

$$n_Q = n, \qquad A_Q = A, \qquad B_Q = B. \tag{38}$$

The structure (38) does not severely limit the synthesis because A_Q and B_Q of the continuous-time dynamic quantizer for the system $\widehat{\Sigma}$ in [15, 16] are also (38). See Appendix B. In other words, $\dot{x}_Q = Ax_Q + Be_Q$ estimates the quantization influence on the system P. Along with this, we fix $\mathcal{Q}$ of (31) as follows:

$$\mathcal{Q} = \begin{bmatrix} Y & V \\ V & V \end{bmatrix}, \quad Y = Y^T > 0, \quad V = V^T > 0. \tag{39}$$

The structure (39) also does not impose a severe limitation on the synthesis because an appropriate choice of the quantizer state coordinates allows us to assume that $\mathcal{Q}$ has the special structure for the full order case $n_Q = n$ [30].

Under some circumstances (38) and (39), we obtain the following synthesis condition.

Theorem 11. *Consider the system Σ_Q composed of P and Q_d with the initial state $x_0 \in \mathbb{R}^n$ and the exogenous input $u \in \mathscr{L}_\infty^m$ in* (15)*. Suppose that the quantization interval $d \in \mathbb{R}_+$, the switching speed $h \in \mathbb{R}_+$, and the performance level $\gamma \in \mathbb{R}_+$ are given. For a scalar $\alpha_h \in [0, 1/2h]$, there exist a continuous-time dynamic quantizer Q_d achieving* (30) *if one of the following equivalent statements holds.*

(i) *There exist matrices $0 < \mathcal{Q} = \mathcal{Q}^T \in \mathbb{R}^{(n+n_Q)\times(n+n_Q)}$, $0 < S = S^T \in \mathbb{R}^{n\times n}$ and a dynamic quantizer Q_d satisfying* (31)*,* (32)*, and* (38)*.*

(ii) *There exist matrices $0 < Y = Y^T \in \mathbb{R}^{n\times n}$, $0 < V = V^T \in \mathbb{R}^{n\times n}$, $W \in \mathbb{R}^{m\times n}$, $0 < S = S^T \in \mathbb{R}^{n\times n}$ satisfying*

$$\begin{bmatrix} \Theta_{Ah} + \Theta_{Ah}^T + 2\alpha_h\Theta_P & \Theta_{Bh} & \sqrt{h}\Theta_{Ah}^T \\ \Theta_{Bh}^T & -2\alpha_h I_m & \sqrt{h}\Theta_{Bh}^T \\ \sqrt{h}\Theta_{Ah} & \sqrt{h}\Theta_{Bh} & -\Theta_P \end{bmatrix} \le 0, \tag{40}$$

$$\begin{bmatrix} \Theta_P & \Theta_C^T & \Theta_{Dh}^T \\ \Theta_C & \gamma^2 I_q - \delta(h)\, CSC^T & 0 \\ \Theta_{Dh} & 0 & S \end{bmatrix} \ge 0, \tag{41}$$

$$S\Omega(\theta) = \Omega(\theta)S, \quad \forall\theta \in [0, h),$$

where

$$\begin{aligned} \Theta_P &:= \begin{bmatrix} Y & V \\ V & V \end{bmatrix}, \qquad \Psi_h := \frac{1}{h}\int_0^h e^{A\tau}d\tau, \\ \Theta_{Ah} &:= \begin{bmatrix} \Psi_h(AY + BW) & \Psi_h(AV + BW) \\ \Psi_h(AV + BW) & \Psi_h(AV + BW) \end{bmatrix}, \\ \Theta_{Bh} &:= \begin{bmatrix} \Psi_h B \\ \Psi_h B \end{bmatrix}, \qquad \Theta_C := \begin{bmatrix} CY & CV \end{bmatrix}, \\ \Theta_{Dh} &:= \begin{bmatrix} \sqrt{\delta(h)}(AY + BW) & \sqrt{\delta(h)}(AV + BW) \end{bmatrix}. \end{aligned} \tag{42}$$

In this case, such a quantizer parameter is given by

$$n_Q = n, \qquad A_Q = A, \qquad B_Q = B, \qquad C_Q = WY^{-1}. \tag{43}$$

Proof. We fix $\mathcal{Q}$ as shown in (39) and introduce the change of variables $W = C_QY$. Hence, (31) and (32) result in (40) and (41). Also, designing C_Q yields $\alpha_h \in [0, 1/2h]$ because $\rho(\mathscr{A})$ is determined by C_Q and $[0, 1/2h - \rho(\mathscr{A})^2/2h] \subseteq [0, 1/2h]$. □

In the limit of $h \to 0$; Ψ_h converges to I and $\delta(h)$ converges to 0; then conditions (40) and (41) also converge to the synthesis condition of the continuous-time dynamic quantizer for the system $\widehat{\Sigma}$ in (34). Also, by setting $S = s_\theta I_n$ for Theorem 11, the quantizer synthesis problem **(E′)** is reduced to the following optimization problem **(Sop)**:

$$\begin{aligned} &\min_{Y=Y>0^T, V=V^T>0, S=s_\theta I_n>0, W, 1/2h\ge\alpha_h\ge0, \gamma>0} \gamma^2 \\ &\text{s.t. } (40) \text{ and } (41). \end{aligned} \tag{44}$$

If **(Sop)** is feasible, **(E′)** is feasible. Therefore, a continuous-time dynamic quantizer considering both spatial and temporal resolution constraints is obtained from Theorem 11.

Remark 12. To consider numerical optimization analysis or synthesis of a quantizer as shown in **(Aop)** and **(Sop)**, we need the signal assumption (15) in Theorems 10 and 11. On the other hand, for the high speed switching such that h is very small, the assumption (15) ensures that solutions to the problem **(E′)** converge to our previous results [15, 16]. Therefore, the results of this paper partly include our previous results [15, 16] although each class of exogenous signals and plants is restricted.

4. Discussion

For the slow switching, we compare the proposed method and existing continuous-time quantizer [15, 16]. Consider the system Σ_Q. The plant P is the stable minimum phase LTI system:

$$\begin{bmatrix} \dot{x}(t) \\ z(t) \end{bmatrix} = \begin{bmatrix} -3 & 3 & 0 \\ 0 & -2 & 2 \\ 1 & 1 & 0 \end{bmatrix} \begin{bmatrix} x(t) \\ v(t) \end{bmatrix}. \tag{45}$$

In the case without the operator HS, an optimal form of the continuous-time quantizer Q_d^{op} [15, 16] is given by (B.2).

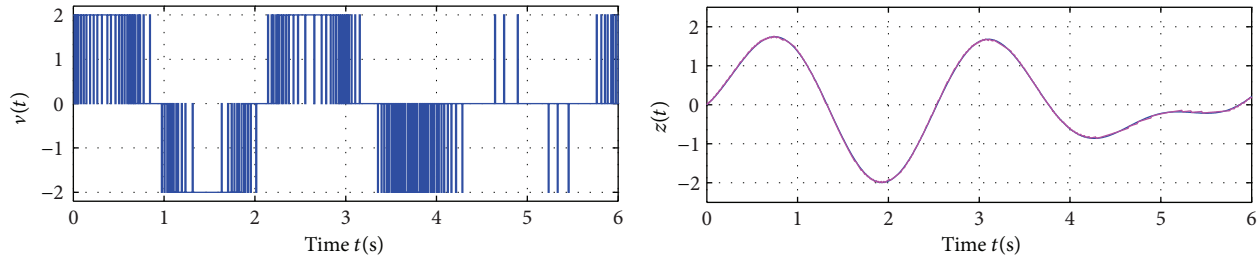

(a) (b)

Figure 4: Time responses of Σ_Q with the proposed quantizer for $h = 0.01$.

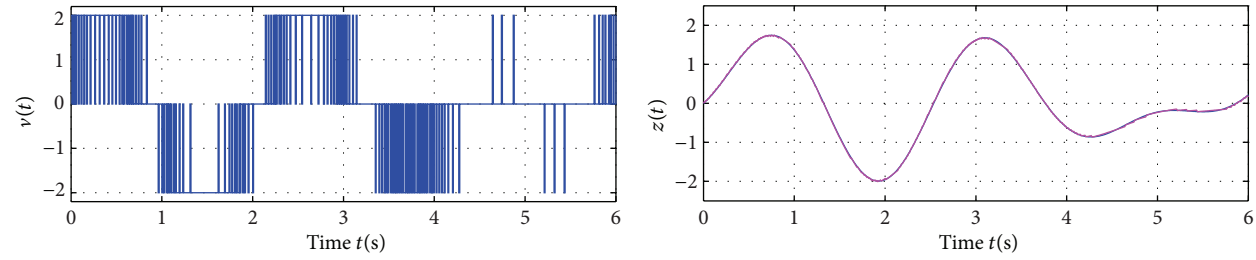

(a) (b)

Figure 5: Time responses of Σ_Q with (B.2) for $h = 0.01$.

See Appendix B. The continuous-time quantizer Q_d^{op} and its performance are parameterized by the free parameter $f \in \mathbb{R}_+$. For the simulation, we consider a two-step design for Q_d^{op}; we first set f and second insert the operator HS in the obtained Q_d^{op}. Also, the achievable performance of $J_{HS}(Q_d^{op})$ is calculated by **(Aop)**.

For the comparison, we set the switching speed $h = 0.01$ [s] and the quantization interval $d = 2$. First, we set $f = 50$ and then obtain Q_d^{op} with $\gamma_c = 0.102$. Also, $\gamma(h) = 0.219$ for $J_{HS}(Q_d^{op})$ is obtained from **(Aop)**. Second, we solve the problem **(Sop)** and obtain $\gamma(h) = 0.219$ and the matrix $C_Q = [-19.26 \ -22.72]$. In this case, both quantizers can approximate well. Figures 4 and 5 illustrate the simulation results of the time responses of Σ_Q with the proposed quantizer and the quantizers Q_d^{op} in (B.2). The initial state $x_0 = [0 \ 0]^T$ and the input $u(t) = \sin \pi t + \cos 0.7\pi t$ are given. In Figures 4 and 5, the thin lines and the thick lines are for the conventional system in Figure 1(b) and the system Σ_Q in Figure 1(a), respectively. We see that the controlled outputs of the discrete-valued input systems with the dynamic quantizers approximate those of the usual systems even if the quantized outputs are applied. Also, the two controlled outputs approximated by both quantizers are exactly the same.

Next, we consider the case $h = 0.1$. In this case, the two controlled outputs approximated by the two quantizers differ. **(Aop)** for Q_d^{op} is infeasible. From **(Sop)**, on the other hand, we obtain $\gamma(h) = 0.949$ and the matrix $C_Q = [-1.1321 \ -3.097]$. Figures 6 and 7 illustrate the simulation results on the time responses of Σ_Q with (B.2) and the proposed quantizer in the same fashion. We see that $z(t)$ of the usual plant P is approximated by $z(t)$ of the system Σ_Q with the proposed quantizer, while $z(t)$ of the system Σ_Q with (B.2) diverges. From this example, we see that the proposed method can address the spatial resolution and the temporal resolution issues, simultaneously. Also, Theorem 10 verifies whether the quantizer Q_d^{op} is applicable to the given switching speed setting.

Remark 13. In the above numerical experiments, the proposed quantizer is designed and the quantizer Q_d^{op} is analyzed for $u = HSF(\sin \pi t + \cos 0.7\pi t)$, while the time responses of the quantizers are simulated for $u = \sin \pi t + \cos 0.7\pi t$. That is, this is the conservativeness caused by the signal assumption (15). However, we see that the above results verify the effectiveness of the proposed method even if the signal conservativeness exists.

Here, we focus on the eigenvalues of $\mathscr{A}$ for the system Σ with Q_d^{op}. The eigenvalues for $f = 50$ and $h = 0.1$ are $\{0.741, 0.819, 0.550, -4.21\}$ and then $\mathscr{A}$ is unstable in the discrete-time domain. From Theorem 10, **(Aop)** is infeasible if $\rho(\mathscr{A})$ is bigger than 1 (in other words, $\mathscr{A}$ is unstable). $\{0.741, 0.819\}$ are the eigenvalues of e^{Ah}. That is, $e^{A_Q h} + \int_0^h e^{A_Q \tau} d\tau B_Q C_Q (=: A_Q(h))$ for Q_d^{op} is unstable. Then, we consider the case in which $f = 3$ and $h = 0.1$ ($\gamma_c = 0.707$) such that $A_Q(h)$ is stable. The corresponding eigenvalues are $\{0.637, 0.354\}$. In this case, $\gamma(h) = 1.085$ for $J_{HS}(Q_d^{op})$ is obtained from **(Aop)**.

From the above results, the existing continuous-quantizer in [15, 16] may be suitable for a two-step design such that $A_Q(h)$ is stable via the parameter f. In terms of the upper

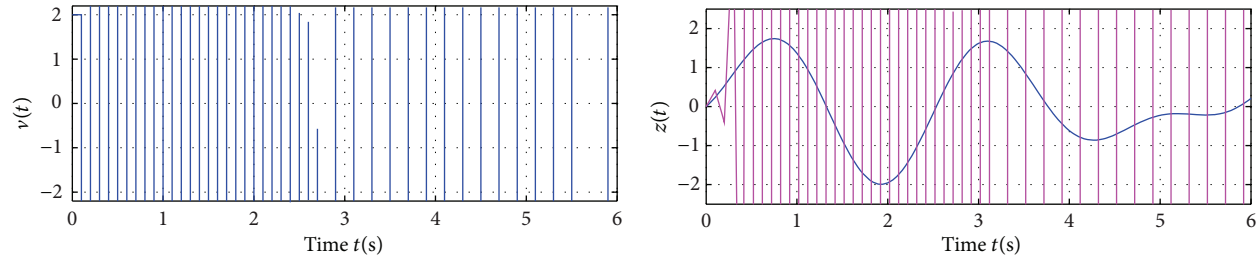

(a) (b)

FIGURE 6: Time responses of Σ_Q with (B.2) for $h = 0.1$.

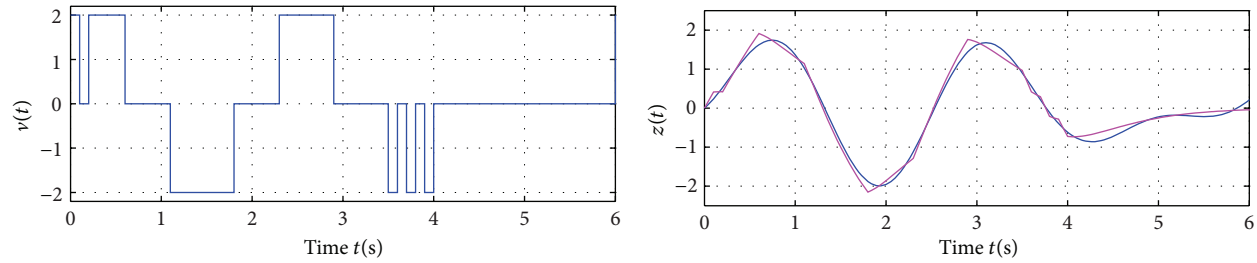

(a) (b)

FIGURE 7: Time responses of Σ_Q with the proposed quantizer for $h = 0.1$.

bound of cost function (B.3), first, let us consider the problem **(P-1)**: maximize f for Q_d^{op} such that

$$\exists X^T = X > 0 \quad \text{s.t. } A_Q(h)^T X A_Q(h) - X < 0, \tag{46}$$

where the parameters (A_Q, B_Q, C_Q) of $A_Q(h)$ are given by (B.2). This problem is LMI for the line search of f. For $h = 0.1$, its solution is $f = 18.9$ ($\gamma_c = 0.173$). However, $\gamma(h) = 113.148$ for $J_{HS}(Q_d^{op})$ is obtained from **(Aop)**. By using Theorem 10, next, let us consider the problem **(P-2)**:

$$\min_{\mathbb{Q}=\mathbb{Q}^T>0, S=s_\theta I_n>0, 1/2h-(\rho(\mathscr{A})^2)/2h\geq\alpha_h\geq 0, f>0, \gamma>0} \gamma^2 \quad \text{s.t. (31) and (32)}, \tag{47}$$

where the parameters (A_Q, B_Q, C_Q) of Ψ_h and Γ_h are given by (B.2). This problem is LMI for the plane search of f and α_h. For $h = 0.1$, its solution is $f = 5.715$ ($\gamma_c = 0.397$) and then $\gamma(h) = 0.949$ for $J_{HS}(Q_d^{op})$ is obtained. This performance is about the same as that of the proposed quantizer. Therefore, we see that Theorem 10 is also helpful for the two-step design of the existing continuous-time quantizer [15, 16] even if the tractable optimization method instead of the plane search remains an issue for future work. Such a method correlates the parameter f with the switching speed h, so its insight is expected not only to result in a new two-step design but also to clarify the relationship between the discrete-time and continuous-time dynamic quantizers. Of course, important future topics also include considering the quantized feedback control system with unstable plants and generalizing the exogenous signal for the evaluation of the cost function.

5. Conclusion

Focusing on the broadbandization and the robustness of the networked control systems, this paper has dealt with the continuous-time quantized control. We have proposed numerical optimization methods analyzing and synthesizing the continuous-time dynamic quantizer on the basis of the invariant set analysis and the sampled-data control technique. The contributions of the proposed method can be summarized as follows.

(i) Both the temporal and spatial resolution constraints can be simultaneously considered, whereas Ishikawa et al. [20] considered the two constraints step-by-step and we [15, 16] previously ignored the temporal constraint in synthesis. As a result, the proposed method is applicable to both the slow and fast switching cases.

(ii) The maximum output difference for each sampling interval is proven to be evaluated numerically via the matrix uncertainty approach, while the existing results [11–14] evaluate that only for each sampling instance.

(iii) The analysis and synthesis conditions are given in terms of BMIs. However, the quantizer analysis and synthesis problems are reduced to tractable optimization problems.

(iv) The new insight is presented for the existing continuous-time quantizer design [15, 16].

Also, this paper has clarified the following areas for future work.

(i) Because of the feedforward structure, the plant is restricted to be stable. To address unstable systems, we

need to propose design methods for feedback control systems.

(ii) The sensors and actuators are distributed in the networked control system [31], so it is necessary to design multiple (decentralized) quantizers rather than a centralized quantizer similar to the existing ones [14, 16].

(iii) The class of exogenous signals evaluating the cost function is restricted. To avoid this conservativeness, it is necessary to propose the equivalent discrete-time expression instead of (11) using adjoint operator similar to sampled-data control [25, 32].

(iv) For networked control applications, it is important to consider the time-varying sampling period, time delay, packet loss, and so on similar to [6–10]. For example, the works [6, 8] using the LMI technique address time-varying sampling period and time delay, so it is expected that our method using the LMI technique also extends to such problems.

Appendix

A. Proof

The proof of Lemma 4 is as follows.

Proof. $z(kh+\theta)$ for $k = 0, 1, 2, \ldots, \theta \in [0, h)$ (which is the behavior of $z(t)$ over the kth sampling interval) is given by the discretized system of P:

$$\begin{aligned} x[k+1] &= e^{Ah}x[k] + \int_0^h e^{A(h-\tau)}Bv(kh+\tau)\,\mathrm{d}\tau \\ z(kh+\theta) &= Ce^{A\theta}x[k] + C\int_0^\theta e^{A(\theta-\tau)}Bv(kh+\tau)\,\mathrm{d}\tau, \end{aligned} \tag{A.1}$$

where $x[k] = x(kh)$. $v(t)$ is given by (9) and $v_Q[k]$ is given by the discretized system of Q:

$$\begin{aligned} x_Q[k+1] &= \left(e^{A_Q h} + \int_0^h e^{A_Q\tau}\mathrm{d}\tau B_Q C_Q\right)x_Q[k] + \int_0^h e^{A_Q\tau}\mathrm{d}\tau B_Q e[k] \\ &\quad + \int_0^h e^{A_Q(h-\tau)}B_Q\widetilde{u}(kh+\tau)\,\mathrm{d}\tau, \\ v_Q[k] &= C_Q x_Q[k], \end{aligned} \tag{A.2}$$

where $x_Q[k] = x_Q(kh)$. This is because e_Q is given by

$$e_Q = \widehat{v}_Q + e + \widehat{u} - u, \qquad \widehat{v}_Q = HSv_Q, \qquad \widehat{u} = HSu. \tag{A.3}$$

Then, $z(kh+\theta, x_0, Q_d(u))$ for $k = 0, 1, 2, \ldots, \theta \in [0, h)$ is expressed by the discretized system of Σ_Q:

$$\Sigma_Q^d : \begin{cases} \begin{bmatrix} x[k+1] \\ x_Q[k+1] \end{bmatrix} \\ \quad = \mathscr{A}\begin{bmatrix} x[k] \\ x_Q[k] \end{bmatrix} + \mathscr{B}e[k] \\ \quad + \begin{bmatrix} \int_0^h e^{A(h-\tau)}Bu[k]\,\mathrm{d}\tau \\ \int_0^h e^{A_Q(h-\tau)}B_Q\widetilde{u}(kh+\tau)\,\mathrm{d}\tau \end{bmatrix}. \\ z(kh+\theta) \\ \quad = \mathscr{C}(\theta)\begin{bmatrix} x[k] \\ x_Q[k] \end{bmatrix} + \mathscr{D}(\theta)e[k] \\ \quad + C\int_0^\theta e^{A(h-\tau)}Bu[k]\,\mathrm{d}\tau \end{cases} \tag{A.4}$$

Also, $z^*(kh+\theta, x_0, u)$ for $k = 0, 1, 2, \ldots, \theta \in [0, h)$ without the quantizer is given by

$$P_d^* : \begin{cases} \widehat{x}[k+1] \\ \quad = e^{Ah}\widehat{x}[k] + \int_0^h e^{A(h-\tau)}Bu(kh+\tau)\,\mathrm{d}\tau \\ z^*(kh+\theta) \\ \quad = Ce^{A\theta}\widehat{x}[k] + C\int_0^\theta e^{A(h-\tau)}u(kh+\tau)\,\mathrm{d}\tau, \end{cases} \tag{A.5}$$

where $\widehat{x}(0) = x_0$ and $\widehat{x}[k] = \widehat{x}(kh)$. From Σ_Q^d and P_d^*, we obtain the system Σ in (11). □

For the proof of Theorem 10, we use the S-procedure [23, 28, 29].

Lemma A.1. *For the real matrices L, M, and N of appropriate size, the inequality*

$$L + M\Delta N + N^T\Delta^T M^T \geq 0 \tag{A.6}$$

holds for any matrix Δ such that $\sigma_{\max}(\Delta) \leq \delta$ if and only if there exists a matrix $S = S^T > 0$ such that

$$\begin{bmatrix} L - \delta MSM^T & \sqrt{\delta}N^T \\ \sqrt{\delta}N & S \end{bmatrix} \geq 0, \quad S\Delta = \Delta S. \tag{A.7}$$

Then, the proof of Theorem 10 is as follows.

Proof. We use Lemmas 9 and A.1 with

$$\begin{aligned} L &= \begin{bmatrix} \mathscr{P} & \widehat{\mathscr{C}}^T \\ \widehat{\mathscr{C}} & \gamma^2 I_q \end{bmatrix}, \qquad M = \begin{bmatrix} 0 \\ C \end{bmatrix}, \\ N &= \begin{bmatrix} \widehat{\mathscr{D}} & 0 \end{bmatrix}, \qquad \Delta = \Omega(\theta). \end{aligned} \tag{A.8}$$

In this case, for the inequalities (25), we obtain their sufficient conditions as follows:

$$\gamma_1 \le \gamma \quad \text{s.t.} \begin{cases} \begin{bmatrix} \mathscr{P} & \widehat{\mathscr{C}}^T & \sqrt{\delta(h)}\widehat{\mathscr{D}}^T \\ \widehat{\mathscr{C}} & \gamma^2 I_q - \delta(h) CSC^T & 0 \\ \sqrt{\delta(h)}\widehat{\mathscr{D}} & 0 & S \end{bmatrix} \ge 0, \\ S\Omega(\theta) = \Omega(\theta) S, \qquad \forall \theta \in [0, h) \end{cases}$$

$$\gamma_2 \le \sigma_{\max}(C)\,\delta(h) \quad \text{s.t.} \quad \Omega(\theta)^T C^T C \Omega(\theta) \le \sigma_{\max}(C)^2 \delta(h)^2 I_n, \quad \forall \theta \in [0, h). \tag{A.9}$$

Then, the upper bound of $J_{HS}(Q_d)$ is given by (30). By substituting $\mathscr{A} = I + h\Phi_h$ and $\mathscr{B} = h\Gamma_h$ into (20), we obtain

$$\begin{bmatrix} \mathscr{A}^T \mathscr{P} \mathscr{A} - (1-\alpha)\mathscr{P} & \mathscr{A}^T \mathscr{P} \mathscr{B} \\ \mathscr{B}^T \mathscr{P} \mathscr{A} & \mathscr{B}^T \mathscr{P} \mathscr{B} - \alpha I_m \end{bmatrix}$$

$$= \begin{bmatrix} (I + h\Phi_h)^T \mathscr{P} (I + h\Phi_h) - (1-\alpha)\mathscr{P} & h(I + h\Phi_h)^T \mathscr{P} \Gamma_h \\ h\Gamma_h^T \mathscr{P} (I + h\Phi_h) & h^2 \Gamma_h^T \mathscr{P} \Gamma_h - \alpha I_m \end{bmatrix}$$

$$= h \begin{bmatrix} \Phi_h^T \mathscr{P} + \mathscr{P}\Phi_h + \alpha/h\mathscr{P} & \mathscr{P}\Gamma_h \\ \Gamma_h^T \mathscr{P} & -\alpha/h I_m \end{bmatrix} + h \begin{bmatrix} \sqrt{h}\Phi_h^T \\ \sqrt{h}\Gamma_h^T \end{bmatrix} \mathscr{P} \begin{bmatrix} \sqrt{h}\Phi_h & \sqrt{h}\Gamma_h \end{bmatrix} \le 0. \tag{A.10}$$

By Schur complement [29], (A.10) is equivalent to (31) where $\mathscr{Q} = \mathscr{P}^{-1}$ and $\alpha_h = \alpha/2h$. Also, (A.9) is equivalent to (32) where $\mathscr{Q} = \mathscr{P}^{-1}$. □

B. Continuous-Time Dynamic Quantizer [15, 16]

For the system $\widehat{\Sigma}$ in (34) without the operator HS, we consider the following non-convex optimization (**OP′**):

$$\min_{\mathscr{P}>0, \mu(\widehat{\mathscr{A}}) \ge \alpha \ge 0, A_Q, B_Q, C_Q, \gamma_c > 0} \gamma_c$$

$$\text{s.t.} \quad \begin{bmatrix} \widehat{\mathscr{A}}^T \mathscr{P} + \mathscr{P}\widehat{\mathscr{A}} + 2\alpha\mathscr{P} & \mathscr{P}\widehat{\mathscr{B}} \\ \widehat{\mathscr{B}}^T \mathscr{P} & -2\alpha I_m \end{bmatrix} \le 0, \quad \begin{bmatrix} \mathscr{P} & \widehat{\mathscr{C}}^T \\ \widehat{\mathscr{C}} & \gamma_c^2 I_q \end{bmatrix} \ge 0. \tag{B.1}$$

The dynamic quantizer without the operator HS is obtained from (**OP′**) and $J(Q_d) \le \gamma_c$ is achieved. Also, an optimal form of the continuous-time quantizer [15, 16] is given by

$$Q_d^{op} : \begin{cases} \dot{x}_Q = Ax_Q + B(v - u) \\ v = q\left(-(CB)^{-1} C(A + fI) x_Q + u\right), \end{cases} \tag{B.2}$$

where its achievable upperbound of $J(Q_d^{op})$ is characterized by

$$\inf \gamma_c = \frac{d\sqrt{m}}{4\sqrt{|g|(f - |g|)}} \sigma_{\max}(CB), \qquad g = \max\left\{\nu(A), \nu\left(A - B(CB)^{-1} C(A + fI)\right)\right\}, \tag{B.3}$$

where $\nu(A) := \max\{\mathrm{Re}(\lambda) : \lambda \in \mathrm{eig}(A)\}$. The continuous-time quantizer Q_d^{op} and its performance are parameterized by the free parameter $f \in \mathbb{R}_+$. Note that the larger values of f not only provide the better approximation performance, but also switch the outputs v, more quickly. In other words, the quantizer from (**OP′**) results in the switching that is too fast and is sometimes not applicable to the slow switching case.

Acknowledgments

The authors would like to thank the reviewers for their valuable comments. This work was partly supported by Grant-in-Aid for Young Scientists (B) no. 24760332 from the Ministry of Education, Culture, Sports, Science and Technology of Japan.

References

[1] W. S. Wong and R. W. Brockett, "Systems with finite communication bandwidth constraints. II: stabilization with limited information feedback," *IEEE Transactions on Automatic Control*, vol. 44, no. 5, pp. 1049–1053, 1999.

[2] N. Elia and S. K. Mitter, "Stabilization of linear systems with limited information," *IEEE Transactions on Automatic Control*, vol. 46, no. 9, pp. 1384–1400, 2001.

[3] M. Fu and L. Xie, "The sector bound approach to quantized feedback control," *IEEE Transactions on Automatic Control*, vol. 50, no. 11, pp. 1698–1711, 2005.

[4] J. Baillieul, "Special issue on networked control systems," *IEEE Transactions on Automatic Control*, vol. 49, no. 9, pp. 1421–1423, 2004.

[5] P. Antsaklis and J. Baillieul, "Special issue on technology of networked control systems," *Proceedings of the IEEE*, vol. 95, no. 1, pp. 5–8, 2007.

[6] D. Yue, E. Tian, Z. Wang, and J. Lam, "Stabilization of systems with probabilistic interval input delays and its applications to networked control systems," *IEEE Transactions on Systems, Man, and Cybernetics A*, vol. 39, no. 4, pp. 939–945, 2009.

[7] W. P. M. H. Heemels, A. R. Teel, N. van de Wouw, and D. Nešić, "Networked control systems with communication constraints: tradeoffs between transmission intervals, delays and performance," *IEEE Transactions on Automatic Control*, vol. 55, no. 8, pp. 1781–1796, 2010.

[8] B. Shen, Z. Wang, and X. Liu, "Sampled-data synchronization control of complex dynamical networks with stochastic sampling," *IEEE Transactions on Automatic Control*, vol. 57, no. 10, pp. 2644–2650, 2012.

[9] W. P. M. H. Heemels, M. C. F. Donkers, and A. R. Teel, "Periodic event-triggered control for linear systems," *IEEE Transactions on Automatic Control*, vol. 58, no. 4, pp. 847–861, 2013.

[10] K. Okano and H. Ishii, "Networked control of uncertain systems over data rate limited and lossy channels," *IEICE Transactions on Fundamentals of Electronics, Communications and Computer Sciences*, vol. E96-A, no. 5, pp. 853–860, 2013.

[11] S. Azuma and T. Sugie, "Optimal dynamic quantizers for discrete-valued input control," *Automatica*, vol. 44, no. 2, pp. 396–406, 2008.

[12] S. Azuma and T. Sugie, "Synthesis of optimal dynamic quantizers for discrete-valued input control," *IEEE Transactions on Automatic Control*, vol. 53, no. 9, pp. 2064–2075, 2008.

[13] K. Sawada and S. Shin, "Synthesis of dynamic quantizers for quantized feedback systems within invariant set analysis framework," in *Proceedings of the American Control Conference (ACC '11)*, pp. 1662–1667, July 2011.

[14] Y. Minami, S. Azuma, and T. Sugie, "Optimal decentralized sigma-delta modulators for quantized feedback control," *IEICE Nonlinear Theory and Its Applications*, vol. 3, no. 3, pp. 386–404, 2012.

[15] K. Sawada and S. Shin, "Synthesis of continuous-time dynamic quantizer for quantized feedback systems," in *Proceedings of the 4th IFAC Conference on Analysis and Design of Hybrid Systems (ADHS '12)*, pp. 2488–2493, 2012.

[16] K. Sawada and S. Shin, "On numerical optimization design of continuous-time feedback type quantizer for networked control systems," in *Proceedings of the 8th IEEE International Conference on Automation Science and Engineering (CASE '12)*, pp. 1140–1145, 2012.

[17] K. Reddy and S. Pavan, "Fundamental limitations of continuous-time delta-sigma modulators due to clock jitter," *IEEE Transactions on Circuits and Systems I*, vol. 54, no. 10, pp. 2184–2194, 2007.

[18] K. Matsukawa, Y. Mitani, M. Takayama, K. Obata, S. Dosho, and A. Matsuzawa, "A fifth-order continuous-time delta-sigma modulator with single-opamp resonator," *IEEE Journal of Solid-State Circuits*, vol. 45, no. 4, pp. 697–706, 2010.

[19] M. Koike and Y. Chida, "Vibration control design considering quantization error for an on-off control system including input time-delay," in *Proceedings of the 50th Annual Conference on Society of Instrument and Control Engineers (SICE '11)*, pp. 760–765, September 2011.

[20] M. Ishikawa, I. Maruta, and T. Sugie, "Practical controller design for discrete-valued input systems using feedback modulators," in *Proceedings of the European Control Conference (ECC '07)*, Kos, Greece, July 2007.

[21] R. Sanchez-Peña and M. Sznaier, *Robust Systems Theory and Applications*, John Wiley & Sons, 1998.

[22] H. Shingin and Y. Ohta, "Optimal invariant sets for discrete-time systems: approximation of reachable sets for bounded inputs," in *Proceedings of the 10th IFAC/IFORS/IMACS/IFIP Symposium on Large Scale Systems, Theory and Applications (LSS '04)*, pp. 401–406, 2004.

[23] Y. Oishi and H. Fujioka, "Stability analysis of aperiodic sampled-data control systems: an improved approach using matrix uncertainty," in *Proceedings of the 19th International Symposium on Mathematical Theory of Networks and Systems (MTNS '10)*, pp. 1147–1152, July 2010.

[24] Y. Oishi and H. Fujioka, "Stability and stabilization of aperiodic sampled-data control systems using robust linear matrix inequalities," *Automatica*, vol. 46, no. 8, pp. 1327–1333, 2010.

[25] T. Chen and B. Francis, *Optimal Sampled-Data Control Systems*, Springer, 1995.

[26] G. H. Golub and C. F. van Loan, *Matrix Computations*, Johns Hopkins Studies in Mathematical Sciences, Johns Hopkins University Press, 3rd edition, 1996.

[27] H. Fujioka, "Command shaping for sampled-data servo systems with constraints," *Transactions of the Institute of Systems, Control and Information Engineers*, vol. 19, no. 7, pp. 284–289, 2006 (Japanese).

[28] M. Fu and N. E. Barabanov, "Improved upper bounds for the mixed structured singular value," *IEEE Transactions on Automatic Control*, vol. 42, no. 10, pp. 1447–1452, 1997.

[29] S. Boyd, L. E. Ghaoui, E. Feron, and V. Balakrishnan, *Linear Matrix Inequalities in System and Control Theory*, vol. 15 of *Studies in Applied Mathematics*, SIAM, 1994.

[30] I. Masubuchi, A. Ohara, and N. Suda, "LMI-based controller synthesis: a unified formulation and solution," *International Journal of Robust and Nonlinear Control*, vol. 8, no. 8, pp. 669–686, 1998.

[31] J. A. Stankovic, "When sensor and actuator networks cover the world," *ETRI Journal*, vol. 30, no. 5, pp. 627–633, 2008.

[32] Y. Hayakawa, S. Hara, and Y. Yamamoto, "H_∞ type problem for sampled-data control systems—a solution via minimum energy characterization," *IEEE Transactions on Automatic Control*, vol. 39, no. 11, pp. 2278–2284, 1994.

Hindawi Publishing Corporation
Mathematical Problems in Engineering
Volume 2013, Article ID 302563, 7 pages
http://dx.doi.org/10.1155/2013/302563

Research Article

Analysis of the Degradation of MOSFETs in Switching Mode Power Supply by Characterizing Source Oscillator Signals

Xueyan Zheng,[1,2] Lifeng Wu,[1,2] Yong Guan,[1,2] and Xiaojuan Li[1,2]

[1] *College of Information Engineering, Capital Normal University, Beijing 100048, China*
[2] *Beijing Engineering Research Center of High Reliable Embedded System, Capital Normal University, Beijing 100048, China*

Correspondence should be addressed to Lifeng Wu; wooleef@gmail.com

Received 5 August 2013; Revised 12 September 2013; Accepted 27 September 2013

Academic Editor: Xiao He

Switching Mode Power Supply (SMPS) has been widely applied in aeronautics, nuclear power, high-speed railways, and other areas related to national strategy and security. The degradation of MOSFET occupies a dominant position in the key factors affecting the reliability of SMPS. MOSFETs are used as low-voltage switches to regulate the DC voltage in SMPS. The studies have shown that die-attach degradation leads to an increase in on-state resistance due to its dependence on junction temperature. On-state resistance is the key indicator of the health of MOSFETs. In this paper, an online real-time method is presented for predicting the degradation of MOSFETs. First, the relationship between an oscillator signal of source and on-state resistance is introduced. Because oscillator signals change when they age, a feature is proposed to capture these changes and use them as indicators of the state of health of MOSFETs. A platform for testing characterizations is then established to monitor oscillator signals of source. Changes in oscillator signal measurement were observed with aged on-state resistance as a result of die-attach degradation. The experimental results demonstrate that the method is efficient. This study will enable a method to predict the failure of MOSFETs to be developed.

1. Introduction

With the rapid development of power electronic technology, SMPS has come to play an important role in electronic equipment. Since the 1970s, SMPSs have been widely used in aeronautics, nuclear power, high-speed railways, and other areas related to national strategy and security.

The failure of SMPS will lead to downtime in electronic systems and cause catastrophic accidents. A recent statistic indicates that approximately 34% of electronic system failures result from the failure of SMPS [1]. Therefore, predicting the impending failure of SMPS is a challenging problem.

The increasing dependence on SMPS, particularly in mission-critical applications, has created an urgent need for real-time techniques that detect incipient faults. According to statistics on the failure of devices relating to two topological structures of DC/DC power supply, the component most prone to failure in switch-mode drives is the controllable power semiconductor (i.e., IGBT and MOSFETs) [2]. In this paper, the focus is on power semiconductors, MOSFETs. Previous work on MOSFETs has focused primarily on three aspects. The first is the reliability design of these components [3]. The second is on predicting the remaining useful life of MOSFETs using off-line accelerated aging tests [4]. An accelerated aging system for the prognostics of discrete power semiconductor devices was built in [5]. Based on accelerated aging with an electrical overstress on MOSFETs, predictions by gate-source voltage are made in [6]. In [7], collector-emitter voltage is identified as a health indicator. In [8], the maximum peak current of the collector-emitter ringing at the turn-off transient is identified as the degradation variable. The third aspect of focus is on the development of degradation models. Degradation models are set up according to the function of the usage time based on accelerated life tests [9]. For example, gate structure degradation modeling of discrete power MOSFETs under ion impurities was presented in [10]. In brief, traditional studies on the degradation of MOSFETs have focused on analyzing nonreal-time data. Predictions of the remaining useful life of MOSFETs have been based on off-line, statistical analyses.

In this paper, the focus is on the detection of incipient faults and on analyzing aging. The primary goal is to realize on-line fault prediction and evaluate the remaining useful life of MOSFETs. The approach that is followed is to use the pulse-width modulation (PWM) signals. PWM is a succession of step functions. The natural characteristic response (oscillator signal) of the source is the output signal. By analyzing the source signal, the paper establishes key parameters of failure related to the natural characteristic response. The key parameters of failure then become the main indicators of the component's state of health. Compared with other methods, the approach has the following several advantages. First, the primary advantage is that there is no need to bring in additional signals. Second, not only can real-time measurements of input and output voltage be realized, but data can also be synchronously processed. Timely judgments and predictions can be made about the state of MOSFETs. Finally, the method is an integration of signal processing with an analytical model. As far as the degradation of MOSFETs is concerned, this is a new perspective. This introductory section is followed by Section 2, which begins by addressing the basic failure mechanism. A nonidealized model of MOSFETs is then introduced. In Section 3, the generation mechanism of oscillator signal and the relationship with key parameters of failure are discussed. In Section 4, the experimental framework is established and the testing procedure is described. In Section 5, the results of the study are summarized and future work is discussed.

2. The Failure Mechanism and a Nonidealized Model of MOSFETs

MOSFETs were first developed in the 1970s. They soon replaced power bipolar junction transistors (BJTs). Unlike BJTs, which are current controlled, MOSFETs are voltage controlled and hence require a simple gate driver circuit. Due to the high current-density capability, low switching loss, and high input impedance of MOSFETs, they are the key components in power conversions. MOSFETs play an especially important role in high-frequency power conversions.

In SMPS, MOSFETs are mainly used for switching. When the MOSFETs are in the on-state, they exhibit resistance between the drain and source terminals. As shown in Figure 1, this resistance is called R_{on}, after the drain-to-source resistance in the on-state. R_{on} is the sum of many elementary contributions [11].

R_s is the source resistance. It represents resistances between the source terminals of the package to the channel of the MOSFETs. R_{ch} is the channel resistance. For a given die size, it is inversely proportional to the channel width and to the channel density. For low-voltage MOSFETs, the channel resistance is one of the main contributors to the R_{on}. A great deal of work has been carried out to reduce the cell size of low-voltage MOSFETs in order to increase the channel density. R_a is the access resistance. It represents the resistance of the epitaxial zone directly under the gate electrode, where the direction of the current changes from horizontal (in the channel) to vertical (to the drain contact). R_j is the detrimental effect of the reduction in cell size mentioned above. The P implantations form the gates of a parasitic transistor that tend to reduce the width of the current flow. R_n is the resistance of the epitaxial layer. As the role of this layer is to sustain the blocking voltage, R_n is directly related to the voltage rating of the device. A high-voltage MOSFET requires a thick, low-doped layer (i.e., highly resistive), whereas a low-voltage transistor only requires a thin layer with a higher doping level (i.e., less resistive). As a result, R_n is the main factor responsible for the resistance of high-voltage MOSFETs. R_d is the equivalent of R_s for the drain. It represents the resistance of the transistor substrate and of the package connections.

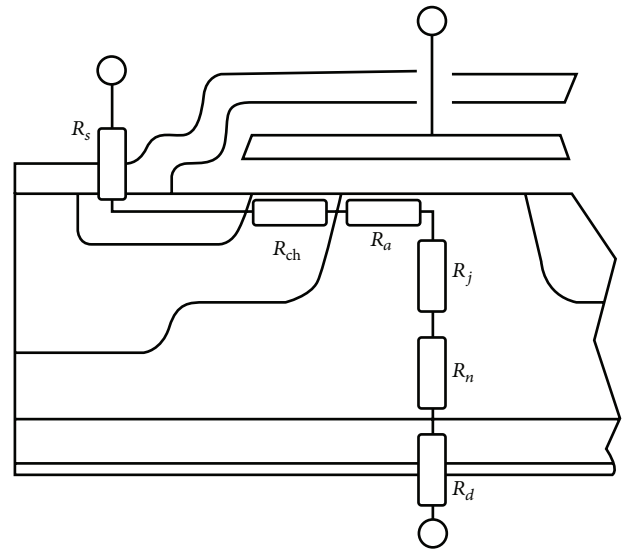

Figure 1: Contribution of the different parts of the MOSFET to the on-state resistance.

In the various aging mechanisms, thermal stress and electrical overstresses are the most common suspects. Both of these mechanisms cause the on-state resistance R_{on} to increase. In the case of thermal stress, the total on-state resistance increases as a result of a reduction in the mobility (μ) of the charge carriers [12]. This mobility reduction is attributed to an increase in the scattering of charge carriers with temperature. The decrease in mobility with temperature is based on the material properties and doping levels of the semiconductor. These changes cause the switch characteristics to change and lead to premature failure. R_{on} is the key indicator of the degradation and state of health of MOSFETs [13]. When MOSFETs degrade, on-state resistance will increase.

The equivalent circuit model of MOSFETs is shown in Figure 2 [14]. In the MOSFETs datasheets, when drain and source terminals are shorted, the input capacitances are often named C_{iss}. The output capacitances are named C_{oss} (gate and source shorted), and the reverse transfer capacitances are named C_{rss} (gate and source shorted). The relationship

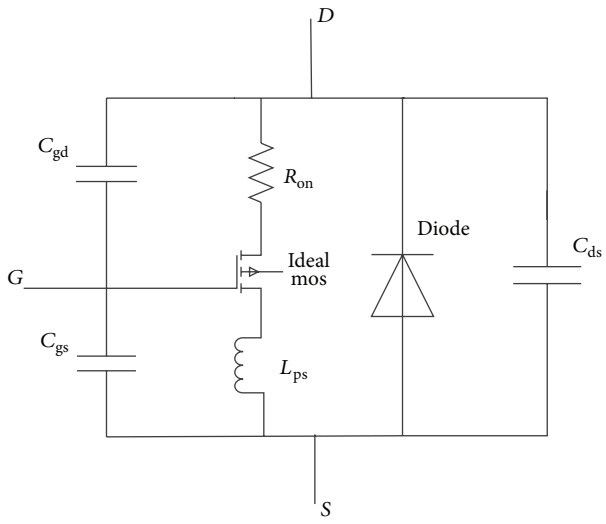

Figure 2: Equivalent circuit model of MOSFETs.

between these capacitances and those described is as follows [15]:

$$\begin{aligned} C_{iss} &= C_{gs} + C_{gd}, \\ C_{oss} &= C_{gd} + C_{ds}, \\ C_{rss} &= C_{gd}. \end{aligned} \tag{1}$$

C_{gs}, C_{gd}, and C_{ds} are the gate-to-source, gate-to-drain, and drain-to-source capacitances, respectively [16]. R_{on} is the on-state resistance. Considering the effect of the distribution parameters, L_{ps} is the source parasitic inductance. Diode is the body diode.

3. Analysis of the Characterization of the Source Oscillator Signal

When MOSFETs turn on, the step inputs drive the gate. The high level of the step signal is set as E. When MOSFETs are suddenly subjected to step inputs, the parasitic capacitance C_{gs} starts charging. The charging voltage E produces a relatively high dv/dt. The value of dv/dt is related to the switching speed. The relationship between these two quantities can be expressed approximately as

$$\frac{dv}{dt} = \frac{E}{t_{on}}. \tag{2}$$

E and t_{on} are the corresponding voltage and conduction time, respectively. Thus, the source displacement current introduced by dv/dt can be expressed as:

$$i_s = C_{gs}\frac{dv}{dt} = C_{gs}\frac{E}{t_{on}}. \tag{3}$$

Between drain and source, due to parasitic capacitance C_{ds}, on-state resistance R_{on}, and distribution inductance L_{ps}, the source will produce an oscillator signal. The source voltage can be expressed as

$$\begin{aligned} V_{ds}(s) &= i_s \cdot Z(s) \\ &= \frac{E}{t_{on}} \cdot \frac{C_{gs}}{C_{ds}} \cdot \frac{S + \left(R_{on}/L_{ps}\right)}{S^2 + \left(R_{on}/L_{ps}\right)S + \left(1/L_{ps}C_{ds}\right)}. \end{aligned} \tag{4}$$

The characteristic equation (4) is a second-order system. $Z(s)$ is the system transfer function in the frequency domain. When the discriminator is less than zero, the Laplace inverse transform can be expressed as

$$u_{ds}(t) = \frac{E}{t_{on}} \cdot \frac{C_{gs}}{C_{ds}} \cdot \left(\sqrt{1 - C_{ds}\frac{R_{on}^2}{4L_{ps}}}\right)^{-1} \cdot e^{-\alpha t}\sin(wt + \theta), \tag{5}$$

where

$$\alpha = \frac{R_{on}}{2L_{ps}}, \quad w = \sqrt{\frac{1}{L_{ps}C_{ds}} - \frac{R_{on}^2}{4 * L_{ps}^2}}, \quad \theta = \arctan\left(\frac{w}{\alpha}\right). \tag{6}$$

Equation (5) represents the damping oscillation curve. The envelope of damping oscillation can be expressed as

$$y = \frac{E}{t_{on}} \cdot \frac{C_{gs}}{C_{ds}} \cdot e^{-\alpha t}. \tag{7}$$

The damping coefficient is shown below in (8) as follows:

$$\alpha = \frac{R_{on}}{2L_{ps}}. \tag{8}$$

The oscillation frequency can be expressed as

$$\omega = \sqrt{\frac{1}{L_{ps}C_{ds}} - \frac{R_{on}^2}{4 * L_{ps}^2}}. \tag{9}$$

Because $R_{on}^2/(4 * L_{ps}^2)$ is far less than $1/L_{ps}C_{ds}$, the oscillation frequency can be expressed as

$$\omega = \sqrt{\frac{1}{L_{ps}C_{ds}}}. \tag{10}$$

According to (8) and (10), R_{on} can be expressed as

$$R_{on} = 2 \cdot \frac{\alpha}{\omega^2 C_{ds}}. \tag{11}$$

When MOSFETs begin degrading, R_{on} will increase. The oscillation envelope of damping oscillation will change. Thus, by the real-time monitoring of the source damping oscillation signal, we can obtain the trend in the variation of the key parameter R_{on}. From the change in R_{on}, the paper can estimate the state of health of MOSFETs. By means of the above, the prognostics and health management of SMPS are realized.

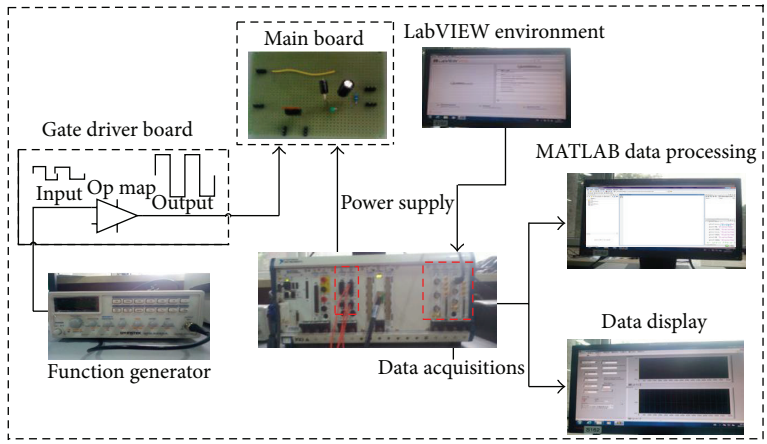

Figure 3: Experimental setup.

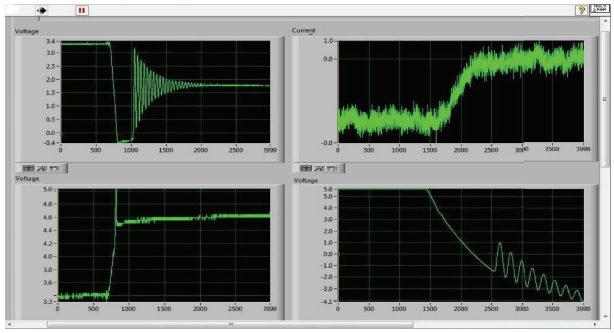

Figure 4: The display of data.

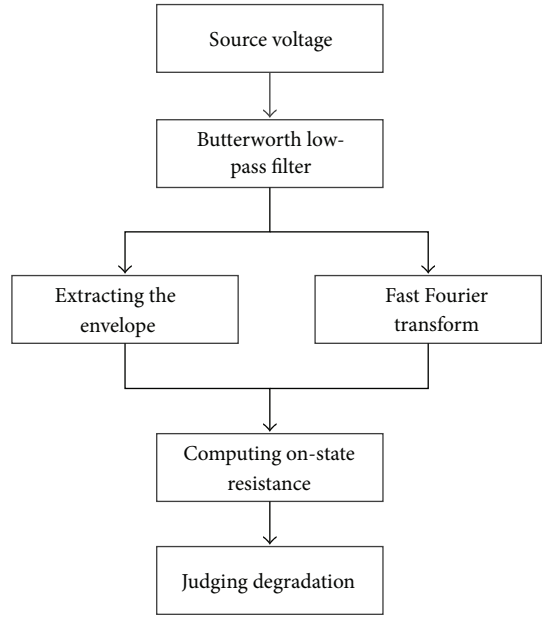

Figure 5: The flow chart for the processing of data.

4. Physics Experiments and the Results of the Data Analysis

4.1. Signal Acquisition Experiments. To monitor the oscillation signal and compute the degradation parameter R_{on}, an aging experimental platform is established. The physics experiments are performed in specialized laboratories. The experimental setup mainly consists of a gate drive board, a main board, a PXI device, and a host computer. The PXI device mainly realizes data acquisition on the basis of LabVIEW 2012. The host computer realizes data processing based on MATLAB 7.0. The main board is a Buck circuit. The input voltage is biased at 6 V dc. The gate drive voltage is produced by a function generator. The gate voltage is a square wave signal with an amplitude of 0~10 V, a frequency of 40 K Hz, and a duty cycle of 50%. The amplifier is used to ensure that enough current is available to charge the gate of MOSFETs.

The main board houses the terminal block for the MOSFETs device and the BNC output ports connected to the terminal block. The source-ground voltage (Vs), gate-ground voltage (Vg), drain-ground voltage (Vd), and drain-source current (Ids) are monitored in situ by the LabVIEW that controls the PXI data acquisition card. In order to ensure synchronous data acquisition, display, and processing, the system applies the producer/consumer mode in LabVIEW. In the circulation of producers, the experimental setup realizes the function of data acquisition and display. In the circulation of consumers, it realizes the function of data storage. Thermal stress is used in the study to cause device damage by applying a controlled temperature. The experimental setup used for the acquisition of signals is shown in Figure 3. The data display is shown in Figure 4.

4.2. Signal Processing Experiments and Degradation Analysis. The effects of the oscillator signal resulting from degraded MOSFETs are evaluated by preprocessing the data. As the MOSFETs age, R_{on} will increase. An appreciable increase in the damping coefficient α is observed. Figure 5 gives the flow chart for the processing of the data. First, the data is filtered using a first-order Butterworth low-pass filter. Second, the envelope of the oscillator signal is extracted.

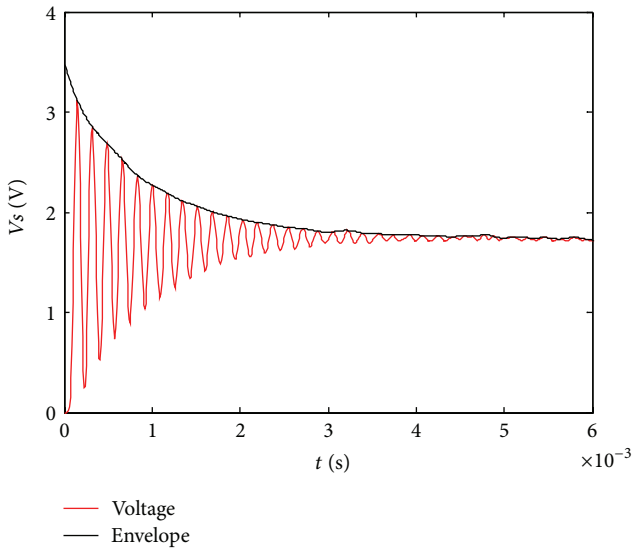

Figure 6: The oscillator signal of the source and the envelope in a normal state.

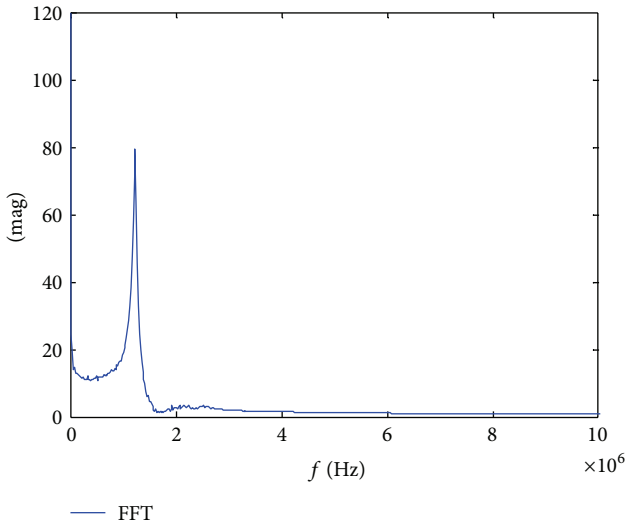

Figure 7: The result of the FFT.

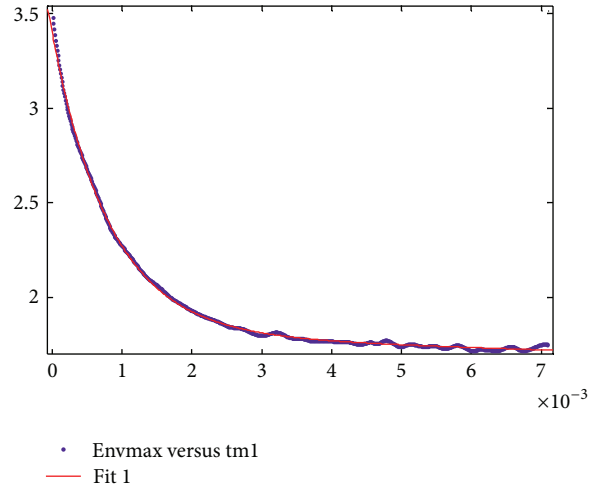

Figure 8: The fitting result.

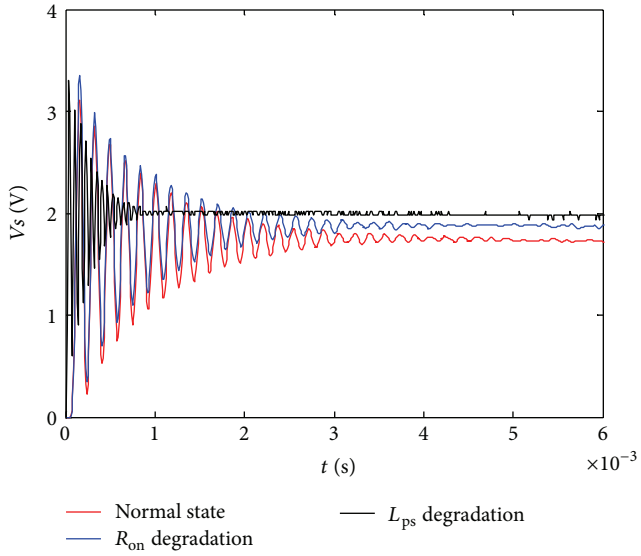

Figure 9: The oscillator signal of source in different states.

Then, the exponential damping of the "cftool toolbox" is used to conduct curve-fitting. Finally, according to (11), the value of on-state resistance is acquired.

After several rounds of processing, an oscillator signal of the source from MOSFETs in normal working condition is acquired. The oscillator signal and envelope are shown in Figure 6. The result of the FFT is shown in Figure 7. The fitting result is shown in Figure 8.

The fitting expression and goodness of fit when MOSFETs are in different states are shown in Table 1. The general model is an exponential model. It is shown in (12) that b, c, and d are coefficients and α is the damping coefficient. The evaluation standard for curve-fitting consists of SSE, R-square, adjusted R-square, and RMSE. SSE represents the sum of squares due to error. R-square is the coefficient of determination. Adjusted R-square represents the degree-of-freedom of the adjusted coefficient of determination. RMSE is the root-mean-square error.

Consider

$$F(x) = b * \exp(-\alpha * x) + c * \exp(d * x). \quad (12)$$

With regard to the failure modes, the potential causes of failure involve high electric fields and high temperatures. In this study, MOSFETs are subjected to thermal overstress to degrade the parts. As the temperature increases, the oscillator signal and envelope will change. Because parasitic capacitance C_{ds} is not prone to damage, when the oscillation frequency remains the same, this means that the change in the envelope is mainly caused by R_{on}. In Figure 9, the red and blue curves, respectively, indicate the oscillation signal in different R_{on} degradation states. The black curve indicates the degradation of distribution inductance L_{ps}. When MOSFETs

Table 1: The results of fitting and goodness of fit.

General model	Goodness of fit			
$F(x) = b * \exp(-\alpha * x) + c * \exp(d * x)$	SSE	R-square	Adjusted R-square	RMSE
$F(x) = 1.408 * \exp(-1321x) + 1.939 * \exp(-6.227x)$	0.1662	0.9973	0.9973	0.01689
$F(x) = 1.423 * \exp(-1408x) + 1.949 * \exp(-6.536x)$	0.1496	0.9975	0.9975	0.01602
$F(x) = 1.493 * \exp(-1493x) + 1.925 * \exp(-11.35x)$	0.1056	0.9984	0.9984	0.01346
$F(x) = 1.604 * \exp(-1604x) + 1.877 * \exp(-1.944x)$	0.0846	0.9986	0.9986	0.01212
$F(x) = 1.350 * \exp(-1832x) + 1.833 * \exp(-4.550x)$	0.0979	0.9977	0.9977	0.01304
$F(x) = 1.368 * \exp(-1990x) + 1.799 * \exp(-0.300x)$	0.1853	0.9953	0.9952	0.01793

Table 2: The results of states of health.

α	ω (Hz)	Experiment R_{on} (mΩ)	Datasheet R_{on} (mΩ)	Error (%)	Health
1321	1.23 * 106	43.66	44	−0.77	Normal
1408	1.23 * 106	46.43	44	5.52	Normal
1493	1.23 * 106	48.35	44	9.89	Degradation
1604	1.23 * 106	58.56	44	33.09	Degradation
1832	1.23 * 106	60.64	44	37.82	Degradation
1990	1.23 * 106	65.77	44	49.48	Degradation

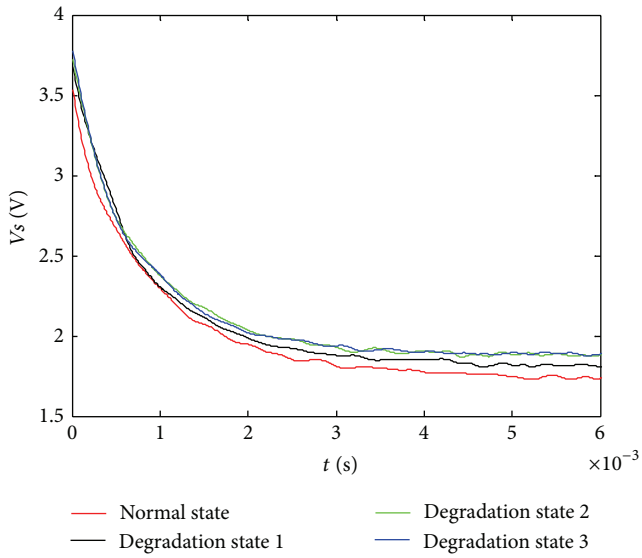

Figure 10: The fitting results in different states.

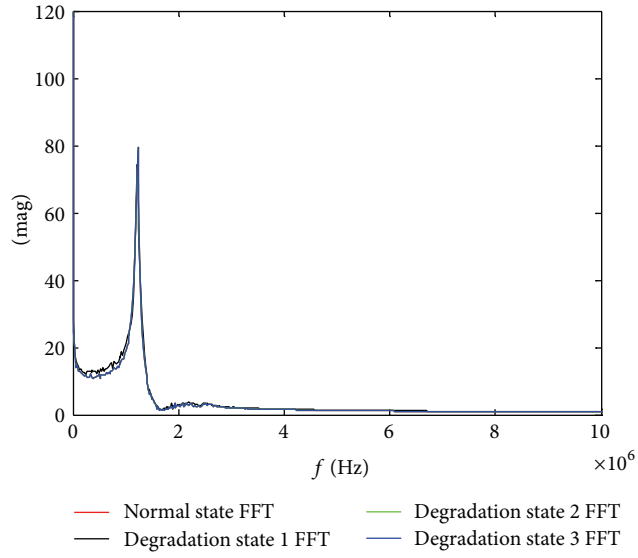

Figure 11: The FFT results in different states.

are different degradation states, the envelope of the oscillator signal and the result of the FFT are, respectively, shown in Figures 10 and 11.

Based on the results of curve-fitting, we obtain different $F(x)$s. When and C_{ds} are obtained, according to (11), the value of R_{on} can be determined. The results are shown in Table 2, with the value of the datasheet given for comparison.

As MOSFETs age, R_{on} will increase. An increasing R_{on} means that the rate of oscillatory decay will increase. This means an increase in the damping coefficient α. As seen in Table 2, when the error is defined as being close to 10%, MOSFETs begin to degrade from the state of normal. When the error is greater than or equal to 50%, MOSFETs fail.

In conclusion, through real-time monitoring and processing the oscillator signal of source, we can obtain the variation tendency of on-state resistance R_{on}. Thus, we can predict the state of health of MOSFETs.

5. Conclusions

A nonidealized model and the degradation mechanism of MOSFETs were described in this paper. In the case of thermal stress, the total on-state resistance R_{on} increases as a result of a reduction in the mobility (μ) of the charge carriers. Thus, in this study, on-state resistance was identified as the key indicator of the degradation and state of health of MOSFETs. According to the relationship between the oscillator signal

and R_{on} in turn-off, on-state resistance R_{on} can be calculated in real-time. An experimental platform was established for the purpose of monitoring the oscillation signal and computing the degradation parameter R_{on}. Without additional incentives, a standard signal was used to predict the state of degradation of MOSFETs in a Buck circuit. The bases for, and a method of, predicting the life and managing the health of MOSFETs were given in this study. Future work is still needed to construct a system for automatically predicting and giving early warnings about the life of MOSFETs.

Acknowledgments

This work received financial support from the National Natural Science Foundation of China (nos. 61070049 and 61202027), the National Key Technology R&D Project (no. 2012DFA11340), the Beijing Natural Science Foundation of China (no. 4122015), the Beijing City Board of Education Science and Technology Development Project (no. KM201210028001), and the Ladder Program of the Beijing Key Laboratory of Electronic System Reliability Technology. The authors also thank Professor Jin for his help throughout this study.

References

[1] Y. Guan, S. Jin, L. Wu, W. Pan, Y. Liu, and J. Zhang, "Power supply prognostics and health management of high reliability electronic systems in rugged environment," *Key Engineering Materials*, vol. 474–476, pp. 1195–1200, 2011.

[2] J. M. Anderson, R. W. Cox, and J. Noppakunkajorn, "An on-line fault diagnosis method for power electronic drives," in *Proceedings of the 4th IEEE Electric Ship Technologies Symposium (ESTS '11)*, vol. 10, pp. 492–497, April 2011.

[3] T. Azoui, P. Tounsi, P. Dupuy, L. Guillot, and J. M. Dorkel, "3D Electro-thermal modelling of bonding and metallization ageing effects for reliability improvement of power MOSFETs," *Microelectronics Reliability*, vol. 51, no. 9-11, pp. 1943–1947, 2011.

[4] V. Smet, F. Forest, J.-J. Huselstein et al., "Ageing and failure modes of IGBT modules in high-temperature power cycling," *IEEE Transactions on Industrial Electronics*, vol. 58, no. 10, pp. 4931–4941, 2011.

[5] J. Celaya, P. Wysocki, and K. Goebel, "Accelerated aging system for prognostics of power semiconductor devices," in *IEEE Autotestcon*, vol. 4, pp. 1–6, 2010.

[6] S. Saha, J. Celaya, V. Vashchenko, S. Mahiuddin, and K. Goebel, "Accelerated aging with electrical overstress and prognostics for power MOSFETs," *Energytech*, vol. 47, pp. 1–6, 2011.

[7] N. Patil, J. Celaya, D. Das, K. Goebel, and M. Pecht, "Precursor parameter identification for insulated gate bipolar transistor (IGBT) prognostics," *IEEE Transactions on Reliability*, vol. 58, no. 2, pp. 271–276, 2009.

[8] G. Sonnenfeld, K. Goebel, and J. R. Celaya, "An agile accelerated aging, characterization and scenario simulation system for gate controlled power transistors," in *IEEE Autotestcon*, vol. 6, pp. 208–215, September 2008.

[9] A. Oukaour, B. Tala-Ighil, B. Pouderoux et al., "Ageing defect detection on IGBT power modules by artificial training methods based on pattern recognition," *Microelectronics Reliability*, vol. 51, no. 2, pp. 386–391, 2011.

[10] A. E. Ginart, I. N. Ali, J. R. Celaya, and P. W. Kalgren, "Modeling SiO_2 ion impurities aging in insulated gate power devices under temperature and voltage stress," in *Proceedings of the Annual Conference of the Prognostics and Health Management Society*, vol. 7, pp. 1–6, 2010.

[11] Y. Zhang, R. Zane, A. Prodic, R. Erickson, and D. Maksimovic, "Online calibration of MOSFET on-state resistance for precise current sensing," *IEEE Power Electronics Letters*, vol. 2, no. 3, pp. 100–103, 2004.

[12] J. R. Celaya, A. Saxena, P. Wysocki, S. Saha, and K. Goebel, "Towards prognostics of power MOSFETs: accelerated aging and precursors of failure," in *Proceedings of the Annual Conference of the Prognostics and Health Management Society*, vol. 5, pp. 1102–1108, 2010.

[13] T. Funaki, H. Arioka, and T. Hikihara, "The influence of parasitic components on power mosfet switching operation in power conversion circuits," *IEICE Electronics Express*, vol. 6, no. 23, pp. 1697–1701, 2009.

[14] Y. Xiao, H. Shah, T. P. Chow, and R. J. Gutmann, "Analytical modeling and experimental evaluation of interconnect parasitic inductance on MOSFET switching characteristics," in *Proceedings of the 19th Annual IEEE Applied Power Electronics Conference and Exposition (APEC '04)*, vol. 1, pp. 516–521, February 2004.

[15] Z. John Shen, Y. Xiong, X. Cheng, Y. Fu, and P. Kumar, "Power MOSFET switching loss analysis: a new insight," in *Proceedings of the 41st IAS Annual Meeting on Industry Applications Conference*, vol. 3, pp. 1438–1442, October 2006.

[16] N. Phankong, T. Funaki, and T. Hikihara, "Characterization of the gate-voltage dependency of input capacitance in a SiC MOSFET," *IEICE Electronics Express*, vol. 7, no. 7, pp. 480–486, 2010.

Hindawi Publishing Corporation
Mathematical Problems in Engineering
Volume 2013, Article ID 520503, 11 pages
http://dx.doi.org/10.1155/2013/520503

Research Article

$\mathscr{H}_\infty$ Control for Two-Dimensional Markovian Jump Systems with State-Delays and Defective Mode Information

Yanling Wei,[1] Mao Wang,[1] Hamid Reza Karimi,[2] and Jianbin Qiu[1]

[1] *Research Institute of Intelligent Control and Systems, Harbin Institute of Technology, Harbin 150001, China*
[2] *Department of Engineering, Faculty of Engineering and Science, University of Agder, 4898 Grimstad, Norway*

Correspondence should be addressed to Yanling Wei; yanlingwei@hit.edu.cn

Received 12 July 2013; Revised 13 September 2013; Accepted 16 September 2013

Academic Editor: Bo Shen

This paper investigates the problem of $\mathscr{H}_\infty$ state-feedback control for a class of two-dimensional (2D) discrete-time Markovian jump linear time-delay systems with defective mode information. The mathematical model of the 2D system is established based on the well-known Fornasini-Marchesini local state-space model, and the defective mode information simultaneously consists of the exactly known, partially unknown, and uncertain transition probabilities. By carefully analyzing the features of the transition probability matrices, together with the convexification of uncertain domains, a new $\mathscr{H}_\infty$ performance analysis criterion for the underlying system is firstly derived, and then the $\mathscr{H}_\infty$ state-feedback controller synthesis is developed via a linearisation technique. It is shown that the controller gains can be constructed by solving a set of linear matrix inequalities. Finally, an illustrative example is provided to verify the effectiveness of the proposed design method.

1. Introduction

During the past decades, two-dimensional (2D) systems have drawn considerable attention due to their extensive applications of both theoretical and practical interests in many modern engineering fields, such as process control (thermal processes, gas absorption, water stream heating, etc.) [1], multidimensional digital filtering [2], and image processing (enhancement, deblurring, seismographic data processing, etc.) [3]. In particular, since the well-known Roesser state-space model and the Fornasini-Marchesini local state-space (FMLSS) model were proposed, theory on 2D systems has progressed greatly [4–11].

On the other hand, as a class of stochastic hybrid systems, Markovian jump linear systems (MJLSs) have been extensively investigated [12–26]. The driving force behind this is that MJLSs can model different classes of dynamic systems subject to random abrupt variations in their structures, for example, manufacturing systems, power systems, and networked control systems, where random failure, repairs, and sudden environment changes may occur in Markov chains [27–29]. It is known that MJLSs are described by a set of classical differential (or difference) equations and a Markov stochastic process (or Markov chain) [30]. As a decisive factor, transition probabilities (TPs) in the jumping process determine the system behavior to a large extent and, so, far, many studies on the analysis and synthesis of MJLSs have been carried out in the context of perfect information on TPs [12–15, 25]. In practice, however, defective mode information is often encountered especially when adequate efforts to obtain the accurate TPs are costly or time consuming. Thus, it is more practical and interesting to study more general jump systems with defective mode information. Recently, there have appeared some results on the analysis and synthesis of MJLSs with uncertain TPs or partially unknown TPs [26, 31–38]. To mention a few, the authors in [31] studied the $\mathscr{H}_\infty$ filter synthesis problem for a class of MJLSs with partially unknown TPs; The author in [32] considered the robust stability analysis and stabilization problems for a class of MJLSs with polytopic uncertain TPs; the authors in [36] addressed the robust stability analysis problem for a class of MJLSs with norm-bounded uncertain TPs.

However, the above-mentioned works were only concerned with one-dimensional (1D) systems. Inevitably, when 2D systems are employed to model dynamic systems with random abrupt changes in their structures or parameters

such as chemical process control, the mathematical modeling of such physical systems would be naturally dependent on jumping parameters. For example, information propagation occurs from pass to pass and along a given pass in a gas absorption, water stream heating, and air drying [39]. Therefore, 2D MJLSs emerge as a more reasonable description to account for the parameter jumping phenomenon and have a great potential in engineering applications. Recently, the stability analysis and synthesis of discrete-time delay-free 2D MJLSs described by Roesser model were reported in [39, 40], which are obtained based on the traditional assumption of complete knowledge on TPs. To the authors' best knowledge, the analysis and synthesis for 2D MJLSs with state-delays and defective mode information have not drawn much attention yet, which motivates us for this study.

In this paper, the $\mathscr{H}_\infty$ control problem for a class of 2D discrete-time MJLSs with state-delays and defective mode information will be studied. The mathematical model of the 2D system is established in terms of the FMLSS model subject to state-delays, and the defective mode information simultaneously includes the exactly known, partially unknown and uncertain TPs. By fully considering the properties of the transition probability matrices, together with the convexification of uncertain domains, a new $\mathscr{H}_\infty$ performance analysis criterion for the closed-loop system will be firstly derived. By a linearisation procedure, the corresponding $\mathscr{H}_\infty$ controller synthesis will then be converted into a convex optimization problem in terms of a set of linear matrix inequalities. Finally, an illustrative example will be performed to show the effectiveness of the proposed controller synthesis method.

Notations. The notations used throughout the paper are standard. $\mathbf{R}^n$ and $\mathbf{R}^{m\times n}$ denote, respectively, the n-dimensional Euclidean space and the set of all $m \times n$ real matrices; $\mathbb{N}^+$ represents the sets of positive integers; the notation $P > 0$ means that P is real symmetric and positive definite; $\mathbf{I}$ and $\mathbf{0}$ represent the identity matrix and a zero matrix, respectively; $(\mathscr{S}, \mathscr{F}, \mathscr{P})$ denotes a complete probability space, in which $\mathscr{S}$ is the sample space, $\mathscr{F}$ is the σ algebra of subsets of the sample space, and $\mathscr{P}$ is the probability measure on $\mathscr{F}$; $\mathbb{E}[\cdot]$ stands for the mathematical expectation; $\|\cdot\|$ refers to the Euclidean norm of a vector or its induced norm of a matrix; $l_2\{[0,\infty),[0,\infty)\}$ denotes the space of square summable sequences on $\{[0,\infty),[0,\infty)\}$. Matrices, if not explicitly stated, are assumed to have appropriate dimensions for algebra operations.

2. Problem Formulation and Preliminaries

Fix a complete probability space $(\mathscr{S}, \mathscr{F}, \mathscr{P})$ and consider the following two-dimensional (2D) discrete-time Markovian jump linear systems (MJLSs), described by the Fornasini-Marchesini local state-space (FMLSS) model with time-delays in the states:

$$\begin{aligned}(\Sigma): x(i+1,j+1) &= A_1(r(i,j+1))\,x(i,j+1)\\ &\quad + A_2(r(i+1,j))\,x(i+1,j)\\ &\quad + A_{d1}(r(i,j+1))\,x(i-d_1,j+1)\\ &\quad + A_{d2}(r(i+1,j))\,x(i+1,j-d_2)\\ &\quad + B_1(r(i,j+1))\,u(i,j+1)\\ &\quad + B_2(r(i+1,j))\,u(i+1,j)\\ &\quad + D_1(r(i,j+1))\,w(i,j+1)\\ &\quad + D_2(r(i+1,j))\,w(i+1,j),\\ z(i,j) &= C(r(i,j))\,x(i,j) + B_3(r(i,j))\,u(i,j)\\ &\quad + D_3(r(i,j))\,w(i,j),\end{aligned} \tag{1}$$

where $x(i,j) \in \mathbf{R}^{n_x}$ is the state vector; $u(i,j) \in \mathbf{R}^{n_u}$ is the control input; $z(i,j) \in \mathbf{R}^{n_z}$ is the controlled output; $w(i,j) \in \mathbf{R}^{n_w}$ denotes the disturbance input vector which belongs to $l_2\{[0,\infty),[0,\infty)\}$; and d_1 and d_2 are two constant positive integers representing delays along vertical and horizontal directions, respectively. $A_1(r(i,j+1))$, $A_2(r(i+1,j))$, $A_{d1}(r(i,j+1))$, $A_{d2}(r(i+1,j))$, $B_1(r(i,j+1))$, $B_2(r(i+1,j))$, $D_1(r(i,j+1))$, $D_2(r(i+1,j))$, $C(r(i,j))$, $B_3(r(i,j))$, and $D_3(r(i,j))$ are real-valued system matrices. These matrices are functions of $r(i,j)$, which is described by a discrete-time, discrete-state homogeneous Markov chain with a finite-state space $\mathscr{I} := \{1,\ldots,N\}$, and a stationary transition probability matrix (TPM) $\Pi = [\pi_{mn}]_{N\times N}$, where

$$\begin{aligned}\pi_{mn} &= \Pr(r(i+1,j+1) = n \mid r(i,j+1) = m)\\ &= \Pr(r(i+1,j+1) = n \mid r(i+1,j) = m), \quad \forall m,n \in \mathscr{I},\end{aligned} \tag{2}$$

with $\pi_{mn} \geq 0$ and $\sum_{n=1}^{N}\pi_{mn} = 1$. For $r(i+1,j) = m \in \mathscr{I}$ or $r(i,j+1) = m \in \mathscr{I}$, the system matrices of the mth mode are denoted by $(A_{1m}, A_{2m}, A_{d1m}, A_{d2m}, B_{1m}, B_{2m}, D_{1m}, D_{2m}, C_m, B_{3m}, D_{3m})$, which are known and with appropriate dimensions. Unless otherwise stated, similar simplification is also applied to other matrices in the following.

In this paper, the transition probabilities (TPs) of the jumping process are assumed to be uncertain and partially accessed; that is, the TPM $\Pi = [\pi_{mn}]_{N\times N}$ is assumed to belong to a given polytope P_Π with vertices Π_s, $s = 1,2,\ldots,M$, $\mathrm{P}_\Pi := \{\Pi \mid \Pi = \sum_{s=1}^{M}\alpha_s\Pi_s;\ \alpha_s \geq 0,\ \sum_{s=1}^{M}\alpha_s = 1\}$, where $\Pi_s = [\pi_{mn}]_{N\times N}$, $m,n \in \mathscr{I}$, are given TPMs containing unknown elements still. For instance, for system (Σ) with four operation modes, the TPM may be as

$$\begin{bmatrix}\pi_{11} & \widetilde{\pi}_{12} & \widehat{\pi}_{13} & \pi_{14}\\ \widehat{\pi}_{21} & \pi_{22} & \widetilde{\pi}_{23} & \pi_{24}\\ \pi_{31} & \widehat{\pi}_{32} & \pi_{33} & \widehat{\pi}_{34}\\ \pi_{41} & \widetilde{\pi}_{42} & \widehat{\pi}_{43} & \widehat{\pi}_{44}\end{bmatrix}, \tag{3}$$

where the elements labeled with "$\widehat{\ }$" and "$\sim$" represent the unknown information and polytopic uncertainties on TPs, respectively, and the others are known TPs. For notational

clarity, for all $m \in \mathcal{I}$, we denote $\mathcal{I} = \mathcal{I}_{\mathcal{K}}^{(m)} \cup \mathcal{I}_{\mathcal{UC}}^{(m)} \cup \mathcal{I}_{\mathcal{UK}}^{(m)}$ as follows:

$$\begin{aligned} \mathcal{I}_{\mathcal{K}}^{(m)} &:= \{n : \pi_{mn} \text{ is known}\}, \\ \mathcal{I}_{\mathcal{UC}}^{(m)} &:= \{n : \widetilde{\pi}_{mn} \text{ is uncertain}\}, \\ \mathcal{I}_{\mathcal{UK}}^{(m)} &:= \{n : \widehat{\pi}_{mn} \text{ is unknown}\}. \end{aligned} \tag{4}$$

Moreover, if $\mathcal{I}_{\mathcal{K}}^{(m)} \neq \emptyset$ and $\mathcal{I}_{\mathcal{UC}}^{(m)} \neq \emptyset$, it is further described as

$$\begin{aligned} \mathcal{I}_{\mathcal{K}}^{(m)} &:= \left\{\mathcal{K}_{1_{(m)}}, \ldots, \mathcal{K}_{t_{(m)}}\right\}, \quad \forall 1 \le t_{(m)} \le N-2, \\ \mathcal{I}_{\mathcal{UC}}^{(m)} &:= \left\{\mathcal{U}_{1_{(m)}}, \ldots, \mathcal{U}_{v_{(m)}}\right\}, \quad \forall 1 \le v_{(m)} \le N, \end{aligned} \tag{5}$$

where $\mathcal{K}_{t_{(m)}} \in \mathbb{N}^+$ represents the $t_{(m)}$th known element with the index $\mathcal{K}_{t_{(m)}}$ in the mth row of the TPM and $\mathcal{U}_{v_{(m)}} \in \mathbb{N}^+$ represents the $v_{(m)}$th uncertain element with the index $\mathcal{U}_{v_{(m)}}$ in the mth row of the TPM. Obviously, $1 \le t_{(m)} + v_{(m)} \le N$. Also, we denote

$$\pi_{\mathcal{UK}}^{(ms)} := \sum_{n \in \mathcal{I}_{\mathcal{UK}}^{(m)}} \widehat{\pi}_{mn} = 1 - \sum_{n \in \mathcal{I}_{\mathcal{K}}^{(m)}} \pi_{mn} - \sum_{n \in \mathcal{I}_{\mathcal{UC}}^{(m)}} \widetilde{\pi}_{mn}^{(s)}, \tag{6}$$

where $\widetilde{\pi}_{mn}^{(s)}$ represents an uncertain TP in the sth polytope, for all $s = 1, \ldots, M$.

The boundary conditions of system (Σ) in (1) are defined by

$$\begin{aligned} &\{x(i,j) = \phi(i,j), \ \forall j \ge 0, \ -d_1 \le i \le 0\}, \\ &\{x(i,j) = \varphi(i,j), \ \forall i \ge 0, \ -d_2 \le j \le 0\}, \\ &\phi(0,0) = \varphi(0,0). \end{aligned} \tag{7}$$

Throughout this paper, the following assumption is made.

Assumption 1. The boundary conditions are assumed to satisfy

$$\begin{aligned} &\lim_{T_1 \to \infty} \mathbb{E}\left\{\sum_{j=0}^{T_1} \sum_{i=-d_1}^{0} \left(\phi^{\mathrm{T}}(i,j)\phi(i,j)\right)\right\} \\ &\quad + \lim_{T_2 \to \infty} \mathbb{E}\left\{\sum_{i=0}^{T_2} \sum_{j=-d_2}^{0} \left(\varphi^{\mathrm{T}}(i,j)\varphi(i,j)\right)\right\} < \infty. \end{aligned} \tag{8}$$

In this paper, we are interested in the $\mathscr{H}_\infty$ controller synthesis for MJLSs (1). The following mode-dependent state-feedback control law is used:

$$u(i,j) = K(r(i,j))\, x(i,j), \tag{9}$$

where $K(r(i,j)) \in \mathbf{R}^{n_u \times n_x}$.

Then the corresponding closed-loop system can be represented as follows:

$$\begin{aligned} \left(\overline{\Sigma}\right) : x(i+1,j+1) &= \overline{A}_1(r(i,j+1))\, x(i,j+1) \\ &\quad + \overline{A}_2(r(i+1,j))\, x(i+1,j) \\ &\quad + A_{d1}(r(i,j+1))\, x(i-d_1,j+1) \\ &\quad + A_{d2}(r(i+1,j))\, x(i+1,j-d_2) \\ &\quad + D_1(r(i,j+1))\, w(i,j+1) \\ &\quad + D_2(r(i+1,j))\, w(i+1,j), \\ z(i,j) &= \overline{C}(r(i,j))\, x(i,j) + D_3(r(i,j))\, w(i,j), \end{aligned} \tag{10}$$

where

$$\begin{aligned} &\overline{A}_1(r(i,j+1)) \\ &\quad := A_1(r(i,j+1)) + B_1(r(i,j+1))\, K(r(i,j+1)), \\ &\overline{A}_2(r(i+1,j)) \\ &\quad := A_2(r(i+1,j)) + B_2(r(i+1,j))\, K(r(i+1,j)), \\ &\overline{C}(r(i,j)) := C(r(i,j)) + B_3(r(i,j))\, K(r(i,j)). \end{aligned} \tag{11}$$

Before proceeding further, we introduce the following definitions.

Definition 2. System (10) is said to be stochastically stable if, for $w(i,j) = 0$ and the boundary conditions satisfying (8), the following condition holds:

$$\mathbb{E}\left\{\sum_{i=0}^{\infty} \sum_{j=0}^{\infty} \left(\|x(i,j+1)\|^2 + \|x(i+1,j)\|^2\right)\right\} < \infty. \tag{12}$$

Definition 3. Given a scalar $\gamma > 0$, system (10) is said to be stochastically stable with an $\mathscr{H}_\infty$ disturbance attenuation performance index γ if it is stochastically stable with $w(i,j) = 0$, and under zero boundary conditions $\phi(i,j) = \varphi(i,j) = 0$ in (7), for all nonzero, $w \in l_2\{[0,\infty), [0,\infty)\}$ satisfies

$$\|\widetilde{z}\|_{\mathbb{E}_2} < \gamma \|\widetilde{w}\|_2, \tag{13}$$

where

$$\begin{aligned} \|\widetilde{z}\|_{\mathbb{E}_2} &:= \sqrt{\mathbb{E}\left\{\sum_{i=0}^{\infty} \sum_{j=0}^{\infty} \left(\|z(i,j+1)\|^2 + \|z(i+1,j)\|^2\right)\right\}}, \\ \|\widetilde{w}\|_2 &:= \sqrt{\sum_{i=0}^{\infty} \sum_{j=0}^{\infty} \left(\|w(i,j+1)\|^2 + \|w(i+1,j)\|^2\right)}. \end{aligned} \tag{14}$$

Therefore, the purpose of this paper is to design a mode-dependent $\mathscr{H}_\infty$ state-feedback controller in the form of (9), such that the resulting closed-loop system (10) with defective mode information is stochastically stable with a prescribed $\mathscr{H}_\infty$ performance index γ.

3. Main Results

In this section, based on a Markovian Lyapunov-Krasovskii functional (MLKF), a new formulation of bounded real lemma (BRL) for the two-dimensional (2D) Markovian jump linear system (MJLS) (10) with state-delays and defective mode information will be firstly given. Then, via a linearisation procedure, the $\mathscr{H}_\infty$ controller synthesis will be developed.

3.1. $\mathscr{H}_\infty$ Performance Analysis. In this subsection, by invoking the properties of the transition probability matrices (TPMs), together with the convexification of uncertain domains, an $\mathscr{H}_\infty$ performance analysis criterion for the closed-loop system (10) with state-delays and defective mode information is presented, which will play a significant role in solving the $\mathscr{H}_\infty$ controller synthesis problem.

Proposition 4. *The 2D MJLS in* (10) *with state-delays and defective mode information is stochastically stable with a guaranteed $\mathscr{H}_\infty$ performance γ if the matrices $\{P_{1m}, P_{2m}, Q_1, Q_2\} \in \mathbf{R}^{n_x \times n_x}$, with $P_{1m} > 0$, $P_{2m} > 0$, $Q_1 > 0$, and $Q_2 > 0$, $m \in \mathscr{I}$, such that the following matrix inequalities hold:*

$$\begin{aligned} &\mathscr{A}_m^T \mathscr{P}_n^{(s)} \mathscr{A}_m + \mathscr{C}_m^T \mathscr{C}_m + \Theta_m < 0, \\ &m \in \mathscr{I}, \quad n \in \mathscr{I}_{\mathscr{UK}}^{(m)}, \quad s = 1, \ldots, M, \end{aligned} \tag{15}$$

where

$$\begin{aligned} \Theta_m &:= \operatorname{diag}\left\{-P_{1m} + Q_1, -P_{2m} + Q_2, -Q_1, -Q_2, -\gamma^2\mathbf{I}, -\gamma^2\mathbf{I}\right\}, \\ \mathscr{A}_m &:= \left[\overline{A}_{1m} \;\; \overline{A}_{2m} \;\; A_{d1m} \;\; A_{d2m} \;\; D_{1m} \;\; D_{2m}\right], \\ \mathscr{C}_m &:= \begin{bmatrix} \overline{C}_m & \mathbf{0} & \mathbf{0}_{n_z \times 2n_x} & D_{3m} & \mathbf{0} \\ \mathbf{0} & \overline{C}_m & \mathbf{0}_{n_z \times 2n_x} & \mathbf{0} & D_{3m} \end{bmatrix}, \\ \mathscr{P}_n^{(s)} &:= \sum_{n \in \mathscr{I}_{\mathscr{K}}^{(m)}} \pi_{mn} \left(P_{1n} + P_{2n}\right) \\ &\quad + \sum_{n \in \mathscr{I}_{\mathscr{UC}}^{(m)}} \widetilde{\pi}_{mn}^{(s)} \left(P_{1n} + P_{2n}\right) + \pi_{\mathscr{UK}}^{(ms)} \underbrace{\left(P_{1n} + P_{2n}\right)}_{n \in \mathscr{I}_{\mathscr{UK}}^{(m)}}, \\ \pi_{\mathscr{UK}}^{(ms)} &:= 1 - \sum_{n \in \mathscr{I}_{\mathscr{K}}^{(m)}} \pi_{mn} - \sum_{n \in \mathscr{I}_{\mathscr{UC}}^{(m)}} \widetilde{\pi}_{mn}^{(s)}. \end{aligned} \tag{16}$$

Proof. Consider the following MLKF for the 2D MJLS (10):

$$\begin{aligned} V(i,j) &:= \sum_{k=1}^{2} V_k\left(x(i,j+1), r(i,j+1)\right) \\ &\quad + \sum_{k=3}^{4} V_k\left(x(i+1,j), r(i+1,j)\right), \end{aligned} \tag{17}$$

where

$$\begin{aligned} &V_1\left(x(i,j+1), r(i,j+1)\right) \\ &\quad := x^{\mathrm{T}}(i,j+1) P_1\left(r(i,j+1)\right) x(i,j+1), \\ &V_2\left(x(i,j+1), r(i,j+1)\right) \\ &\quad := \sum_{k=i-d_1}^{i-1} x^{\mathrm{T}}(k,j+1) Q_1 x(k,j+1), \\ &V_3\left(x(i+1,j), r(i+1,j)\right) \\ &\quad := x^{\mathrm{T}}(i+1,j) P_2\left(r(i+1,j)\right) x(i+1,j), \\ &V_4\left(x(i+1,j), r(i+1,j)\right) \\ &\quad := \sum_{k=j-d_2}^{j-1} x^{\mathrm{T}}(i+1,k) Q_2 x(i+1,k). \end{aligned} \tag{18}$$

Then, based on the MLKF defined in (17), it is known that the following condition (19) guarantees that the 2D closed-loop system (10) is stochastically stable with an $\mathscr{H}_\infty$ performance γ under zero boundary conditions for any nonzero $w(i,j) \in l_2\{[0,\infty), [0,\infty)\}$:

$$\Omega := \Delta V(i,j) + \|\widetilde{z}\|_{\mathbb{E}_2}^2 - \gamma^2 \|\widetilde{w}\|_2^2 < 0, \tag{19}$$

where

$$\begin{aligned} \Delta V(i,j) &:= \mathbb{E}\left\{\sum_{k=1}^{2} V_k\left(x(i+1,j+1), r(i+1,j+1)\right) \mid \right. \\ &\qquad \left. x(i,j+1),\, r(i,j+1) = m\right\} \\ &\quad + \mathbb{E}\left\{\sum_{k=3}^{4} V_k\left(x(i+1,j+1), r(i+1,j+1)\right) \mid \right. \\ &\qquad \left. x(i+1,j), r(i+1,j) = m\right\} \end{aligned}$$

$$- \sum_{k=1}^{2} V_k\left(x\left(i, j+1\right), r\left(i, j+1\right)\right) - \sum_{k=3}^{4} V_k\left(x\left(i+1, j\right), r\left(i+1, j\right)\right), \tag{20}$$

and $\|\widetilde{z}\|_{\mathbb{E}_2}$ and $\|\widetilde{w}\|_2$ are defined in (14).

Taking the time difference of $V(i, j)$ along the trajectories of the 2D system in (10) yields

$$\begin{aligned}
\Delta V_1 &:= \mathbb{E}\left[V_1\left(x\left(i+1, j+1\right), r\left(i+1, j+1\right)\right) \mid x\left(i, j+1\right), r\left(i, j+1\right) = m\right] - V_1\left(x\left(i, j+1\right), r\left(i, j+1\right)\right) \\
&= x^{\mathrm{T}}\left(i+1, j+1\right)\left(\sum_{n\in\mathcal{J}} \pi_{mn} P_{1n}\right) x\left(i+1, j+1\right) - x^{\mathrm{T}}\left(i, j+1\right) P_{1m} x\left(i, j+1\right) \\
&= x^{\mathrm{T}}\left(i+1, j+1\right) \times \left(\sum_{n\in\mathcal{J}_{\mathcal{K}}^{(m)}} \pi_{mn} P_{1n} + \sum_{n\in\mathcal{J}_{\mathcal{UC}}^{(m)}} \left(\sum_{s=1}^{M} \alpha_s \widetilde{\pi}_{mn}^{(s)}\right) P_{1n} + \sum_{n\in\mathcal{J}_{\mathcal{UK}}^{(m)}} \widehat{\pi}_{mn} P_{1n}\right) \\
&\quad \times x\left(i+1, j+1\right) - x^{\mathrm{T}}\left(i, j+1\right) P_{1m} x\left(i, j+1\right), \\
\Delta V_2 &:= \mathbb{E}\left[V_2\left(x\left(i+1, j+1\right), r\left(i+1, j+1\right)\right) \mid x\left(i, j+1\right), r\left(i, j+1\right) = m\right] - V_2\left(x\left(i, j+1\right), r\left(i, j+1\right)\right) \\
&= x^{\mathrm{T}}\left(i, j+1\right) Q_1 x\left(i, j+1\right) - x^{\mathrm{T}}\left(i-d_1, j+1\right) Q_1 x\left(i-d_1, j+1\right), \\
\Delta V_3 &:= \mathbb{E}\left[V_3\left(x\left(i+1, j+1\right), r\left(i+1, j+1\right)\right) \mid x\left(i+1, j\right), r\left(i+1, j\right) = m\right] - V_3\left(x\left(i+1, j\right), r\left(i+1, j\right)\right) \\
&= x^{\mathrm{T}}\left(i+1, j+1\right)\left(\sum_{n\in\mathcal{J}} \pi_{mn} P_{2n}\right) x\left(i+1, j+1\right) - x^{\mathrm{T}}\left(i+1, j\right) P_{2m} x\left(i+1, j\right) \\
&= x^{\mathrm{T}}\left(i+1, j+1\right) \times \left(\sum_{n\in\mathcal{J}_{\mathcal{K}}^{(m)}} \pi_{mn} P_{2n} + \sum_{n\in\mathcal{J}_{\mathcal{UC}}^{(m)}} \left(\sum_{s=1}^{M} \alpha_s \widetilde{\pi}_{mn}^{(s)}\right) P_{2n} + \sum_{n\in\mathcal{J}_{\mathcal{UK}}^{(m)}} \widehat{\pi}_{mn} P_{2n}\right) \\
&\quad \times x\left(i+1, j+1\right) - x^{\mathrm{T}}\left(i+1, j\right) P_{2m} x\left(i+1, j\right), \\
\Delta V_4 &:= \mathbb{E}\left[V_4\left(x\left(i+1, j+1\right), r\left(i+1, j+1\right)\right) \mid x\left(i+1, j\right), r\left(i+1, j\right) = m\right] - V_4\left(x\left(i+1, j\right), r\left(i+1, j\right)\right) \\
&= x^{\mathrm{T}}\left(i+1, j\right) Q_2 x\left(i+1, j\right) - x^{\mathrm{T}}\left(i+1, j-d_2\right) Q_2 x\left(i+1, j-d_2\right).
\end{aligned} \tag{21}$$

Therefore, based on the MLKF defined in (17), together with consideration of (10) and (21), we have

$$\Omega = \varsigma^{\mathrm{T}}(i, j)\left[\boldsymbol{\mathcal{A}}_m^{\mathrm{T}}\left(\overline{\boldsymbol{\mathcal{P}}}_{1n} + \overline{\boldsymbol{\mathcal{P}}}_{2n}\right)\boldsymbol{\mathcal{A}}_m + \boldsymbol{\mathcal{C}}_m^{\mathrm{T}}\boldsymbol{\mathcal{C}}_m + \Theta_m\right] \times \varsigma(i, j), \quad m, n \in \mathcal{J}, \tag{22}$$

where

$$\begin{aligned}
\varsigma(i, j) &:= \left[x^{\mathrm{T}}\left(i, j+1\right)\ x^{\mathrm{T}}\left(i+1, j\right)\ x^{\mathrm{T}}\left(i-d_1, j+1\right)\ x^{\mathrm{T}}\left(i+1, j-d_2\right)\ w^{\mathrm{T}}\left(i, j+1\right)\ w^{\mathrm{T}}\left(i+1, j\right)\right]^{\mathrm{T}}, \\
\Theta_m &:= \operatorname{diag}\left\{-P_{1m} + Q_1, -P_{2m} + Q_2, -Q_1, -Q_2, -\gamma^2\mathbf{I}, -\gamma^2\mathbf{I}\right\}, \\
\boldsymbol{\mathcal{A}}_m &:= \left[\overline{A}_{1m}\ \overline{A}_{2m}\ A_{d1m}\ A_{d2m}\ D_{1m}\ D_{2m}\right], \\
\boldsymbol{\mathcal{C}}_m &:= \begin{bmatrix} \overline{C}_m & \mathbf{0} & \mathbf{0}_{n_z\times 2n_x} & D_{3m} & \mathbf{0} \\ \mathbf{0} & \overline{C}_m & \mathbf{0}_{n_z\times 2n_x} & \mathbf{0} & D_{3m} \end{bmatrix}, \\
\overline{\boldsymbol{\mathcal{P}}}_{ln} &:= \sum_{n\in\mathcal{J}_{\mathcal{K}}^{(m)}} \pi_{mn} P_{ln} + \sum_{n\in\mathcal{J}_{\mathcal{UC}}^{(m)}} \left(\sum_{s=1}^{M} \alpha_s \widetilde{\pi}_{mn}^{(s)}\right) P_{ln} + \sum_{n\in\mathcal{J}_{\mathcal{UK}}^{(m)}} \widehat{\pi}_{mn} P_{ln}, \quad l = 1, 2.
\end{aligned} \tag{23}$$

Considering the fact that $0 \le \alpha_s \le 1$, $\sum_{s=1}^{M} \alpha_s = 1$, and $0 \le \widehat{\pi}_{mn}/\pi_{\mathcal{UK}}^{(ms)} \le 1$, $\sum_{n\in\mathcal{F}_{\mathcal{UK}}^{(m)}} (\widehat{\pi}_{mn}/\pi_{\mathcal{UK}}^{(ms)}) = 1$, (22) can be rewritten as

$$\begin{aligned}\Omega = &\sum_{s=1}^{M}\alpha_s \sum_{n\in\mathcal{F}_{\mathcal{UK}}^{(m)}} \frac{\widehat{\pi}_{mn}}{\pi_{\mathcal{UK}}^{(ms)}} \\ &\times \left[\varsigma^{\mathrm{T}}(i,j)\left[\boldsymbol{\mathcal{A}}_m^{\mathrm{T}}\boldsymbol{\mathcal{P}}_n^{(s)}\boldsymbol{\mathcal{A}}_m + \boldsymbol{\mathcal{C}}_m^{\mathrm{T}}\boldsymbol{\mathcal{C}}_m + \Theta_m\right]\varsigma(i,j)\right], \\ &m\in\mathcal{J},\ n\in\mathcal{J}_{\mathcal{UK}}^{(m)},\ s=1,\ldots,M,\end{aligned} \tag{24}$$

where

$$\begin{aligned}\boldsymbol{\mathcal{P}}_n^{(s)} := &\sum_{n\in\mathcal{F}_{\mathcal{K}}^{(m)}} \pi_{mn}(P_{1n}+P_{2n}) + \sum_{n\in\mathcal{F}_{\mathcal{UC}}^{(m)}} \widetilde{\pi}_{mn}^{(s)}(P_{1n}+P_{2n}) \\ &+ \pi_{\mathcal{UK}}^{(ms)} \underbrace{(P_{1n}+P_{2n})}_{n\in\mathcal{F}_{\mathcal{UK}}^{(m)}}, \\ \pi_{\mathcal{UK}}^{(ms)} := &\ 1 - \sum_{n\in\mathcal{F}_{\mathcal{K}}^{(m)}} \pi_{mn} - \sum_{n\in\mathcal{F}_{\mathcal{UC}}^{(m)}} \widetilde{\pi}_{mn}^{(s)}.\end{aligned} \tag{25}$$

According to (24), it is easy to see that (19) holds if and only if, for all $s = 1,\ldots,M$,

$$\begin{aligned}&\varsigma^{\mathrm{T}}(i,j)\left[\boldsymbol{\mathcal{A}}_m^{\mathrm{T}}\boldsymbol{\mathcal{P}}_n^{(s)}\boldsymbol{\mathcal{A}}_m + \boldsymbol{\mathcal{C}}_m^{\mathrm{T}}\boldsymbol{\mathcal{C}}_m + \Theta_m\right]\varsigma(i,j) < 0, \\ &m\in\mathcal{J},\ n\in\mathcal{J}_{\mathcal{UK}}^{(m)},\end{aligned} \tag{26}$$

which is implied by condition (15). This completes the proof. □

Remark 5. By fully considering the properties of TPMs, together with the convexification of uncertain domains, a new version of BRL has been derived for the 2D MJLS (10) with state-delays and defective mode information in Proposition 4. It is worth mentioning that the results for Fornasini-Marchesini local state-space (FMLSS) model (10) could be readily applied to Roesser model after the similar transformation as performed in [8]. It is also noted that the condition given in (15) is nonconvex due to the presence of product terms between the Lyapunov matrices and system matrices. For the matrix inequality linearisation purpose, in the following, we shall make a decoupling between the Lyapunov matrices and system matrices, which will be convenient for controller synthesis purpose.

In the sequel, we focus on the $\mathscr{H}_\infty$ controller design based on the analysis condition given in Proposition 4.

3.2. $\mathscr{H}_\infty$ Controller Synthesis. In this subsection, based on a linearisation procedure, a unified framework for the solvability of the $\mathscr{H}_\infty$ controller synthesis problem will be proposed. It will be shown that the parametrised representations of the controller gains can be constructed in terms of the feasible solutions to a set of strict linear matrix inequalities (LMIs).

Theorem 6. *Consider 2D MJLS* (1) *with state-delays and defective mode information and the state-feedback controller in the form of* (9)*. The closed-loop system* (10) *is stochastically stable with an $\mathscr{H}_\infty$ performance γ if there exist matrices $\{X_{1m}, X_{2m}, R_1, R_2\} \in \mathbf{R}^{n_x\times n_x}$, with $X_{1m} > 0$, $X_{2m} > 0$, $R_1 > 0$, and $R_2 > 0$ and matrices $G_m \in \mathbf{R}^{n_x\times n_x}$ and $\overline{K}_m \in \mathbf{R}^{n_u\times n_x}$, $m \in \mathcal{J}$, such that the following LMIs hold:*

$$\begin{bmatrix} -\mathcal{X}_{1n}^{(m)} & \mathbf{0} & \mathbf{0} & F_m^{(s)}\overline{\boldsymbol{\mathcal{A}}}_m & \mathbf{0} \\ * & -\mathcal{X}_{2n}^{(m)} & \mathbf{0} & F_m^{(s)}\overline{\boldsymbol{\mathcal{A}}}_m & \mathbf{0} \\ * & * & -\mathbf{I} & \overline{\boldsymbol{\mathcal{C}}}_m & \mathbf{0} \\ * & * & * & -\overline{\Theta}_m & \mathcal{G}_m \\ * & * & * & * & -\mathscr{R} \end{bmatrix} < 0, \tag{27}$$
$$m\in\mathcal{J},\ n\in\mathcal{J}_{\mathcal{UK}}^{(m)},\ s=1,\ldots,M,$$

where

$$\begin{aligned}&\mathcal{X}_{ln}^{(m)} \\ &:= \mathrm{diag}\left\{X_{l\mathcal{K}_{1_{(m)}}},\ldots,X_{l\mathcal{K}_{t_{(m)}}},X_{l\mathcal{U}_{1_{(m)}}},\ldots,X_{l\mathcal{U}_{v_{(m)}}},X_{ln}\right\}, \\ &\qquad l=1,2, \\ &F_m^{(s)} := \left[\sqrt{\pi_{m\mathcal{K}_{1_{(m)}}}}\mathbf{I},\ldots,\sqrt{\pi_{m\mathcal{K}_{t_{(m)}}}}\mathbf{I},\sqrt{\widetilde{\pi}_{m\mathcal{U}_{1_{(m)}}}^{(s)}}\mathbf{I},\ldots,\right. \\ &\qquad \left.\sqrt{\widetilde{\pi}_{m\mathcal{U}_{v_{(m)}}}^{(s)}}\mathbf{I},\sqrt{\pi_{\mathcal{UK}}^{(ms)}}\mathbf{I}\right], \\ &\overline{\boldsymbol{\mathcal{A}}}_m := \left[\overline{\mathcal{A}}_{1m}\ \ \overline{\mathcal{A}}_{2m}\ \ A_{d1m}R_1\ \ A_{d2m}R_2\ \ D_{1m}\ \ D_{2m}\right], \\ &\overline{\boldsymbol{\mathcal{C}}}_m := \begin{bmatrix}\overline{\mathcal{C}}_m & \mathbf{0} & \mathbf{0}_{n_z\times 2n_x} & D_{3m} & \mathbf{0} \\ \mathbf{0} & \overline{\mathcal{C}}_m & \mathbf{0}_{n_z\times 2n_x} & \mathbf{0} & D_{3m}\end{bmatrix}, \\ &\overline{\Theta}_m := \mathrm{diag}\left\{G_m + G_m^{\mathrm{T}} - X_{1m}, G_m\right. \\ &\qquad \left. + G_m^{\mathrm{T}} - X_{2m}, \mathscr{R}, \gamma^2\mathbf{I}, \gamma^2\mathbf{I}\right\}, \\ &\qquad \mathscr{R} := \mathrm{diag}\left\{R_1, R_2\right\}, \\ &\mathcal{G}_m := \begin{bmatrix}G_m & \mathbf{0} & \mathbf{0}_{n_x\times 2(n_x+n_w)} \\ \mathbf{0} & G_m & \mathbf{0}_{n_x\times 2(n_x+n_w)}\end{bmatrix}^{\mathrm{T}}, \\ &\overline{\mathcal{A}}_{lm} := A_{lm} + B_{lm}\overline{K}_m, \\ &\overline{\mathcal{C}}_m := C_m + B_{3m}\overline{K}_m, \\ &\pi_{\mathcal{UK}}^{(ms)} := 1 - \sum_{n\in\mathcal{F}_{\mathcal{K}}^{(m)}} \pi_{mn} - \sum_{n\in\mathcal{F}_{\mathcal{UC}}^{(m)}} \widetilde{\pi}_{mn}^{(s)}.\end{aligned} \tag{28}$$

Moreover, if the above conditions have a set of feasible solutions $(X_{1m}, X_{2m}, R_1, R_2, G_m, \overline{K}_m)$, then the state-feedback controller in the form of (9) *can be constructed as*

$$K_m := \overline{K}_m G_m^{-1}. \tag{29}$$

Proof. It follows from Proposition 4 that, if we can show (15), then the claimed results follow. By Schur complement and with $\mathcal{I}_{\mathcal{K}}^{(m)} := \{\mathcal{K}_{1_{(m)}}, \ldots, \mathcal{K}_{t_{(m)}}\}$ and $\mathcal{I}_{\mathcal{UC}}^{(m)} := \{\mathcal{U}_{1_{(m)}}, \ldots, \mathcal{U}_{v_{(m)}}\}$, (15) is equivalent to

$$\begin{bmatrix} -\mathcal{X}_{1n}^{(m)} & \mathbf{0} & \mathbf{0} & F_m^{(s)}\boldsymbol{\mathcal{A}}_m & \mathbf{0} \\ * & -\mathcal{X}_{2n}^{(m)} & \mathbf{0} & F_m^{(s)}\boldsymbol{\mathcal{A}}_m & \mathbf{0} \\ * & * & -\mathbf{I} & \boldsymbol{\mathcal{C}}_m & \mathbf{0} \\ * & * & * & -\widehat{\Theta}_m & \Lambda \\ * & * & * & * & -\mathcal{Q}^{-1} \end{bmatrix} < 0, \quad (30)$$

$$m \in \mathcal{I},\ n \in \mathcal{I}_{\mathcal{UK}}^{(m)},\ s = 1, \ldots, M,$$

where

$$\mathcal{X}_{ln}^{(m)} := \operatorname{diag}\left\{X_{l\mathcal{K}_{1_{(m)}}}, \ldots, X_{l\mathcal{K}_{t_{(m)}}}, X_{l\mathcal{U}_{1_{(m)}}}, \ldots, X_{l\mathcal{U}_{v_{(m)}}}, X_{ln}\right\}, \quad X_{lm} := P_{lm}^{-1},\ l = 1, 2,$$

$$F_m^{(s)} := \left[\sqrt{\pi_{m\mathcal{K}_{1_{(m)}}}}\mathbf{I}, \ldots, \sqrt{\pi_{m\mathcal{K}_{t_{(m)}}}}\mathbf{I}, \sqrt{\widetilde{\pi}_{m\mathcal{U}_{1_{(m)}}}^{(s)}}\mathbf{I}, \ldots, \sqrt{\widetilde{\pi}_{m\mathcal{U}_{v_{(m)}}}^{(s)}}\mathbf{I}, \sqrt{\pi_{\mathcal{UK}}^{(ms)}}\mathbf{I}\right],$$

$$\boldsymbol{\mathcal{A}}_m := \begin{bmatrix} \overline{A}_{1m} & \overline{A}_{2m} & A_{d1m} & A_{d2m} & D_{1m} & D_{2m} \end{bmatrix},$$

$$\boldsymbol{\mathcal{C}}_m := \begin{bmatrix} \overline{C}_m & \mathbf{0} & \mathbf{0}_{n_z \times 2n_x} & D_{3m} & \mathbf{0} \\ \mathbf{0} & \overline{C}_m & \mathbf{0}_{n_z \times 2n_x} & \mathbf{0} & D_{3m} \end{bmatrix},$$

$$\widehat{\Theta}_m := \operatorname{diag}\left\{X_{1m}^{-1}, X_{2m}^{-1}, \mathcal{Q}, \gamma^2\mathbf{I}, \gamma^2\mathbf{I}\right\}, \quad \mathcal{Q} = \operatorname{diag}\{Q_1, Q_2\},$$

$$\Lambda := \begin{bmatrix} \mathbf{I}_{n_x} & \mathbf{0} & \mathbf{0}_{n_x \times 2(n_x+n_w)} \\ \mathbf{0} & \mathbf{I}_{n_x} & \mathbf{0}_{n_x \times 2(n_x+n_w)} \end{bmatrix}^{\mathrm{T}}. \quad (31)$$

Now, by introducing a nonsingular matrix $G_m \in \mathbf{R}^{n_x \times n_x}$ and pre- and postmultiplying (30) by $\operatorname{diag}\{\mathbf{I}_{2((t_{(m)}+v_{(m)}+1)n_x+n_z)}, G_m^{\mathrm{T}}, G_m^{\mathrm{T}}, Q_1^{-1}, Q_2^{-1}, \mathbf{I}_{2(n_w+n_x)}\}$ and its transpose the following yields:

$$\begin{bmatrix} -\mathcal{X}_{1n}^{(m)} & \mathbf{0} & \mathbf{0} & F_m^{(s)}\overline{\boldsymbol{\mathcal{A}}}_m & \mathbf{0} \\ * & -\mathcal{X}_{2n}^{(m)} & \mathbf{0} & F_m^{(s)}\overline{\boldsymbol{\mathcal{A}}}_m & \mathbf{0} \\ * & * & -\mathbf{I} & \overline{\boldsymbol{\mathcal{C}}}_m & \mathbf{0} \\ * & * & * & -\widetilde{\Theta}_m & \mathcal{G}_m \\ * & * & * & * & -\mathcal{R} \end{bmatrix} < 0, \quad (32)$$

$$m \in \mathcal{I},\ n \in \mathcal{I}_{\mathcal{UK}}^{(m)},\ s = 1, \ldots, M,$$

where

$$\overline{\boldsymbol{\mathcal{A}}}_m := \begin{bmatrix} \overline{\mathcal{A}}_{1m} & \overline{\mathcal{A}}_{2m} & A_{d1m}R_1 & A_{d2m}R_2 & D_{1m} & D_{2m} \end{bmatrix},$$

$$\overline{\boldsymbol{\mathcal{C}}}_m := \begin{bmatrix} \overline{\mathcal{C}}_m & \mathbf{0} & \mathbf{0}_{n_z \times 2n_x} & D_{3m} & \mathbf{0} \\ \mathbf{0} & \overline{\mathcal{C}}_m & \mathbf{0}_{n_z \times 2n_x} & \mathbf{0} & D_{3m} \end{bmatrix},$$

$$\mathcal{G}_m := \begin{bmatrix} G_m & \mathbf{0} & \mathbf{0}_{n_x \times 2(n_x+n_w)} \\ \mathbf{0} & G_m & \mathbf{0}_{n_x \times 2(n_x+n_w)} \end{bmatrix}^{\mathrm{T}},$$

$$\widetilde{\Theta}_m := \operatorname{diag}\left\{G_m^{\mathrm{T}}X_{1m}^{-1}G_m, G_m^{\mathrm{T}}X_{2m}^{-1}G_m, \mathcal{R}, \gamma^2\mathbf{I}, \gamma^2\mathbf{I}\right\}, \quad (33)$$

$$\mathcal{R} = \operatorname{diag}\{R_1, R_2\},$$

$$\overline{\mathcal{A}}_{lm} := A_{lm} + B_{lm}\overline{K}_m, \quad \overline{K}_m := K_m G_m,$$

$$R_l := Q_l^{-1}, \quad l = 1, 2,$$

$$\overline{\mathcal{C}}_m := C_m + B_{3m}\overline{K}_m,$$

and $\mathcal{X}_{1n}^{(m)}$, $\mathcal{X}_{2n}^{(m)}$, and $F_m^{(s)}$ are defined in (31).

It follows from

$$\left(X_{lm} - G_m\right)^{\mathrm{T}} X_{lm}^{-1} \left(X_{lm} - G_m\right) \geq 0, \quad l = 1, 2, \quad (34)$$

that

$$-G_m^{\mathrm{T}}X_{lm}^{-1}G_m \leq -G_m - G_m^{\mathrm{T}} + X_{lm}, \quad l = 1, 2. \quad (35)$$

Then, it is easy to see that (27) implies (32).

On the other hand, the condition in (27) implies that $-G_m - G_m^{\mathrm{T}} < 0$, which means that G_m is nonsingular. Thus, the controller gain can be constructed by (29). The proof is thus completed. □

Remark 7. Theorem 6 provides a sufficient condition on the feasibility of $\mathcal{H}_\infty$ state-feedback controller synthesis problem for the 2D MJLSs with state-delays and defective mode information. It is noted that the $\mathcal{H}_\infty$ state-feedback controller synthesis problem for 2D discrete-time MJLSs has also been considered in [40]. However, there still are some remarkable differences between our results and those in [40]. Firstly, in this paper, the state-delays were introduced in the system (1), whereas the 2D delay-free MJLSs are considered in [40]. In addition, in Theorem 6, the exactly known, partially unknown, and uncertain transition probabilities (TPs) have been simultaneously incorporated into the TPM for 2D MJLSs, while in [40], the TPs were assumed to be completely known. It has been recognized that the scenario containing time-delays and such defective TPs is more general and the underlying MJLSs are thereby more practicable for engineering applications.

4. An Illustrative Example

In this section, we use a simulation example to demonstrate the effectiveness of the proposed state-feedback controller design method to two-dimensional (2D) Markovian jump linear systems (MJLSs).

Consider a 2D MJLS with state-delays in the form of (1) with parameters as follows:

$$\left[\begin{array}{c|c|c|c} A_{11} & A_{d11} & B_{11} & D_{11} \\ \hline A_{21} & A_{d21} & B_{21} & D_{21} \\ \hline C_1 & & B_{31} & D_{31} \end{array}\right] = \left[\begin{array}{cc|cc|cc} -0.5 & 0 & 0 & 0.05 & -0.5 & 0.2 \\ 0 & 0.5 & -0.02 & 0 & 0.5 & 0.6 \\ \hline 0.5 & 1 & 0.04 & 0 & 0.5 & 0.5 \\ 0 & 1 & 0 & 0.02 & 1 & 0.3 \\ \hline 0.2 & 0.5 & & & 0.5 & 0.3 \\ 0.5 & 0.6 & & & 0.2 & -0.5 \end{array}\right],$$

$$\left[\begin{array}{c|c|c|c} A_{12} & A_{d12} & B_{12} & D_{12} \\ \hline A_{22} & A_{d22} & B_{22} & D_{22} \\ \hline C_2 & & B_{32} & D_{32} \end{array}\right] = \left[\begin{array}{cc|cc|cc} 0.6 & 0 & 0 & 0.05 & 0.5 & 0.2 \\ 0.3 & 0.5 & -0.02 & 0.04 & 0.5 & 0.6 \\ \hline 0.5 & 0.5 & 0.04 & 0 & 0.5 & 0.5 \\ 0 & 0.8 & 0.04 & 0.02 & 1 & 0.3 \\ \hline 0.2 & 0.5 & & & 0.5 & 0.3 \\ 0.5 & 0.6 & & & 0.2 & -0.5 \end{array}\right],$$

$$\left[\begin{array}{c|c|c|c} A_{13} & A_{d13} & B_{13} & D_{13} \\ \hline A_{23} & A_{d23} & B_{23} & D_{23} \\ \hline C_3 & & B_{33} & D_{33} \end{array}\right] = \left[\begin{array}{cc|cc|cc} 0.5 & 0 & 0 & 0.05 & 0.5 & 0.2 \\ 0.3 & 0.3 & -0.02 & 0.1 & 0.5 & 0.6 \\ \hline 0.2 & 0.5 & 0.04 & 0 & 0.5 & 0.5 \\ 0 & 0.4 & 0.1 & 0.02 & 0.2 & 0.3 \\ \hline 0.2 & 0.5 & & & 0.5 & 0.3 \\ 0.5 & 0.6 & & & 0.2 & -0.5 \end{array}\right], \tag{36}$$

$$\left[\begin{array}{c|c|c|c} A_{14} & A_{d14} & B_{14} & D_{14} \\ \hline A_{24} & A_{d24} & B_{24} & D_{24} \\ \hline C_4 & & B_{34} & D_{34} \end{array}\right] = \left[\begin{array}{cc|cc|cc} 0.4 & 0 & 0 & 0.05 & 0.3 & 0.2 \\ 0.5 & 0.6 & -0.02 & 0.1 & 0.5 & 0.6 \\ \hline 0.6 & 0.5 & 0.04 & 0 & 0.5 & 0.5 \\ 0 & 0.5 & 0.1 & 0.02 & 0.4 & 0.3 \\ \hline 0.2 & 0.5 & & & 0.5 & 0.3 \\ 0.5 & 0.6 & & & 0.2 & -0.5 \end{array}\right].$$

Four different cases for the transition probability matrix (TPM) are given in Table 1, where the transition probabilities (TPs) labeled with "$\hat{}$" and "$\sim$" represent the unknown and uncertain elements, respectively. Specifically, Case 1, Case 2, Case 3, and Case 4 stand for the completely known TPs, defective mode information (including known, partially unknown, and uncertain TPs), partially unknown TPs, and completely unknown TPs, respectively.

Table 1: Four different TPMs.

Case 1: completely known TPM	Case 2: defective TPM1
$\begin{bmatrix} 0.3 & 0.2 & 0.1 & 0.4 \\ 0.3 & 0.2 & 0.3 & 0.2 \\ 0.1 & 0.5 & 0.3 & 0.1 \\ 0.2 & 0.2 & 0.1 & 0.5 \end{bmatrix}$	$\begin{bmatrix} 0.3 & 0.2 & 0.1 & 0.4 \\ \widehat{\pi}_{21} & \widehat{\pi}_{22} & 0.3 & 0.2 \\ \widehat{\pi}_{31} & \widehat{\pi}_{32} & \widehat{\pi}_{33} & \widehat{\pi}_{34} \\ 0.2 & \widehat{\pi}_{42} & \widehat{\pi}_{43} & \widehat{\pi}_{44} \end{bmatrix}$
Case 3: defective TPM2	**Case 4: completely unknown TPM**
$\begin{bmatrix} 0.3 & 0.2 & 0.1 & 0.4 \\ \widehat{\pi}_{21} & \widehat{\pi}_{22} & 0.3 & 0.2 \\ \widehat{\pi}_{31} & \widehat{\pi}_{32} & \widehat{\pi}_{33} & \widehat{\pi}_{34} \\ 0.2 & \widehat{\pi}_{42} & \widehat{\pi}_{43} & \widehat{\pi}_{44} \end{bmatrix}$	$\begin{bmatrix} \widehat{\pi}_{11} & \widehat{\pi}_{12} & \widehat{\pi}_{13} & \widehat{\pi}_{14} \\ \widehat{\pi}_{21} & \widehat{\pi}_{22} & \widehat{\pi}_{23} & \widehat{\pi}_{24} \\ \widehat{\pi}_{31} & \widehat{\pi}_{32} & \widehat{\pi}_{33} & \widehat{\pi}_{34} \\ \widehat{\pi}_{41} & \widehat{\pi}_{42} & \widehat{\pi}_{43} & \widehat{\pi}_{44} \end{bmatrix}$

Table 2: Comparison of minimum $\mathscr{H}_\infty$ performance for different TPMs.

TPMs	Case 1	Case 2	Case 3	Case 4
$\gamma_{\min}$	0.9884	1.0415	1.0906	2.2398

For Case 2, it is assumed that the uncertain TPs comprise four vertices Π_s, $s = 1, 2, 3, 4$, where the third rows $\Pi_{s(3)}$, $s = 1, 2, 3, 4$, are given by

$$\begin{aligned} \Pi_{1(3)} &= \left[\widehat{\pi}_{31} \;\; 0.2 \;\; \widehat{\pi}_{33} \;\; 0.4\right], \\ \Pi_{2(3)} &= \left[\widehat{\pi}_{31} \;\; 0.5 \;\; \widehat{\pi}_{33} \;\; 0.3\right], \\ \Pi_{3(3)} &= \left[\widehat{\pi}_{31} \;\; 0.3 \;\; \widehat{\pi}_{33} \;\; 0.1\right], \\ \Pi_{4(3)} &= \left[\widehat{\pi}_{31} \;\; 0.1 \;\; \widehat{\pi}_{33} \;\; 0.45\right], \end{aligned} \tag{37}$$

and the other rows in the four vertices are given with the same elements; that is,

$$\begin{aligned} \Pi_{s(1)} &= \left[0.3 \;\; 0.2 \;\; 0.1 \;\; 0.4\right], \\ \Pi_{s(2)} &= \left[\widehat{\pi}_{21} \;\; \widehat{\pi}_{22} \;\; 0.3 \;\; 0.2\right], \\ \Pi_{s(4)} &= \left[0.2 \;\; \widehat{\pi}_{42} \;\; \widehat{\pi}_{43} \;\; \widehat{\pi}_{44}\right], \quad s = 1, 2, 3, 4. \end{aligned} \tag{38}$$

The objective is to design a state-feedback controller of the form (9) for the above system such that the 2D closed-loop system is stochastically stable with an $\mathscr{H}_\infty$ performance γ. By applying Theorem 6, a detailed comparison of the obtained minimum $\mathscr{H}_\infty$ performance indices $\gamma_{\min}$ by the state-feedback controller (9) with four TPM cases being shown in Table 2. It is shown in Tables 1 and 2 that the lower the level of defectiveness of the TPM is, the better the $\mathscr{H}_\infty$ performance can be obtained, which is effective to reduce the design conservatism. Therefore, the introduction of the uncertain TPs is meaningful.

Specifically, in the following, considering the four TPM cases shown in Table 1 and by applying Theorem 6, the feasible

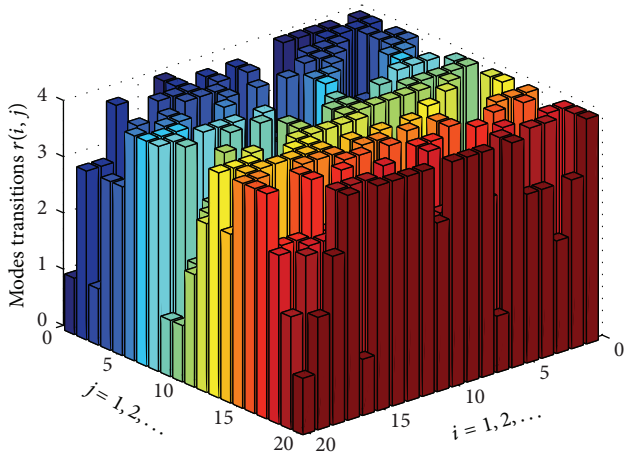

FIGURE 1: One possible system mode evolution.

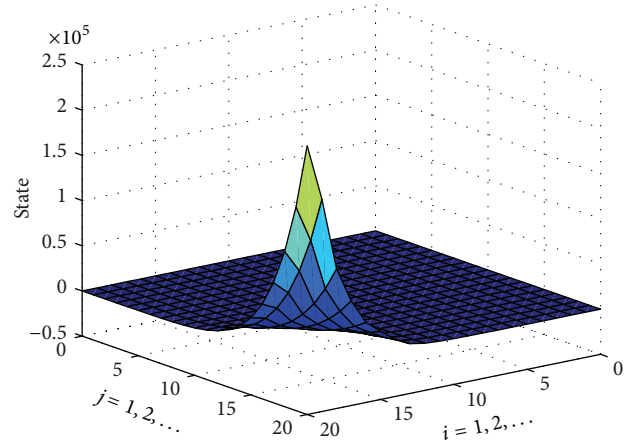

FIGURE 2: State responses of the open-loop system: the 1st component.

solution of $\gamma_{\min} = 1.0415$ for the state-feedback controller is obtained under Case 2 with controller gains given by

$$K_1 = \begin{bmatrix} -0.2467 & -0.7888 \end{bmatrix},$$
$$K_2 = \begin{bmatrix} -0.2125 & -0.7064 \end{bmatrix},$$
$$K_3 = \begin{bmatrix} -0.4563 & -0.5998 \end{bmatrix}, \quad (39)$$
$$K_4 = \begin{bmatrix} -0.2015 & -0.7041 \end{bmatrix}.$$

The feasible solutions for the other three TPM cases in Table 1 are omitted for brevity.

In order to further illustrate the effectiveness of the designed $\mathscr{H}_\infty$ state-feedback controllers, we present some simulation results. Let the boundary conditions be

$$x(t,i) = x(i,t) = \begin{cases} \begin{bmatrix} -1 & 1.4 \end{bmatrix}^{\mathrm{T}}, & 0 \le i \le 10, \\ \begin{bmatrix} 0 & 0 \end{bmatrix}^{\mathrm{T}}, & i > 10, \end{cases} \quad (40)$$

where $-4 \le t \le 0$, and choose the delays $d_1 = 4$ (vertical direction), $d_2 = 4$ (horizontal direction), and disturbance input $w(i, j)$ as

$$w(i,j) = \begin{cases} 0.2, & 0 \le i, j \le 10, \\ 0, & \text{otherwise}. \end{cases} \quad (41)$$

With the previous obtained controllers under Case 2 in Table 1, one possible realization of the Markovian jumping mode is plotted in Figure 1. The state responses for the open-loop and closed-loop systems are shown in Figures 2 and 3 and Figures 4 and 5, respectively, and Figures 6 and 7 are the controlled output trajectories of the closed-loop system. It can be clearly observed from the simulation curves that, despite the defective TPs, the performance of the designed controller is satisfactory.

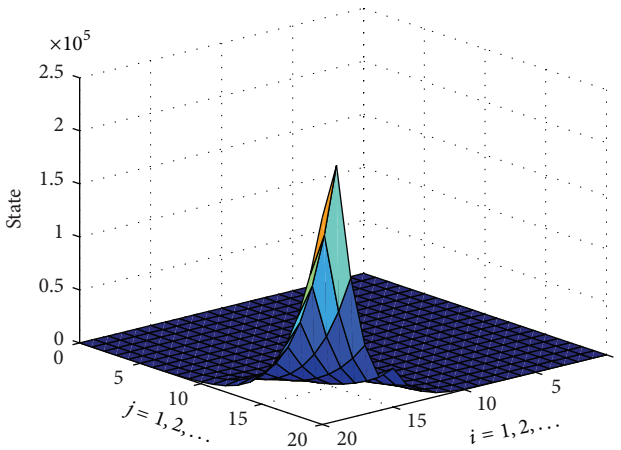

FIGURE 3: State responses of the open-loop system: the 2nd component.

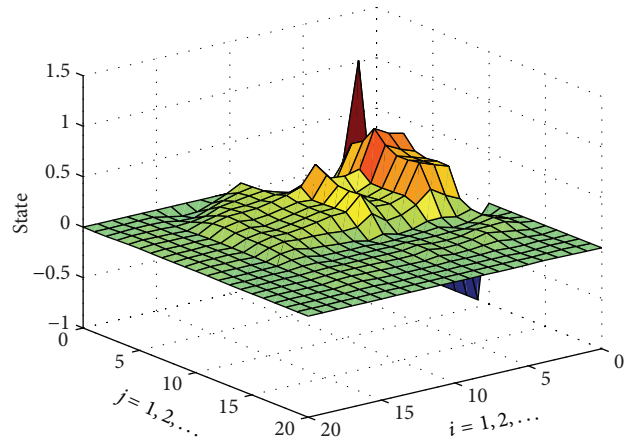

FIGURE 4: State responses of the closed-loop system: the 1st component.

5. Conclusions

This paper has addressed the problem of $\mathscr{H}_\infty$ control for a class of two-dimensional (2D) Markovian jump linear

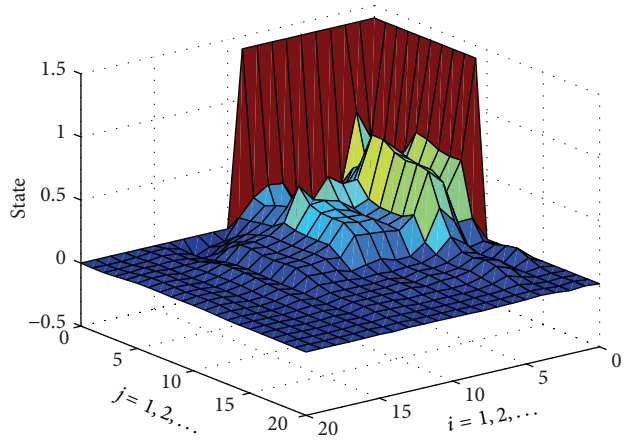

Figure 5: State responses of the closed-loop system: the 2nd component.

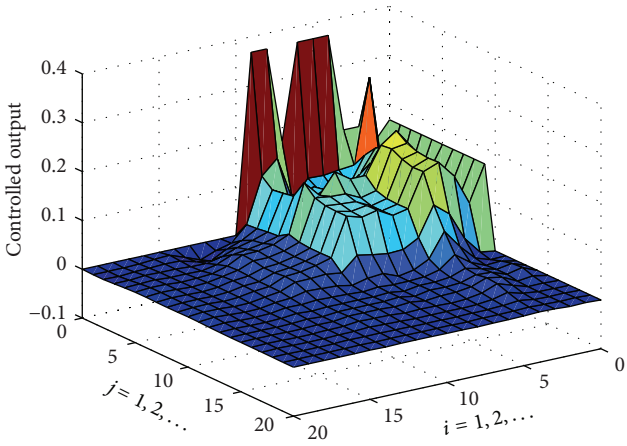

Figure 6: Responses of the controlled output $z(i, j)$ for the closed-loop system: the 1st component.

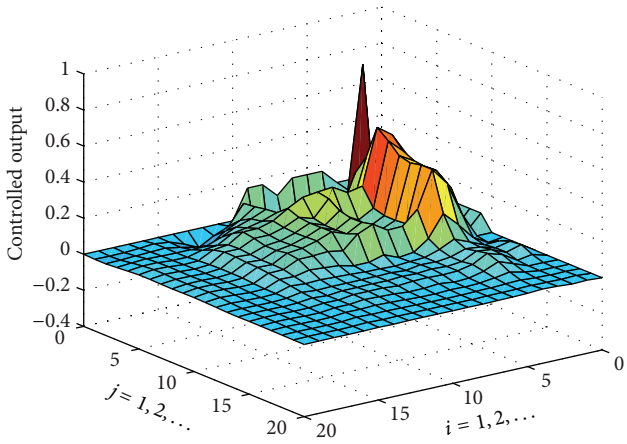

Figure 7: Responses of the controlled output $z(i, j)$ for the closed-loop system: the 2nd component.

systems (MJLSs) with state-delays and defective mode information. Such defective mode information simultaneously includes the exactly known, partially unknown, and uncertain transition probabilities, which contributes to the practicability of 2D MJLSs. By fully considering the properties of the transition probability matrices, together with the convexification of uncertain domains, an $\mathscr{H}_\infty$ performance analysis criterion for the 2D Fornasini-Marchesini local state-space model has been firstly developed, and then via a linearisation procedure, a unified framework has been proposed for the state-feedback controller synthesis that guarantees the stochastic stability of the closed-loop system with an $\mathscr{H}_\infty$ disturbance attenuation level. A simulation example has been given to illustrate the effectiveness of the proposed method.

Acknowledgments

The authors are grateful to the Guest Editors and anonymous reviewers for their constructive comments based on which the presentation of this paper has been greatly improved. This work was supported in part by the National Natural Science Foundation of China (61004038, 61374031), in part by the Program for New Century Excellent Talents in University (NCET-12-0147), in part by the Fundamental Research Funds for the Central Universities (HIT.BRETIII.201214), and in part by the Alexander von Humboldt Foundation of Germany.

References

[1] R. P. Roesser, "A discrete state-space model for linear image processing," *IEEE Transactions on Automatic Control*, vol. 20, pp. 1–10, 1975.

[2] T. Kaczorek, *Two-Dimensional Linear Systems*, vol. 68, Springer, Berlin, Germany, 1985.

[3] W. S. Lu and A. Antoniou, *Two-Dimensional Digital Fiters*, Marcel Dekker, New York, NY, USA, 1992.

[4] S. Xu, J. Lam, Z. Lin, and K. Galkowski, "Positive real control for uncertain two-dimensional systems," *IEEE Transactions on Circuits and Systems I*, vol. 49, no. 11, pp. 1659–1666, 2002.

[5] S. Xu, J. Lam, Z. Lin et al., "Positive real control of two-dimensional systems: Roesser models and linear repetitive processes," *International Journal of Control*, vol. 76, no. 11, pp. 1047–1058, 2003.

[6] L. Xie, C. Du, Y. C. Soh, and C. Zhang, "$\mathscr{H}_\infty$ and robust control of 2-D systems in FM second model," *Multidimensional Systems and Signal Processing*, vol. 13, no. 3, pp. 265–287, 2002.

[7] J. Lam, S. Xu, Y. Zou, Z. Lin, and K. Galkowski, "Robust output feedback stabilization for two-dimensional continuous systems in Roesser form," *Applied Mathematics Letters*, vol. 17, no. 12, pp. 1331–1341, 2004.

[8] W. Paszke, J. Lam, K. Gałkowski, S. Xu, and Z. Lin, "Robust stability and stabilisation of 2D discrete state-delayed systems," *Systems & Control Letters*, vol. 51, no. 3-4, pp. 277–291, 2004.

[9] N. T. Hoang, H. D. Tuan, T. Q. Nguyen, and S. Hosoe, "Robust mixed generalized $\mathscr{H}_2/\mathscr{H}_\infty$ filtering of 2-D nonlinear fractional transformation systems," *IEEE Transactions on Signal Processing*, vol. 53, no. 12, pp. 4697–4706, 2005.

[10] D. Peng and X. Guan, "$\mathscr{H}_\infty$ filtering of 2-D discrete state-delayed systems," *Multidimensional Systems and Signal Processing*, vol. 20, no. 3, pp. 265–284, 2009.

[11] X. Li and H. Gao, "Robust finite frequency $\mathscr{H}_\infty$ filtering for uncertain 2-D Roesser systems," *Automatica*, vol. 48, no. 6, pp. 1163–1170, 2012.

[12] S. Xu, J. Lam, and X. Mao, "Delay-dependent $\mathscr{H}_\infty$ control and filtering for uncertain Markovian jump systems with time-varying delays," *IEEE Transactions on Circuits and Systems I*, vol. 54, no. 9, pp. 2070–2077, 2007.

[13] H. Liu, D. W. C. Ho, and F. Sun, "Design of $\mathscr{H}_\infty$ filter for Markov jumping linear systems with non-accessible mode information," *Automatica*, vol. 44, no. 10, pp. 2655–2660, 2008.

[14] M. Liu, D. W. C. Ho, and Y. Niu, "Stabilization of Markovian jump linear system over networks with random communication delay," *Automatica*, vol. 45, no. 2, pp. 416–421, 2009.

[15] M. Liu, P. Shi, L. Zhang, and X. Zhao, "Fault-tolerant control for nonlinear Markovian jump systems via proportional and derivative sliding mode observer technique," *IEEE Transactions on Circuits and Systems I*, vol. 58, no. 11, pp. 2755–2764, 2011.

[16] Z. Wang, J. Lam, and X. Liu, "Exponential filtering for uncertain Markovian jump time-delay systems with nonlinear disturbances," *IEEE Transactions on Circuits and Systems I*, vol. 51, no. 5, pp. 262–268, 2004.

[17] Z. Wang, J. Lam, and X. Liu, "Robust filtering for discrete-time Markovian jump delay systems," *IEEE Signal Processing Letters*, vol. 11, no. 8, pp. 659–662, 2004.

[18] Z. Wang, Y. Liu, and X. Liu, "Exponential stabilization of a class of stochastic system with Markovian jump parameters and mode-dependent mixed time-delays," *IEEE Transactions on Automatic Control*, vol. 55, no. 7, pp. 1656–1662, 2010.

[19] H. Dong, Z. Wang, and H. Gao, "Distributed filtering for a class of time-varying systems over sensor networks with quantization errors and successive packet dropouts," *IEEE Transactions on Signal Processing*, vol. 60, no. 6, pp. 3164–3173, 2012.

[20] H. Dong, Z. Wang, J. Lam, and H. Gao, "Fuzzy-model-based robust fault detection with stochastic mixed time-delays and successive packet dropouts," *IEEE Transactions on Systems, Man, and Cybernetics B*, vol. 42, no. 2, pp. 365–376, 2012.

[21] Z. Wang, B. Shen, H. Shu, and G. Wei, "Quantized $\mathscr{H}_\infty$ control for nonlinear stochastic time-delay systems with missing measurements," *IEEE Transactions on Automatic Control*, vol. 57, no. 6, pp. 1431–1444, 2012.

[22] B. Shen, Z. Wang, and Y. S. Hung, "Distributed $\mathscr{H}_\infty$-consensus filtering in sensor networks with multiple missing measurements: the finite-horizon case," *Automatica*, vol. 46, no. 10, pp. 1682–1688, 2010.

[23] J. Qiu, G. Feng, and J. Yang, "Improved delay-dependent $\mathscr{H}_\infty$ filtering design for discrete-time polytopic linear delay systems," *IEEE Transactions on Circuits and Systems II*, vol. 55, no. 2, pp. 178–182, 2008.

[24] B. Shen, Z. Wang, Y. S. Hung, and G. Chesi, "Distributed $\mathscr{H}_\infty$ filtering for polynomial nonlinear stochastic systems in sensor networks," *IEEE Transactions on Industrial Electronics*, vol. 58, no. 5, pp. 1971–1979, 2011.

[25] G. He, J.-A. Fang, and X. Wu, "Robust stability of Markovian jumping genetic regulatory networks with mode-dependent delays," *Mathematical Problems in Engineering*, vol. 2012, Article ID 504378, 18 pages, 2012.

[26] Y. Wei, M. Wang, H. R. Karimi, N. Wang, and J. Qiu, "$\mathscr{H}_\infty$ model reduction for discrete-time Markovian jump systems with deficient mode information," *Mathematical Problems in EngineerIng*, vol. 2013, Article ID 537174, 11 pages, 2013.

[27] J. Qiu, G. Feng, and J. Yang, "A new design of delay-dependent robust $\mathscr{H}_\infty$ filtering for discretetime T-S fuzzy systems with time-varying delay," *IEEE Transactions on Fuzzy Systems*, vol. 17, no. 5, pp. 1044–1058, 2009.

[28] J. Qiu, G. Feng, and J. Yang, "Delay-dependent non-synchronized robust $\mathscr{H}_\infty$ state estimation for discrete-time piecewise linear delay systems," *International Journal of Adaptive Control and Signal Processing*, vol. 23, no. 2, pp. 1082–1096, 2009.

[29] J. Qiu, G. Feng, and J. Yang, "New results on robust $\mathscr{H}_\infty$ filtering design for discrete-time piecewise linear delay systems," *International Journal of Control*, vol. 82, no. 1, pp. 183–194, 2009.

[30] E.-K. Boukas, *Stochastic Switching Systems. Analysis and Design*, Birkhäuser, Boston, Mass, USA, 2006.

[31] L. Zhang and E.-K. Boukas, "Mode-dependent $\mathscr{H}_\infty$ filtering for discrete-time Markovian jump linear systems with partly unknown transition probabilities," *Automatica*, vol. 45, no. 6, pp. 1462–1467, 2009.

[32] C. E. de Souza, "Robust stability and stabilization of uncertain discrete-time Markovian jump linear systems," *IEEE Transactions on Automatic Control*, vol. 51, no. 5, pp. 836–841, 2006.

[33] Y. Zhao, L. Zhang, S. Shen, and H. Gao, "Robust stability criterion for discrete-time uncertain Markovian jumping neural networks with defective statistics of modes transitions," *IEEE Transactions on Neural Network*, vol. 22, no. 1, pp. 164–170, 2011.

[34] H. Dong, Z. Wang, D. W. C. Ho, and H. Gao, "Robust $\mathscr{H}_\infty$ filtering for Markovian jump systems with randomly occurring nonlinearities and sensor saturation: the finite-horizon case," *IEEE Transactions on Signal Processing*, vol. 59, no. 7, pp. 3048–3057, 2011.

[35] H. Dong, Z. Wang, and H. Gao, "Fault detection for Markovian jump systems with sensor saturations and randomly varying nonlinearities," *IEEE Transactions on Circuits and Systems I*, vol. 59, no. 10, pp. 2354–2362, 2012.

[36] M. Karan, P. Shi, and C. Y. Kaya, "Transition probability bounds for the stochastic stability robustness of continuous- and discrete-time Markovian jump linear systems," *Automatica*, vol. 42, no. 12, pp. 2159–2168, 2006.

[37] Y. Wei, M. Wang, and J. Qiu, "A new approach to delay-dependent $\mathscr{H}_\infty$ filtering for discrete-time Markovian jump systems with time-varying delay and incomplete transition descriptions," *IET Control Theory and Applications*, vol. 7, no. 5, pp. 684–696, 2013.

[38] Y. Wei, J. Qiu, H. R. Karimi, and M. Wang, "A new design of $\mathscr{H}_\infty$ filtering for continuous-time Markovian jump systems with time-varying delay and partially accessible mode information," *Signal Processing*, vol. 93, no. 9, pp. 2392–2407, 2013.

[39] L. Wu, P. Shi, H. Gao, and C. Wang, "$\mathscr{H}_\infty$ filtering for 2D Markovian jump systems," *Automatica*, vol. 44, no. 7, pp. 1849–1858, 2008.

[40] H. Gao, J. Lam, S. Xu, and C. Wang, "Stabilization and $\mathscr{H}_\infty$ control of two-dimensional Markovian jump systems," *IMA Journal of Mathematical Control and Information*, vol. 21, no. 4, pp. 377–392, 2004.

Hindawi Publishing Corporation
Mathematical Problems in Engineering
Volume 2013, Article ID 836517, 7 pages
http://dx.doi.org/10.1155/2013/836517

Research Article

Performance Reliability Prediction of Complex System Based on the Condition Monitoring Information

Hongxing Wang[1] and Yu Jiang[2]

[1] *Jiangsu Frontier Electric Technology Co., Ltd., Nanjing 211102, China*
[2] *College of Civil Aviation, Nanjing University of Aeronautics and Astronautics, Nanjing 20016, China*

Correspondence should be addressed to Yu Jiang; jiangyu07@nuaa.edu.cn

Received 18 June 2013; Revised 23 September 2013; Accepted 23 September 2013

Academic Editor: Hamid Reza Karimi

Complex system performance reliability prediction is one of the means to understand complex systems reliability level, make maintenance decision, and guarantee the safety of operation. By the use of complex system condition monitoring information and condition monitoring information based on support vector machine, the paper aims to provide an evaluation of the degradation of complex system performance. With degradation assessment results as input variables, the prediction model of reliability is established in Winer random process. Taking the aircraft engine as an example, the effectiveness of the proposed method is verified in the paper.

1. Introduction

The reliability of complex systems is directly related to operation safety, so the reliability prediction is of great importance. Different from the method based on the reliability of fault prediction, complex systems mainly use condition monitoring parameter to predict the complex system performance degradation state. When the threshold of the degradation state goes beyond the prescribed one, timely maintenance and inspection are being done to avoid accidents. Therefore, the reliability of complex systems is mainly aimed at the reliability of the performance degradation prediction.

Complex system reliability prediction has received extensive attention of many scholars. One trend in the research about this problem is using different temporal point data to predict the future level of reliability based on the analysis of the data change trend. Lu et al. [1] presented an evaluation model of real-time performance based on time series method and researched the reliability prediction of the bit excessive wear failure by regarding drill thrust as performance monitoring parameters; Elwany and Gebraeel [2] presented a model for predicting system performance reliability based on Bayesian, and applied to parts replacement and inventory decisions; Li and Masuda [3] discussed the multistate coherent system composed of multistate components. In view of degradation signal monitor parts reliability, Chinnam [4] made use of the reliability condition of some parts which performance degenerate signals were monitored and adopted a general polynomial regression model to describe performance change. In addition, based on the analysis of the relationship between state parameters, the performance change rules on study was put forward, which can be used to predict the reliability level at a particular moment or under specified reliability level of residual life. Condition monitoring is the key to access the operational reliability. Christer et al. [5] used a state space model to predict the erosion condition of the inductors in an induction furnace in which a measure of the conductance ratio (CR) is used to indirectly assess the relative condition of the inductors and to guide replacement decisions. Bharadwaj and Parlos [6] developed a sensorless neural adaptive speed filter for induction motors operating under normal conditions and running off the power supply mains. Chen et al. [7] proposed an integrated RUL prediction method using adaptive neuro-fuzzy inference systems (ANFIS) and high-order particle filtering, which forecast the time evolution of the fault indicator and estimates the probability density function (pdf) of RUL.

Bosnić and Kononenko [8] compared different approaches to estimate the reliability of individual predictions in

regression and to compose a combined estimate that performs better than the individual estimates; Wang and Coit [9] made an analysis of the complex relationship between monitoring variables and proposed a prediction method of correlation between variables with multifunctional parameters and verified the effectiveness of the proposed method by simulation data; Xu et al. [10] established the model of real-time reliability evaluation based on performance degradation by assuming that degradation function conformed to the Brownian motion and drift; Lu et al. [11] presented a technique for predicting system performance reliability in real-time considering multiple failure modes. The technique includes on-line multivariate monitoring and forecasting of selected performance measures and conditional performance reliability estimates based on collaborative filtering; Xu et al. [12] introduced a new real-time reliability prediction method for dynamic systems; Hernando et al. [13] introduced the idea of using a reliability measure associated with the predictions made by recommender systems; in order to improve data utilization results, Li et al. [14] proposed a method based on grey model to predict the reliability and verified the validity of the model by applying it in the manufacturing system data of electronic product; Hu et al. [15] adopted the method of D-S evidence for scientific forecast and verified its validity by its application to engine turbosupercharging system; Moura et al. [16] conducted an analysis of the different sequential points data and made a reliability prediction by the use of support vector machine (SVM) method; Lolas and Olatunbosun [17] presented the first module of an expert system, a neural network architecture that could predict the reliability performance of a vehicle at later stage of its life by using only information from first inspection after the vehicle's prototype production; Hu et al. [18] developed a novel reliability prediction technique based on the evidential reasoning (ER) algorithm which was applied to forecast reliability in turbocharger engine systems. And the experimental results showed that the prediction performance of the ER-based prediction model outperformed several existing methods in terms of prediction accuracy or speed.

The above research is mainly aimed to realize the goal of reliability prediction by using the methods of artificial intelligence and information fusion methods to train and study the data. Due to the complicated system with abundant condition monitoring parameters and small sample system, the paper put forward a method to evaluate complex system performance degeneration by adopting information fusion methods and described the performance degeneration of complex system under random process condition. The main aim of the paper is to realize the goal of improving reliability of forecast accuracy and credibility.

The research results in the paper can be further used in the following areas.

(1) The research results can be applied to control risk in complex system operation. By means of the real-time monitoring and tracking, the major accidents can be avoided.

(2) The research results can be applied to health management field of complex system. The assessment of operational reliability is the core in health management. Improving the accuracy of assessment in operation reliability can increase the operational efficient in healthy management.

(3) The research results can afford supports for the maintenance decision. The complex system is typical repairable system. The maintenance decision is not only related to operational safety but also operational cost. It is necessary to enhance the accuracy of maintenance decision, because that decision basis in maintenance is the reliability standards in complex system.

(4) Improving the value of condition monitoring information can provide new thoughts in design process. In order to ensure the safety and reliability of the operation system and consistently high-quality products, it is still necessary to develop an efficient process monitoring scheme to detect the abnormal situations as early as possible and take corrective actions in time.

2. Framework of the Complex System Reliability Prediction

Complex systems are characterized with abundant condition monitoring parameters and small sample system. Considering these characteristics, support vector machine (SVM) method is used in the research because of its unique advantages in dealing with a small sample data.

Support vector machine (SVM) is a learning system proposed by Vapnik. SVM is put forward according to the structural risk minimization principle in statistical learning theory and uses linear function hypothesis space in high-dimensional feature space. SVM is used to seek the best compromise between complexity and learning ability according to the limited sample information of the model. Because of the forecast superiority in the treatment of small sample, SVM realizes efficient transmission reasoning from training sample to forecast sample. It can reasonably solve the actual problems such as small sample, nonlinear, high dimension, and local minimum point.

Applying SVM method, comprehensive utilization of multisource monitoring parameters and assessment of performance degradation in complex systems can be completed. Because performance retirement leading to reliability is a random course, the paper establishes reliability prediction model for dynamic assessment of the complex systems reliability by choosing Winer process complex system performance degradation.

The process of reliability prediction of complex systems is shown in Figure 1.

The advantages of algorithm in the paper include some aspects.

(1) The algorithm can deal with the prediction of real-timereliability sufficiently in complex system in view

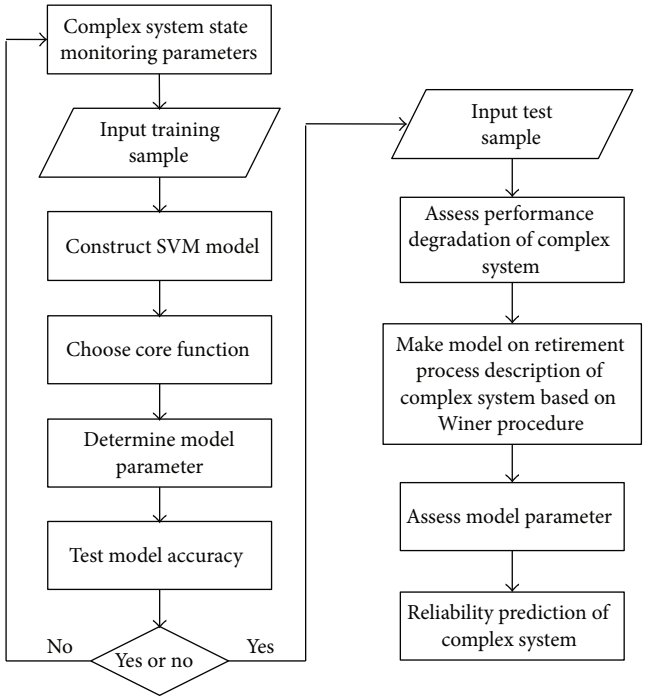

Figure 1: Performance degradation assessment of complex system.

of small sample and solve the question efficiently which is difficult to collect mass data because of the high cost.

(2) The algorithm can exploit multisource monitoring information comprehensively to improve the accuracy of condition monitoring.

(3) The algorithm can indicate the reliable change rules which are lead by the random disturbance of multiple factors, and it confirms to the actual operation of complex system.

(4) The algorithm can analyze the influence on operational reliability accurately produced by condition change. Therefore, it can control the risk efficiently.

3. Performance Degradation Assessment Model of Complex System Based on SVM

Assuming sample training set is $\{(x_i, y_i) \mid i = 1, 2, \ldots, l\}$, $x_i \in R^n$ refers to the input variables, which corresponds to condition monitoring parameters of complex system; $y_i \in R^n$ refers to the output variables. Generally, vector machine can use nonlinear mapping $\varphi(\cdot)$ to get a high-dimensional feature space from the original monitoring parameters, where it can construct the optimal decision function: $f(x) = (w \cdot \varphi(x)) + b$, where $w \cdot \varphi(x)$ means dot-product of vectors w and mapping function. b refers to bias. So the corresponding constraint optimization problem can be expressed as follows:

$$\min_{w,b,\xi,\xi^*} \quad \frac{1}{2}\|w\|^2 \frac{1}{2} + C\sum_{i=1}^{i}(\xi_i + \xi_i^*)$$

$$\text{s.t.} \quad \begin{cases} y_i - w^T \cdot \psi(x_i) - b \le \varepsilon + \xi_i \\ w^T \cdot \psi(x_i) + b - y_i \le \varepsilon + \psi_i^* \\ \xi_i, \xi_i^* \ge 0 \end{cases} \quad (1)$$

$$i = 1, 2, \ldots, l.$$

In formula (1), C is the penalty factor, which implements the empirical risk and confidence range of a compromise, ξ_i, ξ_i^* refer to slack variables, which, respectively, represent the ceiling and floor of training error in the epsilon zero error constraints ($|y_i - [w^T \cdot \psi(x_i) + b]| < \varepsilon$); ε refers to the error defined by insensitive cost function Vapnik-ε. The optimization problem determined by formula (1) is a typical convex quadratic programming one. According to Lagrange theory, weight vector w equals a linear combination of the training data.

$$w = \sum_{i=1}^{i}(\alpha_i - \alpha_i^*)\psi(x_i). \quad (2)$$

Substituting formula (2) into (1), we obtain predictive value of unknown point x. It can be expressed as follows:

$$f(x) = \sum_{i=1}^{l}(\alpha_i - \alpha_i^*)K(x_i, x) + b. \quad (3)$$

In (3), $K(x_i, x) = \psi(x_i) \cdot \psi(x)$ is known as the kernel function.

According to the above optimization problem, the key is the choice of kernel function. There is no general method or theory to select the optimal kernel function so far, so modeling is necessary in the practice to choose a different kernel function for specific objects based on the past experience and simulation. At present more than 10 kinds of kernel function are used. In view of the nature of the question investigated in this paper, the paper chooses Radial Basis Function (RBF) as the kernel function, whose expression is described as follows:

$$K(x, x_i) = \exp\left(\frac{\|x - x_i\|^2}{\delta^2}\right). \quad (4)$$

4. Reliability Prediction of Complex System Based on Wiener Process

Complex system performance degradation is a stochastic process. The paper chooses the Wiener process to describe the process of complex system degradation, denoted by $w(t)$ as follows:

$$w(t) = \eta t + \delta B(t), \quad t \ge 0. \quad (5)$$

The stochastic process is defined as $\{W(t)\}$. If t $>$ 0, $\{W(t)\}$ is defined as Wiener process and satisfies the following assumptions:

(i) $w(0) = 0$;

(ii) $\{w(t)\}; t > 0$ with stationary independent increments;

(iii) for any $t > 0$, $\{w(t)\}$ is normal random variable, whose mean is 0, and the variance is $\delta^2 t$.

For any $0 \le s < \infty$, $[W(t) - W(s)]$ follow Gaussian distributions $N[\eta(t-s), \delta^2(t-s)]$.

Assuming that the complex system failure threshold is w the failure time of complex system is described as follows:

$$T = \inf\{t; w(t) > w\}. \tag{6}$$

The distribution of T is

$$F_T(t) = \phi\left(\frac{\eta}{\delta}\sqrt{t} - \frac{w}{\delta\sqrt{t}}\right) + \phi\left(-\frac{\eta}{\delta}\sqrt{t} - \frac{w}{\delta\sqrt{t}}\right)\cdot e^{2\eta w/\delta^2}, \quad t > 0. \tag{7}$$

Accordingly, at this time the complex systems performance reliability is:

$$R(t) = 1 - \phi\left(\frac{\eta}{\delta}\sqrt{t} - \frac{w}{\delta\sqrt{t}}\right) - \phi\left(-\frac{\eta}{\delta}\sqrt{t} - \frac{w}{\delta\sqrt{t}}\right)\cdot e^{2\eta w/\delta^2}, \quad t > 0. \tag{8}$$

The parameters u and β are described as follows:

$$u = \frac{w}{\eta}, \quad \beta = \frac{\delta^2}{\eta^2}, \quad u > 0,\ \beta > 0, \tag{9}$$

$$F_T(t) = \Phi\left(\frac{\sqrt{t}}{\sqrt{\beta}} - \frac{u}{\sqrt{\beta}\sqrt{t}}\right) + \Phi\left(-\frac{\sqrt{t}}{\sqrt{\beta}} - \frac{u}{\sqrt{\beta}\sqrt{t}}\right)\cdot e^{2u/\beta}, \quad t > 0,\ u > 0,\ \beta > 0. \tag{10}$$

The probability distribution function is described as follows:

$$f_T(t) = \frac{u}{\sqrt{2\pi\beta t^3}} e^{-((t-u)^2/2\beta t)}, \quad t > 0,\ u > 0,\ \beta > 0. \tag{11}$$

Distribution form for the above is Inverse Gaussian, denoted as $t \sim \mathrm{IG}(\mu, \beta)$.

Assuming that $(t_1, t_2, \ldots, t_n)$ is the performance degradation samples to be observed, defining Δx as performance degradation of different time, then do the likelihood function of the probability density function of complex system life distribution, and the expression is shown as follows (12):

$$L(x, u, \beta) = \prod_{i=1}^{n} f(x_i; u, \beta) = \frac{u^n}{(2\pi\beta)^{n/2}\prod_{i=1}^{n}(x_i)^{3/2}} e^{\{-(1/2\beta)\sum_{i=1}^{n}((x_i-\mu)^2/x_i)\}}. \tag{12}$$

Evaluate partial derivative of μ, β and obtain likelihood equations:

$$\frac{\partial \ln L(x_i; \mu, \beta)}{\partial \mu} = \frac{n}{\mu} + \frac{1}{\beta}\sum_{i=1}^{n}\frac{x_i - \mu}{x_i} = 0,$$
$$\frac{\partial \ln L(x_i; \mu, \beta)}{\partial \beta} = \frac{n}{2\beta} + \frac{1}{2\beta^2}\sum_{i=1}^{n}\frac{(x_i - \mu)^2}{x_i} = 0. \tag{13}$$

To solve the likelihood equations, we can get

$$\mu = \frac{1}{n}\sum_{i=1}^{n} x_i,$$
$$\beta = \left(\frac{1}{n}\sum_{i=1}^{n} x_i\right)^2 \left(\frac{1}{n}\sum_{i=1}^{n}\frac{1}{x_i}\right) - \frac{1}{n}\sum_{i=1}^{n} x_i. \tag{14}$$

5. Case Study

Taking aircraft engine as an example, the proposed algorithm is explained. The aircraft engine performance degradation (or efficiency) usually reflects the variation of the monitoring parameters. At present aircraft engine condition monitoring mainly includes the following content.

(1) Pneumatic performance monitoring: the civil aviation engine is the core component gas path system components. Some thermodynamic parameters can reflect the state of engine performance change. The monitoring parameters are turbine gas temperature (EGT) and fuel flow (WF).

(2) Oil lubricating monitoring: the objects of oil lubricating monitoring are lubrication system components and seal system. It is useful for mechanical wear fault monitoring and diagnosis. The monitoring parameters are oil pressure (OP), oil temperature (OT), and oil consumption rate (OCR) parameters, and so forth. The changes of the parameters are useful for engine condition monitoring.

(3) Vibration monitoring: because engine rotor wear or damage will produce a certain degree of vibration signal, mechanical damage of the engine can be observed by observing the vibration of the rotor and its components, including low pressure rotor vibration value deviation (ZVB1F) and the high pressure rotor vibration value deviation (ZVB2R).

EGT overweight, WF increase, and lager ZVB1F, ZVB2R, and OCR are all the indication of aircraft engine performance decline. These indicators can be thought of as internal covariate cause of aeroengine performance decline.

Table 1 is a sample of aircraft which needs to be changed. From the 20 samples data, it can get time since installation (TSI) and flight hour (FH). The paper uses the sample data as training sample to get the relation between performance degeneration degree and condition monitoring parameters.

In Table 2, the engine monitoring information is listed. Related parameter calculation and reliability prediction are

Table 1: Key performance monitoring parameters for some aircraft engine.

Monitoring point	DEGT	GWFM	GPCN25	DPOIL	ZVBIF	ZVB2R	TSI/FH	PDD
1	4.69	2.66	1.83	−3.76	0.31	0.51	3282	0.0975
2	−0.63	4.91	2.00	−5.74	0.43	0.76	3754	0.0459
3	−5.66	3.70	1.95	−3.00	0.29	0.38	2640	0.1078
4	5.25	4.06	2.00	−5.55	0.89	0.65	4740	0.1176
5	−3.94	4.25	1.72	−8.82	0.50	0.46	1707	0.1305
⋮	⋮	⋮	⋮	⋮	⋮	⋮	⋮	⋮
16	17.41	6.03	2.08	9.26	0.29	0.33	6688	0.1892
17	3.17	4.41	2.24	9.39	0.97	0.61	1477	0.1725
18	−3.19	2.00	1.68	13.10	0.00	0.89	6376	0.1572
19	7.52	2.78	1.04	−3.24	0.45	0.99	5021	0.1665
20	4.43	3.77	2.30	−5.96	0.52	0.48	7160	0.1285

Table 2: Performance degradation assessment and reliability prediction for aircraft engine.

No.	Item										
	TSI (h)	GWFM	GPCN25	DPOIL	ZVBIF	ZVB2R	GWFM	DPP	$\widehat{\text{DPP}}$	error	$\hat{R}$
1	1422	5.2515	4.0629	2.0022	0.8911	0.6452	14.0458	0.0792	0.0826	4.29%	0.9728
2	1954	5.3187	4.2168	1.3963	0.0945	0.3609	14.9931	0.1129	0.1135	0.53%	0.9563
3	3330	17.4070	6.0285	2.0803	0.2878	0.3300	22.0301	0.1824	0.1761	−3.45%	0.9195

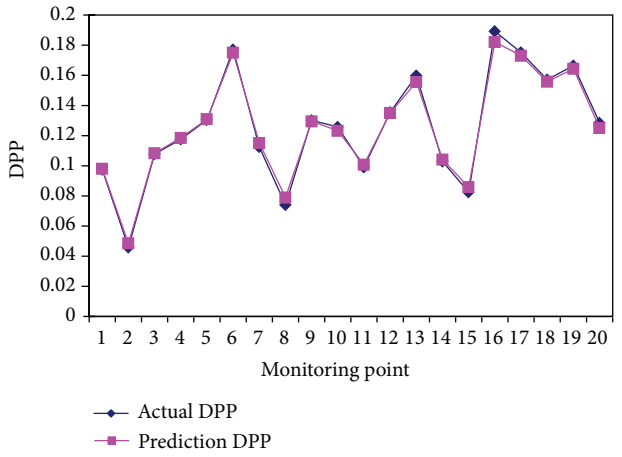

Figure 2: Training sample aircraft engine performance degradation of the actual value compared with forecast figure.

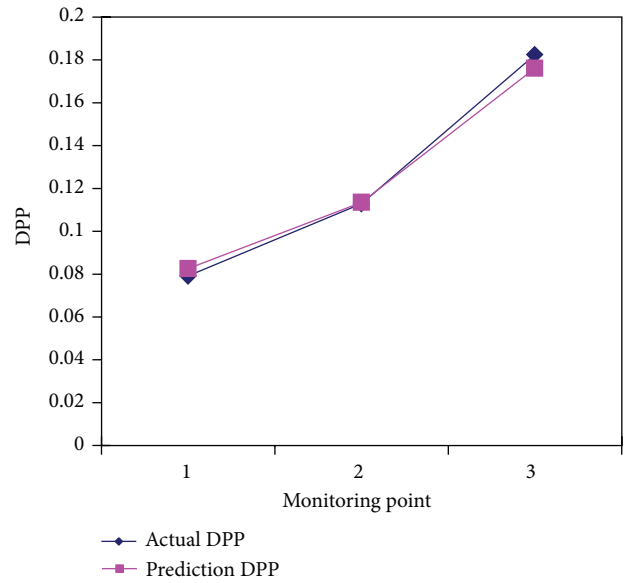

Figure 3: Real value and predictive value of a certain type of aircraft performance degradation.

also listed in Table 2. Performance degradation degree is predicted by monitoring the relationship between parameters by 20 samples. The degree of performance degradation of the actual value (performance degradation degree, PDD) is not directly collected data but calculated by Monte-Carlo simulation method according to the engine under the wing of the remaining life and reliability at a given threshold (90%) cases, when the performance degradation process conforms to the Winer stochastic process.

Using SVM method to extract the relationship between performance degradation and the monitoring parameters, the comparison between predicted values and actual values is shown in Figure 2.

Based on 20 training samples, the SVM method is used to get the relationship between monitoring parameters and the performance degradation, and the calculation results are shown in Table 2. And then compare actual performance degradation calculated by remaining life Backward Pass and the error which are shown in Table 2.

The contrast between real values and predicted values of performance degradation is shown in Figure 3.

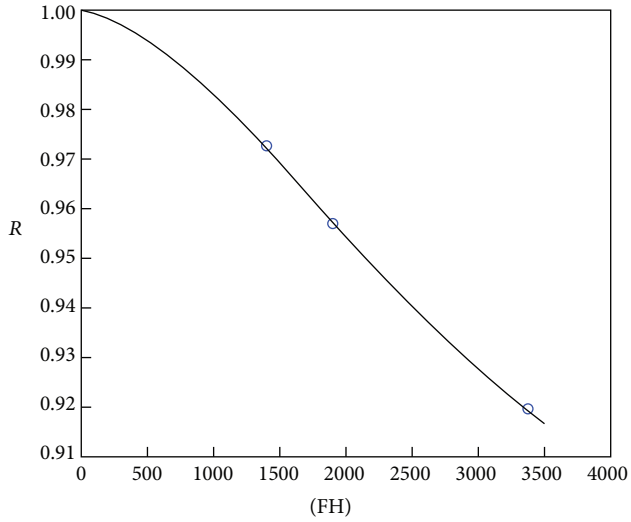

Figure 4: Performance reliability predictions for some aircraft engine.

By the formula (8), the future level of reliability can be predicted. Figure 4 indicates the performance reliability prediction curve of aeroengine. For example, if the cumulative time on wing (TSI) is 3600 flight hours, the result can be expressed as $\overline{R}(3600) = 0.9167$.

The research focuses on exploit condition monitoring to access reliability in the paper at present. The further research will expand to operational reliability assessments of data driven in order to probe more comprehensive data utilization technologies and methods. The further research can expand to design field. The information on operational reliability assessment can be fed back to design process and analyze the influence. It is necessary to enhance the abstraction of related information for sensitive parameters in design process. On the contrary, the data collection demand of sensitive parameters can be reduced. Some scholars have already done some research on it. For example, Yin et al. [19] made a comparison research on basic data-driven methods for process monitoring and fault diagnosis. Yin et al. [20] presented two online schemes for an integrated design of fault-tolerant control systems with application to Tennessee benchmark.

In further, the research on condition monitoring and operational reliability of system integration will be developed.

6. Conclusion

By support vector machine (SVM) method and condition monitoring information, aviation engine performance degradation is evaluated. The result will be used as input variables of the reliability analysis model. Aircraft engine performance degradation process is described by the use of the Winer process in order to forecast aeroengine performance reliability using condition monitoring information. The method integrates the performance monitoring and reliability analysis into one framework, making full use of a variety of condition monitoring information, and so the result is more accurate. Though much research has been done about this method, more studies are needed.

Acknowledgments

This work was supported by the National Natural Science Foundation of China and Civil Aviation Administration of China (no. U1333117), China Postdoctoral Science Foundation (no. 2012M511275), and The Basic Service Foundation of Nanjing University of Aeronautics and Astronautics (no. NS2013067).

References

[1] H. Lu, W. J. Kolarik, and S. S. Lu, "Real-time performance reliability prediction," *IEEE Transactions on Reliability*, vol. 50, no. 4, pp. 353–357, 2001.

[2] A. H. Elwany and N. Z. Gebraeel, "Sensor-driven prognostic models for equipment replacement and spare parts inventory," *IIE Transactions*, vol. 40, no. 7, pp. 629–639, 2008.

[3] J.-A. Li, Y. Wu, K. K. Lai, and K. Liu, "Reliability estimation and prediction of multi-state components and coherent systems," *Reliability Engineering and System Safety*, vol. 88, no. 1, pp. 93–98, 2005.

[4] R. B. Chinnam, "On-line reliability estimation for individual components using statistical degradation signal models," *Quality and Reliability Engineering International*, vol. 18, no. 1, pp. 53–73, 2002.

[5] A. H. Christer, W. Wang, and J. M. Sharp, "A state space condition monitoring model for furnace erosion prediction and replacement," *European Journal of Operational Research*, vol. 101, no. 1, pp. 1–14, 1997.

[6] R. M. Bharadwaj and A. G. Parlos, "Neural state filtering for adaptive induction motor speed estimation," *Mechanical Systems and Signal Processing*, vol. 17, no. 5, pp. 903–924, 2003.

[7] C. Chen, G. Vachtsevanos, and M. E. Orchard, "Machine remaining useful life prediction: an integrated adaptive neuro-fuzzy and high-order particle filtering approach," *Mechanical Systems and Signal Processing*, vol. 28, pp. 597–607, 2012.

[8] Z. Bosnić and I. Kononenko, "Comparison of approaches for estimating reliability of individual regression predictions," *Data and Knowledge Engineering*, vol. 67, no. 3, pp. 504–516, 2008.

[9] P. Wang and D. W. Coit, "Reliability prediction based on degradation modeling f or system s with multiple deggradation measures," *Reliability and Maintainability*, vol. 78, no. 3, pp. 302–307, 2004.

[10] Z. Xu, Y. Ji, and D. Zhou, "Real-time reliability prediction for a dynamic system based on the hidden degradation process identification," *IEEE Transactions on Reliability*, vol. 57, no. 2, pp. 230–242, 2008.

[11] S. Lu, H. Lu, and W. J. Kolarik, "Multivariate performance reliability prediction in real-time," *Reliability Engineering and System Safety*, vol. 72, no. 1, pp. 39–45, 2001.

[12] Z. Xu, Y. Ji, and D. Zhou, "A new real-time reliability prediction method for dynamic systems based on on-line fault prediction," *IEEE Transactions on Reliability*, vol. 58, no. 3, pp. 523–538, 2009.

[13] A. Hernando, J. Bobadilla, F. Ortega, and J. Tejedor, "Incorporating reliability measurements into the predictions of a recommender system," *Information Sciences*, vol. 218, pp. 1–16, 2013.

[14] G.-D. Li, S. Masuda, D. Yamaguchi, and M. Nagai, "A new reliability prediction model in manufacturing systems," *IEEE Transactions on Reliability*, vol. 59, no. 1, pp. 170–177, 2010.

[15] C.-H. Hu, X.-S. Si, and J.-B. Yang, "System reliability prediction model based on evidential reasoning algorithm with nonlinear optimization," *Expert Systems with Applications*, vol. 37, no. 3, pp. 2550–2562, 2010.

[16] M. D. C. Moura, E. Zio, I. D. Lins, and E. Droguett, "Failure and reliability prediction by support vector machines regression of time series data," *Reliability Engineering and System Safety*, vol. 96, no. 11, pp. 1527–1534, 2011.

[17] S. Lolas and O. A. Olatunbosun, "Prediction of vehicle reliability performance using artificial neural networks," *Expert Systems with Applications*, vol. 34, no. 4, pp. 2360–2369, 2008.

[18] C.-H. Hu, X.-S. Si, and J.-B. Yang, "System reliability prediction model based on evidential reasoning algorithm with nonlinear optimization," *Expert Systems with Applications*, vol. 37, no. 3, pp. 2550–2562, 2010.

[19] S. Yin, S. X. Ding, A. Haghani et al., "A comparison study of basic data-driven fault diagnosis and process monitoring methods on the benchmark Tennessee Eastman Process," *Journal of Process Control*, vol. 22, no. 9, pp. 1567–1581.

[20] S. Yin, H. Luo, and S. X. Ding, "Real time implementation of fault-tolerant control systems with performance optimization," *IEEE Transactions on Industrial Electronics*, 2013.

Hindawi Publishing Corporation
Mathematical Problems in Engineering
Volume 2013, Article ID 650354, 8 pages
http://dx.doi.org/10.1155/2013/650354

Research Article

Active Control of Oscillation Patterns in the Presence of Multiarmed Pitchfork Structure of the Critical Manifold of Singularly Perturbed System

Robert Vrabel, Marcel Abas, Michal Kopcek, and Michal Kebisek

Faculty of Materials Science and Technology, Slovak University of Technology in Bratislava, Hajdoczyho 1, 917 01 Trnava, Slovakia

Correspondence should be addressed to Robert Vrabel; robert.vrabel@stuba.sk

Received 2 September 2013; Revised 22 September 2013; Accepted 23 September 2013

Academic Editor: Hamid Reza Karimi

We analyze the possibility of control of oscillation patterns for nonlinear dynamical systems without the excitation of oscillatory inputs. We propose a general method for the partition of the space of initial states to the areas allowing active control of the stable steady-state oscillations. Furthermore, we show that the frequency of oscillations can be controlled by an appropriately positioned parameter in the mathematical model. This paper extends the knowledge of the nature of the oscillations with emphasis on its consequences for active control. The results of the analysis are numerically verified and provide the feedback for further design of oscillator circuits.

1. Introduction

Control of oscillations is a practically important problem in many technical applications (see e.g. [1, 2]), which can generally be stated in terms of two different objectives.

(a) To obtain an asymptotically stable zero solution which attracts all initial conditions in a suitably large region (regulator problem [3]).

(b) To obtain an asymptotically stable periodic solution with desired properties (such as oscillation at the given amplitudes and frequencies) and which attracts all initial states in a suitably large region (oscillator problem).

In this context, usually two-well potential of an unperturbed system was considered by using analytic methods and numerical simulations, (see, e.g., [4–6] and the references therein).

Also, in many biological systems, some form of oscillation control is needed to track the constantly changing resonant frequency or to tune it to a specified frequency while keeping the amplitude constant [7–9].

For example, in [10], the oscillation patterns were analyzed by the symmetric Hopf bifurcation theory applying group theory. Recently, in [11], the oscillation patterns of the bifurcating periodic oscillations of three coupled Van der Pol oscillators were studied.

To our knowledge, no paper exists addressing the question of active control of oscillation patterns for the dynamical systems with potential with multiwell and multibarrier structure. For example, the two-armed pitchfork bifurcation in the presence of Hopf bifurcation in the context of double magneto convection was numerically studied in the work [12]. In the paper [13], the problem of output stability for systems under the oscillatory excitation via Lyapunov approach was analyzed.

The analysis of behavior patterns is of high importance to uncover real-time threats in the industrial systems and to plan a predictive maintenance program. Recently, Yin et al. [14] proposed two online schemes for the fault-tolerant architecture for the purpose of fault-tolerant control. One is a gradient based iterative tuning scheme for the online optimization of the system performance, and the other is an adaptive residual generator scheme for the online identification of the abnormal change of the system parameters.

There are several approaches to the topic of vibration control in industrial equipment; for example, in the work [15], the symbolic computation systems are presented with the

purpose of analyzing the spectrum and waveform vibration allowing bearing defects in low-speed machines via dynamic modeling of patterns of behavior. The paper [16] provides a comparison study on the basic data-driven methods for process monitoring and fault diagnosis. Most recently, in the paper by Palacios-Quinonero et al. [17] by using an approach based on the connected control method, active-passive structural vibration control strategies for seismic protection of multibuilding systems are designed and applied on the proposed linear mathematical model of connected multistructure mechanical systems.

The method we propose could provide the mechanical engineers the mathematical tool for an accurate diagnosis in the vibration analysis and thus prevent or predict future failures of industrial systems. The main advantage of our approach—an analysis of the time-reverse differential equations associated with the problem under consideration—over methods mentioned above lies in its straightforward extension to nonlinear models (continuous and discrete) with time-delay; for the topic, see, e.g., [18–20].

In this paper, we focus our attention on the proof of the existence and the possibility of active control of stable steady-state nonlinear oscillations in the dynamical system describing the singularly perturbed undamped oscillator with a continuous nonlinear restoring force and without the excitation of oscillatory inputs:

$$\begin{aligned} \epsilon^2 y'' + f(t, y) &= 0, \\ y(-\delta) = y_0, \qquad y'(-\delta) &= y_1, \end{aligned} \tag{1}$$

where

$$f(t, y) = \begin{cases} y^{4n+1} & \text{for } t \in [-\delta, 0] \\ y\prod_{i=1}^{2n}\left(y^2 - \left(\dfrac{\mu i h(T) t}{T}\right)^2\right) & \text{for } t \in [0, T] \\ y\prod_{i=1}^{2n}\left(y^2 - \mu^2 i^2 h^2(t)\right) & \text{for } t \in [T, \infty), \end{cases} \tag{2}$$

$[y_0, y_1]$ is an initial state, $y_\epsilon(\cdot, y_0, y_1)$ is a direct output, h is a positive continuous function on $[T, \infty]$, $n \in N$, $\delta > 0$, $T > 0$, and ϵ, $0 < \epsilon \ll 1$ is a singular perturbation parameter. It is instructive for future reference to keep in mind the symmetric manifold $f(t, y) = 0$ (Figure 1). The parameter $\mu > 0$ is a constant determining the distance between pitchfork arms for $t \geq T$, and without loss of generality, we will assume that $\mu = 1$.

Rewriting (1) to an equivalent system of three first order autonomous equations, we obtain

$$\begin{aligned} \epsilon y' &= w \\ \epsilon w' &= -f(t, y) \\ t' &= 1 \end{aligned} \tag{3}$$

$$y(-\delta) = y_0, \qquad w(-\delta) = \epsilon y_1. \tag{4}$$

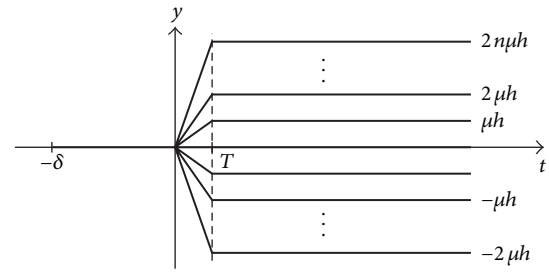

Figure 1: The multiarmed pitchfork manifold $f(t, y) = 0$.

We show that the nonlinear system described by differential equation from (1) can basically exhibit two distinct types of steady-state oscillations, namely.

(i) In-well, small orbit dynamics, where the system state remains within the potential well centered at a stable equilibrium point (center).

(ii) Cross-well, large orbit dynamics, whose trajectories surround the $4n + 1$ equilibrium points (the saddles between centers).

The results of the analysis will be numerically verified and provide valuable insights into dynamics of the control system under consideration.

Further, we show that the singular perturbation parameter ϵ plays role modeling tool for the frequency control of the nonlinear oscillations arising in these systems. Another objective of this paper is to divide the space $\mathbb{E}^2$ of initial states $[y_0, y_1]$ to the areas of stability $A_{-n}(\epsilon)$, $\ldots, A_{-2}(\epsilon), A_{-1}(\epsilon), A_0(\epsilon), A_1(\epsilon), A_2(\epsilon), \ldots, A_n(\epsilon), A_i(\epsilon) \subset \mathbb{E}^2$, $i = -n, \ldots, 0, \ldots, n$ such that for $[y_0, y_1] \in A_i(\epsilon)$ solution of (1) oscillate around $2ih(t)$, $i = -n \ldots, 0, \ldots, n$ and

$$y_\epsilon(t) \in \begin{cases} ((2i-1)h(t), \infty) & \text{for } i = n \\ ((2i-1)h(t), (2i+1)h(t)) & \text{for } i = -(n-1)\ldots, \\ & \qquad 0, \ldots, (n-1) \\ (-\infty, (2i+1)h(t)) & \text{for } i = -n \end{cases} \tag{5}$$

for $t \geq T$.

Finally, we prove that the solutions y_ϵ of (1) will rapidly oscillate for $t \geq T$ with the frequency of the oscillations increasing without bound as $\epsilon \to 0^+$.

System (3) is an example of a singularly perturbed system, because in the limit $\epsilon \to 0^+$, it does not reduce to a differential equation of the same type, but to an algebraic-differential reduced system

$$\begin{aligned} 0 &= w \\ 0 &= -f(t, y) \\ t' &= 1. \end{aligned} \tag{6}$$

Another way to study the singular limit $\epsilon \to 0^+$ is by introducing the new independent variable $\tau = t/\epsilon$ which transforms (3) to the system

$$\begin{aligned} \frac{dy}{d\tau} &= w \\ \frac{dw}{d\tau} &= -f(t,y) \\ \frac{dt}{d\tau} &= \epsilon. \end{aligned} \tag{7}$$

Taking the limit $\epsilon \to 0^+$, we obtain the so-called associated system [21]

$$\frac{dy}{d\tau} = w \tag{8}$$

$$\frac{dw}{d\tau} = -f(t,y) \tag{9}$$

$$\frac{dt}{d\tau} = 0 \quad \text{that is, } t = t^* = \text{constant}, \tag{10}$$

in which t plays the role of a parameter.

Both scalings agree on the level of phase space structure when $\epsilon \neq 0$ but offer very different perspectives since they differ significantly in the limit when $\epsilon = 0$. The main goal of singular perturbation theory is to use these limits to understand structure in the full system when $\epsilon \neq 0$.

The critical manifold S is defined as a solution of the reduced system; that is,

$$S := \{(t,y,w) : t \in \langle -\delta, \infty), f(t,y) = 0, w = 0\}, \tag{11}$$

which corresponds to a set of equilibria for the associated system (8)–(10).

2. Multiarmed Pitchfork Bifurcation of Associated System at $t^* = 0$

Without loss of generality, we will assume hereafter that $n = 1$.

Then, the equations

$$f(t,y) = 0, \qquad w = 0 \tag{12}$$

have one solution for y, w if $t^* \in [-\delta, 0]$ and five if $t^* \in (0, \infty)$; that is, the critical manifold is a multiarmed pitchfork manifold. Due to the fact that the eigenvalues of the Jacobian are

$$\lambda(t^*, y, w) = \pm\sqrt{-\frac{\partial f}{\partial y}(t^*, y)}, \tag{13}$$

the associated system (8), (9), and $t = t^* = \text{const}$ has, for $n = 1$, one equilibrium (degenerate center with a double zero eigenvalue) for $t^* \in (-\delta, 0)$ and five equilibria (two saddles and three centers) for $t^* \in (0, \infty)$. Thus, the two pieces of critical manifold S corresponding to the saddles of associated system (8)–(10) are the normally hyperbolic submanifolds [21].

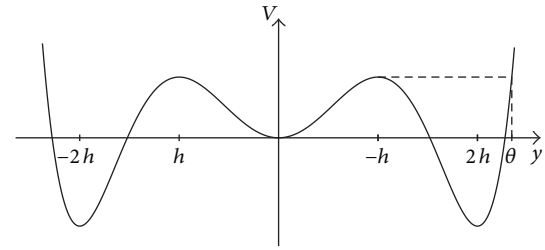

Figure 2: Potential profile V with $h(t) \equiv \text{const}$, $n = 1$, and $\mu = 1$ for $t \geq T$. $V(t,y) = V(y)$.

Consider the total energy functional

$$\begin{aligned} H(t,y,w) &= \frac{1}{2}w^2 + V(t,y), \\ V(t,y) &= \int_0^y f(t,s)\,ds \end{aligned} \tag{14}$$

with potential $V(t,y)$ with multibarrier and multiwell structure (for $n = 1$, see Figure 2).

We use the level surfaces $H(t,y,w) = H(t)$ of H on $[-\delta, \infty)$ to characterize the trajectories of (3). These surfaces in (t,y,w)-space are defined by

$$w = \pm\left(2\left(H(t) - V(t,y)\right)\right)^{1/2}, \tag{15}$$

extending it as long as w remains real. In our case, such trajectories, lying on the surface $w = w(t,y,\epsilon)$, are bounded for every small ϵ. On the interval $[-\delta, 0]$, there is a motion in a single potential well and on the interval $[0, \infty)$, triple well with a barrier in between.

Computing the derivative of H along the solution of (3) ($n = 1$, for $n > 1$, we proceed analogously), we obtain for $t \geq T$

$$\begin{aligned} H'(t) &= w_\epsilon(t)\, w_\epsilon'(t) + f(t, y_\epsilon(t))\, y_\epsilon'(t) \\ &\quad + \int_0^{y_\epsilon(t)} \frac{\partial f}{\partial t}(t,s)\,ds \\ &= 8h(t)\,h'(t)\,y_\epsilon^2(t)\left(h^2(t) - \frac{5}{16}y_\epsilon^2(t)\right). \end{aligned} \tag{16}$$

For potential profile ($t \geq T$), we have

$$\begin{aligned} \frac{\partial V}{\partial t}V(t,0) &= 0, \\ \frac{\partial V}{\partial t}V(t, \pm 2h(t)) &= -8h'(t)\,h^5(t), \\ \frac{\partial V}{\partial t}V(t, \pm h(t)) &= \frac{11}{2}h'(t)\,h^5(t). \end{aligned} \tag{17}$$

As follows from computation above, $h(t) \equiv \text{const} \neq 0$ is a sufficient condition for the existence of nonlinear steady-state oscillations (constant amplitude). In this case, $H(t) = \text{const}$ and $V(t,y) \equiv V(T,y)$ for $t \geq T$.

To characterize input-output relationships, we determine the areas $A_{-1}(\epsilon)$, $A_0(\epsilon)$, $A_1(\epsilon)$ of initial states y_0, y_1 at the

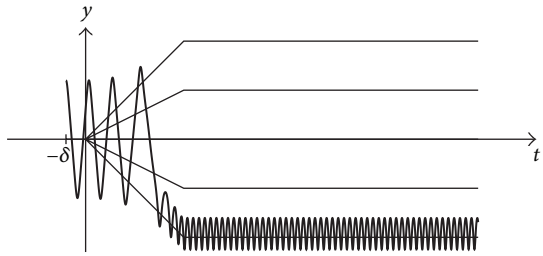

Figure 3: Numerical solution of $\epsilon^2 y'' + f(t, y) = 0$, $y(-\delta) = y_0$, and $y'(-\delta) = y_1$ with $[y_0, y_1] = [1.2, 0] \in A_{-1}(\epsilon)$ and $n = 1$, $h(t) \equiv 1$, $\mu = 1$, $\delta = 0.1$, $T = 0.5$, and $\epsilon = 0.02$.

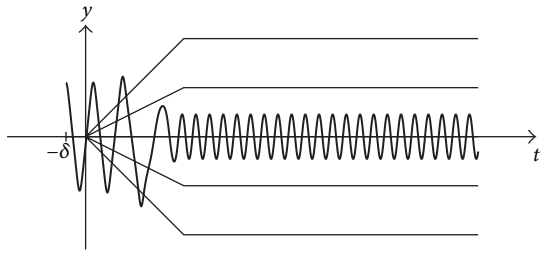

Figure 4: Numerical solution of $\epsilon^2 y'' + f(t, y) = 0$, $y(-\delta) = y_0$, and $y'(-\delta) = y_1$ with $[y_0, y_1] = [1.1, 0] \in A_0(\epsilon)$ and $n = 1$, $h(t) \equiv 1$, $\mu = 1$, $\delta = 0.1$, $T = 0.5$, and $\epsilon = 0.02$.

point $t = -\delta$ by solving associated time-reverse initial value problem

$$\begin{aligned} \epsilon^2 \widetilde{y}'' + f\left(T - t, \widetilde{y}\right) &= 0, \quad t \geq 0 \\ \widetilde{y}(0) &= \widetilde{y}_0, \\ \widetilde{y}'(0) &= \pm\epsilon^{-1}\sqrt{2\left(H(T) - V\left(T, \widetilde{y}_0\right)\right)}, \end{aligned} \tag{18}$$

allowing a specific switching strategy between oscillation patterns.

Let us denote θ_i the real roots of the six-order algebraic equation $V(T, y) = H(T)$.

Thus, taking into consideration the definition of the sets $A_i(\epsilon)$ and the profile of potential V at $t = T$, we obtain

$$\begin{aligned} A_{-1}(\epsilon) = \Big\{\Big[\widetilde{y}_\epsilon(T+\delta), -\widetilde{y}'_\epsilon(T+\delta)\Big] :\ & \widetilde{y}_\epsilon(t) \text{ is a solution of } (18), \\ & \text{where } H(T) \in \left(V(T, \pm 2h), V(T, \pm h)\right), \\ & \widetilde{y}_0 \in [\theta_1, \theta_2], \theta_1 < \theta_2 < -h\Big\}, \\ A_0(\epsilon) = \Big\{\Big[\widetilde{y}_\epsilon(T+\delta), -\widetilde{y}'_\epsilon(T+\delta)\Big] :\ & \widetilde{y}_\epsilon(t) \text{ is a solution of } (18), \\ & \text{where } H(T) \in \left(0, V(T, \pm h)\right), \\ & \widetilde{y}_0 \in [\theta_3, \theta_4], -h < \theta_3 < \theta_4 < h\Big\}, \end{aligned}$$

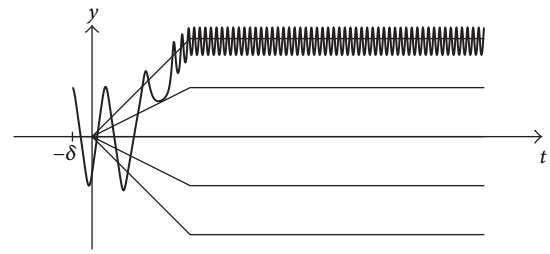

Figure 5: Numerical solution of $\epsilon^2 y'' + f(t, y) = 0$, $y(-\delta) = y_0$, and $y'(-\delta) = y_1$ with $[y_0, y_1] = [1, 0] \in A_1(\epsilon)$ and $n = 1$, $h(t) \equiv 1$, $\mu = 1$, $\delta = 0.1$, $T = 0.5$, and $\epsilon = 0.02$.

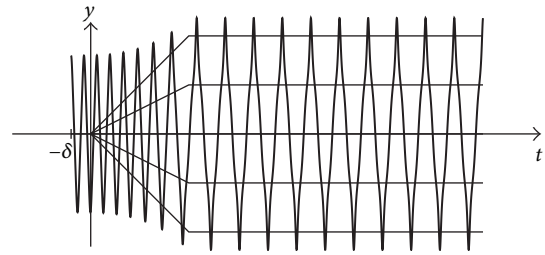

Figure 6: Numerical solution of $\epsilon^2 y'' + f(t, y) = 0$, $y(-\delta) = y_0$, and $y'(-\delta) = y_1$ with $[y_0, y_1] = [1.6, 0] \in A_{\text{all}}(\epsilon)$ and $n = 1$, $h(t) \equiv 1$, $\mu = 1$, $\delta = 0.1$, $T = 0.5$, and $\epsilon = 0.02$.

$$\begin{aligned} A_1(\epsilon) = \Big\{\Big[\widetilde{y}_\epsilon(T+\delta), -\widetilde{y}'_\epsilon(T+\delta)\Big] :\ & \widetilde{y}_\epsilon(t) \text{ is a solution of } (18), \\ & \text{where } H(T) \in \left(V(T, \pm 2h), V(T, \pm h)\right), \\ & \widetilde{y}_0 \in [\theta_5, \theta_6], h < \theta_5 < \theta_6\Big\}. \end{aligned} \tag{19}$$

The Figures 3, 4, and 5 demonstrate all types of oscillations patterns for (1) with the initial values from $A_i(\epsilon)$, $i = -1, 0, 1$, respectively.

Let

$$\begin{aligned} A_{\text{all}}(\epsilon) = \Big\{\Big[\widetilde{y}_\epsilon(T+\delta), -\widetilde{y}'_\epsilon(T+\delta)\Big] :\ & \widetilde{y}_\epsilon(t) \text{ is a solution of } (18), \\ & \text{where } H(T) \in \left(V(T, \pm h), \infty\right), \\ & \widetilde{y}_0 \in [\theta_1, \theta_2]\Big\}. \end{aligned} \tag{20}$$

Then, the solutions of (1) with $[y_0, y_1] \in A_{\text{all}}(\epsilon)$ surround all pitchfork arms for $t > T$ (Figure 6). For analysis of this type of oscillations for double-well potential profile in more detail, see [22]. The selected points of the sets A_{-1}, A_0, A_1, and A_{all} are depicted on the Figure 7.

On the basis of the Kneser and Fukuhara theory, the sets $\overline{A_i(\epsilon)}$, $i = -1, 0, 1$, are continua (i.e., the bounded and connected sets), and A_{all} is connected in $\mathbb{E}^2$ where the overline denotes the closure of a set in the standard topology of $\mathbb{E}^2$. Obviously,

(1) $\{\bigcap A_i(\epsilon) : i = -1, 0, 1, \text{all}\} = \emptyset$

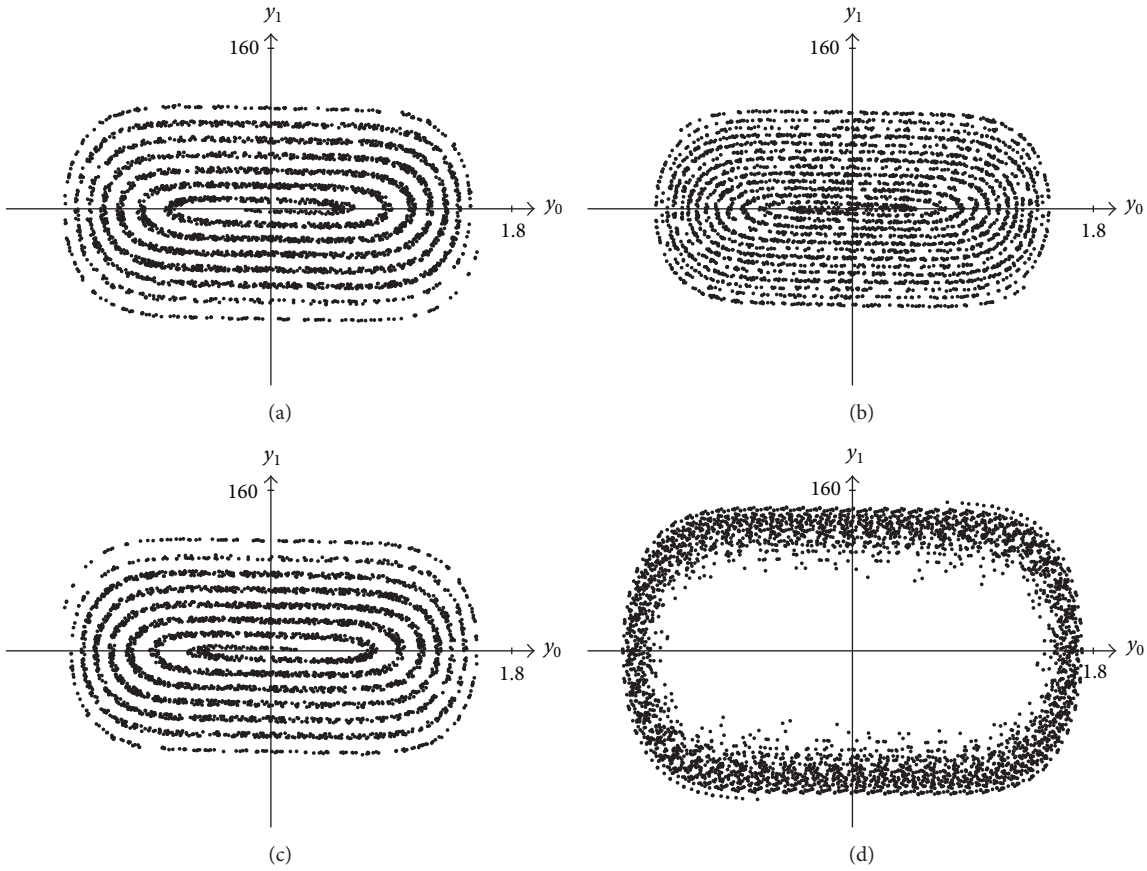

FIGURE 7: The selected points of the spiral-shaped sets A_{-1}, A_0, A_1, and A_{all} for $n = 1$, $h(t) \equiv 1$, $\mu = 1$, $\delta = 0.1$, $T = 0.5$, and $\epsilon = 0.02$ (from (a) to (d)).

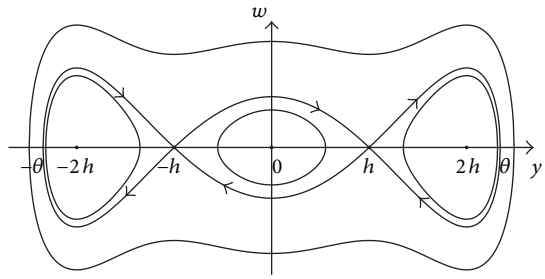

FIGURE 8: The phase portrait of system (3) for $t \geq T$ with $h(t) \equiv$ const and $n = 1$. The solutions of (1) lying in the time $t = T$ on the orbits with arrows are nonoscillatory, and $\lim_{t \to \infty} y_\epsilon(t) = h$ or $-h$.

(2) $\{\bigcup \overline{A_i(\epsilon)} : i = -1, 0, 1, \text{all}\} = \mathbb{E}^2$
for every $\epsilon > 0$.

Also, as a consequence of the oddness of the function f in the variable y for every fixed $t \in [-\delta, \infty)$, we have

(1) $A_i(\epsilon) = -A_{-i}(\epsilon)$, $i \neq 0, \text{all}$

(2) $A_0(\epsilon)$ and $A_{\text{all}}(\epsilon)$ are symmetric about the origin
for every $\epsilon > 0$.

3. Nonoscillatory Solutions

We note that there also exists for $h(t) \equiv$ const a family of the nonoscillatory solutions of (1) for $t \geq T$ with $[y_0, y_1] \in A_{\text{non-osc}}(\epsilon)$ where for $n = 1$

$$A_{\text{non-osc}}(\epsilon) = \left\{ \left[\widetilde{y}_\epsilon (T + \delta), -\widetilde{y}'_\epsilon (T + \delta) \right] : \widetilde{y}_\epsilon (t) \text{ is a solution of (18) with either} \right.$$

(1) $\widetilde{y}_0 = 0$, $H(T) = 0$ or

(2) $\widetilde{y}_0 = \pm h$, $H(T) = V(T, \pm h)$ or

(3) $\widetilde{y}_0 = \pm 2h$, $H(T) = V(T, \pm 2h)$ or

$$\left. H(T) = V(T, \pm h), \widetilde{y}_0 \in [-\theta, \theta], \widetilde{y}_0 \neq \pm h \right\}. \tag{21}$$

In order to facilitate the understanding of the dynamics of dynamical system (3) after the time T, we drew the Figures 8, 9, 10, 11, and 12.

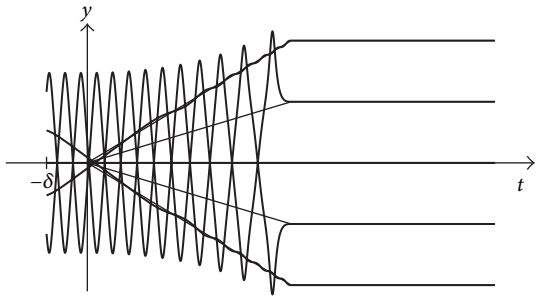

Figure 9: Five solutions ($n = 1$) of (1) with (1) $\tilde{y}_0 = 0$ and $H(T) = 0$ ($y_\epsilon(t) = 0$ on $[-\delta, \infty]$), (2) $\tilde{y}_0 = \pm h$ and $H(T) = V(T, \pm h)$, and (3) $\tilde{y}_0 = \pm 2h$ and $H(T) = V(T, \pm 2h)$.

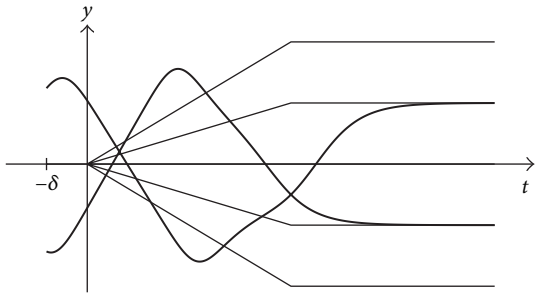

Figure 10: Two of infinitely many solutions of (1) with $\tilde{y}_0 \in (-h, h)$ and $H(T) = V(T, \pm h)$.

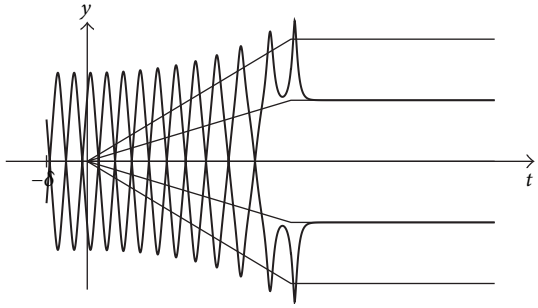

Figure 11: Two of infinitely many solutions of (1) with $H(T) = V(T, \pm h)$ and either $\tilde{y}_0 \in (h, \theta)$, $\tilde{y}'(0) < 0$ or $\tilde{y}_0 \in (-\theta, -h)$, $\tilde{y}'(0) > 0$.

4. Frequency Control of Nonlinear Oscillations

In this section, using the appropriate changes of coordinates, we show that the singular perturbation parameter ϵ plays role modeling tool for control of frequencies of nonlinear oscillations. We will analyze the case $[y_0, y_1] \in A_1(\epsilon)$ only. For the other cases, we proceed in a similar way.

From the theory above, it follows that the solution of (1), $[y_0, y_1] \in A_1(\epsilon)$ will oscillate around the half-line $y = 2h$ for $t \geq T$ (Figure 5).

Let us put $y = 2h + r(t)\cos\gamma(t)$ and $w = -r(t)\sin\gamma(t)$ for $t \geq T$. Due to requirement of steady-state oscillations,

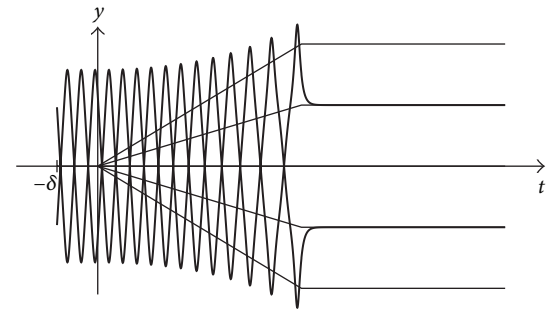

Figure 12: Two of infinitely many solutions of (1) with $H(T) = V(T, \pm h)$ and either $\tilde{y}_0 \in (h, \theta)$, $\tilde{y}'(0) > 0$ or $\tilde{y}_0 \in (-\theta, -h)$, $\tilde{y}'(0) < 0$.

$h(t) \equiv \text{const}$, and consequently, $f(t, y) = f(y)$ for $t \geq T$. Thus,

$$\begin{aligned} y' = \frac{w}{\epsilon} &\Longrightarrow r'\cos\gamma - r\gamma'\sin\gamma = -\frac{r}{\epsilon}\sin\gamma \\ w' = -\frac{f(y)}{\epsilon} &\Longrightarrow -r'\sin\gamma - r\gamma'\cos\gamma = -\frac{f(y)}{\epsilon}. \end{aligned} \tag{22}$$

Multiplying these equations by $\sin\gamma$, $\cos\gamma$, respectively, and after algebraic manipulations, we finally obtain the following differential equation for γ:

$$\gamma' = \frac{1}{\epsilon}\left[\sin^2\gamma + \overline{f}(y)\cos^2\gamma\right], \tag{23}$$

where

$$\begin{aligned} \overline{f}(y) &= \frac{f(y)}{y - 2h}, \\ \overline{f}(2h) &= \frac{\mathrm{d}f}{\mathrm{d}y}(2h). \end{aligned} \tag{24}$$

Denote by θ the root of equation $V(T, y) = V(T, h)$ such that $\theta > h$ (see Figure 2) and let

$$\begin{aligned} \alpha_\Gamma &= \min\left\{\sin^2\gamma + \overline{f}(y)\cos^2\gamma : y \in \Gamma, \gamma \in [0, 2\pi]\right\} \\ \beta_\Gamma &= \max\left\{\sin^2\gamma + \overline{f}(y)\cos^2\gamma : y \in \Gamma, \gamma \in [0, 2\pi]\right\}, \end{aligned} \tag{25}$$

where $\Gamma \subset (h, \theta)$ is a continuum depending on the constant amplitude of oscillations. Obviously, these nonzero values exist because of positivity of function $\overline{f}$ on Γ. Hence,

$$\frac{\alpha_\Gamma}{\epsilon} \leq \gamma' \leq \frac{\beta_\Gamma}{\epsilon}. \tag{26}$$

Now, let us denote by s the spacing between two successive zeros of $y_\epsilon(t) - 2h$ on $[T, \infty)$, where $y_\epsilon(t)$ is a solution of (1) with $[y_0, y_1] \in A_1(\epsilon)$. Then, integrating the inequality (26)

with respect to the variable t between two successive zeros of $y - 2h$, we immediately obtain

$$\begin{aligned}\int_{(j)\text{th zero}}^{(j+1)\text{th zero}} \frac{\alpha_\Gamma}{\epsilon}\mathrm{d}t &\leq \int_{(j)\text{th zero}}^{(j+1)\text{th zero}} \gamma'\mathrm{d}t \\ &\leq \int_{(j)\text{th zero}}^{(j+1)\text{th zero}} \frac{\beta_\Gamma}{\epsilon}\mathrm{d}t \\ \frac{\alpha_\Gamma}{\epsilon}s \leq \pi \leq \frac{\beta_\Gamma}{\epsilon}s.\end{aligned} \tag{27}$$

Hence,

$$\frac{\pi}{\beta_\Gamma}\epsilon \leq s \leq \frac{\pi}{\alpha_\Gamma}\epsilon; \tag{28}$$

that is, the frequency of oscillations increases without bound for ϵ tending to zero. As a consequence of the inequality (28) and the definition of the constant α_Γ, we note that for a fixed value of parameter ϵ, the greater amplitude of oscillations leads to the lower frequency of oscillations.

The data for Figures 3–12 have been worked out with the computer system MAXIMA [23, 24]. The computer code is available from the authors upon request.

5. Conclusions

In this paper, a novel technique to active control of the oscillation patterns and their frequencies for nonlinear dynamical systems with initial condition is proposed. The method is based on solving the time-reverse differential equation on a particular interval. The analytical results are numerically simulated by employing the computer system MAXIMA. The ideas of this paper may be naturally extended and adapted to wide class of the systems to find the basins for different patterns of systems behavior and may be employed without any principal limitation.

References

[1] A. L. Fradkov and A. Y. Pogromsky, *Introduction to Control of Oscillations and Chaos*, World Scientific, River Edge, NJ, USA, 1998.

[2] J. Guckenheimer and P. Holmes, *Nonlinear Oscillations, Dynamical Systems, and Bifurcations of Vector Fields*, Springer, New York, NY, USA, 1983.

[3] S. Park, C.-W. Tan, H. Kim, and S. K. Hong, "Oscillation control algorithms for resonant sensors with applications to vibratory gyroscopes," *Sensors*, vol. 9, no. 8, pp. 5952–5967, 2009.

[4] S. Lenci and G. Rega, "Optimal control of nonregular dynamics in a duffing oscillator," *Nonlinear Dynamics*, vol. 33, no. 1, pp. 71–86, 2003.

[5] A. H. Nayfeh and D. T. Mook, *Nonlinear Oscillations, Pure and Applied Mathematics*, Wiley-Interscience, New York, NY, USA, 1979.

[6] E. Tamaseviciute, A. Tamasevicius, G. Mykolaitis, S. Bumeliene, and E. Lindberg, "Analogue electrical circuit for simulation of the Duffing-Holmes equation," *Nonlinear Analysis: Modelling and Control*, vol. 13, no. 2, pp. 241–252, 2008.

[7] D. E. Nelson, A. E. C. Ihekwaba, M. Elliott et al., "Oscillations in NF-κB signaling control the dynamics of gene expression," *Science*, vol. 306, no. 5696, pp. 704–708, 2004.

[8] T. Williamson, D. Adiamah, J. -M. Schwartz, and L. Stateva, "Exploring the genetic control of glycolytic oscillations in *Saccharomyces cerevisiae*," *BMC Systems Biology*, vol. 6, article 108, 2012.

[9] Z. Zhang, F. Xu, Z. Liu, R. Wang, and T. Wen, "MicroRNA-mediated regulation in biological systems with oscillatory behavior," *BioMed Research International*, vol. 2013, Article ID 285063, 7 pages, 2013.

[10] A. Takamatsu, R. Tanaka, T. Yamamoto, and T. Fujii, "Control of oscillation patterns in a symmetric coupled biological oscillator system," in *Proceedings of the AIP Conference*, pp. 230–235, 2003.

[11] Y. Song, J. Xu, and T. Zhang, "Bifurcation, amplitude death and oscillation patterns in a system of three coupled van der Pol oscillators with diffusively delayed velocity coupling," *Chaos*, vol. 21, no. 2, Article ID 023111, 2011.

[12] A. M. Rucklidge, N. O. Weiss, D. P. Brownjohn, and M. R. E. Proctor, "Oscillations and secondary bifurcations in nonlinear magnetoconvection," *Geophysical and Astrophysical Fluid Dynamics*, vol. 68, no. 1–4, pp. 133–150, 1993.

[13] T. Hu, A. R. Teel, and Z. Lin, "Lyapunov characterization of forced oscillations," *Automatica*, vol. 41, no. 10, pp. 1723–1735, 2005.

[14] S. Yin, H. Luo, and S. X. Ding, "Real-Time implementation of fault-tolerant control systems with performance optimization," *IEEE Transactions on Industrial Electronics*, 2013.

[15] A. Tinnirello, E. Gago, and M. Dadamo, "Spectral vibration patterns by symbolic computation systems," in *Proceedings of the 14th Recent Advances in Applied Mathematics Conference*, Recent Advances in Applied Mathematics, pp. 263–267, 2009.

[16] S. Yin, S. X. Ding, A. Haghani, H. Hao, and P. Zhang, "A comparison study of basic data-driven fault diagnosis and process monitoring methods on the benchmark Tennessee Eastman process," *Journal of Process Control*, vol. 22, pp. 1567–1581, 2012.

[17] F. Palacios-Quinonero, J. M. Rossell, J. Rubi-Masseg, and H. R. Karimi, "Structural vibration control for a class of connected multistructure mechanical systems," *Mathematical Problems in Engineering*, vol. 2012, Article ID 942910, 23 pages, 2012.

[18] J. Qiu, G. Feng, and J. Yang, "A new design of delay-dependent robust H_∞ filtering for discrete-time T-S fuzzy systems with time-varying delay," *IEEE Transactions on Fuzzy Systems*, vol. 17, no. 5, pp. 1044–1058, 2009.

[19] J. Qiu, G. Feng, and J. Yang, "Delay-dependent non-synchronized robust H_∞ state estimation for discrete-time piecewise linear delay systems," *International Journal of Adaptive Control and Signal Processing*, vol. 23, no. 12, pp. 1082–1096, 2009.

[20] Y. Wei, J. Qiu, H. R. Karimi, and M. Wang, "A new design of H_∞ filtering for continuous-time Markovian jump systems with time-varying delay and partially accessible mode information," *Signal Processing*, vol. 93, pp. 2392–2407, 2013.

[21] C. K. R. T. Jones, "Geometric singular perturbation theory," in *C. I. M. E. Lectures, Montecatini Terme*, vol. 1609 of *Lecture Notes in Mathematics*, Springer, Heidelberg, Germany, 1995.

[22] R. Vrabel and M. Abas, "Frequency control of singularly perturbed forced duffing's oscillator," *Journal of Dynamical and Control Systems*, vol. 17, no. 3, pp. 451–467, 2011.

[23] R. H. Rand, "Introduction to Maxima," Department of Theoretical and Applied Mechanics, Cornell University, 2010, http://maxima.sourceforge.net/docs/intromax/intromax.html.

[24] W. F. Schelter, "Maxima 5.26.0 Manual," 2011, http://maxima.sourceforge.net/docs/manual/en/maxima.html.

Hindawi Publishing Corporation
Mathematical Problems in Engineering
Volume 2013, Article ID 369092, 10 pages
http://dx.doi.org/10.1155/2013/369092

Research Article

Nonlinear Robust Control of a Hypersonic Flight Vehicle Using Fuzzy Disturbance Observer

Lei Zhengdong,[1] Wang Man,[1] and Yang Jianying[2]

[1] *College of Engineering, Peking University, Beijing 100871, China*
[2] *State Key Laboratory for Turbulence and Complex Systems, Department of Mechanics and Aerospace Engineering, Peking University, Beijing 100871, China*

Correspondence should be addressed to Yang Jianying; yjy@pku.edu.cn

Received 27 May 2013; Accepted 5 September 2013

Academic Editor: Hongli Dong

This paper is concerned with a novel tracking controller design for a hypersonic flight vehicle in complex and volatile environment. The attitude control model is challengingly constructed with multivariate uncertainties and external disturbances, such as structure dynamic and stochastic wind disturbance. In order to resist the influence of uncertainties and disturbances on the flight control system, nonlinear disturbance observer is introduced to estimate them. Moreover, for the sake of high accuracy and sensitivity, fuzzy theory is adopted to improve the performance of the nonlinear disturbance observer. After the total disturbance is eliminated by dynamic inversion method, a cascade system is obtained and then stabilized by a sliding-mode controller. Finally, simulation results show that the strong robust controller achieves excellent performance when the closed-loop control system is influenced by mass uncertainties and external disturbances.

1. Introduction

The study of the hypersonic flight vehicle (HFV) has been implemented for more than two decades all around the world. As early as 1980s, Chavez and Schmidt had made pivotal works of developing classic longitudinal model of the vehicle dynamics [1, 2]. Afterwards, Bolender and Doman developed the important implicit model: the first-principle model in [3]. In recent years, flexible effect, which results in structure dynamic and may significantly influence the performance of HFV, attracts more and more attention. Some models introduce the flexible modes in the motion equations [4, 5]. The most significant characteristics of HFV are the highly coupled and nonlinear nature of its dynamic behavior. Additionally, complicated flight condition and variability of the vehicle characteristics bring about mass uncertainties for the modeling. Some researchers, such as McNamara and Friedmann, have stated the difficulties faced in the modeling and control in their works [6]. At present, the models are unprecedented, complex, and much closer to the reality.

A large amount of different control methods has been successfully applied to stabilize the system of HFV and accomplish special tasks. Some typical approaches can be much weighted, such as linear parameter-varying control [7], adaptive control [8, 9], sliding-mode control [10], gain-scheduling, dynamic inversion [11], and $\mathscr{H}_\infty$ design [12]. Some other control methods (e.g., linear matrix inequity (LMI)) are based on linearized model by using the small disturbance principle at given trim point [13]. However, most of these methods have much conservation because the controller should be redesigned if the trim points of the system are altered and the calculation is amazingly tremendous. Thus, nonlinear control methods, such as dynamic inversion and adaptive control, seem more effective and present good relationship with physical process.

Despite of recent success of NASA's X-51A experiment, the design of robust guidance and control systems for HFV is still a challenging area [14]. Due to the complex flight environment (e.g., high mach, low air density, and thermal-elasticity), seeking for a strong robust controller is on edge. This kind of controller cannot only adapt to severe environment but also tolerate its own faults. As for HFV, one of the most important tasks is to track the reference trajectory. However, some unknown factors, such as gust wind,

structure dynamic, actuator failure, and sensor fault, bring about great uncertainties to the system performance. Some linearized models have been stabilized by robust controller based on LMI, in which Lyapunov stability theory is widely applied [15]. In [16], energy norm indices have been used for the fault detection problem in discrete-time Markovian jump systems. Some other novel methods also successfully addressed the uncertainties and disturbance problems, such as in [17]; it used extended Kalman filter to solve the problems of stochastic nonlinearities and multiple missing measurements instead of using observing methods. Nevertheless, in [13, 18], the parameters and states in linearized models are all the deviations from the trim point rather than the real ones. Thus, nonlinear analysis methods may be more meaningful in the practical engineering. The study of fault-tolerant control, which is based on nonlinear observer, makes great contributions to the design of strong robust controller. There are lots of various state estimators at present. Such as in [19, 20], state estimators were constructed with data from sensor networks for discrete-time systems to resist bad influence by sensor saturation, delay, and uncertainties. In [14], a fuzzy disturbance observer was proposed to estimate the uncertainties and disturbances. The nonlinear observer cannot only reconfigure the original states but also monitor the total disturbance. Then, the disturbance can be eliminated by using dynamic inverse method. As for this method, descriptions for disturbance and uncertainties are more accurate and rational for the reality.

In order to achieve excellent performance for the disturbance observer, in this paper, we introduce a novel fuzzy disturbance observer (FDO) to monitor the total disturbance, which can intelligently change its behavior according to the error of observation. What we contribute is that we redefine the disturbance as the sum of internal disturbance and external disturbance. This conception was first proposed in active disturbance rejection control (ADRC) by Han [21]. This redefinition reduces the quantity of calculation compared to other online methods, such as adaptive control. Moreover, it becomes feasible to apply this technology to electronic programming [21].

In this paper, our control objective is a kind of HFV similar to High-altitude Test Vehicle-2 (HTV-2). The goal for control is to make the attitude states (angle of attack, angle of the sideslip, and angle of roll) track the reference trajectories as soon as possible, especially when the flight environment contains large scale of uncertainties and disturbances. The rest of the paper is arranged as follows. Section 2 demonstrates the attitude model of the flight vehicle with mass uncertainties in detail. And the disturbance observer based on fuzzy theory is introduced in Section 3. In Section 4, controller is designed based on the disturbance observer. Simulation results in Section 5 confirm the controller's excellent operation and how well the observer monitors the disturbance in real time.

2. Nonlinear Attitude Control Model

2.1. Establishment of Nonlinear Dynamic Model. Some researchers have made great contributions to the modeling for HFV. HFV is usually characterized with strong coupling, strong nonlinear and multiple inputs and multiple outputs (MIMO). It is nearly impossible to do research on a highly accurate model considering all aspects. Thus, tradeoff between the modeling accuracy and simplicity should be considered. According to Newton's second law of motion and three-dimension coordinate transformation, the model of attitude motions for the MIMO flight vehicle model with two inputs (δ_r and δ_l) can be established.

The angle equations are listed as follows:

$$\begin{aligned}
\dot{\alpha} &= \omega_z + \frac{\sin\alpha\sin\beta}{\cos\beta}\omega_y - \frac{\cos\alpha\sin\beta}{\cos\beta}\omega_x \\
&\quad - \frac{\left(-C_A qS - mg\sin\phi_r\cos\psi_r\right)\sin\alpha}{mV_r\cos\beta} \\
&\quad - \left(\left(C_N qS - mg\cos\phi_r\cos\gamma\right.\right. \\
&\qquad \left.\left. -mg\sin\phi_r\sin\psi_r\sin\gamma\right)\cos\alpha\right) \\
&\quad \times \left(mV_r\cos\beta\right)^{-1}, \\
\dot{\beta} &= \omega_y\cos\alpha + \omega_x\sin\alpha \\
&\quad + \frac{C_N qS - mg\left(\cos\phi_r\cos\gamma + \sin\phi_r\sin\psi_r\sin\gamma\right)}{mV_r} \\
&\quad \times \sin\alpha\sin\beta \\
&\quad - \frac{-C_A qS - mg\sin\phi_r\cos\psi_r}{mV_r}\cos\alpha\sin\beta \\
\dot{\gamma} &= \omega_x + \dot{\phi}_r\sin\psi_r.
\end{aligned} \tag{1}$$

And the angle-rate equations are given as

$$\begin{aligned}
&J_x\dot{\omega}_x - J_{xy}\dot{\omega}_y - J_{xz}\dot{\omega}_z + J_z\omega_y\omega_z - J_{xz}\omega_x\omega_y \\
&\quad - J_{yz}\omega_y^2 - J_y\omega_y\omega_z + J_{xy}\omega_x\omega_z + J_{yz}\omega_z^2 \\
&\quad = C_l qSL - \frac{C_{lp}qSL^2\omega_x}{V_r}, \\
&J_y\dot{\omega}_y - J_{xy}\dot{\omega}_x - J_{yz}\dot{\omega}_z + J_x\omega_x\omega_z - J_{xy}\omega_y\omega_z \\
&\quad - J_{xz}\omega_z^2 - J_z\omega_x\omega_z + J_{xz}\omega_x^2 + J_{yz}\omega_x\omega_y \\
&\quad = C_n qSL - \frac{C_{nr}qSL^2\omega_y}{V_r}, \\
&J_z\dot{\omega}_z - J_{xz}\dot{\omega}_x - J_{yz}\dot{\omega}_y + J_y\omega_x\omega_y - J_{xy}\omega_x^2 \\
&\quad - J_{yz}\omega_x\omega_z - J_x\omega_x\omega_y + J_{xy}\omega_y^2 + J_{xz}\omega_y\omega_z \\
&\quad = C_m qSL - \frac{C_{mq}qSL^2\omega_z}{V_r},
\end{aligned} \tag{2}$$

where C_A, C_N, C_Z, C_l, C_m, C_n, C_{lp}, C_{mq}, and C_{nr} are related to one or four parameters (their expressions are listed below) and can be gotten by interpolation method:

$$C_i(\alpha, \beta, \delta_r, \delta_l)\ (i = A, N, Z, l, m, n),$$
$$C_j(\alpha)\ (j = lp, mq, nr). \tag{3}$$

Figure 1 shows the moment and force curves and their fitted functions versus α and β, respectively. As the coefficients are determined by four variables: α, β, δ_r, and δ_l. The inputs δ_r and δ_l are both frozen to 0.1 degree to draw the three-dimensional pictures below.

Therefore, (1) and (2) can be rewritten to (4) by separation of variables:

$$\dot{\boldsymbol{\Theta}} = \mathbf{f}_1(\boldsymbol{\Theta}) + \mathbf{M}(\boldsymbol{\Theta})\,\boldsymbol{\Omega}$$
$$\dot{\boldsymbol{\Omega}} = \mathbf{f}_2(\boldsymbol{\Theta}, \boldsymbol{\Omega}) + \mathbf{B}(\boldsymbol{\Theta})\,\mathbf{u}, \tag{4}$$

where

$$\boldsymbol{\Theta} = \begin{bmatrix}\alpha & \beta & \gamma\end{bmatrix}^T, \qquad \boldsymbol{\Omega} = \begin{bmatrix}\omega_x & \omega_y & \omega_z\end{bmatrix}^T,$$
$$\mathbf{u} = \begin{bmatrix}\delta_r & \delta_l\end{bmatrix}^T,$$
$$\mathbf{M}(\boldsymbol{\Theta}) = \begin{bmatrix} -\cos\alpha\tan\beta & \sin\alpha\tan\beta & 1 \\ \sin\alpha & \cos\alpha & 0 \\ 1 & 0 & 0 \end{bmatrix},$$
$$\mathbf{B}(\boldsymbol{\Theta}) = \begin{bmatrix} J_x & -J_{xy} & -J_{xz} \\ -J_{xy} & J_y & -J_{yz} \\ -J_{xz} & -J_{yz} & J_z \end{bmatrix}^{-1} \begin{bmatrix} C_{C_l}^{\delta_r} & C_{C_l}^{\delta_l} \\ C_{C_n}^{\delta_r} & C_{C_n}^{\delta_l} \\ C_{C_m}^{\delta_r} & C_{C_m}^{\delta_l} \end{bmatrix}. \tag{5}$$

Equation (4) is a typical system that can be stabilized by back-stepping method, in which $\boldsymbol{\Omega}$ can be seen as a pseudoinput. In this system, V_r, ϕ_r, and ψ_r are all determined by the reference trajectory and known for controller design.

2.2. Problem Formulation. As for describing the complex and volatile flight condition, a great amount of parameter uncertainties and stochastic wind disturbance is introduced into this model. The parameter uncertainties and external disturbance (bandlimited and varying slowly) are expressed in the equations as follows:

$$\dot{\boldsymbol{\Theta}} = \left(\mathbf{f}_1(\boldsymbol{\Theta}) + \Delta\mathbf{f}_1(\boldsymbol{\Theta})\right) + \left(\mathbf{M}(\boldsymbol{\Theta}) + \Delta\mathbf{M}(\boldsymbol{\Theta})\right)\boldsymbol{\Omega} + \mathbf{d}_{\mathbf{wind1}},$$
$$\dot{\boldsymbol{\Omega}} = \left(\mathbf{f}_2(\boldsymbol{\Theta}, \boldsymbol{\Omega}) + \Delta\mathbf{f}_2(\boldsymbol{\Theta}, \boldsymbol{\Omega})\right) + \left(\mathbf{B}(\boldsymbol{\Theta}) + \Delta\mathbf{B}(\boldsymbol{\Theta})\right)\mathbf{u} + \mathbf{d}_{\mathbf{wind2}}. \tag{6}$$

In system (6), $\mathbf{f}_1$ and $\mathbf{f}_2$ contain lots of complicated structure information of this model, which are too complicated if they are written into formula expression. For simplicity, some items are rewritten as the following expression:

$$\boldsymbol{\Pi}_1(\boldsymbol{\Theta}, \boldsymbol{\Omega}) = \mathbf{f}_1(\boldsymbol{\Theta}) + \Delta\mathbf{f}_1(\boldsymbol{\Theta}) + \Delta\mathbf{M}(\boldsymbol{\Theta})\,\boldsymbol{\Omega} + \mathbf{d}_{\mathbf{wind}_1},$$
$$\boldsymbol{\Pi}_2(\boldsymbol{\Theta}, \boldsymbol{\Omega}) = \mathbf{f}_2(\boldsymbol{\Theta}, \boldsymbol{\Omega}) + \Delta\mathbf{f}_2(\boldsymbol{\Theta}, \boldsymbol{\Omega}) + \Delta\mathbf{B}(\boldsymbol{\Theta})\,\mathbf{u} + \mathbf{d}_{\mathbf{wind}_2}, \tag{7}$$

thus, system (6) can be rewritten as

$$\dot{\boldsymbol{\Gamma}} = \mathbf{K}(\boldsymbol{\Theta})\,\mathbf{U} + \boldsymbol{\Pi}(\boldsymbol{\Theta}, \boldsymbol{\Omega}), \tag{8}$$

where

$$\boldsymbol{\Gamma} = \begin{bmatrix}\boldsymbol{\Theta} \\ \boldsymbol{\Omega}\end{bmatrix}, \qquad \mathbf{U} = \begin{bmatrix}\boldsymbol{\Omega} \\ \mathbf{u}\end{bmatrix},$$
$$\mathbf{K}(\boldsymbol{\Theta}) = \begin{bmatrix}\mathbf{M}(\boldsymbol{\Theta}) & \mathbf{0} \\ \mathbf{0} & \mathbf{B}(\boldsymbol{\Omega})\end{bmatrix}, \qquad \boldsymbol{\Pi}(\boldsymbol{\Theta}, \boldsymbol{\Omega}) = \begin{bmatrix}\boldsymbol{\Pi}_1(\boldsymbol{\Theta}, \boldsymbol{\Omega}) \\ \boldsymbol{\Pi}_2(\boldsymbol{\Theta}, \boldsymbol{\Omega})\end{bmatrix}. \tag{9}$$

In particular, total disturbance is redefined as $\boldsymbol{\Pi}_i(\boldsymbol{\Theta}, \boldsymbol{\Omega})$ $(i = 1, 2) \in \mathbf{R}^{3\times 1}$, unknown and bandlimited, to represent the sum of partial structure information, model parameter uncertainties, and wind disturbance. From the above consideration, a cascade system with total disturbance is presented. As for the practical hypothesis, the total disturbance, hence, contains wide range of parameter uncertainties, such as force and moment coefficients deviation, inertia deviation, gravity center deviation, and atmosphere density deviation. As the goal for flight control, the goal is to converge the flight attitude and angle-rate $(\boldsymbol{\Theta}(t), \boldsymbol{\Omega}(t))$ into the given reference trajectory $(\boldsymbol{\Theta}^*(t), \boldsymbol{\Omega}^*(t))$ in finite time. And the transient response performance should be as better as the system can achieve. Consider the following:

$$\lim_{t\to+\infty} \left\|\boldsymbol{\Theta}(t) - \boldsymbol{\Theta}^*(t)\right\| = \mathbf{0},$$
$$\lim_{t\to+\infty} \left\|\boldsymbol{\Omega}(t) - \boldsymbol{\Omega}^*(t)\right\| = \mathbf{0}. \tag{10}$$

Dynamic inversion method has been widely used to address such problem; however, the most critical and difficult work is the disturbance estimation. Disturbance estimation relies on identification via inputs and outputs data. As long as the total disturbance is estimated (notated as $\widehat{\boldsymbol{\Pi}}_i$ $(i = 1, 2)$), the problem surely becomes easy to disentangle by dynamic inversion method as the following expression; $\boldsymbol{\Omega}$ behaves as a pseudoinput: $\boldsymbol{\Omega}_c$. Consider the following:

$$\boldsymbol{\Omega}_c = \mathbf{M}^{-1}(\boldsymbol{\Theta})\left(-\widehat{\boldsymbol{\Pi}}_1 + \boldsymbol{\Omega}\right),$$
$$\mathbf{u} = \mathbf{B}^{\dagger}(\boldsymbol{\Theta})\left(-\widehat{\boldsymbol{\Pi}}_2 + \mathbf{u}_c\right). \tag{11}$$

In (11), the inversion matrix $\mathbf{B}^{-1}$ cannot be obtained because $\mathbf{B}$ is not a square matrix. Thus, pseudoinversion $\mathbf{B}^{\dagger}$ is used to replace it, and the error which results from inaccurate dynamic inversion can be reduced by error-integral feedback. If $\widehat{\boldsymbol{\Pi}}_i$ can be perfectly monitored, the plant system (4) can be rewritten as, by replacing with (11),

$$\dot{\boldsymbol{\Theta}} = \boldsymbol{\Omega} + \boldsymbol{\Pi}_1 - \widehat{\boldsymbol{\Pi}}_1,$$
$$\dot{\boldsymbol{\Omega}} = \mathbf{u}_c + \boldsymbol{\Pi}_2 - \widehat{\boldsymbol{\Pi}}_2. \tag{12}$$

Assumption: the observation error $(\widehat{\boldsymbol{\Pi}}_i - \boldsymbol{\Pi}_i)$ is minor, and its effect on the stability of the closed loop system is negligible. This assumption is reasonable because it has been proved

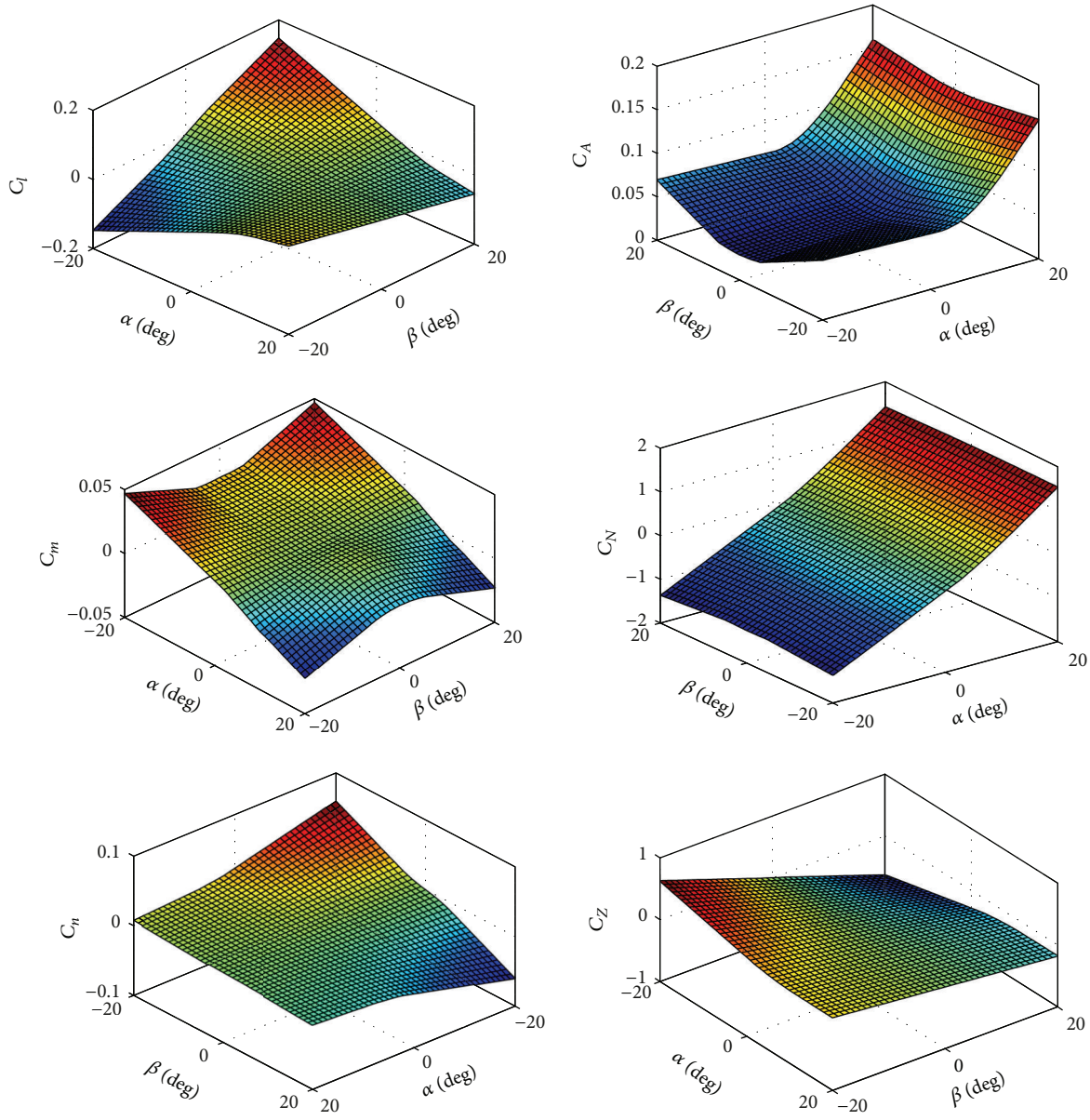

(a) Moment coefficients

(b) Force coefficients

FIGURE 1: Moment and force coefficients at $\delta_r = \delta_l = 0.1$ deg.

that the observation error is uniformly ultimately bounded (UUB, $\in L_\infty$) within a region of arbitrarily small size [14]. Thus, we will neglect the observation error in the following parts.

The estimation of $\widehat{\mathbf{\Pi}}_i$ $(i = 1, 2)$ plays an extremely important role in the whole control system. The total disturbance should be estimated accurately online, and fuzzy theory is quite suitable for this condition. After choosing the membership functions, the fuzzy disturbance observer will have different response time and convergence speed in accordance with which membership area the observation error is located in. This kind of intelligent observer will make the online identification process achieve excellent performance.

3. Disturbance Observer Based on Fuzzy Theory

3.1. Introduction of Extended State. Nonlinear extended state observer (NESO) performs well in not only observing all the system states but also monitoring the uncertainties and external disturbance. Under this framework, NESO can derive various forms due to different nonlinear functions involved. In this paper, fuzzy theory is introduced to deal with disturbance estimation error. The observer behavior will be automatically adjusted by the error level, which makes the observer achieve perfect transient response. According to

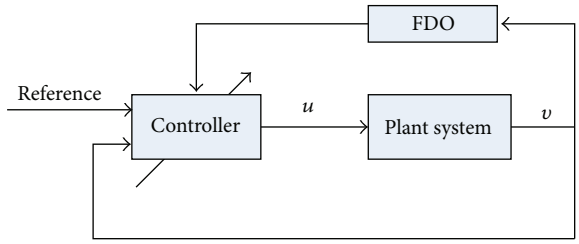

Figure 2: Controlled system based on FDO.

the system (8), the following NESO is designed to estimate the total disturbance:

$$\begin{aligned}\boldsymbol{\Delta\Gamma} &= \boldsymbol{\varrho} - \boldsymbol{\Gamma} = \left[\Delta\alpha \;\; \Delta\beta \;\; \Delta\gamma \;\; \Delta\omega_x \;\; \Delta\omega_y \;\; \Delta\omega_z\right]^T \\ \dot{\boldsymbol{\varrho}} &= \mathbf{K}(\boldsymbol{\Theta})\,\mathbf{U} + \widehat{\boldsymbol{\Pi}} - \mathbf{c}\boldsymbol{\Delta\Gamma} \\ \widehat{\boldsymbol{\Pi}} &= \mathbf{G}(\boldsymbol{\Gamma}, \mathbf{u}),\end{aligned} \tag{13}$$

where

$$\begin{aligned}\boldsymbol{\Delta\Gamma} &= \left[\boldsymbol{\Delta\Theta}^T \boldsymbol{\Delta\Omega}^T\right]^T : \text{reconfigured states error,} \\ \boldsymbol{\varrho} &= \left[\alpha' \;\; \beta' \;\; \gamma' \;\; \omega_x' \;\; \omega_y' \;\; \omega_z'\right]^T : \text{reconfigured states,} \\ \widehat{\boldsymbol{\Pi}} &= \left[\widehat{\boldsymbol{\Pi}}_1^T \;\; \widehat{\boldsymbol{\Pi}}_2^T\right]^T : \text{estimated total disturbance.}\end{aligned} \tag{14}$$

In system (13), the nonlinear function $\mathbf{G}(\boldsymbol{\Gamma}, \mathbf{u})$ is a fuzzy inference engine, which is used to estimate the total disturbance. $\widehat{\boldsymbol{\Pi}}$ is the extended state, which is defined in the subtitle. The $\mathbf{G}(\boldsymbol{\Gamma}, \mathbf{u})$ can be also rewritten as $\mathbf{G}(\boldsymbol{\Gamma})$ because the input $\mathbf{u}(\Gamma)$ is determined by full-state feedback. The constant vector $\mathbf{c}$, if chosen properly, will control the weight the reconfigured error has in the observer equation and it will enhance the stability of the whole system by negative feedback. The goal for this observer is to make the following equation hold:

$$\lim_{t \to +\infty} \left\|\boldsymbol{\varrho} - \boldsymbol{\Gamma}\right\| = \mathbf{0}. \tag{15}$$

Figure 2 depicts the whole controlled system based on fuzzy disturbance observer (FDO).

3.2. Disturbance Observer Based on Fuzzy Theory. In [14], Euntai gave detailed explanations on fuzzy disturbance observer. A typical fuzzy system follows the IF-THEN rules which are characterized by a set of condition $\rightarrow$ action rules, or in IF-THEN form as follows [22]:

$$\text{IF premise THEN consequent,} \tag{16}$$

or

$$\text{IF } \upsilon_1 \text{ is } A_1^i \text{ and}, \ldots, \text{and } \upsilon_n \text{ is } A_n^i \text{ THEN } y^i \text{ is } B. \tag{17}$$

In this paper, the principle of product inference, center-average and singleton fuzzifier is adopted. Then, the expression of the estimated total disturbance is obtained as follows:

$$\mathbf{G}(\boldsymbol{\Gamma}) = \frac{\sum_{i=1}^{m} y^i \left(\prod_{j=1}^{n} \mu_{A_j^i}(\Gamma_j)\right)}{\sum_{i=1}^{m} \left(\prod_{j=1}^{n} \mu_{A_j^i}(\Gamma_j)\right)} = \widehat{\theta}^T \xi(\boldsymbol{\Gamma}), \tag{18}$$

where $\widehat{\theta} \in \mathbb{R}^{27\times 1}, \xi(\boldsymbol{\Gamma}) \in \mathbb{R}^{27\times 1}$. $\widehat{\theta}$ is the adjustable vector, which is composed of y^i, and $\xi(\boldsymbol{\Gamma})$ is the fuzzy basis function. Equation (18) is a general solution formula for every channel of the estimated disturbance vector $\widehat{\boldsymbol{\Pi}}$. The adaptive parameter is shown as follows (take the channel of α, e.g.):

$$\dot{\widehat{\theta}}_\alpha = \lambda_\alpha \Delta\alpha \xi(\alpha, \beta, \gamma), \tag{19}$$

and the fuzzy basis functions are as follows:

$$\xi_i = \frac{\prod_{j=1}^{3} \mu_{A_j^i}(\Gamma_j)}{\sum_{i=1}^{3} \left(\prod_{j=1}^{3} \mu_{A_j^i}(\Gamma_j)\right)}, \tag{20}$$

where $[\Gamma_1\ \Gamma_2\ \Gamma_3] = [\alpha\ \beta\ \gamma]$, $\xi(\alpha, \beta, \gamma) = [\xi_1, \xi_2, \ldots, \xi_{27}]^T$, and

$$\begin{aligned}\mu_{A_1^1}(\Gamma_1) &= \frac{1}{1 + \exp\left(2\left(\Gamma_1 + 0.6\right)\right)}, \\ \mu_{A_1^2}(\Gamma_1) &= \exp\left(-\left(\Gamma_1\right)^2\right), \\ \mu_{A_1^3}(\Gamma_1) &= \frac{1}{1 + \exp\left(-2\left(\Gamma_1 - 0.6\right)\right)}, \\ \mu_{A_2^1}(\Gamma_2) &= \frac{1}{1 + \exp\left(2\left(\Gamma_2 + 0.1\right)\right)}, \\ \mu_{A_2^2}(\Gamma_2) &= \exp\left(-\left(\Gamma_2\right)^2\right), \\ \mu_{A_2^3}(\Gamma_2) &= \frac{1}{1 + \exp\left(-2\left(\Gamma_2 - 0.1\right)\right)}, \\ \mu_{A_3^1}(\Gamma_3) &= \frac{1}{1 + \exp\left(2\left(\Gamma_3 + 0.9\right)\right)}, \\ \mu_{A_3^2}(\Gamma_3) &= \exp\left(-\left(\Gamma_3\right)^2\right), \\ \mu_{A_3^3}(\Gamma_3) &= \frac{1}{1 + \exp\left(-2\left(\Gamma_3 - 0.9\right)\right)}.\end{aligned} \tag{21}$$

For the sake of reducing calculation amount, there are only three fuzzy membership functions for each channel of α, β, and γ, which are shown in Figure 3.

The disturbance observation error $\Delta\Gamma$ will be uniformly ultimately bounded ($\Delta\Gamma \in L_\infty$), which has been proved in [14]. And this method will accelerate the convergence speed of the FDO when the observation error is approaching zero. As for (19), the fuzzy basis functions $\xi(\alpha, \beta, \gamma)$ will be the same when dealing with the channels of α, β, and γ. But when estimating the total disturbance of the channels of ω_x, ω_y, and ω_z, the functions will change to $\xi(\omega_x, \omega_y, \omega_z)$, and the method of obtaining it is similar to the former.

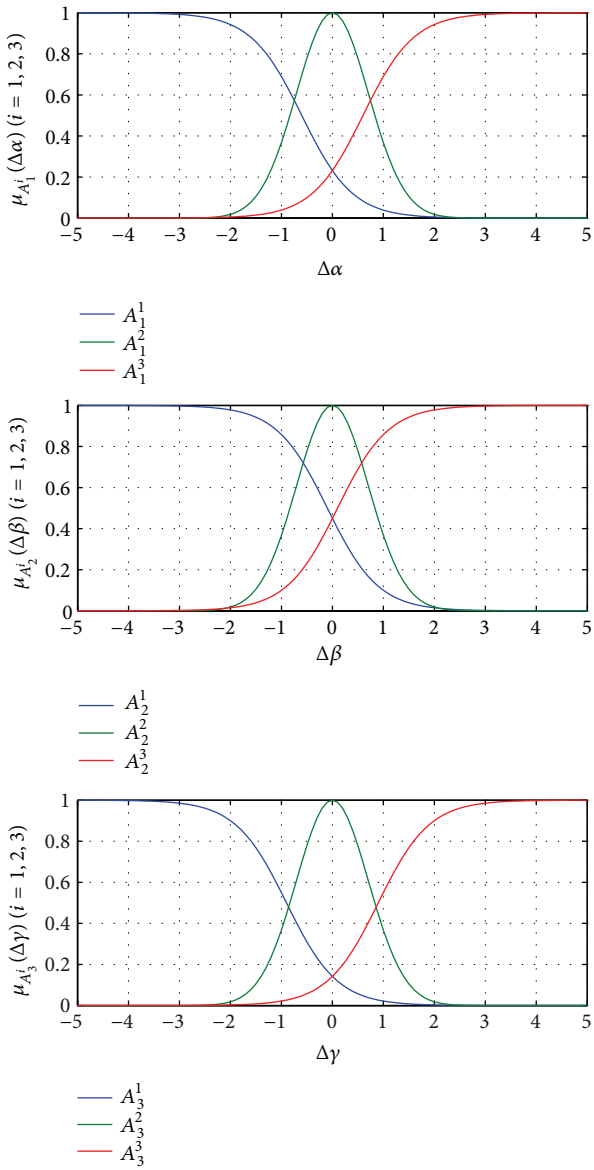

Figure 3: Fuzzy basis functions for α, β, and γ.

4. Controller Design Based on Sliding-Mode Method

After observing and removing the total disturbance, the cascade system (12) is obtained. In this paper, the sliding-mode method is used to deal with the cascade system. Angle tracking errors are defined as follows:

$$\mathbf{e} = \mathbf{\Theta}^* - \mathbf{\Theta}, \tag{22}$$

where $\mathbf{\Theta}^*$ is the given reference trajectory. Differentiating (22),

$$\dot{\mathbf{e}} = \dot{\mathbf{\Omega}}^* - \dot{\mathbf{\Theta}} = \mathbf{\Omega}^* - \mathbf{\Omega}. \tag{23}$$

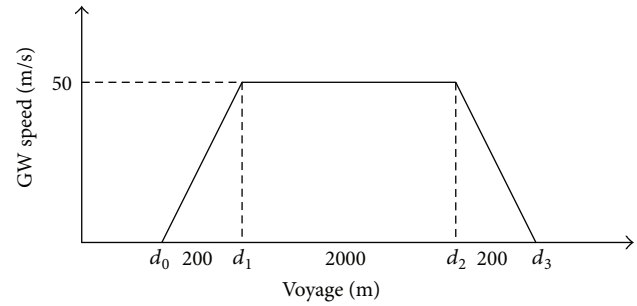

Figure 4: Gust wind model.

Table 1: Distractions of parameters in the plant system model.

Parameter	Distraction	Parameter	Distraction
ΔC_A	20% C_A	ΔC_N	15% C_N
ΔC_Z	20% C_Z	ΔC_l	40% C_l + 0.001
ΔC_n	40% C_n + 0.002	ΔC_m	30% C_m + 0.001
ΔC_{lp}	50% C_{lp}	ΔC_{nr}	50% C_{nr}
ΔC_{mq}	50% C_{mq}	Δm	20% m
ΔJ_X	8% J_X	ΔJ_Y	8% J_Y
ΔJ_Z	8% J_Z	ΔJ_{XY}	15% J_{XY}
ΔJ_{XZ}	0.4	ΔJ_{YZ}	0.4

Table 2: Relationship between stationary wind speed and flight altitude.

Altitude (km)	f_w^{SW} (m/s)	Altitude (km)	f_w^{SW} (m/s)
35.0	64.0	64.5	101.7
39.0	64.0	65.0	101.0
44.0	84.4	69.0	95.4
49.0	112.4	69.5	94.1
59.0	112.4	70.0	92.8
59.5	111.4	74.0	82.4
60.0	110.4	107.0	82.4
64.0	102.4	110.0	80.5

Given $\mathbf{K} = [k_{i1}\ k_{i2}]$, $\mathbf{E} = [\mathbf{e}_i\ \dot{\mathbf{e}}_i]^T$, and $\mathbf{u_c} = [u_{c1}, u_{c2}, u_{c3}]^T, i = 1, 2, 3$, we set the following sliding-mode surface function for any one of the channels:

$$\begin{aligned} \mathbf{s}_i &= \mathbf{KE} = k_{i1}\left(\mathbf{\Theta}_i^* - \mathbf{\Theta}_i\right) + k_{i2}\left(\mathbf{\Omega}_i^* - \mathbf{\Omega}_i\right), \\ \dot{\mathbf{s}}_i &= k_{i1}\left(\dot{\mathbf{\Theta}}_i^* - \mathbf{\Omega}_i\right) + k_{i2}\left(\dot{\mathbf{\Omega}}_i^* - u_{ci}\right) = \text{slaw}_i, \end{aligned} \tag{24}$$

where slaw_i is the sliding-mode approaching law. In order to achieve good tracking performance, in this paper, we choose the exponential approaching law instead of the traditional proportional approaching law:

$$\text{slaw}_i = -\varepsilon_i \operatorname{sgn}\left(\mathbf{s}_i\right) - \beta_i \mathbf{s}_i. \tag{25}$$

In (24), the sliding-mode surface function $\mathbf{s}_i$ satisfies threes conditions: (1) $\mathbf{s}_i(t = t_0) = 0$, (2) $\mathbf{s}_i$ is differentiable, and (3) $\mathbf{s}_i^T \dot{\mathbf{s}}_i < 0$. These conditions guarantee not only the stability of tracking process but also the steady tracking error

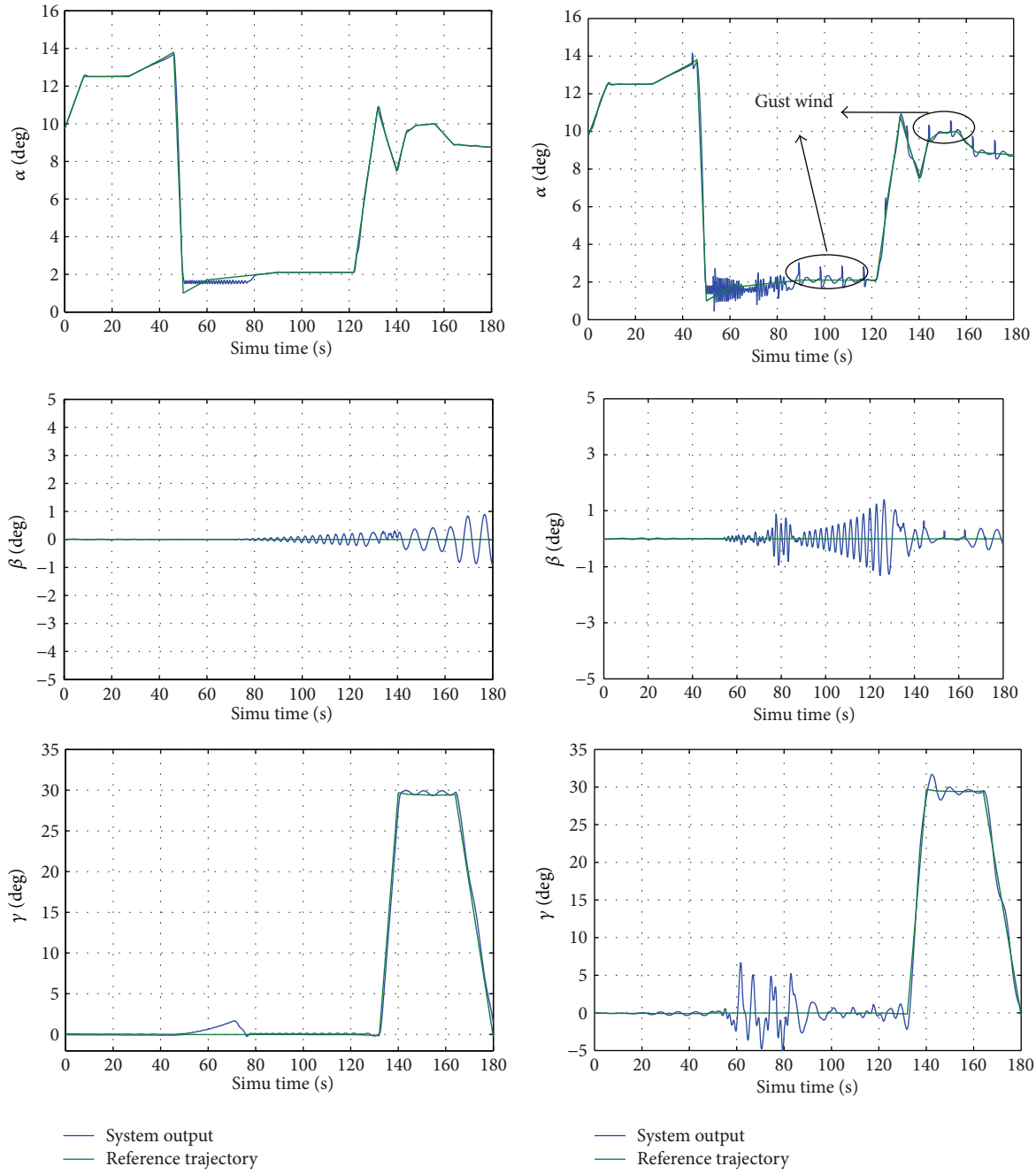

(a) α, β, and γ performance in tracking references without total disturbance

(b) α, β, and γ performance in tracking references with total disturbance

FIGURE 5: Tracking results without and with total disturbance.

asymptotically approaching to zero. Substituting (25) into (24), we get the controlled input as

$$u_{ci} = \frac{1}{k_{i2}} \left(k_{i1} \left(\dot{\boldsymbol{\Theta}}_i^* - \boldsymbol{\Omega}_i \right) + \varepsilon_i \operatorname{sgn}(\mathbf{s}_i) + \beta_i \mathbf{s}_i \right) + \dot{\boldsymbol{\Omega}}_i^*. \quad (26)$$

Remark. According to the repeated trials, it is more likely to achieve good control performance when the parameters are chosen as $\varepsilon_1 = 5$, $\beta_1 = 10$, $k_{11} = 3$, and $k_{12} = 1$. All of these parameters can significantly influence the stability, the rising time and the tracking error of this closed-loop system but no single parameter can determine any of them independently. Thus, so far the adjusting method is one of the best methods to determine these parameters. Substituting (26) into (11), we obtain the final controller expression with the negative feedback of the integral of the tracking error:

$$\mathbf{u} = \mathbf{B}^{\dagger}(\boldsymbol{\Theta}) \left(-\widehat{\boldsymbol{\Pi}}_2 + [u_{c1}, u_{c2}, u_{c3}]^T - \mathbf{K}_a \int \mathbf{e} \right), \quad (27)$$

where

$$\mathbf{K}_a > \mathbf{0}. \quad (28)$$

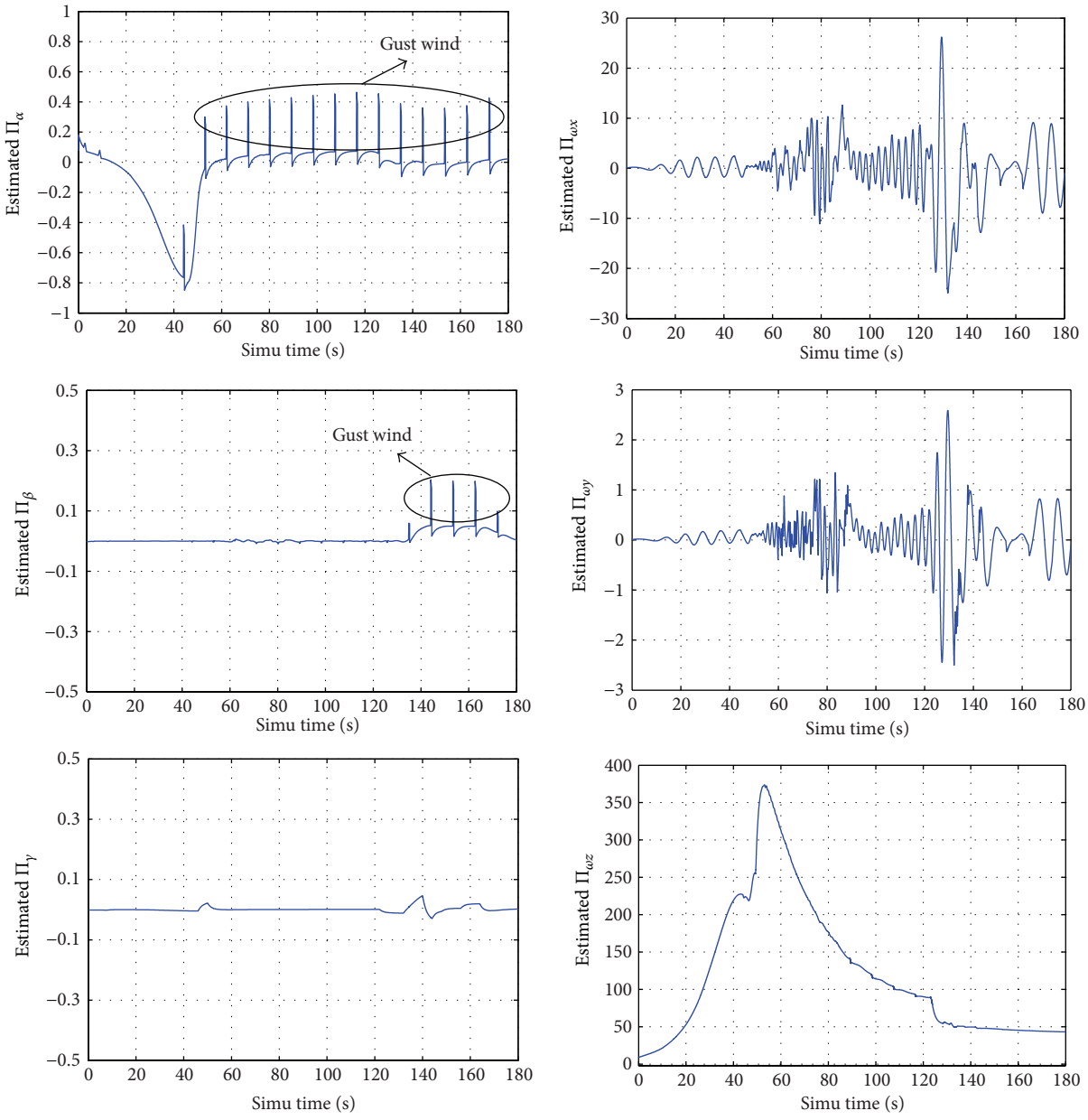

(a) Estimated disturbance of angle channels

(b) Estimated disturbance of angle-rate channels

Figure 6: Total disturbance estimations.

5. Simulations

In this part, a wide range of parameter uncertainties and external disturbance is set for the plant system, and parameter uncertainties are realized by the distractions of relevant parameters in the model of plant system. The goal is to test the ability of the controlled system to resist disturbance and its own uncertainties. It is also expected that the disturbance observer will achieve good performance.

5.1. Parameters Distractions and External Wind Disturbance. In Table 1, all of the distracted parameters are listed, in which numbers expressed in percentage mean relative distractions, while others indicate absolute distractions. All of these changes occur in the model of plant system, which represents the vehicle in the virtual reality environment for flight.

Then, the model for wind disturbance is given as follows. In general, both stationary wind and gust wind will not be taken into consideration until the simulation runs to 60 seconds. The speed of stationary wind will change according to the flight altitude, and the accurate value for this speed can be gotten by linear interpolation. Table 2 demonstrates the relationship between the wind speed and the flight altitude.

As for the gust wind model, a regular model with the period of 50 km is considered, which is illustrated in Figure 4. For each time, the gust wind starts at d_0 and ends at d_3. After

50 km flight, which is at $d_0 + 50$ km, the same wind reappears again.

The directions of both stationary wind and gust wind are stochastic, and A_w denotes the azimuth angle of wind. Thus, the wind vector is as follows:

$$\vec{V}_w = \vec{V}_{\mathrm{SW}} + \vec{V}_{\mathrm{GW}}, \tag{29}$$

where

$$\vec{V}_{\mathrm{SW}} = f_w^{\mathrm{SW}} \times \begin{bmatrix} \cos(A_w) \\ 0 \\ -\sin(A_w) \end{bmatrix},$$
$$\vec{V}_{\mathrm{GW}} = \sqrt{2} \times f_w^{\mathrm{GW}} \times \begin{bmatrix} \cos(A_w) \\ 0 \\ -\sin(A_w) \end{bmatrix} + f_w^{\mathrm{GW}} \times \begin{bmatrix} 0 \\ -1 \\ 0 \end{bmatrix}. \tag{30}$$

The wind vector mainly influences the system outputs (α and β) by changing the speed and direction of the incoming flow. So far, all the modeling work for total disturbance has been finished. In the next subsection, several pictures of simulation results will be shown.

5.2. Simulation Results. The main goal for this paper is to make the HFV track reference trajectory with high performance in severe situation. At first, it only tests the performance of the controller based on sliding-mode method; thus, total disturbance is not added into the plant system. Simulation results are shown in Figure 5(a). It can be clearly learned that the controller has performed an excellent work for the tracking task. Although the tracking performance is not good at about 50 seconds because the angle of attack suddenly drops which results in the rapid declination of lift force, the whole system soon goes back to its stable states under the action of controller and the error is limited within two degrees.

When the total disturbance is added into the system, the performance of the controlled system is shown in Figure 5(b). From these figures, it demonstrates that even though the disturbance exerts negative impact (marked in the figures) on the whole system, it has successfully finished the tracking task and left minor steady error. All these accomplishments benefit from the excellent performance of FDO. Figure 6 demonstrates that the total disturbance is superbly monitored by the FDO. In Figure 6(a), it clearly shows that the periodic gust wind disturbance is totally observed, which is in accordance with the real situation.

6. Conclusions

This study indicates that, although the flight condition for the hypersonic flight vehicle contains mass uncertainties and gust wind disturbance, the fuzzy disturbance observer monitors the total disturbance very well. The definition of total disturbance provides a new way of disentangling complex structure information. This method contains both the analytical dynamic inversion and the numerical online identification, which contributes to its excellent performance when the tracking trajectory varies drastically. In the future, this work is expected to focus on the study of the estimated total disturbance separation and analysis.

Acknowledgments

This work is supported by the National Natural Science Key Foundation of China under Grants nos. 91216124, 91116002, 90916003, 91216304, and 11332001; Foundation of national astronautica key lab (2012-865-6).

References

[1] D. K. Schmidt, "Optimum mission performance and multivariable flight guidance for airbreathing launch vehicles," *Journal of Guidance, Control, and Dynamics*, vol. 20, no. 6, pp. 1157–1164, 1997.

[2] F. R. Chavez and D. K. Schmidt, "Analytical aeropropulsive/aeroelastic hypersonic-vehicle model with dynamic analysis," *Journal of Guidance, Control, and Dynamics*, vol. 17, no. 6, pp. 1308–1319, 1994.

[3] M. A. Bolender and D. B. Doman, "A nonlinear longitudinal dynamical model of an air-breathing hypersonic vehicle," *Journal of Spacecraft and Rockets*, vol. 44, no. 2, pp. 374–387, 2007.

[4] D. Sigthorsson, P. Jankovsky, A. Serrani, S. Yurkovich, M. A. Bolender, and D. B. Doman, "Robust linear output feedback control of an airbreathing hypersonic vehicle," *Journal of Guidance, Control, and Dynamics*, vol. 31, no. 4, pp. 1052–1066, 2008.

[5] J. T. Parker, A. Serrani, S. Yurkovich, M. A. Bolender, and D. B. Doman, "Control-oriented modeling of an air-breathing hypersonic vehicle," *Journal of Guidance, Control, and Dynamics*, vol. 30, no. 3, pp. 856–869, 2007.

[6] J. McNamara and P. Friedmann, "Aeroelastic and aerothermoelastic analysis of hypersonic vehicles: current status and future trends," in *Proceedings of the 48th AIAA/ASME/ASCE/AHS/ASC Structures, Structural Dynamics, and Materials Conference*, pp. 3814–3868, Honolulu, Hawaii, USA, April 2007, AIAA paper no. 2007-2013.

[7] R. Lind, "Linear parameter-varying modeling and control of structural dynamics with aerothermoelastic effects," *Journal of Guidance, Control, and Dynamics*, vol. 25, no. 4, pp. 733–739, 2002.

[8] L. Fiorentini, A. Serrani, M. A. Bolender, and D. B. Doman, "Nonlinear robust adaptive control of flexible air-breathing hypersonic vehicles," *Journal of Guidance, Control, and Dynamics*, vol. 32, no. 2, pp. 401–416, 2009.

[9] L. Fiorentini, A. Serrani, M. A. Bolender, and D. B. Doman, "Nonlinear robust/adaptive controller design for an air-breathing hypersonic vehicle model," in *Proceedings of the AIAA Guidance, Navigation, and Control Conferenc and Exhibit*, pp. 269–284, Hilton Head, SC, USA, August 2007, AIAA paper no. 2007-6329.

[10] H. Xu, M. Mirmirani, and P. Ioannou, "Adaptive sliding mode control design for a hypersonic flight vehicle," *Journal of Guidance, Control, and Dynamics*, vol. 27, no. 5, pp. 829–838, 2004.

[11] Q. Wang and R. F. Stengel, "Robust nonlinear control of a hypersonic aircraft," *Journal of Guidance, Control, and Dynamics*, vol. 23, no. 4, pp. 577–585, 2000.

[12] H. Buschek and A. J. Calise, "Uncertainty modeling and fixed-order controller design for a hypersonic vehicle model," *Journal*

of Guidance, Control, and Dynamics, vol. 20, no. 1, pp. 42–48, 1997.

[13] H. Li, Y. Si, L. Wu, X. Huang, and H. Gao, "Guaranteed cost control with poles assignment for a flexible air-breathing hypersonic vehicle," *International Journal of Systems Science*, vol. 42, no. 5, pp. 863–876, 2011.

[14] K. Euntai, "A fuzzy disturbance observer and its application to control," *IEEE Transactions on Fuzzy Systems*, vol. 10, no. 1, pp. 77–84, 2002.

[15] D. Ye and G. Yang, "Adaptive fault-tolerant tracking control against actuator faults with application to flight control," *IEEE Transactions on Control Systems Technology*, vol. 14, no. 6, pp. 1088–1096, 2006.

[16] H. Dong, Z. Wang, and H. Gao, "Fault detection for Markovian jump systems with sensor saturations and randomly varying nonlinearities," *IEEE Transactions on Circuits and Systems*, vol. 59, no. 10, pp. 2354–2362, 2012.

[17] J. Hu, Z. Wang, H. Gao, and L. K. Stergioulas, "Extended Kalman filtering with stochastic nonlinearities and multiple missing measurements," *Automatica*, vol. 48, no. 9, pp. 2007–2015, 2012.

[18] C. Marrison and R. Stengel, "Design of robust control systems for a hypersonic aircraft," *Journal of Guidance, Control, and Dynamics*, vol. 21, no. 1, pp. 58–63, 1998.

[19] D. Ding, Z. Wang, H. Dong, and H. Shu, "Distributed H1 state estimation with stochastic parameters and nonlinearities through sensor networks: the finite-horizon case," *Automatica*, vol. 48, no. 8, pp. 1575–1585, 2012.

[20] D. Ding, Z. Wang, B. Shen, and H. Shu, "H1 state estimation for discrete-time complex networks with randomly occurring sensor saturations and randomly varying sensor delays," *IEEE Transactions on Neural Networks and Learning Systems*, vol. 23, no. 5, pp. 725–736, 2012.

[21] J. Han, "From PID to active disturbance rejection control," *IEEE Transactions on Industrial Electronics*, vol. 56, no. 3, pp. 900–906, 2009.

[22] M. P. Kevin and S. Yurkovich, *Fuzzy Control*, Addison-Wesley, Reading, Mass, USA, 1997.

Hindawi Publishing Corporation
Mathematical Problems in Engineering
Volume 2013, Article ID 173051, 9 pages
http://dx.doi.org/10.1155/2013/173051

Research Article

Proportional Derivative Control with Inverse Dead-Zone for Pendulum Systems

José de Jesús Rubio, Zizilia Zamudio, Jaime Pacheco, and Dante Mújica Vargas

Sección de Estudios de Posgrado e Investigación, ESIME Azcapotzalco, Instituto Politécnico Nacional, Avenida de las Granjas No. 682, Colonia Santa Catarina, 02250 México, DF, Mexico

Correspondence should be addressed to José de Jesús Rubio; jrubioa@ipn.mx

Received 11 July 2013; Revised 30 August 2013; Accepted 2 September 2013

Academic Editor: Zidong Wang

A proportional derivative controller with inverse dead-zone is proposed for the control of pendulum systems. The proposed method has the characteristic that the inverse dead-zone is cancelled with the pendulum dead-zone. Asymptotic stability of the proposed technique is guaranteed by the Lyapunov analysis. Simulations of two pendulum systems show the effectiveness of the proposed technique.

1. Introduction

Nonsmooth nonlinear characteristics such as dead-zone, backlash, and hysteresis are common in actuators, sensors such as mechanical connections, hydraulic servovalves, and electric servomotors; they also appear in biomedical systems. Dead-zone is one of the most important nonsmooth nonlinearities in many industrial processes, which can severely limit the system performance, and its study has been drawing much interest in the control community for a long time [1].

There is some research about control systems. In [2], the stabilization of the inverted-car pendulum is presented. The stabilization of the Furuta pendulum is introduced in [3]. In [4], the dissipative control problem is investigated for a class of discrete time-varying systems. The distributed H_∞ filtering problem for a class of nonlinear systems is considered in [5]. The recursive finite-horizon filtering problem for a class of nonlinear time-varying systems is addressed in [6, 7]. In [8], the authors present a solution to the problem of the quadratic mini-max regulator for polynomial uncertain systems. The problem of a two-player differential game affected by matched uncertainties with only the output measurement available for each player is considered by [9]. The stability analysis and H_∞ control for a class of discrete time switched linear parameter-varying systems are concerned in [10]. The sliding mode control problem for uncertain nonlinear discrete-time stochastic systems with H_2 performance constraints is designed in [11]. In [12], the sliding mode control problem is considered for discrete-time systems. In [13], the description about the modelling and control of wind turbine system is addressed. A model to describe the dynamics of a homogeneous viscous fluid in an open pipe is introduced in [14]. In [15], the authors consider the problems of robust stability and H_∞ control for a class of networked control systems with long-time delays. The H_∞ control issue for a class of networked control systems with packet dropouts and time-varying delays is introduced in [16]. From the above studies, in [2, 3, 8, 9, 13, 14], the authors propose proportional derivative controls; however, none considers systems with dead-zone inputs.

There is some work about the control of systems with dead-zone inputs. In [17–22], the authors proposed the control of nonlinear systems with dead-zone inputs. Nevertheless, they do not research about the pendulum systems. The pendulum dynamic models have different structures with respect to the nonlinear systems addressed in the above papers; thus, a new design may be developed.

In this paper, a proportional derivative controller with inverse dead-zone is proposed for the control of pendulum systems with dead-zone inputs. One main contribution of this study is that the pendulum dynamic model is rewritten as

a robotic dynamic model to satisfy a property, and later, the property is applied to guarantee the stability of the proposed controller.

The paper is organized as follows. In Section 2, the dynamic model of the robotic arm with dead-zone inputs is presented. In Section 3, the dynamic model of the pendulum systems with dead-zone inputs is presented. In Section 4, the proportional derivative controller with inverse dead-zone is introduced. In Section 5, the proposed method is used for the regulation of two pendulum systems. Section 6 presents conclusions and suggests future research directions.

2. Dynamic Model of the Robotic Arms with Dead-Zone Inputs

The main concern of this section is to understand some concepts of robot dynamics. The equation of motion for the constrained robotic manipulator with n degrees of freedom, considering the contact force and the constraints, is given in the joint space as follows:

$$M(q)\ddot{q} + C(q,\dot{q})\dot{q} + G(q) = \tau, \tag{1}$$

where $q \in \Re^{n\times 1}$ denotes the joint angles or link displacements of the manipulator, $M(q) \in \Re^{n\times n}$ is the robot inertia matrix which is symmetric and positive definite, $C(q,\dot{q}) \in \Re^{n\times n}$ contains the centripetal and Coriolis terms and $G(q)$ are the gravity terms, and τ denotes the dead-zone output. The nonsymmetric dead-zone can be represented by

$$\tau = \mathrm{DZ}(v) = \begin{cases} m_r(v - b_r) & v \geq b_r \\ 0 & b_l < v < b_r \\ m_l(v - b_l) & v \leq b_l, \end{cases} \tag{2}$$

where m_r and m_l are the right and left constant slopes for the dead-zone characteristic and b_r and b_l represent the right and left breakpoints. Note that v is the input of the dead-zone and the control input of the global system.

Define the following two states as follows:

$$\begin{aligned} x_1 &= q \in \Re^{n\times 1}, \\ x_2 &= \dot{q} \in \Re^{n\times 1}, \\ u &= \tau \in \Re^{n\times 1}, \end{aligned} \tag{3}$$

where $x_1 = [x_{11} \quad x_{12}]^T = [q_1 \quad q_2]^T$, $x_2 = [x_{21} \quad x_{22}]^T = [\dot{q}_1 \quad \dot{q}_2]^T$ for $n = 2$. Then (1) can be rewritten as

$$\begin{aligned} \dot{x}_1 &= x_2, \\ M(x_1)\dot{x}_2 + C(x_1,x_2)x_2 + G(x_1) &= u, \end{aligned} \tag{4}$$

where $M(x_1)$, $C(x_1,x_2)$, and $G(x_1)$ are described in (1), the dead-zone u is [17, 19, 20, 22]

$$u = \mathrm{DZ}(v) = \begin{cases} m_r(v - b_r) & v \geq b_r \\ 0 & b_l < v < b_r \\ m_l(v - b_l) & v \leq b_l, \end{cases} \tag{5}$$

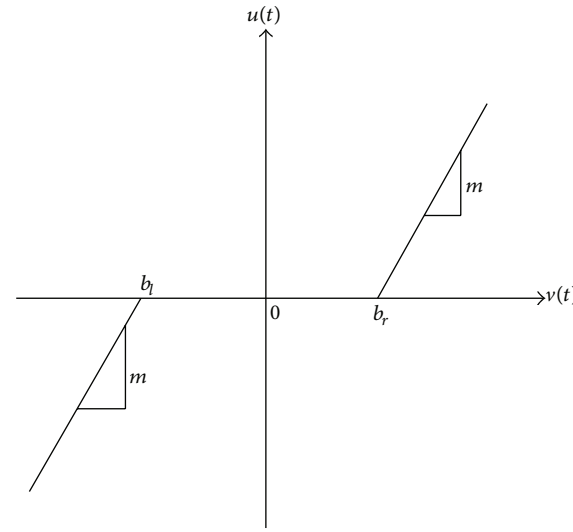

Figure 1: The dead-zone.

the parameters m_r, m_l, b_r, and b_l are described in (2), and v is the control input of the system. Figure 1 shows the dead-zone [17].

Property 1. The inertia matrix is symmetric and positive definite; that is, [23–25]

$$m_1|x|^2 \leq x^T M(x_1)x \leq m_2|x|^2, \tag{6}$$

where m_1, m_2 are known positive scalar constants; $x = [x_1, x_2]^T$.

Property 2. The centripetal and Coriolis matrix is skew-symmetric, that is, satisfies the following relationship [23–25]:

$$x^T\left[\dot{M}(x_1) - 2C(x_1,x_2)\right]x = 0, \tag{7}$$

where $x = [x_1, x_2]^T$.

The normal proportional derivative controller is

$$u = -K_p\tilde{x}_1 - K_d\tilde{x}_2, \tag{8}$$

where $\tilde{x}_1 = x_1 - x_1^d$ and $\tilde{x}_2 = x_2 - x_2^d$ and K_p and K_d are positive definite, symmetric, and constant matrices.

3. Dynamic Model of the Pendulum Systems with Dead-Zone Inputs

The dynamic model of the pendulum systems can be rewritten as the dynamic model of the robotic arms; however Property 2 is not directly satisfied. Pendulum dynamic models are rewritten as the robotic dynamic models because in this study, if the above sentence is true, Property 2 of the robotic systems can be used to guarantee the stability of the controller applied to the pendulum systems. The following lemmas let to modify the Property 2 for its application in the pendulum systems.

Lemma 1. *A pendulum model can be rewritten as a robotic arm model* (4). *Nevertheless, it cannot satisfy Property 2.*

Proof. Consider $n = 2$ for the pendulum systems in (4); it gives

$$\begin{aligned} \dot{x}_1 &= x_2, \\ M(x_1)\dot{x}_2 + C(x_1, x_2)x_2 + G(x_1) &= u, \end{aligned} \tag{9}$$

where

$$\begin{aligned} M(x_1) &= \begin{bmatrix} m_{11} & m_{12} \\ m_{21} & m_{22} \end{bmatrix}, \\ C(x_1, x_2) &= \begin{bmatrix} c_{11} & c_{12} \\ c_{21} & c_{22} \end{bmatrix}, \\ G(x_1) &= \begin{bmatrix} g_1 \\ g_2 \end{bmatrix} \end{aligned} \tag{10}$$

and $M(x_1)$, $C(x_1, x_2)$, and $G(x_1)$ are selected from the pendulum dynamic model, and x_1 and x_2 are defined in (3). Consequently,

$$x^T \left[\dot{M}(x_1) - 2C(x_1, x_2)\right] x \neq 0. \tag{11}$$

□

Lemma 2. *Pendulum model* (4) *can be rewritten as follows:*

$$\begin{aligned} \dot{x}_1 &= x_2, \\ M(x_1)\dot{x}_2 &= -\widehat{C}(x_1, x_2)x_2 - N(x_1, x_2) + u, \end{aligned} \tag{12}$$

where

$$\begin{aligned} M(x_1) &= \begin{bmatrix} m_{11} & m_{12} \\ m_{21} & m_{22} \end{bmatrix}, \\ \widehat{C}(x_1, x_2) &= \begin{bmatrix} \hat{c}_{11} & \hat{c}_{12} \\ \hat{c}_{21} & \hat{c}_{22} \end{bmatrix}, \\ N(x_1, x_2) &= \begin{bmatrix} n_1 \\ n_2 \end{bmatrix} \end{aligned} \tag{13}$$

the input u is given by (5), $c_{11} = \hat{c}_{11} + \bar{c}_{11}$, $c_{12} = \hat{c}_{12} + \bar{c}_{12}$, $c_{21} = \hat{c}_{21} + \bar{c}_{21}$, $c_{22} = \hat{c}_{22} + \bar{c}_{22}$, $n_1 = g_1 + \bar{c}_{11}x_{21} + \bar{c}_{12}x_{22}$, $n_2 = g_2 + \bar{c}_{21}x_{21} + \bar{c}_{22}x_{22}$, *$x_1$ and x_2 are defined in* (3), *and the following modified property is satisfied:*

$$x^T \left[\dot{M}(x_1) - 2\widehat{C}(x_1, x_2)\right] x = 0. \tag{14}$$

Proof. Consider $n = 2$ for the pendulum systems in (4); it gives

$$\begin{aligned} M(x_1)\dot{x}_2 + C(x_1, x_2)x_2 + G(x_1) &= u, \\ M(x_1)\dot{x}_2 &= -C(x_1, x_2)x_2 - G(x_1) + u. \end{aligned} \tag{15}$$

Consequently, a change of variables is used as follows:

$$\begin{aligned} M(x_1)\dot{x}_2 &= -\widehat{C}(x_1, x_2)x_2 - N(x_1, x_2) + u, \\ x^T \left[\dot{M}(x_1) - 2\widehat{C}(x_1, x_2)\right] x &= 0, \end{aligned} \tag{16}$$

where the elements are given in (12). Note that the elements of $\widehat{C}(x_1, x_2)$ and $N(x_1, x_2)$ are selected such that the property (14) is satisfied. □

In the following section, a stable controller for the pendulum systems will be designed.

4. Proportional Derivative Control with Inverse Dead-Zone

The regulation case is considered in this study; that is, the desired velocity is $x_2^d = 0$. The proportional derivative control with inverse dead-zone v is as follows:

$$v = \mathrm{DZ}^{-1}\left(u_{\mathrm{pd}}\right) = \begin{cases} \dfrac{1}{m_r}u_{\mathrm{pd}} + b_r & u_{\mathrm{pd}} > 0 \\ 0 & u_{\mathrm{pd}} = 0 \\ \dfrac{1}{m_l}u_{\mathrm{pd}} + b_l & u_{\mathrm{pd}} < 0, \end{cases} \tag{17}$$

where the parameters m_r, m_l, b_r, and b_l are defined as in (2), and the auxiliary proportional derivative control is

$$u_{\mathrm{pd}} = -K_p\tilde{x}_1 - K_d\tilde{x}_2 + \widehat{N} - K\,\mathrm{sign}\left(\tilde{x}_2\right), \tag{18}$$

where $\tilde{x}_1 = x_1 - x_1^d$ is the tracking error, x_1 and $\tilde{x}_2 = x_2$ are defined in (3), $x_1^d = [x_{11}^d \quad x_{12}^d] \in \Re^{n\times 1}$ is the desired position, K_p, K_d are positive definite, $\widehat{N} \in \Re^{n\times 1}$ is an approximation of $N(x_1, x_2)$, and $N(x_1, x_2) \in \Re^{n\times 1}$ are the nonlinear terms of (12). Figure 2 shows the inverse dead-zone [17, 22] and Figure 3 shows the proposed controller denoted as PDDZ. It is considered that the approximation error $\widetilde{N} = \widehat{N} - N(x_1, x_2)$ is bounded as

$$\left|\widetilde{N}\right| \leq \overline{N}. \tag{19}$$

Now the convergence of the closed-loop system is discussed.

Theorem 3. *The error of the closed-loop system with the proportional derivative control* (17) *and* (18) *for the pendulum systems with dead-zone inputs* (12) *and* (5) *is asymptotically stable, and the error of the velocity parameter $\tilde{x}_2$ will converge to*

$$\limsup_{T\to\infty} \left\|\tilde{x}_2\right\|^2 = 0, \tag{20}$$

where T is the final time, $\tilde{x}_2 = x_2$, $\overline{N} \leq K$, $K_p > 0$, and $K_d > 0$.

Proof. The proposed Lyapunov function is

$$V_1 = \frac{1}{2}\tilde{x}_2^T M(x_1)\tilde{x}_2 + \frac{1}{2}\tilde{x}_1^T K_p\tilde{x}_1. \tag{21}$$

Substituting (17) and (18) into (12) and (5) the closed-loop system is as follows:

$$\begin{aligned} M(x_1)\dot{x}_2 = &-K_p\tilde{x}_1 - K_d x_2 + \widetilde{N} \\ &- K\,\mathrm{sign}\left(x_2\right) - \widehat{C}(x_1, x_2)x_2. \end{aligned} \tag{22}$$

Using the fact $\tilde{x}_2 = x_2$, the derivative of (21) is

$$\dot{V}_1 = \tilde{x}_2^T M(x_1)\dot{x}_2 + \frac{1}{2}\tilde{x}_2^T \dot{M}(x_1)\tilde{x}_2 + \tilde{x}_2^T K_p\tilde{x}_1, \tag{23}$$

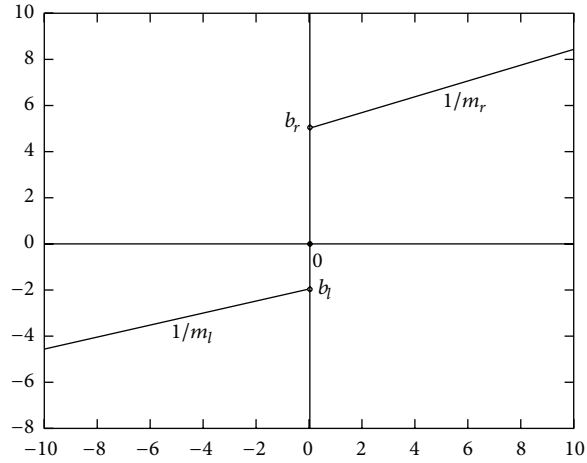

Figure 2: The inverse dead-zone.

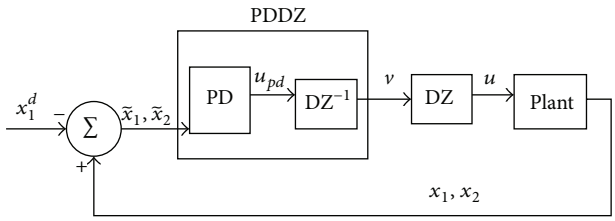

Figure 3: The proposed controller.

where $\dot{\tilde{x}}_1 = \dot{x}_1 - \dot{x}_1^d = x_2 - x_2^d = x_2 = \tilde{x}_2$ and $\dot{\tilde{x}}_2 = \dot{x}_2$. Substituting (22) into (23) gives

$$\begin{aligned} \dot{V}_1 = & -\tilde{x}_2^T K_d \tilde{x}_2 + \tilde{x}_2^T \left[\widetilde{N} - K \operatorname{sign}(x_2)\right] \\ & + \frac{1}{2}\tilde{x}_2^T \left[\dot{M}(x_1) - 2\widehat{C}(x_1, x_2)\right] \tilde{x}_2^T. \end{aligned} \tag{24}$$

Using (14), (17), and $|\tilde{x}_2|^T = \tilde{x}_2^T \operatorname{sign}(x_2)$, it gives

$$\begin{aligned} \dot{V}_1 &\le -\tilde{x}_2^T K_d \tilde{x}_2 + |\tilde{x}_2|^T \overline{N} - |\tilde{x}_2|^T K, \\ \dot{V}_1 &\le -\tilde{x}_2^T K_d \tilde{x}_2, \end{aligned} \tag{25}$$

where $\overline{N} \le K$. Thus, the error is asymptotically stable [26]. Integrating (25) from 0 to T yields

$$\begin{aligned} \int_0^T \tilde{x}_2^T K_d \tilde{x}_2 dt &\le V_{1,0} - V_{1,T} \le V_{1,0}, \\ \frac{1}{T}\int_0^T \tilde{x}_2^T K_d \tilde{x}_2 dt &\le \frac{1}{T} V_{1,0}, \\ \limsup_{T\to\infty} \left(\frac{1}{T}\int_0^T \tilde{x}_2^T K_d \tilde{x}_2 dt\right) &\le V_{1,0}\left[\limsup_{T\to\infty}\left(\frac{1}{T}\right)\right] = 0. \end{aligned} \tag{26}$$

If $T \to \infty$, then $\|\tilde{x}_2\|^2 = 0$; (20) is established. □

Remark 4. The proposed controller is used for the regulation case; that is, the desired velocity is $x_2^d = 0$. The general case when $x_2^d \neq 0$ is not considered in this research.

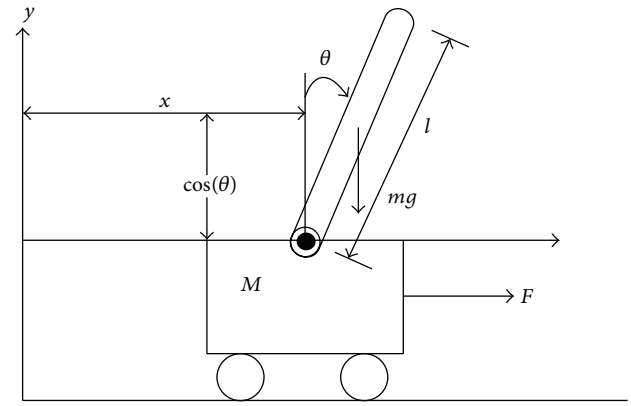

Figure 4: Inverted-car pendulum.

5. Simulations

In this section, the proportional derivative control with inverse dead-zone denoted as PDDZ will be compared with the proportional derivative control with gravity compensation of [23] denoted by PD for the control of two pendulum systems with dead-zone inputs. In this paper, the root mean square error (RMSE) [1, 26, 27] is used for the comparison results and it is given as

$$\text{RMSE} = \left(\frac{1}{T}\int_0^T \tilde{x}^2 dt\right)^{1/2}, \tag{27}$$

where $\tilde{x}^2 = \tilde{x}_{12}^2$ or $\tilde{x}^2 = u_1^2$.

5.1. Example 1. Consider the inverted-car pendulum [2] of Figure 4.

Inverted-car pendulum is written as (1) and it is detailed as follows:

$$\begin{aligned} M(x_1) &= \begin{bmatrix} m_{11} & m_{12} \\ m_{21} & m_{22} \end{bmatrix}, \\ C(x_1, x_2) &= \begin{bmatrix} c_{11} & c_{12} \\ c_{21} & c_{22} \end{bmatrix}, \\ G(x_1) &= \begin{bmatrix} g_1 \\ g_2 \end{bmatrix}, \end{aligned} \tag{28}$$

where $m_{11} = M + m$, $m_{12} = m_{21} = ml\cos(x_{12})$, $m_{33} = I + ml^2$, $c_{12} = -ml\sin(x_{12})x_{22}$, the other parameters of $C(x_1, x_2)$ are zero, $g_2 = -mgl\sin(x_{12})$, and the other parameter of $G(x_1)$ is zero. $\sin(\cdot)$ is the sine function, $\cos(\cdot)$ is the cosine function, $I = 0.5\,\text{kgm}^2$ is the pendulum inertia, $M = 0.136729$ kg is the mass of the car, $m = 0.040691$ kg is the pendulum mass, $l = 0.15$ m is the pendulum length, θ_{12} is the angle with respect of the y axis, $u = F$ is the motion force of the car, $x_{11} = x$ is the motion distance of the car, and $g = 9.81\,\text{m/s}^2$ is the constant acceleration due to gravity. It can be proven that Property 2 of (7) is not satisfied.

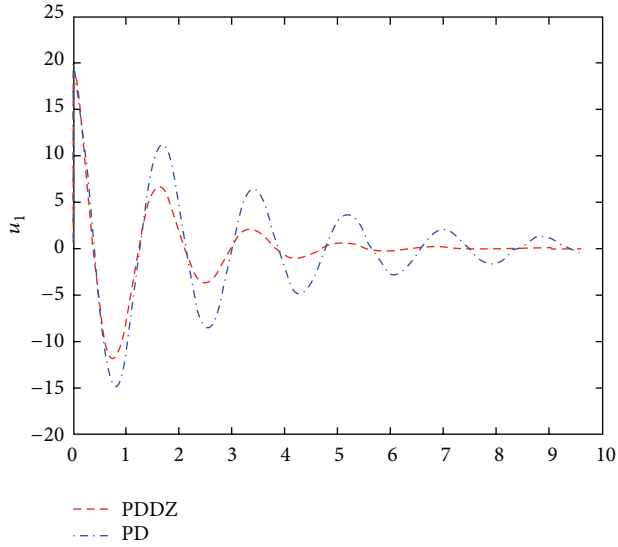

Figure 5: Input for Example 1.

Inverted-car pendulum is written as (12), and it is detailed as follows:

$$M(x_1) = \begin{bmatrix} m_{11} & m_{12} \\ m_{21} & m_{22} \end{bmatrix},$$
$$\widehat{C}(x_1, x_2) = \begin{bmatrix} \widehat{c}_{11} & \widehat{c}_{12} \\ \widehat{c}_{21} & \widehat{c}_{22} \end{bmatrix}, \quad (29)$$
$$N(x_1, x_2) = \begin{bmatrix} n_1 \\ n_2 \end{bmatrix},$$

where $m_{11} = M + m$, $m_{12} = m_{21} = ml\cos(x_{12})$, $m_{33} = I + ml^2$, $\widehat{c}_{12} = \widehat{c}_{21} = -(1/2)ml\sin(x_{12})x_{22}$ and the other parameters of $\widehat{C}(x_1, x_2)$ are zero, $n_1 = -(1/2)ml\sin(x_{12})x_{22}$, $n_2 = -mgl\sin(x_{12}) + (1/2)ml\sin(x_{12})x_{22}$; therefore, it can be proven that the property of the lemma of (14) is satisfied.

PDDZ is given by (17) and (18) as $u_{\text{pd}} = -K_p\widetilde{x}_{12} - K_d\widetilde{x}_{22} + \widehat{n}_1 - K\,\text{sign}(\widetilde{x}_{22})$ with parameters $K_p = 200$, $K_d = 20$, $\widehat{N} = \widehat{n}_1$, and $\widehat{n}_1 = 0.01$, with $K = 0.01$. Conditions given in (20) $\overline{N} \leq K$, $K_p > 0$, and $K_d > 0$ are satisfied; consequently, the error of the closed-loop dynamics of the PDDZ applied for pendulum systems is guaranteed to be asymptotically stable.

PD is given by [23] as $u_{\text{pd}} = -K_p\widetilde{x}_{12} - K_d\widetilde{x}_{22} + g_2$ with parameters $K_p = 400$, $K_d = 20$, and $G(x_1) = g_1$.

Comparison results for the control functions are shown in Figure 5, position states are shown in Figure 6, and comparison results for the controller errors are shown in Figure 7. Comparison of the square norm of the velocity errors $\|\widetilde{x}_2\|^2$ of (20) for the controllers is presented in Figure 8. From the theorem of (20), $\|\widetilde{x}_2\|^2$ will converge to zero for the PDDZ. Table 1 shows the RMSE results using (27).

The most important variable to control is the pendulum angle $x_{12} = \theta$, and this variable may reach zero even if it starts with other value as in this example. Note that the PD technique requires the bigger gains than the PDDZ method to obtain satisfactory results. From Figures 5, 6, and 7, it can be seen that the PDDZ improves the PD because the signal of the plant for the first follows better the desired signal than the second and in the first the inputs are smaller than in the second. From Figure 8, it is shown that the PDDZ improves the PD because the velocity error $\|\widetilde{x}_2\|^2$ presented by the first is smaller than that presented by the second. From Table 1, it

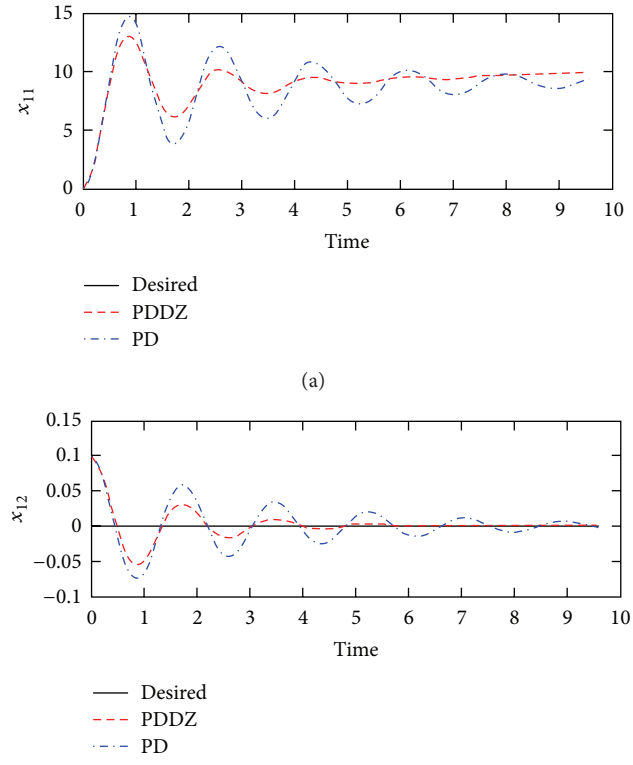

Figure 6: Position states for Example 1.

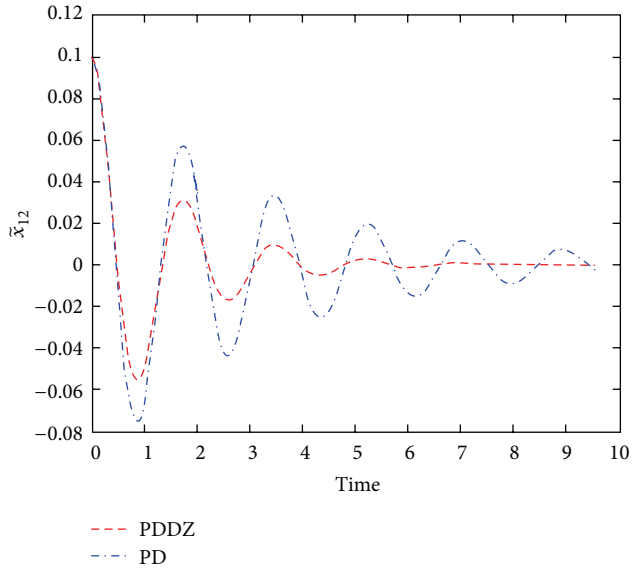

Figure 7: Position state error for Example 1.

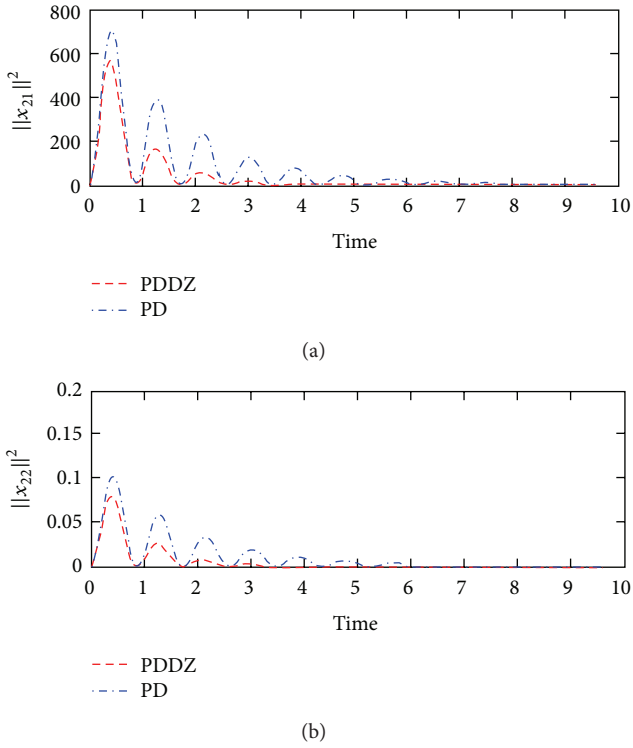

Figure 8: Velocity errors for Example 1.

Table 1: Error results for Example 1.

Methods	RMSE for $\tilde{x}$	RMSE for u
PD	4.2487×10^{-4}	15.5044
PDDZ	2.1995×10^{-4}	7.7534

can be shown that the PDDZ achieves better accuracy when compared with the PD because the RMSE is smaller for the first than for the second.

5.2. Example 2. Consider the Furuta pendulum [3, 27] of the Figure 9.

Furuta pendulum is written as (1) and it is detailed as follows:

$$M(x_1) = \begin{bmatrix} m_{11} & m_{12} \\ m_{21} & m_{22} \end{bmatrix},$$
$$C(x_1, x_2) = \begin{bmatrix} c_{11} & c_{12} \\ c_{21} & c_{22} \end{bmatrix}, \quad (30)$$
$$G(x_1) = \begin{bmatrix} g_1 \\ g_2 \end{bmatrix},$$

where $m_{11} = I_0 + m_1(L_0^2 + l_1^2 \sin^2(x_{12}))$, $m_{12} = m_{21} = m_1 l_1 L_0 \cos(x_{12})$, $m_{33} = J_1 + m_1 l_1^2$, $c_{11} = m_1 l_1^2 \sin(2x_{12}) x_{22}$, $c_{12} = -m_1 l_1 L_0 \sin(x_{12}) x_{22}$, $c_{21} = -m_1 l_1^2 \sin(x_{12}) \cos(x_{12}) x_{21}$, $g_2 = -m_1 g l_1 \sin(x_{12})$, and the other parameter of $G(x_1)$ is zero. $\sin(\cdot)$ is the sine function, $\cos(\cdot)$ is the cosine function, $I_0 = 0.5\,\text{Kgm}^2$ is the arm inertia, $J_1 = 0.5\,\text{kgm}^2$ is the pendulum inertia, $m_2 = 0.34\,\text{kg}$ is the arm mass, $m_1 = 0.24\,\text{kg}$ is the pendulum mass, $L_0 = 0.293\,\text{m}$ is the arm length, $l_1 = 0.28\,\text{m}$ is the pendulum length, $x_{11} = \theta_0$ is the arm angle, $x_{12} = \theta_1$ is the pendulum angle, $u = F$ is the motion torque of the arm, and $g = 9.81\,\text{m/s}^2$ is the constant acceleration due to gravity. It can be proven that Property 2 of (7) is not satisfied.

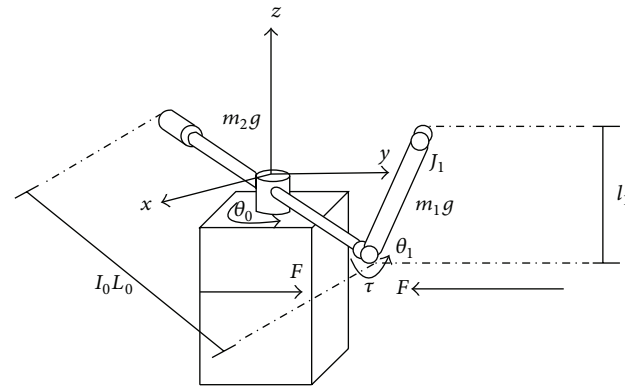

Figure 9: Furuta pendulum.

Furuta pendulum is written as (12), and it is detailed as follows:

$$M(x_1) = \begin{bmatrix} m_{11} & m_{12} \\ m_{21} & m_{22} \end{bmatrix},$$
$$\widehat{C}(x_1, x_2) = \begin{bmatrix} \widehat{c}_{11} & \widehat{c}_{12} \\ \widehat{c}_{21} & \widehat{c}_{22} \end{bmatrix}, \quad (31)$$
$$N(x_1, x_2) = \begin{bmatrix} n_1 \\ n_2 \end{bmatrix},$$

where $m_{11} = M + m$, $m_{12} = m_{21} = ml \cos(x_{12})$, $m_{33} = I + ml^2$, $\widehat{c}_{11} = m_1 l_1^2 \sin(x_{12}) \cos(x_{12}) x_{22}$, $\widehat{c}_{12} = -(1/2) m_1 l_1 L_0 \sin(x_{12}) x_{22}$, $\widehat{c}_{21} = -(1/2) m_1 l_1^2 \sin(x_{12}) \cos(x_{12}) x_{22}$, and the other parameter of $\widehat{C}(x_1, x_2)$ is zero, $n_1 = m_1 l_1^2 \sin(x_{12}) \cos(x_{12}) x_{22} - (1/2) m_1 l_1 L_0 \sin(x_{12}) x_{22}$, $n_2 = -m_1 g l_1 \sin(x_{12}) - (1/2) m_1 l_1^2 \sin(x_{12}) \cos(x_{12})(x_{21} - x_{22})$; therefore, it can be proven that the property of the lemma of (14) is satisfied.

PDDZ is given by (17) and (18) as $u_{\text{pd}} = -K_p \tilde{x}_{12} - K_d \tilde{x}_{22} + \widehat{n}_1 - K \operatorname{sign}(\tilde{x}_{22})$ with parameters $K_p = 200$, $K_d = 20$, $\widehat{N} = \widehat{n}_1$, $\widehat{n}_1 = 0.01$, with $K = 0.01$. Conditions given in (20) $\overline{N} \le K$, $K_p > 0$, and $K_d > 0$ are satisfied; consequently, the error of the closed-loop dynamics of the PDDZ applied for pendulum systems is guaranteed to be asymptotically stable.

PD is given by [23] as $u_{\text{pd}} = -K_p \tilde{x}_{12} - K_d \tilde{x}_{22} + g_2$ with parameters $K_p = 400$, $K_d = 20$, and $G(x_1) = g_2$.

Comparison results for the control functions are shown in Figure 10, position states are shown in Figure 11, and comparison results for the controller errors are shown in Figure 12. Comparison of the square norm of the velocity errors $\|\tilde{x}_2\|^2$ of (20) for the controllers is presented in Figure 13. From the theorem of (20), $\|\tilde{x}_2\|^2$ will converge to zero for the PDDZ. Table 2 shows the RMSE results using (27).

The most important variable to control is the pendulum angle $x_{12} = \theta_1$, and this variable may reach zero even if it

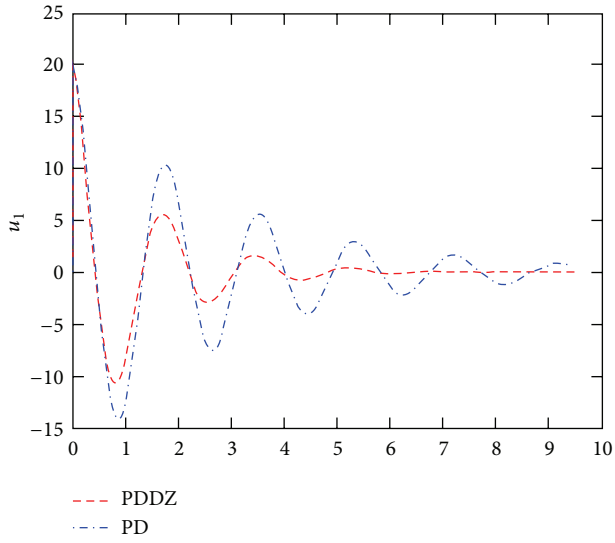

Figure 10: Input for Example 2.

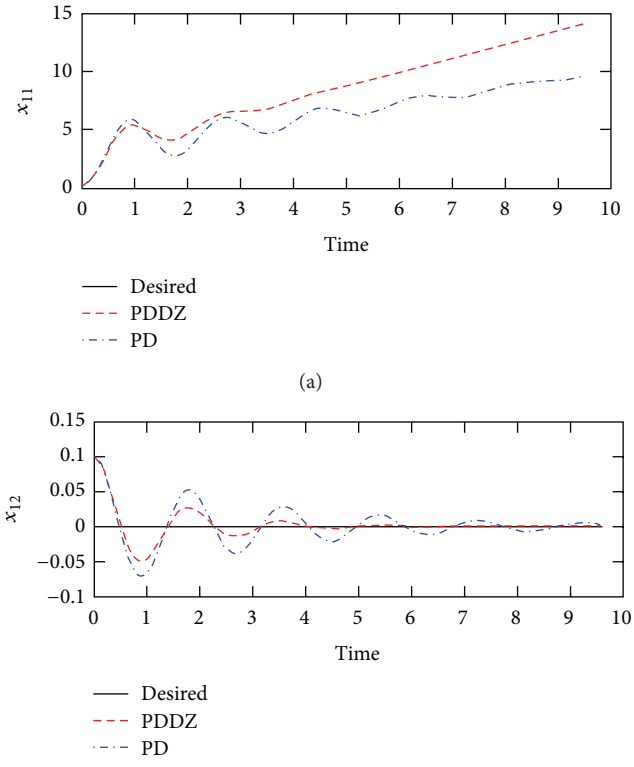

Figure 11: Position states for Example 2.

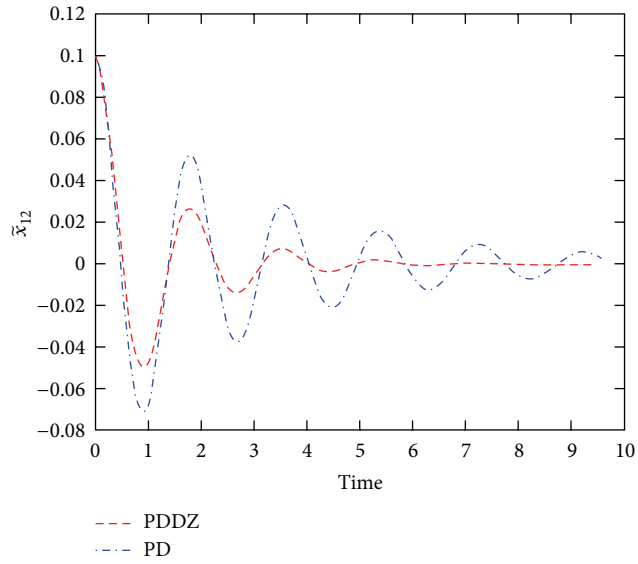

Figure 12: Position state error for Example 2.

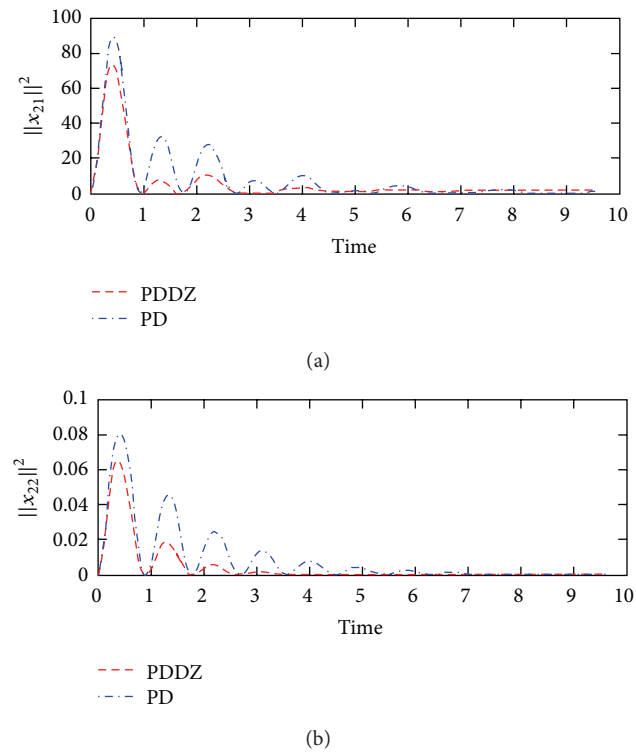

Figure 13: Velocity errors for Example 2.

starts with other value as in this example. Note that the PD technique requires the bigger gains than the PDDZ method to obtain satisfactory results. From Figures 10, 11, and 12, it can be seen that the PDDZ improves the PD because the signal of the plant for the first follows better the desired signal than the second and in the first the inputs are smaller than in the second. From Figure 13, it is shown that the PDDZ improves the PD because the velocity error $\|\tilde{x}_2\|^2$ presented by the first is smaller than that presented by the second. From Table 2, it can be shown that the PDDZ achieves better accuracy when compared with the PD because the RMSE is smaller for the first than for the second.

Table 2: Error results for Example 2.

Methods	RMSE for $\tilde{x}$	RMSE for u
PD	3.7760×10^{-4}	13.6043
PDDZ	2.0158×10^{-4}	6.8328

6. Conclusion

In this research, a proportional derivative control with inverse dead-zone for pendulum systems with dead-zone inputs is presented. The simulations showed that the proposed technique achieves better performance when compared with the proportional derivative control with gravity compensation for the regulation of two pendulum systems, and the results illustrate the viability, efficiency, and the potential of the approach especially important in pendulum systems. As a future research, the proposed study will be improved considering that some parameters of the controller are unknown [28–32], or it will consider the communication delays and packet dropout.

Conflict of Interests

The authors declare no conflict of interests about all the aspects related to this paper.

Acknowledgments

The authors are grateful to the editors and the reviewers for their valuable comments and insightful suggestions, which helped to improve this research significantly. The authors thank the Secretaría de Investigación y Posgrado, the Comisión de Operación y Fomento de Actividades Académicas del IPN, and Consejo Nacional de Ciencia y Tecnología for their help in this research.

References

[1] J. J. Rubio and J. H. Pérez-Cruz, "Evolving intelligent system for the modelling of nonlinear systems with dead-zone input," *Applied Soft Computing*. In press.

[2] C. Aguilar-Ibañez, J. C. Martínez-García, A. Soria-López, and J. D. J. Rubio, "On the stabilization of the inverted-cart pendulum using the saturation function approach," *Mathematical Problems in Engineering*, vol. 2011, Article ID 856015, 14 pages, 2011.

[3] C. Aguilar-Ibañez, M. S. Suárez-Castañón, and O. O. Gutiérres-Frias, "The direct Lyapunov method for the stabilisation of the furuta pendulum," *International Journal of Control*, vol. 83, no. 11, pp. 2285–2293, 2010.

[4] D. Ding, Z. Wang, J. Hu, and H. Shu, "Dissipative control for state-saturated discrete time-varying systems with randomly occurring nonlinearities and missing measurements," *International Journal of Control*, vol. 86, no. 4, pp. 674–688, 2013.

[5] H. Dong, Z. Wang, J. Lam, and H. Gao, "Distributed filtering in sensor networks with randomly occurring saturations and successive packet dropouts," *International Journal of Robust and Nonlinear Control*, 2013.

[6] J. Hu, Z. Wang, B. Shen, and H. Gao, "Quantised recursive filtering for a class of nonlinear systems with multiplicative noises and missing measurements," *International Journal of Control*, vol. 86, no. 4, pp. 650–663, 2013.

[7] J. Hu, Z. Wang, B. Shen, and H. Gao, "Gain-constrained recursive filtering with stochastic nonlinearties and probabilistic sensor delays," *IEEE Transactions on Signal Processing*, vol. 61, no. 5, pp. 1230–1238, 2013.

[8] M. Jimenez-Lizarraga, M. Basin, and P. Rodriguez-Ramirez, "Robust mini-max regulator for uncertain non-linear polynomial systems," *IET Control Theory & Applications*, vol. 6, no. 7, pp. 963–970, 2012.

[9] A. F. de Loza, M. Jimenez-Lizarraga, and L. Fridman, "Robust output nash strategies based on sliding mode observation in a two-player differential game," *Journal of the Franklin Institute*, vol. 349, no. 4, pp. 1416–1429, 2012.

[10] Q. Lu, L. Zhang, H. R. Karimi, and Y. Shi, "H_∞ control for asynchronously switched linear parameter-varying systems with mode-dependent average dwell time," *IET Control Theory & Applications*, vol. 7, no. 5, pp. 677–683, 2013.

[11] L. F. Ma, Z. D. Wang, and Z. Guo, "Robust H_2 sliding mode control for non-linear discrete-time stochastic systems," *IET Control Theory and Applications*, vol. 3, no. 11, pp. 1537–1546, 2009.

[12] Y. Niu, D. W. C. Ho, and Z. Wang, "Improved sliding mode control for discrete-time systems via reaching law," *IET Control Theory & Applications*, vol. 4, no. 11, pp. 2245–2251, 2010.

[13] L. A. Soriano, W. Yu, and J. J. Rubio, "Modeling and control of wind turbine," *Mathematical Problems in Engineering*, vol. 2013, Article ID 982597, 13 pages, 2013.

[14] J. J. Rubio, G. Ordaz, M. Jimenez-Lizarraga, and R. I. Cabrera, "General solution to the Navier-Stokes equation to describe the dynamics of a homogeneous viscous fluid in an open pipe," *Revista Mexicana de Fisica*, vol. 59, no. 3, pp. 217–223, 2013.

[15] Y. Wang, H. R. Karimi, and Z. Xiang, "Delay-dependent H_∞ control for networked control systems with large delays," *Mathematical Problems in Engineering*, vol. 2013, Article ID 643174, 10 pages, 2013.

[16] Y. Wang, H. R. Karimi, and Z. Xiang, "H_∞ control for networked control systems with time delays and packet dropouts," *Mathematical Problems in Engineering*, vol. 2013, Article ID 635941, 10 pages, 2013.

[17] S. Ibrir, W. F. Xie, and C.-Y. Su, "Adaptive tracking of nonlinear systems with non-symmetric dead-zone input," *Automatica*, vol. 43, no. 3, pp. 522–530, 2007.

[18] S. Abrir, "Invarian-manifold approach to the stabilization of feedforward nonlinear systems having uncertain dead-zone inputs," in *Proceedings of the International Sysmposium of Mechatronics and Its Applications*, pp. 1–5, 2012.

[19] J. H. Pérez-Cruz, E. Ruiz-Velázquez, J. J. Rubio, and C. A. de Alva Padilla, "Robust adaptive neurocontrol of SISO nonlinear systems preceded by unknow deadzone," *Mathematical Problems in Engineering*, vol. 2012, Article ID 342739, 23 pages, 2012.

[20] J. H. Pérez-Cruz, J. J. Rubio, E. Ruiz-Velázquez, and G. Sols-Perales, "Tracking control based on recurrent neural networks for nonlinear systems with multiple inputs and unknown deadzone," *Abstract and Applied Analysis*, vol. 2012, Article ID 471281, 18 pages, 2012.

[21] Z. Wang, Y. Zhang, and H. Fang, "Neural adaptive control for a class of nonlinear systems with unknown deadzone," *Neural Computing and Applications*, vol. 17, no. 4, pp. 339–345, 2008.

[22] J. Zhou and X. Z. Shen, "Robust adaptive control of nonlinear uncertain plants with unknown dead-zone," *IET Control Theory and Applications*, vol. 1, no. 1, pp. 25–32, 2007.

[23] F. L. Lewis, D. M. Dawson, and C. T. Abdallah, *Control of Robot Manipulators, Theory and Practice*, CRC Press, New York, NY, USA, 2004.

[24] J. E. Slotine and W. Li, *Applied Nonlinear Control*, Macmillan, Englewood Clifs, NJ, USA, 1991.

[25] M. W. Spong and M. Vidyasagar, *Robot Dynamics and Control*, John Wiley & Sons, 1989.

[26] J. J. Rubio, G. Gutierrez, J. Pacheco, and J. H. Pérez-Cruz, "Comparison of three proposed controls to accelerate the growth of the crop," *International Journal of Innovative Computing, Information and Control*, vol. 7, no. 7, pp. 4097–4114, 2011.

[27] J. J. Rubio, M. Figueroa, J. H. Pérez-Cruz, and J. Rumbo, "Control to stabilize and mitigate disturbances in a rotary inverted pendulum," *Revista Mexicana de Fisica E*, vol. 58, no. 2, pp. 107–112, 2012.

[28] J. A. Iglesias, P. Angelov, A. Ledezma, and A. Sanchis, "Creating evolving user behavior profiles automatically," *IEEE Transactions on Knowledge and Data Engineering*, vol. 24, no. 5, pp. 854–867, 2011.

[29] D. Leite, R. Ballini, P. Costa, and F. Gomide, "Evolving fuzzy granular modeling from nonstationary fuzzy data streams," *Evolving Systems*, vol. 3, no. 2, pp. 65–79, 2012.

[30] E. Lughofer, "Single pass active learning with conflict and ignorance," *Evolving Systems*, vol. 3, pp. 251–271, 2012.

[31] E. Lughofer, "A dynamic split-and-merge approach for evolving cluster models," *Evolving Systems*, vol. 3, pp. 135–151, 2012.

[32] L. Maciel, A. Lemos, F. Gomide, and R. Ballini, "Evolving fuzzy systems for pricing fixed income options," *Evolving Systems*, vol. 3, no. 1, pp. 5–18, 2012.

Hindawi Publishing Corporation
Mathematical Problems in Engineering
Volume 2013, Article ID 169454, 18 pages
http://dx.doi.org/10.1155/2013/169454

Research Article

State-Feedback H_∞ Control for LPV System Using T-S Fuzzy Linearization Approach

Jizhen Liu, Yang Hu, and Zhongwei Lin

State Key Laboratory of Alternate Electrical Power System with Renewable Energy Sources, North China Electric Power University, Beijing 102206, China

Correspondence should be addressed to Yang Hu; hooyoung2011@gmail.com

Received 2 April 2013; Revised 1 July 2013; Accepted 24 July 2013

Academic Editor: Xiao He

This paper discusses the linear parameter varying (LPV) gain scheduling control problem based on the Takagi-Sugeno (T-S) fuzzy linearization approach. Firstly, the affine nonlinear parameter varying (ANPV) description of a class of nonlinear dynamic processes is defined; that is, at any scheduling parameter, the corresponding system is affine nonlinear as usual. For such a class of ANPV systems, a kind of developed T-S fuzzy modeling procedure is proposed to deal with the nonlinearity, instead of the traditional Jacobian linearization approach. More concretely, the evaluation system for the approximation ability of the novelly developed T-S fuzzy modeling procedure is established. Consequently, the LPV T-S fuzzy system is obtained which can approximate the ANPV system with required accuracy. Secondly, the notion of piecewise parameter-dependent Lyapunov function is introduced, and then the stabilization problem and the state-feedback H_∞ control problem of the LPV T-S fuzzy system are studied. The sufficient conditions are given in linear matrix inequalities (LMIs) form. Finally, a numerical example is provided to demonstrate the availability of the above approaches. The simulation results show the high approximation accuracy of the LPV T-S fuzzy system to the ANPV system and the effectiveness of the LPV T-S fuzzy gain scheduling control.

1. Introduction

It is well known that the gain scheduling control is an efficient solution for the control of nonlinear dynamic processes [1, 2]. In particular, due to the advantage to carry forward the stability and dynamic performance analysis, the LPV gain scheduling control has been popularly studied [3–12]. Currently, there are mainly two ways to realize the LPV gain scheduling control: the linear fractional transformation (LFT) gain scheduling technique based on a scaled version of the small gain theorem [5–8] and the quadratic gain scheduling technique based on Lyapunov theory [9–12]. However, both of them adopt the Jacobian linearization approach to deal with the nonlinearity around each steady operating point which means that the number of scheduling parameters is equal to the number of variables relevant to the nonlinearity. As a result, too many scheduling parameters are brought in and too much computation burden is caused for the control design; that is, while the gridding process of scheduling parameters and the parameterization of decision variables in LMIs are executed, the number of LMIs would have a rapid increase. Besides, due to the local linearization around each steady operating point, the control performance is restricted within the local region which would become a weakness when the controlled variables vary widely. Also, it is hard to guarantee the system stability and control performance during the scheduling process. Hence, there requires a further study on the appropriate linearization approach for the ANPV system which can both efficiently reduce the number of scheduling parameters and enlarge the linearization range to extend the effective region of control performance.

On the other hand, the T-S fuzzy model was firstly proposed by Takagi and Sugeno in 1985 [13] and developed by Sugeno and Kang [14], which was data based. To linearize the nonlinearity, the research on the model-based T-S fuzzy modeling procedure was proposed by Kawamoto et al. [15] via the nonlinear sector method which was an exact modeling procedure with constant consequent parts and nonlinear membership functions. Then, Kluska [16]

exploited the local approximation method to establish T-S fuzzy model with homogeneous linear consequent parts. In order to evaluate the approximation ability, Abonyi and Babuska [17] discussed the ways to analyze the relation between the local and global approximation performances of the T-S fuzzy model. Subsequently, Teixeira and Zak [18] gave the T-S fuzzy modeling procedure with homogeneous linear consequent parts by solving a convex optimization problem. And Tanaka and Wang [19] also realized the similar results through uniform partition to the input space of premise variables and proved the universal approximation ability. However, as far as we know, the T-S fuzzy linearization to the ANPV system has been rarely studied in most of the literature.

If the T-S fuzzy linearization is applied to the ANPV system, the choosing of the scheduling parameters and the premise variables can be separated. The nonlinearity of scheduling parameters can remain and that of premise variables should be linearized within their varying regions. As a result, the number of scheduling parameters can be reduced. Meanwhile, because the T-S fuzzy linearization range can be extended to any optional one, the nonlinearity with widely varying state variables can be dealt with for the nonlinear dynamic processes. Due to the above points, it is valuable to study the T-S fuzzy modeling procedure for the ANPV system. Furthermore, in order to efficiently reduce the number of T-S fuzzy rules, an ununiform partition method is utilized, and the evaluation system is also established to adjust the approximation performance. Then, the ANPV system can be linearized on demand and the LPV T-S fuzzy system with required accuracy can be obtained. However, a challenging control problem for such a class of systems is correspondingly formulated. For the T-S fuzzy control, the piecewise Lyapunov functions have been brought in to improve the solvability compared with that based on the common Lyapunov function [20–22]. In addition, considering the approximation error to the ANPV system, the T-S fuzzy H_∞ control has been also studied [23–26]. Hence, the T-S fuzzy control needs to be generalized to the LPV system while improving the solvability by introducing the notion of piecewise Lyapunov function. In addition, for the sake of improving the control performance, the approximation error of LPV T-S fuzzy system to the ANPV system should be considered.

In the paper, the T-S fuzzy modeling procedure with homogeneous linear consequent parts is discussed for the ANPV system while an ununiform partition method is utilized to reduce the number of T-S fuzzy rules. To adjust the approximation accuracy, the evaluation system for the approximation performance of the LPV T-S fuzzy system is established. Then, in order to improve the solvability of the LPV T-S fuzzy gain scheduling control, the notion of piecewise parameter-dependent Lyapunov function is introduced and the LPV T-S fuzzy gain scheduling control design based on the piecewise parameter-dependent Lyapunov functions is studied. Meanwhile, while taking the approximation error to the ANPV system in consideration, the sufficient conditions of the stabilization problem and the state-feedback H_∞ control problem of the LPV T-S fuzzy system are given in LMIs form. More concretely, the main contributions of the paper are listed as follows.

(i) The T-S fuzzy approximation with required accuracy aiming at the ANPV system is studied, and then the nonlinearity of the ANPV system can be dealt with and the LPV T-S fuzzy system with required accuracy can be obtained.

(ii) The stabilization problem of the LPV T-S fuzzy system is studied by bringing in the piecewise parameter-dependent Lyapunov functions while the sufficient conditions are given in LMIs form.

(iii) Considering the approximation error to the ANPV system, the state-feedback H_∞ control problem of the LPV T-S fuzzy system is studied based on the piecewise parameter-dependent Lyapunov functions. The sufficient conditions are given in both Riccati inequalities form and LMIs form.

The rest of the paper is organized as follows. In Section 2, the developed T-S fuzzy modeling procedure utilizing ununiform partition method is proposed aiming at the ANPV system. And the evaluation system for the approximation performance of the LPV T-S fuzzy system with homogeneous consequent parts is established. Then, the LPV T-S fuzzy system with required accuracy can be obtained by applying the above ways to the ANPV system. In Section 3, the notion of piecewise parameter-dependent Lyapunov function is introduced and the stabilization problem of the LPV T-S fuzzy system is studied. In Section 4, the state-feedback H_∞ control problem of the LPV T-S fuzzy system is studied and the sufficient conditions are given in both Riccati inequalities form and LMIs form. In Section 5, a numerical example is provided to demonstrate the availability of the above approaches. Section 6 concludes the paper.

2. Establishment of LPV T-S Fuzzy System

In this section, the ANPV description of a class of nonlinear dynamic processes is defined aiming at which kind of novelly developed T-S fuzzy modeling procedure is proposed and the corresponding evaluation system for the approximation performance is established. Both can be combined to deal with the nonlinearity of the ANPV system to get the LPV T-S fuzzy system with required accuracy.

For a class of nonlinear dynamic processes, if we can achieve their nonlinear descriptions in mathematical models, the ANPV system can be obtained by choosing the proper variables as scheduling parameters. The general form of it can be defined as

$$\begin{bmatrix} \dot{x} \\ z \end{bmatrix} = \begin{bmatrix} f(x,\theta) + d_0(x,\theta)\,\omega + g_0(x,\theta)\,u \\ \varphi(x,\theta) + g_1(x,\theta)\,u \end{bmatrix}, \tag{1}$$

where θ is a vector of the scheduling parameters which may be system parameters, external inputs, or other parameters; x is a column vector of the state variables with n dimensions; and $f(x,\theta), \ldots, g_1(x,\theta)$ are the nonlinear functions of x and θ. Then, referring to the way in [18], the T-S fuzzy modeling

procedure aiming at (1) can be developed to linearize the nonlinearity of the ANPV system.

Considering (1), around the zero state, the Jacobian linearization approach can be easily executed to get homogeneous linear model in the local region. However, for the nonzero states, it would be unavailable. Assume the nonzero operating state x_0^i which can be steady or transient one and corresponds to the ith fuzzy rule, $i = 1, 2, \ldots, L$. It should be noted that x_0^i may include the part or all of the state variables and it is gotten from the partition to the input space of premise variables. Firstly, we establish the homogeneous linear model in the vicinity of x_0^i. Because the local linear model should approximate the local dynamics in the vicinity of x_0^i, we can get

$$\begin{aligned}
&\begin{bmatrix} f(x,\theta) + d_0(x,\theta)\omega + g_0(x,\theta)u \\ \varphi(x,\theta) + g_1(x,\theta)u \end{bmatrix} \\
&\approx \begin{bmatrix} A_i(\theta) & B_1^i(\theta) & B_2^i(\theta) \\ C_1^i(\theta) & 0 & D_{12}^i(\theta) \end{bmatrix} \begin{bmatrix} x \\ \omega \\ u \end{bmatrix}, \\
&\begin{bmatrix} f\left(x_0^i,\theta\right) + d_0\left(x_0^i,\theta\right)\omega + g_0\left(x_0^i,\theta\right)u \\ \varphi\left(x_0^i,\theta\right) + g_1\left(x_0^i,\theta\right)u \end{bmatrix} \\
&= \begin{bmatrix} A_i(\theta) & B_1^i(\theta) & B_2^i(\theta) \\ C_1^i(\theta) & 0 & D_{12}^i(\theta) \end{bmatrix} \begin{bmatrix} x_0^i \\ \omega \\ u \end{bmatrix},
\end{aligned} \tag{2}$$

where ω and u are arbitrarily changed variables and $A_i(\theta), \ldots, D_{12}^i(\theta)$ are parameter-dependent matrices.

Take the first equation $\dot{x} = f(x,\theta) + d_0(x,\theta)\omega + g_0(x,\theta)u$ for example. Due to that, $f(x,\theta), d_0(x,\theta)$, and $g_0(x,\theta)$ are nonlinear functions of operating state x at any θ, and the matrices $A_i(\theta)$, $B_1^i(\theta)$, and $B_2^i(\theta)$ only depend on x. Moreover, because ω and u are arbitrarily changed, we can uniquely determine that

$$\begin{aligned}
d_0\left(x_0^i,\theta\right) &= B_1^i(\theta), \\
g_0\left(x_0^i,\theta\right) &= B_2^i(\theta), \\
f\left(x_0^i,\theta\right) &= A_i(\theta)x_0^i, \\
f(x,\theta) &\approx A_i(\theta)x.
\end{aligned} \tag{3}$$

Define $a_l^i(\theta)^T$, a row vector with n dimensions, as the lth row of the matrix $A_i(\theta)$. Then, condition (3) can be equivalently represented as

$$f_l(x,\theta) \approx a_l^i(\theta)^T x, \quad l = 1, 2, \ldots, n, \tag{4}$$

where $f_l(x,\theta)$ is the lth row of $f(x,\theta)$. Additionally, assume $f_l(0,\theta) = 0$ and $f_l(x,\theta) \in C^1$, which means that f_l and $\partial f_l/\partial x$ are continuous functions on the compact set $\Theta \subset R^n$. Meanwhile, $f(x_0^i,\theta) = A_i(\theta)x_0^i$ can be equivalently represented as

$$f_l\left(x_0^i,\theta\right) = a_l^i(\theta)^T x_0^i, \quad l = 1, 2, \ldots, n. \tag{5}$$

Expanding $f_l(x,\theta)$ of (4) around the operating state x_0^i and neglecting second- and higher-order terms, we can get

$$f_l\left(x_0^i,\theta\right) + \nabla^T f_l\left(x_0^i,\theta\right)\left(x - x_0^i\right) \approx a_l^i(\theta)^T x, \tag{6}$$

where $\nabla f_l(x_0^i,\theta)$ is the gradient, a column vector, of $f_l(x,\theta)$ evaluated at x_0^i. Substituting (5) into (6), we can get

$$\nabla^T f_l\left(x_0^i,\theta\right)\left(x - x_0^i\right) \approx a_l^i(\theta)^T\left(x - x_0^i\right), \tag{7}$$

where x is arbitrarily close to x_0^i. From (7), it can be found that the coefficient vector $a_l^i(\theta)$ needs to be estimated. And in the vicinity of x_0^i, an optimization problem can be constructed by defining an optimal index to evaluate the estimation. Here, define that the notation C^m represents the set of functions which is *m-order* continuous and differentiable on the domain of input variables.

Lemma 1. *Consider the following constrained optimization problem:*

$$\begin{aligned}
&\text{minimize } f(x) \\
&\text{subject to } h(x) = 0,
\end{aligned} \tag{8}$$

where $f(x)$ is $f: R^n \to R$ and $f \in C^1$; it is a convex function on the feasible set $\Omega = \{x \in R^n : h(x) = 0\}$, where $h: R^n \to R^m$ and $h \in C^1$. Assume that Ω is convex and there exist $x^* \in \Omega$ and $\lambda \in R^m$ such that

$$\nabla_\Omega f(x^*) + \lambda \nabla_\Omega h(x^*) = 0, \tag{9}$$

where λ is the Lagrange multiplier. Then, x^* is the optimal solution of f over Ω and λ is the sufficient condition for the convex optimization problem [27]. Particularly, when $h(x)$ is affine linear, Ω is convex.

Considering the estimation of $a_l^i(\theta)$ around $x_0^i \neq 0$ in (7), the optimal index for $f_l(x,\theta)$ corresponding to the ith fuzzy rule can be defined as

$$I_{f_l}^i\left(a_l^i(\theta)\right) = \frac{1}{2}\left\|\nabla f_l\left(x_0^i,\theta\right) - a_l^i(\theta)\right\|_2^2. \tag{10}$$

Then, the optimal problem can be constructed as

$$\begin{aligned}
&\underset{\Omega_{f_l}^i}{\text{minimize}} \quad I_{f_l}^i\left(a_l^i(\theta)\right) \\
&\text{subject to} \quad h_{f_l}^i\left(a_l^i(\theta)\right) = 0,
\end{aligned} \tag{11}$$

where (5) should be fulfilled as an equality constraint and $h_{f_l}^i(a_l^i(\theta)) = f_l(x_0^i,\theta) - a_l^i(\theta)^T x_0^i$.

Transform the objective function in (10) into the form

$$\begin{aligned}
I_{f_l}^i\left(a_l^i(\theta)\right) &= \frac{1}{2}\left\|\nabla f_l\left(x_0^i,\theta\right) - a_l^i(\theta)\right\|_2^2 \\
&= \frac{1}{2}\left(\nabla f_l\left(x_0^i,\theta\right) - a_l^i(\theta)\right)^T\left(\nabla f_l\left(x_0^i,\theta\right) - a_l^i(\theta)\right),
\end{aligned} \tag{12}$$

which is a quadratic function of the unknown coefficient vector $a_l^i(\theta)$ on R^n. Obviously, it means that $I_{f_l}^i(a_l^i(\theta))$ is a convex function. Considering the equality constraint $h_{f_l}^i(a_l^i(\theta))$, it is the linear function of $a_l^i(\theta)$, so the feasible set $\Omega_{f_l}^i = \{a_l^i(\theta) \in R^n : h(a_l^i(\theta)) = 0\}$ is convex. Therefore, the optimal problem is a convex optimization problem and can be solved according to Lemma 1.

Computing the derivative of $I_{f_l}^i(a_l^i(\theta))$ and $h_{f_l}^i(a_l^i(\theta))$ about $a_l^i(\theta)$, we can get

$$\begin{aligned} \nabla_{\Omega_{f_l}^i} I_{f_l}^i\left(a_l^i(\theta)\right) &= a_l^i(\theta) - \nabla f_l\left(x_0^i, \theta\right), \\ \nabla_{\Omega_{f_l}^i} h_{f_l}^i\left(a_l^i(\theta)\right) &= x_0^i. \end{aligned} \tag{13}$$

Then, substituting (13) into (9), we can get

$$a_l^i(\theta) - \nabla f_l\left(x_0^i, \theta\right) + \lambda_{f_l}^i(\theta)\, x_0^i = 0. \tag{14}$$

Considering the equality constraint (5), the Lagrange multiplier $\lambda_{f_l}^i(\theta)$ can be represented as

$$\begin{aligned} \lambda_{f_l}^i(\theta) &= \frac{\nabla^T f_l\left(x_0^i, \theta\right) x_0^i - a_l^i(\theta)^T x_0^i}{\left\|x_0^i\right\|_2^2} \\ &= \frac{\nabla^T f_l\left(x_0^i, \theta\right) x_0^i - f_l\left(x_0^i, \theta\right)}{\left\|x_0^i\right\|_2^2}. \end{aligned} \tag{15}$$

As a result, we can get the column vector

$$\begin{aligned} a_l^i(\theta) &= \nabla f_l\left(x_0^i, \theta\right) \\ &\quad + \frac{f_l\left(x_0^i, \theta\right) - \nabla^T f_l\left(x_0^i, \theta\right) x_0^i}{\left\|x_0^i\right\|_2^2} x_0^i, \qquad x_0^i \neq 0. \end{aligned} \tag{16}$$

Then, the ith T-S fuzzy rule corresponding to the operating state x_0^i can be chosen as

$$\begin{aligned} &\text{Rule } i\text{:} \\ &\text{IF } x_1 \text{ is } A_1^i(x_1), \ldots, \text{ and } x_n \text{ is } A_n^i(x_n), \\ &\text{THEN } \widehat{f}_l^i(x, \theta) = a_l^i(\theta)^T x, \end{aligned} \tag{17}$$

where $\widehat{f}_l^i(x, \theta)$ represents the ith local estimation of the lth row of $f(x, \theta)$, $a_l^i(\theta)$ is the corresponding coefficient vector of the ith fuzzy rule, a column vector, and $A_j^i(x_j)$ represents the fuzzy set and membership function of the jth premise variable, x_j, in the ith fuzzy rule and $j = 1, 2, \ldots, n$.

The activated possibility of the ith fuzzy rule under a group of premise variables x is computed by

$$\omega_i(x) = \prod_{j=1}^{n} A_j^i\left(x_j\right), \quad i = 1, 2, \ldots, L, \;\; j = 1, 2, \ldots, n. \tag{18}$$

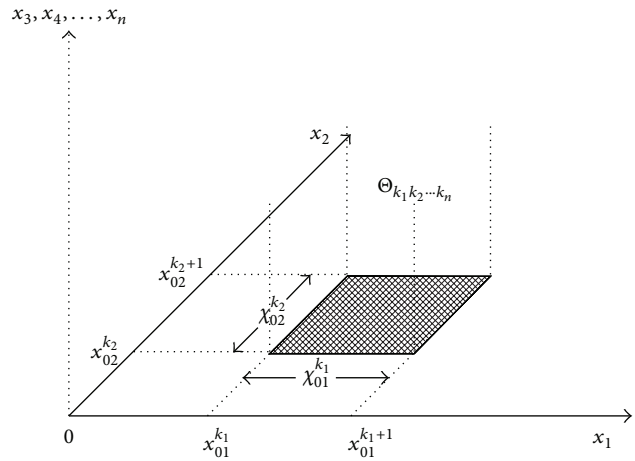

Figure 1: Projection of $\Theta_{k_1 k_2 \cdots k_n}$ on $x_1 x_2$ plane.

The weight coefficients are computed and the center-of-gravity method is used for defuzzification:

$$\alpha_i(x) = \frac{\omega_i(x)}{\sum_{i=1}^{L} \omega_i(x)}, \quad i = 1, 2, \ldots, L, \tag{19}$$

which fulfills that

$$\begin{aligned} &\sum_{i=1}^{L} \alpha_i(x) = 1, \\ &\alpha_i(x) \geq 0. \end{aligned} \tag{20}$$

Finally, the overall T-S fuzzy model can be obtained as

$$\widehat{f}_l(x, \theta) = \sum_{i=1}^{L} \alpha_i(x)\, \widehat{f}_l^i(x, \theta) = \sum_{i=1}^{L} \alpha_i(x)\, a_l^i(\theta)^T x. \tag{21}$$

Usually, based on (21), the evaluation of the overall approximation performance about the nonlinear function $f_l(x, \theta)$ is defined as

$$\left\|e_{f_l}(x, \theta)\right\|_2 = \left\|f_l(x, \theta) - \widehat{f}_l(x, \theta)\right\|_2. \tag{22}$$

Subsequently, a kind of un-uniform partition method is utilized for the above T-S fuzzy modeling procedure which can efficiently reduce the number of T-S fuzzy rules. Meanwhile, define the subset $\Theta_0 = \{x \mid |x_j| < \chi_0\}$ on Θ, where χ_0 is a predefined positive scalar and $a_l^0 = \partial f_l(x, \theta)/\partial x|_{x=0}$ can be gotten at the zero state $x = 0$. Considering the nonzero states, they can be represented as $x_0^{k_1 k_2 \cdots k_n} = (x_{01}^{k_1}, x_{02}^{k_2}, \cdots, x_{0n}^{k_n})^T$, where $\chi_{0j}^{k_j} = x_{0j}^{k_j+1} - x_{0j}^{k_j}$ is a positive scalar and $k_j \in N^+$ is the serial number of partition for x_j. Define the subregion $\Theta_{k_1 k_2 \cdots k_n}$ on Θ (as shown in Figure 1):

$$\Theta_{k_1 k_2 \cdots k_n} = \left\{x \mid x \in \Theta,\, x_{0j}^{k_j} \leq x_j \leq x_{0j}^{k_j+1},\, \chi_{0j}^{k_j} = x_{0j}^{k_j+1} - x_{0j}^{k_j}\right\}. \tag{23}$$

Then, the coefficient vector in (16) can be represented as

$$\begin{aligned} a_l^{k_1k_2\cdots k_n}(\theta) &= \nabla f_l\left(x_0^{k_1k_2\cdots k_n},\theta\right) \\ &\quad - \frac{f_l\left(x_0^{k_1k_2\cdots k_n},\theta\right) - \nabla^T f_l\left(x_0^{k_1k_2\cdots k_n},\theta\right) x_0^{k_1k_2\cdots k_n}}{\left\|x_0^{k_1k_2\cdots k_n}\right\|_2^2} \\ &\quad \times x_0^{k_1k_2\cdots k_n}, \quad x_0^{k_1k_2\cdots k_n} \neq 0. \end{aligned} \tag{24}$$

Consequently, the T-S fuzzy rules can be chosen as follows:

$$\begin{aligned} &\text{Rule 0:} \\ &\text{IF } x_1 \text{ is about } 0,\ldots, \text{ and } x_n \text{ is about } 0, \\ &\text{THEN } \widehat{f}_l^0(x,\theta) = a_l^0(\theta)^T x, \\ &\text{Rule } k_1k_2\cdots k_n\text{:} \\ &\text{IF } x_1 \text{ is about } x_{01}^{k_1},\ldots, \text{ and } x_n \text{ is about } x_{0n}^{k_n}, \\ &\text{THEN } \widehat{f}_l^{k_1k_2\cdots k_n}(x,\theta) = a_l^{k_1k_2\cdots k_n}(\theta)^T x. \end{aligned} \tag{25}$$

For Rule 0, the activated possibility $\alpha_0(x)$ is 1 inside Θ_0 and 0 outside Θ_0. And the activated possibility of the Rule $k_1k_2\cdots k_n$ under a group of premise variables x is computed by

$$\begin{aligned} \omega_{k_1k_2\cdots k_n}(x) &= \prod_{j=1}^{n} A_j^{k_1k_2\cdots k_n}\left(x_j\right), \\ \alpha_{k_1k_2\cdots k_n} &= \frac{\omega_{k_1k_2\cdots k_n}(x)}{\sum_{k_1k_2\cdots k_n}\omega_{k_1k_2\cdots k_n}(x)}, \end{aligned} \tag{26}$$

where the membership function for (26) is given as

$$A_j^{k_1k_2\cdots k_n}\left(x_j\right) = \begin{cases} 1 - \dfrac{\left(x_j - x_{0j}^{k_j}\right)}{\chi_{0j}^{k_j}}, & 0 \le x_j - x_{0j}^{k_j} \le \chi_{0j}^{k_j}, \\ 1 + \dfrac{\left(x_j - x_{0j}^{k_j}\right)}{\chi_{0j}^{k_j-1}}, & 0 \le x_{0j}^{k_j} - x_j \le \chi_{0j}^{k_j-1}, \\ 0, & \text{elsewhere.} \end{cases} \tag{27}$$

Then, $\widehat{f}_l(x,\theta)$ can be written as

$$\widehat{f}_l(x,\theta) = \alpha_0(x)\, a_l^0(\theta)^T x + \sum_{k_1k_2\cdots k_n} \alpha_{k_1k_2\cdots k_n} a_l^{k_1k_2\cdots k_n}(\theta)^T x. \tag{28}$$

Here, the notion of the nonlinear measure along x_j in the partition region $\chi_{0j}^{k_j}$ can be defined as

$$\begin{aligned} M_{0j}^{k_j}\left(\chi_{0j}^{k_j},\theta\right) &= \left\|\nabla f_l\left(x_0^{k_1\cdots k_j+1\cdots k_n},\theta\right)\right. \\ &\quad \left. -\nabla f_l\left(x_0^{k_1\cdots k_j\cdots k_n},\theta\right)\right\|_2 > 0. \end{aligned} \tag{29}$$

Assuming the boundary of $M_{0j}^{k_j}$ is κ_{0j}, the value of κ_{0j} can be set and the proper length of $\chi_{0j}^{k_j}$ can be chosen to guarantee $M_{0j}^{k_j} \le \kappa_{0j}$. Thus, the length of the partition regions, $\chi_{0j}^{k_j}$ ($k_j \in N^+$), of x_j can be different with the same κ_{0j}.

So far, all of the methods show us how to establish the T-S fuzzy system. However, the approximation performance of the T-S fuzzy system is still unknown. Subsequently, the approximation performance of the T-S fuzzy system will be evaluated. Combining with the above T-S fuzzy modeling procedure, the T-S fuzzy system with required approximation accuracy can be obtained at last.

Then, using (24), the approximation performance of the T-S fuzzy system can be evaluated by

$$\begin{aligned} &\left\|e_{f_l}(x,\theta)\right\|_2 \\ &= \left\|f_l(x,\theta) - \widehat{f}_l(x,\theta)\right\|_2 \\ &= \left\|f_l(x,\theta) - \sum_{k_1k_2\cdots k_n} \alpha_{k_1k_2\cdots k_n}(x)\, a_l^{k_1k_2\cdots k_n}(\theta)^T x\right\|_2 \\ &= \left\|f_l(x,\theta) - \sum_{k_1k_2\cdots k_n} \alpha_{k_1k_2\cdots k_n}(x)\, a_l^{k_1k_2\cdots k_n}(\theta)^T x_0^{k_1k_2\cdots k_n}\right. \\ &\qquad \left. - \sum_{k_1k_2\cdots k_n} \alpha_{k_1k_2\cdots k_n}(x)\, a_l^{k_1k_2\cdots k_n}(\theta)^T \left(x - x_0^{k_1k_2\cdots k_n}\right)\right\|_2 \\ &= \left\|f_l(x,\theta) - \sum_{k_1k_2\cdots k_n} \alpha_{k_1k_2\cdots k_n}(x)\, \widehat{f}_l\left(x_0^{k_1k_2\cdots k_n},\theta\right)\right. \\ &\qquad \left. - \sum_{k_1k_2\cdots k_n} \alpha_{k_1k_2\cdots k_n} a_l^{k_1k_2\cdots k_n}(\theta)^T \left(x - x_0^{k_1k_2\cdots k_n}\right)\right\|_2 \\ &\le \sum_{k_1k_2\cdots k_n} \alpha_{k_1k_2\cdots k_n}(x) \left\|f_l(x,\theta) - \widehat{f}_l\left(x_0^{k_1k_2\cdots k_n},\theta\right)\right\|_2 \\ &\quad + \sum_{k_1k_2\cdots k_n} \alpha_{k_1k_2\cdots k_n}(x) \left\|a_l^{k_1k_2\cdots k_n}(\theta)^T \left(x - x_0^{k_1k_2\cdots k_n}\right)\right\|_2 \\ &\le \max_{k_1k_2\cdots k_n} \left\|f_l(x,\theta) - \widehat{f}_l\left(x_0^{k_1k_2\cdots k_n},\theta\right)\right\|_2 \\ &\quad + \max_{k_1k_2\cdots k_n} \left\|a_l^{k_1k_2\cdots k_n}(\theta)^T \left(x - x_0^{k_1k_2\cdots k_n}\right)\right\|_2, \end{aligned} \tag{30}$$

where $x \in \Theta_{k_1k_2\cdots k_n}$ and

$$\begin{aligned} a_l^{k_1k_2\cdots k_n}(\theta)^T &\left(x - x_0^{k_1k_2\cdots k_n}\right) \\ &= \nabla^T f_l\left(x_0^{k_1k_2\cdots k_n}, \theta\right) \\ &\times \left[\left(x - x_0^{k_1k_2\cdots k_n}\right) \right. \\ &\quad \left. - \frac{\left\langle \left(x - x_0^{k_1k_2\cdots k_n}\right), x_0^{k_1k_2\cdots k_n} \right\rangle}{\left\| x_0^{k_1k_2\cdots k_n} \right\|_2^2} x_0^{k_1k_2\cdots k_n} \right] \\ &\quad + \frac{\left\langle \left(x - x_0^{k_1k_2\cdots k_n}\right), x_0^{k_1k_2\cdots k_n} \right\rangle}{\left\| x_0^{k_1k_2\cdots k_n} \right\|_2^2} f_l\left(x_0^{k_1k_2\cdots k_n}, \theta\right). \end{aligned} \tag{31}$$

Because $x \in \Theta_{k_1k_2\cdots k_n}$, the maximum distance between x and any vertex point of $\Theta_{k_1k_2\cdots k_n}$ is less than $\max_{k_1k_2\cdots k_n} \sqrt{n}\chi_{0j}^{k_j}$, which means $\|x - x_0^{k_1k_2\cdots k_n}\|_2 \le \max_{k_1k_2\cdots k_n} \sqrt{n}\chi_{0j}^{k_j}$; besides, in the boundary of $M_{0j}^{k_j}$, the max value of $\|f_l(x) - \widehat{f}_l(x_0^{k_1k_2\cdots k_n})\|_2$ can be adjusted to fulfill the required accuracy.

Thus, the approximation error, $e_{f_l}(x, \theta)$, can be befittingly minimized by properly setting $\chi_{0j}^{k_j}$, which can be shown as

$$\begin{aligned} \left\| e_{f_l}(x, \theta) \right\|_2 \le & \max_{k_1k_2\cdots k_n} \left\| f_l(x, \theta) - \widehat{f}_l\left(x_0^{k_1k_2\cdots k_n}, \theta\right) \right\|_2 \\ & + \max_{k_1k_2\cdots k_n} \left\| a_l^{k_1k_2\cdots k_n}(\theta) \right\|_2 \sqrt{n}\chi_{0j}^{k_j}. \end{aligned} \tag{32}$$

As a result, the evaluation system for the approximation performance of the LPV T-S fuzzy system is established. It provides a useful way to attain the required accuracy of the T-S fuzzy approximation. Then, the nonlinearity in (1) can be dealt with completely. Note that at each known operating state x_0^i, one fuzzy rule is established, which approximates the local dynamics around x_0^i. And the ith T-S fuzzy rule can be represented as

$$\begin{aligned} &\text{Rule } i\text{:} \\ &\text{IF } x_1 \text{ is } A_1^i(x_1), \ldots, \text{ and } x_n \text{ is } A_n^i(x_n), \\ &\text{THEN } \begin{bmatrix} \dot{x} \\ z \end{bmatrix} = \begin{bmatrix} A_i(\theta) & B_1^i(\theta) & B_2^i(\theta) \\ C_1^i(\theta) & 0 & D_{12}^i(\theta) \end{bmatrix} \begin{bmatrix} x \\ \omega \\ u \end{bmatrix}, \end{aligned} \tag{33}$$

where $i = 1, 2, \ldots, L$. More concretely, it is known that $i = k_1k_2\cdots k_n$ and $L = \max\{k_1 \cdot k_2 \cdots k_n\}$.

Finally, the overall LPV T-S fuzzy model can be represented as

$$\begin{aligned} \begin{bmatrix} \dot{x} \\ z \end{bmatrix} &= \begin{bmatrix} A(\alpha, \theta) & B_1(\alpha, \theta) & B_2(\alpha, \theta) \\ C_1(\alpha, \theta) & 0 & D_{12}(\alpha, \theta) \end{bmatrix} \begin{bmatrix} x \\ \omega \\ u \end{bmatrix} \\ &= \begin{bmatrix} \sum_{i=1}^{L} \alpha_i(x) A_i(\theta) & \sum_{i=1}^{L} \alpha_i(x) B_1^i(\theta) & \sum_{i=1}^{L} \alpha_i(x) B_2^i(\theta) \\ \sum_{i=1}^{L} \alpha_i(x) C_1^i(\theta) & 0 & \sum_{i=1}^{L} \alpha_i(x) D_{12}^i(\theta) \end{bmatrix} \begin{bmatrix} x \\ \omega \\ u \end{bmatrix} \\ &= \sum_{i=1}^{L} \alpha_i(x) \begin{bmatrix} A_i(\theta) & B_1^i(\theta) & B_2^i(\theta) \\ C_1^i(\theta) & 0 & D_{12}^i(\theta) \end{bmatrix} \begin{bmatrix} x \\ \omega \\ u \end{bmatrix}. \end{aligned} \tag{34}$$

Remark 2. It is noted that the T-S fuzzy modeling procedure utilizes an un-uniform partition method to reduce the number of T-S fuzzy rules while guaranteeing the approximation accuracy. And the evaluation system for the approximation performance of the LPV T-S fuzzy system can be used to balance the number of T-S fuzzy rules and the approximation performance of the LPV T-S fuzzy system.

3. Piecewise Parameter-Dependent Quadratic Stabilization of LPV T-S Fuzzy System

The LPV T-S fuzzy system (34) represents a class of complex continuous-time systems in a novel form which has both fuzzy inference and locally analytic linear models. In this section, the notion of piecewise parameter-dependent Lyapunov function is introduced for the stabilization problem of the LPV T-S fuzzy system. Firstly, the rth subspace in the state space can be defined as

$$\overline{X}_r = X_r \cup \widetilde{X}_r, \tag{35}$$

where

$$\begin{aligned} X_r &= \left\{ x \mid \alpha_i(x) = \alpha_k(x),\ i, k = 1, 2, \ldots, L,\ i \ne k \right\}, \\ \widetilde{X}_r &= \left\{ x \mid \alpha_i(x) > \alpha_k(x),\ i, k = 1, 2, \ldots, L,\ i \ne k \right\}. \end{aligned} \tag{36}$$

Note that two subspaces are generated around the ith T-S fuzzy rule for the single state x_j. The schematic about the state x_j can be shown in Figure 2. And then, the relation between the rth subspace and the ith T-S fuzzy rule is $i = k_1k_2\cdots k_n$ and $r = (2k_1 - 2/2k_1 - 1)(2k_2 - 2/2k_2 - 1)\cdots(2k_n - 2/2k_n - 1)$ $(i = 1, 2, \ldots, L;$ word $r = 1, 2, \ldots, \overline{L})$, where $L = \max\{k_1 \cdot k_2 \cdots k_n\}$ and $\overline{L} = \max\{2^n \cdot (k_1 - 1) \cdot (k_2 - 1) \cdots (k_n - 1)\}$. Then, the overall model of the LPV T-S system in the rth subspace can be represented as

$$\begin{aligned} &\begin{bmatrix} \dot{x} \\ z \end{bmatrix} \\ &= \begin{bmatrix} \overline{A}_r(\alpha, \theta) & \overline{B}_1^r(\alpha, \theta) & \overline{B}_2^r(\alpha, \theta) \\ \overline{C}_1^r(\alpha, \theta) & 0 & \overline{D}_{12}^r(\alpha, \theta) \end{bmatrix} \begin{bmatrix} x \\ \omega \\ u \end{bmatrix} \\ &= \begin{bmatrix} A_i(\theta) + \widetilde{A}_r(\alpha, \theta) & B_1^i(\theta) + \widetilde{B}_1^r(\alpha, \theta) & B_2^i(\theta) + \widetilde{B}_2^r(\alpha, \theta) \\ C_1^i(\theta) + \widetilde{C}_1^r(\alpha, \theta) & 0 & D_{12}^i(\theta) + \widetilde{D}_{12}^r(\alpha, \theta) \end{bmatrix} \begin{bmatrix} x \\ \omega \\ u \end{bmatrix} \end{aligned} \tag{37}$$

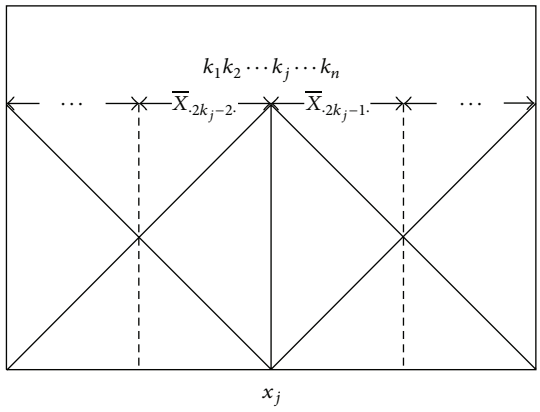

FIGURE 2: Piecewise space partition of x_j.

for $x \in \overline{X}_r$, where

$$\begin{aligned}
\widetilde{A}_r(\alpha,\theta) &= \sum_{k\in\phi_r} \alpha_k(x)\,\widetilde{A}_{ik}(\theta),\\
\widetilde{B}_1^r(\alpha,\theta) &= \sum_{k\in\phi_r} \alpha_k(x)\,\widetilde{B}_1^{ik}(\theta),\\
\widetilde{B}_2^r(\alpha,\theta) &= \sum_{k\in\phi_r} \alpha_k(x)\,\widetilde{B}_2^{ik}(\theta),\\
\widetilde{C}_1^r(\alpha,\theta) &= \sum_{k\in\phi_r} \alpha_k(x)\,\widetilde{C}_1^{ik}(\theta),\\
\widetilde{D}_{12}^r(\alpha,\theta) &= \sum_{k\in\phi_r} \alpha_k(x)\,\widetilde{D}_{12}^{ik}(\theta),
\end{aligned} \tag{38}$$

$$\widetilde{A}_{ik}(\theta) = A_k(\theta) - A_i(\theta),$$

$$\widetilde{B}_1^{ik} = B_1^k(\theta) - B_1^i(\theta), \qquad \widetilde{B}_2^{ik} = B_2^k(\theta) - B_2^i(\theta),$$

$$\widetilde{C}_1^{ik} = C_1^k(\theta) - C_1^i(\theta), \qquad \widetilde{D}_{12}^{ik} = D_{12}^k(\theta) - D_{12}^i(\theta),$$

$$\phi_r = \{k \mid \alpha_k(x) \neq 0,\ \alpha_i(x) \geq \alpha_k(x)\},$$

and ϕ_r is a set including the indexes of the membership functions which are nonzero and less than $\alpha_i(x)$ around the ith rule in the rth subspace. For the overall model, $\widetilde{A}_r(\alpha,\theta)$, $\widetilde{B}_*^r(\alpha,\theta)$, $\widetilde{C}_*^r(\alpha,\theta)$, and $\widetilde{D}_*^r(\alpha,\theta)$ represent the interpolation terms produced by interactions between the ith rule and the other rules in the rth subspace.

In order to find the piecewise parameter-dependent Lyapunov function which is continuous across the rth subspace boundary at a fixed θ, the following constant matrix F_r is established from the structure information of the rth subspace, which fulfills

$$F_r x = F_p x, \quad x \in \overline{X}_r \cap \overline{X}_p,\ r, p = 1, 2, \ldots, \overline{L}. \tag{39}$$

Then, the piecewise parameter-dependent Lyapunov function candidates that are continuous across the rth subspace boundary can be parameterized as

$$V(\theta) = x^T P_r(\theta)\, x, \quad x \in \overline{X}_r, \tag{40}$$

with

$$P_r(\theta) = F_r^T T(\theta)\, F_r, \tag{41}$$

where $T(\theta)$ is the symmetric matrix and characterizes $P_r(\theta)$ with F_r together.

In order to carry forward the control design, the following upper bounds for the interpolation terms in (37) can be defined as

$$\begin{aligned}
\left[\widetilde{A}_r(\alpha,\theta)\right]\left[\widetilde{A}_r(\alpha,\theta)\right]^T &\leq E_{rA}(\alpha,\theta)\,E_{rA}^T(\alpha,\theta),\\
\left[\widetilde{B}_1^r(\alpha,\theta)\right]\left[\widetilde{B}_1^r(\alpha,\theta)\right]^T &\leq E_{rB_1}(\alpha,\theta)\,E_{rB_1}^T(\alpha,\theta),\\
\left[\widetilde{B}_2^r(\alpha,\theta)\right]\left[\widetilde{B}_2^r(\alpha,\theta)\right]^T &\leq E_{rB_2}(\alpha,\theta)\,E_{rB_2}^T(\alpha,\theta),\\
\left[\widetilde{C}_1^r(\alpha,\theta)\right]\left[\widetilde{C}_1^r(\alpha,\theta)\right]^T &\leq E_{rC_1}(\alpha,\theta)\,E_{rC_1}^T(\alpha,\theta),\\
\left[\widetilde{D}_{12}^r(\alpha,\theta)\right]\left[\widetilde{D}_{12}^r(\alpha,\theta)\right]^T &\leq E_{rD_{12}}(\alpha,\theta)\,E_{rD_{12}}^T(\alpha,\theta).
\end{aligned} \tag{42}$$

Since all the information of the interpolation terms in (42) is a priori knowledge, there are many ways to acquire these upper bounds. For example, one simple way is

$$\begin{aligned}
&E_{rA}(\alpha,\theta)\,E_{rA}^T(\alpha,\theta)\\
&\quad= \left(\sum_{k\in\phi_r} \alpha_k(\overline{x})\,\widetilde{A}_{ik}(\theta)\right)\left(\sum_{k\in\phi_r} \alpha_k(\overline{x})\,\widetilde{A}_{ik}(\theta)\right)^T,
\end{aligned} \tag{43}$$

where $\overline{x}$ is the state such that $\alpha_k(\overline{x}) = 0.5$.

Definition 3. On the compact set $\Psi \subset R^s$, one has finite nonnegative numbers $\{\upsilon_q\}_{q=1}^s$. Then the bounded variations set of scheduling parameters can be defined as

$$\Gamma_\Psi^\upsilon = \left\{\theta \in C^1(R, R^s) \mid \theta \in \Psi, \left\|\dot{\theta}_q\right\|_2 \leq \upsilon_q,\ q = 1, \ldots, s\right\}, \tag{44}$$

where C^1 represents the class of functions which are piecewise continuous and one-order differential.

Definition 4. On the compact $\Psi \in R^s$, one has the LPV system

$$\dot{x} = A(\theta)\, x, \tag{45}$$

where $\theta \in \Gamma_\Psi^\upsilon$. If there exists a continuously differentiable symmetric function $P(\theta)$ such that $P(\theta) > 0$ and

$$A^T(\theta)\,P(\theta) + P(\theta)\,A(\theta) + \dot{P}(\theta) < 0, \tag{46}$$

for all $\theta \in \Gamma_\Psi^\upsilon$, then the continuous function $A(\theta)$ is parametrically dependent quadratically stable (or PDQ stable, for short).

Theorem 5. *Consider the LPV T-S fuzzy system* (34) *with* $\omega = u = 0$. *If there exists a symmetric matrix* $T(\theta)$ *satisfying*

$$P_r(\theta) > 0, \tag{47}$$

$$\begin{bmatrix} P_r(\theta)\,A_i^T(\theta) + A_i(\theta)\,P_r(\theta) - \dot{P}_r(\theta) \\ +\varepsilon_{\widetilde{A}_r P_r}(\theta)\,E_{rA}(\alpha,\theta)\,E_{rA}^T(\alpha,\theta) \\ P_r(\theta) \end{bmatrix} \quad \begin{matrix} P_r(\theta) \\ -\varepsilon_{\widetilde{A}_r P_r}(\theta)\,I \end{matrix} < 0 \tag{48}$$

with

$$P_r(\theta) = \left(F_r^T F_r\right)^{-1} F_r^T T(\theta) F_r \left(F_r^T F_r\right)^{-1} \tag{49}$$

for $r = 1, 2, \ldots, \overline{L}$*, then the fuzzy system is globally asymptotically stable.*

Proof. Define the following Lyapunov function $V(\theta)$:

$$V(\theta) = x^T P_r^{-1}(\theta)\, x, \quad x \in \overline{X}_r. \tag{50}$$

From (41), we can get

$$P_r^{-1}(\theta) = F_r^T T^{-1}(\theta) F_r. \tag{51}$$

From (50) and (51), there exist constants $\sigma > 0$ and $\beta > 0$ such that

$$\sigma \|x\|_2^2 \le V(\theta) \le \beta \|x\|_2^2. \tag{52}$$

Thus, using the conditions (47) and (49), $V(\theta)$ is positive and continuous across the subspace boundary. If it can guarantee that the system (37) is asymptotically stable in each subspace, the global asymptotical stability for the system (34) can be attained. Next, we will demonstrate that $V(\theta)$ can guarantee the asymptotical stability in each subspace.

If there exist a constant $\varepsilon_{XY} > 0$ and matrices X and Y with appropriate dimensions, the following matrix inequality can be gotten:

$$X^T Y + Y^T X \le \frac{1}{\varepsilon_{XY}} X^T X + \varepsilon Y^T Y. \tag{53}$$

From (53), define the parameter-dependent positive scalar $\varepsilon_{bc}(\theta)$, where the subscript bc means the relation between b and c just like ε_{XY} means the relation between X and Y. In many cases, $\varepsilon_{ab}(\theta)$ can be set as a constant value. Note that b and c are just used for example and do not have any special significance. However, subscripts of all $\varepsilon_*(\theta)$ are marked as follows to clearly show the meaning of $\varepsilon_*(\theta)$.

Then, from (53) we can get

$$\begin{aligned}
&P_r(\theta)\left(A_i(\theta) + \widetilde{A}_r(\alpha,\theta)\right)^T \\
&\quad + \left(A_i(\theta) + \widetilde{A}_r(\alpha,\theta)\right) P_r(\theta) - \dot{P}_r(\theta) \\
&= P_r(\theta) A_i^T(\theta) + P_r(\theta) \widetilde{A}_r^T(\alpha,\theta) + A_i(\theta) P_r(\theta) \\
&\quad + \widetilde{A}_r(\alpha,\theta) P_r(\theta) - \dot{P}_r(\theta) \\
&\le P_r(\theta) A_i^T(\theta) + A_i(\theta) P_r(\theta) + \frac{1}{\varepsilon_{\widetilde{A}_r P_r}(\theta)} P_r(\theta) P_r(\theta) \\
&\quad + \varepsilon_{\widetilde{A}_r P_r}(\theta) \widetilde{A}_r^T(\alpha,\theta) \widetilde{A}_r(\alpha,\theta) - \dot{P}_r(\theta) \\
&\le P_r(\theta) A_i^T(\theta) + A_i(\theta) P_r(\theta) + \frac{1}{\varepsilon_{\widetilde{A}_r P_r}(\theta)} P_r(\theta) P_r(\theta) \\
&\quad + \varepsilon_{\widetilde{A}_r P_r}(\theta) E_{rA}^T(\alpha,\theta) E_{rA}(\alpha,\theta) - \dot{P}_r(\theta),
\end{aligned} \tag{54}$$

for the system (37). Besides, via the Schur complement lemma, it follows from (48) that

$$\begin{aligned}
&P_r(\theta) A_i^T(\theta) + A_i(\theta) P_r(\theta) + \frac{1}{\varepsilon_{\widetilde{A}_r P_r}(\theta)} P_r(\theta) P_r(\theta) \\
&\quad + \varepsilon_{\widetilde{A}_r P_r}(\theta) E_{rA}(\alpha,\theta) E_{rA}^T(\alpha,\theta) - \dot{P}_r(\theta) < 0.
\end{aligned} \tag{55}$$

Then, from (54) and (55), we have

$$\begin{aligned}
&P_r(\theta)\left(A_i(\theta) + \widetilde{A}_r(\alpha,\theta)\right)^T \\
&\quad + \left(A_i(\theta) + \widetilde{A}_r(\alpha,\theta)\right) P_r(\theta) - \dot{P}_r(\theta) < 0,
\end{aligned} \tag{56}$$

which suggests that

$$\begin{aligned}
&\left(A_i(\theta) + \widetilde{A}_r(\alpha,\theta)\right)^T P_r^{-1}(\theta) \\
&\quad + P_r^{-1}(\theta)\left(A_i(\theta) + \widetilde{A}_r(\alpha,\theta)\right) + \dot{P}_r^{-1}(\theta) < 0,
\end{aligned} \tag{57}$$

where $\dot{P}_r^{-1}(\theta) = -F_r^T T^{-1}(\theta) \dot{T}(\theta) T^{-1}(\theta) F_r = -P_r^{-1}(\theta) \dot{P}(\theta) P_r^{-1}(\theta)$.

Moreover, there exists a constant $\delta > 0$ such that

$$\begin{aligned}
&\left(A_i(\theta) + \widetilde{A}_r(\alpha,\theta)\right)^T P_r^{-1}(\theta) \\
&\quad + P_r^{-1}(\theta)\left(A_i(\theta) + \widetilde{A}_r(\alpha,\theta)\right) + \dot{P}_r^{-1}(\theta) + \delta I < 0.
\end{aligned} \tag{58}$$

As a result, we have

$$\begin{aligned}
\dot{V}(\theta) &= x^T \Big[\left(A_i(\theta) + \widetilde{A}_r(\alpha,\theta)\right)^T P_r^{-1}(\theta) + P_r^{-1}(\theta) \\
&\qquad \times \left(A_i(\theta) + \widetilde{A}_r(\alpha,\theta)\right) + \dot{P}_r^{-1}(\theta)\Big] x \\
&\le x^T(-\delta I)\, x = -\delta \|x\|_2^2,
\end{aligned} \tag{59}$$

which completes the proof of this theorem. □

Remark 6. It is noted that the sufficient conditions in LMIs form are easy to be solved. At a fixed θ, conditions (47) and (49) guarantee that the Lyapunov function is positive and piecewise continuous across each subspace. And the Lyapunov functions solved from condition (48) guarantee that the system (37) is asymptotical in each subspace. All the conditions guarantee that the system (34) is globally asymptotically stable. Besides, in many cases, for the T-S fuzzy control based on the common Lyapunov function, it was hard to find the common Lyapunov function or such a Lyapunov function did not exist at all. Thus, the previous approach can improve the solvability of the LPV T-S fuzzy gain scheduling control.

4. State-Feedback H_∞ Control Design of LPV T-S Fuzzy System

In this section, the state-feedback H_∞ control of the LPV T-S fuzzy system is studied. Considering the approximation error, a controller synthesis approach with H_∞ performance

is presented. In the rth subspace, the state feedback controller can be represented as

$$u = K_r(\theta)\, x, \quad x \in \overline{X}_r. \tag{60}$$

Substituting (60) into (34), the closed-loop system can be obtained as

$$\dot{x} = A_C(\alpha,\theta)\, x + B_C(\alpha,\theta)\, \omega, \qquad z = C_C(\alpha,\theta)\, x, \tag{61}$$

where

$$\begin{aligned} A_C(\alpha,\theta) &= A(\alpha,\theta) + B_2(\alpha,\theta)\, K(\theta), \quad B_C(\alpha,\theta) = B_1(\alpha,\theta), \\ C_C(\alpha,\theta) &= C_1(\alpha,\theta) + D_{12}(\alpha,\theta)\, K(\theta). \end{aligned} \tag{62}$$

In the rth subspace, the system (61) can be represented as

$$\begin{aligned} \dot{x} &= A_{Cr}(\alpha,\theta)\, x + B_{Cr}(\alpha,\theta)\, \omega, \\ z &= C_{Cr}(\alpha,\theta)\, x, \quad x \in \overline{X}_r, \end{aligned} \tag{63}$$

where

$$\begin{aligned} A_{Cr}(\alpha,\theta) &= A_i(\theta) + \widetilde{A}_r(\alpha,\theta) \\ &\quad + \left(B_2^i(\theta) + \widetilde{B}_2^r(\alpha,\theta)\right) K_r(\theta), \\ B_{Cr}(\alpha,\theta) &= B_1^i(\theta) + \widetilde{B}_1^r(\alpha,\theta), \\ C_{Cr}(\alpha,\theta) &= C_1^i(\theta) + \widetilde{C}_1^r(\alpha,\theta) \\ &\quad + \left(D_{12}^i(\theta) + \widetilde{D}_{12}^r(\alpha,\theta)\right) K_r(\theta). \end{aligned} \tag{64}$$

When substituting (37) into (1) and considering the approximating error, the closed-loop nonlinear system in the rth subspace can be represented as

$$\begin{aligned} \begin{bmatrix} \dot{x} \\ z \end{bmatrix} &= \begin{bmatrix} f(x,\theta) + d_0(x,\theta)\,\omega + g_0(x,\theta)\,u \\ \varphi(x,\theta) + g_1(x,\theta)\,u \end{bmatrix} \\ &= \begin{bmatrix} \overline{A}_r(\alpha,\theta) & \overline{B}_1^r(\alpha,\theta) & \overline{B}_2^r(\alpha,\theta) \\ \overline{C}_1^r(\alpha,\theta) & 0 & \overline{D}_{12}^r(\alpha,\theta) \end{bmatrix} \begin{bmatrix} x \\ \omega \\ u \end{bmatrix} \\ &\quad + \begin{bmatrix} \left(f(x,\theta) - \overline{A}_r(\alpha,\theta)\, x\right) + \left(d_0(x,\theta) - \overline{B}_1^r(\alpha,\theta)\right)\omega \\ \quad + \left(g_0(x,\theta) - \overline{B}_2^r(\alpha,\theta)\right)u \\ \left(\varphi(x,\theta) - \overline{C}_1^r(\alpha,\theta)\, x\right) + \left(g_1(x,\theta) - \overline{D}_{12}^r(\alpha,\theta)\right)u \end{bmatrix} \\ &= \begin{bmatrix} \overline{A}_r(\alpha,\theta) + \overline{B}_2^r(\alpha,\theta)\, K_r(\theta) & \overline{B}_1^r(\alpha,\theta) \\ \overline{C}_1^r(\alpha,\theta) + \overline{D}_{12}^r(\alpha,\theta)\, K_r(\theta) & 0 \end{bmatrix} \begin{bmatrix} x \\ \omega \end{bmatrix} \\ &\quad + \begin{bmatrix} \left(f(x,\theta) - \overline{A}_r(\alpha,\theta)\, x\right) + \left(g_0(x,\theta) - \overline{B}_2^r(\alpha,\theta)\right) K_r(\theta)\, x \\ \quad + \left(d_0(x,\theta) - \overline{B}_1^r(\alpha,\theta)\right)\omega \\ \left(\varphi(x,\theta) - \overline{C}_1^r(\alpha,\theta)\, x\right) + \left(g_1(x,\theta) - \overline{D}_{12}^r(\alpha,\theta)\right) K_r(\theta)\, x \end{bmatrix} \\ &= \begin{bmatrix} A_{Cr}(\alpha,\theta) & B_{Cr}(\alpha,\theta) \\ C_{Cr}(\alpha,\theta) & 0 \end{bmatrix} \begin{bmatrix} x \\ \omega \end{bmatrix} + \begin{bmatrix} \Delta f_r(\theta) + \Delta g_0^r(\theta) + \Delta d_0^r(\theta) \\ \Delta\varphi_r(\theta) + \Delta g_1^r(\theta) \end{bmatrix}, \end{aligned} \tag{65}$$

where

$$\begin{aligned} \Delta f_r(\theta) &= f(x,\theta) - \overline{A}_r(x,\theta)\, x, \\ \Delta g_0^r(\theta) &= \left(g_0(x,\theta) - \overline{B}_2^r(\alpha,\theta)\right) K_r(\theta)\, x, \\ \Delta d_0^r(\theta) &= \left(d_0(x,\theta) - \overline{B}_1^r(\alpha,\theta)\right)\omega, \\ \Delta\varphi_r(\theta) &= \varphi(x,\theta) - \overline{C}_1^r(\alpha,\theta)\, x, \\ \Delta g_1^r(\theta) &= \left(g_1(x,\theta) - \overline{D}_{12}^r(\alpha,\theta)\right) K_r(\theta)\, x. \end{aligned} \tag{66}$$

According to (37) and (65), the approximation errors, $\Delta f_r(\theta)$, $\Delta g_0^r(\theta)$, $\Delta d_0^r(\theta)$, $\Delta\varphi_r(\theta)$, and $\Delta g_1^r(\theta)$, of the LPV T-S fuzzy system can be represented as follows:

$$\begin{aligned} \left\|\Delta f_r(\theta)\right\|_2 &= \left\| f(x,\theta) - \overline{A}_r(\alpha,\theta)\, x \right\|_2 \\ &= \left\| f(x,\theta) - \left(A_i(\theta) + \sum_{k\in\phi_r} \alpha_k(x)\, \widetilde{A}_{ik}(\theta) \right) x \right\|_2 \\ &\le \left\| \left(\Delta A_i(\theta) + \sum_{k\in\phi_r} \alpha_k(x)\, \Delta\widetilde{A}_{ik}(\theta) \right) x \right\|_2 \\ &= \left\| \Delta\overline{A}_r(\theta)\, x \right\|_2, \end{aligned} \tag{67}$$

where

$$\begin{aligned} \Delta\overline{A}_r(\theta) &= \Delta A_i(\theta) + \sum_{k\in\phi_r} \alpha_k(x)\, \widetilde{A}_{ik}(\theta) \\ &= \Delta A_i(\theta) + \sum_{k\in\phi_r} \alpha_k(x) \left(\Delta A_k(\theta) - \Delta A_i(\theta)\right) \\ &= \alpha_i(x)\, \Delta A_i(\theta) + \sum_{k\in\phi_r} \alpha_k(x)\, \Delta A_k(\theta) \\ &= \left(\alpha_i(x)\, \delta_{A_r^i}(\theta) + \sum_{k\in\phi_r} \alpha_k(x)\, \delta_{A_r^k}(\theta) \right) \widehat{A}_r(\theta) \\ &= \delta_{\overline{A}_r}(\theta)\, \widehat{A}_r(\theta), \\ \left\|\Delta g_0^r(\theta)\right\|_2 &= \left\| \left(g_0(x,\theta) - \overline{B}_2^r(\alpha,\theta)\right) K_r(\theta) x \right\|_2 \\ &= \left\| \left(g_0(x,\theta) - \left(B_2^i(\theta) + \sum_{k\in\phi_r} \alpha_k(x)\, \widetilde{B}_2^{ik}(\theta) \right) \right)_2 \right. \\ &\quad \left. \times K_r(\theta)\, x \right\|_2 \\ &\le \left\| \left(\Delta B_2^i(\theta) + \sum_{k\in\phi_r} \alpha_k(x)\, \Delta\widetilde{B}_2^{ik}(\theta) \right) K_r(\theta)\, x \right\|_2 \\ &= \left\| \Delta\overline{B}_2^r(\theta)\, K_r(\theta)\, x \right\|_2, \end{aligned} \tag{68}$$

where

$$\begin{aligned}
\Delta\overline{B}_2^r(\theta) &= \Delta B_2^i(\theta) + \sum_{k\in\phi_r}\alpha_k(x)\,\Delta\widetilde{B}_2^{ik}(\theta)\\
&= \Delta B_2^i(\theta) + \sum_{k\in\phi_r}\alpha_k(x)\left(\Delta B_2^k(\theta) - \Delta B_2^i(\theta)\right)\\
&= \alpha_i(x)\,\Delta B_2^i(\theta) + \sum_{k\in\phi_r}\alpha_k(x)\,\Delta B_2^k(\theta)\\
&= \left(\alpha_i(x)\,\delta_{B_2^{i,r}}(\theta) + \sum_{k\in\phi_r}\alpha_k(x)\,\delta_{B_2^{k,r}}(\theta)\right)\widehat{B}_2^r(\theta)\\
&= \delta_{\overline{B}_2^r}\widehat{B}_2^r(\theta),\\
\left\|\Delta d_0^r(\theta)\right\|_2 &= \left\|\left(d_0(x,\theta) - \overline{B}_1^r(\alpha,\theta)\right)\omega\right\|_2\\
&= \left\|\left(d_0(x,\theta) - \left(B_1^i(\theta) + \sum_{k\in\phi_r}\alpha_k(x)\,\widetilde{B}_1^{ik}(\theta)\right)\right)\omega\right\|_2\\
&\le \left\|\left(\Delta B_1^i(\theta) + \sum_{k\in\phi_r}\alpha_k(x)\,\Delta\widetilde{B}_1^{ik}(\theta)\right)\omega\right\|_2\\
&= \left\|\Delta\overline{B}_1^r(\theta)\,\omega\right\|_2,
\end{aligned} \tag{69}$$

where

$$\begin{aligned}
\Delta\overline{B}_1^r(\theta) &= \Delta B_1^i(\theta) + \sum_{k\in\phi_r}\alpha_k(\theta)\,\Delta\widetilde{B}_1^{ik}(\theta)\\
&= \Delta B_1^i(\theta) + \sum_{k\in\phi_r}\alpha_k(x)\left(\Delta B_1^k(\theta) - \Delta B_1^i(\theta)\right)\\
&= \alpha_i(x)\,\Delta B_1^i(\theta) + \sum_{k\in\phi_r}\alpha_k(x)\,\Delta B_1^k(\theta)\\
&= \left(\alpha_i(x)\,\delta_{B_1^{i,r}}(\theta) + \sum_{k\in\phi_r}\alpha_k(x)\,\delta_{B_1^{k,r}}(\theta)\right)\widehat{B}_1^r(\theta)\\
&= \delta_{\overline{B}_1^r}\widehat{B}_1^r(\theta),\\
\Delta\left\|\varphi_r(\theta)\right\|_2 &= \left\|\varphi(x,\theta) - \overline{C}_1^r(\alpha,\theta)\,x\right\|_2\\
&= \left\|\varphi(x,\theta) - \left(C_1^i(\theta) + \sum_{k\in\phi_r}\alpha_k(x)\,\widetilde{C}_1^{ik}(\theta)\right)x\right\|_2\\
&\le \left\|\left(\Delta C_1^i(\theta) + \sum_{k\in\phi_r}\alpha_k(x)\,\Delta\widetilde{C}_1^{ik}(\theta)\right)x\right\|_2\\
&= \left\|\Delta\overline{C}_1^r(\theta)\,x\right\|_2,
\end{aligned} \tag{70}$$

where

$$\begin{aligned}
\Delta\overline{C}_1^r(\theta) &= \Delta C_1^i(\theta) + \sum_{k\in\phi_r}\alpha_k(x)\,\Delta\widetilde{C}_1^{ik}(\theta)\\
&= \Delta C_1^i(\theta) + \sum_{k\in\phi_r}\alpha_k(x)\left(\Delta C_1^k(\theta) - \Delta C_1^i(\theta)\right)\\
&= \alpha_i(x)\,\Delta C_1^i(\theta) + \sum_{k\in\phi_r}\alpha_k(x)\,\Delta C_1^k(\theta)\\
&= \left(\alpha_i(x)\,\delta_{C_1^{i,r}}(\theta) + \sum_{k\in\phi_r}\alpha_k(x)\,\delta_{C_1^{k,r}}(\theta)\right)\\
&\quad\times\widehat{C}_1^r(\theta)\\
&= \delta_{\overline{C}_1^r}(\theta)\,\widehat{C}_1^r(\theta),\\
\left\|\Delta g_1^r(\theta)\right\|_2 &= \left\|\left(g_1(x,\theta) - \overline{D}_{12}^r(\alpha,\theta)\right)K_r(\theta)\,x\right\|_2\\
&= \left\|\left(g_1(x,\theta) - \left(D_{12}^i(\theta)\right.\right.\right.\\
&\qquad\left.\left.\left. + \sum_{k\in\phi_r}\alpha_k(x)\,\widetilde{D}_{12}^{ik}(\theta)\right)\right)\right.\\
&\qquad\left.\times K_r(\theta)\,x\right\|_2\\
&\le \left\|\left(\Delta D_{12}^i(\theta) + \sum_{k\in\phi_r}\alpha_k(x)\,\Delta\widetilde{D}_{12}^{ik}(\theta)\right)\right.\\
&\qquad\left.\times K_r(\theta)\,x\right\|_2\\
&= \left\|\Delta\overline{D}_{12}^r(\theta)\,K_r(\theta)\,x\right\|_2,
\end{aligned} \tag{71}$$

where

$$\begin{aligned}
\Delta\overline{D}_{12}^r(\theta) &= \Delta D_{12}^i(\theta) + \sum_{k\in\phi_r}\alpha_k(x)\,\Delta\widetilde{D}_{12}^{ik}(\theta)\\
&= \Delta D_{12}^i(\theta) + \sum_{k\in\phi_r}\alpha_k(x)\left(\Delta D_{12}^k(\theta) - \Delta D_{12}^i(\theta)\right)\\
&= \alpha_i(x)\,\Delta D_{12}^i(\theta) + \sum_{k\in\phi_r}\alpha_k(x)\,\Delta D_{12}^k(\theta)\\
&= \left(\alpha_i(x)\,\delta_{D_{12}^{i,r}}(\theta) + \sum_{k\in\phi_r}\alpha_k(x)\,\delta_{D_{12}^{k,r}}(\theta)\right)\widehat{D}_{12}^r(\theta)\\
&= \delta_{\overline{D}_{12}^r}(\theta)\,\widehat{D}_{12}^r(\theta).
\end{aligned} \tag{72}$$

Note that not all of the nonlinearities can be given such bounds of approximation error in a linear form. However, for

the nonlinearities satisfying the Lipschitz condition or even the one-order derivable condition, we can usually give the bounds of the approximation error in such a linear form. In addition, it should be noted that $\alpha_i(x) + \sum_{k\in\phi_r} \alpha_k(x) = 1$ and $\|\delta_{A_r^*}(\theta)\|_2 \le 1, \ldots, \|\delta_{\overline{D}_{12}^{*,r}}(\theta)\|_2 \le 1$ for $i = 1, 2, \ldots, L$ and $r = 1, 2, \ldots, \overline{L}$. Then, we can get

$$\begin{bmatrix} \|\Delta f_r(\theta)\|_2 & \|\Delta d_0^r(\theta)\|_2 & \|\Delta g_0^r(\theta)\|_2 \\ \|\Delta \varphi_r(\theta)\|_2 & 0 & \|\Delta g_1^r(\theta)\|_2 \end{bmatrix} \le \begin{bmatrix} \left\|\Delta \overline{A}_r(\theta)\, x\right\|_2 & \left\|\Delta \overline{B}_1^r(\theta)\, \omega\right\|_2 & \left\|\Delta \overline{B}_2^r(\theta)\, K_r(\theta)\, x\right\|_2 \\ \left\|\Delta \overline{C}_1^r(\theta)\, x\right\|_2 & 0 & \left\|\Delta \overline{D}_{12}^r(\theta)\, K_r(\theta)\, x\right\|_2 \end{bmatrix}, \tag{73}$$

for all the x, and describe the bounding matrices as

$$\begin{bmatrix} \Delta \overline{A}_r(\theta) & \Delta \overline{B}_1^r(\theta) & \Delta \overline{B}_2^r(\theta) \\ \Delta \overline{C}_1^r(\theta) & 0 & \Delta \overline{D}_{12}^r(\theta) \end{bmatrix} = \begin{bmatrix} \delta_{\overline{A}_r}(\theta)\, \widehat{A}_r(\theta) & \delta_{\overline{B}_1^r}(\theta)\, \widehat{B}_1^r(\theta) & \delta_{\overline{B}_2^r}(\theta)\, \widehat{B}_2^r(\theta) \\ \delta_{\overline{C}_1^r}(\theta)\, \widehat{C}_1^r(\theta) & 0 & \delta_{\overline{D}_{12}^r}(\theta)\, \widehat{D}_{12}^r(\theta) \end{bmatrix}, \tag{74}$$

where $\|\delta_{\overline{A}_r}(\theta)\|_2 \le 1, \ldots$ and $\|\delta_{\overline{D}_{12}^r}(\theta)\|_2 \le 1$ for $i = 1, 2, \ldots, L$ and $r = 1, 2, \ldots, \overline{L}$.

Theorem 7. *For the closed-loop system* (61)*, while considering the approximation error and a positive scalar* $\gamma > 0$*, if there exist symmetric matrixes* $T(\theta)$ *and* $P_r(\theta) = (F_r^T F_r)^{-1} F_r^T T(\theta) F_r (F_r^T F_r)^{-1}$ *satisfying*

$$P_r(\theta) > 0, \tag{75}$$

$$\begin{aligned} &P_r(\theta)\, A_{C_r}^T(\alpha,\theta) + A_{C_r}(\alpha,\theta)\, P_r(\theta) - \dot{P}_r(\theta) \\ &\quad + \frac{1}{\varepsilon_{\Delta f_r P_r}(\theta)} P_r(\theta)\, \widehat{A}_r^T(\theta)\, \widehat{A}_r(\theta)\, P_r(\theta) \\ &\quad + \frac{1}{\varepsilon_{\Delta g_0^r P_r}(\theta)} P_r(\theta) \left(\widehat{B}_2^r(\theta)\, K_r(\theta)\right)^T \left(\widehat{B}_2^r(\theta)\, K_r(\theta)\right) P_r(\theta) \\ &\quad + \left(\varepsilon_{\Delta f_r P_r}(\theta) + \varepsilon_{\Delta g_0^r P_r}(\theta) + \varepsilon_{\Delta d_0^r P_r}(\theta)\right) \\ &\quad + \left(1 + \varepsilon_{\Delta \varphi_r C_{C_r}}(\theta) + \varepsilon_{\Delta g_1^r C_{C_r}}(\theta)\right) \\ &\quad \times P_r(\theta)\, C_{C_r}^T(\alpha,\theta)\, C_{C_r}(\alpha,\theta)\, P_r(\theta) \\ &\quad + \left(1 + \frac{1}{\varepsilon_{\Delta \varphi_r C_{C_r}}(\theta)} + \frac{1}{\varepsilon_{\Delta \varphi_r \Delta g_1^r}(\theta)}\right) \\ &\quad \times P_r(\theta)\, \widehat{C}_1^r(\alpha,\theta)^T \widehat{C}_1^r(\alpha,\theta)\, P_r(\theta) \\ &\quad + \left(1 + \frac{1}{\varepsilon_{\Delta g_1^r C_{C_r}}(\theta)} + \frac{1}{\varepsilon_{\Delta \varphi_r \Delta g_1^r}(\theta)}\right) P_r(\theta) \\ &\quad \times \widehat{D}_{12}^r(\alpha,\theta)^T \widehat{D}_{12}^r(\alpha,\theta)\, P_r(\theta) \\ &\quad + \left(\gamma^2 I - \frac{1}{\varepsilon_{\Delta d_0^r P_r}(\theta)} \widehat{B}_1^r(\theta)^T \widehat{B}_1^r(\theta)\right)^{-1} \\ &\quad \times B_{C_r}(\alpha,\theta)\, B_{C_r}^T(\alpha,\theta) < 0, \end{aligned} \tag{76}$$

$$\gamma^2 I - \frac{1}{\varepsilon_{\Delta d_0^r P_r}(\theta)} \widehat{B}_1^r(\theta)^T \widehat{B}_1^r(\theta) > 0, \tag{77}$$

the closed-loop system (61) *while considering the approximation error has the* H_∞ *performance with disturbance attenuation* γ*. And it is globally asymptotically stable when* $\omega = 0$*.*

Proof. From (63), the sufficient condition for (46) can be gotten:

$$A_{C_r}^T(\alpha,\theta)\, P_r^{-1}(\theta) + P_r^{-1}(\theta)\, A_{C_r}(\alpha,\theta) + \dot{P}_r^{-1} < 0. \tag{78}$$

According to Theorem 5, if the condition (78) is fulfilled, the system (63) is asymptotically stable. For the system (65) with the approximation error, we can get

$$\begin{aligned} &A_{C_r}^T(\alpha,\theta)\, P_r^{-1}(\theta) + P_r^{-1}(\theta)\, A_{C_r}(\alpha,\theta) \\ &\quad + \dot{P}_r^{-1}(\theta) + \frac{1}{\varepsilon_{\Delta f_r P_r}(\theta)} \widehat{A}_r^T(\theta)\, \widehat{A}_r(\theta) \\ &\quad + \frac{1}{\varepsilon_{\Delta g_0^r P_r}(\theta)} \left(\widehat{B}_2^r(\theta)\, K_r(\theta)\right)^T \widehat{B}_2^r(\theta)\, K_r(\theta) \\ &\quad + \left(\varepsilon_{\Delta f_r P_r}(\theta) + \varepsilon_{\Delta g_0^r P_r}(\theta) + \varepsilon_{\Delta d_0^r P_r}(\theta)\right) P_r^{-1}(\theta)\, P_r^{-1}(\theta) \\ &\quad + \left(1 + \varepsilon_{\Delta \varphi_r C_{C_r}}(\theta) + \varepsilon_{\Delta g_1^r C_{C_r}}(\theta)\right) C_{C_r}^T(\alpha,\theta)\, C_{C_r}(\alpha,\theta) \\ &\quad + \left(1 + \frac{1}{\varepsilon_{\Delta \varphi_r C_{C_r}}(\theta)} + \frac{1}{\varepsilon_{\Delta \varphi_r \Delta g_1^r}(\theta)}\right) \widehat{C}_1^r(\alpha,\theta)^T \widehat{C}_1^r(\alpha,\theta) \\ &\quad + \left(1 + \frac{1}{\varepsilon_{\Delta g_1^r C_{C_r}}(\theta)} + \frac{1}{\varepsilon_{\Delta \varphi_r \Delta g_1^r}(\theta)}\right) \widehat{D}_{12}^r(\alpha,\theta)^T \widehat{D}_{12}^r(\alpha,\theta) \\ &\quad + \left(\gamma^2 I - \frac{1}{\varepsilon_{\Delta d_0^r P_r}(\theta)} \widehat{B}_1^r(\theta)^T \widehat{B}_1^r(\theta)\right)^{-1} P_r^{-1}(\theta)\, B_{C_r}(\alpha,\theta) \\ &\quad \times B_{C_r}^T(\alpha,\theta)\, P_r^{-1}(\theta) < 0 \end{aligned} \tag{79}$$

from (76), which suggests that the condition (78) is fulfilled. Here, the condition (77) needs to be fulfilled. Then, the

system (65) is asymptotically stable. Next, we will show the disturbance attenuation performance.

Considering the Lyapunov function $V(\theta) = x^T P_r^{-1}(\theta)x$ which is piecewise continuous across the rth subspace boundary, we differentiate $V(\theta)$ and then integrate it from zero to infinity in the rth subspace. Then, we can get

$$
\begin{aligned}
&\int_0^\infty \dot{V}(\theta)\,dt \\
&= \int_0^\infty \left(\dot{x}^T P_r^{-1}(\theta)\,x + x^T P_r^{-1}(\theta)\,\dot{x} + x^T \dot{P}_r^{-1}(\theta)\,x\right) dt \\
&= \int_0^\infty \Big[x^T \Big(A_{C_r}^T(\alpha,\theta)\,P_r^{-1}(\theta) + P_r^{-1}(\theta)\,A_{C_r}(\alpha,\theta) \\
&\qquad + \dot{P}_r^{-1}(\theta)\Big)x + \Delta f_r^T(\theta)\,P_r^{-1}(\theta)\,x \\
&\qquad + \Delta g_0^r(\theta)^T P_r^{-1}(\theta)\,x + \Delta d_0^r(\theta)^T P_r^{-1}(\theta)\,x \\
&\qquad + x^T P_r^{-1}(\theta)\,\Delta f_r(\theta) + x^T P_r^{-1}(\theta)\,\Delta g_0^r(\theta) \\
&\qquad + x^T P_r^{-1}(\theta)\,\Delta d_0^r(\theta) + \omega^T B_{C_r}^T(\alpha,\theta)\,P_r^{-1}(\theta)\,x \\
&\qquad + x^T P_r^{-1}(\theta)\,B_{C_r}(\alpha,\theta)\,\omega\Big]\,dt \\
&\le \int_0^\infty \Big[x^T \Big(A_{C_r}^T(\alpha,\theta)\,P_r^{-1}(\theta) + P_r^{-1}(\theta)\,A_{C_r}(\alpha,\theta) \\
&\qquad + \dot{P}_r^{-1}(\theta)\Big)x \\
&\qquad + \frac{1}{\varepsilon_{\Delta f_r P_r}(\theta)}\Delta f_r^T(\theta)\,\Delta f_r(\theta) \\
&\qquad + \varepsilon_{\Delta f_r P_r}(\theta)\,x^T P_r^{-1}(\theta)\,P_r^{-1}(\theta)\,x \\
&\qquad + \frac{1}{\varepsilon_{\Delta g_0^r P_r}(\theta)}\Delta g_0^r(\theta)^T \Delta g_0^r(\theta) \\
&\qquad + \varepsilon_{\Delta g_0^r P_r}(\theta)\,x^T P_r^{-1}(\theta)\,P_r^{-1}(\theta)\,x \\
&\qquad + \frac{1}{\varepsilon_{\Delta d_0^r P_r}(\theta)}\Delta d_0^r(\theta)^T \Delta d_0^r(\theta) \\
&\qquad + \varepsilon_{\Delta d_0^r P_r}(\theta)\,x^T P_r^{-1}(\theta)\,P_r^{-1}(\theta)\,x \\
&\qquad + \omega^T B_{C_r}^T(\alpha,\theta)\,P_r^{-1}(\theta)\,x + x^T P_r^{-1}(\theta)\,B_{C_r}(\alpha,\theta)\,\omega\Big]\,dt \\
&\le \int_0^\infty \Big[x^T \Big(A_{C_r}^T(\alpha,\theta)\,P_r^{-1}(\theta) + P_r^{-1}(\theta)\,A_{C_r}(\alpha,\theta) \\
&\qquad + \dot{P}_r^{-1}(\theta)\Big)x \\
&\qquad + \frac{1}{\varepsilon_{\Delta f_r P_r}(\theta)}\left(\widehat{A}_r(\theta)\,x\right)^T \widehat{A}_r(\theta)\,x + \frac{1}{\varepsilon_{\Delta g_0^r P_r}(\theta)} \\
&\qquad \times \left(\widehat{B}_2^r(\theta)\,K_r(\theta)\,x\right)^T \widehat{B}_2^r(\theta)\,K_r(\theta)\,x \\
&\qquad + \frac{1}{\varepsilon_{\Delta d_0^r P_r}(\theta)}\left(\widehat{B}_1^r(\theta)\,\omega\right)^T \widehat{B}_1^r(\theta)\,\omega \\
&\qquad + \left(\varepsilon_{\Delta f_r P_r}(\theta) + \varepsilon_{\Delta g_0^r P_r}(\theta)\right. \\
&\qquad \left. + \varepsilon_{\Delta d_0^r P_r}(\theta)\right) x^T P_r^{-1}(\theta)\,P_r^{-1}(\theta)\,x \\
&\qquad + \omega^T B_{C_r}^T(\alpha,\theta)\,P_r^{-1}(\theta)\,x + x^T P_r^{-1}(\theta)\,B_{C_r}(\alpha,\theta)\,\omega\Big]\,dt \\
&\le \int_0^\infty \Big[-x^T \Big(\Big(1 + \varepsilon_{\Delta\varphi_r C_{Cr}}(\theta) + \varepsilon_{\Delta g_1^r C_{Cr}}(\theta)\Big) \\
&\qquad \times C_{C_r}^T(\alpha,\theta)\,C_{C_r}(\alpha,\theta) \\
&\qquad + \left(1 + \frac{1}{\varepsilon_{\Delta\varphi_r C_{Cr}}(\theta)} + \frac{1}{\varepsilon_{\Delta\varphi_r \Delta g_1^r}(\theta)}\right)\widehat{C}_1^r(\alpha,\theta)^T \widehat{C}_1^r(\alpha,\theta) \\
&\qquad + \left(1 + \frac{1}{\varepsilon_{\Delta g_1^r C_{Cr}}(\theta)} + \frac{1}{\varepsilon_{\Delta\varphi_r \Delta g_1^r}(\theta)}\right)\widehat{D}_{12}^r(\alpha,\theta)^T \widehat{D}_{12}^r(\alpha,\theta) \\
&\qquad + \left(\gamma^2 I - \frac{1}{\varepsilon_{\Delta d_0^r P_r}(\theta)}\left(\widehat{B}_1^r(\theta)\right)^T \widehat{B}_1^r(\theta)\right)^{-1} P_r^{-1}(\theta) \\
&\qquad \times B_{C_r}(\alpha,\theta)\,B_{C_r}^T(\alpha,\theta)\,P_r^{-1}(\theta)\Big)x \\
&\qquad + \frac{1}{\varepsilon_{\Delta d_0^r P_r}(\theta)}\left(\widehat{B}_1^r(\theta)\,\omega\right)^T \widehat{B}_1^r(\theta)\,\omega \\
&\qquad + \omega^T B_{C_r}^T(\alpha,\theta)\,P_r^{-1}(\theta)\,x \\
&\qquad + x^T P_r^{-1}(\theta)\,B_{C_r}(\alpha,\theta)\,\omega + \gamma^2\omega^T\omega - \gamma^2\omega^T\omega\Big]\,dt \\
&\le \int_0^\infty \Bigg[- z^T z + \gamma^2\omega^T\omega \\
&\qquad - \left\| \left(\gamma^2 I - \frac{1}{\varepsilon_{\Delta d_0^r P_r}(\theta)}\widehat{B}_1^r(\theta)^T \widehat{B}_1^r(\theta)\right)^{1/2}\omega \right. \\
&\qquad \left. - \left(\gamma^2 I - \frac{1}{\varepsilon_{\Delta d_0^r P_r}(\theta)}\widehat{B}_1^r(\theta)^T \widehat{B}_1^r(\theta)\right)^{-1/2} \right. \\
&\qquad \left. \times B_{C_r}^T(\alpha,\theta)\,P_r^{-1}(\theta)\,x \right\|_2^2 \Bigg]\,dt \\
&\le \int_0^\infty \left[-z^T z + \gamma^2\omega^T\omega\right] dt.
\end{aligned}
\tag{80}
$$

That is

$$V(x(\infty),\theta) - V(x(0),\theta) \le \int_0^\infty \left(-z^T z + \gamma^2 \omega^T \omega\right) dt, \tag{81}$$

which suggests that, with $x(0) = 0$,

$$\|z\|_2 \le \gamma \|\omega\|_2. \tag{82}$$

Overall, combining with the condition (75) and $P_r(\theta) = (F_r^T F_r)^{-1} F_r^T T(\theta) F_r (F_r^T F_r)^{-1}$, the system (61), while considering the approximation error, has the H_∞ performance with disturbance attenuation γ and it is globally asymptotically stable when $\omega = 0$. Then, the proof of this theorem is completed. □

Remark 8. Considering the approximation error of the LPV T-S fuzzy system and bringing in the piecewise parameter-dependent Lyapunov functions to the LPV T-S fuzzy gain scheduling control, the state-feedback H_∞ control design is discussed here. And the sufficient conditions are given in Riccati inequalities form which can guarantee the H_∞ performance boundary γ of the closed-loop system.

As follows, based on Theorem 7, the equivalent conditions can be obtained in LMIs form which are easier to be solved.

Theorem 9. *For the closed-loop system* (61)*, while considering the approximation error and a positive scalar $\gamma > 0$, if there exist a symmetric matrix $T(\theta)$, a set of matrices $Q_r(\theta) = K_r(\theta) P_r(\theta)$ and $P_r(\theta) = (F_r^T F_r)^{-1} F_r^T T(\theta) F_r (F_r^T F_r)^{-1}$ satisfying*

$$P_r(\theta) > 0,$$
$$\begin{bmatrix} W_r & P_r(\theta) & Q_r^T(\theta) \\ P_r(\theta) & -M_{Pr}^{-1} & 0 \\ Q_r(\theta) & 0 & -M_{Qr}^{-1} \end{bmatrix} < 0, \tag{83}$$

where

$$\begin{aligned}
W_r &= P_r(\theta) A_i^T(\theta) + A_i(\theta) P_r(\theta) - \dot{P}_r(\theta) \\
&\quad + Q_r^T(\theta) B_2^i(\theta)^T + B_2^i(\theta) Q_r(\theta) \\
&\quad + \varepsilon_{\widetilde{A}_r P_r}(\theta) E_{rA}(\alpha,\theta) E_{rA}^T(\alpha,\theta) \\
&\quad + \varepsilon_{\widetilde{B}_2^r P_r}(\theta) E_{rB_2}(\alpha,\theta) E_{rB_2}^T(\alpha,\theta) \\
&\quad + \left(\gamma^2 I - \frac{1}{\varepsilon_{\Delta d_0^r P_r}(\theta)} \widehat{B}_1^r(\theta)^T \widehat{B}_1^r(\theta)\right)^{-1} \\
&\quad \times \left(1 + \frac{1}{\varepsilon_{B_1^i \widetilde{B}_1^r}(\theta)}\right) B_1^i(\theta) B_1^i(\theta)^T \\
&\quad + \left(\gamma^2 I - \frac{1}{\varepsilon_{\Delta d_0^r P_r}(\theta)} \widehat{B}_1^r(\theta)^T \widehat{B}_1^r(\theta)\right)^{-1} \\
&\quad \times \left(1 + \varepsilon_{B_1^i \widetilde{B}_1^r}(\theta)\right) E_{rB_1}(\alpha,\theta) E_{rB_1}(\alpha,\theta)^T, \\
M_{P_r} &= \frac{1}{\varepsilon_{\widetilde{A}_r P_r}(\theta)} + \frac{1}{\varepsilon_{\Delta f_r P_r}(\theta)} \widehat{A}_r^T(\theta) \widehat{A}_r(\theta) \\
&\quad + \left(1 + \frac{1}{\varepsilon_{\Delta\varphi_r C_{C_r}}(\theta)} + \frac{1}{\varepsilon_{\Delta\varphi_r \Delta g_1^r}(\theta)}\right) \\
&\quad \times \widehat{C}_1^r(\alpha,\theta)^T \widehat{C}_1^r(\alpha,\theta) \\
&\quad + \left(1 + \frac{1}{\varepsilon_{\Delta g_1^r C_{C_r}}(\theta)} + \frac{1}{\varepsilon_{\Delta\varphi_r \Delta g_1^r}(\theta)}\right) \\
&\quad \times \widehat{D}_{12}^r(\alpha,\theta)^T \widehat{D}_{12}^r(\alpha,\theta) \\
&\quad + \left(1 + \varepsilon_{\Delta\varphi_r C_{C_r}}(\theta) + \varepsilon_{\Delta g_1^r C_{C_r}}(\theta)\right) \\
&\quad \times \left(1 + \frac{1}{\varepsilon_{C_1^i \widetilde{C}_1^r}(\theta)} + \frac{1}{\varepsilon_{C_1^i D_{12}^i}(\theta)} + \frac{1}{\varepsilon_{C_1^i \widetilde{D}_{12}^r}(\theta)}\right) \\
&\quad \times C_1^i(\theta)^T C_1^i(\theta) \\
&\quad + \left(1 + \varepsilon_{\Delta\varphi_r C_{C_r}}(\theta) + \varepsilon_{\Delta g_1^r C_{C_r}}(\theta)\right) \\
&\quad \times \left(1 + \varepsilon_{C_1^i \widetilde{C}_1^r}(\theta) + \varepsilon_{D_{12}^i \widetilde{C}_1^r}(\theta) + \frac{1}{\varepsilon_{\widetilde{C}_1^r \widetilde{D}_{12}^r}(\theta)}\right) E_{rC_1}^T \\
&\quad \times E_{rC_1}^T(\alpha,\theta) E_{rC_1}(\alpha,\theta), \\
M_{Q_r} &= \frac{1}{\varepsilon_{\widetilde{B}_2^r P_r}(\theta)} + \frac{1}{\varepsilon_{\Delta g_0^r P_r}(\theta)} \widehat{B}_2^r(\theta)^T \widehat{B}_2^r(\theta) \\
&\quad + \left(1 + \varepsilon_{\Delta\varphi_r C_{C_r}}(\theta) + \varepsilon_{\Delta g_1^r C_{C_r}}(\theta)\right) \\
&\quad \times \left(1 + \varepsilon_{C_1^i D_{12}^i}(\theta) + \frac{1}{\varepsilon_{D_{12}^i \widetilde{C}_1^r}(\theta)} + \frac{1}{\varepsilon_{D_{12}^i \widetilde{D}_{12}^r}(\theta)}\right) \\
&\quad \times D_{12}^i(\theta)^T D_{12}^i(\theta) \\
&\quad + \left(1 + \varepsilon_{\Delta\varphi_r C_{C_r}}(\theta) + \varepsilon_{\Delta g_1^r C_{C_r}}(\theta)\right) \\
&\quad \times \left(1 + \varepsilon_{C_1^i \widetilde{D}_{12}^r}(\theta) + \varepsilon_{\widetilde{C}_1^r \widetilde{D}_{12}^r}(\theta) + \varepsilon_{D_{12}^i \widetilde{D}_{12}^r}(\theta)\right) \\
&\quad \times E_{rD_{12}}^T(\alpha,\theta) E_{rD_{12}}(\alpha,\theta),
\end{aligned} \tag{84}$$

and condition (77)*, the closed-loop system* (61)*, while considering the approximation error, has the H_∞ performance with disturbance attenuation γ and it is globally asymptotically stable when $\omega = 0$. Moreover, the controller gain in the rth subspace is given by*

$$K_r(\theta) = Q_r(\theta) P_r^{-1}(\theta). \tag{85}$$

Proof. According to condition (76) of Theorem 7, we know that the closed-loop system (61), while considering the approximation error, has the H_∞ performance boundary γ.

Then, substituting (37) into (76), we can get

$$\begin{aligned}
&P_r(\theta)A_{Cr}^T(\alpha,\theta)+A_{Cr}(\alpha,\theta)P_r(\theta)\\
&\quad=P_r(\theta)\Big(A_i(\theta)+\widetilde{A}_r(\alpha,\theta)\\
&\qquad+\Big(B_2^i(\theta)+\widetilde{B}_2^r(\alpha,\theta)\Big)K_r(\theta)\Big)^T\\
&\quad+\Big(A_i(\theta)+\widetilde{A}_r(\alpha,\theta)+\Big(B_2^i(\theta)+\widetilde{B}_2^r(\alpha,\theta)\Big)\\
&\qquad\times K_r(\theta)\Big)P_r(\theta)\\
&\quad=P_r(\theta)A_i^T(\theta)+A_i(\theta)P_r(\theta)+Q_r^T(\theta)B_2^i(\theta)^T\\
&\quad+B_2^i(\theta)Q_r(\theta)+P_r(\theta)\widetilde{A}_r^T(\alpha,\theta)\\
&\quad+\widetilde{A}_r(\alpha,\theta)P_r(\theta)+Q_r^T(\theta)\widetilde{B}_2^r(\alpha,\theta)^T\\
&\quad+\widetilde{B}_2^r(\alpha,\theta)Q_r(\theta)\\
&\quad\le P_r(\theta)A_i^T(\theta)+A_i(\theta)P_r(\theta)\\
&\quad+Q_r^T(\theta)B_2^i(\theta)^T+B_2^i(\theta)Q_r(\theta)\\
&\quad+\varepsilon_{\widetilde{A}_rP_r}(\theta)E_{rA}(\alpha,\theta)E_{rA}^T(\alpha,\theta)\\
&\quad+\varepsilon_{\widetilde{B}_2^rP_r}(\theta)E_{rB_2}(\alpha,\theta)E_{rB_2}^T(\alpha,\theta)\\
&\quad+\frac{1}{\varepsilon_{\widetilde{A}_rP_r}(\theta)}P_r(\theta)P_r(\theta)+\frac{1}{\varepsilon_{\widetilde{B}_2^rP_r}(\theta)}Q_r^T(\theta)Q_r(\theta).
\end{aligned}\tag{86}$$

Besides, we also have

$$\begin{aligned}
&P_r(\theta)C_{C_i}^T(\alpha,\theta)C_{C_i}(\alpha,\theta)P_r(\theta)\\
&\quad=P_r(\theta)\Big[C_1^i(\theta)^TC_1^i(\theta)+C_1^i(\theta)^T\widetilde{C}_1^r(\alpha,\theta)\\
&\qquad+\widetilde{C}_1^r(\alpha,\theta)^TC_1^i(\theta)\\
&\qquad+\widetilde{C}_1^r(\alpha,\theta)^T\widetilde{C}_1^r(\alpha,\theta)\Big]P_r(\theta)\\
&\quad+P_r(\theta)C_1^i(\theta)^TD_{12}^i(\theta)Q_r(\theta)\\
&\quad+P_r(\theta)C_1^i(\theta)^T\widetilde{D}_{12}^r(\alpha,\theta)Q_r(\theta)\\
&\quad+P_r(\theta)\widetilde{C}_1^r(\alpha,\theta)^TD_{12}^i(\theta)Q_r(\theta)\\
&\quad+P_r(\theta)\widetilde{C}_1^r(\alpha,\theta)^T\widetilde{D}_{12}^r(\alpha,\theta)Q_r(\theta)\\
&\quad+Q_r^T(\theta)D_{12}^i(\theta)^TC_1^i(\theta)P_r(\theta)\\
&\quad+Q_r^T(\theta)D_{12}^i(\theta)^T\widetilde{C}_1^r(\alpha,\theta)P_r(\theta)\\
&\quad+Q_r^T(\theta)\widetilde{D}_{12}^r(\alpha,\theta)^TC_1^i(\theta)P_r(\theta)\\
&\quad+Q_r^T(\theta)\widetilde{D}_{12}^r(\alpha,\theta)^T\widetilde{C}_1^r(\alpha,\theta)P_r(\theta)\\
&\quad+Q_r^T(\theta)\Big[D_{12}^i(\theta)^TD_{12}^i(\theta)\\
&\qquad+D_{12}^i(\theta)^T\widetilde{D}_{12}^r(\alpha,\theta)\\
&\qquad+\widetilde{D}_{12}^r(\alpha,\theta)^TD_{12}^i(\theta)\\
&\qquad+\widetilde{D}_{12}^r(\alpha,\theta)^T\widetilde{D}_{12}^r(\alpha,\theta)\Big]Q_r(\theta)\\
&\quad\le P_r(\theta)\Bigg[\Bigg(1+\frac{1}{\varepsilon_{C_1^i\widetilde{C}_1^r}(\theta)}+\frac{1}{\varepsilon_{C_1^iD_{12}^i}(\theta)}\\
&\qquad+\frac{1}{\varepsilon_{C_1^i\widetilde{D}_{12}^r}(\theta)}\Bigg)C_1^i(\theta)^TC_1^i(\theta)\\
&\qquad+\Bigg(1+\varepsilon_{C_1^i\widetilde{C}_1^r}(\theta)+\varepsilon_{D_{12}^i\widetilde{C}_1^r}(\theta)\\
&\qquad+\frac{1}{\varepsilon_{\widetilde{C}_1^r\widetilde{D}_{12}^r}(\theta)}\Bigg)E_{rC_1}^T\\
&\qquad\times(\alpha,\theta)E_{rC_1}(\alpha,\theta)\Bigg]P_r(\theta)\\
&\quad+Q_r^T(\theta)\Bigg[\Bigg(1+\varepsilon_{C_1^iD_{12}^i}(\theta)+\frac{1}{\varepsilon_{D_{12}^i\widetilde{C}_1^r}(\theta)}\\
&\qquad+\frac{1}{\varepsilon_{D_{12}^i\widetilde{D}_{12}^r}(\theta)}\Bigg)D_{12}^i(\theta)^TD_{12}^i(\theta)\\
&\qquad+\Big(1+\varepsilon_{C_1^i\widetilde{D}_{12}^r}(\theta)+\varepsilon_{\widetilde{C}_1^r\widetilde{D}_{12}^r}(\theta)\\
&\qquad+\varepsilon_{D_{12}^i\widetilde{D}_{12}^r}(\theta)\Big)\\
&\qquad\times E_{rD_{12}}^T(\alpha,\theta)E_{rD_{12}}(\alpha,\theta)\Bigg]Q_r(\theta),
\end{aligned}\tag{87}$$

$$\begin{aligned}
&B_{Cr}(\alpha,\theta)B_{Cr}^T(\alpha,\theta)\\
&\quad=B_1^i(\theta)B_1^i(\theta)^T+B_1^i(\theta)\widetilde{B}_1^r(\alpha,\theta)^T\\
&\qquad+\widetilde{B}_1^r(\alpha,\theta)B_1^i(\theta)^T+\widetilde{B}_1^r(\alpha,\theta)\widetilde{B}_1^r(\alpha,\theta)^T\\
&\quad\le\left(1+\frac{1}{\varepsilon_{B_1^i\widetilde{B}_1^r}(\theta)}\right)B_1^i(\theta)B_1^i(\theta)^T\\
&\qquad+\Big(1+\varepsilon_{B_1^i\widetilde{B}_1^r}(\theta)\Big)E_{rB_1}(\alpha,\theta)E_{rB_1}^T(\alpha,\theta).
\end{aligned}\tag{88}$$

Substituting (86), (87), and (88) into (76), the complete representation of (76) can be gotten. Then, by defining W_r, M_{P_r}, and M_{Q_r} and using the Schur complement lemma, we can get the sufficient conditions in LMIs form as (83) and (80). The proof of this theorem is completed. □

Remark 10. Based on Theorem 7, the conveniently solvable conditions are obtained in LMIs form in Theorem 9. For some parameter-dependent variables, such as $\varepsilon_*(\theta)$, they can be set as constant values in many cases by which the computation can be further simplified. However, subscripts of all $\varepsilon_*(\theta)$ are marked clearly in Theorem 5, Theorem 7, and Theorem 9 in order to show the meaning of them.

Remark 11. From Theorem 9, the sufficient conditions in LMIs form have been given. Though the solving of the LPV T-S fuzzy gain scheduling control design is different from the solving of the existing LPV gain scheduling control design, most of the procedures are similar. According to [9, 28, 29], the solution of the existing LPV gain scheduling control design has been given. Then, the main procedures of the LPV gain scheduling control design can be shown as follows. Firstly, according to the property of θ, the gridding process may be executed for the nonlinear form of θ or not. In particular, for the affine linear form of θ, the multiconvexity property can be used to guarantee the continuous properties of continuously scheduled θ instead of the gridding process and the number of the LMIs can be reduced which can simplify the computation. Secondly, the parametrization of decision variables in LMIs needs to be executed. Through the two steps, infinite LMIs with infinite decision variables can be gotten. By solving the LMIs, the piecewise parameter-dependent functions can be obtained and then the controller can be determined.

5. Numerical Example

In order to show the availability of the approaches, a numerical example is provided in this subsection. Consider the ANPV system as

$$\begin{aligned} \dot{x} &= f(x,\theta) + B_1\omega + B_2 u, \\ z &= \varphi(x,\theta), \end{aligned} \tag{89}$$

where $f(x,\theta) = \begin{bmatrix} 0.0005\theta x_1^2 + 0.0008 x_2 \\ x_1 - 0.5 x_2 \end{bmatrix}$, $\varphi(x,\theta) = 0.5\theta - x_1$, $B_1 = \begin{bmatrix} 0.0001 & 0 \end{bmatrix}^T$, $B_2 = \begin{bmatrix} 0 & 1 \end{bmatrix}^T$, and $\omega = \sin(t)$ is the sinusoidal interference signal.

Here, define that $\theta = vt + \tau$ is a linear function about time t and set the variation rate $\|v\|_2 \le 1$. Assume that θ changes in the range $[-2, 2]$ and the variation range of x_1 is $[-1, 1]$. From (89), it can be found that the T-S fuzzy linearization is only used to deal with the nonlinearity about x_1. Using the T-S fuzzy modeling procedure given before, the input space of x_1 can be partitioned into $[-1, 0]$ and $[0, 1]$. Then, three T-S fuzzy rules can be obtained as follows:

Rule 1: If x_1 is about -1,

$$\text{then } \begin{cases} \dot{x} = \begin{bmatrix} -0.0005\theta & 0.0008 \\ 1 & -0.5 \end{bmatrix} x + \begin{bmatrix} 0.0001 \\ 0 \end{bmatrix} \omega + \begin{bmatrix} 0 \\ 1 \end{bmatrix} u \\ z = \begin{bmatrix} -0.5\theta - 1 & 0 \end{bmatrix} x, \end{cases} \tag{90}$$

Rule 2: If x_1 is about 0,

$$\text{then } \begin{cases} \dot{x} = \begin{bmatrix} 0 & 0.0008 \\ 1 & -0.5 \end{bmatrix} x + \begin{bmatrix} 0.0001 \\ 0 \end{bmatrix} \omega + \begin{bmatrix} 0 \\ 1 \end{bmatrix} u \\ z = \begin{bmatrix} -1 & 0 \end{bmatrix} x, \end{cases} \tag{91}$$

Rule 3: If x_1 is about 1,

$$\text{then } \begin{cases} \dot{x} = \begin{bmatrix} 0.0005\theta & 0.0008 \\ 1 & -0.5 \end{bmatrix} x + \begin{bmatrix} 0.0001 \\ 0 \end{bmatrix} \omega + \begin{bmatrix} 0 \\ 1 \end{bmatrix} u \\ z = \begin{bmatrix} 0.5\theta - 1 & 0 \end{bmatrix} x. \end{cases} \tag{92}$$

In most cases, the approximation of the LPV T-S fuzzy system to the ANPV system usually has high accuracy, so the approximation error can often be ignored. Here, three T-S fuzzy rules are used at -1, 0, and 1 of x_1 to approximate the nonlinear term x_1^2; the maximum absolute error is $1.1102e-16$. Thus, the approximation error can be ignored.

Meanwhile, using the definition in (35)-(36) and the triangular membership functions, four piecewise subspaces are obtained which are named $\overline{X}_1$, $\overline{X}_2$, $\overline{X}_3$, and $\overline{X}_4$ (as shown in Figure 3). Then, the T-S fuzzy model in each subspace can be represented as

$$\overline{X}_1 : \begin{cases} \dot{x} = \left(\begin{bmatrix} -0.0005\theta & 0.0008 \\ 1 & -0.5 \end{bmatrix} + \alpha_2(x_1) \begin{bmatrix} 0.0005\theta & 0 \\ 0 & 0 \end{bmatrix} \right) x \\ \quad + \begin{bmatrix} 0.0001 \\ 0 \end{bmatrix} \omega + \begin{bmatrix} 0 \\ 1 \end{bmatrix} u \\ z = \left(\begin{bmatrix} -0.5\theta - 1 & 0 \end{bmatrix} + \alpha_2(x_1) \begin{bmatrix} 0.5\theta & 0 \end{bmatrix} \right) x, \quad x_1 \in [-1, -0.5], \end{cases} \tag{93}$$

$$\overline{X}_2 : \begin{cases} \dot{x} = \left(\begin{bmatrix} 0 & 0.0008 \\ 1 & -0.5 \end{bmatrix} + \alpha_1(x_1) \begin{bmatrix} -0.0005\theta & 0 \\ 0 & 0 \end{bmatrix} \right) x \\ \quad + \begin{bmatrix} 0.0001 \\ 0 \end{bmatrix} \omega + \begin{bmatrix} 0 \\ 1 \end{bmatrix} u \\ z = \left(\begin{bmatrix} -1 & 0 \end{bmatrix} + \alpha_1(x_1) \begin{bmatrix} -0.5\theta & 0 \end{bmatrix} \right) x, \quad x_1 \in [-0.5, 0], \end{cases} \tag{94}$$

$$\overline{X}_3 : \begin{cases} \dot{x} = \left(\begin{bmatrix} 0 & 0.0008 \\ 1 & -0.5 \end{bmatrix} + \alpha_3(x_1) \begin{bmatrix} 0.0005\theta & 0 \\ 0 & 0 \end{bmatrix} \right) x \\ \quad + \begin{bmatrix} 0.0001 \\ 0 \end{bmatrix} \omega + \begin{bmatrix} 0 \\ 1 \end{bmatrix} u \\ z = \left(\begin{bmatrix} -1 & 0 \end{bmatrix} + \alpha_3(x_1) \begin{bmatrix} 0.5\theta & 0 \end{bmatrix} \right) x, \quad x_1 \in [0, 0.5], \end{cases} \tag{95}$$

$$\overline{X}_4 : \begin{cases} \dot{x} = \left(\begin{bmatrix} 0.0005\theta & 0.0008 \\ 1 & -0.5 \end{bmatrix} + \alpha_2(x_1) \begin{bmatrix} -0.0005\theta & 0 \\ 0 & 0 \end{bmatrix} \right) x \\ \quad + \begin{bmatrix} 0.0001 \\ 0 \end{bmatrix} \omega + \begin{bmatrix} 0 \\ 1 \end{bmatrix} u \\ z = \left(\begin{bmatrix} 0.5\theta - 1 & 0 \end{bmatrix} + \alpha_2(x_1) \begin{bmatrix} -0.5\theta & 0 \end{bmatrix} \right) x, \quad x_1 \in [0.5, 1]. \end{cases} \tag{96}$$

According to the method in [22], it can be set that $\alpha_k(\overline{x}, \theta) = 0.5$ and the matrices of $E_{rA}(\theta)$ and $E_{rC_1}(\theta)$ for the ith ($i = 1, 2, 3$) fuzzy rule in the rth ($r = 1, 2, 3, 4, k \in \phi_r$) subspace can be obtained. Using the detailed method in [20], the constant matrices F_r can be given.

When the LPV T-S fuzzy system is linear with the scheduling parameter θ, we can parameterize the system

matrices $\overline{A}_r(\theta)$ and $\overline{C}_1^r(\theta)$ and decision variables $P_r(\theta)$ and $Q_r(\theta)$ in the rth subspace as

$$\begin{aligned} \overline{A}_r(\theta) &= \overline{A}_r^0 + \theta\overline{A}_r^1, \qquad \overline{C}_1^r(\theta) = \overline{C}_{1,0}^r + \theta\overline{C}_{1,1}^r, \\ \overline{P}_r(\theta) &= \overline{P}_r^0 + \theta\overline{P}_r^1, \qquad \overline{Q}_r(\theta) = \overline{Q}_r^0 + \theta\overline{Q}_r^1, \end{aligned} \tag{97}$$

where $\overline{A}_r^0, \overline{A}_r^1, \overline{C}_{1,0}^r, \overline{C}_{1,1}^r, \overline{P}_r^0, \overline{P}_r^1, \overline{Q}_r^0$, and $\overline{Q}_r^1$ are constant values and $r = 1, 2, 3, 4$.

Besides, the gridding process is avoided when solving the parameter-dependent Lyapunov functions $P_r(\theta)$ in rth subspace $\overline{X}_r$. Utilizing the multiconvexity property in [30], it just needs to validate the LMIs at the vertexes of θ. Here, the two vertexes at $\theta = -2$ and $\theta = 2$ are tested, respectively.

Following the design algorithm with $\gamma = 0.9$, the solution to the LMIs when $\varepsilon_*(\theta) = 10$ can be obtained:

$$\begin{aligned} P_1(\theta) &= \begin{bmatrix} 0.0265 + 0.0777\theta & -0.2 + 0.996\theta \\ -0.2 + 0.996\theta & 4.475 + 1.5562\theta \end{bmatrix}, \\ Q_1(\theta) &= \begin{bmatrix} 0.1476 + 0.0840\theta & 10.9778 + 0.0191\theta \end{bmatrix}, \\ P_2(\theta) &= \begin{bmatrix} -0.0126 + 0.3006\theta & -0.6849 + 0.0309\theta \\ -0.6849 + 0.0309\theta & 3.6378 + 0.8595\theta \end{bmatrix}, \\ Q_2(\theta) &= \begin{bmatrix} 0.0997 + 0.0373\theta & 7.2065 - 0.1058\theta \end{bmatrix}, \\ P_3(\theta) &= \begin{bmatrix} -0.0126 + 0.3006\theta & -0.6849 + 0.0309\theta \\ -0.6849 + 0.0309\theta & 3.6378 + 0.8595\theta \end{bmatrix}, \\ Q_3(\theta) &= \begin{bmatrix} 0.0997 + 0.0373\theta & 7.2065 - 0.1058\theta \end{bmatrix}, \\ P_4(\theta) &= \begin{bmatrix} -0.0176 + 0.0651\theta & -0.1457 - 1.0275\theta \\ -0.1457 - 1.0275\theta & 6.5439 + 1.5280\theta \end{bmatrix}, \\ Q_4(\theta) &= \begin{bmatrix} 0.0423 - 0.0114\theta & 10.8734 + 0.0179\theta \end{bmatrix}. \end{aligned} \tag{98}$$

Then, the state-feedback controller can be determined as $u = K_r(\theta)x$, where $K_r(\theta) = Q_r(\theta)P_r^{-1}(\theta)$ and $r = 1, 2, 3, 4$.

Because the effective performance region of the controller about x_1 is set as $[-1, 1]$, the scheduling values of θ are chosen to linearly vary from 0.3 to 1.3 with the interval of 0.1 to validate the effectiveness of the controller. The state responses of x_1 and x_2 and the evaluation response of z are shown in Figures 4, 5, and 6, respectively.

Meanwhile, in order to validate the effectiveness of the controller during the scheduling process of θ, θ is scheduled from 0.5 to 1 at 0.5 seconds, which guarantees that the variation rate of θ is 1. The responses of x_1, x_2, and z are shown in Figures 7, 8, and 9, respectively.

From Figures 4, 5, and 6, they suggest the effectiveness of the parameter-dependent controller. At different scheduling points of θ, the system can be stabilized by the state-feedback controller with H_∞ performance boundary $\gamma = 0.9$. From Figures 7, 8, and 9, the performance when switching at different θ points is validated. The time-domain response curves illustrate the stability and control performance of the system when continuously scheduling. Obviously, all the above results suggest the availability of sufficient conditions in Theorems 5, 7, and 9 for the control design of the LPV T-S fuzzy system.

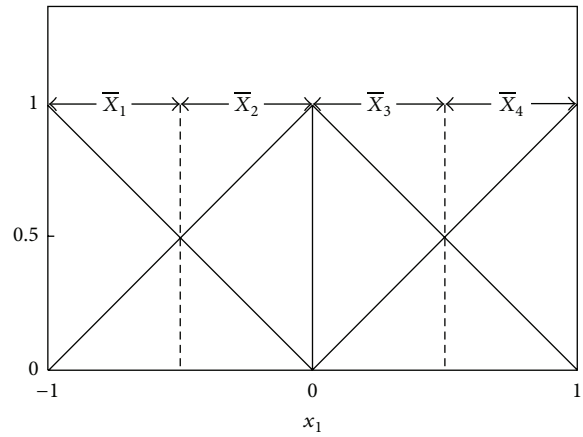

Figure 3: Piecewise space partition of x_1.

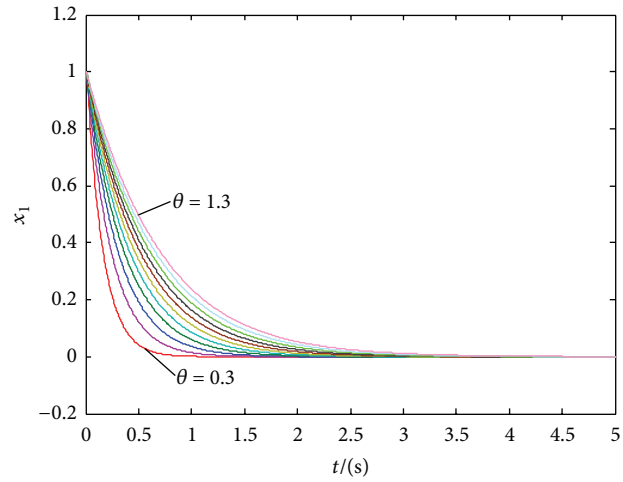

Figure 4: State response of x_1.

6. Conclusion

In order to improve the existing LPV gain scheduling control, the T-S fuzzy modeling procedure was adopted to deal with the nonlinearity and relevant control design was studied in the paper. For the ANPV description of the nonlinear dynamic processes, a kind of developed T-S fuzzy modeling procedure with homogeneous linear consequent parts was proposed to carry forward the linearization. As a result, greater flexibility was obtained by which the number of scheduling parameters could be reduced and the approximation accuracy could be raised in any optional region. Moreover, the un-uniform partition method was utilized and the evaluation system for the approximation ability of the novelly developed T-S fuzzy modeling procedure was established. Through this way, the number of fuzzy rules could be decreased while guaranteeing the approximation performance, and the LPV T-S fuzzy system was obtained with required accuracy. For the LPV T-S fuzzy gain scheduling control, the notion of piecewise parameter-dependent Lyapunov function was introduced to improve the solvability. Subsequently, the stabilization problem and the

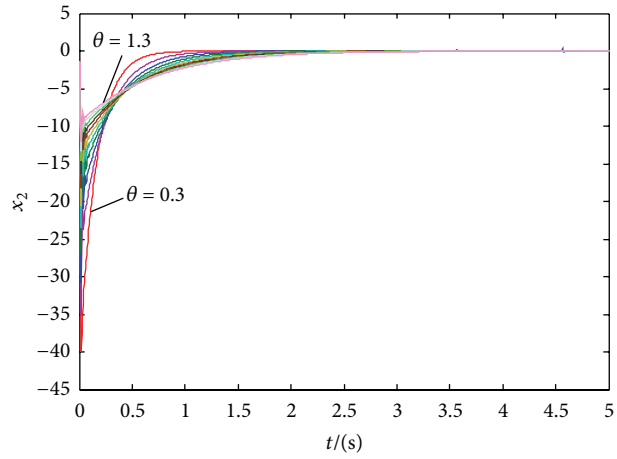

Figure 5: State response of x_2.

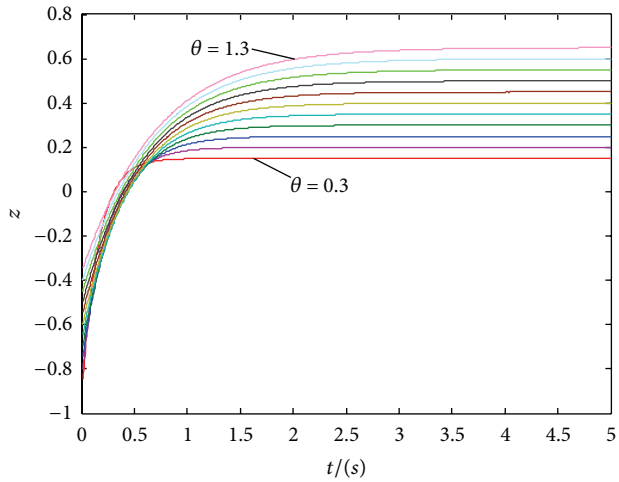

Figure 6: Evaluation response of z.

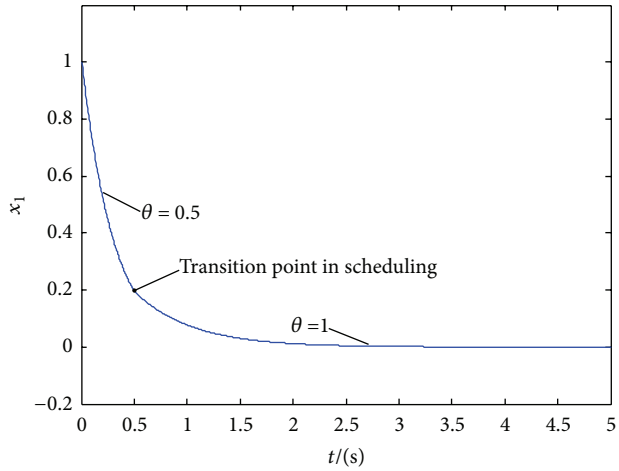

Figure 7: State response of x_1 in scheduling.

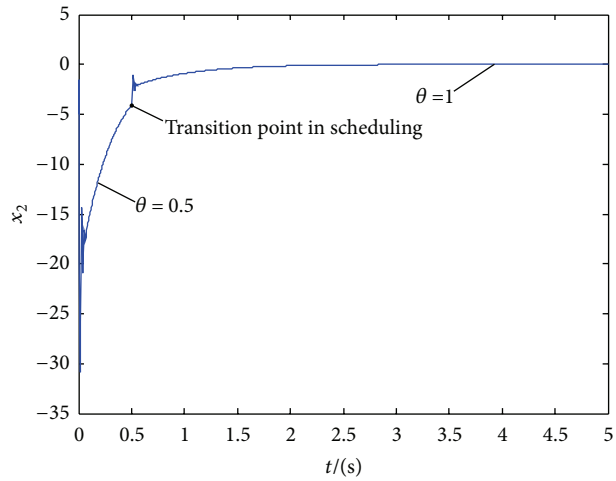

Figure 8: State response of x_2 in scheduling.

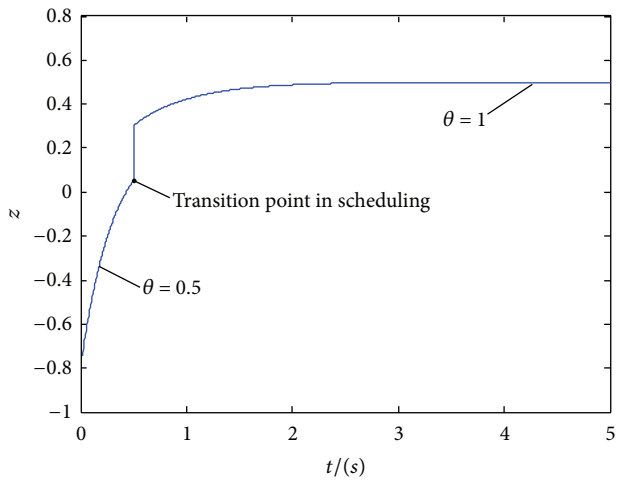

Figure 9: Evaluation response of z in scheduling.

state-feedback H_∞ control problem of the LPV T-S fuzzy system were discussed. The sufficient conditions were given in LMIs form and the approximation error was considered for the H_∞ control. Note that the novel LPV T-S fuzzy system can represent a great class of nonlinear dynamic processes. Based on the LPV T-S fuzzy system framework, more problems could be further studied following such a line, such as the output feedback control design and the corresponding applications.

Acknowledgments

This work is partially supported by the National Basic Research Program of China (973 Program) (Grant no. 2012CB215203), the National Natural Science Foundation of China (no. 51036002 and no. 61203043), and the Fundamental Research Funds for the Central Universities (no. 13XS14).

References

[1] J. S. Shamma and M. Athans, "Analysis of gain scheduled control for nonlinear plants," *IEEE Transactions on Automatic Control*, vol. 35, no. 8, pp. 898–907, 1990.

[2] W. J. Rugh, "Analytical framework for gain scheduling," *IEEE Control Systems Magazine*, vol. 11, no. 1, pp. 79–84, 1991.

[3] J. S. Shamma and M. Athans, "Guaranteed properties of gain scheduled control for linear parameter-varying plants," *Automatica*, vol. 27, no. 3, pp. 559–564, 1991.

[4] J. S. Shamma and M. Athans, "Gain scheduling: potential hazards and possible remedies," *IEEE Control Systems Magazine*, vol. 12, no. 3, pp. 101–107, 1992.

[5] P. Apkarian and P. Gahinet, "A convex characterization of gain-scheduled H_∞ controllers," *IEEE Transactions on Automatic Control*, vol. 40, no. 5, pp. 853–864, 1995.

[6] A. Packard, "Gain scheduling via linear fractional transformations," *Systems & Control Letters*, vol. 22, no. 2, pp. 79–92, 1994.

[7] C. W. Scherer, "LPV control and full block multipliers," *Automatica*, vol. 37, no. 3, pp. 361–375, 2001.

[8] G. Scorletti and L. El Ghaoui, "Improved LMI conditions for gain scheduling and related control problems," *International Journal of Robust and Nonlinear Control*, vol. 8, no. 10, pp. 845–877, 1998.

[9] P. Apkarian and R. J. Adams, "Advanced gain-scheduling techniques for uncertain systems," *IEEE Transactions on Control Systems Technology*, vol. 6, no. 1, pp. 21–32, 1998.

[10] P. Apkarian, P. Gahinet, and G. Becker, "Self-scheduled H_∞ control of linear parameter-varying systems: a design example," *Automatica*, vol. 31, no. 9, pp. 1251–1261, 1995.

[11] G. Becker and A. Packard, "Robust performance of linear parametrically varying systems using parametrically-dependent linear feedback," *Systems & Control Letters*, vol. 23, no. 3, pp. 205–215, 1994.

[12] F. Wu, "A generalized LPV system analysis and control synthesis framework," *International Journal of Control*, vol. 74, no. 7, pp. 745–759, 2001.

[13] T. Takagi and M. Sugeno, "Fuzzy identification of systems and its applications to modeling and control," *IEEE Transactions on Systems, Man and Cybernetics*, vol. 15, no. 1, pp. 116–132, 1985.

[14] M. Sugeno and G. T. Kang, "Structure identification of fuzzy model," *Fuzzy Sets and Systems*, vol. 28, no. 1, pp. 15–33, 1988.

[15] S. Kawamoto, K. Tada, A. Ishigame, and T. Taniguchi, "An approach to stability analysis of second order fuzzy systems," in *Proceedings of the IEEE International Conference on Fuzzy Systems*, pp. 1427–1434, March 1992.

[16] J. Kluska, *Analytical Methods in Fuzzy Modeling and Control*, Springer, Berlin, Germany, 2009.

[17] J. Abonyi and R. Babuska, "Local and global identification and interpretation of parameters in Takagi-Sugeno fuzzy models," in *Proceedings of the 9th IEEE International Conference on Fuzzy Systems*, vol. 2, pp. 835–840, May 2000.

[18] M. C. M. Teixeira and S. H. Zak, "Stabilizing controller design for uncertain nonlinear systems using fuzzy models," *IEEE Transactions on Fuzzy Systems*, vol. 7, no. 2, pp. 133–142, 1999.

[19] K. Tanaka and H. O. Wang, *Fuzzy Control Systems Design and Analysis: A Linear Matrix Inequality Approach*, John Wiley & Sons, New York, NY, USA, 2004.

[20] M. Johansson, A. Rantzer, and K. E. Årzén, "Piecewise quadratic stability of fuzzy systems," *IEEE Transactions on Fuzzy Systems*, vol. 7, no. 6, pp. 713–722, 1999.

[21] G. Feng, "Controller synthesis of fuzzy dynamic systems based on piecewise Lyapunov functions," *IEEE Transactions on Fuzzy Systems*, vol. 11, no. 5, pp. 605–612, 2003.

[22] G. Feng, "H_∞ controller design of fuzzy dynamic systems based on piecewise Lyapunov functions," *IEEE Transactions on Systems, Man, and Cybernetics B*, vol. 34, no. 1, pp. 283–292, 2004.

[23] B. S. Chen, C. S. Tseng, and H. J. Uang, "Robustness design of nonlinear dynamic systems via fuzzy linear control," *IEEE Transactions on Fuzzy Systems*, vol. 7, no. 5, pp. 571–585, 1999.

[24] N. S. D. Arrifano and V. A. Oliveira, "Robust H_∞ fuzzy control approach for a class of Markovian jump nonlinear systems," *IEEE Transactions on Fuzzy Systems*, vol. 14, no. 6, pp. 738–754, 2006.

[25] Z. Lin, Y. Lin, and W. Zhang, "H_∞ stabilisation of nonlinear stochastic active fault-tolerant control systems: fuzzy-interpolation approach," *IET Control Theory & Applications*, vol. 4, no. 10, pp. 2003–2017, 2010.

[26] Z. Lin, J. Liu, W. Zhang, and Y. Niu, "Stabilization of interconnected nonlinear stochastic Markovian jump systems via dissipativity approach," *Automatica*, vol. 47, no. 12, pp. 2796–2800, 2011.

[27] E. K. P. Chong and S. H. Zak, *An Introduction to Optimization*, John Wiley & Sons, New Jersey, NJ, USA, 2013.

[28] F. Wu, *Control of linear parameter varying systems [Ph.D. thesis]*, University of California at Berkeley, Berkeley, Calif, USA, 1995.

[29] F. Wu, X. H. Yang, A. Packard, and G. Becker, "Induced L_2-norm control for LPV systems with bounded parameter variation rates," *International Journal of Robust and Nonlinear Control*, vol. 6, no. 9-10, pp. 983–998, 1996.

[30] P. Gahinet, P. Apkarian, and M. Chilali, "Affine parameter-dependent Lyapunov functions and real parametric uncertainty," *IEEE Transactions on Automatic Control*, vol. 41, no. 3, pp. 436–442, 1996.

Hindawi Publishing Corporation
Mathematical Problems in Engineering
Volume 2013, Article ID 190785, 10 pages
http://dx.doi.org/10.1155/2013/190785

Research Article

Coordinated Control for a Group of Interconnected Pairwise Subsystems

Chen Ma and Xue-Bo Chen

School of Electronics and Information Engineering, Liaoning University of Science and Technology, Anshan 114051, China

Correspondence should be addressed to Xue-Bo Chen; xuebochen@126.com

Received 21 June 2013; Accepted 29 August 2013

Academic Editor: Bo Shen

The implementation of pairwise decomposition is discussed on an interconnected system with uncertainties. Under the concept of system inclusion, two systems with the same expanded system achieved by the same expand transformation are considered as approximations. It is proven that a coordinated controller can be found to stabilize both the two systems. This controller is contracted from the coordinated controller of expanded system, with each pairwise subsystem having information structure constraint taken into consideration. At last, this controller design process is applied on a four-area power system treated as a group of subsystems with information structure constraints.

1. Introduction

Complex systems in real world are usually composed of a large group of interconnected subsystems. The interconnections among the subsystems are commonly presented in dynamics, and not only their weight values but also their connections with others keep evolving from time to time. Decentralized control is an ideal control strategy to handle the structural perturbations. Inclusion principle [1–3] is widely used as a general mathematical framework of decomposition, for example, automatic generation control (AGC) for a four-area power system [4–8], formation control of unmanned aerial vehicles [9], and structural vibration control of tall buildings under seismic excitations [10–12].

Particularly, pairwise decomposition provided in [4–8] can take full use of interconnections in the system, by treating each pair of subsystems with information structure constraint as a basic connected unit. Based on the inclusion principle framework, the system will be expanded into a much bigger space in a recurrent reverse order, so that the system is completely decomposed. Then a pairwise coordinated controller for the expanded system will be constructed by achieving coordinated consensus of each pairwise subsystem in parallel. After properly compensated, the controller can be contracted into the original space to fix the original system.

However, to apply pairwise decomposition methodology, an explicitly defined overall system model in particular superposition form is needed, and this condition may not always be satisfied due to system complexity. The work of this paper is to present an implementation approach of pairwise decomposition for interconnected system with state uncertainties. As the basis of system expansion and contraction, adequate knowledge of interconnection structure between pairwise subsystem is necessary, and this is the presumption to apply pairwise decomposition in this paper. For the system whose model is uncertain, the inclusion principle can not achieve its expansion exactly. But under the circumstance that the interconnection structure of system is available, an approximate expanded system can be constructed instead. Motivated by the idea that the whole system could achieve high performance only if each part could be consistent, an expanded system can be constructed, which comprises all pairwise subsystems with information structure constraints of the original system, and this expanded system is treated as an approximate expansion of the origin. According to the inclusion conditions, the expanded system can be contracted to the original space. A contraction dual to the expansion can always be found, so that the contracted system and original system are approximate in state dynamic. In this way, the coordinated controller that can stabilize the contracted

system is also suitable for the original system. Similar to the system level, the coordinated controller of contracted system is also established by contracting from that of expanded system properly. In fact, this contracted controller can be used directly on the original system. As long as the dynamic of original system is adequately included in the expanded system, the contracted controller can be used as a suboptimal controller of the origin. The approximation of this paper mainly represents how good the expanded system would include the original system state. However, it is difficult to describe the approximation without a comparison of control performances. Considering the uncertainties of system state, a static state feedback controller at each subsystem is designed to robustly stabilize the system dynamics. This control design process mainly depends on the decentralized system form; it can suit a group of systems which can only use local information, for example, the multiagent system. Moreover, just the same as the ordinary pairwise decomposition, this process is also able to deal with the information structure constraints variation.

The organization of this paper is as follows. In the next section, preliminaries of permuted inclusion principle and system contraction are provided. The main result is presented in Section 2, where the approximate expansion under the concept of system inclusion is discussed, as well as the controller design procedure. In Section 3, a simulation example is provided to illustrate the proposed method on a group of subsystems with information structure constraints.

2. Preliminaries

The controller design process provided in this paper mainly relies on the permuted inclusion principle [6, 7] and system contraction [7, 13] that are presented in the following.

2.1. Permuted Inclusion Principle. Suppose that system $\overline{\mathbf{S}}$ is a group of interconnected subsystems and each subsystem $\overline{\mathbf{S}}_i$ is connected to every other counterparts. Then system $\overline{\mathbf{S}}$ can be decomposed into the expanded space of $N(N-1)/2$ pairwise subsystems with a pair recurrent reverse order subscripts as follows:

$$\begin{aligned}\overline{\mathbf{S}}_{ij} : {} & \overline{\mathbf{S}}_{12}, \overline{\mathbf{S}}_{23}, \overline{\mathbf{S}}_{13}, \overline{\mathbf{S}}_{34}, \overline{\mathbf{S}}_{24}, \overline{\mathbf{S}}_{14}, \ldots, \\ & \overline{\mathbf{S}}_{(N-1)N}, \overline{\mathbf{S}}_{(N-2)N}, \ldots, \overline{\mathbf{S}}_{2N}, \overline{\mathbf{S}}_{1N}.\end{aligned} \tag{1}$$

Notice that the pairwise subsystems are arranged by a reverse order of subscript j, and this unnatural order enables the last one or some subsystems of the sequence to disconnect from, or connect to on the contrary, the overall system without impact on the remaining orders. It is convenient for representing the system information structure constraints variations.

The expected pairwise subsystems order is established by both row and column permutation matrices, which are composed of a series of basic permutation matrices representing a special case of nonsingular transformations. Assume that I_k is a subidentity matrix corresponding to the subsystem $\overline{\mathbf{S}}_k$, as provided in [6, 7],

$$\begin{aligned} P &= \overleftarrow{\prod}_{i=1}^{N-2} \overleftarrow{\prod}_{j=1}^{N-i-1} \overleftarrow{\prod}_{k=1+i(i-1)}^{N(N-j)-i(j+1)} p_{k(k+1)} \\ P^{-1} &= \overrightarrow{\prod}_{i=1}^{N-2} \overrightarrow{\prod}_{j=1}^{N-i-1} \overrightarrow{\prod}_{k=1+i(i-1)}^{N(N-j)-i(j+1)} p_{k(k+1)}^{T}, \end{aligned} \tag{2}$$

where the signs "$\leftarrow$" and "$\rightarrow$" indicate right and left directional multiplying operations, and

$$\begin{aligned} p_{k(k+1)} &= \operatorname{blockdiag}\left(I_1, \ldots, I_{k-1}, \begin{bmatrix} 0 & I_k \\ I_{k+1} & 0 \end{bmatrix}, I_{k+2}, \ldots, I_{\widetilde{N}}\right), \\ p_{k(k+1)}^{-1} &= p_{k(k+1)}^{T} \\ &= \operatorname{blockdiag}\left(I_1, \ldots, I_{k-1}, \begin{bmatrix} 0 & I_{k+1} \\ I_k & 0 \end{bmatrix}, I_{k+2}, \ldots, I_{\widetilde{N}}\right) \end{aligned} \tag{3}$$

are the basic permutation matrices for the k and $k+1$ groups of adjacent columns and rows, respectively. The $\widetilde{N}$ in (3) indicates the number of subsystems in the expanded system, and here $\widetilde{N} = N(N-1)$. The literature [8] provides an alternative matrix position-based form to construct this permutation matrix P more simply. Use $P(m,n)_b$ to notate the block position in P of subidentity matrices I_i and I_j corresponding to pairwise subsystem $\overline{\mathbf{S}}_{ij}$ in P; then it comes

$$\begin{aligned} P\left((Ni - j + 1), \left[j(j-1) - 2(i-1) - 1\right]\right)_b &= I_i, \\ P\left(\left[N(j-1) - i + 1\right], \left[j(j-1) - 2(i-1)\right]\right)_b &= I_j, \\ i, j = 1, 2, \ldots, k, \ldots, N, \quad i \neq j. \end{aligned} \tag{4}$$

Example 1. Consider an expansion for system $\overline{\mathbf{S}}$ with full network structure and $N = 3$; its pairwise subsystems can be ordered as

$$\overline{\mathbf{S}}_{ij} : \overline{\mathbf{S}}_{12}, \overline{\mathbf{S}}_{23}, \overline{\mathbf{S}}_{13}. \tag{5}$$

According to (4), the block positions of I_i and I_j to $\overline{\mathbf{S}}_{ij}$ can be obtained as

$$\begin{aligned} \overline{\mathbf{S}}_{12} &: P(2,1)_b = I_1, \qquad P(3,2)_b = I_2, \\ \overline{\mathbf{S}}_{23} &: P(4,3)_b = I_2, \qquad P(5,4)_b = I_3, \\ \overline{\mathbf{S}}_{13} &: P(1,5)_b = I_1, \qquad P(6,6)_b = I_3. \end{aligned} \tag{6}$$

that is to say

$$P = \begin{bmatrix} 0 & 0 & 0 & 0 & I_1 & 0 \\ I_1 & 0 & 0 & 0 & 0 & 0 \\ 0 & I_2 & 0 & 0 & 0 & 0 \\ 0 & 0 & I_2 & 0 & 0 & 0 \\ 0 & 0 & 0 & I_3 & 0 & 0 \\ 0 & 0 & 0 & 0 & 0 & I_3 \end{bmatrix}. \tag{7}$$

It is equivalent to the result of (2) when $N = 3$.

Consider an interconnected system $\overline{\mathbf{S}}$ in compacted form and its expanded system $\widetilde{\mathbf{S}}_P$ as follows:

$$\begin{aligned} \overline{\mathbf{S}} &: \dot{\overline{x}} = \overline{A}\overline{x} + \overline{B}\overline{u}, \qquad \overline{y} = \overline{C}\overline{x}, \\ \widetilde{\mathbf{S}}_P &: \dot{\widetilde{x}}_P = \widetilde{A}_P\widetilde{x}_P + \widetilde{B}_P\widetilde{u}_P, \qquad \widetilde{y}_P = \widetilde{C}_P\widetilde{x}_P, \end{aligned} \tag{8}$$

where $\overline{x}(t) \in \mathbf{R}^{\overline{n}}$, $\overline{u}(t) \in \mathbf{R}^{\overline{m}}$, and $\overline{y}(t) \in \mathbf{R}^{\overline{l}}$ are the state, input, and output vectors of the system $\overline{\mathbf{S}}$; $\widetilde{x}_P(t) \in \mathbf{R}^{\widetilde{n}}$, $\widetilde{u}_P(t) \in \mathbf{R}^{\widetilde{m}}$, and $\widetilde{y}_P(t) \in \mathbf{R}^{\widetilde{l}}$ are those of system $\widetilde{\mathbf{S}}_P$. It is supposed that $\overline{n} \le \widetilde{n}$, $\overline{m} \le \widetilde{m}$, and $\overline{l} \le \widetilde{l}$.

For the input-state-output inclusion principle mentioned in [14, 15], a definition of the permuted inclusion principle is given.

Definition 2. The system $\widetilde{\mathbf{S}}_P$ includes the system $\overline{\mathbf{S}}$, or $\widetilde{\mathbf{S}}_P \supset \overline{\mathbf{S}}$, if there exists a quadruplet of full rank matrices $\{V_P, U_P, Q_P, S_P\}$ satisfying $U_P V_P = I_n$, such that for any $\overline{x}_0 \in \mathbf{R}^{\overline{n}}$ and any $\overline{u} \in \mathbf{R}^{\overline{m}}$, the conditions $\widetilde{x}_{P0} = V_P\overline{x}_0$ and $\overline{u} = Q_P\widetilde{u}_P$ imply $\overline{x}(t; t_0, \overline{x}_0, \overline{u}) = U_P\widetilde{x}_P(t; t_0, \widetilde{x}_{P0}, \widetilde{u}_P)$ and $\overline{y}[\overline{x}(t)] = S_P\widetilde{y}_P[\widetilde{x}_P(t)]$ for all $t \ge t_0$.

Call the system $\overline{\mathbf{S}}$ a contraction of system $\widetilde{\mathbf{S}}_P$. It is supported by the inclusion principle that all information about the behavior of $\overline{\mathbf{S}}$ is included in $\widetilde{\mathbf{S}}_P$, such as stability and optimality. One of the necessary and sufficient conditions for the inclusion is restriction, the following theorem considers the restriction type (d) ([2, 3, 7]).

Theorem 3. *The system $\overline{\mathbf{S}}$ is a typical restriction of the system $\widetilde{\mathbf{S}}_P$, if there is a triplet of full rank matrices $\{V_P, Q_P, S_P\}$ such that*

$$V_P\overline{A} = \widetilde{A}_P V_P, \qquad V_P\overline{B}Q_P = \widetilde{B}_P, \qquad \overline{C} = S_P\widetilde{C}_P V_P. \tag{9}$$

Proof. The proof follows directly from the results in [6, 7, 14, 15].

The systems $\overline{\mathbf{S}}$ and $\widetilde{\mathbf{S}}_P$ are related by

$$\begin{aligned} \widetilde{A}_P &= V_P\overline{A}U_P + M_A^P, \widetilde{B}_P = V_P\overline{B}Q_P + M_B^P, \\ \widetilde{C}_P &= T_P\overline{C}U_P + M_C^P, \end{aligned} \tag{10}$$

where M_A^P, M_B^P, and M_C^P are complementary matrices with proper dimensions. See [6, 7] for details. □

2.2. System Contraction. One of the difficulties in applying system contraction by inclusion principle is that the conditions may be too restrictive, and a complete contraction from the given expanded system $\widetilde{\mathbf{S}}_P$ to system $\overline{\mathbf{S}}$ will not always exist. It is indicated by the restriction conditions of (9) that system $\widetilde{\mathbf{S}}_P$ completely includes $\overline{\mathbf{S}}$ if and only if it is uncontrollable. A natural way to resolve this problem is to introduce an incomplete contraction as an approximation. Split the permuted state matrix $\widetilde{A}_P$ into two parts as

$$\widetilde{A}_P = \widetilde{A}_{RP} + \widetilde{M}_{AP}, \tag{11}$$

where $\widetilde{A}_{RP}$ is the part that can be contracted as (8) implies, $\widetilde{M}_{AP}$ is a complementary matrix with proper dimension standing for the remnant after contraction from the expanded space. System $\overline{\mathbf{S}}$ is a reduced-order model of system $\widetilde{\mathbf{S}}_P$, according to the restriction conditions in (9) and (10), and take the state matrix for example, this incomplete system contraction requires that

$$V_P\overline{A} = \left(\widetilde{A}_P - \widetilde{M}_{AP}\right)V_P. \tag{12}$$

There are arbitrary choices of the expanding transformation matrix V_P. Since this paper is based on the pairwise decomposition methodology, V_P is chosen as the same form of that in [6, 7], which will be presented in next section. Anyway, when V_P is confirmed according to the inclusion condition, here goes

$$\widetilde{M}_{AP}V_P = \widetilde{A}_P V_P - V_P\overline{A}. \tag{13}$$

To satisfy the restriction condition, there must be

$$\overline{A} = \left(V_P^T V_P\right)^{-1} V_P^T \widetilde{A}_P V_P \tag{14}$$

so that $\|\widetilde{M}_{AP}V_P\|$ will be minimum, and this results in the minimal norm solution

$$\widetilde{M}_{AP} = \left[I - V_P\left(V_P^T V_P\right)^{-1}V_P^T\right]\widetilde{A}_P V_P\left(V_P^T V_P\right)^{-1}V_P^T. \tag{15}$$

3. Pairwise Decomposition for a Group of Interconnected Subsystems

Assume that system $\mathbf{S}$ is composed of a group of interconnected subsystems as the coordinated control target,

$$\begin{aligned} \mathbf{S} = \{\mathbf{S}_i\} &: \dot{x} = Ax + Bu, \qquad y = Cx, \\ \mathbf{S}_i &: \dot{x}_i = A_{ii}x_i + B_{ii}u_i \\ &\quad + \sum_{\substack{j=1 \\ j\ne i}}^{N} e_{ij}(t)\, A_{ij}x_j, \qquad y_i = C_{ii}x_i, \\ &\qquad\qquad i = 1, 2, \ldots, N, \end{aligned} \tag{16}$$

where $x_i(t) \in \mathbf{R}^{n_i}$, $u_i(t) \in \mathbf{R}^{m_i}$, and $y_i(t) \in \mathbf{R}^{l_i}$ are the state, input, and output vectors of $\mathbf{S}_i$ at time $t \in \mathbf{R}$ system matrices A, B, and C are compacted forms of A_{ij}, B_{ii}, and C_{ii} in proper dimensions, respectively. Notations $x_i(t; t_0, x_{i0}, u_i)$ and $y_i[x_i(t)]$ denote unique solutions of $\mathbf{S}_i$ for the initial time t_0, the initial state vector x_{i0}, and a fixed control input u_i, $e_{ij}(t)$ is element of the interconnection matrix $E = (e_{ij}) \in \mathbf{R}^{N\times N}$. Under the concept of pairwise decomposition, if at least one of interconnections $e_{ij}(t) \ne 0$ or $e_{ji}(t) \ne 0$, then it appears that subsystems $\mathbf{S}_i$ and $\mathbf{S}_j$ are connected. Call

$$\mathbf{S}_{ij} : \begin{cases} \dot{x}_i = A_{ii}x_i + e_{ij}(t)\, A_{ij}x_j + B_{ii}u_i, & y_i = C_{ii}x_i \\ \dot{x}_j = A_{jj}x_j + e_{ji}(t)\, A_{ji}x_i + B_{jj}u_j, & y_j = C_{jj}x_j \\ & i, j = 1, 2, \ldots, N, \\ & i \ne j \end{cases} \tag{17}$$

a pairwise subsystem with basic interconnection.

The time-varying parameters $e_{ij}(t)$ and $e_{ji}(t)$ in (17) can describe the dynamic weight values between the connected subsystems $\mathbf{S}_i$ and $\mathbf{S}_j$. They represent the information structure constraints of the interconnected system and play a very important role in the system dynamic. In the literature [16], a fundamental interconnection (adjacency) matrix $\overline{E} = (\overline{e}_{ij}) \in \mathbf{R}^{N\times N}$ is defined in order to describe the normal structure of a given system graph. This notation can also be used here to indicate whether there is information structure constraint between a subsystem pair, by the rule

$$\overline{e}_{ij} = \begin{cases} 1, & e_{ij}(t) \neq 0 \\ & \overline{e}_{ii} = 0. \\ 0, & e_{ij}(t) = 0, \end{cases} \tag{18}$$

When $\overline{e}_{ij} = 1$, it indicates that there is interconnection from subsystem $\mathbf{S}_i$ to $\mathbf{S}_j$, and $\overline{e}_{ij} = 0$ indicates not. This binary interconnection matrix $\overline{E}$ will be used later in the inclusion principle framework. If one of $\overline{e}_{ij}$ and $\overline{e}_{ji}$ is equal to 0, the pairwise subsystem $\mathbf{S}_{ij}$ is half connected; the original information structures of $\mathbf{S}_{ij}$ would be changed by using the coordinated control mentioned earlier. In this case, the sequential LQ optimization provided in [3, 17] can be consulted to keep the information structure of $\mathbf{S}_{ij}$. Moreover, note that $\overline{e}_{ij}$ and $\overline{e}_{ji}$ will both be valued 0 under some circumstances, which means that the pairwise subsystem $\mathbf{S}_{ij}$ will be disjointed. The disconnected modes have been discussed in [6, 7]. Particularly, when $\overline{e}_{ij}$ and $\overline{e}_{ji}$ evolute in a dynamical way and enforce $\mathbf{S}_{ij}$ to disjoint and then joint again, the discussion is provided in [8].

Theoretically, any existing control technique can be applied to the coordinated control of this pairwise subsystem $\mathbf{S}_{ij}$. Take pairwise subsystem $\mathbf{S}_{ij}$ as this compact form

$$\mathbf{S}_{ij} : \dot{x}_{ij} = A_{Dij}x_{ij} + B_{Dij}u_{ij}, \qquad y_{ij} = C_{Dij}x_{ij}, \tag{19}$$

with $x_{ij} = [x_i, x_j]^T$, $u_{ij} = [u_i, u_j]^T$, and $y_{ij} = [y_i, y_j]^T$, and

$$A_{Dij} = \begin{bmatrix} A_{ii} & e_{ij}(t)A_{ij} \\ e_{ji}(t)A_{ji} & A_{jj} \end{bmatrix},$$

$$B_{Dij} = \begin{bmatrix} B_{ii} & 0 \\ 0 & B_{jj} \end{bmatrix}, \tag{20}$$

$$C_{Dij} = \begin{bmatrix} C_{ii} & 0 \\ 0 & C_{jj} \end{bmatrix}.$$

Call

$$\mathbf{C}_{ij} : u_{ij} = -K_{Dij}x_{ij} \tag{21}$$

the basic coordinated controller, if it can stabilize the closed loop pairwise subsystem

$$\mathbf{S}_{ij}^{C} : \dot{x}_{ij} = \left(A_{Dij} - B_{Dij}K_{Dij}\right)x_{ij}, \qquad y_{ij} = C_{Dij}x_{ij}. \tag{22}$$

For every pair of subsystems $\mathbf{S}_{ij}$ with information structure constraints $i = j - k$, $j = 2, 3, \ldots, N$, $k = 1, 2, \ldots, j-1$, their basic coordinated controllers can be constructed in this way.

As the fundamental idea of pairwise decomposition, a given system should be expanded following the recurrent reverse order first, so that a coordinated controller can be designed to stabilize all of the pairwise subsystems and then contracted to the original space. However, restricted by the mathematical framework of inclusion principle, it is difficult to expand the system with uncertainties in its dynamics. Consider the procedure of pairwise decomposition, the original states can be almost included in the block-diagonal expanded system which is composed of state functions of all pairwise subsystems,

$$\begin{aligned} \widetilde{\mathbf{S}}_{PD} = \{&\mathbf{S}_{12}, \mathbf{S}_{23}, \mathbf{S}_{13}, \mathbf{S}_{34}, \mathbf{S}_{24}, \mathbf{S}_{14}, \ldots, \mathbf{S}_{2N}, \mathbf{S}_{1N}\} : \\ &\dot{\widetilde{x}}_P = \widetilde{A}_{PD}\widetilde{x}_P + \widetilde{B}_{PD}\widetilde{u}_P, \qquad \widetilde{y}_P = \widetilde{C}_{PD}\widetilde{x}_P, \\ &\widetilde{A}_{PD} = \text{blockdiag}\left(A_{Dij}\right), \\ &\widetilde{B}_{PD} = \text{blockdiag}\left(B_{Dij}\right), \\ &\widetilde{C}_{PD} = \text{blockdiag}\left(C_{Dij}\right). \end{aligned} \tag{23}$$

This block-diagonal system is a reasonable approximate expansion of the origin. To achieve this form, the interconnection structure of system $\mathbf{S}$ should be available, and this is also the restriction in using inclusion principle. The interconnection structure is supposed to be given by the fundamental interconnection matrix $\overline{E} = (\overline{e}_{ij})$. By expanding the original space of system $\mathbf{S}$ into a bigger space of system $\widetilde{\mathbf{S}}_{PD}$ in recurrent reverse order, take the state matrix as an example, the transformation matrices of pairwise decomposition can be selected as

$$\begin{aligned} V = \text{blockdiag}&\left(\frac{\sum_{k=1}^{N}\overline{e}_{1k}}{\overbrace{I_{n_1}\ I_{n_1}\cdots I_{n_1}}}, \ldots, \frac{\sum_{k=1}^{N}\overline{e}_{Nk}}{\overbrace{I_{n_N}\ I_{n_N}\cdots I_{n_N}}}\right)^T, \\ U = \text{blockdiag}&\left(\frac{1}{\sum_{k=1}^{N}\overline{e}_{1k}}\left[\frac{\sum_{k=1}^{N}\overline{e}_{1k}}{\overbrace{I_{n_1}\cdots I_{n_1}}}\right], \ldots, \right. \\ &\left. \frac{1}{\sum_{k=1}^{N}\overline{e}_{Nk}}\left[\frac{\sum_{k=1}^{N}\overline{e}_{Nk}}{\overbrace{I_{n_N}\cdots I_{n_N}}}\right]\right), \end{aligned} \tag{24}$$

R, Q, T, and S have the same structure as their counterparts, respectively. Notice that there are arbitrary choices of these transformation matrices, and their forms are bound up with the inclusion form. Since the structure of expanded system $\widetilde{\mathbf{S}}_{PD}$ is confirmed, then the transformation matrices are also fixed, just as (24).

Consider the permuted inclusion principle; the transformation matrices will be permuted as

$$\begin{aligned} V_P &= P_A^{-1}V, \qquad U_P = UP_A, \\ R_P &= P_B^{-1}R, \qquad Q_P = QP_B, \\ T_P &= P_C^{-1}T, \qquad S_P = SP_C. \end{aligned} \tag{25}$$

Therefore the state matrices of systems $\mathbf{S}$ and $\widetilde{\mathbf{S}}_{PD}$ are related by (12), and the relationship of the state, input, and output vectors can be obtained by Definition 2 as

$$x = U_P \tilde{x}_P, \qquad u = Q_P \tilde{u}_P, \qquad y = S_P \tilde{y}_P. \tag{26}$$

At the same time, a virtual system $\overline{\mathbf{S}}$ can be constructed as another contraction of system $\widetilde{\mathbf{S}}_{PD}$. The state dynamic of system $\overline{\mathbf{S}}$ is in a certain form, and $\overline{\mathbf{S}}$ is raised as an estimation of the original system $\mathbf{S}$. According to the contraction condition, it is possible to use the transformation matrix V_P such that system $\widetilde{\mathbf{S}}_{PD}$ can be contracted to $\overline{\mathbf{S}}$ by (12) after an appropriate compensation. This process will also lead to the same relationship as (26). In this way, systems $\mathbf{S}$ and $\overline{\mathbf{S}}$ may share the same state, input, and output vectors, since they have the same expanded system $\widetilde{\mathbf{S}}_{PD}$ which is calculated by the same transformation matrices. It can be concluded that systems $\mathbf{S}$ and $\overline{\mathbf{S}}$ represent a pair of systems with approximate dynamics, and the bias between them is mainly reflected in compensation $\widetilde{M}_{AP}$ of the contraction procedure.

Suppose that the expanded system $\widetilde{\mathbf{S}}_{PD}$ comprises every state function of pairwise subsystem $\mathbf{S}_{ij}$ in system $\mathbf{S}$, and the pairwise subsystems are arranged in the recurrent reverse order as (23). Each $\mathbf{S}_{ij}$ is stabilized by the basic coordinated controller (21); then the coordinated controller for $\widetilde{\mathbf{S}}_{PD}$ can be constructed in a block-diagonal form as

$$\widetilde{\mathbf{C}}_{PD} = \left(\mathbf{C}_{ij}\right) : \tilde{u}_P = -\widetilde{K}_D \tilde{x}_P = -\text{blockdiag}\left(K_{Dij}\right) \tilde{x}_P. \tag{27}$$

It is clear that a redundant control set is established with all pairwise controllers, which contains all necessary coordinated information K_{Dij} for both system $\mathbf{S}$ and $\overline{\mathbf{S}}$. When the structure form of the estimator $\overline{\mathbf{S}}$ is determined, the coordinated controller of system $\mathbf{S}$ can be obtained by contracting $\widetilde{K}_D$ together with a proper compensator $\widetilde{M}_{KP}$. The contraction is checked by the following theorem.

Theorem 4. *For the systems mentioned above, system $\widetilde{\mathbf{S}}_{PD}$ is the expansion for both systems $\mathbf{S}$ and $\overline{\mathbf{S}}$. The state feedback controller $C : u = -Kx$ can stabilize the closed loop system of $\mathbf{S}$, if the controller $\overline{C}$ of system $\overline{\mathbf{S}}$ can be contracted from $\widetilde{C}_P$, and it satisfies*

$$K = \overline{K} = Q_P \left(\widetilde{K}_D + \widetilde{M}_{KP}\right) V_P. \tag{28}$$

Proof. Since system $\overline{\mathbf{S}}$ is a contraction system $\widetilde{\mathbf{S}}_{PD}$, supported by the contraction condition (12), the state function of system $\widetilde{\mathbf{S}}_{PD}$ is rewritten as

$$\dot{\tilde{x}}_P = \left(\widetilde{A}_{PD} - \widetilde{M}_{AP}\right) \tilde{x}_P + \widetilde{B}_{PD} \tilde{u}_P, \tag{29}$$

and it apparently indicates the controller form of (5). According to the inclusion principle, here goes

$$x = U_P \tilde{x}_P, \qquad u = Q_P \tilde{u}_P. \tag{30}$$

moreover, the approximation between systems $\mathbf{S}$ and $\overline{\mathbf{S}}$ may indicate that $x = \overline{x}$ and $u = \overline{u}$, so that the controllers of systems $\mathbf{S}$ and $\widetilde{\mathbf{S}}_{PD}$ are related as

$$u = -Kx, \qquad \tilde{u}_P = -\left(\widetilde{K}_D + \widetilde{M}_{KP}\right) \tilde{x}_P. \tag{31}$$

Notice that $U_P V_P = I_n$, then (30) and (31) will conclude that $K = Q_P(\widetilde{K}_D + \widetilde{M}_{KP})V_P$. □

Remark 5. The literature [6] provides a sufficient condition of connective stability. But since far more information might be accumulated in the largest singular values of subsystem matrices, the criterion of connective stability might be somewhat conservative.

The virtual system $\overline{\mathbf{S}}$ is used as the estimator of system $\mathbf{S}$, and it may have many possible forms. This diversity will mainly impact on the controller design process in determining the compensator $\widetilde{M}_{KP}$. One of the most challenging problems in controller design for multiagent systems is the estimation of information structures among agents. The further research of this paper on implementation of pairwise decomposition in systems with dynamic information structure constraints, as well as the estimation of the interconnection structure, is undergoing. This issue is based on inclusion principle for time-varying system ([18]) and method in dealing with the structure perturbation under the concept of pairwise decomposition ([8]). However, in a particular case when the state function of each subsystem satisfies the linear superposition principle, there is a way to determine the structure of $\widetilde{M}_{KP}$ much more easily.

Consider the mathematical framework of permuted inclusion principle; this position information can be concluded with (8) by using the block row-order of sub-identity matrices. Consider that system $\mathbf{S}$ is in full network structure, the row-order of a particular pairwise subsystem $\mathbf{S}_{ij}$ is

$$c_i = j\left(j-1\right) - 2\left(i-1\right) - 1, \qquad c_j = j\left(j-1\right) - 2\left(i-1\right). \tag{32}$$

Besides, the row-order of every pairwise subsystem can also be concluded in this way as

$$c_{ik_i} = \begin{cases} k_i\left(k_i-1\right) - 2\left(i-1\right) - 1, & i < k_i \\ i\left(i-1\right) - 2\left(k_i-1\right), & i > k_i \end{cases}$$

$$c_{jk_j} = \begin{cases} k_j\left(k_j-1\right) - 2\left(j-1\right) - 1, & j < k_j \\ j\left(j-1\right) - 2\left(k_j-1\right), & j > k_j \end{cases}$$

$$i, j = 1, 2, \ldots, N, \quad k_i, k_j = 1, 2, \ldots, N, \quad i \neq j, \quad k_i, k_j \neq i, j. \tag{33}$$

so that the complementary matrix $\widetilde{M}_{KP}$ can be constructed by the following lemma.

Lemma 6. *Suppose that system $\mathbf{S}$ is in full network structure; the row-order of subsystems in each pairwise subsystem is concluded as* (32) *and* (33)*, and $\widetilde{M}_{KP}$ complements the information structure constraints bias between system $\mathbf{S}$ and system*

$\overline{\mathbf{S}}$. *Then* $\widetilde{M}_{KP}$ *can be presented by the information structure of corresponding pairwise subsystem* $\mathbf{S}_{ij}$ *as*

$$\widetilde{M}_{KP}\left(c_{ik_i}, c_j\right)_b = K_{ij}, \qquad \widetilde{M}_{KP}\left(c_{jk_j}, c_i\right)_b = K_{ji}$$
$$i, j = 1, 2, \ldots, N, \quad k_i, k_j = 1, 2, \ldots, N, \quad i \neq j, \quad k_i, k_j \neq i, j. \tag{34}$$

This matrix structure-based lemma is convenient for calculation, especially for real-time control in practice.

Example 7. Also consider system $\mathbf{S}$ with $N = 3$ subsystems, and its recurrent reverse order is presented as (5). According to (32) and (33), the calculation is proceeded as

$$\begin{aligned}
&\mathbf{S}_{12} : c_i = 1, \quad c_j = 2,\\
&\quad k_i = k_j = 3, \quad c_{ik_i} = 5, \quad c_{jk_j} = 3,\\
&\Longrightarrow \widetilde{M}_{KP}(5,2)_b = K_{12}, \quad \widetilde{M}_{KP}(3,1)_b = K_{21}\\
&\mathbf{S}_{23} : c_i = 3, \quad c_j = 4,\\
&\quad k_i = k_j = 1, \quad c_{ik_i} = 2, \quad c_{jk_j} = 6,\\
&\Longrightarrow \widetilde{M}_{KP}(2,4)_b = K_{23}, \quad \widetilde{M}_{KP}(6,3)_b = K_{32}\\
&\mathbf{S}_{13} : c_i = 5, \quad c_j = 6,\\
&\quad k_i = k_j = 2, \quad c_{ik_i} = 1, \quad c_{jk_j} = 4,\\
&\Longrightarrow \widetilde{M}_{KP}(1,6)_b = K_{13}, \quad \widetilde{M}_{KP}(4,5)_b = K_{31}.
\end{aligned} \tag{35}$$

So that the matrix $\widetilde{M}_{KP}$ can be constructed by Lemma 6:

$$\widetilde{M}_{KP} = \begin{bmatrix} 0 & 0 & 0 & 0 & 0 & K_{13} \\ 0 & 0 & 0 & K_{23} & 0 & 0 \\ K_{21} & 0 & 0 & 0 & 0 & 0 \\ 0 & 0 & 0 & 0 & K_{31} & 0 \\ 0 & K_{12} & 0 & 0 & 0 & 0 \\ 0 & 0 & K_{32} & 0 & 0 & 0 \end{bmatrix}. \tag{36}$$

4. Automatic Generation Control (AGC) for a Four-Area Power System

A four-area power system is shown in Figure 1; assume that areas 1, 2, and 3 contain three reheat turbine type thermal units and area 4 contains a hydro unit, respectively. Each pairwise subsystem is interconnected by tie line indicated by solid lines, and its information structure constraint is indicated by dotted ellipse. Details of the system description can be found in [19, 20]. References [4–8] implement the pairwise decomposition methodology in the procedure of coordinated control to this four-area power system AGC. As a counterpart, the controller design procedure of the new pairwise decomposition modality in this paper is presented here. Consider the system dynamic bias between system $\mathbf{S}$ and system $\overline{\mathbf{S}}$ taken as approximation; each pairwise subsystem is robustly stabilized in terms of linear matrix inequalities (LMI) ([21, 22]).

Suppose that the system graph is undirected and $e_{ij}(t) = e_{ji}(t) = 1$ for description convenience. The pairwise subsystem model is provided in (17) as

$$\begin{aligned}
\mathbf{S}_{ij} : \begin{bmatrix} \dot{x}_i \\ \dot{x}_j \end{bmatrix} &= \begin{bmatrix} A_{ii} & A_{ij} \\ A_{ji} & A_{jj} \end{bmatrix} \left(\begin{bmatrix} x_i \\ x_j \end{bmatrix} + \begin{bmatrix} w_i \\ w_j \end{bmatrix} \right)\\
&\quad + \begin{bmatrix} B_{ii} & 0 \\ 0 & B_{jj} \end{bmatrix} \begin{bmatrix} u_i \\ u_j \end{bmatrix} + \begin{bmatrix} G_{ii} & 0 \\ 0 & G_{jj} \end{bmatrix} \begin{bmatrix} \xi_i \\ \xi_j \end{bmatrix},\\
\begin{bmatrix} y_i \\ y_j \end{bmatrix} &= \begin{bmatrix} C_{ii} & 0 \\ 0 & C_{jj} \end{bmatrix} \begin{bmatrix} x_i \\ x_j \end{bmatrix}\\
i, j &= 1, 2, \ldots, N, \quad i \neq j,
\end{aligned} \tag{37}$$

where $x_{ij} = [x_i^T, x_j^T]^T$, $u_{ij} = [u_i^T, u_j^T]^T$, $\xi_{ij} = [\xi_i^T, \xi_j^T]^T$, and $y_{ij} = [y_i^T, y_j^T]^T$ are the state, control input, disturbance, and output vectors, respectively. $w_{ij} = [w_i^T, w_j^T]^T$ is the unmodeled or uncertain state dynamic. $A_{Dij} = (A_{ij})$, $B_{Dij} = (B_{ii})$, $G_{Dij} = (G_{ii})$, and $C_{Dij} = (C_{ii})$ are system matrices with proper dimensions, respectively. The numerical values of the system matrices are given by

$$A_{11} = \begin{bmatrix} -0.05 & 6 & 0 & 0 & 0 & -6 \\ 0 & -0.1 & -1.01 & 1.11 & 0 & 0 \\ 0 & 0 & -3.33 & 3.33 & 0 & 0 \\ -2.08 & 0 & 0 & -5 & 5 & 0 \\ -0.255 & 0 & 0 & 0 & 0 & -0.06 \\ 1.33 & 0 & 0 & 0 & 0 & 0 \end{bmatrix},$$

$$A_{12} = \begin{bmatrix} 0_{5\times1} & 0_{5\times5} \\ -0.444 & 0_{1\times5} \end{bmatrix}, \qquad A_{13} = \begin{bmatrix} 0_{4\times1} & 0_{4\times4} & 0_{4\times1} \\ 0 & 0_{1\times4} & 0.06 \\ -0.444 & 0_{1\times4} & 0 \end{bmatrix},$$

$$A_{14} = A_{21} = A_{32} = A_{13}, \quad A_{23} = A_{31} = A_{41} = A_{12},$$

$$A_{44} = \begin{bmatrix} -0.0769 & 6.15 & 0 & 0 & 0 & -6.15 \\ 8.78 \times 10^{-4} & -2 & 2.2 & -0.198 & 2.11 \times 10^{-3} & 0 \\ -4.39 \times 10^{-4} & 0 & -0.1 & 0.0989 & 1.05 \times 10^{-3} & 0 \\ -8.56 \times 10^{-3} & 0 & 0 & -0.0205 & 0.0205 & 0 \\ -0.0255 & 0 & 0 & 0 & 0 & -0.06 \\ 0.444 & 0 & 0 & 0 & 0 & 0 \end{bmatrix},$$

$$B_{11} = B_{22} = B_{33} = \begin{bmatrix} 0 & 0 & 0 & 5 & 0 & 0 \end{bmatrix}^T,$$

$$B_{44} = \begin{bmatrix} 0 & 0 & 0 & 0.0205 & 0 & 0 \end{bmatrix}^T,$$

$$G_{11} = G_{22} = G_{33} = \begin{bmatrix} -6 & 0 & 0 & 0 & 0 & 0 \end{bmatrix}^T,$$

$$G_{44} = \begin{bmatrix} -6.15 & 0 & 0 & 0 & 0 & 0 \end{bmatrix}^T,$$

$$C_{11} = C_{22} = C_{33} = C_{44} = I_6. \tag{38}$$

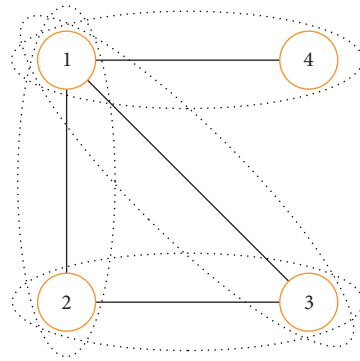

Figure 1: Schematic diagram of the four-area power system.

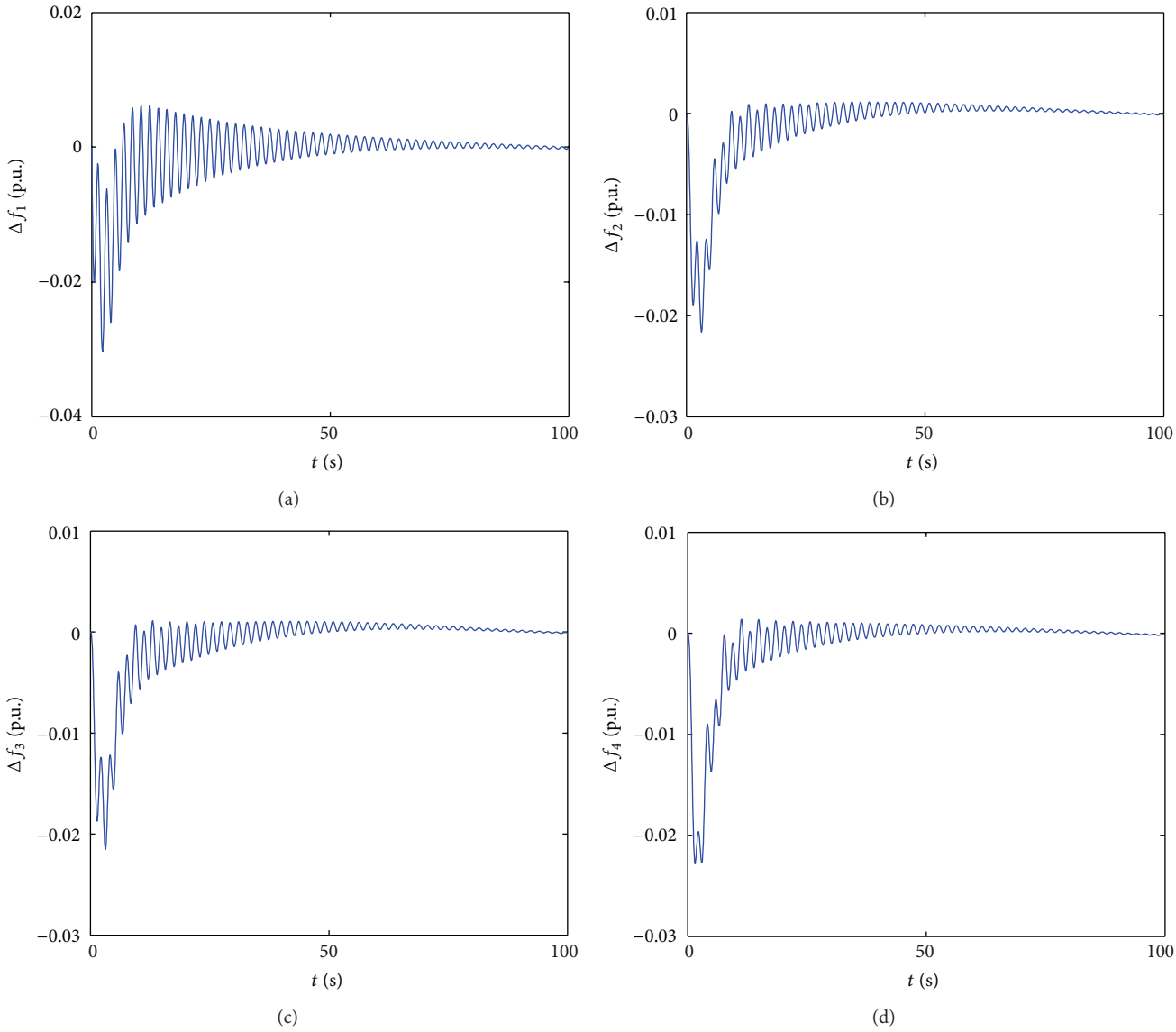

Figure 2: Deviations of frequency among the power system.

A_{22} and A_{33} are the same as A_{11} except that $A_{22}(6,1) = A_{33}(6,1) = 0.888$, respectively.

The quadratic constraints are imposed on the state uncertainty w_{ij} as follows:

$$w_{ij}^T w_{ij} \le \alpha_{ij}^2 x_{ij}^T W_{ij}^T W_{ij} x_{ij}, \tag{39}$$

where α_{ij} is a positive number to be maximized and W_{ij} is a full rank constant matrix; it can be set as an identity matrix in case that the information of uncertainty is unavailable. Pairwise subsystem (37) is robustly stabilizable with arbitrarily large basic coordinated controller degree α by the basic coordinated controller (21), a LMI problem that can be obtained as

$$\begin{aligned} &\text{minimize} \quad \gamma_{ij} \\ &\text{subject to} \quad Y_{ij} > 0 \\ &\begin{bmatrix} A_{Dij}Y_{ij} + Y_{ij}A_{Dij}^T + B_{Dij}L_{ij} + L_{ij}^T B_{Dij}^T & A_{Dij} & Y_{ij}W_{ij}^T \\ A_{Dij}^T & -I & 0 \\ W_{ij}^T Y_{ij} & 0 & -\gamma_{ij} I \end{bmatrix} \\ &< 0, \end{aligned} \tag{40}$$

where $L_{ij} = K_{Dij}Y_{ij}$ and $\gamma_{ij} = 1/\alpha_{ij}^2$. Further details of this robust control procedure can be found in [21, 22].

According to the permuted inclusion principle, the expanded system $\widetilde{\mathbf{S}}_P$ is supposed to contain those particular pairwise subsystems listed as following:

$$\widetilde{\mathbf{S}}_P = \{\mathbf{S}_{12}, \mathbf{S}_{23}, \mathbf{S}_{13}, \mathbf{S}_{14}\}. \tag{41}$$

Then compose the coordinated controller of system $\widetilde{\mathbf{S}}_P$ by arranging the basic coordinated controllers of pairwise subsystems $\mathbf{S}_{12}$, $\mathbf{S}_{23}$, $\mathbf{S}_{13}$, and $\mathbf{S}_{14}$ in this exact recurrent reverse order,

$$\begin{aligned} \widetilde{K}_D &= \text{blockdiag}\left(K_{D12}, K_{D23}, K_{D13}, K_{D14}\right) \\ &= \text{blockdiag}\left(\begin{bmatrix} K_{11} & K_{12} \\ K_{21} & K_{22} \end{bmatrix}, \begin{bmatrix} K_{22} & K_{23} \\ K_{32} & K_{33} \end{bmatrix}, \right. \\ &\qquad \left. \begin{bmatrix} K_{11} & K_{13} \\ K_{31} & K_{33} \end{bmatrix}, \begin{bmatrix} K_{11} & K_{14} \\ K_{41} & K_{44} \end{bmatrix}\right). \end{aligned} \tag{42}$$

Choose the transformation matrices by (24)

$$\begin{aligned} V &= \text{blockdiag}\left(\begin{bmatrix} I_1^A & I_1^A & I_1^A \end{bmatrix}^T, \begin{bmatrix} I_2^A & I_2^A \end{bmatrix}^T, \begin{bmatrix} I_3^A & I_3^A \end{bmatrix}^T, I_4^A\right) \\ Q &= \text{blockdiag}\left(\frac{1}{3}\begin{bmatrix} I_1^B & I_1^B & I_1^B \end{bmatrix}, \frac{1}{2}\begin{bmatrix} I_2^B & I_2^B \end{bmatrix}, \frac{1}{2}\begin{bmatrix} I_3^B & I_3^B \end{bmatrix}, I_4^B\right), \end{aligned} \tag{43}$$

and the permutation matrix P_A can be constructed by (2); P_B is in the same structure as P_A,

$$P_A = \begin{bmatrix} 0 & 0 & 0 & 0 & 0 & 0 & I_1^A & 0 \\ 0 & 0 & 0 & 0 & I_1^A & 0 & 0 & 0 \\ I_1^A & 0 & 0 & 0 & 0 & 0 & 0 & 0 \\ 0 & I_2^A & 0 & 0 & 0 & 0 & 0 & 0 \\ 0 & 0 & I_2^A & 0 & 0 & 0 & 0 & 0 \\ 0 & 0 & 0 & I_3^A & 0 & 0 & 0 & 0 \\ 0 & 0 & 0 & 0 & 0 & I_3^A & 0 & 0 \\ 0 & 0 & 0 & 0 & 0 & 0 & 0 & I_4^A \end{bmatrix}, \tag{44}$$

where the dimensions of I_k^A and I_k^B are determined by the system state and control input vector, respectively. In this simulation example, $I_k^A = I_{6\times 6}$, $I_k^B = 1$.

Use (34) to construct the complementary matrix $\widetilde{M}_{KP}$ as follows:

$$\widetilde{M}_{KP} = \begin{bmatrix} 0 & 0 & 0 & 0 & 0 & K_{13} & 0 & K_{14} \\ 0 & 0 & 0 & K_{23} & 0 & 0 & 0 & 0 \\ K_{21} & 0 & 0 & 0 & 0 & 0 & 0 & 0 \\ 0 & 0 & 0 & 0 & K_{31} & 0 & 0 & 0 \\ 0 & K_{12} & 0 & 0 & 0 & 0 & 0 & K_{14} \\ 0 & 0 & K_{32} & 0 & 0 & 0 & 0 & 0 \\ 0 & K_{12} & 0 & 0 & 0 & K_{13} & 0 & 0 \\ 0 & 0 & 0 & 0 & 0 & 0 & 0 & 0 \end{bmatrix}. \tag{45}$$

Finally, the coordinated controller of $\mathbf{S}$ can be contracted as

$$\begin{aligned} K = \overline{K} &= Q_P\left(\widetilde{K}_D + \widetilde{M}_{KP}\right)V_P \\ &= \begin{bmatrix} K_{11} & K_{12} & K_{13} & K_{14} \\ K_{21} & K_{22} & K_{23} & 0 \\ K_{31} & K_{32} & K_{33} & 0 \\ K_{41} & 0 & 0 & K_{44} \end{bmatrix}. \end{aligned} \tag{46}$$

Figures 2 and 3 illustrate the frequency and tie-line power perturbations of the group of subsystems. The respond curves are very similar to those of [4–7].

5. Conclusion

This paper presents a theoretical study of the pairwise decomposition, which can be seen as a reverse modality of this methodology. The proposed approach is able to coordinated the interconnected system with uncertainties, and it can achieve high quality control performance as well. Moreover, this process is convenient for a group of interconnected subsystems without a superposition-form overall system model, which is in the case that only local information is available. Further research is ongoing, and one task is to determine the structure of system $\overline{\mathbf{S}}$ as an estimator of the original system $\mathbf{S}$. For this purpose, an update law which can fit the features of pairwise decomposition is needed as well as a calculation framework to deal with the structure perturbations effectively enough. The proposed approach can also motivate the application of pairwise decomposition to a nonlinear time-variant system.

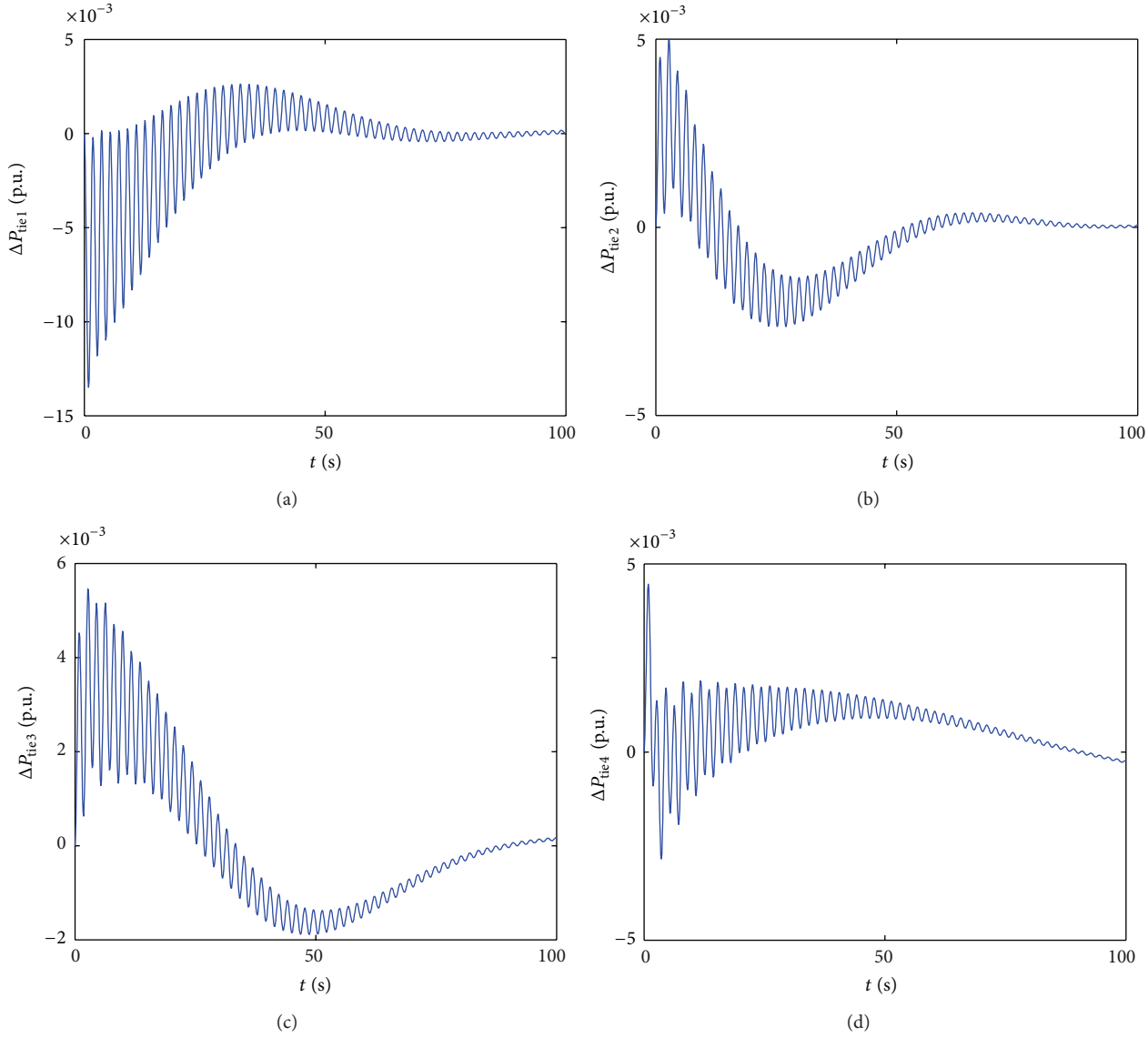

Figure 3: Deviations of tie-line power among the power system.

Acknowledgment

This research reported herein was supported by the NSF of China under Grant no. 60874017.

References

[1] M. Ikeda and D. D. Šiljak, "Overlapping decompositions, expansions and contractions of dynamic systems," *Large Scale Systems*, vol. 1, no. 1, pp. 29–38, 1980.

[2] M. Ikeda, D. D. Šiljak, and D. E. White, "An inclusion principle for dynamic systems," *IEEE Transactions on Automatic Control*, vol. 29, no. 3, pp. 244–249, 1984.

[3] D. D. Šiljak, *Decentralized Control of Complex Systems*, Academic Press, New York, NY, USA, 1991.

[4] X.-B. Chen and S. S. Stanković, "Decomposition and decentralized control of systems with multi-overlapping structure," *Automatica*, vol. 41, no. 10, pp. 1765–1772, 2005.

[5] X.-B. Chen and S. S. Stanković, "Overlapping decentralized approach to automation generation control of multi-area power systems," *International Journal of Control*, vol. 80, no. 3, pp. 386–402, 2007.

[6] X.-B. Chen, W.-B. Xu, T.-Y. Huang, X.-Y. Ouyang, and S. S. Stanković, "Pair-wise decomposition and coordinated control of complex systems," *Information Sciences*, vol. 185, no. 1, pp. 78–99, 2012.

[7] X.-B. Chen, *System Inclusion Principle and Its Application*, Science Press, Beijing, PRC, 2012, (Chinese).

[8] X.-B. Chen and C. Ma, "Coordinated control of a four-area power system under structural perturbation," in *Proceedings of the 9th Asian Control Conference*, Istanbul, Turkey, 2013.

[9] D. M. Stipanović, G. Inalhan, R. Teo, and C. J. Tomlin, "Decentralized overlapping control of a formation of unmanned aerial vehicles," *Automatica*, vol. 40, no. 8, pp. 1285–1296, 2004.

[10] F. Palacios-Quiñonero, J. Rodellar, and J. M. Rossell, "Sequential design of multi-overlapping controllers for longitudinal multi-overlapping systems," *Applied Mathematics and Computation*, vol. 217, no. 3, pp. 1170–1183, 2010.

[11] F. Palacios-Quiñonero, J. M. Rossell, and H. R. Karimi, "Semi-decentralized strategies in structuralm vibration control," *Modeling, Identification and Control*, vol. 32, no. 2, pp. 57–77, 2011.

[12] F. Palacios-Quiñonero, J. Rubió-Massegú, J. M. Rossell et al., "Discretetime multioverlapping controller design for structural vibration control of tall buildings under seismic excitation," *Mathematical Problems in Engineering*, vol. 2012, Article ID 636878, 20 pages, 2012.

[13] M. E. Sezer and D. D. Šiljak, "Validation of reduced-order models for control systems design," *Journal of Guidance, Control, and Dynamics*, vol. 5, no. 5, pp. 430–437, 1982.

[14] M. Ikeda and D. D. Šiljak, "Overlapping decentralized control with input, state, and output inclusion," *Control Theory and Advanced Technology*, vol. 2, no. 2, pp. 155–172, 1986.

[15] S. S. Stanković, X.-B. Chen, M. R. Matausek et al., "Stochastic inclusion principle applied to decentralized overlapping suboptimal LQG control," *International Journal of Control*, vol. 72, no. 3, pp. 276–288, 1999.

[16] D. D. Šiljak, "Dynamic graphs," *Nonlinear Analysis: Hybrid Systems*, vol. 2, no. 2, pp. 544–567, 2008.

[17] S. S. Stanković and D. D. Šiljak, "Sequential LQG optimization of hierarchically structured systems," *Automatica*, vol. 25, no. 4, pp. 545–559, 1989.

[18] S. S. Stanković and D. D. Šiljak, "Inclusion principle for linear time-varying systems," *SIAM Journal on Control and Optimization*, vol. 42, no. 1, pp. 321–341, 2003.

[19] C. S. Chang and W. Fu, "Area load frequency control using fuzzy gain scheduling of PI controllers," *Electric Power Systems Research*, vol. 42, no. 2, pp. 145–152, 1997.

[20] H. L. Zeynelgil, A. Demiroren, and N. S. Sengor, "The application of ANN technique to automatic generation control for multi-area power system," *International Journal of Electrical Power and Energy Systems*, vol. 24, no. 5, pp. 345–354, 2002.

[21] S. Boyd, L. El Ghaoui, E. Feron et al., *Linear Matrix Inequalities in System and Control Theory*, SIAM, Philadelphia, PA, USA, 1994.

[22] D. D. Šiljak and D. M. Stipanović, "Robust stabilization of nonlinear systems: the LMI approach," *Mathematical Problems in Engineering*, vol. 6, no. 5, pp. 461–493, 2000.

Hindawi Publishing Corporation
Mathematical Problems in Engineering
Volume 2013, Article ID 172608, 11 pages
http://dx.doi.org/10.1155/2013/172608

Research Article

Synchronization of Complex Dynamical Networks with Nonidentical Nodes and Derivative Coupling via Distributed Adaptive Control

Miao Shi, Junmin Li, and Chao He

Department of Mathematics, Xidian University, Xi'an 710071, China

Correspondence should be addressed to Miao Shi; miaomiao_90@aliyun.com

Received 23 May 2013; Revised 19 August 2013; Accepted 19 August 2013

Academic Editor: Jun Hu

Adaptive synchronization control is proposed for a new complex dynamical network model with nonidentical nodes and nonderivative and derivative couplings. The distributed adaptive learning laws of periodically time-varying and constant parameters and distributed adaptive control are designed. The new method which can obtain the synchronization error of closed-loop complex network system is asymptotic convergence in the sense of square error norm. What is more, the coupling matrix is not assumed to be symmetric or irreducible. Finally, a simulation example shows the feasibility and effectiveness of the approach.

1. Introduction

Complex dynamical networks have become a focus issue and have attracted increasing attention in many fields. The structure of many real systems in nature can be modeled by complex networks, such as biological neural networks, ecosystems, food webs, and World Wide Web [1, 2]. It has been demonstrated that many cooperative behavior mechanisms and complex phenomena in nature and society have close relationships with network synchronization [3]. Thus, the synchronization of complex systems has been widely studied, and many control schemes, such as adaptive control [4, 5], sliding mode control [6], and state observer-based control [7], have been focused on this topic. However, many existing works on synchronization are based on the networks with same nodes. Since almost all complex dynamical networks in engineering have different nodes, it is unrealistic to assume that all network nodes are the same. For example, in a multirobot system, the robots can have distinct structures or have different parameters such as masses and inertias. With much more complicated behaviors, the synchronization schemes for complex networks with identical nodes cannot be directly applied to the dynamical networks with nonidentical nodes. Therefore, it is strongly necessary to conduct further investigation of new synchronization schemes for a complex dynamical network with nonidentical nodes.

Recently, some papers have studied the synchronization problem with nonidentical nodes. A pinning control scheme was developed to realize the cluster synchronization of community networks with nonidentical nodes [8]. Moreover, other weaker forms of synchronization, namely, output synchronization and bounded synchronization, were proposed in [9, 10]. It is so difficult for a complex network with nonidentical nodes to achieve asymptotic synchronization that little work has been reported to deal with the problem. By constructing a common Lyapunov function for all the nodes, a synchronization criterion for a nonidentical nodes system was given in [11]. Some local robust controllers were designed for the network with strictly different nodes to achieve generalized synchronization in [12]. In [13], the asymptotic synchronization for complex dynamical networks with nonidentical nodes was studied. Based on solving a number of lower dimensional matrix inequalities and scalar inequalities, global synchronization criteria were given. Except the propriety of nonidentical nodes, the time-varying parameter and unknown system parameters should be considered meanwhile. Reference [14] introduced the adaptive synchronization of complex network systems

with unknown time-varying nonlinear coupling. Although it considered nonlinearly parameterized complex dynamical networks with unknown time-varying parameters, the nonidentical nodes were not considered yet.

On the other hand, the aforementioned papers only considered nonderivative coupling. Taking into account the complexity of the network, such as population ecology [15] and robots in contact with rigid environments [16], there always exist delayed coupling [17], derivative coupling, and so on. In [18], the authors proposed a general complex dynamical network with non-derivative and derivative coupling. Under the designed adaptive controllers, the network system can asymptotically synchronize to a given trajectory. The paper was limited to the inner coupling matrix of derivative being identity matrix. A complex dynamic network model with derivative coupling and nonidentical nodes was studied in [19]. By designing the adaptive strategy with time derivative terms, the authors have dealt with the known derivative coupling successfully. However, they did not consider nonlinear parameterized complex network with time-varying coupling strength and the unknown derivative coupling strength.

In recent years, the adaptive learning control has been proposed to deal with the unknown constant or time-varying parameters of the system in order to obtain control input [20, 21]. Under the designed adaptive learning control, the convergence of tracking error can be proved by using the composite energy function. Meanwhile, the sliding mode control (SMC) strategy has been successfully applied to a class of systems with nonlinearities and uncertainties [22–24]. The advantage of using SMC method is the concepts of sliding mode surface design and equivalent control. In this paper, under the adaptive control strategy and inequality technique, we solve the proposed problem successfully. For the nonlinearities function, further work can focus on SMC method.

Motivated by the above discussion, the synchronization problem via new distributed adaptive control is proposed for nonlinear parametric complex dynamical networks with derivative coupling and nonidentical nodes. The main difficulty is how to deal with the unknown derivative coupling. Using the adaptive control and skill of inequality zoom, we find a way to overcome this challenge. By designing the distributed adaptive laws, the effect of derivative coupling can be eliminated. Based on a Lyapunov-Krasovskii-like composite energy function (CEF) [25, 26], the adaptive asymptotical synchronization is obtained for nonlinearly parameterized complex dynamical networks with nonidentical nodes and derivative coupling. The theoretical analysis shows that the designed effective distributed adaptive strategy guarantees that the system asymptotically stable in the L_T^2 norm sense and all closed-loop signals are bounded. And it is worth mentioning that the coupling configuration matrix may be arbitrary matrix with appropriate dimensions [27].

The rest of the paper is organized as follows. The problem formulation and preliminaries are given in Section 2. In Section 3, adaptive synchronization scheme of the complex dynamical networks is presented. In Section 4, a simulation example is provided to illustrate the effectiveness of the proposed controller. Finally, conclusion is given in Section 5.

2. Problem Statement and Preliminaries

A complex dynamical network consisting of N nonidentical nodes is described as

$$\begin{aligned}\dot{x}_i(t) &= f_i(t, x_i(t)) \\ &\quad + \sum_{j=1}^{N} a_{ij}\Gamma g\left(x_j(t), \varphi_i(t)\right) \\ &\quad + \sum_{j=1}^{N} \alpha_i b_{ij}\Gamma \dot{x}_j(t), \quad i = 1, 2, \ldots, N,\end{aligned} \tag{1}$$

where $x_i(t) = [x_{i1}(t), x_{i2}(t), \ldots, x_{in}(t)]^T \in R^n$ is the state vector of the ith node, $f_i : R^+ \times R^n \to R^n$ is a vector-valued continuous function, $g : R^n \times R \to R^n$ is an unknown continuous nonlinear vector-valued function, $\varphi_i(t)$ represents the unknown time-varying function, and α_i is an unknown constant parameter. The inner coupling matrix $\Gamma = (\gamma_{ij}) \in R^{n\times n}$ is nonnegative definite. $A = (a_{ij})_{N\times N}$ and $B = (b_{ij})_{N\times N}$ are the coupling configuration constant matrices, which are defined as follows: if there is a connection from node i to node j $(i \neq j)$, then $a_{ij} > 0$, $b_{ij} > 0$; otherwise, $a_{ij} = b_{ij} = 0$. And the coupling matrices that satisfy $\sum_{j=1}^{N} a_{ij} = \sum_{j=1}^{N} b_{ij} = 0$.

Remark 1. In this paper, we assume that the strength of matrix Γ is unknown, which is more general than the inner coupling matrices assumed to be diagonal matrix in [18]. As the authors in papers [19] and [21] only consider the known coupling matrix strength, it should be pointed out that the unknown derivative coupling consists of more information than the dynamical model in [19, 21]. The coupling configuration matrices A and B need not be symmetric or irreducible. Thus, the results can be suitable to more complex dynamical networks.

Let $s(t) \in R^n$ be a solution of the dynamics of the isolated node to which all $x_i(t)$ are expected to synchronize.

Define synchronization error vectors

$$e_i(t) = x_i(t) - s(t), \quad i = 1, 2, \ldots, N. \tag{2}$$

In order to obtain the synchronized dynamics of network (1), we add an adaptive control strategy to nodes in network (1). Then, the controlled network is given by

$$\begin{aligned}\dot{x}_i(t) &= f_i(t, x_i(t)) \\ &\quad + \sum_{j=1}^{N} a_{ij}\Gamma g\left(x_j(t), \varphi_i(t)\right) \\ &\quad + \sum_{j=1}^{N} \alpha_i b_{ij}\Gamma \dot{x}_j(t) + u_i(t), \quad i = 1, 2, \ldots, N,\end{aligned} \tag{3}$$

where $u_i(t) = [u_{i1}(t), u_{i2}(t), \ldots, u_{in}(t)]^T \in R^n$, $i = 1, 2, \ldots, N$ are the adaptive controllers to be designed.

Since the row sum of coupling matrix is zero, we have the following dynamical error equation:

$$\begin{aligned}\dot{e}_i(t) &= \dot{x}_i(t) - \dot{s}(t)\\ &= f_i(t, x_i(t))\\ &\quad + \sum_{j=1}^{N} a_{ij}\Gamma\left(g\left(x_j(t), \varphi_i(t)\right) - g\left(s(t), \varphi_i(t)\right)\right)\\ &\quad + \sum_{j=1}^{N} \alpha_i b_{ij}\Gamma\left(\dot{x}_i(t) - \dot{s}(t)\right) - \dot{s}(t) + u_i(t)\\ &= f_i(t, x_i(t))\\ &\quad + \sum_{j=1}^{N} a_{ij}\Gamma\left(g\left(x_j(t), \varphi_i(t)\right) - g\left(s(t), \varphi_i(t)\right)\right)\\ &\quad + \sum_{j=1}^{N} \alpha_i b_{ij}\Gamma\dot{e}_j(t) - \dot{s}(t) + u_i(t).\end{aligned} \tag{4}$$

Our objective is to design adaptive control laws $u_i(t)$ such that the synchronization errors converge to zero in the norm sense.

In order to derive the main results, some assumptions and lemmas are introduced as follows.

Assumption 2. For the unknown continuous function $g(\cdot,\cdot)$, the following inequality holds:

$$\begin{aligned}&\left\|g\left(x_j(t), \varphi_i(t)\right) - g\left(s(t), \varphi_i(t)\right)\right\|^2\\ &\quad \le \left\|x_j(t) - s(t)\right\|^2 h\left(x_j(t), s(t)\right)\lambda\left(\varphi_i(t)\right).\end{aligned} \tag{5}$$

Here $h(\cdot,\cdot)$ is a known nonnegative continuous function with constant upper bounded H, and $\lambda(\cdot)$ is an unknown nonnegative continuous function.

Remark 3. According to separation principle [28], Assumption 2 can be easily satisfied. Under the assumption, we can "separate" the parameters from the nonlinear function. For the unknown parameters, we can solve the problem using adaptive method.

Assumption 4 (Lipschitz condition). For system (1), there exist positive constants $l_i > 0, i = 1, \ldots, N$ such that

$$\begin{aligned}&\left\|f_i(t, x) - f_i(t, y)\right\| \le l_i\left\|x - y\right\|,\\ &\qquad \forall x, y \in R^n, \quad i = 1, 2, \ldots, N.\end{aligned} \tag{6}$$

Assumption 5. In network (1), $\varphi_i(t)$ is an unknown time-varying function with a known period T; thus, $\lambda(\varphi_i(t))$ is also a periodic function with the same period T. Suppose

$$\lambda\left(\varphi_i(t)\right) = \phi_i(t) + \theta_i, \tag{7}$$

where $\phi_i(t)$ is an unknown continuous function with a known period T and θ_i is an unknown constant parameter.

Assumption 6. In the network (1), the inner coupling matrix Γ satisfies

$$\max\left(\|\Gamma\|, \max\left(\left|\gamma_{ij}\right|\right)\right) \le \gamma, \quad \forall i, j = 1, 2, \ldots, N, \tag{8}$$

where γ is positive constant.

Assumption 7. Assume that the state and the state derivative of system (1) are measurable.

Remark 8. This assumption is necessary to design controller and adaptive laws. Assumption 7 seems to be restrictive. The observer for state derivative will be considered in the near future.

Lemma 9 (Young's inequality). *For any vectors $x, y \in R^n$, and any $c > 0$, the following matrix inequality holds:*

$$x^T y \le cx^T x + \frac{1}{4c} y^T y. \tag{9}$$

Lemma 10. *For a positive constant T, if for all $t \ge 0$, $f(t)$ is a continuous function, $\int_{t-T}^{t} f(\tau)d\tau$ exists and is bounded with M. Then, $f(t)$ is bounded.*

Proof. In fact, if $f(t)$ is unbounded, we can get, for all $N > 0$, $\exists\tau \in [t - T, t]$, $f(\tau) > N$. As $f(t)$ is a continuous function, according to the properties of the continuous functions, we have $\exists\varepsilon > 0$ for all $k \in [\tau - \varepsilon, \tau + \varepsilon] \subset [t - T, t]$, $f(k) > N$; then $\int_{t-T}^{t} f(\tau)d\tau \ge \int_{\tau-\varepsilon}^{\tau+\varepsilon} f(t)dt \ge 2\varepsilon N$. We can choose $N = M/2\varepsilon + 1$; then $\int_{t-T}^{t} f(\tau)d\tau > M$. This is a contradiction with the assumption. The proof is completed. □

3. Adaptive Synchronization of the Complex Dynamical Networks

In this section, adaptive controller is designed to make the states of (1) synchronize to the trajectory $s(t)$, and some sufficient conditions are given to ensure the asymptotic stability of the synchronization process.

For network (1), we design the controller $u_i(t) \in R^n$ as follows:

$$\begin{aligned}u_i(t) &= \dot{s}(t) - f_i(t, s(t))\\ &\quad - \gamma H e_i(t)\sum_{j=1}^{N} a_{ji}^2\left(\widehat{\phi}_j(t) + \widehat{\theta}_j(t)\right)\\ &\quad - \sum_{j=1}^{N}\left|b_{ij}\right|\gamma\widehat{\alpha}_i(t)\,\mathrm{sign}\left(e_i(t)\right)\left|\dot{e}_{j\cdot}(t)\right|,\end{aligned} \tag{10}$$

where γ, H satisfy Assumption 6, N is the node number of network (1), and $\widehat{\phi}_i(t)$, $\widehat{\theta}_i(t)$, $\widehat{\alpha}_i(t)$ are the estimations of $\phi_i(t)$, θ_i, α_i, respectively. We denote

$$\begin{aligned}\mathrm{sign}\left(e_i(t)\right) &= \left(\mathrm{sign}\left(e_{i1}(t)\right), \ldots, \mathrm{sign}\left(e_{in}(t)\right)\right)^T,\\ \left|\dot{e}_{j\cdot}(t)\right| &= \sum_{k=1}^{n}\left|\dot{e}_{jk}(t)\right|.\end{aligned} \tag{11}$$

Remark 11. The main design difficulty is how to deal with the unknown derivative coupling and Γ. In this paper, we use the known upper bound to magnify the inner coupling matrix. Thus, the controller is related to every element of the synchronization error vector. Under the new controller, we can deal with the derivative terms easily.

The constant parameter distributed update laws are designed as follows:

$$\dot{\widehat{\theta}}_i(t) = r_i \sum_{j=1}^{N} a_{ij}^2 e_j^T(t)\, e_j(t), \tag{12}$$

$$\dot{\widehat{\alpha}}_i(t) = g_i \sum_{k=1}^{n} \left|e_{ik}(t)\right| \sum_{j=1}^{N} \left|b_{ij}\right| \left|\dot{e}_{j\cdot}(t)\right|. \tag{13}$$

The time-varying distributed periodic adaptive learning law is designed as

$$\widehat{\phi}_i(t) = \begin{cases} 0, & t \in [-T, 0), \\ q_{i0}(t) \sum_{j=1}^{N} a_{ij}^2 e_j^T(t)\, e_j(t), & t \in [0, T), \\ \widehat{\phi}_i(t-T) + q_i \sum_{j=1}^{N} a_{ij}^2 e_j^T(t)\, e_j(t), & t \in [T, +\infty), \end{cases} \tag{14}$$

where r_i, g_i, q_i are positive constants and $q_{i0}(t)$ is a continuous and strictly increasing nonnegative function which satisfies $q_{i0}(0) = 0, q_{i0}(T) = q_i$, which ensure $\widehat{\phi}_i(t)$ is continuous when $t = iT, i = 1, 2, \ldots, N$.

The following theorem will give a sufficient condition of asymptotical synchronization for the controlled network (3).

Theorem 12. *Under Assumptions 2–6, the control law* (10) *with the distributed adaptive learning laws* (12)–(14) *guarantees that the controlled network* (4) *achieves asymptotic synchronization in the L_T^2 norm sense; that is to say,*

$$\lim_{t \to \infty} \int_{t-T}^{t} \left\|e_i(\tau)\right\|^2 d\tau = 0, \qquad i = 1, 2, \ldots, N. \tag{15}$$

Moreover, all closed-loop signals are bounded.

Proof. Define a Lyapunov-Krasovskii function as follows: for $t \in [0, \infty)$

$$\begin{aligned} V(t) = {} & \frac{1}{2} \sum_{i=1}^{N} e_i^T e_i + \frac{\gamma H}{2} \sum_{i=1}^{N} \int_{t-T}^{t} q_i^{-1} \widetilde{\phi}_i^2(\tau)\, d\tau \\ & + \frac{\gamma H}{2} \sum_{i=1}^{N} r_i^{-1} \left(\widetilde{\theta}_i(t) + L\right)^2 + \frac{\gamma}{2} \sum_{i=1}^{N} g_i^{-1} \widetilde{\alpha}_i^2(t), \end{aligned} \tag{16}$$

where

$$\begin{aligned} \widetilde{\phi}_i(t) &= \phi_i(t) - \widehat{\phi}_i(t), \\ \widetilde{\theta}_i(t) &= \theta_i - \widehat{\theta}_i(t), \qquad \widetilde{\alpha}_i(t) = \alpha_i - \widehat{\alpha}_i(t), \end{aligned} \tag{17}$$

and L is a sufficiently large positive constant which will be determined later.

It should be noted that we define

$$\phi_i(t) = \phi_i(0), \qquad t \in [-T, 0), \tag{18}$$

from the distributed adaptive law (14), and we get

$$\widetilde{\phi}_i^2(t-T) = \phi_i^2(t-T) = \phi_i^2(0), \qquad t \in [0, T]. \tag{19}$$

Firstly, the finiteness property of $V(t)$ for the period $[0, T)$ is given. Consider (4) and the proposed distributed control laws (12)–(14), it can be seen that the right-hand side of (4) is continuous with respect to all arguments. According to the existence theorem of differential equation, (4) has unique solution in the interval $[0, T_1) \subset [0, T)$, with $0 < T_1 \leq T$. This can guarantee the boundedness of $V(t)$ over $[0, T_1)$. Therefore, we need only focus on the interval $[T_1, T)$.

For any $\in [T_1, T)$, the derivative of $V(t)$ with respect to time is given by

$$\begin{aligned} \dot{V}(t) = {} & \sum_{i=1}^{N} e_i^T(t)\, \dot{e}_i(t) \\ & + \frac{\gamma H}{2} \left(\sum_{i=1}^{N} q_i^{-1} \widetilde{\phi}_i^2(t) - \sum_{i=1}^{N} q_i^{-1} \widetilde{\phi}_i^2(t-T) \right) \\ & + \gamma H \sum_{i=1}^{N} r_i^{-1} \left(\widetilde{\theta}_i(t) + L\right) \dot{\widetilde{\theta}}_i(t) \\ & + \gamma \sum_{i=1}^{N} g_i^{-1} \widetilde{\alpha}_i(t)\, \dot{\widetilde{\alpha}}_i(t). \end{aligned} \tag{20}$$

Let us introduce some notations as

$$\begin{aligned} \Phi &= f_i\left(t, x_i(t)\right) - f_i\left(t, s(t)\right), \\ \Lambda &= g\left(x_j(t), \varphi_i(t)\right) - g\left(s(t), \varphi_i(t)\right). \end{aligned} \tag{21}$$

Along the trajectory of (4), we get

$$\begin{aligned} & \sum_{i=1}^{N} e_i^T(t)\, \dot{e}_i(t) \\ & = \sum_{i=1}^{N} e_i^T(t) \left[f_i\left(t, x_i(t)\right) + \sum_{j=1}^{N} a_{ij} \Gamma \Lambda \right. \\ & \qquad \left. + \sum_{j=1}^{N} \alpha_i b_{ij} \Gamma \dot{e}_j(t) - \dot{s}(t) + u_i(t) \right]. \end{aligned} \tag{22}$$

Substituting (10) into the above equation, from Assumption 6 and Lemma 9, we have

$$\begin{aligned}
&\sum_{i=1}^{N} e_i^T(t)\,\dot{e}_i(t)\\
&\quad\le \sum_{i=1}^{N}\Bigg[e_i^T\Phi+\sum_{j=1}^{N}a_{ij}e_i^T\Gamma\Lambda+\sum_{j=1}^{N}\alpha_i b_{ij}e_i^T\Gamma\dot{e}_j\\
&\qquad -\gamma H e_i^T e_i\sum_{j=1}^{N}a_{ji}^2\left(\widehat{\phi}_j(t)+\widehat{\theta}_j(t)\right)\\
&\qquad -e_i^T\sum_{j=1}^{N}\left|b_{ij}\right|\gamma\widehat{\alpha}_i(t)\,\mathrm{sign}\left(e_i(t)\right)\left|\dot{e}_{j\cdot}(t)\right|\sum_{j=1}^{N}\Bigg]\\
&\quad\le \sum_{i=1}^{N}\Bigg[\left(ce_i^Te_i+\frac{1}{4c}\Phi^T\Phi\right)\\
&\qquad +\sum_{j=1}^{N}\left(de_i^Te_i+\frac{1}{4d}a_{ij}^2\Lambda^T\Gamma^T\Gamma\Lambda\right)\\
&\qquad +\sum_{j=1}^{N}\alpha_i b_{ij}e_i^T(t)\,\Gamma\dot{e}_j(t)\\
&\qquad -\gamma H e_i^Te_i\sum_{j=1}^{N}a_{ji}^2\left(\widehat{\phi}_j(t)+\widehat{\theta}_j(t)\right)\\
&\qquad -\sum_{j=1}^{N}\left|b_{ij}\right|\gamma\widehat{\alpha}_i(t)\sum_{k=1}^{n}\left|e_{ik}(t)\right|\left|\dot{e}_{j\cdot}(t)\right|\Bigg].
\end{aligned}\tag{23}$$

Using inequality properties, we obtain

$$\sum_{j=1}^{N}\alpha_i b_{ij}e_i^T(t)\,\Gamma\dot{e}_j(t)\le\sum_{j=1}^{N}\left|b_{ij}\right|\gamma\alpha_i\sum_{k=1}^{n}\left|e_{ik}(t)\right|\left|\dot{e}_{j\cdot}(t)\right|.\tag{24}$$

Then, according to Assumptions 2–5 and the previous inequality, we have

$$\begin{aligned}
\sum_{i=1}^{N}e_i^T(t)\,\dot{e}_i(t)\le\sum_{i=1}^{N}\Bigg[&\left(ce_i^Te_i+\frac{1}{4c}l_i^2e_i^Te_i\right)\\
&+\sum_{j=1}^{N}de_i^Te_i+\sum_{j=1}^{N}a_{ij}^2\left(\phi_i(t)+\theta_i\right)\frac{H\gamma^2}{4d}e_j^Te_j\\
&+\sum_{j=1}^{N}\left|b_{ij}\right|\gamma\alpha_i\sum_{k=1}^{n}\left|e_{ik}(t)\right|\left|\dot{e}_{j\cdot}(t)\right|\\
&-\sum_{j=1}^{N}a_{ji}^2\gamma H\left(\widehat{\phi}_j(t)+\widehat{\theta}_j(t)\right)e_i^Te_i\\
&-\sum_{j=1}^{N}\left|b_{ij}\right|\gamma\widehat{\alpha}_i(t)\sum_{k=1}^{n}\left|e_{ik}(t)\right|\left|\dot{e}_{j\cdot}(t)\right|\Bigg],
\end{aligned}\tag{25}$$

where c and d are positive constants. If choosing

$$c=\frac{1}{2},\qquad d=\frac{\gamma}{4},\tag{26}$$

we have

$$\begin{aligned}
\sum_{i=1}^{N}e_i^T(t)\,\dot{e}_i(t)\le&\sum_{i=1}^{N}\left(\frac{1}{2}+\frac{1}{2}l_i^2+\frac{N\gamma}{4}\right)e_i^Te_i\\
&+\sum_{i=1}^{N}\sum_{j=1}^{N}a_{ij}^2\gamma H\left(\widetilde{\phi}_i(t)+\widetilde{\theta}_i(t)\right)e_j^Te_j\\
&+\sum_{j=1}^{N}\left|b_{ij}\right|\gamma\widetilde{\alpha}_i\sum_{k=1}^{n}\left|e_{ik}(t)\right|\left|\dot{e}_{j\cdot}(t)\right|.
\end{aligned}\tag{27}$$

From (12), the third term on the right-hand side of (20) satisfies

$$\gamma H\sum_{i=1}^{N}r_i^{-1}\left(\widetilde{\theta}_i(t)+L\right)\dot{\widetilde{\theta}}_i(t)=-\gamma H\sum_{i=1}^{N}\left(\widetilde{\theta}_i(t)+L\right)\sum_{j=1}^{N}a_{ij}^2e_j^Te_j,\tag{28}$$

while the fourth term on the right-hand side of (20) satisfies

$$\gamma\sum_{i=1}^{N}g_i^{-1}\widetilde{\alpha}_i(t)\,\dot{\widetilde{\alpha}}_i(t)=-\sum_{i=1}^{N}\gamma\widetilde{\alpha}_i(t)\sum_{k=1}^{n}\left|e_{ik}(t)\right|\sum_{j=1}^{N}\left|b_{ij}\right|\left|\dot{e}_{j\cdot}(t)\right|.\tag{29}$$

Since $q_{i0}(t)$ is a continuous function and strictly increasing in $[T_1,T)\subset[0,T)$, $q_i^{-1}\le q_{i0}^{-1}(t)<\infty$ is ensured. Focusing on the second term on the right-hand side of (20), from (19), we can get, when $t\in[0,T)$,

$$\begin{aligned}
&\frac{\gamma H}{2}\left(\sum_{i=1}^{N}q_i^{-1}\widetilde{\phi}_i^2(t)-\sum_{i=1}^{N}q_i^{-1}\widetilde{\phi}_i^2(t-T)\right)\\
&\quad\le\frac{\gamma H}{2}\sum_{i=1}^{N}q_{i0}^{-1}\widetilde{\phi}_i^2(t)\\
&\quad=\frac{\gamma H}{2}\sum_{i=1}^{N}q_{i0}^{-1}\left[\phi_i^2(t)+2\widehat{\phi}_i^2(t)-2\phi_i(t)\,\widehat{\phi}_i(t)\right.\\
&\qquad\left.-\widehat{\phi}_i^2(t)\right]\\
&\quad\le\frac{\gamma H}{2}\sum_{i=1}^{N}q_{i0}^{-1}\left[\phi_i^2(t)+2\widehat{\phi}_i^2(t)-2\phi_i(t)\,\widehat{\phi}_i(t)\right]\\
&\quad=\frac{\gamma H}{2}\sum_{i=1}^{N}q_{i0}^{-1}\phi_i^2(t)-\gamma H\sum_{i=1}^{N}\sum_{j=1}^{N}a_{ij}^2\widetilde{\phi}_i(t)\,e_j^Te_j.
\end{aligned}\tag{30}$$

Substituting (27)–(30) into (20), we have

$$\begin{aligned}
\dot{V}(t)\le&\sum_{i=1}^{N}\left(\frac{1}{2}+\frac{1}{2}l_i^2+\frac{N\gamma}{4}-L\sum_{j=1}^{N}a_{ji}^2\right)e_i^Te_i\\
&+\frac{\gamma H}{2}\sum_{i=1}^{N}q_{i0}^{-1}(t)\,\phi_i^2(t).
\end{aligned}\tag{31}$$

We can choose the appropriate L such that

$$\sum_{i=1}^{N}\left(\frac{1}{2}+\frac{1}{2}l_i^2+\frac{N\gamma}{4}-L\sum_{j=1}^{N}a_{ji}^2\right)<0. \tag{32}$$

According to (31), we have

$$\dot{V}(t)\le\frac{\gamma H}{2}\sum_{i=1}^{N}q_{i0}^{-1}(t)\,\phi_i^2(t),\quad t\in[0,T). \tag{33}$$

Since $\phi_i(t)$ is continuous and periodic, the boundedness can be obtained. The boundedness of $\phi_i(t)$ leads to the boundedness of $\dot{V}(t)$. For $V(T_1)$ is bounded, the finiteness of $V(t)$ is obvious, for all $t\in[0,T)$.

Next, we will prove the asymptotical convergence of $e(t)$.

According to (16), for all $t\ge T$, we get

$$\begin{aligned}\Delta V(t)&=V(t)-V(t-T)\\&=\frac{1}{2}\sum_{i=1}^{N}e_i^T(t)\,e_i(t)-\frac{1}{2}\sum_{i=1}^{N}e_i^T(t-T)\,e_i(t-T)\\&\quad+\frac{\gamma H}{2}\sum_{i=1}^{N}\int_{t-T}^{t}\left[q_i^{-1}\widetilde{\phi}_i^2(\tau)-q_i^{-1}\widetilde{\phi}_i^2(\tau-T)\right]d\tau\\&\quad+\frac{\gamma H}{2}\sum_{i=1}^{N}r_i^{-1}\left(\widetilde{\theta}_i(t)+L\right)^2\\&\quad-\frac{\gamma H}{2}\sum_{i=1}^{N}r_i^{-1}\left(\widetilde{\theta}_i(t-T)+L\right)^2+\frac{\gamma}{2}\sum_{i=1}^{N}g_i^{-1}\widetilde{\alpha}_i^2(t)\\&\quad-\frac{\gamma}{2}\sum_{i=1}^{N}g_i^{-1}\widetilde{\alpha}_i^2(t-T).\end{aligned} \tag{34}$$

Considering the first two terms on the right-hand side of (34), with Newton-Leibniz formula, we obtain

$$\begin{aligned}&\frac{1}{2}\sum_{i=1}^{N}e_i^T(t)\,e_i(t)-\frac{1}{2}\sum_{i=1}^{N}e_i^T(t-T)\,e_i(t-T)\\&=\sum_{i=1}^{N}\int_{t-T}^{t}e_i^T(\tau)\,\dot{e}_i(\tau)\,d\tau\\&\le\sum_{i=1}^{N}\int_{t-T}^{t}\left(\left(\frac{1}{2}+\frac{1}{2}l_i^2+\frac{N\gamma}{4}\right)e_i^T(\tau)\,e_i(\tau)\right.\\&\qquad\left.+\sum_{j=1}^{N}a_{ij}^2\gamma He_j^T(\tau)\,e_j(\tau)\,\widetilde{\phi}_i(\tau)\right)d\tau\\&\quad+\sum_{i=1}^{N}\sum_{j=1}^{N}\int_{t-T}^{t}a_{ij}^2\gamma He_j^T(\tau)\,e_j(\tau)\,\widetilde{\theta}_i(\tau)\,d\tau\\&\quad+\sum_{i=1}^{N}\sum_{j=1}^{N}\int_{t-T}^{t}\left|b_{ij}\right|\gamma\widetilde{\alpha}_i\sum_{k=1}^{n}\left|e_{ik}(\tau)\right|\left|\dot{e}_{j\cdot}(\tau)\right|d\tau.\end{aligned} \tag{35}$$

Use the algebraic relation

$$\begin{aligned}&(a-b)^TH(a-b)-(a-c)^TH(a-c)\\&\quad=(c-b)^TH[2(a-b)+(b-c)],\end{aligned} \tag{36}$$

where $a,b,c\in R^p$, $H\in R^{p\times p}$.

Choosing $H=1$, $a=\phi_i(\tau)$, $b=\widehat{\phi}_i(\tau)$, $c=\widehat{\phi}_i(\tau-T)$, $\phi_i(\tau)=\phi_i(\tau-T)$, then $a-c=\widetilde{\phi}_i(\tau-T)$, $a-b=\widetilde{\phi}_i(\tau)$. The following equality can be obtained:

$$\begin{aligned}&\frac{\gamma H}{2}\sum_{i=1}^{N}q_i^{-1}\widetilde{\phi}_i^2(\tau)-\frac{\gamma H}{2}\sum_{i=1}^{N}q_i^{-1}\widetilde{\phi}_i^2(\tau-T)\\&=\frac{\gamma H}{2}\sum_{i=1}^{N}q_i^{-1}\left[2\widetilde{\phi}_i(\tau)+\widehat{\phi}_i(\tau)-\widehat{\phi}_i(\tau-T)\right]\\&\qquad\times\left[\widehat{\phi}_i(\tau-T)-\widehat{\phi}_i(\tau)\right]\\&=-\gamma H\sum_{i=1}^{N}\left(\widetilde{\phi}_i(\tau)+\frac{1}{2}q_i\sum_{j=1}^{N}a_{ij}^2e_j^Te_j\right)\sum_{k=1}^{N}a_{ik}^2e_k^Te_k.\end{aligned} \tag{37}$$

Taking the third term on the right-hand side of (34), from (37), one obtains

$$\begin{aligned}&\frac{\gamma H}{2}\sum_{i=1}^{N}\int_{t-T}^{t}\left[q_i^{-1}\widetilde{\phi}_i^2(\tau)-q_i^{-1}\widetilde{\phi}_i^2(\tau-T)\right]d\tau\\&=-\gamma H\sum_{i=1}^{N}\int_{t-T}^{t}\left[\widetilde{\phi}_i(\tau)+\frac{1}{2}q_i\sum_{j=1}^{N}a_{ij}^2e_j^Te_j\right]\\&\qquad\times\sum_{k=1}^{N}a_{ik}^2e_k^Te_k\,d\tau.\end{aligned} \tag{38}$$

The other terms on right-hand side of (34) can be simplified as follows:

$$\begin{aligned}&\frac{\gamma H}{2}\sum_{i=1}^{N}r_i^{-1}(\widetilde{\theta}_i(t)+L)^2\\&\qquad-\frac{\gamma H}{2}\sum_{i=1}^{N}r_i^{-1}(\widetilde{\theta}_i(t-T)+L)^2\\&=\gamma H\sum_{i=1}^{N}\int_{t-T}^{t}r_i^{-1}\left(\widetilde{\theta}_i(\tau)+L\right)\dot{\widetilde{\theta}}_i(\tau)\,d\tau\\&=-\gamma H\sum_{i=1}^{N}\int_{t-T}^{t}\left(\widetilde{\theta}_i(\tau)+L\right)\sum_{j=1}^{N}a_{ij}^2e_j^T(\tau)\,e_j(\tau)\,d\tau,\\&\frac{\gamma}{2}\sum_{i=1}^{N}g_i^{-1}\widetilde{\alpha}_i^2(t)-\frac{\gamma}{2}\sum_{i=1}^{N}g_i^{-1}\widetilde{\alpha}_i^2(t-T)\\&=\gamma\sum_{i=1}^{N}\int_{t-T}^{t}g_i^{-1}\widetilde{\alpha}_i(\tau)\,\dot{\widetilde{\alpha}}_i(\tau)\,d\tau\\&=-\gamma\sum_{i=1}^{N}\sum_{j=1}^{N}\int_{t-T}^{t}\left|b_{ij}\right|\widetilde{\alpha}_i\sum_{k=1}^{n}\left|e_{ik}(t)\right|\left|\dot{e}_{j\cdot}(t)\right|d\tau.\end{aligned} \tag{39}$$

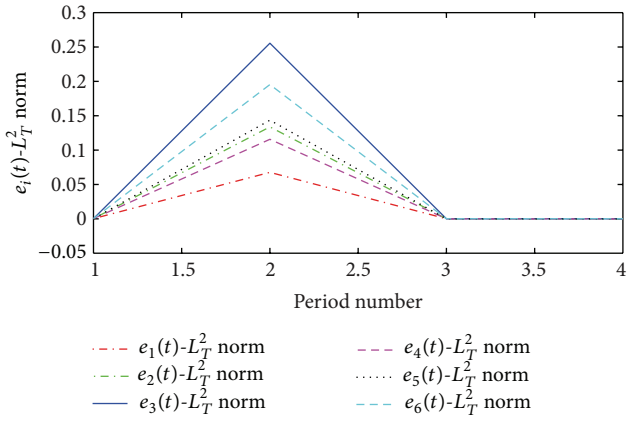

FIGURE 1: The change of synchronization error $e_i(t)$ along period number $i = 1, \ldots, 6$.

Substituting (35), (38)-(39) into (34), we can attain

$$\Delta V(t) \le -\sum_{i=1}^{N} \int_{t-T}^{t} \left(L \sum_{j=1}^{N} a_{ji}^2 - \frac{1}{2} - \frac{1}{2} l_i^2 - \frac{N\gamma}{4} \right) \times e_i^T(\tau)\, e_i(\tau)\, d\tau. \tag{40}$$

Obviously, there exists L such that

$$L > \frac{\left(1/2 + (1/2)\, l_i^2 + N\gamma/4\right)}{\sum_{j=1}^{N} a_{ji}^2}, \quad i = 1, \ldots, N. \tag{41}$$

We can obtain

$$\Delta V(t) < 0. \tag{42}$$

Applying (40) repeatedly for any $t \in [lT, (l+1)T]$, $l = 1, 2, \ldots$ and denoting $t_0 = t - lT$, we have

$$V(t) = V(t_0) + \sum_{j=0}^{l-1} \Delta V(t - jT). \tag{43}$$

Considering $t_0 \in [0, T)$ and the positive of $V(t)$, according to (43), we obtain

$$V(t) < \max_{t_0 \in [0,T)} V(t_0) - \sum_{j=0}^{l-1} \sum_{i=1}^{N} \int_{t-(j+1)T}^{t-jT} \left(L \sum_{j=1}^{N} a_{ji}^2 - \frac{1}{2} - \frac{1}{2} l_i^2 - \frac{N\gamma}{4} \right) \times e_i^T(\tau)\, e_i(\tau)\, d\tau. \tag{44}$$

Since $V(t_0)$ is bounded in the interval $[0, T)$, according to the convergence theorem of the sum of series and (44), the error $e_i(t)$ converges to zero asymptotically in the L_T^2 norm sense. That is to say, we have

$$\lim_{t \to \infty} \int_{t-T}^{t} e_i^T(\tau)\, e_i(\tau)\, d\tau = 0. \tag{45}$$

Finally, for all $t \in [T, \infty)$, we prove that all the closed-loop signals are bounded, and the derivative of $V(t)$ is

$$\begin{aligned} \dot{V}(t) &= \sum_{i=1}^{N} e_i^T(t)\, \dot{e}_i(t) + \frac{\gamma H}{2} \sum_{i=1}^{N} q_i^{-1} \widetilde{\phi}_i^2(t) - \frac{\gamma H}{2} \sum_{i=1}^{N} q_i^{-1} \widetilde{\phi}_i^2(t - T) \\ &\quad + \gamma H \sum_{i=1}^{N} r_i^{-1} \left(\widetilde{\theta}_i(t) + L \right) \dot{\widetilde{\theta}}_i(t) + \gamma \sum_{i=1}^{N} g_i^{-1} \widetilde{\alpha}_i(t)\, \dot{\widetilde{\alpha}}_i(t) \\ &\le -\frac{\gamma H}{2} \sum_{i=1}^{N} q_i \left(\sum_{j=1}^{N} a_{ij}^2 e_j^T e_j \right)^2 \\ &\quad - \sum_{i=1}^{N} \left(L \sum_{j=1}^{N} a_{ji}^2 - \frac{1}{2} - \frac{1}{2} l_i^2 - \frac{N\gamma}{4} \right) e_i^T e_i. \end{aligned} \tag{46}$$

By (46), one can obtain

$$\begin{aligned} V(t) &\le V(T) - \frac{\gamma H}{2} \sum_{i=1}^{N} \int_{T}^{t} q_i \left(\sum_{j=1}^{N} a_{ij}^2 e_j^T e_j \right)^2 d\tau \\ &\quad - \sum_{i=1}^{N} \int_{T}^{t} \left(L \sum_{j=1}^{N} a_{ji}^2 - \frac{1}{2} - \frac{1}{2} l_i^2 - \frac{N\gamma}{4} \right) e_i^T e_i d\tau. \end{aligned} \tag{47}$$

Choosing

$$L > \frac{\left(1/2 + (1/2)\, l_i^2 + N\gamma/4\right)}{\sum_{j=1}^{N} a_{ji}^2}, \quad i = 1, \ldots, N, \tag{48}$$

we have

$$V(t) < V(T). \tag{49}$$

From the boundedness of $V(t)$ and (16), we conclude that e_i, $\int_{t-T}^{t} \widetilde{\phi}_i^2(\tau) d\tau$, $\widetilde{\theta}_i(t)\widetilde{\alpha}_i(t)$ are all bounded. Since $\widetilde{\phi}_i(t)$ is continuous function and θ_i, α_i are constants, it implies the boundedness of $\widehat{\theta}_i(t)$ and $\widehat{\alpha}_i(t)$. According to Lemma 10, the boundedness of $\widetilde{\phi}_i(t)$ is obviously obtained. As $\phi_i(t)$ is a continuous periodic function, we can get that $\widehat{\phi}_i(t)$ is bounded. According to (10), the boundedness of the control input $u_i(t)$ is obtained. Since $e_i(t)$ is bounded, the boundedness of $x_i(t)$ is received. So the proof is completed. □

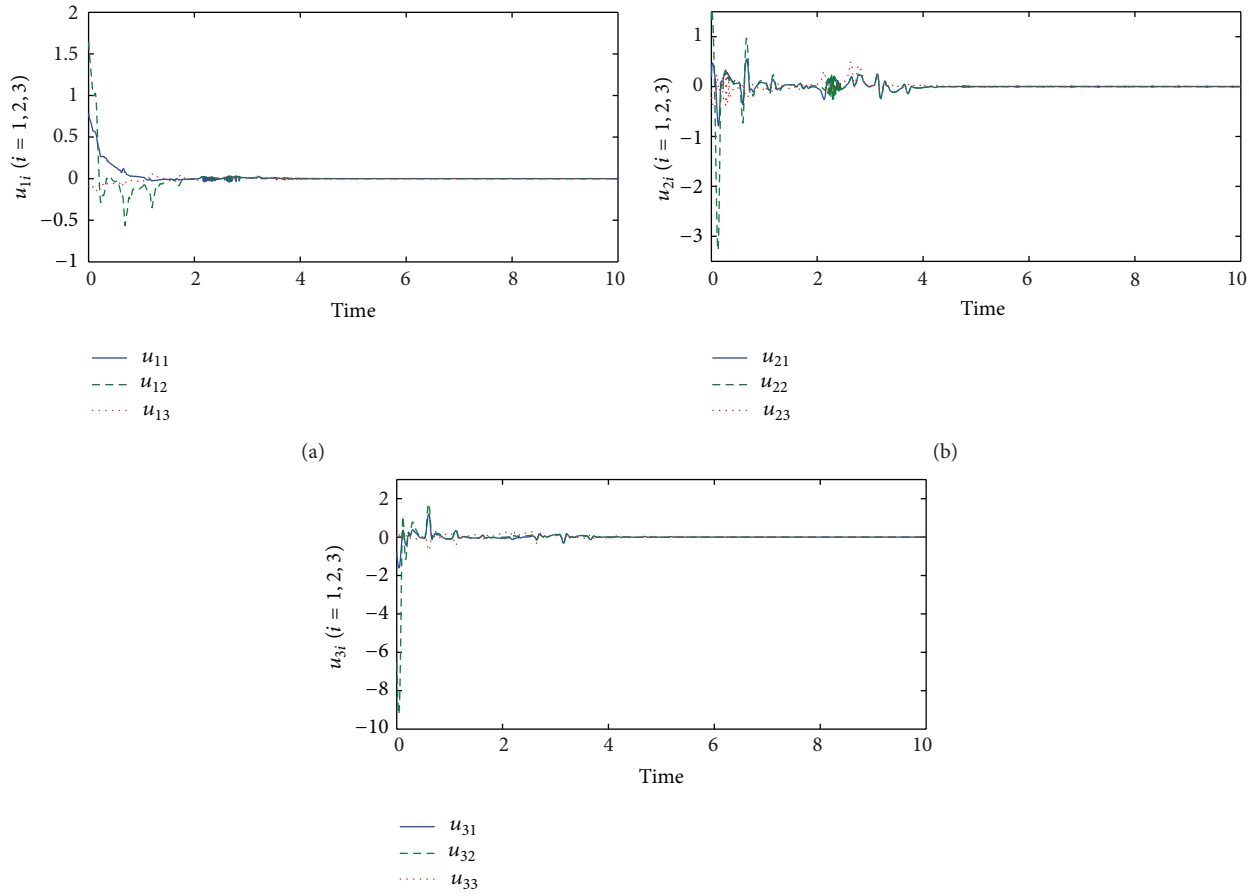

FIGURE 2: The change of control $u_i(t)$ along time: (a) u_{1i}, $i = 1, 2, 3$, (b) u_{2i}, $i = 1, 2, 3$, and (c) u_{3i}, $i = 1, 2, 3$.

4. Simulation Example

To demonstrate the theoretical result obtained in Section 3, we consider the following dynamical network with six nonidentical nodes

$$\begin{aligned}\dot{x}_i(t) &= f_i(t, x_i(t)) \\ &+ \sum_{j=1}^{N} a_{ij}\Gamma \exp\left(-\varphi_i(t)\begin{pmatrix} x_{j1}^2(t) \\ x_{j2}^2(t) \\ x_{j3}^2(t)\end{pmatrix}\right) \\ &+ \sum_{j=1}^{N} \alpha_i b_{ij}\Gamma \dot{x}_j(t) + u_i(t), \quad i = 1, \ldots, 6,\end{aligned} \tag{50}$$

where

$$f_1(t, x_1) = \begin{pmatrix} -2.5x_{11} + 0.3x_{12} + 0.9x_{13} + 3x_{13}^2 \\ 0.6x_{11} - 2.6x_{12} + 3x_{12}^2 + x_{13} \\ -2.8x_{11} + \sin x_{11} \cos x_{12} - 2.2x_{13}\end{pmatrix},$$

$$f_2(t, x_2) = \begin{pmatrix} -2.5x_{21} + x_{22} + x_{21}x_{22} + x_{23} \\ 0.5x_{21} - 0.8x_{22} - \sin x_{22} + x_{23} - x_{23}^2 \\ -2x_{21} - 0.8x_{23} - 0.5\sin(2x_{23})\end{pmatrix},$$

$$f_3(t, x_3) = \begin{pmatrix} -2.5x_{31} + x_{31}\sin x_{31} + x_{32} + 1.4x_{33} \\ 0.5x_{31} - 2.5x_{32} + x_{33} \\ -2x_{31} + x_{32}x_{33} - 0.6x_{33} - x_{33}\cos x_{33}\end{pmatrix},$$

$$f_4(t, x_4) = \begin{pmatrix} -2.5x_{41} + 1.5x_{42} + 1.5x_{43} \\ x_{41} - 2.5x_{42} + x_{42}^2 + 1.5x_{43} + x_{43}^2 \\ -2x_{41} + x_{41}x_{43} - 2.5x_{43}\end{pmatrix},$$

$$f_5(t, x_5) = \begin{pmatrix} -2.1x_{51} + 0.5x_{51}^2 + 1.4x_{52} + x_{53} \\ 0.9x_{51} - 2.1x_{52} + x_{52}x_{53} + x_{53} \\ -2x_{51} + 0.4x_{52} - 2.1x_{53}\end{pmatrix},$$

$$f_6(t, x_6) = \begin{pmatrix} -3.2x_{61} + 10x_{62} + 2.95\left(|x_{61} + 1| - |x_{61} - 1|\right) \\ x_{61} - x_{62} + x_{63} \\ -14.7x_{62}\end{pmatrix},$$

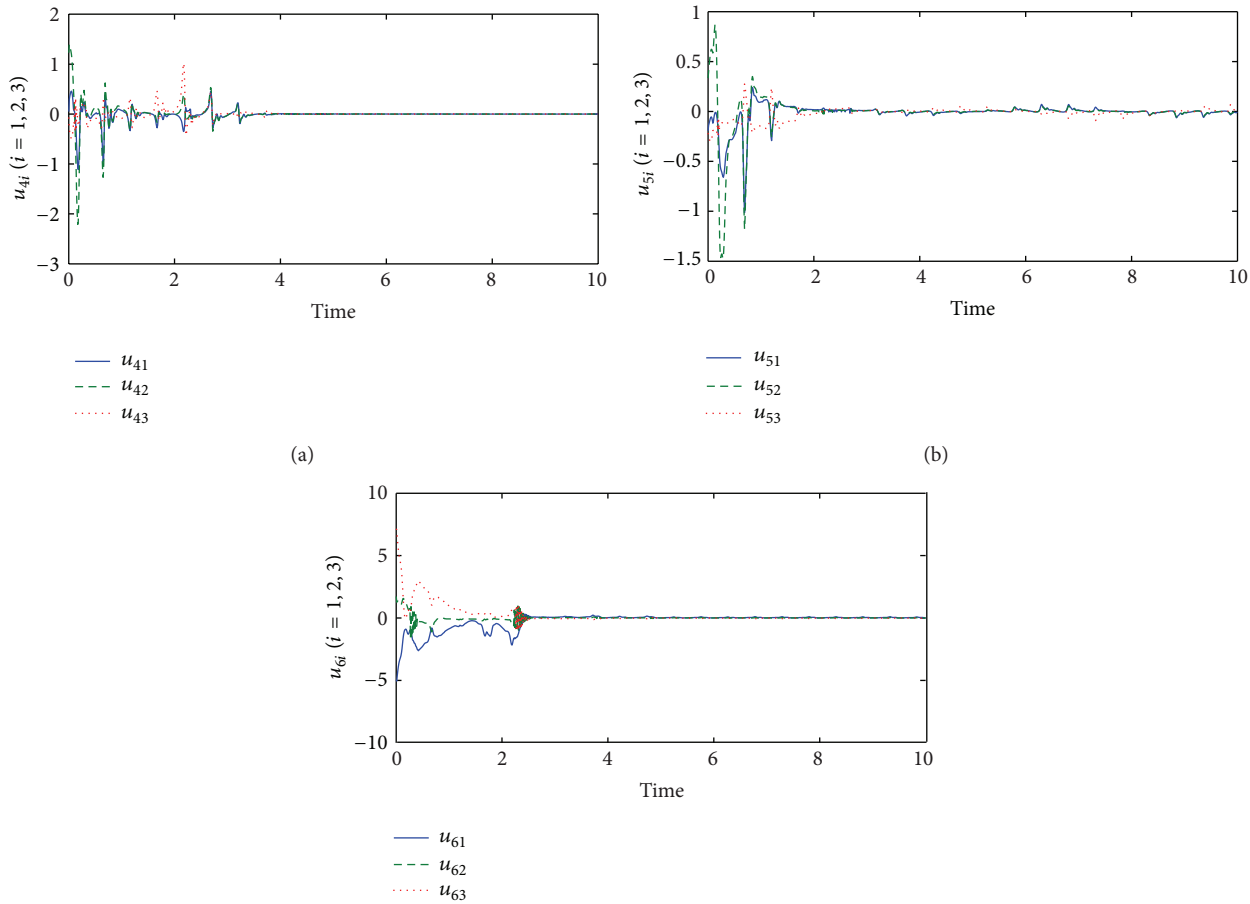

FIGURE 3: The change of curve of control $u_i(t)$ along time: (a) u_{4i}, $i = 1, 2, 3$, (b) u_{5i}, $i = 1, 2, 3$, and (c) u_{6i}, $i = 1, 2, 3$.

$$\Gamma = \begin{bmatrix} 1 & 0 & 0 \\ 0 & 1 & 0 \\ 0 & 0 & 1 \end{bmatrix},$$

$$A = \begin{bmatrix} -3 & 0 & 2 & 1 & 0 & 0 \\ 2 & -5 & 0 & 0 & 2 & 1 \\ 0 & 3 & -4 & 0 & 0 & 1 \\ 1 & 1 & 0 & -5 & 2 & 1 \\ 0 & 0 & 1 & 3 & -4 & 0 \\ 0 & 1 & 1 & 1 & 0 & -3 \end{bmatrix},$$

$$B = \begin{bmatrix} -3 & 2 & 0 & 1 & 0 & 0 \\ 0 & -3 & 0 & 0 & 1 & 2 \\ 0 & 1 & -3 & 2 & 0 & 0 \\ 1 & 0 & 2 & -4 & 0 & 1 \\ 0 & 0 & 1 & 1 & -2 & 0 \\ 2 & 0 & 0 & 0 & 1 & -3 \end{bmatrix}. \tag{51}$$

Nonlinearly parameterized function satisfies

$$\left\| \exp\left(-\varphi_i(t) \begin{pmatrix} x_{j1}^2(t) \\ x_{j2}^2(t) \\ x_{j3}^2(t) \end{pmatrix} \right) - \exp\left(-\varphi_i(t) \begin{pmatrix} s^2(t) \\ s^2(t) \\ s^2(t) \end{pmatrix} \right) \right\|^2 \leq \left\| e_j(t) \right\|^2 2\varphi_i(t) \exp(-1). \tag{52}$$

We choose $\dot{s}(t) = f_6(t, s(t))$, and the parameters are selected as follows:

$$\begin{aligned} &N = 6, \quad T = 0.5, \quad \gamma = 1, \quad H = 5, \\ &\phi_1(t) = 0.2 \sin 8\pi t + 2, \quad \phi_2(t) = 2 \cos 4\pi t + 2, \\ &\phi_3(t) = -\sin 8\pi t + 2, \quad \phi_4(t) = \cos 8\pi t + 2, \\ &\phi_5(t) = -2 \sin 8\pi t + 2, \quad \phi_6(t) = 2 \sin 4\pi t + 2, \\ &\theta = (1, 2, 3, 1.1, 1.5, 1.3)^T, \\ &\alpha = (0.01, 0.01, 0.01, 0.01, 0.01, 0.01)^T. \end{aligned} \tag{53}$$

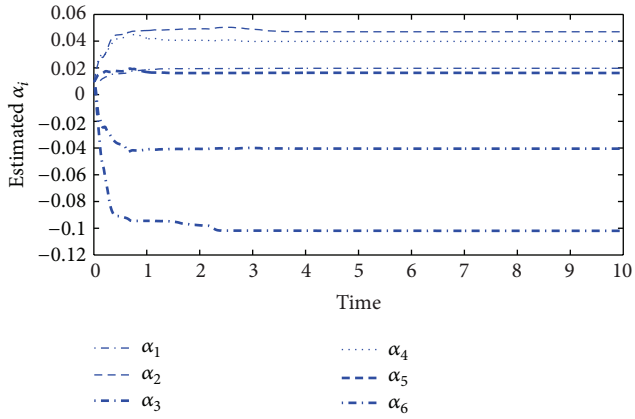

FIGURE 4: The evaluations of parameters α_i along time with $i = 1, \ldots, 6$.

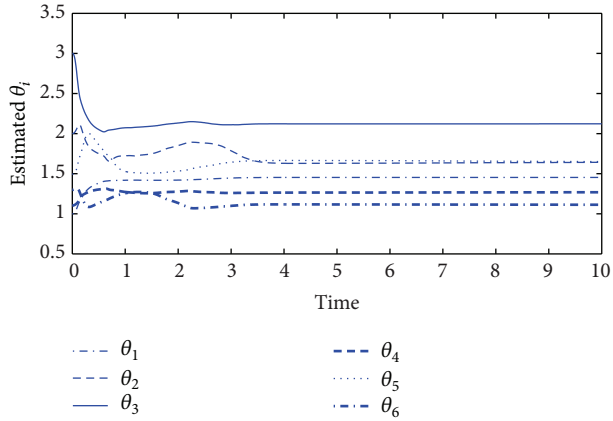

FIGURE 5: The evaluations of parameters θ_i along time with $i = 1, \ldots, 6$.

In the following simulation, we choose

$$q_1 = 1, \quad q_2 = 3, \quad q_3 = 2,$$
$$q_4 = 5, \quad q_5 = 1, \quad q_6 = 2,$$
$$q_{10}(t) = 2tq_1, \quad q_{20}(t) = 2tq_2, \quad q_{30}(t) = 2tq_3,$$
$$q_{40}(t) = 2tq_4, \quad q_{50}(t) = 2tq_5, \quad q_{60}(t) = 2tq_6. \tag{54}$$

The initially estimated values of the unknown parameters are

$$\widehat{\phi}(0) = \begin{pmatrix} 1 & 1 & 1 & 1 & 1 & 1 \end{pmatrix}^T,$$
$$\widehat{\theta}(0) = (1, 2, 3, 1.1, 1.5, 0)^T, \quad \widehat{\alpha}(0) = (0, 0, 0, 0, 0, 0)^T, \tag{55}$$

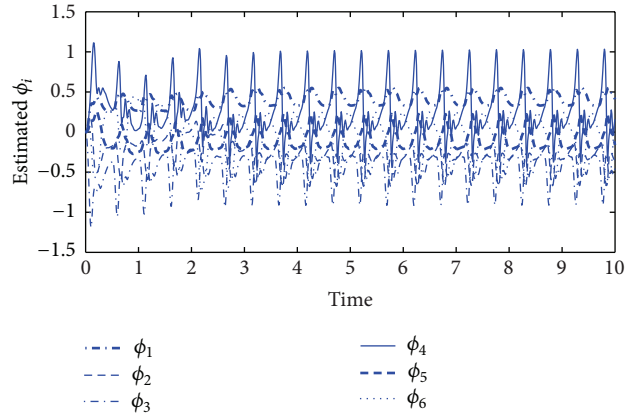

FIGURE 6: The evaluations of parameters ϕ_i along time with $i = 1, \ldots, 6$.

and the initial states are chosen as

$$x_1 = \begin{bmatrix} 0.01 & 0.03 & 0.02 \end{bmatrix}^T, \quad x_2 = \begin{bmatrix} 0.03 & 0.02 & 0.03 \end{bmatrix}^T,$$
$$x_3 = \begin{bmatrix} 0.04 & 0.02 & 0 \end{bmatrix}^T, \quad x_4 = \begin{bmatrix} 0 & 0.05 & 0.03 \end{bmatrix}^T,$$
$$x_5 = \begin{bmatrix} 0.1 & 0 & 0 & .03 \end{bmatrix}^T, \quad x_6 = \begin{bmatrix} 0.1 & 0.01 & 0 \end{bmatrix}^T,$$
$$s = \begin{bmatrix} 0.1 & 0.5 & 0 \end{bmatrix}^T. \tag{56}$$

According to Theorem 12, the synchronization of the complex dynamical network can be guaranteed by the distributed adaptive controllers (10) and the distributed adaptive learning laws (12)–(14). Figure 1 shows the error evolutions under the designed controllers. Figures 2-3 depict the time evolution of the controllers, and Figures 4, 5, and 6 show the evolution of the estimated time-varying parameters. Figures 2–6 show that all signals in the network are bounded.

5. Conclusion

In this paper, a new distributed adaptive learning control method is applied to the synchronization of complex dynamical networks with nonidentical nodes, nonlinear nonderivative coupling, and derivative coupling. The coupling matrix is not assumed to be symmetric or irreducible. By combining inequality techniques and the parameter separation, introducing the composite energy function, the convergence of the tracking error and the boundedness of the system signals are derived. Simulation results demonstrate the effectiveness of the proposed control method. Future effort is needed to design the observer for state derivative.

Acknowledgment

This work was supported by the National Natural Science Foundation of China under Grant no. 60974139.

References

[1] S. H. Strogatz, "Exploring complex networks," *Nature*, vol. 410, no. 6825, pp. 268–276, 2001.

[2] S. Boccaletti, V. Latora, Y. Moreno, M. Chavez, and D.-U. Hwang, "Complex networks: structure and dynamics," *Physics Reports*, vol. 424, no. 4-5, pp. 175–308, 2006.

[3] J. Lü and G. Chen, "A time-varying complex dynamical network model and its controlled synchronization criteria," *IEEE Transactions on Automatic Control*, vol. 50, no. 6, pp. 841–846, 2005.

[4] D. H. Ji, S. C. Jeong, J. H. Park, S. M. Lee, and S. C. Won, "Adaptive lag synchronization for uncertain complex dynamical network with delayed coupling," *Applied Mathematics and Computation*, vol. 218, no. 9, pp. 4872–4880, 2012.

[5] X.-Y. Guo and J.-M. Li, "Stochastic synchronization for time-varying complex dynamical networks," *Chinese Physics B*, vol. 21, no. 2, Article ID 020501, 2012.

[6] J. Hu, Z. D. Wang, H. J. Gao, and L. K. Stergioulas, "Robust sliding mode control for discrete stochastic systems with mixed time delays, randomly occurring uncertainties, and randomly occurring nonlinearities," *IEEE Transactions on Industrial Electronics*, vol. 59, no. 7, pp. 3008–3015, 2012.

[7] G.-P. Jiang, W. K.-S. Tang, and G. Chen, "A state-observer-based approach for synchronization in complex dynamical networks," *IEEE Transactions on Circuits and Systems I*, vol. 53, no. 12, pp. 2739–2745, 2006.

[8] K. Wang, X. Fu, and K. Li, "Cluster synchronization in community networks with nonidentical nodes," *Chaos*, vol. 19, no. 2, Article ID 023106, 2009.

[9] N. Chopra and M. W. Spong, "Output synchronization of nonlinear systems with time delay in communication," in *Proceedings of the 45th IEEE Conference on Decision and Control (CDC '06)*, pp. 4986–4992, December 2006.

[10] S. Jie, E. M. Bollt, and T. Nishikawa, "Constructing generalized synchronization manifolds by manifold equation," *SIAM Journal on Applied Dynamical Systems*, vol. 8, no. 1, pp. 202–221, 2009.

[11] J. Xiang and G. Chen, "On the V-stability of complex dynamical networks," *Automatica*, vol. 43, no. 6, pp. 1049–1057, 2007.

[12] J. G. B. Ramirez and R. Femat, "On the controlled synchronization of dynamical networks with nonidentical nodes," in *Proceedings of the 3rd International IEEE Scientific Conference on Physics and Control*, pp. 1253–1257, 2007.

[13] J. Zhao, D. J. Hill, and T. Liu, "Synchronization of dynamical networks with nonidentical nodes: criteria and control," *IEEE Transactions on Circuits and Systems I*, vol. 58, no. 3, pp. 584–594, 2011.

[14] T. F. Wang, J. M. Li, and S. Tang, "Adaptive synchronization of nonlinearly parameterized complex dynamical networks with unknown time-varying parameters," *Mathematical Problems in Engineering*, vol. 2012, Article ID 592539, 16 pages, 2012.

[15] Y. Kuang, *Delay Differential Equations with Applications in Population Dynamics*, Academic Press, Boston, Mass, USA, 1993.

[16] S.-I. Niculescu, *Delay Effects on Stability: A Robust Control Approach*, Springer, Berlin, Germany, 2001.

[17] D. W. Gong, H. G. Zhang, Z. S. Wang, and B. Huang, "New global synchronization analysis for complex networks with coupling delay based on a useful inequality," *Neural Computing and Applications*, vol. 22, no. 2, pp. 205–210, 2013.

[18] Y. H. Xu, W. N. Zhou, J. A. Fang, and W. Sun, "Adaptive synchronization of the complex dynamical network with non-derivative and derivative coupling," *Physics Letters A*, vol. 374, no. 15-16, pp. 1673–1677, 2010.

[19] J. Wang, L. Feng, and S.-K. Li, "Adaptive synchronization between two delayed complex networks with derivative coupling and non-identical nodes," in *Proceedings of the International Conference on Information and Automation (ICIA '11)*, pp. 135–140, June 2011.

[20] Z. Jia, X. C. Fu, G. M. Deng, and K. Z. Li, "Group synchronization in complex dynamical networks with different types of oscillators and adaptive coupling schemes," *Communications in Nonlinear Science and Numerical Simulation*, vol. 18, no. 10, pp. 2752–2760, 2013.

[21] J. Xiao, Y. H. Yang, and J. S. Long, "Synchronisation of complex networks with derivative coupling via adaptive control," *International Journal of Systems Science*, vol. 44, no. 12, pp. 2183–2189, 2013.

[22] J. Hu, Z. D. Wang, H. J. Gao, and L. K. Stergioulas, "Robust H_∞ sliding mode control for discrete time-delay systems with stochastic nonlinearities," *Journal of the Franklin Institute*, vol. 349, no. 4, pp. 1459–1479, 2012.

[23] J. Hu, Z. D. Wang, Y. G. Niu, and L. K. Stergioulas, "H_∞ sliding mode observer design for a class of nonlinear discrete time-delay systems: a delay-fractioning approach," *International Journal of Robust and Nonlinear Control*, vol. 22, no. 16, pp. 1806–1826, 2012.

[24] J. Hu, Z. D. Wang, and H. J. Gao, "A delay fractioning approach to robust sliding mode control for discrete-time stochastic systems with randomly occurring non-linearities," *IMA Journal of Mathematical Control and Information*, vol. 28, no. 3, pp. 345–363, 2011.

[25] J.-X. Xu and Y. Tan, "A composite energy function-based learning control approach for nonlinear systems with time-varying parametric uncertainties," *IEEE Transactions on Automatic Control*, vol. 47, no. 11, pp. 1940–1945, 2002.

[26] J. Zhou, J.-A. Lu, and J. H. Lü, "Adaptive synchronization of an uncertain complex dynamical network," *IEEE Transactions on Automatic Control*, vol. 51, no. 4, pp. 652–656, 2006.

[27] Z. S. Wang and H. G. Zhang, "Synchronization stability in complex interconnected neural networks with nonsymmetric coupling," *Neurocomputing*, vol. 108, pp. 84–92, 2013.

[28] W. Lin and C. J. Qian, "Adaptive control of nonlinearly parameterized systems: the smooth feedback case," *IEEE Transactions on Automatic Control*, vol. 47, no. 8, pp. 1249–1266, 2002.

Hindawi Publishing Corporation
Mathematical Problems in Engineering
Volume 2013, Article ID 163769, 8 pages
http://dx.doi.org/10.1155/2013/163769

Research Article

Robust H_∞ Control for Discrete-Time Stochastic Interval System with Time Delay

Shengchun Yu,[1] Guici Chen,[1,2] and Yi Shen[3]

[1] *Hubei Province Key Laboratory of Systems Science in Metallurgical Process, Wuhan University of Science & Technology, Wuhan 430081, China*
[2] *School of Hydropower & Information Engineering, Huazhong University of Science & Technology, Wuhan 430074, China*
[3] *School of Automation, Huazhong University of Science & Technology, Wuhan 430074, China*

Correspondence should be addressed to Guici Chen; gcichen@aliyun.com

Received 23 April 2013; Accepted 26 August 2013

Academic Editor: Bo Shen

The robust H_∞ control problem for discrete-time stochastic interval system (DTSIS) with time delay is investigated in this paper. The stochastic interval system is equivalently transformed into a kind of stochastic uncertain time-delay system firstly. By constructing the appropriate Lyapunov-Krasovskii functional, the sufficient conditions for the existence of the robust H_∞ controller for DTSIS are obtained in terms of linear matrix inequality (LMI) form, and the robust H_∞ controller is designed. Finally, a numerical example with simulation is given to show the effectiveness and correctness of the designed robust H_∞ controller.

1. Introduction

In the past few years, much research effort has paid to the robust control problems for stochastic systems which have come to play an important role in many fields including communication network, image processes, and mobile robot localization. So far, plenty of significant results also have been published; see, for example, [1–3] and the references therein. In the meantime, we all know that time delay arises naturally in many mathematical (non) linear models of real phenomena, such as communication, circuits theory, biology, mechanics, electronics, hydraulic, rolling mill, chemical systems, and computer controlled systems, and which is frequently one of the main sources of instability, oscillation and poor performance of control systems. So the stability analysis and robust control for dynamic time-delay systems have attracted a number of researchers; see, for example, [4–8] and the references therein.

Meanwhile, from Hinrichsen who presented the H_∞ control problems for stochastic systems in 1998 [9], more and more experts begin to study the stochastic H_∞ control problems [10–17]. In the view of dissipation, Berman develops a H_∞-type theory for a large class of time-continuous stochastic nonlinear systems. In particular, it introduces the notion of stochastic dissipative systems by analogy with the familiar notion of dissipation associated with the deterministic systems. The problem of H_∞ output feedback control for uncertain stochastic systems with time-varying delay is discussed in [12], and the parameter uncertainties are assumed to be time-varying norm-bounded. Xu et al. [13] investigate the problems of robust stochastic stabilization and robust H_∞ control for uncertain neutral stochastic time-delay systems.

On the other hand, when modeling real-time plants, the parameter uncertainties are unavoidable, which are very often the cause of instability and poor performance, such as modeling error, external perturbation, and parameter fluctuation during the physical implementation. As a result, the parameters of a system matrix are estimated only within certain closed intervals. We call this kind of system interval system or stochastic interval system (SIS) with the following form:

$$\dot{x}(t) = Ax(t), \tag{1}$$

or

$$dx(t) = Ax(t)\,dt + Hx(t)\,d\omega(t), \tag{2}$$

where $A \in [\underline{A}, \overline{A}]$, $H \in [\underline{H}, \overline{H}]$, and $\underline{\cdot}, \overline{\cdot}$ denote the lower and upper bounds of the interval for the coefficients, respectively. Interval system and stochastic interval system have been well known for their importance in practice applications. And in recent years, the stability analysis and stabilization problems of various interval systems have received plenty of research attention; see, for example, [18–24] and the references therein. Of course, there are a lot of research works on stability analysis and stabilization problems for stochastic interval system that have been reported; see, for example, [25–29] and the references therein. However, to the best of authors' knowledge, so far little results on robust H_∞ control problem for stochastic interval system with time-delay are available in the existing literature.

Inspired by the above discussions, in this paper we study the robust H_∞ control problem for discrete-time stochastic interval system (DTSIS) with time delay. The stochastic interval system will be equivalently transformed into a kind of stochastic uncertain time-delay system firstly. By constructing appropriate Lyapunov-Krasovskii functional, the sufficient conditions for the existence of the robust H_∞ controller for DTSIS are obtained in terms of linear matrix inequality (LMI) form, and the robust H_∞ controller can be designed by MATLAB LMI control toolbox.

2. Problems Formulation and Preliminaries

Consider the following discrete-time stochastic interval system (DTSIS) with time delay:

$$\begin{aligned} x(k+1) &= A^l x(k) + A_d^l x(k-d) + Bu(k) + Dv(k) \\ &\quad + \left[H^l x(k) + H_d^l x(k-d)\right]\omega(k), \\ z(k) &= C^l x(k) + C_d^l x(k-d), \\ x(k) &= \varphi(k), \quad k \in [-d, 0], \end{aligned} \tag{3}$$

where $x(k) \in \mathbb{R}^n$ is the state vector; $d > 0$ is the time delay; $u(k) \in \mathbb{R}^m$ is the control input; $z(k) \in \mathbb{R}^q$ is the control output; $v(k) \in \mathbb{R}^p$ is the exogenous disturbance input, which satisfies $v(k) \in L_2([0,\infty), \mathbb{R}^p)$, where $L_2([0,\infty), \mathbb{R}^p)$ is the space of nonanticipatory square-summable stochastic process with respect to $(\mathcal{F}_k)_{k\in I^+}$ with the following norm:

$$\|v(k)\|_2^2 = \mathbb{E}\left\{\sum_{k=0}^{\infty}\|v(k)\|^2\right\} = \sum_{k=0}^{\infty}\mathbb{E}\left\{\|v(k)\|^2\right\}. \tag{4}$$

$\omega(k) \in \mathbb{R}^l$ is a scalar Brownian motion defined on a complete probability space $(\Theta, \mathcal{F}, P)$ with

$$\mathbb{E}[\omega(k)] = 0, \qquad \mathbb{E}\left[\omega^2(k)\right] = 1. \tag{5}$$

In the system (3), A^l is an interval matrix with appropriate dimension, which means

$$\begin{aligned} A^l &= \left[\underline{A}, \overline{A}\right] \\ &= \left\{\left(a_{ij}\right) \in \mathbb{R}^{n\times n} \mid \underline{a}_{ij} \le a_{ij} \le \overline{a}_{ij}, i, j = 1, 2, \ldots, n\right\}, \end{aligned} \tag{6}$$

where $\underline{A} = (\underline{a}_{ij})_{n\times n}$, $\overline{A} = (\overline{a}_{ij})_{n\times n}$ are determinate matrices.

Remark 1. It is not difficult to see that the matrices $A^l, A_d^l, H^l, H_d^l, C^l, C_d^l$ can also be time-dependent as long as the mappings $A^l : R_+ \to [\underline{A}, \overline{A}]$, $A_d^l : R_+ \to [\underline{A}_d, \overline{A}_d]$, $H^l : R_+ \to [\underline{H}, \overline{H}]$, $H_d^l : R_+ \to [\underline{H}_d, \overline{H}_d]$, $C^l : R_+ \to [\underline{C}, \overline{C}]$, and $C_d^l : R_+ \to [\underline{C}_d, \overline{C}_d]$ are continuous.

Set

$$\begin{aligned} A &= \frac{1}{2}\left[\underline{A} + \overline{A}\right], \\ \Delta &= \frac{1}{2}\left[\overline{A} - \underline{A}\right] = \left(\delta_{ij}\right)_{n\times n}, \\ D_1 &= \left(\sqrt{\delta_{11}}e_1, \ldots, \sqrt{\delta_{1n}}e_1, \ldots, \sqrt{\delta_{n1}}e_n, \ldots, \sqrt{\delta_{nn}}e_n\right), \\ G_1 &= \left(\sqrt{\delta_{11}}e_1, \ldots, \sqrt{\delta_{1n}}e_1, \ldots, \sqrt{\delta_{n1}}e_n, \ldots, \sqrt{\delta_{nn}}e_n\right)^T, \end{aligned} \tag{7}$$

where $e_i (i = 1, 2, \ldots, n)$ is the ith column of $n\times n$ identification matrix, setting

$$\overline{F} = \left\{f \mid f = \operatorname{diag}\left\{\alpha_{11}, \ldots, \alpha_{1n}, \ldots, \alpha_{n1} \ldots, \alpha_{nn}\right\}\right\}, \tag{8}$$

where $\|\alpha_{ij}\| \le 1$. Obviously, we have $F_1 F_1^T \le I_{n^2}$; here I_{n^2} is the $n^2 \times n^2$ identification matrix. So the interval matrix A^l can equivalently be written as

$$\begin{aligned} A^l &= \left[\underline{A}, \overline{A}\right] = A + \Delta A \\ &= A + D_1 F_1 G_1, \quad F_1 \in \overline{F}. \end{aligned} \tag{9}$$

Similar to the above derivation, we can have

$$\begin{aligned} A_d^l &= \left[\underline{A}_d, \overline{A}_d\right] = A_d + \Delta A_d = A_d + D_2 F_2 G_2, \\ H^l &= \left[\underline{H}, \overline{H}\right] = H + \Delta H = H + D_3 F_3 G_3, \\ H_{\mathrm{d}}^l &= \left[\underline{H}_d, \overline{H}_d\right] = H_d + \Delta H_d = H_d + D_4 F_4 G_4, \\ C^l &= \left[\underline{C}, \overline{C}\right] = C + \Delta C = C + D_5 F_5 G_5, \end{aligned} \tag{10}$$

$$C_d^l = \left[\underline{C}_d, \overline{C}_d\right] = C_d + \Delta C_d = C_d + D_6 F_6 G_6; \tag{11}$$

where $F_i \in \overline{F}$, $i = 1, 2, \ldots, 6$; let

$$\begin{aligned} \widetilde{F} &= \operatorname{diag}\{F_1, F_2, \ldots, F_6\}, \\ E_1 &= (D_1, D_2, 0, 0, 0, 0), \\ E_2 &= (0, 0, D_3, D_4, 0, 0), \\ E_3 &= (0, 0, 0, 0, D_5, D_6), \\ N_1^T &= (G_1^T, 0, G_3^T, 0, G_5^T, 0), \\ N_2^T &= (0, G_2^T, 0, G_4^T, 0, G_6^T). \end{aligned} \tag{12}$$

Then (9)–(11) can be rewritten as

$$\begin{pmatrix} \Delta A & \Delta A_d \\ \Delta H & \Delta H_d \\ \Delta C & \Delta C_d \end{pmatrix} = \begin{pmatrix} E_1 \\ E_2 \\ E_3 \end{pmatrix} \widetilde{F} \begin{pmatrix} N_1 & N_2 \end{pmatrix}. \tag{13}$$

So the system (3) can be readily derived as

$$\begin{aligned} x(k+1) &= (A + \Delta A)\, x(k) + (A_d + \Delta A_d)\, x(k-d) \\ &\quad + Bu(k) + Dv(k) + (H + \Delta H)\, x(k)\, \omega(k) \\ &\quad + (H_d + \Delta H_d)\, x(k-d)\, \omega(k), \\ z(k) &= (C + \Delta C)\, x(k) + (C_d + \Delta C_d)\, x(k-d), \\ x(k) &= \varphi(k), \quad k \in [-d, 0]. \end{aligned} \tag{14}$$

For system (14), we design the following state feedback controller:

$$u(k) = Kx(k), \tag{15}$$

where the matrix K is the controller gain, which is to be designed. Then the closed-loop stochastic control system can be rewritten as

$$\begin{aligned} x(k+1) &= \widetilde{A}x(k) + \widetilde{A}_d x(k-d) + Dv(k) \\ &\quad + \left[\widetilde{H}x(k) + \widetilde{H}_d x(k-d)\right] \omega(k), \\ z(k) &= \widetilde{C}x(k) + \widetilde{C}_d x(k-d), \end{aligned} \tag{16}$$

where $\widetilde{A} = A + BK + \Delta A$, $\widetilde{A}_d A_d + \Delta A_d$, $\widetilde{H} = H + \Delta H$, $\widetilde{H}_d = H_d + \Delta H_d$, $\widetilde{C} = C + \Delta C$, $\widetilde{C}_d = C_d + \Delta C_d$.

Definition 2. Discrete-time stochastic interval system (DTSIS) with time delay (3) is said to be stochastic exponentially stable in mean square, if there exist scalars $c > 0$, $\mu > 1$, such that

$$\mathbb{E}|x(N)|^2 \le c\mu^{-N} \max_{-d \le i \le 0} \mathbb{E}\left|\varphi(i)\right|^2. \tag{17}$$

In this paper, we aim to design the controller gain matrix K in (16) such that the requirements are simultaneously satisfied.

(a) The zero-solution of the closed-loop stochastic control system (16) with $v(k) = 0$ is stochastic exponentially stable in mean square.

(b) Under the zero-initial condition, the control output $z(k)$ satisfies

$$\sum_{k=0}^{\infty} \mathbb{E}\left\{\|z(k)\|^2\right\} \le \gamma^2 \sum_{k=0}^{\infty} \mathbb{E}\left\{\|v(k)\|^2\right\} \tag{18}$$

for all nonzero $v(k)$.

Which is also said the closed-loop stochastic control system (16) is stochastic exponentially stable in mean square with disturbance attenuation level $\gamma > 0$.

Lemma 3 (see [30]). *For given symmetric matrix Σ, and matrices H, E with appropriate dimension, $\Sigma + HFE + E^T F^T H^T < 0$ with F satisfying $F^T F \le I$ holds if and only if $\Sigma + a^{-1} HH^T + aE^T E < 0$ holds for any $a > 0$.*

3. Main Results

Theorem 4. *If there exist two positive definite matrices P and Q, and for a given positive constant $\gamma > 0$, such that the following matrix inequality holds:*

$$\Sigma = \begin{pmatrix} Q - P & 0 & 0 & \widetilde{A}^T & \widetilde{H}^T & \widetilde{C}^T \\ * & -Q & 0 & \widetilde{A}_d^T & \widetilde{H}_d^T & \widetilde{C}_d^T \\ * & * & -\gamma^2 I & D^T & 0 & 0 \\ * & * & * & -P^{-1} & 0 & 0 \\ * & * & * & * & -P^{-1} & 0 \\ * & * & * & * & * & -I \end{pmatrix} < 0, \tag{19}$$

then the closed-loop stochastic control system (16) is stochastic exponentially stable in mean square with disturbance attenuation level γ.

Proof. Let $v(k) = 0$; we construct the Lyapunov-Krasovskii functional as

$$V(k) = x^T(k) Px(k) + \sum_{i=1}^{d} x^T(k-i) Qx(k-i). \tag{20}$$

Calculating the difference of $V(k)$ along with the system (16) and taking the mathematical expectation, we have

$$\begin{aligned} \mathbb{E}\{\Delta V(k)\} &= E\{V(k+1) - V(k)\} \\ &= x^T(k+1) Px(k+1) - x^T(k) Px(k) \\ &\quad + x^T(k) Qx(k) - x^T(k-d) Qx(k-d) \\ &= \begin{pmatrix} x(k) \\ x(k-d) \end{pmatrix}^T \Pi_1 \begin{pmatrix} x(k) \\ x(k-d) \end{pmatrix}, \end{aligned} \tag{21}$$

where

$$\begin{aligned} \Pi_1 &= \begin{pmatrix} Q - P & 0 \\ 0 & -Q \end{pmatrix} + \begin{pmatrix} \widetilde{A}^T \\ \widetilde{A}_d^T \end{pmatrix} P \begin{pmatrix} \widetilde{A}^T \\ \widetilde{A}_d^T \end{pmatrix}^T \\ &\quad + \begin{pmatrix} \widetilde{H}^T \\ \widetilde{H}_d^T \end{pmatrix} P \begin{pmatrix} \widetilde{H}^T \\ \widetilde{H}_d^T \end{pmatrix}^T. \end{aligned} \tag{22}$$

It is clear form $\Sigma < 0$ that there exists a sufficient scalar $a > 0$, such that

$$\Sigma + a \operatorname{diag}\{I_{n\times n}, 0\} < 0. \tag{23}$$

Therefore, we have

$$\mathbb{E}\{\Delta V(k)\} \le -a\mathbb{E}\left\{|x(k)|^2\right\}. \tag{24}$$

We now in a position to analyze of the exponential stable in mean square for the stochastic interval delay system (16). According to the definition of $V(k)$, we have

$$\mathbb{E}\{V(k)\} \le \rho_1\mathbb{E}\left\{|x(k)|^2\right\} + \rho_2\sum_{k=1}^{d}\mathbb{E}\left\{|x(k-i)|^2\right\}, \tag{25}$$

where $\rho_1 = \lambda_{\max}(P)$ and $\rho_2 = \lambda_{\max}(Q)$. For any scalar $\mu > 1$, the earlier inequality, together with (23), implies that

$$\begin{aligned}
&\mu^{k+1}\mathbb{E}\{V(k+1)\} - \mu^k\mathbb{E}\{V(k)\| \\
&\quad = \mu^{k+1}\mathbb{E}\|\Delta V(k)\| + \mu^k(\mu-1)\mathbb{E}\{V(k)\} \\
&\quad \le \beta_1(\mu)\mu^k\mathbb{E}\left\{|x(k)|^2\right\} \\
&\qquad + \beta_2(\mu)\mu^k\sum_{i=1}^{d}\mathbb{E}\left\{|x(k-i)|^2\right\},
\end{aligned} \tag{26}$$

where $\beta_1(\mu) = -a\mu + \rho_1(\mu-1), \beta_2(\mu) = (\mu-1)\rho_2$.

Furthermore, summing up both sides of the earlier inequality from 0 to $N-1$ with respect to k, we get

$$\begin{aligned}
&\mu^N\mathbb{E}\{V(N)\} - \mathbb{E}\{V(0)\} \\
&\quad \le \beta_1(\mu)\sum_{k=0}^{N-1}\mu^k\mathbb{E}\left\{|x(k)|^2\right\} \\
&\qquad + \beta_2(\mu)\sum_{k=0}^{N-1}\sum_{i=1}^{d}\mu^k\mathbb{E}\left\{|x(k-i)|^2\right\}.
\end{aligned} \tag{27}$$

For $d > 1$,

$$\begin{aligned}
&\sum_{k=0}^{N-1}\sum_{i=1}^{d}\mu^k\mathbb{E}\left\{|x(k-i)|^2\right\} \\
&\quad \le \left(\sum_{i=-d}^{-1}\sum_{k=0}^{i+d} + \sum_{i=0}^{N-1-d}\sum_{k=i+1}^{i+d} + \sum_{i=N-1-d}^{N-1}\sum_{k=i+1}^{N-1}\right)\mu^k\mathbb{E}\left\{|x(i)|^2\right\} \\
&\quad \le \sum_{i=-d}^{-1}\mu^{i+d}\mathbb{E}\left\{|x(i)|^2\right\} + d\sum_{i=0}^{N-1-d}\mu^{i+d}\mathbb{E}\left\{|x(i)|^2\right\} \\
&\qquad + d\sum_{i=N-1-d}^{N-1}\mu^{i+d}\mathbb{E}\left\{|x(i)|^2\right\} \\
&\quad \le d\mu^d\max_{-d\le i\le 0}\mathbb{E}\left\{|\varphi(i)|^2\right\} + d\mu^d\sum_{i=0}^{N-1}\mathbb{E}\left\{|x(i)|^2\right\}.
\end{aligned} \tag{28}$$

Then, from (27) and (28), it follows that

$$\begin{aligned}
\mu^N\mathbb{E}\{V(N)\} &\le \mathbb{E}\{V(0)\} + \left(\beta_1(\mu) + d\mu^d\beta_2(\mu)\right) \\
&\quad \times \sum_{k=0}^{N-1}\mu^k\mathbb{E}\left\{|x(k)|^2\right\} \\
&\quad + d\mu^d\beta_2(\mu)\max_{-d\le i\le 0}\mathbb{E}\left\{|\varphi(i)|^2\right\}.
\end{aligned} \tag{29}$$

Let $\rho_0 = \lambda_{\min}(P)$ and $\rho = \max\{\rho_1, \rho_2\}$; we have

$$\mathbb{E}\{V(N)\} \ge \rho_0\mathbb{E}\left\{|x(N)|^2\right\}. \tag{30}$$

It also follows that

$$\mathbb{E}\{V(0)\} \le \rho\max_{-d\le i\le 0}\mathbb{E}\left\{|\varphi(i)|^2\right\}. \tag{31}$$

We can choose appropriate scalar $\sigma > 0$ such that

$$\beta_1(\sigma) + d\sigma^d\beta_2(\sigma) = 0, \tag{32}$$

which implies

$$\mathbb{E}\left\{|x(N)|^2\right\} \le c\mu^{-N}\max_{-d\le i\le 0}\mathbb{E}\left\{|\varphi(i)|^2\right\}, \tag{33}$$

where $c = (1/\rho_0)(\rho + d\sigma^d\beta_2(\sigma))$. Hence the closed-loop stochastic control system (16) with $v(k) = 0$ is stochastic exponentially stable in mean square according to Definition 2.

Under the zero-initial condition, let $v(k) \ne 0$, setting

$$\begin{aligned}
J(N) &= \mathbb{E}\left\{\sum_{k=0}^{N}\left[z^T(k)z(k) - \gamma^2v^T(k)v(k)\right]\right\} \\
&= \mathbb{E}\left\{\sum_{k=0}^{N}\left[z^T(k)z(k) - \gamma^2v^T(k)v(k) \right.\right. \\
&\qquad \left.\left. + V(k+1) - V(k)\right]\right\} \\
&\quad - V(N+1) \\
&\le \mathbb{E}\left\{\sum_{k=0}^{N}\left[z^T(k)z(k) - \gamma^2v^T(k)v(k) + \Delta V(k)\right]\right\} \\
&= \sum_{k=0}^{N}\begin{pmatrix} x(k) \\ x(k-d) \\ v(k)\end{pmatrix}^T\Pi_2\begin{pmatrix} x(k) \\ x(k-d) \\ v(k)\end{pmatrix},
\end{aligned} \tag{34}$$

where

$$\begin{aligned}
\Pi_2 &= \begin{pmatrix} Q-P & 0 & 0 \\ 0 & -Q & 0 \\ 0 & 0 & -\gamma^2I\end{pmatrix} + \begin{pmatrix} \widetilde{A}^T \\ \widetilde{A}_d^T \\ \\ D^T\end{pmatrix}P\begin{pmatrix} \widetilde{A}^T \\ \widetilde{A}_d^T \\ \\ D^T\end{pmatrix}^T \\
&\quad + \begin{pmatrix} \widetilde{H}^T \\ \widetilde{H}_d^T \\ 0\end{pmatrix}P\begin{pmatrix} \widetilde{H}^T \\ \widetilde{H}_d^T \\ 0\end{pmatrix}^T + \begin{pmatrix} \widetilde{C}^T \\ \widetilde{C}_d^T \\ 0\end{pmatrix}\begin{pmatrix} \widetilde{C}^T \\ \widetilde{C}_d^T \\ 0\end{pmatrix}^T.
\end{aligned} \tag{35}$$

So (19) implies that $\Pi_2 < 0$; hence, $J(N) < 0$. Thus $N \to \infty$, $J(\infty) < 0$, such that (18) holds. The proof is completed. □

To design the controller (15), matrix inequality (15) must be solvable and matrix inequality (15) in Theorem 4 must be inverted into LMI form. In the following section, we will find a way for the solution of (15).

Remark 5. The results obtained in the paper are based on the Lyapunov-Krasovskii functional and the corresponding technique used in the proof of Theorem 4, and it is easy to extend the results to stochastic system with time-varying delay or multiple delays. Details are omitted here due to page length consideration.

Theorem 6. *If there exist two positive definite matrices $X, \widetilde{Q}$, a matrix Y with appropriate dimension, and a positive constant ε, for a given positive constant $\gamma > 0$, such that the following linear matrix inequality (LMI) holds*

$$\begin{pmatrix} \widetilde{Q}-X & 0 & 0 & \Omega & XH^T & XC^T & XN_1^T & 0 \\ * & -\widetilde{Q} & 0 & XA_d^T & XH_d^T & XC_d^T & XN_2^T & 0 \\ * & * & -\gamma^2 I & D^T & 0 & 0 & 0 & 0 \\ * & * & * & -X & 0 & 0 & 0 & \varepsilon E_1 \\ * & * & * & * & -X & 0 & 0 & \varepsilon E_2 \\ * & * & * & * & * & -I & 0 & \varepsilon E_3 \\ * & * & * & * & * & * & -\varepsilon I & 0 \\ * & * & * & * & * & * & * & -\varepsilon I \end{pmatrix} < 0, \tag{36}$$

where $\Omega = Y^T B^T + XA^T$, then the closed-loop stochastic control system (16) *is stochastic exponentially stable in mean square with disturbance attenuation level γ with the controller designed as $K = YX^{-1}$.*

Proof. By (13) and (19), we have

$$\Pi + \Theta_1 \widetilde{F}^T \Theta_2^T + \Theta_2 \widetilde{F} \Theta_1^T < 0, \tag{37}$$

where

$$\Pi = \begin{pmatrix} Q-P & 0 & 0 & (A+BK)^T & H^T & C^T \\ * & -Q & 0 & A_d^T & H_d^T & C_d^T \\ * & * & -\gamma^2 I & D^T & 0 & 0 \\ * & * & * & -P^{-1} & 0 & 0 \\ * & * & * & * & -P^{-1} & 0 \\ * & * & * & * & * & -I \end{pmatrix} \tag{38}$$

$$\Theta_1^T = \left(N_1, N_2, 0_{1\times 4}\right), \qquad \Theta_2^T = \left(0_{1\times 3}, E_1^T, E_2^T, E_3^T\right).$$

By Lemma 3, we know that

$$\Pi + \varepsilon^{-1} \Theta_1 \Theta_1^T + \varepsilon \Theta_2 \Theta_2^T < 0. \tag{39}$$

Using Schur complement lemma and contragradient transformation, we can get the LMI (36) holds. The proof is completed. □

Without considering of interval matrices, the system (3) changes into the following discrete-time stochastic time-delay system:

$$\begin{aligned} x(k+1) &= Ax(k) + A_d x(k-d) + Bu(k) \\ &\quad + Dv(k) + \left[Hx(k) + H_d x(k-d)\right] \omega(k), \\ z(k) &= Cx(k) + C_d x(k-d), \\ x(k) &= \varphi(k), \quad k \in [-d, 0]. \end{aligned} \tag{40}$$

We can design the controller (15) by the following the corollary without proof.

Corollary 7. *If there exist two positive definite matrices $X, \widetilde{Q}$ and a matrix Y with appropriate dimension, for a given positive constant $\gamma > 0$, such that the following linear matrix inequality (LMI) holds*

$$\begin{pmatrix} \widetilde{Q}-X & 0 & 0 & \Omega & XH^T & XC^T \\ * & -\widetilde{Q} & 0 & XA_d^T & XH_d^T & XC_d^T \\ * & * & -\gamma^2 I & D^T & 0 & 0 \\ * & * & * & -X & 0 & 0 \\ * & * & * & * & -X & 0 \\ * & * & * & * & * & -I \end{pmatrix} < 0, \tag{41}$$

where Ω is defined in (36)*, then the closed-loop stochastic control system* (40) *is stochastic exponentially stable in mean square with disturbance attenuation level γ with the controller designed as $K = YX^{-1}$.*

If we do not consider the stochastic disturbance in system (3), the system (3) can be written as

$$\begin{aligned} x(k+1) &= A^l x(k) + A_d^l x(k-d) \\ &\quad + Bu(k) + Dv(k), \\ z(k) &= C^l x(k) + C_d^l x(k-d), \\ x(k) &= \varphi(k), \quad k \in [-d, 0]. \end{aligned} \tag{42}$$

Then the robust H_∞ controller can be designed by the following corollary.

Corollary 8. *If there exist two positive definite matrices $X, \widetilde{Q}$, a matrix Y with appropriate dimension, and a positive constant ε, for a given positive constant $\gamma > 0$, such that the following linear matrix inequality (LMI) holds*

$$\begin{pmatrix} \widetilde{Q}-X & 0 & 0 & \Omega & XC^T & XN_1^T & 0 \\ * & -\widetilde{Q} & 0 & XA_d^T & XC_d^T & XN_2^T & 0 \\ * & * & -\gamma^2 I & D^T & 0 & 0 & 0 \\ * & * & * & -X & 0 & 0 & \varepsilon E_1 \\ * & * & * & * & -I & 0 & \varepsilon E_3 \\ * & * & * & * & * & -\varepsilon I & 0 \\ * & * & * & * & * & * & -\varepsilon I \end{pmatrix} < 0, \tag{43}$$

where Ω *is defined in* (36)*, then the closed-loop stochastic control system* (42) *is exponentially stable with disturbance attenuation level* γ *with the controller designed as* $K = YX^{-1}$.

4. Numerical Example with Simulation

In this section, an example is given to show the usefulness of the designed controller. Consider the following discrete-time stochastic interval system with time delay:

$$\begin{aligned} x(k+1) &= \begin{pmatrix} 1 & [0.5, 0.7] \\ 0.2 & [0.1, 0.3] \end{pmatrix} x(k) + \begin{pmatrix} 0.2 \\ 0.3 \end{pmatrix} u(k) \\ &\quad + \begin{pmatrix} [-0.1, 0.1] & 0 \\ 0.15 & [-0.5, 0.2] \end{pmatrix} x(k-10) \\ &\quad + \begin{pmatrix} -0.1 & 0.1 \\ -0.1 & 0.2 \end{pmatrix} \begin{pmatrix} e^{-0.2k} \sin k \\ -e^{-0.1k} \cos 2k \end{pmatrix} \\ &\quad + \left\{ \begin{pmatrix} [0.1, 0.3] & 0 \\ 0.3 & [-0.2, 0.1] \end{pmatrix} x(k) \right. \\ &\quad \left. + \begin{pmatrix} -0.1 & [-0.1, 0.1] \\ 0 & [-0.1, 0.2] \end{pmatrix} x(k-10) \right\} \omega(k), \\ z(k) &= \begin{pmatrix} [-0.1, 0.1] & 0.1 \\ 0 & 0.2 \end{pmatrix} x(k) \\ &\quad + \begin{pmatrix} [0, 0.1] & [0.1, 0.3] \\ -0.1 & 0 \end{pmatrix} x(k-10), \\ x(k) &= \varphi(k), \quad k \in [-10, 0]. \end{aligned} \tag{44}$$

Without considering the state-feedback control, we see that the open-loop stochastic interval system is unstable from Figure 1.

We aim at designing a state-feedback controller for stochastic interval system (44), such that the closed-loop stochastic interval system is stochastic exponentially stable in mean square with disturbance attenuation level γ.

By using the method discussed in the previous section, we can calculate the matrices $A, A_d, H, H_d, C, C_d, D_i, G_i$, $i = 1, 2, \ldots, 6$, setting $\gamma = 0.9$, solving the LMI (36) in Theorem 6 and then obtain the matrices as follows:

$$\begin{aligned} X &= \begin{pmatrix} 0.7147 & 0.0706 \\ 0.0706 & 1.3303 \end{pmatrix}, \\ \widetilde{Q} &= \begin{pmatrix} 0.2442 & 0.0285 \\ 0.0285 & 0.9091 \end{pmatrix}, \\ Y &= \begin{pmatrix} -2.8706 & -0.5642 \end{pmatrix}, \\ \varepsilon &= 2.2710. \end{aligned} \tag{45}$$

Note that in expression of Theorem 6, we can design the controller as

$$K = YX^{-1} = \begin{pmatrix} -3.9954 & -0.2119 \end{pmatrix}. \tag{46}$$

The response of the closed-loop stochastic interval system (44) is shown in Figures 2 and 3, which demonstrate that the designed controller for the stochastic interval system (44) is effective.

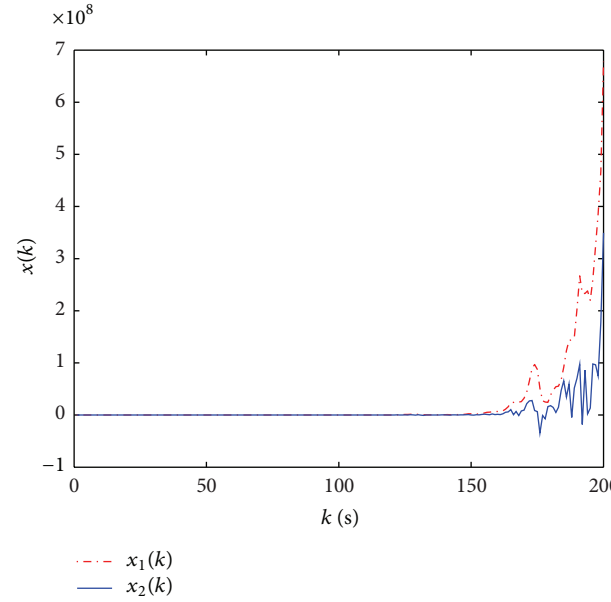

Figure 1: Response of open-loop DTSIS (44) to initial state $(5, -3)$.

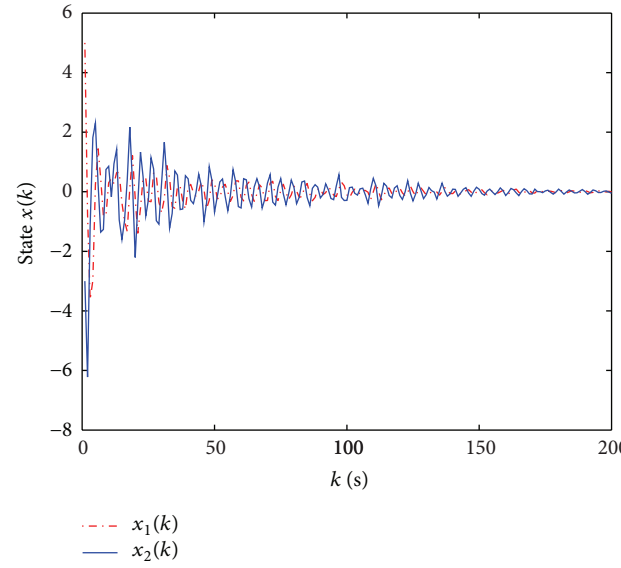

Figure 2: Response of closed-loop DTSIS (44) to initial state $(5, -3)$.

5. Conclusions

In this paper, we have studied the robust H_∞ control problem for discrete-time stochastic interval system (DTSIS) with time delay. The stochastic interval system was equivalently transformed into a kind of stochastic uncertain time-delay system firstly. By constructing appropriate Lyapunov-Krasovskii functional, the sufficient conditions for the existence of the robust H_∞ controller for DTSIS have been obtained in terms of linear matrix inequality (LMI) form,

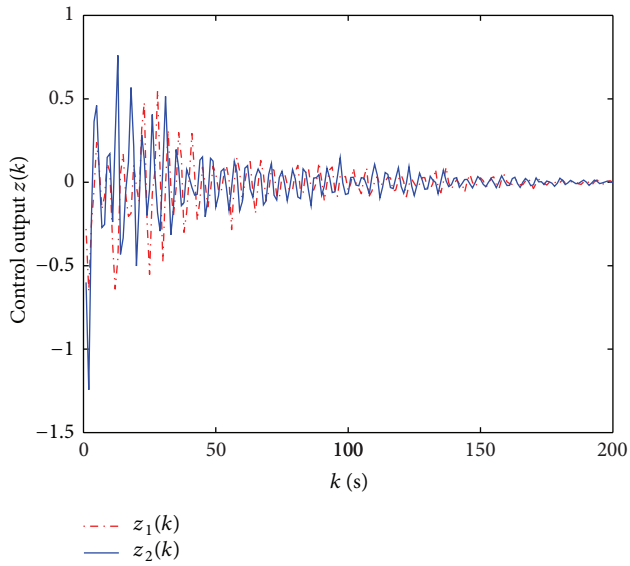

FIGURE 3: Response of control output $z(k)$ of closed-loop DTSIS (44).

and the robust H_∞ controller has been designed easily by MATLAB LMI control toolbox. A numerical example with simulation has been given to demonstrate the feasibility and effectiveness of the proposed method.

Of course, this method proposed in this paper also can be used to the the state estimation problem and the sampled-data synchronization control problem for the complex networks, which has been studied in [31, 32] and is one of our future research topics.

Acknowledgments

The authors thank the referee and the associate editor for their very helpful comments and suggestions. This work is supported by National Science Foundation of China (NSFC) under Grant nos. 61104127, 51079057, and 61134012, China Postdoctoral Science Foundation with Grant no. 2012M521428, and Hubei Province Key Laboratory of Systems Science in Metallurgical Process (Wuhan University of Science and Technology) under Grant no. Y201101.

References

[1] X. Mao, N. Koroleva, and A. Rodkina, "Robust stability of uncertain stochastic differential delay equations," *Systems and Control Letters*, vol. 35, no. 5, pp. 325–336, 1998.

[2] Y. Niu, D. W. C. Ho, and J. Lam, "Robust integral sliding mode control for uncertain stochastic systems with time-varying delay," *Automatica*, vol. 41, no. 5, pp. 873–880, 2005.

[3] V. B. Kolmanovskii and A. D. Myshkis, *Introduction To the Theory and Applications of Functional Differential Equations*, Kluwer Academic Publishers, Dordrecht, The Netherlands, 1999.

[4] Z. Zeng, J. Wang, and X. Liao, "Global exponential stability of a general class of recurrent neural networks with time-varying delays," *IEEE Transactions on Circuits and Systems*, vol. 50, no. 10, pp. 1353–1358, 2003.

[5] Z. Zeng, J. Wang, and X. Liao, "Stability analysis of delayed cellular neural networks described using cloning templates," *IEEE Transactions on Circuits and Systems*, vol. 51, no. 11, pp. 2313–2324, 2004.

[6] Z. Zeng and J. Wang, "Improved conditions for global exponential stability of recurrent neural networks with time-varying delays," *IEEE Transactions on Neural Networks*, vol. 17, no. 3, pp. 623–635, 2006.

[7] Z. Zeng, J. Wang, and X. Liao, "Global asymptotic stability and global exponential stability of neural networks with unbounded time-varying delays," *IEEE Transactions on Circuits and Systems*, vol. 52, no. 3, pp. 168–173, 2005.

[8] X. X. Liao, J. Wang, and Z. Zeng, "Global asymptotic stability and global exponential stability of delayed cellular neural networks," *IEEE Transactions on Circuits and Systems*, vol. 52, no. 7, pp. 403–409, 2005.

[9] D. Hinrichsen and A. J. Pritchard, "Stochastic H_∞," *SIAM Journal on Control and Optimization*, vol. 36, no. 5, pp. 1504–1538, 1998.

[10] N. Berman and U. Shaked, "H_∞-like control for nonlinear stochastic systems," *Systems and Control Letters*, vol. 55, no. 3, pp. 247–257, 2006.

[11] G. Wei, Z. Wang, and H. Shu, "Nonlinear H_∞ control of stochastic time-delay systems with Markovian switching," *Chaos, Solitons and Fractals*, vol. 35, no. 3, pp. 442–451, 2008.

[12] S. Xu and T. Chen, "H_∞ output feedback control for uncertain stochastic systems with time-varying delays," *Automatica*, vol. 40, no. 12, pp. 2091–2098, 2004.

[13] S. Xu, P. Shi, Y. Chu, and Y. Zou, "Robust stochastic stabilization and H_∞ control of uncertain neutral stochastic time-delay systems," *Journal of Mathematical Analysis and Applications*, vol. 314, no. 1, pp. 1–16, 2006.

[14] Z. Wang, F. Yang, D. W. C. Ho, and X. Liu, "Robust variance-constrained H_∞ control for stochastic systems with multiplicative noises," *Journal of Mathematical Analysis and Applications*, vol. 328, no. 1, pp. 487–502, 2007.

[15] N. Berman and U. Shaked, "H_∞ control for discrete-time nonlinear stochastic systems," *IEEE Transactions on Automatic Control*, vol. 51, no. 6, pp. 1041–1046, 2006.

[16] B.-S. Chen and W. Zhang, "Stochastic H2/H_∞ control with state-dependent noise," *IEEE Transactions on Automatic Control*, vol. 49, no. 1, pp. 45–57, 2004.

[17] H. Gao, C. Wang, and J. Wang, "On H_∞ performance analysis for continuous-time stochastic systems with polytopic uncertainties," *Circuits, Systems, and Signal Processing*, vol. 24, no. 4, pp. 415–429, 2005.

[18] Y.-T. Juang and C.-S. Shao, "Stability analysis of dynamic interval systems," *International Journal of Control*, vol. 49, no. 4, pp. 1401–1408, 1989.

[19] H. Zhang, Z. Wang, and D. Liu, "Robust stability analysis for interval Cohen-Grossberg neural networks with unknown time-varying delays," *IEEE Transactions on Neural Networks*, vol. 19, no. 11, pp. 1942–1955, 2008.

[20] K. D. Kim and N. K. Bose, "Vertex implications of stability for a class of delay-differential interval system," *IEEE Transactions on Circuits and Systems*, vol. 37, no. 7, pp. 969–972, 1990.

[21] X. Liao and J. Yu, "Robust stability for interval Hopfield neural networks with time delay," *IEEE Transactions on Neural Networks*, vol. 9, no. 5, pp. 1042–1045, 1998.

[22] S. Hu and J. Wang, "On stabilization of a new class of linear time-invariant interval systems via constant state feedback control," *IEEE Transactions on Automatic Control*, vol. 45, no. 11, pp. 2106–2111, 2000.

[23] C. Li, X. Liao, and R. Zhang, "Global robust asymptotical stability of multi-delayed interval neural networks: an LMI approach," *Physics Letters A*, vol. 328, no. 6, pp. 452–462, 2004.

[24] A. Chen, J. Cao, and L. Huang, "Global robust stability of interval cellular neural networks with time-varying delays," *Chaos, Solitons and Fractals*, vol. 23, no. 3, pp. 787–799, 2005.

[25] X. X. Liao and X. Mao, "Exponential stability of stochastic delay interval systems," *Systems and Control Letters*, vol. 40, no. 3, pp. 171–181, 2000.

[26] X. Mao, "Exponential stability of stochastic delay interval systems with Markovian switching," *IEEE Transactions on Automatic Control*, vol. 47, no. 10, pp. 1604–1612, 2002.

[27] X. Mao and C. Selfridge, "Stability of stochastic interval systems with time delays," *Systems and Control Letters*, vol. 42, no. 4, pp. 279–290, 2001.

[28] X. Mao, J. Lam, S. Xu, and H. Gao, "Razumikhin method and exponential stability of hybrid stochastic delay interval systems," *Journal of Mathematical Analysis and Applications*, vol. 314, no. 1, pp. 45–66, 2006.

[29] G. Wei, Z. Wang, H. Shu, and J. Fang, "Delay-dependent stabilization of stochastic interval delay systems with nonlinear disturbances," *Systems and Control Letters*, vol. 56, no. 9-10, pp. 623–633, 2007.

[30] L. Xie, "Output feedback H_∞ control of systems with parameter uncertainty," *International Journal of Control*, vol. 63, no. 4, pp. 741–750, 1996.

[31] B. Shen, Z. D. Wang, and X. H. Liu, "Sampled-data synchronization control of dynamical networks with stochastic sampling," *IEEE Transactions on Automatic Control*, vol. 57, no. 10, pp. 2644–2650, 2012.

[32] D. Ding, Z. D. Wang, B. Shen, and H. Shu, "H_∞ state estimation for discrete-time complex networks with randomly occurring sensor saturations and randomly varying sensor delays," *IEEE Transactions on Neural Networks and Learning Systems*, vol. 23, no. 5, pp. 725–736, 2012.

Hindawi Publishing Corporation
Mathematical Problems in Engineering
Volume 2013, Article ID 107450, 11 pages
http://dx.doi.org/10.1155/2013/107450

Research Article

On the Multipeakon Dissipative Behavior of the Modified Coupled Camassa-Holm Model for Shallow Water System

Zhixi Shen,[1] Yujuan Wang,[1] Hamid Reza Karimi,[2] and Yongduan Song[1]

[1] *School of Automation, Chongqing University, Chongqing 400044, China*
[2] *Department of Engineering, Faculty of Technology and Science, University of Agder, N-4898 Grimstad, Norway*

Correspondence should be addressed to Yongduan Song; ydsong@cqu.edu.cn

Received 9 May 2013; Accepted 26 June 2013

Academic Editor: Hongli Dong

This paper investigates the multipeakon dissipative behavior of the modified coupled two-component Camassa-Holm system arisen from shallow water waves moving. To tackle this problem, we convert the original partial differential equations into a set of new differential equations by using skillfully defined characteristic and variables. Such treatment allows for the construction of the multipeakon solutions for the system. The peakon-antipeakon collisions as well as the dissipative behavior (energy loss) after wave breaking are closely examined. The results obtained herein are deemed valuable for understanding the inherent dynamic behavior of shallow water wave breaking.

1. Introduction

The study of the dynamic behavior of shallow water wave represents an important research topic in view of its potential application in surface and underwater vehicle systems design, control, deployment, and monitoring. There are several classical models describing the motion of waves at the free surface of shallow water under the influence of gravity, the best known of which are the Korteweg-de Vries (KdV) equation [1, 2] and the Camassa-Holm (CH) equation [3–5]. The KdV equation admits solitary wave solutions but does not model the phenomenon of breaking for water waves. The CH equation, modeling the unidirectional propagation of shallow water waves over a flat bottom [4–6] as well as water waves moving over an underlying shear flow [7], has many remarkable properties like solitary waves with singularities called peakons [4, 6] and breaking waves [4, 8] which set it apart from KdV. The peaked solitary waves mean that they are smooth except at the crests, where they are continuous but have a jump discontinuity in the first derivative, while the presence of breaking waves means that the solution remains bounded while its slope becomes unbounded in finite time [8, 9]. After wave breaking the solutions of the CH equation, as shown by several works [10–16], become uniquely as either global conservative or global dissipative solutions.

Recently, the CH equation has been extended to many multicomponent generalizations, which can better reflect the feature of the shallow water moving. In this paper, we consider the following modified coupled two-component Camassa-Holm system [17]:

$$\begin{aligned} &m_t + 2mu_x + m_x u + (mv)_x + nv_x = 0, \quad t > 0,\ x \in R,\\ &n_t + 2nv_x + n_x v + (nu)_x + mu_x = 0, \quad t > 0,\ x \in R,\\ &m = u - u_{xx}, \quad t > 0,\ x \in R,\\ &n = v - v_{xx}, \quad t > 0,\ x \in R, \end{aligned} \tag{1}$$

which is a modified version of the coupled two-component Camassa-Holm system as established by Fu and Qu in [18], allowing for peakon solitons in the form of a superposition of multipeakons. System (1) can be rewritten as a Hamiltonian system,

$$\frac{\partial}{\partial t}\begin{pmatrix} m \\ n \end{pmatrix} = -\begin{pmatrix} \partial m + m\partial & \partial m + n\partial \\ \partial n + m\partial & \partial n + n\partial \end{pmatrix}\begin{pmatrix} \dfrac{\delta H}{\delta m} = u \\ \dfrac{\delta H}{\delta n} = v \end{pmatrix} \tag{2}$$

with the Hamiltonian $H = (1/2)\int (mG*m+nG*n)dx$, where $G * m = u$, $G * n = v$, and $G = (1/2)e^{-|x|}$. Particularly, when

$u = 0$ (or $v = 0$), the degenerated equation (1) has the same peakon solitons as the CH equation. We are interested in such system because it exhibits the following conserved quantities, as can be easily verified:

$$E_1(u) = \int_R u\,dx, \qquad E_2(v) = \int_R v\,dx,$$
$$E_3(u) = \int_R m\,dx, \qquad E_4(u) = \int_R n\,dx, \tag{3}$$
$$E_5(u,v) = \int_R \left(u^2 + u_x^2 + v^2 + v_x^2\right) dx.$$

It has been shown that system (1) is locally well-posed and also has global strong solutions which blow up in finite time [17, 18]. Moreover, the existence issue for a class of local weak solutions for such system was also addressed in [17]. It is interesting to know that whether the two remarkable properties associated with the original CH equation persist in this modified coupled two-component Camassa-Holm system. In our recent work [19, 20], we studied the problem of solution continuation beyond wave breaking of system (1), where it was established that the system admits either global conservative solutions or global dissipative solutions.

Just as with the CH equation, the multipeakon dissipative solution represents an important aspect related to the solutions near wave breaking, it is interesting to know whether or not system (1) also exhibits the similar feature. Thus far very little effort has been made on studying the multipeakon dissipative solution associated with the modified coupled two-component Camassa-Holm system of the form as expressed in (1) in the literature. Based on our recent work [20] where a global continuous semigroup of dissipative solutions of system (1) is established, in this paper we show how to construct globally defined multipeakon solutions in the dissipative case for the modified coupled two-component Camassa-Holm system.

It should be stressed that the system considered in this work is a heavily coupled one; it is the mutual effect between the two components that makes the analysis and computation much more involved than the system with single component as studied in [16]. The key to circumvent the difficulty is to utilize a skillfully defined characteristic and several new variables to obtain a new set of ordinary differential equations, from which the dissipative multipeakons are globally determined. Such feature discovered is deemed useful in further understanding the dynamic behavior of the wave breaking associated with the system. Examples are presented to illustrate the feature of the multipeakons with peakon-antipeakon collisions.

The rest of this paper is organized as follows. Section 2 represents the construction of the global dissipative solutions of the modified coupled Camassa-Holm system. Section 3 is devoted to the establishment of the dissipative multipeakon solutions of system (1). The method is illustrated by explicit calculations in the case $n = 1$ and by numerical computations when $n = 2$ with peakon-antipeak on *collisions* in Section 4. The paper is concluded in Section 5.

2. Global Dissipative Solutions of the Modified Coupled Camassa-Holm System

We represent the construction of the global dissipative solutions of system (1) obtained in [20] in this section. System (1) can be rewritten as

$$\begin{aligned} u_t + (u+v)\,u_x + P_1 + P_{2,x} &= 0, \quad t > 0,\ x \in R,\\ v_t + (u+v)\,v_x + P_3 + P_{4,x} &= 0, \quad t > 0,\ x \in R, \end{aligned} \tag{4}$$

where P_1, P_2, P_3, P_4 are given by

$$\begin{aligned} P_1(t,x) &= G * (uv_x) = \frac{1}{2}\cdot\int_R e^{-|x-x'|}(uv_x)(t,x')\,dx',\\ P_2(t,x) &= G * \left(u^2 + \frac{u_x^2}{2} + u_xv_x + \frac{v^2}{2} - \frac{v_x^2}{2}\right)\\ &= \frac{1}{2}\cdot\int_R e^{-|x-x'|}\left(u^2 + \frac{u_x^2}{2} + u_xv_x + \frac{v^2}{2} - \frac{v_x^2}{2}\right)\\ &\quad\times(t,x')\,dx',\\ P_3(t,x) &= G * (vu_x) = \frac{1}{2}\cdot\int_R e^{-|x-x'|}(vu_x)(t,x')\,dx',\\ P_4(t,x) &= G * \left(v^2 + \frac{v_x^2}{2} + u_xv_x + \frac{u^2}{2} - \frac{u_x^2}{2}\right)\\ &= \frac{1}{2}\cdot\int_R e^{-|x-x'|}\left(v^2 + \frac{v_x^2}{2} + u_xv_x + \frac{u^2}{2} - \frac{u_x^2}{2}\right)\\ &\quad\times(t,x')\,dx', \end{aligned} \tag{5}$$

with $G = e^{-|x|}/2$ the Green's function such as $G * f(x) = 1/2\cdot\int_R e^{-|x-x'|}f(x')dx'$ for all $f \in L^2(R)$ and $*$ the spatial convolution.

By using a skillfully defined characteristic $y_t(t,\xi) = (u+v)(t, y(t,\xi))$, which can be decomposed as $y(t,\xi) = \varsigma(t,\xi) + \xi$, and a new set of Lagrangian variables; namely,

$$\begin{aligned} h(t,\xi) &= \left(u^2 + u_x^2 + v^2 + v_x^2\right)\circ yy_\xi,\\ U(t,\xi) &= u(t, y(t,\xi)),\\ V(t,\xi) &= v(t, y(t,\xi)),\\ M(t,\xi) &= u_x(t, y(t,\xi)),\\ N(t,\xi) &= v_x(t, y(t,\xi)), \end{aligned} \tag{6}$$

where h corresponds to the Lagrangian energy density and U, V the Lagrangian velocity, we derive an equivalent system of the modified coupled Camassa-Holm system,

$$\begin{aligned}
\varsigma_t &= U + V, \qquad U_t = -P_1 - P_{2,x},\\
V_t &= -P_3 - P_{4,x},\\
M_t &= \left(-\frac{M^2}{2} - \frac{N^2}{2} + U^2 + \frac{V^2}{2} - P_{1,x} - P_2\right),\\
N_t &= \left(-\frac{N^2}{2} - \frac{M^2}{2} + V^2 + \frac{U^2}{2} - P_{3,x} - P_4\right),\\
h_t &= \left(3U^2 - 2P_2\right)U_\xi - 2UP_{2,x}y_\xi\\
&\quad + \left(3V^2 - 2P_4\right)V_\xi - 2VP_{4,x}y_\xi.
\end{aligned} \tag{7}$$

It is shown in [20] that the existence, uniqueness, and stability of solutions of system (7) are obtained in a Banach space, which is transformed into the conservative solution of the original system (4), while dissipative solutions differ from conservative solutions when particles collide, that is, when $y_\xi(t,\xi) = 0$ for ξ in an interval of positive length. To obtain the dissipative solution, we impose that when particles collide, they lose their energy; that is, if $y_\xi(\tau,\xi) = 0$ for some τ, then we set $h(\tau,\xi) = 0$. Thus we define $\tau(\xi)$ as the first time when $y_\xi(t,\xi)$ vanishes; namely,

$$\tau(\xi) = \sup\left\{t \in R^+ \mid y_\xi\left(t',\xi\right) > 0 \ \forall 0 \le t' < t\right\}, \tag{8}$$

and the expressions for P_i and $P_{i,x}$ $(i = 1,2,3,4)$ become

$$\begin{aligned}
P_1(t,\xi) &= \frac{1}{2}\cdot\int_{t<\tau(\xi)} e^{-|y(\xi)-y(\xi')|}\\
&\quad\times\left[(UN)\,y_\xi\right]\left(\xi'\right)d\xi',\\
P_{1,x}(t,\xi) &= -\frac{1}{2}\cdot\int_{t<\tau(\xi)} \operatorname{sgn}\left(\xi-\xi'\right)e^{-|y(\xi)-y(\xi')|}\\
&\quad\times\left[(UN)\,y_\xi\right]\left(\xi'\right)d\xi',\\
P_2(t,\xi) &= \frac{1}{4}\cdot\int_{t<\tau(\xi)} e^{-|y(\xi)-y(\xi')|}\\
&\quad\times\left[h + \left(U^2 + 2MN - N^2\right)y_\xi\right]\\
&\quad\times\left(\xi'\right)d\xi',\\
P_{2,x}(t,\xi) &= -\frac{1}{4}\cdot\int_{t<\tau(\xi)} \operatorname{sgn}\left(\xi-\xi'\right)e^{-|y(\xi)-y(\xi')|}\\
&\quad\times\left[h + \left(U^2 + 2MN - N^2\right)y_\xi\right]\\
&\quad\times\left(\xi'\right)d\xi',\\
P_3(t,\xi) &= \frac{1}{2}\cdot\int_{t<\tau(\xi)} e^{-|y(\xi)-y(\xi')|}\\
&\quad\times\left[(VM)\,y_\xi\right]\left(\xi'\right)d\xi',\\
P_{3,x}(t,\xi) &= -\frac{1}{2}\cdot\int_{t<\tau(\xi)} \operatorname{sgn}\left(\xi-\xi'\right)e^{-|y(\xi)-y(\xi')|}\\
&\quad\times\left[(VM)\,y_\xi\right]\left(\xi'\right)d\xi',\\
P_4(t,\xi) &= \frac{1}{4}\cdot\int_{t<\tau(\xi)} e^{-|y(\xi)-y(\xi')|}\\
&\quad\times\left[h + \left(V^2 + 2MN - M^2\right)y_\xi\right]\\
&\quad\times\left(\xi'\right)d\xi',\\
P_{4,x}(t,\xi) &= -\frac{1}{4}\cdot\int_{t<\tau(\xi)} \operatorname{sgn}\left(\xi-\xi'\right)e^{-|y(\xi)-y(\xi')|}\\
&\quad\times\left[h + \left(V^2 + 2MN - M^2\right)y_\xi\right]\\
&\quad\times\left(\xi'\right)d\xi',
\end{aligned} \tag{9}$$

and the modified system to be solved here reads

$$\begin{aligned}
\varsigma_t &= U + V, \qquad U_t = -P_1 - P_{2,x},\\
V_t &= -P_3 - P_{4,x},\\
M_t &= \left(-\frac{M^2}{2} - \frac{N^2}{2} + U^2 + \frac{V^2}{2} - P_{1,x} - P_2\right),\\
N_t &= \left(-\frac{N^2}{2} - \frac{M^2}{2} + V^2 + \frac{U^2}{2} - P_{3,x} - P_4\right).
\end{aligned} \tag{10}$$

$$\varsigma_{\xi t} = \begin{cases} U_\xi + V_\xi & \text{if } t < \tau(\xi),\\ 0 & \text{otherwise,}\end{cases}$$

$$U_{\xi t} = \begin{cases} \dfrac{h}{2} + \left(\dfrac{U^2}{2} + MN - N^2 - P_2 - P_{1,x}\right)y_\xi & \text{if } t < \tau(\xi),\\ 0 & \text{otherwise,}\end{cases}$$

$$V_{\xi t} = \begin{cases} \dfrac{h}{2} + \left(\dfrac{V^2}{2} + MN - M^2 - P_4 - P_{3,x}\right)y_\xi & \text{if } t < \tau(\xi),\\ 0 & \text{otherwise,}\end{cases} \tag{11}$$

$$h_t = \begin{cases} \left(3U^2 - 2P_2\right)U_\xi - 2UP_{2,x}y_\xi\\ \quad + \left(3V^2 - 2P_4\right)V_\xi - 2VP_{4,x}y_\xi & \text{if } t < \tau(\xi),\\ 0 & \text{otherwise.}\end{cases}$$

Note that, in this definition, we do not reset the energy density h to zero for $t \geq \tau(\xi)$ but keep the value it reached just before the collision, which has the advantage of rendering the right hand of (11) continuous across the value $t = \tau(\xi)$ and the behavior of the system remains unchanged.

The local existence of solutions is proved in the Banach space E where

$$E = L^\infty \cap W \cap W \cap W \cap W \cap W \cap W \cap L^1, \quad W = L^2 \cap L^\infty. \tag{12}$$

The global solutions of (10) may not exist for all initial data in E; however, they exist when the initial data $X_0 = (\varsigma_0, U_0, V_0, M_0, N_0, h_0) \in \Gamma$, where Γ is defined as follows.

Definition 1. The set Γ is composed of all $(\varsigma, U, V, M, N, h)$ such that

$$X = \left(\varsigma, U, V, M, N, \varsigma_\xi, U_\xi, V_\xi, h\right) \in E, \tag{13}$$

$$y_\xi \geq 0, \qquad h \geq 0 \text{ almost everywhere}, \tag{14}$$

$$y_\xi h = y_\xi^2 U^2 + U_\xi^2 + y_\xi^2 V^2 + V_\xi^2, \text{ almost everywhere}, \tag{15}$$

$$\frac{1}{\left(y_\xi + h\right)} \in L^\infty(R), \tag{16}$$

$$g\left(y, U, V, y_\xi, U_\xi, V_\xi, h\right) - 1 \in W, \tag{17}$$

where $g(\mathbf{x})$ is given by

$$g(\mathbf{x}) = \begin{cases} \left|x_5\right| + \left|x_6\right| + 2\left(1 + x_2^2 + x_3^2\right)x_4, & \text{if } x \in \Omega, \\ x_4 + x_7, & \text{otherwise}, \end{cases} \tag{18}$$

for $\mathbf{x} = (x_1, x_2, x_3, x_4, x_5, x_6, x_7) \in R^7$, where Ω is the following subset of R^7

$$\Omega = \left\{\mathbf{x} \in R^7 \mid \left|x_5\right| + \left|x_6\right| + 2\left(1 + x_2^2 + x_3^2\right) \times x_4 \leq x_4 + x_7, x_5, x_6 \leq 0\right\}. \tag{19}$$

The main result in [20] is stated in the following theorem.

Theorem 2. *Let $z_0 = (u_0, v_0) \in H^1 \times H^1$ be given. If one denotes $t \to z(t) = T_t(z_0)$ the corresponding trajectory, then $z = (u, v)$ is a weak dissipative solution of the modified coupled two-component Camassa-Holm system, which constructs a continuous semigroup with respect of the metric d_{H^1} on bounded sets of H^1; that is, for any $M > 0$ and any sequence $z_n \in H^1$ such that $\|z_n\|_{H^1} \leq M$, one has that $\lim_{n\to\infty} d_{H^1}(z_n, z) = 0$ implies $\lim_{n\to\infty} d_{H^1}(T_t(z_n), T_t(z)) = 0$.*

3. Multipeakon Dissipative Solutions of the Original System

In this section, we derive a new system of ordinary differential equations for the multipeakon solutions which is well-posed even when collisions occur, and the variables (y, U, V, M, N, H) are used to characterize multipeakons in a way that avoids the problems related to blowing up.

Solutions of the modified coupled two-component Camassa-Holm system may experience wave breaking in the sense that the solution develops singularities in finite time, while keeping the H^1 norm finite. Continuation of the solution beyond wave breaking imposes significant challenge as can be illustrated in the case of multipeakons, which are special solutions of the modified coupled two-component Camassa-Holm system of the form

$$(u, v)(t, x) = \left(\sum_{i=1}^n p_i(t)\, e^{-|x - q_i(t)|}, \sum_{i=1}^n r_i(t)\, e^{-|x - q_i(t)|}\right), \tag{20}$$

where $(p_i(t), r_i(t), q_i(t))$ satisfy the explicit system of ordinary differential equations

$$\begin{aligned} \dot{p}_i &= \sum_{j=1, i\neq j}^n \left(p_i p_j + r_i r_j\right) \operatorname{sgn}\left(q_j - q_i\right) e^{-|q_i - q_j|}, \\ \dot{r}_i &= \sum_{j=1, i\neq j}^n \left(p_i p_j + r_i r_j\right) \operatorname{sgn}\left(q_j - q_i\right) e^{-|q_i - q_j|}, \\ \dot{q}_i &= -\sum_{j=1}^n \left(p_j + r_j\right) e^{-|q_i - q_j|}. \end{aligned} \tag{21}$$

Let us consider initial data $z_0 = (u_0, v_0)$ given by

$$(u_0, v_0)(x) = \left(\sum_{i=1}^n p_i e^{-|x - \xi_i|}, \sum_{i=1}^n r_i e^{-|x - \xi_i|}\right). \tag{22}$$

Peakons interact in a way similar to that of solitons of the CH equation, and wave breaking may appear when at least two of the q_i coincide. In the case that $p_i(0)$ and $r_i(0)$ have the same sign for all $i = 1, 2, \ldots n$ and $q_i(t)$ remain distinct, (21) allows for a unique global solution, where the peakons are traveling in the same direction. By inserting that solution into (20), it is not hard to know that $z = (u, v)$ is a global weak solution of system (4). However, when two peakons have opposite signs, collisions may occur, and if so, the system (21) blows up. Without loss of generality, we assume that the p_i and r_i are all nonzero, and that the ξ_i are all distinct. The aim is to characterize the unique and global weak solution from Theorem 2 with initial data (22) explicitly. Since the variables p_i and r_i blow up at collisions, they are not appropriate to define a multipeakon in the form of (20). We consider the following characterization of multipeakons given as continuous solutions $z = (u, v)$, which are defined on intervals $[y_i, y_{i+1}]$ as the solutions of the Dirichlet problem

$$z - z_{xx} = 0, \tag{23}$$

with boundary conditions $z(t, y_i(t)) = z_i(t)$, $z(t, y_{i+1}(t)) = z_{i+1}(t)$. The variables y_i denote the position of the peaks, and the variables z_i denote the values of z at the peaks. In the following part we will show that this property persists for dissipative solutions.

We introduce $\overline{X} = (\overline{y}, \overline{U}, \overline{V}, \overline{M}, \overline{N}, \overline{h})$ as a representative of $z = (u, v)$ in Lagrangian equivalent system; that is, $\overline{X} = L(\overline{z})$, which is given by

$$\overline{y}(\xi) = \xi, \tag{24}$$

$$\begin{aligned} \overline{U}(\xi) &= \overline{u}(\xi), \qquad \overline{V}(\xi) = \overline{v}(\xi), \\ \overline{M}(\xi) &= \overline{u}_x(\xi), \qquad \overline{N}(\xi) = \overline{v}_x(\xi), \end{aligned} \tag{25}$$

$$\overline{h}(\xi) = \overline{u}^2 + \overline{u}_x^2 + \overline{v}^2 + \overline{v}_x^2. \tag{26}$$

Let $I = \bigcup_{i=0}^{n} I_i$, where I_i denote the open interval (ξ_i, ξ_{i+1}) with the conventions that $\xi_0 = -\infty$ and $\xi_{n+1} = \infty$. For each interval I_i, we define $\tau_i = \inf\{\tau(\xi) \mid \xi \in (\xi_i, \xi_{i+1})\}$ such that $\tau_i > 0$ for all $i = 1, \ldots, n$. By the linearity of the governing equations (10), and the bounds which hold on the solution X and $P_i, P_{i,x} (i = 1, 2, 3, 4)$, it is not hard to check that $y, U, V \in C([0, \tau_i], C^2(I_i))$, while $h \in C([0, \tau_i], C^1(I_i))$.

Thus the existence of multipeakon solutions is given by the next theorem.

Theorem 3. *For any given multipeakon initial data* $\overline{z}(x) = (\overline{u}, \overline{v})(x) = (\sum_{i=1}^{n} p_i e^{-|x-\xi_i|}, \sum_{i=1}^{n} r_i e^{-|x-\xi_i|})$, *let* (y, U, V, M, N, h) *be the solution of system* (10), (11) *with initial data* $(\overline{y}, \overline{U}, \overline{V}, \overline{M}, \overline{N}, \overline{H})$ *given by* (24), (25), *and* (26). *Between adjacent peaks, if* $x_i = y(t, \xi_i) \neq x_{i+1} = y(t, \xi_{i+1})$, *the solution* $z(t, x) = (u, v)(t, x)$ *is twice differentiable with respect to the space variable, and one has*

$$(z - z_{xx})(t, x) = 0 \quad \text{for } x \in (x_i, x_{i+1}). \tag{27}$$

Proof. For a given time t, we consider two adjacent peaks $x_i = y(t, \xi_i)$ and $x_{i+1} = y(t, \xi_{i+1})$. If $x_i = x_{i+1}$, then the two peaks have collided and, since y_ξ is positive, we must have $y_\xi(t, \xi) = 0$ for all $\xi \in I_i$. Hence, $t \geq \tau_i$, which conversely implies that $t < \tau_i$ when $x_i(t) < x_{i+1}(t)$. There exists $\xi \in I_i$ such that $x = y(t, \xi)$ for any $x \in (x_i(t), x_{i+1}(t))$. Since $\xi \in I_i$ and $t < \tau_i$, we have $y_\xi(t, \xi) \neq 0$. It follows from the implicit function theorem that $y(t, \cdot)$ is invertible in a neighborhood of ξ and its inverse is C^2, and therefore $(u, v)(t, x') = (U, V)(t, y^{-1}(t, x'))$ are C^2 with respect to the spatial variable and the quantity $(z - z_{xx})(t, x)$ is defined in the classical sense.

We now prove that $(z - z_{xx})(t, x) = 0$ for $x \in (x_i, x_{i+1})$. Let us first prove that $u - u_{xx} = 0$. Assuming that $y_\xi(t, \xi) \neq 0$, we have that

$$\begin{aligned} u_x \circ y &= M, \\ u_{xx} \circ y &= \frac{M_\xi}{y_\xi} = \frac{\left(U_{\xi\xi} y_\xi - y_{\xi\xi} U_\xi\right)}{y_\xi^3}, \end{aligned} \tag{28}$$

and therefore

$$(u - u_{xx}) \circ y = \frac{\left(U y_\xi^3 - U_{\xi\xi} y_\xi + y_{\xi\xi} U_\xi\right)}{y_\xi^3}. \tag{29}$$

We set

$$R = U y_\xi^3 - U_{\xi\xi} y_\xi + y_{\xi\xi} U_\xi. \tag{30}$$

For a given $\xi \in I$ and $t < \tau_i$, differentiating (30) with respect to t, it then follows from (10) and (11) that

$$\begin{aligned} \frac{dR}{dt} &= 3U y_\xi^2 y_{\xi t} + U_t y_\xi^3 - U_{\xi\xi t} y_\xi - U_{\xi\xi} y_{\xi t} \\ &\quad + y_{\xi\xi t} U_\xi + y_{\xi\xi} U_{\xi t} \\ &= 2U\left(U_\xi + V_\xi\right) y_\xi^2 - 2N\left(M_\xi - N_\xi\right) y_\xi^2 \\ &\quad - \frac{h_\xi y_\xi}{2} + \frac{h y_{\xi\xi}}{2}. \end{aligned} \tag{31}$$

Differentiating (15) with respect to ξ, we get

$$\begin{aligned} y_{\xi\xi} h + y_\xi h_\xi &= 2 y_\xi y_{\xi\xi} U^2 + 2 y_\xi^2 U U_\xi + 2 U_\xi U_{\xi\xi} \\ &\quad + 2 y_\xi y_{\xi\xi} V^2 + 2 y_\xi^2 V V_\xi + 2 V_\xi V_{\xi\xi}. \end{aligned} \tag{32}$$

We have, after inserting the value of $y_\xi h_\xi$ given by (32) into (31) and multiplying the equation by y_ξ, that

$$\begin{aligned} y_\xi \frac{dR}{dt} &= U U_\xi y_\xi^3 - U_\xi U_{\xi\xi} y_\xi \\ &\quad + \left(h y_\xi - y_\xi^2 U^2 - y_\xi^2 V^2 - V_\xi^2\right) y_{\xi\xi} \\ &\quad + U V_\xi y_\xi^3 - U_{\xi\xi} V_\xi y_\xi + U_\xi V_\xi y_{\xi\xi}. \end{aligned} \tag{33}$$

Since $y_{\xi t} = (U_\xi + V_\xi)$, it follows from (15) that

$$y_\xi \frac{dR}{dt} = y_{\xi t} \cdot R. \tag{34}$$

For any $\xi \in I$, as $\overline{u}$ is a multipeakon initial data, we have $R(0, \xi) = (\overline{u} - \overline{u}_{xx}) \cdot y_\xi^3 = 0$. It thus follows from Gronwall's lemma that $R(t, \xi) = 0$ and therefore $(u - u_{xx})(t, \xi) = 0$ for $t \in [0, \tau_i]$. Similarly, we can obtain that $(v - v_{xx})(t, \xi) = 0$. □

Thus, the system of ordinary differential equations that the dissipative multipeakon solutions satisfy can be derived based on the fact that the multipeakon structure is preserved by the semigroup of dissipative solutions.

Let us define

$$H_i = \int_{\xi_i}^{\xi_{i+1}} h(\xi)\, d\xi. \tag{35}$$

For each $i = 1, 2 \ldots, n$, by using (11), we obtain the following system of O.D.E.; namely,

$$\begin{aligned} \frac{dy_i}{dt} &= u_i + v_i, \qquad \frac{du_i}{dt} = -P_{1,i} - P_{2,xi}, \\ \frac{dv_i}{dt} &= -P_{3,i} - P_{4,xi}, \\ \frac{dH_i}{dt} &= \left(u_{i+1}^3 - 2u_{i+1} P_{2,i+1} + v_{i+1}^3 - 2v_{i+1} P_{4,i+1}\right) \\ &\quad - \left(u_i^3 - 2u_i P_{2,i} + v_i^3 - 2v_i P_{4,i}\right), \end{aligned} \tag{36}$$

where $(y_i, u_i, v_i) = (y, U, V)(t, \xi_i)$, $P_{k,i} = P_k(t, \xi_i)$, $P_{k,xi} = P_{k,x}(t, \xi_i)$, $(k = 1, 2, 3, 4)$, respectively. We have

$$P_{2,i} = \frac{1}{4} \cdot \int_{\{t<\tau(\xi')\}} e^{-|y_i - y(\xi')|} \times \left[h + \left(U^2 + 2MN - N^2\right) y_\xi\right](\xi')\, d\xi'. \tag{37}$$

We denote $B = \{\xi' \in R \mid y_\xi(t, \xi') > 0\}$. Thus, we get

$$\begin{aligned} P_{2,i} &= \frac{1}{2} \cdot \int_B e^{-|y_i - y(\xi')|} \left(u^2 + \frac{u_x^2}{2} + u_x v_x + \frac{v^2}{2} - \frac{v_x^2}{2}\right) \circ y(\xi')\, y_\xi(\xi')\, d\xi' \\ &= \frac{1}{2} \cdot \int_{y(B)} e^{-|y_i - x|} \left(u^2 + \frac{u_x^2}{2} + u_x v_x + \frac{v^2}{2} - \frac{v_x^2}{2}\right) \times (x)\, dx, \end{aligned} \tag{38}$$

where we have used the fact that $h = (u^2 + u_x^2 + v^2 + v_x^2) \circ y y_\xi$ on B and $t < \tau(\xi')$ if and only if $y_\xi(t, \xi') > 0$. Since $y_\xi(\xi) = 0$ on B^c, that means $(y(B^c)) = \int_{y(B^c)} dx = \int_{B^c} y_\xi(\xi) d\xi = 0$, which implies that the domain of integration in (37) can be extended to the whole axis,

$$P_{2,i} = \frac{1}{2} \cdot \int_R e^{-|y_i - x|} \left(u^2 + \frac{u_x^2}{2} + u_x v_x + \frac{v^2}{2} - \frac{v_x^2}{2}\right) dx. \tag{39}$$

Similarly, we can get that

$$\begin{aligned} P_{1,i} &= \frac{1}{2} \cdot \int_R e^{-|y_i - x|} (u v_x)\, dx, \\ P_{1,xi} &= -\frac{1}{2} \cdot \int_R \operatorname{sgn}(y_i - x)\, e^{-|y_i - x|} (u v_x)\, dx, \\ P_{2,xi} &= -\frac{1}{2} \cdot \int_R \operatorname{sgn}(y_i - x)\, e^{-|y_i - x|} \times \left(u^2 + \frac{u_x^2}{2} + u_x v_x + \frac{v^2}{2} - \frac{v_x^2}{2}\right) dx, \\ P_{3,i} &= \frac{1}{2} \cdot \int_R e^{-|y_i - x|} (v u_x)\, dx, \\ P_{3,xi} &= -\frac{1}{2} \cdot \int_R \operatorname{sgn}(y_i - x)\, e^{-|y_i - x|} (v u_x)\, dx, \\ P_{4,i} &= \frac{1}{2} \cdot \int_R e^{-|y_i - x|} \times \left(v^2 + \frac{v_x^2}{2} + u_x v_x + \frac{u^2}{2} - \frac{u_x^2}{2}\right) dx, \\ P_{4,xi} &= -\frac{1}{2} \cdot \int_R \operatorname{sgn}(y_i - x)\, e^{-|y_i - x|} \times \left(v^2 + \frac{v_x^2}{2} + u_x v_x + \frac{u^2}{2} - \frac{u_x^2}{2}\right) dx. \end{aligned} \tag{40}$$

Between two adjacent peaks located at y_i and y_{i+1}, we know that $z = (u, v)$ satisfies $(z - z_{xx}) = 0$ and therefore $z = (u, v)$ can be written as

$$z(x) = (u, v)(x) = \left(A_i e^x + B_i e^{-x}, C_i e^x + D_i e^{-x}\right) \tag{41}$$

for $x \in [y_i, y_{i+1}]$, $i = 1, 2, \ldots, n-1$, where the constants A_i, B_i, C_i, and D_i depend on u_i, u_{i+1}, v_i, v_{i+1}, y_i, and y_{i+1} and read

$$\begin{aligned} A_i &= \frac{e^{-\overline{y}_i}}{2} \left[\frac{\overline{u}_i}{\cosh(\delta y_i)} + \frac{\delta u_i}{\sinh(\delta y_i)}\right], \\ B_i &= \frac{e^{\overline{y}_i}}{2} \left[\frac{\overline{u}_i}{\cosh(\delta y_i)} - \frac{\delta u_i}{\sinh(\delta y_i)}\right], \\ C_i &= \frac{e^{-\overline{y}_i}}{2} \left[\frac{\overline{v}_i}{\cosh(\delta y_i)} + \frac{\delta v_i}{\sinh(\delta y_i)}\right], \\ D_i &= \frac{e^{\overline{y}_i}}{2} \left[\frac{\overline{v}_i}{\cosh(\delta y_i)} - \frac{\delta v_i}{\sinh(\delta y_i)}\right], \end{aligned} \tag{42}$$

where

$$\begin{aligned} \overline{y}_i &= \frac{1}{2} \cdot (y_i + y_{i+1}), & \delta y_i &= \frac{1}{2} \cdot (y_i - y_{i+1}), \\ \overline{u}_i &= \frac{1}{2} \cdot (u_i + u_{i+1}), & \delta u_i &= \frac{1}{2} \cdot (u_i - u_{i+1}), \\ \overline{v}_i &= \frac{1}{2} \cdot (v_i + v_{i+1}), & \delta v_i &= \frac{1}{2} \cdot (v_i - v_{i+1}). \end{aligned} \tag{43}$$

Thus, the constants A_i, B_i, C_i, and D_i uniquely determine $z = (u, v)$ on the interval $[y_i, y_{i+1}]$, and we compute

$$\begin{aligned} \delta H_i &= H_{i+1} - H_i = \int_{y_i}^{y_{i+1}} \left(u^2 + u_x^2 + v^2 + v_x^2\right) dx \\ &= 2\overline{u}_i^2 \tanh(\delta y_i) + 2\delta u_i^2 \coth(\delta y_i) \\ &\quad + 2\overline{v}_i^2 \tanh(\delta y_i) + 2\delta v_i^2 \coth(\delta y_i) \\ &= \delta H_{1i} + \delta H_{2i}, \end{aligned} \tag{44}$$

with $\delta H_{1i} = 2\overline{u}_i^2 \tanh(\delta y_i) + 2\delta u_i^2 \cosh(\delta y_i)$ and $\delta H_{2i} = 2\overline{v}_i^2 \tanh(\delta y_i) + 2\delta v_i^2 \cosh(\delta y_i)$. We now turn to the computation of $P_{k,i}$ $(k = 1, 2, 3, 4)$ given by (39) and (40). Let us write $z = (u, v)$ as

$$\begin{aligned} z(t,x) &= (u,v)(t,x) \\ &= \left(\sum_{j=0}^{n} \left(A_j e^{x} + B_j e^{-x} \right) \chi_{(y_j, y_{j+1})}(x), \right. \\ &\qquad \left. \sum_{j=0}^{n} \left(C_j e^{x} + D_j e^{-x} \right) \chi_{(y_j, y_{j+1})}(x) \right). \end{aligned} \tag{45}$$

Set $y_0 = -\infty$, $y_{n+1} = \infty$, $u_0 = u_{n+1} = 0$, $v_0 = v_{n+1} = 0$, $A_0 = u_1 e^{-y_1}$, $B_0 = 0$, $A_n = 0$, $B_n = u_n e^{y_n}$, $C_0 = v_1 e^{-y_1}$, $D_0 = 0$, $C_n = 0$, and $D_n = v_n e^{y_n}$. We have

$$\begin{aligned} uv_x &= \sum_{j=0}^{n} \left(A_j C_j e^{2x} - A_j D_j + B_j C_j \right. \\ &\qquad \left. - B_j D_j e^{-2x} \right) \chi_{(y_j, y_{j+1})}, \\ u^2 + \frac{u_x^2}{2} + u_x v_x + \frac{v^2}{2} - \frac{v_x^2}{2} &= \sum_{j=0}^{n} \left(\left(\frac{3}{2} \cdot A_j^2 + A_j C_j \right) e^{2x} \right. \\ &\qquad + \left(A_j B_j - A_j D_j - B_j C_j + 2 C_j D_j \right) \\ &\qquad \left. + \left(\frac{3}{2} \cdot B_j^2 + B_j D_j \right) e^{-2x} \right) \chi_{(y_j, y_{j+1})}, \\ vu_x &= \sum_{j=0}^{n} \left(A_j C_j e^{2x} - C_j B_j + D_j A_j \right. \\ &\qquad \left. - B_j D_j e^{-2x} \right) \chi_{(y_j, y_{j+1})}, \\ v^2 + \frac{v_x^2}{2} + u_x v_x + \frac{u^2}{2} - \frac{u_x^2}{2} &= \sum_{j=0}^{n} \left(\left(\frac{3}{2} \cdot C_j^2 + A_j C_j \right) e^{2x} \right. \\ &\qquad + \left(C_j D_j - C_j B_j - D_j A_j + 2 A_j B_j \right) \\ &\qquad \left. + \left(\frac{3}{2} \cdot D_j^2 + D_j B_j \right) e^{-2x} \right) \chi_{(y_j, y_{j+1})}. \end{aligned} \tag{46}$$

By inserting (46) into (39) and (40), we get

$$\begin{aligned} P_{1,i} &= \frac{1}{2} \cdot \sum_{j=0}^{n} \int_{y_j}^{y_{j+1}} e^{-k_{ij}(y_i - x)} \\ &\qquad \times \left(A_j C_j e^{2x} - A_j D_j + B_j C_j - B_j D_j e^{-2x} \right) dx, \\ P_{2,i} &= \frac{1}{2} \sum_{j=0}^{n} \int_{y_j}^{y_{j+1}} e^{-k_{ij}(y_i - x)} \\ &\qquad \times \left(\left(\frac{3}{2} A_j^2 + A_j C_j \right) e^{2x} \right. \\ &\qquad + \left(A_j B_j - A_j D_j - B_j C_j + 2 C_j D_j \right) \\ &\qquad \left. + \left(\frac{3}{2} B_j^2 + B_j D_j \right) e^{-2x} \right) dx, \\ P_{3,i} &= \frac{1}{2} \cdot \sum_{j=0}^{n} \int_{y_j}^{y_{j+1}} e^{-k_{ij}(y_i - x)} \\ &\qquad \times \left(A_j C_j e^{2x} - C_j B_j + D_j A_j - B_j D_j e^{-2x} \right) dx, \\ P_{4,i} &= \frac{1}{2} \sum_{j=0}^{n} \int_{y_j}^{y_{j+1}} e^{-k_{ij}(y_i - x)} \\ &\qquad \times \left(\left(\frac{3}{2} C_j^2 + A_j C_j \right) e^{2x} \right. \\ &\qquad + \left(C_j D_j - C_j B_j - D_j A_j + 2 A_j B_j \right) \\ &\qquad \left. + \left(\frac{3}{2} D_j^2 + D_j B_j \right) e^{-2x} \right) dx, \end{aligned} \tag{47}$$

where $k_{ij} = -1$ if $i \le j$, $k_{ij} = 1$ if $i > j$. It then follows from (42) and (44) that

$$\begin{aligned} A_j^2 &= \frac{e^{-2\overline{y}_j}}{\sinh^2(2\delta y_j)} \left[\overline{u}_j^2 \sinh^2(\delta y_j) + 2\overline{u}_j \delta u_j \sinh(\delta y_j) \right. \\ &\qquad \left. \times \cosh(\delta y_j) + \delta u_j^2 \cosh^2(\delta y_j) \right] \\ &= \frac{e^{-2\overline{y}_j}}{4 \sinh(2\delta y_j)} \cdot \left[\delta H_{1j} + 4\overline{u}_j \delta u_j \right], \\ A_j B_j &= \frac{1}{4 \sinh(2\delta y_j)} \cdot \left[4\overline{u}_j^2 \tanh(\delta y_j) - \delta H_{1j} \right], \\ A_j C_j &= \frac{e^{-2\overline{y}_j}}{2 \sinh(2\delta y_j)} \left[\overline{u}_j \overline{v}_j \tanh(\delta y_j) + \delta u_j \overline{v}_j + \delta v_j \overline{u}_j \right. \\ &\qquad \left. + \delta u_j \delta v_j \coth(\delta y_j) \right], \end{aligned}$$

$$
\begin{aligned}
A_jD_j &= \frac{1}{2\sinh\left(2\delta y_j\right)}\left[\overline{u}_j\overline{v}_j\tanh\left(\delta y_j\right)+\delta u_j\overline{v}_j-\delta v_j\overline{u}_j\right.\\
&\qquad\left.-\delta u_j\delta v_j\coth\left(\delta y_j\right)\right],\\
B_jC_j &= \frac{1}{2\sinh\left(2\delta y_j\right)}\left[\overline{u}_j\overline{v}_j\tanh\left(\delta y_j\right)+\delta v_j\overline{u}_j-\delta u_j\overline{v}_j\right.\\
&\qquad\left.-\delta u_j\delta v_j\coth\left(\delta y_j\right)\right],\\
B_jD_j &= \frac{e^{2\overline{y}_j}}{2\sinh\left(2\delta y_j\right)}\left[\overline{u}_j\overline{v}_j\tanh\left(\delta y_j\right)-\delta u_j\overline{v}_j-\delta v_j\overline{u}_j\right.\\
&\qquad\left.+\delta u_j\delta v_j\coth\left(\delta y_j\right)\right],\\
B_j^2 &= \frac{e^{2\overline{y}_j}}{4\sinh\left(2\delta y_j\right)}\cdot\left[\delta H_{1j}-4\overline{u}_j\delta u_j\right].
\end{aligned}
\tag{48}
$$

Thus, from (48), we can obtain that

$$
\begin{aligned}
&\int_{y_j}^{y_{j+1}} e^{-k_{ij}(y_i-x)}A_j^2e^{2x}dx\\
&\quad=\frac{e^{-k_{ij}y_i}\cdot e^{k_{ij}\overline{y}_j}}{2\left(2+k_{ij}\right)\sinh\left(2\delta y_j\right)}\\
&\qquad\times\sinh\left(\left(2+k_{ij}\right)\delta y_j\right)\left[\delta H_{1j}+4\overline{u}_j\delta u_j\right],\\
&\int_{y_j}^{y_{j+1}} e^{-k_{ij}(y_i-x)}A_jC_je^{2x}dx\\
&\quad=\frac{e^{-k_{ij}y_i}\cdot e^{k_{ij}\overline{y}_j}}{\left(2+k_{ij}\right)\sinh\left(2\delta y_j\right)}\\
&\qquad\times\sinh\left(\left(2+k_{ij}\right)\delta y_j\right)\\
&\qquad\cdot\left[\overline{u}_j\overline{v}_j\tanh\left(\delta y_j\right)+\delta u_j\overline{v}_j+\delta v_j\overline{u}_j\right.\\
&\qquad\quad\left.+\delta u_j\delta v_j\coth\left(\delta y_j\right)\right],\\
&\int_{y_j}^{y_{j+1}} e^{-k_{ij}(y_i-x)}A_jB_jdx\\
&\quad=\frac{e^{-k_{ij}y_i}\cdot e^{k_{ij}\overline{y}_j}}{2\sinh\left(2\delta y_j\right)}\sinh\left(\delta y_j\right)\\
&\qquad\times\left[4\overline{u}_j^2\tanh\left(\delta y_j\right)-\delta H_{1j}\right],\\
&\int_{y_j}^{y_{j+1}} e^{-k_{ij}(y_i-x)}A_jD_jdx\\
&\quad=\frac{e^{-k_{ij}y_i}\cdot e^{k_{ij}\overline{y}_j}}{\sinh\left(2\delta y_j\right)}\sinh\left(\delta y_j\right)\\
&\qquad\cdot\left[\overline{u}_j\overline{v}_j\tanh\left(\delta y_j\right)+\delta u_j\overline{v}_j-\delta v_j\overline{u}_j\right.\\
&\qquad\quad\left.-\delta u_j\delta v_j\coth\left(\delta y_j\right)\right],\\
&\int_{y_j}^{y_{j+1}} e^{-k_{ij}(y_i-x)}B_jC_jdx\\
&\quad=\frac{e^{-k_{ij}y_i}\cdot e^{k_{ij}\overline{y}_j}}{\sinh\left(2\delta y_j\right)}\sinh\left(\delta y_j\right)\\
&\qquad\cdot\left[\overline{u}_j\overline{v}_j\tanh\left(\delta y_j\right)+\delta v_j\overline{u}_j-\delta u_j\overline{v}_j\right.\\
&\qquad\quad\left.-\delta u_j\delta v_j\coth\left(\delta y_j\right)\right],\\
&\int_{y_j}^{y_{j+1}} e^{-k_{ij}(y_i-x)}C_jD_jdx\\
&\quad=\frac{e^{-k_{ij}y_i}\cdot e^{k_{ij}\overline{y}_j}}{2\sinh\left(2\delta y_j\right)}\sinh\left(\delta y_j\right)\\
&\qquad\times\left[4\overline{v}_j^2\tanh\left(\delta y_j\right)-\delta H_{2j}\right],\\
&\int_{y_j}^{y_{j+1}} e^{-k_{ij}(y_i-x)}B_j^2e^{-2x}dx\\
&\quad=\frac{e^{-k_{ij}y_i}\cdot e^{k_{ij}\overline{y}_j}}{2\left(k_{ij}-2\right)\sinh\left(2\delta y_j\right)}\\
&\qquad\times\sinh\left(\left(k_{ij}-2\right)\delta y_j\right)\left[\delta H_{1j}-4\overline{u}_j\delta u_j\right],\\
&\int_{y_j}^{y_{j+1}} e^{-k_{ij}(y_i-x)}B_jD_je^{-2x}dx\\
&\quad=\frac{e^{-k_{ij}y_i}\cdot e^{k_{ij}\overline{y}_j}}{\left(k_{ij}-2\right)\sinh\left(2\delta y_j\right)}\\
&\qquad\times\sinh\left(\left(k_{ij}-2\right)\delta y_j\right)\\
&\qquad\cdot\left[\overline{u}_j\overline{v}_j\tanh\left(\delta y_j\right)-\delta u_j\overline{v}_j-\delta v_j\overline{u}_j\right.\\
&\qquad\quad\left.+\delta u_j\delta v_j\coth\left(\delta y_j\right)\right].
\end{aligned}
\tag{49}
$$

It thus follows from (49) that

$$
P_{1,i}=\sum_{j=0}^{n}P_{1,ij},\qquad P_{2,i}=\sum_{j=0}^{n}P_{2,ij},
\tag{50}
$$

where

$$P_{1,ij}=\begin{cases}\dfrac{1}{6}\cdot u_1v_1e^{y_1-y_i}, & \text{for } j=0,\\ \dfrac{e^{-k_{ij}y_i}\cdot e^{k_{ij}\overline{y}_j}}{6\cosh\left(\delta y_j\right)}\\ \times\left[2k_{ij}\overline{u}_j\overline{v}_j\sinh^2\left(\delta y_j\right)\tanh\left(\delta y_j\right)\right.\\ \quad +2k_{ij}\delta u_j\delta v_j\sinh\left(\delta y_j\right)\cosh\left(\delta y_j\right)\\ \quad +2\delta u_j\overline{v}_j\cosh^2\left(\delta y_j\right)+2\delta v_j\overline{u}_j\cosh^2\left(\delta y_j\right)\\ \quad +\delta u_j\overline{v}_j+\delta v_j\overline{u}_j-3\overline{u}_j\overline{v}_j\tanh\left(\delta y_j\right)\\ \quad \left.+3\delta u_j\delta v_j\coth\left(\delta y_j\right)\right], & \text{for } j=1,\ldots,n-1,\\ -\dfrac{1}{6}\cdot u_nv_ne^{-y_n+y_i} & \text{for } j=n,\end{cases}$$

$$P_{2,ij}=\begin{cases}\dfrac{1}{4}\cdot u_1^2e^{y_1-y_i}+\dfrac{1}{6}\cdot u_1v_1e^{y_1-y_i}, & \text{for } j=0,\\ \dfrac{e^{-k_{ij}y_i}\cdot e^{k_{ij}\overline{y}_j}}{4\cosh\left(\delta y_j\right)}\\ \times\left[\delta H_{1j}\cosh^2\left(\delta y_j\right)+4k_{ij}\overline{u}_j\delta u_j\sinh^2\left(\delta y_j\right)\right.\\ \quad +2\overline{u}_j^2\tanh\left(\delta y_j\right)+4\overline{v}_j^2\tanh\left(\delta y_j\right)\\ \quad -\delta H_{2j}-\dfrac{4}{3}\overline{u}_j\overline{v}_j\tanh\left(\delta y_j\right)+\dfrac{8}{3}\delta u_j\delta v_j\\ \quad \times\coth\left(\delta y_j\right)+\dfrac{4}{3}\overline{u}_j\overline{v}_j\cosh\left(\delta y_j\right)\sinh\left(\delta y_j\right)\\ \quad +\dfrac{4}{3}\delta u_j\delta v_j\cdot\coth\left(\delta y_j\right)\cosh^2\left(\delta y_j\right)\\ \quad +\dfrac{4}{3}k_{ij}\delta u_j\overline{v}_j\sinh^2\left(\delta y_j\right)+\dfrac{4}{3}\\ \quad \left.\times k_{ij}\delta v_j\overline{u}_j\sinh^2\left(\delta y_j\right)\right], & \text{for } j=1,\ldots,n-1,\\ \dfrac{1}{4}\cdot u_n^2e^{-y_n+y_i}+\dfrac{1}{6}\cdot u_nv_ne^{-y_n+y_i}, & \text{for } j=n.\end{cases}\tag{51}$$

The terms $P_{3,i}$, $P_{4,i}$, and $P_{k,ix}$ $(k=1,2,3,4)$ can be computed in the same way and we have

$$P_{k,ix}=-\sum_{j=0}^{n}k_{ij}P_{k,ij}\cdot(k=1,2,3,4).\tag{52}$$

The result can be summarized in the following theorem.

Theorem 4. *Assume* $\overline{y}_i=\xi_i$, $\overline{z}_i=(\overline{u}_i,\overline{v}_i)=(\overline{u}(\xi_i),\overline{v}(\xi_i))$ *and* $\overline{H}_i=\int_{\xi_i}^{\xi_{i+1}}(\overline{u}^2+\overline{u}_x^2+\overline{v}^2+\overline{v}_x^2)dx$ *for* $i=1,\ldots,n$ *with a multipeakon initial data* $\overline{z}=(\overline{u},\overline{v})$ *as given by* (22). *Then, there exists a global solution* (y_i,u_i,v_i,H_i) *of* (36), (50), *and* (52) *with initial data* $(\overline{y}_i,\overline{u}_i,\overline{v}_i,\overline{H}_i)$. *On each interval* $[y_i(t),y_{i+1}(t)]$, *one defines* $z(t,x)=(u,v)(t,x)$ *as the solution of the Dirichlet problem* $z-z_{xx}=0$ *with boundary conditions* $z(t,y_i(t))=z_i(t)$, $z(t,y_{i+1}(t))=z_{i+1}(t)$ *for each time* t. *Thus* $z=(u,v)$ *is a dissipative solution of the modified coupled two-component Camassa-Holm system, which is the dissipative multipeakon solution.*

4. Examples

In this section, we give the examples with the case $n=1$ by explicit calculations and the case $n=2$ by numerical computations with peakon-antipeakon collisions.

(i) Let $n=1$. From (50) and (52), we can compute that $P_{1,1}=\sum_{j=0,1}P_{1,1j}=u_1v_1/6-u_1v_1/6=0$ and $P_{2,x1}=-k_{1j}\sum_{j=0,1}P_{2,1j}=-u_1^2/4-u_1v_1/6+u_1^2/4+u_1v_1/6=0$, which imply that $u_{1t}=-P_{1,1}-P_{2,x1}=0$ and therefore $u_1=c_1$. Similarly, we can get that $v_1=c_2$. Thus from (36), we can obtain that $y_{1t}=u_1+v_1=c_1+c_2=c$, which yields $y_1=ct+a$ with c_1, c_2, c, a some constants. There is no collision and we find the familiar one peakon $(u,v)(t,x)=(c_1e^{-|x-c_1t-a|},c_2e^{-|x-c_2t-a|})$.

(ii) Let $n=2$. We first consider the case of an antisymmetric pair of peakons where the two peakons collide. We take the initial conditions as

$$\begin{aligned}&y_2(0)=-y_1(0)=\overline{y},\qquad u_2(0)=-u_1(0)=\overline{u},\\ &v_2(0)=-v_1(0)=\overline{v},\qquad \delta H_1(0)=E^2\end{aligned}\tag{53}$$

for some strictly positive constants $\overline{y}$, $\overline{u}$, $\overline{v}$, and E the initial total energy of the system, that is, the H^1 norm of the solution; we denote $\tau=\tau_1$, the time of collision. For $t<\tau$, the solution is identical to the conservative case. After collision, for $t\geq\tau$, the solution remains antisymmetric. Let us assume this for the moment and write

$$\begin{aligned}&y=y_2=-y_1,\qquad u=u_2=-u_1,\\ &v=v_2=-v_1,\qquad h=\delta H_1,\\ &P_2=P_{2,1}=P_{2,2},\qquad P_4=P_{4,1}=P_{4,2},\\ &P_1=P_{1,1}=-P_{1,2},\qquad P_3=P_{3,1}=-P_{3,2},\\ &P_{2,x}=P_{2,x1}=-P_{2,x2},\qquad P_{4,x}=P_{4,x1}=-P_{4,x2}.\end{aligned}\tag{54}$$

By using (50) and (52) and after some calculations, we can compute P_k and $P_{k,x}$ $(k=1,2,3,4)$ and obtain that

$$\begin{aligned}P_1&=\sum_{j=0,2}P_{1,1j}=\frac{1}{6}\cdot uv\left(1-e^{-2y}\right),\\ P_2&=\sum_{j=0,2}P_{2,1j}=\left(\frac{1}{4}\cdot u^2+\frac{1}{6}\cdot uv\right)\left(1+e^{-2y}\right),\\ P_3&=\sum_{j=0,2}P_{3,1j}=\frac{1}{6}\cdot uv\left(1-e^{-2y}\right),\\ P_4&=\sum_{j=0,2}P_{4,1j}=\left(\frac{1}{4}\cdot v^2+\frac{1}{6}\cdot uv\right)\left(1+e^{-2y}\right),\\ P_{2,x}&=-\left(-\sum_{j=0,2}k_{1,j}P_{2,1j}\right)\\ &=-\left(\frac{1}{4}\cdot u^2+\frac{1}{6}\cdot uv\right)\left(1-e^{-2y}\right),\\ P_{4,x}&=-\left(-\sum_{j=0,2}k_{1,j}P_{4,1j}\right)\\ &=-\left(\frac{1}{4}\cdot v^2+\frac{1}{6}\cdot uv\right)\left(1-e^{-2y}\right).\end{aligned}\tag{55}$$

Thus we are led to the following system of ordinary differential equations:

$$y_t = u + v, \qquad u_t = \frac{1}{4}\cdot u^2\left(1 - e^{-2y}\right),$$
$$v_t = \frac{1}{4}\cdot v^2\left(1 - e^{-2y}\right), \tag{56}$$
$$h_t = \left(u^3 + v^3\right)\left(1 - e^{-2y}\right) - \frac{2}{3}\cdot uv\,(u+v)\left(1 + e^{-2y}\right).$$

Note that this system holds before collision. With the initial condition $y(\tau) = u(\tau) = v(\tau) = 0$, the solution of (56) is $y(t) = u(t) = v(t) = 0$ and $h(t) = h(\tau)$. It means that the multipeakon solution remains identically equal to zero after the collision.

If we consider a more general case with two colliding peakons by using the Hamiltonian system before collision, then from (50) and (52), the system (36) can be rewritten as

$$\frac{dy_1}{dt} = u_1 + v_1, \qquad \frac{dy_2}{dt} = u_2 + v_2,$$
$$\frac{du_1}{dt} = \frac{1}{4}\cdot u_1^2 - \frac{1}{4}\cdot u_2^2 e^{y_1 - y_2},$$
$$\frac{du_2}{dt} = \frac{1}{4}\cdot u_1^2 e^{y_1 - y_2} - \frac{1}{4}\cdot u_2^2,$$
$$\frac{dv_1}{dt} = \frac{1}{4}\cdot v_1^2 - \frac{1}{4}\cdot v_2^2 e^{y_1 - y_2}, \tag{57}$$
$$\frac{dv_2}{dt} = \frac{1}{4}\cdot v_1^2 e^{y_1 - y_2} - \frac{1}{4}\cdot v_2^2,$$
$$\frac{dH_1}{dt} = \left(u_2^3 - 2u_2P_{2,2} + v_2^3 - 2v_2P_{4,2}\right) - \left(u_1^3 - 2u_1P_{2,1} + v_1^3 - 2v_1P_{4,1}\right).$$

Thus we have

$$y_1 = \ln\left(\frac{c_1 - c_2}{c_1 e^{-c_1(t-\tau)} - c_2 e^{-c_2(t-\tau)}}\right),$$
$$y_2 = \ln\left(\frac{c_1 e^{c_1(t-\tau)} - c_2 e^{c_2(t-\tau)}}{c_1 - c_2}\right),$$
$$u_1 = \frac{\left(c_1^1\right)^2 - \left(c_2^1\right)^2 e^{(c_1^1 - c_2^1)(t-\tau)}}{c_1^1 - c_2^1 e^{(c_1^1 - c_2^1)(t-\tau)}},$$
$$u_2 = \frac{\left(c_2^1\right)^2 - \left(c_1^1\right)^2 e^{(c_1^1 - c_2^1)(t-\tau)}}{c_2^1 - c_1^1 e^{(c_1^1 - c_2^1)(t-\tau)}}, \tag{58}$$
$$v_1 = \frac{\left(c_1^2\right)^2 - \left(c_2^2\right)^2 e^{(c_1^2 - c_2^2)(t-\tau)}}{c_1^2 - c_2^2 e^{(c_1^2 - c_2^2)(t-\tau)}},$$
$$v_2 = \frac{\left(c_2^2\right)^2 - \left(c_1^2\right)^2 e^{(c_1^2 - c_2^2)(t-\tau)}}{c_2^2 - c_1^2 e^{(c_1^2 - c_2^2)(t-\tau)}},$$

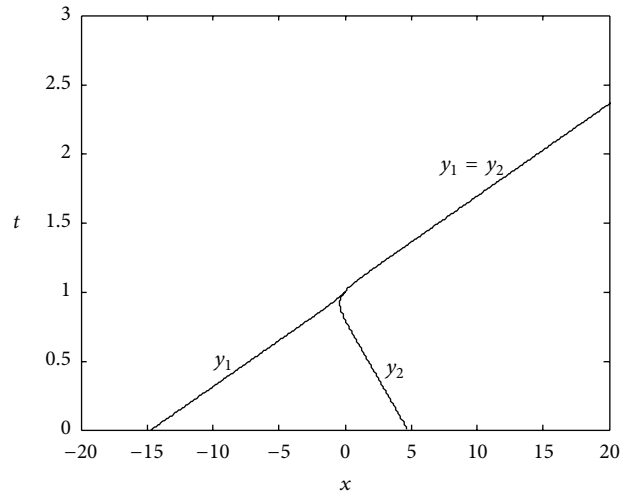

Figure 1: Position of the peakons.

where $c_1 = c_1^1 + c_1^2$ and $c_2 = c_2^1 + c_2^2$ denote the speed of the peaks y_1 and y_2, respectively. At collision time, we have

$$y_1(\tau) = y_2(\tau) = 0,$$
$$u_1(\tau) = u_2(\tau) = c_1^1 + c_2^1, \tag{59}$$
$$v_1(\tau) = v_2(\tau) = c_1^2 + c_2^2.$$

For the initial data given by (59), the solution of (57) is

$$u_1(t) = u_2(t) = c_1^1 + c_2^1, \qquad v_1(t) = v_2(t) = c_1^2 + c_2^2,$$
$$y_1 = y_2 = (c_1 + c_2)\,t, \qquad H_1(t) = H_1(\tau), \tag{60}$$

with $c_1 = c_1^1 + c_1^2$, $c_2 = c_2^1 + c_2^2$, and after the collision we obtain a single peakon traveling at speed $c_1 + c_2$.

We know that if $p_i(0)$ and $r_i(0)$ have the same sign for all $i = 1, 2, \ldots, n$ and $q_i(t)$ remain distinct, (57) admits a unique global solution, where the peakons are traveling in the same direction. However, when two peakons have opposite signs, collisions may occur, and if so, the system (57) blows up. In Figures 1 and 2, the solution is plotted with $c_1 = 15$, $c_2 = -5$, and $\tau = 1$.

5. Conclusion

Considered in this paper is the dissipative property of the modified coupled two-component Camassa-Holm system after wave breaking. Based on the obtained global dissipative solutions of the modified coupled two-component Camassa-Holm system, we construct the dissipative multipeakon solutions, a useful result for understanding the inevitable multipeakon phenomenon near wave breaking. Some interesting issues worthy of further investigation include the computational complexity of the algorithms and the impact of the multipeakon dissipative behavior on the system performance when blended into control system design.

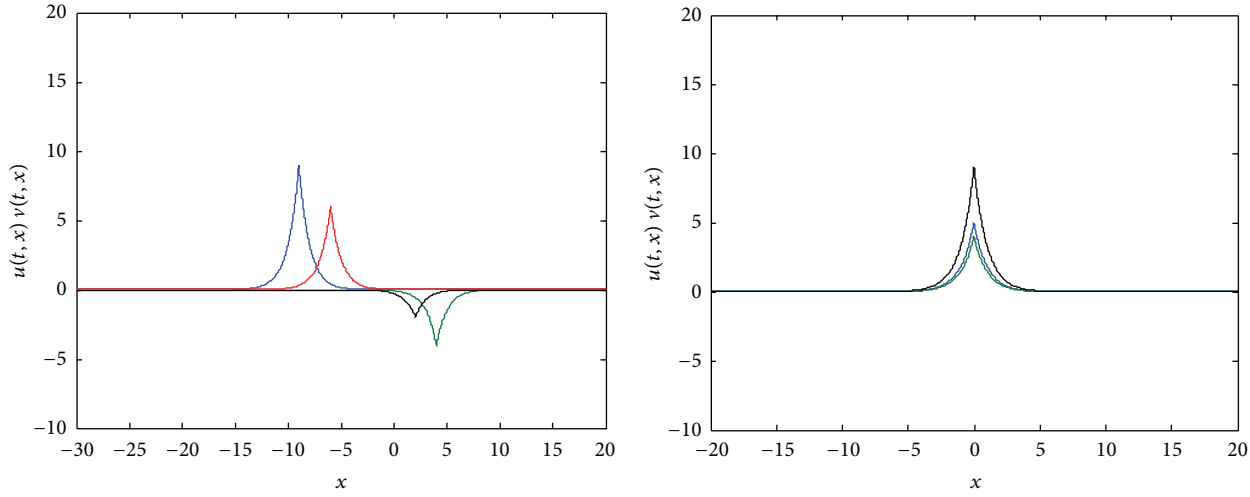

Figure 2: (a) Initial configuration. (b) The two peakons collide.

Acknowledgments

The paper is supported by the Major State Basic Research Development Program 973 (no. 2012CB215202), the National Natural Science Foundation of China (no. 61134001), and the Fundamental Research Funds for the Central Universities (no. CDJXS12170003). The authors would like to thank the referees.

References

[1] G. A. Nariboli, "Nonlinear longitudinal dispersive waves in elastic rods," *Journal of Mathematical Physics*, vol. 4, pp. 64–73, 1970.

[2] G. B. Whitham, *Linear and Nonlinear Waves*, John Wiley & Sons, New York, NY, USA, 1980.

[3] A. Constantin, "The Hamiltonian structure of the Camassa-Holm equation," *Expositiones Mathematicae*, vol. 15, no. 1, pp. 53–85, 1997.

[4] R. Camassa and D. D. Holm, "An integrable shallow water equation with peaked solitons," *Physical Review Letters*, vol. 71, no. 11, pp. 1661–1664, 1993.

[5] H. R. Dullin, G. A. Gottwald, and D. D. Holm, "An integrable shallow water equation with linear and nonlinear dispersion," *Physical Review Letters*, vol. 87, no. 19, Article ID 194501, 4 pages, 2001.

[6] A. Constantin and D. Lannes, "The hydrodynamical relevance of the Camassa-Holm and Degasperis-Procesi equations," *Archive for Rational Mechanics and Analysis*, vol. 192, no. 1, pp. 165–186, 2009.

[7] R. S. Johnson, "The Camassa-Holm equation for water waves moving over a shear flow," *Japan Society of Fluid Mechanics: Fluid Dynamics Research*, vol. 33, no. 1-2, pp. 97–111, 2003.

[8] A. Constantin and J. Escher, "Wave breaking for nonlinear nonlocal shallow water equations," *Acta Mathematica*, vol. 181, no. 2, pp. 229–243, 1998.

[9] A. Constantin, "Existence of permanent and breaking waves for a shallow water equation: a geometric approach," *Annales de l'Institut Fourier*, vol. 50, no. 2, pp. 321–362, 2000.

[10] A. Bressan and A. Constantin, "Global conservative solutions of the Camassa-Holm equation," *Archive for Rational Mechanics and Analysis*, vol. 183, no. 2, pp. 215–239, 2007.

[11] H. Holden and X. Raynaud, "Global conservative solutions of the Camassa-Holm equation—a Lagrangian point of view," *Communications in Partial Differential Equations*, vol. 32, no. 10–12, pp. 1511–1549, 2007.

[12] H. Holden and X. Raynaud, "Periodic conservative solutions of the Camassa-Holm equation," *Annales de l'Institut Fourier*, vol. 58, no. 3, pp. 945–988, 2008.

[13] A. Bressan and A. Constantin, "Global dissipative solutions of the Camassa-Holm equation," *Analysis and Applications*, vol. 5, no. 1, pp. 1–27, 2007.

[14] H. Holden and X. Raynaud, "Dissipative solutions for the Camassa-Holm equation," *Discrete and Continuous Dynamical Systems A*, vol. 24, no. 4, pp. 1047–1112, 2009.

[15] H. Holden and X. Raynaud, "Global conservative multipeakon solutions of the Camassa-Holm equation," *Journal of Hyperbolic Differential Equations*, vol. 4, no. 1, pp. 39–64, 2007.

[16] H. Holden and X. Raynaud, "Global dissipative multipeakon solutions of the Camassa-Holm equation," *Communications in Partial Differential Equations*, vol. 33, no. 10–12, pp. 2040–2063, 2008.

[17] Y. Fu, Y. Liu, and C. Qu, "Well-posedness and blow-up solution for a modified two-component periodic Camassa-Holm system with peakons," *Mathematische Annalen*, vol. 348, no. 2, pp. 415–448, 2010.

[18] Y. Fu and C. Qu, "Well posedness and blow-up solution for a new coupled Camassa-Holm equations with peakons," *Journal of Mathematical Physics*, vol. 50, no. 1, Article ID 012906, 25 pages, 2009.

[19] L. Tian, Y. Wang, and J. Zhou, "Global conservative and dissipative solutions of a coupled Camassa-Holm equations," *Journal of Mathematical Physics*, vol. 52, no. 6, Article ID 063702, 29 pages, 2011.

[20] Y. Wang and Y. Song, "On the global existence of dissipative solutions for the modified coupled Camassa-Holm system," *Soft Computing*. In press.

Hindawi Publishing Corporation
Mathematical Problems in Engineering
Volume 2013, Article ID 574571, 8 pages
http://dx.doi.org/10.1155/2013/574571

Research Article

Robust H_∞ Filtering for a Class of Uncertain Markovian Jump Systems with Time Delays

Yi Yang[1,2] and Junwei Lu[3]

[1] *Reliability and Systems Engineering School, Beihang University, Beijing 100191, China*
[2] *China Astronaut Research and Training Center, Beijing 100094, China*
[3] *School of Electrical and Automation Engineering, Nanjing Normal University, 78 Bancang Street, Nanjing 210042, China*

Correspondence should be addressed to Yi Yang; zzpcissy2006@163.com

Received 5 May 2013; Accepted 1 July 2013

Academic Editor: Jun Hu

This paper studies the problem of robust H_∞ filtering for a class of uncertain time-delay systems with Markovian jumping parameters. The system under consideration is subject to norm-bounded time-varying parameter uncertainties. The problem to be addressed is the design of a Markovian jump filter such that the filter error dynamics are stochastically stable and a prescribed bound on the $\mathscr{L}_2$-induced gain from the noise signals to the filter error is guaranteed for all admissible uncertainties. A sufficient condition for the existence of the desired robust H_∞ filter is given in terms of two sets of coupled algebraic Riccati inequalities. When these algebraic Riccati inequalities are feasible, the expression of a desired H_∞ filter is also presented. Finally, an illustrative numerical example is provided.

1. Introduction

In the past decades, much attention has been focused on the celebrated Kalman filtering which seems to be one of the most popular estimation approaches; see, for example, [1]. Such a kind of filtering approach assumes that the system is subjected to stationary Gaussian noises with known statistics. However, in practical applications, the statistics of the noise sources may not be exactly known. To deal with this problem, an alternative approach named H_∞ filtering was proposed, and a great number of results on this topic have been reported in the literature; see, for example, [2–5]. Note that in the H_∞ filtering setting, the exogenous input signals are assumed to belong to $\mathscr{L}_2[0,\infty)$; furthermore, no exact statistics are required to be known. When parameter uncertainties appear not only in the exogenous input but also in the system model, the problem of robust H_∞ filtering has been investigated and algebraic Riccati equation approach and linear matrix inequality (LMI) approach have been adopted to solve this problem; see [6–9] and the references therein.

Systems with Markovian jumping parameters have been extensively studied due to their both practical and theoretical importance; many issues, such as filtering, stability analysis, and synthesis, on this kind of systems have been studied [10–13]. The problem of H_∞ filtering for Markovian jumping systems has received much attention. Sufficient conditions for the solvability of this problem were presented in [14], and a design methodology was also proposed based on LMI approach. These results were further extended to uncertain Markovian jump linear systems in [15–18].

In this paper, we consider the problem of robust H_∞ filtering for a class of continuous-time uncertain systems with Markovian jump parameters in all system matrices and time delays in the state variables. We consider uncertain systems with norm-bounded time-varying parameter uncertainties. The objective of this paper is to design a Markovian jump linear filter which guarantees both the stochastic stability and a prescribed H_∞ performance of the filtering error dynamics for all admissible uncertainties. An algebraic Riccati inequalities approach is developed to solve the previous problem and the desired H_∞ filter can be constructed by solving two sets of coupled algebraic Riccati inequalities.

Notation. Throughout this paper, for symmetric matrices X and Y, the notation $X \geq Y$ (resp., $X > Y$) means

that the matrix $X - Y$ is positive semidefinite (resp., positive definite); I is the identity matrix with appropriate dimension. The notation M^T represents the transpose of the matrix M; $\mathscr{E}\{\cdot\}$ denotes the expectation operator with respect to some probability measure $\mathscr{P}$; $L_2[0,\infty)$ is the space of square-integrable vector functions over $[0,\infty)$; $|\cdot|$ refers to the Euclidean vector norm; $\|\cdot\|_2$ stands for the usual $L_2[0,\infty)$ norm, while $\|\cdot\|_{E_2}$ denotes the norm in $L_2((\Omega,\mathscr{F},\mathscr{P}),[0,\infty))$; $(\Omega,\mathscr{F},\mathscr{P})$ is a probability space; $\lambda_{\min}(M)$ is used to denote the minimum eigenvalue of the matrix M. Matrices, if not explicitly stated, are assumed to have compatible dimensions.

2. Problem Formulation

Fix a complete probability space $(\Omega,\mathscr{F},\mathscr{P})$ and consider the following class of uncertain stochastic linear systems with Markovian jumping parameters and time delay:

$$\Sigma:\begin{cases}\dot{x}(t) = [A(r(t)) + \Delta A(t,r(t))]\,x(t) \\ \quad + [A_d(r(t)) + \Delta A_d(t,r(t))] \\ \quad \times x(t-d) + B(r(t))\,\omega(t), \\ y(t) = [C(r(t)) + \Delta C(t,r(t))] \\ \quad \times x(t) + D(r(t))\,\omega(t), \\ z(t) = L(r(t))\,x(t), \\ x(t) = \phi(t), \quad \forall t \in [-d,0],\ d>0,\ r(0) = r_0,\end{cases} \tag{1}$$

where $x(t) \in \mathbb{R}^n$ is the system state; $y(t) \in \mathbb{R}^r$ is the measurement; $\omega(t) \in \mathbb{R}^m$ is the noise signal which belongs to $L_2[0,\infty)$; $z(t) \in \mathbb{R}^l$ is a linear combination of state variables to be estimated; $d > 0$ is the time delay of the system; and $\phi(t) \in \mathbb{R}^n$ is the continuous initial-value function. The parameter $r(t)$ represents a continuous discrete-state Markov process taking values in a finite set $\mathscr{S} = \{1,2,\ldots,s\}$ with transition probability matrix $\Pi \triangleq \{\pi_{ij}\}$ given by

$$\Pr\{r(t+h) = j \mid r(t) = i\} = \begin{cases}\pi_{ij}h + o(h), & i \neq j, \\ 1 + \pi_{ii}h + o(h), & i = j,\end{cases} \tag{2}$$

where $h > 0$, $\lim_{h\to\infty}(o(h)/h) = 0$, and $\pi_{ij} \geq 0$ is the transition rate from mode i at time t to mode j at time $t+h$ and

$$\pi_{ii} = -\sum_{j=1, j\neq i}^{s} \pi_{ij}. \tag{3}$$

In system Σ, $A(r(t)), \Delta A(t,r(t)), A_d(r(t)), \Delta A_d(t,r(t)), B(r(t)), C(r(t)), \Delta C(t,r(t), D(r(t))$, and $L(r(t))$ are appropriately dimensioned real-valued matrix functions of $r(t)$. For simplicity of notations, in the sequel, for each possible $r(t) = i, i \in \mathscr{S}$, we will denote the matrices associated with the ith mode by

$$\begin{gathered} A_i \triangleq A(r(t)), \qquad \Delta A_i(t) \triangleq \Delta A(t,r(t)), \\ A_{di} \triangleq A_d(r(t)), \qquad \Delta A_{di}(t) \triangleq \Delta A_d(t,r(t)), \\ B_i \triangleq B(r(t)), \qquad C_i \triangleq C(r(t)), \\ \Delta C_i(t) \triangleq \Delta C(t,r(t)), \qquad D_i \triangleq D(r(t)), \end{gathered} \tag{4}$$

$$L_i \triangleq L(r(t)), \tag{5}$$

where $A_i, A_{di}, B_i, C_i, D_i$, and L_i, are known constant matrices representing the nominal system for each $i \in \mathscr{S}$ and $\Delta A_i(t)$, $\Delta A_{di}(t)$, and $\Delta C_i(t)$ are unknown matrices representing time-varying parameter uncertainties and are assumed to be of the form

$$\begin{aligned} \Delta A_i(t) &= M_{Ai}F_{Ai}(t)N_{Ai}, \\ \Delta A_{di}(t) &= M_{di}F_{di}(t)N_{di}, \\ \Delta C_i(t) &= M_{Ci}F_{Ci}(t)N_{Ci}, \end{aligned} \tag{6}$$

where M_{Ai}, N_{Ai}, M_{di}, N_{di}, M_{Ci}, and N_{Ci}, for each $i \in \mathscr{S}$, are known constant matrices and $F_{Ai}(t)$, $F_{di}(t)$, and $F_{Ci}(t)$, for each $i \in \mathscr{S}$, are the uncertain time-varying matrices satisfying

$$\begin{gathered} F_{Ai}(t)^T F_{Ai}(t) \leq I, \qquad F_{di}(t)^T F_{di}(t) \leq I, \\ F_{Ci}(t)^T F_{Ci}(t) \leq I, \quad \forall i \in \mathscr{S}. \end{gathered} \tag{7}$$

It is assumed that all the elements of $F_{Ai}(t)$, $F_{di}(t)$, and $F_{Ci}(t)$ are Lebesgue measurable. $\Delta A_i(t)$, $\Delta A_{di}(t)$, and $\Delta C_i(t)$, for each $i \in \mathscr{S}$, are said to be admissible if both (6) and (7) hold.

Throughout the paper we will use the following concept of stochastic stability.

Definition 1. Consider the following stochastic jump system:

$$\begin{aligned} \dot{x}(t) &= A(r(t))\,x(t) + A_d(r(t))\,x(t-d), \\ x(t) &= \phi(t), \quad \forall t \in [-d,0],\ d>0,\ r(0) = r_0. \end{aligned} \tag{8}$$

The system (8) is said to be stochastically stable, if, for finite $\phi(t) \in \mathbb{R}^n$ defined on $[-d,0]$ and $r_0 \in \mathscr{S}$, there exists a scalar $c > 0$ such that

$$\begin{aligned} \lim_{t\to\infty} \mathscr{E}\left\{\int_0^t x^T(\tau,\phi,r_0)\,x(\tau,\phi,r_0)\,d\tau \mid \phi, r_0\right\} \\ \leq c \sup_{-d\leq\tau\leq 0} |\phi(\tau)|^2, \end{aligned} \tag{9}$$

where $x(t,\phi,r_0)$ denotes the solution of system (8) at time t under the initial conditions $\phi(t)$ and r_0.

Now, for each $i \in \mathscr{S}$, consider a Markovian filter of the form

$$\Sigma_F:\begin{cases}\dot{\hat{x}}(t) = \widehat{A}_i\hat{x}(t) + \widehat{K}_i y(t), \\ \hat{z}(t) = \widehat{L}_i\hat{x}(t),\end{cases} \tag{10}$$

where $\hat{x}(t) \in \mathbb{R}^n$ is the estimator state and the matrices $\widehat{A}_i$, $\widehat{K}_i$, and $\widehat{L}_i$ are to be chosen. The filtering error is defined by

$$e(t) \triangleq z(t) - \hat{z}(t). \tag{11}$$

Then the robust H_∞ filtering problem to be dealt with in this paper can be formulated as determining a filter of the form (10) such that, for all admissible uncertainties $\Delta A_i(t)$, $\Delta A_{di}(t)$, and $\Delta C_i(t)$, $i \in \mathcal{S}$, the following requirements are satisfied:

(R1) the augmented system from system Σ and the filter Σ_F is stochastically stable;

(R2) with zero initial conditions, the following holds:

$$\|e(t)\|_{E_2} < \gamma \|\omega(t)\|_2, \tag{12}$$

for all nonzero $\omega(t) \in L_2[0,\infty)$, where $\gamma > 0$ is a prescribed scalar.

Before concluding this section, we introduce the following lemma which will be used in the proof of our main results in the next section.

Lemma 2 (see [19, 20]). *Let A, D, E, F, and P be real matrices of appropriate dimensions with $P > 0$ and F satisfying $F^TF \le I$. Then one has the following:*

(1) *for any scalar $\epsilon > 0$,*

$$DFE + (DFE)^T \le \epsilon^{-1} DD^T + \epsilon E^T E, \tag{13}$$

(2) *for any scalar $\epsilon > 0$ such that $P - \epsilon E^T E > 0$,*

$$(A + DFE) P^{-1} (A + DFE)^T \le A\left(P - \epsilon E^T E\right)^{-1} A^T + \epsilon^{-1} DD^T, \tag{14}$$

(3) $AD + (AD)^T \le APA^T + D^T P^{-1} D$.

3. Main Results

In this section, a Riccati-like inequality approach is proposed to design a robust H_∞ filter for uncertain stochastic linear systems with Markovian jumping parameters and time delay. Our main result is presented in the next theorem.

Theorem 3. *Consider the uncertain jump linear system Σ. If there exist scalars $\varepsilon_{1i} > 0$, $\varepsilon_{2i} > 0$, $\varepsilon_{3i} > 0$, and $\varepsilon_{4i} > 0$ and matrices $P_{1i} > 0$, $P_{2i} > 0$, $i = 1, \ldots, s$, $Q_1 > 0$, and $Q_2 > 0$, such that $Q_1 - \varepsilon_{3i} N_{di}^T N_{di} > 0$, $i = 1, \ldots, s$, and the following coupled Riccati matrix inequalities hold:*

$$\begin{aligned} &A_i^T P_{1i} + P_{1i} A_i + \sum_{j=1}^{s} \pi_{ij} P_{1j} + P_{1i} W_i P_{1i} \\ &\quad + \varepsilon_{1i} N_{Ai}^T N_{Ai} + \varepsilon_{2i} N_{Ci}^T N_{Ci} + Q_1 < 0, \\ &\widehat{A}_i^T P_{2i} + P_{2i} \widehat{A}_i + \sum_{j=1}^{s} \pi_{ij} P_{2j} + P_{2i} U_i P_{2i} + L_i^T L_i + Q_2 < 0, \end{aligned} \tag{15}$$

where

$$\begin{aligned} W_i &= \varepsilon_{1i}^{-1} M_{Ai} M_{Ai}^T + \varepsilon_{3i}^{-1} M_{di} M_{di}^T \\ &\quad + A_{di}\left(Q_1 - \varepsilon_{3i} N_{di}^T N_{di}\right)^{-1} \\ &\quad \times A_{di}^T + \gamma^{-2} B_i B_i^T, \\ U_i &= \varepsilon_{1i}^{-1} M_{Ai} M_{Ai}^T + \varepsilon_{3i}^{-1} M_{di} M_{di}^T \\ &\quad + A_{di}\left(Q_1 - \varepsilon_{3i} N_{di}^T N_{di}\right)^{-1} A_{di}^T \\ &\quad + \gamma^{-2} B_i \left(I - D_i^T H_i^{-1} D_i\right) B_i^T, \\ \widehat{A}_i &= A_i + \left[\varepsilon_{1i}^{-1} M_{Ai} M_{Ai}^T + \varepsilon_{3i}^{-1} M_{di} M_{di}^T \right. \\ &\quad \left. + A_{di}\left(Q_1 - \varepsilon_{3i} N_{di}^T N_{di}\right)^{-1} A_{di}^T\right] P_{1i} \\ &\quad + \gamma^{-2} B_i \left(I - D_i^T H_i^{-1} D_i\right) B_i^T P_{1i} - B_i D_i^T H_i^{-1} C_i, \\ H_i &= D_i D_i^T + \gamma^2 \varepsilon_{2i}^{-1} M_{Ci} M_{Ci}^T + \varepsilon_{4i} I, \end{aligned} \tag{16}$$

for $i = 1, \ldots, s$, then the robust H_∞ filtering problem is solvable. In this case, a suitable robust H_∞ filter Σ_F is given in form (10) *with parameters as follows:*

$$\widehat{K}_i = B_i D_i^T H_i^{-1}, \quad \widehat{L}_i = L_i, \quad i \in \mathcal{S}. \tag{17}$$

Proof. Let the mode at time t be i, that is; $r(t) = i$, $i \in \mathcal{S}$, and define

$$\overline{x}(t) = x(t) - \hat{x}(t), \tag{18}$$

then from system Σ and filter Σ_F, it is easy to show that

$$\begin{aligned} \dot{\overline{x}}(t) &= \widehat{A}_i \overline{x}(t) + \left[A_i + \Delta A_i(t) - \widehat{A}_i - \widehat{K}_i\left(C_i + \Delta C_i(t)\right)\right] x(t) \\ &\quad + \left[A_{di} + \Delta A_{di}(t)\right] x(t-d) + \left(B_i - \widehat{K}_i D_i\right) \omega(t). \end{aligned} \tag{19}$$

Therefore, by defining $\widetilde{x}(t)^T \triangleq [x(t)^T, \overline{x}(t)^T]^T$, we obtain the augmented system from Σ and Σ_F as

$$\Sigma_{\text{aug}}: \begin{cases} \dot{\widetilde{x}}(t) = \widetilde{A}_i(t)\widetilde{x}(t) + \widetilde{A}_{di}(t)\widetilde{x}(t-d) + \widetilde{B}_i \omega(t), \\ e(t) = \widetilde{C}_i \widetilde{x}(t), \\ \widetilde{x}(t) = \varphi(t), \quad \forall t \in [-d, 0], \ d > 0, \ r(0) = r_0, \end{cases} \tag{20}$$

where

$$\widetilde{A}_i(t) = \widetilde{A}_i + \Delta\widetilde{A}_i(t), \qquad \widetilde{A}_{di}(t) = \widetilde{A}_{di} + \Delta\widetilde{A}_{di}(t),$$

$$\widetilde{A}_i = \begin{bmatrix} A_i & 0 \\ A_i - \widehat{A}_i - \widehat{K}_i C_i & \widehat{A}_i \end{bmatrix},$$

$$\Delta\widetilde{A}_i(t) = \begin{bmatrix} \Delta A_i(t) & 0 \\ \Delta A_i(t) - \widehat{K}_i \Delta C_i(t) & 0 \end{bmatrix}, \tag{21}$$

$$\widetilde{A}_{di} = \begin{bmatrix} A_{di} & 0 \\ A_{di} & 0 \end{bmatrix}, \qquad \Delta\widetilde{A}_{di}(t) = \begin{bmatrix} \Delta A_{di}(t) & 0 \\ \Delta A_{di}(t) & 0 \end{bmatrix},$$

$$\widetilde{B}_i = \begin{bmatrix} B_i \\ B_i - \widehat{K}_i D_i \end{bmatrix}, \qquad \widetilde{C}_i = \begin{bmatrix} 0 & L_i \end{bmatrix}.$$

For $r(t) = i, i \in \mathcal{S}$, we define a matrix $P_i > 0$ by

$$P_i = \begin{bmatrix} P_{1i} & 0 \\ 0 & P_{2i} \end{bmatrix}. \tag{22}$$

Next, we will show that under the conditions of the theorem, the following matrix inequality

$$\begin{aligned} Z_i(t) &:= \widetilde{A}_i(t)^T P_i + P_i \widetilde{A}_i(t) + \sum_{j=1}^{s} \pi_{ij} P_j \\ &\quad + P_i \widetilde{A}_{di}(t) Q^{-1} \widetilde{A}_{di}(t)^T P_i + Q + \widetilde{C}_i^T \widetilde{C}_i \\ &\quad + \gamma^{-2} P_i \widetilde{B}_i \widetilde{B}_i^T P_i \le \begin{bmatrix} V_{1i} & 0 \\ 0 & V_{2i} \end{bmatrix} \end{aligned} \tag{23}$$

holds, when $r(t) = i, i \in \mathcal{S}$, where

$$\begin{aligned} Q &= \begin{bmatrix} Q_1 & 0 \\ 0 & Q_2 \end{bmatrix} > 0, \\ V_{1i} &= A_i^T P_{1i} + P_{1i} A_i + \sum_{j=1}^{s} \pi_{ij} P_{1j} + P_{1i} W_i P_{1i} \\ &\quad + \varepsilon_{1i} N_{Ai}^T N_{Ai} + \varepsilon_{2i} N_{Ci}^T N_{Ci} + Q_1, \\ V_{2i} &= \widehat{A}_i^T P_{2i} + P_{2i} \widehat{A}_i + \sum_{j=1}^{s} \pi_{ij} P_{2j} \\ &\quad + P_{2i} U_i P_{2i} + L_i^T L_i + Q_2. \end{aligned} \tag{24}$$

To this end, we use Lemma 2 to obtain the following matrix inequalities:

$$\begin{aligned} &P_i \Delta\widetilde{A}_i(t) + \Delta\widetilde{A}_i(t)^T P_i \\ &\le \varepsilon_{1i}^{-1} P_i \begin{bmatrix} M_{Ai} \\ M_{Ai} \end{bmatrix} \begin{bmatrix} M_{Ai}^T & M_{Ai}^T \end{bmatrix} P_i \\ &\quad + \varepsilon_{1i} \begin{bmatrix} N_{Ai}^T \\ 0 \end{bmatrix} \begin{bmatrix} N_{Ai} & 0 \end{bmatrix} \\ &\quad + \varepsilon_{2i}^{-1} P_i \begin{bmatrix} 0 \\ -\widehat{K}_i M_{Ci} \end{bmatrix} \begin{bmatrix} 0 & -M_{Ci}^T \widehat{K}_i^T \end{bmatrix} P_i \\ &\quad + \varepsilon_{21i} \begin{bmatrix} N_{Ci}^T \\ 0 \end{bmatrix} \begin{bmatrix} N_{Ci} & 0 \end{bmatrix} \\ &= \begin{bmatrix} H_{1i} & \varepsilon_{1i}^{-1} P_{1i} M_{Ai} M_{Ai}^T P_{2i} \\ \varepsilon_{1i}^{-1} P_{2i} M_{Ai} M_{Ai}^T P_{1i} & H_{2i} \end{bmatrix}, \\ &P_i \widetilde{A}_{di}(t) Q^{-1} \widetilde{A}_{di}(t)^T P_i \\ &\le P_i \widetilde{A}_{di} \left(Q - \varepsilon_{3i} \begin{bmatrix} N_{di}^T \\ 0 \end{bmatrix} \begin{bmatrix} N_{di} & 0 \end{bmatrix} \right)^{-1} \\ &\quad \times \widetilde{A}_{di}^T P_i + \varepsilon_{3i}^{-1} P_i \begin{bmatrix} M_{di} \\ M_{di} \end{bmatrix} \begin{bmatrix} M_{di}^T & M_{di}^T \end{bmatrix} P_i \\ &= \begin{bmatrix} G_{1i} & G_{2i}^T \\ G_{2i} & G_{3i} \end{bmatrix}, \end{aligned} \tag{25}$$

where (7) and

$$Q_1 - \varepsilon_{3i} N_{di}^T N_{di} > 0, \quad i = 1, \ldots, s, \tag{26}$$

are used and

$$\begin{aligned} H_{1i} &= \varepsilon_{1i}^{-1} P_{1i} M_{Ai} M_{Ai}^T P_{1i} + \varepsilon_{1i} N_{Ai}^T N_{Ai} + \varepsilon_{2i} N_{Ci}^T N_{Ci}, \\ H_{2i} &= P_{2i} \left(\varepsilon_{1i}^{-1} M_{Ai} M_{Ai}^T + \varepsilon_{2i}^{-1} \widehat{K}_i M_{Ci} M_{Ci}^T \widehat{K}_i^T \right) P_{2i}, \\ G_{1i} &= P_{1i} \left[\varepsilon_{3i}^{-1} M_{di} M_{di}^T + A_{di} \left(Q_1 - \varepsilon_{3i} N_{di}^T N_{di} \right)^{-1} A_{di}^T \right] P_{1i}, \\ G_{2i} &= P_{2i} \left[A_{di} \left(Q_1 - \varepsilon_{3i} N_{di}^T N_{di} \right)^{-1} A_{di}^T + \varepsilon_{3i}^{-1} M_{di} M_{di}^T \right] P_{1i}, \\ G_{3i} &= P_{2i} \left[A_{di} \left(Q_1 - \varepsilon_{3i} N_{di}^T N_{di} \right)^{-1} A_{di}^T + \varepsilon_{3i}^{-1} M_{di} M_{di}^T \right] P_{2i}. \end{aligned} \tag{27}$$

Hence

$$\begin{aligned} &Z_i(t) \\ &\le \widetilde{A}_i^T P_i + P_i \widetilde{A}_i \\ &\quad + \sum_{j=1}^{s} \pi_{ij} P_j + Q + \widetilde{C}_i^T \widetilde{C}_i + \gamma^{-2} P_i \widetilde{B}_i \widetilde{B}_i^T P_i \\ &\quad + \begin{bmatrix} H_{1i} + G_{1i} & \varepsilon_{1i}^{-1} P_{1i} M_{Ai} M_{Ai}^T P_{2i} + G_{2i}^T \\ \varepsilon_{1i}^{-1} P_{2i} M_{Ai} M_{Ai}^T P_{1i} + G_{2i} & H_{2i} + G_{3i} \end{bmatrix}. \end{aligned} \tag{28}$$

Substituting (16) and (17) into the right-hand side of the previous inequality and using algebraic manipulations we have that (23) holds.

Now, we will show the stochastic stability of the augmented system Σ_{aug} when $\omega(t) = 0$. In the following we will simply use $\widetilde{x}(t)$ to stand for the solution of the system Σ_{aug} at time t with the initial conditions $\varphi(t)$ and r_0.

Introduce the following stochastic Lyapunov functional candidate for system Σ_{aug}:

$$V(\widetilde{x}(t), r(t)) = \widetilde{x}(t)^T P(r(t)) \widetilde{x}(t) + \int_{t-d}^{t} \widetilde{x}(\tau)^T Q \widetilde{x}(\tau)\, d\tau. \tag{29}$$

It can then be shown that the weak infinitesimal generator $\mathscr{A}$ of the random process $\{\widetilde{x}(t), r(t)\}$ is given by

$$\begin{aligned}\mathscr{A}V(\widetilde{x}(t), i) &= \lim_{h\longrightarrow\infty}\frac{1}{h}\left[\mathscr{E}\left\{V(\widetilde{x}(t+h), r(t+h)) \mid \widetilde{x}(t), \right.\right. \\ &\qquad \left.\left. r(t) = i\right\} - V(\widetilde{x}(t), r(t) = i)\right] \\ &= \widetilde{x}(t)^T\left[\widetilde{A}_i(t)^T P_i + P_i\widetilde{A}_i(t) + \sum_{j=1}^{s}\pi_{ij}P_j + Q\right] \\ &\quad \times \widetilde{x}(t) + \widetilde{x}(t)^T P_i\widetilde{A}_{di}(t)\,\widetilde{x}(t-d) \\ &\quad + \widetilde{x}(t-d)^T\widetilde{A}_{di}(t)^T P_i\widetilde{x}(t) \\ &\quad - \widetilde{x}(t-d)\,Q\widetilde{x}(t-d),\end{aligned} \tag{30}$$

for any $r(t) = i$, $i \in \mathcal{S}$. Then, from Lemma 2, it follows that

$$\begin{aligned}&\mathscr{A}V(\widetilde{x}(t), i) \\ &\le \widetilde{x}(t)^T\left[\widetilde{A}_i(t)^T P_i + P_i\widetilde{A}_i(t)\right. \\ &\qquad \left. + \sum_{j=1}^{s}\pi_{ij}P_j + P_i\widetilde{A}_{di}(t)\,Q^{-1}\widetilde{A}_{di}(t)^T P_i + Q\right]\widetilde{x}(t).\end{aligned} \tag{31}$$

Using (23), we have

$$\mathscr{A}V(\widetilde{x}(t), i) \le \widetilde{x}(t)^T\begin{bmatrix} V_{1i} & 0 \\ 0 & V_{2i}\end{bmatrix}\widetilde{x}(t) \le -\beta_1\widetilde{x}(t)^T\widetilde{x}(t), \tag{32}$$

where $\beta_1 = \min_{i\in\mathcal{S}}\{\lambda_{\min}(-V_{1i}), \lambda_{\min}(-V_{2i})\}$. From (15), it is easy to see that $\beta_1 > 0$.

Now using Dynkin's formula, we have, for each $r(t) = i$, $i \in \mathcal{S}$, $t > 0$,

$$\begin{aligned}&\mathscr{E}\{V(\widetilde{x}(t), i)\} - V(\widetilde{x}_0, r_0) \\ &\quad = \mathscr{E}\left\{\int_0^t \mathscr{A}V(\widetilde{x}(\tau), r(\tau))\,d\tau\right\} \\ &\quad \le -\beta_1\int_0^t \mathscr{E}\left\{\widetilde{x}(\tau)^T\widetilde{x}(\tau)\right\}d\tau.\end{aligned} \tag{33}$$

On the other hand, for each $r(t) = i$, $i \in \mathcal{S}$, we can show that

$$\begin{aligned}\mathscr{E}\{V(\widetilde{x}(t), i)\} &= \mathscr{E}\left\{\widetilde{x}(t)^T P_i\widetilde{x}(t)\right\} \\ &\quad + \mathscr{E}\left\{\int_{t-d}^t \widetilde{x}(\tau)^T Q\widetilde{x}(\tau)\,d\tau\right\} \\ &\ge \beta_2\mathscr{E}\left\{\widetilde{x}(t)^T\widetilde{x}(t)\right\},\end{aligned} \tag{34}$$

where $\beta_2 = \min_{i\in\mathcal{S}}\{\lambda_{\min}(P_i)\}$ and $\beta_2 > 0$. The previous inequality and (33) imply that

$$\begin{aligned}\mathscr{E}\left\{\widetilde{x}(t)^T\widetilde{x}(t)\right\} &\le -\lambda_1\int_0^t \mathscr{E}\left\{\widetilde{x}(\tau)^T\widetilde{x}(\tau)\right\}d\tau \\ &\quad + \lambda_2 V(\widetilde{x}_0, r_0),\end{aligned} \tag{35}$$

where $\lambda_1 = \beta_1\beta_2^{-1} > 0$ and $\lambda_2 = \beta_2^{-1} > 0$. Then, it can be verified that

$$\mathscr{E}\left\{\widetilde{x}(t)^T\widetilde{x}(t)\right\} \le \lambda_2\exp(-\lambda_1 t)\,V(\widetilde{x}_0, r_0). \tag{36}$$

Therefore,

$$\begin{aligned}&\mathscr{E}\left\{\int_0^t \widetilde{x}(\tau)^T\widetilde{x}(\tau)\,d\tau \mid \varphi, r_0\right\} \\ &\qquad \le \lambda_1^{-1}\lambda_2\left[1 - \exp(-\lambda_1 t)\right]V(\widetilde{x}_0, r_0).\end{aligned} \tag{37}$$

Taking limit as $t \to \infty$, we have

$$\lim_{t\to\infty}\mathscr{E}\left\{\int_0^t \widetilde{x}(\tau)^T\widetilde{x}(\tau)\,d\tau \mid \varphi, r_0\right\} \le \lambda_1^{-1}\lambda_2 V(\widetilde{x}_0, r_0). \tag{38}$$

Note that there always exists a scalar $c > 0$ such that

$$\lambda_1^{-1}\lambda_2 V(\widetilde{x}_0, r_0) \le c\sup_{-d\le\tau\le 0}\left|\varphi(\tau)\right|^2. \tag{39}$$

Considering (38), we have that the augmented system Σ_{aug} is stochastically stable. Next we will show that

$$\|e(t)\|_{E_2} < \gamma\|\omega(t)\|_2, \tag{40}$$

for all nonzero $\omega(t) \in L_2[0, \infty)$. To this end, we introduce

$$J = \mathscr{E}\left\{\int_0^\infty\left[e(\tau)^T e(\tau) - \gamma^2\omega(\tau)^T\omega(\tau)\right]d\tau\right\}. \tag{41}$$

For any $r(t) = i$, $i \in \mathcal{S}$, $\omega(t) \ne 0$, we have

$$\begin{aligned}\mathscr{A}V(\widetilde{x}(t), i) &= \widetilde{x}(t)^T\left[\widetilde{A}_i(t)^T P_i + P_i\widetilde{A}_i(t) + \sum_{j=1}^{s}\pi_{ij}P_j + Q\right] \\ &\quad \times \widetilde{x}(t) + \widetilde{x}(t)^T P_i\widetilde{A}_{di}(t)\,\widetilde{x}(t-d) \\ &\quad + \widetilde{x}(t-d)^T\widetilde{A}_{di}(t)^T P_i\widetilde{x}(t) \\ &\quad - \widetilde{x}(t-d)^T Q\widetilde{x}(t-d) \\ &\quad + \widetilde{x}(t)^T P_i\widetilde{B}_i\omega(t) + \omega(t)^T\widetilde{B}_i^T P_i\widetilde{x}(t).\end{aligned} \tag{42}$$

Thus, under zero initial condition, for any $t > 0$, $r(t) = i$, $i \in \mathcal{S}$, $\omega(t) \neq 0$,

$$\begin{aligned} J_1 &= \mathscr{E}\left\{\int_0^t \left[e(\tau)^T e(\tau) - \gamma^2 \omega(\tau)^T \omega(\tau)\right] d\tau\right\} \\ &= \mathscr{E}\left\{\int_0^t \left[e(\tau)^T e(\tau) - \gamma^2 \omega(\tau)^T \omega(\tau) \right.\right. \\ &\qquad \left.\left. + \mathscr{A}V(\tilde{x}(\tau), i)\right] d\tau\right\} \\ &\quad - \mathscr{E}\left\{\int_0^t \mathscr{A}V(\tilde{x}(\tau), i)\, d\tau\right\} \\ &= \mathscr{E}\left\{\int_0^t \left[\tilde{x}(\tau)^T Z_i(\tau)\tilde{x}(\tau) \right.\right. \\ &\qquad - \left(\tilde{x}(t-d)^T - \tilde{x}(t)^T P_i \widetilde{A}_{di}(t) Q^{-1}\right) \\ &\qquad \times Q\left(\tilde{x}(t-d) - Q^{-1}\widetilde{A}_{di}(t)^T P_i \tilde{x}(t)\right) \\ &\qquad - \gamma^2\left(\omega(\tau)^T - \gamma^{-2}\tilde{x}(t)^T P_i \widetilde{B}_i\right) \\ &\qquad \left.\left. \times \left(\omega(\tau) - \gamma^{-2}\widetilde{B}_i^T P_i \tilde{x}(t)\right)\right] d\tau\right\} \\ &\quad - \mathscr{E}\{V(\tilde{x}(t), i)\}. \end{aligned} \tag{43}$$

Hence

$$J \leq \mathscr{E}\left\{\int_0^\infty \tilde{x}(\tau)^T Z_i(\tau)\tilde{x}(\tau)\, d\tau\right\}. \tag{44}$$

Finally, from (23), (40) follows immediately. This completes the proof. □

Remark 4. Theorem 3 provides a sufficient condition for the solvability of robust H_∞ filtering problem for uncertain stochastic time-delay systems with Markovian jumping parameters, and the desired filter can be constructed by solving two sets of coupled algebraic Riccati inequalities.

In the case when $\mathcal{S} = \{1\}$, that is, there is only one mode operation, we have $\pi_{ii} = 0, i \in \mathcal{S} = \{1\}$, and system Σ reduces to the following uncertain time-delay system with no jumping parameters:

$$\Sigma_1 : \begin{cases} \dot{x}(t) = [A + \Delta A(t)]\, x(t) \\ \quad + [A_d + \Delta A_d(t)]\, x(t-d) + B\omega(t), \\ y(t) = [C + \Delta C(t)]\, x(t) + D\omega(t), \\ z(t) = Lx(t), \\ x(t) = \phi(t), \quad \forall t \in [-d, 0],\ d > 0,\ r(0) = r_0, \end{cases} \tag{45}$$

where $\Delta A(t)$, $\Delta A_d(t)$, and $\Delta C(t)$ are unknown matrices and are assumed to be of the form

$$\begin{aligned} \Delta A(t) = M_A F_A(t) N_A, \qquad \Delta A_d(t) = M_d F_d(t) N_d, \\ \Delta C(t) = M_C F_C(t) N_C, \end{aligned} \tag{46}$$

where M_A, N_{Ai}, M_d, N_d, M_C, and N_C are known constant matrices and $F_A(t)$, $F_d(t)$, and $F_C(t)$ are the uncertain time-varying matrices satisfying

$$\begin{aligned} F_A(t)^T F_A(t) \leq I, \qquad F_d(t)^T F_d(t) \leq I, \\ F_C(t)^T F_C(t) \leq I. \end{aligned} \tag{47}$$

Then, from Theorem 3, we have the following robust H_∞ filtering result for the previous system.

Corollary 5. *Consider the uncertain time-delay system* (Σ_1). *If there exist scalars* $\varepsilon_i > 0$, $i = 1, \ldots, 4$, *and matrices* $P_1 > 0$, $P_2 > 0$, $Q_1 > 0$, *and* $Q_2 > 0$, *such that* $Q_1 - \varepsilon_3 N_d^T N_d > 0$, *and the following coupled Riccati matrix inequalities hold:*

$$\begin{aligned} A^T P_1 + P_1 A + P_1 W P_1 + \varepsilon_1 N_A^T N_A + \varepsilon_2 N_C^T N_C + Q_1 < 0 \\ \widehat{A}^T P_2 + P_2 \widehat{A} + P_2 U P_2 + L^T L + Q_2 < 0, \end{aligned} \tag{48}$$

where

$$\begin{aligned} W &= \varepsilon_1^{-1} M_A M_A^T + \varepsilon_3^{-1} M_d M_d^T + A_d\left(Q_1 - \varepsilon_3 N_d^T N_d\right)^{-1} A_d^T \\ &\quad + \gamma^{-2} B B^T, \\ U &= \varepsilon_1^{-1} M_A M_A^T + \varepsilon_3^{-1} M_d M_d^T + A_d\left(Q_1 - \varepsilon_3 N_d^T N_d\right)^{-1} A_d^T \\ &\quad + \gamma^{-2} B\left(I - D^T H^{-1} D\right) B^T, \\ \widehat{A} &= A + \left[\varepsilon_1^{-1} M_A M_A^T + \varepsilon_3^{-1} M_d M_d^T \right. \\ &\qquad \left. + A_d\left(Q_1 - \varepsilon_3 N_d^T N_d\right)^{-1} A_d^T\right] P_1 \\ &\quad + \gamma^{-2} B\left(I - D^T H^{-1} D\right) B^T P_1 - B D^T H^{-1} C, \\ H &= DD^T + \gamma^2 \varepsilon_2^{-1} M_C M_C^T + \varepsilon_4 I, \end{aligned} \tag{49}$$

then the robust H_∞ *filtering problem is solvable. In this case, a suitable robust* H_∞ *filter is given by*

$$\begin{aligned} \dot{\hat{x}}(t) = \widehat{A}\hat{x}(t) + \widehat{K} y(t), \\ \hat{z}(t) = \widehat{L}\hat{x}(t), \end{aligned} \tag{50}$$

where

$$\widehat{K} = B D^T H^{-1}, \qquad \widehat{L} = L. \tag{51}$$

Remark 6. The solvability for robust H_∞ filtering problem for uncertain continuous delay-free systems can be easily derived from Corollary 5, in this case. It can be shown that the result coincides with that proposed in [8].

4. Numerical Example

In this section, we will give a numerical example to demonstrate the applicability of the proposed approach.

Consider the uncertain time-delay stochastic linear systems with Markovian jumping parameters in form (1) with two modes. For mode 1, the dynamics of the system are described as follows:

$$A_1 = \begin{bmatrix} -5 & 2 & 0 \\ 0 & -4 & 1 \\ 0 & 0 & -5 \end{bmatrix}, \quad A_{d1} = \begin{bmatrix} -1 & 0 & 0.2 \\ 0 & 0.5 & 1 \\ 0.5 & 0 & 0 \end{bmatrix},$$
$$B_1 = \begin{bmatrix} 1 & -2.3 \\ 0 & 1 \\ 0.5 & 0 \end{bmatrix}, \quad C_1 = \begin{bmatrix} -1 & 0 & 2 \\ 0 & 1 & 1 \end{bmatrix},$$
$$D_1 = \begin{bmatrix} 1 & 0 \\ 0 & 1 \end{bmatrix}, \quad M_{C1} = \begin{bmatrix} 0.5 & 1 \\ 0 & 0.5 \end{bmatrix},$$
$$N_{C1} = \begin{bmatrix} 0 & 0.5 & 1 \\ 0 & -0.5 & 1 \end{bmatrix}, \quad M_{A1} = \begin{bmatrix} 1 & 0 \\ 0 & 1 \\ 0.5 & 1 \end{bmatrix},$$
$$M_{d1} = \begin{bmatrix} 0 & 0.5 \\ 0.5 & 1 \\ 0.5 & 0 \end{bmatrix}, \quad N_{A1}^T = \begin{bmatrix} -0.2 \\ 0.1 \\ 0 \end{bmatrix},$$
$$N_{d1}^T = \begin{bmatrix} -0.1 \\ 0 \\ 0.2 \end{bmatrix}, \quad L_1 = \begin{bmatrix} 0.2 & 0 & 0 \\ 0 & 0.3 & -0.1 \end{bmatrix}. \tag{52}$$

For mode 2, the dynamics of the system are described as follows:

$$A_2 = \begin{bmatrix} -6 & 1 & 0.5 \\ -1 & -7 & 0 \\ 0 & 0.5 & -6 \end{bmatrix}, \quad A_{d2} = \begin{bmatrix} 0 & 1 & 0 \\ 0.5 & -1 & -0.1 \\ 0 & 0 & 1 \end{bmatrix},$$
$$B_2 = \begin{bmatrix} -1 & 0.5 \\ -3 & 1 \\ 0 & 1 \end{bmatrix}, \quad C_2 = \begin{bmatrix} 0.5 & 1 & 2 \\ -1 & 0 & 2 \end{bmatrix},$$
$$D_2 = \begin{bmatrix} -1 & 0.5 \\ 0.2 & 1 \end{bmatrix}, \quad M_{C2} = \begin{bmatrix} 0.1 & -0.3 \\ 0.5 & 0 \end{bmatrix},$$
$$N_{C2} = \begin{bmatrix} -1 & 0.2 & 0.3 \\ 0.5 & 0.5 & 0 \end{bmatrix}, \quad M_{A2} = \begin{bmatrix} 0.5 & 0.3 \\ 0 & 0.5 \\ 0.2 & 1 \end{bmatrix},$$
$$M_{d2} = \begin{bmatrix} -0.6 & 0.5 \\ 0 & 1 \\ 0.5 & 1 \end{bmatrix}, \quad N_{A2}^T = \begin{bmatrix} 0 \\ 0.1 \\ 0 \end{bmatrix},$$
$$N_{d2}^T = \begin{bmatrix} 0.2 \\ 0 \\ 0 \end{bmatrix}, \quad L_2 = \begin{bmatrix} -0.2 & 0.1 & 0 \\ 0.3 & 0 & 0.5 \end{bmatrix}. \tag{53}$$

Let the transition probability matrix be given by

$$\Pi = \begin{bmatrix} -0.5 & 0.5 \\ 1 & -1 \end{bmatrix}. \tag{54}$$

In this example, we set $\gamma = 2.8$. By solving (15), we obtain

$$P_{11} = \begin{bmatrix} 2.1592 & 0.3579 & -0.0589 \\ 0.3579 & 3.2018 & 0.1337 \\ -0.0589 & 0.1337 & 4.0867 \end{bmatrix},$$
$$P_{12} = \begin{bmatrix} 2.9083 & -0.0024 & -0.2047 \\ -0.0024 & 1.6855 & 0.0031 \\ -0.2047 & 0.0031 & 2.0020 \end{bmatrix},$$
$$Q_1 = \begin{bmatrix} 11.1343 & -0.4670 & -0.3949 \\ -0.4670 & 10.5734 & -0.6361 \\ -0.3949 & -0.6361 & 11.8166 \end{bmatrix},$$
$$P_{21} = \begin{bmatrix} 0.2157 & 0.1094 & 0.0221 \\ 0.1094 & 0.3324 & 0.0524 \\ 0.0221 & 0.0524 & 0.1848 \end{bmatrix},$$
$$P_{22} = \begin{bmatrix} 0.1572 & -0.0161 & 0.0122 \\ -0.0161 & 0.0989 & -0.0176 \\ 0.0122 & -0.0176 & 0.1414 \end{bmatrix},$$
$$Q_2 = \begin{bmatrix} 0.7630 & -0.0624 & -0.0257 \\ -0.0624 & 0.7896 & -0.0205 \\ -0.0257 & -0.0205 & 0.8370 \end{bmatrix},$$
$$\varepsilon_{11} = 12.1023, \quad \varepsilon_{21} = 9.2498,$$
$$\varepsilon_{31} = 12.1293, \quad \varepsilon_{41} = 0.0032,$$
$$\varepsilon_{12} = 12.1346, \quad \varepsilon_{22} = 10.1634,$$
$$\varepsilon_{32} = 12.1219, \quad \varepsilon_{42} = 0.0012. \tag{55}$$

Therefore, using Theorem 3, a suitable Markovian robust H_∞ filter can be constructed with parameters given as follows:

$$\widehat{A}_1 = \begin{bmatrix} -3.5504 & 4.4496 & 0.3304 \\ 0.0239 & -3.8366 & 0.9941 \\ 0.2927 & 0.4860 & -4.7540 \end{bmatrix},$$
$$\widehat{K}_1 = \begin{bmatrix} 0.9411 & -2.2211 \\ -0.1821 & 0.8865 \\ 0.2611 & -0.0911 \end{bmatrix},$$
$$\widehat{L}_1 = \begin{bmatrix} 0.2 & 0 & 0 \\ 0 & 0.3 & -0.1 \end{bmatrix},$$
$$\widehat{A}_2 = \begin{bmatrix} -5.9695 & 0.0301 & -1.2747 \\ -2.8680 & -9.2528 & -4.3890 \\ 0.7840 & 0.5184 & -7.3116 \end{bmatrix},$$
$$\widehat{K}_1 = \begin{bmatrix} 0.9452 & -0.0162 \\ 2.7441 & -0.4287 \\ 0.1826 & 0.7602 \end{bmatrix},$$
$$\widehat{L}_2 = \begin{bmatrix} -0.2 & 0.1 & 0 \\ 0.3 & 0 & 0.5 \end{bmatrix}. \tag{56}$$

5. Conclusions

In this paper, we have studied the problem of robust H_∞ filtering for a class of uncertain Markovian jump systems

with time-delay and norm-bounded time-varying parameter uncertainties. A Markovian jump filter is designed which guarantees the stochastic stability of the filter error dynamics and a prescribed bound on the $\mathscr{L}_2$-induced gain from the noise signals to the filter error irrespective of the parameter uncertainties. It has been shown that the desired robust H_∞ filter can be constructed by solving two sets of coupled algebraic Riccati inequalities.

Acknowledgments

This work was supported in part by the National Natural Science Foundation of China (61104132) and Director of the foundation (SJ201002).

References

[1] B. D. O. Anderson and J. B. Moore, *Optimal Filtering*, Prentice-Hall, Englewood Cliffs, NJ, USA, 1979.

[2] D. S. Bernstein and W. M. Haddad, "Steady-state Kalman filtering with an H_∞ error bound," *Systems & Control Letters*, vol. 12, no. 1, pp. 9–16, 1989.

[3] M. J. Grimble and A. Elsayed, "Solution of the H_∞ optimal linear filtering problem for discrete-time systems," *Institute of Electrical and Electronics Engineers*, vol. 38, no. 7, pp. 1092–1104, 1990.

[4] K. M. Nagpal and P. P. Khargonekar, "Filtering and smoothing in an H_∞ setting," *Institute of Electrical and Electronics Engineers*, vol. 36, no. 2, pp. 152–166, 1991.

[5] B. O. S. Teixeira, J. Chandrasekar, H. J. Palanthandalam-Madapusi, L. A. B. Tôrres, L. A. Aguirre, and D. S. Bernstein, "Gain-constrained Kalman filtering for linear and nonlinear systems," *IEEE Transactions on Signal Processing*, vol. 56, no. 9, pp. 4113–4123, 2008.

[6] M. Fu, C. E. de Souza, and L. Xie, "H_∞ estimation for uncertain systems," *International Journal of Robust and Nonlinear Control*, vol. 2, pp. 87–105, 1992.

[7] H. Li and M. Fu, "An LMI approach to robust H_∞ filtering for linear systems," in *Proceedings of the 34th IEEE Conference Decision and Control*, pp. 3608–3613, New Orleans, La, USA, December 1995.

[8] L. Xie and C. E. de Souza, "On robust filtering for linear systems with parameter uncertainty," in *Proceedings of the 34th IEEE Conference Decision and Control*, pp. 2087–2092, New Orleans, La, USA, December 1995.

[9] L. Xie, C. E. de Souza, and M. Fu, "H_∞ estimation for discrete-time linear uncertain systems," *International Journal of Robust and Nonlinear Control*, vol. 1, pp. 111–123, 1991.

[10] H. J. Chizeck, A. S. Willsky, and D. Castañon, "Discrete-time Markovian-jump linear quadratic optimal control," *International Journal of Control*, vol. 43, no. 1, pp. 213–231, 1986.

[11] X. Feng, K. A. Loparo, Y. Ji, and H. J. Chizeck, "Stochastic stability properties of jump linear systems," *Institute of Electrical and Electronics Engineers*, vol. 37, no. 1, pp. 38–53, 1992.

[12] Y. Ji and H. J. Chizeck, "Controllability, stabilizability, and continuous-time Markovian jump linear quadratic control," *Institute of Electrical and Electronics Engineers*, vol. 35, no. 7, pp. 777–788, 1990.

[13] B. Zhang and Y. Li, "Exponential L_2-H_∞ filtering for distributed delay systems with Markovian jumping parameters," *Signal Processing*, vol. 93, pp. 206–216, 2013.

[14] C. E. de Souza and M. D. Fragoso, "H_∞ filtering for Markovian jump linear systems," *In Proceedings of the 35th IEEE Conference on Decision and Control*, pp. 4814–4818, Kobe, Japan, December 1996.

[15] C. E. de Souza and M. D. Fragoso, "Robust H_∞ filtering for Markovian jump linear systems," *In Proceedings of the 35th IEEE Conference Decision and Control*, pp. 4808–4813, Kobe, Japan, December 1996.

[16] C. E. de Souza and M. D. Fragoso, "Robust H_∞ filtering for uncertain Markovian jump linear systems," *International Journal of Robust and Nonlinear Control*, vol. 12, no. 5, pp. 435–446, 2002.

[17] S. Wen, Z. Zeng, and T. Huang, "Reliable H_∞ filter design for a class of mixed-delay Markovian jump systems with stochastic nonlinearities and multiplicative noises via delay-partitioning method," *International Journal of Control, Automation and Systems*, vol. 10, pp. 711–720, 2012.

[18] R. Zhang, Y. Zhang, C. Hu, M. Q.-H. Meng, and Q. He, "Delay-range-dependent H_∞ filtering for two-dimensional Markovian jump systems with interval delays," *IET Control Theory & Applications*, vol. 5, no. 18, pp. 2191–2199, 2011.

[19] X. Li and C. E. de Souza, "Criteria for robust stability and stabilization of uncertain linear systems with state delay," *Automatica*, vol. 33, no. 9, pp. 1657–1662, 1997.

[20] X. Li and C. E. de Souza, "Delay-dependent robust stability and stabilization of uncertain linear delay systems: a linear matrix inequality approach," *Institute of Electrical and Electronics Engineers*, vol. 42, no. 8, pp. 1144–1148, 1997.

Hindawi Publishing Corporation
Mathematical Problems in Engineering
Volume 2013, Article ID 825143, 8 pages
http://dx.doi.org/10.1155/2013/825143

Research Article

Finite-Frequency Filter Design for Networked Control Systems with Missing Measurements

Dan Ye,[1,2] Yue Long,[3] and Guang-Hong Yang[1]

[1] *College of Information Science and Engineering, Northeastern University, Liaoning, Shenyang 110004, China*
[2] *State Key Laboratory of Robotics, Shenyang Institute of Automation, (CAS), Liaoning, Shenyang 110016, China*
[3] *College of Information, Shenyang Institute of Engineering, Liaoning, Shenyang 110136, China*

Correspondence should be addressed to Dan Ye; yedan@ise.neu.edu.cn

Received 26 March 2013; Revised 22 May 2013; Accepted 2 June 2013

Academic Editor: Bo Shen

This paper is concerned with the problem of robust filter design for networked control systems (NCSs) with random missing measurements. Different from existing robust filters, the proposed one is designed in finite-frequency domain. With consideration of possible missing data, the NCSs are first modeled to Markov jump systems (MJSs). A finite-frequency stochastic H_∞ performance is subsequently given that extends the standard H_∞ performance, and then a sufficient condition guaranteeing the system to be with such a performance is derived in terms of linear matrix inequality (LMI). With the aid of this condition, a procedure of filter synthesis is proposed to deal with noises in the low-, middle-, and high-frequency domains, respectively. Finally, an example about the lateral-directional dynamic model of the NASA High Alpha Research Vehicle (HARV) is carried out to illustrate the effectiveness of the proposed method.

1. Introduction

Due to the rapid development in communication network and computer technology, networked control systems (NCSs) have received much more research attentions. Networked control systems (NCSs) are control systems in which controller and plant are connected via a communication channel. The defining feature of an NCS is that information (reference input, plant output, control input, etc.) is exchanged using a network among control system components (sensors, controller, actuators, etc.). NCSs have many advantages such as easy diagnosis, low cost, and high mobility. And thus NCSs have been applied in many industrial systems such as automobiles, manufacturing plants, and aircrafts; see, for example, [1, 2]. Motivated by this wide spectrum of applications, the new problems arising from the limit resources of the communication channel are gradually taken into account when designing the NCSs. For example, the issues of network-induced delay, packet dropout, and quantization are considered in [3–12], respectively.

On the other hand, state estimation has been widely studied and has found many practical applications over the past decades [13]. When a priori statistical information on the external noise signals is unknown, the celebrated Kalman filtering cannot be employed. To address this issue, H_∞ filtering is introduced, which aims to make the worst case H_∞ norm from the process noise to the estimation error minimized. More recently, there have appeared a few results on H_∞ filter design [14–18]. However, it should be noticed that all the aforementioned methods are proposed in full-frequency domain. Nevertheless, practical industry systems often employ large, complex, or lightweight structures, which include finite-frequency fundamental vibration modes [19]. In these situations, it is more reasonable and precise to design filters in finite-frequency domain. Fortunately, the Kalman-Yakubovich-Popov (KYP) lemma is generalized in [20] to characterize frequency domain inequalities with (semi)finite-frequency ranges in terms of linear matrix inequalities (LMIs). The generalized KYP lemma is an effective tool to deal with the finite-frequency problem of linear time-invariant systems [20–26]. There are some results concerned with this meaningful problem, for example, [27] proposed an effective filter for fuzzy nonlinear systems. However, to the best of the author's knowledge, for system engaging random

packet dropout, few results have been published for such class of NCSs. This instance motivates our present investigation.

This paper studies the robust filter design problem with finite-frequency specifications for networked control systems (NCSs) subject to random missing measurements. First, the considered systems are modeled in the framework of Markov jump systems (MJSs). Motivated by Iwasaki et al. [22], a definition of finite-frequency stochastic H_∞ norm is subsequently given to measure the robustness, which extends the standard H_∞ norm and contains the frequency information of noises. Then based on Projection Lemma, an analysis condition is presented to guarantee the MJS being with such a performance in the framework of linear matrix inequalities (LMIs). Further, a procedure of filter synthesis is designed to deal with noises in low-, middle-, and high-frequency domains, respectively. Finally, an example about the lateral-directional dynamic model of the NASA High Alpha Research Vehicle (HARV) is given to illustrate the effectiveness of the proposed method.

The rest of the paper is organized as follows. The problem statement for NCSs with random packet dropout is formulated in Section 2. Section 3 provides sufficient condition to meet the performance request and a design procedure of the robust filter. In Section 4, an example is given to illustrate the effectiveness of the proposed method. Finally, some conclusions end the paper in Section 5.

Notations. Throughout the paper, the superscripts T and -1 stand for, respectively, the transposition and the inverse of a matrix; $M > 0$ means that M is real symmetric and positive definite; $\|\cdot\|$ denotes the Euclidean norm; l_2 denotes the Hilbert space of square integrable functions. In block symmetric matrices or long matrix expressions, we use $*$ to represent a term that is induced by symmetry. The sum of a square matrix A and its transposition A^T is denoted by $He(A) := A + A^T$.

2. Problem Formulation

Considering the NCS depicted in Figure 1, the continuous-time plant model is

$$\begin{aligned} \dot{x}(t) &= Ax(t) + Bw(t), \\ y(t) &= Cx(t) + Dw(t), \\ z(t) &= Ex(t), \end{aligned} \tag{1}$$

where $x(t) \in \mathbb{R}^n$ is the state, $y(t) \in \mathbb{R}^m$ is the measured output, $z(t) \in \mathbb{R}^p$ is the controlled output, and $w(t) \in \mathbb{R}^d$ is the exogenous disturbance which belongs to $l_2[0, \infty)$. A, B, C, D, and E are known real constant matrices with appropriate dimensions.

It is assumed that, as shown in Figure 1, the measurement signals will be transmitted via the networks wherein missing data may occur. Further, assume the interval between the kth and the $(k+1)$th successfully received measurements at the filter is $\alpha_k h$, where h is the sampling period of the sensor. It is obvious that the number of the missed packets at time instant $(k+1)h$ is $\alpha_k - 1$, which can be modeled

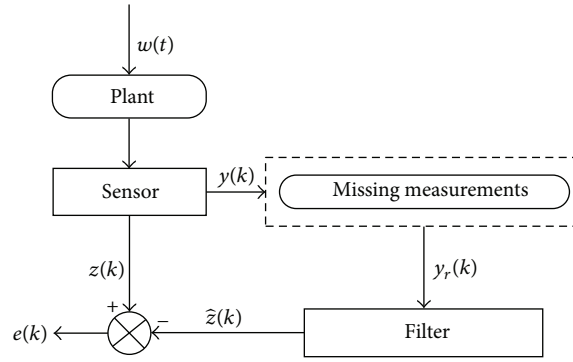

Figure 1: The structure of the NCSs.

by a time-homogeneous Markov chain α_k with the range set $\mathbb{S} = \{1, 2, \ldots, N\}$ and the transition probability matrix

$$\begin{aligned} \Lambda &= \left(\lambda_{ij}\right)_{i,j\in\mathbb{S}} = \left(\mathbf{P}\left(\alpha_{k+1} = j \mid \alpha_k = i\right)\right)_{i,j\in\mathbb{S}} \\ &= \begin{bmatrix} \lambda_{11} & \lambda_{12} & \cdots & \lambda_{1N} \\ \lambda_{21} & \lambda_{22} & \cdots & \lambda_{2N} \\ \vdots & \vdots & \ddots & \vdots \\ \lambda_{N1} & \lambda_{N2} & \cdots & \lambda_{NN} \end{bmatrix}. \end{aligned} \tag{2}$$

In this situation, the dynamics of plant (1) together with the missing measurements at time instant t_k can be approximated by

$$\begin{aligned} x(k+1) &= A_{\alpha_k} x(k) + B_{\alpha_k} w(k), \\ y_r(k) &= Cx(k) + Dw(k), \\ z(k) &= Ex(k), \end{aligned} \tag{3}$$

where $t_0 = 0$, $t_k = \sum_{i=0}^{k-1} \alpha_i h$ $(k \geq 1)$, $x(k) = x(t_k)$, $A_{\alpha_k} = e^{A_c(\alpha_k h)}$, and $B_{\alpha_k} = \int_0^{\alpha_k h} e^{A_c t} B_c dt$. It can be seen that, after the above treatment, the possible missing measurements can be converted to the jumping parameter of the MJS (3) with the transition probability Λ.

In this paper, the filter is chosen as the following form:

$$\begin{aligned} \hat{x}(k+1) &= A_{f\alpha_k} \hat{x}(k) + B_{f\alpha_k} y_r(k), \\ \hat{z}(k) &= C_{f\alpha_k} x(k) + D_{f\alpha_k} y_r(k), \end{aligned} \tag{4}$$

where $\hat{x}(k) \in \mathbb{R}^n$ is the filter's state, $\hat{z}(k)$ is the estimated output, and $A_{f\alpha_k}$, $B_{f\alpha_k}$, $C_{f\alpha_k}$, and $D_{f\alpha_k}$ are filter gains to be designed.

To ensure the achievement of filter design objective, a basic assumption, that is, A_c is stable, is also assumed to be valid.

Remark 1. This assumption is required to get a stable filtering error dynamics. If this assumption is not satisfied, a stabilizing output feedback controller is required.

For convenience, A_{α_k}, B_{α_k}, $A_{f\alpha_k}$, $B_{f\alpha_k}$, $C_{f\alpha_k}$, and $D_{f\alpha_k}$ are notated as A_i, B_i, A_{fi}, B_{fi}, C_{fi}, and D_{fi} when $\alpha_k = i$,

respectively. Denoting $\eta(k) = [x^T(k)\ \hat{x}^T(k)]^T$ and $e(k) = z(k) - \hat{z}(k)$, the filtering error system can be described by the following system:

$$\begin{aligned} \eta(k+1) &= \mathscr{A}_i \eta(k) + \mathscr{B}_i w(k), \\ e_r(k) &= \mathscr{C}_i \eta(k) + \mathscr{D}_i w(k), \end{aligned} \tag{5}$$

where

$$\left[\begin{array}{c|c} \mathscr{A}_i & \mathscr{B}_i \\ \hline \mathscr{C}_i & \mathscr{D}_i \end{array}\right] = \left[\begin{array}{cc|c} A_i & 0 & B_i \\ B_{fi}C & A_{fi} & B_{fi}D \\ \hline E - D_{fi}C & -C_{fi} & -D_{fi}D \end{array}\right]. \tag{6}$$

In order to present the objective of this paper clearly, the following definition is first given.

Definition 2 (MSS). The filter error system (5) is said to be mean-square stable (MSS) with $w(k) = 0$, if

$$\lim_{k\to\infty} \mathbb{E}\left\{\|\eta(k)\|^2\right\} = 0 \tag{7}$$

holds for all $\alpha_k = i \in \mathbb{S}$.

Definition 3 (finite-frequency stochastic H_∞ norm). For all the solutions of (5) which satisfied the following inequalities under zero initial condition for nonzero disturbance:

(i) for the low-frequency range $|\theta| \le \vartheta_l$

$$\begin{aligned} &\sum_{k=0}^{\infty} \left(\eta(k+1) - \eta(k)\right)\left(\eta(k+1) - \eta(k)\right)^T \\ &\quad \le \left(2\sin\frac{\vartheta_l}{2}\right)^2 \sum_{k=0}^{\infty} \eta(k)\,\eta(k)^T, \end{aligned} \tag{8}$$

(ii) for the middle-frequency range $\vartheta_1 \le \theta \le \vartheta_2$

$$\begin{aligned} &e^{j\vartheta_w} \sum_{k=0}^{\infty} \left(\eta(k+1) - e^{j\vartheta_1}\eta(k)\right) \\ &\qquad \times \left(\eta(k+1) - e^{-j\vartheta_2}\eta(k)\right)^T \le 0, \end{aligned} \tag{9}$$

where $\vartheta_w = (\vartheta_2 - \vartheta_1)/2$,

(iii) for the high-frequency range $|\theta| \ge \vartheta_h$

$$\begin{aligned} &\sum_{k=0}^{\infty} \left(\eta(k+1) - \eta(k)\right)\left(\eta(k+1) - \eta(k)\right)^T \\ &\quad \ge \left(2\sin\frac{\vartheta_h}{2}\right)^2 \sum_{k=0}^{\infty} \eta(k)\,\eta(k)^T. \end{aligned} \tag{10}$$

the given constant $\gamma > 0$ is said to be the finite-frequency stochastic H_∞ norm of (5) if the following inequality

$$\mathbb{E}\left(\sum_{k=0}^{\infty} \|e_r(k)\|^2\right) \le \gamma^2 \mathbb{E}\left(\sum_{k=0}^{\infty} \|w(k)\|^2\right) \tag{11}$$

holds.

Remark 4. Definition 3 is motivated by the work of [20, 27], which can be regarded as an extension in finite-frequency domain of standard H_∞ norm. Noticeably, it expresses the robustness from $w(k)$ to $e(k)$ in finite-frequency, that is, the smaller it is, the more robust to $w(k)$ the error $e(k)$ becomes.

Now, the problem to be addressed in this paper can be formulated as follows: design a stable filter (4) such that the filter error system (5) is mean-square stable, and with prescribed finite-frequency stochastic H_∞ norm γ for the external disturbance $w(k)$.

3. Main Results

The filter design problem proposed in the above section will be discussed in this section.

3.1. Conditions for Robustness. Before proceeding further, the following lemma will be recalled to help us derive our main results.

Lemma 5 (Projection Lemma [27]). *For arbitrary* Γ, Λ, Θ, *there exists matrix* F *satisfying* $\Gamma F \Lambda + (\Gamma F \Lambda)^T + \Theta < 0$ *if and only if the following two conditions hold:*

$$\Gamma^{\perp}\Theta\Gamma^{\perp^T} < 0, \qquad \Lambda^{T^{\perp}}\Theta\Lambda^{T^{\perp^T}} < 0. \tag{12}$$

The following lemma will be given which provides a sufficient condition for the desired performance (11) of system (5).

Lemma 6. *Assume the MJLS* (5) *is mean-square stable; let* $\gamma > 0$ *be a given constant, then system* (5) *has a finite-frequency stochastic* H_∞ *norm* γ *if there exist mode-dependent matrices* $P_i = P_i^T$, $Q_i = Q_i^T > 0$, $i \in \mathbb{S}$ *such that the following inequalities hold:*

$$\begin{aligned} &\begin{bmatrix} \mathscr{A}_i & \mathscr{B}_i \\ I & 0 \end{bmatrix}^T \Xi_i \begin{bmatrix} \mathscr{A}_i & \mathscr{B}_i \\ I & 0 \end{bmatrix} \\ &\quad + \begin{bmatrix} \mathscr{C}_i & \mathscr{D}_i \\ 0 & I \end{bmatrix}^T \Pi \begin{bmatrix} \mathscr{C}_i & \mathscr{D}_i \\ 0 & I \end{bmatrix} < 0, \end{aligned} \tag{13}$$

where $\Pi = \left[\begin{smallmatrix} I & 0 \\ 0 & -\gamma^2 I \end{smallmatrix}\right]$ *and*

(i) *for the low-frequency range* $|\theta| \le \vartheta_l$

$$\Xi_i = \begin{bmatrix} -\overline{P}_i & Q_i \\ Q_i & P_i - 2\cos\vartheta_l Q_i \end{bmatrix}, \tag{14}$$

(ii) *for the middle-frequency range* $\vartheta_1 \le \theta \le \vartheta_2$

$$\Xi_i = \begin{bmatrix} -\overline{P}_i & e^{j\vartheta_c}Q_i \\ e^{-j\vartheta_c}Q_i & P_i - 2\cos\vartheta_w Q_i \end{bmatrix}, \tag{15}$$

where $\vartheta_c = (\vartheta_2 + \vartheta_1)/2$, $\vartheta_w = (\vartheta_2 - \vartheta_1)/2$,

(iii) *for the high-frequency range* $|\theta| \ge \vartheta_h$

$$\Xi_i = \begin{bmatrix} -\overline{P}_i & -Q_i \\ -Q_i & P_i + 2\cos\vartheta_h Q_i \end{bmatrix}, \tag{16}$$

where $\overline{P}_i = \sum_{j\in\mathbb{S}} \lambda_{ij} P_j$.

Proof. We first consider the middle-frequency case for the system (5). Assume (13) holds, before and after multiplying it by $\left[\eta^T(k) \;\; w^T(k)\right]$ and its transpose, then we can derive

$$\begin{aligned}\eta^T(k)P_i\eta(k) - \eta^T(k+1)\overline{P}_i\eta(k+1) + e_r^T(k)e_r(k)\\ - \gamma^2 w^T(k)w(k) + \mathrm{tr}\left\{Q\left(e^{j\vartheta_c}\eta(k)\eta^T(k+1)\right.\right.\\ + e^{-j\vartheta_c}\eta(k+1)\eta^T(k)\\ \left.\left.-2\cos\vartheta_w\eta(k)\eta^T(k)\right)\right\} \le 0.\end{aligned} \tag{17}$$

Since $\eta(0) = 0$ and system (5) is mean-square stable, summing up (17) from 0 to ∞ with respect to k, it is straightforward to see that (17) is equal to

$$\mathbb{E}\left(\sum_{k=0}^{\infty}\left(e_r^T(k)e_r(k) - \gamma^2 w^T(k)w(k)\right) + \mathrm{tr}\{Q_iS\}\right) \le 0, \tag{18}$$

where

$$\begin{aligned}S := \sum_{k=0}^{\infty}\left(e^{j\vartheta_c}\eta(k)\eta^T(k+1) + e^{-j\vartheta_c}\eta(k+1)\eta^T(k)\right.\\ \left.-2\cos\vartheta_w\eta(k)\eta^T(k)\right).\end{aligned} \tag{19}$$

It is easy to prove that $-S$ is equal to the left-hand side of (9), so the S is semipositive definite. Also, since $Q_i > 0$, the term $\mathrm{tr}\{Q_iS\}$ is nonnegative when (9) is satisfied. Hence, we have $\mathbb{E}(\sum_{k=0}^{\infty}(e_r^T(k)e_r(k) - \gamma^2 w^T(k)w(k)) \le 0$, which is equivalent to condition (11) for middle frequency in Definition 3.

Similarly, the results follow by choosing $\vartheta_1 := -\vartheta_l$ and $\vartheta_2 := \vartheta_l$ for low-frequency case and $\vartheta_1 := \vartheta_h$ and $\vartheta_2 := 2\pi - \vartheta_h$ for high-frequency case, respectively. The proof is completed. □

Remark 7. If all the matrices in Lemma 6 are independent on i, the MJS will be reduced to a determinate linear system. In this case, Lemma 6 is equivalent to the GKYP in [20], which has been proved to be an effective tool to deal with the finite-frequency problem of linear time-invariant systems.

Theorem 8. *Consider system* (5) *for all $\alpha_k = i \in \mathbb{S}$; assume it is mean-square stable; for a given scalar $\gamma > 0$, the performance of* (11) *is guaranteed if there exist matrices U_i, W_i, V_i, $\mathscr{A}_{fi}$, $\mathscr{B}_{fi}$, C_{fi}, D_{fi}, and*

$$P_i^T = P_i = \begin{bmatrix}P_{i1} & *\\ P_{i2} & P_{i3}\end{bmatrix}, \qquad Q_i^T = Q_i = \begin{bmatrix}Q_{i1} & *\\ Q_{i2} & Q_{i3}\end{bmatrix}, \tag{20}$$

such that the following LMIs hold:

$$\begin{bmatrix}-\overline{P}_{i1} & * & * & * & * & *\\ -\overline{P}_{i2} & -\overline{P}_{i3} & * & * & * & *\\ Q_{1i}-U_i & Q_{2i}^T - V_i & \Psi_3^3 & * & * & *\\ Q_{2i}-W_i & Q_{3i}-V_i & \Psi_3^4 & \Psi_4^4 & * & *\\ 0 & 0 & \Psi_3^5 & \Psi_4^5 & -\gamma^2 I & *\\ 0 & 0 & D_fC & C_f & D_fD & -I\end{bmatrix} < 0, \tag{21}$$

where $\overline{P}_i = \sum_{j\in\mathbb{S}}\lambda_{ij}P_j$ and

$$\begin{aligned}\Psi_3^3 &= P_{i1} - 2\cos\vartheta_l Q_{i1} + He\left(U_iA_i + \mathscr{B}_{fi}C\right)\\ &\quad + E^TE - He\left(C^TD_{fi}^TE\right),\\ \Psi_3^4 &= P_{i2} - 2\cos\vartheta_l Q_{i2} + W_iA_i + \mathscr{B}_{fi}C + \mathscr{A}_{fi}^T - C_{fi}^TE,\\ \Psi_4^4 &= P_{i3} - 2\cos\vartheta_l Q_{i3} + He\left(\mathscr{A}_{fi}\right),\\ \Psi_3^5 &= B_i^TU_i^T + D^T\mathscr{B}_{fi}^T - D^TD_f^TE,\\ \Psi_4^5 &= B_i^TW_i^T + D^T\mathscr{B}_{fi}^T.\end{aligned} \tag{22}$$

Proof. It can be concluded from Lemma 6 that if inequality (13) holds for all $\alpha_k = i \in \mathbb{S}$, the performance of (11) can be reached. Further, (13) is equivalent to

$$\begin{bmatrix}\mathscr{A}_i & \mathscr{B}_i\\ I & 0\\ 0 & I\end{bmatrix}^T\Theta_i\begin{bmatrix}\mathscr{A}_i & \mathscr{B}_i\\ I & 0\\ 0 & I\end{bmatrix} < 0, \tag{23}$$

where

$$\Theta_i = J\Xi_iJ^T + H_i\Pi H_i^T, \tag{24}$$

with $J = \left[\begin{smallmatrix}I & 0\\ 0 & I\\ 0 & 0\end{smallmatrix}\right]$ and $H_i = \left[\begin{smallmatrix}0 & 0\\ \mathscr{C}_i & 0\\ \mathscr{D}_i & I\end{smallmatrix}\right]$.

On the other hand, (13) implies that

$$\begin{bmatrix}I & 0 & 0\\ 0 & 0 & I\end{bmatrix}^T\Theta_i\begin{bmatrix}I & 0 & 0\\ 0 & 0 & I\end{bmatrix} = \begin{bmatrix}-\overline{P}_i & 0\\ 0 & \mathscr{D}_i^T\mathscr{D}_i - \gamma^2 I\end{bmatrix} < 0. \tag{25}$$

Combining (23) and (25), from Lemma 5, one can easily derive that (13) holds if and only if

$$\Theta_i + He\left(\begin{bmatrix}-I\\ \mathscr{A}_i^T\\ \mathscr{B}_i^T\end{bmatrix}X_i^T\begin{bmatrix}0 & I & 0\end{bmatrix}\right) < 0, \tag{26}$$

where matrix X_i^T is the slack variable with appropriate dimensions which is introduced by Lemma 5.

Rewrite X_i as the form of

$$X_i = \begin{bmatrix}U_i & V_i\\ W_i & V_i\end{bmatrix}. \tag{27}$$

One can conclude that the following inequality provides a sufficient condition for (26):

$$\begin{bmatrix}-\overline{P}_i & * & *\\ Q_i - X_i & \psi & *\\ 0 & \mathscr{B}_i^TX_i^T + \mathscr{D}_i^T\mathscr{C}_i & \mathscr{D}_i^T\mathscr{D}_i - \gamma^2 I\end{bmatrix} < 0, \tag{28}$$

where $\psi = P_i - 2\cos\vartheta_l Q_i + He(X_i\mathscr{A}_i) + \mathscr{C}_i^T\mathscr{C}_i$.

After partitioning the matrices P_i and Q_i as the following form

$$P_i = \begin{bmatrix}P_{i1} & *\\ P_{i2} & P_{i3}\end{bmatrix}, \qquad Q_i = \begin{bmatrix}Q_{i1} & *\\ Q_{i2} & Q_{i3}\end{bmatrix} \tag{29}$$

and defining the following new variables

$$\mathscr{A}_{fi} = V_i A_{fi}, \qquad \mathscr{B}_{fi} = V_i B_{fi}, \tag{30}$$

inequality (21) can be derived. The proof is completed. □

Remark 9. In Theorem 8, by introducing a variable X_i, the coupling between the variable P_i and the filter gains will be eliminated. Such a matrix does not present any structure constraint; on the contrary, it may lead to potentially less conservative results.

3.2. Conditions for Stability. Theorem 8 can guarantee the filtering error system to be with a specific robust performance in a certain frequency range of relevance. However, the stability has not been captured, and hence, one may wish to include a stability constraint as an additional design specification. The following theorem will give a result for stability.

Theorem 10. *The system* (5) *is mean-square stable with* $w(k) = 0$ *if there exist matrices* U_i, W_i, V_i, $\mathscr{A}_{fi}$, $\mathscr{B}_{fi}$, C_{fi}, D_{fi}, *and*

$$P_{si}^T = P_{si} = \begin{bmatrix} P_{si1} & * \\ P_{si2} & P_{si3} \end{bmatrix} > 0, \tag{31}$$

such that the following inequality holds:

$$\begin{bmatrix} \overline{P}_{si1} - He\left(U_i\right) & * & * & * \\ \overline{P}_{si2} - V_i^T - W_i & \overline{P}_{si3} - He\left(V_i\right) & * & * \\ A_i^T U_i^T + C^T \mathscr{B}_{fi}^T & A_i^T W_i^T + C^T \mathscr{B}_{fi}^T & -P_{si1} & * \\ \mathscr{A}_{fi}^T & \mathscr{A}_{fi}^T & -P_{si2} & -P_{si3} \end{bmatrix} < 0, \tag{32}$$

where $\overline{P}_{si} = \sum_{j\in\mathbb{S}} \lambda_{ij} P_{sj}$.

Proof. Combing the knowledge of the existing stability criteria for MJSs and the lemma, following the line of the proof for Theorem 8, the conclusion can be derived easily. We do not explain it specifically here. □

Remark 11. It should be pointed out that inequalities (28)–(33) are all linear matrix inequalities which can be solved through LMI toolbox of MATLAB.

Based on the above analysis, a set of optimal solutions $\mathscr{A}_{fi}$, $\mathscr{B}_{fi}$, C_{fi}, and D_{fi} can be obtained by solving the following optimization problem:

$$\begin{aligned} &\min \quad \gamma \\ &\text{s.t.} \quad (21), (32). \end{aligned} \tag{33}$$

Then the filter gains can be computed by the following equalities:

$$\begin{aligned} A_{fi} &= V^{-1} \mathscr{A}_{fi}, \qquad B_{fi} = V^{-1} \mathscr{B}_{fi}, \\ C_{fi} &= C_{fi}, \qquad D_{fi} = D_{fi}. \end{aligned} \tag{34}$$

4. An Illustrative Example

In this section, an example is given to illustrate the effectiveness of the proposed method.

According to some previous researches of the aircraft dynamic model such as [28, 29], it is easily concluded that the nonlinear aircraft dynamic model can be established according to Newton's Second Law of motion. Furthermore, in order to decouple the nonlinear dynamics, the model is decomposed into two models along with longitudinal- and lateral-directional motions, respectively.

The model used in this example is the lateral-directional dynamic model of the NASA High Alpha Research Vehicle (HARV) utilized in [30], that is,

$$\begin{aligned} \dot{x}(t) &= \begin{bmatrix} -0.166 & 0.629 & -0.9971 \\ -12.97 & -1.761 & 0.5083 \\ 3.191 & -0.1417 & -0.1529 \end{bmatrix} x(t) \\ &\quad + \begin{bmatrix} 1.8 \\ 0.7 \\ -1.46 \end{bmatrix} w(t), \\ y(t) &= \begin{bmatrix} 0 & 1 & 0 \\ 0 & 0 & 1 \end{bmatrix} x(t) + \begin{bmatrix} 0.96 \\ -0.4 \end{bmatrix} w(t), \\ z(t) &= \begin{bmatrix} 2.8 & -0.52 & 1.3 \\ 1.7 & 0.9 & -0.4 \end{bmatrix} x(t), \end{aligned} \tag{35}$$

where the system state and output are, respectively,

$$\begin{aligned} \text{state} &= \begin{bmatrix} \text{sideslip angle}\,(^\circ) \\ \text{roll rate}\,(^\circ/s) \\ \text{yaw rate}\,(^\circ/s) \end{bmatrix}, \\ \text{output} &= \begin{bmatrix} \text{roll rate}\,(^\circ/s) \\ \text{yaw rate}\,(^\circ/s) \end{bmatrix}. \end{aligned} \tag{36}$$

Assume that the sampling period is $h = 1$ s, and the sampled data are transmitted through a network, where the data packets may be lost. Further, the quantity of the lost packet $(\alpha_k - 1)$, $\alpha_k \in \mathbb{S} = \{1, 2, 3\}$ at each sampling period is shown in Figure 2, which is subject to the following transition probability matrix:

$$\Lambda = \begin{bmatrix} 0.9 & 0.1 & 0 \\ 0.8 & 0.1 & 0.1 \\ 0.8 & 0.2 & 0 \end{bmatrix}. \tag{37}$$

For prescribed $\vartheta_l = 0.8$, solving the optimization problem (33), we can obtain the optimal value for finite-frequency

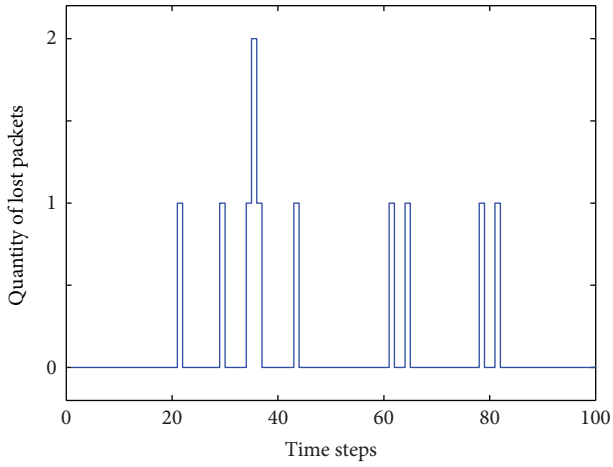

FIGURE 2: The quantity of the dropped packet.

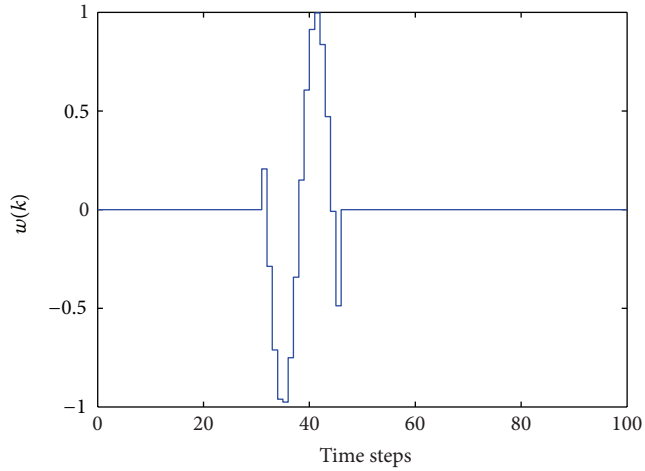

FIGURE 3: The disturbance input $w(t)$.

stochastic H_∞ norm, that is, the robust performance is $\gamma = 0.001$ with the corresponding filter gains as follows:

$$A_{f1} = \begin{bmatrix} -0.5552 & 0.2072 & 1.8402 \\ 1.0360 & -1.5484 & -10.5804 \\ 0.4397 & 0.4041 & 2.0462 \end{bmatrix},$$

$$B_{f1} = \begin{bmatrix} 0.2367 & 1.8933 \\ -1.3950 & -11.7654 \\ 0.2054 & 1.8380 \end{bmatrix},$$

$$C_{f1} = \begin{bmatrix} -2.8000 & -1.1960 & -5.4184 \\ -1.7000 & 0.0944 & 2.7866 \end{bmatrix},$$

$$D_{f1} = \begin{bmatrix} -1.7160 & -4.1184 \\ 0.9944 & 2.3866 \end{bmatrix},$$

$$A_{f2} = \begin{bmatrix} 0.2543 & 0.0869 & -0.3916 \\ -0.2131 & -0.2798 & 3.0482 \\ 0.0533 & 0.0319 & -0.4729 \end{bmatrix},$$

$$B_{f2} = \begin{bmatrix} 0.0765 & -0.3750 \\ -0.5082 & 3.0383 \\ 0.0340 & -0.7283 \end{bmatrix},$$

$$C_{f2} = \begin{bmatrix} -2.8000 & -0.2844 & -3.2306 \\ -1.7000 & -0.3677 & 1.6775 \end{bmatrix},$$

$$D_{f2} = \begin{bmatrix} -0.8044 & -1.9306 \\ 0.5323 & 1.2775 \end{bmatrix},$$

$$A_{f3} = \begin{bmatrix} -0.1377 & -0.0739 & 0.0753 \\ 0.3593 & 0.4907 & -0.6657 \\ 0.0806 & -0.1414 & 0.0216 \end{bmatrix},$$

$$B_{f3} = \begin{bmatrix} -0.0615 & 0.0800 \\ 0.5174 & -0.9498 \\ -0.1909 & -0.0263 \end{bmatrix},$$

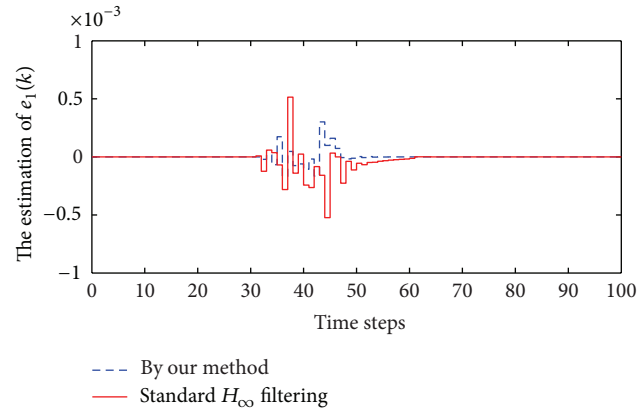

FIGURE 4: The estimation error $e_1(k)$.

$$C_{f3} = \begin{bmatrix} -2.8000 & 0.7070 & -0.8511 \\ -1.7000 & -0.7467 & 0.7680 \end{bmatrix},$$

$$D_{f3} = \begin{bmatrix} 0.1870 & 0.4489 \\ 0.1533 & 0.3680 \end{bmatrix}. \tag{38}$$

In order to show the advantage of the proposed method, we compare it with standard H_∞ filtering method for MJSs which can be found in many researches. In the following, the system will be simulated under zero initial condition, and the disturbance input $w(t)$ is

$$w(t) = \begin{cases} \sin(0.5t), & 0\,\text{s} \le t \le 40\,\text{s}, \\ 0, & \text{otherwise}, \end{cases} \tag{39}$$

which is shown in Figure 3. It is easy to see that the disturbance considered in the this paper is an instantaneous sinusoidal disturbance and its frequency is considered as zero, which belongs to the low frequency.

The simulation results are shown in Figures 4 and 5, which confirm that all the expected system performance requirement are well achieved. Compared with the standard

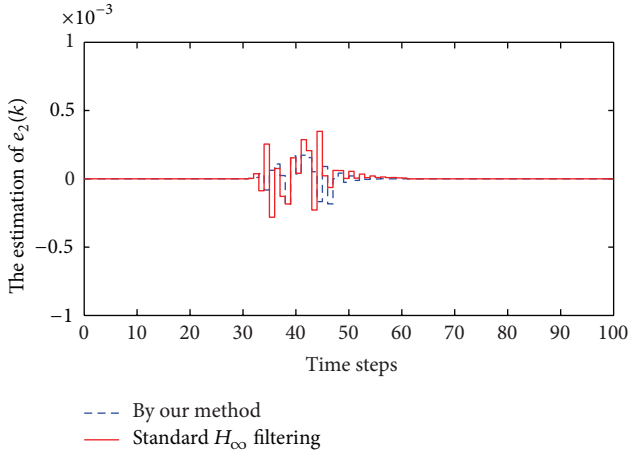

FIGURE 5: The estimation error $e_2(k)$.

H_∞ filtering method, our method performs better even in the case of possible missing measurements.

5. Conclusions

In this paper, we have studied the robust filtering with finite-frequency specifications for NCSs subject to random missing measurements. Here, the NCSs are first modeled into MJLs. Then, a new robust filtering method has been proposed that makes full use of the frequency information of noises to reduce design conservatism by the introduction of finite-frequency stochastic H_∞ index for MJLSs. The design problem is formulated into solving a set of linear matrix inequalities, which can be computed by the LMI Control Toolbox. An example is included to show the effectiveness of the obtained theoretical results.

Acknowledgments

This work is supported by National Natural Science Foundation of China (nos. 61273155, 61273148), New Century Excellent Talents in University (no. NCET-11-0083), a Foundation for the Author of National Excellent Doctoral Dissertation of P.R. China (no. 201157), the Fundamental Research Funds for the Central Universities (Grant no. N120504003), and the Foundation of State Key Laboratory of Robotics (no. 2012-001).

References

[1] P. Seiler and R. Sengupta, "An H_∞ approach to networked control," *IEEE Transactions on Automatic Control*, vol. 50, no. 3, pp. 356–364, 2005.

[2] Y. Shi and H. Fang, "Kalman filter-based identification for systems with randomly missing measurements in a network environment," *International Journal of Control*, vol. 83, no. 3, pp. 538–551, 2010.

[3] H. R. Karimi and H. Gao, "New delay-dependent exponential Hco synchronization for uncertain neural networks with mixed time delays," *IEEE Transactions on Systems, Man, and Cybernetics B*, vol. 40, no. 1, pp. 173–185, 2010.

[4] H. L. Dong, Z. D. Wang, and H. J. Gao, "Robust H_∞ filtering for a class of nonlinear networked systems with multiple stochastic communication delays and packet dropouts," *IEEE Transactions on Signal Processing*, vol. 58, no. 4, pp. 1957–1966, 2010.

[5] B. Shen, Z. D. Wang, and X. H. Liu, "Sampled-data synchronization control of dynamical networks with stochastic sampling," *IEEE Transactions on Automatic Control*, vol. 57, no. 10, pp. 2644–2650, 2012.

[6] D. R. Ding, Z. D. Wang, B. Shen, and H. S. Shu, "H_∞ state estimation for discrete-time complex networks with randomly occurring sensor saturations and randomly varying sensor delays," *IEEE Transactions on Neural Networks and Learning Systems*, vol. 23, no. 5, pp. 725–736, 2012.

[7] D. Yue, Q.-L. Han, and J. Lam, "Network-based robust H_∞ control of systems with uncertainty," *Automatica*, vol. 41, no. 6, pp. 999–1007, 2005.

[8] J. P. Hespanha, P. Naghshtabrizi, and Y. Xu, "A survey of recent results in networked control systems," *Proceedings of the IEEE*, vol. 95, no. 1, pp. 138–162, 2007.

[9] J. Wu and T. W. Chen, "Design of networked control systems with packet dropouts," *IEEE Transactions on Automatic Control*, vol. 52, no. 7, pp. 1314–1319, 2007.

[10] S. Hu and W.-Y. Yan, "Stability robustness of networked control systems with respect to packet loss," *Automatica*, vol. 43, no. 7, pp. 1243–1248, 2007.

[11] G. N. Nair, F. Fagnani, S. Zampieri, and R. J. Evans, "Feedback control under data rate constraints: an overview," *Proceedings of the IEEE*, vol. 95, no. 1, pp. 108–137, 2007.

[12] M. Y. Fu and L. H. Xie, "Finite-level quantized feedback control for linear systems," *IEEE Transactions on Automatic Control*, vol. 54, no. 5, pp. 1165–1170, 2009.

[13] J. Hu, Z. D. Wang, B. Shen, and H. J. Gao, "Gain-constrained recursive filtering with stochastic nonlinearities and probabilistic sensor delays," *IEEE Transactions on Signal Processing*, vol. 61, no. 5, pp. 1230–1238, 2013.

[14] Z. D. Wang, F. W. Yang, D. W. C. Ho, and X. H. Liu, "Robust H_∞ filtering for stochastic time-delay systems with missing measurements," *IEEE Transactions on Signal Processing*, vol. 54, no. 7, pp. 2579–2587, 2006.

[15] G.-H. Yang and D. Ye, "Adaptive reliable H_∞ filtering against sensor failures," *IEEE Transactions on Signal Processing*, vol. 55, no. 7, pp. 3161–3171, 2007.

[16] B. Shen, Z. D. Wang, H. S. Shu, and G. L. Wei, "On nonlinear H_∞ filtering for discrete-time stochastic systems with missing measurements," *IEEE Transactions on Automatic Control*, vol. 53, no. 9, pp. 2170–2180, 2008.

[17] J. Liu, J. L. Wang, and G.-H. Yang, "Reliable guaranteed variance filtering against sensor failures," *IEEE Transactions on Signal Processing*, vol. 51, no. 5, pp. 1403–1411, 2003.

[18] X. He, Z. D. Wang, and D. H. Zhou, "Robust H_∞ filtering for time-delay systems with probabilistic sensor faults," *IEEE Ignal Processing Letters*, vol. 16, no. 5, pp. 442–445, 2009.

[19] L. J. Karam and J. H. McClellan, "Chebyshev digital FIR filter design," *Signal Processing*, vol. 76, no. 1, pp. 17–36, 1999.

[20] T. Iwasaki and S. Hara, "Generalized KYP lemma: unified frequency domain inequalities with design applications," *IEEE Transactions on Automatic Control*, vol. 50, no. 1, pp. 41–59, 2005.

[21] Y.-S. Chou, C.-C. Lin, and Y.-L. Chang, "Robust H-infinity filtering in finite frequency domain for polytopic systems with application to in-band quantisation noise reduction in uncertain cascaded sigma-delta modulators," *IET Control Theory & Applications*, vol. 6, no. 9, pp. 1155–1171, 2012.

[22] T. Iwasaki, S. Hara, and A. L. Fradkov, "Time domain interpretations of frequency domain inequalities on (semi)finite ranges," *Systems & Control Letters*, vol. 54, no. 7, pp. 681–691, 2005.

[23] T. Iwasaki and S. Hara, "Feedback control synthesis of multiple frequency domain specifications via generalized KYP lemma," *International Journal of Robust and Nonlinear Control*, vol. 17, no. 5-6, pp. 415–434, 2007.

[24] X. W. Li and H. J. Gao, "Robust finite frequency H_∞ filtering for uncertain 2-D Roesser systems," *Automatica*, vol. 48, no. 6, pp. 1163–1170, 2012.

[25] H. Wang and G.-H. Yang, "A finite frequency approach to filter design for uncertain discrete-time systems," *International Journal of Adaptive Control and Signal Processing*, vol. 22, no. 6, pp. 533–550, 2008.

[26] H. J. Gao and X. W. Li, "H_∞ filtering for discrete-time state-delayed systems with finite frequency specifications," *IEEE Transactions on Automatic Control*, vol. 56, no. 12, pp. 2935–2941, 2011.

[27] D.-W. Ding and G.-H. Yang, "Fuzzy filter design for nonlinear systems in finite-frequency domain," *IEEE Transactions on Fuzzy Systems*, vol. 18, no. 5, pp. 935–945, 2010.

[28] D. Mcituer, I. Ashkenas, and D. Graham, *Aircraft Dynamics and Automatic Control*, Princeton University Press, Princeton, NJ, USA, 1973.

[29] R. J. Adams, J. M. Buffngton, A. G. Sparks, and S. S. Banda, "An introduction to multivariable flight control system design," Wright Lab. Report WL-TR-92-3110, Wright Lab Wright-Patterson AFB, Wright-Patterson AFB, Ohio, USA, 1992.

[30] W. Siwakosit, S. A. Snell, and R. A. Hess, "Robust flight control design with handling qualities constraints using scheduled linear dynamic inversion and loop-shaping," *IEEE Transactions on Control Systems Technology*, vol. 8, no. 3, pp. 483–494, 2000.